सत्यमेव जयते

INDIAN AGRICULTURAL
RESEARCH INSTITUTE, NEW DELHI.

I. A. R. I. 6.
MGIPC—S1—6 AR/54—7-7-54—10,000.

The Journal of
PHYSICAL CHEMISTRY

(Founded by Wilder D. Bancroft)

Editor

S. C. LIND

Associate Editors

E. J. BOWEN
FARRINGTON DANIELS
HERBERT FREUNDLICH
GEORGE GLOCKLER
C. N. HINSHELWOOD
GEORGE S. PARKS
J. R. PARTINGTON

Assistant Editor

LOUISE KELLEY

Volume 44

IMP. AGRI. RES. INST. NEW DELHI
10. FEB. 1941
LIBRARY

BALTIMORE
1940

10. FEB. 1941
LIBRARY

CONTENTS

NUMBER 1, JANUARY, 1940

The Colloidal Behavior of Clays as Related to their Crystal Structure. T. F. Ford, A. G. Loomis, and J. F. Fidiam 1
Chemical Preparation of Colloidal Suspensions in Non-aqueous Solvents. I. Methyl Alcohol and Benzene. Arthur A. Vernon and Harrison A. Nelson 12
Chemical Preparation of Colloidal Suspensions in Non-aqueous Solvents. II. Ether, Dioxane, and Acetone. Arthur A. Vernon and Harrison A. Nelson. 21
The Influence of Brownian Movement on the Viscosity of Solutions. R. Simha 25
The Growth, Orientation, and Preparation of the Surface of Single Crystals of Copper. Allen T. Gwathmey and Arthur F. Benton 35
Mechanism of Photographic Development II. Development by Hydroquinone. T. H. James 42
Studies of Silicic Acid Gels. IX. The Effect of a Change of pH upon the Time of Set of Some Acid Gels. Charles B. Hurd and Harris W. Paton. 57
The Influence of Sol Concentration on Flocculation Values. E. D. Fisher and C. H. Sorum 62
Activated Carbon as a Catalyst in Certain Oxidation-Reduction Reactions. Elmer C. Larsen and James H. Walton 70
Wetting Characteristics of Solid Surfaces Covered with Adsorbed Films. F. E. Bartell and Kenneth E. Bristol 86
On Quasi-reversible Conduction and Galvanic Cells with Liquid-Liquid Junctions. F. O. Koenig 101
New Books:
- Der disperse Bau der festen Systeme. By D. A. Balarew Reviewed by C. H. Desch 136
- Mellor's Modern Inorganic Chemistry. Reviewed by Arthur A. Vernon 137
- Précis de Chimie Physique. By A. Berthoud. Reviewed by F. H. MacDougall 137
- Essentials of Physiological Chemistry. By Arthur K. Anderson. Reviewed by L. Earle Arnow 138
- A Text-Book of Light. By A. W. Barton. Reviewed by Allan Ferguson 138

NUMBER 2, FEBRUARY, 1940

Asphaltic Bitumen as Colloid System. J. Ph. Pfeiffer and R. N. J. Saal 139
Rheological Properties of Asphaltic Bitumen. R. N. J. Saal and J. W. A. Labout 149
The Solubility of Calcium Oxalate in Various Salt Solutions. H. Shehyn and D. B. Pall 166
The Effect of Roentgen Irradiation upon Erythrocytes. D. H. Drummond, J. P. Tollman, and F. L. Richards 172
Catalysis by Metallized Bentonites. Geoffrey Broughton 180

The Structure of Gelatin Sols and Gels. VI. The Absorption of Water Vapor and the Electrical Conductivity. S. E. Sheppard, R. C. Houck, and C. Dittmar 185

The Solubilities of Certain Inorganic Compounds in Ordinary Water and in Deuterium Water. Robert D. Eddy and Alan W. C. Menzies 207

The Catalytic Oxidation of Hydrogen on Platinum. A Search for Chemiluminescence and Ionization. R. Potvin and C. Ouellet 235

pH Change in Gold Sol Formation. C. L. Throckmartin and C. H. Sorum 247

The System Silver Sulfate—Aluminum Sulfate—Water. J. A. Addlestone, L. R. Marsh, and G. C. Hall . 256

Hydrous Lanthanum Hydroxide as an Emulsifying Agent. Therald Moeller 259

NUMBER 3, MARCH, 1940

Electrokinetics. XXII. Electrokinetic Potentials of Barium Sulfate in Solutions of Electrolytes and in Fifty Per Cent Ethanol. R. G. Ruyssen . 265

Physical Properties of the Alkyl Fluorides and a Comparison of the Alkyl Fluorides with the Other Alkyl Halides and with the Alkyls of the Elements of Period II. Aristid V. Grosse, Richard C. Wackher, and Carl B. Linn 275

Intramolecular Folding of Polypeptide Chains in Relation to Protein Structure. Hans Neurath 296

Calculation of Solute Activities from Activities of the Solvent. Limiting Behavior of the *h* and *j* Functions in Dilute Solutions. Merle Randall and Bruce Longtin 306

Approximate Rules for Solute Activities in Dilute Solutions of Non-electrolytes. Generalized Form of Bury's Rule. Merle Randall, W. F. Libby, and Bruce Longtin . . 313

Polyiodides of Ammonium. I. Ammonium Iodide and Iodine. T. R. Briggs and K. H. Ballard 322

Polyiodides of Ammonium. II. The Ternary System Ammonium Iodide, Iodine, and Water T. R. Briggs, K. H. Ballard, Miss F. R. Alrich, and J. P. Wikswo.. 325

Polyiodides of Potassium. II. The Ternary System Potassium Iodide–Iodine–Water. T. R. Briggs, K. D. G. Clack, K. H. Ballard, and W. A. Sassaman 350

Note on the System Sodium Iodide–Water. T. R. Briggs and W. F. Geigle '. 373

The Physical Properties of the Ternary System Butyl Alcohol–Ethyl Acetate–Toluene. E. E. Litkenhous, J. D. Van Arsdale, and I. W. Hutchinson, Jr. 377

The Conductance of Salts in Monoethanolamine. H. T. Briscoe and Thedford P. Dirkse 388

New Books:

An Introduction to the Principles of Physical Chemistry. By O. Maass and E. W. R. Steacie. Reviewed by F. E. Bartell 397

Electromagnetics: A Discussion of Fundamentals. By Alfred O'Rahilly. Reviewed by W. F. G. Swann. 397

Thorpe's Dictionary of Applied Chemistry. By Jocelyn Field Thorpe and M. A. Whiteley. Reviewed by Jas. Lewis Howe. 399

NUMBER 4, APRIL, 1940

Translucent Films of Aluminum Oxide. Richard E. Vollrath 401

The Azeotropic System Alcohol–Water–Benzene. Walter D. Bonner and Max B. Williams. 404

A Note concerning Ion Adsorption by Pectin. Glenn H. Joseph. . . . 409

Photovoltaic Cells with Silver-Silver Bromide Electrodes. III. Optical Sensitizing by Dyes. S. E. Sheppard, W. Vanselow, and G. P. Happ 411
Silicic Acid as a Protective Colloid for Manganese Dioxide Sols. Fred Hazel 422
Freezing Points in Mixtures of Strong Electrolytes. Merle Randall and Bruce Longtin 427
The Preparation of Fluorescent Calcite. Gorton R. Fonda 435
The Copper Sulfate-Sodium Silicate Reaction. Harold V. Anderson and Frank P. Hochgesang . . 439
Convergence of Tie Lines in Ternary Liquid Systems. Irvin Bachman 446
The Effect of Variation in Ionic Strength and Temperature on the Apparent Dissociation Constants of Thirty Substituted Barbituric Acids. M. E. Krahl 449
On the Theory of Galvanic Cells Subject to Fields of Force. I. The Gravitational Field. F. O. Koenig and S. W. Grinnell 463
The Specific Heats of Some Aqueous Sodium and Potassium Chloride Solutions at Several Temperatures. I. C. B. Hess and Bruce E. Gramkee.. 483
The Specific Heats of Some Aqueous Sodium and Potassium Chloride Solutions at Several Temperatures. II. Chester M. White 494
X-ray Studies of Crystallite Orientation in Cellulose Fibers. III. Fiber Structures from Coagulated Cellulose. Wayne A. Sisson . 513
New Books:
Explosions- und Verbrennungs-vorgänge in Gasen. By Wilhelm Jost. Reviewed by Oliver C. de C. Ellis .. . 529
Technische Adsorptionstoffe in der Kontaktkatalyse. By Franz Krczil. Reviewed by L. H. Reyerson .. . 530
Applied Mathematics in Chemical Engineering. By T. K. Sherwood and C. F. Reed. Reviewed by C. C. Furnas. 530
Ferromagnetismus. By R. Becker and W. Döring. Reviewed by Edmund C. Stoner. 531
Reine Metalle. Edited by A. E. van Arkel. Reviewed by C. H. Desch .. 531
Principles of Mineral Dressing. By A. M. Gaudin. Reviewed by Oliver C. Ralston 532
Lectures on Osmosis. By F. A. H. Schreinemakers. Reviewed by F. E. Bartell 533
Colloid Chemistry. By Harry Boyer Weiser. Reviewed by Karl Sollner 534

NUMBER 5, MAY, 1940

The Inhibiting Action of Minute Amounts of Sodium Hexametaphosphate on the Precipitation of Calcium Carbonate from Ammoniacal Solutions. I. Quantitative Studies of the Inhibition Process. R. F. Reitemeier and T. F. Buehrer 535
The Inhibiting Action of Minute Amounts of Sodium Hexametaphosphate on the Precipitation of Calcium Carbonate from Ammoniacal Solutions. II. Mechanism of the Process, with Special Reference to the Formation of Calcium Carbonate Crystals. T. F. Buehrer and R. F. Reitemeier 552
A Sensitive Static Vapor Pressure Apparatus. Ray Calvin Chandler. . . 574
Particle Size Determination of Colloidal Systems by the Supercentrifuge. E. A. Hauser and H. K. Schachman............ 584
Cybotaxis at Interfaces. T. H. Hazlehurst and Harvey A. Neville. .. . 592
The Photochemical Oxidation of Oxalic Acid Sensitized by Ferric Ion. Robert Livingston 601

Figures in Thin Layers of Grease and Viscous Liquids. W. D. Kumler.. .. 612
Molal Volumes of Solute. IV. Otto Redlich....... 619
The Ternary Systems Ethylene Glycol–Potassium Carbonate–Water and Dioxane–Potassium Carbonate–Water. Kenneth A. Kobe and Joseph P. Stong, Jr. 629
Solid Polyiodides of Rubidium. H. W. Foote and Michael Fleischer. . . 633
Addition Compounds of Iodine with Alkali Bromides and Thiocyanates. H. W. Foote and Michael Fleischer 640
The Iodides of Some Polyvalent Metals. H. W. Foote and Michael Fleischer 647
The Coefficient of Thixotropy of Suspensions of Carbon Black in Mineral Oil. J. E. Arnold and C. F. Goodeve 652
Mixed Copper–Chromium Oxide Hydrogenation Catalysts. V. N. Ipatieff, B. B. Corson, and J. D. Kurbatov 670
New Books:
Theoretical Electrochemistry. By N. C. McKenna. Reviewed by I. M. Kolthoff 679
Volumetric and Phase Behavior of Hydrocarbons. By Bruce H. Sage and William N. Lacey. Reviewed by B. T. Brooks 680
Quantitative Biological Spectroscopy. By Elmer S. Miller. Reviewed by Joseph Valasek . . 680
The Raman Effect. By James H. Hibben. Reviewed by Geo. Glockler . 681
Molecular Spectra and Molecule Structure. I. Diatomic Molecules. By Gerhard Herzberg. Reviewed by Geo. Glockler 682

NUMBER 6, JUNE, 1940

The Quaternary System Acetic Acid–Chloroform–Acetone–Water at 25°C. A. V. Brancker, T. G. Hunter, and A. W. Nash . 683
The Derivation of the Equilibrium Conditions in Physical Chemistry on the Basis of the Work Principle. J. N. Brønsted 699
Brønsted's Criticism of Classical Thermodynamics. F. H. MacDougall 713
The Dielectric Properties of the System Gelatin–Water. II. Hugo Fricke and Edward Parker 716
Catalytic Hydrolysis of Chlorobenzene in the Vapor Phase. Arthur A. Vernon and Francis X. Thompson 727
Boiling Point Relationships among Aliphatic Hydrocarbons. Gustav Egloff, J. Sherman, and R. B. Dull 730
Light Scattering in Normal Human Dentine. The Calculation of Absorption and Scattering Constants. Richard S. Manly, John F. Bonner, and Harold C. Hodge 745
The Precipitation of Silver Chromate. Andrew Van Hook 751
Intermicellar Hole and Tube System in Fiber Structure. H. Mark. ... 764
Hevea Latex: Effect of Proteins and Electrolytes on Colloidal Behavior. A. R. Kemp and W. G. Straitiff 788
The Liquid State of the Elements. William Hume-Rothery 808
Radioactive Standards 824
New Books:
M. K. S. Units and Dimensions and a Proposed M. K. O. S. System. By G. E. M. Jauncey and A. S. Langsdorf. Reviewed by F. H. MacDougall... 825
Thermodynamics and Chemistry. By F. H. MacDougall. Reviewed by Kenneth S. Pitzer 825
Einführung in die technische Fliesskunde. By G. W. Scott Blair. Reviewed by Eugene C. Bingham 826

The Nature of the Chemical Bond. By Linus Pauling. Reviewed by Robert S. Mulliken 827
The Cyclotron. By W. B. Mann. Reviewed by S. C. Lind . 828
Abridged Scientific Publications from the Kodak Research Laboratories. Vol. XX. 829
Rheological Memoirs. Edited by Eugene C. Bingham. Reviewed by S. C. Lind . . 829
The Physics and Chemistry of Surfaces. By N. K. Adam. Reviewed by L. H. Reyerson 829
Kurzes Lehrbuch der physikalischen Chemie. Heft 2. By K. Jellinek. Reviewed by James F. Spencer 829
Introduction to Atomic Physics. By Henry Semat. Reviewed by Geo. Glockler . . 830
The Physical Examination of Metals. Vol. I. Optical Methods. By Bruce Chalmers. Reviewed by Ralph L. Dowdell . 831
Statistical Thermodynamics. By R. H. Fowler and E. Guggenheim. Reviewed by E. L. Hill . 831
Rutherford. By A. S. Eve. Reviewed by S. C. Lind 832
Some Problems in Adsorption. By J. K. Roberts. Reviewed by A. B. Van Cleave . . 833
Casein and its Industrial Applications. By Edwin Sutermeister and Frederick L. Browne. Reviewed by L. H. Reyerson 834
Errata . 834

NUMBER 7, OCTOBER, 1940

Gas Imperfection. I. Experimental Determination of Second Virial Coefficients for Seven Unsaturated Aliphatic Hydrocarbons. EDWIN E. ROPER 835
Studies on Silicic Acid Gels. X. The Time of Set of Gel Mixtures Containing High Concentrations of Mineral Acids. Charles B. Hurd and Raymond W. Barclay . . 847
The Yellow and Red Zinc Silicate Phosphors. Gorton R. Fonda 851
Sugar Alcohols. XXI. A Study of the Effect of the Anhydrides of Sorbitol on the Dissociation Constant of Boric Acid. Frederick K. Bell, C. Jelleff Carr, and John C. Krantz, Jr. . 862
The Quantum Yields of Some Dye-sensitized Photoöxidations. Frank Hurd and Robert Livingston 865
The Reaction of Formaldehyde with Amino Acids: X-ray Diffraction Patterns. Allan K. Smith, Philip Handler, and J. N. Mrgudich 874
The Effects of Certain Salts on the Dissociation of Alanine. II. Experiments on Cells without Liquid-junction Potentials. A. C. Batchelder and Carl L. A. Schmidt . . 880
The Effects of Certain Salts on the Dissociation of Aspartic Acid, Arginine, and Ornithine. A. C. Batchelder and Carl L. A. Schmidt 893
Equilibria in the Systems $Na_2O-SiO_2-H_2O$ and $Na_2O-Al_2O_3-H_2O$ at 25°C. J. W. Sprauer and D. W. Pearce. . 909
The Activity of the Constituents in Mixtures of *n*-Butyl Alcohol and Water at 30°C. Merle Randall and Heinz P. Weber 917
Studies on Aging and Coprecipitation. XXXIII. The Thermal Aging of Imperfect Barium Sulfate. I. M. Kolthoff and W. M. MacNevin 921
Photovoltaic Behavior of Pure Silver Bromide. Herbert L. Sanders and I. M. Kolthoff 936

Application of the Hydrogen-bridge Theory to Sorption from Solution by Silica Gel. Albert L. Elder and Robert A. Springer.......... 943
Communication to the Editor:
Photochemical Reduction of Ferric Ion by Oxalic Acid. Gertrud Kornfeld. . 949
New Books:
A Dictionary of Metals and their Alloys. By F. J. Camm. Reviewed by Ralph L. Dowdell 950
Theoretical and Applied Electrochemistry. By Maurice de Kay Thompson. Reviewed by Hiram S. Lukens 950
Chemical Computations and Errors. By Thomas B. Crumpler and John H. Yoe. Reviewed by Robert Livingston . . 951
Chemistry and Medicine. Maurice B. Visscher, *Editor*. Reviewed by W. D. Armstrong . . 951
Introduction to Bessel Functions By F. Bowman. Reviewed by Allan Ferguson 952
The Nature of the Chemical Bond. By Linus Pauling. Reviewed by Robert S. Mulliken 952
The Ultracentrifuge. By The Svedberg and Kai O. Pedersen. Reviewed by H. Freundlich . . 952
Electrocapillarity. By J. A. V. Butler. Reviewed by H. Freundlich 953
Physicochemical Methods. By Joseph Reilly and William Norman Rae. Reviewed by Robert Livingston . . 953
A New Dictionary of Chemistry. Edited by Stephen Miall. Reviewed by J. R. Partington . . 954
Molecular Spectra and Molecule Structure. I. Diatomic Molecules. By Gerhard Herzberg 954

NUMBER 8, NOVEMBER, 1940

Absolute Rates of Solid Reactions: Diffusion. Allen E. Stearn and Henry Eyring........... 955
A Theory of Diffusion in Liquids. Allen E. Stearn, Edwin M. Irish, and Henry Eyring 981
Water Bound to Gelatin as Shown by Molecular Structure Studies. O. L. Sponsler, Jean D. Bath, and J. W. Ellis . .. 996
The Macleod Constant and its Dependence on Physicochemical Factors. David T. Lewis . 1007
New Books:
Electrochemistry and Electrochemical Analysis. Vol. II. By H. J. S. Sand. Reviewed by James F. Spencer 1011
Principles of Inorganic and Analytical Chemistry. By E. J. Baldwin. Reviewed by I. M. Kolthoff 1012

NUMBER 9, DECEMBER, 1940

A Phase Rule Study of the System Sodium Stearate–Water. James W. McBain, Robert D. Vold, and Mary Frick.... 1013
The Time of Set of Silica Gels. V. The Effect of Alcohols and pH on the "Heat of Activation." L. A. Munro and J. A. Pearce............... 1024
An Anomalous Concentration Cell. The Constitution of Solutions of Stannous Chloride in Water and in Hydrochloric Acid. L. R. Allison, E. J. Hartung, and E. Heymann.................................... 1033
Viscosities of Several Common Gases between 90°K. and Room Temperature. Herrick L. Johnston and Kenneth E. McCloskey...................... 1038

Systems of Sodium Palmitate in Organic Liquids. Robert D. Vold, Charles W. Leggett, and James W. McBain 1058
Quantitative Capillary Luminescence Analysis. Frank E. E. Germann and James W. Hensley 1071
An Electron Diffraction Study of Hydrous Oxides Amorphous to X-rays. Harry B. Weiser and W. O. Milligan 1081
Skin Reactions. IX. The Electrophoretic Demonstration of the Patent Pores of the Living Human Skin; its Relation to the Charge of the Skin. Harold A. Abramson and Manuel H. Gorin 1094
Electric Moments and Relaxation Times of Protein Molecules. J. L. Oncley 1103
A Study of Some Properties of Thixotropic Gels Containing Egg Albumin as the Disperse Phase. William G. Myers and Wesley G. France 1113
The Infrared Absorption of Proteins in the 3μ Region. XII. A. M. Buswell, Karl F. Krebs, and W. H. Rodebush 1126
Ultracentrifugation Studies on Tobacco Mosaic and Bushy Stunt Viruses. Max A. Lauffer 1137
New Books:
Kinetics of Chemical Change. By C. N. Hinshelwood. Reviewed by S. C. Lind 1147
Electrochemistry and Electrochemical Analysis. Vol. I. Electrochemical Theory. By Henry J. S. Sand. Reviewed by S. Glasstone 1147
Intermediate Chemical Calculations. By Partington and Stratton. Reviewed by Robert Livingston . 1147
Electronic Structure and Chemical Binding. By O. K. Rice. Reviewed by Geo. Glockler . . . 1148
International Union of Chemistry, Tables and Committee Reports. Reviewed by S. C. Lind . . . 1149

ERRATA

Volume 44, Number 6

Page 809: In the second equation substitute

$$\text{“}\frac{L_p}{(T_b)_p}\text{”} \quad \text{for} \quad \text{“}\frac{F_p}{(T_b)_p}\text{”}$$

Page 815: In the fifth line below table 3 substitute "*a*" for "*g*."

Page 817: Line 14 should read "The boiling point is the temperature at which the liquid and vapor are in equilibrium, . . ."

Page 819: In column 9 of table 5 substitute "Hf" for "Hg."

Page 812: The second sentence in paragraph No. 6 should be omitted.

LIBRARY

THE COLLOIDAL BEHAVIOR OF CLAYS AS RELATED TO THEIR CRYSTAL STRUCTURE[1]

T. F. FORD, A. G. LOOMIS, AND J. F. FIDIAM

Shell Development Company, Emeryville, California

Received August 31, 1939

INTRODUCTION

Most salts cause precipitation or gelation of clay suspensions. Small amounts of sodium tannate, sodium hexametaphosphate, or sodium silicate, on the other hand, remarkably reduce their viscosity. Advantage is taken of this fact in oil well drilling by the rotary method to produce mobile clay drilling fluids of high density, and such treated suspensions serve various practical purposes (1).

Experiments here described develop in detail the view, which has been also suggested by Garrison (6), that these chemicals are adsorbed on specific portions of the exterior of clay particles, and that they reduce the viscosity of suspensions by destroying the aggregation of the particles into structures.

VISCOSITY REDUCTION PRODUCED BY VARIOUS CHEMICALS

The curves of figure 1 show the viscosity reduction produced by the chemicals which have been mentioned and by sodium pyrophosphate, one of the most effective reducers (4). In figure 2 similar curves are given for a series of sodium polyphosphates, of which sodium pyrophosphate is the first member. The sodium polyphosphates have the general formula $Na_nP_{n-2}O_{3n-5}$ (18) and probably differ only in the length of the PO_2 chain, according to the structure

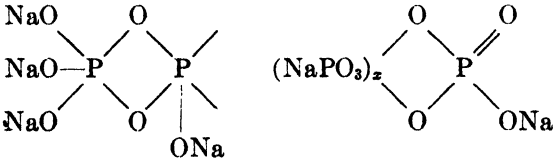

In these experiments the viscosities were determined at room temperature with the Störmer viscosimeter. The clay is one found near Frazier Mountain, California, and employed in the Los Angeles area to make

---

[1] Presented at the Sixteenth Colloid Symposium, held at Stanford University, California, July 6–8, 1939.

14685

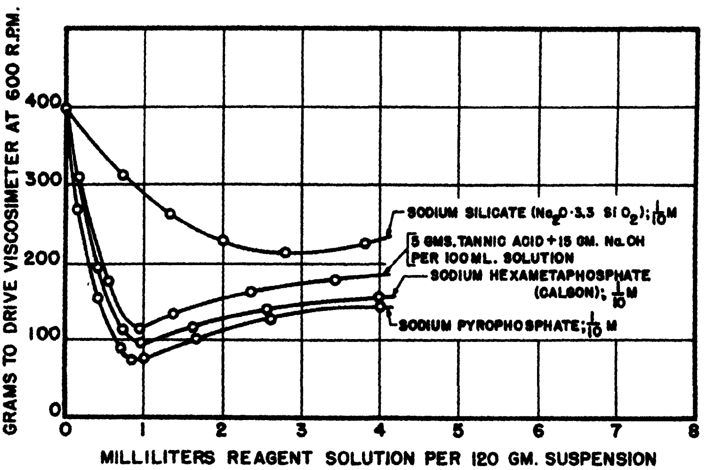

FIG. 1. Viscosity reduction produced by various chemicals. All curves corrected for dilution.

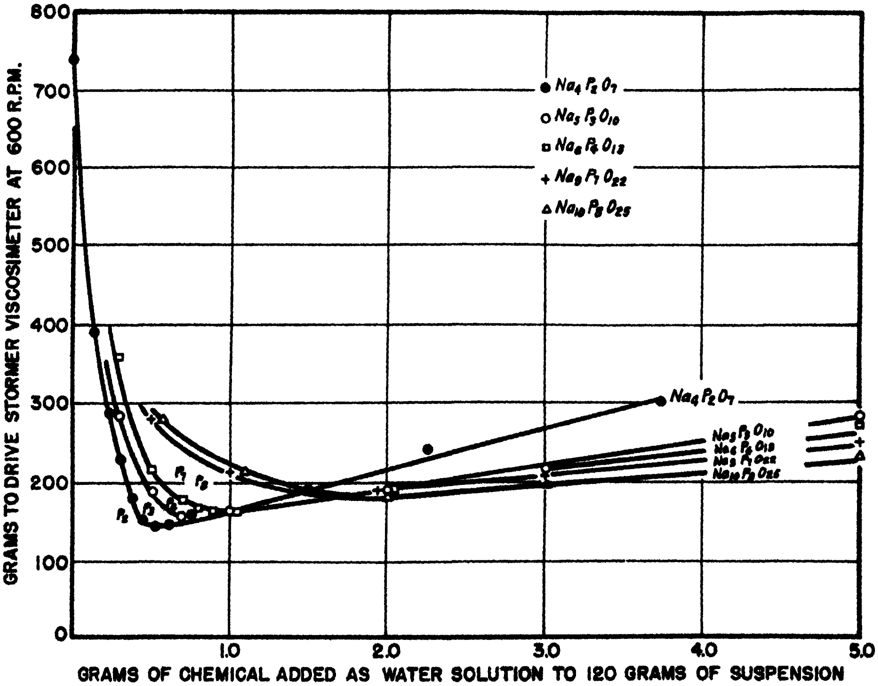

FIG. 2. Viscosity reduction produced by sodium polyphosphates. All curves corrected for dilution.

suspensions for well drilling. The suspensions used were at least 3 weeks old.

EVIDENCE FOR ADSORPTION OF VISCOSITY-REDUCING CHEMICALS IN THE CLAY–WATER INTERFACE

The amount of sodium tetraphosphate required to reduce the viscosity of Frazier Mountain clay is greater per gram of clay for fine fractions than for coarse fractions as obtained in the De Laval and Sharples centrifuges. Since the analyses of these fractions (table 1) appear to eliminate any explanation based on differences of chemical composition, at least the initial effect of this chemical must be on the outside surfaces of the particles. Similar results have been obtained with graded Wyoming bentonites.

TABLE 1

Chemical analysis of Frazier Mountain clay fractions

	MEDIUM FRACTION	FINE FRACTION
	per cent	*per cent*
SiO_2	52.43	52.11
Fe_2O_3	9.34	9.48
Al_2O_3	19.01	19.60
CaO	2.17	2.14
MgO	4.12	4.08
Na_2O/K_2O as Na_2O	3.20	3.60
SO_4^{--}		
Cl^-		
Loss on ignition	10.56	9.95
Total	100.83	100.96

The viscosities of treated suspensions tend to revert to original or even higher values after several hours or days, especially if there is agitation. Among the polyphosphates reversion is the most rapid for the pyrophosphate. Possibly these agents are slowly lost by diffusion into inner particle surfaces where they cannot prevent aggregation but may, on the other hand, promote splitting of crystal sheets with multiplication of particles.

The amounts of polyphosphates required to produce the maximum viscosity reduction in 120 g. of suspension containing 14 g. of clay, as calculated from figure 2, are as follows:

For $Na_4P_2O_7$	0.00021 mole
For $Na_5P_3O_{10}$, prepared by fusing $Na_4P_2O_7$ + 1/6 $Na_6P_6O_{18}$	0.00019 mole
For $Na_6P_4O_{13}$, prepared by fusing $Na_4P_2O_7$ + 1/3 $Na_6P_6O_{18}$	0.00018 mole
For $Na_9P_7O_{22}$, prepared by fusing Na_3PO_4 + $Na_6P_6O_{18}$	0.00020 mole
For $Na_{10}P_8O_{25}$, prepared by fusing $Na_4P_2O_7$ + $Na_6P_6O_{18}$	0.00018 mole approximately

The experiments suggest that these compounds produce equal effects per molecule because they cover equal areas per molecule.

Tannic acid evidently coats the same area as pyrophosphate, since one-fifth as many moles are required for maximum effect (figure 1), but the cross-sectional area of the molecule, $C_6H_7O_6[\text{—}COC_6H_2(OH)_2OCOC_6H_2(OH)_3]_5$, is about five times the cross-sectional area of the pyrophosphate molecule.

EVIDENCE FOR STRUCTURAL BREAKDOWN IN CLAY SUSPENSIONS ON CHEMICAL TREATMENT

Left undisturbed, clay suspensions tend to develop considerable mechanical strength or yield value, but most of this mechanical strength is lost immediately on chemical treatment, as shown by the curves of figure 3. In these experiments the torque just necessary to initiate rotation of a metal cylinder imbedded in the suspension was taken as a measure of the mechanical strength, or gel strength. Similar data are reported by Garrison (6).

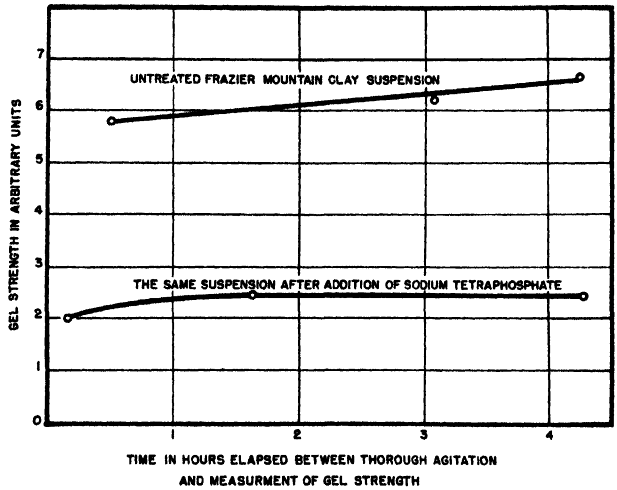

FIG. 3. The relation of gel strength to time of setting, and the effect of sodium tetraphosphate on gel strength.

Structural breakdown of suspensions on treatment is shown not only by loss of gel strength, but by the disappearance of structural viscosity as shown by the curves of figure 4. The relation between viscosity and concentration for treated suspensions is in fact often described fairly well by the Einstein equation

$$\eta/\eta_0 = 1 + 2.5C\nu$$

derived for spherical particles.

CRYSTAL STRUCTURE

Clays are hydrated aluminum silicates, most of which may be classed as either kaolins, $Al_2O_3 \cdot 2SiO_2 \cdot 2H_2O$, or montmorillonites, $Al_2O_3 \cdot 4SiO_2 \cdot H_2O$. These formulas represent ideal analyses of the acid or amphoteric clays. Both the kaolins and the montmorillonites (or bentonites) are composed of superimposed layers of aluminum and silicon bound together through oxygen bridges (2). The structures of the kaolin and montmorillonite unit sheets as given by Hofmann, Endell, and Wilm (10) are reproduced in figure 5. Many of these unit sheets may be combined in individual clay particles. Water may penetrate between the unit sheets in montmorillonite and presumably may even cause their complete separation (9, 19).

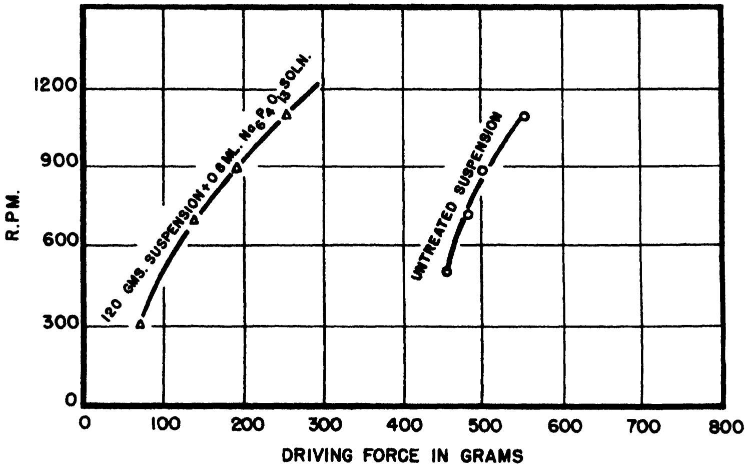

FIG. 4. Relations between shearing stress and rate of shear for treated and untreated suspensions of Frazier Mountain clay. Stórmer viscosimeter.

Clay particles, like the unit sheets of which they are composed, are themselves plates, as can be directly observed in some cases or inferred either from streaming in polarized light or from the nature of the twinkling in the ultramicroscope.

GROSS STRUCTURE IN CLAY SUSPENSIONS

The plate-like character of clay particles is emphasized by Lewis, Squires, and Thompson (14), who suggest that overlapping will build up structural agglomerates. Broughton and Squires (3) suggest edge-to-edge contact. The chief objection (9) is that gelation occurs in fine bentonite suspensions so dilute (0.1 per cent) that, for continuous contact, ratios of length and breadth to thickness of square platelets of the order of 1000 to 2000:1 are necessary. This objection holds only for suspensions to which salt has been added, however, and in the absence of added electrolytes gelation has not been observed below 1.4 per cent (8). The particles used to produce these latter gels might have had ratios of length and breadth to thickness which do permit edge-to-edge contact in semi-rigid structures.

To explain gelation Salmang (20) has postulated immobilization in microscopically thick hulls of bound water, but calculations based on the sorption capacity for exchangeable ions (11) and on heats of sorption (17) lead to the conclusion that the thickness of the solvation mantle cannot exceed 25 to 40 Å; and decreasing setting time with rising temperature is also inconsistent with the bound water theory, as solvation is generally considered to decrease with temperature (9). Although the existence of compressed water in bentonite suspensions is shown by increasing apparent density with concentration (9), at low concentrations apparent densities are found which are equal to or even less than the dry density of bentonite. This suggests that the compressed water is not bound as solvation hulls to single particles but that it must be entrapped between particles. The forces primarily responsible for structure, therefore, do not arise from the bound water.

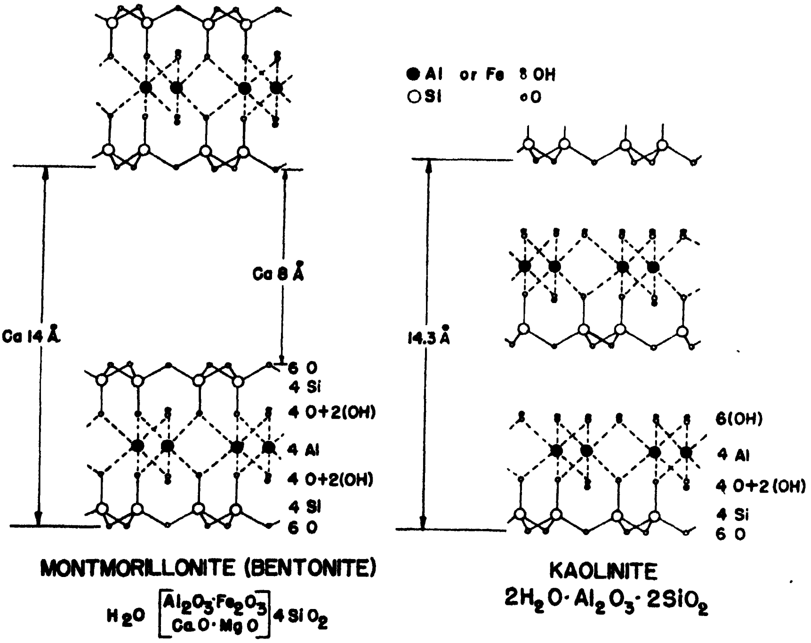
● Al or Fe
8 OH
O Si
∘ O
Ca 8 Å
Ca 14 Å
6 O
4 Si
4 O+2(OH)
4 Al
4 O+2(OH)
4 Si
6 O
14.3 Å
6(OH)
4 Al
4 O+2 (OH)
4 Si
6 O
MONTMORILLONITE (BENTONITE)
$H_2O \begin{bmatrix} Al_2O_3 \cdot Fe_2O_3 \\ CaO \cdot MgO \end{bmatrix} 4SiO_2$
KAOLINITE
$2H_2O \cdot Al_2O_3 \cdot 2SiO_2$

FIG. 5. Crystal structures of kaolin and montmorillonite (from Hofmann, Endell, and Wilm (10)).

Another view, due to Freundlich and Hamaker (5, 7, 12), is that the particles in thixotropic clay suspensions are held at equilibrium distances such that forces of repulsion due to interpenetration of the diffuse ionic clouds are just balanced by forces of attraction which are assumed to be the London-van der Waals forces. Langmuir (13) substitutes for long-range van der Waals forces the Coulomb attraction between the micelles and the oppositely charged ions in solution.

The theories of Freundlich, Hamaker, and Langmuir apply to uniformly charged particles, but variations of exchange capacity with SiO_2–R_2O_3 ratio (21), orientation in an electric field (15), and the high electrical conductivity of masses deposited on the anode membrane in electrodialysis, as opposed to the low conductivity in non-oriented thixotropic systems (16), all suggest that positive as well as negative areas are to be found on clay particles.

According to the crystal structures, the planar and transverse surfaces of particles should differ radically. Since all transverse surfaces must be formed by breaking the lattice, they should expose both aluminum atoms with unsaturated valences or unsaturated aluminum–oxygen groups, which normally will react with water to form hydroxides, and unsaturated oxygen atoms attached to silicon, which normally will react with water to form silicic acid. Over the planar silica surfaces secondary valence forces will induce acid hydrolysis of adsorbed water, and over planar alumina surfaces (as are found in kaolin) the reverse may be expected. Thus, in the same particles, both positive and negative reactive areas, points, or edges are available.

Between like surfaces of clay particles, according to the analysis of Freundlich, Hamaker, and Langmuir, high equilibrium distances of separation are possible. However, between different kinds of broken bonds on the transverse surfaces or at the edges or corners of the particles, or between edges and planar surfaces of the opposite charge, or between dissimilar planar surfaces, actual contact which may be regarded as chemical reaction should be expected. Structures in untreated clay suspensions may be attributed, then, to the combined effects of attraction between dissimilar surfaces, edges, or corners, and to repulsion or large equilibrium distances of separation which occur primarily between like planar surfaces.

The clay particle may be considered a colloid molecule and symbolized by the following formulas: for montmorillonite (bentonite), in neutral solution,

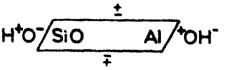

$$H^+O^- \underset{\mp}{\overset{\pm}{/\,SiO \quad Al\,/}} {}^+OH^-$$

or for kaolin,

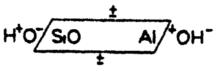

$$H^+O^- \underset{\pm}{\overset{\pm}{/\,SiO \quad Al\,/}} {}^+OH^-$$

KAOLIN AND BENTONITE

According to the formulas which have been written, in suspensions of hydrogen bentonite elimination of water between particles may occur as indicated by the equation,

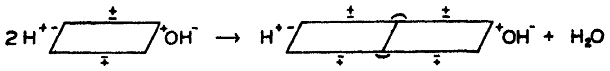

Since the particles are never of completely regular shape, less ideal configurations result which permit structures in three dimensions. In the case of hydrogen bentonite, however, the planar ionic clouds are so feeble that there is little or no mutual repulsion; consequently there is no thixotropic structure, but dense aggregates may be formed. Hence well-dialyzed bentonites swell only to a limited extent in water, and some clays low in alkaline salts, such as are found in wet climates, will not form thixotropic suspensions unless small amounts of electrolytes are added. The hydrogen clays are but little dissociated, in contrast to the ionic clouds which are formed where hydrogen has been substituted by other metallic ions.

For kaolin the condensation between the ends of particles should be analogous to that for bentonite, but the dissimilar planar faces should permit the formation of more compact structures, even in the presence of electrolytes. In strong alkalies, however, it is possible that both faces of kaolin may hydrolyze acidically with multiplication of particles and improved thixotropic behavior.

Since the dissimilar natures of the planar faces of the kaolin unit sheets do not permit separation in water to such an extent as is possible with bentonite, there is ordinarily a large difference in particle size between kaolin and bentonite particles. This difference can be observed microscopically or inferred from wide differences in settling rate.

THE PLATING ACTION OF VISCOSITY-REDUCING AGENTS

Experiments have been described which indicate that viscosity reduction by small amounts of certain large negative ions is a surface effect. Presumably these ions react with the exposed aluminum atoms on the broken transverse surfaces. Considering only bentonite and representing the viscosity reducing chemical by $Na_x\theta$, the reaction can be symbolized thus:

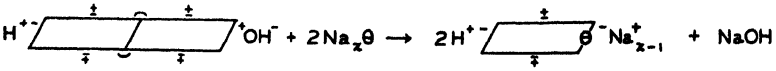

The contact structure has been destroyed, unipolar particles formed, and the structural viscosity, therefore, reduced.

THE GELLING ACTION OF SALTS

Figures 6 and 7 show that the amounts of specific viscosity-reducing chemicals required for maximum effect with Frazier Mountain clay are almost in proportion to the amounts of clay, but the amounts of salts required to produce gelation seem independent of the amount of clay in a given amount of water. This should be true if viscosity-reducing chemicals plate certain parts of the exteriors of clay particles, and salts affect the ionic atmospheres.

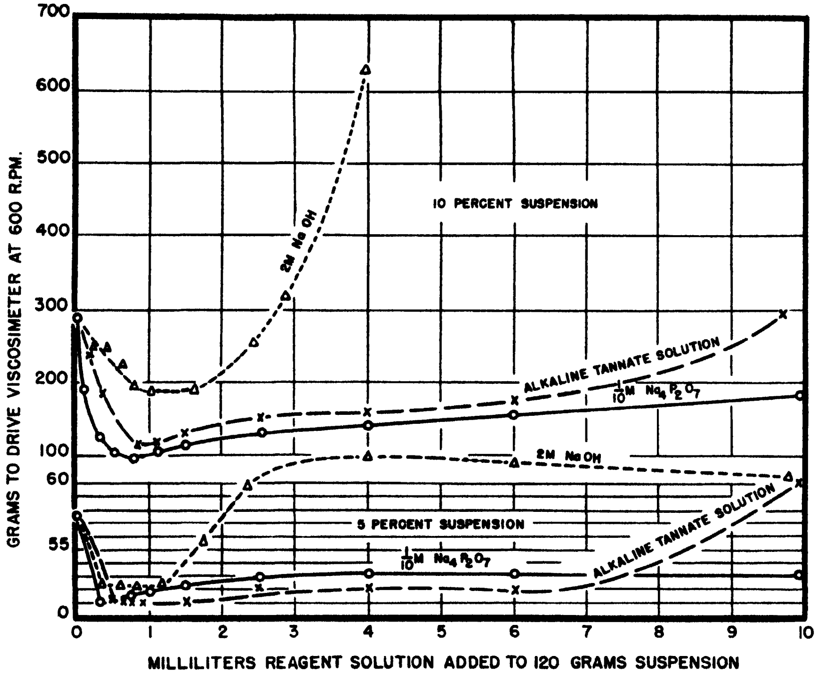

FIG. 6. Amounts of viscosity-reducing chemicals required at different concentrations of clay.

With increasing concentration ordinary salts first raise and then lower the yield point and the apparent viscosity of a suspension. According to the ideas of Freundlich and Vinograd (12), with increasing ionic concentration the thickness of the double layer is progressively reduced while the forces of attraction are constant, and therefore the force required to move the particles out of their oriented positions is greatest at an intermediate salt concentration.

These effects of ordinary salts are superimposed upon and apparently are independent of the presence of specific viscosity reducers. The latter are needed only in small amounts and so do not appreciably affect the ionic atmospheres but perform the single function of preventing adhesion between particles with consequent destruction of that portion of the gel strength and viscosity attributable to structural contact. The gel strength may be reduced by adding one of the polyphosphates and then progressively increased by adding salt, or the salt may be added first, so that many possibilities exist for the control of this or other properties.

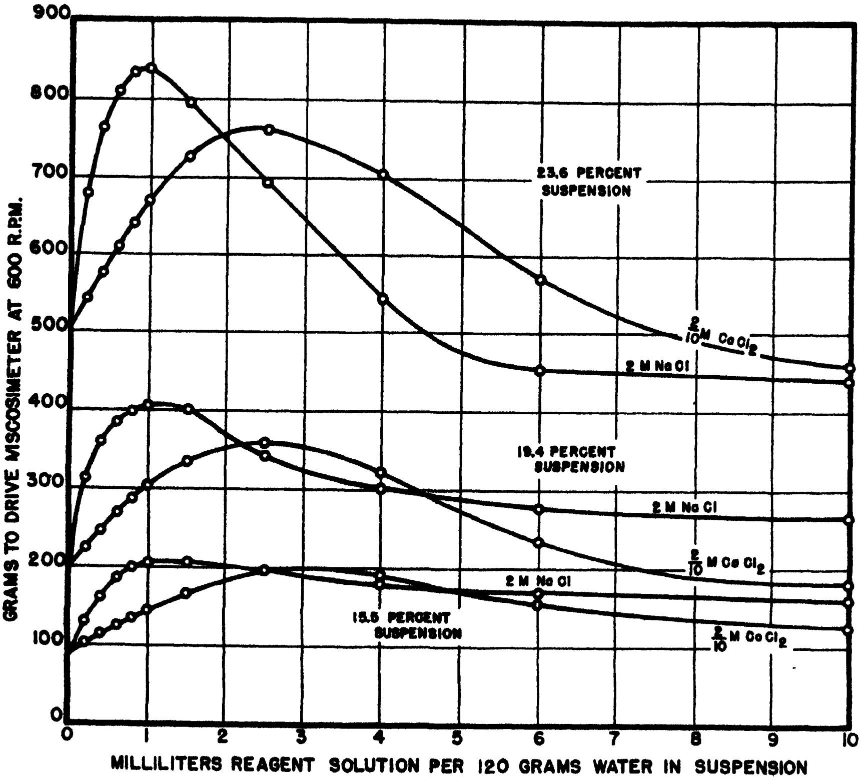

FIG. 7. Amounts of salt required for gelation at different concentrations of clay

The effectiveness of salts in both gelation and coagulation of clay suspensions increases steeply with the valence of the positive ion, just as in the coagulation of other colloids.

AMPHOTERIC REACTIONS AND THE EFFECTS OF ALKALIES

Addition of water to a dry montmorillonite particle may be indicated by

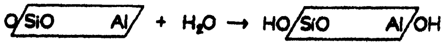

and for this hydrated particle the possible reactions of hydrolysis are:

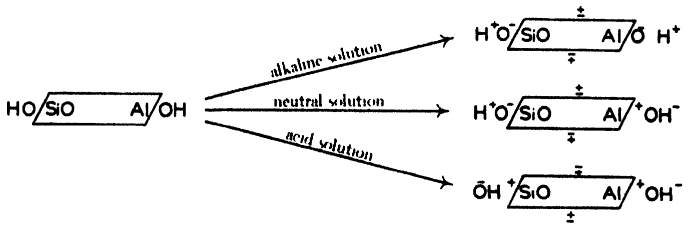

In accordance with these formulas, two minima in viscosity or yield point curves are observed with increasing pH (1, 14).

On adding sodium hydroxide to a neutral suspension the first effect is to induce the acidic hydrolysis of alumina and then to affect the ionic clouds in the same way as salts. This dual action is illustrated by the curves of figure 6. The viscosity is reduced at low concentrations of sodium hydroxide because particles with uniform sign of charge are formed, and at higher concentrations the viscosity is increased because the ionic clouds are affected. The viscosity reduction obtained is less than with pyrophosphate because the acidic hydrolysis is induced by a mass action effect of the alkali, and this electrolyte concentration required for viscosity reduction also simultaneously produces some gelation.

SUMMARY

1. Certain chemicals, such as sodium tannate and various phosphates, which in low concentration reduce the apparent viscosity of concentrated clay suspensions appear to be adsorbed on specific parts of the crystal faces of the clay particles, and to destroy the aggregation of the particles into structures.

2. The gelling and coagulating effects of most salts are attributed to changes in concentration of the inter-particle ionic atmospheres.

3. On the basis of the detailed crystal structures of clays, chemical formulas are written for colloidal clay particles and are used in explaining the various phenomena encountered with clay suspensions.

REFERENCES

(1) Ambrose and Loomis: Physics **1**, 129 (1931).
(2) Bragg: Proc. Roy. Inst. Gt. Brit. **30**, 39 (1938).
(3) Broughton and Squires: J. Phys. Chem. **40**, 1041 (1936).
(4) Byck, H. T.: Unpublished results, Shell Development Laboratory, Emeryville, California.
(5) Freundlich: *Thixotropy*. Hermann et Cie., Paris (1935).
(6) Garrison: Mining Technology **3**, No. 2, and Petroleum Technology **2**, No. 1, Technical Publication 1027 (1939).
(7) Hamaker: Rec. trav. chim. **55**, 1015 (1936).

(8) Hauser and leBeau: J. Phys. Chem. **42**, 1031 (1938).
(9) Hauser and Reed: J. Phys. Chem. **41**, 911 (1937).
(10) Hofmann, Endell, and Wilm: Z. Krist. **86**, 340 (1933).
(11) Houwink: *Elasticity, Plasticity, and Structure of Matter*, p. 336. University Press, Cambridge (1937).
(12) Houwink: *Elasticity, Plasticity, and Structure of Matter*, p. 338. University Press, Cambridge (1937).
(13) Langmuir: J. Chem. Phys. **6**, 873 (1938).
(14) Lewis, Squires, and Thompson: Trans. Am. Inst. Mining Met. Engrs. **114**, 39 (1935).
(15) Marshall: Trans. Faraday Soc. **26**, 173 (1930).
(16) Marshall: J. Phys. Chem. **41**, 935 (1937).
(17) Mattson: Soil Sci. **33**, 301 (1931).
(18) Mellor: *Treatise on Inorganic Chemistry*, Vol. VIII, p. 990. Longmans, Green and Company, London (1928).
(19) Reed: Petroleum Eng. **9**, No. 4, 48 (1938).
(20) Salmang: Kolloid-Z. **48**, 377 (1929).
(21) Winterkorn: Soil Sci. **41**, 25 (1936).

CHEMICAL PREPARATION OF COLLOIDAL SUSPENSIONS IN NON-AQUEOUS SOLVENTS. I

Methyl Alcohol and Benzene[1]

ARTHUR A. VERNON[2] and HARRISON A. NELSON[3]
Department of Chemistry, Rhode Island State College, Kingston, Rhode Island

Received February 23, 1939

Tomaschewsky (9) prepared fairly stable alkali-metal organosols by the simultaneous condensation of the vapors of the metal and the dispersion medium. Fodiman and Kargin (1) used a method by which they condensed metallic vapors in an organic liquid. The change of solvent method was used by Horiba, Otagari, and Kiyota (5) and by Von Hoessle (10), while Svedberg (7) used an electrical dispersion system.

A silver suspension in alcohol was prepared by Formstecher (2) by reduction of silver nitrate with formaldehyde. Hydrogen sulfide was used by Lottermoser (6) to suspend cupric sulfide and mercuric sulfide in alcohol. In view of the scant information on the subject it seemed of value to try the methods of Gorbowski (3) and Gutbier (4) with organic solvents.

---

[1] This article is condensed from a thesis submitted by Harrison A. Nelson to the Faculty of Rhode Island State College in partial fulfillment of the requirements for the degree of Master of Science in Chemistry, June, 1938.

[2] Present address: Department of Chemistry, Northeastern University, Boston, Massachusetts.

[3] Present address: Department of Chemistry, The Rice Institute, Houston, Texas.

EXPERIMENTAL

Materials

All materials used were of C.P. grade. The solvents were methyl alcohol and benzene and were redistilled before use.

Procedure

The procedure was essentially the same in all cases; a dilute solution was prepared in the dispersion medium to be used and the protective colloid was added. The reducing agent was added directly or hydrogen sulfide was bubbled through the solution. All colloids were filtered and examined with a dark-field microscope attachment.

It was found preferable to filter unprotected sols immediately, rubber-protected sols after 24 hr., and cellulose nitrate-protected sols in from 2 to 4 days. A suction filter was used, with a medium-pore filter paper.

Owing to the general insolubility of metallic salts in benzene, a concentrated solution of the salt was prepared in ether or acetone, and enough of this solution added to the benzene to produce the desired concentration. The solutions prepared for reductions were generally very dilute. In the case of colored solutions, a dilution was made up in which the ion coloration was scarcely visible, so that the optical properties of the sol might not be interfered with to too great an extent. Non-colored ions were used in a range of concentrations from 0.001 to 2.0 per cent.

Two compounds were found especially suitable as protective agents. Collodion, added on the basis of cellulose nitrate in amounts of 0.2 per cent or more, successfully protected suspensions in alcohol. In benzene, rubber was generally the protecting agent. Two methods of producing a suitable rubber material for this purpose were employed with almost equal success. In one method, a 40 per cent commercial latex suspension was dried out in a film which was then cut into small pieces and shaken with benzene. Not all of the material dissolved, but the solution adequately protected suspensions when added in small amounts before reaction. In the other procedure, pale crepe rubber was cut up and dissolved in benzene. This method was found to produce a more viscous solution with less undissolved material. In both cases standing for 24 hr. was necessary to produce a suitable solution. Filtering the rubber solution before adding it to the solution to be reduced did not materially impair its stabilizing effect, but it was generally found more satisfactory to add the mixture, reduce or react the solution in the presence of the undissolved lumps, and filter the resulting suspension. "Gold nuclear solution", as mentioned in connection with the formation of certain sols, was merely a stable red gold sol, made up in the dispersion medium in use and reduced by hydrazine hydrate.

Reducing agents

(*1*) Hydrazine hydrate: A very small quantity of a 40 per cent aqueous solution of this material was introduced into the salt solution on the end of a glass rod. (*2*) Phosphorus: A solution of phosphorus in carbon disulfide was diluted twenty times with the dispersion medium and a few drops of the dilute solution were added to the solution to be reduced. (*3*) Phosphorus and hydrazine (phosphorus-hydrazine): This combination of the two preceding reducing agents was found capable of reducing many salts upon which other reagents had no effect. The phosphorus was first added in slight excess, eight to ten drops of the dilute solution, followed by one drop of 40 per cent hydrazine hydrate solution. (*4*) Tannin: A freshly prepared alcoholic solution of tannic acid was added dropwise until the first faint signs of color developed. (*5*) Stannous chloride: A concentrated alcoholic solution of stannous chloride was added dropwise until the development of color in the reduction of auric chloride solution. (*6*) Hydrogen: Hydrogen gas was passed through a solution of silver oxide at a moderate rate for about 20 min., or until the development of a color.

Reductions at a raised temperature were attempted with the first five reducing agents mentioned. The reagent was added to the protected salt solution, and the mixture sealed in a tube and heated to 100°C. for 20 min.

Before filtering the benzene sols, the ether or acetone added in the salt solution was removed by boiling.

RESULTS

The investigation has resulted in the preparation of many metallic and metallic sulfide organosols and the compilation of data on various possibilities of organosol formation. In tables 1, 2, and 3 are listed all the more stable sols produced from alcohol and benzene, which were observed over a period of several months.

The more significant results of the experiment are summarized below.

1. Alcohol as dispersion medium

(*a*) *Gold:* It was not possible to produce red gold sols without first adding cellulose nitrate. Reducing an unprotected auric chloride solution gave a blue sol which had a life of 90 min. Phosphorus, tannic acid, and other organic acids did not reduce auric chloride at room temperature.

(*b*) *Silver:* Silver oxide was not reduced by hydrogen at room temperature. At a temperature of 50°C. hydrogen when passed through the solution produced a stable sol with cellulose nitrate; without a protective colloid the sol was stable for only 5 hr.

(*c*) *Lead:* Lead nitrate solution was reduced to a good sol in the presence of a small amount of gold nuclear solution, but without the nuclear solution a white cloud formed. Phosphorus at 100°C. reduced lead nitrate to a brown sol, but the phosphorus-hydrazine combination was the only other successful reducing agent. Phosphorus reduced lead acetate in 7 hr. at room temperature, producing a black sol stable for 3 days.

(*d*) *Bismuth:* Bismuth nitrate and bismuth chloride crystals added to alcohol produced the white flocculent oxide complex. Filtering removed the undissolved material and left a solution reducible to a good brown sol. The phosphorus-hydrazine combination was the only successful reducing agent for bismuth.

TABLE 1

Metallic sols in alcohol (with protective colloid)

DISPERSED PHASE	COMPOUND REDUCED	REDUCING AGENT	COLOR	
			By transmitted light	By reflected light
Au	$AuCl_3$	Hydrazine	Ruby	Brown
Au	$AuCl_3$	Hydrazine	Purple	Gray-brown
Au	$AuCl_3$	Stannous chloride	Ruby	Red-brown
Au	$AuCl_3$	Stannous chloride	Purple	Dull gold
Ag	$AgNO_3$	Hydrazine	Amber	Olive
Ag	$AgNO_3$	Tannin	Deep red	Gray-brown
Ag	$AgNO_3$	Phosphorus	Brown	Black
Ag	Ag_2O	Hydrogen	Yellow	Brown
Pb	$Pb(NO_3)_2$	Phosphorus-hydrazine	Yellow to red (slow change)	Green to black (slow change)
Bi	BiOCl	Hydrazine	Brown	Black
Sb	$SbCl_3$	Hydrazine	Yellow	Yellow
Ni	$NiNO_3$	Hydrazine	Amber	Lavender
Cr	$CrCl_3$	Phosphorus	Yellow	Green
Co	$CoCl_2$	Hydrazine	Amber	Gray-green
Cu	$CuBr_2$	Hydrazine	Yellow	Green
Hg	$HgNO_3$	Hydrazine	Yellow	Gray-green
Sn	$SnCl_2$	Hydrazine	Red-amber	Tan

(*e*) *Antimony:* Gold nuclear solution was necessary in antimony trichloride solution for the formation of stable sols. The phosphorus-hydrazine combination was the only suitable reducing agent.

(*f*) *Nickel:* In the presence of gold nuclear solution, hydrazine hydrate reduced nickel nitrate to nickel. Without the nuclear solution, the suspension was an unstable cloudy white. Other reducing agents produced unstable sols or no sols at all.

(*g*) *Copper:* Cupric chloride and cupric acetate were precipitated by reducing agents. Hydrazine hydrate reduced them to suspensions with a life of about 24 hr. Cupric bromide was reduced only with the phosphorus-hydrazine combination.

(*h*) *Cobalt:* Cobaltous chloride was precipitated by hydrazine hydrate, reduced by phosphorus-hydrazine, and unaffected by other reducing agents. A small amount of cobaltous sulfate, added to the cobaltous chloride solution to be reduced, was found to increase the stability very greatly.

TABLE 2

Metallic sols in benzene (with protective colloid)

DISPERSED PHASE	COMPOUND REDUCED	REDUCING AGENT	COLOR	
			By transmitted light	By reflected light
Au	$AuCl_3$	Hydrazine	Red	Brown-purple
Au	$AuCl_3$	Excess hydrazine	Purple-blue	Gray-tan
Au	$AuCl_3$	Stannous chloride	Pink	Pink-gold
Ag	$AgNO_3$	Phosphorus-hydrazine	Yellow	Green-gray
Ag	$AgNO_3$	Phosphorus	Amber	Brown
Bi	$BiONO_3$	Phosphorus-hydrazine	Orange	Brown

TABLE 3

Stable metallic sulfide sols in methyl alcohol and benzene (with protective colloid)

SULFIDE OF	SALT USED	COLOR IN ALCOHOL		COLOR IN BENZENE	
		By transmitted light	By reflected light	By transmitted light	By reflected light
Ag	$AgNO_3$	Red-brown	Black	Yellow	Gray
Pb	$Pb(NO_3)_2$	Brown	Black	Brown	Black
Bi	$Bi(NO_3)_3$	Red	Black	Yellow	Tan
Sb	$SbCl_3$	Orange	Tan		
Hg	$HgNO_3$	Brown	Black		
Ni	$Ni(NO_3)_2$	Black	Black	Black	Black
Co	$Co(NO_3)_2$	Black	Black	Gray	Black
Sn	$SnCl_2$	Amber	Tan	Amber	Tan
Fe	$FeCl_2$				
Cu	$CuCl_2$	Light green	Gray	Light green	Gray
As	$AsCl_3$	Amber	Yellow	Red	Yellow
Cd	$CdCl_2$				

(*i*) *Chromium:* Reducing agents, with the exception of phosphorus-hydrazine, had no effect on solutions of chromic chloride. Dilute solutions which had been reduced with phosphorus-hydrazine precipitated in a few weeks, but more concentrated chromic chloride solutions, in which the green color was very evident, were reduced to form very stable sols.

(*j*) *Mercury:* Mercurous nitrate was similar to chromic chloride in that concentrated solutions were necessary for stability. Phosphorus reduced mercurous nitrate to a black sol stable for 2 months, while other reducing agents gave precipitates.

(*k*) *Strontium:* Strontium nitrate was reduced by phosphorus-hydrazine, in the presence of gold nuclear solution, to a yellow sol stable for 2 months.

(*l*) *Tin:* Stannous chloride was reduced by phosphorus-hydrazine alone. Only very dilute solutions gave stable sols. Sols produced from solutions of a concentration of 0.2 per cent or more flocculated almost immediately.

2. Benzene as dispersion medium

The possibility of sol formation in benzene depended on the use of salts soluble in acetone or ether, since most salts are insoluble in benzene. Those salts giving satisfactory acetone or ether solutions were added to benzene as described in the method of procedure, and the various reducing agents were used with each. Although salts of antimony, gold, silver, lead, bismuth, tin, nickel, chromium, cobalt, copper, mercury, and silver were tried, only with salts of gold, silver, bismuth, and tin were stable sols possible.

A pink suspension of gold in benzene, prepared by the use of stannous chloride, was stable for 24 hr. without the addition of a second organic protective colloid.

Silver sols were stable for 4 hr. without a protective colloid, but bismuth and tin suspensions were possible only in the presence of rubber.

DISCUSSION

The following observations are given to show the general behavior of various sols and the problems involved in their preparation:

(*1*) *Gold:* This was the most easily prepared suspension. It was found possible to form almost any shade of blue, purple, or red gold suspension desired. For example, if a light red sol were desired, a dilute solution of auric chloride was reduced with hydrazine in the presence of cellulose nitrate. If a blue suspension were desired, it could be prepared by introducing the reducing agent before adding the cellulose nitrate. Deeper colors were obtained by using higher concentrations of auric chloride.

During the course of these experiments, it was noticed that the color of gold sols reduced in the presence of cellulose nitrate developed from a blue to a deep red, and in no case was a red sol formed immediately. This phenomenon was very strongly evident in solutions containing a high concentration of both salt and cellulose nitrate. In this case the introduction of hydrazine hydrate produced a very light blue color, which slowly darkened to black, then to purple, then to red.

It has been suggested by Svedberg that the difference between blue and red gold sols may be due to a difference in the size of the particles, the blue sols containing larger particles than the red. This suggestion, however, is not supported by the above observations. It seems improbable that reduction should first form large aggregates which on standing would break down into smaller particles. The tendency is rather for condensation than for dispersion.

But the proposition of Thiessen (8), that colored aurous oxide may be partly responsible for the color of blue sols, is apparently supported. It is quite possible that reduction is at first incomplete, thus producing aurous oxide instead of gold in suspension, giving a blue color. Reduction continuing, the metal stage is finally reached, and the sol becomes red.

(*2*) *Silver:* The silver sols prepared were quite uniform in color, transmitting yellow to brown light, and reflecting brown-gray to black. These sols were unique in appearance under the dark-field apparatus, showing white particles in a deep blue field. The microscopic field was practically colorless with other sols.

(*3*) *Lead:* Some reduction of lead salts was possible with phosphorus at 100°C., but phosphorus-hydrazine was much more successful. With the latter reducing agent, the first color observed was light yellow. This slowly changed to a deeper yellow in transmitted light and a green-yellow in reflected light. There was then no change in coloration for several days, when a gradual darkening set in, finally producing a typical dark lead sol transmitting brown light and appearing black in reflected light.

This gradual change of appearance might be analogous to the blue or red color change observed in gold sols. It might then be assumed that the reduction is slow, and that the first sol contains oxides, or other incompletely reduced compounds.

In the case of lead, as with several other metals, the addition of a small amount of a gold nuclear solution was found to assist greatly in stabilizing sols. The action of the nuclear solution was merely to furnish a large number of nuclei, upon which the lead molecules might deposit. In the absence of the nuclear material, the first few particles of metal acted as nuclei for the agglomeration of the lead subsequently reduced. These particles enlarged rapidly and soon precipitated, subsequent lead produced by reduction in the solution depositing on the precipitated mass.

(*4*) *Cobalt:* Gold nuclear solutions greatly facilitated the preparation of stable cobalt sols, but in this case the addition of a small amount of cobaltous sulfate apparently served the same purpose. Evidently the cobaltous sulfate was unreduced and partially dissociated, providing some stabilizing ions on the particle surface. This procedure might conceivably be as successful with other metals, but in this investigation it was not attempted with metals other than cobalt and nickel.

(*5*) *Iron:* Iron sols prepared with phosphorus–hydrazine were first deep red, very similar to the red of a gold sol, but later changed to a green or black. The red sol was proved by dark-field examination to contain colloidal particles. The other colored suspensions might possibly have contained compounds instead of the metal. It is even possible that the red sol was of ferric oxide, as a slight amount of water was introduced with the hydrazine in reduction.

(*6*) *Chromium:* The unusual behavior of chromium sols in the matter of stability with respect to concentration might well be investigated. The fact that higher dilutions are less stable is in direct opposition to what appeared to be the general rule in all other cases. It is possible that a strong excess of unreduced ions is necessary to form the stabilizing layer.

Protective colloids

A wide variety of material was used in an attempt to stabilize the sols, but few substances were satisfactory. The protective properties of cellulose nitrate have not been investigated thoroughly. Rubber, on the other hand, has often been used. Among the many compounds employed were stearates, linoleates, glycols, and Glyco products, shellac, waxes, and paraffin.

Ammonium stearate prolonged the life of a blue gold sol in alcohol by 8 hr., but was otherwise ineffectual, as were all other compounds tried.

Effect of aging

During the first few weeks after the formation of a stable sol, some changes were noticed. By the end of the first week, a slight precipitate was often present in the bottom of the vessel. This preliminary precipitation was almost universally noted in greater or lesser degree. The characteristic appearance and stability of the residual sol were, however, in no wise affected, and if the sol were filtered after several weeks' standing, no further change or precipitation was noted. It is probable that the precipitated material consisted of irregular shaped particles and particles of greater than colloidal dimensions. It is also possible that some organic compounds were included in the precipitate as the result of side reactions in the organic liquids.

Sulfide sols

The table of sulfide sols is rather complete, and little need be said of the results. It is fairly simple to suspend sulfides in organic liquids, owing to their general insolubility. But some attempts were unsuccessful, owing to precipitation of the sulfide. Removal of the excess hydrogen sulfide after reaction could be accomplished by passing a current of air through the solution or by boiling, but a somewhat greater general stability was evident if some hydrogen sulfide were left, it being apparently sufficiently dissociated to supply stabilizing ions.

SUMMARY

1. By the use of hydrazine hydrate, phosphorus, stannous chloride, tannin, and other reducing agents, stable colloidal suspensions of several metals were prepared in methyl alcohol and benzene. The concentration of salts used varied from 0.001 to 2.0 per cent. A combination of phosphorus and hydrazine was necessary to reduce salts of copper, lead, tin, and antimony.

2. Colloidal suspensions of metallic sulfides were prepared in the same dispersion media by passing dry hydrogen sulfide through dilute solutions of metallic salts.

3. Protective colloids were generally found necessary for stability. Cellulose nitrate, in concentrations of 0.2 per cent or more, successfully protected sols in alcohol, while rubber was found to be necessary for benzene. Some sulfide sols were very stable without protective colloids, but unprotected metal sols were short-lived.

REFERENCES

(1) Fodiman and Kargin: J. Phys. Chem. (U. S. S. R.) **5**, 423–30 (1934).
(2) Formstecher: Phot. Ind. **30**, 6 (1932).
(3) Gorbowski: Ber. **36**, 125 (1903).
(4) Gutbier: Z. anorg. Chem. **31**, 448; **32**, 348 (1902).
(5) Horiba, Otagari, and Kiyota: Japanese patent 101,948 (July 13, 1933).
(6) Lottermoser: J. prakt. Chem. [2] **75**, 293–306 (1907).
(7) Svedberg: Ber. **36**, 3616 (1905); **39**, 1705 (1906); J. Am. Chem. Soc. **46**, 1980 (1924); Kolloid-Z. **25**, 154 (1919).
(8) Thiessen: Z. anorg. Chem. **134**, 393 (1924).
(9) Tomaschewsky: Kolloid-Z. **54**, 79 (1931).
(10) Von Hoessle: German patent 623,075 (December 12, 1935).

CHEMICAL PREPARATION OF COLLOIDAL SUSPENSIONS IN NON-AQUEOUS SOLVENTS. II

Ether, Dioxane, and Acetone

ARTHUR A. VERNON[1] AND HARRISON A. NELSON[2]
Department of Chemistry, Rhode Island State College, Kingston, Rhode Island

Received April 11, 1939

In a previous paper the authors (1) have described the preparation and properties of some inorganic colloids in methyl alcohol and benzene. This paper gives the results of similar experiments with diethyl ether, 1,4-dioxane, and acetone as the solvents.

EXPERIMENTAL

Materials

All materials used were of C.P. grade. The solvents, diethyl ether, 1,4-dioxane, and acetone, were redistilled before use.

Procedure

The methods by which the colloids were prepared were the same as those reported in the previous paper. The observations there made about the use of reducing agents and of hydrogen sulfide were found to apply equally well to ether, dioxane, and acetone as solvents. The protective agents used were collodion for acetone and dioxane and rubber for ether. These were used in the same way as described previously.

RESULTS

The results of the investigation are shown in tables 1, 2, 3 and 4, which list the stable metal and metallic sulfide sols prepared.

The more significant results of the experiments are set forth below, classified under the dispersion medium and dispersed phase.

1. Ether as dispersion medium

(*a*) *Gold:* Stable gold sols were easily prepared with phosphorus, hydrazine hydrate, and stannous chloride in the presence of rubber. Without protective colloids, purple or blue sols of 30 to 60 min. stability were formed with the same reducing agents.

(*b*) *Silver:* Salts of silver are insoluble in ether, and sols were therefore impossible in the pure solvent. Addition of a very small amount of an alcohol solution of silver nitrate produced a sufficient concentration to give a sol when reduced, but the dispersion medium could no longer be considered pure ether.

---

[1] Present address: Department of Chemistry, Northeastern University, Boston, Massachusetts.

[2] Present address: Department of Chemistry, The Rice Institute, Houston, Texas.

(*c*) *Other elements:* With the exception of bismuth, tin, and iron, other metals presented a problem similar to that met in silver. Although some salts were slightly soluble, none of those used was capable of producing sols on reduction.

TABLE 1

Metallic sols in ether (with protective colloid)

DISPERSED PHASE	COLOR		REDUCING AGENT	METALLIC SALT REDUCED
	By transmitted light	By reflected light		
Au	Rose	Tan	Hydrazine	$AuCl_3$
Au	Rose	Tan	Phosphorus	$AuCl_3$
Bi	Red-brown	Brown-gray	Phosphorus-hydrazine	$BiONO_3$
Sn	Yellow	Green	Phosphorus-hydrazine	$SnCl_2$
Fe	Green-yellow	Dark-gray green	Phosphorus-hydrazine	$FeCl_3$
Pb	Yellow	Green-yellow	Phosphorus-hydrazine	$Pb(C_2H_3O_2)_2$

TABLE 2

Metallic sols in dioxane (with protective colloid)

DISPERSED PHASE	COLOR		REDUCING AGENT	METALLIC SALT REDUCED
	By transmitted light	By reflected light		
Au	Purple-red	Brown	Hydrazine	$AuCl_3$
Au	Purple	Brown	Stannous chloride	$AuCl_3$
Au	Purple-blue	Brown	Excess hydrazine	$AuCl_3$
Fe	Red	Brown	Phosphorus-hydrazine	$FeCl_3$
Sb	Yellow	Yellow	Phosphorus-hydrazine	$SbCl_3$
Ag	Light yellow	Gray	Hydrazine	Ag_2O
Pb	Red-brown	Brown-gray	Phosphorus-hydrazine	$Pb(C_2H_3O_2)_2$
Bi	Red-brown	Brown	Phosphorus-hydrazine	$BiONO_3$
Ni	Yellow	Gray	Phosphorus-hydrazine	$Ni(NO_3)_2$
Co	Amber	Tan	Phosphorus-hydrazine	$Co(NO_3)_2$
Hg	Tan	Dark gray	Phosphorus-hydrazine	$HgNO_3$
Cu	Red-brown	Tan-gray	Phosphorus-hydrazine	$CuCl_2$

2. Dioxane as dispersion medium

(*a*) *Gold:* A blue sol was formed by reducing auric chloride in dioxane without a protective colloid. Precipitation was complete in one minute. Stannous chloride reduced auric chloride to a deep blue sol in the presence of cellulose nitrate, the color changing to light purple on long standing.

Phosphorus–hydrazine gave a definite green sol with auric chloride, stable for several months.

TABLE 3

Metallic sols in acetone (with protective colloid)

DISPERSED PHASE	COLOR		REDUCING AGENT	METALLIC SALT REDUCED
	By transmitted light	By reflected light		
Au	Amber	Tan	Phosphorus-hydrazine	$AuCl_3$
Ag	Yellow	Yellow-gray	Hydrazine	$AgNO_3$
Ag	Red-brown	Black	Phosphorus	$AgNO_3$
Bi	Yellow	Yellow-green	Phosphorus-hydrazine	$BiONO_3$
Ni	Red-brown	Black	Phosphorus-hydrazine	$Ni(NO_3)_2$

TABLE 4

Stable metallic sulfide sols in ether, dioxane, and acetone (with protective colloid)

SULFIDE OF	IN ETHER		IN DIOXANE		IN ACETONE		SALT USED
	Color by transmitted light	Color by reflected light	Color by transmitted light	Color by reflected light	Color by transmitted light	Color by reflected light	
Ag			Brown	Gray	Light brown	Gray	$AgNO_3$
Pb			Light brown	Gray	Brown	Black	$Pb(NO_3)_2$
Bi			Light brown	Light brown	Red-brown	Brown	$Bi(NO_3)_3$
Sb	Red	Orange	Red	Orange	Red	Orange	$SbCl_3$
Hg	Gray	Gray	Black	Black	Gray	Black	$HgNO_3$
Ni	Gray	Black	Black	Black	Gray	Black	$Ni(NO_3)_2$
Co	Gray-brown	Black	Brown	Black	Brown	Black	$Co(NO_3)_2$
Sn	Amber	Olive	Amber	Yellow			$SnCl_2$
Fe			Light brown	Gray	Green	Gray	$FeCl_2$
Cu	Amber	Gray					$CuCl_2$
As	Orange	Yellow	Amber	Yellow	Yellow	Green	$AsCl_3$
Cd					Orange	Yellow	$CdCl_2$

(*b*) *Silver:* Silver oxide was used in dioxane, as silver nitrate is insoluble in this solvent. Silver oxide was reduced to stable sols with most reducing agents.

(*c*) *Lead:* Lead salts were reduced by phosphorus-hydrazine alone in dioxane. Lead acetate was reduced to a very stable sol, while lead nitrate was reduced to unstable sols.

(*d*) *Nickel and cobalt:* Nickel and cobalt nitrates were reduced by phosphorus-hydrazine to stable sols, while their chlorides formed unstable sols. A small amount of cobaltous sulfate solution or a small amount of a gold nuclear solution added to cobaltous nitrate solution before reduction guaranteed stability.

(*e*) *Copper:* Copper chloride was reduced to a stable sol by phosphorus–hydrazine, but the nitrate formed unstable sols.

(*f*) *Chromium:* Chromium salts were reduced by phosphorus-hydrazine, but precipitation was immediate.

3. Acetone as dispersion medium

(*a*) *Gold:* Reduction by hydrazine in acetone solution was impaired by the reaction between acetone and hydrazine. Auric chloride was reduced to a blue or purple suspension with hydrazine hydrate in the presence of cellulose nitrate, but on standing the sol reverted to a clear yellow solution, evidently auric chloride, which again formed a blue sol on addition of hydrazine hydrate. The sol disappeared for a second time and further addition of hydrazine hydrate failed to bring it back. Stannous chloride added to auric chloride solution produced a tan colored sol, evidently not of metallic gold. Other reducing agents were ineffective with auric chloride.

(*b*) *Silver:* Silver nitrate was reduced to a stable sol by phosphorus. Hydrazine hydrate had an effect similar to that observed with auric chloride, except that on the third addition of the reagent a stable sol was formed.

(*c*) *Lead:* Lead acetate solution reduced with phosphorus-hydrazine was cloudy, and precipitated in 8 hr. Lead nitrate reduced with an excess of phosphorus followed by hydrazine produced a lead sol stable for several weeks.

(*d*) *Antimony:* Reduction of antimony trichloride by phosphorus–hydrazine gave a white flocculent precipitate.

(*e*) *Nickel:* Nickel nitrate solution reacted with hydrazine hydrate in the same manner as silver. Three separate reductions were necessary to produce a stable sol.

(*f*) *Chromium:* Chromic nitrate dissolved in acetone and was apparently partially reduced by the solvent, producing a cloudy sol, which precipitated in a short time.

DISCUSSION

The general characteristics of sols in methyl alcohol and benzene as given in the previous paper were found to apply equally well to ether, dioxane, and acetone. A comparison of the results of experiments with the five solvents showed that the stability of the suspensions decreased in the order alcohol, dioxane, benzene, ether, and acetone. The general problem of stability of sols in non-aqueous media appears to be very interesting and should merit further investigation. It is hoped that more work may be done in this laboratory to determine changes and precipitation characteristics.

SUMMARY

1. Suspensions of several metals in ether, dioxane, and acetone have been prepared by reduction methods.

2. Colloidal suspensions of metallic sulfides in the same solvents have been prepared by double decomposition reaction with hydrogen sulfide.

3. As reported in previous work on methyl alcohol and benzene, protective materials were necessary to ensure stability. Cellulose nitrate was used with dioxane and acetone, while rubber was the best agent with ether.

4. A comparison with results published in a previous paper shows that the suspensions decrease in stability in the order alcohol, dioxane, benzene, ether, acetone.

REFERENCE

(1) VERNON, ARTHUR A., AND NELSON, HARRISON A.: J. Phys. Chem. **44**, 12 (1940).

THE INFLUENCE OF BROWNIAN MOVEMENT ON THE VISCOSITY OF SOLUTIONS[1]

R. SIMHA

Department of Chemistry, Columbia University, New York City, New York

Received May 12, 1939

INTRODUCTION

The study of the internal friction of pure liquids is of great technical as well as scientific interest. From the latter point of view it has become especially important, since a more intensive study of the liquid state has been undertaken. The viscosity and its dependence on other quantities have been shown to furnish substantial information about the structure of the medium considered.

No less important is the study of the viscosity of solutions, especially in the study of the high polymers. Besides technical problems this question arose: On the basis of the viscosity of a solution, to what extent is it possible to draw quantitative conclusions as to the shape and size of particles suspended therein? Although it is not yet possible to give a comprehensive answer, much progress has been made both by experiment and theory. A detailed representation of these problems is found elsewhere (7, 15; also the last paper mentioned in reference 3).

---

[1] Presented at the Ninety-seventh Meeting of the American Chemical Society, held at Baltimore, Maryland, April, 1939.

Einstein (2) was the first to calculate the viscosity of a suspension of spheres on the basis of the phenomenological hydrodynamic equations. Here a necessary assumption is that the suspended particles are large compared with the molecules of the solvent. It is further assumed that no gliding between solid and liquid occurs. Jeffery (11) treated the same problem for ellipsoids. Both authors restrict themselves to dilute solutions and rigid particles and obtain proportionality between the specific viscosity and the concentration, c:

$$\frac{\mu - \mu_0}{\mu_0} = \nu c$$

(μ_0 is the viscosity of the solvent; μ is the viscosity of the solution.) The factor ν has the value 2.5 for spheres and is a function of the axial ratio for ellipsoids. We shall refer to this paper. Recently Eirich, Guth, Simha, and coworkers (3, 7) tried to extend the theory and at the same time to investigate the validity of the underlying assumptions by experiments on models of known characteristics.

THE PURELY HYDRODYNAMIC CASE

Before considering the influence of Brownian movement on the behavior of suspended particles, such of Jeffery's results as are used in this paper may be briefly discussed. He calculates the motion of an ellipsoid suspended in a liquid with a velocity $u_i^{(0)}$.[2] $u_i^{(0)}$ is composed by a rotation and a distortion, as a pure translation of the fluid is not disturbed by the presence of the ellipsoid, if inertia forces are neglected. One must therefore find a solution of Stokes' equations

$$\left.\begin{aligned} \mu_0 \nabla^2 u_i &= \frac{\partial p}{\partial x_i} \\ \frac{\partial u_r}{\partial x_r} &= 0 \end{aligned}\right\} \qquad (1)$$

which gives at infinite distance from the particle

$$u_i = u_i^{(0)} = a_{ir} x_r + \xi_k x_l - \xi_l x_k$$

---

[2] In the following i, k, l follow from each other by cyclic permutation; summations are performed only on twice occurring indices r, s.

(a_{ik} and ξ_k are constant components of distortion and rotation, respectively.) The x_k refer to axes fixed in the particle, which will perform a rotation with the angular velocities ω_i, so that on the surface of the ellipsoid

$$u_i = \omega_k x_l - \omega_l x_k$$

The resultant couple acting on the particle must vanish, as inertia forces were neglected. This gives the values of ω_i.

Finally Jeffery considers the special case of a motion between two flat plates, where the one moves uniformly against the other, as approximately realized in a Couette apparatus:

$$u_1' = u_2' = 0, \quad u_3' = \kappa x_2'$$

The primed quantities refer to a system fixed in space. On introducing the Eulerian angles φ, ϑ, ψ, one obtains for an ellipsoid of revolution with the semi-axes a_1 and a_2

$$\left(\beta = \frac{a_1^2 - a_2^2}{a_1^2 + a_2^2}\right)$$

the equations of motion of the immersed particles:

$$\left.\begin{aligned} &\dot{\varphi} = \frac{\kappa}{2}(1 + \beta \cos 2\varphi), \quad \dot{\vartheta} = \frac{\kappa\beta}{4} \sin 2\vartheta \sin 2\varphi, \quad \dot{\varphi} \cos \vartheta + \psi = \frac{\kappa}{2} \cos \vartheta \\ &\text{and therefore} \\ &\qquad tg\varphi = \frac{a_1}{a_2} tg\left(\frac{\kappa a_1 a_2}{a_1^2 + a_2^2} t\right), \qquad tg^2 \vartheta = \frac{2a_1^2 a_2^2}{k^2(a_1^2 + a_2^2)(1 + \beta \cos 2\varphi)} \end{aligned}\right\} \quad (2)$$

For $t = 0$, $\varphi = 0$. k is an integration constant determined by the initial value of ϑ which, however, is unknown. It is a measure for the angle of the cone described by the axis of revolution about the normal to the plane of the undisturbed motion. Every k value is consistent with the equations 1. At the present state of the theory, where inertia and the non-stationary terms in the hydrodynamic equations are neglected, it is not possible to eliminate this undeterminateness without additional assumptions. This lack is felt not only in problems of double refraction of flow, but also here, as k enters in the expression for the dissipated energy and therefore determines the viscosity. For the increase of energy dissipated per unit time and due to the presence of the particle, one obtains

$$\frac{dW}{dt} = \frac{4\pi}{3} \mu_0 \kappa^2 \left\{ \left(\frac{\alpha_1''}{2a_2^2 \alpha_1' \alpha_2''} + \frac{1}{2a_2^2 \alpha_1'} - \frac{2}{\alpha_2'(a_1^2 + a_2^2)} \right) \sin^2 2\omega \sin^4 \vartheta \right.$$
$$\left. + \frac{\cos^2 \vartheta}{a_2^2 \alpha_1'} + \frac{2 \sin^2 \vartheta}{\alpha_2'(a_1^2 + a_2^2)} \right\} \quad (3)$$

In equation 3 ϑ has to be expressed by φ and k with the aid of equation 2; the α_i', α_i'' are functions of a_1 and a_2, defined in Jeffery's paper. $\mathrm{d}W/\mathrm{d}t$ is a function of the time t. The average value is found by computing the integral

$$\overline{\frac{\mathrm{d}W}{\mathrm{d}t}} = \frac{\int_0^{2\pi} \frac{\mathrm{d}W}{\mathrm{d}t}(\varphi, k) \frac{\mathrm{d}\varphi}{\varphi}}{\int_0^{2\pi} \frac{\mathrm{d}\varphi}{\dot{\varphi}}} \tag{3a}$$

Jeffery assumes that the particles are orientated in a manner which corresponds to a minimum of $\overline{\mathrm{d}W/\mathrm{d}t}$. This gives for prolate ellipsoids $k = \infty$, $\vartheta = 0$, i.e., the axis of revolution is normal to the plane of flow, whereas $k = 0$, $\vartheta = \frac{\pi}{2}$ corresponds to a maximum, and *vice versa* for oblate spheroids. Experiments on models show that long particles strike into the plane of flow with increasing axial ratio and there orientate themselves parallel to the direction of flow in contradistinction to the minimum hypothesis.[3] Using the method of small vibrations, the author (18) was able to show that the more elongated the particles, the more stable becomes the position in the plane of flow.

PARTICLES WITH BROWNIAN MOVEMENT

With decreasing particle size and velocity gradient and increasing temperature, the influence of the rotatory Brownian movement must be considered. The heat motion of the solvent molecules by means of collisions with the solute particles tends to bring about an isotropic angular distribution of the ellipsoids. The ratio κ/D (D = rotational diffusion constant of the spheroids) is a measure for this influence, which shows a certain analogy to the orientation of dipoles in an external field. Also in this case the distribution function $F(\varphi)$ of all possible directions is determined by a generalized diffusion equation. With the aid of F the average value $\overline{\mathrm{d}W/\mathrm{d}t}$ can be calculated. In the purely hydrodynamic case characterized by $\frac{\kappa}{D} \rightarrow \infty$ the distribution function is proportional to $\frac{1}{\dot{\varphi}}$, as is evident from equation 3a. We shall not go here into details concerning this problem of so-called "partial Brownian movement." For a critical discussion see references 3 and 7. The $\varphi - \vartheta$ coupling and therefore the undeterminateness mentioned before persists so long as there is any orientation tendency effective in the flow. This is no longer the case for complete Brownian movement. Here the gradient κ is so small and the thermal motion of the particles is so intensive that the ratio κ/D tends toward zero. The macroscopic flow is no longer able to bring about a regular rotation of the ellipsoids. Their axes on the average are uniformly distributed through the liquid. At the same time, however, a change must be made in expressing the dissipated energy as a function of the orientation. The hitherto used formula 3 was derived with the aid of the equations of motion 2. It therefore implicitly involves a coupling of the angles φ and ϑ. Now if the particles have no regular motion within the plane of flow,[4] then the same must hold for the motion referring to ϑ, which would in any case induce an orientation tendency. Therefore no mutual dependence of the angles which described the gyroscopical motion of the ellipsoids in the hydrodynamical case exists. In this way two modifications in the former considerations occur: (*a*) The problem to be dealt with depends on two independent variables φ and ϑ. The distribution function F therefore equals $N/4\pi$ (N = number of suspended ellipsoids). (*b*) One must assume vanishing spins ω_i and calculate the energy increase due to ellipsoids at rest, orientated under all possible angles ϑ, φ against the direction of the undisturbed flow.

---

[3] J. M. Burgers in the Second Report on Viscosity and Plasticity (Amsterdam, 1938) remarks that the orientation for long particles parallel to the undisturbed velocity gives practically the same value for the viscosity as Jeffery's minimum value. It is, however, much smaller than that found in the experiments mentioned. This fact seems to be due essentially to concentration effects (*cf.* page 33).

For this purpose we can use Jeffery's solution of equations 1 in inserting $\omega_i = 0$ in his formulas 22, 24, and 26. In order to calculate dW/dt one describes as usual a sphere of finite radius R around the particle, but so that $R \gg a_1, a_2$. Then the rate at which work is done by the hydrodynamical stresses on the surface of the sphere is computed. As explained in Jeffery's paper, one considers for this purpose a motion which assumes on the boundary of the sphere the velocities $u_i^{(0)}$ of the undisturbed motion. As R is finite, to the solution of equation 1 used hitherto a second motion has to be added, so that the resultant solution fulfills the condition mentioned before. The calculation gives:

$$\left.\begin{aligned}
u_i &= u_i^{(0)} - \frac{4x_i}{R^5 r^5}(R^5 - r^5)\Phi + \frac{5(R^2 - r^2)}{R^5}\frac{\partial \Phi}{\partial x_i}\\
&\qquad + \frac{4}{3}\left\{(A_{il} - A'_{il})x_l - (A_{ik} - A'_{ik})x_k\right\}\frac{R^3 - r^3}{R^3 r^3};\\
&\text{with}\\
A_{ik} &= \frac{\alpha_i a_{ik} - a_k^2 \alpha'_l \xi_l}{2\alpha'_l(a_i^2\alpha_i + a_k^2\alpha_k)}, \quad A'_{ik} = \frac{\alpha_k a_{ik} + a_i^2 \alpha'_l \xi_l}{2\alpha'_l(a_i^2\alpha_i + a_k^2\alpha_k)}\\
A_{ii} &= \frac{1}{6}\,\frac{2\alpha''_i a_{ii} - \alpha''_k a_{kk} - \alpha''_l a_{ll}}{(\alpha''_1\alpha''_2 + \alpha''_3\alpha''_1 + \alpha''_2\alpha''_3)}, \quad \Phi = A_{rr}x_r^2 + (A_{rs} + A'_{rs})x_r x_s
\end{aligned}\right\} \tag{4}$$

---

[4] This motion tends to drive elongated ellipsoids in the direction of flow ($\varphi = \pi/2$), as in this position $\dot{\varphi}$ reaches its minimum.

The rate of work done is given by the integral

$$\iint u_r^{(0)} p_r \, \mathrm{d}S$$

extended over the surface of the sphere. Here the p_r are the components of the stress acting normal to the surface:

$$p_r = p_{rs} \frac{x_s}{r}$$

and

$$p_{rs} = -p\delta_{rs} + \mu_0 \left(\frac{\partial u_r}{\partial x_s} + \frac{\partial u_s}{\partial x_r} \right)$$

Inserting from equation 4 one obtains for the heat increase due to an ellipsoid of revolution $a_2 = a_3$,

$$\left.\begin{aligned} \frac{\mathrm{d}W}{\mathrm{d}t} = \frac{16\pi\mu_0}{3} \Bigg\{ & \frac{\alpha_1'' a_{11}^2}{2a_2^2 \alpha_1' \alpha_2''} + \frac{a_{22}^2 + a_{33}^2 + 2a_{23}^2}{2a_2^2 \alpha_1'} + \frac{2(a_{12}^2 + a_{13}^2)}{\alpha_2'(a_1^2 + a_2^2)} \\ & + \frac{[\alpha_2'(a_1^2 + a_2^2) + 2\alpha_2''](a_{12}^2 + a_{13}^2) - \alpha_2'(a_1^2 - a_2^2)(a_{13}\xi_2 - a_{12}\xi_3)}{\alpha_2'[2a_1^2 a_2^2 \alpha_2' + (a_1^2 + a_2^2)\alpha_2'']} \Bigg\} \end{aligned}\right\} \quad (5)$$

The terms in the first line are Jeffery's. As expected, an increase of energy results from the assumption that the particles do not follow the motion of the fluid.

For the Couette streaming one obtains:

$$\left.\begin{aligned} \frac{\mathrm{d}W}{\mathrm{d}t}(\vartheta, \varphi) = & \left[\frac{\mathrm{d}W}{\mathrm{d}t}(\vartheta, \varphi) \right]_{\mathrm{Jeff.}} \\ & + \frac{4\pi}{3}\mu_0 \kappa^2 \Bigg\{ \frac{[\alpha_2'(a_1^2 + a_2^2) + 2\alpha_2''](\sin^2\vartheta - \sin^4\vartheta \sin^2 2\varphi)}{\alpha_2'[2a_1^2 a_2^2 \alpha_2' + (a_1^2 + a_2^2)\alpha_2'']} \\ & + \frac{\alpha_2'(a_1^2 - a_2^2)\sin^2\vartheta \cos 2\varphi}{\alpha_2'[2a_1^2 a_2^2 \alpha_2' + (a_1^2 + a_2^2)\alpha_2'']} \\ & - \frac{2}{\alpha_2'(a_1^2 + a_2^2)} (\sin^2\vartheta - \sin^4\vartheta \sin^2 2\varphi) \Bigg\} \end{aligned}\right\} \quad (5a)$$

where $\left[\frac{\mathrm{d}W}{\mathrm{d}t}\right]_{\mathrm{Jeff.}}$ is given by equation 3. Now as the average value

$$\overline{\frac{\mathrm{d}W}{\mathrm{d}t}} = \frac{N}{4\pi} \int_0^{\pi} \int_0^{2\pi} \frac{\mathrm{d}W}{\mathrm{d}t}(\vartheta, \varphi) \sin\vartheta \, \mathrm{d}\vartheta \, \mathrm{d}\varphi$$

the final result for the factor ν is:

$$\left.\begin{aligned}\nu = \frac{1}{a_1 a_2^2}\Bigg\{&\left(\frac{\alpha_1''}{2a_2^2\alpha_1'\alpha_2''} + \frac{1}{2a_2^2\alpha_1'} - \frac{2}{\alpha_2'(a_1^2 + a_2^2)}\right)\frac{4}{15} + \frac{1}{3a_2^2\alpha_1'} \\ &+ \frac{4}{3\alpha_2'(a_1^2 + a_2^2)}\Bigg\} + \frac{1}{a_1 a_2^2}\Bigg\{\frac{\alpha_2'(a_1^2 + a_2^2) + 2\alpha_2''}{\alpha_2'[2a_1^2 a_2^2\alpha_2' + (a_1^2 + a_2^2)\alpha_2'']} \\ &- \frac{2}{\alpha_2'(a_1^2 + a_2^2)}\Bigg\}\frac{2}{5}\end{aligned}\right\} \tag{6}$$

In the limit $f \gg 1$ one gets:

$$\left.\begin{aligned}&\text{Rods:} \quad \nu \approx \frac{f^2}{15(\log 2f - \frac{3}{2})} + \frac{f^2}{5(\log 2f - \frac{1}{2})} + \frac{14}{15}, \quad f = \frac{a_1}{a_2} \\ &\text{Disks:} \quad \nu \approx \frac{16}{15}\frac{f}{\operatorname{tang}^{-1} f} \qquad\qquad f = \frac{a_2}{a_1}\end{aligned}\right\} \tag*{(6a)[5]}$$

DISCUSSION

The first part in the first line of expression 6a was derived by Eisenschitz (8) in starting from the energy formula 3 for the case without heat motion. From our assumptions results a rather large increase in the calculated viscosity. The approximately quadratic dependence on the axial ratio f for rigid rods, and only on f, however, is preserved. Whatever assumptions may be made concerning the orientation in the purely hydrodynamic case, one obtains always approximate proportionality with the first power of f for rods. The disorientation tendency of the thermal agitation therefore increases the viscosity in the solution as compared with the viscosity without Brownian movement, as expected.

These results are valid for every motion with constant components of rotation and distortion, as was shown by the author (19). Although only proved in using expression 3, one can assume that the result will continue to be valid in this case. However, the only streaming of that kind which has been produced is the laminar Couette flow previously considered.

---

[5] *Note added in proof:* Polson (Kolloid-Z. **88**, 51 (1939)) measured the viscosity of solutions of various proteins, whose molecules had axial ratios varying from about 3 to 10. Using an empirical equation

$$\nu = 4.0 + 0.098 f^2$$

and diffusion data, he obtained values for the molecular weights agreeing satisfactorily with those found by ultracentrifugal measurements, being slightly greater, while the theoretical expressions used always gave values that were too low.

Our expressions 6 and 6a on the other hand give values for the molecular weights slightly lower than those resulting from the empirical formula, and in this way satisfying agreement with the experimental data.

In many cases viscosity measurements were carried on in a capillary tube viscosimeter, so that our formulas should not be directly applied. Theory predicts (20) the same viscosity values for dilute solutions in both types of flow without Brownian movement influence and neglecting inertia. The latter effect presumably lowers the viscosity, according to experiments by Eirich and Goldschmid (4) and some preliminary calculations. When the heat motion enters into play in the solution, fundamental differences between the results obtained in the two cases are to be expected, as the distribution function F and thus also the dissipated energy will depend on the velocity gradient which varies from point to point in the tube. In approaching the limit of complete Brownian movement, however, one should get equal viscosity values for dilute solutions in Couette and Poiseuille, since inertia forces will be of much less importance for small particles than for the big ones in the hydrodynamic case.

Results of a direct quantitative comparison of these considerations with experimental data do not appear to be very illuminating. Staudinger's measurements (21), for instance, for polystyrene solutions combined with formula 6a would provide values for the chain length in fair agreement with those found by other methods. These results, however, do not differ enough from those found with the aid of Eisenschitz's expression to make a decisive conclusion concerning the basic assumptions in the derivation of our viscosity formula.

It appears interesting to evaluate Meyer and van der Wyk's (16, 17) very exact measurements on paraffin solutions in carbon tetrachloride in the light of results furnished by the hydrodynamic theory. The values found for the factor ν are in several cases lower than that calculated by Einstein for spheres, in disagreement with the theory, so that we must assume with Burgers (1) that the addition of the solute changes the solvent, or that the hydrodynamic treatment is quite inadequate for these cases.

On the other hand, discrepancies between the theoretically calculated dependence of the viscosity increase on the dimensions of the solute particles and that deduced by Staudinger from his measurements clearly show that flexibility of the chains must be taken into account.[6] This effect not only changes the relation between molecular weight and chain length according to the theory developed by Kuhn and Mark (10, 12, 13, 14), but also reduces the energy dissipated in the flow. For flexible particles do not disturb the distortional part of the viscosimeter flow to the same extent as rigid ones. This follows also from recent experiments by Eirich and Sverak (5), who found a remarkable viscosity decrease with increasing degree of swelling of their models. Theory and experiment further show (6, 9) that the linear range of the viscosity *versus* concentration graph decreases rather rapidly with increasing axis ratio, so that neglect of the hydrodynamic reciprocal action of the solute particles is no longer justified, although the flexibility effect may counteract this tendency. This influence of concentration must be considered also in the case of overwhelming thermal motion.

---

[6] For an interesting treatment of flexibility using Kuhn's (Z. physik. Chem. **A161,** 1 (1932)) approximations, see M. L. Huggins (J. Phys. Chem. **42,** 911 (1938); **43,** 439 (1939)).

On principle it must further be examined, whether the theoretical methods used are still appropriate in the case considered, where the particles of the solute sometimes are of almost molecular size, at least in one dimension. The experimental material and the points mentioned indicate that a complete elucidation of these questions can not be expected from a purely hydrodynamic theory in the form hitherto used, because of the complex superposition of such factors as concentration, degree of dispersity, rigidity of the suspended molecules, Brownian movement, and solvation. Therefore a statistical and kinetical treatment of these phenomena similar to that started in pure liquids should parallel the phenomenological one, although the treatment in this case appears to be more complicated than in the case where only molecules of one kind are present. Further experiments, especially in respect to the temperature dependence of all operative influences, appear to be necessary also. Nevertheless it seemed desirable to discuss some aspects of the problem at the present state of theory and experiment, in order to establish a point of departure for investigations in the directions indicated.

SUMMARY

The calculation of the viscosity of dilute solutions of non-spherical particles as a function of their dimensions and of the concentration was discussed. Three different cases must be distinguished according to the magnitude of the factor κ/D (D = rotational diffusion constant of the particles assumed as spheroids and κ = velocity gradient of the flow in the viscosimeter). κ/D infinite characterizes the purely hydrodynamic case, treated by Jeffery for the case of a Couette streaming.

Finite κ/D means that the irregular thermal motion is superimposed upon the orientation tendency of the shear. This problem and its difficulties, due to the incompleteness of the hydrodynamic solution, were not further discussed, but the third case of complete Brownian movement $\left(\frac{\kappa}{D} \rightarrow 0\right)$ was considered. Here the macroscopic flow is no longer able to bring about a regular rotational motion of the ellipsoids against the thermal motion, which, on the average, effects an isotropic distribution of the particle axes in the fluid. The specific viscosity $\frac{\mu - \mu_0}{\mu_0}$ was calculated.

Possible extensions of these results to other types of flow, especially the streaming in a capillary tube, were discussed. Theoretical considerations as well as experimental results show improvements in the theory and further experiments to be necessary.

The author wishes to thank the Faculty Fellowship Fund for the grant which enabled him to carry on this work. He is especially indebted to Professor V. K. La Mer, in whose laboratory the work was done.

REFERENCES

(1) BURGERS, J. M.: Second Report on Viscosity and Plasticity. Amsterdam (1938).

(2) EINSTEIN, A.: Ann. Physik **19,** 289 (1906); **34,** 591 (1911).

(3) EIRICH, F., GUTH, E., SIMHA, R., AND OTHERS: *Untersuchungen über die Viskosität von Suspensionen und Lösungen,* Kolloid-Z., 1936–39; Monatsh. **71,** 67 (1937).

(4) EIRICH, F., AND GOLDSCHMID, O.: Kolloid-Z. **81,** 7 (1937).

(5) EIRICH, F., AND SVERAK, A.: Kolloid-Z., in press.

(6) EIRICH, F., MARGARETHA, H., AND BUNZL, M.: Kolloid-Z. **75,** 20 (1936).

(7) EIRICH, F., AND SIMHA, R.: Reports on Progress in Physics **6** (1939), in press.

(8) EISENSCHITZ, R.: Z. physik. Chem. **A163,** 133 (1933).

(9) GOLD, O.: Thesis, Vienna, 1937.

(10) GUTH, E., AND MARK, H.: Monatsh. **65,** 93 (1934).

(11) JEFFERY, G. B.: Proc. Roy. Soc. (London) **A102,** 163 (1923).

(12) KUHN, W.: Kolloid-Z. **68,** 2 (1934).

(13) KUHN, W.: Kolloid-Z. **76,** 258 (1936).

(14) MARK, H.: Chem. Rev. **25,** 121 (1939).

(15) MARK, H.: *High Polymers.* Elsevier, Amsterdam (in press).

(16) MEYER, K. H., AND VAN DER WYK, A.: Helv. Chim. Acta **18,** 1067 (1935).

(17) MEYER, K. H., AND VAN DER WYK, A.: Kolloid-Z. **76,** 278 (1936).

(18) SIMHA, R.: Unpublished work.

(19) SIMHA, R.: Thesis, Vienna, 1935.

(20) SIMHA, R.: Kolloid-Z. **76,** 16 (1936).

(21) STAUDINGER, H.: *Die hochmolekularen Verbindungen.* Julius Springer, Berlin (1932).

THE GROWTH, ORIENTATION, AND PREPARATION OF THE SURFACE OF SINGLE CRYSTALS OF COPPER

ALLAN T. GWATHMEY AND ARTHUR F. BENTON

Department of Chemistry, University of Virginia, Charlottesville, Virginia

Received April 11, 1939

A satisfactory understanding of the properties of a polycrystalline metal is dependent on a knowledge of the properties of the individual crystals. Especially is this true of the important surface phenomena such as photoelectric and thermionic emissions, extraction of electrons by intense fields, thermoelectricity, diffraction of low-voltage electrons, adsorption of gases, corrosion, and contact catalysis. Many of these properties have been shown to vary with the crystal plane along which the surface is prepared.

In an effort to prepare single crystals of copper for use in the study of adsorbed gas by means of the diffraction of low-voltage electrons, considerable difficulty was encountered in obtaining satisfactory and reproducible surfaces. Very little information seemed to be available on the proper etching reagent to be used in developing a smooth surface parallel to a particular crystallographic plane. The method herein described offers a simple way of preparing very smooth surfaces on single crystals for use in the study of any of the surface phenomena of copper. The surface may be made parallel to any desired crystallographic plane. In making measurements on metallic surfaces it should be emphasized that a slight improvement in the preparation of the surface will often be of far more value than a painstaking improvement in the method of making the measurement.

THE GROWTH OF SINGLE CRYSTALS OF COPPER

The furnace used for the growth of the single crystals is a modification of the furnace developed by Quimby (3), who employed the Bridgman method (1) for metals with melting points as high as 1500°C. A few changes have been made in the furnace described by Quimby to simplify its construction and operation for the growth of crystals of copper. A front view is shown in figure 1. Only the parts which differ essentially from those used in the furnace developed by Quimby will be described.

The crucible E is made from a graphite rod of the highest purity, 9 in. long and 1 in. in diameter, with a hole $\frac{5}{8}$ in. in diameter and 5 in. long drilled in one end, the lower $1\frac{1}{4}$ in. being tapered to a point. The crucible is supported on an alundum rod, which in turn is supported by means of a piece of $\frac{1}{2}$-in. iron pipe which floats in mercury in tube O.

The crucible containing the molten metal is slowly lowered by lowering the leveling bulb L, which is partially filled with mercury and connected to the pipe O by a piece of rubber pressure tubing and a section of glass tubing as shown in figure 1. The top of the leveling bulb is also connected to the furnace through the base-plate by means of rubber tubing, the weight of which is carried by counterweights suspended from pulleys K. The leveling bulb is suspended by a piece of strong string which is wound around the ½-in. shaft at J. The shaft is turned by a variable-speed electric motor connected to the pulley J through two sets of reducing gears and the necessary belts. The motor and reducing gears are mounted

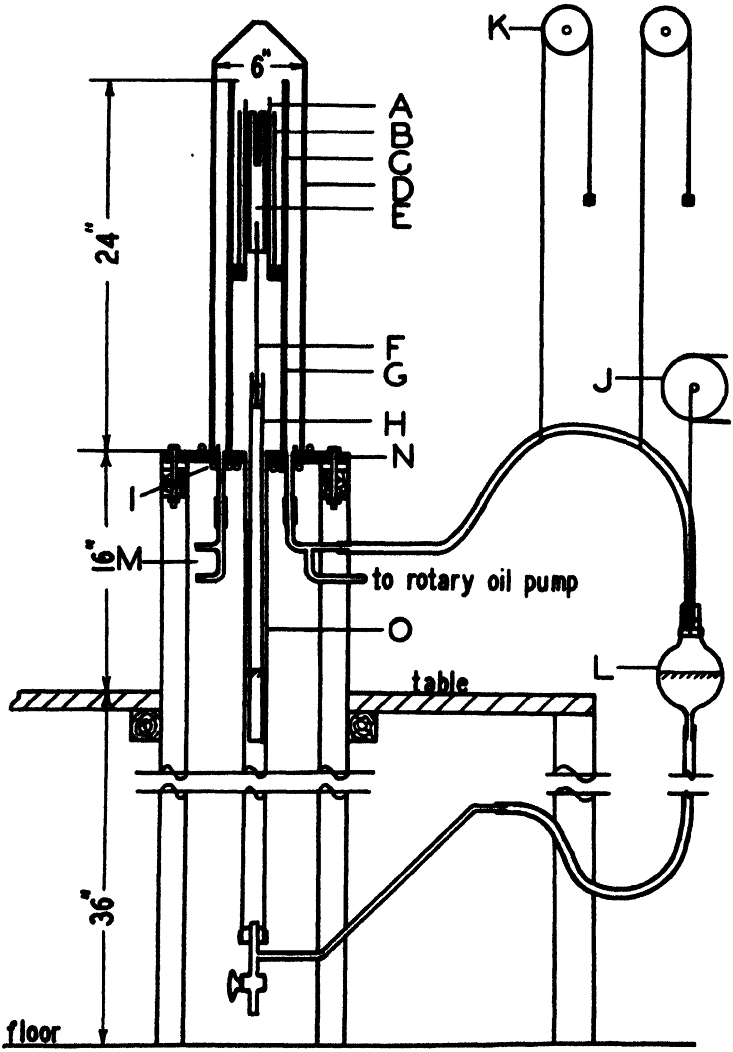

FIG. 1. Vacuum furnace for growing single crystals

on a separate stand in order to prevent vibrations in the furnace. For the growth of a single crystal of copper, ⅝ in. in diameter and 5 in. long, the crucible was lowered at the rate of ⅝ in. per hour. The use of the leveling bulb for lowering the crucible was found to be more satisfactory than the revolving stopcock (3), since it avoided the difficulty of keeping the latter well greased.

The opaque fused-silica tube D is sealed to the steel base-plate N by means of a vacuum-tight joint. This is obtained by using stopcock grease between two brass rings, one of which is sealed by picein wax to the bottom of the silica tube and the other to the base-plate. The wax and grease are kept cool by circulating water through five turns of ⅜-in. copper tubing soldered to the bottom and one turn to the top of the plate as shown.

The electrical leads to the furnace windings are brought into the furnace through a glass arm M, which is attached by a piece of rubber tubing to a ¼-in. steel tube which in turn is soldered into the base-plate. The leads are sealed to the ends of the glass tube by means of picein wax, giving a vacuum-tight joint. Through a similar glass arm, not shown in figure 1 but connected to the base-plate at the rear, helium gas is led into the inside of the tube C at the rate of about 4 cc. per minute. A pressure of less than 1 mm. of mercury is maintained within the furnace by means of a Hyvac pump.

The power input required to keep the furnace at a temperature of at least 100°C. above the melting point of copper was about 1000 watts at 85 volts. The power was supplied by a 115-volt D.C. motor-generator set which furnished a sufficiently steady voltage for the purpose desired. About 2 hr. were required to bring the furnace up to temperature, about 14 hr. for the total time of lowering the crucible, and about 2 hr. for cooling the furnace before it could be opened. Care is required in removing the crystal from the crucible. In some cases the crystal could be removed by simply inverting the crucible and shaking it slightly. Quite often it is necessary to break open the crucible by forcing small wedges into three saw cuts made lengthwise in its outer surface.

THE IDENTIFICATION AND ORIENTATION OF THE SINGLE CRYSTALS

The identification and orientation may be most easily determined by the reflection pattern from one complete set of planes. Tammann and Sartorius (4) have studied the etching of single crystals of copper in the form of a sphere with various reagents. We have found three of these to produce reflection patterns which are satisfactory for determining the orientation. It should be mentioned, however, that these reagents are not satisfactory for imparting the final polish to surfaces parallel to one definite crystallographic plane, since they leave the surface in a slightly roughened condition.

The reagents are, in decreasing order of their preference as regards the brightness of the reflections: (*1*) Ten grams of silver nitrate in 350 cc. of concentrated nitric acid (sp. gr. 1.42) and enough water to make 1 liter. This solution develops the (111) planes. (*2*) Forty grams of cupric chloride in 1000 cc. of concentrated hydrochloric acid (sp. gr. 1.19). This solution develops the 100 planes. (*3*) One hundred grams of ammonium persulfate in 350 cc. of concentrated ammonium hydroxide (sp. gr. 0.90) and enough water to make 1 liter. This solution develops the 111 planes. In order to remove any grease which has been left on the surface due to handling, the part of the crystal which is to be etched is first washed with soap and water and then rinsed in ether followed by alcohol. Since the silver nitrate in the first reagent produces a deposit of silver on the surface of the crystal, either of the latter two reagents may be satisfactorily used if it is desired not to contaminate the surface with the silver. The period of etching for each of the solutions is about 3 min.

After treating the crystal rod with the reagent which will develop the set of planes along which it is desired to prepare the surface, the reflection pattern is determined in the following manner, the general principle of which is attributed to Langmuir (1): A convenient source of light is an incandescent lamp in the ceiling of a high-pitched and partially darkened room. The end of the crystal rod is attached to a cork ball, 1 in. in diameter or larger, by sticking the tapered end snugly into a ¼-in. hole cut in the ball. A spherical fishing cork was actually used. The rod is now held in the hand at arm's length toward the floor with the light above and over one shoulder, and the rod is rotated until a definite reflection flashes in from the illuminated side of the rod. The orientation with respect to the beam of light is now marked on the ball by the following device. A piece of plane mirror, the back of which is smeared with a little printer's ink, is held in one hand, the other maintaining the rod in the position of regular reflection, and the mirror is rotated until the source of light is also visible in it. The mirror is now touched lightly to the cork ball, the ink on the back side marking the position. This procedure is repeated until the positions of all of the reflections are marked on the ball. We have found it convenient to stick straight pins normally into the ball at each of the ink spots, since they allow the observer to see at one time the locations of all of the poles of the reflecting planes. In the case of a copper crystal, the poles of the (111) planes are located in the faces of an octahedron, and those of the (100) planes are located in the faces of a cube. If more than one crystal exists in the rod, it can be determined from the position of the poles marked on the ball.

THE PREPARATION OF THE SURFACE ALONG A DEFINITE PLANE

It is assumed that the surface is to be prepared parallel to a (111) plane and that the crystal has been treated with the proper reagent for developing this set of planes.

The crystal rod is clamped in position in the vice of a milling machine in the manner described below and a surface is cut parallel to the (111) plane by means of a circular saw revolving on the arbor (or shaft) of the machine. The saw used is 4 in. in diameter and specially made for cutting copper. The method of clamping the crystal is shown in figure 2. It is held in a holder B, which consists of a brass block ¾ in. by ¾ in. by 2 in. long, with a hole the size of the crystal drilled lengthwise through the center. A slit is made lengthwise through the top of the holder in order to allow a slight adjustment in the size of the hole by pressing on the sides of the holder. From the midpoint of two opposite sides of the holder extend small shafts (C) ⅛ in. in diameter and ¼ in. long. These two shafts rest in holes drilled into brass blocks (D, D), which fit over the jaws of the vice of the milling machine. With the jaws E, E of the vice not pressed tightly against the holder, the crystal rod A may be revolved about its own longitudinal axis, about the vertical axis of the vice of the milling

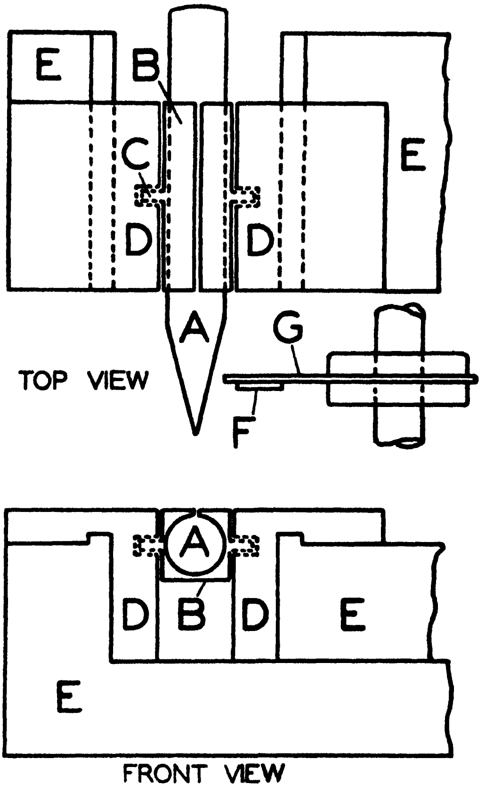

Fig. 2. Clamp for holding single crystal

machine, and about the axis formed by the two shafts (C). A small piece of plane mirror F is now attached by means of an adhesive to the front and near the outside edge of the circular saw G. By moving the table (which carries the vice) of the milling machine, the crystal in the holder is now moved to a position until it nearly touches the edge of the saw. With the room partially darkened, one person stands about 6 ft. distant from the saw in a line perpendicular to the plane of the saw at the point where the mirror is attached. An ordinary flash light with an adjustable focus is held in one hand and a concentrated beam of light is thrown normally onto the mirror. By sighting along the side of the light, directions are given to a second person for changing the orientation of the crystal until a reflection from the crystal flashes into view at the same time as the reflection from the mirror attached to the saw. If the reflections, resulting from the first etching made for the purpose of identifying the single crystal, are not sufficiently bright, the crystal may be polished electrolytically by the method to be described presently and then treated again with the desired reagent. The original etching is generally satisfactory, but the brightness of the reflections depends on the roughness of the surface as the crystal comes from the crucible and on the amount of oxidation which has taken place since the time of the first etching.

After the position of the crystal has been definitely established, the jaws of the vice on the milling machine are clamped tightly against the holder and the plane of the saw is then parallel to one of the (111) planes of the crystal. The small mirror is now removed from the saw and a cut is made through the crystal rod with the saw revolving at a speed of about 300 R.P.M. If more than one specimen is desired, additional cuts parallel to the same plane may be made by moving the table of the milling machine. If it is desired to cut a second plane, different from the first, on the same specimen, it may be done by means of a jeweler's handsaw, locating the position of the second plane by measuring off the known angle which it makes with the first plane. The final adjustment of the second plane can be made by filing or grinding.

The sawed surfaces are now made plane by grinding on a metallurgical grinding belt of medium grade. They are then rubbed successively on metallographic polishing papers Nos. 1, 0, 00, 000, and 0000 placed on a sheet of plate glass. Care is taken to remove any grit left on the surface by one paper before rubbing on the next finer grade.

In preparing a metallographic specimen, it is customary, after using the above polishing papers, to give the surface a final polish by pressing it lightly against a revolving disk covered with a cloth on which is poured a suspension of some fine abrasive such as alumina. This is considered to produce an amorphous layer on the surface which, together with any strained layers and fragments of broken crystals previously produced by sawing and rubbing, is removed by treating with an etching reagent. This latter treatment generally produces a slightly irregular surface. In an effort to avoid this, it has been found that a very bright and smooth finish can be produced by using the electrolytic etching method developed by Jacquet (2) for the preparation of surfaces on polycrystalline specimens. Under the conditions employed, etching takes place parallel to the geometric face, so that it is only necessary to cut the surface parallel to the desired plane. This electrolytic method is not only more rapid than the mechanical method but it has the decided advantage of removing any amorphous layer or broken crystals simultaneous with the polishing. It is carried out as follows:

After the surface to be polished has been rubbed on the five grades of metallographic paper as described above, the single crystal is thoroughly degreased by first washing in a soap solution, and is then connected as a cathode in a dilute solution of sodium hydroxide for about 15 min. with a current density sufficient to give a strong evolution of gas. The specimen is rinsed thoroughly in water and given its final polish by connecting it as an anode in an electrolytic cell containing orthophosphoric acid at a concentration of one volume of commercial acid (sp. gr. 1.71) to one volume of water. The cathode consists of ordinary sheet copper, $\frac{1}{16}$ in. thick and of a surface slightly greater than the surface of the anode. The cell should be operated at a voltage just below the value at which gas is evolved from the anode. This depends on the concentration of the solution and the position of the cathode, and may best be determined by a preliminary experiment. It was found convenient to use a cell which consists of a vertical glass tube, 2 in. in diameter and closed at the bottom, to the opposite sides of which are sealed at a point about 2 in. from the bottom two side arms, 1 in. in diameter. The side arms are bent upwards to a vertical position. The anode is placed in the center of the larger tube opposite the entrance to the side arms. A cathode is placed in each of the vertical side arms in order that the gas evolved therefrom may escape to the surface of the liquid before it has an opportunity to stick to the anode and produce an uneven surface. For an anode of total surface equal to 1.2 sq. in. and with the cell described above, a very bright surface is obtained after 7 min. with a current of 0.65 ampere and a voltage drop across the cell of 4.4 volts. If a 500-cc. beaker is used as a cell with the cathodes placed $\frac{3}{4}$ in. from the anode, 2 volts is required. If, after the electrolytic etching has been completed, any scratches on the surface due to the initial rubbing on the metallographic paper can be seen with a microscope, the surface should be rubbed again on the 4/0 paper and etched electrolytically a second time. A brilliant and smooth surface is finally obtained.

SUMMARY

Single crystals of copper, $\frac{5}{8}$ in. in diameter and 5 in. long, are grown in a vacuum furnace using a modified form of the Bridgman method.

A simple method of preparing a surface on these crystals parallel to a desired crystallographic plane is described. A very bright and smooth finish may be produced by using the electrolytic polishing method. This has the decided advantage of removing any strained or amorphous layers on the surface simultaneous with the polishing.

The specimens so prepared may be used for studying any of the surface phenomena of single crystals of copper.

We are indebted to Professor S. L. Quimby of Columbia University and to Mr. J. Zacharias for furnishing us with details of their furnace used for growing single crystals of nickel.

REFERENCES

(1) Bridgman, P.: Proc. Am. Acad. Arts Sci. **60**, 305 (1925).
(2) Jacquet, P.: Trans. Electrochem. Soc. **69**, 629 (1936).
(3) Quimby, S.: Phys. Rev. **39**, 345 (1932).
(4) Tammann and Sartorius: Z. anorg. allgem. Chem. **175**, 97 (1928).

MECHANISM OF PHOTOGRAPHIC DEVELOPMENT. II

Development by Hydroquinone

T. H. JAMES

Kodak Research Laboratories,[1] *Eastman Kodak Company, Rochester, New York*

Received May 10, 1939

In a preceding paper (3) it was demonstrated that, in the normal course of development (absence of strong silver halide solvent action), the ions or molecules of the reducing agent must penetrate the double-layer electric barrier before reacting with the silver halide grain. The changes which occur in the potential barrier during the course of development and the variation from grain to grain in the magnitude of the original barrier significantly alter the kinetics of development by the ionic reducing agents; further, the barrier effect becomes more pronounced as the negative charge increases. The induction period observed in development by such agents as hydroquinone and *p*-hydroxyphenylglycine may be attributed largely to a decrease in the potential barrier as the reduction proceeds.

---

[1] Communication No. 724 from the Kodak Research Laboratories.

A more detailed investigation of the kinetics of development by hydroquinone has been made with the view of obtaining a clearer understanding of the mechanism of the chemical reaction itself. The apparatus and procedure were the same as those previously employed. The majority of the experiments were with sulfite-free solutions of pH 8.0 to 8.9. All solutions were prepared from components carefully freed from oxygen, and development was carried out under an atmosphere of pure nitrogen. The development rates were conveniently slow, and development could be carried to apparent completion without formation of stain or significant fog. The emulsion employed was, as before, an unsensitized motion picture positive silver bromide material of thin and very uniform coating. Borax–boric acid buffers were used throughout. All temperatures, unless otherwise specified, were 20°C. ± 0.05°. Silver determinations were made by potentiometric titration at 70°C. with 0.0002 *M* potassium iodide. The determinations were of the amount of silver in a circular area of film $\frac{5}{16}$ in. in diameter, cut from the sensitometer strip by means of a steel punch.

EXPERIMENTAL DATA

The pronouncedly S-shaped density-time curve obtained with a pure hydroquinone developer was illustrated in figure 2 of the preceding paper. Obviously, such curves cannot be represented by the simple formulas proposed in the literature (7). The upper third of the curves may be represented approximately by the simple formula

$$\mathrm{d}D/\mathrm{d}t = k(D_{\mathrm{max.}} - D) \qquad (1)$$

but this relation fails badly for the lower portion.

Three methods of expressing the rate of development have been employed and found to give results consistent among themselves for the simple case of the pure hydroquinone developer. These are as follows: (*1*) determination of k in equation 1 from the data for the upper third of the curve; (*2*) determination of the slope of the density-time curve at a fixed density (usually $\frac{1}{2}$ D_{max}, since the curve at this point is a reasonably straight line); (*3*) determination of the reciprocal of the time required to attain a given density. The rates so expressed are largely independent of the density chosen when we deal with change of pH or change of developer concentration. In all of these cases, if a plot of density against log t is made, the curves obtained may be largely superimposed by the proper shift along the log t axis.

The maximum density obtainable with a given exposure did not vary with the concentration of developing agent used or with the pH of the solution over the range employed. Likewise, the maximum amount of silver did not change. An example of the results is given in table 1.

These data show further that, over a considerable range of exposure, the ratio D/Ag is constant when development is carried to completion. The ratio therefore does not depend upon the number of grains developed over this range of exposure. If, however, data for a fixed exposure and varying degrees of development are examined, it is found that the ratio D/Ag increases with decreasing degree of development. A plot of log Ag against log D yields a reasonably straight line of slope 1.45; i.e.,

TABLE 1

Variation of maximum density with exposure

LOG E	pH	$D_{max.}$	D/Ag*
1.15	8.89	2.50	1.68
0.85	8.89	2.02	1.68
0.85	8.29	2.01	1.71
0.85	8.00	1.98	1.68
0.55	8.29	1.55	1.64
0.40	8.48	1.30	1.63

* Silver expressed as milliliters of 0.001 M potassium iodide used in titration.

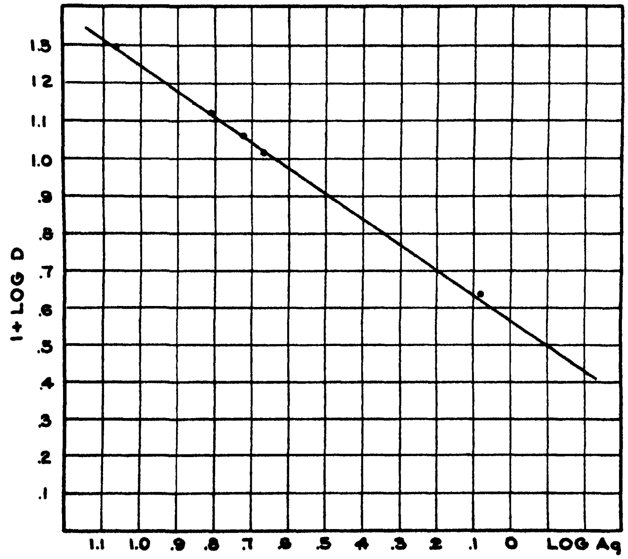

FIG. 1. Silver-density relationship. Log E = 0.85

$$\log \text{Ag} = 1.45 \log D + \text{Constant} \qquad (2)$$

(see figure 1).

This relationship is interesting in connection with the results reported by Eggert and Küster (1). They found that, over a rather wide range of conditions, the ratio Ag/D is a linear function of the mean grain diameter. From the relations:

$$\mathrm{Ag}/D = k_1 d + C$$

$$\mathrm{Ag} = k_2 d^3$$

where d is the mean grain diameter, it follows for constant grain number that

$$\log \mathrm{Ag} = 1.5 \log D + 1.5 \log (K + C\mathrm{Ag}^{-1/3}) \qquad (3)$$

This expression is in good agreement with our experimental results, since the constant C is very small.

The agreement between the experimental results and equation 3 is good evidence that we have to deal largely with rates of reduction of the silver halide grains, and not with rates of initiation of the reduction process, since, in the latter case, the ratio D/Ag would be nearly constant for the fairly uniform grain sizes of the experimental emulsion.

This conclusion is supported by observations on the bromide effect. The pure hydroquinone developer is very sensitive to small concentrations of bromide, and the effect is markedly to extend the toe of the development curve without appreciably altering the rate of development beyond the toe region (*cf.* table 4). The effect is more pronounced at lower exposures than at higher. These facts point to a strongly preferential action of bromide at the start of development,—a phenomenon readily understandable on the basis of considerations given in the preceding paper of this series (3). Experiment shows, however, that if development is started in a bromide-free developer and continued to a suitable density (say 0.30 for $\log E = 0.85$), addition of 0.1 g. potassium bromide per liter results in only a slight decrease in the development rate. The same amount of bromide, present at the start of development, would increase fivefold the time required to obtain a density of 0.10.

The dependence of the rate of development upon the solution pH is indicated in figure 2. A plot of the logarithm of the rate against the pH conforms approximately to a straight line of slope 1.0. Hence the rate varies as the first power of the hydroxyl-ion concentration.[2]

The rate varies approximately as the square root of the hydroquinone concentration. This is shown for two sets of data by the constancy of the ratios given in columns V and VI of table 2.

The temperature dependence of the development rate is given in table 3. Temperature coefficient calculations from rates determined at the start of

[2] More accurately the data, corrected for change in concentration of hydroquinone which is due to ionization, indicate a dependence on the 1.08 power of the hydroxyl-ion concentration and the 0.55 power of the hydroquinone concentration.

development and at the midpoint are in fair agreement, although a dependence upon exposure appears in the former case, but is not definitely indicated in the latter.

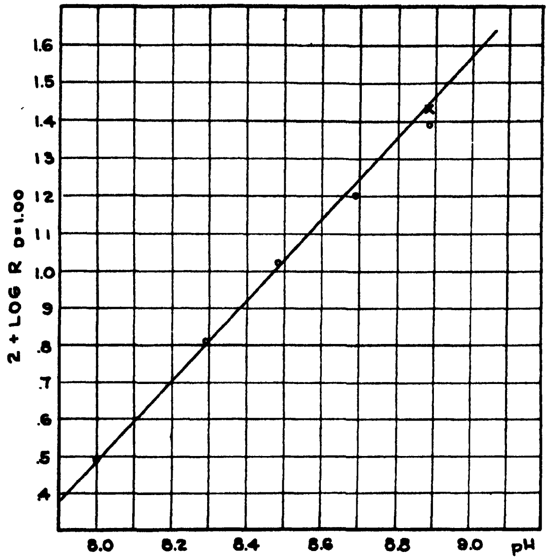

FIG. 2. Variation of rate with pH. Log E = 1.15. x, correction applied for change in concentration of unionized hydroquinone.

TABLE 2

Variation of rate with hydroquinone concentration

pH = 8.75

I HYDROQUINONE	II $(10 \times Hq)^{1/2}$	III LOG E = 0.85 R_D = 1.00	IV LOG E = 1.75 R_D = 1.5	V RATIO II/III	VI RATIO II/IV
grams per 300 ml.					
6.60	8.12	0.270	0.397	30.0	20.5
3.30	5.74	0.170	0.280	33.7	20.5
1.65	4.06	0.123	0.192	33.0	21.2
0.825	2.87	0.082	0.130	35.0	22.2
0.412	2.03	0.058	0.090	35.0	22.5

The pure hydroquinone developers employed in this investigation are highly sensitive to the bromide-ion concentration. The major effect of small concentrations of bromide is exerted at the start of development. Larger quantities of bromide, however, affect the entire course of development. This is indicated by the data in table 4. The times employed in determining the rate of initiation of development are for different densities (i.e., 0.20 and 0.10) for the two exposures recorded, the densities having been chosen to give equal rates of reaction in the absence of soluble bromide.

The depressing effect of small amounts of bromide (less than 0.2 g. per liter) is thus confined almost exclusively to the early stages of development, and is most pronounced in the region of low exposures (13). If development is started in the absence of added bromide and then continued in a developer to which 0.10 g. of potassium bromide has been added, no significant change occurs in the rate, provided the initial development is carried to about the end of the induction period. Larger amounts of bromide, however, exert a significant influence over the entire course of development, as indicated by the much smaller rate observed at $D = 1.00$ when the solution contained 1.00 g. of potassium bromide per liter.

TABLE 3

Dependence of rate upon temperature

Hydroquinone concentration = 0.05 M; pH (at 20°C.) = 8.89

LOG E	R AT 8.0°C. $D = 1/2$ max.	R AT 20.0°C. $D = 1/2$ max.	TEMPERATURE COEFFICIENT	TEMPERATURE COEFFICIENT FROM $1/t$; $D = 0.10$
1.75	0.090	0.315	2.90	2.95
1.15	0.070	0.245	2.9	3.1
0.85	0.056	0.208	3.1	3.3
0.25	Accurate values could not be determined			3.9

TABLE 4

Effect of added bromide

Hydroquinone = 0.05 M; pH = 8.71

KBr ADDED	LOG E = 1.45			LOG E = 0.85	
	t $D = 0.20$	Rate $1/t$	Rate $D = 1.00$	t $D = 0.10$	Rate $1/t$
grams per liter					
0	9.3	0.107	0.192	9.2	0.109
0.025	19.3	0.052	0.190	24.1	0.0415
0.10	36.7	0.0272	0.190	46	0.0217
0.25	53	0.019	0.12	65	0.0154
1.00	102	0.0098	0.030	143	0.0070
Washed film	8.1	0.123	0.192	8.0	0.125

It has already been demonstrated that the addition of quinone to the hydroquinone solution increases the development rate. Accordingly, it was desirable to check the kinetic results already obtained by similar measurements made in the presence of added quinone and in the presence of sodium sulfite (which rapidly removes the quinone formed during development). The same dependence of the reaction rate upon the square root of the hydroquinone concentration and the first power of the hydroxyl-ion concentration was obtained in these experiments as in those involving only hydroquinone. This is illustrated by the data in tables 5 and 6.

It will be observed that, both in the presence of added quinone and in the presence of sulfite, a fourfold change in the concentration of hydroquinone results in only a twofold change in the development rate. From table 5 we see that a change of 0.39 in pH results in a change in log R of 0.35 and 0.42, respectively, while in table 6 a change of 0.22 in pH is accompanied by a change of 0.22 in log R. Hence the rate of development once more is proportional to the hydroxyl-ion concentration and the square root of the hydroquinone concentration.

TABLE 5

The reaction rate in the presence of added quinone

Added quinone = 0.001 M

HYDROQUINONE CONCENTRATION	pH	LOG E = 0.85 RATE D = 0.40	LOG E = 1.45 RATE D = 0.60
0.05	8.67	0.100	0.150
0.0125	8.67	0.050	0.077
0.05	8.28	0.045	0.057

TABLE 6

The reaction rate in the presence of sodium sulfite

Sodium sulfite = 0.005 M

HYDROQUINONE CONCENTRATION	pH	LOG E = 0.85		LOG E = 1.45	
		Rate	Log R	Rate	Log R
0.05	8.67	0.0196	0.1292	0.0296	0.471
0.05	8.89	0.0336	0.526	0.049	0.69
0.025	8.89			0.034	0.53
0.10	8.89			0.068	0.83

Figure 2 of the preceding paper (3) shows that the induction period of hydroquinone development decreases with increasing concentration of added quinone. Further experiment showed that the maximum density obtained for a given exposure is sharply decreased by the addition of quinone. Figure 3 is based upon data obtained at pH 8.29. A direct plot of silver against development time has been made here. Curve I is for pure hydroquinone solution; curve II is for hydroquinone solution containing 0.001 *M* quinone. The maximum amount of silver has decreased from 1.11 to 0.82 (× 10^{-3} millimoles), and the maximum density from 2.01 to 1.32. This decrease cannot be due to a shift in the equilibrium

$$2Ag^+ + C_6H_4O_2^{--} \rightleftharpoons 2Ag + C_6H_4O_2$$

since thermodynamic considerations show that the reduction would go practically to completion in both cases. The behavior of the photometric equivalent gives the clue to the true cause.

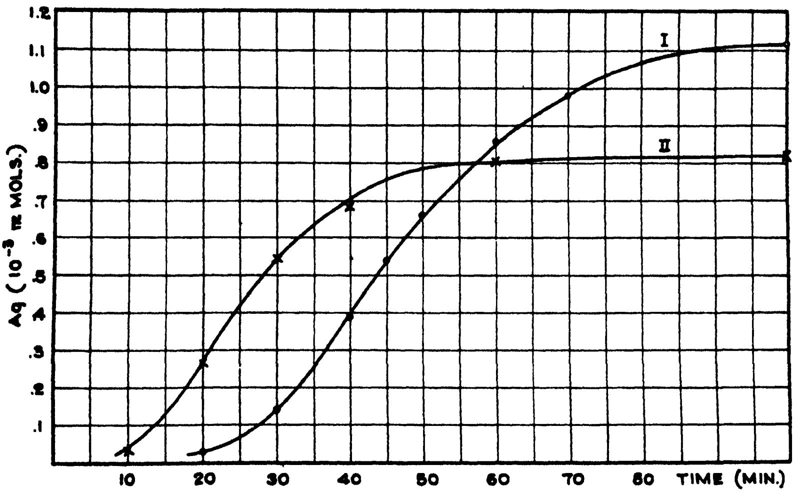

FIG. 3. Effect of quinone (0.001 *M*) on development by hydroquinone (0.05 *M*). I, pure hydroquinone; II, quinone added.

In table 7 the ratio of silver obtained by development in the hydroquinone–quinone solution to that obtained without the addition of quinone (development carried to the same density) is given for several density values. If, instead of comparing equal densities for the same exposure, we compare equal *maximum* densities, we find that there is no significant difference in the photometric equivalent. For example, the maximum density obtained in the presence of quinone is 1.32 for log E = 0.85. This density is matched by the hydroquinone developer for log E = 0.41. The experimental ratio of the amounts of silver obtained was 1.005. Hence, the effect of quinone upon the maximum density is equivalent to a *reduction in the amount of exposure.* The data are accounted for if we assume that the presence of quinone effects no change in the diameter of the developed grains, but reduces the number of grains developed. The data are not accounted for on the assumption that the number of developed grains remains unchanged, but that each attains a smaller maximum size in the presence of quinone. Further evidence in this direction appears from the fact that, if development is started in the absence of added quinone, carried to a density of 0.25 (log E = 0.85), then continued in the quinone-containing solution after thorough washing, a maximum density of 1.95 is obtained in comparison with 2.0 for the pure hydroquinone solution.

The ratio Ag(added quinone)/Ag(no added quinone) drops to 1.03.

In an attempt to determine to what extent continued development is influenced by the quinone formed in the reaction, a series of tests was made in which the sensitometer strips were partially developed, then thoroughly washed in running water, and finally subjected to continued development in fresh hydroquinone solution. In part of the runs, hydroquinone itself was used for the initial development; in the rest, a ferrous oxalate developer was employed. An examination of the data obtained showed that, when the initial development was slight, the intermediate washing process had no effect upon the course of continued development, and the results obtained with initial development by ferrous oxalate checked those obtained with initial development by hydroquinone. As the amount of initial development increased, more and more divergence appeared between the course of the secondary development and that of the uninterrupted development, and the decrease in the rate of secondary development was significantly greater when ferrous oxalate was used for the primary development. If, however, the initial development is carried out by hydroquinone in the presence of a small amount of sodium sulfite, the rate of continued development in pure hydroquinone solution is approximately equal to that found when the initial development is by ferrous oxalate. Under these circumstances, the initial rate of the secondary development does not diverge greatly from the rate of development by a hydroquinone

TABLE 7

Ratio of silver obtained by development in the hydroquinone-quinone solution to that obtained without the addition of quinone

Log E = 0.85

DENSITY	RATIO Ag(QUINONE)/Ag(NO ADDED QUINONE)
1.32*	1.30
1.19	1.23
1.00	1.28
0.58	1.21

* Maximum development in hydroquinone-quinone solution.

solution containing sulfite or resorcinol when the latter rate is measured at the same density. Some comparative results are given in table 8. The rates given for secondary development apply to experiments in which the initial development was carried to densities 0.02 to 0.04 unit less than the densities at which the rate measurements were made.

These results clearly show that quinone catalysis is not responsible for the induction period in hydroquinone development. However, an accelerating effect of quinone or some degradation product thereof does persist throughout the entire course of development If development started in a pure hydroquinone solution is interrupted and the film washed in running water for 30 min. or bathed in sodium bisulfite solution for 10 min., continued development in a fresh hydroquinone solution proceeds at a rate comparable with that of uninterrupted development. This indicates that the immediate presence of quinone is not essential for the "catalytic" effect. A quinone catalysis of the type which exists in the autoxidation of durohydroquinone (4) is therefore eliminated. An effect of quinone upon the electric barrier may still be involved, since this might persist after the quinone had been removed. However, a comparison of the relative accelerating action of benzoquinone, toluquinone, and *m*-xyloquinone upon development by the respective hydroquinones indicates that a decomposition product of the quinone, rather than the quinone itself, is largely responsible for the effect.

TABLE 8

Effect of removal of quinone during development upon the rate of continued development

TYPE OF DEVELOPMENT	SOLUTION	LOG E = 1.45 R_D=0.40	LOG E = 0.85 R_D=0.30
Primary	Pure hydroquinone	0.11	0.078
Secondary	Initial development by pure hydroquinone	0.10	0.07
Secondary	Initial development by hydroquinone-sulfite	0.038	0.023
Secondary	Initial development by ferrous oxalate	0.054	0.025
Primary	Hydroquinone plus 0.05 M resorcinol	0.034	0.023
Primary	Hydroquinone plus 0.10 M resorcinol	0.031	0.022
Primary	Hydroquinone plus 0.005 M sulfite	0.028	0.020
Primary	Hydroquinone plus 0.05 M sulfite	0.028	0.020
Primary	Hydroquinone, 0.005 M sulfite, 0.10 M resorcinol	0.028	0.023

In table 9, T_1 represents the time required to obtain a density of 0.50 (log E = 1.15) with the pure hydroquinone developer; T_2 represents the time required in a developer containing 0.001 mole of the corresponding quinone. The pH and hydroquinone concentration were adjusted to give approximately the same development rate in the absence of added quinone.

TABLE 9

Accelerating effect of quinone homologues on development by the corresponding hydroquinone

Quinone = 0.001 *M*

DEVELOPING AGENT	CONCENTRATION	pH	TIME REQUIRED FOR $D = 0.50$		
			T_1 (No addition)	T_2 (Quinone added)	T_1/T_2
Hydroquinone	*M*/20	8.29	28	15.5	1.80
Toluhydroquinone	*M*/20	*ca.* 8.0	24.5	18.8	1.30
m-Xylohydroquinone	*M*/80	*ca.* 8.0	27.0	25.0	1.08

TABLE 10

Comparative measurements with substituted hydroquinones

Sulfite-free developers; phosphate buffer

COMPOUND	DEVELOPMENT RATE $D_7 = 0.50$ CONCENTRATION = *M*/80 pH~7.9	RELATIVE RATE	AUTOXIDATION RATE, $K/2.3$ pH = 7.44	RELATIVE RATE
Hydroquinone	0.014	1.00	0.00123	1.00
Toluhydroquinone	0.021	1.5	0.00479	3.9
m-Xylohydroquinone	0.044	3.1	0.0234	19.0
Chlorohydroquinone	0.057	4.0	0.0092	7.5
3-Chlorotoluhydroquinone	0.100	7.1		(30)*
Dichlorohydroquinone	0.066	4.7	(0.0142)	(11.5)
Bromohydroquinone	0.065	4.6	(0.0132)	(10.7)
Hydroxyhydroquinone	0.053	3.8	(0.310)	(250)

* Values enclosed in parentheses are approximate only.

TABLE 11

Comparative measurements with substituted hydroquinones

Sulfite-containing developers; borate buffer

COMPOUND	DEVELOPMENT RATE $D_7=0.50$ pH = 8.9	RELATIVE RATE	AUTOXIDATION RATE pH = 7.81	RELATIVE RATE	REDUCTION OF Ag^+ pH~8.9	RELATIVE RATE
Hydroquinone	0.020	1.00	0.0046	1.00	0.038	1.00
Toluhydroquinone	0.039	1.95	0.0180	3.8	0.027	0.71
m-Xylohydroquinone	0.0846	4.23	0.076	16.5	0.10	2.6
Chlorohydroquinone	0.089	4.45		(7.1)	0.47	12.4
3-Chlorotoluhydroquinone	0.108	5.40		(30.0)		
Dichlorohydroquinone	0.146	7.3	(0.077)	(16.7)		
Bromohydroquinone	0.109	5.45	(0.052)	(11.3)		
Sodium hydroquinonemonosulfonate		0.10	0.00053	0.115	0.0038	0.10

Clearly, the accelerating effect of the quinone decreases sharply as its stability increases.

COMPARATIVE RATES OF DEVELOPMENT, AUTOXIDATION, AND SILVER-ION REDUCTION

Comparative measurements were made with a number of substituted hydroquinones of the development rate, the autoxidation rate, and the rate of the silver-catalyzed reduction of silver ion. The autoxidation rates were determined according to the procedure given by James and Weissberger (4) and are expressed as "first-order" constants. The rates of the silver-catalyzed reduction of silver ion were determined as described in a previous paper (2), except that sodium sulfite was employed to decrease the silver-ion concentration and thus allow measurements to be made at a higher pH. Some check experiments showed that the presence of the sulfite effected no significant change in the mechanism of the reduction and the silver sulfite complex was not attacked to a detectable extent by the hydroquinone. The comparative rates are given in tables 10 and 11.

DISCUSSION

The work of Sheppard and Mees (13) and of Luther and Leubner (6) indicated that the divalent hydroquinonate ion is responsible for the reduction of silver bromide by the hydroquinone developer. Our data lend themselves to the same interpretation. In the pH range of 8.0 to 8.9 we may write for constant amount of added hydroquinone:

$$[C_6H_4O_2^{--}] = K[OH^-]^2 \tag{4}$$

since the concentration of unionized hydroquinone will be constant within 10 per cent. Further, at constant pH but varying hydroquinone concentration:

$$[C_6H_4O_2^{--}] = K'[C_6H_6O_2] \tag{5}$$

From these equations, it follows that the *square root* of the divalent ion varies as the first power of the hydroxyl-ion concentration and as the square root of the hydroquinone concentration. The rate of development shows the same dependence upon hydroxyl-ion concentration and hydroquinone concentration, and hence varies as the square root of the concentration of divalent ion. This we interpret to mean that the divalent ion is the entity which reduces the silver halide in development.

The occurrence of a $\frac{1}{2}$ power in the rate equation may be taken as direct evidence that adsorption plays an important rôle in the development process. The kinetics are quite analogous to those frequently observed in heterogeneous reactions in which adsorption follows approximately the Freundlich isotherm and the rate obeys the equation

$$\text{Rate} = kc^{1/n} \tag{6}$$

Whether the adsorption is to the silver nuclei, the silver halide itself, or the silver–silver halide interface is not indicated.

Rabinowitsch and his coworkers (8, 10) believe that the adsorption is to silver. However, their experiments were so complicated by the occurrence of a large amount of oxygen oxidation that their claims to establishing adsorption must be regarded with suspicion. This is particularly the case since recent measurements made in these Laboratories by Sheppard, Ballard, and Perry failed to show any adsorption within experimental error. Further, it is not apparent why, if adsorption to the silver is the essential thing, the adsorption effects may be detected so readily in the development kinetics but not appear in the silver-catalyzed reduction of free silver ion. The silver nucleus is present in both cases.

On the other hand, Wulff and Seidl (16) showed that resorcinol was adsorbed by silver bromide from *alkaline* solution, and argued by analogy that hydroquinone would be so adsorbed, in agreement with Sheppard's theory (14). Their experimental evidence for adsorption of hydroquinone, i.e., that resorcinol decreases the rate of development by hydroquinone, is untenable, but the analogy appears reasonable. Further, Rabinowitsch's failure to detect adsorption of hydroquinone from *acid* solution furnishes no rebuttal, since Rabinowitsch's measurements would not have revealed adsorption of the *divalent ion* or even of the univalent ion.

We may conclude with reasonable certainty that, in the process of development by hydroquinone, the reduction occurs heterogeneously at the silver–silver halide interface. The Ostwald–Abegg supersaturation mechanism can offer no explanation either of the general kinetics of the development process or of the potential barrier effect which appears so strongly under the conditions we have employed. An alternative mechanism, that of solution of the silver halide followed by silver-catalyzed reduction of the silver ions, is likewise ruled out by the fact that the development kinetics conform neither to those of solution of silver halide nor of catalyzed reduction of silver ions present initially in the solution. The hydroquinone, as the divalent ion, reacts only after adsorption, presumably at the silver–silver halide interface. This adsorption undeniably affects the kinetics of the reduction process. However, the deformation experienced by the silver ions "adsorbed" at the active boundary lines of the silver–silver halide interfaces in the developing grains is probably a more fundamental reason for the enhanced reactivity of the nucleated grains which makes possible differential reduction (12).

The picture of the development process which we have presented in this and the preceding paper appears to correlate satisfactorily the existing data on sulfite-free hydroquinone developers and solutions containing low concentrations of sulfite. When strong silver halide solvent action is present, other processes may, and probably do, take a significant part in the development process.

Some further support is to be found in an examination of the relative rates of development, autoxidation, and silver ion reduction given in tables 10 and 11. There is no correlation between the rates of development and those of silver-ion reduction. Some correlation exists, however, between the development rates and the autoxidation rates. This is explainable on the basis that the active species in each case is the divalent ion, in contrast to the silver-ion reduction where the reaction of the univalent ion predominates. The correlation is simplest in the series: hydroquinone, toluhydroquinone, *m*-xylohydroquinone. Here, when sulfite is present in the development process, the rate of development varies almost exactly as the square root of the autoxidation rate,—a relation which is interesting in connection with the dependence of the development rate upon the square root of the divalent-ion concentration. The divergence from this simple relationship shown by the rates measured in the absence of sulfite is due to the quinone effect already discussed. It thus appears that the autoxidation rates furnish a clue to the rates to be expected for development by substituted hydroquinones, provided the substituent group or groups are not highly ionized. In the latter event, the electric barrier effect may become dominant.

The extent to which the electric barrier effect may influence the relative development rates exhibited by agents belonging chemically to the same class is indicated by a comparison of hydroquinone with its monosulfonate (charge group -3) and its disulfonate (charge group -4). At pH 8.9, the pure sulfite-free solution of the monosulfonate develops at only about 0.08 times the hydroquinone rate. When $M/20{,}000$ phenosafranine is present, however, the monosulfonate rate has been increased to about 0.2 that of hydroquinone. The phenosafranine effects a threefold increase in the hydroquinone rate and a sevenfold increase in the monosulfonate rate. Only the faintest trace of an image was obtained in 4 hr. with potassium hydroquinonedisulfonate at pH = 9.5. When $M/10{,}000$ phenosafranine was added, a good image was obtained in 20 min. This shows that the apparent weakness of the disulfonate as a developer is due to the inability of the highly charged ions to penetrate the electric barrier, rather than to a lack of reactivity.

The potential barrier effect enters significantly into the action of elon-hydroquinone developers. The density obtained in a given time of development by a hydroquinone-elon mixture is greater than the sum of the densities obtained by development with the two agents separately.

This phenomenon has been attributed by various writers (5, 15) to the action of a "metoquinone" possessed of special developing properties or to an elon–hydroquinone adsorption complex. However, much the same effect can be obtained if the development is started in an elon solution and, after thorough intermediate washing, is continued in a hydroquinone solution. It appears, therefore, that the preliminary development in elon merely accomplishes a partial breakdown of the electric barrier and thus allows a greater rate of penetration by the more sensitive hydroquinone ions. Such action should be kept in mind when considering the rôle which the sulfonates play in development.

The experimental results given in the preceding pages do not support the contention of Reinders (11) that "it may certainly be concluded that there is a close relation between the velocity of development and ΔE." The dependence of the rate upon the solution pH and the concentration of the developing agent appears quite clear from the kinetic considerations, and requires no association with the thermodynamic quantity for elucidation. The marked dependence of the reaction rate upon the size of the developed silver speck (9) does not follow from Reinders' argument, while the accelerating effect which quinone has upon the development process is exactly contrary to that argument. It may be noted, likewise, that the decrease in "maximum density" observed when quinone was added to the pure hydroquinone developer is not a true equilibrium phenomenon, and should not be associated with the change in ΔE.

SUMMARY

1. The rate of development by hydroquinone in the absence of sodium sulfite and oxygen varies as the square root of the hydroquinone concentration and the first power of the hydroxyl-ion concentration in the pH range 8.0 to 8.9. The rates measured approximate the average rates of development of the individual silver bromide grain.

2. The addition of quinone to the developer results in an increase in the development rate, which is due to an effect, presumably of a decomposition product of the quinone, upon the double-layer electric barrier. The quinone likewise attacks the development centers, resulting in a decrease in the number of developed grains for a given exposure.

3. The divalent ion is the active developing agent. Reduction occurs heterogeneously at the silver–silver halide interface.

4. Comparative rates are given for the development reaction, autoxidation, and the silver-catalyzed reaction of silver ion with a series of substituted hydroquinones.

The writer is indebted to Dr. S. E. Sheppard of these Laboratories for many valuable suggestions and criticisms.

REFERENCES

(1) Eggert, J., and Küster, A.: Kinotech. **18**, 381 (1936).
(2) James, T. H.: J. Am. Chem. Soc. **61**, 648 (1939).
(3) James, T. H.: J. Phys. Chem. **43**, 701 (1939).
(4) James, T. H., and Weissberger, A.: J. Am. Chem. Soc. **60**, 98 (1938).
(5) Lumière, A., Lumière, L., and Seyewetz, A.: Phot. Korr. **62**, 183 (1926).
(6) Luther, R., and Leubner, A.: Brit. J. Phot. **59**, 632 et seq. (1912).
(7) *cf.* Nietz, A. H.: *Theory of Development.* D. Van Nostrand Company, New York (1922).
(8) Rabinowitsch, A. J.: Trans. Faraday Soc. **34**, 920 (1938).
(9) Rabinowitsch, A. J.: Trans. Faraday Soc. **34**, 921 (1938).
(10) Rabinowitsch, A. J., and Peissachowitsch, S.: Z. wiss. Phot. **33**, 94 (1934).
(11) Reinders, W.: Trans. Faraday Soc. **34**, 936 (1938).
(12) *cf.* Schwab, G. M.: Z. Elektrochem. **35**, 584 (1929).
(13) *cf.* Sheppard, S. E., and Mees, C. E. K.: *Investigations on the Theory of the Photographic Process.* Longmans, Green and Company, London (1907).
(14) Sheppard, S. E., and Meyer, G.: J. Am. Chem. Soc. **42**, 689 (1920).
(15) Shiberstov, V.: Photo-Kino Chem. Ind., **2**, 141 (1933).
(16) Wulff, P., and Seidl, K.: Z. wiss. Phot. **28**, 239 (1930).

STUDIES ON SILICIC ACID GELS. IX

The Effect of a Change of pH upon the Time of Set of Some Acid Gels

CHARLES B. HURD and HARRIS W. PATON[1]

Department of Chemistry, Union College, Schenectady, New York

Received January 20, 1939

INTRODUCTION

A recent study of the time of set of silicic acid gels, prepared from solutions of sodium silicate and acetic acid in this laboratory (5), has shown that, for mixtures of acid reaction, the time of set is proportional to the hydrogen-ion concentration. A report by Hurd, Frederick, and Haynes (2) showed a similar result when hydrochloric, nitric, or sulfuric acid was used. A discussion of the theory has also been given (1). .

It was observed, incidentally, that addition of extra acid to mixtures already prepared delayed their setting. We have thought that it would be very important to discover whether there might be some particular time, during the setting of the already prepared mixture, when the introduction of the extra acid would have a particularly marked effect. If such a point were found, it would mark the time during the setting of the gel mixture when the process would be taking place which is so sensitive to the hydrogen-ion concentration. If no significant point were found, it would indicate that the whole process would appear to be equally sensitive to the hydrogen-ion concentration.

---

[1] Present address: Corning Glass Works, Corning, New York.

The experiments to be described were devised to test this point. They cover, unfortunately, only a part of the pH range, namely, from 4.57 to 5.08, but appear worth reporting because of their bearing upon the theory.

EXPERIMENTAL

The technique employed has been reported several times in this Journal (5, 2). A solution of sodium silicate equivalent to 1.26 *N* sodium hydroxide was obtained by dilution of "E" brand sodium silicate, prepared by the Philadelphia Quartz Company. This silicate has a soda:silica weight ratio of 1 to 3.19. A 2.01 *N* solution of acetic acid was used. The tests were carried out at 25°C. in an electrically controlled water thermostat. The solution of sodium silicate was always poured into the acetic acid solution. Double quantities of the mixtures were prepared, and were mixed by pouring back and forth. The time of set was determined in one sample in a 100-cc. Pyrex Griffin beaker by the "tilted rod" method of Hurd and Letteron (4). The pH was measured in the other sample by the quinhydrone method, as recommended by Hurd and Griffeth (3).

Since addition of a solution of acid to any silicic acid gel mixture decreases the silica concentration, parallel series were carried out where equal volumes of pure water in the one series and acetic acid solution in the other were used. The length of time from the preparation of the original mixture to the addition of the acid solution of water was varied from zero, where the mixtures were made up complete at first, to about 85 per cent of the time required for the original mixture to set. Beyond that point the gel was set sufficiently so that liquid could not be mixed with it homogeneously.

The concentrations are easily calculated. For example, in the first mixture of the second section of table 1 they are as follows: SiO_2, 0.86; CH_3COONa, 0.52; CH_3COOH, 0.65; all concentrations are in gram-moles per liter.

A word of explanation may be useful. In the first result in table 1, the extra 5 cc. of acid solution was added at the start, and the mixture set in 88 min. at 25°C. In other words, 25 cc. of silicate solution was poured into 30 cc. of acid solution. The second result was obtained by mixing first 25 cc. of silicate solution and 25 cc. of acid solution. This 50 cc. of mixture was placed in the 25°C. thermostat in a 100-cc. beaker, and covered with a watch glass. At exactly 15 min. after mixing, an extra 5 cc. of acid solution was introduced and the result mixed. It set 79 min. after the

TABLE 1

The effect of addition of extra acetic acid solution or of water upon the time of set and the pH of various mixtures of sodium silicate solution and acetic acid

ACID ADDED	WATER ADDED	TIME OF ADDITION	TIME OF SET	pH
Original mixture = 25.0 cc. of silicate solution and 30.0 cc. of acetic acid solution				
cc.	*cc.*		*minutes*	
5.0	0.0	0.0	88.0	4.57
5.0	0.0	15.0	79.0	4.57
5.0	0.0	26.0	75.0	4.57
5.0	0.0	39.0	65.5	4.57
0.0	0.0		57.0	4.82
0.0	5.0	0.0	67.5	4.82
0.0	5.0	8.0	66.5	4.82
0.0	5.0	15.0	64.5	4.82
0.0	5.0	20.5	63.0	4.82
0.0	5.0	30.0	61.0	4.82
0.0	5.0	40.0	60.0	4.82
0.0	5.0	45.0	58.0	4.82
0.0	5.0	46.0	59.0	4.82
0.0	0.0		57.0	4.82
Original mixture = 25.0 cc. of silicate solution and 25.0 cc. of acetic acid solution				
10.0	0.0	0.0	88.0	4.57
10.0	0.0	8.0	74.0	4.57
10.0	0.0	15.0	60.0	4.57
10.0	0.0	22.0	49.0	4.57
0.0	0.0		32.0	4.98
0.0	10.0	0.0	46.0	5.03
0.0	10.0	10.0	42.0	5.03
0.0	10.0	15.0	39.5	5.03
0.0	10.0	20.0	37.5	5.03
0.0	0.0		32.0	4.98
Original mixture = 25.0 cc. of silicate solution and 20.0 cc. of acetic acid solution				
15.0	0.0	0.0	88.0	4.57
15.0	0.0	3.0	67.5	4.57
15.0	0.0	6.0	47.5	4.57
15.0	0.0	8.0	36.0	4.57
0.0	0.0		11.0	5.08
0.0	15.0	0.0	21.0	5.42
0.0	15.0	3.0	20.0	5.42
0.0	15.0	6.0	17.5	5.42
0.0	15.0	8.0	15.3	5.42
0.0	0.0		11.0	5.08

time of first mixing. The last result in the first section of table 1 set 57 min. after mixing. No extra acid had been added.

The pH in each case is for the mixture which actually set.

The data of these three tables are plotted on figure 1. The straight-line relation is very evident.

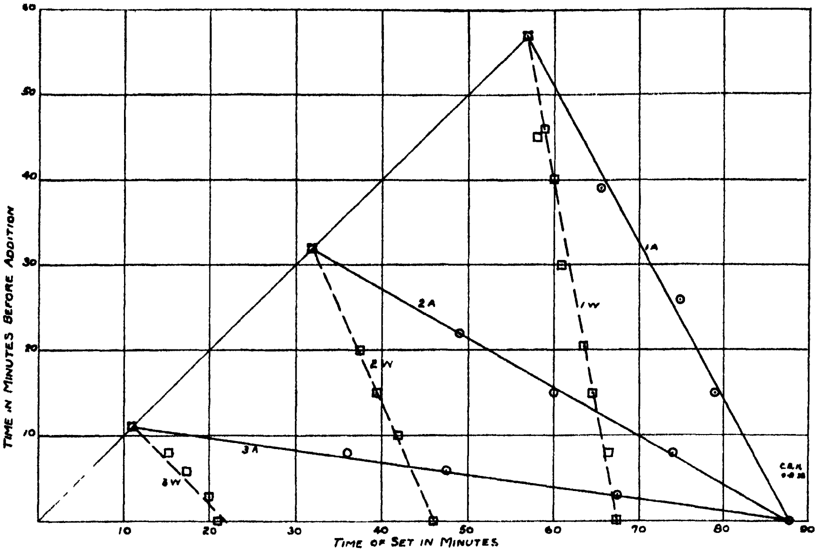

FIG. 1. Effect of addition of extra acid upon the time of set of silicic acid gels

DISCUSSION

The data show, quantitatively, a straight-line relation between the time of set of the mixture and the time which had elapsed from the time of mixing the original solution to the time of addition of the extra acid or water. The limits of these straight lines are a maximum time of set, when the extra acetic acid solution, or water, was added at the start,—that is, as part of the original mixture,—and a minimum time of set when the original mixture set without addition. These linear relations are very significant.

For example, if we consider the second line of the first section of table 1, we see that the extra 5 cc. of acid added 15 min. after the gel mixture was prepared gave a mixture whose setting time was 79 min. If this extra acid had been added at the start, the time of set would have been 88 min., while if it had never been added, the original mixture would have set in 57 min.

We may consider that this setting process is proceeding in the original solution at a rate such as to make it set in 57 min., and that, after the addition of the extra acid, the rate became much slower, so that 88 min. would have been required for setting. Calculating that after the original

15 min., the fraction $\frac{57 - 15}{57}$ must still occur at a rate such that $\frac{57 - 15}{57} \times$ 88 min. are necessary, we have for our total time of set

$$t = 15.0 + \frac{57 - 15}{57} \times 88 = 15.0 + 64.7 = 79.7 \text{ min.}$$

The time measured was 79.0 min. It is obvious that such a calculation is possible for all points and that these calculated setting times will agree with the actually measured values as well as the coincidence of the points with the straight lines. The latter agree with the straight-line relations within the experimental error, except for one value at 30 min. on curve 1 for acid and several values for water.

It would appear, then, that we may change the rate of the setting process by dilution or by addition of more acid; the latter includes both a dilution of the solution and an increase in the hydrogen-ion concentration. The effect of either of these procedures is to change the time of set by an amount capable of calculation, namely, as the sum of two time intervals.

It appears to make no difference where the extra acid solution or water is added between the limits of the original mixing time and 85 per cent of the setting time. Over this wide range, the time of set of the final mixture appears to be equal to the sum of the two time intervals. It would be very interesting if an addition of either were possible even nearer to the time of set, but it proved impossible to mix the result uniformly.

The general weight of opinion of workers in this field favors the polysilicic acid fibrillar theory to explain the formation of silicic acid gels (7, 6). The theory postulates that a monosilicic acid is first formed and that condensation reactions occur, building up more and more complex acids (1) until finally the whole mass sets.

There is, apparently, no especially significant point in the setting process at which addition of more acid has a particularly marked effect.

SUMMARY

The time of set of a silicic acid gel mixture, produced by mixing solutions of sodium silicate and acetic acid, may be increased by addition of more water or more acetic acid solution. The original mixtures were acid and the temperature was kept constant at 25°C.

There is, apparently, no time during the setting when the process shows any unusual sensitivity to change in the hydrogen-ion concentration, the process being uniformly affected.

The time of set may be calculated, if the time of the addition of water or acetic acid solution is known, since the relation is linear. The total

time is shown to be the sum of two intervals, each dependent on the concentration of silica and of hydrogen ion.

The bearing of this experiment upon the fibrillar condensation theory of silicic acid gel structure has been discussed.

REFERENCES

(1) Hurd, C. B.: Chem. Rev. **22**, 403 (1938).
(2) Hurd, C. B., Frederick, K. J., and Haynes, C. R.: J. Phys. Chem. **42**, 85 (1938).
(3) Hurd, C. B., and Griffeth, R. L.: J. Phys. Chem. **39**, 1155 (1935).
(4) Hurd, C. B., and Letteron, H. A.: J. Phys. Chem. **36**, 604 (1932).
(5) Hurd, C. B., Raymond, C. L., and Miller, P. S.: J. Phys. Chem. **38**, 663 (1934).
(6) Jordis, E.: Z. anorg. Chem. **44**, 200 (1905).
(7) Treadwell, W. D., and König, W.: Helv. Chim. Acta **16**, 54 (1933).

THE INFLUENCE OF SOL CONCENTRATION ON FLOCCULATION VALUES

E. D. FISHER and C. H. SORUM

Department of Chemistry, University of Wisconsin, Madison, Wisconsin

Received March 24, 1939

INTRODUCTION

The influence of sol concentration on the flocculation values of pure ferric oxide and chromium hydroxide hydrosols has been previously reported (3, 5). With these pure sols the flocculation values decreased for monovalent ions, remained constant for divalent ions, and decreased for trivalent and tetravalent ions as the sols were diluted. This behavior conformed to the flocculation rule formulated by Burton and Bishop (1). When these pure sols were made impure by adding small amounts of stabilizing electrolytes, the flocculation values for all ions decreased as the sols were diluted. In this paper a more detailed study of the behavior of chromium hydroxide sols will be presented, as well as observations on other typical systems. Changes in flocculation values when the sols were diluted with alcohol are also included.

CHROMIUM HYDROXIDE

Table 1 shows the effect of the addition of chromium chloride on the flocculation values of a pure chromium hydroxide sol at various dilutions. The monovalent coagulating ions chosen are widely separated in the Hofmeister series; two polyvalent ions are also included. The sol was prepared by precipitating the hydroxide from a chromium chloride solution

TABLE 1

Effect of the addition of chromium chloride on the flocculation values of a chromium hydroxide sol

COAGULATING SALT	MILLIMOLES OF $CrCl_3$ PER LITER	SOL CONCENTRATION			
		100%	80%	60%	40%
NaCl	0.0	1.3	1.7	2.0	2.4
	0.1	3.4	3.7	3.8	4.1
	0.2	8.0	7.0	7.0	7.0
	0.3	11.0	10.0	9.5	9.0
	0.4	16.0	15.0	14.0	13.5
	0.5	20.0	18.0	16.0	14.5
$NaC_2H_3O_2$	0.0	1.1	1.3	1.5	1.6
	0.1	2.0	2.2	2.0	1.5
	0.2	3.7	3.8	3.6	3.3
	0.3	4.9	5.0	4.6	4.2
	0.4	5.5	4.5	4.0	3.5
	0.5	6.0	5.5	5.0	4.0
NaI	0.0	1.2	1.6	2.2	3.0
	0.1	3.6	3.9	4.1	4.3
	0.2	10.0	10.0	10.0	10.0
	0.3	15.0	14.0	13.8	13.5
	0.4	23.0	22.0	21.0	19.0
	0.5	27.0	26.0	22.0	20.0
NaSCN	0.0	1.0	1.4	1.6	1.8
	0.1	1.9	2.1	2.2	2.3
	0.2	4.0	4.2	4.0	3.8
	0.3	5.5	5.0	5.0	4.5
	0.4	8.0	7.5	7.0	6.0
	0.5	10.0	9.5	9.0	8.0
Na_2SO_4	0.0	0.06	0.06	0.06	0.06
	0.1	0.08	0.07	0.07	0.06
	0.2	0.14	0.12	0.10	0.09
	0.3	0.18	0.16	0.13	0.11
	0.4	0.19	0.16	0.14	0.12
	0.5	0.23	0.20	0.15	0.12
$K_3Fe(CN)_6$...	0.0	0.040	0.030	0.025	0.020
	0.1	0.050	0.045	0.035	0.025
	0.2	0.080	0.065	0.055	0.045
	0.3	0.110	0.085	0.070	0.050
	0.4	0.125	0.085	0.075	0.060
	0.5	0.140	0.110	0.090	0.060

by means of ammonia in a manner previously described (3). In the final purified state it contained 0.940 g. of chromium per liter. The original sol is referred to as 100 per cent, and the lower percentages are in terms of the original concentration. Unless otherwise stated, all dilutions were obtained by adding water.

The flocculation values of the pure sol for the various coagulating ions again have shown that a pure chromium hydroxide sol follows the rule of Burton and Bishop when coagulated by ions of varying valences.

When a sufficient amount of chromium chloride was added the flocculation values of all ions were higher, and those of the monovalent coagulating ions decreased as the sol was diluted. This behavior of the impure sol is contrary to that predicted by the Burton–Bishop rule. As the sols were made more impure by the addition of chromium chloride, the flocculation values for all ions showed a more distinct decrease with sol dilution.

TABLE 2

Changes in the flocculation values of sodium chloride when a chromium hydroxide sol is diluted with liquids

DILUTING AGENT	SOL CONCENTRATION							
	90%	80%	70%	60%	50%	40%	30%	20%
Water	0.4	0.5	0.6	0.7	0.8	0.9	1.4	1.8
Alcohol (20%)	0.35	0.35	0.40	0.40	0.40	0.40	0.40	0.45
Alcohol (40%)	0.35	0.35	0.35	0.30	0.25	0.20	0.20	0.20
Alcohol (60%)	0.35	0.40	0.35	0.25	0.15	0.15	0.15	0.10
Alcohol (80%)	0.35	0.40	0.35	0.30	0.30	0.20	0.15	0.05
Alcohol (90%)	0.30	0.40	0.10	0.10	0.08	0.06	0.05	0.05
Alcohol (100%)	0.40	0.30	0.10	0.05	0.001			
Methyl alcohol (100%)	0.35	0.40	0.50	0.45	0.30	0.10	0.05	0.01
Acetone (100%)	0.35	0.40	0.45	0.20	0.15	0.20	0.20	0.20

The changes in the flocculation values of sodium chloride when a pure chromium hydroxide sol was diluted with absolute ethyl alcohol and similar liquids are shown in table 2. The original sol contained 0.825 g. of chromium per liter and had a flocculation value of 0.25 millimole of sodium chloride per liter.

The sol showed a distinct increase in flocculation values when dilutions were made with water. As the dilutions were made with an increasing amount of alcohol the extent of increase diminished, and finally the flocculation values showed a decrease when a sufficient amount of alcohol was added. The results with methyl alcohol and acetone were similar to those exhibited with ethyl alcohol. In all instances the first diluting portions seemed to increase the sol stability toward sodium chloride, but as the amount of alcohol increased the flocculation values passed through a maximum and then decreased. Table 3 shows the effect of the addition of stabilizing electrolyte on this maximum flocculation value. The sol used contained 0.631 g. of chromium per liter. A 60 per cent solution of ethyl alcohol in water was used as the diluting agent.

With the addition of chromium chloride the observed maximum decreased and soon disappeared, as shown by table 3. The changes observed when a pure chromium hydroxide sol is diluted with methyl and ethyl alcohols and acetone may be attributed to the dehydrating nature of the diluting liquids, since a pure sol quite definitely owes a major portion of its stability to hydration. The first dilution with these liquids is similar to dilution with water, since the flocculation values for monovalent ions increased. But with increasing dilution sensitization and dehydration became more acute and the flocculation values showed a decrease. When chromium chloride was added to a hydrated sol a large part of the sol stability was due to ion adsorption. When this is the case, dilution with alcohol and other liquids becomes more similar to dilutions with water.

TABLE 3

Effect of the addition of stabilizing electrolyte on the maximum flocculation value

MILLIMOLES OF $CrCl_3$ PER LITER	SOL CONCENTRATION						
	100%	90%	80%	70%	60%	50%	40%
0.0	0.50	0.60	0.65	0.60	0.40	0.30	0.15
0.1	1.8	1.9	1.8	1.7	1.6	1.4	1.3
0.2	3.9	3.2	2.9	2.6	2.3	2.1	1.9
0.3	5.6	5.1	4.6	4.3	4.0	3.7	3.3

ARSENIC TRISULFIDE

That the flocculation values for monovalent ions for an arsenic trisulfide sol increase as the sol is diluted has long been known. This work shows how the addition of stabilizing electrolyte impurity changes the ordinary behavior with dilution. The sol was prepared by bubbling hydrogen sulfide through a saturated solution of arsenious oxide (4). The resultant sol was dialyzed in collodion bags for 24 hr. at 50°C. In the final purified state it contained 1.18 g. of arsenic per liter. Table 4 shows the flocculation values with water and 95 per cent ethyl alcohol as the diluting agents.

When the dilutions were made with alcohol the flocculation values for potassium chloride increased more than when the dilutions were made with water. A possible reason for this can be found in an ordinary rule of adsorption, which states that adsorption in solution is largely dependent upon the surface tension of the solvent. The addition of alcohol lowered the surface tension of the liquid phase; consequently adsorption was lessened and the presence of a larger amount of coagulating electrolyte was necessary for flocculation.

Table 5 shows the flocculation values for potassium chloride when stabilizing electrolyte was added.

It is evident that as the sol was made impure with stabilizing electrolyte the flocculation values became higher and the increase with dilution was much less. Larger amounts of sodium sulfide were not added, as its solvent action tended to destroy the colloidal nature of the sol.

TABLE 4

Flocculation value for arsenic trisulfide sol with water and alcohol as diluents

SALTS	SOL CONCENTRATION				
	100%	80%	60%	40%	20%
	Dilutions with water				
KCl	78.	84.	90.	94.	98.
$BaCl_2$	0.6	0.6	0.6	0.6	0.6
$CrCl_3$	0.025	0.023	0.020	0.017	0.015
	Dilutions with alcohol (95 per cent)				
KCl	78.	90.	95.	105.	130.
$BaCl_2$	0.6	0.8	0.8	0.8	0.7
$CrCl_3$	0.025	0.023	0.020	0.018	0.015

TABLE 5

Flocculation values for potassium chloride in presence of stabilizing electrolyte

STABILIZING ELECTROLYTE	SOL CONCENTRATION				
	100%	80%	60%	40%	20%
1 millimole of Na_2S per liter	140	140	145	148	150
2.5 millimoles of Na_2S per liter	150	150	150	152	155
Sol saturated with H_2S	125	125	130	132	135

MANGANESE DIOXIDE

The sol was prepared by the reduction of permanganate by ammonia (2). In the final purified state it contained 0.320 g. of manganese dioxide per liter. Flocculation values are shown in table 6.

Table 6 readily shows that the Burton–Bishop rule applies to the flocculation of manganese dioxide if the sols are made sufficiently pure by dialysis. When dilutions were made with alcohol some flocculation values first increased, then decreased with dilution,—behavior characteristic of a highly hydrated sol. This sol exhibited an "irregular series" with the polyvalent coagulating ions. Between the ranges of concentration shown for the flocculation values the sol was completely coagulated; at either end it was stable. The lower limit represents the flocculation values for a negative sol, and the upper limit was the point at which the sol had adsorbed a sufficient amount of positive ions to become a positive sol.

TABLE 6

Flocculation values for manganese dioxide sol

SALT	SOL CONCENTRATION				
	100%	80%	60%	40%	20%
Sol dialyzed for 24 hr. at 90°C. Dilutions with water					
NaCl	10.0	10.0	9.0	8.5	8.0
LiCl	12.0	11.0	10.5	9.0	7.0
$BaCl_2$	0.15	0.15	0.15	0.15	0.15
$CrCl_3$	0.12-0.06	0.09-0.05	0.08-0.04	0.05-0.03	0.03-0.02
$AlCl_3$	0.13-0.07	0.10-0.06	0.08-0.05	0.06-0.04	0.03-0.02
$Th(NO_3)_4$	0.05-0.03	0.045-0.025	0.030-0.020	0.020-0.015	0.015-0.010
Sol dialyzed for 72 hr. at 90°C. Dilutions with water					
NaCl	1.0	1.1	1.3	1.4	1.6
LiCl	1.9	2.1	2.2	2.4	2.6
KCl	0.8	0.7	0.65	0.60	0.50
$BaCl_2$	0.06	0.06	0.06	0.06	0.07
$CrCl_3$	0.065-0.015	0.055-0.015	0.045-0.010	0.030-0.007	0.015-0.004
$Th(NO_3)_4$	0.018-0.008	0.018-0.006	0.016-0.005	0.012-0.004	0.007-0.003
Sol dialyzed for 72 hr. at 90°C. Dilutions with 95 per cent ethyl alcohol					
NaCl	1.0	1.25	1.1	0.8	0.5
LiCl	1.6	1.65	1.5	1.0	0.7
KCl	0.8	0.6	0.45	0.3	0.1
$BaCl_2$	0.06	0.04	0.03	0.02	0.008
$CrCl_3$	0.065-0.015	0.040-0.015	0.025-0.013	0.015-0.009	0.013-0.006
$Th(NO_3)_4$	0.018-0.008	0.014-0.008	0.009-0.005	0.008-0.003	0.006-0.002

FERRIC OXIDE

The ferric oxide sol has been previously shown to follow the Burton-Bishop rule (5). This work was for the purpose of following changes in flocculation values when dilutions were made with ethyl alcohol. The sol was prepared and purified according to the method described by Sorum (6). In the final purified state it contained 1.708 g. of iron per liter. Table 7 shows flocculation values when dilutions were made with 95 per cent ethyl alcohol. Here again it seems probable that the decreasing stability with dilution is caused by the dehydrating action of the diluting alcohol.

A stannic oxide sol was prepared by peptizing the precipitated hydroxide with ammonia, and was dialyzed for 2 days at room temperature. In the final purified state it contained 2.88 g. of stannic oxide per liter. Table 8 shows flocculation values.

Table 9 shows the results obtained with an aluminum hydroxide sol prepared by washing the precipitated hydroxide until it was peptized.

TABLE 7

Flocculation values for ferric oxide sol when dilutions were made with ethyl alcohol

SALTS	SOL CONCENTRATION				
	100%	80%	60%	40%	20%
NaCl	10.5	8.5	7.8	6.5	5.5
$NaC_2H_3O_2$	4.0	3.7	3.3	2.8	2.0
NaSCN	6.5	5.0	4.3	3.7	3.0
KCl	10.0	8.5	7.8	6.5	5.5
LiCl	10.5	8.5	8.0	7.5	7.0

TABLE 8

Flocculation values for stannic oxide sol

SALTS	SOL CONCENTRATION				
	100%	80%	60%	40%	20%
Dilutions with water					
NaCl	0.7	0.8	0.9	1.0	1.0
LiCl	0.6	0.7	0.8	1.0	1.2
KCl	0.65	0.68	0.70	0.75	0.80
$BaCl_2$	0.04	0.04	0.04	0.04	0.04
$AlCl_3$	0.015	0.012	0.010	0.009	0.007
Dilutions with alcohol					
NaCl	0.70	0.60	0.55	0.50	0.50
LiCl	0.60	0.60	0.55	0.45	0.40
KCl	0.65	0.60	0.50	0.40	0.30
0.01 g. of NH_3 per liter; dilutions with water					
NaCl	5.0	4.0	3.2	2.5	2.0
LiCl	5.5	5.0	4.5	4.0	3.8

Sols of titanium oxide and thorium hydroxide were prepared and purified by dialysis. Attempts to purify the sols to a high degree failed, as they coagulated in the dialyzer. With these sols the flocculation values for all ions decreased as the sol was diluted. However, the extent of decrease for the monovalent ions was noticeably diminished as the sols were dialyzed to higher degrees of purity.

DISCUSSION

The results have shown that with pure sols flocculation values increased for monovalent ions, remained about the same for divalent ions, and decreased with polyvalent ions as the sols were diluted. When the sols were made impure with stabilizing electrolyte, flocculation values for all electrolytes decreased. These results indicate that the applicability of the Burton–Bishop rule is determined by the purity of the sol.

One of the possible factors contributing to the increased stability of diluted systems is the increased adsorption of the stabilizing ion of the coagulating electrolyte with dilution (7). When relatively large amounts of stabilizing electrolyte are already present it may prevent any great adsorption of ions of added electrolyte. Hence the above-mentioned factor in increasing sol stability with dilution may not function.

TABLE 9

Flocculation values for an aluminum hydroxide sol

SALTS	SOL CONCENTRATION			
	100%	80%	60%	40%
Dilutions with water				
NaCl	29.0	32.0	34.0	38.0
$NaC_2H_3O_2$	7.0	8.0	8.5	9.0
Na_2SO_4	0.09	0.09	0.09	0.09
$K_3Fe(CN)_6$	0.05	0.03	0.01	0.003
Dilutions with alcohol				
NaCl	29.0	21.0	12.0	4.0
Undialyzed sol; dilutions with water				
NaCl	175	170	160	155

When hydration was a factor in sol stability, dilution with dehydrating agents naturally resulted in a decrease in flocculation values. This dehydrating effect more than balanced any stabilizing effects of dilution, as shown in tables 2, 3, and 6, where the flocculation values first increased but then decreased as further amounts of alcohol were added.

SUMMARY

The applicability of the Burton–Bishop rule to hydrosols of chromium hydroxide, ferric oxide, arsenic trisulfide, manganese dioxide, stannic oxide, aluminum hydroxide, titanium oxide, and thorium hydroxide seems to be a function of the purity of the sol. Highly purified sols followed the

rule; sols containing relatively large amounts of stabilizing electrolyte did not.

REFERENCES

(1) Burton and Bishop: J. Phys. Chem. **24**, 701 (1920).
(2) Cuy, E. J.: J. Phys. Chem. **25**, 415 (1921).
(3) Fisher and Sorum: J. Phys. Chem. **39**, 283 (1935).
(4) Freundlich and Nathanson: Kolloid-Z. **28**, 258 (1921).
(5) Judd and Sorum: J. Am. Chem. Soc. **52**, 2598 (1930).
(6) Sorum: J. Am. Chem. Soc. **50**, 1263 (1928).
(7) Weiser: *Hydrous Oxides*. The McGraw-Hill Book Company, Inc., New York (1926).

ACTIVATED CARBON AS A CATALYST IN CERTAIN OXIDATION-REDUCTION REACTIONS[1]

ELMER C. LARSEN and JAMES H. WALTON

Department of Chemistry, University of Wisconsin, Madison, Wisconsin

Received June 20, 1939

I. The Decomposition of Hydrogen Peroxide

Lemoine (17) in 1907 first reported that carbon is an effective catalyst for the decomposition of hydrogen peroxide solutions. In 1923 Firth and Watson (5) found that heating ordinary sugar carbon *in vacuo* increases its activity greatly, but that after the reaction has proceeded for about 10 hr. the catalyst becomes ineffective. They also found (6) that the rate of decomposition is proportional to the quantity of catalyst used. It has since been observed (15) that heating in an atmosphere of moist oxygen results in a still more active carbon. King (11) obtained a carbon of maximum activity on activating sugar carbon at 900°C. and a product of minimum activity at 450°C. He found the catalyst to become ineffective after the reaction had continued for about 90 min. He attributed the decay in activity to a chemical reaction between the peroxide and the surface oxide of the carbon.

It is the purpose of this investigation to develop a technique for obtaining samples of activated carbon whose catalytic properties can be reproduced, and to use this carbon to obtain more accurate data on the factors affecting the rate of decomposition of hydrogen peroxide. Special emphasis is given to the decay of catalytic activity. In part II of this paper

---

[1] This investigation was financed by a grant from the Research Committee of the University of Wisconsin, Dean E. B. Fred, *Chairman*.

the activity of carbon when used as a catalyst in two autoxidation reactions is discussed.

EXPERIMENTAL PROCEDURE

Preparation of carbon

Mallinckrodt's "reagent quality" sucrose was used in all the work reported here unless otherwise specified. Fifty-gram portions of sucrose were heated in silica dishes in a muffle furnace at 500°C., and the charred residue ground to less than 100 mesh in an agate mortar. Ten grams of the ground carbon were placed in a long-necked quartz flask and heated in a muffle furnace at 1000°C. until no more gases were evolved. The resulting carbon contained less than 0.04 per cent ash. The carbon was activated in an all-quartz system consisting of a large opaque silica cylinder into which was inserted a long-necked quartz tube with an activating chamber 15 cm. long and 4 cm. in diameter. Ten-gram portions of carbon were placed in the activating chamber, the system flushed out first with nitrogen, then with oxygen, and moist oxygen passed over the carbon at the rate of 5 ml. per minute. The oxygen train was the same as that used by King and Lawson (13) and consisted of one wash flask filled with water and two with a saturated solution of calcium chloride. The activation was continued for 12 hr., since King (11) found that for carbon activated at 800°C. the activity of the carbon becomes nearly constant after 10 to 12 hr. of heating. The temperature of the furnace was held constant to ±5°C. At the end of 12 hr. the carbon was quickly poured out into small beakers, allowed to cool a moment in air, and then placed under vacuum until used. The loss in weight during activation represented about 40 per cent of the total carbon.

Materials

Merck's "reagent quality" superoxol, which is free from stabilizer, was simply diluted to the desired concentrations with double-distilled water. These results agreed with those obtained using redistilled C.P. quality superoxol. All other materials used were of the highest quality obtainable, and were used without further purification.

Apparatus

The rate of decomposition of hydrogen peroxide was followed by measuring the rate of oxygen evolution in an apparatus similar to that described by Filson and Walton (4). Fifteen milliliters of peroxide solution were placed in the flask, and the carbon was suspended in a glass vial which broke immediately upon starting the run. It was necessary to apply a correction for the gases evolved on wetting the carbon.

Unless otherwise stated, all work was carried out at 25°C., using as catalyst carbon activated at 850°C. The results obtained in duplicate runs in experiments involving carbon and peroxide only (runs in which no foreign substances were added) agreed to within 2 per cent when the same batch of active carbon was used, and to within 5 per cent when carbon activated in two different batches was used.

Concentrations are expressed as milliliters of available oxygen per 15 ml. of solution, corrected to standard conditions.

FACTORS AFFECTING THE RATE OF DECOMPOSITION

Temperature of activation

Carbon was activated at approximately 75°C. intervals over the range from 335° to 1045°C. Half-gram portions were allowed to react with 15 ml. of peroxide solution containing 75 ml. of available oxygen. The volume of oxygen evolved in the interval from 5 to 35 min. was taken as an index of its activity. The results are shown in figure 1. The carbon is inactive when activated below 350°C.; the activity reaches a maximum for carbons activated at 825–875°C. King (11) reported a pronounced minimum in activity at 400°C. and a large increase in activity at lower temperatures. The activity of his "unactivated" carbon was equivalent

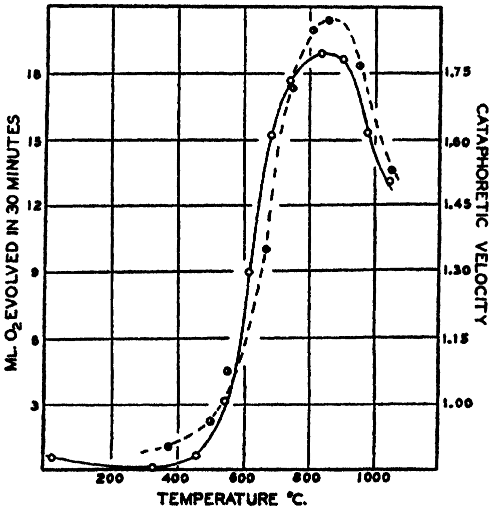

FIG. 1

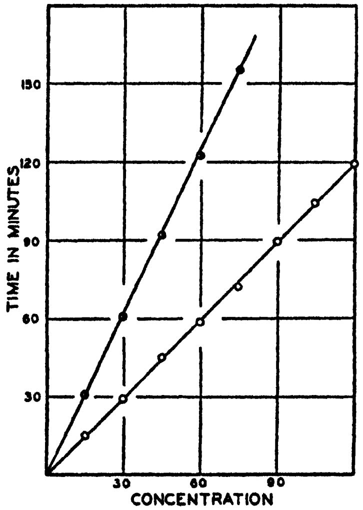

FIG. 2

FIG. 1. Effect of temperature of activation of carbon: O, on rate of decomposition of hydrogen peroxide (work of present authors); ◑, on cataphoretic velocity in μ per second per volt per centimeter (from King).

FIG. 2. Effect of initial concentration of hydrogen peroxide (in milliliters of available oxygen): ◑, on the time of half-life of the decomposition; O, on the time of third-life of the decomposition.

to that of his carbon activated at about 650° to 700°C. The present authors found that carbon which had not been activated possessed slight catalytic activity, and attribute this to activation which occurred when the sugar was charred. It is probable that the carbon used by King was prepared under such conditions that appreciable activation took place, and the activity he reports for low-temperature carbons is probably due to failure to reëstablish the surface characteristic of low-temperature carbon after the activation which occurred on charring.

Figure 1 also gives the data of King (12) for the effect of temperature of activation on the cataphoretic velocity of activated carbon. The form of the two curves is practically identical. It is probable that the same surface condition which gives rise to the high negative charge on the carbon is also that which is responsible for its catalytic activity in the decomposition of hydrogen peroxide.

TABLE 1

Oxygen liberated from peroxide solution by carbon from different sources

SOURCE OF CARBON	VOLUME OF OXYGEN EVOLVED IN 5 TO 35 MINUTES
	ml.
Gelatin	Immeasurably fast
Lactose	15.35
Dextrose	14.35
Sucrose	11.40
Starch	9.75
Acetylene black	0.65

Source of carbon

Carbon was prepared in the usual manner from lactose, dextrose, starch, and ash-free gelatin. In addition, a sample of Shawinigan acetylene black was procured. Samples (0.3 g.) of the activated carbon were allowed to react with 15 ml. of peroxide solution containing 60 ml. of available oxygen. In table 1 is listed the amount of oxygen evolved in the interval from 5 to 35 min.

The carbon prepared from gelatin was extremely active. When only 0.1 g. was used, 40 ml. of oxygen was evolved in 7.5 min. In an experiment with 0.01 g. of catalyst and 817 ml. of available oxygen, 33.2 ml. of oxygen was evolved in 10 min., as compared to 1.05 ml. of oxygen evolved when sucrose carbon was used. This high activity is in agreement with the observations of Farmer and Firth (3), who found that carbons of highest activity are those derived from substances containing basic nitrogen. The active gelatin carbon contained 1.6 per cent nitrogen.

The low activity of the acetylene black is likely related to its graphitic structure, since it is produced at temperatures above 1500°C.

Initial peroxide concentration

To determine the effect of the concentration of peroxide on the rate of decomposition, 0.3 g. of active carbon was allowed to react with 15 ml. of peroxide solution whose initial concentration was varied from 15 ml. to 120 ml. of available oxygen. From figure 2 it is seen that the times of half-life and of third-life are proportional to the initial peroxide concentration. This is not a zero-order reaction, however, for the rate of the reaction decreases as the reaction proceeds. This decay in activity is discussed at length later in the paper.

Since the amount of peroxide decomposed per unit time is proportional to the quantity of catalyst present (6), it is probable that the reaction takes place with peroxide adsorbed on the surface. If this is true, then the amount of oxygen evolved per unit time at different concentrations should be an index of the amount of peroxide adsorbed. It is then possible to calculate indirectly the constant n of Freundlich's adsorption equation

$$x/m = ac^n$$

Plotting the volume of oxygen evolved in 10 min. against the mean peroxide concentration gives a curve resembling an adsorption isotherm. Plotting the logarithm of the volume evolved against the logarithm of the mean concentration gives a straight line of slope 0.39. If 30 min. is chosen as the unit of time, the value of the slope is smaller because of the decay factor. If a smaller unit could conveniently be taken, a value greater than 0.39 would result. In later calculations the value 0.45 has been used.

If one attempts to determine reaction rate constants in the usual manner it is found that the reaction follows no apparent order of reaction until from 15 to 20 per cent of the peroxide has been decomposed. From 20 to 45 per cent decomposition the reaction appears to be a second-order reaction, and beyond 45 per cent decomposition it appears to be a first-order reaction. This regularity was observed in all the reactions, regardless of the concentration of the peroxide, the amount of catalyst, or temperature of the reaction, providing that a fresh sample of catalyst was employed in each run.

Variation of the quantity both of catalyst and of peroxide

The quantity of catalyst and the initial concentration of peroxide were increased progressively from 0.075 g. of carbon and 15 ml. of available oxygen to 0.6 g. of carbon and 120 ml. of available oxygen. The ratio of carbon to peroxide was kept constant at 0.1 g. carbon to 20 ml. of available oxygen. The period of half-life is a linear function of the reciprocal of the initial peroxide concentration. This is shown in figure 3.

Temperature of reaction (temperature coefficient)

In determining the influence of the temperature on the rate of peroxide decomposition, 0.3 g. of carbon was allowed to react with 15 ml. of peroxide solution containing 50 ml. of available oxygen at intervals of 5°C. from 15° to 35°C. The temperature coefficient, calculated from the reciprocal of period of half-life, was 1.90 over the range from 15° to 25°C., 1.97 from 20° to 30°C., and 2.03 from 25° to 35°C. This compares with the value of 2.1 reported by Allmand and Style (1) for the thermal decomposition of hydrogen peroxide. The high value of the coefficient indicates that the rate of chemical reaction rather than the rate of diffusion is the limiting factor in determining the speed of reaction.

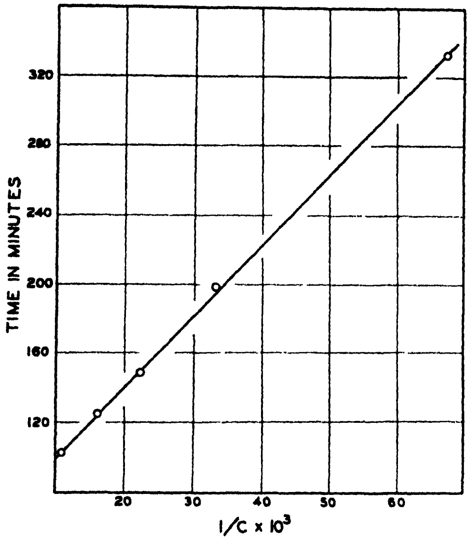

Fig. 3

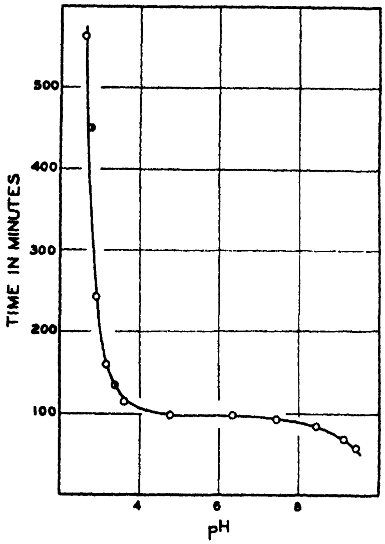

Fig. 4

Fig. 3. Variation of time of half-life with reciprocal of initial peroxide concentration when amounts of carbon and of hydrogen peroxide are increased in the same proportion.

Fig. 4. Effect of pH on time of half-life. ◑ represents runs using hydrochloric acid in place of sulfuric acid to adjust the pH in the acid range.

Hydrogen-ion concentrations

The period of half-life for the decomposition of hydrogen peroxide solution containing 50 ml. of available oxygen and catalyzed by 0.3 g. of active carbon was determined over the pH range 2.6 to 9.5. Sodium hydroxide was used to adjust the pH over the alkaline range, and sulfuric acid over the acid range, though it was found that hydrochloric acid gave identical results. The pH measurements were made with a glass electrode. The results are shown graphically in figure 4.

Metallic salts

Salts of many heavy metals are in themselves effective catalysts for the decomposition of hydrogen peroxide. Iron salts (2) are known to be the most effective, but copper salts (14) are able to effect appreciable decomposition. In this work the catalytic activity of ferric sulfate and copper sulfate when used in conjunction with active carbon was determined. Samples (0.3 g.) of carbon and varying amounts of the salt were allowed to react with a peroxide solution containing 50 ml. of available oxygen. The results are shown in figure 5 for ferric sulfate and figure 6 for copper sulfate. In both cases, the presence of small quantities of the salt reduced the total activity. This is probably due to the preferential adsorption of the salt by the carbon. As the concentration of the salt is further increased,. the rate of decomposition begins to increase. With ferric sulfate this increase is very great and indicates a promoter reaction, since when ferric sulfate is used alone, the rate of increase of the speed of reaction tends to fall off over the same range of concentration.

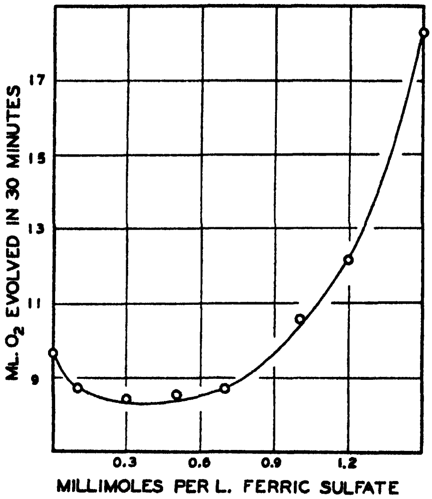

FIG. 5

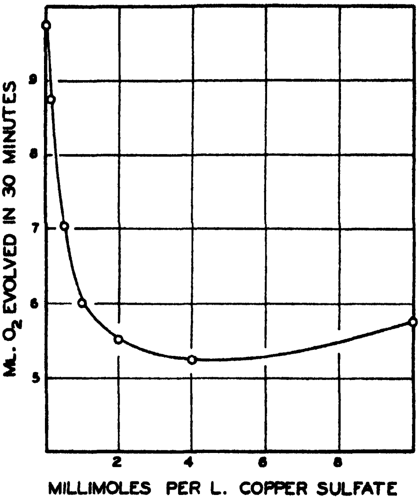

FIG. 6

FIG. 5. Combined effect of ferric sulfate and active carbon on the rate of peroxide decomposition.

FIG. 6. Combined effect of copper sulfate and active carbon on the rate of peroxide decomposition.

THE DECAY IN CATALYTIC ACTIVITY OF CARBON

The effect of moisture and oxygen

The time of half-life was determined for the decomposition of 15 ml. of hydrogen peroxide solution containing 50 ml. of available oxygen, using as catalyst 0.3 g. of carbon which had been treated in a variety of ways. With no special treatment the period of half-life was 100 min. When the carbon had been moistened with water and dried in an oven for 6 hr. at 110°C., the time of half-life was 108 min. A sample kept in a bomb at an oxygen pressure of 40 atmospheres for 3 days gave a half-life of 114 min. When the carbon was moistened with water and placed in the bomb at an oxygen pressure of 40 atmospheres, the time of half-life was increased to 148 min. Another sample was suspended in water and tank oxygen bubbled through the suspension for 8 days. The time of half-life was 173 min. The carbon is most readily deactivated by the combined action of moisture and oxygen.

Maintaining constant concentration of peroxide

To determine the rate of decomposition of hydrogen peroxide under conditions such that the peroxide concentration remained sensibly constant, 0.1 g. of carbon was allowed to react with 15 ml. of peroxide solution containing 817 ml. of available oxygen. During the course of the observations a total of 42 ml. of oxygen was evolved,—about 5 per cent of the total available quantity. The rate of decomposition over the same period decreased from 2.09 to 0.22 ml. of oxygen per minute. Compared to this enormous decrease in activity, the 5 per cent decrease in peroxide concentration is almost negligible, and can be regarded as remaining constant throughout the experiment.

In figure 7 the variation of both the total amount of oxygen evolved and the rate of decomposition with time are given. In determining this rate of decomposition, a correction factor of 0.01 ml. per minute was applied to allow for the spontaneous decomposition of the concentrated peroxide solution. At the end of the run, 422 ml. of oxygen had been decomposed per gram of carbon, and decomposition was still taking place at the rate of 2.2 ml. of oxygen per gram of carbon per minute. The activity was decreasing very slowly over this range. King (11) has postulated that active carbon is not a true catalyst, but that a reaction occurs between active carbon and the high-temperature surface oxide, converting it into the low-temperature type with the liberation of oxygen. However, he reported *complete* decay in activity of 850°C. carbon when only 70 ml. of oxygen had been evolved per gram of carbon. It is possible that the surface oxide is changing during the reaction, but in light of the data presented here, the simple stoichiometric change postulated by King is not sufficient to explain the observed facts.

Repeated use of the same carbon

The rate of decomposition of a hydrogen peroxide solution containing 50 ml. of available oxygen with 0.3 g. of carbon as catalyst was followed in the usual manner. Then this same carbon, whose activity had greatly decreased, was allowed to react a second and then a third time with the same quantity of hydrogen peroxide. In another series the procedure was changed. The carbon was allowed to react with a solution containing 100 ml. of available oxygen. When this carbon was used a second time, its activity was comparable with that of carbon used in the third run described above. The total quantity of hydrogen peroxide decomposed is then the important factor.

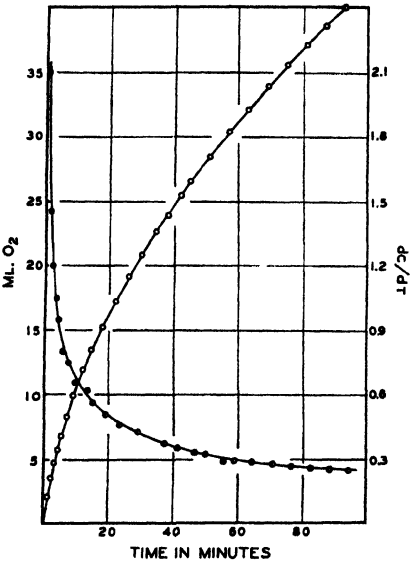

FIG. 7

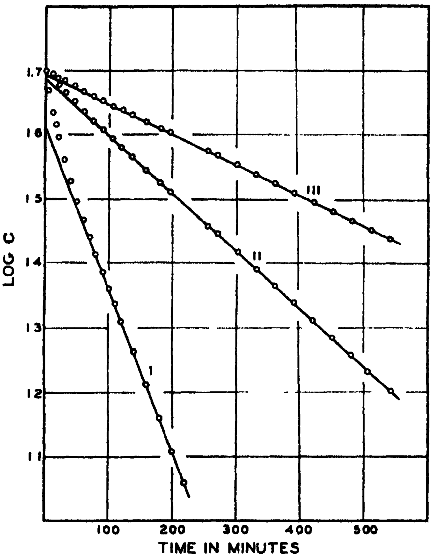

FIG. 8

FIG. 7. Rate of decomposition with large excess of hydrogen peroxide; O, total volume of oxygen; ◐, dc/dt.

FIG. 8. Log c *versus* time for three consecutive reactions using the same catalyst

In figure 8 the logarithm of concentration is plotted against time for these three consecutive reactions. The first reaction was carried to 80 per cent completion (4 hr.), the second to 68 per cent completion (9 hr.), and the third to 45 per cent completion (9 hr.). In each case they appear to follow a first-order reaction during the greater part of the decomposition. There was no tendency to deviate from the straight line for as long a time as the course of the reaction was followed. However, although these linear relationships are found to hold within a run, the values for the reaction rate constants for the three runs differ widely. For the reaction in which fresh carbon was used the first-order reaction constant was 97 × 10^{-6}, for the second run 40 × 10^{-6}, and for carbon used a third time 18 × 10^{-6} reciprocal seconds.

In the calculation of the reaction rate constants just given, no consideration was given to the influence of adsorption. When a correction is made for adsorption, the equation for the first-order reaction constant becomes (18)

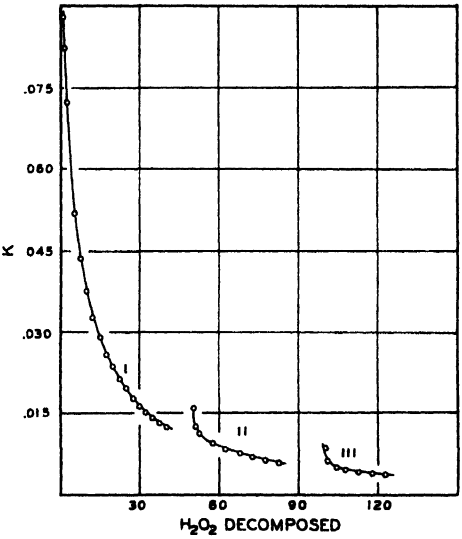

FIG. 9

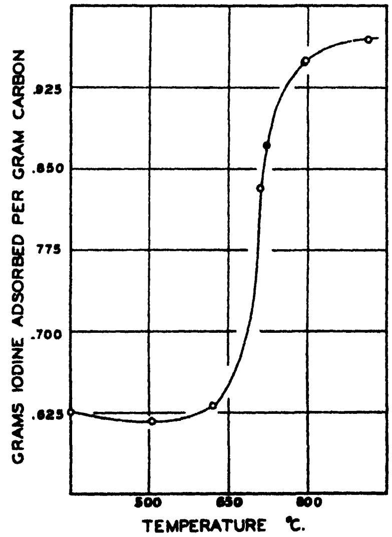

FIG. 10

FIG. 9. Variation of first-order reaction constant, corrected for adsorption, with amount of hydrogen peroxide decomposed in three consecutive reactions.

FIG. 10. Effect of temperature of activation of carbon on adsorptive capacity for iodine. ●, 795°C. carbon left in water 12 hr. and dried; ◑, same left in hydrogen peroxide solution.

$$c_0^{1-n} - c_t^{1-n} = kt$$

where n is the Freundlich adsorption constant. Plotting c^{1-n} against time should give a straight line of slope k.

Calculations were made for the series of three consecutive reactions, using for n the value 0.45. For these calculations the concentration of peroxide was expressed in moles per liter, and time in seconds. These calculations give a continuously decreasing value for the first-order "constant". In figure 9 the values of the constants thus calculated are plotted against the total volume of oxygen evolved during the reactions. Though in each of the three trials there is a sharp decrease in the value of the constant during the first part of the reaction, taken as a whole the values so obtained show a continuous decay in catalytic activity rather than the three sharp breaks obtained when calculations are made without taking adsorption into consideration.

ADSORPTION OF IODINE FROM AQUEOUS SOLUTIONS

Iodine has been used extensively to determine the relative surface area of carbon because it has been assumed (11) that not only are the molecules small enough to enter the ultra-fine pore structure, but that, unlike acids and bases, it is adsorbed equally well by high- and low-temperature carbons. A determination of the adsorption capacity for iodine of carbons activated at different temperatures seemed advisable.

The adsorption experiments were carried out according to the method of Kruyt and deKadt (16), using 0.5 g. samples of carbon and 50 ml. of 0.1084 *N* iodine solution. The results, calculated on the basis of grams of iodine adsorbed per gram of carbon, are shown in figure 10. There is a minimum in the amount of iodine adsorbed by carbon activated at 500°C. This minimum occurs at the same temperature of activation for which Schilow (20) reports a minimum in acid adsorption. It is scarcely probable that increasing the temperature of activation would decrease the total surface area. It would indicate, rather, that the nature of the carbon surface influences the amount of iodine adsorbed as well as the amount of acids and bases.

To one sample of 795°C. carbon, distilled water was added; to another some stabilizer-free hydrogen peroxide. Both samples were allowed to stand overnight, then filtered and dried *in vacuo* at 65°C. for 6 hr. The carbon that had been kept in water adsorbed the same quantity of iodine as before this treatment, while that which had reacted with the peroxide adsorbed considerably less. The total surface area in each case should be the same. King (11) has postulated that the reaction with peroxide converts the surface oxide of the carbon from the high-temperature to the low-temperature form. This decrease in the amount of iodine adsorbed after a reaction between peroxide and carbon lends further support to the postulate, and indicates that the nature of the surface influences the amount of iodine adsorbed. One would scarcely expect the amount of adsorption to be equivalent to that of low-temperature carbon, for activation at high temperatures would increase the surface area. The large increase in iodine adsorption for high-temperature carbons is caused by the combined effect of increased surface area *and* the formation of a new surface oxide.

DISCUSSION OF RESULTS

In spite of the regularity observed in the rate of decomposition of hydrogen peroxide when catalyzed by active carbon, the reaction is too complex to permit a simple quantitative analysis of the observed facts. In addition to the complications due to considerations of adsorption, there is superimposed an additional complicating factor,—the decay in activity of the carbon as the reaction proceeds.

Most investigators now favor the hypothesis that the specific properties of active carbons are a result of the surface oxides formed at different temperatures of activation (19). At least two types of surface oxides are believed to exist. Schilow (20) postulates three types of surface oxides,—A, B, and C. At temperatures above 800°C., oxide B alone is present. At lower temperatures the oxide B is replaced by C, but B is present again in increasing amounts below 500°C. Since 850°C. carbon is most effective in the decomposition of peroxide, oxide B must be the catalyst. If this is true, then the activity should increase for carbons activated below 500°C., but this does not occur. The existence of only two oxides as postulated by King,—an alkaline oxide formed at high temperatures and an acid oxide formed at low temperatures,—explains the observed facts much better.

The data of King on the pH of charcoal suspensions and the measurements of iodine adsorption reported here support the view that deactivation of the carbon and a change in the nature of the surface occur simultaneously. However, contrary to the reports of previous investigators, complete destruction of catalytic activity was not observed, even after the reaction had continued for more than 20 hr. The carbon used in the extremely concentrated peroxide solution was still active even after it had decomposed six times the amount of peroxide that completely deactivated the carbon used by King. This indicates that the stoichiometric change in surface oxide does not adequately describe the change that occurs. Qualitatively, at least, these results can be rationalized by picturing the reaction as proceeding through a chain mechanism, the length of chain increasing with increasing peroxide concentration. Haber and Weiss and coworkers offer a variety of evidence to show that the catalytic decomposition of hydrogen peroxide by enzymes (9, 23), by various metals (23), and by ferrous and ferric ions (8) proceeds through a short chain mechanism involving the radicals OH and HO_2.

If the chain mechanism is assumed, then as long as the concentration of the peroxide remains constant, the rate of decomposition should be proportional to the quantity of catalyst present. Increasing the concentration increases the length of the chains and more peroxide molecules are decomposed for a given number of initial chains. Thus, even if the initiation of a chain results in a portion of the surface being changed from the alkaline to acid type of oxide, the actual quantity of peroxide decomposed would depend upon the concentration of the peroxide and would not be fixed, as King suggests. The effect of concentration on the length of chain would also explain the increase in velocity constant observed each time a fresh portion of peroxide was added to a partially deactivated sample of carbon.

II. THE AUTOXIDATION OF STANNOUS CHLORIDE AND POTASSIUM URATE

In part I of this paper the activity of activated carbon was measured by its effect on the rate of decomposition of hydrogen peroxide. In this part of the paper its activity will be measured by its effect on the rate of autoxidation of stannous chloride in an acid solution and of potassium urate in an alkaline solution.

Apparatus and procedure

The rate of autoxidation of these substances was followed by observing the decrease in volume of oxygen above the solution, using the method described by Filson and Walton (4). The stock solution of stannous chloride (Merck's "reagent quality") was 0.354 N with respect to stannous chloride and 0.8 N with respect to hydrochloric acid. The stock solution of potassium urate contained 20 g. of uric acid (Merck's) per liter and 25 g. of potassium hydroxide per liter. Both solutions were kept under an atmosphere of nitrogen. Samples (0.5 g.) of carbon were allowed to react with 15 ml. of the stock solution at 25°C. For the stannous chloride the rate of autoxidation in air was determined; for potassium urate the rate of autoxidation in oxygen.

Autoxidation of stannous chloride

Haring and Walton (10) found that ordinary powdered willow charcoal accelerates the rate of autoxidation of stannous chloride in acid solution very greatly, but no work was done on the effect of activated sugar carbon. In this investigation carbons activated at temperatures ranging from 350° to 850°C. were employed as catalysts. In figure 11 the speed of reaction, expressed as the reciprocal of the time required for oxidation of half the stannous chloride present, is plotted against the temperature of activation of the catalyst. It is seen that the speed of reaction is greatest when carbons activated in the neighborhood of 575°C. are used as catalysts. The rate of reaction decreases rapidly when carbons activated at temperatures above 650°C. and below 450°C. are used. It was found that this reaction is a zero-order reaction. There was no indication that the activity of the catalyst decays as the reaction proceeds, as is the case in the decomposition of hydrogen peroxide.

It is interesting to compare these results with those obtained by Schilow (20) and coworkers for the adsorption of acids and alkali on carbons activated at different temperatures. The results they obtained for the adsorption of hydrochloric acid are also shown in figure 11. They found a maximum adsorption of alkali and a minimum adsorption of acids on carbon activated at 540°C. Thus it is seen that those carbons which are capable of adsorbing the least amount of acid are those which are most effective in catalyzing the autoxidation of stannous chloride. The decrease in rate of autoxidation when carbons activated at higher or lower temperatures are used can be attributed to the preferential adsorption of acid from the acid solution of stannous chloride, the acid occupying surface which would otherwise be available for stannous chloride.

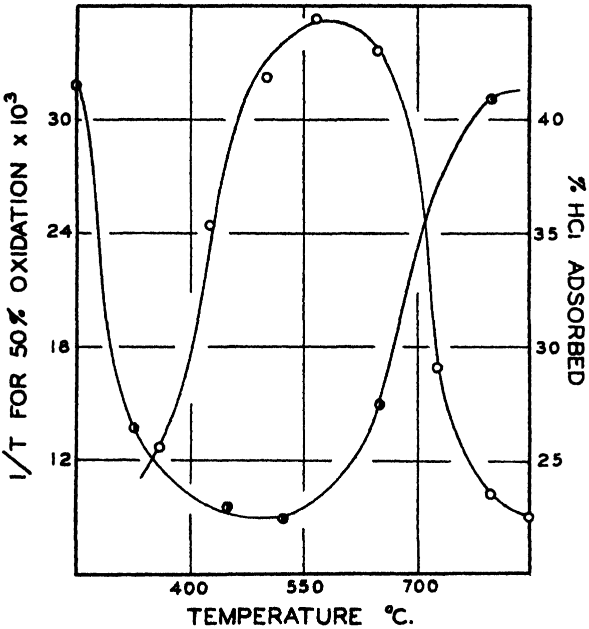

FIG. 11. Effect of temperature of activation: ○, on the rate of autoxidation of stannous chloride (work of the present authors); ◐, on adsorption of hydrogen chloride (from Schilow).

Autoxidation of potassium urate

Frèrejacque (7) found that, using commercial activated charcoal in the ratio of 1 part of charcoal to 20 parts of water, the time required for the autoxidation of a quantity of potassium urate was reduced from 15 hr. to 10 min. No work was reported for the effect of activated sugar carbon. In this work carbons activated at temperatures from 350° to 850°C. were employed as catalysts. In table 2 the time required to oxidize half the potassium urate present in solution is recorded for each type of carbon.

These experiments were difficult to reproduce. They were carried out in triplicate and the mean of the three trials recorded. The individual runs differed from each other by as much as 10 per cent. The reaction was a zero-order reaction, and was independent of the rate of shaking the solution. As in the autoxidation of stannous chloride, here too there was no indication of decay in catalytic activity of the carbon.

Approximately 2 moles of oxygen were absorbed for every 3 moles of potassium urate. This agrees with the observations of Frèrejacque, who found that between one and two atoms of oxygen are needed to oxidize one molecule of uric acid.

TABLE 2

Effect of temperature of activation on the rate of autoxidation of potassium urate

TEMPERATURE OF ACTIVATION	TIME FOR HALF-OXIDATION
°C.	*minutes*
No carbon	133
Unactivated	67
360	32.5
430	30
500	27
570	24.5
650	22
730	21.5
800	19.5
850	20

From table 2 it is seen that the rate of reaction increases as the temperature of activation is increased. There is no range of pronounced activity, as was observed for both the decomposition of hydrogen peroxide and the autoxidation of stannous chloride. Truszkowski (21) found that active carbon adsorbed no alkali urate from a solution whose pH value varied from 6 to 10, and concluded that the oxidation is purely a contact process. The increase in rate of reaction observed here can be attributed to the larger surface area per unit weight of carbon that is produced as the temperature of activation is increased. This is quite different from the decomposition of hydrogen peroxide, in which reaction the type of oxide present on the surface is the factor which decides whether or not a particular sample of carbon is to be an active catalyst.

SUMMARY

The activity of activated carbon was measured by its effect on the rate of decomposition of hydrogen peroxide, and on the rate of autoxidation

of stannous chloride and potassium urate. The effect of temperature of activation on the amount of iodine adsorbed from aqueous solutions was determined.

The effect on the rate of decomposition of hydrogen peroxide when catalyzed by activated carbon was determined for the temperature of activation, source of carbon, initial peroxide concentration, variation of both quantity of catalyst and of peroxide, temperature of reaction, pH, metallic salts, and repeated use of the same catalyst.

The decay in activity of the carbon during peroxide decomposition was discussed from the point of view of surface oxides of carbon and the chain mechanism of peroxide decomposition.

REFERENCES

(1) Allmand, A. J., and Style, D. W. G.: J. Chem. Soc. **1930,** 598–606.
(2) Bohnson, V. L.: J. Phys. Chem. **25,** 19 (1921).
(3) Farmer, W., and Firth, J. B.: J. Phys. Chem. **28,** 1136 (1924).
(4) Filson, G. W., and Walton, J. H.: J. Phys. Chem. **36,** 740 (1932).
(5) Firth, J. B., and Watson, F. S.: J. Chem. Soc. **123,** 1750 (1923).
(6) Firth, J. B., and Watson, F. S.: J. Phys. Chem. **29,** 987 (1925).
(7) Frèrejacque, M.: Compt. rend. **191,** 949 (1930).
(8) Haber, F., and Weiss, J.: Naturwissenschaften **20,** 948 (1932); Proc. Roy. Soc. (London) **A147,** 332 (1934).
(9) Haber, F., and Willstätter, R.: Ber. **64,** 2844 (1931).
(10) Haring, R. C., and Walton, J. H.: J. Phys. Chem. **37,** 375 (1933).
(11) King, A.: J. Chem. Soc. **1936,** 1688–92.
(12) King, A.: J. Chem. Soc. **1938,** 991–7.
(13) King, A., and Lawson, C. G.: Kolloid-Z. **69,** 21 (1934).
(14) Kiss, A., and Lederer, E.: Rec. trav. chim. **46,** 453 (1927).
(15) Kolthoff, I. M.: J. Am. Chem. Soc. **54,** 4473 (1932).
(16) Kruyt, H. R., and de Kadt, G. S.: Kolloid-Beihefte **32,** 249 (1931).
(17) Lemoine, G.: Compt. rend. **144,** 357 (1907).
(18) MacInnes, D. A.: J. Am. Chem. Soc. **36,** 878 (1914).
(19) Miller, E. J.: J. Phys. Chem. **36,** 2967 (1932).
(20) Schilow, N., Schatunowskaja, H., and Tschmutow, K.: Z. physik. Chem. **A149,** 211 (1930).
(21) Truszkowski, R.: Biochem. J. **24,** 1349 (1930).
(22) Weiss, J.: J. Phys. Chem. **41,** 1107 (1937).
(23) Weiss, J.: Trans. Faraday Soc. **31,** 1547 (1935).

WETTING CHARACTERISTICS OF SOLID SURFACES COVERED WITH ADSORBED FILMS

F. E. BARTELL AND KENNETH E. BRISTOL

Department of Chemistry, University of Michigan, Ann Arbor, Michigan

Received April 1, 1939

Clean solid surfaces exposed to the atmosphere adsorb constituents of the atmosphere almost immediately. This adsorption alters the free surface energy of the solid and hence the wetting characteristics of the solid. The extent of alteration depends upon the constituent adsorbed and upon its concentration in the atmosphere. An alteration of the free surface energy of a solid is readily detected by measurement of the contact angle of a liquid upon the solid.

We had observed that hydrophilic solids such as glass and quartz might give different contact angle measurements on different days. It seemed likely that the contact angle values were closely related to the degree of humidity of the atmosphere. Subsequent study showed this to be true.

In the present investigation, clean hydrophilic surfaces and clean organophilic surfaces were treated with water vapor and with organic liquid vapors, respectively, so as to produce definite and controlled adsorption. Contact angle measurements were made with different liquids upon such surfaces. The method employed for measuring contact angles was the sessile-drop method.

I. MEASUREMENT OF CONTACT ANGLES ON HYDROPHILIC SURFACES

Apparatus

In order to measure, by the sessile-drop method, both the advancing and the receding contact angles of a given system, an apparatus was designed with which liquid could be added to the drop or removed from the drop very slowly. The solid surface used was of Pyrex or quartz made in the form of a tip, S, which fitted a ground-glass joint (figure 1). The horizontal surface of this tip was polished optically plane, and a small capillary extended from the center of this surface down through the solid. The tip was mounted in a cell, C, which had parallel plate-glass windows and was sealed by a ground-glass joint, E. The liquid, of which the contact angle was to be measured, was contained in a reservoir, R. This could be raised or lowered so as to control the direction of flow of the liquid through the syphon tube, T. The rate of flow was controlled by the accurately ground stopcock, A; also, the flow of liquid could be stopped when desired.

Control of water vapor concentration

The amount of adsorption of water on the solid surface was regulated by controlling the concentration of water vapor in contact with the solid. Solutions (or solid materials) capable of maintaining a constant aqueous tension were placed in the bottom of the cell C, and the system was kept in an air thermostat at 25°C. These materials were so placed in the cell that the surface of the tip was 2 or 3 cm. above the materials. The substances used to obtain the different aqueous tension conditions are given in table 1.

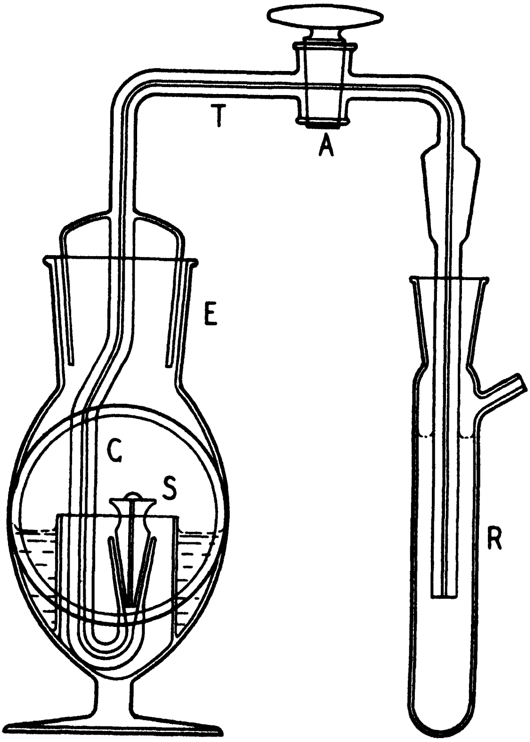

FIG. 1. Apparatus for the measurement of angles of contact in atmospheres of controlled vapor concentrations

Method of making the measurements

The solid was first treated with boiling benzene for 0.5 hr., was next heat-treated in a furnace at 425°C., and was then slowly cooled in the furnace to remove strains. When cool it was removed from the furnace and quickly placed in the cell C, where the solid surface was allowed to come to equilibrium with the gas phase in the cell. One hour was found to be sufficient for the hydrophilic surfaces to reach sorption equilibrium in the system at 25°C.

The organic liquid to be used was forced over through the syphon tube and allowed to form a drop on the surface of the solid. The rate of flow of the liquid was adjusted so that the drop grew very slowly (i.e., approximately 5 min. were allowed for the drop to grow from a diameter of 1 mm. to 3 mm.). The contact angle formed with this advancing liquid-air interface against the solid will be referred to in this paper as the dynamic advancing angle. Photomicrographs of the drop were taken at intervals as the interface advanced. The direction of the flow of the liquid was then reversed and the interface was allowed to recede and the drop, having a dynamic receding angle, was photographed. The drop was made to grow again until the previously wet surface was entirely covered; then as the liquid advanced further, the dynamic advancing angle was again observed. The flow of liquid was then stopped and the system was allowed to stand. The drop now was observed to advance very slowly and in 0.5 hr. it came to rest with the liquid forming a definite and reproducible contact angle, which in this paper is referred to as a "static advancing angle" (meaning that it has been formed after the forced flow of liquid was stopped and after the liquid was allowed to advance under the influence of surface forces only until no further change occurred). This drop also was photographed.

TABLE 1

*Aqueous tension values of materials used in controlling the concentration of water vapor**

NO.	SUBSTANCE	WATER VAPOR PRESSURE AT 25°C.
		mm. of Hg
1	P_2O_5	0 (approximately)
2	Anhydrous $CaCl_2$	0 (approximately)
3	Saturated solution of $MgCl_2$	7.6
4	Saturated solution of $Zn(NO_3)_2$	9.5
5	Saturated solution of $Ca(NO_3)_2$	12.1
6	Saturated solution of NH_4NO_3	14.7
7	Saturated solution of $NH_4Cl + KNO_3$	17.1
8	Saturated solution of $(NH_4)_2SO_4$	19.3
9	Saturated solution of KCl	20.5
10	Saturated solution of $BaCl_2$	21.5
11	14% water solution of concentrated H_2SO_4	22.5
12	Saturated solution of K_2SO_4	23.0
13	10% water solution of concentrated H_2SO_4	23.4
14	Double-distilled water	23.8

* These data were obtained from the International Critical Tables.

In table 2 are given the data for the contact angles of acetylene tetrabromide on Pyrex and quartz surfaces over the range of aqueous tension values. Figures 2 and 3 are curves drawn by plotting aqueous tension values against the values of the contact angles.

Those dotted portions of the curves representing measurements at aqueous tension values higher than 23.8 mm. were obtained in the following manner: Double-distilled water was placed on the surface of the tip, which was then allowed to stand at 25°C. in the closed cell containing an atmosphere saturated with water vapor. The system was allowed to stand until the visible film of water had evaporated from the surface. In this condition the surface gave, with the organic liquid, a dynamic receding angle which was very nearly the same as the dynamic advancing angle, and was also nearly the same as the static advancing angle.

TABLE 2

Contact angles of acetylene tetrabromide on Pyrex and on quartz in systems having controlled water vapor concentrations

AQUEOUS TENSION VALUE OF GAS PHASE AT 25°C.	CONTACT ANGLES ON PYREX			CONTACT ANGLES ON QUARTZ		
	θ_{da}*	θ_{dr}*	θ_{sa}*	θ_{da}*	θ_{dr}*	θ_{sa}*
mm. of Hg						
0	10°	0	0	10°	6°	9°
7.6	17°	0	0			
9.5	17°	0	0	19°	10°	15°
12.1	19°	0	0	23°	10°	18°
14.7	21°	0	5°	28°	13°	21°
17.1	28°	0	11°	30°	14°	24.5°
19.3	36°	0	14.5°			
20.5	36.5°	18°	18°	31°	18°	26°
21.5	36°	18°	19°			
22.5	36°	25°	26.5°			
23.0	38°	25°	26°	37.5°	29°	31°
23.4	36.5°	28°	29°	38°	34°	36°
23.8 (saturation)	38°	32°	36°	38°	34°	37°
(above saturation)	38°	35°	36°	38°	34°	37°

* The meanings of the symbols used in this paper are as follows: θ_{da} refers to a dynamic advancing angle; θ_{dr} refers to a dynamic receding angle; θ_{sa} refers to a "static advancing angle."

Contact angles on Pyrex

In the case of Pyrex, the dynamic advancing contact angles varied between fairly wide limits as the concentration of water vapor was varied between the zero value and the value represented by an aqueous tension of about 19 mm. A very decided change of the dynamic advancing angle

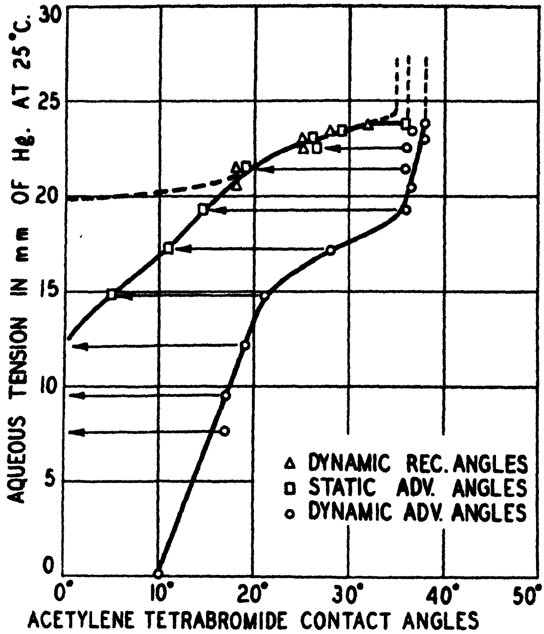

Fig. 2. The system Pyrex-air (water vapor)-acetylene tetrabromide

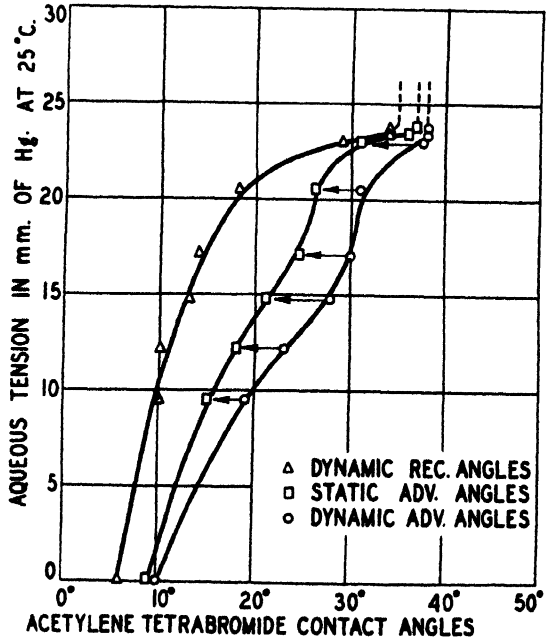

Fig. 3. The system quartz-air (water vapor)-acetylene tetrabromide

occurred when the aqueous tension values were raised from 15 to 19 mm. With aqueous tension values of 19 mm. and higher, the magnitude of the dynamic advancing angle remained practically constant. This variation of contact angle with water vapor concentration would account to a large extent for the differences in contact angles observed when no attempt is made to control the partial pressure of water vapor (figure 2).

The dynamic receding angles were not measurable (i.e., were zero) from zero concentration of water vapor to a concentration represented by an aqueous tension value of about 21 mm. Above this concentration of water vapor, the dynamic receding angle became greater in magnitude as the concentration of water vapor was increased. The dynamic receding angle values approached the dynamic advancing angle value at the saturation pressure of water vapor.

In an atmosphere having an aqueous tension value below 15 mm., a drop of the organic liquid, allowed to stand for a half hour, spread completely over the Pyrex surface, giving what is interpreted as a 0° static advancing angle. In atmospheres with aqueous tension values of 15 mm. or more, the static advancing angle values became larger as the concentration of water vapor was increased, and approached the value of the dynamic advancing angle at the saturation pressure of water vapor.

Contact angles on quartz

When quartz was used as the solid surface, the dynamic advancing angle of acetylene tetrabromide was found to have a value of 10° at zero concentration of water vapor. The angle was larger at higher aqueous tension values, until at 20.5 mm. it had a value of 31°. At a somewhat higher vapor pressure of water, the angle reached a value of 38°. At the saturation pressure of water vapor, the value of the dynamic advancing contact angle was not greater than 38° (figure 3).

For a given vapor pressure of water, the static advancing angle was always less than the dynamic advancing angle. In a system saturated with water vapor, the static advancing angle did not differ from the dynamic advancing angle by more than 1°.

The dynamic receding contact angle of acetylene tetrabromide on quartz in a system dried with calcium chloride or phosphorus pentoxide had a magnitude of 6°. This was somewhat surprising, since acetylene tetrabromide did not give a measurable receding angle on Pyrex until the vapor pressure of water had reached a value of 20.5 mm.

Thickness or completeness of water film dependent on aqueous tension

Such investigators as McHaffie and Lenher (9), Frazer (6), Lenher (8), and d'Huart (5) have shown that quartz and glasses adsorb increasing amounts of water as the aqueous tension values become greater. It is believed by them that the solid adsorbs the water vapor as a film whose thickness is governed by the concentration of water vapor in the gas phase (at constant temperature). These workers differ in their conclusions as to the number of molecular layers in the films, but they all state that the film must be multimolecular in thickness at high humidities. Findings of these investigators, together with our data on the contact angle values, indicate quite conclusively that the magnitude of the contact angle depends upon the completeness and thickness of the adsorbed film of water molecules.

Measurements on hydrophilic surfaces other than Pyrex or quartz

Surface properties of several insoluble hydrophilic minerals were next investigated. These crystalline minerals were freshly cleaved and placed in a cell containing an atmosphere saturated with water vapor at 25°C.

TABLE 3

Contact angles of acetylene tetrabromide and alpha-bromonaphthalene on solids in systems saturated with water vapor (at 25°C.)

SOLID	STATIC ADVANCING CONTACT ANGLES	
	Acetylene tetrabromide	Alpha-bromo-naphthalene
Pyrex	36°	35°
Quartz	37°	36°
Gypsum	37.5°	37°
Mica	39°	35.5°
Fluorite	37.5°	37°
Celestite	38°	35.3°

The system was allowed to stand so that the solid surface could come to sorption equilibrium with the gas phase. Drops of organic liquids were placed on the solid by means of a freshly drawn glass pipet. The height and diameter of the drops were measured with a microscope, and the contact angles were calculated by means of the formula

$$\tan \tfrac{1}{2} \theta = 2h/d$$

Table 3 gives the results obtained using acetylene tetrabromide and alpha-bromonaphthalene drops on the surfaces exposed to an atmosphere saturated with water vapor at 25°C. The drops were placed by pipet rather than by the more complicated syphon system, since the experiments on glass and quartz had shown that in atmospheres saturated with water vapor the advancing and receding angles had practically the same value, hence the method of placing the drop made little difference.

Adsorbed film masks the adhesive forces of the solid

The data in table 3 show that acetylene tetrabromide on each of the hydrophilic solids gave a contact angle which in each case was the same, within experimental error, and had an average value of 37.5°. Alpha-bromonaphthalene also gave contact angles on the different solids which were of the same value for the different solids, namely, about 36° (the values were practically the same as those obtained with acetylene tetrabromide). Since these solids have different wetting characteristics in the dry condition, the fact that the contact angles on the different film-covered solids were the same for a given liquid shows that the surface of each solid had been altered so that each had the same wetting properties. At high humidities, the hydrophilic solids must sorb a film of water which is thick enough to mask the adhesive forces of the underlying solid and to give surfaces having energy values peculiar only to an adsorbed film of oriented water molecules. If the apparent surface energy of the solid is due entirely to the water film or layer, this film must be continuous even under the drop of the organic liquid. During the period of the experiment, apparently no stripping of the water film occurred.

Persistence of the water film

That adsorbed water is strongly held by a hydrophilic surface has been demonstrated repeatedly by experiments showing the high temperatures necessary to remove all of the adsorbed water from glass and quartz surfaces. Bunsen (4) found that glass must be heated to about 500°C. before it will give up all of its sorbed water. Langmuir (7) found that when glass was heated as high as 450°C., 22 cc. of water vapor was given off per 10,000 sq. cm. of surface. Bartell and Wooley (3) found that by heating Pyrex and quartz to 425°C. for 1 hr., these solids were made less hydrophilic and attained a condition such that further heating did not affect their wetting characteristics. This heat treatment probably caused the removal of water which had been sorbed by the Pyrex or quartz, and so made them less hydrophilic.

In the present investigation experiments were made to determine whether such a drying agent as phosphorus pentoxide could remove the adsorbed water from Pyrex and quartz at room temperature. Pyrex and quartz surfaces were allowed to stand for 1 hr. in air saturated with water vapor at 25°C. These surfaces were then placed in a closed cell containing air dried with fresh phosphorus pentoxide and allowed to stand 24 hr. At the end of this time, the dynamic advancing angles of acetylene tetrabromide on these surfaces were measured. The values of these angles were about 20°. As has been reported in this paper, Pyrex and quartz surfaces which have not been exposed to water vapor have dynamic advancing contact angles with acetylene tetrabromide of 10°, while the presence of adsorbed water on the Pyrex and quartz surfaces causes the dynamic advancing angle of acetylene tetrabromide to have values higher than 10°. It appears, therefore, since the measured angle was greater than 10°, that adsorbed water must have been left on the Pyrex and quartz surfaces even after the surfaces stood over fresh phosphorus pentoxide.

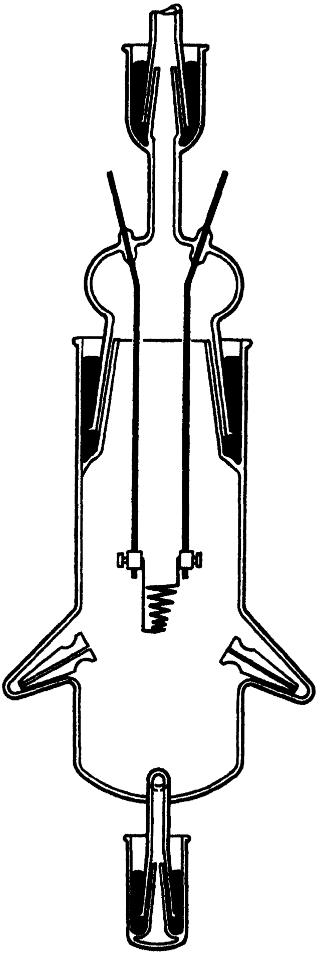

Fig. 4. Coating apparatus

II. MEASUREMENT OF CONTACT ANGLES ON ORGANOPHILIC SURFACES

In the investigation of the wetting characteristics of organophilic solids upon which films of organic liquids had been adsorbed, the contact angles of water drops upon such solids were measured. Crystals of organophilic solids were cleaved and an attempt was made to drill a small capillary from the bottom of the crystal to the smooth top surface. Such drilling was not successful, because the surface immediately around the hole was roughened in the process, and the roughened surface did not permit of uniform spreading of the water drop. Pyrex or quartz tips (figure 1) coated with organophilic solids by sublimation in a high vacuum were therefore used.

The coating process

The coating apparatus (figure 4) was similar to that described by Bartell and Hatch (2). The heating coil, made of No. 26 gauge tungsten wire, was in the shape of a cone with the apex pointing downward. Small crystals of the solid to be sublimed were placed in this coil. Since many of these substances broke up into finer particles when heated, the surfaces to be coated were held in position at the side of the coil (see figure 4). This method of coating gave a smooth, mirror-like surface, free from roughness such as would have been caused by falling particles of solid.

Preliminary to coating, the tips were placed in the coating chamber and the system was evacuated. When the pressure had been reduced to 10^{-5} mm. of mercury, the current was started through the tungsten heating coil. Just enough heat was used to vaporize the mineral slowly. If the vaporization was too rapid, most minerals did not give smooth shiny coatings. It was also found that if the surface to be coated was allowed to become too hot, owing to heat radiated from the coil, a spongy deposit was formed. For this reason the walls of the coating chamber were cooled with ice water during the coating process. It was found to be unnecessary to flush out the apparatus with nitrogen before evacuation to 10^{-5} mm. of mercury, since surfaces formed after such precaution was taken had the same wetting characteristics as the others.

Solids used

The organophilic solids upon which measurements were made included galena (PbS), cinnabar (HgS), sphalerite (ZnS), antimony metal, and stibnite (Sb_2S_3). Measurements were also made on surfaces of stibnite which had been altered by oxidation.

The unoxidized stibnite surface was designated as "stibnite 1". Some "stibnite 1" samples were heated in air at different temperatures and for different lengths of time, and gave surfaces indicated as follows:

"Stibnite 2": "stibnite 1" heated at 180°C. for 3 hr.
"Stibnite 3": "stibnite 1" heated at 200°C. for 3 hr.
"Stibnite 4": "stibnite 1" heated at 220°C. for 2 hr.

Considerable difficulty was encountered in oxidizing the stibnite coatings simply by heating in air. No appreciable oxidation occurred until the temperature was over 210°C., and it was found that if the temperature was allowed to rise above this point, the stibnite coating usually would loosen from the glass tip. In order to effect oxidation at a lower temperature, a little nitrogen dioxide gas was introduced with air into the furnace tube where the tip was being heated. After a few minutes, this nitrogen dioxide was blown out of the furnace tube by a stream of air, and the heating was then continued in air. The presence of the small amount of nitrogen dioxide caused the oxidation to begin at a lower temperature, but the oxidation progressed too rapidly if nitrogen dioxide was allowed to remain in the furnace tube after the first few minutes. After the stibnite surface had become slightly oxidized, further oxidation would occur slowly in pure air even at a comparatively low temperature. Using this method, other oxidized stibnite coatings were prepared from "stibnite 1" and are indicated as follows:

"Stibnite 5": "stibnite 1" heated in nitrogen dioxide and air at 180°C. for 5 min., then heated in air at 205°C. for 2 hr.

"Stibnite 6": "stibnite 1" heated in nitrogen dioxide and air at 180°C. for 15 min., then heated in air at 210°C. for 3 hr.

"Stibnite 7": "stibnite 1" heated in nitrogen dioxide and air at 180°C. for 10 min., then heated in air at 180°C. for 2 hr.

The original "stibnite 1" mirrors were brown in color. The oxidized stibnite surfaces were a silvery gray. The galena mirrors were gray, a little darker than a silver mirror. The cinnabar films were pale yellow and transparent. The antimony mirrors had a bright silvery appearance. The sphalerite films were colorless and transparent; when they were peeled off the glass, they looked like little sheets of mica.

Measurement of the water contact angles

A tip with its coating was placed in the holder B (figure 1) and put in position in the cell C. After the tip came to constant temperature at 25°C., water was forced over onto the surface from the reservoir R. The water drop was formed and allowed to stand, and the static advancing angle was photographed. The liquid–air interface did not advance after the water supply was shut off. Thus it appeared that the static advancing angle was the same as the dynamic advancing angle. Photographs were also taken of receding drops provided a measurable receding angle was formed. Data obtained from water contact angle measurements on the pure organophilic surfaces are given in columns 2 and 3 of table 4. These data show that sphalerite, galena, cinnabar, and antimony metal surfaces have quite different wetting characteristics, and that the wetting characteristics of the stibnite mirror surfaces may be changed by oxidation treatments.

Formation of films on organophilic solids

When the surface S (figure 1) is coated with an organophilic solid and is then placed in the cell C, containing a small amount of organic liquid at 50–80°C., and allowed to cool, organic vapors will be sorbed by the solid and will form a complete film on the organophilic surface. If a suitable length of time is allowed for the visible layer of condensed organic liquid to evaporate from the solid, a uniform adsorbed film will be left on the surface.

TABLE 4

Contact angles of water on pure organophilic surfaces and on organophilic surfaces covered with organic liquid films

SOLID	PURE SURFACE		ACETYLENE TETRABROMIDE FILMS		ALPHA-BROMONAPHTHALENE FILMS		DECALIN FILMS	
	θ_{sa}	θ_{dr}	θ_{sa}	θ_{dr}	θ_{sa}	θ_{dr}	θ_{sa}	θ_{dr}
Stibnite 1	80°	0°	75°	40°	80°	32°	90°	27°
Stibnite 2	79°	0°						
Stibnite 3	75°	0°						
Stibnite 4	64°	0°						
Stibnite 5	70°	0°	78°	43°				
Stibnite 6	55°	0°	75°	40°				
Stibnite 7	39°	0°	61°	0°				
Galena	88°	0°	77°	75°	79°	55°	94°	84°
Cinnabar	113°	47°	75°	67°	78°	54°	92°	56°
Sphalerite	46°	0°	54°	0°				
Antimony metal	55°	0°						

Persistence of films on organophilic surfaces

Experiments were made to determine the relative degrees of adsorption of different types of organic liquids on the different organophilic solids. It was found that liquids with a strong permanent dipole, such as acetylene tetrabromide and alpha-bromonaphthalene, could not be removed by unaided evaporation at 25°C. in an atmosphere free from vapors of the adsorbate. But when non-polar or but slightly polar liquids, such as decalin, *n*-octane, or mesitylene, were used as the adsorbate, the film of organic liquid disappeared within about a half-hour.

Measurement of water contact angles on adsorbed films of organic liquids on organophilic surfaces

After the organic liquid vapors in the cell had come to sorption equilibrium with the organophilic solid on the surface S, a water drop was caused to form on the solid surface. As in the previous experiments, the drops were photographed as the liquid advanced, remained fixed, or receded.

Columns 4 and 5 of table 4 give the results obtained with water drops on acetylene tetrabromide films adsorbed on the different organophilic solids. These data show that the static advancing angles of water on acetylene tetrabromide films on coatings of the stibnites, galena, and cinnabar all have angles between 75° and 78°. The surfaces which failed to give an advancing angle of this magnitude were films of acetylene tetrabromide on those solids which, in the absence of organic vapors (i.e., in the pure state), gave static advancing angles with water of less than 40° to 50°. Such solids were "stibnite 7" and sphalerite. When these solids were covered with an adsorbed film of acetylene tetrabromide, the water static advancing angles were much lower than the 75° to 78° value which was common to the other solids. A notable fact was that the water dynamic receding angles on these film-covered surfaces were 0°, or the same as the water dynamic receding angles on the pure "stibnite 7" and sphalerite. This indicates that the sorbed organic liquid film was removed from these solids by the advancing water interface. On those solids from which water did not remove the acetylene tetrabromide film, the film apparently masked the wetting characteristics of the underlying solid and the advancing contact angle measurement was a measurement of the wetting characteristics of the acetylene tetrabromide film.

Columns 6 and 7 and columns 8 and 9 of table 4 give the results obtained from water contact angle measurements on adsorbed films of alpha-bromonaphthalene and decalin on different organophilic surfaces. Alpha-bromonaphthalene films on "stibnite 1," galena, and cinnabar gave surfaces on which water has a static advancing contact angle of about 79°. The dynamic receding angles were 30° to 60°. Adsorbed films of the non-polar liquids decalin, mesitylene, and *n*-octane were also formed on the above three solids, but decalin was the only one which gave a surface on which a stable advancing water angle formed. Water on the decalin films on the three solids gave an advancing contact angle of about 92°. With the three solids both alpha-bromonaphthalene and decalin films appear to have masked the underlying solid so completely that the advancing water angles are a measure of the wetting properties of the films rather than of the solids.

Measurements of water contact angles on the organic liquid films on the "stibnite 1," galena, and cinnabar surfaces were repeated using new tips with new deposited mirrors, and it was found that the advancing angles gave good checks. The receding water angles varied between fairly wide limits, however, and gave values anywhere between 30° and the advancing angle value. The probable cause for the differences observed in the receding angle values was difference in the thickness or the completeness of the adsorbed films of organic liquid in the different ex periments. If it had been possible to control the thickness of the films of organic liquids adsorbed on the organophilic solids, as it was possible to control the thickness of the adsorbed water film of the hydrophilic solid, the receding angles probably would have given better agreement.

Surface tension of adsorbed films

The surface tension of adsorbed water or organic liquid films can be calculated, using the well-known Young equation (10), if it be assumed that the interfacial tension existing between the liquid drop used and the liquid film under it is the same as the interfacial tension, S_{23}, between the two liquids in bulk (admittedly, such an assumption is questionable). If the surface tension of the water film is designated as S_3', and the surface tension of the organic film as S_2', the following equations can be set up (S_3 = surface tension of water; S_2 = surface tension of organic liquid):

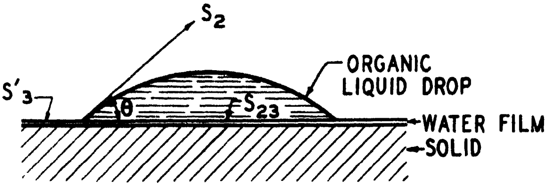

FIG. 5. Drop of organic liquid on surface covered with water

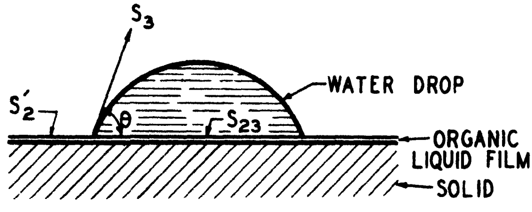

FIG. 6. Drop of water on surface covered with organic liquid

$$S_3' = S_{23} + S_2 \cos \theta_{sa} \quad \text{(see figure 5)} \qquad (1)$$

$$S_2' = S_{23} + S_3 \cos \theta_{sa} \quad \text{(see figure 6)} \qquad (2)$$

Since S_{23}, S_2, and S_3 are all known, S_2' and S_3' can be calculated by using the cosines of the appropriate static advancing angles.

Using the acetylene tetrabromide or alpha-bromonaphthalene values of θ_{sa} in saturated water vapor from table 2, S_3' is calculated to be about 77 dynes. This is the same value as that indicated by the empirical equations of Bartell and Bartell (10) to be the value of the surface tension of a complete film of oriented water molecules.

If the value of 77 dynes is correct it can be seen from equation 1 that only those organic liquids whose $S_{23} + S_2$ values are greater than 77 dynes will give measurable angles on water films. Table 5 gives a list of S_2 and S_{23} values for six liquids. Carbon disulfide is the only liquid in this group which gave a measurable angle on the water film, and is the only liquid of this group whose $(S_2 + S_{23})$ value is greater than 77 dynes. The other liquids spread completely over the surfaces. Only mutually insoluble liquids can be used for such tests. Liquids which show any appreciable solubility in water give anomalous results.

TABLE 5

S_2 and S_{23} values for six liquids

ORGANIC LIQUID	S_2	S_{23}	$(S_2 + S_{23})$
Benzene	28.2	34.8	63.0
Toluene	27.9	35.9	63.8
Nitrobenzene	43.3	25.3	68.6
n-Octane	21.3	50.6	71.9
Carbon tetrachloride	26.2	44.5	70.7
Carbon disulfide	31.6	48.1	79.7

TABLE 6

Calculated values of surface tensions of adsorbed organic liquid films ($S_3 = 72$)

LIQUID	S_{23}	θ_{sa}	S'_2	S_2
Acetylene tetrabromide	38.3*	76°	55.7	49.1*
Alpha-bromonaphthalene	41.6*	79°	55.3	44.0*
Decalin	34.2	92°	31.8	31.6

* These values were taken from the International Critical Tables.

From equation 2 the surface tension of some organic liquid films can be calculated if the cosines of the appropriate values of θ_{sa} from table 4 are used. Table 6 gives the calculated values of the surface tension of some adsorbed organic liquid films.

The polar liquids acetylene tetrabromide and alpha-bromonaphthalene give calculated values of S'_2 considerably higher than the corresponding values of S_2 for the liquids in question, as was the case for the polar water film. The non-polar liquid decalin gives a value for surface tension of the liquid film practically the same as the surface tension of the liquid itself.

SUMMARY

Using dynamic advancing and receding contact angles, as well as static advancing contact angles, as measures of the wetting properties of solid surfaces, it has been shown that hydrophilic solids in atmospheres of high

humidity, and extremely organophilic solids in atmospheres saturated with organic liquid vapors, adsorb films upon their surfaces sufficiently thick to mask the original surface properties. Less organophilic solids adsorb organic films, but these films may be stripped away by water advancing upon the surface.

The values of the surface tensions of some films adsorbed upon some solids have been calculated. In order to make the calculation, one assumption had to be made: namely, that the interfacial tension between a liquid drop placed upon a film is the same as the interfacial tension between the two liquids in bulk. The calculations indicate that the surface tensions of films of polar liquids are higher than the surface tensions of the polar liquids, but that the surface tensions of films of non-polar liquids are the same as the surface tensions of the non-polar liquids.

REFERENCES

(1) Bartell and Bartell: J. Am. Chem. Soc. **56**, 2205 (1934).
(2) Bartell and Hatch: J. Phys. Chem. **39**, 11 (1935).
(3) Bartell and Wooley: J. Am. Chem. Soc. **55**, 3518 (1933).
(4) Bunsen: Wied. Ann. Physik **24**, 321 (1885).
(5) d'Huart: Compt. rend. **180**, 1594 (1925).
(6) Frazer: Phys. Rev. **33**, 97 (1929).
(7) Langmuir: J. Am. Chem. Soc. **38**, 2283 (1916).
(8) Lenher: J. Chem. Soc. **1926**, 1785.
(9) McHaffie and Lenher: J. Chem. Soc. **127**, 1561, 1565 (1925).
(10) Young: Trans. Roy. Soc. (London), p. 65 (1805).

ON QUASI-REVERSIBLE CONDUCTION AND GALVANIC CELLS WITH LIQUID-LIQUID JUNCTIONS

F. O. KOENIG

Department of Chemistry, Stanford University, California

Received February 4, 1939

I. Introduction

THERMODYNAMIC AND KINETIC METHODS IN THE THEORY OF LIQUID-LIQUID JUNCTIONS

The problem of liquid-liquid junctions, like many problems in physical chemistry, has been attacked theoretically by both thermodynamic and kinetic methods. The thermodynamic method was first applied to this problem by Helmholtz (11) and has been further developed chiefly by Nernst (20), Henderson (13), Lewis and Randall (18), Taylor (23), and Guggenheim (4, 5, 6, 9). The kinetic method was originated by Nernst

(19) and Planck (21), and has been further developed chiefly by Johnson (14) and Pleijel (22). The present paper is concerned with the thermodynamic method alone.

FOUR DEFECTS OF THE EXISTING THERMODYNAMIC THEORY

The existing thermodynamic theory of cells with liquid–liquid junctions appears to us to be defective or incomplete in a number of respects, of which we emphasize the following four:

(*i*) *Artificiality in manner of neglecting diffusion.* In any thermodynamic theory of cells with liquid–liquid junctions it is necessary at some point in the argument and in some manner to disregard changes of state due to diffusion. The above-mentioned authors of the existing theory have all done this by treating the solution in the cell as if it were "frozen," i.e., as if diffusion were not taking place at all, so that, when an infinitesimal electric current is passed through the cell, the only change of state is the change in composition due to transport of components by the current. Actually, however, since rate of diffusion is in general finite, the change in composition at any point of the solution, due to an *infinitesimal* current flowing during any time interval, must itself be infinitesimal compared with the change due to spontaneous diffusion during the same time interval. In view of this fact the existing treatment of the solution as "frozen" is evidently highly artificial.

(*ii*) *Incomplete definition of transport numbers.* In order to calculate the change of composition caused by an infinitesimal current, transport numbers (or mobilities) must be introduced. Transport numbers, however, have been defined hitherto only for the special case of uniform solutions not subject to diffusion in the absence of a current. The unqualified extension of the transport number concept thus defined to the diffusing solutions constituting liquid–liquid junctions is clearly an error in logic. This error has moreover caused some confusion, as an example of which we cite the attitude of P. B. Taylor (23), who maintains that the equations for the E.M.F., in order to be exact, must include terms for the transport of solvent, but fails to explain why transport numbers calculated from experimental E.M.F.'s are generally in perfect agreement (within experimental error) with the Hittorf numbers obtained from migration experiments under the convention that the transport number of the solvent is zero.

Of the other thermodynamic authors referred to above (11, 20, 13, 18, 4, 5, 6, 9), all but Helmholtz (11) have simply ignored the entire question, no doubt because they have been guided by the intuition (which we prove below to be correct) that the use of the Hittorf numbers is valid; in this they have of course been supported by the experimental findings. Helmholtz studied the case of a single electrolyte in a non-electrolyte solvent and indicated plainly that the Hittorf numbers are *sufficient* for an exact theory in this particularly simple case; however, he left untouched the question as to whether the Hittorf numbers are *necessary* for an exact theory (we prove below that they are not necessary) and as to what the situation is when two or more electrolytes are present.

(*iii*) *Restriction to cylindrical symmetry.* Hitherto all treatments except that of Helmholtz (11) have been limited to the special case of junctions with cylindrical symmetry, i.e., junctions in which all concentration gradients are parallel to a fixed straight line (*cf.* 5). The treatment of Helmholtz, however, besides being restricted to the case of a single electrolyte, is based upon a special method whose extension to systems of more complex composition is not obvious; this method consists in calculating the transport of *solvent* just necessary to keep the composition of the solution at each point *unchanged* when current flows through the cell. It is therefore clear that the laws for arbitrary junctions of any composition are as yet unknown.

(*iv*) *Obscurity of the relation to gravity cells.* The relation of cells with liquid-liquid junctions to gravity cells of the types studied by Des Coudres (1) and Tolman (24) is obscure. That a relation must exist is evident from the facts that (*a*) gravity cells, like cells with liquid-liquid junctions, are subject to diffusion ("sedimentation") and (*b*) transport numbers can be calculated from the E.M.F.'s of gravity cells as well as from the E.M.F.'s of cells with liquid-liquid junctions.

OBJECTS AND PLAN OF THE PRESENT PAPER

Corresponding to the above-mentioned defects of the existing thermodynamic theory are the four chief objects of the present paper: (*i*) to show that it is possible to neglect the effects of diffusion in a manner less artificial than in the existing theory; (*ii*) to extend the definition of transport number so as to include solutions subject to diffusion, and thus to clarify the relationship between migration experiments and cells with liquid-liquid junctions; (*iii*) to discover what thermodynamic laws hold if the restriction to cylindrical symmetry is abandoned; (*iv*) to prepare the way for a unified theory of cells with liquid-liquid junctions and gravity cells.[1]

In order to achieve these objects we propose: (*i*) to state the assumptions and definitions underlying the thermodynamic theory of cells with liquid-liquid junctions as exactly as possible and in a form general enough to take into account arbitrary gradients of concentration and of gravitational potential; (*ii*) to deduce from these assumptions and definitions a certain general theorem concerning liquid–liquid junctions; and (*iii*) to deduce with the help of this theorem the thermodynamic laws of cells with liquid-liquid junctions.

---

[1] The detailed theory of gravity cells from the point of view of this paper has been worked out in collaboration with Dr. S. W. Grinnell and will be reported in a later paper.

Among the assumptions needed we shall find one which is of more special importance for the problem in hand than all the others. For reasons apparent below we suggest that this outstanding assumption be known as the *assumption of quasi-reversible conduction*, or, abbreviated, as the *qrc. assumption*. The other assumptions we shall refer to as *auxiliary assumptions*. We furthermore suggest that the theorem to be deduced be known as the *condition for quasi-reversible conduction* or the *qrc. condition*.

II. ASSUMPTIONS AND DEFINITIONS

DEFINITION 1. DESCRIPTION OF THE SYSTEM TO BE STUDIED; CONFIGURATION OF THE SYSTEM

We shall consider a system made up of two electrodes in contact with an electrically conducting solution which is liquid and non-metallic. Each of these electrodes may consist either of a single metallic phase or of a set of contiguous phases, at least one of which is metallic, e.g., Ag | AgCl. We denote the *entire set of phases* constituting one of these electrodes by α, that constituting the other electrode by α', the layer of solution immediately contiguous to α by β, and the layer of solution immediately contiguous to α' by β'. We shall of course assume electrodes and solution to consist of mutually insoluble materials, so that no matter can enter or leave the solution at the electrodes save by flow of current. We shall also assume that no matter ever enters the solution save at the electrodes. The solution we shall assume to be subject to diffusion under gradients of concentration and of gravitational potential, and we shall allow these gradients, together with the volume and shape of the solution, to be arbitrary, except for the following restrictions: (*i*) The solution is at each instant in hydrostatic and thermal equilibrium (see definition 3 below), and the temperature of the solution and the electrodes is at all times constant. (*ii*) At each instant all points of the layer of solution β are in the same electrochemical state (see definition 4 below) and likewise are all points of the layer β'. (*iii*) The layers of solution β and β' are at each instant in electrochemical equilibrium (see definition 5 below) with their respective electrodes α and α'. (*iv*) The electrodes α, α' are so arranged that any volume changes undergone by any of their various phases take place (*a*) reversibly, (*b*) only in directions parallel to the equipotential surfaces of the gravitational field, and (*c*) in such a manner that volume, shape, and position of the solution are unaffected. The reasons for these restrictions will appear later.

By the *configuration of the system* we shall mean the volume, shape, and position—i.e., the complete geometrical description—of the solution and the electrodes.

DEFINITION 2. COMPONENTS

We shall classify the components of the system described above as charged components and neutral components, respectively. The charged components are regarded as arising from the dissociation of electrolyte components. A detailed account of this classification has been given by the author elsewhere (15); here it suffices to recall that in general the number of charged components in a system is one greater than the number of electrolyte components. We shall refer to electrolyte components by the symbol *el*, to neutral components by the symbol *nt*, to charged and neutral components indiscriminately by the symbol *i*.

AUXILIARY ASSUMPTION 1. SUBPHASES AND GIBBSIAN EQUATIONS

We shall assume that the system described above behaves as if made up of infinitesimal electrically neutral regions—to be called subphases—each of which is at each instant subject to the fundamental thermodynamic equations of Gibbsian type obeyed by electrically conducting systems in complete equilibrium in an external gravitational field. Of these Gibbsian equations, which have been deduced elsewhere by the author (16), we shall here use only that for the Helmholtz free energy A; this equation may be written in the form:

$$\mathrm{d}(\delta A) = -\delta S \mathrm{d}T - P\mathrm{d}(\delta V) + \delta M \mathrm{d}\varphi + \sum_i \mu_i \mathrm{d}(\delta n_i) \tag{1}$$

Here S denotes entropy, T temperature, P pressure, V volume, M mass, φ gravitational potential, μ_i the potential (total potential) per mole of component i, and n_i a number of moles of i. The symbol d refers to an *infinitesimal change in the value* of the quantity following it, and the symbol δ to the *infinitesimal value, for the subphase,* of the (extensive) variable following it. The assumption of the electroneutrality of the subphases means that the quantities δn_i in equation 1 are subject to the restriction

$$\sum_i z_i \delta n_i = 0 \tag{2}$$

where

$$z_i = \begin{cases} \text{the valence, with regard to sign, of the component } i \text{ if it is charged} \\ \text{zero, if the component } i \text{ is neutral} \end{cases} \tag{3}$$

Division of equation 2 by δV yields the electroneutrality condition in a form needed later: namely,

$$\sum_i z_i c_i = 0 \tag{4}$$

where c_i is the concentration of i in moles per unit volume.

DEFINITION 3. HYDROSTATIC AND THERMAL EQUILIBRIUM

For fluids in complete equilibrium the conditions for hydrostatic equilibrium in a gravitational field and for thermal equilibrium are, respectively,

$$\operatorname{grad} P + \rho \operatorname{grad} \varphi = 0 \tag{5}$$

$$\operatorname{grad} T = 0 \tag{6}$$

where ρ denotes density. For a fluid undergoing diffusion and therefore not in complete equilibrium, we accordingly *define* hydrostatic and thermal equilibrium by equations 5 and 6. The physical meaning of these equations is then as follows: Equation 5 requires that in spite of the irreversible processes, bulk movement is reversible, i.e., such that at each instant the hydrostatic force on a subphase balances the gravitational force; equation 6 requires that in spite of the irreversible processes, flow of heat is reversible, i.e., isothermal.

DEFINITION 4. ELECTROCHEMICAL STATE AND CHEMICAL STATE

The electrochemical state of a subphase we shall regard as defined by the set of variables

$$T, \varphi, \mu_i \tag{7}$$

or any set sufficient to fix the set 7. The chemical state of a subphase we shall regard as defined by the set of variables

$$T, \varphi, \mu_{el}, \mu_{nl} \tag{8}$$

or any set sufficient to fix the set 8. The concepts involved in these definitions have been explained by E. A. Guggenheim (4, 7, 8) and by E. Lange and K. P. Miscenko (17).

AUXILIARY ASSUMPTION 2. CHEMICAL STATE DETERMINED BY ELECTROCHEMICAL STATE

In a system in complete equilibrium the potentials, μ_{el}, of the electrolyte components are determined by the potentials of the charged components through equilibrium conditions, and therefore the chemical state is determined by the electrochemical state. The converse of this is of course not true, simply because the number of variables in the set 7 is one greater than that in the set 8. We shall assume that in each subphase of the diffusing solution here considered, the chemical state is at each instant fixed by the electrochemical state through equilibrium between the charged and the electrolyte components.

DEFINITION 5. NOTATION FOR ELECTRODE PROCESS AND ELECTROCHEMICAL EQUILIBRIUM

For the purposes in hand we need to describe electrode processes in a form somewhat out of the ordinary. We classify the components participating in the electrode process at any electrode, say α, into (*i*) the electron, El^-, which is added to or removed from the metals in α by the process; (*ii*) the other components added to or removed from any of the phases of α by the process; (*iii*) the components, charged and neutral, added to or removed from the contiguous layer of solution β by the process. We denote the chemical formula of any of the components *ii* by X_q, and of any of the components *iii* by X_r, and write the chemical equation for the electrode process in the form

$$[\sum_r \nu_r X_r]^\beta = [\sum_q \nu_q X_q]^\alpha + [El^-]^\alpha \tag{9}$$

where ν_q, ν_r are stochiometric coefficients of proper sign and the meaning of the superscripts α and β is obvious. If the positive current passes from α to β, the process proceeds from left to right and *vice versa.* Since the electric charge entering or leaving β through α is equivalent to the charge carried by the electrons produced or consumed in α, the coefficients ν_r are subject to the condition

$$\sum_r z_r \nu_r = -1 \tag{10}$$

It is furthermore evident that the terms $[\sum \nu_q X_q]^\alpha$ in equation 9 represent the net amounts of *all electrolyte components and neutral components* gained by α when one faraday of positive electricity passes from α to β (or lost by α when one faraday of positive electricity passes from β to α). We may illustrate these principles by writing equation 9 for the particular case of the electrode Hg | HgO in contact with a basic aqueous solution:

$$OH^- - \tfrac{1}{2}H_2O = \tfrac{1}{2}HgO - \tfrac{1}{2}Hg + El^- \tag{11}$$

If the electrode process is reversible, the electrode α is in electrochemical equilibrium with the solution β and equation 9 permits us to write the equilibrium condition in the form

$$\sum_r \nu_r \mu_r^\beta = \sum_q \nu_q \mu_q^\alpha + \mu_{El^-}^\alpha \tag{12}$$

For the electrode α of the system postulated by definition 1 above we shall accordingly have equations 9, 10, 12, and for the electrode α' the analogous equations

$$[\sum_{r'} \nu_{r'} X_{r'}]^{\beta'} = [\sum_{q'} \nu_{q'} X_{q'}]^{\alpha'} + [El^-]^{\alpha'} \tag{13}$$

$$\sum_{r'} z_{r'} \nu_{r'} = -1 \tag{14}$$

$$\sum_{r'} \nu_{r'} \mu_{r'}^{\beta'} = \sum_{q'} \nu_{q'} \mu_{q'}^{\alpha'} + \mu_{\mathrm{El}^-}^{\alpha'} \tag{15}$$

where the components $X_{q'}$, $X_{r'}$ are in general not the same as X_q, X_r.

DEFINITION 6. FLOW VECTORS AND CURRENT VECTOR

To each of the charged and neutral components of the diffusing solution here considered we assign a flow vector, $\vec{\Phi}_i$, whose direction at any point is the direction of the flow of the component at that point, and whose magnitude is given by the number of moles of the component crossing a fixed infinitesimal plane normal to the direction of the flow, per unit area and per second. We also assign to each point of the solution a current vector $\vec{I}$, whose direction is that of the positive electric current and whose magnitude is given by the number of faradays of electricity crossing an infinitesimal plane normal to the direction of the current, per unit area and per second. From the fact that the electric current results from the flow of charged components, it is readily shown that

$$\vec{I} = \sum_i z_i \vec{\Phi}_i \tag{16}$$

The values of $\vec{\Phi}_i$ and $\vec{I}$ for any case in which the current *between the electrodes α and α′* is zero, we shall denote by $\vec{\Phi}_i^{\mathrm{spont}}$ and $\vec{I}^{\mathrm{spont}}$, respectively, to indicate that the movement of the components is due to spontaneous diffusion alone. It is worth recalling that although $\vec{I}^{\mathrm{spont}} = 0$ in certain simple spontaneously diffusing solutions, as for instance those with cylindrical symmetry, it is not true that $\vec{I}^{\mathrm{spont}} = 0$ in general. Thus in the ring-shaped solution with three liquid–liquid junctions, which has been studied by Dolezalek and Krüger (2), diffusion proceeds in such a way that there is an electric current around the ring.

THE ASSUMPTION OF QUASI-REVERSIBLE CONDUCTION (QRC. ASSUMPTION)

In the system postulated by definition 1 let the electric current between the electrodes α and α' be zero, and let diffusion proceed spontaneously, keeping volume, shape, and position of the solution constant. Owing to the continual change of composition at each point of the solution, there will be a continual change of pressure at each point of the system, and this will in turn produce a continual change in the volumes of the electrodes α and α', which volume change, according to restriction *iv* of definition 1, will take place reversibly and parallel to the gravitational equipotentials. At each instant the system is in a definite state characterized by (*i*) a definite configuration, (*ii*) definite values of the variables 7 and therefore a definite electrochemical state at each point, (*iii*) definite values of the variables 8 and therefore a definite chemical state at each point, and (*iv*) definite values of the vectors $\vec{\Phi}_i$ and $\vec{I}$ at each point. We select the system at an arbitrary instant, and let Z^{spont} denote its state at this instant, as characterized by *i*, *ii*, *iii*, and *iv*. We then consider the course of events during the infinitesimal time interval dt, following the instant at which the system is in Z^{spont}. During dt there occurs a change in the Helmholtz free energy, A, of the system, which we denote by $\mathrm{d}A^{\text{spont}}$. Since electrodes and solution are both changing, we may write

$$\mathrm{d}A^{\text{spont}} = \mathrm{d}A^{\alpha,\text{spont}} + \mathrm{d}A^{\alpha',\text{spont}} + \mathrm{d}A^{\text{soln},\text{spont}} \tag{17}$$

where the superscript "soln" indicates solution. During dt, furthermore, the surroundings do a quantity of work upon the system because of the volume changes of the electrodes; let $\mathrm{d}w^{\text{spont}}$ denote this quantity of work. Since the volume changes are reversible we have

$$\mathrm{d}w^{\text{spont}} = -[\sum P\mathrm{d}(\delta V)]^{\alpha,\text{spont}} - [\sum P\mathrm{d}(\delta V)]^{\alpha',\text{spont}} \tag{18}$$

where the two summations are extended over all the subphases of α and α', respectively.

Now we consider the system when a steady infinitesimal electric current is flowing through the solution from α to α' while at the same time spontaneous diffusion is proceeding. We suppose volume, shape, and position of the solution to be the same as before and to be held constant. We assume that the flow of current is brought about by the continual reversible and isothermal transfer of an equivalent quantity of electrons *externally* from the metal in α to the metal in α' or *vice versa.* Under these conditions there is a continual change of composition at each point of the solution due to (*i*) spontaneous diffusion, (*ii*) transport of components by the current, and (*iii*) change in chemical content of the solution by the electrode processes. This change of composition produces as before a continual change of pressure at each point of the system. Owing partly to this change of pressure and partly to the change in chemical content of the electrodes by the electrode processes, the electrodes again suffer a continual volume change which is reversible and parallel to the gravitational equipotentials. We now assume that the system has been so arranged that at some instant it passes through a *state Z^* which has exactly the same configuration as the state Z^{spont} and exactly the same chemical state at each point as Z^{spont}.* Since the electrode current is infinitesimal, Z^* will differ infinitesimally from Z^{spont} in (*i*) the electrochemical state at each point and (*ii*) the vectors $\vec{\Phi}_i$ and $\vec{I}$ at each point. During the infinitesimal time interval dt following the instant in which the system is in Z^*, there occurs a change in Helmholtz free energy which we denote by $\mathrm{d}A^*$ and for which we may evidently write

$$\mathrm{d}A^* = \mathrm{d}A^{\alpha,*} + \mathrm{d}A^{\alpha',*} + \mathrm{d}A^{\mathrm{soln},*} \tag{19}$$

The work done by the surroundings upon the system is due partly to the volume changes of the electrodes, and partly to the external transfer of the electrons; let $\mathrm{d}w^*$ denote the quantity of this work during $\mathrm{d}t$. Since the work is done isothermally and reversibly we have, according to well-known principles of thermodynamics,

$$\mathrm{d}w^* = -[\sum P\mathrm{d}(\delta V)]^{\alpha,*} - [\sum P\mathrm{d}(\delta V)]^{\alpha',*} - (\mu_{\mathrm{El}^-}^{\alpha',*} - \mu_{\mathrm{El}^-}^{\alpha,*})\,\mathrm{d}\xi \tag{20}$$

where $\mathrm{d}\xi$ is the number of moles of electrons transferred during $\mathrm{d}t$ from α to α'.

Our principal assumption consists in setting

$$\mathrm{d}A^* - \mathrm{d}A^{\mathrm{spont}} = \mathrm{d}w^* - \mathrm{d}w^{\mathrm{spont}} \tag{21}$$

That is, we treat the work, $\mathrm{d}w^* - \mathrm{d}w^{\mathrm{spont}}$, *due solely to the flow of an infinitesimal electrode current,* as if this flow constituted a reversible process. In reality the flow of electrode current superimposed upon spontaneous diffusion is not reversible in the ordinary sense, because after the system has once passed through the state Z^*, this state can obviously not be restored by reversing the direction of the electrode current. For this reason we shall refer to the assumption expressed by equation 21 as the assumption of *quasi-reversible* conduction, or qrc. assumption. The qrc. assumption appears to constitute a natural means of avoiding the artificiality of treatment noted in section I above.

The question might arise whether the artificiality in question could not also be avoided by sending through the solution, instead of an infinitesimal current, a finite current of such magnitude that during the time $\mathrm{d}t$

$$|\,\mathrm{d}A^*\,| \gg |\,\mathrm{d}A^{\mathrm{spont}}\,| \tag{22}$$

$$|\,\mathrm{d}w^*\,| \gg |\,\mathrm{d}w^{\mathrm{spont}}\,| \tag{23}$$

so that instead of equation 21 we could write

$$\mathrm{d}A^* \sim \mathrm{d}w^* \tag{24}$$

which would enable us without artificiality to regard the solution to a first approximation as "frozen." This question must, however, be answered in the negative, because for a finite current, the heat irreversibly generated is no longer negligible. This heat is evidently of the order of

$$\left(\frac{\mathrm{d}\xi}{\mathrm{d}t}\right)^2 \mathrm{d}t, \quad \text{i.e.,} \quad \frac{\mathrm{d}\xi}{\mathrm{d}t}\,\mathrm{d}\xi$$

In order that the process be treated as reversible, this quantity of heat must, as Helmholtz (11) first pointed out, be negligible compared with $\mathrm{d}\xi$ itself. But obviously this is the case only if $\mathrm{d}\xi/\mathrm{d}t$, i.e., the current, is infinitesimal.

By substitution of equations 17, 18, 19, 20 into equation 21 we obtain the qrc. assumption in more expanded form:

$$\begin{aligned}(\mathrm{d}A^{\alpha,*} - \mathrm{d}A^{\alpha,\mathrm{spont}}) + (\mathrm{d}A^{\alpha',*} - \mathrm{d}A^{\alpha',\mathrm{spont}}) + (\mathrm{d}A^{\mathrm{soln},*} - \mathrm{d}A^{\mathrm{soln,spont}}) \\ = (\mu_{\mathrm{El}^-}^{\alpha',*} - \mu_{\mathrm{El}^-}^{\alpha,*})\mathrm{d}\xi - [\textstyle\sum P\mathrm{d}(\delta V)]^{\alpha,*} - [\textstyle\sum P\mathrm{d}(\delta V)]^{\alpha',*} \\ + [\textstyle\sum P\mathrm{d}(\delta V)]^{\alpha,\mathrm{spont}} + [\textstyle\sum P\mathrm{d}(\delta V)]^{\alpha',\mathrm{spont}} \qquad (25)\end{aligned}$$

Equation 25 serves as the starting point for the deduction of the qrc. condition (section III below).

AUXILIARY ASSUMPTION 3. CONCERNING THE CHANGE OF FLOW VECTORS PRODUCED BY AN INFINITESIMAL ELECTRODE CURRENT

Let $\vec{\Phi}_i^{\mathrm{spont}}$ and $\vec{I}^{\mathrm{spont}}$ now denote the values of $\vec{\Phi}_i$ and $\vec{I}$ in the particular state Z^{spont}, and $\vec{\Phi}_i^*$ and $\vec{I}^*$ the values in the corresponding state Z^*. Then the infinitesimal vectors $\partial\vec{\Phi}_i$ and $\partial\vec{I}$, defined by

$$\partial\vec{\Phi}_i = \vec{\Phi}_i^* - \vec{\Phi}_i^{\mathrm{spont}} \qquad (26)$$

$$\partial\vec{I} = \vec{I}^* - \vec{I}^{\mathrm{spont}} \qquad (27)$$

may evidently be regarded as the contributions of the infinitesimal electrode current to the vectors $\vec{\Phi}_i^*$ and $\vec{I}^*$, respectively.[2] From equations 16, 26, and 27 it follows that

$$\partial\vec{I} = \sum_i z_i \partial\vec{\Phi}_i \qquad (28)$$

We now make the reasonable assumption that any one of the infinitesimal vectors $\partial\vec{\Phi}_i$ at a given point is either parallel or antiparallel to any other. From this assumption and equation 28 it then follows that the infinitesimal vector $\partial\vec{I}$ is either parallel or antiparallel to any given $\partial\vec{\Phi}_i$.

DEFINITION 7. TRANSPORT NUMBERS

For a given state Z^{spont}, we may now define the transport number t_i of any charged or neutral component at each point of the solution by the equation

$$\bar{z}_i \partial\vec{\Phi}_i + \bar{z}_i c_i \partial\vec{v} = t_i \partial\vec{I} \qquad (29)$$

---

[2] The symbol ∂ used here has no connection with partial differentiation; its purpose is merely to distinguish infinitesimals arising from comparison of the states Z^* and Z^{spont} from (*i*) infinitesimals arising from change of state during $\mathrm{d}t$ and here denoted by d, and from (*ii*) infinitesimals arising from the extension of a subphase and here denoted by δ.

where $\overrightarrow{\partial v}$ is an infinitesimal vector of arbitrary magnitude either parallel or antiparallel to $\overrightarrow{\partial I}$, and

$$\bar{z}_i = \begin{cases} z_i, \text{ if the component } i \text{ is charged} \\ \text{unity, if the component } i \text{ is neutral} \end{cases} \tag{30}$$

In order that equation 29 lead to particular values of t_i at any point, the magnitude and sense of the vector $\partial\vec{v}$ must in general be fixed by some suitable convention, such as that of assigning an arbitrary numerical value to the transport number of a particular component.

AUXILIARY ASSUMPTION 4. TRANSPORT NUMBERS ARE SCALAR FUNCTIONS OF PRESSURE, TEMPERATURE AND COMPOSITION

We now assume that at any interior point of the diffusing solution here considered, the values of t_i, fixed at that point by any convention for $\partial\vec{v}$ depend only on this convention and on the pressure, the temperature, and the composition at the point. That is, we assume the t_i to be scalars, which, when pressure, temperature, composition, and the convention for $\partial\vec{v}$ are fixed, are independent of (*i*) the configuration of the system, (*ii*) the electrode processes, (*iii*) the gradients of the variables 7 defining the electrochemical state, (*iv*) the magnitudes and directions of the vectors $\vec{\Phi}_i^{\text{spont}}$, $\vec{\Phi}_i^*$, and therefore of $\vec{I}^{\text{spont}}$, $\vec{I}^*$, and (*v*) the rate at which the electrochemical state is changing. Since P, T, and composition at a point are fixed when the variables 8 defining the chemical state are fixed at the point, it follows that the t_i are functions of the *chemical* state.

We shall now show that by virtue of this assumption the novel definition of transport number here adopted leads directly to the usual definition of Hittorf number. Consider the special case of a long cylindrical tube filled with a chemically uniform aqueous solution and fitted at the two ends with electrodes which are movable so that the volume of the solution may be kept constant when an infinitesimal current flows. Suppose gravitational effects to be negligible. If we set $t_{H_2O} = 0$ and $\bar{z}_{H_2O} = 1$ we obtain from equation 29 for $\partial\vec{v}$

$$\partial\vec{v} = -\frac{\partial\vec{\Phi}_{H_2O}}{c_{H_2O}} \tag{31}$$

and hence for the transport number of any component i

$$t_i = \frac{\bar{z}_i\,\partial\vec{\Phi}_i - \bar{z}_i c_i \dfrac{\partial\vec{\Phi}_{H_2O}}{c_{H_2O}}}{\partial\vec{I}} \tag{32}$$

According to our assumption the t_i so determined are the same regardless of the nature of the electrodes. Suppose now we choose a special pair of electrodes such that, while the current flows, the pressure in the solution remains constant. Then the expression on the right-hand side of equation 32 is the Hittorf number of i. To prove this, we imagine a plane which is normal to the cylinder axis and can move parallel to this axis with a velocity $\partial\vec{v}_i$ such that, while the current flows, none of the component i passes through the plane. Then evidently

$$c_i\partial\vec{v}_i = \partial\vec{\Phi}_i \tag{33}$$

$$c_{H_2O}\partial\vec{v}_{H_2O} = \partial\vec{\Phi}_{H_2O} \tag{34}$$

and equation 32 becomes

$$t_i = \frac{z_i c_i(\partial\vec{v}_i - \partial\vec{v}_{H_2O})}{\partial\vec{I}}. \tag{35}$$

But the expression on the right-hand side of equation 35 is clearly equal to the ratio of the number of equivalents of i *moved through the water* to the number of faradays of electricity moved through the tube (with due regard to the directions of these movements and, if i is charged, to the sign of the charge) at constant pressure, i.e., it is equal to the Hittorf number of i.

It may be remarked that if one dispenses with auxiliary assumptions 3 and 4, it is still possible to define transport numbers by equation 29, but that such transport numbers will be tensors rather than scalars.

AUXILIARY ASSUMPTION 5 AND DEFINITION 8. SPECIFIC ELECTROLYTIC FLOW VECTORS AND SPECIFIC ELECTROLYTIC CURRENT VECTORS

When the state Z^{spont} is fixed, the infinitesimal vectors $\partial\vec{\Phi}_i$ evidently depend upon the magnitude of the total infinitesimal electrode current, $d\xi/dt$, in the corresponding state Z^*. We now introduce the reasonable assumptions that (*i*) the magnitude of $\partial\vec{\Phi}_i$ is an infinitesimal of the same order as $d\xi/dt$, (*ii*) configuration of the system and chemical state at each point being fixed, the *direction* of $\partial\vec{\Phi}_i$ at any point is *independent* of $d\xi/dt$, and the *magnitude* of $\partial\vec{\Phi}_i$ is *directly proportional* to $d\xi/dt$. In analytical form these assumptions are

$$\partial\vec{\Phi}_i = \vec{\Psi}_i\frac{d\xi}{dt} \tag{36}$$

where $\vec{\Psi}_i$ is a finite vector whose direction and magnitude at *any* point depend upon the configuration of the system and upon the chemical state at *all* points. From equations 36 and 28 we deduce

$$\partial\vec{I} = \vec{J}\frac{d\xi}{dt} \tag{37}$$

where $\vec{J}$ is a finite vector given by

$$\vec{J} = \sum_i z_i \vec{\Psi}_i \tag{38}$$

and is thus determined at any point by the configuration of the system and the chemical state at all points. From equations 36, 37, and 29 it is evident that $\vec{J}$ and the $\vec{\Psi}_i$ are related not only by equation 38 but also by the equations

$$z_i \vec{\Psi}_i = t_i^{[0]} \vec{J} \tag{39}$$

where the $t_i^{[0]}$ are the transport numbers under the particular convention $\partial \vec{v} = 0$. We shall call the $\vec{\Psi}_i$ the specific electrolytic flow vectors and $\vec{J}$ the specific electrolytic current vector. We point out that equation 37 shows the assumptions leading to $\vec{\Psi}_i$ and $\vec{J}$ to be in accord with the requirement of Ohm's law, to the effect that the tubes of equal electric flow through a conductor be independent of the total current (superposition principle of conduction; Helmholtz, 1853 (12)).

To illustrate the principles involved we calculate the vectors $\vec{\Psi}_i$ and $\vec{J}$ for the case of cylindrical symmetry. Since $\partial \vec{I}$ is everywhere constant we have

$$\vec{q} \cdot \partial \vec{I} = \frac{d\xi}{dt} \tag{40}$$

where $\vec{q}$ is the cross-section vector in the direction from α to α'. By comparison with equation 37 it follows that

$$\vec{J} = \vec{q}^{\,-1} \tag{41}$$

where $\vec{q}^{\,-1}$ has the direction from α to α'. For $\vec{\Psi}_i$ we obtain by equation 39

$$\vec{\Psi}_i = \frac{t_i^{[0]}}{z_i} \vec{q}^{\,-1} \tag{42}$$

For this simple case, therefore, $\vec{\Psi}_i$ at a point is a function of the configuration and of the chemical state only at *that* point, rather than at *all* points, and $\vec{J}$ is a function of the configuration alone.

DEFINITION 9. ELECTROCHEMICALLY LAMELLAR AND CHEMICALLY LAMELLAR SOLUTIONS

We shall call a mass of solution electrochemically lamellar if through each point at which any of the variables 7 have finite gradients, there passes one and only one surface over which the electrochemical state is constant, and chemically lamellar if through each point at which any of the variables 8 have finite gradients, there passes one and only one surface over which the chemical state is constant. Liquid-liquid junctions with cylindrical symmetry represent a special case of chemical lamellarity.

DEFINITION 10. SIMPLY AND MULTIPLY CONNECTED SOLUTIONS

We shall need to apply to the solution postulated by definition 1 the mathematical concepts of simple and multiple connectivity. We shall call a solution simply connected if any two paths joining any two fixed points within the solution can be made to coincide by continuous deformation without ever cutting a boundary of the solution; otherwise we shall say the solution is multiply connected. Ordinarily the solutions in galvanic cells are simply connected. An interesting example of a multiply connected solution is the ring-shaped system of Dolezalek and Krüger (2) mentioned above.

AUXILIARY ASSUMPTION 6. CONCERNING SIMPLY CONNECTED CHEMICALLY LAMELLAR SOLUTIONS

Since chemical state is determined by electrochemical state, every electrochemically lamellar solution is chemically lamellar. But the converse of this is not true, for whenever an electric current is sent through a chemically lamellar solution in any direction save that normal to the surfaces of constant chemical state, the solution is surely not electrochemically lamellar. We shall however assume that in the *absence of currents between electrodes*, every *simply connected chemically lamellar* solution is also electrochemically lamellar.

III. DEDUCTION OF THE CONDITION FOR QUASI-REVERSIBLE CONDUCTION

DEDUCTION OF THE QRC. CONDITION IN GENERAL FORM

The qrc. condition is obtained by transforming equation 25 with the help of some of the foregoing definitions and auxiliary assumptions. We begin by using equation 1 to calculate the terms on the left-hand side of equation 25. Since all changes are isothermal, the results will contain no terms in dT.

Scrutinizing the electrodes α, α' we note that since their volume changes occur in directions parallel to the gravitational equipotentials (definition 1), we have $d\varphi = 0$ for each of the subphases. We also note, with the help of equations 9 and 13, that when $d\xi$ moles of electrons are transferred from α to α', the electrode α *gains* $\nu_q d\xi$ moles of each of the (electrolyte or neutral) components X_q and electrode α' *loses* $\nu_{q'} d\xi$ moles of each of the (electrolyte or neutral) components $X_{q'}$. Equation 1 accordingly yields for the electrodes

$$\mathrm{d}A^{\alpha,\mathrm{spont}} = -[\sum P\mathrm{d}(\delta V)]^{\alpha,\mathrm{spont}} \tag{43}$$

$$\mathrm{d}A^{\alpha',\mathrm{spont}} = -[\sum P\mathrm{d}(\delta V)]^{\alpha',\mathrm{spont}} \tag{44}$$

$$\mathrm{d}A^{\alpha,*} = -[\sum P\mathrm{d}(\delta V)]^{\alpha,*} + \sum_q \nu_q \mu_q^{\alpha,*}\,\mathrm{d}\xi \tag{45}$$

$$\mathrm{d}A^{\alpha',*} = -[\sum P\mathrm{d}(\delta V)]^{\alpha',*} - \sum_{q'} \nu_{q'} \mu_{q'}^{\alpha',*}\,\mathrm{d}\xi \tag{46}$$

Turning to the solution, we note that since its volume, shape, and position remain constant (qrc. assumption), the volume δV and the gravitational potential φ of each subphase may be taken as constant. Equation 1 therefore yields for each subphase of the solution

$$\mathrm{d}(\delta A)^{\mathrm{soln,spont}} = \sum_i \mu_i^{\mathrm{soln,spont}}\,\mathrm{d}(\delta n_i)^{\mathrm{soln,spont}} \tag{47}$$

$$\mathrm{d}(\delta A)^{\mathrm{soln},*} = \sum_i \mu_i^{\mathrm{soln},*}\,\mathrm{d}(\delta n_i)^{\mathrm{soln},*} \tag{48}$$

Since δV is constant we have, furthermore,

$$\mathrm{d}(\delta n_i)^{\mathrm{soln,spont}} = \mathrm{d}c_i^{\mathrm{soln,spont}}\,\delta V \tag{49}$$

$$\mathrm{d}(\delta n_i)^{\mathrm{soln},*} = \mathrm{d}c_i^{\mathrm{soln},*}\,\delta V \tag{50}$$

Substitution of equations 49 and 50 into equations 47 and 48, and integration over the volume, V, of the solution gives

$$\mathrm{d}A^{\mathrm{soln,spont}} = \int_V \mu_i^{\mathrm{soln,spont}}\,\mathrm{d}c_i^{\mathrm{soln,spont}}\,\delta V \tag{51}$$

$$\mathrm{d}A^{\mathrm{soln},*} = \int_V \mu_i^{\mathrm{soln},*}\,\mathrm{d}c_i^{\mathrm{soln},*}\,\delta V \tag{52}$$

When equations 43, 44, 45, 46, 51, and 52 are substituted into equation 25, the terms in $P\mathrm{d}(\delta V)$ cancel and we are left with

$$\int_V \sum_i (\mu_i^{\mathrm{soln},*}\,\mathrm{d}c_i^{\mathrm{soln},*} - \mu_i^{\mathrm{soln,spont}}\,\mathrm{d}c_i^{\mathrm{soln,spont}})\delta V$$
$$= (\mu_{\mathrm{El}^-}^{\alpha',*} + \sum_{q'} \nu_{q'}\mu_{q'}^{\alpha',*} - \mu_{\mathrm{El}^-}^{\alpha,*} - \sum_q \nu_q \mu_q^{\alpha,*})\,\mathrm{d}\xi \tag{53}$$

Since at each point of Z^* the chemical state is the same as at the corresponding point of Z^{spont} (qrc. assumption) and since X_q, $X_{q'}$ are electrolyte or neutral components, we have

$$\mu_q^{\alpha,*} = \mu_q^{\alpha,\mathrm{spont}} \tag{54}$$

$$\mu_q^{\alpha',*} = \mu_q^{\alpha',\mathrm{spont}} \tag{55}$$

Since at each point of Z^* the electrochemical state differs infinitesimally from that at the corresponding point of Z^{spont} (qrc. assumption), we have, furthermore,

$$\mu_{\mathrm{El}^-}^{\alpha,*} = \mu_{\mathrm{El}^-}^{\alpha,\mathrm{spont}} + \partial\mu_{\mathrm{El}^-}^{\alpha} \tag{56}$$

$$\mu_{\mathrm{El}^-}^{\alpha',*} = \mu_{\mathrm{El}^-}^{\alpha',\mathrm{spont}} + \partial\mu_{\mathrm{El}^-}^{\alpha'} \tag{57}$$

$$\mu_i^{\mathrm{soln},*} = \mu_i^{\mathrm{soln},\mathrm{spont}} + \partial\mu_i^{\mathrm{soln}} \tag{58}$$

with $\partial\mu_i^{\mathrm{soln}} = 0$ for such of the i as are neutral components. Substitution of equations 54 to 58 into equation 53 gives, after neglect of infinitesimals of higher order,

$$\begin{aligned}\int_V \sum_i \mu_i^{\mathrm{soln},\mathrm{spont}} (\mathrm{d}c_i^{\mathrm{soln},*} - \mathrm{d}c_i^{\mathrm{soln},\mathrm{spont}})\delta V \\ = \Big(\mu_{\mathrm{El}}^{\alpha',\mathrm{spont}} + \sum_{q'} \nu_{q'}\mu_{q'}^{\alpha',\mathrm{spont}} - \mu_{\mathrm{El}^-}^{\alpha,\mathrm{spont}} - \sum_q \nu_q\mu_q^{\alpha,\mathrm{spont}}\Big)\,\mathrm{d}\xi\end{aligned} \tag{59}$$

Since the changes in c_i^{soln} are due to the action of the flow vectors $\vec{\Phi}_i$ over the time dt, we have, referring to equation 26,

$$\mathrm{d}c_i^{\mathrm{soln},\mathrm{spont}} = -\mathrm{d}t \operatorname{div} \vec{\Phi}_i^{\mathrm{spont}} \tag{60}$$

$$\mathrm{d}c_i^{\mathrm{soln},*} = -\mathrm{d}t \operatorname{div} \vec{\Phi}_i^* \tag{61}$$

$$\begin{aligned}\therefore \mathrm{d}c_i^{\mathrm{soln},*} - \mathrm{d}c_i^{\mathrm{soln},\mathrm{spont}} &= -\mathrm{d}t(\operatorname{div} \vec{\Phi}_i^* - \operatorname{div} \vec{\Phi}_i^{\mathrm{spont}}) \\ &= -\mathrm{d}t \operatorname{div} (\vec{\Phi}_i^* - \vec{\Phi}_i^{\mathrm{spont}}) \\ &= -\mathrm{d}t \operatorname{div} \partial\vec{\Phi}_i\end{aligned} \tag{62}$$

Henceforth we shall need to consider only the state Z^{spont}, and can therefore dispense with the superscript "spont." We shall also omit as no longer necessary the superscript "soln." With the notation thus simplified, substitution of equation 62 into equation 59 yields

$$-\mathrm{d}t \int_V \sum_i \mu_i \operatorname{div} \partial\vec{\Phi}_i\delta V = \Big(\mu_{\mathrm{El}}^{\alpha'} + \sum_{q'} \nu_{q'}\mu_{q'}^{\alpha'} - \mu_{\mathrm{El}^-}^{\alpha} - \sum_q \nu_q\mu_q^{\alpha}\Big)\,\mathrm{d}\xi \tag{63}$$

Since the electrodes are in electrochemical equilibrium (definitions 1, 5), equations 12 and 15 apply; introduction of these into equation 63 yields

$$-\mathrm{d}t \int_V \sum_i \mu_i \operatorname{div} \partial\vec{\Phi}_i\delta V = \Big(\sum_{r'} \nu_{r'}\mu_{r'}^{\beta'} - \sum_r \nu_r\mu_r^{\beta}\Big)\,\mathrm{d}\xi \tag{64}$$

Equation 64 reduces to the desired qrc. condition when the volume integral is transformed as follows. First we write

$$\begin{aligned}-\mathrm{d}t \int_V \sum_i \mu_i \operatorname{div} \partial\vec{\Phi}_i\delta V = -\,\mathrm{d}t \int_V \operatorname{div} \sum_i \mu_i\partial\vec{\Phi}_i\delta V \\ + \mathrm{d}t \int_V \sum_i \partial\vec{\Phi}_i \operatorname{grad} \mu_i\delta V\end{aligned} \tag{65}$$

and then we apply Gauss' integral theorem to the first integral on the right-hand side of equation 65; we obtain

$$-\mathrm{d}t \int_V \operatorname{div} \sum_i \mu_i \overrightarrow{\partial\Phi}_i \delta V = \mathrm{d}t \int_\sigma \sum_i \mu_i \overrightarrow{\partial\Phi}_i \cdot \delta\vec{\sigma} \tag{66}$$

where σ denotes the boundary surface of the solution and $\delta\vec{\sigma}$ is the vector element of boundary surface in the direction of the *inner* normal. But the surface integral is given by

$$\mathrm{d}t \int_\sigma \sum \mu_i \overrightarrow{\partial\Phi}_i \cdot \delta\vec{\sigma} = \sum_{r'} \nu_{r'} \mu_{r'}^{\beta'} \mathrm{d}\xi - \sum_r \nu_r \mu_r^{\beta} \mathrm{d}\xi \tag{67}$$

We establish equation 67 as follows: Since matter enters or leaves the solution only at the electrodes α and α' (definition 1), the vectors $\overrightarrow{\partial\Phi}_i$ are either parallel to the boundary surface or zero at all parts of the boundary save the two parts which lie respectively between α and β and between α' and β'. It is therefore only these parts that contribute at all to the surface integral. Since β is a layer of constant electrochemical state (definition 1), each of the μ_i is constant within β and therefore all the vectors $\overrightarrow{\partial\Phi}_i$ are zero at the boundary between α and β except the vectors $\overrightarrow{\partial\Phi}_r$ of those components X_r which, owing to the reversible electrode process (equation 9), are *leaving* β in amounts $\nu_r \mathrm{d}\xi$. The contribution of the boundary between α and β is therefore given by the second term on the right-hand side of equation 67. Similarly the contribution of the boundary between α' and β', at which the components $X_{r'}$ are *entering* β' in amounts $\nu_{r'}\mathrm{d}\xi$, is given by the first term on the right-hand side of equation 67. From equations 67, 66, and 65 we obtain

$$-\mathrm{d}t \int_V \sum_i \mu_i \operatorname{div} \overrightarrow{\partial\Phi}_i \delta V = \Big[\sum_{r'} \nu_{r'} \mu_{r'}^{\beta'} - \sum_r \nu_r \mu_r^{\beta}\Big] \mathrm{d}\xi + \mathrm{d}t \int_V \sum_i \overrightarrow{\partial\Phi}_i \cdot \operatorname{grad} \mu_i \delta V \tag{68}$$

the substitution of which into equation 64 yields the qrc. condition in the form

$$\int_V \sum_i \overrightarrow{\partial\Phi}_i \cdot \operatorname{grad} \mu_i \delta V = 0 \tag{69}$$

By virtue of equation 36 we may replace the infinitesimal vectors $\overrightarrow{\partial\Phi}_i$ in equation 69 by the specific electrolytic flow vectors $\vec{\Psi}_i$, which are finite, and thus obtain the qrc. condition in the form

$$\int_V \sum_i \vec{\Psi}_i \cdot \operatorname{grad} \mu_i \delta V = 0 \tag{70}$$

Yet another useful form of the qrc. condition is obtained from equation 69 by eliminating $\partial\vec{\Phi}_i$ by means of equation 29; this gives

$$\int_V \partial\vec{I}\cdot\sum_i \frac{t_i}{\bar{z}_i}\operatorname{grad}\mu_i\delta V - \int_V \partial\vec{v}\cdot\sum_i c_i\operatorname{grad}\mu_i\delta V = 0 \qquad (71)$$

The second integral on the left-hand side of this equation however vanishes, as proved below; this leaves the desired result

$$\int_V \partial\vec{I}\cdot\sum_i \frac{t_i}{\bar{z}_i}\operatorname{grad}\mu_i\delta V = 0 \qquad (72)$$

In equation 72, finally, we may by virtue of equation 37 replace the infinitesimal vector $\partial\vec{I}$ by the specific electrolytic current vector $\vec{J}$, which is finite, and thus obtain the qrc. condition in the form

$$\int_V \vec{J}\cdot\sum_i \frac{t_i}{\bar{z}_i}\operatorname{grad}\mu_i\delta V = 0 \qquad (73)$$

To prove that the second integral on the left-hand side of equation 71 is zero, we need to recall that the equation of Gibbs–Duhem type deducible from equation 1 may be written (*cf.* 16) as

$$-\mathrm{d}P - \rho\,\mathrm{d}\varphi + s\,\mathrm{d}T + \sum_i c_i\,\mathrm{d}\mu_i = 0 \qquad (74)$$

where s denotes entropy per unit volume. Since at any instant all intensive variables vary continuously from subphase to adjacent subphase, it follows that in general in a diffusing solution

$$-\operatorname{grad}P - \rho\operatorname{grad}\varphi + s\operatorname{grad}T + \sum_i c_i\operatorname{grad}\mu_i = 0 \qquad (75)$$

Since the solution here considered is in hydrostatic and thermal equilibrium (definitions 1, 3), equations 5 and 6 apply; introduction of these into equation 75 shows our solution to be at all times subject to the requirement

$$\sum_i c_i\operatorname{grad}\mu_i = 0 \qquad (76)$$

in consequence of which the integral in question vanishes.

INVARIANCE OF THE QRC. CONDITION

We emphasize that the disappearance of the term in $\partial\vec{v}$ from equation 71 signifies that equations 72 and 73 are independent of any convention used to fix the numerical values of the t_i. A confirmatory proof of this invariance, here omitted for the sake of brevity, is readily given with the help of equation 76. The behavior of the t_i in the qrc. condition is thus very similar to that of the surface densities, Γ_i, in Gibbs' adsorption theorem (*cf.* 10).

As will be shown below, it is through the qrc. condition in the form of 72 or 73 that the transport numbers t_i enter the equations for the E.M.F. of cells with liquid-liquid junctions. Because of the invariance in question, it is in general permissible to set the transport number of a particular component equal to zero and therefore to drop the corresponding term for that component from the equations for the E.M.F. The use of the *Hittorf* numbers in the theory of liquid-liquid junctions is thus seen to be *completely justified* theoretically, but *not necessary.*

SIMPLIFICATION OF THE QRC. CONDITION FOR SIMPLY CONNECTED CHEMICALLY LAMELLAR SYSTEMS

Whenever the solution is simply connected and chemically lamellar, the general qrc. condition simplifies to

$$\int_C \sum_i \frac{t_i}{\bar{z}_i} \operatorname{grad} \mu_i \cdot \delta \vec{s} = 0 \tag{77}$$

Here C is *any* curve joining any point of β with any point of β', and $\delta\vec{s}$ is the vector element of length along this curve. The volume integral of equations 72 and 73 has thus been reduced to a line integral.

In order to prove this result we note that since the t_i are functions of chemical state alone (auxiliary assumption 4), the surfaces of constant chemical state are also surfaces of constant t_i. We note further that since in the state Z^{spont} the solution is free of currents between electrodes (qrc. assumption), the surfaces of constant chemical state are also surfaces of constant electrochemical state (auxiliary assumption 6). It follows that all the vectors grad μ_i and grad t_i are mutually parallel or antiparallel. From this conclusion we deduce

$$\begin{aligned} \operatorname{curl} \sum_i \frac{t_i}{\bar{z}_i} \operatorname{grad} \mu_i &= \sum_i \operatorname{curl} \frac{t_i}{\bar{z}_i} \operatorname{grad} \mu_i \\ &= \sum_i \left(\operatorname{grad} \frac{t_i}{\bar{z}_i} \times \operatorname{grad} \mu_i + \frac{t_i}{\bar{z}_i} \operatorname{curl} \operatorname{grad} \mu_i \right) \\ &= 0 \end{aligned} \tag{78}$$

Since the solution is simply connected it follows from equation 78 that there exists throughout the solution a single-valued function, ω, *of the coördinates,* such that at each instant

$$\sum_i \frac{t_i}{\bar{z}_i} \operatorname{grad} \mu_i = \operatorname{grad} \omega \tag{79}$$

Substitution of equation 79 into equation 72 leads to

$$\begin{aligned} 0 &= \int_V \delta\vec{I}\cdot\operatorname{grad}\omega\delta V \\ &= \int_V \operatorname{div}\omega\delta\vec{I}\delta V - \int_V \omega \operatorname{div}\delta\vec{I}\delta V \end{aligned} \tag{80}$$

But by virtue of equations 28, 26, 62, and 4 we have

$$\operatorname{div}\delta\vec{I} = \sum_i z_i \operatorname{div}\delta\vec{\Phi}_i = -\sum_i z_i \frac{dc_i^{\text{soln},*} - dc_i^{\text{soln, spont}}}{dt} = 0 \tag{81}$$

so that the second integral on the right-hand side of equation 80 vanishes. For the first integral we obtain by Gauss' theorem

$$\int_V \operatorname{div}\omega\delta\vec{I}\delta V = -\int_\sigma \omega\delta\vec{I}\cdot\delta\vec{\sigma} \tag{82}$$

Now according to equation 79 the vector grad ω is parallel or antiparallel to a given grad μ_i, and therefore the surfaces of constant μ_i are surfaces of constant ω. It then follows from considerations similar to those leading to equation 67 that

$$-\int_\sigma \omega\delta\vec{I}\cdot\delta\vec{\sigma} = (\omega^{\beta'} - \omega^{\beta})\frac{d\xi}{dt} \tag{83}$$

But again according to equation 79

$$\omega^{\beta'} - \omega^{\beta} = \int_C \sum_i \frac{t_i}{z_i}\operatorname{grad}\mu_i\cdot\delta\vec{s} \tag{84}$$

where C is any path from β to β'. It follows that, as stated above, the qrc. condition reduces to equation 77.

If the chemically lamellar solution is multiply connected, equation 78 still holds, and a function ω satisfying equation 79 still exists, but this function is not necessarily single-valued, and so Gauss' theorem, and the fundamental theorem on line integrals involved in equation 84, do not apply unqualifiedly.

REMARK ON THE APPLICATION OF THE QRC. CONDITION

It must be noted that the applicability of the qrc. condition in any of its forms is not limited to systems so arranged that the volume changes of their electrodes take place parallel to the gravitational equipotentials and that volume, shape, and position of the solution remain constant in all changes, as described under the qrc. assumption. This restriction is obviously of the nature of a scaffolding necessary for constructing the definitions of $\delta\vec{\Phi}_i$, $\delta\vec{I}$, t_i, $\vec{\Psi}_i$, $\vec{J}$, and the proof of the qrc. condition; having served this purpose, the restriction may be discarded.

IV. Application of the Condition for Quasi-reversible Conduction to Cells with Liquid–Liquid Junctions

A. PRELIMINARY CONSIDERATIONS

Nature of the problem

The objects of a thermodynamic theory of cells with liquid–liquid junctions appear to us to be twofold: (*i*) To discover if possible the manner in which the E.M.F. depends upon the chemical state at all points and upon the configuration of the system. (*ii*) To discover if possible the manner in which the respective contributions of (*a*) the two electrodes jointly and (*b*) the junction alone depend upon the chemical state at all points and upon the configuration of the system.

Hitherto these problems have been discussed only for the special case of cylindrical symmetry. For this case problem (*i*) has been completely solved, and it has been recognized that problem (*ii*) is not thermodynamically determinate except for ideal solutions. For non-ideal solutions Guggenheim has, however, obtained an important result (4, 6, 9) which we shall refer to as "Guggenheim's theorem"; it is that the E.M.F. may be expressed as the sum of (*a*) an ideal contribution from the two electrodes jointly (*b*) an ideal contribution from the junction alone, and (*c*) a "salt effect" contribution due to the deviations from ideality in every part of the solution. This theorem arises from the discussion of problem (*ii*), but is in reality the solution of problem (*i*) couched in an especially suggestive and useful form.

In the following sections we shall show how with the help of the qrc. condition, problems (*i*) and (*ii*) may be treated without the restriction to cylindrical symmetry. We shall deal first with the completely general case described under definition 1 and then with the more special case of simply connected chemically lamellar solutions. In each case we shall find that problem (*i*) is completely solvable and that the discussion of problem (*ii*) leads to Guggenheim's theorem. Finally, as a check on our general formulae, we shall deduce from them the familiar fact, first pointed out by Helmholtz (11), that in the special case of solutions consisting of a single electrolyte component and a single neutral component, the E.M.F. is independent of the structure of the junction.

Auxiliary formulae and theorems

(*i*) In what follows we shall assume that the gravitational potential is everywhere zero, so that P may be taken as constant throughout the system. In that case the potentials of the electrolyte components and the neutral components *of the electrodes* become functions of P and T alone and therefore we may write

$$\sum_{q} \nu_q \mu_q^{\alpha} - \sum_{q'} \nu_{q'} \mu_{q'}^{\alpha'} = B(P, T) \tag{85}$$

(*ii*) We shall need the formula

$$\operatorname{div} \vec{J} = 0 \tag{86}$$

which follows immediately from equations 81 and 37.

(*iii*) We shall need the formula

$$\sum_i \frac{z_i t_i}{\bar{z}_i} = 1 \tag{87}$$

which is obtained by multiplying equation 29 by $z_i/\bar{z}_i$, summing over all i, and comparing the result with equations 4 and 28.

(*iv*) We shall need the well-known formulae

$$\mu_i = \tau_i + z_i F \psi \tag{88}$$

$$\tau_i = \tau_i^0(P, T) + RT \log N_i + RT \log f_i \tag{89}$$

Here τ_i is a function of P, T, and composition and therefore of the chemical state, ψ a function of the electrochemical state called the electric potential, $\tau_i^0(P, T)$ a function of P and T, N_i the mole fraction of the component i, f_i the activity coefficient of the component i (a function of P, T, and composition and therefore of the chemical state), and F Faraday's equivalent.[3] Guggenheim has repeatedly emphasized (7, 4, 6, 3, 8) that the functions τ_i and f_i for charged components and the function ψ are indeterminate, because neither experiment nor thermodynamic theory yields any relation among these functions which is independent of equations 88, 89.

(*v*) We shall need the fact that the E.M.F., $E^{\alpha\alpha'}$, of the electrode α with respect to the electrode α', is always given by

$$FE^{\alpha\alpha'} = \overset{\alpha'}{\mu}_{\mathrm{El}^-} - \overset{\alpha}{\mu}_{\mathrm{El}^-} \tag{90}$$

(*vi*) We shall for simplicity assume that the *terminal* metals of the two electrodes α and α' are *identical*; this obviously causes no loss of generality. Denoting the terminal metal of α by I and that of α' by II, we have, since τ_i depends on chemical state alone,

$$\overset{\mathrm{I}}{\tau}_{\mathrm{El}^-} - \overset{\mathrm{II}}{\tau}_{\mathrm{El}^-} = 0 \tag{91}$$

Furthermore, since now

$$\overset{\alpha}{\mu}_{\mathrm{El}^-} = \overset{\mathrm{I}}{\mu}_{\mathrm{El}^-}, \quad \overset{\alpha'}{\mu}_{\mathrm{El}^-} = \overset{\mathrm{II}}{\mu}_{\mathrm{El}^-} \tag{92}$$

we have from equations 90, 88, and 91,

$$E^{\alpha\alpha'} = \psi^{\mathrm{I}} - \psi^{\mathrm{II}} \tag{93}$$

---

[3] Equation 88 applies only in the absence of gravity; to take gravity into account it is, however, merely necessary to add to the right-hand side of equation 88 the term $M_i\varphi$, where M_i is the formula weight of i.

(*vii*) We shall need the following theorems which depend upon the electroneutrality condition and upon auxiliary assumption 2 above, and which are due (in slightly different form) to Guggenheim (7, 6, 3, 8). Let λ_i be a set of scalar coefficients corresponding to the components i, defined at each point of a system, and subject to the condition

$$\sum_i z_i \lambda_i = 0 \tag{94}$$

Then the linear combination

$$\sum_i \lambda_i \mu_i \tag{95}$$

is a function of the λ_i and of the *chemical state* at the point, in spite of the fact that the individual μ_i (for charged components) are functions of the electrochemical state. Furthermore the linear combination

$$\sum_i \lambda_i \log f_i \tag{96}$$

is a determinate function of the λ_i and the chemical state at the point, in spite of the fact that the individual f_i (for charged components) are indeterminate. We shall also need the obvious extension of these theorems to the linear combinations

$$\sum_i \lambda_i \operatorname{grad} \mu_i \quad \text{and} \quad \sum_i \lambda_i \operatorname{grad} \log f_i \tag{97}$$

respectively.

B. THE GENERAL CASE

E.M.F. as a function of chemical state and configuration

By subtracting equation 12 from equation 15 we obtain

$$\mu_{\mathrm{El}^-}^{\alpha'} - \mu_{\mathrm{El}^-}^{\alpha} = \sum_q \nu_q \mu_q^{\alpha} - \sum_{q'} \nu_{q'} \mu_{q'}^{\alpha'} + \sum_{r'} \nu_{r'} \mu_{r'}^{\beta'} - \sum_r \nu_r \mu_r^{\beta} \tag{98}$$

which by equations 90 and 85 yields

$$E^{\alpha\alpha'} = \frac{1}{F} [B(P, T) + \sum_{r'} \nu_{r'} \mu_{r'}^{\beta'} - \sum_r \nu_r \mu_r^{\beta}] \tag{99}$$

Introduction of equation 64 gives

$$E^{\alpha\alpha'} = \frac{1}{F} \left[B(P, T) - \frac{\mathrm{d}t}{\mathrm{d}\xi} \int_V \sum_i \mu_i \operatorname{div} \partial\vec{\Phi}_i \, \delta V \right] \tag{100}$$

which by virtue of equation 36 becomes

$$E^{\alpha\alpha'} = \frac{1}{F} \left[B(P, T) - \int_V \sum_i \mu_i \operatorname{div} \vec{\Psi}_i \, \delta V \right] \tag{101}$$

Since by equations 38 and 86

$$\sum_i z_i \operatorname{div} \vec{\Psi}_i = \operatorname{div} \vec{J} = 0 \tag{102}$$

the div $\vec{\Psi}_i$ satisfy equation 94 and therefore the integral in equation 101 is a function of the div $\vec{\Psi}_i$ and of the chemical state at every point; the $\vec{\Psi}_i$, however, and therefore the div $\vec{\Psi}_i$, are functions of chemical state and configuration. Equation 101 thus shows the manner in which the E.M.F. of any galvanic cell with reversible electrodes whatever depends upon the chemical state at every point and the configuration of the system, and therefore constitutes a solution of problem (*i*) of section IV A above.

The solution may also be obtained in terms of the specific electrolytic current vector $\vec{J}$ in place of the specific electrolytic flow vectors $\vec{\Psi}_i$. For this purpose we calculate the term $\sum_{r'} \nu_{r'} \mu_{r'}^{\beta'}$ with the help of equation 37, Gauss' theorem, and equation 86, as follows:

$$\sum_{r'} \nu_{r'} \mu_{r'}^{\beta'} - \sum_{r'} \nu_{r'} \mu_{r'}^{\beta} = -\frac{\mathrm{d}t}{\mathrm{d}\xi} \int_\sigma \partial \vec{I} \cdot \sum_{r'} \nu_{r'} \mu_{r'} \delta \vec{\sigma} \tag{103}$$

$$\begin{aligned} \therefore \sum_{r'} \nu_{r'} \mu_{r'}^{\beta'} &= \sum_{r'} \nu_{r'} \mu_{r'}^{\beta} - \int_\sigma \vec{J} \cdot \sum \nu_{r'} \mu_{r'} \cdot \delta\sigma \\ &= \sum_{r'} \nu_{r'} \mu_{r'}^{\beta} + \int_V \operatorname{div} \vec{J} \sum_{r'} \nu_{r'} \mu_{r'} \delta V \\ &= \sum_{r'} \nu_{r'} \mu_{r'}^{\beta} + \int_V \vec{J} \cdot \sum_{r'} \nu_{r'} \operatorname{grad} \mu_{r'} \delta V \end{aligned} \tag{104}$$

Substitution of equation 104 into equation 99 yields

$$E^{\alpha\alpha'} = \frac{1}{F} \left[B(P, T) + \sum_{r'} \nu_{r'} \mu_{r'}^{\beta} - \sum_{r'} \nu_r \mu_r^{\beta} + \int \vec{J} \cdot \sum_{r'} \nu_{r'} \operatorname{grad} \mu_{r'} \delta V \right] \tag{105}$$

In order to show this expression to be a function of chemical state we introduce into it the qrc. condition in the form of equation 73 and obtain

$$\begin{aligned} E^{\alpha\alpha'} = \frac{1}{F} \Bigg[& B(P, T) + \sum_{r'} \nu_{r'} \mu_{r'}^{\beta} - \sum_{r} \nu_r \mu_r^{\beta} \\ & + \int_V \vec{J} \cdot \left(\sum_{r'} \nu_{r'} \operatorname{grad} \mu_{r'} + \sum_i \frac{t_i}{\bar{z}_i} \operatorname{grad} \mu_i \right) \delta V \Bigg] \end{aligned} \tag{106}$$

Now by equations 10 and 14 we have

$$\sum_{r'} z_{r'} \nu_{r'} - \sum_r z_r \nu_r = 0 \tag{107}$$

and by equations 14 and 87

$$\sum_{r'} z_{r'} \nu_{r'} + \sum_i \frac{z_i t_i}{\bar{z}_i} = 0 \tag{108}$$

Hence the right-hand side of equation 106 is a function of the chemical state at every point and the configuration, and constitutes a solution of the problem in terms of $\vec{J}$. By starting with an equation for $\sum_r \nu_r \mu_r^\beta$ analogous to equation 104 for $\sum_{r'} \nu_{r'} \mu_{r'}^{\beta'}$, we obtain an alternative solution: namely,

$$E^{\alpha\alpha'} = \frac{1}{F}\Big[B(P, T) + \sum_{r'} \nu_{r'} \mu_{r'}^{\beta'} - \sum_r \nu_r \mu_r^{\beta'} \tag{108}$$

$$+ \int_V \vec{J}\cdot\Big(\sum_r \nu_r \operatorname{grad} \mu_r + \sum \frac{t_i}{z_i} \operatorname{grad} \mu_i\Big)\,\delta V\Big] \tag{109}$$

Formulae 106 and 109, although less compact than formula 101, are instructive because they are very similar to the formulae, obtained below, for the simply connected chemically lamellar case.

Guggenheim's theorem

By virtue of equation 93 we may write

$$E^{\alpha\alpha'} = (\psi^{\mathrm{I}} - \psi^\beta) + (\psi^{\beta'} - \psi^{\mathrm{II}}) + (\psi^\beta - \psi^{\beta'}) \tag{110}$$

The three parentheses represent, in order from left to right, the contribution to the E.M.F. of the electrode α, the electrode α', and the junction.

To calculate the "electrode potential," $(\psi^{\mathrm{I}} - \psi^\beta)$, we note that according to equations 88 and 89

$$\mu_r^\beta = \tau_r^0(P, T) + RT \log N_r^\beta + RT \log f_r^\beta + z_r F \psi^\beta \tag{111}$$

$$\mu_{\mathrm{El}^-}^{\mathrm{I}} = \tau_{\mathrm{El}^-}^{\mathrm{I}} - F\psi^{\mathrm{I}} \tag{112}$$

Upon substituting equations 111 and 112 into equation 12 and taking account of equation 10, we obtain

$$\psi^{\mathrm{I}} - \psi^\beta = \frac{1}{F}\,[\tau_{\mathrm{El}^-}^{\mathrm{I}} + \sum_q \nu_q \mu_q^\alpha - \sum_r \nu_r \tau_r^0(P, T)$$

$$- RT \sum_r \nu_r \log N_r^\beta - RT \sum_r \nu_r \log f_r^\beta] \tag{113}$$

For the "electrode potential" $(\psi^{\beta'} - \psi^{\mathrm{II}})$ we obtain in similar fashion

$$\psi^{\beta'} - \psi^{\mathrm{II}} = \frac{1}{F}\,[-\tau_{\mathrm{El}^-}^{\mathrm{II}} - \sum_{q'} \nu_{q'} \mu_{q'}^{\alpha'} + \sum_{r'} \nu_{r'} \tau_{r'}^0(P, T)$$

$$+ RT \sum_{r'} \nu_{r'} \log N_{r'}^{\beta'} + RT \sum_{r'} \nu_{r'} \log f_{r'}^{\beta'}] \tag{114}$$

Adding equations 113 and 114 and taking account of equations 91 and 85 gives for the contribution of both electrodes together to the E.M.F.

$$(\psi^{\mathrm{I}} - \psi^{\beta}) + (\psi^{\beta'} - \psi^{\mathrm{II}}) = \frac{1}{F}\left[B(P, T) + \sum_{r'} \nu_{r'}\tau^{0}_{r'}(P, T) - \sum_{r} \nu_{r}\tau^{0}_{r}(P, T)\right]$$

$$+ \frac{RT}{F} \log \prod_{r,r'} (N^{\beta}_{r})^{-\nu_r}(N^{\beta'}_{r'})^{\nu_{r'}}$$

$$+ \frac{RT}{F} [\sum_{r'} \nu_{r'} \log f^{\beta'}_{r'} - \sum_{r} \nu_r \log f^{\beta}_{r}] \qquad (115)$$

The "junction potential," $\psi^{\beta} - \psi^{\beta'}$, we now calculate from the qrc. condition as follows: Substituting equations 88 and 89 into equation 70 we obtain

$$RT \int_V \sum_i \vec{\Psi}_i \cdot \text{grad} \log N_i \delta V + RT \int_V \sum_i \vec{\Psi}_i \cdot \text{grad} \log f_i \delta V$$

$$+ F \int_V \text{grad}\, \psi \cdot \sum_i z_i \vec{\Psi}_i \delta V = 0 \qquad (116)$$

The term in grad ψ we transform with the help of equations 38 and 86 and Gauss' theorem, as follows

$$\int_V \text{grad}\, \psi \cdot \sum_i z_i \vec{\Psi}_i \delta V = \int_V \text{grad}\, \psi \cdot \vec{J} \delta V$$

$$= \int_V \text{div}\, \psi \vec{J} \delta V - \int_V \psi \,\text{div}\, \vec{J} \delta V$$

$$= - \int_\sigma \psi \vec{J} \cdot \delta\vec{\sigma}$$

$$= \psi^{\beta'} - \psi^{\beta} \qquad (117)$$

From equations 116 and 117 it follows that

$$\psi^{\beta} - \psi^{\beta'} = \frac{RT}{F} \int_V \sum_i \vec{\Psi}_i \cdot \text{grad} \log N_i \delta V + \frac{RT}{F} \int_V \sum_i \vec{\Psi}_i \cdot \text{grad} \log f_i \delta V \qquad (118)$$

An alternative formula for $(\psi^{\beta} - \psi^{\beta'})$, obtained from equation 73 in the same manner as equation 118 from equation 70, is

$$\psi^{\beta} - \psi^{\beta'} = \frac{RT}{F} \int_V \vec{J} \cdot \sum_i \frac{t_i}{\bar{z}_i} \text{grad} \log N_i \delta V + \frac{RT}{F} \int_V \vec{J} \cdot \sum_i \frac{t_i}{\bar{z}_i} \text{grad} \log f_i \delta V \qquad (119)$$

By adding equations 115 and 118 and comparing the result with equation 110 we deduce

$$E^{\alpha\alpha'} = E_{\text{electrodes, ideal}} + E_{\text{junction, ideal}} + E_{\text{salt effect}} \qquad (120)$$

where

$$E_{\text{electrodes, ideal}} = E^0(P, T) + \frac{RT}{F}\log\prod_{r,r'}(N_r^\beta)^{-\nu_r}(N_{r'}^{\beta'})^{\nu_{r'}} \tag{121}$$

$$E_{\text{junction, ideal}} = \frac{RT}{F}\int_V \sum_i \vec{\Psi}_i\cdot\text{grad}\log N_i\,\delta V \tag{122}$$

$$\begin{aligned} E_{\text{salt effect}} = \frac{RT}{F}\Bigg[\sum_{r'}\nu_{r'}\log f_{r'}^{\beta'} - \sum_r \nu_r\log f_r^\beta \\ + \int_V \sum_i \vec{\Psi}_i\cdot\text{grad}\log f_i\,\delta V\Bigg] \end{aligned} \tag{123}$$

$$E^0(P, T) = \frac{1}{F}[B(P, T) + \sum \nu_{r'}\tau_{r'}^0(P, T) - \sum \nu_r\tau_r^0(P, T)] \tag{124}$$

The expression for $E_{\text{salt effect}}$ is simplified and shown to be determinate by transforming the integral by means of Gauss' theorem etc. to give

$$\begin{aligned} \int_V \sum_i \vec{\Psi}_i\cdot\text{grad}\log f_i\,\delta V &= \int_V \text{div}\sum_i \vec{\Psi}_i\log f_i\,\delta V - \int_V \sum_i \log f_i\,\text{div}\,\vec{\Psi}_i\,\delta V \\ &= \int_\sigma \sum_i \vec{\Psi}_i\log f_i\cdot\vec{\delta\sigma} - \int_V \sum_i \log f_i\,\text{div}\,\Psi_i\,\delta V \\ &= \sum_r \nu_r\log f_r^\beta - \sum_{r'}\nu_{r'}\log f_{r'}^{\beta'} \\ &\quad - \int_V \sum_i \log f_i\,\text{div}\,\Psi_i\,\delta V \end{aligned} \tag{125}$$

Substitution of equation 125 into equation 123 yields

$$E_{\text{salt effect}} = -\frac{RT}{F}\int_V \sum_i \log f_i\,\text{div}\,\vec{\Psi}_i\,\delta V \tag{126}$$

a result which is confirmed by inspection of equation 101. The integral is seen to be determinate on comparison with equation 102. Equations 120, 121, 122, 124, 126 constitute the extension of Guggenheim's theorem to the most general type of cell with liquid-liquid junction. The theorem may be obtained in terms of the vector $\vec{J}$ in place of the vectors $\vec{\Psi}_i$ by adding equation 119 to equation 115 and proceeding as in the deduction of equations 120 to 126 above. The resulting equations for $E_{\text{electrodes, ideal}}$ and $E^0(P, T)$ are of course identical with equations 121 and 124, but for $E_{\text{junction, ideal}}$ we obtain, instead of equation 122,

$$E_{\text{junction, ideal}} = \frac{RT}{F}\int_V \vec{J}\cdot\sum \frac{t_i}{z_i}\,\text{grad}\log N_i\,\delta V \tag{127}$$

and for $E_{\text{salt effect}}$ we obtain, instead of equation 126, the alternative equations

$$E_{\text{salt effect}} = \frac{RT}{F}\left[\sum_{r'} \nu_{r'} \log f_{r'}^{\beta} - \sum_{r} \nu_r \log f_r^{\beta} + \int_V \vec{J}\cdot\left(\sum_{r'} \nu_{r'} \operatorname{grad} \log f_{r'} + \sum_{i} \frac{t_i}{\bar{z}_i} \operatorname{grad} \log f_i\right) \delta V\right] \tag{128}$$

$$E_{\text{salt effect}} = \frac{RT}{F}\left[\sum_{r'} \nu_{r'} \log f_{r'}^{\beta'} - \sum_{r} \nu_r \log f_r^{\beta'} + \int_V \vec{J}\cdot\left(\sum_{r} \nu_{r} \operatorname{grad} \log f_{r} + \sum_{i} \frac{t_i}{\bar{z}_i} \operatorname{grad} \log f_i\right) \delta V\right] \tag{129}$$

These expressions are confirmed by inspection of equations 106 and 109, and are seen to be determinate on comparison with equations 107 and 108.

C. THE SIMPLY CONNECTED CHEMICALLY LAMELLAR CASE

E.M.F. as a function of chemical state

In analogy to equation 104 we have

$$\sum_{r'} \nu_{r'} \mu_{r'}^{\beta'} = \sum_{r'} \nu_{r'} \mu_{r'}^{\beta} + \int_C \sum_{r'} \nu_{r'} \operatorname{grad} \mu_{r'} \cdot \delta s \tag{130}$$

where C is any path from β to β'. Substitution of equation 130 into equation 99 gives

$$E^{\alpha\alpha'} = \frac{1}{F}\left[B(P, T) + \sum_{r'} \nu_{r'} \mu_{r'}^{\beta} - \sum_{r} \nu_r \mu_r^{\beta} + \int_C \sum_{r'} \nu_{r'} \operatorname{grad} \mu_{r'} \cdot \delta \vec{s}\right] \tag{131}$$

Into this expression we introduce the qrc. condition for the simply connected chemically lamellar case, i.e., equation 77, and obtain

$$E^{\alpha\alpha'} = \frac{1}{F}\left[B(P, T) + \sum_{r'} \nu_{r'} \mu_{r'}^{\beta} - \sum_{r} \nu_r \mu_r^{\beta} + \int_C \left(\sum_{r'} \nu_{r'} \operatorname{grad} \mu_{r'} + \sum_{i} \frac{t_i}{\bar{z}_i} \operatorname{grad} \mu_i\right) \cdot \delta \vec{s}\right] \tag{132}$$

This expression, on comparison with equations 107 and 108, is seen to be a function of the chemical state at each point of the path C, and thus to constitute a solution of problem (*i*) of section IV A above. An alternative solution is obviously

$$E^{\alpha\alpha'} = \frac{1}{F}\left[B(P, T) + \sum_{r'} \nu_{r'} \mu_{r'}^{\beta'} - \sum_{r} \nu_r \mu_r^{\beta'} + \int_C \left(\sum_{r} \nu_{r} \operatorname{grad} \mu_{r} + \sum_{i} \frac{t_i}{\bar{z}_i} \operatorname{grad} \mu_i\right) \cdot \delta \vec{s}\right] \tag{133}$$

Equations 132 and 133 are seen to be closely analogous to equations 106 and 109 for the general case.

Guggenheim's theorem

In the simply connected chemically lamellar case, the "electrode potentials" $(\psi^{\mathrm{I}} - \psi^{\beta})$ and $(\psi^{\beta'} - \psi^{\mathrm{II}})$ are given by the same formulae as in the general case, namely, equations 113 and 114, and so equation 115 still holds. The "junction potential," $(\psi^{\beta} - \psi^{\beta'})$, however, has a simpler form; we obtain it by substituting equations 88 and 89 into the qrc. condition in the form of equation 77:

$$RT \int_C \sum_i \frac{t_i}{\bar{z}_i} \operatorname{grad} \log N_i \cdot \delta\vec{s} + RT \int_C \sum_i \frac{t_i}{\bar{z}_i} \operatorname{grad} \log f_i \cdot \delta\vec{s} + F \int_C \sum_i \frac{z_i t_i}{\bar{z}_i} \operatorname{grad} \psi \cdot \delta\vec{s} = 0 \qquad (134)$$

$$\therefore \quad \psi^{\beta} - \psi^{\beta'} = \frac{RT}{F} \int_C \sum_i \frac{t_i}{\bar{z}_i} \operatorname{grad} \log N_i \cdot \delta\vec{s} + \frac{RT}{F} \int_C \sum_i \frac{t_i}{\bar{z}_i} \operatorname{grad} \log f_i \cdot \delta\vec{s} \qquad (135)$$

By adding equations 115 and 135 and comparing the result with equation 110 we deduce

$$E^{\alpha\alpha'} = E_{\text{electrodes, ideal}} + E_{\text{junction, ideal}} + E_{\text{salt effect}} \qquad (136)$$

where

$$E_{\text{electrodes, ideal}} = E^0(P, T) + \frac{RT}{F} \log \prod_{r,r'} (N_r^{\beta})^{-\nu_r} (N_{r'}^{\beta'})^{\nu_{r'}} \qquad (137)$$

$$E_{\text{junction, ideal}} = \frac{RT}{F} \int_C \sum_i \frac{t_i}{\bar{z}_i} \operatorname{grad} \log N_i \cdot \delta\vec{s} \qquad (138)$$

$$E_{\text{salt effect}} = \frac{RT}{F} \left[\sum_{r'} \nu_{r'} \log f_{r'}^{\beta'} - \sum_r \nu_r \log f_r^{\beta} + \int_C \sum_i \frac{t_i}{\bar{z}_i} \operatorname{grad} \log f_i \cdot \delta\vec{s} \right] \qquad (139)$$

$$E^0(P, T) = \frac{1}{F} \left[B(P, T) + \sum_{r'} \nu_{r'} \tau_{r'}^0(P, T) - \sum_r \nu_r \tau_r^0(P, T) \right] \qquad (140)$$

Equation 139 may evidently be transformed into either of the equations

$$E_{\text{salt effect}} = \frac{RT}{F} \left[\sum_{r'} \nu_{r'} \log f_{r'}^{\beta} - \sum_r \nu_r \log f_r^{\beta} + \int_C \left(\sum_{r'} \nu_{r'} \operatorname{grad} \log f_{r'} + \sum_i \frac{t_i}{\bar{z}_i} \operatorname{grad} \log f_i \right) \cdot \delta\vec{s} \right] \qquad (141)$$

$$E_{\text{salt effect}} = \frac{RT}{F}\left[\sum_{r'} \nu_{r'} \log f_{r'}^{\beta'} - \sum_{r} \nu_r \log f_r^{\beta'} + \int_C \left(\sum_r \nu_r \operatorname{grad} \log f_r + \sum_i \frac{t_i}{z_i} \operatorname{grad} \log f_i\right) \cdot \delta \vec{s}\,\right] \tag{142}$$

Expressions 141, 142 for $E_{\text{salt effect}}$ are confirmed by inspection of equations 132 and 133 and are seen to be determinate by comparison with equations 107 and 108. Equations 136, 137, 138, 140, 141, and 142 constitute Guggenheim's theorem for simply connected chemically lamellar liquid liquid junctions. On comparison with the result for the general case we find, as we should expect, that equations 136, 137, 140 are identical with equations 120, 121, 124 and that equations 138, 141, 142 are closely analogous to equations 127, 128, 129.

Remark

It will be noted that equations 137, 138, 140, 141, 142 for simply connected chemically lamellar junctions have a form essentially identical with that of the equations obtained by Guggenheim (6, 4, 9) for the special cases with cylindrical symmetry studied by him. It thus appears that junctions with cylindrical symmetry have no advantages of theoretical simplicity over junctions which are merely simply connected and chemically lamellar. The special importance of cylindrical symmetry resides in the fact that it represents that type of simply connected chemical lamellarity which is most easily obtained in practice.

D. SOLUTION CONSISTING OF A SINGLE ELECTROLYTE COMPONENT AND A SINGLE NEUTRAL COMPONENT

In order to verify the general formulae for E.M.F. obtained above and to illustrate their use, we shall deduce from them the familiar laws for solutions consisting of a single electrolyte component and a single neutral component.

For this case it follows from auxiliary assumption 2 and equation 76 that

$$c_{el} \operatorname{grad} \mu_{el} + c_{nt} \operatorname{grad} \mu_{nt} = 0 \tag{143}$$

from which it appears that grad μ_{el} and grad μ_{nt} always have opposite directions, and that therefore, in the absence of gravitational effects, *the solution must always be chemically lamellar.* It follows that as long as the solution is simply connected, formulae 132, 133 always apply. For the sake of completeness it is however desirable to consider also the multiply connected case and we therefore base our treatment not on equation 132 or 133, but rather on the analogous, more general equation 106 or 109.

If we refer to the cation and the anion by the subscripts + and −, respectively, it is clear from the foregoing that for the case in hand equation 106 may be written in the form

$$E^{aa'} = \frac{1}{F}\left[B(P, T) + \sum_{r'} \nu_{r'}\mu_{r'}^{\beta} - \sum_{r} \nu_r \mu_r^{\beta} \right.$$
$$\left. + \int_V \vec{J}\cdot(\lambda_+ \operatorname{grad} \mu_+ + \lambda_- \operatorname{grad} \mu_- + \lambda_{nt} \operatorname{grad} \mu_{nt})\delta V\right] \tag{144}$$

where λ_+, λ_-, λ_{nt} are functions of the chemical state defined at each point of the system and subject to the condition

$$z_+\lambda_+ + z_-\lambda_- = 0 \tag{145}$$

The potentials μ_+, μ_-, μ_{el} are subject to the equilibrium condition

$$\frac{\mu_+}{z_+} - \frac{\mu_-}{z_-} = \frac{\mu_{el}}{n} \tag{146}$$

where n is the number of equivalents of electrolyte component per mole. By means of equations 145 and 146 the quantities grad μ_+ and grad μ_- can be eliminated from the integral in equation 144, and if at the same time grad μ_{nt} is eliminated by means of equation 143, this integral becomes

$$\int_V \vec{J}\cdot\left(\pm\frac{z_\pm}{n}\lambda_\pm - \frac{c_{el}}{c_{nt}}\lambda_{nt}\right) \operatorname{grad} \mu_{el}\delta V \tag{147}$$

where one may take either the upper or the lower sign. Since P and T are constant throughout, the chemical state at each point of the solution and therefore the quantities λ_+, λ_-, λ_{nt} are functions of μ_{el} alone, and therefore we may write

$$\left(\pm\frac{z_\pm}{n}\lambda_\pm - \frac{c_{el}}{c_{nt}}\right) = \theta(\mu_{el}) \tag{148}$$

where $\theta(\mu_{el})$ is a single-valued function of μ_{el} alone. If we now define the function $\zeta(\mu_{el})$ by means of a definite integral as follows

$$\zeta(\mu_{el}'') - \zeta(\mu_{el}') = \int_{\mu_{el}'}^{\mu_{el}''} \theta(\mu_{el})\, d\mu_{el} \tag{149}$$

where μ_{el}', μ_{el}'' are arbitrary values of μ_{el}, then evidently

$$\left(\pm\frac{z_\pm}{n}\lambda_\pm - \frac{c_{el}}{c_{nt}}\lambda_{nt}\right) \operatorname{grad} \mu_{el} = \theta(\mu_{el}) \operatorname{grad} \mu_{el}$$
$$= \operatorname{grad} \zeta(\mu_{el}) \tag{150}$$

For the integral 147 we accordingly obtain

$$\int_V \vec{J}\cdot\left(\pm\frac{z_\pm}{n}\lambda_\pm - \frac{c_{el}}{c_{nt}}\lambda_{nt}\right) \operatorname{grad} \mu_{el}\delta V = \int_V \vec{J}\cdot\operatorname{grad} \zeta(\mu_{el})\delta V \tag{151}$$

The integral on the right-hand side of equation 151 may be transformed in the manner of equations 80 to 83, giving

$$\begin{aligned}\int_V \vec{J}\cdot\operatorname{grad}\zeta(\mu_{el})\delta V &= \int_V \operatorname{div}\zeta(\mu_{el})\vec{J}\delta V - \int_V \zeta(\mu_{el})\operatorname{div}\vec{J}\delta V\\ &= -\int_\sigma \zeta(\mu_{el})\vec{J}\cdot\delta\vec{\sigma}\\ &= \zeta(\mu_{el}^{\beta'}) - \zeta(\mu_{el}^{\beta}) \end{aligned} \tag{152}$$

Comparison of equations 152, 151, 144, 148 shows that

$$\int_V \vec{J}\cdot\left(\pm\frac{z_\pm}{n}\lambda_\pm - \frac{c_{el}}{c_{nt}}\lambda_{nt}\right)\operatorname{grad}\mu_{el}\delta V = \int_{\mu_{el}^{\beta}}^{\mu_{el}^{\beta'}}\left(\pm\frac{z_\pm}{n}\lambda_\pm - \frac{c_{el}}{c_{nt}}\lambda_{nt}\right)d\mu_{el} \tag{153}$$

Equation 144 for the E.M.F. accordingly becomes

$$E^{\alpha\alpha'} = \frac{1}{F}\left[B(P, T) + \sum_{r'}\nu_{r'}\mu_{r'}^{\beta} - \sum_{r}\nu_r\mu_r^{\beta} + \int_{\mu_{el}^{\beta}}^{\mu_{el}^{\beta'}}\left(\pm\frac{z_\pm}{n}\lambda_\pm - \frac{c_{el}}{c_{nt}}\lambda_{nt}\right)d\mu_{el}\right. \tag{154}$$

Equation 154 represents the exact and general theoretical proof that $E^{\alpha\alpha'}$ depends only upon the nature of the electrodes and upon the chemical states in β and β', and is independent of the structure of the junction. For the simply connected case equation 154 follows immediately from equation 132 or 133.

As a final check on our formulae we shall deduce from equation 154 the well-known formulae for the case in which the electrodes are identical and respond simply to one of the ions. In this case we have

$$B(P, T) = 0 \tag{155}$$

$$\sum_{r'}\nu_{r'}\mu_{r'} = \sum_{r}\nu_r\mu_r \tag{156}$$

$$= \begin{cases} -\dfrac{\mu_+}{z_+}, & \text{if the electrodes respond to the cation} \quad (157)\\[2ex] -\dfrac{\mu_-}{z_-}, & \text{if the electrodes respond to the anion} \quad (158)\end{cases}$$

We introduce Hittorf numbers by setting

$$t_{nt} = 0 \tag{159}$$

and note also that according to equations 30 and 87

$$\bar{z}_+ = z_+;\quad \bar{z}_- = z_- \tag{160}$$

$$t_+ + t_- = 1 \tag{161}$$

Substitution of equations 157, 159, 160, 161 into the integral in equation 106 shows that when the electrodes respond to the cation, this integral is equal to

$$\int_V \vec{J}\cdot\left(-\frac{t_-}{z_+}\,\mathrm{grad}\,\mu_+ + \frac{t_-}{z_-}\,\mathrm{grad}\,\mu_-\right)\delta V \tag{162}$$

whence, by comparison with the integral in equation 144, we deduce

$$\lambda_+ = -\frac{t_-}{z_+} \tag{163}$$

$$\lambda_- = \frac{t_-}{z_-} \tag{164}$$

$$\lambda_{nt} = 0 \tag{165}$$

Substitution of equations 163, 164, 165 and also of equations 155 and 156 into equation 154 with the upper sign gives the familiar formula

$$E^{\alpha\alpha'} = -\frac{1}{nF}\int_{\mu^{\beta}_{el}}^{\mu^{\beta'}_{el}} t_-\,\mathrm{d}\mu_{el} \tag{166}$$

In similar fashion it follows that if the electrodes respond to the anion, then

$$E^{\alpha\alpha'} = \frac{1}{nF}\int_{\mu^{\beta}_{el}}^{\mu^{\beta'}_{el}} t_+\,\mathrm{d}\mu_{el} \tag{167}$$

V. SUMMARY

Four defects of the existing thermodynamic theory of cells with liquid-liquid junctions are pointed out. In the attempt to remedy these defects, the assumptions and definitions underlying the theory are revised, account being taken of arbitrary gradients of concentration and gravitational potential. In the course of this revision, a new manner of neglecting spontaneous diffusion is adopted, transport numbers are defined in a way more general than hitherto, and two new vectors are introduced, the specific electrolytic flow vector, $\vec{\Psi}_\iota$, of a component, and the specific electrolytic current vector, $\vec{J}$. It is then shown that the assumptions and definitions in question lead to a theorem, which, although implicit in previous treatments of cells with liquid-liquid junctions, is here for the first time stated explicitly and generally, and is called the condition for quasi-reversible conduction, or the qrc. condition. With the help of the qrc. condition the thermodynamic laws of cells with liquid-liquid junctions are deduced. It is found that the well-known laws for junctions with cylindrical symmetry apply unaltered to junctions which are merely chemically lamellar and simply connected, and that for the general case of junctions with any continuous distribution of chemical states and any configuration whatever, closely analogous more complicated laws hold. The general formulae for E.M.F. here obtained for the first time are verified by deducing from them the familiar laws for the case of a single electrolyte in a non-electrolyte solvent.

The author takes pleasure in thanking Professor J. W. McBain, Professor P. J. Van Rysselberghe, and Dr. S. W. Grinnell for a number of helpful suggestions and comments.

REFERENCES

(1) DES COUDRES, T.: Wied. Ann. **49**, 284 (1893); **57**, 232 (1896).
(2) DOLEZALEK, F., AND KRÜGER, F.: Z. Elektrochem. **12**, 669 (1910).
(3) DONNAN, F. G., AND GUGGENHEIM, E. A.: Z. physik. Chem. **A162**, 346 (1932).
(4) GUGGENHEIM, E. A.: *Modern Thermodynamics by the Methods of Willard Gibbs*, pp. 133–151. Methuen, London (1933).
(5) GUGGENHEIM, E. A.: J. Am. Chem. Soc. **52**, 1315 (1930).
(6) GUGGENHEIM, E. A.: J. Phys. Chem. **34**, 1758 (1930).
(7) GUGGENHEIM, E. A.: J. Phys. Chem. **33**, 842 (1929); **34**, 1540 (1930).
(8) GUGGENHEIM, E. A.: Article in *A Commentary on the Scientific Writings of J. Willard Gibbs, etc.*, Vol. I, p. 181. Yale University Press, New Haven (1936).
(9) GUGGENHEIM, E. A.: Phil. Mag. **23**, 983 (1936).
(10) GUGGENHEIM, E. A., AND ADAM, N. K.: Proc. Roy. Soc. (London) **A139**, 218 (1933).
(11) HELMHOLTZ, H.: Berl. Monatsber. for the year 1877, pp. 713–726; or Wied. Ann. **3**, 201 (1878); or (somewhat revised and extended) *Wissenschaftliche Abhandlungen*, Vol. I, p. 840 (Barth, Leipzig (1882)); or Ostwald's *Klassiker*, Nr. 124, p. 1 (Engelmann, Leipzig (1902)).
(12) HELMHOLTZ, H.: Pogg. Ann. **89**, 211, 253 (1853); or *Wissenschaftliche Abhandlungen*, Vol. I, p. 475 (Barth, Leipzig (1882)).
(13) HENDERSON, P.: Z. physik. Chem. **59**, 118 (1907); **63**, 325 (1908).
(14) JOHNSON, K. R.: Ann. Physik [4] **14**, 995 (1904).
(15) KOENIG, F. O.: J. Phys. Chem. **38**, 111 (1934).
(16) KOENIG, F. O.: J. Phys. Chem. **40**, 373 (1936).
(17) LANGE, E., AND MISCENKO, K. P.: Z. physik. Chem. **A149**, 1 (1930).
(18) LEWIS, G. N., AND RANDALL, M.: *Thermodynamics and the Free Energy of Chemical Substances*, pp. 337–40. The McGraw-Hill Book Company, Inc., New York (1923).
(19) NERNST, W.: Z. physik. Chem. **2**, 613 (1888).
(20) NERNST, W.: Z. physik. Chem. **4**, 129 (1889).
(21) PLANCK, M.: Wied. Ann. **39**, 161 (1890); **40**, 561 (1890).
(22) PLEIJEL, H.: Z. physik. Chem. **72**, 1 (1910).
(23) TAYLOR, P. B.: J. Phys. Chem. **31**, 1478 (1927).
(24) TOLMAN, R. C.: Proc. Am. Acad. Arts. Sci. **46**, 109 (1910); J. Am. Chem. Soc. **33**, 121 (1911).

NEW BOOKS

Der disperse Bau der festen Systeme. Allgemeine Theorie der Verunreinigung fester Systeme. By D. BALAREW. 23.5 x 15.5 cm.; vi + 240 pp. Dresden and Leipzig: Theodor Steinkopff, 1939. Price: unbound, 7.50 RM; bound, 8.62 RM.

Theories of the mosaic structure of real, as distinguished from ideal, crystals have been constructed by many writers with the object of accounting for special properties of solids, such as their behavior on deformation or their action on x-rays. The work of Balarew is concerned rather with the chemical properties of crystals, especially their tendency to retain impurities when separating from solution. The author has carried out many experiments in this field, which he has described in numerous papers. His main idea is that a crystal is always built up of small blocks, often so small that their composition departs markedly from the stoichiometric ratio, and that these blocks are separated by irregular channels, in which foreign molecules, atoms, or ions are retained. This is described as internal adsorption. If barium sulfate be precipitated in the presence of potassium permanganate, the crystals are colored red, and this color is not removed even by long contact with reducing agents. Other similar examples are described. The formation of submicrons when a crystal is in process of dissolving is also taken as evidence for a block structure.

The bearing of such observations on gravimetric analysis is discussed, and means are described for obtaining precipitates with the least possible contamination, internal adsorption being regarded as of greater importance than adsorption at the free surface. X-ray evidence is referred to but not discussed quantitatively. Again, although reference is made to the appearance of crystals under the microscope, this method is not applied in any systematic way.

The presentation of the author's ideas involves a great deal of repetition, and the work might have been condensed with great advantage. There are many references to the literature, but also some surprising omissions. Thus, although mention is made of the action of impurities in modifying the habit of crystals, there are no references to the work of such investigators as Beudant, Tertsch, and Buckley, although their experiments, especially those of Buckley, have thrown much light on the way in which foreign ions and molecules are built into the structure of a growing crystal.

The general impression derived from reading the book is that the author has collected many useful observations on crystals which support the view that some kind of block structure is usually present, but that they fall short of providing an explanation of that structure. The concluding theoretical argument is unconvincing.

C. H. DESCH.

Mellor's Modern Inorganic Chemistry. Revised and edited by G. D. Parker in collaboration with J. W. Mellor. 6 x 9 in.; xix + 915 pp.; 241 figures; 68 tables. New York: Longmans Green and Company, 1939. Price: $4.50.

This is the ninth edition of what has come to be generally accepted as one of the standard books of inorganic chemistry. The contents have been entirely rearranged and largely rewritten. The first sixteen chapters are devoted to theoretical material and include: properties of gases; chemical change; molecular theory; atomic and equivalent weight; classification of the elements and constitution of matter; solutions and their properties; electrolysis and electrolytic dissociations; thermochemistry; chemical equilibrium; reaction velocity; and the colloidal state. The other twenty chapters are devoted to the chemistry of the elements and their compounds. The separate headings are: hydrogen and water; oxygen; carbon, nitrogen; the atmosphere; sulphur; the halogens; the inert gases; the alkali metals; copper, silver, and gold; the alkaline earth metals; zinc, cadmium, and mercury; the elements of Group III; the elements of Group IV; the elements of Group V; selenium and tellurium; chromium, masurium, and rhenium; iron, cobalt, nickel, and the platinum metals; radioactivity and the radioelements.

The general plan is thus to treat the theoretical and physical-chemical material in the first part of the book and the factual inorganic material in the second part. The salts are discussed under the heading of the metal concerned, which brings the book more in line with current practice. A little more space might have been devoted to the treatment of the modern theory of electrolytic dissociation and uses of the Brönsted theory.

This revised edition is a valuable work and contains a great deal of useful material. The binding and cover are very good. The book is to be recommended to students and teachers both as an advanced textbook and as a reference work.

ARTHUR A. VERNON.

Précis de Chimie Physique. By A. BERTHOUD. 10 x 6½ in.; 133 figures; vi + 498 pp. Paris: Gauthier-Villars, 1939.

In this book Professor Berthoud has given a lucid, able, and interesting survey of the field of physical chemistry. By omitting details of experimental arrangements and, above all, by avoiding verbose discussions, he has contrived to include in a volume of moderate dimensions a treatment of virtually all the topics that are the concern of physical chemists. For students who can read French easily, this book will be an excellent introduction to physical chemistry. Although the book throughout is characterized by clarity of style and attractiveness of presentation, I am of the opinion that the discussions of thermodynamics, of heterogeneous equilibria, and of the electronic theory of valence are to be especially commended.

On the other hand, the treatment of the Debye and Hückel theory, even in an introductory textbook, seems to be less than adequate. A more controversial point is the rather extensive use of results of quantum theory and of wave mechanics without laying, in my opinion, a sufficient foundation.

F. H. MACDOUGALL.

Essentials of Physiological Chemistry. Second Edition. By ARTHUR K. ANDERSON. 6 x 9 in.; ix + 323 pp.; 36 figures. New York: John Wiley and Sons, Inc., 1939. Price: $2.75.

Dr. Anderson's two decades of teaching and research in biochemistry at the University of Minnesota and at Pennsylvania State College adequately qualify him to write a textbook of physiological chemistry.

This book is designed to be an introduction to animal biochemistry, and has been written primarily for the use of students of home economics. A conventional order of presentation of subjects is followed: physical chemistry; chemistry of carbohydrates, lipids, and proteins; foods; enzymes; digestion; absorption; metabolism of carbohydrates, fats, and proteins; calorimetry; composition of tissues; blood; urine; hormones; and vitamins. Some students may be dismayed by the rather large amount of chemical information contained between the covers of the book, but they will appreciate Dr. Anderson's clear, informative style of writing. The few errors observed by the reviewer were minor, and will be picked up readily by any teacher of physiological chemistry. The author perhaps ascribes more physiological potency to some of the vitamins than they actually possess: for example, "A generous supply of vitamin A in the diet promotes longevity." The vitamins discussed are vitamin A, thiamin, riboflavin, nicotinic acid amide, vitamin B_6, ascorbic acid, vitamins D, the tocopherols, and vitamin K. Where possible, the chemical names of the vitamins have been indicated, but the author appears to prefer the older vitamin terminology. The use of vitamin K in the treatment of human disease is not mentioned. References to original literature are not given; in the reviewer's opinion, this omission in a textbook for undergraduate students is a desirable feature. A short list of standard textbooks of biochemistry and nutrition are included at the end of each chapter. The book is well indexed. It contains no appendix and no laboratory exercises.

The book is bound attractively in green cloth. Heavy type, rather than italics, is used to indicate emphasis. Most of the thirty-six illustrations are line drawings. The type is readable, and the paper used is of good quality.

The reviewer predicts a generous reception for this useful little book.

L. EARLE ARNOW.

A Text-Book of Light. By A. W. BARTON. 22 x 14 cm.; vii + 426 pp. London, New York, and Toronto: Longmans, Green and Company, 1939. Price: 8 s.

Dr. Barton's textbook, which deals with geometrical and physical optics, is of Higher Certificate and University Intermediate standard; the treatment is, however, sufficiently comprehensive to make the work serviceable, with a little supplementing, for students reading for a pass degree.

Those who know Dr. Barton's useful little treatise on heat will expect this work to be characterized by the same qualities of originality and clarity of exposition. They will not be disappointed.

Many treatises on optics are accurate, logical, and arid in their development of their subject; Dr. Barton has adopted a mode of presentation which is at once accurate, vivid, and stimulating,—"historical in the sense that the discovery of facts and the development of ideas are presented as they occur historically." It is not, as Dr. Barton remarks, a logical method, but it does not suffer on that account. The treatment is up-to-date, and the chapter on photometry may be singled out for special commendation, for Dr. Barton insists on the importance of illumination photometry,—a topic until quite recently, singularly neglected in orthodox exposition of the subject. The section dealing with physical optics covers the usual topics and ends with a chapter on the renaissance of the corpuscular theory.

The book is well produced, has a large number of illustrative queries appended to each chapter, and the photographs of aberrations, interference, and diffraction effects are most striking. It should be assured of success.

ALLAND FERGUSON.

1940
LIBRARY

ASPHALTIC BITUMEN AS COLLOID SYSTEM[1]

J. PH. PFEIFFER AND R. N. J. SAAL

Laboratorium N. V. de Bataafsche Petroleum Maatschappij, Amsterdam, Holland

Received August 7, 1939

The conception due to Nellensteyn (2) that asphaltic bitumens must be looked upon as colloid systems has been further developed by Pfeiffer and his collaborators (5) in the Laboratory of the N. V. de Bataafsche Petroleum Maatschappij at Amsterdam (the Netherlands). According to these theories, the great differences in rheological properties found can be accounted for by the fact that asphaltic bitumens consist of dispersions of micelles in heavy, purely viscous oils and that these micelles are peptized to different degrees resulting in differences in the tendency to form gels. To make the discussion in the subsequent pages quite clear, it is necessary first to give details about our conception of such systems, after which a brief survey will be given of experimental data which fully substantiate these ideas. A more extensive survey will shortly appear elsewhere.

I. GENERAL CONCEPTION OF THE CONSTITUTION OF ASPHALTIC BITUMENS

The majority of asphaltic bitumens contain substances which are insoluble in low-molecular aliphatic hydrocarbons, and which when heated do not soften, but decompose, swell, and finally sinter together. This fraction is generally called the "asphaltene" fraction, as distinguished from the soluble or "maltene" fraction consisting of heavy, purely viscous oil. The asphaltenes in all probability consist of high-molecular hydrocarbons of a predominantly aromatic character, with a comparatively low hydrogen content, formed by condensation and dehydrogenation from aromatic–naphthenic hydrocarbons of lower molecular weight. As a rule some oxygen, some sulfur, and a still smaller quantity of nitrogen are present.

Depending upon the intensity of the heat treatment to which the base material or the bitumen formed from it has been subjected, different asphaltenes are obtained which comprise a continuous range of products of increasing carbon content up to "carbenes," "carboids," and ultimately coke. The latter are especially produced by high level cracking according to the Dubbs process. Even this so-called coke is not pure elementary carbon, but still contains a certain proportion of hydrocarbon chains or rings, which may be quite firmly bound to a carbon nucleus (4). In the discussion which follows, it is quite immaterial whether the binding of these hydrocarbons is of a predominantly chemical or physical nature.

---

[1] Presented at the Sixteenth Colloid Symposium, held at Stanford University, California, July 6–8, 1939.

A point of great importance is that most asphaltenes have a marked tendency to adsorb aromatic hydrocarbons of lower molecular weight, and that this faculty is the more pronounced the less severe the heat treatment has been.

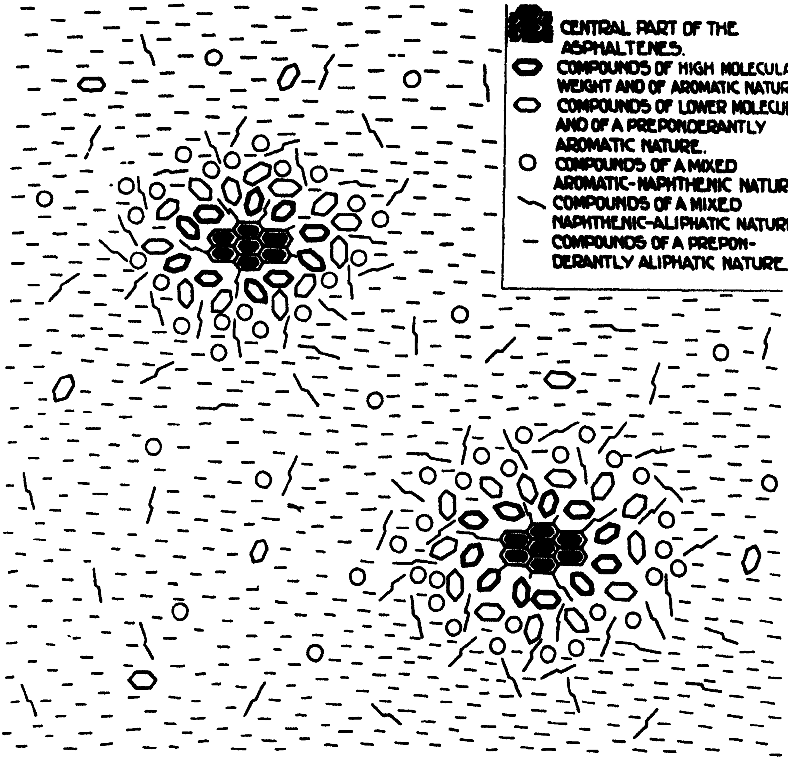
CENTRAL PART OF THE ASPHALTENES.
COMPOUNDS OF HIGH MOLECULAR WEIGHT AND OF AROMATIC NATURE.
COMPOUNDS OF LOWER MOLECULAR AND OF A PREPONDERANTLY AROMATIC NATURE.
COMPOUNDS OF A MIXED AROMATIC-NAPHTHENIC NATURE.
COMPOUNDS OF A MIXED NAPHTHENIC-ALIPHATIC NATURE.
COMPOUNDS OF A PREPONDERANTLY ALIPHATIC NATURE.

FIG. 1. Schematic representation of peptized asphaltene micelles

The asphaltenes, as they are found in natural crudes or in carefully steam-distilled residues, represent the first stages of condensation and have dimensions that defy observation under any ordinary or dark-field microscope.

In the asphaltic bitumens the asphaltenes are the centers of micelles which are formed by adsorption, and perhaps partly by absorption, of part of the maltenes on the surfaces or in the interiors of the asphaltene particles. This part of the maltenes consists chiefly of hydrocarbons of an aromatic or of a combined aromatic–naphthenic–aliphatic nature and is by some authors referred to as resins. The other part of the maltenes is often referred to as oily constituents or petrolenes.

According to our conception, the structure of such a micelle is such that the bulk of the substances with the greatest molecular weight and with the most pronounced aromatic nature are arranged the most closely to the nucleus. These again are surrounded by lighter constituents of less aromatic nature and so on, until a gradual and nearly continuous transition to the intermicellar phase is formed (figure 1). In other words, there is no distinct interface; neither at the outside of the micelle, nor around the nucleus, is there a contact of substances with distinct differences, for instance, in surface tension. It is therefore clear that it is impossible to make a sharp and rigid distinction between fractions such as the so-called resins and the oily constituents.

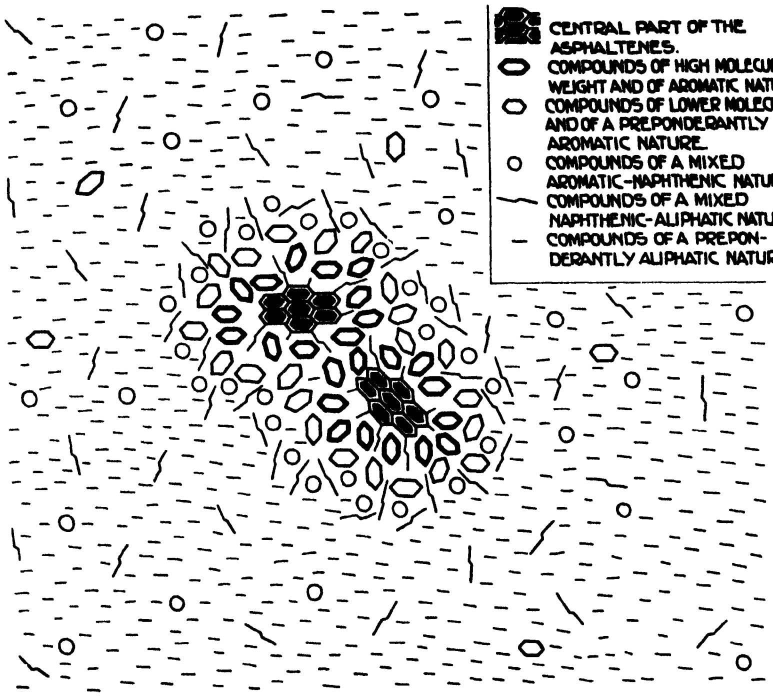
CENTRAL PART OF THE ASPHALTENES.
COMPOUNDS OF HIGH MOLECULAR WEIGHT AND OF AROMATIC NATURE.
COMPOUNDS OF LOWER MOLECULAR AND OF A PREPONDERANTLY AROMATIC NATURE.
COMPOUNDS OF A MIXED AROMATIC-NAPHTHENIC NATURE.
COMPOUNDS OF A MIXED NAPHTHENIC-ALIPHATIC NATURE.
COMPOUNDS OF A PREPONDERANTLY ALIPHATIC NATURE.

FIG. 2. Schematic representation of flocculated asphaltene micelles

When the entire system contains sufficient constituents for the formation of the outer regions of the micelles, the asphaltenes are fully peptized and able to move through the bitumen as freely as the viscosity of the intermicellar phase permits. Such a system will show almost purely viscous flow, except for a marked intramicellar elasticity (3).

If, however, there is a shortage of "asphaltic resins," part of the forces causing the formation of the micelle are not compensated by adsorption of asphaltic resins, and the micelles will be subjected to mutual attraction. The micelles will form a kind of bond (figure 2) in places where they accidentally approach so closely as to get into a region of minimum potential energy formed by the counterbalance of mutual attractive and repulsive forces. A certain force is then required to remove them from this region.

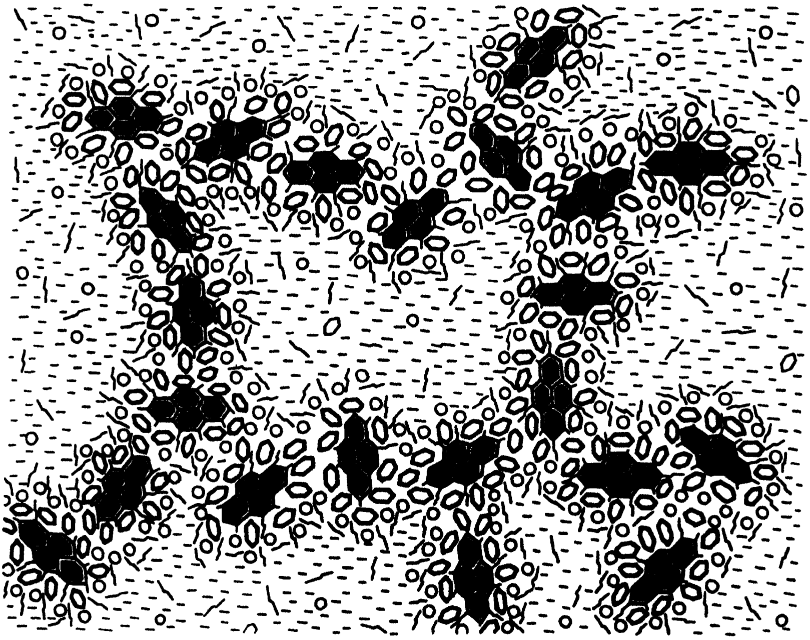

FIG. 3. Schematic representation of the structure of an asphaltic bitumen of the blown type

Thus a gel structure is formed (figure 3) that may be described as irregular open packing, the spaces of which are filled by the intermicellar liquid. Such a system may exhibit all the characteristics of complex flow, such as elasticity and thixotropy. In this case the elasticity is composed of intramicellar and intermicellar elasticity. There is reason to presume that the intramicellar elasticity predominates and that its effect is enhanced by the presence of the structure and its (intermicellar) elasticity. A more detailed discussion of such systems and their properties is given by one of us elsewhere (3).

In the following pages a brief survey will be given of the experimental data on the properties of asphaltic bitumens which have been obtained by the authors and their collaborators.

II. PROPERTIES OF ASPHALTIC BITUMENS AND OF THEIR COMPONENTS

The usual way to discriminate between different asphaltic bitumens is according to hardness, which is in practice expressed by the penetration of a standard needle under standard conditions. Bitumens of the same hardness frequently show differences in other rheological properties.

In a previous publication by Pfeiffer and van Doormaal (5) it has been explained that for practical purposes the temperature susceptibility of asphaltic bitumens can be expressed by a single number, the penetration index (*P.I.*). In the form of an index figure it gives the mean slope of the log penetration–temperature curve in the temperature interval between 15° or 25°C. and the temperature of the softening point R & B.

TABLE 1

Relationship between properties

P.I.	$\frac{\text{d LOG PENETRATION}}{\text{d TEMPERATURE}}$	DEGREE OF ELASTIC DEFORMABILITY	THIXOTROPY	NATURE OF THE MATERIAL IS THAT OF
−2.5	0.060	None	None	Coal-tar pitch
0	0.040	Moderate	Slight	Normal asphaltic bitumen
2	0.030	Rather great	Moderate	
5	0.020	Great	Great	Rubber

A drop of one point in *P.I.* approximately corresponds to a rise of 15 per cent in (d log penetration)/(d temperature).

As has been stated in the introduction, deviations from purely viscous flow are assumed to be due to the colloid nature of the bitumen, and to be particularly great when the micelles form more or less coherent structures.

Thus the temperature-susceptibility as indicated by (d log penetration)/(d temperature) and *P.I.* is related to the degree of elasticity and thixotropy attributable to the micellar structure of the mass. These relationships are shown in table 1.

The best way of splitting asphaltic bitumen into fractions is by mixing them with an excess of some low-boiling saturated hydrocarbon. The quantities of the soluble part (the maltenes) and the insoluble part (the asphaltenes) vary for the same bitumen with the nature and the quantity of solvent used, with the temperature of mixing, and with the time elapsing between mixing and separation of the precipitate. Therefore the procedure has to be thoroughly standardized.

We shall refer to these fractions as 60/80 asphaltenes or pentane asphaltenes, according as an aromatic-free gasoline having a boiling range of 60° to 80°C. or pentane is used as a solvent.

We have studied such properties of these fractions as are expected to influence the properties of the whole system, by examining fractions obtained from several bitumens produced by different processes and with widely varying rheological properties.

Asphaltenes

The important properties of the asphaltenes are the chemical composition and the particle size and shape.

Little difference was found between the C/H ratios of the asphaltenes of most steam-refined and blown products examined; these varied in most cases from 0.8 to 0.9. The asphaltenes from cracked residue showed far higher ratios up to about 1.3. Different fractions obtained from single asphaltenes by extraction usually show only slight differences in C/H ratios.

The influence of the C/H ratio on the ability of the asphaltenes to adsorb aromatic compounds was investigated by studying the relative viscosities of dispersions of different asphaltenes in benzene. Evidence was found that micelles formed with asphaltenes having a C/H ratio of less than 0.9 occupy about four times the volume of the asphaltenes alone as originally added, and that the asphaltenes having a C/H ratio of over 1.1 occupy only about twice the volume of the original asphaltenes.

These conclusions depend upon the assumption, for the validity of which there are several indications, that the shape of the bitumen micelle approaches that of a sphere.

Now and again, widely different data on the "molecular weight" of asphaltenes have been published. From our point of view it is more correct to speak of the "mean micelle weight." It will, however, be clear that it is impossible to conceive of the "micelle" as a sharply delimited unit. Not only do the micelles perhaps differ widely in size, but their composition depends on the medium in which the asphaltenes are dispersed. By solving asphaltenes in some solvent, part of the high-molecular protective substances (asphaltic resins) will, dependent on the adsorption equilibrium, remain attached to the asphaltene nuclei and form part of the micelles, whereas the remainder will be present in a molecularly dispersed condition in the liquid phase.

It will be clear from the above that the usual methods of determining molecular weights by measuring the depression of freezing points or the lowering of vapor pressures will at most give only rough indications of the micelle size. Figures ranging from about 10^3 to 10^4 are usually obtained by these methods.

An attempt to estimate the micelle size of asphaltenes by studying the behavior of "monomolecular" films according to the method of Langmuir (1) gave the values collected in table 2.

The results found by this method were not influenced by variations in the concentration of the solution, in the area over which the solution was spread, or in the duration of the test. It is, however, clear that these figures can give only a rough estimation of the mean weight of the micelle. The values found are probably too high, as deviations from spherical shape (though too small to influence viscosity) as well as the packed arrangements of large and small particles in the film may greatly affect the results.

Maltenes

From our conception of the structure of asphaltic bitumens it follows that the peptizing power of the maltenes depends mainly on (*1*) the content of aromatics, by which is meant the proportion of the maltenes consisting of aromatic rings, and (*2*) the molecular weight of the aromatic fractions.

TABLE 2

Size of micelles of asphaltenes

ASPHALTENES	MEAN "MOLECULAR WEIGHT" OF MICELLE
Mexican, steam-refined . . .	80,000
Mexican, blown .	80,000
Venezuelan, steam-refined	110,000
Venezuelan, blown	140,000
Blown East India distillate	9,000
Egyptian, cracked . . .	18,000

To verify these ideas a number of asphaltic bitumens of different types and with divergent rheological properties were split into a number of fractions rich and poor in aromatics by means of solvent extractions. The aromaticity of these fractions was further judged by various methods. The study of these data is too complicated to be discussed here.

Bitumens of the gel type (generally blown bitumens) have been found to contain only small amounts of high-molecular liquid aromatic compounds (or resins) and to contain maltenes which are comparatively poor in aromatics, whereas all of the constituents of bitumens derived from cracked residues, which bitumens are of the sol or coal-tar pitch type, are found to be of a predominantly aromatic nature.

III. RELATIONSHIP BETWEEN THE PROPERTIES OF ASPHALTIC BITUMENS AND THEIR COMPOSITION

In order to establish the influence of the nature of the components on the properties of asphaltic bitumens, we have investigated "synthetic" products made by combining maltene fractions and asphaltene fractions, which fractions were obtained by solvent extractions of representative asphaltic bitumens. These fractions were derived in some cases from a single bitumen and in other cases from different bitumens. The preparation of synthetic asphaltic bitumens was effected by dissolving all of the components together in carbon disulfide and then distilling off the carbon disulfide. Blank experiments in which bitumens were split into various fractions and subsequently recomposed have shown slight increases in hardness, but never changes of the characteristic rheological properties which together determine the type of a bitumen.

By omitting certain fractions and comparing the properties of the products thus obtained with the "complete product," we were able to determine the influence of these omitted fractions. By replacing such fractions by similar ones from other types of bitumens it was possible to compare their influences on the resulting systems.

The rheological properties of the synthetic bitumens thus obtained were examined by means of the conicylindrical rotation viscometer (6).

With the data thus obtained it could be shown that the nature of the maltenes has a marked influence on the tendency of asphaltic bitumens to form gel structures. For a given asphaltene content this tendency is absent in the presence of a certain excess of aromatics and increases as the aromatic content of the maltenes is lowered.

It has further been demonstrated that the particular nature of the asphaltenes is of importance. Asphaltenes having a relatively low C/H ratio are easily solvated and hold the solvation mantles firmly, but when the maltenes contain insufficient lower aromatic constituents to supply a mantle, these asphaltenes lead to the formation of gels. Asphaltenes having a high C/H ratio require maltenes of high aromatic content to form stable sols, and with maltenes of low aromatic content flocculation rather than gelation may occur.

The latter fact is the basis of the "Oliensis" test, which aims at showing the presence of cracked material in an asphaltic bitumen.

The high elastic deformability of bitumens may be ascribed to intramicellar and intermicellar elasticity. Intramicellar elasticity, as measured by elastic recovery, increases regularly with the shearing stress. Intermicellar elasticity, although more marked at low shearing stresses, is limited by structural failure. The intramicellar elasticity decreases with increasing C/H ratio of the asphaltenes; this may be attributed to smaller micelles, or to more compact structure of the micelles, or to combinations of these.

IV. EQUILIBRIA IN THE MALTENE–ASPHALTENE SYSTEM

The relative volumes of the two phases in systems composed of asphaltenes and maltenes is of importance, but it is difficult to determine them because they are always altered by any change to which the system is subjected. The quantities of precipitate obtained by mixing with other liquids such as aliphatic hydrocarbons give little information as to the total volume of the micelles.

These ratios can be found, however, at least for bitumens of the blown type (with a distinct gel structure), by taking advantage of the phenomenon of "sweating", which is similar to the syneresis of aqueous gels. Sweating involves the separation of small quantities of the intermicellar phase from the system, and is due presumably to contractive forces in the micelle skeleton. Neither the usual asphaltic bitumens nor those examined here exhibit this phenomenon to the extent that they yield separated intermicellar liquid of themselves. It is, however, possible to effect this separation by contact with porous materials.

This was done by spreading a suitable powder evenly on a layer of the bitumen being examined, and, after contact for a given time at a specified temperature, removing the powder and carefully extracting from it the sweated oil.

TABLE 3

Comparison of maltenes with oil sweated at 50°C.

	60/80 MALTENES	SWEATED OIL
Density, 25°/4°	0.963	0.943
Percentage by weight of saturated hydrocarbons present	39	49
Per cent by weight insoluble in 60/80 gasoline	0.0	0.2

The properties of the sweated oil thus obtained were found in most cases to differ materially from those of the maltenes separated from the bitumen with 60/80 gasoline, which shows that the composition of the micelles differs from that of the 60/80 asphaltenes. For a blown Mexican bitumen containing 32 per cent by weight of 60/80 asphaltenes, figures comparing the maltenes with the oil sweated at 50°C. are given in table 3. The sweated oil proves to be practically free from asphaltenes, showing that the continuous phase of the system has therefore actually been separated off.

From these figures the quantity of intermicellar liquid can be calculated, if it be assumed that no saturated hydrocarbons have been bound by the micelles.

By this method we have examined various bitumens of the same *P.I.*, hence of nearly the same rheological properties and the same type, but differing in asphaltene content. The data obtained are given in table 4 and point to substantial quantitative differences in the ratio of the phases. Thus, bitumen No. 1 has a much smaller quantity of intermicellar liquid than No. 3. In agreement with this, No. 1 shows a lower rate of oil sweating, although the viscosity of the sweated oil is lower than that of No. 3.

Moreover, the specific gravity of the sweated oil from No. 3 is lower than that of No. 1, which points to a more saturated character of the sweated oil from No. 3. This accounts for the fact that these bitumens do not differ much in rheological properties, as is roughly indicated by the *P.I.* The more saturated nature of the intermicellar liquid implies that the mutual binding in the structure is stronger and thus the smaller quantity of micelles in No. 3 are yet able to form a structure with about the same rheological properties as No. 1. In addition, the particular nature of the micelles may be a factor, the asphaltenes of No. 3 having absorbed fewer constituents of the maltenes, and being thus less "protected." This would also be expected for asphaltenes differing in composition.

TABLE 4

Comparison of the quantities of intermicellar liquid in bitumens of the same type and hardness

ANALYSIS	BITUMEN NO.		
	1	2	3
Density, 25°/4°	1.044	1.028	1.019
R & B melting point, °C	86.5	85.5	86
Penetration at 25°C	24	25.5	29
P.I.	3.4	3.4	3.8
Viscosity, 150°C., centistokes	5400	3900	2530
Per cent by weight insoluble in 60/80 gasoline	32.2	30.4	26.7
SWEATING TESTS			
Quantity of sweated oil, 10 days at 50°C.	0.25	0.45	0.88
Density, 25°/4°	0.953	0.943	0.938
Viscosity, 50°C., centipoises	230	310	910
Quantity of intermicellar liquid:			
Per cent by weight at 50°C	36	52	About 58
Per cent by volume at 50°C	39.5	56	About 63

It follows from these few examples that at normal temperature the micelles in asphaltic bitumens consist of asphaltenes to which a substantial portion of the maltenes may be bound. Since the quantitative ratio between the volume of the micelles and asphaltenes is not constant, the quantity of asphaltenes is to be considered only as a very approximate indication of the micelle content.

REFERENCES

(1) Langmuir, I.: J. Am. Chem. Soc. **39**, 1848 (1917).
(2) Nellensteyn, F. J.: Bereiding en constitutie van asphalt (Manufacture and constitution of asphaltic bitumen); Dissertatie Technische Hoogeschool, Delft, 1923.
(3) Pfeiffer, J. Ph.: De Ingenieur **54**, P4-P10 (1939).
(4) Pfeiffer, J. Ph.: De Ingenieur **54**, Mk41-Mk47 (1939).
(5) Pefiffer, J. Ph., and Doormaal, P. M. van: J. Inst. Petroleum Tech. **22**, 414 (1936).
(6) Saal, R. N. J., and Labout, J. W. A.: J. Phys. Chem. **43**, 149 (1939).

RHEOLOGICAL PROPERTIES OF ASPHALTIC BITUMENS[1]

R. N. J. SAAL and J. W. A. LABOUT

Laboratorium N. V. de Bataafsche Petroleum Maatschappij, Amsterdam, Holland

Received August 7, 1939

I. INTRODUCTION

In numerous investigations, the rheological properties of asphaltic bitumens have been found to vary widely in elastic deformability and thixotropy (5, 6). From the point of view of their thixotropic properties, they may be divided arbitrarily into two groups—those of the sol type and those of the gel type (3). Elasticity may be due to the elastic deformability either of the separate micelles or of a structure built up by coherent micelles; it may therefore occur both in bitumens of the sol type and in those of the gel type (4).

The wide and continuous range of chemical composition observed in all asphaltic bitumens makes it likely that free (sol) micelles or isolated small agglomerates of micelles, which may themselves be considered free micelles, may be present in bitumens of the gel type as well as in those of the sol type. Among the technical asphaltic bitumens, therefore, many representatives of mixed gel-sol types may be expected.

In order to be able to judge in how far the rheological properties of asphaltic bitumens may be explained by regarding them either as sols or as gels, a close study was made of the rheological properties of two quite different bitumens, not only the deformation under constant shearing stress being investigated, but also the elastic recovery or the relaxation of the stress. The measurements were carried out in a concentric rotation viscometer with a conical bottom.

---

[1] Presented at the Sixteenth Colloid Symposium, held at Stanford University, California, July 6-8, 1939.

The chief characteristics of the bitumens used in this investigation are given in table 1. The rheological measurements were made at 35°C., a temperature at which the deformations could be accurately observed. On the strength of the penetration index bitumen A would seem to belong to the gel type, bitumen B to the sol type (3). The low C/H ratio of the asphaltenes should be expected to give both of these bitumens a high elastic deformability (4).

The following rheological measurements were made: (*1*) The change in deformation with time under constant shearing stress (subsequently referred to here as "deformation"). (*2*) The degree of elastic recovery after various deformations. (*3*) The relaxation of the internal stress with time after various deformations. The internal stress will be referred to here as the relaxation stress. (*4*) The recovery with time after deformation and partial relaxation of the stress. (*5*) The relaxation of the internal stress with time after deformation and partial recovery.

TABLE 1

Chief characteristics of bitumens A and B

PROPERTIES	BITUMEN A	BITUMEN B
Penetration at 25°C	64	17
R & B melting point, °C.	68	62.5
Penetration index	3.2	−0.7
Insoluble in 60/80 gasoline, per cent by weight	25.0	25.3
C/H ratio of asphaltenes	0.90	0.85
Penetration at 35°C	100	50

II. THEORETICAL CONSIDERATIONS

For mathematical analysis asphaltic bitumens or colloidal systems in general may be typified as (*1*) pure sols in which each micelle is independently mobile, (*2*) pure gels in which all the micelles are interconnected to form a structure, or (*3*) gel–sols in which part of the micelles form a structure, but others are independently mobile.

Using a rough theoretical model somewhat different from that of Burgers (1), flow equations for the mixed gel–sol type may be derived. Figure 1 represents in two dimensions a unit of volume containing one free micelle. The dimensions of the free micelle, the elasticity of which is indicated by G_1, are given by p and q. The deformation of the element is indicated by s, that of the free micelle by s'. Further, there is an elastic element of the structure G_2, to which, for the sake of simplicity, no volume has been assigned. Rotations of the free micelle are left out of consideration. The theoretical analyses of the five types of rheological measurements reported are here indicated briefly.

1. *Deformation*

For the deformation of this model system the following equations may be set up:

$$\tau = (1 - p)\eta \frac{ds}{dt} + p\eta \frac{1}{1 - q}\left(\frac{ds}{dt} - \frac{ds'}{dt}\right) + G_2 s$$

which says that the stress resisting deformation of the element is equal to the sum of the viscous stress in compartments II and I and the elastic stress $G_2 s$; and

$$\frac{s'}{q} G_1 = \frac{\eta}{1 - q}\left(\frac{ds}{dt} - \frac{ds'}{dt}\right)$$

which says that the elastic stress in the micelle is equal to the viscous stress in compartment I above it.

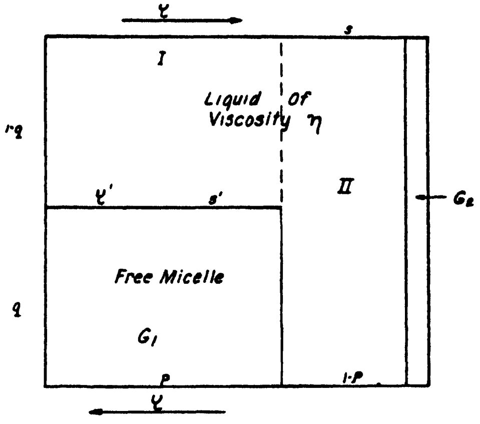

FIG 1. Theoretical model of mixed gel-sol system

When solved for the case of a particular value of the constant τ these equations give

$$s = \frac{\tau}{\gamma G_2}\{\gamma + (\beta + \lambda_2)e^{\lambda_1 t} - (\beta + \lambda_1)e^{\lambda_2 t}\} \tag{1}$$

in which

$$\lambda_1 \text{ and } \lambda_2 = -\tfrac{1}{2}\{(1 - q + pq)\alpha + \beta\} \pm \tfrac{1}{2}\gamma$$

Here

$$\alpha = \frac{G_1}{(1 - p)q\eta}, \quad \beta = \frac{G_2}{(1 - p)\eta}$$

and

$$\gamma = \lambda_1 - \lambda_2 = \sqrt{\{(1 - q + pq)\alpha + \beta\}^2 - 4\alpha\beta(1 - p)(1 - q)}$$

As elements with different properties must be combined to obtain a real material, the dependence of the deformation on time becomes more complicated. The integral values of the deformation, however, probably will be proportional to the stress whenever time is taken to be constant making

$$s = \tau f_1(t) \tag{1a}$$

At large deformations real structures will be destroyed and the applicability of equation 1a is, therefore, limited.

2. *Recovery*

Recovery phenomena may be derived from differential equations similar to those used above:

$$0 = (1 - p)\eta \frac{ds}{dt} + \frac{p\eta}{1 - q}\left(\frac{ds}{dt} - \frac{ds'}{dt}\right) + G_2 s$$

and

$$\frac{s'}{q} G_1 = \frac{\eta}{1 - q}\left(\frac{ds}{dt} - \frac{ds'}{dt}\right)$$

If these differential equations are solved for the case in which recovery follows immediately upon a deformation with shearing stress τ_0 during time t_0, an equation of the same type as equation 1 is obtained, which can be reduced to

$$s_e = \tau_0\{f_1(t_0 + t) - f_1(t)\} \tag{2}$$

where s_e is the part of the total recovery s_{e0} which the bitumen still has to cover at the end of the time of recovery t. Referred to the previous deformation s_0 or to the total recovery s_{e0}, equation 2 becomes

$$\frac{s_e}{s_0} = \frac{s_e}{s_{e0}} = \frac{f_1(t_0 + t) - f_1(t)}{f_1(t_0)} \tag{2a}$$

3. *Relaxation*

Relaxation is possible only with free micelles. Therefore the formula cannot be of type 1 or 2. If the relaxation follows immediately after a deformation during t_0 under τ_0, then

$$\tau_R = G_2 s_0 + \tau_0 \frac{p\alpha}{\gamma}\left(e^{\lambda_1 t_0} - e^{\lambda_2 t_0}\right)e^{-\epsilon t} \tag{3}$$

where

$$\epsilon = (1 - p)\,(1 - q)\alpha$$

In more general forms this equation is

$$\tau_R/\tau_0 = G_2 f_1(t_0) - f_2(t_0)e^{-\epsilon t} \tag{3a}$$

or even

$$\tau_R/\tau_0 = G_2 f_1(t_0) - f_3(t_0, t) \tag{3b}$$

Therefore relative relaxation stress-time curves must coincide with equal times of previous deformation, and it should further be possible to make relaxation curves with differing t_0, but with equal s_0, coincide by shifting them in the direction of the time axis.

4. Recovery after partial relaxation

If, after deformation s_0, a certain relaxation to the stress τ_{R0} takes place, followed by recovery, a recovery curve will have to be found coinciding with one after a deformation of s_0 under a smaller shearing stress, of such a magnitude that its relaxation stress at the first moment equals τ_{R0}.

5. Relaxation after partial recovery

In deformations to s_0 by τ_0 during t_0 and partial recovery to s_e during t_e followed by relaxation, the value of the elastic deformation of the free micelle after the partial recovery must first be calculated. With large enough recoveries this deformation can be negative, in which case during the relaxation following, the stress will *rise*.

For this case the following formula can be obtained:

$$\tau_R = \tau_{R(t_0 + t_e)} - \tau_{Rt_e} \tag{4}$$

This equation says that the relaxation stress in question is equal to the difference between the relaxation stresses after deformations with the same shearing stress during times $(t_0 + t_e)$ and t_e, if the three values of τ_R are taken after equal relaxation time.

The above formulas are derived for mixed gel-sol type systems and therefore also comprise the separate cases of the pure sol and pure gel type. Since the particular bitumens we examined showed pronounced relaxation which occurs only with free micelles, only the equations for the pure sol type need to be deduced.

(*1*) Deformation in connection with time is then found to be

$$s = \frac{\tau}{G_1}\frac{q}{1 - q + pq}\left\{(1 - p)(1 - q)\alpha t + \frac{p}{1 - q + pq}(1 - e^{-\gamma t})\right\} \tag{5}$$

in which $\gamma = (1 - q + pq)\alpha$. More generally this becomes

$$s = \tau\{At + f_3(t)\} \tag{5a}$$

(*2*) The recovery is represented by

$$s_e = \frac{\tau_0}{G_1} \frac{pq}{(1 - q + pq)^2} (1 - e^{-\gamma t_0}) e^{-\gamma t} \tag{6}$$

and the total recovery is therefore given by

$$s_{e0} = \tau_0 f_3(t_0) \tag{6a}$$

so that formula 5a can also be written as

$$s - s_{e0} = \tau A t \tag{5b}$$

Furthermore, formula 6 may be reduced to

$$\frac{s_e}{s_{e0}} = \frac{f_3(t_0 + t) - f_3(t)}{f_3(t_0)} \tag{6b}$$

so that for the sol type we must always refer the recovery to the total recovery.

(*3*) For the relaxation

$$\tau_R = \tau_0 \frac{p}{1 - q + pq} (1 - e^{-\gamma t_0}) e^{-\epsilon t} \tag{7}$$

so that the generalized form

$$\tau_R = \tau_0 f_4(t_0, t) \tag{7a}$$

becomes analogous to equation 3b.

(*4*) When after deformation partial relaxation is followed by recovery, the relationships are the same for the sol type as for the more general gel–sol type.

(*5*) When after deformation partial recovery is followed by relaxation, for the pure sol type no rise in the relaxation stress is possible but only a regular decrease to zero. It is not quite certain, however, that this will continue to apply with a more generalized model.

Before ascertaining in how far measurements are in agreement with the formulas, the following remarks have to be made: Owing to the continuous transition in chemical nature between the components that form the bitumen, it cannot be expected that there should be a sharp distinction between free and bound micelles in the mixed gel–sol type. Continuous transition may also be expected in the force with which the micelles are bound together. If loosely bound micelles are present, the theories given above may not fully apply.

The theory is based on the contrast between free and bound micelles. A similar mathematical analysis might be based on differences in the rate of mutual binding of micelles.

III. MEASUREMENTS

1. *Deformation*

In figures 2 and 3 curves for deformations under constant shearing stress have been drawn for bitumen A and bitumen B by plotting the logarithm of the deformation (log *s*) against the logarithm of the time of deformation (log *t*), *s* being expressed in centimeters of shear per centimeter of layer thickness and *t* in seconds. It appears that with small deformations the distances between the lines at the same times are approximately equal to the logarithms of the ratios of the shearing stresses applied, which is in agreement with formula 1 or formula 5.

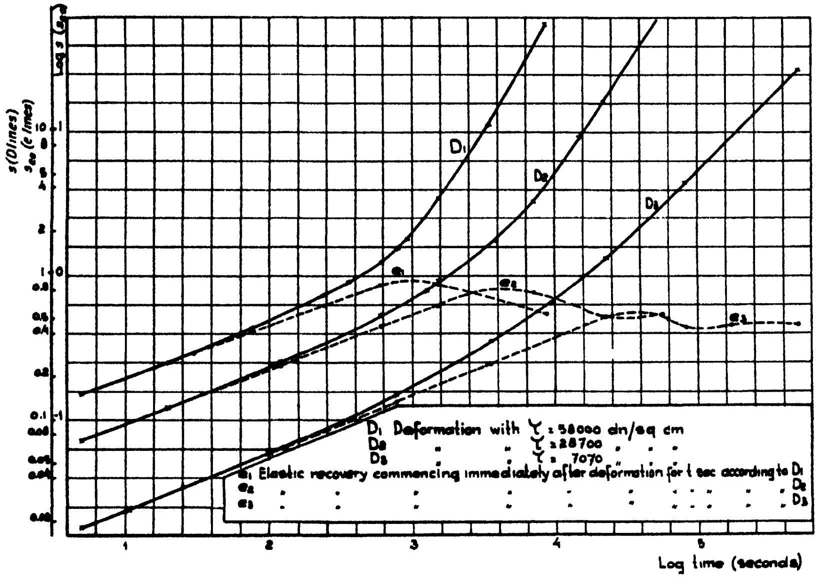

FIG. 2. Relation between deformation and time. Bitumen A

With greater deformations this rule no longer holds for bitumen A. When the rate of deformation for different values of *t* is calculated, it further appears for curves D_1 and D_2 for bitumen A that the rate of deformation increases with the time for greater deformations, which in the graph is clear from the slope of the curves. This is in agreement with the assumption that bitumen A contains a skeleton which is broken down at a certain deformation. It has further appeared that after a sufficient time of rest (1 to 3 days) the curve can be completely reproduced, whereas this is not possible at once, which indicates that this bitumen has the property of self-healing or thixotropy. Beyond the deformation at which structure is temporarily destroyed the curves cannot be derived from the model.

For small deformations the curves for bitumen A are practically straight and can therefore be represented by

$$s = \tau a t^n \tag{8}$$

Hence in formula 1a, $f_1(t) = at^n$, where $a = 1.38 \times 10^{-6}$ and $n = 0.38$.

Curves for bitumen B have been found to display a distinct curvature at small deformations, but after great deformations the slope becomes practically 1, so that ds/dt is constant. Hence there are here no indications for skeleton breakdown.

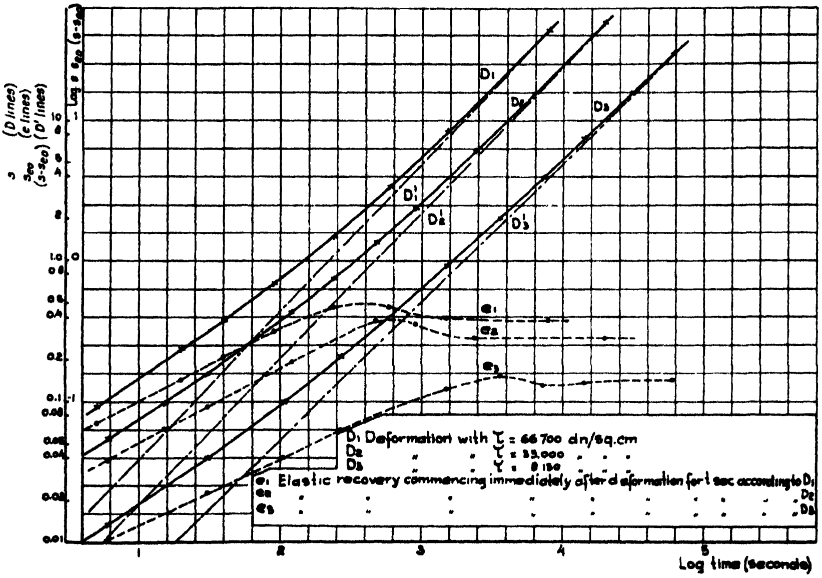

FIG. 3. Relation between deformation and time. Bitumen B

2. Recovery

In figures 2 and 3 are also plotted the curves e_1, e_2, and e_3, which indicate the total elastic recovery observed on releasing the external stress immediately after deformation during the period indicated on the abscissa. The distance between the corresponding lines D and e therefore gives for each time of deformation that part of the deformation which is permanent. It is clear that for bitumen A the total recovery after small deformation is complete, whereas this is not true in the case of great deformations. This makes it probable that in the case of small deformation bitumen A must be considered to have a coherent structure. In the case of bitumen B such a structure seems to be absent from the start.

With bitumen A the e lines display a distinct maximum near the deformation at which the *D* lines display the greatest curvature, indicating that after breakdown of the skeleton the total recovery becomes smaller. The order of magnitude at which serious breakdown occurs corresponds with that calculated by Kratky (2).

With bitumen B also the *e* lines afford indications of a breakdown either of a weak structure or of structures in small agglomerates, although for this asphalt the *D* lines do not disclose this property. In any case the behavior of bitumen B seems to approach that of the sol type, and for this reason we have further plotted, in figure 3, log $(s - s_{e0})$ against log time (curves D'), obtaining straight lines of slopes very close to 1 which approximately satisfy equation 5b. The secondary effects which account for the small deviations have been treated in previous publications (5).

It may further be noted that also in the case of bitumen A, log $(s - s_{e0})$ plotted against log time gives practically a straight line but the slope of this line is not always 1, and it is therefore described by the equation

$$s - s_{e0} = bt^m \tag{9}$$

where m may be >1 and can to a certain extent be used as a measure for thixotropy (4).

In figure 2 the first parts of the *e* lines coincide with the *D* lines and can therefore be represented, for these or even greater deformations, by the formula

$$s_{e0} = \tau_0 a t_0^n \tag{10}$$

In figure 3 the first part of the *e* lines, unlike that of the *D* lines, is straight and hence can also be represented by formula 10, where $a = 0.49 \times 10^{-6}$ and $n = 0.50$.

It is important to define the conditions under which no skeleton breakdown occurs. It was found that immediately after one experiment good duplicate results could be obtained as long as the previous deformation did not exceed $s = 0.6$ to 1.0 at most.

For bitumens A and B the rates of recovery are given in figures 4 and 5 by plotting s_e/s_{e0} against time. This permits comparison of the results with the theoretical recovery equation (2a), into which it has now become possible to introduce the specific form of the function as given by equations 8 and 10, so that we have

$$\frac{s_e}{s_{e0}} = \frac{(t_0 + t)^n - t^n}{t_0^n} = \left(1 + \frac{t}{t_0}\right)^n - \left(\frac{t}{t_0}\right)^n \tag{11}$$

In figures 4 and 5 there is a regular displacement of the lines dependent upon the duration of the preceding deformation as shown on the graphs, and apparently independent of other conditions. Quantitatively there is reasonable agreement, points of equal t/t_0 which according to equation 11 should have equal values of s_e/s_{e0}, and which in a few cases have been connected by lines, displaying differences between maxima and minima of 0.05. Direct calculation of s_e/s_{e0} by means of formula 11 gives values for bitumen A that are somewhat lower than those found experimentally,

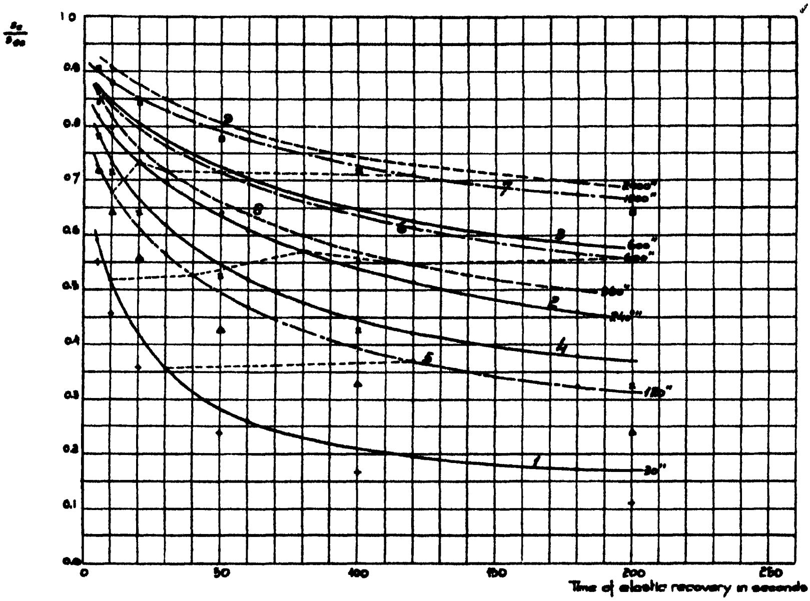

FIG. 4. Relation between s_e/s_{e0} and time after various deformations at different shearing stresses. Bitumen A. Times on curves refer to duration of previous deformation. Horizontal dotted lines connect points of equal t/t_0.

NO.	s_0	s_{e0}	t_0	τ_0	CALCULATED
			seconds	*dynes per sq.cm.*	
1	0.30	0.30	30	58,000	+
2	0.75	0.64	240	58,000	×
3	1.27	0.87	600	58,000	○
4	27.5	0.615	6000	58,000	
5	0.255	0.245	120	28,700	△
6	0.55	0.46	600	28,700	
7	0.87	0.625	1500	28,700	
8	0.135	0.12	360	7,080	
9	0.375	0.255	2400	7,080	□

the maximum difference being 0.10; for bitumen B the equation applies within the limits of error of our experiments. There therefore appears to be satisfactory agreement with the model.

With values of s_0 greater than 1, on the contrary, no agreement is found, probably owing to breakdown of structure.

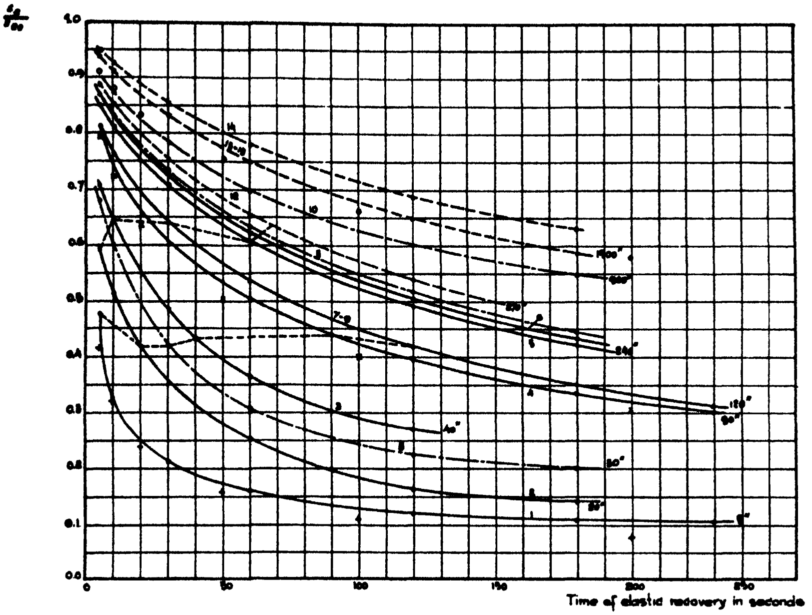

FIG. 5. Relation between s_e/s_{e0} and time after various deformations at different shearing stresses. Bitumen B. Times on curves refer to duration of previous deformation. Horizontal dotted lines connect points of equal t/t_0.

NO.	s_0	s_{e0}	t_0	τ_0	CALCULATED
			seconds	*dynes per sq.cm.*	
1	0.090	0.071	5	66,700	+
2	0.24	0.146	20	66,700	
3	0.382	0.21	40	66,700	
4	0.69	0.32	90	66,700	×
5	1.51	0.465	240	66,700	
6	3.37	0.473	600	66,700	○
7	45.4	0.38	7740	66,700	
8	0.161	0.094	30	33,000	
9	0.438	0.195	120	33,000	
10	2.40	0.356	900	33,000	
11	15.8	0.282	6000	33,000	
12	0.225	0.064	270	8,130	
13	0.945	0.128	1500	8,130	
14	4.22	0.131	7200	8,130	
15	7.5	0.135	14100	8,130	

3. *Relaxation*

In figures 6 and 7 the relaxation stress after various previous deformations under different shearing stresses have been plotted against time as

τ_R/τ_0. Here, too, the phenomenon discussed in the previous section is observed: up to deformations of s_0 = about 1 the curves fall in the expected order in accordance with the theoretical relaxation equation (3b), but at greater deformations these curves again lie in reversed order.

A second possibility of checking the relaxation equation is to compare the relaxation curves at equal values of s_0 but different values of t_0, since by displacing them in a τ_R–t diagram in the direction of the time axis it should be possible to make them coincide in accordance with equation 3. A few cases have been illustrated in figures 6 and 7, which must now be read as τ_R–t diagrams according to the scale division at the right-hand side of the diagrams. In these figures relaxation curves for a low shearing stress have been laid with their first points on a curve of higher shearing stress with the same previous deformation s_0. The agreement proves to be satisfactory.

4. Recovery after partial relaxation

In figure 8 the curves *A* and *D* are ordinary recovery curves of bitumen A, while curves *E* to *G* represent recoveries after partial relaxation. In all cases s_0 is about 1. It appears that the curves are of the same shape for both groups. The relaxation stress at the beginning of recovery agrees with that predicted by the model. The conditions of the deformation in experiment B are practically the same as those employed in the experiment represented by curve 14 of figure 6, for which by extrapolation a relaxation stress at $t = 0$ is obtained of about 26,000 to 28,000 dynes per square centimeter. It will be seen that this recovery curve *B* coincides fairly well with curve *F*, representing an experiment where a higher stress was released to 29,000 dynes per square centimeter before recovery started. Similar results were obtained using bitumen B.

5. Relaxation after partial recovery

This type of experiment has little accuracy, since calculation of the results by means of the model involves a difference between two measurements of relaxation stress.

In figure 9 is given the result of a single experiment using bitumen A. In agreement with the model it is found that the relaxation stress can rise at first.

Calculation of the relaxation stresses by means of equation 4, using the data of figure 6, gives reasonable agreement with the observations indicated by figure 9.

The gradual decrease of the stress shown by the bitumen after longer relaxation time is not in agreement with the model, for according to the model the relaxation stress must approach a constant value $G_2 s_e$. Here again the discrepancy may be attributed to skeleton breakdown, and better agreement would be expected at lower deformations.

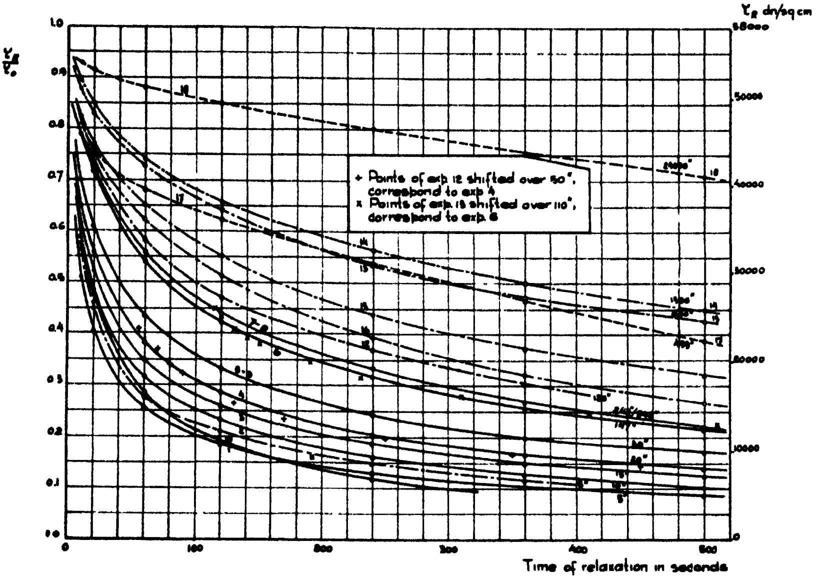

FIG. 6. Relation between τ_R/τ_0 and time after various deformations at different shearing stresses. Bitumen A. Times on curves refer to duration of previous deformation.

NO.	s_0	t_0	τ_0
		seconds	*dynes per sq.cm.*
1	0.176	5	58,000
2	0.203	10	58,000
3	0.225	15	58,000
4	0.247	20	58,000
5	0.262	30	58,000
6	0.53	147	58,000
7	0.75	242	58,000
8	1.27	546	58,000
9	3.26	1559	58,000
10	27.2	6660	58,000
11	0.083	5	28,700
12	0.247	120	28,700
13	0.53	600	28,700
14	0.90	1500	28,700
15	3.86	7200	28,700
16	16.9	21720	28,700
17	0.13	499	7,080
18	1.50	24000	7,080

In the case of bitumen B similar phenomena are observed, as shown by figure 10. Here, too, a maximum occurs in the relaxation stress-time curve after which, however, the relaxation stress decreases in the normal

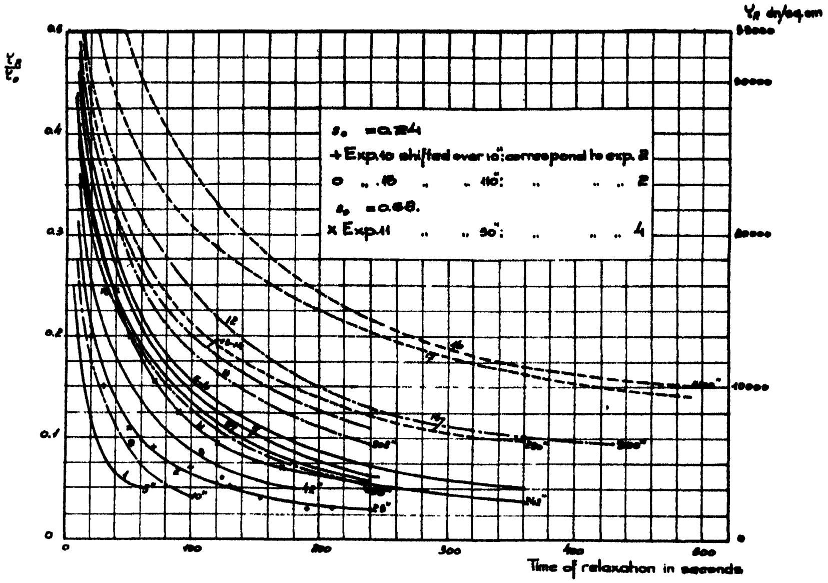

Fig. 7. Relation between τ_R/τ_0 and time after various deformations at different shearing stresses. Bitumen B. Times on curves refer to duration of previous deformation.

NO.	s_0	t_0	τ_0
		seconds	*dynes per sq.cm.*
1	0.097	5	66,700
2	0.24	23	66,700
3	0.375	42.4	66,700
4	0.68	92.4	66,700
5	1.50	242	66,700
6	3.34	603	66,700
7	8.4	1481	66,700
8	44.2	7525	66,700
9	0.052	10	33,000
10	0.24	58	33,000
11	0.68	208	33,000
12	2.24	900	33,000
13	16.1	6000	33,000
14	40.3	15600	33,000
15	0.24	280	8,130
16	2.68	5100	8,130
17	7.5	13780	8,130

way. These results indicate a weak structure for bitumen B as contrasted to a stronger structure for bitumen A.

From the foregoing discussions it has become clear that there is a satisfactory agreement between material and model.

From the data given it appears that in the two bitumens examined there must be a certain amount of coherence between the micelles. In the case of bitumen A this follows from the complete recovery after small deformations, from the maximum in the curve for the total recovery and from the higher rate of deformation, recovery, and relaxation at high deformations,

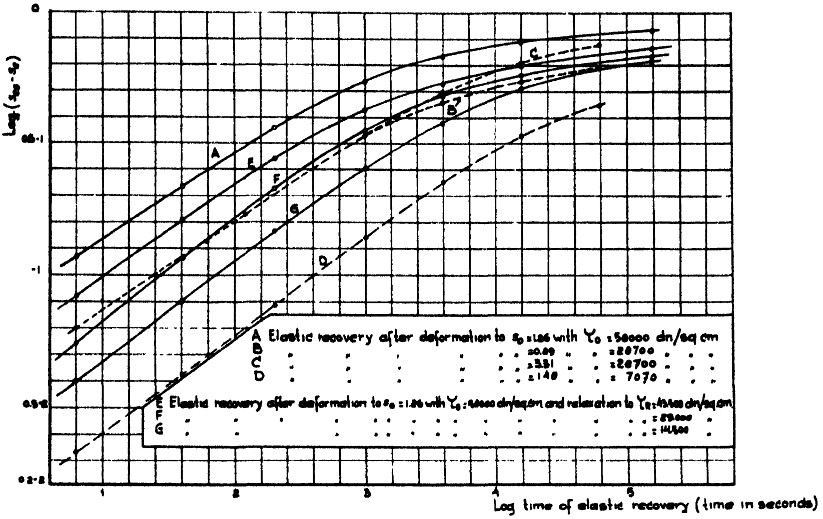

FIG. 8. Relation between elastic recovery and time after partial relaxation. Bitumen A

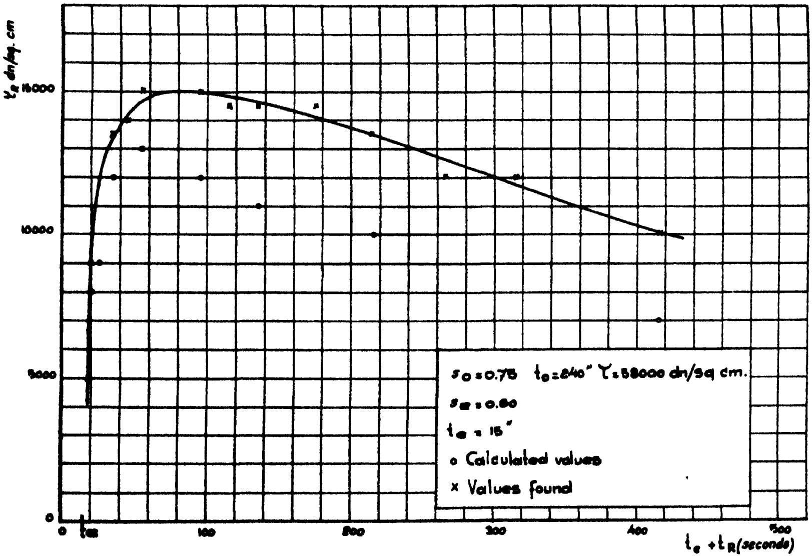

FIG. 9. Changes in relaxation stress after partial elastic recovery. Bitumen A

the last four factors pointing to breakdown of structure. In the case of bitumen B only the maximum in the curve for the total recovery and the higher rate of recovery and relaxation at high deformations were observed.

At deformations small enough to show no serious breakdown of the skeleton, a satisfactory agreement with the model system, representing a mixed gel–sol system, was found in the five different ways of investigation used. From this we conclude that the model in the main represents the constitution of the bitumen.

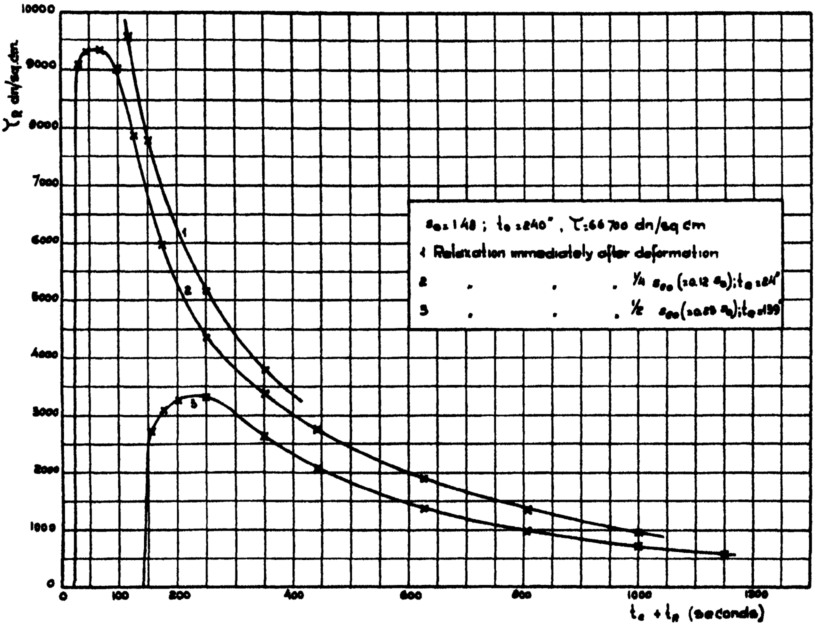

FIG. 10. Changes in relaxation stress after partial elastic recovery. Bitumen B

As bitumen A showed complete recovery at small deformation and pronounced skeleton breakdown at larger deformations, this bitumen must possess a marked gel structure. As bitumen B showed incomplete recovery and skeleton breakdown to only a slight degree, this product must be considered as containing either free agglomerates of micelles or very slight coherence throughout the material and is therefore more in the nature of a sol. This is in agreement with the theories formerly given by Pfeiffer and van Doormaal (3).

It will not be possible, however, always to account for still more complicated treatment. The following experiment may serve as an instance: The bitumen was deformed to $s = 1$, then by an opposite stress to $s = -0.4$, and then released. There was at first recovery to $s = +0.15$, when the movement was reversed. After reaching $s = +0.10$ it was again reversed, reaching a final position of $s = +0.12$. To explain such phenomena it will be necessary to assume coupling of differently formed elementary systems (1).

IV. SUMMARY

1. Rheological measurements in a conicylindrical rotation viscometer were carried out on two asphaltic bitumens of different types, employing methods of investigation involving deformations under constant stress, elastic recovery, relaxation, and combinations of these.

2. The experimental results were found to be in satisfactory agreement with the properties of a theoretical model representing the simplest form of a mixed gel-sol system.

3. It is concluded, in accordance with the views of Pfeiffer and van Doormaal, that asphaltic bitumens must be considered such mixed gel-sol systems and that the degrees of structure exhibited can vary widely with composition.

The authors are indebted to the Management of the N. V. de Bataafsche Petroleum Maatschappij for their permission to publish this paper and to their collaborators in these investigations.

REFERENCES

(1) BURGERS, J. M.: First Report on Viscosity and Plasticity. Academy of Sciences, Amsterdam (1935).

(2) KRATKY, O.: Kolloid-Z. **70**, 14 (1935).

(3) PFEIFFER, J. PH., AND DOORMAAL, P. M. VAN: J. Inst. Petroleum Tech. **22**, 414 (1936).

(4) PFEIFFER, J. PH., AND SAAL, R. N. J.: J. Phys. Chem. **43**, 139 (1939).

(5) SAAL, R. N. J.: J. Inst. Petroleum Tech. **19**, 176 (1933); Proc. World Petroleum Congr., London, **1933**, II, 515.

(6) TRAXLER, R. N., AND COLLABORATORS, *a.o.*: J. Applied Phys. **8**, 291 (1937); J. Phys. Chem. **40**, 1133 (1936).

THE SOLUBILITY OF CALCIUM OXALATE IN VARIOUS SALT SOLUTIONS

H. SHEHYN AND D. B. PALL

Analytical Laboratories, Aluminum Company of Canada, Arvida, Quebec, Canada

Received November 24, 1938

INTRODUCTION

Complementary to some analytical investigations, the solubility of calcium oxalate in various salt solutions has been established over a range of temperatures. The accuracy of these results appears to be greater than that of any previously reported work, making them of sufficient general interest to warrant publication.

MATERIALS

Calcium oxalate monohydrate was made from Baker's C.P. analyzed calcium chloride and oxalic acid. The material first obtained by direct addition of the reagents in hot solution, was recrystallized after dissolving in hot hydrochloric acid, by addition of ammonia solution. Finally it was filtered and washed with hot water and dried at 105°C. The soft cake so obtained was reduced to a powder by grinding in a mortar.

Sodium sulfate was prepared from sodium hydroxide and sulfuric acid used in equivalent proportions, crystallized by evaporation, and dried at 105°C.

Ammonium sulfate was prepared from the acid and base and crystallized by evaporation, keeping the mother liquor alkaline to methyl red by small additions of ammonia solution. The crystals were dried at room temperature. When results obtained with this material were compared with those using ammonium sulfate of Baker's C.P. analyzed grade, excellent agreement was found.

All other salts and all starting materials were of Baker's C.P. analyzed grade.

EXPERIMENTAL METHOD

At room temperature: To 250 ml. of salt solution of the required concentration, 125 mg. or more of $CaC_2O_4 \cdot H_2O$ was added. The mixture was then stirred mechanically for at least 10 min. After filtration, and without washing, the filtrate was acidified with 10 ml. of 1:1 sulfuric acid and titrated with 0.02 N potassium permanganate. Blanks were run in all cases. Temperatures were measured just before filtration and are good to about 0.5°C. The error due to hold-up in the filter paper is about 0.5 per cent; this was neglected. The highest concentration of chloride ion used did not affect the permanganate titration.

At 50°C.: The mixture, made up as before, was placed in a covered beaker and mechanically stirred in a water bath maintained at 50°C.; it was then filtered through a funnel in a bath kept at 55°C.; in this manner the temperature of the mixture was maintained at 50°C. ± 1° throughout the whole of the manipulation.

At 95°C.: The solution was first made up with about 20 ml. of water in excess and heated to boiling with an excess of calcium oxalate. The mixture was then poured into a specially constructed flask (A in figure 1).

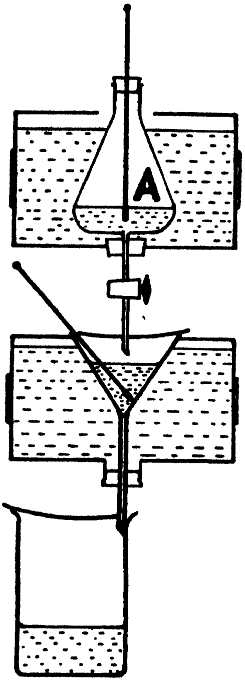

FIG. 1. Set-up for determining solubilities at 95°C.

After a temperature of 99°C. had been reached, as indicated by the thermometer in A, filtration was begun by opening the stopcock. When the lower bath was maintained at 100°C., the material in the filter was at 95°C. This was then assumed to be the temperature to which the measured solubility corresponded. This assumption seems justified, because the filtration was relatively slow and because while the solution, which had been previously saturated at a higher temperature, was in the funnel it was in intimate contact with crystalline monohydrate. The volume and temperature of the filtrate were now measured, and the volume calculated to room temperature. In order to obtain the results calculated to the volume at 95°C., 4 per cent should be subtracted from the values listed in the tables.

TIME REQUIRED FOR EQUILIBRIUM

This point is dealt with rather fully, because it is believed that some of the data appearing in the literature are low, owing to lack of equilibrium conditions.

In figure 2 curves are given in which the amount of calcium oxalate monohydrate dissolved is plotted against the time during which the mixture was rapidly stirred. If stirring were "occasionally by hand," as is reported by at least one investigator (3), the curves would be considerably flatter, and especially if insufficient excess oxalate were added, low results might easily be obtained. From an examination of figure 2, it was easy to decide on a minimum excess of calcium oxalate and a stirring time which would still make certain the establishment of equilibrium.

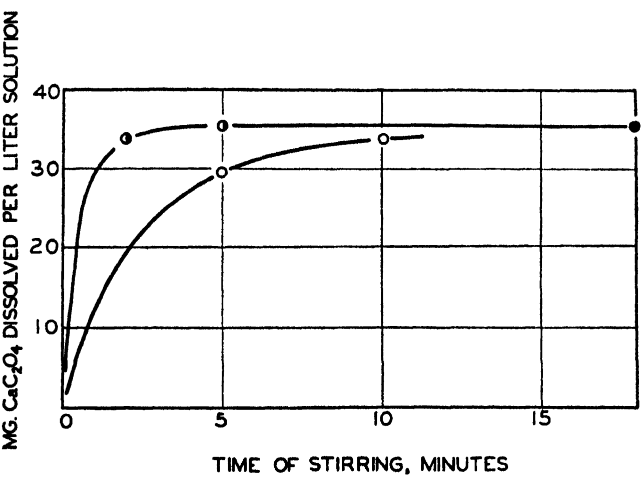

FIG. 2. Plot of calcium oxalate monohydrate dissolved against the time during which the mixture was rapidly stirred. ○, 200 mg. of CaC_2O_4 added per liter of solution; ◑, 400 mg. of CaC_2O_4 added per liter of solution; ●, 2000 mg. of CaC_2O_4 added per liter of solution.

SOLUBILITIES

The solubilities are summarized in table 1. They are plotted against the concentrations at the three temperatures in figures 3 and 4.

The solubility of calcium oxalate in water was determined by the same method and found to be 8.27 mg. per liter at 30°C., and 14.5 mg. per liter at 95°C. The value at 50°C. was obtained by interpolation, using a straight line on a log solubility–reciprocal temperature plot, and was found to be 10.0 mg. of CaC_2O_4 per liter.

The units of solubility are milligrams of anhydrous salt per liter of solution.

TABLE 1

Solubility of calcium oxalate in various salt solutions

SALT SOLUTION	MILLIGRAMS OF CaC_2O_4 PER LITER OF SOLUTION AT				
	27.5°C.	28°C.	30°C.	50°C.	95°C.
Sodium sulfate:					
3 g. Na_2SO_4 per liter		17.18		24.97	39.9
15 g. Na_2SO_4 per liter		34.08		49.75	83.5*
40 g. Na_2SO_4 per liter		55.19		84.30	144.0
Ammonium chloride:					
3 g. NH_4Cl per liter	16.40			21.62	34.2
15 g. NH_4Cl per liter	28.63			41.42	66.9
40 g. NH_4Cl per liter	41.22			61.14	104.7
Ammonium nitrate:					
3 g. NH_4NO_3 per liter	14.66				
40 g. NH_4NO_3 per liter	35.77†				
80 g. NH_4NO_3 per liter	46.49				
Ammonium sulfate:					
3 g. $(NH_4)_2SO_4$ per liter			21.5	28.85	47.5
15 g. $(NH_4)_2SO_4$ per liter			42.4	56.8	
25 g. $(NH_4)_2SO_4$ per liter					134.0‡
27.5 g. $(NH_4)_2SO_4$§ per liter			57.0		
40.0 g. $(NH_4)_2SO_4$§ per liter			70.2		
40 g. $(NH_4)_2SO_4$ per liter			72.1	97.8	
90 g. $(NH_4)_2SO_4$ per liter			109.4	147.2	314.5¶

* Average of two results (83.1 and 83.9).

† Average of two results (35.72 and 35.82).

‡ Average of two results (133.0 and 135.0).

§ Baker's C.P. analyzed.

¶ Average of two results (313.5 and 315.5).

CORRELATION

While the results with ammonium chloride are in rough agreement with those of Maljaroff and Gluschakoff (3), those with ammonium sulfate and ammonium nitrate differ by factors of four and three, respectively. This serious discrepancy made some sort of absolute check desirable. This is available in the rule which states that the effect of the addition of a second salt on the solubility of a given slightly soluble salt is the same for all salts and depends only on the ionic strength (2).

Thus if we read from the curves of figures 3 and 4, the solubilities of

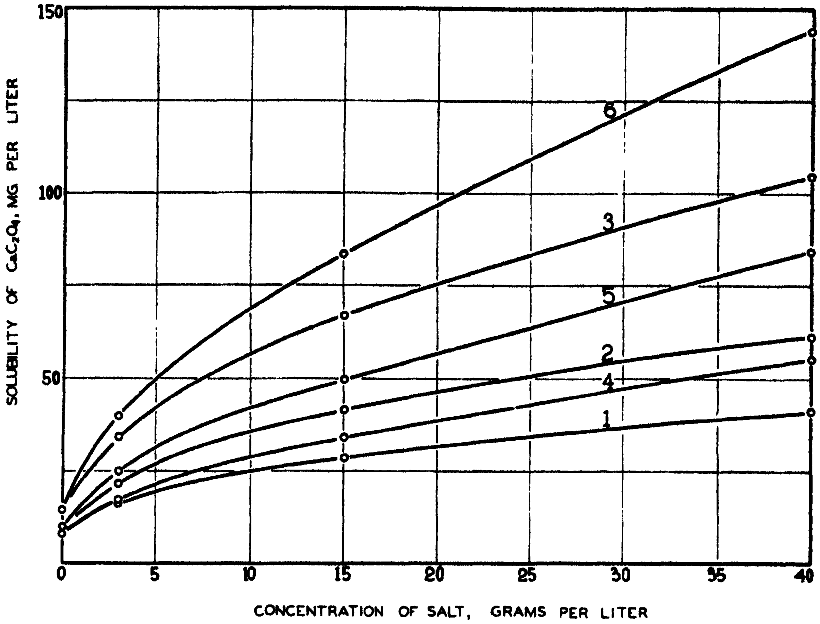

FIG. 3. Plot of solubility of calcium oxalate against the concentration of the salt solution. Curve 1, ammonium chloride at 27.5°C.; curve 2, ammonium chloride at 50°C.; curve 3, ammonium chloride at 95°C.; curve 4, sodium sulfate at 28°C.; curve 5, sodium sulfate at 50°C.; curve 6, sodium sulfate at 95°C.

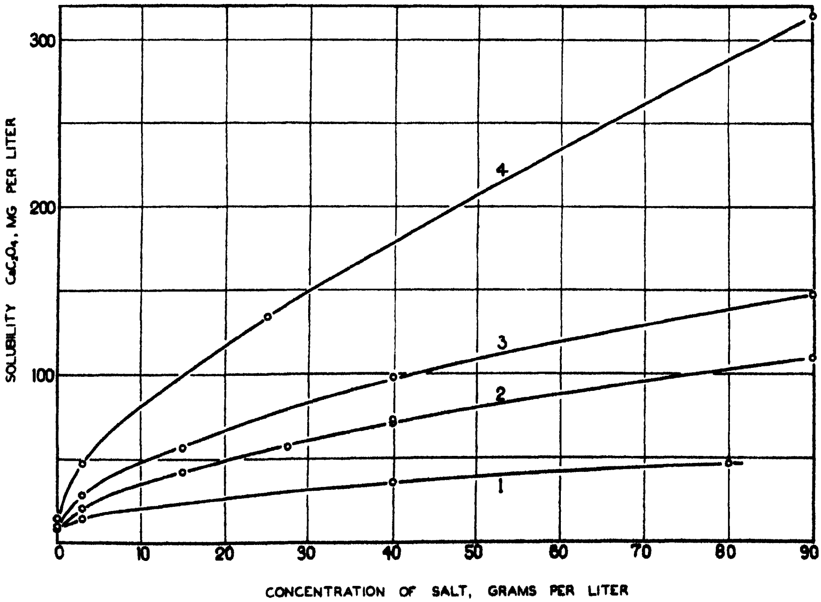

FIG. 4. Plot of solubility of calcium oxalate against the concentration of the salt solution. Curve 1, ammonium nitrate at 27.5°C.; curve 2, ammonium sulfate at 30°C.; curve 3, ammonium sulfate at 50°C.; curve 4, ammonium sulfate at 95°C.

calcium oxalate should be the same at the same "ionic strength concentration" of the second salt, regardless of the specific salt chosen.

The ionic strength is defined as:

$$1/2 \sum_{\mu} m_{\mu} e_{\mu}^2$$

where m_{μ} is the molarity of the μ^{th} ion, and e_{μ} is the charge of the μ^{th} ion.

For sodium sulfate and ammonium sulfate, the ionic strength is three times the molar salt concentration. For ammonium chloride and ammonium nitrate the ionic strength equals the molar salt concentration.

In table 2 the solubilities of calcium oxalate are compared for various ionic strengths of the second salt. The small temperature extrapolations required were easily made using a plot of the logarithm of the solubility against the whole range of the reciprocal of the temperature, which should give a straight-line relationship. The agreement is fairly good. It seems probable that the deviations at higher concentration are not experimental, and simply show that at these concentrations the rule of ionic strength no longer holds better than the experimental accuracy. The data for sodium chloride are from the work of Hammarsten (1).

TABLE 2

Solubility of calcium oxalate in various salt solutions, compared at the same ionic strengths at 28°C.

IONIC STRENGTH	MILLIGRAMS OF CaC_2O_4 PER LITER OF SOLUTION				
	NH_4NO_3	NH_4Cl	$(NH_4)_2SO_4$	Na_2SO_4	NaCl
0.01	10.4	10.0	10.3	10.0	11.3
0.02	12.1	11.6	12.0	11.6	11.6
0.05	16.1	15.9	16.6	15.8	13.3
0.10	21.6	20.2	22.8	21.1	18.6
0.20	28.0	25.9	33.6	26.5	23.0

SUMMARY

The solubility of calcium oxalate in ammonium chloride, ammonium sulfate, and sodium sulfate solutions has been determined at room temperature, 50°C., and 95°C., and over a range of salt concentrations. The solubility in ammonium nitrate solutions is given at room temperature only. The solubilities at room temperatures are correlated using the rule of ionic strength, and found to be consistent among themselves, and also with outside data for sodium chloride solutions.

REFERENCES

(1) Hammarsten, G.: Compt. rend. trav. lab. Carlsberg **17,** No. 11 (1929).

(2) Lewis, G. N., and Randall, M.: Thermodynamics, p. 374. McGraw-Hill Book Company, Inc., New York (1923).

(3) Maljaroff, K. L., and Gluschakoff, A. J.: Z. anal. Chem. **93,** 266 (1933).

THE EFFECT OF ROENTGEN IRRADIATION UPON ERYTHROCYTES

D. H. DRUMMOND, J. P. TOLLMAN, AND F. L. RICHARDS

Department of Pathology, University of Nebraska Medical School, Omaha, Nebraska

Received May 10, 1939

It was suggested by Failla (2) that as a result of irradiation the proteins of the cells were broken down to compounds of lower molecular weight. This raised the intracellular osmotic pressure, causing entrance of water into the cell with swelling. In order to test this theory Miss Woodard (7) studied the effects of irradiation with x-rays on the colloidal properties of sheep erythrocytes. Although red blood cells are quite radio-resistant, these were chosen since they presented a relatively simple single membrane equilibrium which would not be the case in nucleated cells. Miss Woodard found that cells which were suspended in hypertonic saline showed swelling after irradiation; those suspended in isotonic or hypotonic saline showed a decrease in volume after irradiation, as the result of the extensive hemolysis which occurred. Cells which had been kept in the ice-box for 6 or more days showed some spontaneous swelling and showed a decrease in volume after irradiation. This was considered to be due to a coagulating effect on the proteins. She felt that there was no primary damage to the cell membrane as a result of stretching in those cells which showed marked swelling.

Since the effect of imbibition of water would raise the concentration of electrolytes in the suspending solution, it was felt that a study of the concentration changes in the saline would give more information on this problem. Also, injury to the cell membrane would cause an opposite effect by allowing diffusion of salt into the cell. In the present work we studied these relationships by measuring the cell volume, the chloride concentration of the solution in which the cells were suspended, and the per cent of hemolysis.

EXPERIMENTAL

Sheep blood was used for the work, since it is quite resistant to hemolysis. The blood was collected in a flask containing sufficient sodium citrate to prevent coagulation. The blood was then centrifuged to throw down the cells, and the serum was removed. The cells were then washed four times with saline of the concentration to be used in the experiment and finally suspended in saline, the volume being made up to a value somewhat above that of the original blood volume. The washed cells were kept in the ice-box. Before each series of experiments the cells were washed once more, and then 15-cc. samples of the suspension were removed and transferred to Pyrex test tubes which were stoppered. These were then exposed for 45 min. to irradiation from a therapy tube at 22 cm. distance, using 200 kilovolts and 18 milliamperes and producing 365 r. per minute, giving a total irradiation of 16,425 r. The only filtration was by the wall of the Pyrex tube, which was about 1 mm. thick. At varying times after irradiation blood from one of the tubes was transferred to a hematocrit tube which was then centrifuged and the supernatant fluid was removed. After suitable dilution, to adjust the chloride-ion concentration to the correct range, the chloride content was determined by the method of Whitehorn for chlorides in urine (6). The same determinations were made on the control tubes. The cells in the control tubes were hemolyzed by adding distilled water and making up to a volume equal to the initial volume of the suspension. This was designated as 100 per cent hemolysis. This solution after dilution to approximately the same hemoglobin concentration as the supernatant saline was used as a standard for the colorimetric determination of hemolysis. Some of the original control tubes were centrifuged to pack the red cells. The supernatant fluid was carefully removed and then more dilute saline was added up to the original volume. After the cells were thoroughly mixed with the saline, a specimen was removed for a hematocrit determination. The contents of the test tube were then centrifuged again and the supernatant fluid analyzed for chloride and degree of hemolysis. Results of preliminary work with isotonic solutions are recorded in table 1. Since the marked hemolysis made these results unsatisfactory, the work was then carried out in hypertonic solutions. These results are recorded in table 2.

TABLE 1

Results of preliminary work with isotonic solutions

	NO.	HEMATOCRIT	HEMOLYSIS
			per cent
Cells equilibrated with 0.145 *m* NaCl	1	37.6	3.0
	2	37.6	4.0
	3	38.1	2.4
		37.4 (mean)	
Cells centrifuged and reëquilibrated with 0.145 *m* NaCl. .. .	1	38.3	10.0
	2	36.1	2.5
	3	36.1	3.1
		36.8 (mean)	
Cells irradiated after 15 hr. in ice-box	1	22.0	51.5
	2	18.0	39.0
	3	18.0	41.0

TABLE 2

Results with hypertonic solutions

A. Fresh cells

NO.	HEMATOCRIT	HEMOLYSIS	CHLORIDE CONCENTRATION	RELATIVE VOLUME
Control equilibrated with 0.336 *m* NaCl after washing with 0.142 *m* NaCl				
		per cent		
1	28.5	0.5	0.263	1.00
2	28.2	0.7	0.273	0.99
	28.4 (mean)		0.268 (mean)	
Reëquilibrated with 0.154 *m* NaCl				
1	36.0	1.0	0.190	1.26
2	36.0	0.9	0.178	1.26
Cells equilibrated with 0.336 *m* NaCl and then treated with x-ray; 2 hr. after irradiation				
1	32.0	1.1	0.270	1.13
2	32.0	1.8	0.272	1.14
Same after standing 15 hr. after irradiation				
1	31.0	4.5	0.280	1.13
2	32.0	4.3	0.284	1.17

B. Cells after being kept in ice-box for 5 days

NO.	HEMATOCRIT	HEMOLYSIS	CHLORIDE CONCENTRATION	RELATIVE VOLUME
Control equilibrated with 0.314 *m* NaCl				
		per cent		
1	28.5	0.5	0.267	1.00
2	28.5	0.5	0.267	1.00
Reëquilibrated with 0.142 *m* NaCl				
1	34.0	0.5	0.173	1.19
2	35.0	0.5	0.174	1.23
Cells equilibrated with 0.314 *m* NaCl; 15 hr. after irradiation				
1	32.5	1.5	0.258	1.16
2	32.0	1.5	0.260	1.13
3	32.0	1.5	0.262	1.13
4	32.0	1.5	0.260	1.13

TABLE 2—*Concluded*

C. Cells after being kept in ice-box for 10 days

NO.	HEMATOCRIT	HEMOLYSIS	CHLORIDE CONCENTRATION	RELATIVE VOLUME
Control equilibrated with 0.308 *m* NaCl				
		per cent		
1	30.5	0.2	0.243	1.07
2	30.5	0.2	0.245	1.07
Reëquilibrated with 0.135 *m* NaCl				
1	36.3	0.8	0.167	1.28
2	36.3	0.8	0.167	1.28
Cells equilibrated with 0.308 *m* NaCl; 4 hr. after irradiation				
1	32.5	1.0	0.223	1.18
2	32.5	1.0	0.223	1.18
3	32.5	1.0	0.222	1.18
4	32.5	1.0	0.222	1.18

DISCUSSION

It is seen from table 2 that after irradiation the cells showed uniform swelling and some degree of hemolysis. Also the chloride concentration decreased, showing that some chloride had diffused into the cells. If there were no injury to the membrane then water would be withdrawn from the saline with the swelling, causing a rise in the concentration of the saline. It is evident that both water and chloride diffused into the irradiated cells. The question now arises as to whether or not the entire swelling is due to membrane injury. If the cell membrane were injured so that it would freely transmit ions from the outside, sodium chloride would diffuse into the cell. The osmotic concentrations inside and outside would then be equalized and the cell would assume a volume equal to that which it would assume if it were placed in an isotonic solution. Consequently it is necessary to know volume changes in the normal cell for different concentrations of the saline.

Since the cells had been repeatedly washed with saline, the ions which could be replaced by chloride within the cells have been entirely replaced, owing to repeated equilibration according to the Gibbs-Donnan law. Consequently the concentration of chloride outside the cells is a measure of the hypertonicity of the solution, since no chloride shift can occur. In figure 1 there is plotted relative volume against chloride-ion concentration in millimoles per liter. The results obtained in this work are indicated by circles. In the higher concentrations there is quite good agreement. The scattering in the lower concentrations may be due to some difference in time of standing before the hematocrit determination, since Ponder and Saslow (3) have shown that there is some change in cell volume with time after change in the concentration of the suspending medium. These authors (4) have shown that the red cell does not act as a perfect osmometer, although Davson (1) has reported that the red cell is more nearly an ideal osmometer than Saslow and Ponder have found and that there is no diffusion of cations into the cell in hypertonic solutions. Warburg and Winge (5) have studied this problem, and their results are represented in the form of a graph showing the relative volume of erythrocytes on the abscissa and the relative salt concentration on the ordinate. It is seen that in the higher concentrations their curve approached a straight line, which is the nearest graphic representation of our data. By re-

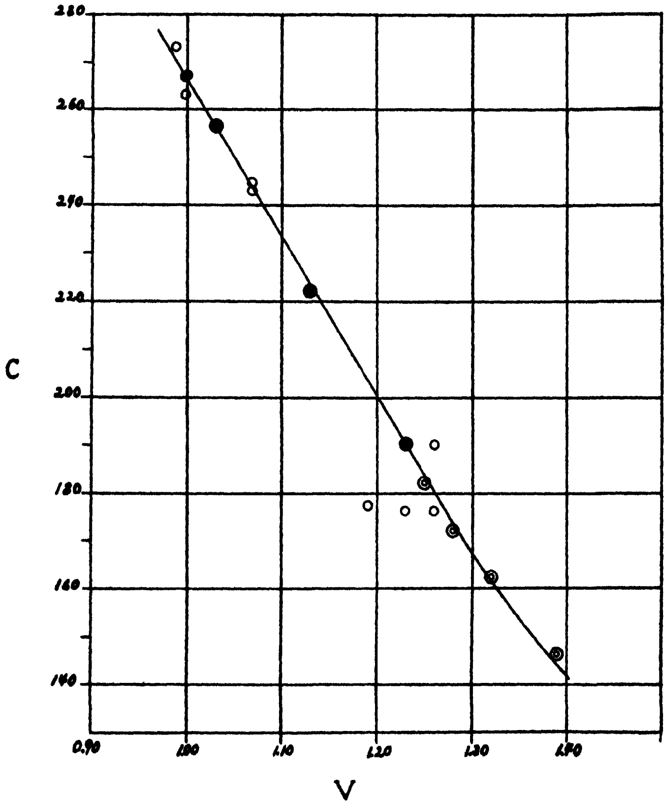

FIG. 1. Plot of relative volume of the cells against chloride-ion concentration in millimoles per liter

computing their results in the same terms as our graph it was possible to incorporate their results. Their figures, taken from arbitrary points on their curve, are represented by the double circles in figure 1. It is seen that at higher concentrations their curve straightens out into that represented by our results. The curve drawn in figure 1 is chosen to give the best representation of the combined points of our results and the Warburg and Winge curve. The curve on the graph is defined in the equation:

$$H = -0.00287C + 1.76 + (12.7 \times 10^4)/C^3 \qquad (1)$$

The solid points represent the recomputed ideal results given by Ponder and Saslow (4) for cells acting as perfect osmometers without diffusion of ions. It is not the purpose of this paper to discuss in detail the question of ionic permeability of red cells in hypertonic solution. It is nevertheless evident that there is some marked impermeability, since cells shrink in hypertonic solutions. Furthermore there is a relationship between cell volume and saline concentration represented by figure 1. In subsequent developments this graph will be used for reading off relative cell volume for any given saline concentration.

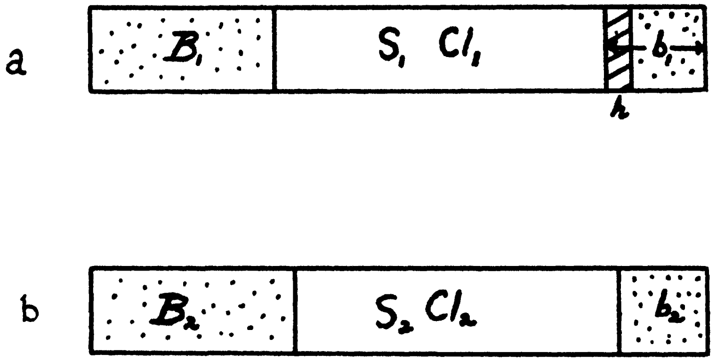

FIG. 2. (a) A tube before irradiation with an arbitrary separation of cells; (b) a tube after irradiation

The problem now presents itself to determine from the data how much of the swelling is due to injury to the membrane and how much is due to swelling of the cytoplasm due to irradiation.

In figure 2 the upper drawing represents a tube before irradiation with an arbitrary separation of cells. B_1 represents cells which will change volume without membrane injury after irradiation. b_1 represents cells which will swell as a result of injury to the membrane with diffusion inward of sodium chloride, together with the component h, which will hemolyze. After irradiation B_1 changes to B_2. Also the unhemolyzed portion of b_1, namely,

$(b_1 - h)$, has changed to b_2. The actual ratio of volumes irrespective of hemolysis and membrane changes is

$$B_2/B_1 = k \tag{2}$$

where k is an arbitrary swelling due to irradiation, which is to be computed. If H_1 and H_2 are the initial and final hematocrit readings, then

$$H_1 = b_1 + B_1 \quad \text{and} \quad H_2 = b_2 + B_2 \tag{3}$$

Since the total chloride present has not changed, although the concentration has done so, owing to diffusion into b_1, it is evident that

$$S_1Cl_1 = (S_2 + b_1)Cl_2 \tag{4}$$

and hence,

$$b_1 = \frac{S_1Cl_1 - S_2Cl_2}{Cl_2}$$

where S and Cl represent the volume and chloride-ion concentration of the saline, respectively.

To find B_2 two factors must be taken into account. One of these is the swelling due to irradiation and is measured by the factor k in equation 2. If k were unity there would still be a change in B_2 because of a change in chloride concentration from Cl_1 to Cl_2. This volume change can be read off from the graph; it is the factor read on the abscissa labeled V and denoted here by f_c.

Therefore

$$B_2 = B_1 \cdot k \cdot f_c \tag{5}$$

Similarly the volume b_2 is equal to the unhemolyzed portion of b_1 multiplied by the volume factor f_i, which is that for an isotonic solution and is seen from the graph to be 1.38.

$$b_2 = (b_1 - h) \times 1.38 \tag{6}$$

This relationship holds, since if b_1 is completely permeable to sodium chloride and water, then the osmotic pressure inside the cell will be equal to that outside; consequently it will assume a volume equal to that which it would assume in an isotonic solution.

The quantity h is the per cent actually hemolyzed as seen in figure 2. The per cent of hemolysis given in table 2 is based on 100 per cent hemolysis of the initial cell volume. Therefore h = per cent hemolysis (ϕ) times H_1. Finally, writing $H_2 - b_2$ for B_2 and $H_1 - b_1$ for B_1 (equation 3) and substituting from equation 6:

$$H_2 - (b_1 - \phi H_1) \times 1.38 = (H_1 - b_1)f_c \cdot k \tag{7}$$

Solving for k:

$$k = \frac{H_2 - (b_1 - \phi H_1) \times 1.38}{(H_1 - b_1)f_c} \tag{8}$$

Using equation 8 the values for k were calculated and recorded in table 3. It is seen that the fresh blood shows the highest values for k. After standing for some time there is a decrease and finally k becomes less than unity, representing a shrinking corresponding to the coagulation described by Miss Woodard. As for the nature of this process, it is felt that neither these results nor those of Miss Woodard throw any light upon this. Certainly there is some injury to the membrane of the cell. However, it is impossible to say whether this is primarily due to irradiation, or is due to injury from swelling. It might be that as the result of the swelling from irradiation some membranes are injured enough to produce hemolysis, while those more hardy or those subjected to less distension allowed free access to ions without releasing proteins. Further, the idea of Miss Woodard that this process is due to increase in the number of molecules in the protein is very questionable. Her idea would suggest more of a physical change of the molecular form of the protein, which one would expect to be independent of changes in its chemistry produced by standing. It would seem equally plausible that there are some colloidal changes, possibly related to changes in isoelectric point, which produced some swell-

TABLE 3

Calculated values of k

	NO.	VALUE OF k
A. Fresh cells 2 hr. after irradiation.....	1	1.16
	2	1.16
Fresh cells 15 hr. after irradiation.	1	1.21
	2	1.26
		1.20 (mean)
B. Cells 5 days old; 15 hr. after irradiation ..	1	1.06
	2	1.06
	3	1.08
	4	1.06
		1.07 (mean)
C. Cells 10 days old; 4 hr. after irradiation...	1	0.85
	2	0.85
	3	0.84
	4	0.84
		0.85 (mean)

ing on a chemical basis resulting in imbibition of water. This mechanism would be essentially different from inflow of water to equalize osmotic relationships. It would seem that the only answer to this would be direct molecular weight determinations on irradiated hemoglobin rather than dependence upon such complex relationships as those studied.

SUMMARY

1. It was found that irradiation by Roentgen rays caused swelling of erythrocytes.

2. Associated membrane damage was found dependent either upon irradiation or upon minimal injury due to swelling of the cell.

3. Diminution of volume after irradiation was found in those cells stored in the ice-box for some time.

4. The findings of Miss Woodard are in general confirmed, although it is felt that no adequate explanation can be given for the phenomenon.

The authors wish to express their appreciation to Dr. H. B. Hunt of the Radiology Department for the use of the therapy equipment and to Miss Gladys Anderson for carrying out the irradiations.

REFERENCES

(1) Davson, H.: Biochem. J. **30**, 391 (1936).
(2) Failla, G.: Address given at the meeting of the American Association for the Advancement of Science, December, 1936.
(3) Ponder, E., and Saslow, G.: J. Physiol. **70**, 169 (1930).
(4) Ponder, E., and Saslow, G.: J. Physiol. **73**, 267 (1931).
(5) Warburg, E., and Winge, K.: Acta Med. Scand., Supplement xvl, p. 500 (1928).
(6) Whitehorn, J. C.: J. Biol. Chem. **45**, 449 (1921).
(7) Woodard, H. Q.: J. Phys. Chem. **42**, 47 (1938).

CATALYSIS BY METALLIZED BENTONITES

GEOFFREY BROUGHTON

Department of Chemical Engineering, Massachusetts Institute of Technology, Cambridge, Massachusetts

Received March 4, 1939

Clays have long been known to possess catalytic activity, some varieties finding considerable industrial use as catalysts. Metallic ions present in the clays undoubtedly influence their activity; in some cases acid clays, i.e., clays which have undergone electrodialysis or treatment with acid to remove metallic ions, are found to be more active than the original clays. Nevertheless, no attempt appears to have been made to investigate the effect of single specific metallic ions upon the catalytic properties of a clay. Because bentonite is catalytically active and possesses a high base-exchange value, it was chosen for the present experiments. Specific metallic ions were combined with acid bentonite, and the catalysis of three typical reactions—the decomposition of hydrogen peroxide, the polymerization of pinene, and the thermal decomposition of 2-propanol (isopropyl alcohol)—was studied.

PREPARATION OF METALLIZED BENTONITES

A 4 per cent suspension of Wyoming bentonite was electrodialyzed in a cell of the Mattson type until the catholyte liquor was no longer alkaline. The acid clay, free from exchangeable cations, was suspended for 48 hr. in a saturated solution of the desired metallic chloride, centrifuged, and washed with distilled water until no chloride ion could be detected in the wash waters. After centrifuging, the samples were dried at 95°C. Analyses of the iron (ferric), nickel, and copper bentonites thus prepared showed 3.53, 2.22, and 1.25 per cent of metal, respectively.

TABLE 1

The decomposition of hydrogen peroxide

CLAY	HYDROGEN PEROXIDE REACTION CONSTANT (*K*) AT 27°C.	MAXIMUM TEMPERATURE RISE IN PINENE POLYMERIZATION
		°*C.*
Bentonite (raw)	4.4×10^{-4}	0.5
Acid bentonite	3.4	10
Sodium bentonite*	4.9	0.7
Calcium bentonite*	5.3	1.5
Iron bentonite (ferric)	13	12
Nickel bentonite	4.6	3.3

* Prepared by using 1 *N* instead of saturated chloride solutions.

HYDROGEN PEROXIDE DECOMPOSITION

Half a gram of the clay was added to 5.0 ml. of 2.98 per cent hydrogen peroxide solution in a mechanically shaken, small Erlenmeyer flask. The gas evolved was collected in a gas buret. The temperature was carefully controlled, and readings were made of the time and of the volume of gas evolved. Blank runs were made, using ferric chloride as catalyst and allowing decomposition to become complete.

All the clays tested catalyzed the reaction to some degree, the rate being represented by the equation:

$$\theta = \frac{2.303}{K} \log_{10} \frac{a}{a - x}$$

where a = the original concentration of hydrogen peroxide or the milliliters of total oxygen evolved when the reaction is allowed to proceed to completion, and x = the milliliters of oxygen evolved at time θ in minutes.

The reaction constants given in table 1 are, therefore, a measure of the catalytic activities of the different metallized bentonites. Because reaction velocity was found to be dependent upon particle size, all samples were ground to just pass a 100 mesh screen; grinding from 48 to 100 mesh increased the rate by about 25 per cent.

PINENE POLYMERIZATION

Half a gram of the clay sample, ground to just pass a 100 mesh screen, was added to a mixture of 1 ml. of pinene and 1 ml. of xylene (added as a diluent) contained in a test tube supported in a Dewar flask. The temperature of the mixture was noted every 30 sec., the maximum usually occurring after 2 or 3 min. Measurements were made on all the clays used in the hydrogen peroxide and 2-propanol reactions.

2-PROPANOL DECOMPOSITION

The thermal decomposition of alcohols can proceed with the elimination of hydrogen or water, the course of the reaction being dependent upon the catalyst. In the case of secondary alcohols, dehydrogenation rarely gives the ether (2). The reactions possible for 2-propanol are:

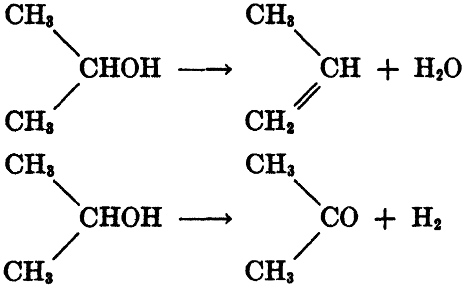

(I)

(II)

Reaction I is favored by catalysts such as sulfuric acid, thoria, clay, phosphoric acid, and boric anhydride; reaction II is favored by finely divided metals, nickel, copper, cobalt, iron, etc. The attachment of metals, such as nickel, to a clay surface may result, therefore, in changing the latter from a dehydrating to a dehydrogenating catalyst. This possibility was studied for 2-propanol.

From a buret, similar to that of Paik, Swann, and Keyes (1), mercury forced 2-propanol over into vaporizing coils set in an oil thermostat. The rate of flow of the alcohol could be measured in milliliters per minute to within about 5 per cent. The alcohol vapors were adjusted to catalyst temperature by passing through preheating coils in the electric furnace, the temperature of which was measured by a thermocouple external to the tube. This was calibrated against a thermocouple inside the tube in a preliminary run. Such procedure was necessary to avoid any catalysis by the thermocouple itself. Unreacted 2-propanol and any condensable reaction products were condensed out, and the gases evolved were collected over water at constant pressure. Analysis of the gas was made with an Orsat apparatus, propylene being determined by absorption in bromine water. In all cases the same amount of catalyst, ground to pass through a 4 onto a 28 mesh screen was used. Knowing the volume of gas collected and the volume of 2-propanol fed to the apparatus in the same time, the amount of decomposition could readily be calculated.

The 2-propanol used was dehydrated over solid caustic soda and distilled (b.p., 81.9°C.; $d_{23°}^{23°}$, 0.7889; $n_D^{20°}$, 1.3780).

TABLE 2

Thermal decomposition of 2-propanol

CATALYST	2-PROPANOL DECOMPOSITION AT 295°C.	COMPOSITION OF GAS EVOLVED		PINENE POLYMERIZATION OF CATALYST	
		C_3H_6	H_2	Before	After
	per cent	*per cent*	*per cent*	*°C.*	*°C.*
Alumina	22	100	0		
Acid kaolin	17	100	0	3.4	
Acid bentonite	33	100	0	11.1	5.1
Acid bentonite (250°C.)	16	100	0	11.1	5.1
Iron bentonite	18	100	0	11.5	5.6
Iron bentonite (250°C.)	7.5	100	0	11.5	5.6
Copper bentonite	53	97	3	7.1	3.0
Nickel bentonite	43	97	3	5.8	4.5

The results, together with the maximum temperature rises caused by the catalysts (both before and after use) in the pinene polymerization, are shown in table 2. Fractional distillation using a Podbielniak column indicated the presence of nothing but unchanged 2-propanol and water, with the possible exception of a trace of isopropyl ether from the acid bentonite condensate.

DISCUSSION

Tables 1 and 2 indicate that metallic ions attached to a clay do modify its catalytic properties to a considerable extent. Furthermore, their action varies with the reaction investigated. In some cases they appear to lower the activity of the catalyst; acid bentonite causes a greater temperature rise in pinene polymerization than any of the metallized bentonites with the exception of iron. Acid bentonite is also active in 2-propanol decomposition, being even more active than precipitated alumina. On the other hand, its activity towards the decomposition of hydrogen peroxide is small. Much more effective is iron bentonite, the ferric ions apparently remaining excellent catalysts in spite of their attachment to the clay. Pinene polymerization appears to be no guide to the influence of the clay catalyst upon the 2-propanol reaction. Copper and nickel bentonites, most active catalysts for the latter, show the least effect upon the former. In their case also the metallic ions act to some extent as dehydrogenating catalysts, as would the free metals, while the activity of the clay as a dehydrating catalyst is promoted by their presence. From the results as a whole there seems but little doubt that the clay and the combined metal behave independently to a considerable degree.

The diminished activities of the clays towards pinene polymerization after use in the thermal decomposition of 2-propanol are interesting. Alumina used as a dehydrating catalyst in the alcohol reaction becomes poisoned after a time and can be reactivated by ignition in a current of air. Presumably carbon is deposited upon some of the active areas of the catalyst, affecting its activity not only in the 2-propanol reaction but in other reactions as well.

SUMMARY

The catalytic activity of a number of metallized bentonites in three typical reactions has been investigated. The combined metal plays an important part, metal and clay apparently acting independently to a considerable degree.

REFERENCES

(1) Paik, Swann, and Keyes: Ind. Eng. Chem. 30, 173 (1938).
(2) Sabatier and Reid: Catalysis in Organic Chemistry. D. Van Nostrand Company, New York (1938).

THE STRUCTURE OF GELATIN SOLS AND GELS. VI

The Adsorption of Water Vapor and the Electrical Conductivity[1]

S. E. SHEPPARD, R. C. HOUCK, AND C. DITTMAR

Kodak Research Laboratories, Eastman Kodak Company, Rochester, New York

Received June 27, 1939

Part I. The Adsorption of Water Vapor

It has been pointed out elsewhere (17) by one of the authors that considerable information about the structure of xerogels—among which "air-dry" gelatin may be included—is obtainable by measurements of the sorption of vapors. Apart from this general interest for colloid science, the moisture regain of gelatin has a particular interest for photographic technology because of the considerable effect which the relative humidity, i.e., the moisture content, has upon the sensitivity of photographic emulsions (22).

Data found in the literature on the subject are rather scanty. Wilson and Fuwa (26) have given some data on the moisture regain of a gelatin at various humidities, but the data seem to have been recorded before (approximate) equilibrium had been reached, being much smaller than any we have obtained. Data given by J. R. Katz (6) are more comparable, although since the pH of coating is not stated, nor the concentration of the jelly, it is not possible to make a precise comparison. Making certain reasonable assumptions as to these factors, and as to the temperature, we have plotted his data in comparison with some of our own in figure 1.

MATERIALS USED

The gelatins used were (*a*) a lime-processed calfskin gelatin deashed to about 0.02 per cent ash (Eastman Kodak purified gelatin No. 70), having an isoelectric point at pH 4.8 ∓ 0.03, and an acid-processed pigskin gelatin, with an ash content of 0.07 per cent and an isoelectric point at pH 8.2. In order to give a relatively reproducible and controllable history and form to the samples, the gelatins were made to 7.0 per cent sols at the pH desired, coated on cellulose nitrate surfaces, and dried at 24°C. and 47 per cent relative humidity (R. H.) except when these factors—namely, concentration of sol and drying conditions—were specifically varied (*q. v. infra*). The gelatin skins were stripped from the support, and samples 3.8 cm. x 6.3 cm. x 0.0046 cm. were used for each experiment.

PROCEDURE

The samples were weighed in wide-mouth weighing bottles, then dried out over phosphorus pentoxide in large desiccators for 2 weeks. They were then weighed again, and placed in desiccators over sulfuric acid-water mixtures of known vapor pressures. A valuable summary of the vapor pressure *versus* density values of such mixtures has been given by R. E. Wilson (25). In our experiments the mixtures were prepared to give the desired vapor pressures or relative humidities, and the composition checked by density determinations. In the cases where a large number of comparisons were being made at the same relative humidity, the samples after drying over phosphorus pentoxide were placed in a large air-conditioned testing room at 24°C. (75°F.) and 47 to 50 per cent relative humidity. In every case the moisture regain or loss was determined after 2 weeks in the desiccators, which was found to be sufficient to attain (apparent) equilibrium. This was checked by accelerating the adjustment toward the end by operating an agitating fan within the desiccator and noting when no appreciable change of weight occurred. The accuracy of the procedure was controlled in certain cases by independent experiments which were made by P. T. Newsome, using an adsorption balance (16), and which gave excellent agreement. The "dry weight" over phosphorus pentoxide was checked at the end of each experiment by drying the sample

---

[1] Communication No. 732 from the Kodak Research Laboratories.

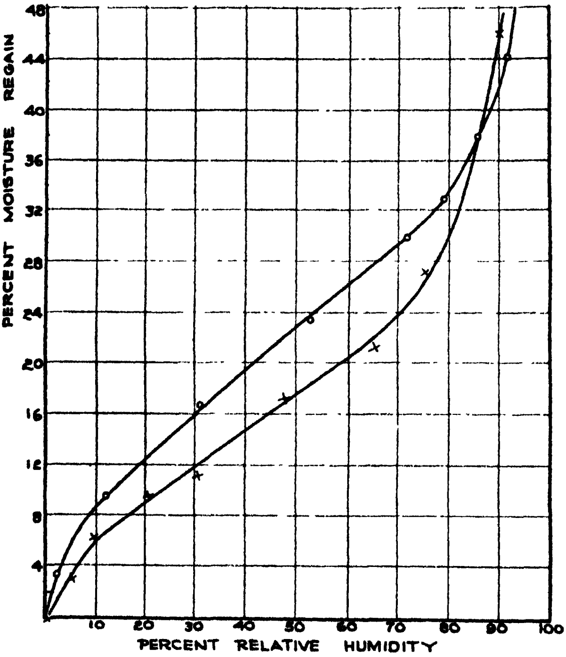

FIG. 1. Moisture regain of gelatin. O, values of Katz (Kolloid-Beihefte 9, a (1917); no mention of pH or temperature. X, values of Sheppard, Houck, and Dittmar, obtained with deashed gelatin (Eastman Kodak No. 70) at pH 6 and 1 temperature of 25°C.

overnight at 105–107°C. The measurements described here were all made at 25°C. ∓ 1°.

Various factors were investigated in regard to their influence on the adsorption isotherms at 25°C. The experimental results are now described separately.

RESULTS

1. *Effect of pH of gelatin sol at coating*

Neither Wilson and Fuwa (26) nor Katz (6) mentioned the pH of their gelatin. Probably this was in the neighborhood of pH 6, since the gelatins used were not deashed. In the first series, at 60 per cent relative humidity, deashed gelatin (Eastman Kodak No. 70) was used, coatings being made from 7 per cent sols adjusted to pH values from 2.8 to 9.0. The results are shown in table 1 and figure 2.

TABLE 1

Effect of pH of gelatin (Eastman Kodak No. 70) on the moisture regain

Samples 0.036 to 0.051 mm. thick; temperature, 24°C.; relative humidity, 60 per cent

pH	MOISTURE REGAIN
	per cent
2.8	15.2
4.0	17.4
4.9	19.56
6.0	20.01
7.0	20.3
8.0	20.14
9.0	20.9

The moisture regain increases rather sharply from pH 2.8 to pH 5.0, and then much more gradually.[2] There is no indication of a minimum at the isoelectric point (pH 4.9), as is found for the absorption of liquid water by this type of gelatin. This suggests a difference in the mechanism of the adsorption of water vapor to gelatin compared to that for liquid water absorption.

The general character of the relation between moisture regain and pH remains much the same at different humidities, so that the isotherms for different pH values are similar, only being displaced *en bloc* as shown in figure 3.

2. *Effect of concentration of the gelatin in the sol at coating*

Solutions of gelatin (Eastman Kodak No. 70) were made up at pH 4.77, concentrations being varied from 2 per cent to 15 per cent. They were coated with varying volumes so as to secure skins of the same thickness. Moisture regains obtained are given in table 2 and figure 4.

---

[2] D. R. Briggs (J. Phys. Chem. 35, 2914 (1939)) showed in the case of casein that the moisture regain increased as the pH was raised from pH 4.8 to 10.1.

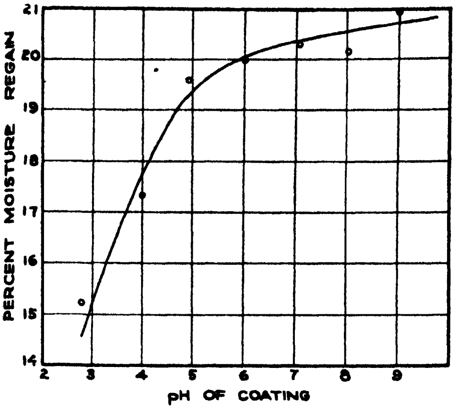

FIG. 2. Effect of pH of gelatin sol at coating on the moisture regain of deashed gelatin (Eastman Kodak No. 70); temperature, 25°C.; relative humidity, 60 per cent.

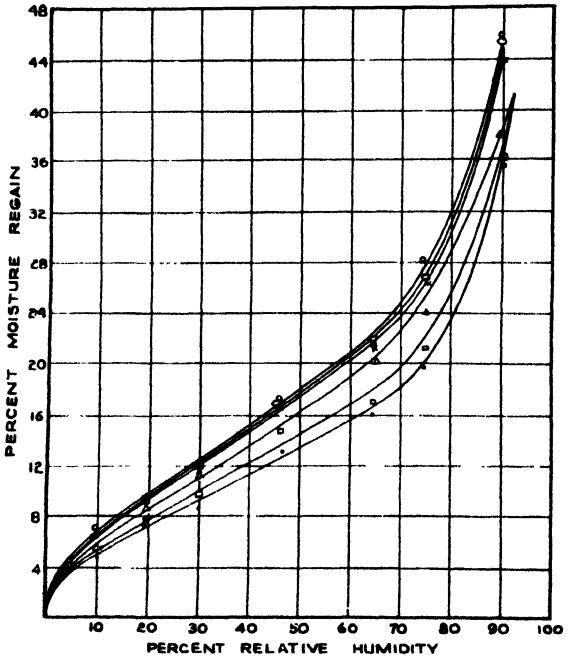

FIG. 3. Effect of pH of gelatin sol at coating on the moisture adsorption isotherm of deashed gelatin (Eastman Kodak No. 70), at 25°C. ●, pH 2.0; □, pH 2.9; △, pH 4.79; ×, pH 6.10; ⬭, pH 7.89; ○, pH 10.02.

In this case, the behavior is similar to that of gelatin with liquid water, in that there is a definite diminution of the take-up of water vapor as the concentration of the solution used in coating is increased. It appears that any internal structure difference with concentration, whether in regard to pore dimensions or to orientation of hydrophile groups, must be similarly effective in both cases.

3. Effect of thickness of gelatin layer

Coatings of 7 per cent concentration of gelatin (Eastman Kodak No. 70) at pH 4.77 were made to different thicknesses. The data are given in table 3. Above a thickness of 0.076 mm., the moisture regain remains practically constant, while a skin of 0.051 mm. showed a definitely lower regain. These results, and others confirming them, agree with those we have obtained with liquid water, in which case the absorption (swelling) was independent of the thickness up to 0.29 mm., above which it decreased somewhat.

TABLE 2

Effect of concentration of gelatin (Eastman Kodak No. 70) sol used in making gelatin coating on moisture regain

Temperature, 25°C.; pH, 4.77; relative humidity, 57–60 per cent

CONCENTRATION OF GELATIN SOL	THICKNESS OF COATING	MOISTURE REGAIN OF RESULTING GELATIN COATING
per cent	*mm.*	*per cent*
2	0.040	18.75
5	0.043	18.3
10	0.048	17.49
15	0.050	14.6

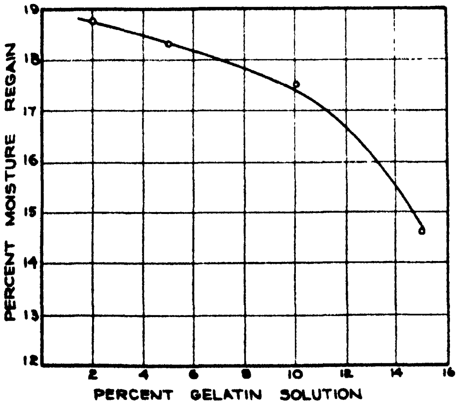

FIG. 4. Effect of concentration of gelatin sol at coating on moisture regain of deashed gelatin (Eastman Kodak No. 70) at a temperature of 25°C. and a relative humidity of 60 per cent.

4. Effect of hydrolytic degradation of gelatin

Deashed lime-processed calfskin gelatin (Eastman Kodak No. 67) was hydrolyzed in water at 90°C. for increasing periods of time, the degree of hydrolytic degradation being followed by the fall in viscosity of 5 per cent sols. Data are given in table 4.

In figure 5 are given comparisons of the adsorption isotherms for the original and the partly hydrolyzed gelatins. Apparently hydrolysis of this order has little effect upon the moisture regain.

TABLE 3

Effect of thickness of coating on moisture regain of gelatin (Eastman Kodak No. 70); various volumes of 7 per cent gelatin sol

Temperature, 25°C.; pH, 4.77; relative humidity, 45–47 per cent

THICKNESS OF COATING	MOISTURE REGAIN
mm.	*per cent*
0.050	14.67
0.076	17.24
0.101	17.55
0.127	17.39
0.152	17.56
0.179	17.66
0.203	17.60

5. Predrying conditions

It is known that the conditions of first drying of a gelatin jelly affect the degree of swelling in liquid water.[3] Some experiments were made to ascertain what influence this might have upon moisture regain. Gelatin (Eastman Kodak No. 70) was coated at pH 6 and dried under two conditions as follows:

WET BULB	DRY BULB	MOISTURE REGAIN AT 60 PER CENT RELATIVE HUMIDITY
°C.	*°C.*	[illegible]
17.2	24	20.4
25.0	50	19.0

The sample dried at the higher temperature had a slightly smaller regain. This difference was checked repeatedly, so it appears to be real. It is in the same sense as that for the absorption of liquid water, but less in magnitude, since in the latter case differences of 40 to 50 per cent are observed with similar preconditioning.

---

[3] Numerous investigations, including the one reported in reference 11.

6. *Type of gelatin and moisture adsorption*

Gelatins might be classified according to the original stock or source of origin, e.g., as hide, bone, or as calfskin, pigskin, etc. However, the principal difference is established by the pretreatment of the stock in preparation for the extraction, rather than by the original material,—at least so far as the ordinary industrially available materials are concerned. We expect to deal with this elsewhere, but in the present connection have compared the moisture adsorption isotherms at 25°C. of two contrasted types of gelatin, *viz.*, a lime-processed gelatin (Eastman Kodak No. 70) having an isoelectric point at pH 4.77, and an acid-processed pigskin

TABLE 4

Effect of degree of degradation on moisture regain of gelatin (Eastman Kodak No. 67)
Samples 0.050 mm. thick; temperature, 25°C.; pH, 5.02; relative humidity, 47 per cent

TIME HYDROLYZED	η IN C.P. AT 40°C.; 5 PER CENT SOL	MOISTURE REGAIN
hours		*per cent*
0.0	5.1	17.28
2.0	2.2	16.70
8.0	1.4	16.76

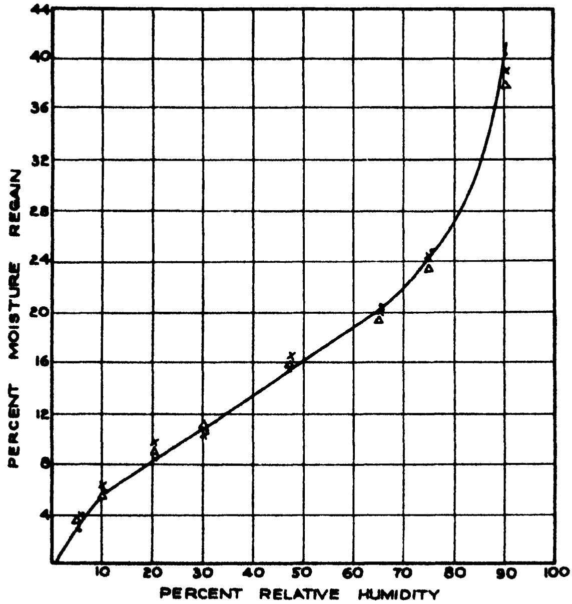

FIG. 5. Effect of degree of degradation of deashed gelatin (Eastman Kodak No. 70) on moisture regain at a pH of 4.77 and a temperature of 25°C. ●, original gelatin No. 70; △, hydrolyzed 2.5 hr. at 90–100°C.; ×, dialyzed hydrolyzed gelatin.

gelatin of isoelectric point 8.2. The data for moisture regains are shown in figure 6.

Both gelatin sols were adjusted to pH 6.0 at coating. It will be seen that no difference in moisture regain was observed until high humidities were reached, when the lime-processed gelatin began to adsorb considerably more water vapor. The values for the acid-processed gelatin at pH 8.2, its isoelectric point, are slightly higher than at 6.2. The differences in moisture adsorption of these two gelatins are much less than for the adsorption of liquid water. Lime-processed gelatin shows a well-defined minimum at its isoelectric point, *ca.* pH 5, the adsorption then rising sharply at higher pH values, while acid-processed gelatin of, e.g., isoelectric point pH 8, shows a zone of minimum swelling sometimes extending from pH 5 to pH 11.

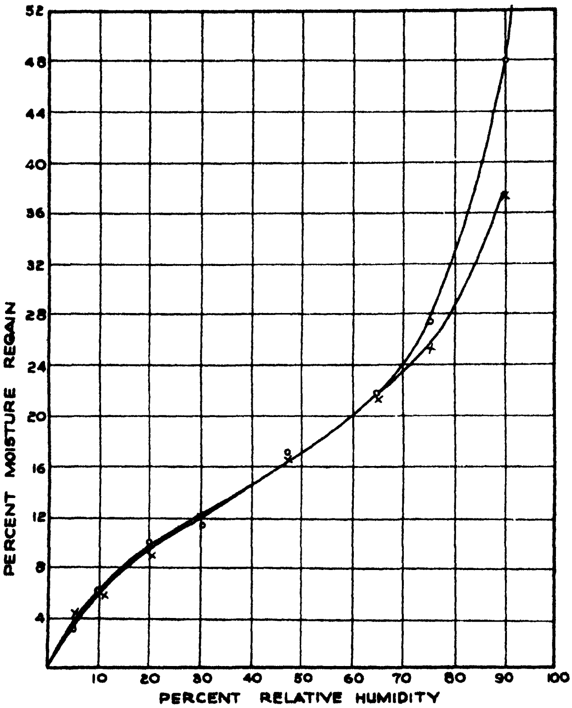

FIG. 6. Effect of isoelectric point of gelatin on moisture regain at 25°C. O, lime-processed gelatin (Eastman Kodak No. 70), pH 6.0, isoelectric point at pH 4.77; ×, acid-processed gelatin, pH 6.0, isoelectric point at pH 8.2.

GENERAL DISCUSSION OF THE ADSORPTION ISOTHERM

The general character of the isotherm is shown in figures 1, 3, 5, and 6. The typical S-shaped curve resembles those obtained for silk, wool, and cellulose. On desorption, similar hysteresis phenomena are observed (see figure 7).

It seems probable that much the same mechanism is involved. In the case of cellulose, Sheppard and Newsome (21) concluded that "There are two main forces influencing the adsorption of water vapor. First, water is initially adsorbed at inner surfaces by the free hydroxyls of the cellulose material (i.e., those lying exposed, not holding each other in the formation of the crystallized portion) and secondly, further adsorption consists mainly in the condensation of water vapor in the voids of the structure." In the case of gelatin, the initial adsorption is probably chiefly due to the amino groups, which are freed on the alkaline side of the isoelectric point. But the rapid fall of moisture regain as the pH is lowered to 3 is not easy to interpret, particularly as it is so opposed to the behavior in liquid water. Possibly we may suppose that the carboxyl groups are so mutually oriented, with hydrogen bridge formation, that they cannot readily solvate in vapor phases.

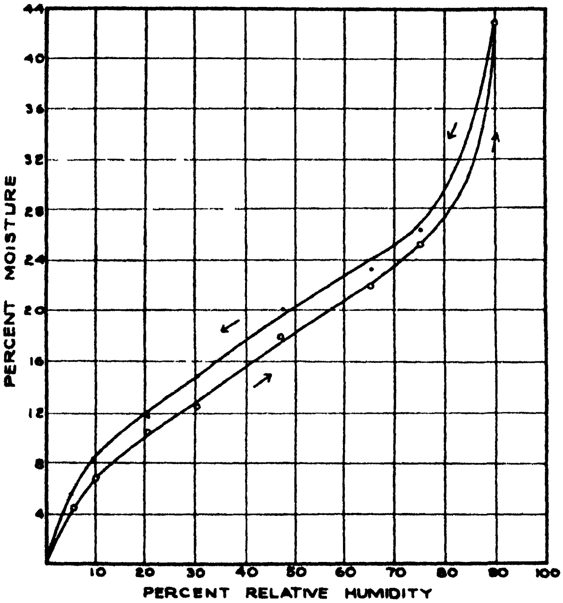

FIG. 7. Sorption hysteresis of deashed gelatin (Eastman Kodak No. 70) at pH 6 and 25°C. ○, adsorption; ●, desorption.

A further experimental aspect of the problem is furnished by the electrical conductance properties to be described in Part II.

In photographic practice the gelatin of emulsions is often "hardened," i.e., tanned by treatment with various substances, either incorporated in the emulsion before coating or used in solutions in the course of processing.

Of these, chrome salts, such as potassium chrome alum, and formaldehyde are typical. It was of interest to ascertain what effect they have on moisture adsorption. The isotherms plotted in figure 8 show that the effect is slight for adsorption from the vapor phase, although swelling in liquid water is greatly reduced.

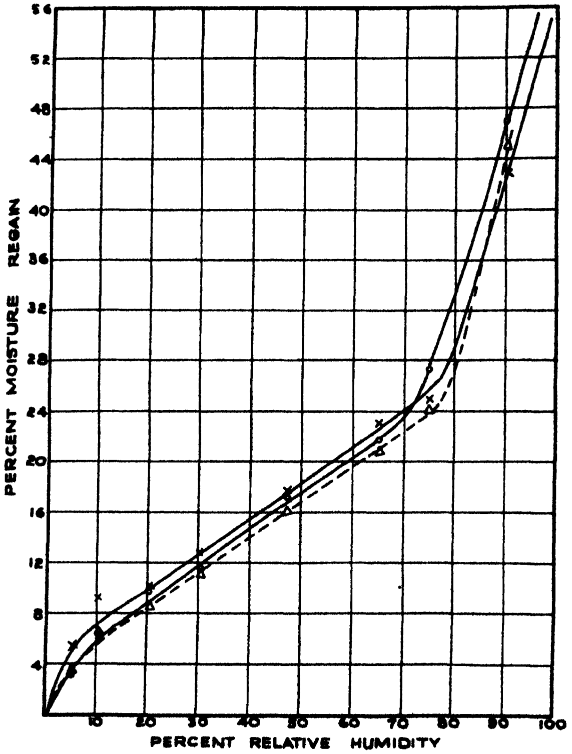

FIG. 8. Effect of hardeners on moisture regain of deashed gelatin (Eastman Kodak No. 70) at pH 6.08 and 25°C. ○, gelatin No. 70 (per cent liquid absorbed = 1704); ×, chrome alum-hardened gelatin (per cent liquid absorbed = 343); △, formaldehyde-hardened gelatin (per cent liquid absorbed = 266).

PART II. THE ELECTRICAL CONDUCTIVITY OF GELATIN GELS

MATERIAL AND PROCEDURE

The gelatin skins used were prepared from the deashed gelatin (Eastman Kodak No. 70) used for moisture regain experiments. Coatings were made on glass and dried at 24°C. and 47 per cent relative humidity. The thickness, when not specifically varied, was 0.046 ∓ 0.002 mm. The samples, held in special glass racks, were conditioned for 2 days at 27.8°C. and the desired relative humidity.

The humidor in which the conditioning and the measurements were made is shown in figure 9. It is a large air-tight metal box in which air circulation is obtained with a small blower. This drew the air down from the top of the box over the samples, then over trays of sulfuric acid water

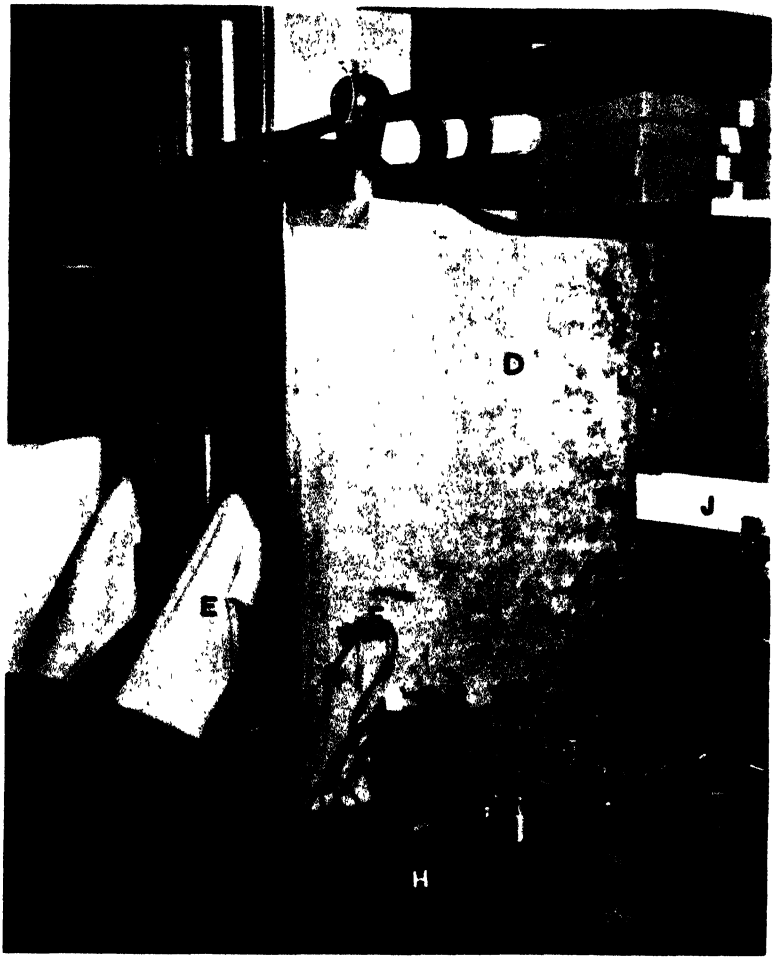

Fig 9 Humidor G, galvanized humidity box; E, long gauntlet gloves. F, Bakelite plug; G, variable mica condenser; H, discharge switch, J, scale

mixtures and so back to the blower. The actual relative humidity was checked by wet-bulb and dry-bulb thermometers, and the humidor was thermostated at 27.8°C. The electrodes and samples could be manipulated in the box by using long rubber gauntlet gloves sealed to the outside. Very great care is necessary in maintaining the samples at constant humidity, since, as will be seen, the conductivity changes very rapidly with change of humidity.

The electrodes consisted of brass strips 3 mm. wide by 2.5 cm. long mounted on Tenite, as shown in figure 10. The contacting metal surfaces were given a matte surface by engraving a half-tone line-screen image of 150 lines per inch, using a regular copper plate etching bath.[4] This gave a uniform dot formation over the electrode surface, and with sufficient weighting gave a very reliable contact. The electrodes were separated by an interval of 25 mm. Leads to the measuring apparatus were carried through a special Bakelite plug. The actual resistance was measured by a ballistic method. A condenser in series with the sample bridging the electrodes was charged at a known voltage for a definite time, then discharged through a high sensitivity ballistic galvanometer. The hook-up is shown diagrammatically in figure 11. The applied voltage and the capacity of the condenser were varied according to the order of the resistance being measured.

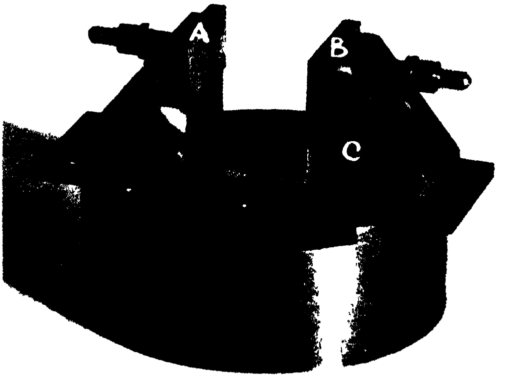

FIG. 10. Electrode mounting. A and B, etched brass electrodes; C, Tenite

The measurement was made by placing the conditioned coated plate across the electrodes, weighting with a 2-kg. weight to insure good contact, charging for a definite length of time, and noting the deflection of the galvanometer on discharge.

The resistance was calculated according to the equation:

$$2.303\left(\log \frac{d_\infty - d_T}{d_\infty}\right) = -\frac{T}{RC} \quad \text{or} \quad R = \frac{T}{C \times 2.3 \log\left(\frac{d_\infty}{d_\infty - d_T}\right)}$$

---

[4] Our thanks are due to Mr. G. Wilhelm of the Photoengraving Department of these Laboratories for the engraving.

in which d_∞ = deflection when condenser is completely charged,
d_T = deflection at time T,
T = time of charging in seconds,
C = capacity of condenser in microfarads, and
R = unknown resistance in megohms.

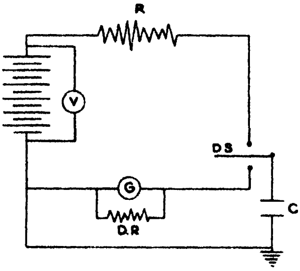

FIG. 11

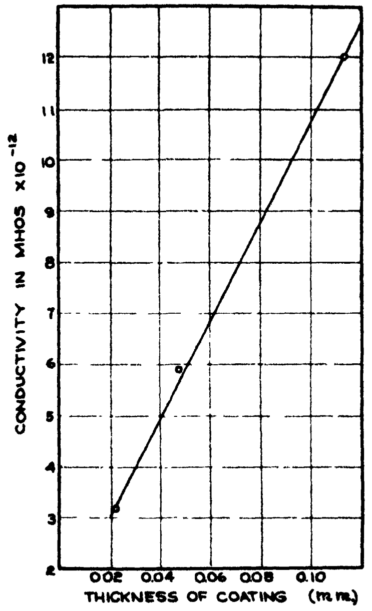

FIG. 12

FIG. 11. Hook-up for measurement of resistance. V = voltmeter; R = unknown resistance; C = high-grade mica condenser (a Leeds and Northrup variable condenser); G = high-sensitivity ballistic galvanometer; D.R. = damping resistance (40,000 ohms); D.S. = discharge switch.

FIG. 12. Effect of thickness of coating on conductivity of emulsion A; pH, 6.3; relative humidity, 45 per cent; temperature, 27.8°C.

The d_∞ for any charge up to 0.15 microcoulomb is determined by direct measurement. The d_∞ for charges greater than 0.15 microcoulomb is calculated from the equation:

$$d_\infty = \frac{V \times C}{0.15} \times d_{0.15}$$

in which V = applied voltage, C = capacity of condenser in microfarads, and $d_{0.15} = d_\infty$ for a charge of 0.15 microcoulomb. All the conductivities are given for a 25-mm. separation of the electrodes.

This method of determination and calculation was checked against the leakage method of determining high resistance, using known high resistances. The results obtained checked quite satisfactorily, as shown by table 5.

TABLE 5

Comparison of stated and experimentally determined values of resistances

RESISTANCE (GIVEN BY MANUFACTURER)	DETERMINED RESISTANCE	
	Charge and discharge method	Leakage method
ohms	*ohms*	*ohms*
5.9×10^9	4.4×10^9	4.1×10^9
1.5×10^{10}	1.2×10^{10}	1.19×10^{10}
1.6×10^{11}	1.52×10^{11}	1.58×10^{11}

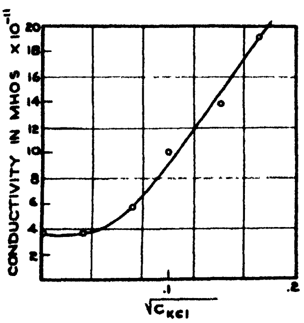

FIG. 13

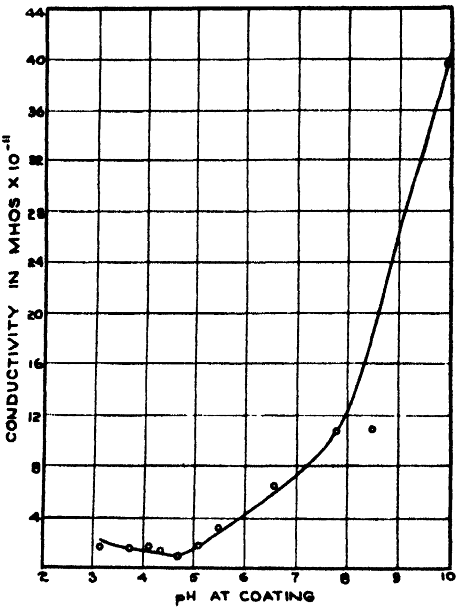

FIG. 14

FIG. 13. Effect of concentration of potassium chloride on conductivity of deashed gelatin (Eastman Kodak No. 70) at pH 6.1 and a relative humidity of 48 per cent.

FIG. 14. Effect of pH of gelatin sol at coating on conductivity of deashed gelatin (Eastman Kodak No. 70) at 27.8°C. and a relative humidity of 51 per cent.

1. *Effect of thickness of coating*

Over the range of thickness studied the conductivity is directly proportional to the thickness (*cf.* figure 12). This shows that the conductance is a volume effect, in agreement with the conclusion of Marsh and Earp (13) on the electrical conductivity of wool fibers.

2. The effect of neutral salts

Coatings of gelatin (Eastman Kodak Company No. 70) at pH 6.1 were measured with varying content of potassium chloride (*cf.* figure 13). A similar result was obtained with potassium bromide in a gelatino-silver bromide emulsion.

TABLE 6

Effect of pH at coating on the conductivity of gelatin (Eastman Kodak No. 70)

Temperature, 27.8°C.; relative humidity, 51 per cent

pH AT COATING	CONDUCTIVITY	WATER IN SAMPLE
	mhos	*per cent*
3.17	1.65×10^{-11}	15.05
3.74	1.5×10^{-11}	15.60
4.14	1.59×10^{-11}	15.5
4.31	1.07×10^{-11}	15.69
4.77	8.916×10^{-12}	16.55
5.05	1.81×10^{-11}	16.79
5.5	3.19×10^{-11}	16.96
6.62	6.58×10^{-11}	17.41
7.8	1.1×10^{-10}	18.45
8.48	1.1×10^{-10}	18.48
9.95	3.95×10^{-10}	17.77 (?)

TABLE 7

Effect of pH at coating on the conductivity of gelatin (Eastman Kodak No. 70)

Temperature, 27.8°C.; relative humidity, 48 per cent

pH AT COATING	CONDUCTIVITY	WATER IN SAMPLE
	mhos	*per cent*
2.19	4.25×10^{-11}	11.5
3.23	7.07×10^{-12}	15.15
3.82	7.36×10^{-12}	15.6
4.42	4.69×10^{-12}	16.15
4.83	5.0×10^{-12}	16.7
5.61	1.18×10^{-11}	16.95

3. Effect of pH

Solutions of deashed gelatin (Eastman Kodak No. 70) were adjusted to various pH values with sulfuric acid and sodium hydroxide, the pH values being measured with a glass electrode prior to coating. The coatings, after drying at 24°C. and 47 per cent relative humidity, were conditioned at 51 per cent relative humidity. Control samples were identically treated to obtain moisture contents, and the conductivities were measured. The data obtained are given in tables 6 and 7 and are graphed in figure 14.

These results show some indication of a minimum conductance at the isoelectric point pH 4.77.[5] The moisture regain values, as noted before, do not show this. Further data definitely establish this (*cf.* figure 15), and the presence of solid silver halide, as in photographic emulsions, did not interfere. The divergence in character of the effect of pH on moisture adsorption and on electrical conductance will be discussed later. Here it should be noted that the contour of the graphs of conductivity against pH given here is not a correct representation of the actual relation, because the water content—at the same relative humidity—is varying also with the pH (*cf.* figure 2). The correct comparison would be conductivities of gelatins of different pH but constant water content. This means changing

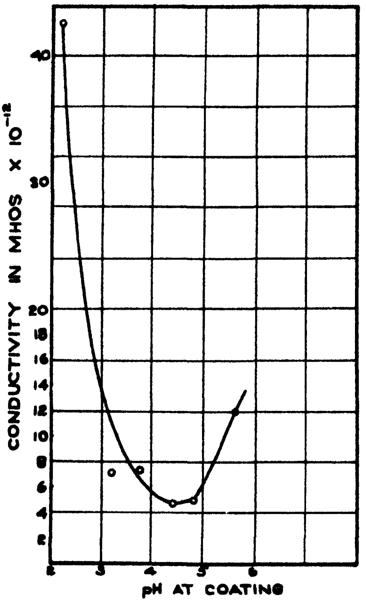

FIG. 15

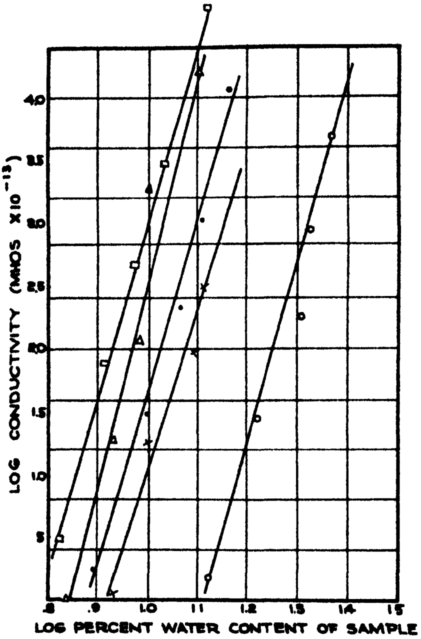

FIG. 16

FIG. 15. Effect of pH of gelatin sol at coating on the conductivity of deashed gelatin (Eastman Kodak No. 70) at 27.8°C. and a relative humidity of 48 per cent.

FIG. 16. Effect of water content of sample on the conductivity of gelatin and of photographic emulsions at 27.8°C. Plot of log conductivity against log water content of sample. ○, deashed gelatin (Eastman Kodak No. 70), pH 6.10; ×, photographic emulsion A, pH 6.20; ●, photographic emulsion B, pH 6.21; △, photographic emulsion C, pH 6.14; □, photographic emulsion D, pH 6.21.

---

[5] This result is in agreement with that obtained by W. S. Denham, E. A. Hulton, and T. Lonsdale (Trans. Faraday Soc. **31**, 511 (1935)), who reported that the resistance of silk cloth showed a maximum at a pH *ca.* 4.2. They considered this pH to be approximately the pH of the isoelectric point of thin silk.

the relative humidity to secure the constant moisture content, and such determinations are being made. But it is evident that this can only tend to narrow the amplitude of the graph and increase the sharpness of the minimum in the neighborhood of the isoelectric point.

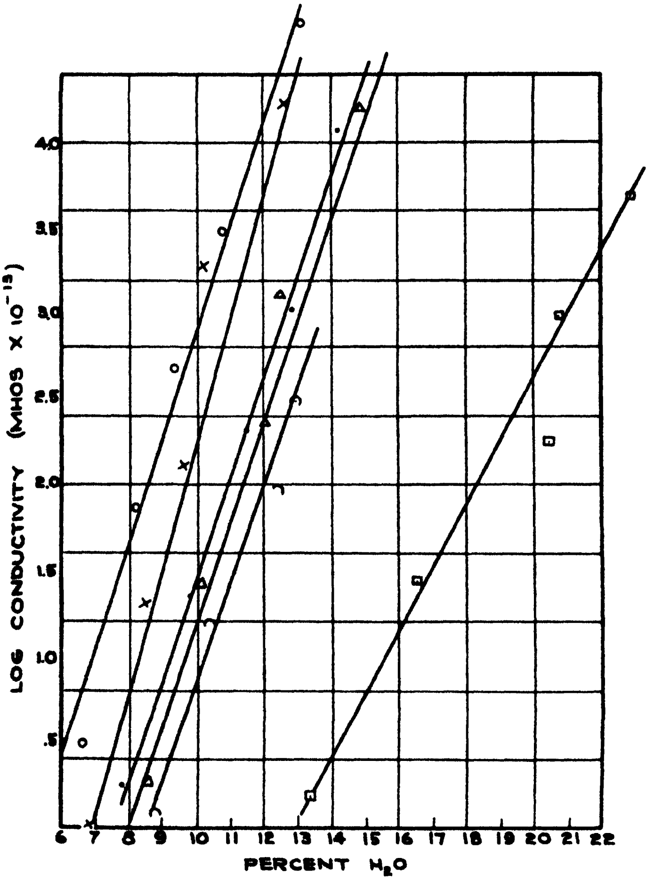

FIG. 17. Effect of water content of sample on the conductivity of gelatin and of photographic emulsions at 27.8°C. Plot of log conductivity against water content of sample. ⊡, deashed gelatin (Eastman Kodak No. 70), pH 6.10; ∩, photographic emulsion A, pH 6.20; ●, photographic emulsion B, pH 6.21; ×, photographic emulsion C, pH 6.14; ○, photographic emulsion D, pH 6.21; △, photographic emulsion E, pH 8.2.

4. *Relative humidity, moisture content, and conductivity*

Measurements were made on gelatin (Eastman Kodak No. 70) conditioned at various humidities. The experiments were started at 69 per cent relative humidity, and the humidities were progressively reduced. Moisture contents were determined in a similar order. In any such series, the measurements should always be made on the same sample throughout, and with the humidity varied progressively in one direction or the other, on account of the hysteresis.

Data obtained have been plotted logarithmically (see figures 16 and 17) over a considerable range—from 20 to 70 per cent relative humidity. The logarithm of the conductivity is a linear function of the logarithm of the water content. This relation was found to hold for cotton thread by Murphy and coworkers (15) and was confirmed by Marsh and Earp (13) for wool fibers. It is evident from the shape of the moisture sorption isotherms that this relation cannot hold over the whole isotherm. Walker (24) has suggested different empirical equations, of logarithmic type, depending upon the order of the moisture regain. Over a somewhat more restricted range, it is possible to get a linear relation between the logarithm of the conductivity and the moisture content itself.[6] The relations suggested by Walker are, on conversion to conductivities:

Below 3 per cent moisture content ($M.C.$):

$$\log_{10}\lambda = A_1(M.C.) + B_1$$

Between 3 and 10 per cent moisture content:

$$\log_{10}\lambda = A_2 \log_{10}(M.C.) + B_2$$

Between 10 per cent moisture content and saturation:

$$\log_{10}\lambda = A_3(R.H.) + B_3$$

Walker points out that the slope constant A depends (among other factors) on the history or pretreatment (hysteresis).

DISCUSSION

The most interesting results of these conductivity measurements for the nature of gelatin gels is the apparent discrepancy between the effect of change of pH on moisture regain and on electrical conductivity, respectively. In the latter case the results indicate that the electrical condition—and some value corresponding to pH—exists in the xerogel and is determined by the pH of the sol before drying. This is shown by the shape of the conductance–pH curve. On the other hand, this does not hold for the actual adsorption of water. The explanation may lie in a lowered intramicellar sorption of water vapor at low pH values, while surface or intermicellar sorption may remain sufficient to affect the conductance.

The relation of the absorption of liquid water, and the swelling of gelatin at different pH values, has been rather successfully (quantitatively) accounted for by application of the Donnan membrane equilibrium theory to the osmotic pressures set up (3). The concentrations of certain ions inside the gelatin (membrane) will differ from those in the liquid outside because of the non-diffusibility of the gelatin (dipole) ions. However, it must be noted that there are other hydrophilic properties which are not so readily explained on this basis. One of these is the still considerable swelling of isoelectric gelatin in water. Northrop and Kunitz (10) have attempted to explain this on lines consistent with the membrane theory by postulating that gelatin consists inherently of an insoluble and a soluble (at low temperatures) component. The latter, in sols, is supposed to form minute sacs or capsules enclosing the soluble portion. The sacs are supposed to be permeable to water, but not to the "soluble" gelatin. Also, they are capable of elastic distention. At the isoelectric point they absorb water until the osmotic pressure of this solution balances the elastic resistance of the sac wall. These authors consider that they had given experimental support for this conception by fractionating out from gelatin an insoluble component, repetition of their procedure producing smaller increments of the insoluble portion, but an increasingly "soluble" residue. We consider it probable that the "insoluble fraction" of Northrop and Kunitz is actually nothing but the "coagulable protein," or albuminous impurity, present more or less in all gelatins. Evidence for this has been presented by Sheppard and Hudson (19). If this is the case, the swelling at the isoelectric point is not connected with "insoluble capsules," but is a phenomenon general with high molecular substances, although they may be organophile or hydrophile.

---

[6] This relation has been used by Mr. R. Pinoir, in unpublished work of the Research Laboratory of the Kodak-Pathé Company in France.

The other property referred to is the relation of *viscosity* of gelatin solutions to pH. As shown previously by two of the present authors (18), while the viscosity, in consequence of hydrolysis, (above a certain temperature) steadily diminishes with time, there is an initial relation of viscosity to pH which is similar to that between swelling and pH. Loeb (12), who used solutions actually at too low temperatures, considered that the viscosity-pH characteristic was, equally with swelling, determined by membrane equilibrium, but in the sol by independent micellar capsules,—a view, as will be seen, somewhat similar to Northrop and Kunitz's picture. However, there is considerable evidence, which cannot be discussed here, that the "micelles" in gelatin solutions above a certain temperature are either the long-chain macromolecules of the polypeptide, or else casual "knots" or tangles of such macromolecules. Whether such kinetic elements as these could enforce a Donnan equilibrium appears doubtful. The general features of the viscosity-pH relation remain the same even in very dilute solutions,[7] so that it appears to be a direct consequence of the relation of the *molecular* (zwitter ion) constitution to pH. This is substantiated by the electrometric titration curves of gelatin, i.e., the acid $\sim$ base combination as function of pH. Moreover, amino acids themselves show an electroviscous effect varying with the pH. It becomes necessary to consider the bearing of x-ray diffraction and optical (birefringence) studies of gelatin on the problem of moisture adsorption. Early investigations by J. R. Katz and O. Gerngross (9) indicated a rather complicated x-ray diffraction diagram. Arguing from Katz' observation of a paracrystalline condition in stretched rubber, Gerngross (4) tried the effect of stretching gelatin gels, and found that the dried stretched gelatin gave a quasi-fiber diagram very similar to that given by collagen. Trillat (23) concluded from his x-ray study of gelatin that it consisted of a highly polymerized portion mixed with a less polymerized portion. In 1930, K. Herrmann, O. Gerngross and W. Abitz (5) made more extended studies, including the effect of swelling in water. In unstretched "air-dry" gelatin they distinguished the diffraction rings shown in table 8. While I_1, I_2, S, and K had the appearance of crystalline interferences, either from very small crystallites, or imperfect lattices, the F halos resembled more "liquid" halos. They could not be attributed to water, and indicate a completely amorphous component or constituent.

---

[7] Work done in these Laboratories; to be published.

TABLE 8

Diffraction rings in unstretched "air-dry" gelatin

NAME	*d* BRAGG	REMARKS
	Å.	
I_1	23.0	Only with chromium radiation; apparently crystalline interference
I_2	11.3	Apparently crystalline interference
S	7.5	Only on very long exposure (faint); apparently crystalline interference
K	2.8	Apparently crystalline interference
F_1	4.3	With copper radiation; Debye camera
F_2	2.1	

The effect of swelling with water on the x-ray interferences is significant, as shown in table 9.

Of the so-called crystalline interference rings, K remains completely unaffected, while I_2 is steadily widened with increased swelling. The conclusion is that water is taken up *within* the crystallite or micelle (intramicellar swelling, according to Katz) but only in a preferred direction. This anisotropy of water sorption is confirmed by many other (macroscopic) phenomena, particularly birefringence (20). It appears that the swelling is oriented so that water is taken up only between the principal valency chains, or, in terms of the polypeptide picture of protein structure, in extending the side-chain interval. These results were confirmed and amplified by J. R. Katz and J. C. Derksen (7), who correlated the swelling of a gelatin[8] in water vapor with the x-ray diffraction. Operating both in the direction moist → dry and dry → moist, they observed that the hysteresis had little effect (on the x-ray spectrum as a function of moisture). No discontinuity was observed either in the sorption isotherm or in the x-ray diffraction series.

These workers observed further that at low humidities, or low moisture content, the x-ray diagram indicated only amorphous material. They pointed out the resemblance of this to the amorphous α-gelatin state observed (8) in a melted gelatin gel of about 15 per cent water, indicating that, on melting, the gelatin becomes dehydrated. The x-ray analysis of gelatin and of other proteins has been investigated by W. T. Astbury and collaborators (1, 2). In the case of gelatin, Astbury suggests as the "principal" spacing of the polypeptide chain, the 2.8 Å. ring, regarding the actual spacing as three condensed amino acid residues with a slight contraction due to twist, equal, therefore, to 8.4 Å.,—some evidence for which was found by G. von Susich (14). This he regards as in agreement with the rather large "side-chain" spacings of 5 Å.[9] and 11 Å.

TABLE 9

Diffraction interval from Bragg's equation

NAME	RATIO OF DRY GELATIN TO WATER					
	1:0 Dry	1:0.18 Air-dry	1:0.50	1:2.5	1:3.7	1:4.3
I_2	10.4	11.3	13.0	17.1		
S........	*	7.5	7.5		7.5	7.5
K........	2.8	2.8	2.8		2.8	2.8
F_1........	4.4	4.3	3.7		3.6	3.3

* pH values, origin, etc. not given.

In dried sheets, the crystallite orientation is undoubtedly with the axes or the chains, parallel to the plane of the sheet (20). There is also definite evidence that, in specimens dried to the same moisture content, but in one case at higher, and in the other at lower temperatures, the planar orientation of the crystallites is more marked in the latter, with consequent greater preponderance of side chains perpendicular to the surface. Differences in lateral swelling in water parallel this arrangement.

If we apply these conclusions to the sorption of water vapor in relation to pH (*cf.* figure 3), it appears probable that on the acidic side of the isoelectric point—or from a certain pH down—there is an increasing interlocking of side-chain groups which is not unloosed by water vapor, perhaps because the water molecules cannot achieve favorable penetration and orientation. The *amorphous* α-gelatin structure described by Katz *et al.* at low humidities would probably favor this. Whether it is due to association of carboxyl groups or to some type of lactonization cannot yet be stated.

---

[8] pH values, origin, etc. were not given.

[9] Apparently the 4.6 Å. spacing of Katz *et al.*, which gets narrower on moistening.

SUMMARY

1. The sorption of water vapor by dry gelatin has been studied at 25°C., using two types of "ash-free," purified gelatin, *viz.* "lime-processed" gelatin, isoelectric point pH 4.8, and "acid-processed" gelatin, isoelectric point pH 8.2. Little difference was observed until the vapor pressure approached saturation, when the "lime-processed" material showed greater adsorption.

2. The adsorption (and desorption) isotherms are curves of double flexure, resembling those obtained with cotton cellulose, wool, silk, and other fibrous materials.

3. The moisture regain varies with pH (of the sol at coating), decreasing from high to low pH, but no minimum was found at the isoelectric point.

4. The electrical conductivity increases with moisture content, as found for cotton and wool. Over a considerable range the logarithm of the conductance is a linear function of the moisture content.

5. The electrical conductance shows a decided minimum at the isoelectric point.

6. The results are discussed in connection with x-ray diffraction studies of the structure of gelatin. The sorption of water vapor appears to be largely conditioned by the fine structure of the xerogel, but this again is conditioned by chemical interactions of the protein molecules.

REFERENCES

(1) Astbury, W. T.: Trans. Faraday Soc. **29**, 193 (1933).
(2) Astbury, W. T., and Lomax, R.: J. Chem. Soc. **1935**, 847.
(3) *cf.* Bolam, T. R.: *The Donnan Equilibrium.* G. Bell and Sons, London (1932).
(4) Gerngross, O.: Kolloid-Z. **33**, 254 (1923).
(5) Herrmann, K., Gerngross, O., and Abitz, W.: Z. physik. Chem. **B10**, 371 (1930).
(6) Katz, J. R.: Kolloid-Beihefte **9**, 182 (1917).
(7) Katz, J. R., and Derksen, J. C.: Rec. trav. chim. **51**, 513 (1932).
(8) Katz, J. R., Derksen, J. C., and Bon, W. F.: Rec. trav. chim. **50**, 725 (1931).
(9) Katz, J. R., and Gerngross, O.: Naturwissenschaften **13**, 900 (1925); Kolloid-Z. **39**, 181 (1926).
(10) Kunitz, M., and Northrop, J. H.: J. Gen. Physiol. **12**, 379 (1929).
(11) Lloyd, D. J., and Pleass, W.: Biochem. J. **21**, 1352 (1927).
(12) Loeb, J.: *Proteins and the Theory of Colloidal Behavior.* The McGraw-Hill Book Company, New York (1922).
(13) Marsh, M. C., and Earp, K.: *The Colloid Aspects of Textile Materials and Related Topics.* The Faraday Society, September, 1932, p. 173.

(14) Meyer, K. H.: Biochem. Z. **214**, 265 (1929).
(15) Murphy, E., and Walker, A. C.: J. Phys. Chem. **32**, 1761 (1928); **33**, 200, 509 (1929).
(16) Newsome, P. T.: Ind. Eng. Chem. **20**, 827 (1928).
(17) Sheppard, S. E.: Trans. Faraday Soc. **29**, 77 (1933).
(18) Sheppard, S. E., and Houck, R. C.: J. Phys. Chem. **36**, 2219 (1932).
(19) Sheppard, S. E., and Hudson, J. H.: J. Am. Chem. Soc. **53**, 760 (1931).
(20) Sheppard, S. E., and McNally, J. G.: Colloid Symposium Monograph **7**, 17 (1930).
(21) Sheppard, S. E., and Newsome, P. T.: J. Phys. Chem. **34**, 1158 (1930).
(22) Sheppard, S. E., and Wightman, E. P.: Ber. 8th Intern. Kongr. Phot., Dresden, **1931**, p. 157.
(23) Trillat, J. J.: Compt. rend. **190**, 265 (1930).
(24) Walker, A. C.: J. Textile Inst. **24**, T146 (1933).
(25) Wilson, R. E.: Ind. Eng. Chem. **13**, 326 (1921).
(26) Wilson, R. E., and Fuwa, T.: Ind. Eng. Chem. **14**, 915 (1922).

THE SOLUBILITIES OF CERTAIN INORGANIC COMPOUNDS IN ORDINARY WATER AND IN DEUTERIUM WATER[1]

ROBERT D. EDDY[2] AND ALAN W. C. MENZIES

Frick Chemical Laboratory, Princeton University, Princeton, New Jersey

Received August 1, 1939

INTRODUCTION

In the field of solubility in deuterium water, little work has hitherto been published (32, 28, 21). In the present article we contribute the results of solubility measurements, with a 1 per cent accuracy, of fifteen solids in deuterium water, with a comparison of analogous systems in ordinary water, embracing temperatures in the range from near 0°C. to 105–180°C. It is hoped that the collection of such data of reasonably good precision and through a wide temperature range may help in throwing light on the general question of solubility in non-ideal solutions.

METHOD

The method used was that described by Menzies (20), which uses about 1 g. of solvent (later completely recovered), gives an accuracy of the order of 1 per cent, and is adaptable to both high and low solubilities and to high and low temperatures. The details of the apparatus have been set forth in earlier publications (20, 21), but, in order to assist others who may wish to use this method, certain comments are here added to the earlier descriptions.

---

[1] This article reports essential portions of the dissertation presented by Robert D. Eddy to the Faculty of Princeton University in partial fulfillment of the requirements for the degree of Doctor of Philosophy, October, 1938.

[2] Present address: Department of Chemistry, Tufts College, Massachusetts.

(*a*) Before opening the seal after the apparatus has been charged, it is well to reduce the aqueous pressure above the water by cooling it. Otherwise a portion of the seal when melted may be carried over into and admixed with the solid under investigation. (*b*) It is better to place the constriction for the seal on the side of the apparatus distant from, rather than next to, the part containing the solute. (*c*) A mixture of silver chloride with silver iodide containing 43.9 molecular per cent of the former was found most satisfactory. (*d*) Silver iodide containing, as here used, a low concentration of silver chloride in solid solution undergoes enantiomorphic change somewhat below 135°C. The (cubic) high-temperature form has a smaller specific volume than the (hexagonal) low-temperature form. For this reason, the seal is particularly close-fitting below 135°C. In order that leakage shall not occur immediately above 135°C., it is essential that the constriction in the glass which is to be closed by the silver salts shall be of hour-glass shape, and not merely tubular. Consideration of the adjacent schematic diagram (figure 1) will show that, if the plug of silver halides occupies the volume *AABB* at 130°C., it may be expected to occupy the new volume *A'A'B'B'* at 140°C. and that the plug will still be tight because it shrinks alike in each dimension. (*e*) Because of the considerable increase in volume of silver iodide (3) as it passes upon cooling through its inversion point above 135°C., mixtures of the chloride and iodide that are too rich in iodide may cause fracture of a thick-walled cylindrical Pyrex capillary when the temperature falls below 135°C. (*f*) Complete assurance of absence of leakage through the seal is furnished by identity of the volume of unused water before and after each experiment. (*g*) Because of the high viscosity exhibited by certain of the solutions encountered in the present work, the dimensions of the tube containing

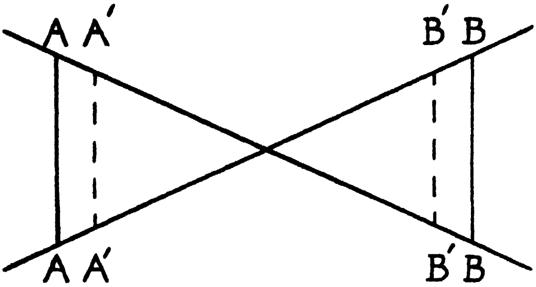

FIG. 1. Contraction of a solid in an hour-glass container

the solute were modified from their former values to a length of 6 cm. and a bore of 8 mm. This tube was attached to the rest of the apparatus through an upright tube of 6-mm. bore. (*h*) A few graduations were etched upon the tube that contained the solution, so that its volume at any temperature could be measured as an aid in determining the volume of water present above the solution in the vapor phase.

Securing and measuring temperatures for equilibrium

For temperatures below 25°C., the apparatus was, in a few cases, immersed in a stirred water thermostat of 320-liters capacity. More usually, for all temperatures below 85°C., the apparatus was submerged in a 4-liter beaker of water, suitably jacketed and adequately stirred. Heat was supplied either by the air of the room (when this was warmer than the experimental vessel), by the lamp bulb used for illumination, suitably screened, or by the additional aid of two knife-form resistance heaters supplied with regulated and metered current. For temperatures above 85°C., the apparatus was placed in a well-insulated air oven, of 1-cu. ft. capacity, with strong internal illumination, distributed heating elements supplied with metered and controlled current, and fan stirring.

Temperatures were measured as previously described (20) but in certain cases with an accuracy of ±0.02°C. instead of ±0.1°C. in the region below 85°C., as controlled by certificated thermometers.

Correction for weight of water in the vapor phase

The volume of such water vapor, which is obviously absent from the liquid solution, was readily obtained from the known volume of the apparatus. But recorded values for the aqueous pressure over the saturated salt solutions at various temperatures are scanty in the case of solutions in ordinary water and entirely lacking for solutions in deuterium water. The value of such correction becomes significant only above 70°C. In the present work, the correction exceeded 2.7 per cent of the solubility value only in one case, an observation at 203.8°C. It can thus be understood that a knowledge of the aqueous pressure over the saturated solutions need not usually be more accurate than 5 per cent, and this only for temperatures above 150°C. A sufficiently accurate value of the aqueous pressures over saturated solutions in deuterium water could be obtained by reducing the values for solutions of like concentration in ordinary water in the ratio of the vapor pressure of pure deuterium water to that of ordinary water at the temperature concerned. These ratios are known (22).

In order to obtain estimates of the aqueous pressure over our solutions in ordinary water, we employed the method of plotting *R*, relative molal lowering, against molal concentration (18), utilizing the values of *R* for 100°C. found in the *International Critical Tables* (16 (b)). When the change of R with temperature for identical solutions was known it was small in amount, but due correction was applied for such departure from Babo's law. In case better values for these aqueous pressures should later become available, we have been careful to state in the "a" tables below the actual values of the pressures as used by us for this correction in each case.

In the case of sodium sulfate, direct measurements of the aqueous pressure over its saturated solutions were available. In the cases of cadmium iodide and mercuric chloride we were able with some confidence to utilize Raoult's law to obtain approximate values. The work of Beckmann (1) and of Landsberger (17) has shown that aqueous solutions of these salts are little abnormal.

PURITY OF MATERIALS

Ordinary water. Water from a block-tin still of 350-gallons capacity was boiled in a Pyrex flask for 10 min., and then the flask was stoppered, to keep out air. Investigation had previously shown that the specific conductivity of water thus treated is 5.3×10^{-6} mhos.

Deuterium water. Thirty cubic centimeters of a 2 per cent solution of sodium deuteroxide in 92 per cent deuterium water was electrolyzed to one-sixth of its volume. This was normalized with dried carbon dioxide and distilled twice under reduced pressure at 60°C. The resulting water had a freezing point of 3.80°C.±0.02°, corresponding to a purity of 99.4 per cent. Of the original 5 cc. prepared, but 1 cc. remained at the end, the rest having been lost by accidental dilution during the course of the investigation.

Sodium chloride. Merck's "reagent" sodium carbonate was recrystallized twice above 36°C., and sodium chloride was obtained from this by precipitation from a concentrated solution with an excess of redistilled Grasselli "reagent" hydrochloric acid. This was twice recrystallized from distilled water, and dried by heating to incipient fusion for 20 min.

Sodium bromide. Baker's C.P. sodium bromate was recrystallized twice from water and then decomposed by fusion to sodium bromide. Fusion was continued until the addition of a few drops of sulfuric acid to a solution of the salt failed to give a brown coloration. This salt was recrystallized twice from distilled water and dried at 400°C. for 2 hr.

Sodium iodide. Baker's C.P. ammonium iodide and Merck's "reagent" sodium carbonate were recrystallied twice from water solution, the latter above 36°C. An excess of the ammonium iodide was added to a concentrated solution of the sodium carbonate, the resulting solution evaporated, and the solid material heated to fusion. The salt was then recrystallized three times from water, and dried for 3 hr. at 350°C. A solution of this salt was found to be colorless and neutral to litmus.

Sodium sulfate. Merck's "reagent" sodium sulfate was recrystallized three times above 35°C. and dried for 2 hr. at 500°C.

Potassium bromide. Merck's "reagent" potassium bromate was twice recrystallized from water and then decomposed by fusion in the same manner as was the sodium bromate. The resulting potassium bromide was recrystallized twice from water and dried by heating to 500°C. for 2 hr.

Potassium iodide. Baker's C.P. potassium iodide was recrystallized three times from water and dried for 3 hr. at 350°C.

Barium chloride. Baker's "reagent" barium chloride was recrystallized once from water alone and twice by dissolving it in a minimum amount of water and precipitating it by the addition of alcohol. It was again recrystallized from water and dried for 3 hr. at 350°C.

Cadmium iodide. Merck's "reagent" cadmium iodide was recrystallized once from water solution, once from 95 per cent ethyl alcohol solution, and again from water solution. It was then dried for 2 days at 150°C.

Mercuric chloride. Baker's "reagent" mercuric chloride was tested for impurities and used without further purification. It was dried for 2 days at 150°C.

MANNER OF CALCULATING AND OF STATING RESULTS, AND THEIR ESTIMATED ACCURACY

Solubilities are here stated in number of moles of anhydrous salt per 55.51 moles of water considered as H_2O or D_2O, respectively, conformably to the practice of *International Critical Tables.* This we shall call the molal solubility. The method of reducing the experimental results has been already described elsewhere (28). The density of our (99.4 per cent) deuterium water was taken as $d_{25°}^{25°} = 1.1076$. The molecular weight of H^1 was taken as 1.0081 and of H^2 as 2.0134.

For each salt two tables are given; those lettered "a" stating experimental values and those lettered "b" stating values at rounded temperatures obtained by the graphic method outlined elsewhere (20).

In both "a" and "b" tables, T signifies temperature Centigrade, M molal solubility as above defined; m following a value of M means that the solid phase is metastable.

In "a" tables, S refers to the grams of anhydrous salt used in the apparatus, W to the number of grams of water measured into the solution side of the apparatus, V to the estimated volume of the vapor phase in cubic centimeters, P to the estimated pressure of the water vapor in millimeters of mercury, C to the number of grams of water calculated to be present as vapor. The letter "a" following a few values of S in tables 4a, 5a, and 9a indicates that these points were obtained by measurements made in individual sealed Pyrex tubes by the customary synthetic method.

In "b" tables, in which the style and symbology of *International Critical Tables* have been followed, the heading "I.C.T." designates values of M_{H_2O} extracted from these tables, an asterisk * indicates a value of M_{H_2O} derived from other work not our own, D represents $M_{H_2O} - M_{D_2O}$, $\%D$ represents $D \times 100/M_{H_2O}$, and U placed after a value of M indicates that a transition in the solid phase occurs at this concentration and temperature.

A discussion of error in this method of solubility determination has been given elsewhere (20). It may be stated broadly that molal solubilities are estimated to be accurate within 1 per cent. Since the difference values tabulated under D and $\%D$ are arrived at by subtraction of two much larger quantities, their percentage error is much higher and can be estimated by inspection of the molal solubilities from which they are derived. The terminal digits of these values therefore often lack rigid significance.

TABLE 1a

Observed solubility of sodium chloride (58.454) in ordinary water and in deuterium water

(1) Ordinary water

T	S	W	V	P	C	M
°C.	*grams*	*grams*	*cc.*	*mm.*	*grams*	
101.9	0.3394	0.8691	3.21	601.	0.0015	6.69
168.3	0.3394	0.7780	3.17	3968.	0.0082	7.54

(2) Deuterium water

T	S	W	V	P	C	M
°C.	*grams*	*grams*	*cc.*	*mm.*	*grams*	
−3.8	0.3040	1.0454				5.53
1.7	0.3040	1.0356				5.58
11.7	0.3040	1.0181				5.68
19.7	0.2753	0.9134				5.73
28.2	0.3040	0.9957				5.81
61.5	0.2753	0.8679				6.04
110.8	0.2753	0.8007	3.51	787.	0.0023	6.55
144.1	0.3040	0.8400	3.33	2166.	0.0055	6.92
180.3	0.3040	0.7910	3.40	5258.	0.0127	7.42

The accuracy of transition temperatures arrived at from points of intersection of solubility curves is dependent on their angle of intersection, and absolute values can seldom be expected to be better than ±0.2°C. in the present work.

COMMENTS UPON THE INDIVIDUAL SALTS

Sodium chloride. The values for the molal solubility of this salt in ordinary water as given in *International Critical Tables* are stated to have an estimated accuracy of 0.2 per cent below 55°C., and of 0.5 per cent in the range 60°C. to 110°C., above which the accuracy is unknown. As tests in the higher temperature ranges we made the two measurements recorded in table 1a. At 101.9°C. and 168.3°C. the molal solubilities found were

6.69 and 7.54, respectively, while interpolation from I.C.T. values yields 6.72 and 7.55. This concordance was sufficiently satisfactory to warrant

TABLE 1b

Solubilities of sodium chloride in ordinary water and in deuterium water at rounded temperatures

T	I.C.T.	M_{D_2O}	D	% D
°C.				
−5		(5.53)		
0	6.10 m	5.56	0.54	8.$_9$
0.15	6.10 U	5.56	0.54	8.$_9$
5	6.10	5.60	0.50	8.$_2$
10	6.11	5.64	0.47	7.$_7$
15	6.12	5.68	0.44	7.$_2$
20	6.13	5.72	0.41	6.$_7$
25	6.145	5.76	0.385	6.$_3$
30	6.165	5.79	0.375	6.$_1$
35	6.18	5.83	0.35	5.$_7$
40	6.215	5.87	0.345	5.$_6$
45	6.24	5.91	0.33	5.$_3$
50	6.26	5.95	0.31	5.$_0$
55	6.29	5.99	0.30	4.$_8$
60	6.33	6.03	0.30	4.$_7$
65	6.37	6.07	0.30	4.$_7$
70	6.41	6.12	0.29	4.$_5$
75	6.45	6.16	0.29	4.$_5$
80	6.50	6.21	0.29	4.$_5$
85	6.55	6.26	0.29	4.$_4$
90	6.60	6.31	0.29	4.$_4$
95	6.65	6.36	0.29	4.$_4$
100	6.70	6.42	0.28	4.$_2$
105		6.47		
110	6.81	6.52	0.29	4.$_3$
115		6.58		
120	6.93	6.64	0.29	4.$_2$
125		6.70		
130	7.06	6.76	0.30	4.$_2$
135		6.82		
140	7.19	6.88	0.31	4.$_3$
145		6.95		
150	7.32	7.01	0.31	4.$_2$
155		7.08		
160	7.45	7.14	0.31	4.$_2$
165		7.21		
170	7.58	7.28	0.30	4.$_0$
175		7.35		
180	7.71	7.42	0.29	3.$_8$

our utilizing unchanged the I.C.T. values for the solubility of sodium chloride in ordinary water.

One determination of the solubility of sodium chloride in 92 per cent deuterium water at 25°C. is to be found in the literature (32). Converted to molal solubility in 100 per cent deuterium water on the assumption that divergencies in solubility are linear with the change in solvent, this determination gives $M_{D_2O} = 5.72$ at 25°C., with which our value, 5.76, is in satisfactory concordance.

Sodium bromide. Values for the solubility in ordinary water of this salt are reported in I.C.T. up to 120°C. only, and with an estimated accuracy of 2 per cent. We believe their accuracy is higher than this, for no one of these values differs by as much as 2 per cent from the values reported by us in table 2b. Intersection of our solubility curves for the dihydrate and the anhydrous salt occurs at 50.8°C. Richards and Wells (26) reported 50.67°C. for this transition temperature.

In the case of the corresponding system with deuterium water, our value of 47.4°C. for the transition temperature may be compared with that of Bell (2), 47.7°C.

Sodium iodide. I.C.T. reports values for solubility in ordinary water only to 100°C., with an accuracy estimated at 2 per cent. We believe the degree of accuracy is here again understated, for our values, reported in table 3b, in no case diverge by as much as 2 per cent. The temperature of the transition from dihydrate to anhydrous sodium iodide is given by Panfilow (23) as 64.3°C. and by I.C.T. as 68.9°C. Our solubility curves for these salts intersect at 68.2°C. For the analogous system with deuterium water our value is 66.0°C.

While seeking for metastable points on the solubility curves of the anhydrous salts below these transition temperatures, we discovered the existence of a metastable hydrate which has not hitherto been reported. Three experimental points on the solubility curve of this new hydrate are shown in table 3a, as are also three points on the solubility curve of the analogous deuterate. The temperatures of transition to anhydrous salt, as shown by the points of intersection of the appropriate solubility curves, are 60.0°C. and 58.2°C. for hydrate and deuterate, respectively. We were unable to determine with certainty the formulae of these new compounds because of their instability when removed from a closed glass system.

Sodium sulfate. At temperatures below 50°C. the viscosity of the solutions caused some inconvenience. Since the solubility of the decahydrate has been much studied, the values of I.C.T. are there stated to have a 1 per cent accuracy. We therefore confined ourselves to a single measurement at 24.8°C., which showed concordance to 0.5 per cent with these values.

In the case of the metastable heptahydrate, the experimental work has been scanty (10, 19, 24) and has been interpreted very differently by different tabulators. As a consequence of this, the transition temperature

TABLE 2a

Observed solubility of sodium bromide (102.913) in ordinary water and in deuterium water

(1) Ordinary water

T	*S*	*W*	*V*	*P*	*C*	*M*
$NaBr\cdot 2H_2O$						
°C.	*grams*	*grams*	*cc.*	*mm.*	*grams*	
−3.1	1.0074	1.2852				7.62
8.4	1.0074	1.1912				8.22
24.3	1.0074	1.0681				9.16
40.5	1.0074	0.9443				10.37
49.0	1.0074	0.8771				11.16
50.1_5	1.0074	0.8658				11.31
50.9_5	1.0074	0.8578				11.41 m
NaBr						
47.1	1.0074	0.8605				11.38 m
53.9	1.0074	0.8578				11.41
72.9	1.0074	0.8465				11.56
97.3	1.0074	0.8278	3.21	348.	0.0009	11.84
120.1	1.0074	0.8059	3.25	730.	0.0017	12.17
144.6	1.0074	0.7739	3.30	1440.	0.0033	12.70
171.2	1.0074	0.7380	3.38	2599.	0.0057	13.37

(2) Deuterium water

T	*S*	*W*	*V*	*P*	*C*	*M*
$NaBr\cdot 2D_2O$						
°C.	*grams*	*grams*	*cc.*	*mm.*	*grams*	
−2.3	0.6817	0.9814				7.50
10.1	0.6817	0.9038				8.15
23.4	0.6817	0.8241				8.94
35.4	0.6817	0.7475				9.85
39.9_5	0.9892	1.0438				10.24
44.0	0.6817	0.6911				10.66
46.6	0.6817	0.6731				10.94
47.5	0.6817	0.6699				10.99 m
NaBr						
35.0	0.6817	0.6731				10.94 m
50.2	0.6817	0.6699				10.99
57.9	0.6817	0.6667				11.05
75.7	0.6817	0.6581				11.19
99.7	0.6817	0.6395	3.50	369.	0.0011	11.53
122.9	0.9892	0.8979	3.20	786.	0.0020	11.92
132.9	0.6817	0.6093	3.56	1023.	0.0029	12.14
164.9	0.6817	0.5774	3.63	2297.	0.0061	12.88

TABLE 2b

Solubilities of sodium bromide in ordinary water and in deuterium water at rounded temperatures

T	M_{H_2O}	I.C.T.	M_{D_2O}	*D*	*% D*
			NaBr·2Aq		
°*C.*					
−5	(7.53)		(7.37)	0.16	$2._1$
0	7.77	7.71	7.61	0.16	$2._1$
5	8.03		7.86	0.17	$2._1$
10	8.30	8.17	8.13	0.17	$2._0$
15	8.59		8.42	0.17	$2._0$
20	8.89	8.77	8.73	0.16	$1._8$
25	9.20		9.07	0.13	$1._4$
30	9.54	9.46	9.44	0.10	$1._0$
35	9.91		9.84	0.07	$0._7$
40	10.32	10.31	10.27	0.05	$0._5$
45	10.78		10.75	0.03	$0._3$
47.4	10.98		10.98 U	0.00	$0._0$
50	11.29	11.29 U			
50.8	(11.39) U				
			NaBr		
35			10.93 m		
40			10.95 m		
45	(11.37)		10.97 m	0.40	$3._5$
50	11.38	11.29	11.00	0.38	$3._3$
55	11.41		11.03	0.38	$3._3$
60	11.44	11.38	11.07	0.37	$3._2$
65	11.48		11.11	0.37	$3._2$
70	11.52		11.16	0.36	$3._1$
75	11.57		11.21	0.36	$3._1$
80	11.62	11.60	11.27	0.35	$3._0$
85	11.67		11.33	0.34	$2._9$
90	11.73		11.40	0.33	$2._8$
95	11.80		11.47	0.33	$2._7$
100	11.87	11.84	11.54	0.33	$2._8$
105	11.94		11.62	0.32	$2._7$
110	12.02		11.70	0.32	$2._7$
115	12.10		11.78	0.32	$2._6$
120	12.19	12.13	11.87	0.32	$2._6$
125	12.28		11.96	0.32	$2._6$
130	12.38		12.06	0.32	$2._6$
135	12.49		12.16	0.33	$2._6$
140	12.60		12.27	0.33	$2._6$
145	12.71		12.38	0.33	$2._6$
150	12.83		12.49	0.34	$2._7$
155	12.96		12.61	0.35	$2._7$
160	13.08		12.74	0.34	$2._6$
165	13.22		(12.87)	0.35	$2._6$
170	13.35		(13.01)	0.34	$2._5$

TABLE 3a

Observed solubility of sodium iodide (149.92) in ordinary water and in deuterium water

(1) Ordinary water

T	*S*	*W*	*V*	*P*	*C*	*M*
			$NaI \cdot 2H_2O$			
°C.	*grams*	*grams*	*cc.*	*mm.*	*grams*	
2.3	1.4218	0.8777				10.81
13.0_8	2.2352	1.2976				11.49
37.6_7	2.2352	1.0991				13.56
47.9_7	2.2352	0.9986				14.93
58.9_3	2.2352	0.8808				16.93
62.7_8	2.2352	0.8343				17.87
64.5_7	2.2352	0.8136				18.32
65.6_8	2.2352	0.7957				18.74
67.6_3	2.5465	0.8802				19.30
68.4_3	2.5465	0.8667				19.60 m
			$NaI \cdot xH_2O$			
46.1_6	2.2352	0.8136				18.32 m
51.6_4	2.2352	0.7957				18.74 m
58.3_0	2.5465	0.8802				19.30 m
			NaI			
72.2_9	2.5465	0.8667				19.60
85.2	2.5465	0.8567				19.83
103.0	2.5465	0.8437				20.13
126.9	2.5465	0.8161	2.75	384.	0.0008	20.83
147.7	2.5465	0.7901	2.77	680.	0.0013	21.53
182.9	2.5465	0.7410	2.80	1733.	0.0031	23.02

(2) Deuterium water

T	*S*	*W*	*V*	*P*	*C*	*M*
			$NaI \cdot 2D_2O$			
12.4	1.5440	1.0204				11.22
27.7_8	1.5440	0.9211				12.43
42.5_0	1.5440	0.8140				14.07
54.0_4	2.2352	1.0427				15.89
60.4_5	2.2352	0.9511				17.43
64.0_2	2.4085	0.9657				18.49
64.0_7	2.2352	0.8958				18.49
65.4_4	2.2352	0.8746				18.95
65.5_5	2.4085	0.9400				19.00
			$NaI \cdot xD_2O$			
46.4_5	2.4085	0.9861				18.11 m
51.7	2.2352	0.8958				18.50 m
56.9_0	2.2352	0.8746				18.95 m
			NaI			
62.1	2.4085	0.9337				19.13 m
77.7	2.4085	0.9237				19.33
112.2	2.4085	0.8917				20.03

TABLE 3b

Solubilities of sodium iodide in ordinary water and in deuterium water at rounded temperatures

T	m_{H_2O}	I.C.T.	m_{D_2O}	D	% D
			NaI·2Aq		
°C.					
0	(10.68)	10.72	(10.47)	0.21	$2._{0}$
5	10.96		(10.75)	0.21	$1._{9}$
10	11.26	11.31	(11.05)	0.21	$1._{9}$
15	11.59		11.39	0.20	$1._{7}$
20	11.95	11.98	11.77	0.18	$1._{5}$
25	12.34		12.18	0.16	$1._{3}$
30	12.78	12.75	12.64	0.14	$1._{1}$
35	13.28		13.15	0.13	0.9_{8}
40	13.85	13.75	13.73	0.12	0.8_{7}
45	14.50		14.40	0.10	0.6_{9}
50	15.24	15.13	15.17	0.07	0.4_{6}
55	16.10		16.09	0.01	0.0_{6}
60	17.15	17.18	17.23	−0.07	-0.4_{1}
65	18.47		18.80	−0.33	$-1._{8}$
66.0	18.78		(19.15) U	−0.37	$-2._{0}$
68.2	19.56 U				
68.9		19.59 U			
			NaI·xAq		
45	(18.24) m		(18.00) m	0.24	$1._{3}$
50	18.61 m		18.39 m	0.22	$1._{2}$
55	19.01 m		18.80 m	0.21	$1._{1}$
58.2	19.26 m		(19.06) m U	0.20	$1._{0}$
60.0	(19.43) m U				
			NaI		
55	(19.38) m		(19.02) m	0.36	$1._{9}$
60	(19.44) m		(19.08) m	0.36	$1._{9}$
65	(19.51) m		19.14	0.37	$1._{9}$
70	(19.58)	19.60	19.21	0.37	$1._{9}$
75	19.65		19.28	0.37	$1._{9}$
80	19.72	19.80	19.36	0.36	$1._{8}$
85	19.80		19.45	0.35	$1._{8}$
90	19.89	20.00	19.54	0.35	$1._{8}$
95	19.99		19.64	0.35	$1._{8}$
100	20.10	20.24	19.75	0.35	$1._{7}$
105	20.22		19.87	0.35	$1._{7}$
110	20.35		19.99	0.36	$1._{8}$
115	20.48		(20.12)	0.36	$1._{8}$
120	20.63				
125	20.77				

TABLE 3b—*Concluded*

T	m_{H_2O}	I.C.T.	m_{D_2O}	D	% D
	NaI—*Continued*				
°*C.*					
130	20.92				
135	21.09				
140	21.27				
145	21.45				
150	21.63				
155	21.82				
160	22.02				
165	22.23				
170	22.45				
175	22.67				
180	22.89				

to anhydrous salt found as 24.4°C. from the data of Loewel (19) has been incorporated unchanged in numerous tables, while I.C.T. prefers 28.2°C. The appropriate intersection of our solubility curves lies at 23.7°C. Since our work was completed, an accurate redetermination of this point has been undertaken by Washburn and Clem (34), who find 23.465°C.

The solubility of the anhydrous salt has been much studied, and the values of I.C.T. are therein estimated as accurate to 1 per cent. We found this salt difficult to work with because of its small change in solubility with temperature, and, in this instance, do not prefer our values to those of I.C.T. Only one of our experimental points (at 82.2°C.) gives, however, a solubility differing from these by more than 1 per cent. In comparing solubilities in deuterium water, we have, nevertheless, utilized our own values for solubility in ordinary water, since both our sets of experiments would be subject to similar systematic error (see table 4a). Our solubility curve for the anhydrous salt intersects the solubility curve for decahydrate based upon I.C.T. values at 32.5°C., while I.C.T. reports this intersection at 32.48°C. (16(c)). The accepted value is 32.384°C. (11, 25), which is raised only 0.01°C. by 35 additional atmospheres of pressure.

In the case of the systems with deuterium water, we found the transition temperatures of deca- and hepta-deuterate to anhydrous salt as 34.2°C. and 26.7°C., respectively, from the points of intersection of the appropriate solubility curves. The former point has been reported by others at 34.48°C. (31), 34.5°C. (2), and 34.6–34.9°C. (14); and the latter at 26.6–27.0°C. (14).

Potassium chloride. The solubility of this salt in ordinary water and in deuterium water has already been studied in this laboratory (28). Because

TABLE 4a

Observed solubility of sodium sulfate (142.05) in ordinary water and in deuterium water

(1) Ordinary water

T	*S*	*W*	*V*	*P*	*C*	*M*
			$Na_2SO_4\cdot 10H_2O$			
°C.	*grams*	*grams*	*cc.*	*mm.*	*grams*	
24.8	0.3093	1.1268				1.93_2
			$Na_2SO_4\cdot 7H_2O$			
2.9	0.2303 a	1.0994				1.47_5 m
8.1	0.3093	1.1268				1.93_2 m
13.4	0.3093	0.8885				2.45_1 m
17.8	0.3864	0.9296				2.92_6 m
20.8	0.3864	0.8258				3.29 m
21.4	0.3093	0.6526				3.34 m
24.1	0.3864	0.7326				3.71 m
			Na_2SO_4			
21.0	0.3093	0.5810				3.75 m
47.5	0.3864	0.8258				3.29
82.2	0.4025 a	0.9486				2.99
114.0	0.3864	0.9296	3.48	1097.	0.0028	2.93_5
134.5	0.3864	0.9296	3.46	2119.	0.0052	2.94
165.8	0.4025 a	0.9486	0.54	5020	0.0018	2.99

(2) Deuterium water

T	*S*	*W*	*V*	*P*	*C*	*M*
			$Na_2SO_4\cdot 10D_2O$			
°C.	*grams*	*grams*	*cc.*	*mm.*	*grams*	
8.7	0.0499	0.8389				0.466
11.5	0.0776	1.0878				0.558
16.2	0.0499	0.4721				0.827
22.4	0.0499	0.2903				1.34_5
26.2	0.2564	1.1124				1.80_4
29.0	0.2564	0.9134				2.19_7
30.5_5	0.2564	0.7933				2.52_9
			$Na_2SO_4\cdot 7D_2O$			
7.7	0.0499	0.2509				1.55_6 m
10.3	0.2564	1.1124				1.80_4 m
14.3	0.2564	0.9134				2.19_7 m
17.9	0.2564	0.7933				2.52_9 m
24.7	0.4709	1.1124				3.31 m
27.0	0.4709	1.0101				3.65 m
			Na_2SO_4			
24.8	0.4709	1.0101				3.65 m
42.8	0.4709	1.1124				3.31
124.2	0.2564	0.6943	2.35	1468.	0.0028	2.90
152.0	0.2564	0.6950	2.35	3500.	0.0062	2.91
192.7	0.2564	0.6943	2.30	9280.	0.0147	2.95

TABLE 4b

Solubilities of sodium sulfate in ordinary water and in deuterium water at rounded temperatures

T	M_{H_2O}	I.C.T.	M_{D_2O}	D	$\% D$
$Na_2SO_4 \cdot 10Aq$					
°C.					
0	0.342*	0.342	(0.267)	0.075	2_2.
5	0.428*	0.428	(0.350)	0.078	1_8.
10	0.628*	0.628	0.512	0.116	1_8.
15	0.920*	0.920	0.770	0.150	1_6.
20	1.33*	1.33	1.12	0.21	1_6.
25	1.96*	1.96	1.65	0.31	1_6.
30	2.88*	2.88	2.42	0.46	1_6.
32.48		3.50 U	2.95	0.55	1_6.
32.5	3.52 U*		2.97	0.55	1_6.
34.2			3.45 U		
$Na_2SO_4 \cdot 7Aq$					
0	(1.25) m	1.34 m	(0.99) m	0.26	2_1.
5	1.64 m		(1.36) m	0.28	1_7.
10	2.10 m	2.14 m	1.77 m	0.33	1_6.
15	2.62 m		2.24 m	0.38	1_5.
20	3.18 m	2.94 m	2.76 m	0.42	1_3.
23.7	3.69 m U		3.20 m	0.49	1_3.
25			3.36 m		
26.7			3.60 m U		
28.2		3.59 m U			
Na_2SO_4					
25	3.67 m		3.66 m	0.01	$0._3$
30	3.57 m		3.55 m	0.02	$0._6$
35	3.47	3.45	3.44	0.03	$0._9$
40	3.39	3.40	3.36	0.03	$0._9$
50	3.26	3.28	3.22	0.04	$1._2$
60	3.16	3.19	3.12	0.04	$1._3$
70	3.07	3.11	3.03	0.04	$1._3$
80	3.01	3.05	2.98	0.03	$1._0$
90	2.96	3.00	2.94	0.02	$0._7$
100	2.94	2.97	2.92	0.02	$0._7$
110	2.93	2.96	2.91	0.02	$0._7$
120	2.92	2.95	2.90	0.02	$0._7$
130	2.93	2.95	2.91	0.02	$0._7$
140	2.95	2.96	2.92	0.03	$1._0$
150	2.97		2.92	0.05	$1._7$
160	2.99	3.01	2.93	0.06	$2._0$
170	(3.01)		2.94	0.07	$2._3$
180	(3.02)	3.09	2.95	0.07	$2._3$

of the unexpected position of the curve for potassium chloride in figure 3 below, in relation to the curves for the bromide and iodide of potassium, solubilities in deuterium water were redetermined for potassium chloride at the three temperatures 13.1°, 33.85°, and 151.9°C. In each case the molal solubility found was about 0.5 per cent lower than that of the earlier work. As this falls within the error of experiment, no change in the earlier values was required.

TABLE 5a

Observed solubility of potassium bromide (119.012) in ordinary water and in deuterium water

(1) Ordinary water

T	*S*	*W*	*V*	*P*	*C*	*M*
°C.	*grams*	*grams*	*cc.*	*mm.*	*grams*	
5.0_7	0.7033 a	1.2553				4.71
11.3_8	0.7896 a	1.3168				5.04
18.1_2	1.0975 a	1.7218				5.36
25.2_5	0.6791	0.9968				5.72
34.5_2	0.4683 a	0.6385				6.16
44.6_0	0.6851	0.8736				6.59
60.9	0.6851	0.7961				7.23
76.8	0.7352 a	0.7837				7.88
94.2	0.6851	0.6715	2.48	430.4	0.0008	8.58
101.5	0.3753 a	0.3553	1.58	552.3	0.0007	8.89
129.7	0.8090 a	0.6823	1.55	1306.	0.0015	9.98
159.3	1.0959 a	0.8226	0.81	2717.	0.0015	11.21
193.7	0.7325	0.4948	3.64	5507.	0.0124	12.76

(2) Deuterium water

T	*S*	*W*	*V*	*P*	*C*	*M*
°C.	*grams*	*grams*	*cc.*	*mm.*	*grams*	
8.0	0.4599	1.0321				4.16
12.2	0.4102	0.8678				4.42
20.1	0.4599	0.8847				4.86
31.1_0	0.4102	0.7085				5.41
48.9_8	0.3817	0.5753				6.20
68.7	0.4599	0.6097				7.05
82.7	0.4599	0.5641				7.62
96.2	0.3817	0.4360	2.90	447.4	0.0011	8.19
126.9	0.4599	0.4609	2.88	1198.	0.0022	9.36
167.2	0.4599	0.3975	2.93	3296.	0.0070	11.00
203.8	0.4599	0.3459	2.97	6686	0.0134	12.91

Potassium bromide. The solubility values for this salt found in I.C.T. are therein estimated to have accuracy within 1 per cent below 100°C. and within 5 per cent above 100°C. We believe their accuracy above

100°C. is better than estimated, for our results between 0° and 170°C. nowhere diverge by as much as 1 per cent from their values. We have not carried our table 5b higher than 170°C., because our experimental points above this temperature indicate a change of slope of the solubility curves for both varieties of water which our experimental values are not sufficiently numerous to define. According to Kracek (15) and others, potas-

TABLE 5b

Solubilities of potassium bromide in ordinary water and in deuterium water at rounded temperatures

T	M_{H_2O}	I.C.T.	M_{D_2O}	D	% D
°C.					
0	(4.44)	4.49	(3.63)	0.81	1_8.
5	(4.71)		(3.97)	0.74	1_6.
10	4.97	4.97	4.28	0.69	1_4.
15	5.23		4.57	0.66	1_3.
20	5.48	5.42	4.84	0.64	1_2.
25	5.71		5.10	0.61	1_1.
30	5.94	5.88	5.35	0.59	$9._9$
35	6.16		5.59	0.57	$9._3$
40	6.38	6.31	5.83	0.55	$8._6$
45	6.59		6.05	0.55	$8._3$
50	6.80		6.27	0.53	$7._8$
55	7.01		6.48	0.53	$7._6$
60	7.21		6.69	0.52	$7._2$
65	7.41		6.90	0.51	$6._9$
70	7.61		7.11	0.50	$6._6$
75	7.81		7.31	0.50	$6._4$
80	8.01		7.51	0.50	$6._2$
85	8.21		7.71	0.50	$6._1$
90	8.41		7.91	0.50	$5._9$
95	8.61		8.11	0.50	$5._8$
100	8.81	8.84	8.31	0.50	$5._7$
105	9.01		8.51	0.50	$5._5$
110	9.21	9.2	8.71	0.50	$5._4$
115	9.41		8.91	0.50	$5._3$
120	9.61	9.7	9.11	0.50	$5._2$
125	9.81		9.31	0.50	$5._1$
130	10.01		9.51	0.50	$5._0$
135	10.21		9.71	0.50	$4._9$
140	10.41	10.5	9.91	0.50	$4._8$
145	10.61		10.11	0.50	$4._7$
150	10.81		10.31	0.50	$4._6$
155	11.01		10.51	0.50	$4._5$
160	11.21	11.3	10.71	0.50	$4._5$
165	11.41		10.91	0.50	$4._4$
170	11.61		11.11	0.50	$4._3$

sium iodide likewise shows at higher temperatures a faster increase with temperature of solubility in ordinary water.

Potassium iodide. In the region above 100°C., the solubility values in I.C.T. have been found to be seriously in error by Kracek (15), whose measurements, however, did not embrace temperatures below 50°C. We considered it unnecessary to repeat the work of Kracek, but made the three measurements recorded in table 6a, which agree within 1 per cent with I.C.T. values, in order to extend Kracek's results to 0°C.

TABLE 6a

Observed solubility of potassium iodide (166.02) in ordinary water and in deuterium water

(1) Ordinary water

T	*S*	*W*	*V*	*P*	*C*	*M*
°C.	*grams*	*grams*	*cc.*	*mm.*	*grams*	
6.2	1.0154	0.7655				7.99
11.2	1.0154	0.7434				8.23
56.6_5	1.0154	0.5866				10.4_3

(2) Deuterium water

T	*S*	*W*	*V*	*P*	*C*	*M*
°C.	*grams*	*grams*	*cc.*	*mm.*	*grams*	
2.6	1.0130	1.0136				6.69
10.7	1.0130	0.9391				7.22
17.8	1.0130	0.8860				7.65
34.0	1.0130	0.7925				8.55
60.3	1.4968	1.0167				9.86
62.7	1.0130	0.6788				9.99
88.6	1.4968	0.8907				11.2_5
118.1	1.4968	0.7894	2.98	744.	0.0018	12.7_2
146.1	1.4968	0.7169	3.01	1597.	0.0037	14.0_5

Barium chloride. No estimate is given in I.C.T. of the accuracy of the stated values of solubility of barium chloride dihydrate. Their maximum discrepancy from our values is little over 1 per cent. We have not tabulated the values of Etard (13) for the monohydrate, because of their lack of precision. Our solubility curves for these two hydrates intersect in the neighborhood of 102°C. Collins and Menzies (9) found this transition at 101.94°C. ± 0.05°.

Taylor, Caley, and Eyring (32) measured the solubility of barium chloride in 92 per cent deuterium water at 20°C. Converted, as described for the similar case of sodium chloride, to solubility in 100 per cent deuterium water, their value for molal solubility is 1.51, as compared with 1.48 found in the present work. The transition temperature of di- to mono-deuterate is found near 93.3°C. Since the two solubility curves intersect at a very unfavorable angle, this temperature is uncertain by 2°C.

Cadmium iodide. Since the solubility values in I.C.T. up to 40°C. taken from the data of Cohen and coworkers (6, 7), are estimated to have

TABLE 6b

Solubilities of potassium iodide in ordinary water and in deuterium water at rounded temperatures

T	M_{H_2O}	Kracek (15)	M_{D_2O}	*D*	% *D*
°*C.*					
0	(7.66)	7.78	(6.52)	1.14	1_5.
5	(7.92)		6.85	1.07	1_4.
10	8.17	8.24	7.17	1.00	1_2.
15	8.42		7.48	0.94	1_1.
20	8.66	8.70	7.78	0.88	1_0.
25	8.90		8.07	0.83	$9._3$
30	9.14	9.17	8.34	0.80	$8._8$
35	9.38		8.60	0.78	$8._3$
40	9.62	9.63	8.85	0.77	$8._0$
45	9.85		9.09	0.76	$7._7$
50	10.09*	10.09	9.34	0.75	$7._4$
55	10.32*		9.59	0.73	$7._1$
60	10.56*	10.56	9.84	0.72	$6._8$
65	10.79*		10.09	0.70	$6._5$
70	11.02*	11.02	10.33	0.69	$6._3$
75	11.25*		10.58	0.67	$6._0$
80	11.49*	11.49	10.82	0.67	$5._8$
85	11.72*		11.06	0.66	$5._6$
90	11.96*	11.96	11.31	0.65	$5._4$
95	12.20*		11.55	0.65	$5._3$
100	12.43*	12.43	11.80	0.63	$5._1$
105	12.67*		12.04	0.63	$5._0$
110	12.91*	12.91	12.29	0.62	$4._8$
115	13.15*		12.53	0.62	$4._7$
120	13.39*	13.39	12.77	0.62	$4._6$
125	13.63*		13.02	0.61	$4._5$
130	13.87*	13.87	13.26	0.61	$4._4$
135	14.12*		13.51	0.61	$4._3$
140	14.37*	14.37	13.75	0.62	$4._3$
145	14.61*		13.99	0.62	$4._2$
150	14.86*	14.86	(14.24)	0.62	$4._2$

an accuracy of ±0.1 per cent, we did not repeat any measurements in this range. Our experimental values for higher temperatures show wide discordance from the values in I.C.T., amounting to 10 per cent at 140°C. (see table 8a). These values are based, apparently, on the work of Etard (13) and on two values of Dietz (12), whose preparations may have differed from ours (5, 29, 8).

Mercuric chloride. Values for M_{H_2O} for this salt differ widely from those in I.C.T. While the accuracy claimed for these latter is but 10 per cent over the whole range 0–100°C., we find closer agreement over most of the range. Nevertheless even wider deviation is found at 60°, 70° and 80°C.,

TABLE 7a

Observed solubility of barium chloride (208.27) in ordinary water and in deuterium water

(1) Ordinary water

T	*S*	*W*	*V*	*P*	*C*	*M*
			$BaCl_2 \cdot 2H_2O$			
°*C.*	*grams*	*grams*	*cc.*	*mm.*	*grams*	
9.7	0.3053	0.9223				1.59
29.2	0.3053	0.8078				1.81
53.1	0.3053	0.6946				2.11
65.1	0.5200	1.0935				2.28
78.3	0.3053	0.5895				2.49
98.5	0.5200	0.8911	2.81	612.9	0.0013	2.81
			$BaCl_2 \cdot H_2O$			
102.8	0.5200	0.8672	2.82	711.2	0.0015	2.88
113.1	0.5200	0.8499	2.85	1001.	0.0021	2.95
127.8	0.5200	0.8259	2.87	1585.	0.0033	3.04
153.0	0.5200	0.7807	2.92	3193.	0.0063	3.22
168.7	0.5200	0.7567	2.94	4718.	0.0091	3.34
180.0	0.5200	0.7328	2.96	6111.	0.0115	3.46

(2) Deuterium water

T	*S*	*W*	*V*	*P*	*C*	*M*
			$BaCl_2 \cdot 2D_2O$			
°*C.*	*grams*	*grams*	*cc.*	*mm.*	*grams*	
4.1	0.2046	0.8766				1.24
21.2	0.2046	0.7299				1.50
21.6	0.3074	1.0879				1.51
37.0	0.3074	0.9463				1.73
53.1	0.3074	0.8400				1.95
77.1	0.3402	0.7900				2.30
80.7	0.3074	0.6954				2.36
			$BaCl_2 \cdot D_2O$			
95.5	0.3402	0.7092	3.35	528.1	0.0015	2.56
104.8	0.3402	0.7006	3.37	739.3	0.0021	2.60
119.8	0.3402	0.6751	3.39	1217.	0.0034	2.70
135.0	0.3402	0.6539	3.42	1936.	0.0052	2.80
159.3	0.3402	0.6178	3.47	3751.	0.0097	2.98
179.7	0.3402	0.5869	3.50	6075.	0.0151	3.17

TABLE 7b

Solubilities of barium chloride in ordinary water and in deuterium water at rounded temperatures

T	m_{H_2O}	I.C.T.	m_{D_2O}	D	% D
			$BaCl_2 \cdot 2Aq$		
°C.					
0	(1.50)	1.52	(1.19)	0.31	$2_1.$
5	(1.55)		1.26	0.29	$1_9.$
10	1.61	1.61	1.33	0.28	$1_7.$
15	1.66		1.41	0.25	$1_5.$
20	1.72	1.72	1.48	0.24	$1_4.$
25	1.78		1.55	0.23	$1_3.$
30	1.83	1.83	1.62	0.21	$1_1.$
35	1.89		1.70	0.19	$1_0.$
40	1.96	1.94	1.77	0.19	$9._7$
45	2.02		1.84	0.18	$8._9$
50	2.08		1.92	0.16	$7._7$
55	2.15		1.99	0.16	$7._4$
60	2.22		2.06	0.16	$7._2$
65	2.29		2.14	0.15	$6._6$
70	2.37		2.21	0.16	$6._8$
75	2.44		2.28	0.16	$6._6$
80	2.52		2.35	0.17	$6._7$
85	2.60		2.43	0.17	$6._5$
90	2.68		2.50	0.18	$6._7$
93.3	2.74		2.54 U	0.20	$7._8$
95	2.76				
100	2.85	2.82			
102.1	2.88 U				
			$BaCl_2 \cdot Aq$		
95			2.55		
100			2.58		
105	2.89		2.61	0.28	$9._7$
110	2.92		2.64	0.28	$9._6$
115	2.95		2.67	0.28	$9._5$
120	2.98		2.70	0.28	$9._4$
125	3.01		2.73	0.28	$9._3$
130	3.04		2.76	0.28	$9._2$
135	3.07		2.79	0.28	$9._1$
140	3.11		2.83	0.28	$9._0$
145	3.15		2.87	0.28	$8._9$
150	3.19		2.91	0.28	$8._8$
155	3.23		2.95	0.28	$8._7$
160	3.27		2.99	0.28	$8._6$
165	3.31		3.03	0.28	$8._5$
170	3.36		3.08	0.28	$8._3$
175	3.41		3.12	0.29	$8._5$
180	3.46		(3.17)	0.29	$8._4$

temperatures for which other experimental data are scarce. The solubility of this salt changes fifteenfold in the range studied. When this is represented on a single graph, error in graphing causes the greatest percentage error at low solubility, where also the percentage error of experiment is greatest. In the neighborhood of 70°C., however, such error is no longer excessive. Our value is there about 16 per cent higher than that of I.C.T. and about 2 per cent lower than a value published by Sugden (30) in 1929.

TABLE 8a

Observed solubility of cadmium iodide (366.25) in ordinary water and in deuterium water

(1) Ordinary water

T	*S*	*W*	*V*	*P*	*C*	*M*
°C.	*grams*	*grams*	*cc.*	*mm.*	*grams*	
76.9	1.0513	0.9642				2.98
99.1	0.6024	0.4813	3.30	708.0	0.0018	3.43
131.2	1.0513	0.7009	3.42	1950.	0.0048	4.12
155.1	1.0513	0.6012	3.51	3801.	0.0090	4.85

(2) Deuterium water

T	*S*	*W*	*V*	*P*	*C*	*M*
°C.	*grams*	*grams*	*cc.*	*mm.*	*grams*	
1.7	0.4266	0.8491				1.52
11.1	0.4266	0.8026				1.61
24.4	0.4266	0.7395				1.75
44.4	0.3900	0.6008				1.97
57.7	0.7027	1.0104				2.11
78.9	0.7027	0.8800				2.42
96.9	0.7027	0.7708	3.64	653.0	0.0019	2.77
115.0	0.7027	0.6893	3.70	1175.	0.0035	3.11
125.9	0.7027	0.6289	3.76	1652.	0.0048	3.42
137.4	0.7027	0.5812	3.85	2333.	0.0068	3.71
149.4	0.7027	0.5356	3.94	3251.	0.0095	4.05

EXPRESSION OF SOLUBILITY DIFFERENCES

One may, for example, plot the values of $\%D$ for each salt either (*a*) against temperature or (*b*) against M_{H_2O}, the molal solubility of the saturated solution in ordinary water at the temperature of comparison. With the salts here studied, a more open diagram is obtained by method (*b*), which we have employed for figure 2. On this are included for comparison, in addition to salts described above, cupric sulfate pentaquate, strontium chloride hexaquate and diaquate, and potassium chloride from other work in this laboratory (21, 28). Figure 3 shows a plot by method (*a*) for halides of potassium and sodium.

It should be emphasized that the smaller the values of $\%D$, the more subject are they to inevitable uncertainty.

TABLE 8b

Solubilities of cadmium iodide in ordinary water and in deuterium water at rounded temperatures

T	M_{H_2O}	I.C.T.	M_{D_2O}	D	$\%\ D$
°C.					
0	2.16	2.155	(1.50)	0.66	3_1.
5	2.19		1.54	0.65	3_0.
10	2.23	2.230	1.59	0.64	2_9.
15	2.27		1.64	0.63	2_8.
20	2.31	2.312	1.69	0.62	2_7.
25	2.35		1.74	0.61	2_6.
30	2.40	2.404	1.79	0.61	2_5.
35	2.45		1.84	0.61	2_5.
40	2.51	2.506	1.90	0.61	2_4.
45	2.56		1.96	0.60	2_3.
50	2.62		2.02	0.60	2_3.
55	2.68		2.09	0.59	2_2.
60	2.74	2.77	2.16	0.58	2_1.
65	2.81		2.23	0.58	2_1.
70	2.88		2.30	0.58	2_0.
75	2.95		2.38	0.57	1_9.
80	3.03	3.09	2.46	0.57	1_9.
85	3.11		2.54	0.57	1_8.
90	3.19		2.63	0.56	1_8.
95	3.28		2.72	0.56	1_7.
100	3.38	3.48	2.81	0.57	1_7.
105	3.48		2.91	0.57	1_6.
110	3.59		3.01	0.58	1_6.
115	3.70		3.12	0.58	1_6.
120	3.82	3.96	3.24	0.58	1_5.
125	3.94		3.36	0.58	1_5.
130	4.07		3.48	0.59	1_4.
135	4.21		3.61	0.60	1_4.
140	4.35	4.74	3.75	0.60	1_4.
145	4.50		3.89	0.61	1_4.
150	4.67		(4.04)	0.63	1_3.
155	4.84				
160	(5.02)				

TRANSITION TEMPERATURES AND MELTING POINTS

In table 10 we have set down data for nine transitions studied in this laboratory. In comparing, in column 4, by difference in temperature the transition points in systems with ordinary and dueterium water, we have utilized values for each obtained by like methods, when two such values were available.

Inspection of table 10 makes clear that the differences of temperature for analogous transitions may be in either direction. Pure water, sodium sulfate heptahydrate, and sodium sulfate decahydrate show difference values of −3.82°, −3.0°, and −2.1°C. at 0°, 23.7°, and 32.4°C., respectively, an orderly succession not out of harmony with a suggestion of Bernal and Fowler (4) that water in certain hydrates is in an ice-like arrangement.

TABLE 9a

Observed solubility of mercuric chloride (271.524) in ordinary water and in deuterium water

(1) Ordinary water

T	*S*	*W*	*V*	*P*	*C*	*M*
°C.	*grams*	*grams*	*cc.*	*mm.*	*grams*	
0.9	0.1344 a	2.8674				0.173
20.9_3	0.0627	0.9477				0.244
39.2_5	0.0627	0.6082				0.380
55.8_5	0.0627	0.4078				0.566
62.7	0.1766	0.9467				0.687
75.4	0.1766	0.6539				0.995
91.6	0.4132	0.9457	3.15	542.	0.0014	1.612
99.7	0.4132	0.7230	3.36	724.	0.0019	2.110
105.6	0.4132	0.5511	3.60	880.	0.0024	2.773

(2) Deuterium water

T	*S*	*W*	*V*	*P*	*C*	*M*
°C.	*grams*	*grams*	*cc.*	*mm.*	*grams*	
8.1	0.0279	0.8831				0.129
18.7	0.0279	0.6733				0.170
27.2	0.0279	0.5366				0.213
48.9	0.0796	0.8831				0.369
57.4	0.0796	0.7037				0.463
67.3	0.0796	0.5382				0.605
91.2	0.2612	0.8831	3.30	510.	0.0015	1.212
105.1	0.2612	0.5308	3.73	835.	0.0028	2.024

These transition temperatures are points of incongruent melting. The congruent melting points for these hydrates would lie at concealed maxima on the solubility–temperature curves. The molecular composition of corresponding hydrates and deuterates is, of course, identical. Thus the maxima, for corresponding salts, fall at the same position on the composition axis. The relative positions and slopes of the two analogous solubility curves, as they approach this identical composition, will indicate which will cross this composition at the lower temperature, that is, which will have the lower congruent melting point. Inspection of figure 2 shows if and where any two analogous solubility curves cross, thus making it possible to predict which of the two curves will be at the higher temperature when it reaches its maximum at the composition of the hydrate. Consequently we see that the congruent melting points of $SrCl_2 \cdot 6D_2O$, $SrCl_2 \cdot 2D_2O$, $NaBr \cdot 2D_2O$ and $NaI \cdot 2D_2O$ must lie at lower temperatures than do those of the corresponding hydrates. For example, if one extrapolates the solubility curves of $NaI \cdot 2H_2O$ and $NaI \cdot 2D_2O$ to maxima at the composition M = 27.75 (which corresponds to the formula), one finds that the congruent melting points should lie near 80°C., with the deuterate melting point a degree or two lower than that of the hydrate.

TABLE 9b

Solubilities of mercuric chloride in ordinary water and in deuterium water at rounded temperatures

T	M_{H_2O}	I.C.T.	M_{D_2O}	D	$\%D$
°C.					
0	(0.172)	0.170	(0.100)	0.072	4_2.
5	0.184		(0.120)	0.064	3_5.
10	0.200	0.204	0.140	0.060	3_0.
15	0.220		0.160	0.060	2_7.
20	0.243	0.246	0.180	0.063	2_6.
25	0.269		0.202	0.067	2_5.
30	0.300	0.300	0.226	0.074	2_5.
35	0.335		0.253	0.082	2_4.
40	0.376	0.366	0.284	0.092	2_4.
45	0.426		0.321	0.105	2_5.
50	0.486	0.466	0.367	0.119	2_4.
55	0.557		0.426	0.131	2_4.
60	0.640	0.554	0.496	0.144	2_3.
65	0.738		0.569	0.169	2_3.
70	0.853	0.714	0.651	0.202	2_4.
75	0.985		0.748	0.237	2_4.
80	1.140	0.980	0.865	0.275	2_4.
85	1.325		1.006	0.319	2_4.
90	1.546	1.41	1.177	0.369	2_4.
95	1.801		1.378	0.423	2_3.
100	2.151	2.06	1.637	0.514	2_4.
105	2.705		2.018	0.687	2_5.

The contrary case is exhibited by $Na_2SO_4 \cdot 10Aq$. Inspection of figure 2 shows that the solubility curve of $Na_2SO_4 \cdot 10D_2O$ is quite unlikely to lie lower in temperature than the curve for $Na_2SO_4 \cdot 10H_2O$ as they pass through their maxima at M = 5.55, for there is no indication that the curves will cross before reaching that composition. The graph on figure 2 will approach nowhere near the zero per cent horizontal if extrapolated to M = 5.55.

It thus appears that, when deuterium water forms compounds with salts entirely analogous to compounds with ordinary water, the congruent melting points of the deuterium compounds may be either higher or lower than those of their analogues. Such congruent melting points may doubtless be realized, and not merely predicted for metastable phases, in suitably chosen cases.

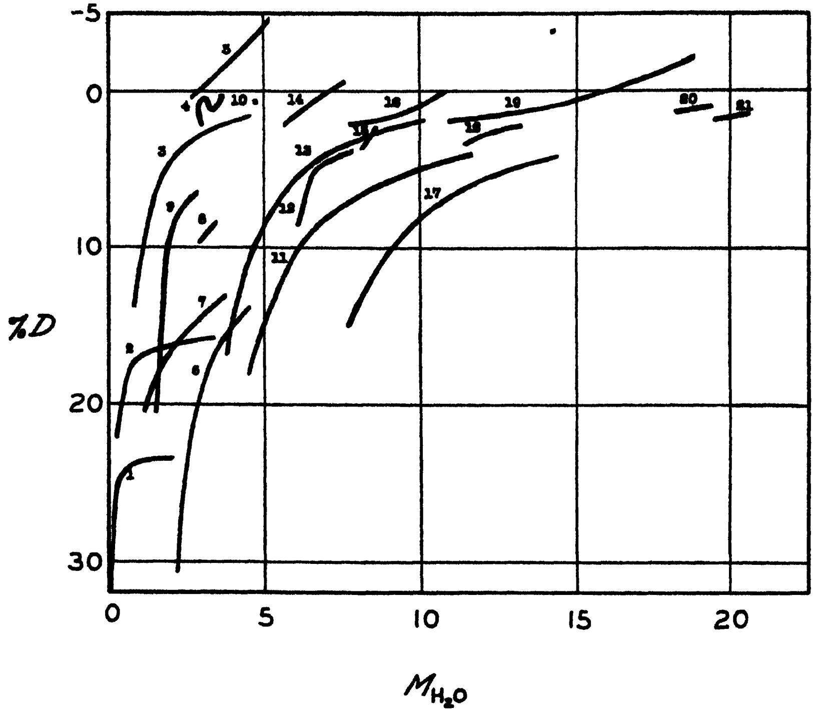

FIG. 2. Graph of %D against M_{H_2O} for certain salts and salt aquates

NO.	SOLID PHASE	RANGE IN °C.	NO.	SOLID PHASE	RANGE IN °C.
1	$HgCl_2$	10–105	11	KBr	0–170
2	$Na_2SO_4 \cdot 10Aq$	0–32	12	NaCl	0–180
3	$CuSO_4 \cdot 5Aq$	3–95	13	KCl	0–180
4	Na_2SO_4	25–180	14	$SrCl_2 \cdot 2Aq$	62–128
5	$SrCl_2 \cdot 6Aq$	0–56	15	$SrCl_2 \cdot Aq$	135–145
6	CdI_2	0–150	16	NaBr·2Aq	45–170
7	$Na_2SO_4 \cdot 7Aq$	0–23	17	KI	0–150
8	$BaCl_2 \cdot Aq$	105–180	18	NaBr	45–170
9	$BaCl_2 \cdot 2Aq$	0–93	19	NaI·2Aq	0–66
10	$CuSO_4 \cdot 3Aq$	100–110	20	NaI·xAq	45–60
			21	NaI	55–115

An examination of merely the few cases before us might make it appear that the relative temperatures of the (unrealized) congruent melting

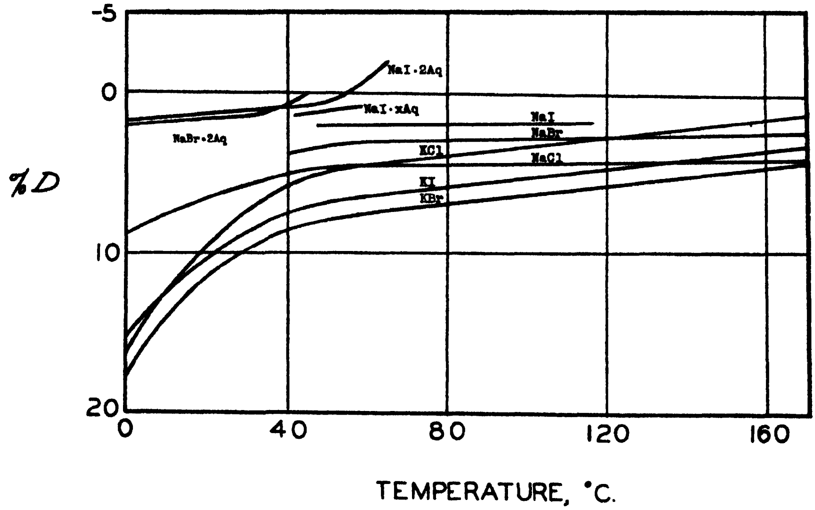

FIG. 3. Graph of %D against temperature in °C. for halides of sodium and potassumi

TABLE 10

The transition temperatures of some salt deuterates and their corresponding hydrates

TRANSITION	TEMPERATURES		
	Hydrates	Deuterates	Difference
	°C.	°C.	°C.
$NaBr \cdot 2Aq \rightleftharpoons NaBr + 2Aq$	50.8	47.4	3.4
	50.674 (26)	47.7 (2)	
$NaI \cdot 2Aq \rightleftharpoons NaI + 2Aq$	68.2	66.0	2.2
	64.3 (23)		
$NaI \cdot xAq \rightleftharpoons NaI + xAq$	60.0	58.2	1.8
$Na_2SO_4 \cdot 10Aq \rightleftharpoons Na_2SO_4 + 10Aq$	32.5	34.2	
	32.384 (11)	34.48 (31)	−2.1
		34.5 (2)	
		34.6–34.9 (14)	
$Na_2SO_4 \cdot 7Aq \rightleftharpoons Na_2SO_4 + 7Aq$	23.7	26.7	−3.0
	23.46 (34)	26.6–27 (14)	
$CuSO_4 \cdot 5Aq \rightleftharpoons CuSO_4 \cdot 3Aq + 2Aq$	95.9 (9)	96.2 (21)	−0.3
$BaCl_2 \cdot 2Aq \rightleftharpoons BaCl_2 \cdot Aq + Aq$	102.1	93.3	8.8
	101.94 (9)		
$SrCl_2 \cdot 6Aq \rightleftharpoons SrCl_2 \cdot 2Aq + 4Aq$	61.4 (20)	56.4 (21)	5.0
	61.34 (27)	56.5 (2)	
$SrCl_2 \cdot 2Aq \rightleftharpoons SrCl_2 \cdot Aq + Aq$	134.4 (20)	128.5 (21)	5.9

points were always in the same sense as those of the (realized) incongruent melting points. This is not necessarily the case, for the extrapolated graph for $CuSO_4 \cdot 5Aq$ in figure 2 may, for example, cross the zero line before reaching the composition $M = 11.1$ (which corresponds to the formula).

Further discussion will find place in the light of additional experimental facts.

SUMMARY

1. The solubilities in ordinary water of NaCl, $NaBr \cdot 2H_2O$, NaBr, $NaI \cdot 2H_2O$, $NaI \cdot xH_2O$, NaI, $Na_2SO_4 \cdot 10H_2O$, $Na_2SO_4 \cdot 7H_2O$, Na_2SO_4, KBr, KI, $BaCl_2 \cdot 2H_2O$, $BaCl_2 \cdot H_2O$, CdI_2, and $HgCl_2$ have been studied, chiefly by a method proposed by Menzies, over their ranges of existence within the interval 0°C. to 105–180°C.

2. A similar study has been made of the analogous systems in deuterium water.

3. The resulting molal solubility values and their differences in the two systems have been tabulated for rounded temperatures at intervals of 5°C. Differences were found to range from -2.0 to $+42$ per cent.

4. From the intersection of solubility curves, the transition temperatures of six hydrates and six analogous deuterates have been evaluated and compared. These were all incongruent melting points, and were sometimes lower and sometimes higher for deuterates than for their analogous hydrates. It is predicted that the same will be true for congruent melting points of such compounds.

5. The existence has been uncovered of a new hydrate of sodium iodide, and of the analogous deuterate.

REFERENCES

(1) Beckmann, E.: Z. physik. Chem. **6**, 460 (1890).
(2) Bell: J. Chem. Soc. **1937**, 459.
(3) Benedicks: Orig. Com. Intern. Congr. Appl. Chem. **22**, 13 (1912).
(4) Bernal and Fowler: J. Chem. Phys. **1**, 515 (1933).
(5) Clarke and Kebler: Am. Chem. J. **5**, 235 (1883).
(6) Cohen and Bruins: Z. physik. Chem. **93**, 43 (1919).
(7) Cohen, Hetterschij, and Moesveld: Z. physik. Chem. **94**, 210 (1920).
(8) Cohen and Moesveld: Z. physik. Chem. **94**, 450 (1920).
(9) Collins and Menzies: J. Phys. Chem. **40**, 379 (1936).
(10) De Coppet: Z. physik. Chem. **22**, 239 (1897).
(11) Dickenson and Mueller: Bull. Bur. Standards **3**, 641 (1907).
(12) Dietz: Z. anorg. Chem. **20**, 240 (1899).
(13) Etard: Ann. chim. phys. **2**, 503 (1894).
(14) Higuchi, I.: J. Chem. Soc. Japan **58**, 193 (1937).
(15) Kracek: J. Phys. Chem. **35**, 947 (1931).
(16) *International Critical Tables:* (a) Volume IV, page 216 and ff.: (b) Volume III, page 292 and ff.: (c) Volume IV, page 236. The McGraw-Hill Book Company, New York (1925).
(17) Landsberger: Z. anorg. Chem. **17**, 453 (1898).

(18) Leopold and Johnston: J. Am. Chem. Soc. **49**, 1974 (1927).
(19) Loewel: Ann. chim. phys. **49**, 32 (1857).
(20) Menzies, A. W. C.: J. Am. Chem. Soc. **58**, 934 (1936).
(21) Miles and Menzies: J. Am. Chem. Soc. **59**, 2392 (1937).
(22) Miles and Menzies: J. Am. Chem. Soc. **58**, 1067 (1936).
(23) Panfilow: J. Russ. Ges. (Chem.) **25**, 273 (1893).
(24) Pascal and Ero: Bull. soc. chim. **25**, 35 (1919).
(25) Richards and Wells: Z. physik. Chem. **43**, 465 (1903).
(26) Richards and Wells: Z. physik. Chem. **56**, 348 (1906).
(27) Richards and Yngve: J. Am. Chem. Soc. **40**, 89 (1918).
(28) Shearman and Menzies: J. Am. Chem. Soc. **59**, 185 (1937).
(29) Snell: J. Am. Chem. Soc. **29**, 1288 (1909).
(30) Sugden: J. Chem. Soc. **1929**, 488.
(31) Taylor, H. S.: J. Am. Chem. Soc. **56**, 2643 (1934).
(32) Taylor, Caley, and Eyring: J. Am. Chem. Soc. **55**, 4334 (1933).
(33) Taylor and Selwood: J. Am. Chem. Soc. **56**, 998 (1934).
(34) Washburn and Clem: J. Am. Chem. Soc. **60**, 754 (1938).
(35) Wuite: Z. physik. Chem. **86**, 349 (1914).

THE CATALYTIC OXIDATION OF HYDROGEN ON PLATINUM. A SEARCH FOR CHEMILUMINESCENCE AND IONIZATION

R. POTVIN and C. OUELLET

Laboratory of Physical Chemistry, Laval University, Quebec, Canada

Received June 20, 1939

INTRODUCTION

Numerous investigations have shown that the radiation and ionization in hot flames can be accounted for by a purely thermal mechanism. Although part of the energy responsible for these phenomena could be derived directly from the chemical reaction, as in cold chemiluminescence, it is difficult to obtain direct evidence of such chemical excitation in the presence of the intense thermal excitation in hot flames of hydrogen, hydrocarbons, and carbon monoxide, as shown by Bonhoeffer (2), Konradjew (7), Garner and Saunders (4), and Gill (5). The present paper describes an attempt to eliminate the thermal background by causing the reaction to proceed at low temperatures on a catalyst. Any effect detected under such conditions should be ascribed a chemical origin.

The oxidation of hydrogen on platinum at temperatures ranging from 80°C. to 170°C. has been investigated, and the light measurements have been limited to the ultraviolet part of the spectrum. Although the net reaction heat is only 57 kg-cal., a number of intermediate steps involving energies above 100 kg-cal., corresponding to ultraviolet radiation, have been assumed to take place, such as:

$$H + H \rightarrow H_2 + 101 \text{ kg-cal.}$$

$$O + O \rightarrow O_2 + 117 \text{ kg-cal.}$$

$$H + OH \rightarrow H_2O + 112 \text{ kg-cal.}$$

$$H + O_2 + H \rightarrow H_2O + OH + 102 \text{ kg-cal.}$$

Photoelectric counters were used as detectors of radiation, and the emission of electricity by the platinum catalyst was measured by means of an electrometer.

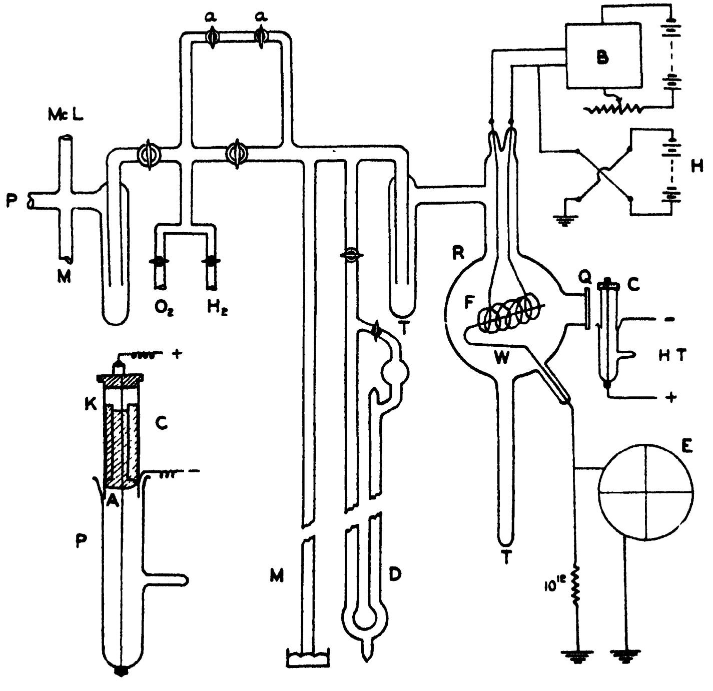

FIG. 1. The reaction system.

APPARATUS AND PROCEDURE

The reaction system

As shown in figure 1, a 500-cc. Pyrex reaction chamber was provided with a quartz window, Q, 3 cm. in diameter, and two traps T, and was connected through 20-mm. tubing with the mercury diffusion and Hyvac pumps P and a McLeod gauge (McL). Small amounts of gases were admitted through a by-pass aa′, and pressures down to 0.05 mm. were read on a mercury manometer M and a differential manometer D, filled with Hyvac oil. The 0.35-mm. thick platinum filament, F, wound into seven spirals 1 cm. in diameter, constituted one of the branches of a bridge, B, by means of which its temperature was measured. A tungsten wire, W, coaxial with the platinum coil, acted as a collecting electrode and was connected with an electrometer, E, shunted through a 10^{12}-ohm resistance and giving a deflection of 1 mm. for a current of 10^{-14} ampere. The oxygen and hydrogen were prepared electrolytically and stored over phosphorus pentoxide.

In doing a run, the traps T were immersed in a mixture of acetone and carbon dioxide to condense the water formed during the reaction; the filament was glowed during a few minutes in a vacuum and then during 5 sec. at 700°C. in oxygen at the pressure at which the reaction was to take place. The filament was then allowed to cool and hydrogen admitted. The reaction was then started by heating the filament again to the desired temperature, and this temperature was kept constant throughout the reaction by means of a variable rheostat placed in the heating circuit.

The photoelectric counters

Photoelectric tube counters C (figure 1), of the type described by Rajewski (10) and others, were used as detectors of ultraviolet light. A quartz tube, K, one end of which was sealed into the slightly conical end of a Pyrex tube, P, contained the cathode, made of copper or aluminum foil bent into a cylinder 1.5 cm. in diameter and 4 cm. long, with an 0.8-cm. longitudinal slit through which light could enter. The anode consisted of chromel wire, about 0.2 cm. thick, which was subjected to no other treatment than washing in distilled water and alcohol. The general behavior of chromel wire (sharp impulses and 75–100 volts characteristics) compares favorably with that of platinum, tungsten, and iron wires used in previous work by one of the authors (9). The counters were filled at pressures $\sim$5 cm. of mercury with air that had been dried by calcium chloride and purified of dust by bubbling through Hyvac oil.

The photoelectric thresholds of the cathodes were determined approximately by displacing the counters in front of a small quartz spectrograph, using a carbon arc as a source. They were found to lie at 2800 Å. for copper and 3500 Å. for aluminum, although in this case a region of low sensitivity extended as far as 4000 Å. The sensitivity of the counters is discussed below, together with the experimental results.

The counting circuit is shown in figure 2. The high tension was supplied by a GM high voltage unit, the primary current of which was stabilized by a Raytheon voltage regulator. Further stabilization of the output voltage was ensured by means of a circuit embodying a neon lamp and pentode, similar to that described by Gingreich (6), a 20,000-ohm variable rheostat being added to obtain finer regulation. The high tension, generally about 1400 volts, was applied to the cathode of the counter through a 10^7-ohm protective resistance. The impulses from the anode wire were transmitted through a 5.5×10^9-ohm resistance to a three-stage amplifier and a FG 17 thyratron tube which operated a mechanical telephone recorder R. The amplifying circuit, based on that published by Barasch (1), was completely shielded and contained only metal tubes. The first stage was mounted separately and clamped near the counter, so as to eliminate long leads.

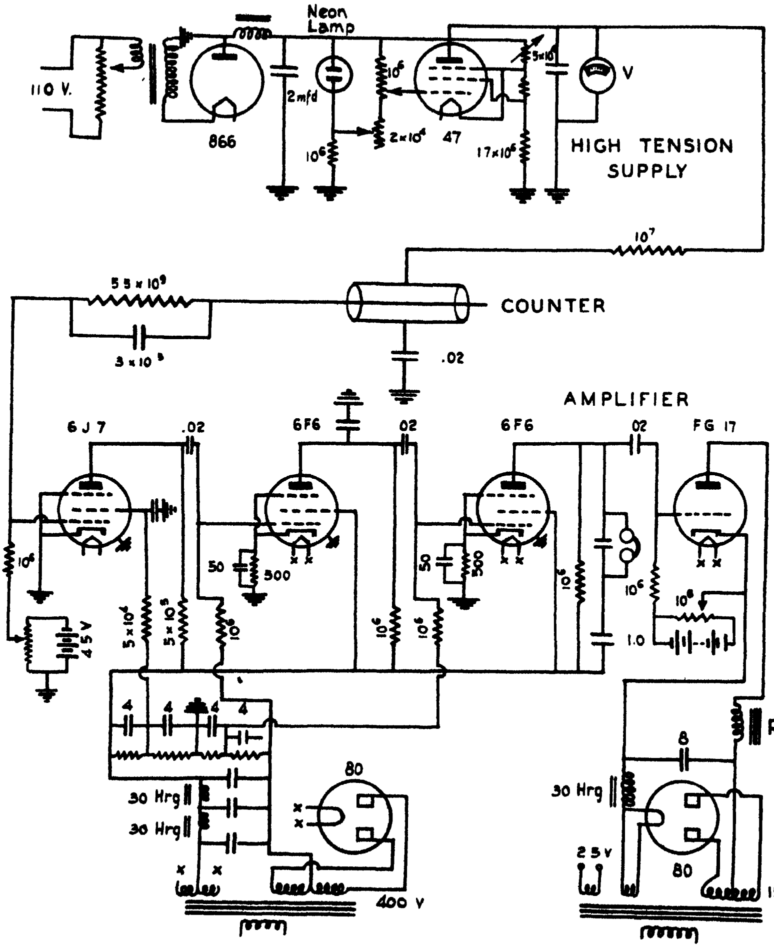

FIG. 2. The counting circuit

RESULTS AND DISCUSSION

The kinetics of the reaction

The reaction was studied at pressures of the order of 10 mm. of mercury, safely below the lower explosion limit. Langmuir (8), Wiig (13), and others have investigated its kinetics at very low pressures, but no data seem to be available concerning its behavior under the conditions used in this work. Although no systematic investigation of the kinetics has been undertaken, the velocity of the reaction has been determined at different temperatures of the filament, and some of the curves obtained are shown in figure 3. These results were reproducible within 5 per cent at intervals of several weeks, showing that the surface of the catalyst had suffered no alteration.

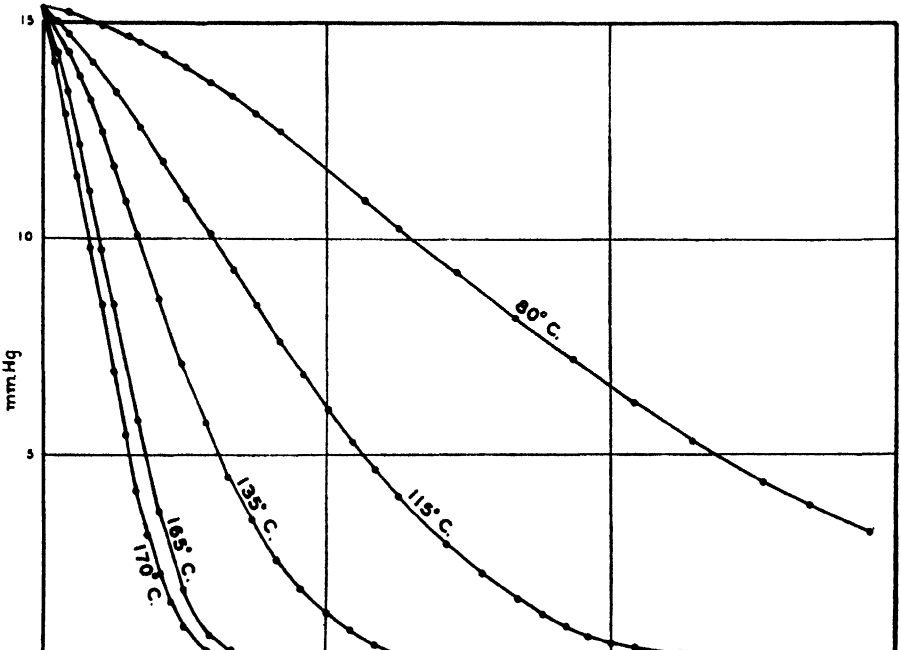

FIG. 3. Velocity of the reaction at different temperatures of the filament

It is clear that the rate tends towards a maximum value as the temperature increases and may remain constant or possibly decrease at temperatures above 200°C. As the cold reaction only was of interest in this work, this point was left for further investigation. The shape of the curves suggests that the reaction is autocatalytic at the lower temperatures and gradually loses this character as the temperature increases. This is to be expected if active centers are developed on the catalyst by the reaction itself. At the higher temperatures, however, the concentration of the centers being already near saturation, the reaction will proceed at once with almost its maximum velocity.

Without going into the details of the mechanism, an equation which fits the experimental curves can be derived from the somewhat arbitrary assumptions that the velocity is proportional to the second power of the total pressure p of the stoichiometric mixture and to the concentration, α, of the active centers on the surface of the catalyst.

$$-\frac{dp}{dt} = k_1 \alpha p^2 \tag{1}$$

The rate of increase of α is taken as

$$\frac{d\alpha}{dt} = k_2(a + \alpha)$$

where a is the initial concentration of the centers and is constant at a given temperature. By integration, we obtain

$$\alpha = C_1 e^{k_2 t} - a \tag{2}$$

which, introduced into equation 1, gives

$$-\frac{dp}{dt} = k_1(C_1 e^{k_2 t} - a)p^2$$

Integrating and combining the constants, we finally have

$$\frac{p_0}{p} = e^{k_2 t} - k_3 t \tag{3}$$

where k_2 and k_3 are constants, and p_0 is the pressure at time $t = 0$. Table 1 gives a comparison of the observed values of p with those calculated from equation 3. In all three cases $p_0 = 13.5$ mm. of mercury.

The measurement of radiation

In looking for an emission of ultraviolet radiation during the reaction, the counter was placed in front of the quartz window Q and the number of impulses recorded over periods of 10 or 20 min. during which the reaction was proceeding, and over equal and alternate control periods during which the filament was in a vacuum. Tables 2 and 3 give, as an example, the detailed results of a series of 20-min. periods and the sum of all the counts. In each case, the initial pressure of the gases is indicated.

It is seen from these results that the difference between the number of counts during the reaction and control periods keeps well within the limits of the statistical fluctuations ($\pm\sqrt{4207} = \pm 65$ and $\pm\sqrt{3175} = \pm 56$). If radiation is emitted, its intensity is below the limit of sensitivity of the detectors used in these experiments.

TABLE 1

Comparison of observed values of p with those calculated from equation 3

TIME	80°C.		115°C.		135°C.	
	$k_2 = 0.025$ $k_3 = 0.02$		$k_2 = 0.06$ $k_3 = 0.055$		$k_2 = 0.1$ $k_3 = 0.09$	
	p calculated	p observed	p calculated	p observed	p calculated	p observed
minutes	*mm.*	*mm.*	*mm.*	*mm.*	*mm.*	*mm.*
3	13.2	13.3	13.0	12.8	12.5	12.3
5	13.0	13.1	12.4	12.0	11.2	11.0
8	12.7	12.8	11.4	11.2	9.0	9.0
10	12 5	12.6	10.8	10.5	7.4	7.6
15			9.3	9.1	4.3	4.4
20	10.8	11.0	6.2	6.7	2.4	2.3
30	8.9	9.2	4.0	3.7	0.8	0.2
40	7.1	7.3	1 5	1.5		
50	5.4	5.5	0.8	0.6		
60	4.1	4.0				
70	3.1	2.5				

TABLE 2

Results with a copper cathode (2000–2800 Å.)

O_2 PRESSURE	H_2 PRESSURE	IMPULSES	
		Reaction	Control
mm. Hg	*mm. Hg*		
0.7	2.0	286	281
0.8	2.6	248	275
4.8	12.0	230	222
4.6	9.6	254	254
4.6	9.3	234	240
5.5	11.0	235	215
		291	305
4.6	10.0	247	229
5.0	10.9	231	232
4.6	9.3	217	238
		2473	2491 ±50
Other counts.		1826	1716 ±42
Total.		4299	4207 ±65

In determining the sensitivity of the counters towards ultraviolet light, the catalytic filament itself was used as a light source. This method does away with the problematic corrections concerning the geometry of the apparatus and the losses by absorption and reflection, and gives directly the number of impulses per minute caused by the emission of a known number of photons from the surface of the catalyst under the actual experimental arrangement. The projection of the platinum wire on a plane perpendicular to the direction going from the coil to the counter was taken as the effective emitting area and estimated at 0.5 cm.^{2} The filament was brought to temperatures of 1775°K. for the copper counter and 1550°K. for the aluminum counter, and respective increases of 65 and 29 impulses per minute were recorded. The amounts of radiation emitted were calculated by means of Wien's equation:

TABLE 3

Results with an aluminum cathode (2000-4000 Å.)

O_2 PRESSURE	H_2 PRESSURE	IMPULSES	
		Reaction	Control
mm. Hg	*mm.* Hg		
5.2	10.2	258	256
5.0	10.0	250	240
5.0	10.0	228	215
4.6	10.0	248	285
		265	215
0.7	1.7	253	264
1.4	3.0	250	280
0.7	1.4	276	269
		2028	2024 ±45
Other counts..........................		1153	1151 ±34
Total..................................		3181	3175 ±56

$$E(\lambda) = \frac{c_1}{\lambda^5}\cdot e^{-c_2/\lambda T}$$

where λ is the mean wave length of the sensitivity interval for each counter, T is the absolute temperature of the filament, $c_1 = 10^{-5}$ erg per second cm.^{2}, and $c_2 = 1.4$ cm. degree. Taking $\lambda = 2500$ Å., $\Delta\lambda = 1000$ Å., and $T = 1775$°K., the amount of radiation emitted by the filament is found to be 1.75×10^{-1} erg per second or 1.5×10^{10} $h\nu$ per second. The part of this radiation which entered the copper counter caused an increase of 65 impulses per minute over a dark rate averaging 13 per minute. An increase 100 times smaller, corresponding to $\sim 10^8$ photons per second, could have been detected.

The number of elementary reactions taking place per second when the reaction was proceeding to completion in 20 min. from an initial pressure of 10 mm. of mercury in the 500-cc. bulb, was calculated to be $\sim 10^{16}$. Therefore, less than 10^8 photons in the region $\lambda = 2500$ Å. are emitted by 10^{16} reacting molecules, i.e., less than 1 photon by 10^8 molecules.

Emission of electricity

Several processes may be responsible for the passage of a current between the catalyst and the collecting electrode. Electrons may be emitted from the metal by a purely thermionic process or under the influence of the chemical reaction, as was shown by Denisoff and Richardson (3) in the case of alkali metals reacting with halogens. The adsorbed gases may also form ions, positive or negative, which are removed by the applied field. Any one of these processes may mask the effect which was looked for in the present experiments, i.e., the production of ions by the reaction itself. In order to distinguish between these various possible sources of current, experiments were conducted under different conditions as follows:

In investigating the emission of negative electricity, the platinum filament was first glowed in a vacuum for several hours and then raised to a potential of −135 volts respective to the collecting electrode. The lowest temperature at which a thermionic emission was recorded was 750°C. Measurements were then made in the presence of the reaction mixture. The gases were first admitted and the filament heated to 250°C. to start the reaction. No emission was observed before the setting in of the reaction. During the reaction the gas pressure, the current, and the temperature of the filament (which was not controlled) were measured. Some of the results obtained with different mixtures are shown in figure 4. The upper part contains the time–pressure curves, while the corresponding time–current curves are shown in the lower part of the figure. Both temperature and current rose to a peak during the first seconds and then went down very rapidly. Curve V was obtained with a potential difference of −500 volts; after 3 min. the pressure had decreased to such a point that a gas discharge set in.

The very weak currents observed do not seem to be due to the reaction itself, since their intensity is not proportional to the velocity of the reaction. It is improbable also that they be emitted by a mechanism similar to that found by Denisoff and Richardson (3), as the energy of the reaction (57 kg-cal.) is much smaller than the lowest value of the work-function of platinum (4.1 volts or 96 kg-cal.) observed by Suhrmamn (12) in the presence of hydrogen. Only the possible intermediate steps with energies above 100 kg-cal. could give rise to such an emission. These negative currents may be accounted for by a simple thermionic emission, assuming that, under the influence of the reaction, active spots on the platinum surface are raised to temperatures far above that of the bulk of the filament as measured by the Wheatstone bridge.

The emission of positive electricity was found to be very much the same during the reaction as in the presence of oxygen alone, as indicated by the curves on figure 5. In order to obtain a sharper definition of the threshold temperature, the feet of the curves were determined again with an increased sensitivity of the electrometer and are plotted on an enlarged scale in the upper left-hand corner of the figure. The vacuum emission was obtained after the filament had been glowed overnight at about 1000°C. in a vacuum of 10^{-5} mm. of mercury. Similar measurements were carried out in oxygen at 10 mm. of mercury and in a stoichiochemical mixture of

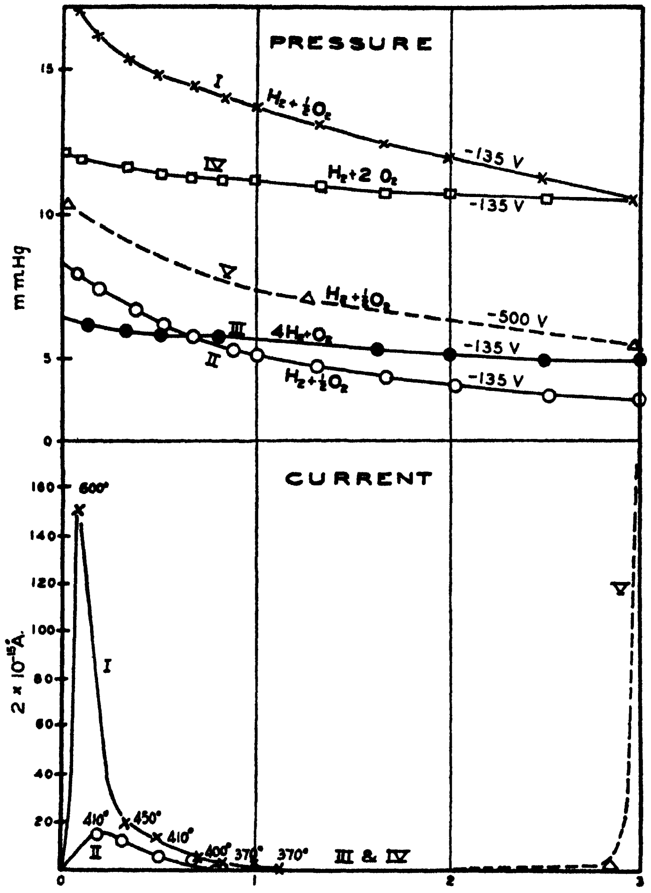

FIG. 4. Negative emission with different mixtures

oxygen and hydrogen at a total pressure of 10 mm. of mercury. It is clear that the effect of the reacting mixture does not differ appreciably from that of oxygen alone. Moreover, the emission begins at the same temperature, about 340°C., in a vacuum and in oxygen, with the sole difference that its intensity is lower in a vacuum. It seems that in all

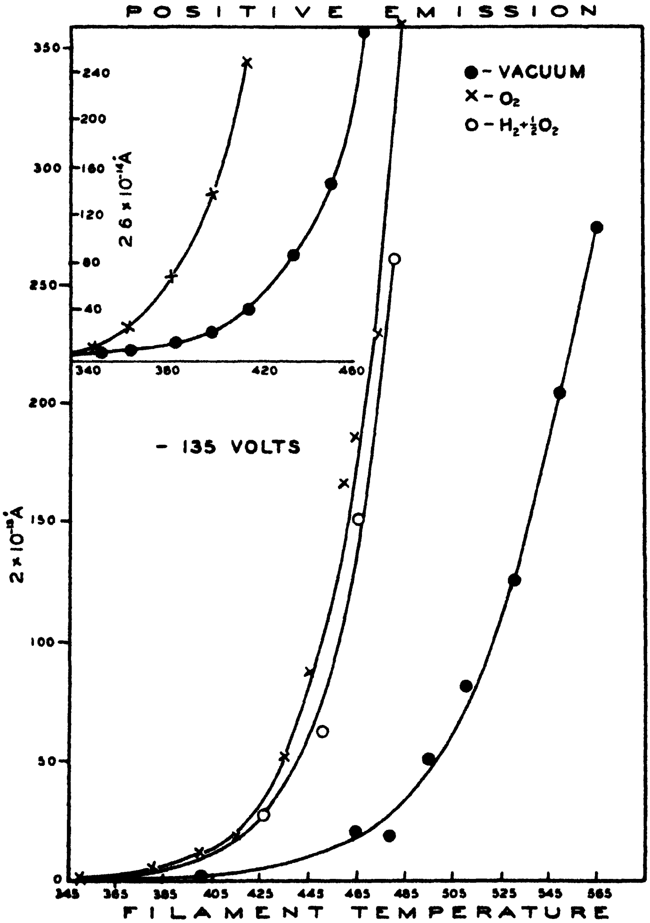

Fig. 5. Positive ion emission

three cases, the emission is connected with the presence of oxygen on the surface of the platinum, the gas being imperfectly removed by the preheating of the filament.

If the charged particles were produced directly by the reaction their removal by a field might be expected to alter the velocity of the reaction. That such is not the case was shown by repeating the curves of figure 3 with the filament 135 volts positive as well as negative respective to the collecting electrode. No difference in the reaction velocity was detected.

It is interesting to note that the temperature of 340°C., at which positive emission sets in, is very nearly the same as that at which Reischauer (11) observed the beginning of an activated adsorption of oxygen.

SUMMARY

1. The reaction $H_2 + \frac{1}{2}O_2 \rightarrow H_2O$, catalyzed by a platinum filament, has been studied at pressures of the order of 10 mm. of mercury and temperatures ranging from 80°C. to 170°C. The velocity curves have been determined.

2. Photoelectric tube counters have been used to detect an emission of ultraviolet radiation by the reaction. If such radiation is emitted, its intensity must be below 1 photon per 10^8 reacting molecules.

3. Negative electricity is emitted from the filament during the reaction and may be due to a localized thermionic effect. The emission of positive electricity seems to be independent of the reaction and sets in at a temperature of about 340°C., at which an activated adsorption of oxygen has been reported to take place.

REFERENCES

(1) Barasch, H. P.: Proc. Phys. Soc. (London) **47**, 824 (1935).
(2) Bonhoeffer, K. F.: Z. Elektrochem. **42**, 499 (1936).
(3) Denisoff, A. K., and Richardson, O. W.: Proc. Roy. Soc. (London) **A144**, 46 (1934).
(4) Garner, K., and Saunders, S. W.: Trans. Faraday Soc. **23**, 243 (1927).
(5) Gill, F.: Trans. Faraday Soc. **26**, 49 (1930).
(6) Gingreich, N. S.: Rev. Sci. Instruments **7**, 105 (1936).
(7) Konratjew, V.: Acta Phys. Polon. **5**, 71 (1936).
(8) Langmuir, I.: Trans. Faraday Soc. **17**, 621 (1922).
(9) Ouellet, C., and Rideal, E. K.: J. Chem. Phys. **3**, 150 (1935).
(10) Rajewski, B.: Physik. Z. **32**, 121 (1931).
(11) Reischauer, H.: Z. physik. Chem. **B26**, 399 (1934).
(12) Suhrmann, R.: Ann. Physik. **67**, 43 (1922).
(13) Wiig, E. O.: J. Am. Chem. Soc. **55**, 2673 (1933).

pH CHANGE IN GOLD SOL FORMATION

C. L. THROCKMARTIN[1] AND C. H. SORUM

Department of Chemistry, University of Wisconsin, Madison, Wisconsin

Received July 24, 1939

When colloidal gold is prepared by reduction of an alkaline solution of potassium aurate by formaldehyde the nature of the color change that takes place indicates that the reaction is probably autocatalytic. Thus, at a given temperature and with a given concentration of reactants the reaction mixture remains colorless for several minutes; then the color begins to appear, very slowly at first, then more rapidly until, finally, the end of the reaction is reached with what might be described as a rush of color. If the concentration of the reactants, the temperature, and the rate of addition of the reactants are carefully controlled, the sol obtained has a clear orange-red color. However, in arriving at this final color, the sol generally goes through a color change from lavender to blue to violet to violet-red to orange-red.

Zsigmondy and Hückel (3) have followed the rate of this reaction by comparing the color of the reaction mixture at any time with a set of standards of known colloidal gold content. Their results indicate that the reaction is autocatalyzed and is complete when the color intensity reaches a maximum. Zsigmondy and Hückel prepared their sols under such conditions that the blue color noted above did not appear. When this blue color appears, as was the case in the present study, a color comparison method for following the rate of the reaction is not satisfactory. Since the reduction of potassium aurate by formaldehyde is accompanied by a change in the pH of the system, this pH change was used as a means of following the reaction.

PREPARATION OF SOLS

All sols were prepared by the reduction, with formaldehyde, of a solution of gold chloride made alkaline with potassium carbonate. A small amount of resorcinol was added to aid in the formation of nuclei. The following directions are typical: To 1945 cc. of water add, in turn, 20 cc. of a 1 per cent solution of gold chloride, 20 cc. of a 2 per cent solution of potassium carbonate, 5 cc. of 0.001 *M* resorcinol, and 10 cc. of a 1 per cent solution of formaldehyde. Stir for 1 min. and allow to stand at 20°C. until the reaction is complete.

The above directions were varied by changing, in turn, the temperature, the concentration of potassium carbonate, the concentration of formaldehyde, and the concentration of resorcinol. Within limits, these variations

---

[1] Wisconsin Alumni Research Foundation Assistant.

TABLE 1

Reaction mixture: 1940 cc. H_2O, *20 cc. of 1 per cent* $HAuCl_4$, *20 cc. of 2 per cent* K_2CO_3, *10 cc. of 0.001 M resorcinol, 10 cc. of 1 per cent* HCHO

$T = 24°C.$

A NITROGEN BUBBLED THROUGH SOL DURING FORMATION		B SOL FORMED IN ATMOSPHERE OF NITROGEN		C SOL FORMED IN ATMOSPHERE OF NITROGEN	
Time	pH	Time	pH	Time	pH
minutes		*minutes*		*minutes*	
10	9.53	15	9.55	5	9.66
31	9.38	30	9.44	30	9.50
50	9.31	60	9.32	90	9.34
75	9.19	90	9.28	120	9.29
100	9.03	105	9.31	130	9.23
135	8.44	120	9.29	140	9.03
141	8.32	130	9.26	150	8.41
150	8.22	140	9.19	160	7.65
160	8.14	150	8.74	170	7.42
170	8.10	160	7.81	180	7.36
180	8.07	170	7.50	190	7.34
200	8.05	180	7.43	200	7.33
		190	7.38		
		200	7.36		

TABLE 2

Reaction mixture: 1940 cc. H_2O, *20 cc. of 2 per cent* K_2CO_3, *20 cc. of 1 per cent* $HAuCl_4$, *10 cc. of 1 per cent* HCHO

$T = 20°C.$

A 5 cc. OF 0.001 *M* RESORCINOL		B 10 cc. OF 0.001 *M* RESORCINOL	
Time	pH	Time	pH
minutes		*minutes*	
5	9.59	2	9.63
20	9.50	10	9.50
40	9.43	50	9.43
60	9.40	100	9.33
130	9.21	110	9.28
136	9.12	120	9.25
140	8.88	130	9.00
150	8.29	135	8.52
160	7.91	140	8.21
170	7.84	145	8.06
190	7.72	150	7.90
225	7.60	165	7.80
265	7.51	183	7.67
300	7.41	202	7.61
		220	7.59

changed the rate of sol formation but did not appreciably alter either the color of the final sol or the fundamental shape of the rate curve.

All water used was redistilled from potassium permanganate in a Pyrex still. Steamed Pyrex glassware was used in all operations.

MEASUREMENT OF pH

The pH was measured by a Leeds and Northrup glass electrode unit No. 7685. In this unit the potential of the electrode is measured against a calomel cell which is so constructed that connection between the sol and the saturated potassium chloride solution is made through a ground-glass joint. The amount of potassium chloride entering the sol is negligible, so that coagulation of the colloid about the electrode does not take place. The electrode comes to equilibrium very quickly, so that a pH determination can be made in a few moments. The error in reading the instrument is not more than 0.02 of a pH unit.

TABLE 3

Reaction mixture: 1945 cc. H_2O, *20 cc. of 1 per cent* $HAuCl_4$, *5 cc. of 0.001 M resorcinol, 10 cc. of 1 per cent* HCHO

$T = 20°C.$

A 20 CC. OF 2 PER CENT K_2CO_3		B 18 CC. OF 2 PER CENT K_2CO_3		C 17 CC. OF 2 PER CENT K_2CO_3		D 16 CC. OF 2 PER CENT K_2CO_3	
Time	pH	Time	pH	Time	pH	Time	pH
minutes		*minutes*		*minutes*		*minutes*	
1	9.73	2	9.63	2	9.19	1	8.73
15	9.50	3	9.57	3	9.10	5	7.90
30	9.46	4	9.54	4	9.07	10	7.80
50	9.42	5	9.49	5	8.99	30	7.72
70	9.33	16	9.41	14	8.85	60	7.65
90	9.32	34	9.35	30	8.71	90	7.57
110	9.27	60	9.25	60	8.50	120	7.53
130	9.23	120	9.10	90	8.33	150	7.50
140	9.20	140	9.05	162	7.91	200	7.45
151	9.13	160	8.97	210	7.84	240	7.43
160	8.90	180	8.88	313	7.67	340	7.38
166	8.43	190	8.80	690	7.38	435	7.35
172	7.98	200	8.69			1095	7.35
180	7.80	210	8.47				
190	7.66	216	8.31				
200	7.60	222	8.17				
267	7.36	230	8.04				
300	7.36	240	7.91				
		310	7.38				
		335	7.36				

TABLE 4

Reaction mixture: 1940 cc. H_2O, *20 cc. of 1 per cent* $HAuCl_4$, *20 cc. of 2 per cent* K_2CO_3, *10 cc. of 0.001 M resorcinol, 10 cc. of 1 per cent* HCHO

A $T = 12°C.$		B $T = 30°C.$	
Time	pH	Time	pH
minutes		*minutes*	
5	9.83	5	9.74
17	9.68	17	9.66
30	9.57	30	9.51
60	9.54	73	9.43
90	9.48	100	9.38
108	9.46	150	9.31
140	9.46	180	9.27
200	9.46	200	9.25
400	9.31	220	9.17
430	9.27	230	9.04
460	9.21	240	8.65
480	9.04	250	8.10
495	8.84	260	7.86
510	8.38	270	7.73
580	7.72	285	7.64
650	7.58	300	7.53
680	7.58		

TABLE 5

Reaction mixture: 1940 cc. H_2O, *20 cc. of 1 per cent* $HAuCl_4$, *10 cc. of 0.001 M resorcinol*
$T = 20°C.$

A 10 cc. OF 1 PER CENT HCHO		B 12 cc. OF 1 PER CENT HCHO		C 14 cc. OF 1 PER CENT HCHO	
Time	pH	Time	pH	Time	pH
minutes		*minutes*		*minutes*	
5	9.66	5	9.64	5	9.61
30	9.30	30	9.44	30	9.36
90	9.34	60	9.30	60	9.20
120	9.29	90	9.16	90	8.65
140	9.03	100	9.00	100	8.50
150	8.41	120	8.20	120	7.46
160	7.65	140	7.50	140	7.37
170	7.42	150	7.32	150	7.24
180	7.36	160	7.28	160	7.23
190	7.34				
200	7.33				

TABLE 6

Reaction mixture: 1945 cc. H_2O, *20 cc. of 1 per cent* $HAuCl_4$, *20 cc. of 2 per cent* K_2CO_3, *5 cc. of 0.001 M resorcinol*

T = 20°C.; no formaldehyde added

A		B	
Time	pH	Time	pH
minutes		*minutes*	
1	9.73	1	9.72
5	9.66	5	9.66
10	9.59	10	9.57
15	9.50	15	9.51
20	9.48	20	9.48
30	9.46	30	9.45
50	9.43	50	9.44
60	9.40	60	9.42
80	9.40	80	9.40
90	9.40	90	9.40
120	9.40	120	9.40

TABLE 7

Reaction mixture: The reaction mixtures from table 6, which had been allowed to stand for 2 hr. at 20°C., were treated with 10 cc. of 1 per cent formaldehyde

A		B	
Time from addition of formaldehyde	pH	Time from addition of formaldehyde	pH
minutes		*minutes*	
1	9.33	1	9.32
5	9.32	5	9.32
20	9.33	20	9.32
30	9.27	30	9.28
50	9.25	50	9.25
100	9.17	100	9.13
120	9.00	120	9.02
130	8.50	130	8.52
140	8.20	140	8.10
150	8.04	150	8.02
160	7.88	160	7.90
180	7.56	180	7.60
200	7.51	200	7.50
220	7.40	220	7.37

EXPERIMENTAL RESULTS

Sols were prepared at various temperatures within the working range of the pH apparatus, and the change in the pH of the reaction mixture during the course of the formation of the sol was noted. In order to

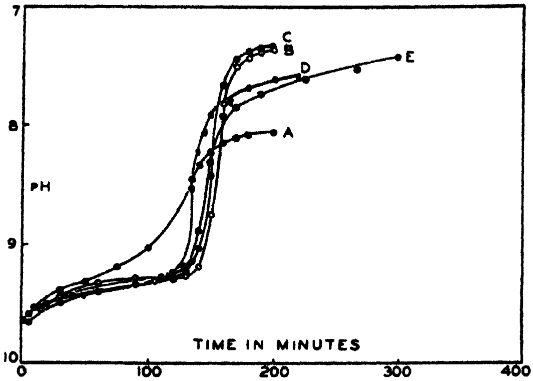

FIG. 1. pH change in gold sol formation. Curve A, data from table 1A, nitrogen gas bubbled through sol during formation. Curves B and C, data from tables 1B and 1C, respectively; sol formed in atmosphere of carbon dioxide-free nitrogen. Curves D and E, data from tables 2B and 2A, respectively, showing influence of varying amount of resorcinol on pH change.

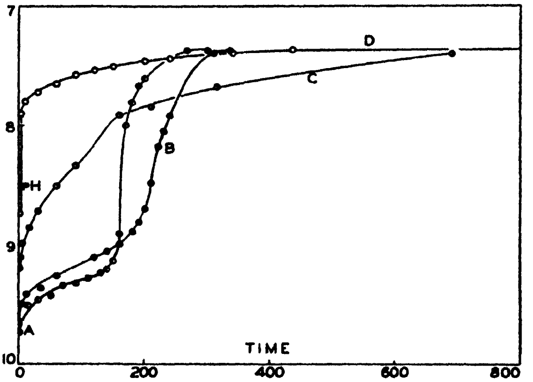

FIG. 2. The influence of concentration of potassium carbonate on pH change in gold sol formation. Curves A, B, C, and D represent data from tables 3A, 3B, 3C, and 3D, respectively.

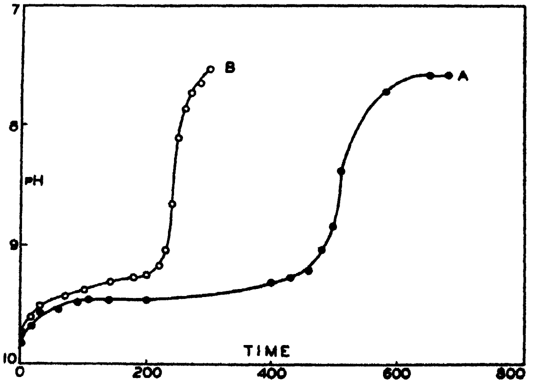

FIG. 3. The influence of temperature on the rate of pH change in gold sol formation. Curves A and B represent data from tables 4A and 4B, respectively.

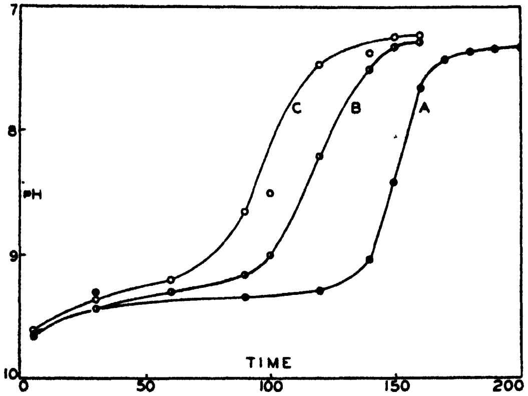

FIG. 4. The influence of concentration of formaldehyde upon the rate of pH change in gold sol formation. Curves A, B, and C represent the data from tables 5A, 5B, and 5C, respectively.

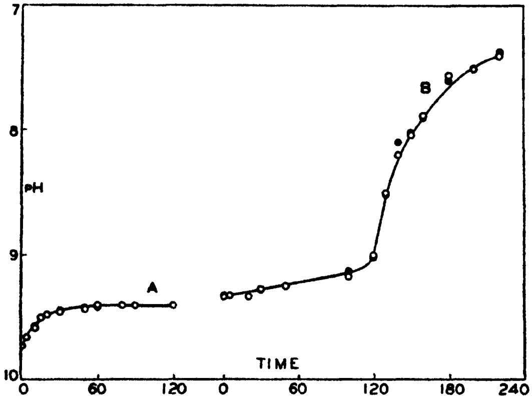

FIG. 5. Curve A, data from table 6, pH change in formation of potassium aurate; curve B, data from table 7, pH change in reduction of potassium aurate by formaldehyde.

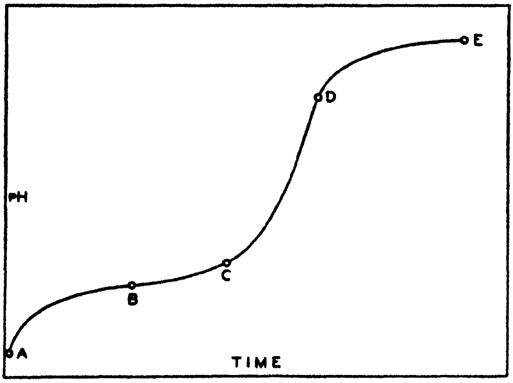

FIG. 6. Rate of pH change in gold sol formation

prevent a change in pH due to carbon dioxide dissolving from the air the sols were formed in an atmosphere of nitrogen. The results obtained are summarized in tables 1 to 7 and figures 1 to 6.

DISCUSSION

The typical curve obtained when the pH of the reduction mixture is plotted against time consists of four parts (figure 6). The first part of the curve, *A–B*, in which the rate of change of pH is decreasing with time, probably represents the reaction of potassium carbonate with chloroauric acid to form potassium aurate. The experimental data represented in figure 5a, in which the pH of a mixture of potassium carbonate, gold chloride, and resorcinol is plotted against time, support this contention. It is to be noted that the curve in figure 5A is of the same general form as *A–B*. The data represented in figure 5B also support the above contention. When the potassium carbonate and gold chloride are allowed to react before the formaldehyde is added, part *A–B* of the type curve disappears. The chemical reaction taking place through *A–B* is generally considered to be:

$$2HAuCl_4 + 4K_2CO_3 + 2H_2O = 2Au(OH)_3 + 4CO_2 + 8KCl$$

$$2Au(OH)_3 + K_2CO_3 = 2KAuO_2 + CO_2 + 3H_2O$$

The second part of the curve, *B–C*, which shows a very slowly accelerated increase in pH, is the induction period, during which nuclei are forming. The rate of the reaction becomes marked at *C*, increasing to a point where, approaching *D*, there is a rush of color. The increased rate of the reaction in part *C–D* may be interpreted as being due to the catalytic effect on the reduction process of the increased amount of surface of the colloidal particles which have been formed. As this surface area increases the rate of change of pH, that is, the rate of the reaction, increases very rapidly to a maximum.

The fourth part of the curve, *D–E*, may arise from two separate factors. First, there is the normal decrease in the rate of the reaction, due to decrease in concentration of the reactants. The fact that the color of the sol does not change after point *D* is passed may appear to contradict this contention. However, the relative amount of colloid formed from *D* to *E* is so small that the color change is not noticeable. The second factor may be the adsorption of hydroxyl ions from solution by the colloidal particles. Additional experiments, intended to verify or disprove this factor, are now under way.

The normal color changes that accompany the change in pH are as follows: From *A* to *B* the reaction mixture is colorless. At *B* a very faint lavender tint begins to appear. Between *C* and *D* the color ranges from blue to violet to violet-red, finally becoming a clear orange-red. The exact origin of these colors can not be stated at this time. It seems probable that the potassium aurate is first reduced to blue colloidal aurous oxide, which is subsequently reduced to orange-red colloidal gold. The color changes observed could then be due to a change in the absolute and relative amounts of these two colloidal substances. It is hoped that studies with the polarograph, which are now under way in this laboratory, will throw more light on the cause of the color change.

Table 4 and figure 3 emphasize the temperature dependence of the reaction. If the reaction mixture is heated to 90–95°C. the entire reaction is complete in about 10 min.

The specific rôle of the resorcinol is being studied in more detail. As noted in table 2 and figure 1, however, an excess of resorcinol does not seem to alter the rate of the reaction.

Table 3 and figure 2 simply confirm a fact already noted by other investigators, among them Beaver and Muller (1) and Kharasch and Isbell (2): namely, that the rate of reduction of the aurate increases with increase in the alkalinity of the system.

Table 5 and figure 4 emphasize the mass law effect insofar as the concentration of formaldehyde is concerned. In all cases the pH–time curve conforms to the general type already discussed.

SUMMARY

The changes in pH during the formation of gold sols have been measured. The experimental results appear to verify the fact that the reduction of potassium aurate by formaldehyde is an autocatalytic reaction.

REFERENCES

(1) Beaver and Muller: J. Am. Chem. Soc. **50**, 304 (1928).
(2) Kharasch and Isbell: J. Am. Chem. Soc. **52**, 2919 (1930); **53**, 2701, 3053 (1931).
(3) Zsigmondy and Hückel: Z. Physik **116**, 291 (1925).

THE SYSTEM SILVER SULFATE-ALUMINUM SULFATE-WATER[1]

J. A. ADDLESTONE, L. R. MARSH, AND G. C. HALL

Department of Chemistry, Virginia Polytechnic Institute, Blacksburg, Virginia

Received May 25, 1939

There are conflicting reports in the literature concerning the existence of silver alum. Kern (3) reported having made typical crystals of silver alum by evaporation of a mixed solution of silver sulfate and aluminum sulfate. Church and Northcote (2) described the preparation of this alum by heating a mixture of silver sulfate, aluminum sulfate, and water in a sealed tube until all the silver salt had dissolved. Both of these methods have been employed by other investigators (1) without being able to produce silver alum. Caven and Mitchell (1) investigated the system silver sulfate–aluminum sulfate–water and concluded that a crystalline silver alum does not form at 30°C. The present study was undertaken with the purpose of obtaining isotherms for this system at 0°C., 25°C., and 45°C.

EXPERIMENTAL PROCEDURE

Solutions were made, using C.P. silver sulfate and aluminum sulfate. For each isotherm a series of solutions was prepared containing varying concentrations of aluminum sulfate in contact with solid silver sulfate, and other solutions containing silver sulfate solutions in contact with solid aluminum sulfate. The solutions were placed in a constant-temperature water bath for the 25°C. and 45°C. isotherms, and in a water–ice mixture for the 0°C. isotherm. The solutions were shaken several times daily for a week and then allowed to settle completely so that the supernatant liquid was clear. It was shown by duplicate analyses that this allowed sufficient time for equilibrium to be reached.

Samples of the clear liquid were taken for analysis through pipets with cotton filters. The solid phase was sampled with a glass spoon and as much of the liquid as possible was allowed to drain off.

Silver was determined volumetrically by the thiocyanate method, and aluminum was determined by precipitation and ignition to the oxide. The silver was calculated to silver sulfate and the aluminum to aluminum sulfate; water was determined by difference. The composition of the solid phase in equilibrium with the various solutions was determined

---

[1] This paper is an abstract of theses submitted by L. R. Marsh and G. C. Hall in partial fulfillment of the requirements for the B.S. degree in chemistry.

FIG. 1. Solubility isotherms for the system silver sulfate–aluminum sulfate–water

graphically by means of intersecting tie-lines on a large-scale triangular diagram.

TABLE 1

0°C. isotherm

LIQUID PHASE		WET RESIDUE			SOLID PHASE
Moles Ag_2SO_4 per 1000 g. H_2O	Moles $Al_2(SO_4)_3$ per 1000 g. H_2O	Ag_2SO_4	$Al_2(SO_4)_3$	H_2O	
moles	*moles*	*per cent*	*per cent*	*per cent*	
0.0177	0				Ag_2SO_4
0.0179	0.0828				Ag_2SO_4
0.0185	0.1674	54.74	2.17	43.09	Ag_2SO_4
0.0205	0.2506				Ag_2SO_4
0.0211	0.3294	62.36	3.92	33.72	Ag_2SO_4
0.0211	0.5245				Ag_2SO_4
0.0213	0.5956	47.26	8.10	44.64	Ag_2SO_4
0.0218	0.8488	27.45	30.35	43.20	Ag_2SO_4 and $Al_2(SO_4)_3 \cdot 18H_2O$
0	0.9938				$Al_2(SO_4)_3 \cdot 18H_2O$

TABLE 2

25°C. isotherm

LIQUID PHASE		WET RESIDUE			SOLID PHASE
Moles Ag_2SO_4 per 1000 g. H_2O	Moles $Al_2(SO_4)_3$ per 1000 g. H_2O	Ag_2SO_4	$Al_2(SO_4)_3$	H_2O	
moles	*moles*	*per cent*	*per cent*	*per cent*	
0.0272	0				Ag_2SO_4
0.0277	0.1085				Ag_2SO_4
0.0289	0.2946	71.42	3.27	25.31	Ag_2SO_4
0.0290	0.3856				Ag_2SO_4
0.0304	0.5141				Ag_2SO_4
0.0307	0.6068	61.66	6.26	32.08	Ag_2SO_4
0.0309	0.8564				Ag_2SO_4
0.0310	1.047	59.10	10.32	30.58	Ag_2SO_4
0.0311	1.099	8.23	40.18	51.59	Ag_2SO_4 and $Al_2(SO_4)_3 \cdot 18H_2O$
0.0169	1.117	0.19	40.00	59.81	$Al_2(SO_4)_3 \cdot 18H_2O$
0	1.157				$Al_2(SO_4)_3 \cdot 18H_2O$

DATA AND CONCLUSIONS

The data for the three isotherms are given in tables 1 to 3 and shown graphically in figure 1. An inspection of these curves indicates that each isotherm consists of two solubility curves with no evidence of compound formation.

TABLE 3

45°C. isotherm

LIQUID PHASE		WET RESIDUE			SOLID PHASE
Moles Ag_2SO_4 per 1000 g. H_2O	Moles $Al_2(SO_4)_3$ per 1000 g. H_2O	Ag_2SO_4	$Al_2(SO_4)_3$	H_2O	
moles	*moles*	*per cent*	*per cent*	*per cent*	
0.0333	0				Ag_2SO_4
0.0351	0.0961	52.87	2.25	44.88	Ag_2SO_4
0.0376	0.1911				Ag_2SO_4
0.0386	0.3587	41.83	7.04	51.13	Ag_2SO_4
0.0397	0.5568				Ag_2SO_4
0.0399	0.7384	42.89	12.14	44.97	Ag_2SO_4
0.0402	1.284	40.56	18.07	41.37	Ag_2SO_4 and $Al_2(SO_4)_3 \cdot 18H_2O$
0	1.365				$Al_2(SO_4)_3 \cdot 18H_2O$

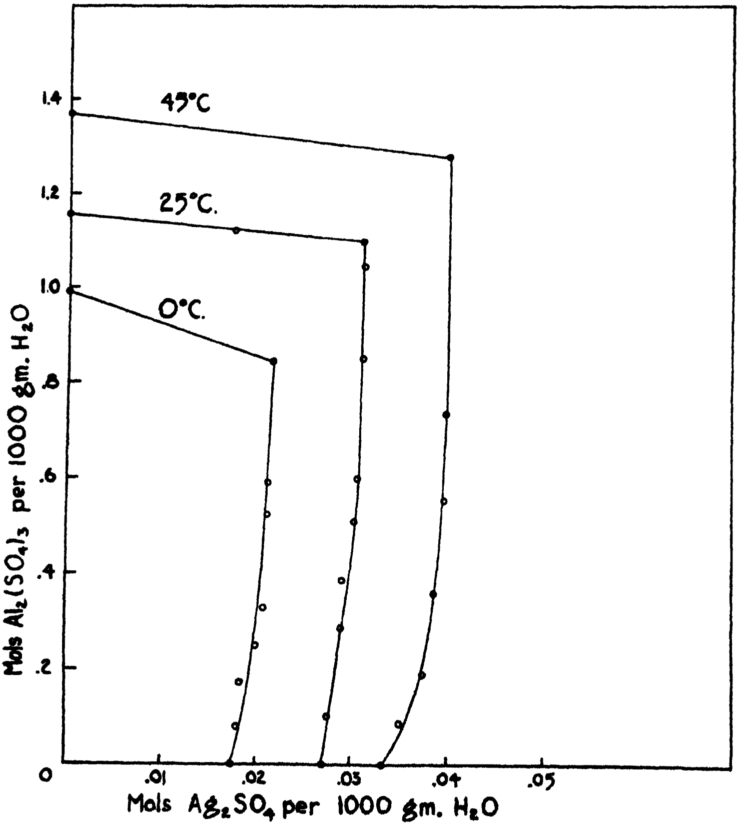

FIG. 1

SUMMARY

The 0°C., 25°C., and 45°C. isotherms for the system silver sulfate–aluminum sulfate–water have been determined.

The stable solid phases at these temperatures are Ag_2SO_4 and $Al_2(SO_4)_3 \cdot 18H_2O$.

There is no evidence of the formation of silver alum as a solid phase at the temperatures used in this study.

REFERENCES

(1) Caven and Mitchell: J. Chem. Soc. **127**, 2550 (1925).
(2) Church and Northcote: Chem. News **9**, 155 (1864).
(3) Kern: Chem. News **31**, 209 (1875).

HYDROUS LANTHANUM HYDROXIDE AS AN EMULSIFYING AGENT

THERALD MOELLER[1]

Laboratory of General Chemistry, University of Wisconsin, Madison, Wisconsin

Received July 24, 1939

INTRODUCTION

Very little information exists relative to agitating hydrous oxide and hydroxide sols with immiscible liquids, although it has been recognized that certain oxides and hydroxides can stabilize emulsions. Reinders (6) shook several sols, among them ferric oxide, with a number of organic liquids and found the suspended matter to concentrate at the interface in nearly all cases. Briggs (1) found that a hydrous ferric oxide sol when shaken with either benzene or kerosene gave rise to oil-in-water emulsions providing a small amount of a weakly flocculating electrolyte were present. Klein (2) was unable to precipitate such sols as ferric and aluminum oxides with various organic compounds.

In a preliminary experiment in which portions of a hydrous lanthanum hydroxide sol were shaken with equal volumes of different immiscible organic liquids, it was found that white foam-like emulsions floated to the top with benzene, toluene, and xylene. With ether, isoamyl alcohol, carbon tetrachloride, and chloroform, however, emulsions were not produced.

---

[1] Present address: Noyes Chemical Laboratory, University of Illinois, Urbana, Illinois.

EXPERIMENTAL

For the experiments which follow a sol was prepared which contained 1.492 g. of lanthanum oxide and 0.031 g. of chloride per liter, the purity ratio being 15.7 (3, 4). Carbon dioxide-free water was used throughout, and the organic compounds were of analytical reagent quality.

A. Effect of sol concentration

To each of a series of glass-stoppered bottles containing the amounts of the sol indicated in table 1 was added 15 ml. of toluene. Each bottle was shaken vigorously for 2 min. and observed at once.

TABLE 1

Effect of sol concentration using toluene

BOTTLE	SOL	WATER	OBSERVATIONS
	ml.	*ml.*	
0	0	15	Immediate separation to two layers
1	1	14	Concentration of La(OH)$_3$ at interface
2	2	13	
3	3	12	
4	4	11	
5	5	10	White foamy emulsion on top
6	6	9	
7	7	8	
8	8	7	
9	9	6	
10	10	5	
11	11	4	
12	12	3	
13	13	2	
14	14	1	
15	15	0	

In the bottle containing no sol, no emulsion resulted. Bottles 1, 2, 3, and 4 showed a definite white layer of lanthanum hydroxide at the water-toluene interface. Beginning with bottle 5, an emulsion formed in each instance, the size of the droplets decreasing with increasing sol concentration. It would thus appear that insufficient lanthanum hydroxide to promote emulsion stability was present until bottle 5 was reached. In the formation of the emulsions, considerable lanthanum hydroxide was removed from the water layer.

Similar results were obtained with benzene. The emulsions produced with either liquid were extremely stable and showed no tendency to break.

B. Effect of colloidal gold

Into a series of test tubes were measured the amounts of hydrous lanthanum hydroxide sol and gold sol (containing 0.05 g. of gold per liter, undialyzed) indicated in table 2. Five milliliters of toluene was added to each, followed by shaking for 30 sec.

Stable emulsions formed until 1.8 ml. of the gold sol had been added, this quantity of gold sol being that required to produce immediate flocculation when added to the lanthanum hydroxide sol. From this point on, although emulsions did not form, there was a concentration of reddish floc at the water–toluene interface in all cases.

TABLE 2

Effect of colloidal gold using toluene

TUBE	La(OH)$_3$ SOL	GOLD SOL	OBSERVATIONS (AT ONCE)
	ml.	*ml.*	
1	5.0	0	Stable emulsion
2	4.8	0.2	
3	4.6	0.4	
4	4.4	0.6	
5	4.2	0.8	
6	4.0	1.0	
7	3.8	1.2	
8	3.6	1.4	
9	3.4	1.6	
10	3.2	1.8	No emulsion
11	3.0	2.0	
12	2.8	2.2	
13	2.6	2.4	
14	2.4	2.6	
15	2.2	2.8	
16	2.0	3.0	

The gold was carried into the emulsion, apparently because of adsorption on the lanthanum hydroxide, for the gold sol alone was incapable of stabilizing an emulsion. As the amount of gold increased, the emulsions became increasingly reddish in color and appeared jewel-like by reflected light. Emulsions containing moderate amounts of gold were stable for indefinite periods.

C. Effect of flocculating electrolytes

In order to determine the effects of the presence of various ions, 5-ml. portions of the hydrous lanthanum hydroxide sol were flocculated with excesses of a number of electrolytes. When the flocs had definitely settled, 5 ml. of toluene was added to each, followed by vigorous shaking. An emulsion, accompanied by the removal of the coagulum from the aqueous layer, resulted in the presence of potassium ferrocyanide, potassium ferricyanide, potassium arsenate, primary, secondary, and tertiary potassium phosphates, potassium dichromate, potassium chromate, potassium sulfate, potassium fluoride, potassium chloride, potassium bromide, potassium iodide, potassium thiocyanate, sodium sulfate, sodium thiosulfate, sodium tetraborate, magnesium sulfate, and lithium chloride. With sodium carbonate and sodium sulfite, however, emulsions were not formed, nor was there any concentration of the hydroxide at the water–toluene interface.

D. Action of precipitated hydrous lanthanum hydroxide

A sample of hydrous lanthanum hydroxide was precipitated from a hot solution of lanthanum chloride with ammonium hydroxide and washed until chloride-free. Portions of an aqueous suspension of this were placed in glass-stoppered bottles and shaken with various liquids. With ether, isoamyl alcohol, carbon tetrachloride, and chloroform there was an immediate separation into two liquid layers, and the hydroxide settled out in the water layer. With benzene, toluene, xylene, mesitylene, kerosene, gasolene, and turpentine, however, very stable emulsions were produced, and the lanthanum hydroxide was completely removed from the aqueous layer.

DISCUSSION

These emulsions were of the oil-in-water type. For toluene-containing emulsions this was easily proved by treatment with small amounts of an iodine solution. The emulsions were colored pink, and closer examination revealed them to be made up of tiny pink droplets.

That hydrous lanthanum hydroxide was the emulsifying agent follows not only from the fact that aqueous solutions of lanthanum salts failed to produce emulsions when shaken with the various liquids but also from the fact that the addition of small amounts of hydrochloric acid (which would dissolve the lanthanum hydroxide) immediately broke the emulsions, causing the separation of two liquid layers. Hydrous lanthanum hydroxide must, therefore, concentrate at the interface between the oil and the water, and since the oil is always the dispersed phase, the hydroxide must be wetted better by water than by the organic liquid (5).

Apparently the physical character of the emulsifying agent had little to do with its action. The ability of colloidally dispersed hydrous lanthanum hydroxide to stabilize these emulsions distinguishes it from the colloidal ferric oxide reported by Briggs (1). It is also interesting to note that when mutually flocculated by colloidal gold lanthanum hydroxide loses its emulsifying power. Inasmuch as the gold is adsorbed on the floc, it is probable that the lanthanum hydroxide thereby loses some of its surface activity, although such an explanation does not account for the formation of an emulsion when a sol is flocculated by various electrolytes.

It is to be noted that of the liquids investigated only the hydrocarbons were emulsified.

SUMMARY

1. Hydrous lanthanum hydroxide, whether colloidally dispersed, flocculated from a sol by certain electrolytes, or precipitated from lanthanum salt solutions, stabilizes oil-in-water emulsions. The dispersed phase may be benzene, toluene, xylene, mesitylene, kerosene, gasolene, or turpentine.

2. Emulsions are not produced with ether, isoamyl alcohol, carbon tetrachloride, or chloroform.

REFERENCES

(1) Briggs: Ind. Eng. Chem. **13**, 1008 (1921).
(2) Klein: Kolloid-Z. **29**, 247 (1921).
(3) Moeller and Krauskopf: J. Am. Chem. Soc. **60**, 726 (1938).
(4) Moeller and Krauskopf: J. Phys. Chem. **43**, 363 (1939).
(5) Pickering: J. Chem. Soc. **91**, 2001 (1907).
(6) Reinders: Kolloid-Z. **13**, 235 (1913).

22. APR. 1940
LIBRARY

ELECTROKINETICS. XXII

ELECTROKINETIC POTENTIALS OF BARIUM SULFATE IN SOLUTIONS OF ELECTROLYTES AND IN FIFTY PER CENT ETHANOL[1]

R. G. RUYSSEN[2]

Division of Agricultural Biochemistry, University of Minnesota, St. Paul, Minnesota

Received February 11, 1939

Streaming potential measurements on barium sulfate diaphragms were suggested by the studies of Julien (2) on silver bromide. Julien found that capillaries obtained by fusing the salt had a permanent negative electrokinetic charge against all concentrations of silver nitrate in the streaming liquid. It is nevertheless generally admitted that silver halide sols acquire a positive charge in even very dilute silver nitrate solutions, as does barium sulfate in an excess of barium chloride. We have shown (4) that barium sulfate crystals with regular walls and an even shape (natural barite or barium sulfate precipitated in very dilute solutions) remain negative in barium chloride solutions of concentrations (0.001 mole per liter) such that streaming potentials are still measurable. Finely precipitated crystals with a great adsorptive surface behaved differently, and their charge was reversed to a positive sign at very low barium chloride concentrations (± 2 μ moles per liter[3]). However, the diaphragms used did not permit measurements of the surface conductance, and the potential could only be calculated by introducing, in the well-known von Smoluchowski formula, the conductivity of the liquid in the bulk.

We have resumed these experiments, using the technique of this laboratory, in which both the streaming potential and the conductivity of the liquid in the diaphragm are measured with the same electrodes.

EXPERIMENTAL

Preparation of the barium sulfate

The mode of formation of the crystals has a great influence on their electrical and adsorptive properties. Attention must be paid to the temperature of the solution, the concentration of the SO_4^{--} or Ba^{++} ions in excess during the formation, and the conditions for the growing and aging of the crystals. The sign was always negative when the barium sulfate was formed from exactly equimolar (0.1 M) barium chloride and potassium sulfate (or sodium sulfate) solutions, at the boiling temperature, and after being subjected to an aging and desorption procedure for several weeks. During these experiments we obtained some information about the influence of some factors on the charge and the adsorption of barium chloride by the formation of barium sulfate in an excess of barium ions. The main factor in obtaining negatively charged crystals was to leave the mother solution (containing the potassium chloride formed) in contact with the precipitate for 24 hr. If the solution was siphoned off and replaced by cold conductivity water, the desorption of the barium ions in the presence of potassium chloride was not complete and the barium sulfate (samples No. 10 and No. 12) was still positively charged even after several weeks aging and washing with water. This positive barium sulfate could be rendered negative by treatment with potassium chloride (see below).

---

[1] Paper No. 1692 of the Scientific Series of the Minnesota Agricultural Experiment Station.

[2] Advanced Fellow of the Belgian-American Educational Foundation. Professor of Pharmaceutical Chemistry in the University of Ghent, Belgium.

[3] 1μ mole = 1×10^{-6} mole.

After numerous tests the following method of preparation was adopted: One liter of distilled water was heated to boiling in a 4-liter Pyrex beaker. Separate portions of 1 liter each of exactly 0.100 M barium chloride and 0.100 M potassium sulfate (or sodium sulfate) solutions were brought to boiling. Aliquots of these hot solutions (50 ml.) were poured into two separatory funnels, from which they were dropped at slow and equal rates into pure water which was maintained at the boiling point. The entire precipitating process required approximately 1 hr. The boiling solution was kept stirred for a further 2 min. and was then allowed to settle for 15 min. The clear supernatant liquid was siphoned off and replaced with distilled water, which was left in contact with the precipitate for 24 hr. The water was then poured off and the precipitate was transferred to a sintered-glass filter with 100 cc. of boiling water and washed thoroughly to the absence of chlorides. The crystals were then transferred to a 1-liter flask with distilled water, shaken, and washed by decantation during 2 or 3 weeks, the water being renewed twice a day. The conductivity of the water remained constant after 2 weeks' washing.

The measuring device

The diaphragm and the streaming potential apparatus were essentially as used by Martin and Gortner (7), although the cell used was that of Lauffer and Gortner (6).

In order to prevent the fine barium sulfate from being carried away with the streaming liquid, the perforated platinum electrodes were covered by a double disc of ash-free, washed filter paper. The relative resistance to flow through this cellulose membrane was negligible as compared to the resistance to flow through the barium sulfate diaphragm. A tight packing of the powder in the diaphragm was secured, as this was essential for reproducible and constant streaming potentials. The rate of flow in the different diaphragms was kept in the same range and averaged about 0.0522 cc. per second, for a pressure difference of 26.5 cm. of mercury.

The potentials were measured with a Leeds and Northrup precision potentiometer, using a Dolezalek quadrant electrometer as a null instrument. The absolute accuracy was about 0.5 millivolt.

The specific conductivity of the liquids in the pores of the diaphragms and in equilibrium with the crystals was measured with the ordinary Wheatstone bridge, using a 1000-cycle current and telephones. The precision even in pure water was quite satisfactory. In the determination of the cell constant the streaming liquid was replaced by $N/10$ potassium chloride solution, which was repeatedly sucked and streamed through the diaphragm until, after several hours of treatment, the resistance remained constant.

The electrokinetic potentials were calculated from the well-known formula

$$\zeta = \frac{4\pi\eta\kappa_s E}{\epsilon P}$$

where η represents the coefficient of viscosity, E the measured potential, P the pressure, and ϵ the dielectric constant of the liquid. When E and ζ are expressed in millivolts, P in cm. of mercury, and κ_s in reciprocal ohms,

$$\zeta = 84.76 \times \eta \times \kappa_s \times \frac{1}{\epsilon} \times \frac{E}{P} \times 10^7$$

For electrolyte solutions in water ($\epsilon = 80.0$ and $\eta = 0.01$),

$$\zeta = 1.06 \times 10^6 \times \frac{E\kappa_s}{P}$$

Bull and Gortner (1) proposed that electrokinetic measurements be expressed in terms of qd, the electric moment per unit area, following the equation

$$qd = \frac{\eta\kappa_s E}{P}$$

which does not involve the dielectric constant, as we do not know its exact value in the double layer where it is probably different from the ϵ of the bulk solution. In electrostatic units, $qd = 226{,}200\eta\kappa_s \times E/P$.

DATA

The streaming potentials were largely determined on the same sample of barium sulfate (No. 13, prepared as above from equimolar solutions) against water or barium chloride or other electrolyte solutions, saturated with barium sulfate at room temperature. The liquid was always streamed through the diaphragm until the potential remained constant. The electrolyte solution was also frequently replaced by a fresh one, as the concentration could have changed by desorption or by the displacement of the weaker solution from the preceding determination. The effects of polarization of the electrodes or of differences in the liquid levels were cancelled by taking the average of the potentials measured in both streaming directions. The absolute value as well as the sign of the potentials were checked with a normal Weston element. As the diaphragms were tightly packed, the streaming potential was independent of pressure in the experimental range. This is illustrated in table 1 (results in the successive order of the experiments).

TABLE 1

Constancy of E/P for various determinations of the electrokinetic potential in a barium sulfate diaphragm against 100 µ molar barium chloride solution

Cell constant = 6.713

EXPERIMENT NO.	*E*	*P*	*E/P*	EXPERIMENT NO.	*E*	*P*	*E/P*
	mv.	*cm. Hg*			*mv.*	*cm. Hg*	
1	+118.0	20.65	+5.71	9	91.5	16.10	5.68
2	115.5	20.45	5.65	10	72.0	12.60	5.72
3	163.0	28.35	5.75	11	69.5	12.45	5.60
4	162.0	28.10	5.76	12	61.5	10.80	5.70
5	180.5	31.95	5.65	13	46.5	8.20	5.67
6	179.5	31.45	5.71	14	45.5	8.1	5.61
7	168.0	29.75	5.66	15	43.5	7.55	5.71
8	146.5	25.50	5.75	16	42.0	7.30	5.75

TABLE 2

The effect of the concentration of barium chloride in the streaming liquid on the sign and magnitude of the electrokinetic potential on barium sulfate crystals

Cell constant = 6.713

EXPERIMENT NO.	STREAMING LIQUID	*E*	*P*	*E/P*	κ_s	ζ	*qd*
		mv.	*cm. Hg*		*mhos* × 10^5	*mv.*	*E.S.U.* × 10^5
1	H_2O	−90.5	21.60	−4.190	1.76	−7.81	−16.70
2	25µ molar $BaCl_2$	+94.5	21.50	+4.399	1.34	+6.21	+13.22
3	100µ molar $BaCl_2$	+146.5	25.50	+5.750	3.00	+18.30	+39.02
4	250µ molar $BaCl_2$	+71.0	20.85	+3.410	7.73	+27.87	+59.50
5	500µ molar $BaCl_2$	+56.5	23.60	+2.372	14.06	+35.31	+75.60
6	1000µ molar $BaCl_2$	+33.5	24.20	+1.385	28.17	+41.20	+87.80

In table 2 and figure 1 are presented the equilibrium values acquired in successive barium chloride solutions of increasing concentrations. A sharp reversal in charge of the initially negative crystals occurred at a concentration which we can estimate by interpolation to approximate a barium chloride concentration of 5 μ moles.

In table 3 and figure 1 are presented the data obtained using potassium chloride in the streaming liquid with a freshly prepared diaphragm of the same barium sulfate. After a first inflection in the curve, the potential values remained nearly constant; no charge reversal was observed.

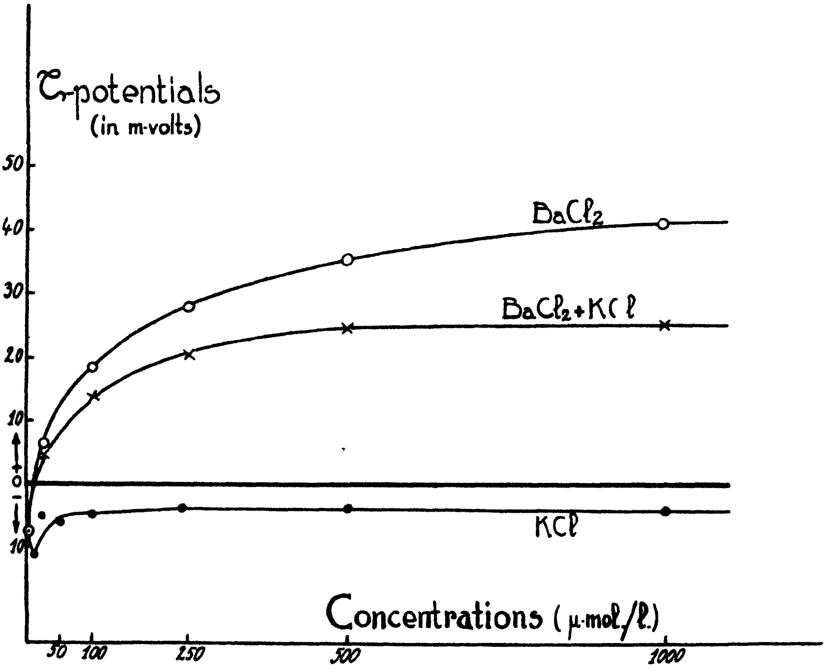

FIG. 1. Showing electrokinetic potential curves of barium sulfate in solutions of potassium chloride, barium chloride, and mixtures of potassium chloride and barium chloride.

The potentials of mixed barium chloride and potassium chloride, presented in table 4 and figure 1, illustrate the antagonism between these two electrolytes, already demonstrated for cellulose and potassium chloride–calcium chloride systems (8). It is important to notice that the barium ions were not desorbed by a saturated barium sulfate solution. This desorption could be followed by the decrease of the ζ-potential when, after the determination with 1000 μ molar barium chloride (experiment 6), the electrolyte solution was displaced by distilled water. Table 5 shows this decrease as a function of the time of thorough streaming (the liquid being renewed every hour).

The diaphragm was next streamed with 250 μ molar potassium chloride and 1000 μ molar potassium chloride, with the measured values shown in table 6. When the electrolyte solution was washed away and twice-renewed distilled water (saturated with barium sulfate) was streamed for

TABLE 3

The effect of the concentration of potassium chloride in the streaming liquid on the sign and magnitude of the electrokinetic potential on barium sulfate crystals

Cell constant = 5.337

EXPERIMENT NO.	STREAMING LIQUID	E	P	E/P	κ_s	ζ	qd
		mv.	*cm. Hg*		*mhos* × 10^6	*mv.*	*E.S.U.* × 10^6
7	H_2O	−94.0	27.90	−3.373	2.050	−7.31	−15.61
8	10μ molar KCl	−128.0	25.60	−4.925	2.133	−11.10	−23.65
9	20μ molar KCl	−78.5	23.40	−3.358	1.557	−5.31	−11.83
10	50μ molar KCl	−63.5	23.90	−2.658	2.123	−5.98	−12.79
11	100μ molar KCl	−38.5	23.20	−1.660	2.780	−4.89	−10.43
12	240μ molar KCl	−16.5	22.65	−0.728	4.960	−3.83	−8.17
13	500μ molar KCl	−9.8	23.10	−0.424	8.910	−4.01	−8.50
14	1000μ molar KCl	−8.5	23.70	−0.274	15.08	−4.37	−9.35

TABLE 4

The effect of the concentration of potassium chloride and barium chloride in a mixed solution in the streaming liquid on the sign and magnitude of the electrokinetic potential on barium sulfate crystals

Cell constant = 5.465

EXPERIMENT NO.	STREAMING LIQUID	E	P	E/P	κ_s	ζ	qd
		mv.	*cm. Hg*		*mhos* × 10^6	*mv.*	*E.S.U.* × 10^6
15	H_2O	−89.0	22.80	−3.908	1.717	−7.12	−15.18
16	25μ molar $BaCl_2$ 25μ molar KCl	+54.0	23.3	+2.319	1.890	+4.64	+9.90
17	100μ molar $BaCl_2$ 100μ molar KCl	68.5	22.9	+2.920	4.525	+13.98	29.80
18	250μ molar $BaCl_2$ 250μ molar KCl	50.5	30.1	+1.678	11.50	+20.41	43.55
19	500μ molar $BaCl_2$ 500μ molar KCl	26.75	24.8	+1.080	21.45	+24.60	52.48
20	1000μ molar $BaCl_2$ 1000μ molar KCl	17.5	28.0	+0.632	37.48	+25.07	53.50

30 min., the charge of the crystals again became negative. A new run with a 250 μ molar barium chloride solution of barium sulfate similarly treated reproduced closely the value of experiment 4; No. 23: 250 μ moles of barium chloride per liter, E = 80.0 millivolts, P = 24.65 cm. of mercury, E/P = 3.245, κ_s = 8.378 mhos × 10^5, ζ = 28.8 millivolts.

The desorption of the positively charged barium ions by an excess of potassium chloride was confirmed with other barium sulfate samples prepared in the same way. Sample No. 10 was prepared by the described procedure but using a 0.110 M barium chloride solution, so that the mother liquor after precipitation contained 0.066 mole of potassium chloride and 0.0033 mole of barium chloride per liter. The mother liquor was siphoned off after 15 min. This barium sulfate was positively charged and the charge could be reversed in the same way by treatment with $M/10$ potassium chloride followed by washing out the potassium chloride. When, after the precipitation, the mother solution remained for 24 hr. in contact with the crystals, the electrokinetic potential was negative and of the same order of magnitude (ζ = -6.38 millivolts, cell constant = 5.854) as for barium sulfate precipitated from equivalent solutions.

TABLE 5

Change in electrokinetic potential on barium sulfate crystals as the streaming liquid progressively changes from 1000 μ molar barium chloride solution to pure water

TIME	ζ	TIME	ζ
hours	*mv.*	*hours*	*mv.*
0	+41.2	6	9.31
2	16.22	8	7.08
4	12.17	10	6.35

TABLE 6

Change produced in electrokinetic potential of the barium sulfate crystals remaining from the experiments of table 5 as potassium chloride solutions are streamed through the mass

EXPERIMENT NO.	STREAMING LIQUID	E	P	E/P	κ_s	ζ	qd
		mv.	*cm.* Hg		*mhos* × 10^5	*mv.*	*E.S.U.* × 10^6
21	250 μ molar KCl	+37.0	22.50	+1.635	3.788	+6.55	+13.96
22	1000 μ molar KCl	+10.0	23.45	+0.426	16.670	+7.54	+16.08

It is important to notice that the curve of the change in the ζ-potential with barium chloride concentration does not follow the Freundlich adsorption isotherm. We have here a typical adsorption of a positive potential-determining ion (Ba^{++}) (5, 10, 9), assuming the potentials (or the electric moment) as being regularly proportional to the number of ions adsorbed.

Figure 2 shows a linear relationship between ζ and log C and not between log ζ and log C.

Kolthoff and MacNevin (3) found that the adsorption of barium salts on barium sulfate and of salts having no ion in common with the lattice is much greater from 50 per cent ethanol than from water. Here the adsorption of barium salts (chloride and nitrate) was a molecular adsorption and followed the Freundlich adsorption isotherm; potassium bromate also gave an equivalent adsorption of cations and anions.

With the same sample of barium sulfate (No. 13) the streaming potentials of barium chloride, barium nitrate, and potassium bromate were measured in a 50 per cent ethanol solution saturated with barium sulfate. This solvent was prepared by mixing equal volumes of pure ethanol and distilled water. The viscosity of this solvent, containing 500 μ molar barium chloride, was measured with an Ostwald viscosimeter ($\eta = 0.0282$), and the value for ϵ (48.5) introduced in the calculations was taken from the *International Critical Tables*. The different values measured are shown in table 7 and figure 3. The potentials in this alcohol solution are much higher than in the corresponding aqueous solutions. The slope of the curve also is different, and a saturation charge was obtained at a lower concentration, and remained unchanged by the higher concentrations.

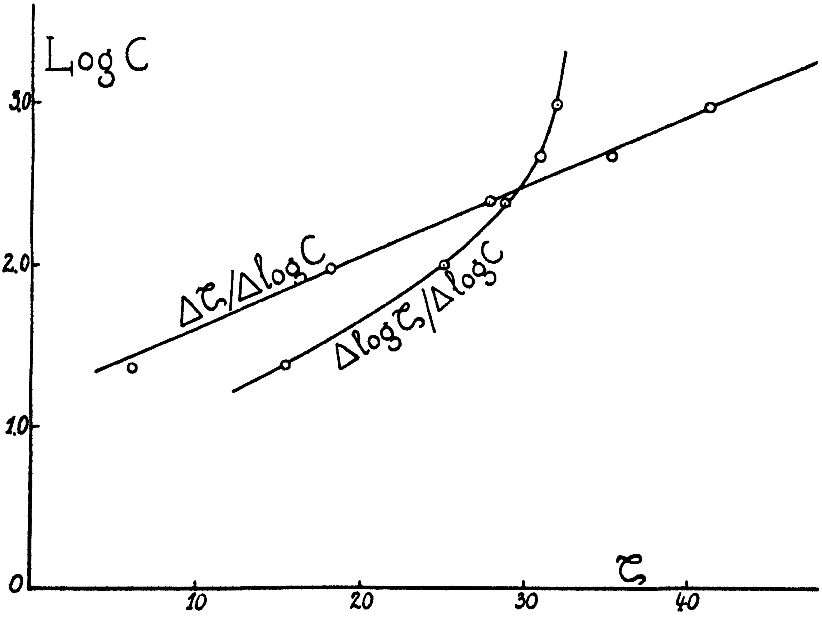

FIG. 2. Showing relationships between the electrokinetic potential of barium sulfate and the concentration of barium chloride in the streaming liquid.

TABLE 7

Changes produced in the electrokinetic potential when various electrolytes dissolved in 50 per cent ethanol were streamed through a barium sulfate diaphragm

EXPERIMENT NO.	ELECTROLYTE IN STREAMING LIQUID	E	P	E/P	κ_s	ζ	qd
		mv.	*cm.* Hg		*mhos* × 10^6	*mv.*	E.S.U. × 10^6
24	250μ molar $BaCl_2$	+104 5	21.8	+4.78	3.34	+86.6	+104.4
25	500μ molar $BaCl_2$	62.0	21.7	2.86	5.62	87.0	105.1
26	1000μ molar $BaCl_2$	44.0	23.7	1.85	8.79	88.4	106.9
27	20μ molar $Ba(NO_3)_2$	107.0	23.8	4.49	1.34	32.6	39.3
28	100μ molar $Ba(NO_3)_2$	101.0	23.5	5.10	2.26	62.5	77.0
29	500μ molar $Ba(NO_3)_2$	119.5	24.2	4.95	3.60	96 6	
30	1000μ molar $Ba(NO_3)_2$	60 0	23.0	2.61	6.60	93.3	
31	20μ molar $KBrO_3$	209.5	24.5	8.55	0.40	18 6	22.4
32	100μ molar $KBrO_3$	90.0	24.1	3.72	0.86	17.3	20.9
33	500μ molar $KBrO_3$	42.5	27.6	1.57	2.95	25.1	32.6
34	2500μ molar $KBrO_3$	12.5	33.5	0.37	14.65	29.6	35.7
34b	Washed	509.5	37.0	13.75	0 13	9.7	11.7
35	500μ molar KCl	58.0	21.7	2.66	3.04	44.0	52.9

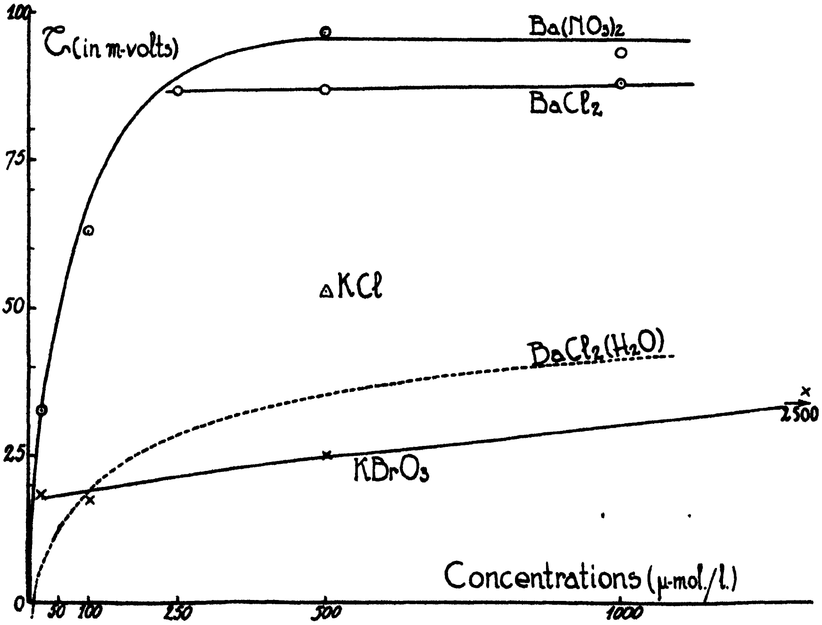

FIG. 3. Showing electrokinetic potential curves of barium sulfate as influenced by various electrolyte concentrations in 50 per cent ethanol solutions.

The increase of potentials appears to be in opposition with the Coehn Raydt rule, since, according to this rule, a decrease in the dielectric constant difference between the liquid and the solid in contact should also give rise to a decrease of the electrokinetic potential. However, if any credit could be given to this rule, it should be only in its application to an inert apolar wall with no ion exchange.

Quite unexpected also was the increase in positive charge and potential in potassium bromate and even in potassium chloride solutions (experiments 31 to 35). Could we, under these changed conditions, postulate a preferential orientation of the cations towards the barium sulfate walls? Such an effect was not observed in the aqueous potassium chloride solution (experiments 7 to 14), since the negative ζ there remained unchanged at the higher electrolyte concentrations. We should prefer to suggest a change in the dipolar orientation on the moving liquid boundaries, but any final answer must remain for further investigation.

Following experiment 34 (2500 μ molar potassium bromate) the diaphragm was washed out and flooded with pure water for several hours. This caused the barium sulfate to regain a negative charge ($E/P = 3.71$). The water was again displaced by 50 per cent ethanol, and the charge on the barium sulfate again became positive (see experiment 34b). It appears probable that even after thorough washing and treatment with pure water, some traces of electrolyte were still adsorbed and produced the positive charge. Indeed, subsequently repeated experiments on new barium sulfate samples showed that the equilibrium charge in pure 50 per cent ethanol in the absence of any electrolyte was always negative, and became positive only when potassium chloride was present.

SUMMARY

The streaming potentials on precipitated and negatively charged barium sulfate show a charge reversal by barium chloride solution; the ζ-potential–concentration curve is a typical one for the adsorption of a potential-determining ion.

The adsorbed barium ions are liberated and desorption of barium ions takes place in a strong potassium chloride solution ($M/10$).

The positive potential curve displayed a great charge increase in 50 per cent ethanolic solutions of barium chloride and barium nitrate. The charge reversal of the negative barium sulfate was also observed for potassium bromate and potassium chloride in 50 per cent ethanol.

The author wishes to express his sincere thanks to Prof. R. A. Gortner and Dr. D. R. Briggs for their highly appreciated hospitality.

REFERENCES

(1) **Bull, H. B., and Gortner, R. A.: Physics 2, 21 (1932).**

(2) **Julien, P. F.: Thesis, Utrecht, 1933.**

(3) KOLTHOFF, I. M., AND MACNEVIN, W. H.: J. Am. Chem. Soc. **58**, 1543 (1936).
(4) KRUYT, H. R., AND RUYSSEN, R. G.: Koninkl. Akad. Wetenschappen Amsterdam **37**, 9 (1934).
(5) LANGE, E., AND BERGER, R.: Z. Elektrochem. **36**, 171 (1930).
(6) LAUFFER, M. A., AND GORTNER, R. A.: J. Phys. Chem. **42**, 641 (1938).
(7) MARTIN, W. McK., AND GORTNER, R. A.: J. Phys. Chem. **34**, 1509 (1930).
(8) MOYER, L. S., AND BULL, H. B.: J. Gen. Physiol. **19**, 239 (1935).
(9) VERWEY, E. J. W.: Kolloid-Z. **72**, 187 (1935).
(10) VERWEY, E. J. W., AND KRUYT, H. R.: Z. physik. Chem. **A167**, 149 (1933).

PHYSICAL PROPERTIES OF THE ALKYL FLUORIDES AND A COMPARISON OF THE ALKYL FLUORIDES WITH THE OTHER ALKYL HALIDES AND WITH THE ALKYLS OF THE ELEMENTS OF PERIOD II

ARISTID V. GROSSE, RICHARD C. WACKHER, AND CARL B. LINN

Research Laboratories, Universal Oil Products Co., Riverside, Illinois

Received February 4, 1939

Only meager knowledge exists concerning alkyl[1] fluorides, in contrast to the extensive literature relative to the other halogen alkyls. Until recently the methods of preparation for alkyl fluorides were cumbersome, and larger quantities of them were available only with difficulty. The ease of decomposition of the tertiary and secondary alkyl fluorides, particularly in the presence of impurities, added another determent to their accurate investigation.

Our new method of their preparation (23, 24)—namely, the addition of hydrogen fluoride to olefins and the splitting of cyclopropane (or its alkyl derivatives) with hydrogen fluoride—makes them readily available in large quantities. It permitted us to complete their study, which was pioneered by the investigations of Dumas (19), Fremy (21), Moissan (38, 37), Meslans (38, 33, 34, 35, 36) and in more recent years by F. Swarts (56, 57, 58, 59, 60, 61, 62).

In Part I of this paper our measurements of the following physical properties—melting and boiling points, vapor pressures, densities, indices of refraction, and their respective temperature coefficients—will be given for methyl, ethyl, normal propyl, secondary propyl, secondary butyl, tertiary butyl, and tertiary amyl fluorides. Reliable literature data on other fluorides are included.

---

[1] The term "alkyl", as defined in reference 30, page 5, comprises both the aryl and the alphyl (C_nH_{2n+1}) groups. In view of the fact that the latter term is practically unknown in English-speaking countries, the term "alkyl" will be used in this article to denote only C_nH_{2n+1} groups.

With the data now available it is possible to make a general comparison of the fluorine alkyls with the other halogen alkyls, as well as with alkyls of neighboring elements of Period II of the Periodic Table. Such a comparison is made in Part II.

PART I

SOURCE OF ALKYL FLUORIDES

Ethyl, *n*-propyl, *sec*-propyl, *sec*-butyl, *tert*-butyl, and *tert*-amyl fluorides were prepared by the direct addition of hydrogen fluoride to ethylene, cyclopropane, propylene, 1-butene, isobutylene, and trimethylethylene, respectively. The hydrofluorination of the first three substances is described in the article cited (23, 24). The preparation of the butyl and amyl fluorides will appear in an early publication.

Methyl fluoride, which cannot be prepared from the corresponding olefin, was prepared by the method of Collie (31, 11, 12). Tetramethylammonium fluoride, when heated to 190°C., decomposes into methyl fluoride and trimethylamine, the latter substance being removed in a sulfuric acid wash. This method was selected rather than other described preparations as being the one likely to give the purest methyl fluoride. Methyl fluoride prepared by Fremy's method (21) may contain dimethyl ether, carbon dioxide, ethylene, water, and sulfur dioxide (3, 2). F. G. Nunez' statement that methyl fluoride prepared by Collie's method is contaminated with methane present in a constant-boiling mixture (42) was not substantiated. Our product corresponds exactly in its vapor pressure with the very pure fluoride (obtained by Fremy's method), prepared by Moles and Batuecas (39, 40, 41) for their atomic weight determination (see also 45, 9, 1) of fluorine. F. Swarts' latest method (61) came to our attention belatedly.

PURIFICATION OF REAGENTS

The respective alkyl fluorides were first distilled on a low-temperature Podbielniak column (with the exception of the amyl and butyl fluorides, which were distilled on an efficient laboratory column of the total reflux type), and five to eight cuts were made on the main plateau of the substance. The refractive indices of these cuts were taken, with the exception of methyl fluoride, and a fraction which showed no significant differences in refraction and boiling point from neighboring cuts was used for further purification. As a check of their composition they were analyzed for fluorine. They were then sealed into a Stock[2] high-vacuum, all-glass apparatus equipped with the Stock type of mercury seal valves. The alkyl fluoride was frozen out in a liquid nitrogen bath and degassed several times by alternate melting, freezing, and evacuation. While being automatically stirred the sample was then fractionated at 1–2 mm. under its own vapor pressure into four cuts. The purest cut, as indicated by the individual vapor pressures or melting points, was used in the determination of the physical constants. Usually the vapor pressures of the extreme cuts did not vary more than 5 per cent.

---

[2] See reference 54. The appendix of this book contains brief descriptions of high-vacuum apparatus and methods and many references to the original literature.

EXPERIMENTAL

Analysis for fluorine

To analyze for fluorine the compounds were burned with air or oxygen in a platinum tube of the design shown in figure 1. The hydrogen fluoride produced, together with the other products of combustion, was absorbed in an alkaline solution and the fluorine determined as thorium fluoride by the method of Rowley and Churchill (47). Samples were volatilized using the standard technique of organic combustion analysis. Fluorides boiling below 50°C., however, were condensed in a volatilizing chamber, the temperature being adjusted so that the vapor pressure of the substance was 10–20 mm., and the sample was volatilized in a stream of oxygen.

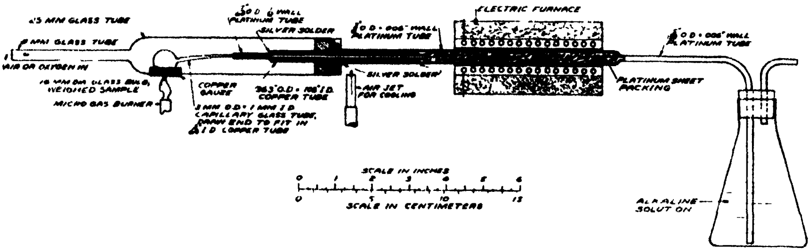
15 MM GLASS TUBE
8 MM GLASS TUBE
AIR OR OXYGEN IN
16 MM DIA GLASS BULB, WEIGHED SAMPLE
MICRO GAS BURNER
.50 O D .6 WALL PLATINUM TUBE
SILVER SOLDER
COPPER GAUZE
.363" O.D. × .185" I.D. COPPER TUBE
3 MM O.D. × 1 MM I D CAPILLARY GLASS TUBE, DRAW END TO FIT IN .1 I D COPPER TUBE
O D × .005" WALL PLATINUM TUBE
SILVER SOLDER
AIR JET FOR COOLING
ELECTRIC FURNACE
PLATINUM SHEET PACKING
O D × .005" WALL PLATINUM TUBE
ALKALINE SOLUTION
SCALE IN INCHES
0 1 2 3 4 5 6
0 5 10 15
SCALE IN CENTIMETERS

FIG. 1. Apparatus for the determiantion of fluorine

Temperature

Temperatures below −30°C. were determined by means of Stock (53) vapor pressure thermometers containing ammonia, carbon dioxide, and ethylene. Samples of these materials were fractionated in the high-vacuum apparatus and the best fraction, as determined by its vapor pressure, was used for the thermometer. The thermometers were calibrated at standard reference points, using carbon disulfide (m.p. −111.6°C.), carbon dioxide (sublimes at −78.5°C.), and mercury (m.p. −38.87°C.), by comparison with the accurate vapor pressures of ammonia, carbon dioxide, and ethylene, measured by Stock. For temperatures above −30°C. a mercury thermometer, together with an iron-Constantan thermocouple and Leeds and Northrop potentiometer, was used.

Melting points

Melting points, reproducible within ±0.1°C., were determined by the method of Stock (52). The melting points of the various fluorides are given in table 1. All the fluorides solidified to white, transparent, needle-like or prismatic crystals. Additional literature values for melting points of alkyl fluorides are given in table 1a to complete our above data.

Boiling points and vapor pressures

Vapor pressures were determined from approximately 10–800 mm. by the static method described by Stock, using a cathetometer accurate to ±0.1 mm. These values have been corrected to 0°C. The data showed that log p was not a straight-line function of $1/T$. The data, however, were found to agree very closely with values calculated from the Rankine formula,

TABLE 1

Melting points of some alkyl fluorides

COMPOUND	MELTING POINT
	°C.
CH_3F	−141.8
C_2H_5F	−143.2
n-C_3H_7F	−159
sec-C_3H_7F	−133.4
sec-C_4H_9F	−121.4
tert-C_4H_9F	−77
tert-$C_5H_{11}F$	−121

TABLE 1a

Melting points of other alkyl fluorides

COMPOUND	MELTING POINT	REFERENCE
	°C.	
n-$C_5H_{11}F$	Below −80	(58)
3(?)-$C_6H_{13}F$	−104	(43, 44)
n-$C_7H_{15}F$	About −73	(57)
x-$C_{10}H_{21}F$	Solid in dry ice	(58)
x-$C_{16}H_{33}F$	Solid at room temperature	(58)

$$\text{Log}_{10} P = -A/T - B \log_{10} T + C \qquad (1)$$

in which p is the vapor pressure in millimeters of mercury and T is the absolute temperature. The constants for the various fluorides for equation 1, calculated by the method of least squares, are given in table 2. To compare our experimental vapor pressures with vapor pressures calculated from equation 1, table 3 gives experimental and calculated vapor pressures in a typical case, that of normal propyl fluoride. The final results are correlated in table 4.

Our data are in full agreement with those of Moles and Batuecas (39, 41) on methyl fluoride prepared by Dumas' method (760 mm. at −78.2°C. and 200 mm. at −99.8°C.), and with those of Desreux (17) on *sec*-butyl fluoride (765 mm. at 25.26°C.). Additional accurate literature data on boiling points are given in table 4a.

TABLE 2

Constants for the fluorides for equation 1

CONSTANTS	CH_3F	C_2H_5F	*n*-C_3H_7F	*sec*-C_3H_7F	*tert*-C_4H_9F	*sec*-C_4H_9F	*tert*-$C_5H_{11}F$
A	1016.6	1507.7	1582.9	1482.5	1358.5	2068.9	1502.6
B	1.187	4.304	2.729	2.217	0	5.478	0
C	10.8206	19.4859	15.3743	13.8746	7.6439	23.3755	7.6071
Average deviation in per cent . ..	0.7	0.7	0.7	1.0	1.3	0.6	1.4

TABLE 3

Vapor pressure data for n-propyl fluoride

TEMPERATURE	EXPERIMENTAL VAPOR PRESSURE	CALCULATED VAPOR PRESSURE	PER CENT DEVIATION
°C.	*mm.*	*mm.*	*per cent*
0.0	860.1	852.1	−0.9
−4.2	715.7	721.6	+0.8
−14.8	462.6	461.7	−0.2
−20.3	362.1	360.2	−0.5
−30.9	215.3	215.4	0.0
−38.7	142.8	142.7	0.0
−51.3	67.7	68.6	+0.3
−51.7	66.7	66.9	+1.3
−68.8	20.8	21.0	+1.0
−75.5	12.8	12.6	−1.6

The following *critical data* are available in the literature and are added to complete the record:

COMPOUND	CRITICAL TEMPERATURE	CRITICAL PRESSURE	CRITICAL VOLUME	REFERENCE
	°C.	*atmospheres*	*cc. per gram*	
CH_3F	44.55	58.0 ± 0.2	333	(9)
CH_3F	52.2			(39)
C_2H_5F	102.16 ± 0.02	49.62 ± 0.05		(4)

TABLE 4

Vapor pressure data for the fluorides

PRESSURE	CH_3F	C_2H_5F	*n*-C_3H_7F	*sec*-C_3H_7F	*sec*-C_4H_9F	*tert*-C_4H_9F	*tert*-$C_5H_{11}F$
mm. of Hg.							
760 (N.B.P.)	**−78.5**	**−37.1**	**−2.5**	**−9.4**	**+25.1**	**+12.1**	**+44.8**
200	−99.7	−63.5	−32.4	−38.5	−7.7	−18.8	+10.1
100	−108.9	−74.5	−44.9	−50.8	−21.5	−32.4	−5.1
50	−117.2	−84.4	−56.3	−61.9	−33.5	−44.6	−18.8
20	−126.7	−95.8	−69.4	−74.8	−47.8	−58.9	−34.8
10	−133.1	−103.6	−78.2	−83.7	−57.1	−68.6	−45.7
dt_B/dp (°C./mm. Hg.)...	0.0236	0.0298	0.0331	0.0323	0.0374	0.0342	0.0384
Heat of vaporization at N.B.P. in Cal. per mole	4196	4884	5780	5626	6225	6215	6874
Trouton's constant in E.U..........	21.6	20.7	21.4	21.3	20.9	21.8	21.6

TABLE 4a

Data on boiling points of alkyl fluorides

COMPOUND	BOILING POINT	REFERENCE
	°*C.*	
n-Butyl fluoride*.........................	31.97 at 746 mm. (= 32.50 at 760 mm.)	(17)
n-Amyl fluoride......................	62.8 at 760 mm.	(58)
Isoamyl fluoride†......................	53.5 at 760 mm.	(58)
n-Hexyl fluoride...................	93.15 at 753 mm. (= 93.43 at 760 mm.)	(17)
sec-Hexyl fluoride..................	81.15 at 758 mm. (= 81.23 at 760 mm.)	(17)
3(?)-Fluorohexane	82.86 at 760 mm.	(43, 44)
n-Heptyl fluoride....................	120.55 at 765 mm. (= 120.40 at 760 mm.) 119.5 at 755 mm.	(17) (57, 58)
n-Octyl fluoride......................	142.5 at 754 mm. (= 142.7 at 760 mm.)	(57, 58)
sec-Octyl fluoride......................	139.3 at 760 mm.	(58)
x-Decyl fluoride	183.6 at 760 mm.	(58)
x-Hexadecyl fluoride..................	287.5 at 760 mm.	(58)

* The boiling point of *tert*-butyl fluoride is also given as 11–14°C. or "about 13°" (25, 13).

† The boiling point values of isoamyl fluoride given by Young (67, see also 49) as 72–92°C., and by Tronow and Kreuger (66) as 46.7°C. at 755 mm. are definitely wrong. The liquefaction point of isobutyl fluoride is given as +16°C. (38); the expected correct boiling point is around 25°C.

Densities

The dilatometer method was employed. The dilatometer, of about 2.5-cc. capacity, was sealed on to the high-vacuum apparatus, the fluoride was distilled into it, and then it was sealed off. The volume was measured over a considerable temperature range and the corresponding densities calculated after the weight of the contents had been determined. The weighings were corrected to vacuum and for the vapor present. The equation giving density as a function of temperature was calculated by the method of least squares. The density–temperature function for the alkyl fluorides studied may be found by substituting data from table 5 in equation 2:

TABLE 5

Density constants for fluorides for equation 2

	CH_3F	C_2H_5F	*n*-C_3H_7F	*sec*-C_3H_7F	*sec*-C_4H_9F	*tert*-C_4H_9F	*tert*-$C_5H_{11}F$
A.	0.7078	0.7684	0.7782	0.7551	0.7865	0.7688	0.7985
B.	$0.0_2 2369$	$0.0_2 1327$	$0.0_2 1431$	$0.0_2 1523$	$0.0_2 122$	$0.0_2 1311$	$0.0_2 1005$
C.	$0.0_5 196$	0	$0.0_5 150$	$0.0_5 190$	0	$0.0_5 121$	0
Average deviation of density curve (density units)	$0.0_3 1$	0.0_{31}	$0.0_3 6$	$0.0_3 1$		$0.0_3 1$	$0.0_3 7$

TABLE 6

Density data for tert-butyl fluoride

TEMPERATURE	EXPERIMENTAL DENSITY	$d^t_{4°}$ CALCULATED FROM EQUATION 2	DEVIATION × 10^4
°*C.*			
9.8	0.7559	0.7559	0
2.0	0.7658	0.7661	+3
0.0	0.7690	0.7688	−2
−10.0	0.7817	0.7818	+1
−33.2	0.8111	0.8110	−1
−42.4	0.8221	0.8222	+1

$$d^t_{4°}\ (\text{vac.}) = 4 - Bt - Ct^2 \qquad (2)$$

where *t* is in °C. The comparison of experimental and calculated densities for tertiary butyl fluoride given in table 6 shows the extent to which equation 2 fits the data in a typical case.

Complete data for the fluorides studied are given in table 7.

A comparison with literature data is possible only in the case of sec-

TABLE 7

Densities of alkyl fluorides in grams per cubic centimeter at different temperatures
$d_{4°}^{t}$ (vacuum corrected)

T	CH_3F	C_2H_5F	n-C_3H_7F	*sec*-C_3H_7F	*sec*-C_4H_9F	*tert*-C_4H_9F	*tert*-$C_5H_{11}F$
°C.							
Normal boiling point	**0.8817**	**0.8176**	**0.7818**	**0.7692**	**0.7559**	**0.7527**	**0.7535**
−130	0.9827						
−100	0.9251	0.9011	0.9063	0.8884			
−80	0.8848	0.8746	0.8831	0.8647			
−60	0.8428	0.8480	0.8587	0.8397		0.8431	
−40		0.8215	0.8330	0.8130		0.8193	
−20			0.8062	0.7848	0.8109	0.7945	0.8186
0			0.7782	0.7551	0.7865	0.7688	0.7985
+10			0.7638	0.7397	0.7743	0.7559	0.7885
+20			0.7490	0.7238	0.7621		0.7784
+30					0.7499		0.7683
Average dd/dT	−0.00192	−0.00133	−0.00146	−0.00157	−0.00122	−0.00129	−0.00101
In the temperature range......	−130° to −100°C.	−100° to 35°C.	0° to 20°C.	0° to 20°C.	−20° to +30°C.	0° to +10°C.	−20° to +30°C.

TABLE 7a

Densities of alkyl fluorides from the literature

COMPOUND	$d_{4°}^{0°}$	$d_{4°}^{15°}$	$d_{4°}^{20°}$	$d_{4°}$ AT T		−dD/dT	REFERENCE
					°C.		
n-C_4H_9F.................	0.8005	0.7824	0.7763			0.00122	(17, 18)
sec-C_4H_9F..................	0.7884	0.7700	0.7639 (calcd.)			0.00123	(17, 18)
n-$C_5H_{11}F$*...............	0.7905		0.7880	0.7960	10.5	0.00084	(58, 18)
n-$C_6H_{13}F$................	0.8200	0.8052	0.8004			0.00099	(17, 18)
sec-$C_6H_{13}F$..............	0.8115		0.7914			0.00099	(17, 18)
n-$C_7H_{15}F$................			0.8071	0.8029	21		(58, 18)
n-$C_8H_{17}F$................				0.8036	21	0.0012	(58)
				0.8120	14		
x-$C_{10}H_{21}F$...............				0.792	10.2		(58)
x-$C_{16}H_{33}F$...............				0.809	17.5		(58)
3(?)-$C_6H_{13}F$..............	0.819						

* Tronow's highly improbable density of isoamyl fluoride, given as 0.69415 at 19.6°C. (66), combined with his low boiling point value (see page 7), definitely indicates a product consisting mainly of amylenes.

ondary butyl fluoride (see table 7a). Our data show a slight but definite deviation from the values of Desreux (17, 18). Since our sample was pure according to rigorous criteria and all corrections were accurately made, we give preference to our values. In table 7a are given additional reliable data from the literature to complete our list.

Refractive indices

The adaptation of the Abbe refractometer for the determination of indices of refraction at low temperatures has been recently described by one of us (22). Briefly, the method consists in circulating a low-boiling liquid through the prism chambers of the refractometer, the cooling medium being refluxed under a condenser cooled with carbon dioxide. The temperature may be lowered by reducing the pressure on the system.

TABLE 8

Refractive indices (n_D) of alkyl fluorides

TEMPERATURE	C_2H_5F	*n*-C_3H_7F	*sec*-C_3H_7F	*sec*-C_4H_9F	*tert*-C_4H_9F	*tert*-$C_5H_{11}F$
°C.						
Normal boiling point	**1.3033**	**1.3225**	**1.3282**	**1.3299**	**1.3241**	**1.3375**
−70	1.3229					
−60	1.3169	1.3553	1.3461			
−50	1.3110	1.3496	1.4306	1.3691	1.3580	1.3859
−40	1.3050	1.3439	1.3351	1.3639	1.3526	1.3808
−30	1.2990	1.3382	1.3296	1.3587	1.3471	1.3756
−20		1.3326	1.3240	1.3534	1.3417	1.3705
−10		1.3268	1.3185	1.3482	1.3363	1.3653
0		1.3211	1.3130	1.3430	1.3309	1.3603
+10		1.3154	1.3075	1.3379		1.3552
+20				1.3326		1.3502
$-dn_D/dT$	0.00060	0.00057	0.00055	0.00052	0.00054	0.00051
In the temperature range	−70° to −30°C.	−60° to +10°C.	−60° to +10°C.	−50° to +20°C	−50° to 0°C.	−50° to +20°C.

The refractometer was checked both with the standard prism and water before and after measurements. The refractive indices of the respective substances studied fell upon a straight line within the limits of experimental error (±0.0002). Table 8 summarizes refractometric data of the alkyl fluorides studied. The data included are read from curves plotted from experimental values. The refractive index of methyl fluoride was not measured, since even at −100°C. the index of refraction of this substance is below the scale of the Abbe refractometer (minimum reading, 1.3000).

The only possible case for comparison with literature data is our n_D of secondary butyl fluoride, 1.3369 at 12°C. This is in good agreement with the value of Desreux for that compound given in table 8a, which lists additional refractometric data from the literature.

It is worthwhile to emphasize that the n_D values of the alkyl fluorides are very near to the values for the corresponding paraffins. For example, $n_D^{20°}$ of normal pentane = 1.3576, of normal hexane = 1.3751, of normal heptane = 1.3877, and of normal octane = 1.3976. Thus in mixtures with paraffins the presence of fluorides is not revealed by the refractive index of the solution, in contrast to the other halides. In line with the other halides, however, the alkyl fluorides have higher densities than the corresponding paraffins.

TABLE 8a

Refractive indices of alkyl fluorides from the literature

COMPOUND	H_α	T	H_β	T	H_γ	T	D	T	REFERENCE
		°C.		°C.		°C.		°C.	
n-C_4H_9F	1.3404	15	1.3457	15	1.3488	15	1.3419	15	(17)
sec-C_4H_9F	1.3350	12	1.3403	12			1.3366	12	(17)
n-$C_5H_{11}F$	1.35622	20	1.36183	20	1.36533	20			(58)
n-$C_6H_{13}F$	1.3730	20	1.3791	30	1.3826	30	1.3748	20	(17)
sec-$C_6H_{13}F$	1.3677	20	1.3736	20	1.3771	20	1.3693	20	(17)
n-$C_7H_{15}F$	1.38358	21.5	1.3899	21.5	1.39358	21.5	1.3855	21.5	(58)
n-$C_8H_{17}F$	1.3952	14.1	1.40175	14.1	1.43565	14.1	1.3970	14.1	(58)
3(?)-Fluorohexane							1.3683	26.2	(43, 44)

PART II

Now that many of the previously undetermined properties of the fluorine alkyls are available, a comparison with alkyls of other elements from the standpoint of systematic chemistry[3] is possible. This comparison does not include the high members of the series. With increasing molecular weight of the alkyl group the influence of the element becomes less and less pronounced, and with the present accuracy of experimentation the practical limit is reached at about C_{10}-alkyls.

Melting and boiling points

The following rule expresses the relationship between the halogen alkyls: "The melting and boiling points of the halides of any particular alkyl group always increase in the order F → Cl → Br → I." Table 9 illustrates this rule. The only known exception is the low melting point of secondary propyl iodide; this measurement is probably in error.

The relationship in respect to the different alkyl groups is not as simple.

---

[3] For a definition of this term see reference 30.

TABLE 9

*Melting points and boiling points (at 760 mm.) of alkyl halides**

HALOGEN	H	CH_3	C_2H_5	C_3H_7		C_4H_9				C_5H_{11}		n-C_6H_{13}	n-C_7H_{15}	n-C_8H_{17}
				n-	*sec-*	*n-*	iso-	*sec-*	*tert-*	*n-*	*tert-*			
Melting points														
	°C.	°C.	°C.	°C.	°C.	°C.	°C.	°C.	°C.	°C.	°C.	°C.	°C.	°C.
F	−83	−141.8	−143.2	−159.0	−133.4	?	?	−121.4	−77	−80	−121	?	−73	?
Cl	−111.5	−97.6	−138.7	−122.8	−117.0	−123.1	131.2	?	−27.1	?	−72.9	?	?	?
Br	−86.5	−93	−119.0	−110.0	−89	−112.4	?	−111.9	−16.2	?	?	?	?	?
I	−50.8	−66.45	−111.1	−101.3	−90	−103.0	−93.5	−104.0	?	?	?	?	?	−45.9
Boiling points														
F	19.6	−78.5	−37.1	−2.5	−9.4	32.5	?	25.1	12.1	62.8	44.8	93.4	120.4	142.7
Cl	−85.1	−23.73	13.1	46.60	34.8	78.50	68.85	68.25	50.7	108.4	85.7	134	159.5	184.6
Br	−66.7	4.5	38.40	71.00	59.35	101.60	91.40	91.20	73.25	127.9	107.8	156	178.8	204
I	−35.7	42.50	72.30	102.45	89.45	130.40	121.0	120.0	?	154.2	127.0	180	203.8	225.5

* The values for the halides other than fluorides used in this table are taken from Beilstein's *Handbuch der organischen Chemie,* the *International Critical Tables,* and the publications of J. Timmermans (a to e) and his coworkers, published in the *Journal de chimie physique* from 1926 to 1934. The data on hydrides were obtained from Gmelin's *Handbuch der anorganischen Chemie.*

(a) Timmermans, J., and Martin, F.: J. chim. phys. **23,** 733 (1926). Paper I.
(b) Timmermans, J., and Martin, F.: J. chim. phys. **23,** 747 (1926). Paper II.
(c) Timmermans, J., and Martin, F.: J. chim. phys. **25,** 411 (1928). Paper III.
(d) Timmermans, J., and Hennant-Roland, Mme.: J. chim. phys. **27,** 401 (1930). Paper IV.
(e) Timmermans, J., and Hennant-Roland, Mme.: J. chim. phys. **29,** 529 (1932). Paper V.

The melting points show no simple relationship, as a study of table 9 indicates. Since small changes in the symmetry of a molecule will affect to a substantial extent the crystal lattice energy, the lack of a regular change in melting point is not surprising.

The boiling points, however (see table 9), in the series of normal alkyl groups always increase with the molecular weight. Among the isomeric groups the highest boiling point is always associated with the normal group; it is followed by the iso and the secondary groups, while the tertiary group has always the lowest boiling point. In more complex cases it will generally be found that the greater the branching and symmetry of the alkyl group, the higher the vapor pressure of the corresponding halide.

TABLE 10

*Melting and boiling points (at 760 mm.) of the alkyls of the non-metals of Period II**

R	CR_4	NR_3	OR_2	FR
		Melting points		
	°C.	°C.	°C.	°C.
	←			
CH_3	−19.5	−124.0	−138.0	−141.8
C_2H_5	−41	−114.8	-166.3^{α} -123.3^{β}	−143.2
n-C_3H_7	Compound unknown	−93.5	−122.0	−159.0
		Boiling points		
CH_3	9.4	3.5	−24.9	−78.5
C_2H_5	139.2	89.0	34.6	−37.1
n-C_3H_7	Compound unknown	156.5	90.1	−2.5
	←			

* Sources of data same as for table 9.

A horizontal comparison in Period II (i.e., with alkyls of oxygen, nitrogen, and carbon) also shows the great regularity in the properties of fluorine alkyls. Both melting and boiling points always increase in the order F → O → N → C, as illustrated in table 10.

Densities and molecular volumes

The fluorine alkyls always have the lowest densities in the row of halogen alkyls, as can be readily seen from table 11. They have, however, the highest densities in the row of the Period II elements; in all cases their densities are higher than those of the corresponding ethers (table 12).

The densities of the other halides were corrected to the N.B.P. by using a second-order equation. The first constant of this equation was generally obtainable from the literature. A second-order constant of

TABLE 11

*Densities and molecular volumes of halogen alkyls**

HALOGEN	AT RESPECTIVE NORMAL BOILING POINTS (SEE TABLE 9)						AT 20°C.									
	H	CH_3	C_2H_5	C_3H_7		n-C_4H_9	C_4H_9				C_5H_{11}		n-C_6H_{13}	n-C_7H_{15}	n-C_8H_{17}
				n-	*sec*-		*n*-	iso-	*sec*-	*tert*-	*n*-	*tert*-			
	Densities														
F......	0.9593(a)	0.8817	0.8176	0.7818	0.7692	0.7610	0.7763	?	0.7621	0.7546	0.7880	0.7784	0.8004	0.8039	0.8046
Cl......	1.187(b)	0.9915	0.9062	0.8581 (0.8923^{20})	0.8424 (0.8617^{20})	0.8161	0.8865	0.8773	0.8732	0.8414	0.8782	0.8657	0.872	0.877	0.872
Br......	2.158(c)	1.7206	1.4223	1.2620 (1.3513^{20})	1.2953 (1.3139^{20})	1.1470	1.2757	1.2646	1.2609	1.2209	1.2175	1.2157	1.173	1.130	1.112
I......	2.799(d)	2.2174 (2.2790^{20})	1.8149 (1.9359^{20})	1.5844 (1.7489^{20})	1.5662 (1.7042^{20})	1.4232	1.6154	1.6035	1.5975	1.3670	1.5095	1.4955	1.441	1.382	1.335
	Molecular volume														
F......	20.86	38.60	58.78	79.42	80.72	100.02	98.03		99.86	100.84	114.36	115.77	130.10	146.97	164.27
Cl......	30.72	50.92	71.20	91.54	93.25	113.43	104.41	105.50	106.00	110.01	121.36	123.11	138.29	153.49	170.44
Br..	37.50	55.18	76.62	97.47	98.80	119.47	107.41	108.35	108.67	112.23	124.05	124.23	140.71	158.47	173.64
I...	45.71	64.02	85.94	107.30	108.55	129.31	113.92	114.76	115.20	134.6	131.20	132.42	147.16	163.58	179.84

* Sources of data same as for table 9.

(a) Simons, J. H., and Bouknight, J. W.: J. Am. Chem. Soc. **54**, 129 (1932); see also Gmelin's *Handbuch*, Volume 5, p. 35.

(b) McIntosh and Steele: Z. physik. Chem. **55**, 142 (1906); see also Gmelin's *Handbuch*, Volume 6, p. 114.

(c) McIntosh and Steele: Z. physik. Chem. **55**, 142 (1906); see also Gmelin's *Handbuch*, Volume 7, p. 196.

(d) McIntosh and Steele: Proc. Roy. Soc. (London) **A73**, 451 (1904); Z. physik. Chem. **55**, 140 (1906); see also Gmelin's *Handbuch*, Volume 8, p. 270.

-0.0_515t° was used, since this constant for all of our fluorides and all other halides available in the literature was always between 0.0_51 and 0.0_52. For the few on which no first-order constant could be found in the literature a probable value was obtained by plotting the first-order coefficients of the different compounds, as a function of the alkyl group or halogen, at corresponding (T_x/T_b) temperatures and interpolating. This value was then combined with the second-order constant above.

The molecular volumes show the greatest regularities, particularly when compared at "corresponding" temperatures (see table 11). In figure 2 the volumes of the first four alkyls are compared at their respective normal boiling points. They form a straight-line relationship within experimental accuracy. The increments per CH_2 group for all four families are nearly equal, showing only a slight increase from fluorides to iodides (20.6 → 20.9 → 21.4 → 21.7). The volumes of the higher alkyls (compared at 20°C. in view of the uncertainty of extrapolating to the boiling points) show, as is to be expected, small deviations from the relationship expressed in figure 2. It is noteworthy that among all the butyl halides the volumes always increase in the order normal → iso → secondary → tertiary; the same order prevails among the normal and ter-

TABLE 12

Properties of the alkyls of the elements of Period II

Temperatures at 20°C. unless indicated

ALKYLS	CH_3	C_2H_5	n-C_3H_7	n-C_4H_9	n-C_5H_{11}
		Densities			
CR_4	0.6130^{0°	0.7522		0.7700	
NR_3	$0.6537^{+2.5^\circ}$	0.7302	0.7570	0.7768	
OR_2	$0.7340^{-24.9^\circ}$	0.7146	0.7470	0.7682	0.7830
		Molecular volumes			
CR_4	117.70^{0°	170.45		312.24	
NR_3	$90.42^{+2.5^\circ}$	138.54	189.22	238.60	
OR_2	$62.76^{-24.9^\circ}$	103.70	136.75	169.49	202.12
		Indices of refraction, n_D			
CR_4	1.3513^{0°	1.4197		1.4357	
NR_3	$1.3610^{+2.5^\circ}$	1.4003	1.4174		
OR_2	$1.3363^{-24.9^\circ}$	1.3528	1.3804	1.3968	1.4118
		Molecular refractions, MR_D^{LL}			
CR_4	25.40^{0°	43.12		81.60	
NR_3	$19.99^{+2.5^\circ}$	33.62	47.63		
OR_2	$13.02^{-24.9^\circ}$	22.48	31.71	40.80	50.28

tiary amyl halides. The literature value for the easily decomposable tertiary butyl iodide (see table 11) is definitely in error.

Data showing the relationship of the fluorine alkyls to the alkyls of the elements of Period II are given in table 12. Again the molecular volumes of the fluorine, oxygen, nitrogen, and carbon alkyls show straight-line relationships, as expressed in figure 3.

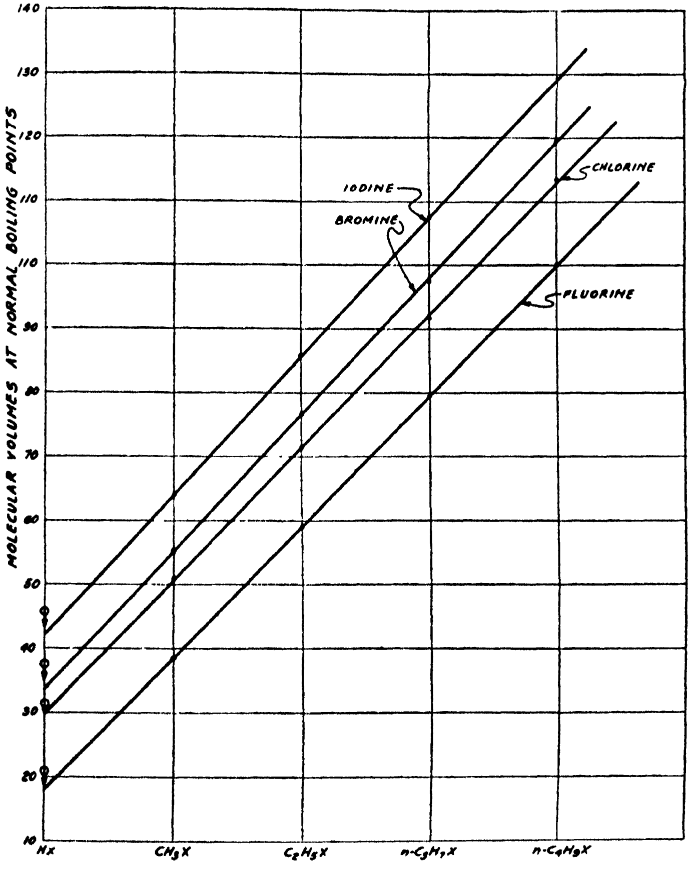

FIG. 2. Comparison of the molecular volumes of alkyl halides at their normal boiling points

Indices and molecular refractions

The experimental material is correlated in table 13; the calculated Lorentz–Lorenz molecular refractions for the D line are given in table 14. The indices for one particular alkyl group always increase in the order F → Cl → Br → I. They increase in the row of normal alkyl groups with increasing molecular weight for the fluorides and chlorides, while the opposite is true for the iodides. The molecular refractions, MR^{LL}_D, of all normal alkyl halides up to and including the normal octyl group show a straight-line relationship, as illustrated in figure 4. It will be noted that the value for normal amyl chloride is low.

The atomic refractions of the four halogens[4] were calculated from the above data using the procedure of F. Swarts (reference 59, page 35) and G. Schiemann (48), i.e., subtracting from the molar refractions of the halides the molar refractions of the corresponding paraffins and adding to the difference the atomic refraction of hydrogen. The values obtained, using, respectively, Eisenlohr's (20) and van der Hulst's (28) values for the atomic refractions of hydrogen, are as follows:

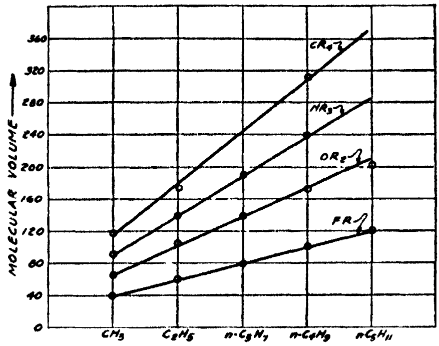

FIG. 3. Comparison of the molecular volumes of the fluorine, oxygen, nitrogen, and carbon alkyls

EXPERIMENTER	ATOMIC REFRACTIONS AT 20°C., AR^{LL}_D				
	H	F	Cl	Br	I
Eisenlohr	**1.100**	**0.945**	**5.958**	**8.851**	**13.962**
van der Hulst	1.025	0.870	5.883	8.776	13.887
Eisenlohr's old values	1.100	?	5.967	8.865	13.900

For comparison the old and still accepted values of Eisenlohr are included. A similar lawful relationship exists in regard to the alkyls of the elements of Period II. This is shown graphically in figure 5. An examination of figures 3 and 5, respectively, brings out the close relationship between the molecular volumes and refractions.

The data given here have been presented from the standpoint of *systematic chemistry*, because this enables one rapidly to overlook the entire

---

[4] Our complete data on the atomic refraction of fluorine will be published separately.

TABLE 13

Indices of refraction, n_D, of halogen alkyls

Temperatures at 20°C. unless otherwise indicated

HALOGEN	CH_3	C_2H_5	C_3H_7		C_4H_9				C_5H_{11}		n-C_6H_{13}	n-C_7H_{15}	n-C_8H_{17}
			n-	*sec-*	*n-*	iso-	*sec-*	*tert-*	*n-*	*tert-*			
F.....	?	$1.3033^{-37.1°}$	$1.3225^{-2.5°}$	$1.3182^{-9.4°}$	1.3393	?	1.3326	$1.3241^{12.1°}$	1.3578	1.3502	1.3748	1.3862	1.3940
Cl....	$1.3712^{-23.7°}$	$1.3724^{13.1°}$	1.3886	1.3783	1.4023	1.3989	1.3973	1.3851	1.4119	1.4056	1.4194	?	?
Br....	$1.4269^{4.5°}$	$1.4130^{38.4°}$	1.4349	1.4256	1.4421	1.4366	1.4370	1.4285	1.4444	1.4421	1.4478	?	?
I.....	1.5311	1.5137	1.5057	1.4992	1.4999	1.4864	1.5001	?	1.4955	?	1.4929	?	1.4890 ↓

TABLE 14

*Molecular refractions, MR^{LL}_{D}, of halogen alkyls**

Temperatures at 20°C. unless otherwise indicated

HALOGEN	CH_3	C_2H_5	C_3H_7		C_4H_9				C_5H_{11}		n-C_6H_{13}	n-C_7H_{15}	n-C_8H_{17}
			n-	*sec-*	*n-*	iso-	*sec-*	*tert-*	*n-*	*tert-*			
F.....	?	$11.13^{-37.1°}$	$15.87^{-2.5°}$	$15.93^{-9.4°}$	20.51	?	19.98	$19.76^{12.1°}$	25.07	24.92	29.76	34.53	39.17
Cl....	$11.62^{-23.7°}$	$16.29^{13.1°}$	20.80	21.03	25.44	25.52	25.55	25.79	28.84	30.22	34.17	?	?
Br....	$14.16^{4.5°}$	$19.10^{38.4°}$	23.75	23.97	28.43	28.37	28.47	28.90	32.98	32.88	37.66	?	?
I.....	19.27	24.25	28.87	29.30	33.51	32.98	33.90	?	38.30	?	42.77	?	51.92

* The values of $d_{4°}^{20°}$ used in our calculations are given in table 11. The other densities were at the respective boiling points (table 9).

field and to correlate immediately a large variety of data concerning many compounds. The examination of a chemical individual fitting into the field covered by such a survey is markedly aided. One can predict properties with considerable accuracy. Likewise one is enabled reasonably to discount data which do not fit into the scheme properly. This serves the experimenter as a check upon his own work and as a powerful and valuable means of evaluating the work of others. The lack of any systematic measurements of other properties, such as viscosity or surface tension, precluded their general comparison at this time.

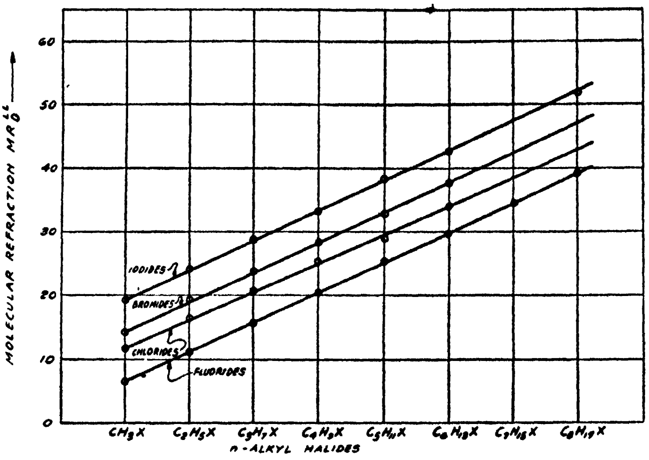

FIG. 4. Comparison of the molecular refractions of the alkyl halides

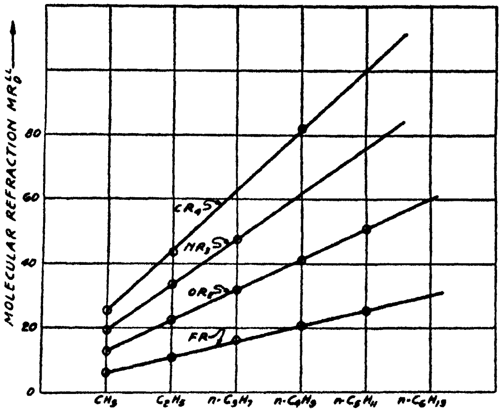

FIG. 5. Comparison of the molecular refractions of the fluorine, oxygen, nitrogen, and carbon alkyls

TABLE 15

Refractometric and density data for several alkyl halides

TEMPERATURE	REFRACTIVE INDICES, n_D^t						DENSITIES, $d_{4°}^{t°}$ (VAC.)		
							Our data	Data of Maass*	
	CH_3Cl	CH_3Br	C_2H_5Cl	C_2H_5Br	$(CH_3)_2O$	$(CH_3)_3N$	$(CH_3)_2O$	$(CH_3)_2O$	$(CH_3)_3N$
°C.									
−80							0.7999		
−70							0.7883		
−60		1.4697	1.4142		1.3538	1.3990	0.7767		
−50		1.4631	1.4085		1.3488	1.3930	0.7653		
−40	1.3773	1.4565	1.4028	1.4608	1.3438	1.3870	0.7538	0.7556(?)	0.7016
−30	1.3736	1.4499	1.3971	1.4547	1.3388	1.3810	0.7413	0.7416	0.6906
−20	1.3698	1.4432	1.3913	1.4486	1.3338	1.3750	0.7272	0.7275	0.6796
−10	1.3661	1.4367	1.3856	1.4425	1.3288	1.3690	0.7133	0.7133	0.6686
0		1.4301	1.3798	1.4364	[illegible]	1.3631	0.6994		0.6576
10		1.4234	1.3742	1.4303					0.6466
20					—				0.6356
$-\Delta n/\Delta T$	0.00037	0.00066	0.00057	0.00061	0.00050	0.00060			
n_D at N.B.P. (table 9)	1.3712	1.4269	1.3724	1.4130	$1.3363^{-24.9°}$	$1.3610^{+3.5°}$			
Density at N.B.P							$0.7340^{-24.9°}$	$0.7343^{-24.9°}$	$0.6537^{+3.5°}$
$-\Delta d/\Delta t$							0.00132		0.00110

---

* Maass and Boomer: J. Am. Chem. Soc. **44**, 1709 (1922).

APPENDIX

In order to complete the literature data for our comparisons we have determined and given in table 15 refractometric and density data for several alkyl halides, and also for the nitrogen and oxygen methyls discussed above. The compounds were obtained from pure commercial preparations which in turn were further purified as described in Part I for our fluorides.

REFERENCES[5]

(1) Batuecas, F.: J. chim. phys. **29**, 269 (1932).
(2) Bennett, W. H.: J. Am. Chem. Soc. **51**, 377 (1929).
(3) Bennett, W. H., and Meyer, C. F.: Phys. Rev. [2] **32**, 888 (1928).
(4) Booth, H. S., and Swinehart, C. F.: J. Am. Chem. Soc. **57**, 1337 (1935).
(5) Braus, D. H.: J. Am. Chem. Soc. **56**, 1421 (1934).
(6) Brockway, L. O.: J. Phys. Chem. **41**, 185 (1937).
(7) Brockway, L. O.: J. Phys. Chem. **41**, 747 (1937).
(8) Calloway, N. O.: J. Am. Chem. Soc. **59**, 1474 (1937).
(9) Cawood, W., and Patterson, H.: J. Chem. Soc. **1932**, 2180.
(10) Chadwell, H. M., and Titani, T.: J. Am. Chem. Soc. **55**, 1363 (1933).
(11) Collie, N.: J. Chem. Soc. **55**, 110 (1889).
(12) Collie, N.: J. Chem. Soc. **85**, 1317 (1904).
(13) Cooper, K. A., and Hughes, E. D.: J. Chem. Soc. **1937**, 1183.
(14) Cusas, H. L.: J. Am. Chem. Soc. **49**, 1270 (1927).
(15) DeForcrand, R.: Compt. rend. **135**, 960 (1902).
(16) Dennison, D. M., and Johnston, M.: Phys. Rev. [2] **47**, 93 (1935).
(17) Desreux, V.: Bull. acad. roy. Belg. [5] **20**, 457 (1934).
(18) Desreux, V.: Bull. acad. roy. Belg. **44**, 249 (1935).
(19) Dumas, J., and Peligot, E.: Ann. **15**, 59 (1835); Ann. chim. phys. **59**, 193 (1836).
(20) Eisenlohr, F.: *Spektrochemie organischer Verbindungen*, p. 48. F. Enke, Stuttgart (1912).

---

[5] The bibliography covers the literature on alkyl fluorides to November 1, 1938. The references not cited by us in this article are given below: methods of preparation and chemical properties: 15, 14, 27, 26, 10, 64, 8, 32; thermochemical data: 56, 57, 58, 63; optical data: 48, 5; dipole moments and atomic polarization: 50, 51, 46; parachor: 18; surface tension: 18; molecular structure: 65, 16, 55, 29, 61, 7.

The following table gives the references in chronological order:

YEAR	REFERENCES	YEAR	REFERENCES	YEAR	REFERENCES	YEAR	REFERENCES
1835	(19)	1894	(34, 35)	1921	(58)	1931	(48, 45, 60)
1854	(21)	1896	(36)	1922	(42)	1932	(9, 65, 26, 1)
1881	(67)	1902	(15)	1923	(59)	1933	(10, 50)
1885	(49)	1904	(12)	1926	(66)	1934	(17, 25, 5, 51)
1888	(31, 38)	1907	(43, 44)	1927	(14, 63)	1935	(18, 4, 16, 55, 29)
1889	(11)	1912	(56)	1928	(3)	1936	(61, 64, 46)
1890	(37)	1919	(57, 39)	1929	(2)	1937	(23, 62, 6, 7, 8, 32, 13)
1893	(33)	1920	(40, 41)	1930	(27)	1938	(24)

(21) **Fremy**: Ann. **92**, 247 (1854).

(22) **Grosse, A. V.**: J. Am. Chem. Soc. **59**, 2739 (1937).

(23) **Grosse, A. V., and Linn, C. B.**: Abstracts of Papers presented before the Division of Organic Chemistry at the Ninety-fourth Meeting of the American Chemical Society, held at Rochester, New York, September, 1937 (page 9).

(24) **Grosse, A. V., and Linn, C. B.**: J. Org. Chem. **3**, 26 (1938).

(25) **Hannum, C. W.**: Thesis (under the direction of M. S. Kharasch), University of Chicago, December, 1934.

(26) **Hartel, H. von, Meer, N., and Polanyi, M.**: Z. physik. Chem. **B19**, 139 (1932).

(27) **Hartel, H. von, and Polanyi, M.**: Z. physik. Chem. **B11**, 316 (1931).

(28) **Hulst, L. J. N. van der**: Rec. trav. chim. **54**, 518 (1935).

(29) **Johnston, M., and Dennison, D. M.**: Phys. Rev. [2] **48**, 868 (1935).

(30) **Krause, E., and Grosse, A. V.**: *Die Chemie der metallorganischen Verbindungen*, p. 749. Bornträger, Berlin (1938).

(31) **Lawson, A. T., and Coolie, N.**: J. Chem. Soc. **53**, 624 (1888).

(32) **Meerwein, H., Hinz, G., Hoffmann, P., Kroning, E., and Pfeil, E.**: J. prakt. Chem. [N.F.] **147**, 257 (1937).

(33) **Meslans, M.**: Bull. soc. chim. [3] **9**, 109 (1893).

(34) **Meslans, M.**: Z. anal. Chem. **33**, 470 (1894).

(35) **Meslans, M.**: Ann. chim. [7] **1**, 363 (1894).

(36) **Meslans, M.**: Ann. chim. [7] **7**, 94 (1896).

(37) **Moissan, H.**: Ann. chim. [6] **19**, 272 (1890).

(38) **Moissan, H., and Meslans, M.**: Compt. rend. **107**, 1155 (1888); Jahresbericht, p. 931 (1888).

(39) **Moles, E., and Batuecas, F.**: J. chim. phys. **17**, 537 (1919).

(40) **Moles, E., and Batuecas, F.**: J. chim. phys. **18**, 353 (1920).

(41) **Moles, E., and Batuecas, F.**: Anales soc. españ. fís. quím. [2] **18**, 211 (1920); Chem. Zentr. **1921**, III, 766.

(42) **Nunez, F. G.**: Anales soc. españ. fís. quím. **20**, 539 (1922).

(43) **Paternò, E., and Spallino, R.**: Gazz. chim. ital. **37**, II, 310 (1907).

(44) **Paternò, E., and Spallino, R.**: Atti. accad. Lincei [5] **16**, II, 161 (1907).

(45) **Patterson, H., Whytlaw-Gray, R., and Cawood, W.**: Nature **128**, 375 (1931).

(46) **Ramaswamy, K. L.**: Proc. Indian Acad. Sci. **A4**, 108 (1936).

(47) **Rowley, R. J., and Churchill, H. V.**: Ind. Eng. Chem., Anal. Ed. **9**, 551 (1937).

(48) **Schiemann, G.**: Z. physik. Chem. **A156**, 397 (1931).

(49) **Seubert, K.**: Ber. **18**, 2647 (1885).

(50) **Smyth, C. P.**: J. Chem. Phys. **1**, 247 (1933).

(51) **Smyth, C. P., and McAlpine, K. B.**: J. Chem. Phys. **2**, 499 (1934).

(52) **Stock, Alfred**: Ber. **50**, 156 (1917).

(53) **Stock, Alfred**: Z. Elektrochem. **29**, 354, 357 (1923).

(54) **Stock, Alfred**: *Hydrides of Boron and Silicon.* Cornell University Press, Ithaca, New York (1934).

(55) **Sutherland, G. B. B. M., and Dennison, D. M.**: Proc. Roy. Soc. (London) **A148**, 250 (1935).

(56) **Swarts, F.**: Bull. acad. roy. Belg. **1912**, 481.

(57) **Swarts, F.**: J. chim. phys. **17**, 3–70 (1919).

(58) **Swarts, F.**: Bull. acad. roy. Belg. [5] **7**, 438 (1921).

(59) **Swarts, F.**: J. chim. phys. **20**, 30–76 (1923).

(60) Swarts, F.: J. chim. phys. **28**, 622 (1931).
(61) Swarts, F.: Bull. acad. roy. Belg. [5] **22**, 781 (1936).
(62) Swarts, F.: Bull. soc. chim. Belg. **13**, 10 (1937).
(63) Swietoslawski, M. W., and Bolinska, J.: J. chim. phys. **24**, 545 (1927).
(64) Tang, Chao-Lun, Ho, Teh-Sen, and Huan, Kun: Sci. Repts. Natl. Univ. Peking **1**, 9 (1936); Chem. Zentr. **1937**, II, 3311.
(65) Teller, E., and Tisza, L.: Z. Physik **73**, 791 (1932).
(66) Tronow, B., and Kreuger, E.: J. Russ. Phys. Chem. Soc. **58**, 1270 (1926); Chem. Zentr. **1927**, II, 1145.
(67) Young, S.: J. Chem. Soc. **39**, 489 (1881).

INTRAMOLECULAR FOLDING OF POLYPEPTIDE CHAINS IN RELATION TO PROTEIN STRUCTURE[1]

HANS NEURATH

Department of Biochemistry, School of Medicine, Duke University, Durham, North Carolina

Received June 12, 1939

Recently H. B. Bull and the author (10) have presented a critical examination of the available data regarding the properties of protein monolayers. From considerations of space requirements, the conclusion was drawn that only the structure of fully extended polypeptide chains can account for the observed film areas, whereas the assumption of folded or cyclized polypeptide chains would result in film areas much smaller than those observed. As the surface area of protein films is determined by the dimensions and orientation of the side chains, the question arose whether the discrepancy between observed and calculated film areas may not be due to steric difficulties inherent in the structures that have been suggested. It is the object of the present investigation to examine the structures of fully extended, folded, and cyclized polypeptide chains in regard to the orientation and space requirements of amino acid residues. Evidently any structure, if it is to represent the actual facts, must meet certain physical and chemical requirements which may briefly be stated as follows: (*1*) Proteins are built up of amino acids which are structurally related to the *levo-rotatory* isomer of lactic acid. (*2*) There must not be any unreasonable deviation from accepted bond angles and interatomic distances. (*3*) The distribution and orientation of amino acid residues must be such as to allow sufficient room for their accommodation.

---

[1] Presented at the Ninety-seventh Meeting of the American Chemical Society, held in Baltimore, Maryland, April, 1939.

Acknowledgment is made to the Lederle Laboratories, Pearl River, New York, for a grant-in-aid.

For evaluating the relative positions of atoms and groups, atomic models have been used which Dr. Edward Mack, Jr., of the University of North Carolina very kindly placed at my disposal. Such models, which have been described by Mack (11), are made on a scale of 10^8 to 1, or 1 cm. = 1 Å. The C—C interatomic distance has been taken as 1.54 Å., C—N as 1.47 Å., C—H as 1.08 Å., and C—O as 1.43 Å.[2] Tetrahedral bond angles have been assumed for carbon and nitrogen, and the angle of the oxygen bond has been taken as 111°. The radii of the atomic domains of hydrogen and oxygen atoms, beyond the nucleus, have been chosen as 1.1 Å. and 1.35 Å., respectively.

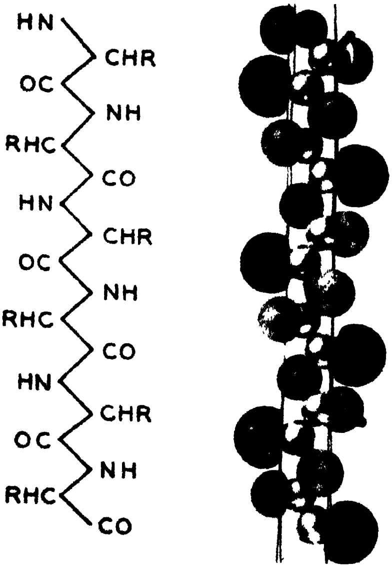

FIG. 1. Scaled model of a fully extended polypeptide chain viewed from above

Beta-keratin

Figure 1 illustrates the structure of a fully extended polypeptide chain, sometimes referred to as the beta-keratin structure (3, 4), viewed from above. The carbon, nitrogen, and oxygen atoms of the main chain, formed by successive peptide linkages, are all lying in one plane. The hydrogen atoms are oriented in a spiral-like fashion around the main chain, and the side chains, formed by that part of the amino acid residues which extends beyond the alpha-carbon atom, are oriented at about right angles to the plane. Stereochemical considerations demand that in such a fully extended zigzag chain the side chains protrude alternately from the upper and lower surface of the plane, as indicated by the match sticks in figure 2, which is a picture of the same model viewed from the side.

---

[2] The values for carbon-nitrogen and carbon-oxygen distances used here are somewhat larger than those found recently by Albrecht and Corey for glycine crystals (J. Am. Chem. Soc. **61**, 1087 (1939)).

The spacings indicated by x-ray analysis (3, 4) are as follows: 3.33 Å. for the distance between the points of attachment of two side chains in the longitudinal direction, 4.65 Å. for the distance of closest approach of main chains in their own plane (backbone spacing), and 9.7 Å. for the distance between main chains in the direction of the side chains (side-chain spacing). These values are in full accord with those to be expected from the known values of interatomic distances and bond angles, respectively. The backbone distance of 4.5 Å. can be accounted for if it is assumed that the oxygen atoms of one chain tuck into the recesses between oxygen atoms of the neighboring chain, while the side-chain spacing is due to the alternately arranged side chains, of an average length of about 4.5 Å. The minimum area available for one side chain is, therefore, 4.65 × 3.33 × 2 = 31 sq. Å. This leaves definitely enough room for their accommodation, as the average cross-sectional area of amino acid residues is about 17 to 25 sq. Å. Values of the cross-sectional areas of various amino acid residues, as determined with the use of scaled atomic models, are listed in table 1. These values, determined for straight chains, are average values. The effective cross-sectional area may be somewhat larger if the side chains are rotating, whereas somewhat smaller areas would result if under the influence of attractive forces the atoms of one side chain would fit into the recesses between atoms of the neighboring chain.

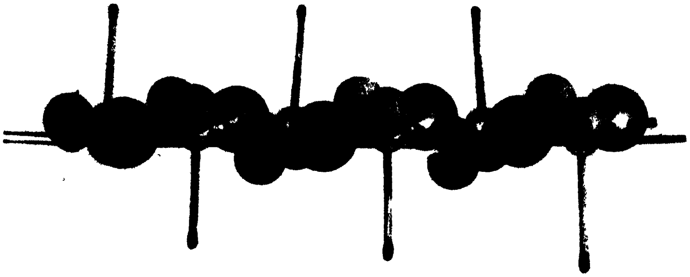

FIG. 2. Scaled model of a fully extended polypeptide chain viewed from the side. The orientation of the side chains is indicated by the match sticks.

The complete structure of a hypothetical, fully extended polypeptide chain is shown in figure 3. In this particular model, the non-polar residues of leucine, phenylalanine, and valine emerge from the upper surface, whereas the polar residues of aspartic acid, cysteine, and arginine protrude from the lower surface. This model illustrates the surprisingly large space taken up by the residues.

TABLE 1

Cross-sectional areas and lengths of amino acid residues (estimated from scaled atomic models)

AMINO ACID RESIDUE	MAXIMUM CHAIN LENGTH BEYOND ALPHA CARBON ATOM	CROSS-SECTIONAL AREA (APPROXIMATE)
	A.	sq. Å.
Glycine	1.4	4
Alanine	2.2	11.5
Valine	3.8	26
Leucine	5.0	26
Phenylalanine Tyrosine	7.1	35
Cysteine	4.2	17
Aspartic acid	5.1	22
Arginine	8.4	25

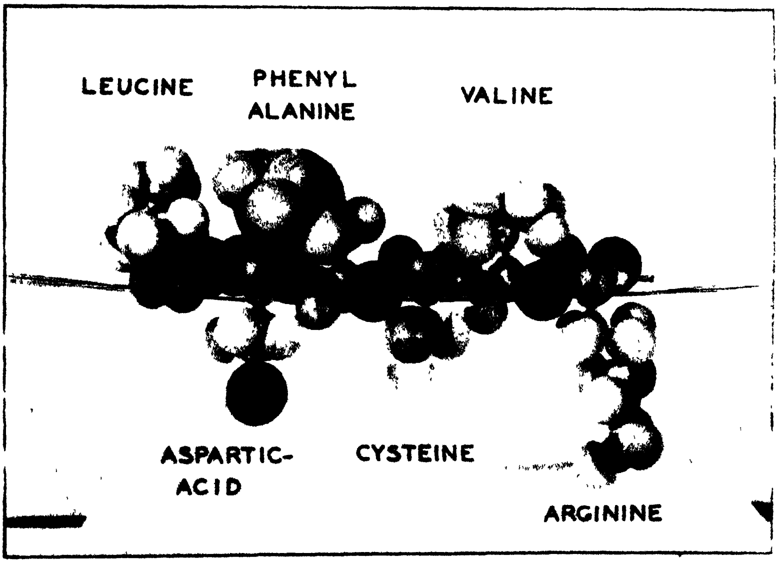

FIG. 3. Scaled model of a hypothetical fully extended polypeptide chain viewed from the side.

The structure of fully extended polypeptide chains can account, almost quantitatively, for the observed properties and surface areas of protein monolayers (10). Most proteins, when spread under comparable conditions, occupy a film area of 1.4 to 1.6 square meters per milligram in the most expanded state, corresponding to a film thickness of about 5 Å. Fully compressed, homogeneous protein films have an area of about 0.77 square meter per milligram and a thickness of about 10 Å. If we take into account the alternate orientation of side chains and the values for the average molecular weight per residue, we can calculate the mean film area per side chain. The results and implications of such calculations have been discussed previously (10) and are summarized in table 2. The agreement between the values calculated from surface film data on the one hand, and molecular models on the other, is extremely good, in the case of both most expanded and compressed films, if we assume that in the most expanded state the side chains are lying flat on the surface, and if we assume that they are oriented perpendicular to the surface when the films are compressed. In the latter case only one half of the side chains will contribute to the surface area, the other half being buried in the water phase. The distribution of side chains between the water and the air phases will, in compressed films, be such that polar side chains are preferably directed towards the water, and non-polar ones towards the air. Such a selected orientation may readily be provided for by fully extended polypeptide chains. (Whether the composition of the proteins permits such a general scheme remains, of course, to be proved.)

TABLE 2

Observed and calculated film areas of proteins

PROTEIN	AVERAGE RESIDUE WEIGHT	MOST EXPANDED FILMS			COMPRESSED FILMS		
		Area per milligram	Film thickness	Mean area per side chain	Area per milligram	Film thickness	Mean area per side chain
		square meters	*Å.*	*sq. Å.*	*square meters*	*Å.*	*sq. Å.*
Calculated from beta-keratin (model)			4.5-5	32		9-10	31
Egg albumin	124	1.3	5.7	27.5	0.77	9.6	31.8
Insulin	122	1.65	4.5	33.0	0.77	9.6	31.0
Serum albumin	134	1.45	5.1	32.0	0.79	9.4	34.2
Cytochrome C	120	1.55	4.9	30.6	0.70	10.0	28.0

Alpha-keratin

Naturally, one must anticipate that, owing to free rotation about single bonds, fully extended polypeptide chains may undergo intramolecular folding. As a result of their investigation of the mechanism of reversible stretching and contraction of wool and other fibrous proteins, Astbury and his associates have, in their early publications (3, 4, 1), suggested a folded polypeptide structure which is known as alpha-keratin.

This folded configuration may be derived from fully extended polypeptide chains by assuming that the main chains contract to about one-half of their original length. The spacings indicated by x-ray measurements (3, 4) are, respectively, 5.1 Å. for the distance of separation between three amino acid residues in the longitudinal direction, and 9.7 Å. for the side-chain spacing. Assuming no deviation, or only slight deviation, from tetrahedral bond angles, it becomes at once apparent that the transformation of beta-keratin into alpha-keratin must be accompanied by profound changes in the orientation of the side chains. There are at least two ways of arranging the side chains, depending on the configuration of the hexagonal rings. If one chooses the puckered ring of the "diamond type," in which the atoms are alternately above and below the median plane, one of the two side chains, carried by carbon atoms of the rings, will point *upwards*, whereas the other one will point *sidewards*. If the hexagonal rings are of the "camphor type," two atoms above the median plane and four below it, *both* side groups will be directed *upwards*. The side groups which are attached to those carbon atoms which bridge two adjoining rings are, in both cases, directed *outwards*.

Figure 4 illustrates diagrammatically both types of configuration. The hydrogen atoms and one of the oxygen atoms have, for purposes of demonstration, been omitted in this diagram.

It may readily be seen that the "diamond ring" configuration cannot accommodate those side chains which are directed sidewards. Even if we assume drastic distortions of the tetrahedral bond angles, it seems impossible to accommodate them, as the space above the neighboring ring is fully occupied by the vertical side chain. We may, therefore, by mere considerations of space requirements, exclude this configuration from the discussion. In the "camphor ring" structure, certain side groups may get into the required positions. The distance of separation between the points of attachment of successive side chains, in the longitudinal direction, is alternately about 3 Å. and 2 Å. While residues with small cross-sectional areas, such as glycine or alanine, may be accommodated, it seems utterly impossible to accommodate any of the larger amino acid residues. Still greater obstacles appear if one tries to get the hydrogen atoms into the required position. The hydrogen atoms carried by the 4-carbon atom of one ring and the 1-carbon atom of the neighboring ring should point outwards, towards each other. However, the free space between these carbon atoms is only about 0.5 Å., whereas the space required by the domains of two hydrogens is about 2.6 Å.

One way out of this difficulty would be to assume that the folded main chain does not lie in one plane, but that each successive hexagon lies, for instance, 2 Å. above the preceding one. Such a stepwise configuration of the main chain would remove the obstacle of accommodating the hydrogen

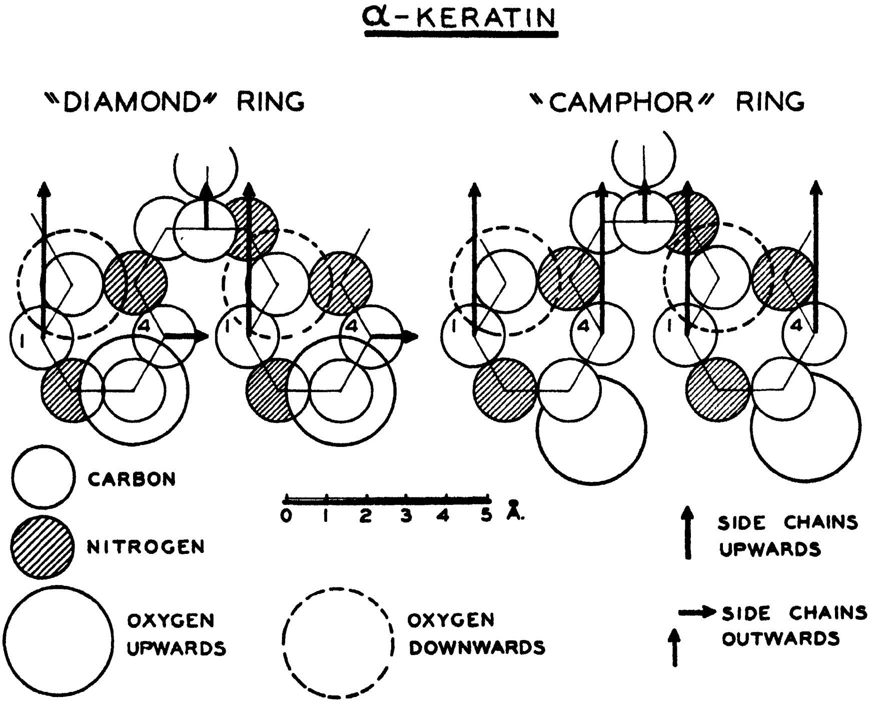

FIG. 4. Showing the orientation of side chains in two different configurations of alpha-keratin. The hydrogen atoms have been omitted. Drawn roughly to scale.

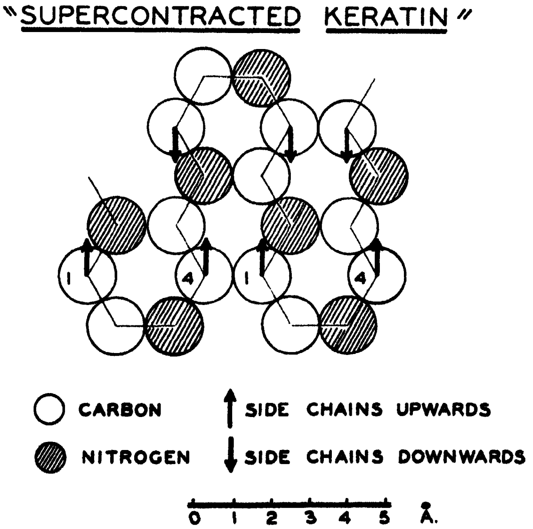

FIG. 5. Showing the orientation of side chains and the packing of carbon and nitrogen atoms in supercontracted keratin. Drawn roughly to scale.

atoms, but it would not aid in fitting the vertical side chains. Another alternative would be either to evoke a keto–enol interchange, in the manner suggested by Astbury and Miss Wrinch (5, 2), or to use actual diketopiperazine rings which, as Corey (6) has shown recently, are virtually coplanar. Both alternatives, however, would still leave unsolved the problem of accommodating the vertical side chains of successive rings, as the distance of separation between the carbon atoms to which they are attached is only 3 Å. Moreover, it is very unlikely that reversible opening and closure of diketopiperazine rings could be accomplished by mere forces of mechanical stress.

Supercontracted keratin

More drastic folding of polypeptide chains may result in a structure the skeleton of which is illustrated by figure 5. In this structure, which has been suggested by Astbury for the *supercontracted* form of keratin (3, 4, 1), the side chains attached to one hexagon are directed *upwards* and those attached to the next one *downwards* (figure 5). The steric difficulties of accommodating hydrogen atoms and side chains are, in this structure, probably greater still, as there is no free space left between adjoining hexagonal rings.

Cyclol structure

Complete cyclization of polypeptide chains leads to the cyclol structure which has been described in detail by Miss Wrinch (12). Suffice it to recall that cyclol units of different configurations may be obtained, depending on the number of amino acid residues which participate in cyclization. The "cyclol 6," comprising six amino acid residues, has been used for the construction of the so-called C_2 molecule which contains 288 residues, arranged on the surface of a truncated polyhedron. Higher members of the cyclol series may be obtained by cyclization of 18, 42, 66, etc. amino acid residues. All cyclol units are alike, however, in that they are essentially dorsiventral, i.e., all side chains emerge initially from one surface and none from the other. If the cyclol network consists of polymers of "cyclol 6," as has been suggested for the insulin and pepsin molecules (13, 14), the area per amino acid residue is, according to Miss Wrinch (12), about 10 sq. Å. Comparison of this value with the cross-sectional areas of amino acid residues demonstrates at once that the cyclol 6 polymer cannot accommodate the side chains, unless they consist exclusively of hydrogen atoms (glycine) and alanine residues. Miss Wrinch has contended that the orientation of side chains refers only to the beta-carbon atom and that, owing to free rotation, the rest of the side chains may bend around so as to emerge from the other side of the network. Such an assumption would not solve the problem for two reasons: First, it is evident that a bent side chain requires more space than if it were straight; and since it is impossible to accommodate a straight side chain, it is likewise impossible to accommodate a bent side chain. Secondly, it has to be emphasized that the value for the area per amino acid residue, just given, is a maximum value, owing to the uneven distribution of side chains within the network and the space taken up by those hydroxyl groups which likewise protrude from the upper surface. The actual available area per residue must be considerably smaller than is indicated by Miss Wrinch's calculations.[3]

CONCLUSIONS

From the above considerations the conclusion must be drawn that free rotation of polypeptide chains around carbon-carbon and carbon-nitrogen bonds is greatly restricted, owing to the space requirements of the side chains.

If both optical isomers of amino acids were to occur in proteins, a great variety of stereochemically permissible structures would be conceivable. The fact that all naturally occurring amino acids are identical in respect to their optical configuration limits, apparently, the possible structures to that of beta-keratin.[4]

Yet experimental evidence indicates strongly that, in proteins, polypeptide chains must exist in configurations other than that of the fully extended type. The long-range contraction of the fibrous proteins (2, 4), the apparent shapes of the globular proteins (9), and the shape changes accompanying denaturation (3, 4) call for some radical type of intramolecular rearrangement. It will be noted that all structures discussed in the preceding paragraphs are alike in that the carbon and nitrogen atoms of the rings, formed by the main chains, lie essentially in one plane. This fact is responsible for the steric difficulties of accommodating side chains and hydrogen atoms. More recently, Astbury (2) has emphasized that the folding of polypeptide chains must in general take place in planes transverse to the side chains. This could only be possible if the folds are far from coplanar. The question suggests itself, therefore, whether a contracted form of polypeptide chains may not be arrived at by evoking a three-dimensional (spiralled) folding of the main chains, which would still preserve the alternate orientation of the side chains.

---

[3] A very detailed demonstration of the steric difficulties inherent in the cyclol structure has been given recently by Mack (11).

[4] Wrinch and Lloyd (15), Mirsky and Pauling (8), and Huggins (7) have drawn attention to the rôle which hydrogen bonds may play in protein structure. Huggins (7) recently suggested patterns and cage molecule structures closely related to Miss Wrinch's models but involving the use of hydrogen bonds.

SUMMARY

The space requirements and orientation of amino acid residues in fully extended and folded polypeptide chains have been investigated with the use of scaled atomic models.

Accommodation of the side chains, formed by the amino acid residues, may be readily brought about in fully extended polypeptide chains, chiefly owing to the fact that the side chains protrude alternately from the upper and lower surface of the plane formed by the main chain. This structure can account, almost quantitatively, for the observed film areas and properties of protein monolayers.

Folding of polypeptide chains, in the manner suggested for alpha-keratin and supercontracted keratin, respectively, results in drastic changes in the orientation of the side chains. The data indicate that, unless unreasonable distortions of bond angles are assumed, these configurations are too condensed to permit residues, other than those of glycine and alanine, and hydrogen atoms to get into the positions called for by the carbon atoms of the hexagonal rings to which they are attached. From considerations of space requirements of amino acid residues it follows also that the cyclol structure is too condensed to permit the accommodation of side chains.

The significance of these considerations for the problem of protein structure is discussed.

REFERENCES

(1) Astbury: Chem. Weekblad **33**, 778 (1936).
(2) Astbury: Trans. Faraday Soc. **34**, 377 (1938); Compt. rend. trav. lab. Carlsberg **22**, 45 (1938).
(3) Astbury and Lomax: J. Chem. Soc. **1935**, 847.
(4) Astbury and Woods: Nature **126**, 913 (1930); Phil. Trans. Roy. Soc. **A232**, 333 (1933); Astbury, Dickinson, and Baily: Biochem. J. **29**, 2351 (1935).
(5) Astbury and Wrinch: Nature **139**, 798 (1937).
(6) Corey: J. Am. Chem. Soc. **60**, 1698 (1938).
(7) Huggins: J. Am. Chem. Soc. **61**, 755 (1939).
(8) Mirsky and Pauling: Proc. Natl. Acad. Sci. U. S. **22**, 439 (1936).
(9) Neurath: J. Am. Chem. Soc. **61**, 1841 (1939).
(10) Neurath and Bull: Chem. Rev. **23**, 391 (1938).
(11) Symposium on Reaction Rates, held at the meeting of the American Association for the Advancement of Science, Richmond, Virginia, December 27, 1938; also Mack: J. Am. Chem. Soc. **54**, 2141 (1932).
(12) Wrinch: Nature **137**, 411 (1936); Proc. Roy. Soc. (London) **A160**, 59 (1937); Phil. Mag. **25**, 705 (1938).
(13) Wrinch: Phil. Mag. **24**, 940 (1937).
(14) Wrinch and Langmuir: J. Am. Chem. Soc. **60**, 2247 (1938).
(15) Wrinch and Lloyd: Nature **138**, 758 (1936).

CALCULATION OF SOLUTE ACTIVITIES FROM ACTIVITIES OF THE SOLVENT. LIMITING BEHAVIOR OF THE *h* AND *j* FUNCTIONS IN DILUTE SOLUTIONS[1]

MERLE RANDALL AND BRUCE LONGTIN[2]

Department of Chemistry, University of California, Berkeley, California

Received June 12, 1939

To facilitate the calculation of solute activities from solvent activities, Lewis and Randall (2) defined the function *h* by the equation

$$h = (\ln a_1)/r + 1 \qquad (1)$$

where a_1 is the activity of the solvent and r is the ratio, $\mathrm{N}_2/\mathrm{N}_1$, of the mol fraction of solute to that of solvent in the given solution. Making use of the generalized Duhem equation, they showed that the solute activity is given by the expression

$$-\mathrm{d} \ln (a_2/r) = \mathrm{d}h + h\mathrm{d}r/r \qquad (2)$$

Since the molality, *m*, of solute in an aqueous solution is equal to $55.51r$, equation 2 is equally valid with the mol ratio r replaced by the molality m.

Equation 2 is convenient for the evaluation of the activity coefficient (a_2/m) expressed in terms of molalities. In non-aqueous solutions the coefficient (a_2/N_2) based upon the mol fraction of solute is more important. The coefficients a_2/N_2 and a_2/r are related through the definition of r as $\mathrm{N}_2/\mathrm{N}_1$. Thus if the coefficient a_2/r has previously been calculated, the coefficient a_2/N_2 may be obtained by the equation

$$\log (a_2/\mathrm{N}_2) = \log \gamma_{\mathrm{N}_2} = \log (a_2/r) - \log \mathrm{N}_1 \qquad (3)$$

If a_2/r has not already been calculated it is simpler to calculate a_2/N_2 directly with the help of a new function h', defined by the equation

$$h'r = \ln (a_1/\mathrm{N}_1) \qquad (4)$$

The generalized Duhem equation takes the form (2)

$$-\mathrm{d} \ln a_2 = (1/r)\,\mathrm{d} \ln a_1 \qquad (5)$$

and must be identically satisfied by all binary solutions. Taking into account the mathematical identity

$$-\mathrm{d} \ln \mathrm{N}_2 \equiv (1/r)\,\mathrm{d} \ln \mathrm{N}_1 \qquad (6)$$

---

[1] Clerical assistance of the Works Progress Administration O. P. No. 665-08-3-144 is gratefully acknowledged.

[2] Shell Fellow in Chemistry, 1938–39.

we may write

$$-\mathrm{d}\ln(a_2/\mathrm{N}_2) = (1/r)\,\mathrm{d}\ln(a_1/\mathrm{N}_1) = (1/r)\,\mathrm{d}\,(h'r) = \mathrm{d}h' + (h'/r)\,\mathrm{d}r \quad (7)$$

Equation 7 has exactly the same form as equation 2, but expresses the coefficient a_2/N_2 in terms of the function h'.

The solution of equations 2 and 7 requires a graphical integration in which the area under a curve of either (h/r) or (h'/r) plotted against r must be determined between the limits of infinite dilution ($r = 0$) and the given concentration. The validity of the result depends upon the accuracy with which the functions h/r and h'/r may be extrapolated to infinite dilution.

IDEAL SOLUTIONS

In an ideal solution the activity, a_1, of the solvent is equal to its mol fraction N_1 at all concentrations. Thus equation 4 shows that for an ideal solution the function (h'/r) must vanish for all concentrations of solute, since $\ln(a_1/\mathrm{N}_1)$ is zero. The non-vanishing of (h'/r) is always an indication that the solution is not ideal.

The two functions h and h' are closely related, as may be seen by comparing equations 1 and 4. If the value of $\ln a_1$ obtained from equation 4 is substituted in equation 1, the result

$$h = h' + [1 + (\ln \mathrm{N}_1)/r] \quad (8)$$

is obtained. For an ideal solution, therefore, h must have the value $[1 + (\ln \mathrm{N}_1)/r]$. For an imperfect solution h differs from the ideal solution value by the amount h'.

For an ideal solution the function h/r must have the value $[1 + (\ln \mathrm{N}_1)/r](1/r)$. This function is represented as curve 1 in figure 1. Since the mol fraction N_1 may be expressed in terms of the mol ratio as $1/(1 + r)$, the function $[1 + (\ln \mathrm{N}_1)/r](1/r)$ may be expanded in the series

$$\begin{aligned}[1 + (\ln \mathrm{N}_1)/r](1/r) &= [1 - (1/r)\ln(1 + r)](1/r) \\ &= 1/2 - r/3 + r^2/4 - r^3/5 + \cdots \quad (9)\end{aligned}$$

valid in the neighborhood of infinite dilution ($r = 0$). Thus for an ideal solution the curve of h/r *vs.* r has the limiting value 1/2 and the limiting slope $-1/3$ at infinite dilution. Observing that m is $55.51r$, the limiting value of h/m must be $1/111.0 = 0.0090$ and the limiting slope $-1/3(55.51)^2 = 0.000108$ for the ideal solution.

SOLUTIONS OBEYING HENRY'S LAW

A solution is said to obey a generalized Henry's law if the activity coefficient a_2/N_2 is constant in dilute solutions. In general the coefficient a_2/N_2 approaches a finite limit (2) at infinite dilution. However, it can be said to approach constancy only if its rate of change approaches zero. Thus Henry's law can be said to be obeyed only in that portion of the region of dilute solutions for which d ln $(a_2/N_2)/dr$ vanishes. With the exception of ideal solutions, it is extremely unlikely that Henry's law is exactly obeyed in any region other than in the limit of infinite dilution. For a_2/N_2 to remain constant up to any finite concentration and then deviate from that constant value would require a type of discontinuity which, so far, we have been unable to observe in nature.

Whether or not a solution obeys Henry's law is clearly indicated in the nature of the curve of h'/r *vs.* r. Equation 7 requires that $h'r$ be constant in every region in which d ln $(a_2/N_2)/dr$ vanishes. At infinite dilution

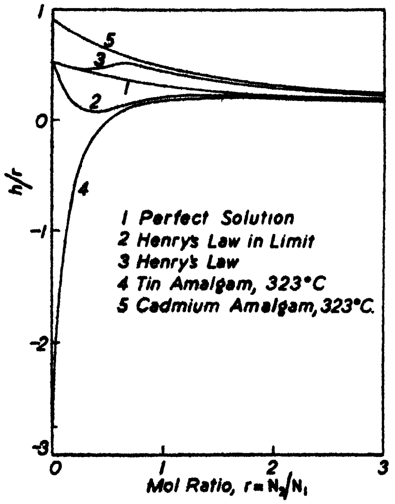

FIG. 1. h/r *versus* r for various typical solutions

a_1/N_1 is always given the value of unity by the choice of pure solvent as the standard state. Hence equation 4 requires that $h'r$ have the value zero at infinite dilution. Consequently, if Henry's law is to hold at infinite dilution and at higher concentrations as well, $h'r$ and likewise h'/r must vanish over the whole region in which Henry's law is obeyed. Furthermore, if Henry's law is only approached in the limit, equation 7 shows that $h'r$ must approach zero at least as rapidly as r^3, and hence h'/r must approach zero as rapidly as does r. In general the extent to which Henry's law is obeyed is indicated by the extent to which h'/r approaches zero at high dilution.

Many solutions which are not ideal and hence do not obey Raoult's law nevertheless approach Raoult's law in the limit of the pure solute ($r \rightarrow \infty$). By this it is meant that a_2/N_2 becomes constant again in the concentrated solutions, but with a value different from that in the dilute solutions (if the pure solute is chosen as a standard state, the new constant value is unity). In this case $h'r$ must approach a constant limit as r becomes very large. The value of this constant may differ from zero. Thus the Raoult's law limit is indicated in the h'/r *vs.* r curve by an asymptotic approach to a curve for which (h'/r) is proportional to $1/r^2$.

These two general features of a curve of h'/r *vs.* r for a solution obeying Henry's law in dilute solution and approaching Raoult's law in concentrated solutions are indicated by curves 2 and 3 of figure 2. The corresponding curve of h/r differs from the ideal limit by the amount h'/r. Curves 2 and 3 of figure 1 correspond to curves 2 and 3 (respectively) of figure 2, being obtained by adding the ordinates of the curve in figure 2 to those of curve 1 in figure 1. In general these curves will deviate from the ideal curve to different extents (the asymptotic curve $h'/r \propto 1/r^2$ may deviate widely or only slightly from zero) depending on the extent of imperfectness of the solution. Curve 2 represents a case in which Henry's law is obeyed approximately up to fairly high concentrations, while curve 3 gives the case in which Henry's law is obeyed only in the limit.

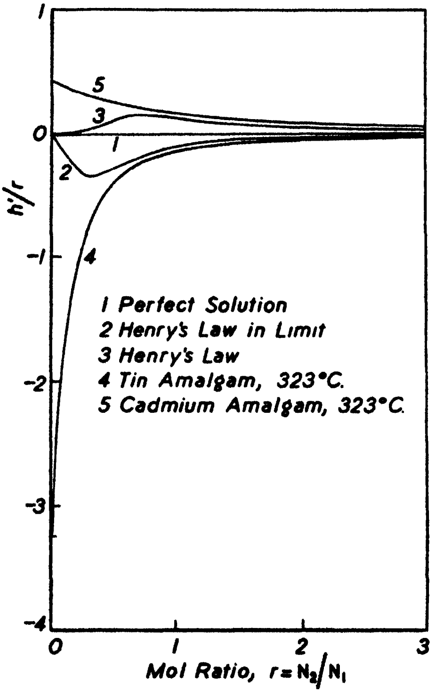

FIG. 2. h'/r *versus* r for various typical solutions

VAN LAAR SOLUTIONS

Van Laar (3) has given the theoretical equation

$$\ln (a_2/N_2) = \alpha/(1 + \beta r)^2 \qquad (10)$$

for the general behavior of imperfect solutions. This equation has been shown to hold experimentally for a wide class of solutions (1). Substituting this expression in equation 7 we obtain the differential equation

$$(1/r)d(h'r) = 2\alpha\beta dr/(1 + \beta r)^2 \qquad (11)$$

which defines the function h' for a Van Laar solution. On integration, this equation gives

$$h'/r = -\alpha\beta/(1 + \beta r)^2 \qquad (12)$$

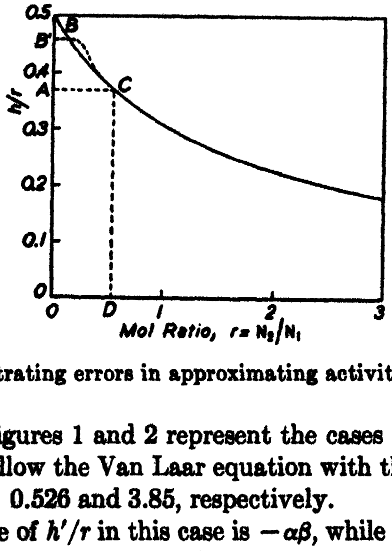

FIG. 3. Illustrating errors in approximating activity coefficients

Curves 4 and 5 of figures 1 and 2 represent the cases of cadmium and tin amalgams, which follow the Van Laar equation with the values $\alpha = 0.393$ and -3.26 and $\beta = 0.526$ and 3.85, respectively.

The limiting value of h'/r in this case is $-\alpha\beta$, while the limiting slope of the curve of h'/r is $+2\alpha\beta^2$. The coefficient β is often approximately equal to the ratio of molal volume of the two components (1), while α depends on the degree of imperfectness of the solution; both may vary over wide ranges. The curve of h/r *vs.* r has the limiting value $(1/2 - \alpha\beta)$ and the limiting slope $(1/3 + \alpha\beta^2)$. Only in rare cases will the limiting slope be zero, namely, when $\alpha\beta^2$ has the value $+1/3$. The limiting value of h/r may be either positive or negative.

THE LEWIS AND RANDALL RULE

Lewis and Randall (2) have suggested that in cases of uncertainty the function h/m might be extrapolated as constant at high dilution. This rule is equivalent to the assumption of a definite way in which the activity coefficient a_2/N_2 behaves in dilute solutions. Since h/m is proportional to

h/r, the rule says that h must be proportional to r. If we write $h = cr$, equation 2 may be integrated to give

$$\ln (a_2/r) = 2cr + c' \tag{13}$$

Expressed in terms of mol fractions,

$$\ln (a_2/N_2) = 2cN_2/N_1 + \ln N_1 + c' \tag{14}$$

Such an equation cannot possibly hold over any wide range of concentrations, since in general it gives an infinite value to $\ln (a_2/N_2)$ in the limit of pure solute.

In figure 3 the area $OACD$ has the value $(h/r)r = h$. Inspection of equation 2 shows that $-\ln (a_2/r)$ is given by the sum of this area plus the whole area, $OBCD$, under the curve. According to the rule of Lewis and Randall the curve BC would be replaced by the approximate dotted curve $B'C$, which is horizontal in the limit of infinite dilution. Obviously this substitution will not produce any serious errors unless the true curve BC is very steep in the dilute region.

While the rule of Lewis and Randall leads to a good approximate answer, a much closer approximation may be had by assuming that the curve of h/r *vs.* r approaches a straight line (slope not necessarily zero) as limit in dilute and even fairly concentrated solutions. Such an assumption can lead to serious error only in the case of dissociating solutes, in which case h/r approaches infinity asymptotically at infinite dilution.

EFFECTS OF EXPERIMENTAL ERRORS

Experimental errors in the determination of the function h'/r will most often enter in the form of constant percentage errors in the activity coefficient a_1/N_1. Thus $\ln (a_1/N_1)$ will most likely be in error by a constant amount ϵ on the average. Such an error is equivalent to an average error ϵ/r^2 in the function h'/r (likewise in h/r). An error so slight as 0.01 per cent in a_1/N_1 at $r = 0.001$ (approximately 0.05 M) will produce an error of 100 in h/r; at infinite dilution any experimental error whatever in a_1/N_1 will produce an infinite error in h/r.

Any finite error made in extrapolating h/r (resp. h'/r) to infinite dilution cannot produce as much error in the final result as is produced by the smallest experimental errors. Thus if it is possible to make the extrapolation without more than a finite error, the values of $\ln (a_2/m)$ obtained from the extrapolated h/r plot will be far more accurate in the region of high dilution than could possibly have been obtained from the experimental data on solvent activities alone.

In many cases—in particular, solutions which follow a Henry's law, Raoult's law, a Van Laar equation or any similar law—it is to be expected that h/r will approach a finite limit at infinite dilution. For any such solution the extrapolation of the h/r *vs.* r curve can certainly be made to within a finite error. Thus in such cases the h/r *vs.* r plot may be used to give a result far more accurate than the data.

On the other hand, for solutions of electrolytes and other dissociating substances, h/r may approach an infinite limit. In the case of dissociating non-electrolytes, the infinite limit may be removed by expressing the mol ratio r in terms of the dissociation products rather than the undissociated substance (reference 2, page 304). In the case of electrolytes it is necessary to introduce the function $h/m^{\frac{1}{2}}$ (in view of the Debye–Hückel theory) in order to make the limit finite. By such special devices these unusual cases may be handled as readily as the more regular cases.

Because of the possibility of true as well as spurious infinite limits of h/r, it becomes necessary to examine the data critically before making a finite extrapolation. Purely accidental experimental errors will be evidenced in the h/r plot by randomly positive and negative values of h/r, which become increasingly great at high dilution. In this case an extrapolation to a finite limit is probably quite safe. However, a systematic error will produce values of h/r which tend definitely to a spurious infinite limit (or very rarely may mask a true infinite limit by cancellation). Thus it becomes important to determine whether an apparent infinite limit of h/r is due to dissociation or to systematic errors.

THE FUNCTION j

The activity of the solvent is frequently determined from data on freezing point lowering. To facilitate the use of such data, Lewis and Randall defined the function

$$j = 1 - (\theta/\lambda m) \tag{15}$$

where θ is the freezing point lowering for a solution of molality m and λ is an appropriate constant. For aqueous solutions the function j is identical with the function h up to moderate concentrations. Thus a plot of j/m *vs.* m for any aqueous solution should coincide with the curve of h/m *vs.* m, at least in the region of dilute solutions. Consequently all that has been said of the function h may be said as well of j in the region of dilute solutions. Fortunately this is the region in which the preceding considerations are of much importance.

SUMMARY

1. A new function $h' = (\mathrm{N}_1/\mathrm{N}_2) \ln (a_1/\mathrm{N}_1)$ is defined which allows the direct calculation of the activity coefficient (a_2/N_2) of the solute from that of the solvent to be made in the same manner that the coefficient (a_2/m) may be calculated from the function h defined by Lewis and Randall.

2. Experimental errors in determining a_1 produce infinite errors in the functions $h/(\mathrm{N}_2/\mathrm{N}_1)$ and $h'/(\mathrm{N}_2/\mathrm{N}_1)$ at infinite dilution.

3. If the curves of $h/(N_2/N_1)$ and $h'/(N_2/N_1)$ *vs.* (N_2/N_1) can be extrapolated to infinite dilution with no more than a finite error, the values of the solute activity coefficients (a_2/N_2) and (a_2/m) obtained from the extrapolated curves will be infinitely more accurate at infinite dilution (i.e., the error is reduced by a factor of ∞) than could be obtained from the experimental data alone. The extrapolation can be made to within a finite error provided the functions $h/(N_2/N_1)$ and $h'(N_2/N_1)$ have finite limits.

4. For an ideal solution $h'/(N_2/N_1)$ should be everywhere zero, while $h/(N_2/N_1)$ has a definite form as a function of (N_2/N_1) with the limiting value of 1/2 and the limiting slope $-1/3$. Different types of deviations from ideality and their effects on the limiting values and limiting slopes of the $h/(N_2/N_1)$ and $h'/(N_2/N_1)$ *vs.* (N_2/N_1) curves are discussed.

REFERENCES

(1) *cf.* HILDEBRAND, J. H.: *Solubility of Non-electrolytes.* American Chemical Society Monograph No. 17. Reinhold Publishing Corporation, New York (1936).

(2) LEWIS AND RANDALL: *Thermodynamics and the Free Energy of Chemical Substances.* McGraw-Hill Book Company, New York (1923).

(3) VAN LAAR: Z. physik. Chem. **72**, 723 (1910); **83**, 599 (1913).

APPROXIMATE RULES FOR SOLUTE ACTIVITIES IN DILUTE SOLUTIONS OF NON-ELECTROLYTES. GENERALIZED FORM OF BURY'S RULE[1]

MERLE RANDALL, W. F. LIBBY, AND BRUCE LONGTIN[2]

Department of Chemistry, University of California, Berkeley, California

Received June 12, 1939

A recent article (3) described the general nature of the function h/r (used in calculating solute activities from solvent activities) for various types of deviation from the ideal solution laws. The behavior and significance of this and related functions in the limit of high dilution, together with a number of other problems, may be made still clearer by the use of series expansions of the various functions involved.

[1] Clerical assistance of the Works Progress Administration O. P. No. 665-08-3-144 is gratefully acknowledged.

[2] Shell Fellow in Chemistry, 1938–39.

POWER SERIES EXPANSION BY METHOD OF RESIDUES

Let y denote any empirical function of x which is capable of expansion into a power series in x. Let the series expansion be

$$y = A_0 + A_1x + A_2x^2 + \ldots + A_nx^n + \ldots \qquad (1)$$

The essential requirement is that all of the derivatives of y exist and be finite at $x = 0$.

It is desired to obtain the coefficients A_0, A_1, A_2, ... A_n, ... etc., directly from the experimental data. This may be accomplished by a relatively simple device. Let us define the series of functions

$$Y' = (y - A_0)/x = A_1 + A_2x + A_3x^2 + \ldots \qquad (2)$$

$$Y'' = (Y' - A_1)/x = A_2 + A_3x + \ldots \qquad (3)$$

$$Y''' = (Y'' - A_2)/x = A_3 + \ldots, \text{ etc.} \qquad (4)$$

Each function is obtained from the preceding function as the difference between that function and the limit which it approaches at $x = 0$, divided by the value of x. The limit approached by each of these functions as x approaches zero is one of the desired coefficients A_0, A_1, A_2, ..., A_n, ...

This procedure is the basis of the special graphical methods developed by Lewis and Randall (2) for the calculation of solute activities. Thus the functions ln (a_1/r) and h/r are the first and second derived functions (Y' and Y'') which would be used in obtaining the series expansion of ln a_1 in terms of the mol ratio r. Likewise the functions θ/m and $-\lambda(j/m)$ are those which would be used in obtaining a series expansion of the freezing point lowering, θ, in terms of the molality m, as is explained later.

The application of this method is further illustrated in figures 1 and 2 by means of a set of experimental data. From the data it is estimated that y approaches the limit A_0 (figure 1). The value of $(y - A_0)$ corresponding to any one point is given by the vertical distance from the point to the horizontal line $y = A_0$. The value of the function Y' corresponding to this point is given as the ratio of this distance to the abscissa (x coördinate) of the point. If the experimental data should fall on a straight line through the point ($x = 0$, $y = A_0$), then Y' would have the same numerical value for all of the experimental points.

The values of Y' obtained from the experimental data are plotted in figure 2. From these values the function Y'' may be obtained by a repetition of the above process. It is to be noted that the points scatter widely in the neighborhood of $x = 0$. This occurs because the experimental errors in y are magnified by dividing by x. The estimated limit A_1 was based chiefly on extrapolation from the higher values of x, where the experimental errors are not so greatly magnified.

As the process is repeated to obtain the higher order coefficients, the experimental errors will become seriously magnified up to successively higher values of x. The estimated values of the coefficients will be based chiefly on the experimental data at higher and higher values of x, until finally the data scatter too widely to allow any reliable estimate of the values of higher coefficients. This merely means that with this number of terms in the series and the estimated coefficients, equation 1 has been made to fit the data within the limits of error. The addition of further terms might alter the shape of the resulting curve slightly but would not cause it to fit the data better.

The proper choice of the coefficient A_0 assures that the curve represented by equation 1 will approach the correct limit at $x = 0$. If there were only the one additional term A_1x, the curve would be a straight line whose slope is so chosen as to fit the experimental data near $x = 0$. The higher terms are present to insure that the curve will fit the data at higher values of x as well. Thus it is only natural that their coefficients should be determined chiefly by the data at higher values of x. When the curve has been made to fit the data up to the highest value of x, the information which the data can give is exhausted, and it is futile to include higher terms in the series.

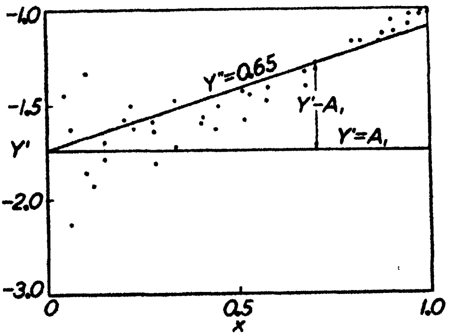

FIG. 1

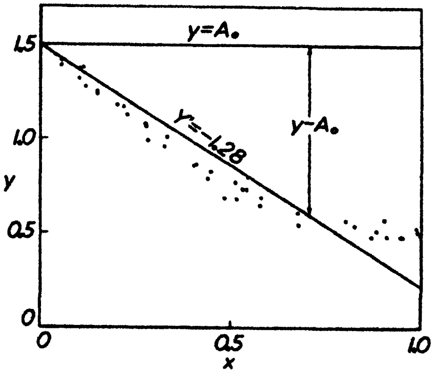

FIG. 2

FIG. 1. Direct plot of a set of data
FIG. 2. Plot of first derived function of the set of data of figure 1

It is always likely that a small error ϵ will be made in estimating the limit A_0 approached by y. The function Y'' will then have the apparent value $(y - A_0 \pm \epsilon)/x$ instead of the correct value $(y - A_0)/x$. Thus an error $(\pm \epsilon/x)$ is produced in Y'. While this error is infinite at $x = 0$, it becomes smaller—until negligible—at higher values of x. Thus if the region in the neighborhood of $x = 0$ is disregarded, the errors made in estimating A_0, A_1, etc. are not cumulative in the estimation of the higher coefficients.

The series expansion may be expressed analytically as a Maclaurin's series. From this standpoint the coefficients $A_1, A_2, \ldots, A_n, \ldots$ can be expressed in terms of the limiting values of the derivatives $\mathrm{d}y/\mathrm{d}x$, $\mathrm{d}^2y/\mathrm{d}x^2, \ldots, \mathrm{d}^ny/\mathrm{d}x^n, \ldots$ at $x = 0$. Thus we obtain the limiting laws

$$\lim_{x\to 0} Y' = A_1 = \lim_{x\to 0} \mathrm{d}y/\mathrm{d}x \tag{5}$$

$$\lim_{x\to 0} Y'' = A_2 = \frac{1}{2!}\lim_{x\to 0} \mathrm{d}^2y/\mathrm{d}x^2 \tag{6}$$

$$\lim_{x\to 0} Y^{(n)} = A_n = \frac{1}{n!}\lim_{x\to 0} \mathrm{d}^ny/\mathrm{d}x^n \tag{7}$$

Thus the coefficient A_1 gives the limiting slope of the curve of y *vs.* x, while the coefficient A_2 depends upon the limiting curvature, and the higher coefficients depend upon the way in which the curvature changes.

One might have started with the derived function Y' rather than the function y, obtaining Y'' as the *first* function derived from Y'. Thus we may also establish the rules

$$\lim_{x\to 0} Y'' = \lim_{x\to 0} \mathrm{d}Y'/\mathrm{d}x \tag{8}$$

$$\lim_{x\to 0} Y^{(n)} = \frac{1}{(n-1)!}\lim_{x\to 0} \mathrm{d}^{(n-1)}Y'/\mathrm{d}x \tag{9}$$

and many similar sets based on the higher functions Y'', etc. as the *first* of the set.

THE h/m RULES

The function $\ln a_1$ (the natural logarithm of the solvent activity, a_1) may be considered as a function of the mol ratio r (i.e., the ratio N_2/N_1 of mol fraction of the solute to that of the solvent), which may in many cases be expressed by a power series in r. To find the coefficients of the series we define the functions

$$y = \ln a_1 \qquad \left[\lim_{r\to 0} y = 0\right] \tag{10}$$

$$Y' = (y - 0)/r = (1/r)\ln a_1 \qquad \left[\lim_{r\to 0} Y' = -1\right] \tag{11}$$

$$Y'' = h/r = (Y' + 1)/r = (1/r)[1 + (1/r)\ln a_1], \quad \text{etc.} \tag{12}$$

The function Y'' is the function h/r used in calculating solute activities.

An interesting rule may be obtained by combining equations 11 and 12 with equation 9. Thus for very dilute solutions

$$\lim_{r\to 0} (h/r) = \lim_{r\to 0} \mathrm{d}(1/r)\ln a_1/\mathrm{d}r = \lim_{r\to 0} \mathrm{d}h/\mathrm{d}r \tag{13}$$

The final member of equation 13 appears, since h differs from $(1/r)\ln a_1$ only by the term unity, which contributes nothing to the derivative. Equation 13 shows that the limiting value of h/r is the limiting slope of a curve of $(1/r)\ln a_1$ *vs.* r. The accuracy to which the limiting slope of this curve may be estimated directly is certainly no greater than the accuracy of the data at high dilution. However, it was shown in the previous article (3) that the limiting value of (h/r) could under some circumstances be estimated far more accurately than the data alone would permit. Thus the plot of (h/r) *vs.* r furnishes a more sensitive means of estimating the limiting slope of the curve of $(1/r)\ln a_1$ *vs.* r.

Lewis and Randall (2) have shown that the solute activity, a_2, is to be obtained by the differential equation

$$-\mathrm{d}\ln(a_2/r)/\mathrm{d}r = \mathrm{d}h/\mathrm{d}r + h/r \tag{14}$$

If $\ln(a_2/r)$ can be expressed by a power series in r and has the value $\ln\gamma_0$ at infinite dilution, equation 5 shows that $\mathrm{d}\ln(a_2/r)/\mathrm{d}r$ has the same limit as $(1/r)\ln(a_2/r\gamma_0)$. Remembering equations 13 and 14, one may therefore write

$$\lim_{r\to 0}(1/r)\ln(a_2/r\gamma_0) = -2\lim_{r\to 0}(h/r) \tag{15}$$

This is an exact statement of the approximate rule of Lewis and Randall that $\ln(a_2/r\gamma_0)$ is equal to $-2h$. For aqueous solutions, in which the activity is taken equal to the molality ($m = 55.51r$) at infinite dilution, it may be written in the form

$$\lim_{m\to 0}\frac{1}{m}\ln(a_2/m) = -2\lim_{m\to 0}(h/m) \tag{16}$$

It is a simple matter to determine the limits within which equation 16 will give the activity coefficient (a_2/m) accurately. To a first approximation (h/r) may be expressed as $(h/r)_0 + Br$, where B is the limiting slope of the curve of (h/r) *vs.* r. To this approximation $\mathrm{d}h/\mathrm{d}r = (h/r)_0 + 2Br$, since h is given as $(h/r)_0 r + Br^2$. Thus integration of equation 14 gives (to this degree of approximation)

$$\ln(a_2/r\gamma_0) = 2(h/r)_0 r + (3/2)Br^2 \tag{17}$$

and for aqueous solutions

$$\ln(a_2/m) = 2(h/m)_0 m + (3/2)B'm^2 \tag{18}$$

where B' is the limiting slope $(B/(55.51)^2)$ of the curve of (h/m) *vs.* m.

Equations 17 and 18 differ from equations 15 and 16 only by the presence of the terms containing the coefficient B. The limiting laws of equations 15 and 16 will give the activity coefficient accurately if the term $(3/2)Br^2$ is negligible. In general they will hold to within an accuracy of 0.01 per cent in $(a_2/r\gamma_0)$ up to the concentration at which $(3/2)Br^2$ has the value $\ln 1.0001 = 10^{-4}$.

It was previously shown (3) that for an ideal solution B has the value $-1/3$. In this case the highest value of r at which this accuracy will obtain is 0.014, corresponding to a molality of 0.80. For cadmium and tin amalgams, with values of $B = 24.4$ and -0.75, respectively, the accuracy of 0.01 per cent in $(a_2/r\gamma_0)$ will hold up to $r = 1.65 \times 10^{-3}$ (0.092 M) and 0.009 (0.53 M), respectively. These last two are cases in which the deviations from ideality are fairly large. In general it may be said that the Lewis and Randall rule, namely, $\ln a_2/r\gamma_0 = -2h$, should hold quite accurately up to at least 0.1 M except in extreme cases. On the other hand, equations 17 and 18 should hold accurately up to the neighborhood of 5 M ($r = 0.1$), as is indicated by the data for cadmium and tin amalgams (3).

In the region in which equation 18 holds, the activity coefficient (a_2/m) is given as

$$\exp\,[2(h/m)_0 m + (3/2)B'm^2]$$

This may be expanded in series to give

$$a_2/m = 1 + 2(h/m)_0 m + [(3/2)B' + 2(h/m)_0^2]m^2 \qquad (19)$$

to the order of approximation of m^2. An exactly similar equation may be written for $(a_2/r\gamma_0)$, with r and B substituted in the right-hand member for m and B'. Noting that r can be expanded as $(N_2 + N_2^2 + \ldots + N_2^n + \ldots)$, this latter equation may be rearranged to give

$$a_2/\gamma_0 N_2 = 1 + [1 + 2(h/r)_0]N_2 + [1 + 2(h/r)_0 + 2(h/r)_0^2 + (3/2)B]N_2^2 \qquad (20)$$

Equations 19 and 20 may be used to calculate the activity directly from the limiting value and limiting slope of the plot of h/r *vs.* r, and are valid up to moderately high concentrations.

FREEZING POINT LOWERING

The freezing point lowering, θ, produced by the presence of solute to the extent of m molal, is a function of the molality, which ordinarily is capable of being expressed by a power series in m. By definition it approaches zero as limit at infinite dilution. In determining the coefficients of the series expansion the functions $\Theta' = \theta/m$, $\Theta'' = (\theta/m - \lambda)/m$, etc. (where

$\lambda = 1.858$ is the limiting value of θ/m) would be defined. The function j/m defined by Lewis and Randall (2) is $-\Theta''/\lambda$.

Equation 6 thus shows that the limiting value of j/m at infinite dilution is given as

$$\lim_{m\to 0} (j/m) = -(\lambda/2) \lim_{m\to 0} d^2\theta/dm^2 \tag{21}$$

This limiting value depends on the curvature of the freezing point *vs.* molality curve. Thus it is evident that the limiting value of (j/m) may be made uncertain by a common tendency to extrapolate to infinite dilution along a straight line.

Similarly equations 7 and 8 show that the limiting slope of the (j/m) *vs.* m plot is given by the equation

$$\begin{aligned}\lim_{m\to 0} d(j/m)/dm &= -(1/\lambda) \lim_{m\to 0} d\Theta''/dm = \\ -(1/\lambda) \lim_{m\to 0} \Theta''' &= -(1/6\lambda) \lim_{m\to 0} d^3\theta/dm^3\end{aligned} \tag{22}$$

The limiting slope depends upon the rate of change of curvature of the freezing point lowering curve at infinite dilution, and is made even more uncertain by the tendency toward linear extrapolation.

Since both θ and θ/m are functions of m, θ/m is also a function of θ. Bury (1) has assumed that (θ/m) can be expanded in a power series in θ, with the limiting value λ at infinite dilution. Thus by equation 5 the limiting value of $[(\theta/m) - \lambda]/\theta$ is equal to the limiting slope, $d(\theta/m)/d\theta$ of a plot of (θ/m) *vs.* θ. Since θ approaches λm in the limit, the limiting value of $[(\theta/m) - \lambda]/\theta$ is also equal to the limiting value of $-j/m$. Bury's rule states that

$$\lim_{m\to 0} (-j/m) = \lim_{m\to 0} d(\theta/m)/d\theta \tag{23}$$

This rule can be given several generalized forms. If θ/m is considered as being expressed by a power series in m, then equation 8 gives

$$\lim_{m\to 0} (-j/m) = (1/\lambda) \lim_{m\to 0} d(\theta/m)/dm \tag{24}$$

since Θ'' differs from θ/m only by the additive constant λ. This particular form is analogous to equation 13. From the considerations established there, it is evident that the plot of j/m *vs.* m or θ together with Bury's rule furnishes a more sensitive and more accurate method of determining the slopes $d(\theta/m)/d\theta$ and $d(\theta/m)/dm$ than the plots of θ/m itself. This is a reversal of Bury's proposal. Bury's rule is valuable in giving better values of θ/m rather than better values of j/m.

In aqueous solutions the activity of water is given to a high degree of approximation in terms of the freezing point lowering as (2)

$$\ln a_1 = -(1/55.51)\,[(\theta/\lambda) + 2.85 \times 10^{-4}\theta^2 + 8.8 \times 10^{-7}\theta^3] + 2.303x \qquad (25)$$

The coefficient of the term in θ^3 is at present quite doubtful, and this term is ordinarily omitted. The function x is that defined by Lewis and Randall[3] to take into account the difference in $\ln a_1$ between the given temperature and the freezing point of the solution. It depends on the heats of mixing, is everywhere zero for ideal solutions, and vanishes at least as rapidly as m^2 in other cases.

From equation 25 and the definition of h/m, it follows that

$$h/m = j/m - 2.85 \times 10^{-4}\,(\theta/m)^2 - 8.8 \times 10^{-7}\,(\theta/m)^2\theta + (55.51 \times 2.303)x/m^2 \qquad (27)$$

In the limit of infinite dilution

$$\lim_{m\to 0}\,(h/m) = \lim_{m\to 0}\,(j/m) - 2.85 \times 10^{-4}\lambda^2 + 55.51X_0 \qquad (28)$$

where X_0 is the finite limit approached by $2.303x/m^2$. Equation 28 gives the value of $(h/m)_0$ needed in equation 19, directly in terms of the freezing point data.

Equation 19 also requires the limiting value, B', of the slope, $\mathrm{d}(h/m)/\mathrm{d}m$, of the curve of h/m *vs.* m. Since by equation 5

$$\lim_{m\to 0}\,[h/m - (h/m)_0]/m = \lim_{m\to 0}\,\mathrm{d}(h/m)/\mathrm{d}m \qquad (29)$$

and

$$\lim_{m\to 0}\,[j/m - (j/m)_0]/m = \lim_{m\to 0}\,\mathrm{d}(j/m)/\mathrm{d}m \qquad (30)$$

these limiting values may be obtained by subtracting equation 28 from equation 27, dividing by m, and passing to the limit. Thus

$$B' = \lim_{m\to 0}\,\mathrm{d}(h/m)/\mathrm{d}m = \lim_{m\to 0}\,\mathrm{d}(j/m)/\mathrm{d}m - 2.85 \times 10^{-4}\lim_{m\to 0}\,[(\theta/m)^2 - \lambda^2]/m - 8.8 \times 10^{-7}\lim_{m\to 0}\,(\theta/m)^3 + 55.51\lim_{m\to 0}\,[2.303x/m^2 - X_0]/m \qquad (31)$$

---

[3] Reference 2, page 289:

$$x = -(1/2.303R)\int_{T'}^{T''}[(\bar{\mathrm{H}}_1 - \bar{\mathrm{H}}_1^0)/T^2]\,\mathrm{d}T \qquad (26)$$

Again equation 5 shows that

$$\lim_{m\to 0}\,[(\theta/m)^2 - \lambda^2]/m$$

has the value

$$\lim_{m\to 0}\,2(\theta/m)\mathrm{d}(\theta/m)/\mathrm{d}m$$

which by equation 24 becomes $-2\lambda^2(j/m)_0$. The term in $(\theta/m)^3$ has the limit λ^3, while we will write X_1 for

$$\lim_{m\to 0}\,[2.303x/m^2 - X_0]/m$$

Equation 31 takes the final form

$$B' = \lim_{m\to 0}\,\mathrm{d}(j/m)/\mathrm{d}m + 5.7 \times 10^{-4}\lambda^2(j/m)_0 + 8.8 \times 10^{-7}\lambda^3 + 55.51X_1 \quad (32)$$

The values of $(h/m)_0$ and B' obtained from freezing points by means of equations 28 and 32 can be used in equation 19 to calculate solute activities with the same accuracy as values obtained from other types of data.

SUMMARY

1. A simple general method of residues is given for obtaining the coefficients in a Maclaurin's series directly from experimental data. The functions (h/m) and (j/m) used in calculating solute activities are shown to form special cases of the application of this method.

2. Equations are given whereby the solute activity may be calculated accurately for solutions up to about 5 *M* from a knowledge of the limiting values of the function (h/m) and the slope of a curve of (h/m) *vs.* m (likewise (j/m) and the slope of a curve of (j/m) *vs.* m) at infinite dilution.

3. It is shown that Bury's rule and analogous rules may be useful in obtaining improved values of freezing point lowerings and solvent activities from extrapolated curves of j/m and h/m *vs.* m, respectively. This follows since in some cases it is possible to extrapolate (j/m) and (h/m) with an accuracy greater than that of the experimental data.

REFERENCES

(1) Bury: J. Am. Chem. Soc. **48**, 3123 (1926).

(2) Lewis and Randall: *Thermodynamics and the Free Energy of Chemical Substances.* McGraw-Hill Book Company, New York (1923).

(3) Randall and Longtin: J. Phys. Chem. **44**, 306 (1940).

POLYIODIDES OF AMMONIUM. I

AMMONIUM IODIDE AND IODINE

T. R. BRIGGS AND K. H. BALLARD

Department of Chemistry, Cornell University, Ithaca, New York

Received June 12, 1939

In the course of a polythermal phase rule investigation of the system ammonium iodide–iodine–water, recently completed in this laboratory, it became necessary to determine the temperature–composition diagram of the system ammonium iodide–iodine. The report on this system, though brief, is offered in the form of a separate paper in the series on the binary systems (1, 2, 3).

TABLE 1

Temperature arrests

NH_4I	FIRST ARREST	SECOND ARREST
per cent	°*C.*	°*C.*
0	114	None
2	111.6	?
4	108.2	?
6	102.4	88.6
8	95.4	88.8
9	92.0	88.8
9.5	90.0	88.9
10	89.2	88.9
11	98.3	88.8
12	106.1	88.8
14	119.0	88.8
16	131.2	88.6
19	146.5	88.1
21	153.2	87.9
22	157.0	87.8
26	169.3	87.6
30	175	?
34	175	?
38	175	None
42	175	None
50	175	None

Before the work was undertaken, however, a few exploratory tests were

TABLE 2

Analyses of the saturated melt

TEMPERATURE	NH₄I
°C.	*per cent*
88.8	10.5
175	29.9
194	31.1
213	30.7
228	31.1
230	31.2

TABLE 3

Boiling points

TEMPERATURE	NH₄I
°C.	*per cent*
184	0
192	12.0
203	20.2
230	31.2
230	42.0
230	50.0

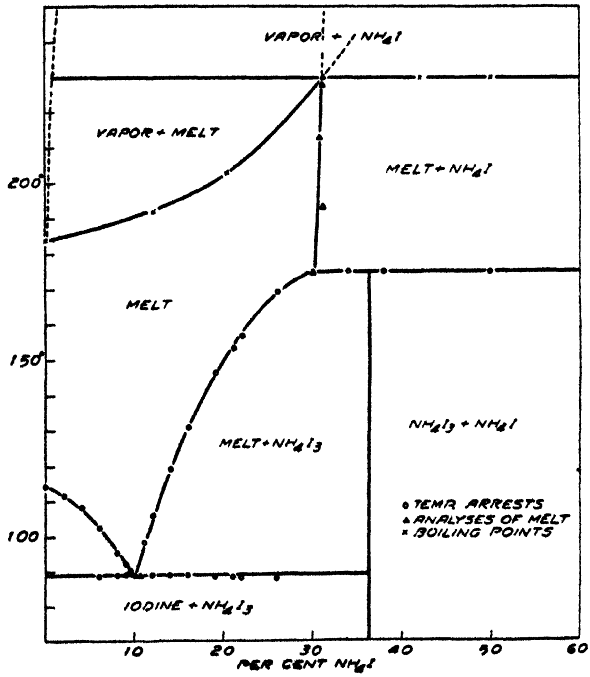

Fig. 1. Ammonium iodide–iodine at approximately 1 atmosphere

made on a small scale in order to find out if danger was to be expected from iodides of nitrogen (4). Accordingly, mixtures of the two components (ammonium iodide was found to be quite soluble in liquid iodine) were melted together and kept in a fused condition for considerable periods of time, after which they were cooled and examined (by percussion) for the presence of explosive substances. None such was ever found.

EXPERIMENTAL

The experimental technique has been described in the paper on potassium iodide and iodine. The data were obtained mainly from cooling curves and analyses of the saturated melt. A few boiling point determinations, made under the prevailing atmospheric pressure (*ca.* 745 mm.), completed the upper part of the phase diagram. The data (compositions in weight per cent) are shown in tables 1, 2, and 3 and the diagram in figure 1.

The temperature–composition diagram requires little discussion. It is entirely similar to the diagram of the system rubidium iodide–iodine. A single polyiodide, melting incongruently at 175°C., separates from the melt; this polyiodide is undoubtedly the triiodide NH_4I_3 (theory 36.3 per cent NH_4I), though no elaborate study of the persistence of the eutectic arrests at 88.9°C. was made to prove this point. The liquid at the eutectic point contains 10.5 per cent ammonium iodide, and the liquid saturated with ammonium iodide as solid phase contains 31.2 per cent ammonium iodide at its boiling point (230°C.). At the transition point (175°C.) it contains 29.9 per cent ammonium iodide, whence it is evident that the solubility of ammonium iodide in liquid iodine, like that of the iodides of potassium, rubidium, and cesium in the same solvent, changes only slightly with the temperature.

REFERENCES

(1) Briggs: J. Phys. Chem. **34**, 2260 (1930); the cesium iodide–iodine system.

(2) Briggs and Geigle: J. Phys. Chem. **34**, 2250 (1930); the potassium iodide–iodine system.

(3) Briggs and Patterson: J. Phys. Chem. **36**, 2621 (1932); the rubidium iodide–iodine system.

(4) *cf.* Johnson: J. Chem. Soc. **33**, 397 (1878).

POLYIODIDES OF AMMONIUM[1] II

THE TERNARY SYSTEM AMMONIUM IODIDE, IODINE, AND WATER

T. R. BRIGGS, K. H. BALLARD, MISS F. R. ALRICH, AND
J. P. WIKSWO

Department of Chemistry, Cornell University, Ithaca, New York

Received June 12, 1939

While there is now no valid reason for questioning the reality of solid ammonium triiodide (*cf.* 7, 3) or for doubting that it can crystallize from aqueous mixtures containing ammonium iodide and iodine (*cf.* 12), no quantitative phase rule studies of the system ammonium iodide–iodine–water have yet been made, though such studies (hitherto always isothermal) have been published for the systems containing the iodides of potassium (15, 9), cesium (5), and barium (16). Accordingly, the investigation to be described in the present paper was undertaken; it consists of two parts,—one a preliminary isothermal study made by Miss Alrich and Mr. Wikswo, and the other an elaborate polythermal study carried out subsequently by Mr. Ballard. The latter's polythermal phase diagram is the first of its type for any polyhalide system.

EXPERIMENTAL

PART I. ISOTHERMAL STUDIES

The isothermal studies were somewhat exploratory in nature and were completed before the polythermal work was begun. Their primary purpose was to find out what solid polyiodides of ammonium are formed in the aqueous system, and to try to identify these solid phases by the method of indirect analysis. The low temperatures (0° and −15°C.) were chosen for the studies because it was thought that they might be favorable for the discovery of new solvated forms. This expectation was borne out by the facts, as will be seen.

The procedure used was essentially the same as that already described in connection with the cesium iodide system (5). The constant-temperature bath was similar to the one developed by Foote and Akerloff (6). Because of the low temperatures which were employed, special precautions had to be taken regarding the sampling of the saturated liquid and the wet solid residues, as well as to prevent condensation of moisture from the air during these operations.

The work at 0°C. was carried out by Miss Alrich. Her data appear in table 1, and her isothermal diagram, showing the details of the extrapolations through the wet solid residues, appears in figure 1. Compositions are in percentages by weight.

TABLE 1

*Ammonium iodide–iodine–water at 0°C.**

SERIAL NO.	SOLUTION		WET SOLID		EXTRAPOLATED SOLID
	NH_4I	I	NH_4I	I	
1	60.8	0			NH_4I
2	57.4	8.4	78.1	4.3	
3	54.5	14.4	72.5	8.8	
4	51.0	22.4	69.6	13.7	
5	49.2	26.1	67.0	16.9	
6	46.8	31.3	66.5	19.8	
7	46.6	31.0	60.6	27.8	NH_4I and NH_4I_3
8	46.5	31.3	52.2	38.3	
9	46.1	32.0	50.0	42.1	
(Mean........	46.4	31.5)			
10	41.9	37.1	38.5	55.4	NH_4I_3
11	39.1	40.9	37.4	56.4	
12	34.0	49.1	35.9	59.0	
13	33.3	50.3	35.6	58.2	
14	28.8	58.0	34.5	61.5	
15	25.9	63.8	32.7	63.6	
16	25.8	64.0	27.1	68.0	NH_4I_3 and NH_4I_5 (?)
17	25.8	63.9	24.2	70.2	NH_4I_5 (?)
18	25.0	64.2	23.8	69.8	
19	24.1	65.4	22.8	70.2	NH_4I_5 (?) and iodine
20	24.0	64.9	11.7	83.2	Iodine
21	23.8	61.4	9.6	85.2	
22	23.5	56.4	9.5	84.0	
23	23.3	52.7	11.1	77.4	
24	22.2	45.6	8.2	80.1	
25	17.4	27.6	4.6	81.5	
26	12.2	15.0	3.3	82.0	
27	3.5	2.9	0.9	80.9	

* Data by Miss Alrich.

The diagram shows definitely that NH_4I_3 (theory 36.3 per cent NH_4I) is one of the solid phases and that it is congruently soluble. But a more interesting matter is the clear indication of a second polyiodide, the solubility curve of which is very short. The data are not numerous enough to permit one to be sure about the formula of this new polyiodide, but the evidence (based upon two tie lines) points to a pentaiodide. If so, it is not congruently soluble.

It will be noticed that Miss Alrich's diagram has been marked "partly metastable." This is because it was later found in the polythermal study that her isothermal curves in the region of the polyiodides, while correct insofar as they represent solid–liquid systems in equilibrium, do not correspond to the stable conditions. This matter will be considered later in more detail.

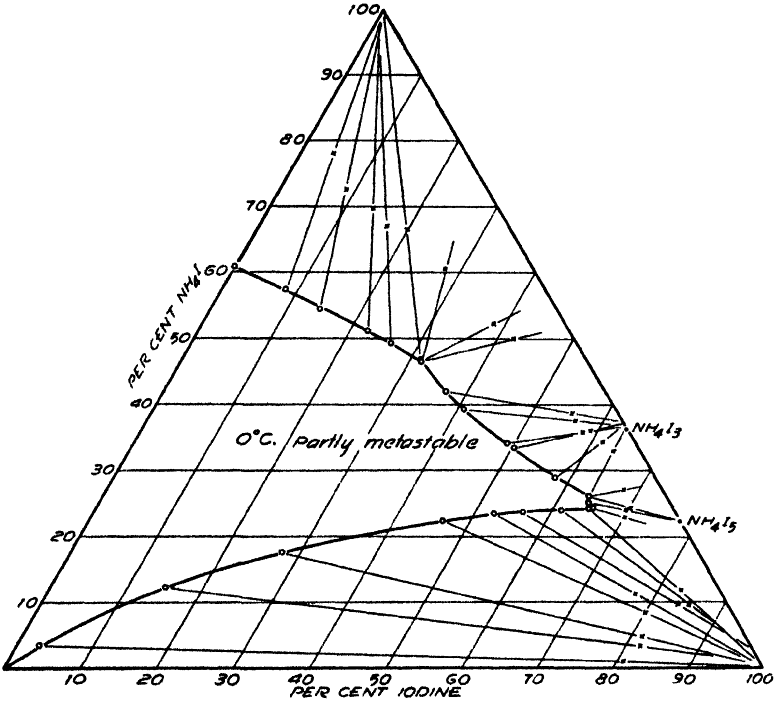

FIG. 1. Isothermal diagram at 0°C.

The work at −15°C. was done by Mr. Wikswo. His data appear in table 2 and his diagram in figure 2. The latter indicates that the solid phases are ice, ammonium iodide, and a polyiodide. The isothermal is apparently stable throughout. The test mixtures used in this work were kept in the thermostat for at least one month before the first analysis was made, and during that time they were shaken each day and the solid residue ground fine with a glass rod.

Fortunately, in the work at −15°C. the trouble due to metastability was detected in time so that the stable diagram could be obtained. The liquidus curves for the ice and for the ammonium iodide were determined first, and what later proved to be metastable systems were found in the course of this work. The metastable systems are serial Nos. 4 and 5 (saturated with ammonium iodide) and Nos. 19, 20, 21, and 22 (in equilibrium with ice) in table 2. They give points on the metastable extensions, respectively, of the liquidus curves of ammonium iodide and ice, as shown in figure 2 by means of the broken lines.

TABLE 2

*Ammonium iodide–iodine–water at −15°C.**

SERIAL NO.	SOLUTION		WET SOLID		EXTRAPOLATED SOLID
	NH_4I	I	NH_4I	I	
1	53.38	0			NH_4I
2	56.91	4.25	80.78	1.94	
3	55.14	8.85	78.38	4.43	
4	53.96 m	11.23 m	73.90	6.39	
5	49.76 m	20.95 m	69.63	12.81	
6	54.67	10.08	41.74	38.40	NH_4I and $NH_4I_3 \cdot 3H_2O$
7	54.61	9.93	67.05	14.96	
8	54.58	9.94	49.05	29.87	
(Mean........	54.6_2	10.0_0)			
9	50.55	9.91	41.56	32.97	$NH_4I_3 \cdot 3H_2O$
10	47.83	9.68	39.69	34.03	
11	45.81	9.78	37.02	40.53	
12	42.03	9.93	37.25	32.36	
13	40.47	10.30	34.47	41.80	
14	39.12	10.19	35.62	32.17	
15	37.08	10.52	33.86	37.13	
16	37.12	10.67	30.51	32.69	$NH_4I_3 \cdot 3H_2O$ and ice
17	37.02	10.52	28.03	22.20	
18	36.72	10.74	22.23	8.53	
(Mean........	36.9_6	10.6_4)			
19	31.74 m	34.38 m	23.30	24.91	Ice
20	34.54 m	21.10 m	25.85	15.70	
21	36.30 m	13.63 m	23.62	8.92	
22	37.03 m	11.06 m	24.62	7.22	
23	38.61	4.40	23.36	2.70	
24	39.54	0			

* Data by J. P. Wikswo; m, metastable.

Finally—and purely by chance—one of the mixtures (serial No. 5 in table 2) gave the invariant solution (serial No. 7) later found to be in equilibrium with ammonium iodide and the polyiodide. Solid taken from this mixture was thereupon used to inoculate other mixtures with the polyiodide (obviously the solid which was failing to appear); whereupon No. 4 changed to No. 6 (ammonium iodide-polyiodide invariant), and Nos. 19, 20, and 21 changed to Nos. 16, 17, and 18, respectively (ice-polyiodide invariant). After this, it was a simple matter to locate the solubility curve of the polyiodide itself (Nos. 9 to 15, inclusive).

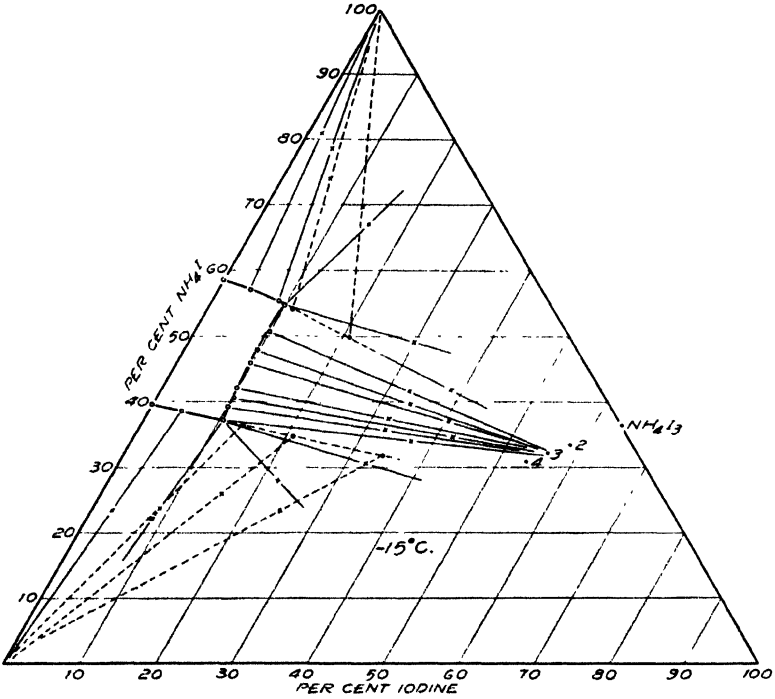

FIG. 2. Isothermal diagram at −15°C.

The tie lines used in ascertaining the composition of the polyiodide at −15°C. have been drawn with great care in figure 2. The points numbered 2, 3, and 4 in the diagram correspond respectively to the dihydrate, trihydrate, and tetrahydrate of NH_4I_3. It is evident from the diagram that the tie lines converge in close proximity to the point (32.0 per cent ammonium iodide, 56.1 per cent iodine) representing the trihydrate; hence the polyiodide has the formula $NH_4I_3 \cdot 3H_2O$. It is not congruently soluble at −15°C.

It is quite evident, from what has gone before, that the isothermal studies were productive of several important results. They showed that at least three polyiodide phases were to be expected in any polythermal study of the ternary system,—i.e., the anhydrous triiodide NH_4I_3, the hydrated triiodide $NH_4I_3 \cdot 3H_2O$, and a third polyiodide which is possibly a pentaiodide. They also gave warning of the difficulties arising from suspended transformation, especially as regards the hydrated triiodide, and indicated that systematic inoculation would have to be used in all future work.

PART II. THE POLYTHERMAL SYSTEM

A. The binary systems

The solubility of iodine in water has been determined at a number of temperatures by Hartley and Campbell,[1] and is so small that it may be neglected in the present work. The ice–iodine eutectic temperature is therefore virtually the same as the melting point of ice, and the eutectic solution contains almost no iodine.

TABLE 3

Solubility of ammonium iodide

TEMPERATURE	NH_4I	TEMPERATURE	NH_4I
°C.	*per cent*	*°C.*	*per cent*
−20	57.6	40	65.6
−10	59.1	50	66.6
0	60.5	60	67.6
10	62.0	70	68.6
15	62.7	80	69.6
20	63.1	100	71.4
25	63.9	120	73.1
30	64.4	140	75.0

When the present investigation was begun, temperature–composition data for the system ammonium iodide–iodine were non-existent and had to be found by means of a special investigation. The results have been presented in a separate communication (3). As expected, the compound NH_4I_3 was found; it decomposes at 175°C. (incongruent melting point) into solid ammonium iodide and melt. The temperature of the eutectic between iodine and NH_4I_3 is 88.9°C., and the eutectic melt contains 10.5 per cent ammonium iodide by actual analysis.

As regards the system ammonium iodide–water, Smith and Eastlack (17) have determined the solubility of the salt, which forms no hydrates, between −19° and 136°C. Their data, interpolated for rounded temperatures and converted into per cent ammonium iodide, are given in table 3.

---

[1] See reference 11; the solubility is 0.028 per cent at 18°C. and 0.092 per cent at 55°C. *Cf.* also the more complete study of the system iodine–water by Kracek (J. Phys. Chem. **35**, 417 (1931)).

According to Guthrie (10) the ice–ammonium iodide eutectic is at −27.6°C. and 55.6 per cent ammonium iodide. Data enabling one to locate the fusion curve of ice, however, were lacking, and had to be determined separately. The data, for rounded temperatures down to the eutectic point, are given in table 4.

At this point mention should be made of the fact that in no case, either in the binary systems containing ammonium iodide or in the ternary system, was there found any indication of an ammonium iodide transition point. While Bridgman (2; *cf.* 17) has shown that there is a second polymorphic modification which is stable below an estimated temperature of −17.6°C. at normal pressure, it is formed too slowly to be observed under the conditions prevailing in the present work.

TABLE 4

Freezing points of ammonium iodide solutions

TEMPERATURE	NH_4I	TEMPERATURE	NH_4I
°C.	*per cent*	*°C.*	*per cent*
0	0	−16	40.7
−3	11.8	−21	47.7
−6	20.7	−24	51.5
−9	28.0	−27.4 E	55.5 E
−13	35.8		

B. Procedure

The procedure employed in the polythermal study was basically the same as that described by Briggs and Geigle (4) in their work on the system potassium iodide–iodine. Cooling curves of various mixtures of the three components contained in a specially constructed jacketed tube were obtained with extreme care. The tube, which was partly immersed in a suitable cooling mixture contained in a large Dewar flask, was fitted with a cork stopper (painted with collodion) carrying the thermometer, a high-speed stirrer, and an opening for sampling and inoculation. All thermometers (marked for stem immersion) were calibrated by intercomparison and by means of a number of standard fixed temperatures.

The first attempts to obtain reproducible cooling curves resulted in complete failure at the low temperatures. Undercooling was extreme,—so much so that a first arrest was often followed by a second which was as much as 10°C. higher. The trouble, however, disappeared immediately after a suitable system of inoculation was employed. The inoculating solid was obtained by dipping a number of fine glass rods into the fused mixture being cooled, and keeping these rods in a stoppered tube held well below the temperature of the arrest being determined.

The procedure finally adopted was to make a preliminary determination of the cooling curve so as to establish the approximate position of each arrest, and to follow this with a second determination accompanied by repeated inoculations begun well above the temperature of the expected arrest. Perfectly reproducible cooling curves were thus obtained, in which consecutive arrests differing from each other by as little as 0.5°C. could be found with certainty.

After the cooling curve had been determined to the satisfaction of the operator, the mixture was remelted, cooled slowly, and subjected to analysis of the liquid phase at appropriate temperatures as determined by a consideration of the cooling curve. Since the operation is really a determination of solubility, care was taken to hold the temperature of the mixture constant at the point decided upon for a sufficient length of time. A period of 15 min. (with rapid stirrings) was found by test to be sufficient for the accuracy necessary in work of this kind. Inoculation, of course, was again essential.

C. *Crystallization from ternary melts*

Before proceeding to the data, the general considerations governing crystallization (i.e., separation of solid phases) in ternary systems will be reviewed. Although the matter was considered in detail by Geer (8) many years ago, it will be presented here again, but in a somewhat different way.

Figure 3 shows a typical triangular projection diagram of a system giving a ternary compound, ABC, melting incongruently. The direction of falling temperature along each boundary line between adjacent fields is indicated on the diagram and is in agreement with the theorem stated by Bancroft (1) and attributed by him to van Rijn van Alkemade (18). Points *E* and *F* are therefore ternary eutectics and *T* is a transition point, while *P* and *Q* are positions of maximum temperature (i.e., dystectics) on their respective boundary lines.

As temperature falls along the boundary *DE*, solid A and solid B separate simultaneously from the melt and the composition of the latter follows the boundary to *E*, where a third solid phase (compound ABC) appears and solidification proceeds to completion at constant temperature and constant composition of the melt (i.e., *E* is an end point of crystallization). If one takes any point on this boundary (such as the one indicated on the diagram by the pair of diverging arrows), and draws through this point the tie lines to A and B, respectively, it is easy to see that separation of A from the melt tends to shift the composition of the melt along the corresponding tie line *away* from A, while separation of B tends to shift the composition along the other corresponding tie line *away* from B. The direction of these individual composition shifts may be represented by means of arrows (i.e., composition vectors) as shown on the diagram; whence it becomes obvious at once that the net effect or resultant of the two simultaneous separations of solid is a shift in the composition of the melt (necessarily along the boundary line) in the direction of the eutectic at *E*,—that is to say, in the direction of *falling* temperature.

Along the boundary *DE*, of course, the two solid phases separate simultaneously as the system is cooled. Such is not the case, however, along the incongruently saturated boundary *EQT*, for, as one of the two solids separates (ABC in this case), the other (B) actually dissolves. The latter phenomenon will be called *negative* separation (or *negative* crystallization) in order to distinguish it conveniently from the opposite case where the solid actually separates, which case will be called *positive*. In figure 3, as a matter of fact, we have positive separation of A and B along *DE* during cooling, positive separation of A and C along *HF*, of B and C along *TG*, of ABC and C along *FT*, and of A and ABC along *EF*; but along *ET* we have *positive* separation of ABC and *negative* separation of B. The composition of the melt will remain on the boundary *ET* during cooling, only

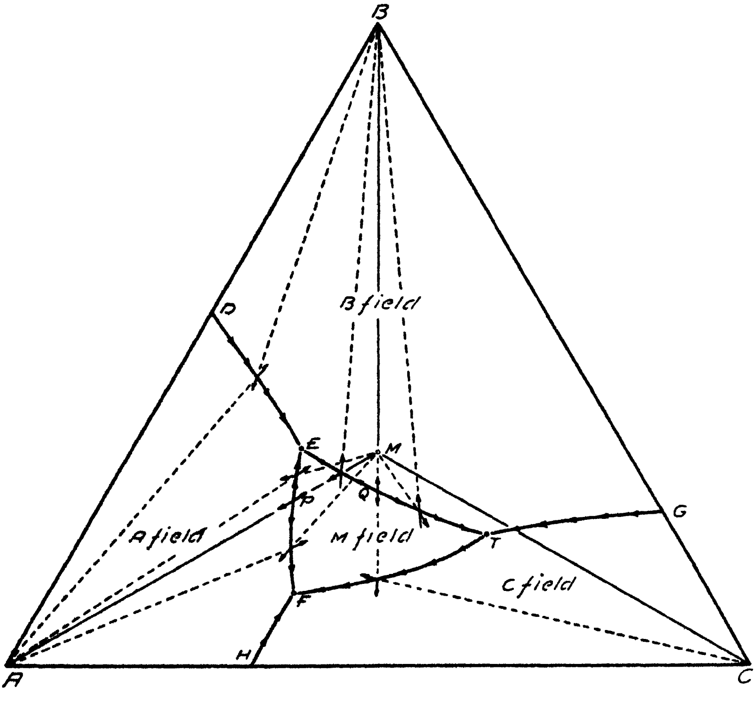

FIG. 3. Typical triangular projection diagram of a system giving a ternary compound, ABC, melting incongruently

so long as a supply of solid B remains to be dissolved. When the solid B is used up, the melt departs from the boundary. Several instances of such a departure were encountered during the work on the ternary system, and until it was clearly understood, the cooling curves were difficult to interpret.

Departure from a boundary is possible whenever one of the two co-existing solid phases exhibits negative separation along the boundary. It is therefore necessary to be able to predict the type of separation which prevails along any part of any given boundary, and in doing this one will find it extremely helpful to make use of the semi-quantitative vectorial method which has been indicated above. The general rule governing the method may be stated as follows:

> "The vectors (arrows) drawn at any point on a boundary curve in order to represent the individual composition shifts which result from the separation, *either positive or negative*, of the respective solid phases during cooling, must conform to the facts that their resultant is *tangential* to the boundary at the place under consideration, and is pointed in the direction of *falling temperature* along the boundary."

The direction of falling temperature, of course, is taken from the point under consideration on the boundary; and the direction must be known from the experimental facts or from the application of van Alkemade's theorem. It is then a simple matter to apply the rule, give the vectors (arrows) their proper direction at any point on a boundary, and find whether the separation required of each solid is positive or negative. Several examples of the application of the rule are shown in figure 3 and are discussed in the next two paragraphs.

If we take any point on the congruent boundary *FT* in figure 3, or any point other than the dystectic *P* on the congruent boundary *FPE*, it is evident that the rule requires that the vectors (arrows) be drawn and directed as shown on the diagram. Positive separation of both solid phases (ABC and C, ABC and A for the two boundaries, respectively) is thus indicated during cooling. It should be observed that at the dystectic *P* the tangential resultant has become equal to zero and there is neither a temperature fall nor a change in the composition of the melt while the two solids are separating.

As regards the boundary *EQT*, the only possible arrangement of the arrows which conforms to the rule is also as shown on the diagram; hence ABC separates positively and B negatively. At the dystectic *Q* the same kind of separation takes place, but the resultant composition shift is again zero and the melt remains at *Q* (temperature constant) as long as any solid B remains undissolved.

In figure 3A part of the same triangular diagram is reproduced on a larger scale, so that some of the crystallization phenomena may be more easily followed. Lines have been drawn (also in figure 3) from *M* (ABC) to the three apexes *A*, *B*, and *C*, respectively, dividing the triangular diagram into three delimiting areas which enable one to tell what *final* solid phases will result when any given melt is cooled to the point of complete solidification. Thus, if the composition of the melt lies in the area bounded by *AMCA*, the final solid phases must be A, ABC, and C, and the end point of solidification (crystallization) must be the eutectic *F*. Similarly, A, ABC, and B must be the final solids in the area *ABMA* and the eutectic *E* the end point, while in the area *BMCB*, C, ABC, and B must be the final solids, and the end point must be the transition point *T*, even though B separates negatively at that point.[2] All of this, of course, is predicated on the assumption that equilibrium between the various phases is constantly maintained.

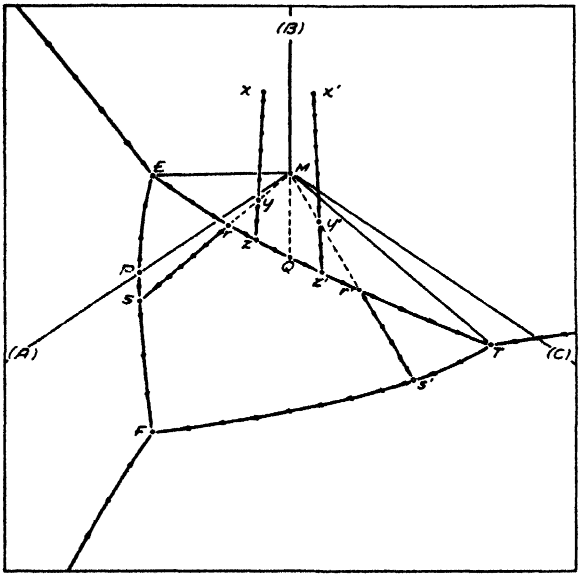

FIG. 3A. Crystallization paths

We are now ready to deduce a few theoretical crystallization paths, beginning, for example, with melt of the composition *x* in figure 3A. Since *x* lies in the delimiting area giving A, ABC, and B as the *final* solids, the eutectic *E* must be the end point of crystallization.

Since *x* also lies in the field of B as solid phase, the latter will be the first to appear on cooling. The temperature will fall continuously as B separates, and the composition of the melt will move along the tie line

---

[2] At a eutectic, of course, all three solids separate positively, but at other three-solid invariants depending on the type, we have negative separation of one solid or negative separation of two solids.

Bxz toward z. When z (on the boundary EQT) is reached, solid ABC will begin to separate, and B will begin to *redissolve* (i.e., separate negatively). The temperature will continue to fall until the eutectic at E is reached, where solidification to a mixture of A, ABC, and B will go on to completion at constant temperature. Between z and E, however, *some but not all* of the solid B separating between x and z will have redissolved. The cooling curve will show a partial arrest at x (separation of B), a second partial arrest at z (separation of ABC), and a complete and final arrest at the eutectic E.

Melt of the composition y (below the critical line EM) follows a more complicated crystallization path in which departure from a boundary line occurs. Since y happens to lie in the delimiting area $AMCA$, the final solids must be A, ABC, and C, and the second eutectic at F is the crystallization end point. As before, solid B appears first on cooling (note however that B cannot be one of the final solid phases), the composition of the melt shifts to z and then along the boundary EQT in the direction of E. It never reaches E, however, but instead at the point r (on the extension of the tie line joining y with M), the melt leaves the boundary line and crosses over the ABC field to the boundary FPE at s.

At the "critical" point r the system consists of melt, solid ABC, and the last trace of solid B, for the solid B which separated between y and z is about to disappear on account of negative separation between z and r. It is not difficult to understand why this must be so, if one keeps in mind the fact that the composition shift from y to the critical point r could have been made stoichiometrically by the removal of ABC *alone* from the original melt. At the point r, of course, the system gains a degree of freedom.

The rest is obvious. When the critical point is reached, the melt moves across the ABC field to s, the temperature falling continuously and ABC separating positively. At s solid A also begins to separate positively, and finally the eutectic is reached at F.

The cooling curve is also worth considering. A partial arrest will be observed at y when B begins to separate, and another at z when ABC starts to form. Some change in the slope of the cooling curve should be noticed at the critical point r, followed by a third partial arrest at s. There will be, of course, a complete and final arrest at the eutectic F.

Melt of the composition x' in figure 3A lies in the delimiting area giving A, ABC, and C as the final solid phases and the transition point T as the end point of crystallization. By following the same line of reasoning as before, it is not difficult to see that the crystallization path follows the tie line $Bx'z'$ to z', and then the boundary EQT to T. Similarly, melt of the composition y' (which lies in the delimiting area giving A, ABC, and C as the final solids, and F as the end point of crystallization) follows the path y' to z', the path z' to r' (critical point where solid B disappears), then departs from the boundary EQT across to s', and finally follows the boundary FT to F.

If one has followed this discussion carefully, it is now apparent that the region (hereinafter called a "critical" area) which is bounded by EQT and the straight lines EM and MT, includes all possible melts which show departure from the boundary EQT on cooling. The recognition of these critical areas is important for the purposes of the present investigation, since several areas of the type appear in the ternary diagram, as will be seen later. For further details, the paper by Geer should be consulted.

D. The ternary diagram

Table 5 contains the temperature-composition data, the compositions being expressed in percentages by weight, as before. The data marked "W" are taken from table 2. The ordinary type of polythermal projection diagram is shown in figure 4. The value given for each invariant is the mean of several independent determinations. Thus, for example, the invariant K was found during four different surveys, with the following results:

Temperature, °C	0.1	0.2	0.2	0.2	
Ammonium iodide	23.84	23.90	23.98	23.91	23.91 ± 0.04 (mean)
Iodine	65.38	65.40	65.51	65.40	65.42 ± 0.04 (mean)

Table 6 contains the various binary and ternary invariants, collected together for the sake of convenience. Some of these, of course, are taken from the paper by Briggs and Ballard on the system ammonium iodide–iodine (3).

Most of the actual composition data are shown on the triangular diagram (figure 4), except in the pentaiodide region, where they have been omitted for the sake of clearness. Figure 5 is the corresponding Jänecke projection on the ammonium iodide–iodine plane. The invariants B and L are eutectics; P and Q are dystectics. The peculiar appearance of the ice–iodine boundary SL on the Jänecke projection should be noted.

Some of the boundary lines merit further comment. A discussion of these boundaries follows.

The boundary SL (ice–iodine). Mention already has been made of the fact that the position of this boundary is most unusual. If one applies the vectorial method described in the preceding section of this paper, one finds that iodine separates negatively along all but a negligible part of the boundary, the critical region being the area inclosed by the boundary and a straight line drawn from the invariant L to a point which is virtually the same as S. Any mixture having a composition within this area will ultimately depart from the boundary during cooling, the crystallization path

TABLE 5

Boundary lines

POSITION ON DIAGRAM	TEMPERATURE	LIQUID		SOLID PHASES
		NH_4I	I	
	°C.			
S	0	0	(0.016)	
SL	−1.9	7.81	8.30	Ice and iodine
SL	−3.2	13.48	18.36	
SL	−4.5	18.53	31.22	
SL	−5.9	21.51	43.50	
SL	−6.9	22.80	48.63	
L	−8.3	23.20	52.48	
LB	−8.1	23.21	51.50	Ice and $NH_4I_3 \cdot 3Aq$
LB		23.61	44.35	
LB	−7.6	23.82	43.40	
LB	−7.6	23.51	43.00	
LB	−7.7	23.82	36.81	
LB	−8.1	24.20	32.60	
LB	−9.0	25.90	23.84	
LB	−10.5	28.91	17.10	
LB	−12.8	33.12	12.32	
LB	−15.0	36.95 W*	10.64 W	
LB	−16.9	39.52	8.97	
LB	−19.1	43.22	7.09	
LB	−23.4	48.70	5.76	
B	−27.9	53.50	4.60	
BC	−23.4	54.41	5.92	NH_4I and $NH_4I_3 \cdot 3Aq$
BC	−19.1	54.62	7.49	
BC	−16.9	54.61	8.61	
BC	−15.0	54.62 W	10.00 W	
BC	−14.9	54.50	9.75	
BC	−12.8	54.13	11.20	
BC	−10.5	53.48	13.33	
BC	−7.2	52.22	17.08	
BC	−4.2	50.49	21.91	
BC	−2.2	48.50	26.35	
C	−0.8	46.72	30.02	
CD	2.0	46.12	31.42	NH_4I and NH_4I_3
CD	9.7	44.79	35.11	
CD	18.0	43.22	39.02	
CD	25.0	42.19	41.89	
CD	61.5	37.92	53.02	
CD	78.7	36.41	55.72	
D	175	29.92	70.13	

---

* The data marked "W" are taken from table 2.

TABLE 5—*Continued*

POSITION ON DIAGRAM	TEMPERATURE	LIQUID		SOLID PHASES
		NH_4I	I	
	°C.			
CG	0.9	44.02	33.72	$NH_4I_3 \cdot 3Aq$ and NH_4I_3
CG	2.9	40.31	39.21	
CG	4.4	37.38	43.82	
CG	5.9	34.61	48.28	
CG	6.7	32.61	51.52	
CG	7.0	30.78	54.13	
CG	6.6	29.31	56.51	
CG	6.0	28.31	58.93	
CG	5.6	27.91	59.90	
CG	5.1	27.36	60.41	
CG	4.1	26.58	62.12	
CG	3.4	25.92	63.52	
CG	2.9	25.51	64.23	
G	2.4	25.08	64.64	
GF	3.0	24.91	65.10	Pentaiodide and NH_4I_3
GF	5.0	24.41	66.13	
GF	5.3	24.45	66.05	
GF	7.0	24.02	67.00	
GF	7.6	23.90	67.10	
F	9.8	23.22	68.75	
GK	1.6	24.78	65.10	$NH_4I_3 \cdot 3Aq$ and pentaiodide
GK	1.2	24.61		
GK	0.6	24.07	65.23	
K	0.2	23.91	65.42	
KL	−0.3	24.00	64.71	$NH_4I_3 \cdot 3Aq$ and iodine
KL	−0.8	23.90	64.21	
KL	−1.8	23.81	63.00	
KL	−2.7	23.82	61.75	
KL	−3.8	23.81	60.50	
KL	−5.0	23 80	58.90	
KL	−6.9	23.63	55.40	
L	−8.3	23.20	52.48	
KF	2.2	23.71	66.12	Pentaiodide and iodine
KF	3.2	23.82	66.50	
KF	4.2	23.71	66.96	
KF	4.4	23.58	67.00	
KF	5.7	23.50	67.00	
KF	6.0	23.62	67.21	
KF	6.8	23.40	67.90	
KF	8.7	23.30	68.13	
KF	8.9	23.16	68.45	
F	9.8	23.22	68.75	

TABLE 5—*Concluded*

POSITION ON DIAGRAM	TEMPERATURE	LIQUID		SOLID PHASES
		NH₄I	I	
	°C.			
FE	11.3	22.93	69.10	NH_4I_3 and iodine
FE	12.0	22.80	69.41	
FE	15.1	22.41	70.17	
FE	20.1	22.02	71.56	
FE	25.0	21.52	72.62	
FE	33.4	20.03	75.03	
FE	45.6	17.88	78.22	
FE	59.2	15.13	82.46	
E	88.9	10.52	89.48	

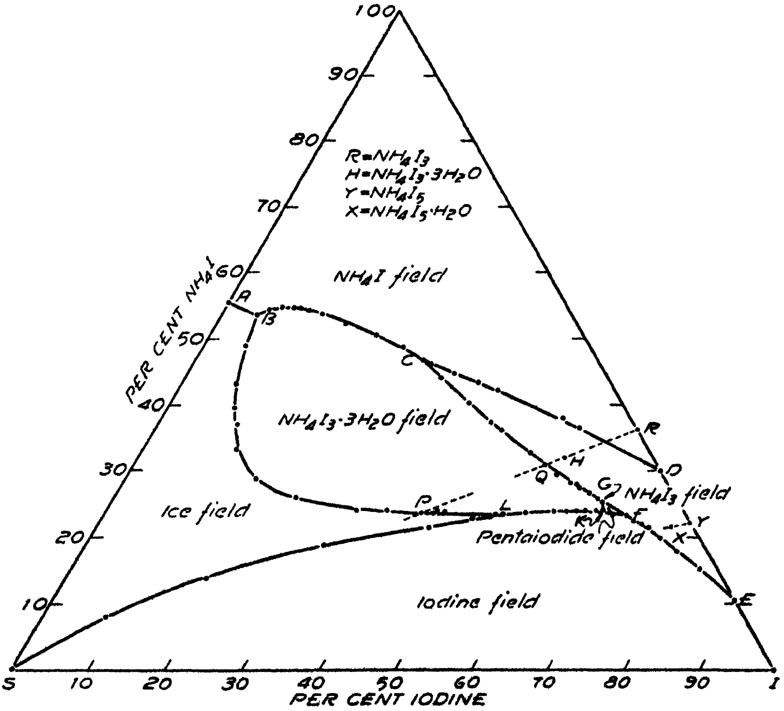

FIG. 4. Polythermal projection diagram

then cutting across the ice field to the boundary *BL*. An interesting study of the theoretical crystallization paths may be made in this region.

The boundary LB (*ice*–$NH_4I_3 \cdot 3H_2O$). The vector test shows that both solid phases separate positively during cooling. The experimental data show a definite though slight temperature maximum (i.e., the dystectic

TABLE 6

Invariant points

POSITION ON DIAGRAM	TEMPERATURE	LIQUID		SOLID PHASES
		NH_4I	I	
	°C.			
A	−27.4	55.5	0	Ice and NH_4I
S	0	0	(0.016)	Ice and iodine
D	175	29.9	70.1	NH_4I and NH_4I_3
E	88.9	10.5	89.5	NH_4I_3 and iodine
I	114	0	100	Iodine
B	−27.9	53.5_0	4.6_0	Ice, $NH_4I_3 \cdot 3Aq$, and NH_4I
L	−8.3	23.2_0	52.4_8	Ice, $NH_4I_3 \cdot 3Aq$, and iodine
C	−0.8	46.7_2	30.0_2	NH_4I, $NH_4I_3 \cdot 3Aq$, and NH_4I_3
G	2.4	25.0_5	64.6_4	$NH_4I_3 \cdot 3Aq$, NH_4I_3, and pentaiodide
K	0.2	23.9_1	65.4_2	$NH_4I_3 \cdot 3Aq$, pentaiodide, and iodine
F	9.8	23.2_2	68.7_6	Pentaiodide, NH_4I_3, and iodine

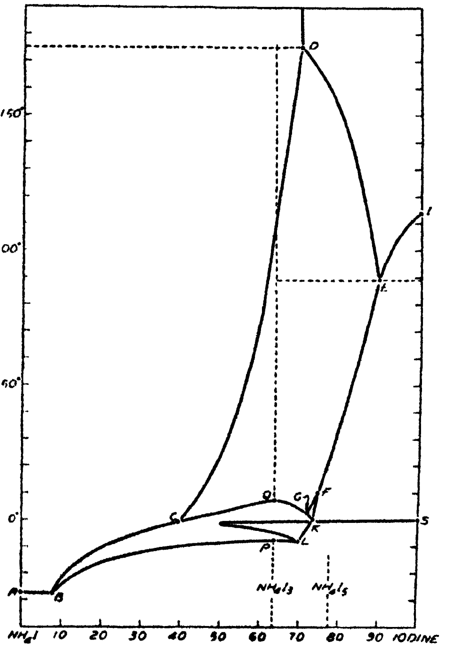

FIG. 5. Jänecke projection on the ammonium iodide–iodine plane

P), not far from the invariant *L*. When the data used in constructing the Jänecke projection (temperature *versus* per cent iodine in the total of ammonium iodide and iodine) were plotted separately on a suitable scale, the position of the maximum temperature (−7.6°C.) was estimated to be at about 64 per cent iodine. Since the theoretical iodine content of ammonium triiodide is 63.7 per cent, all this is evidence (based upon the van Alkemade principle) that the polyiodide present at this boundary is a triiodide. Since it cannot be the anhydrous triiodide, it must be a hydrated form—evidently the trihydrate discovered by Mr. Wikswo in his isothermal study. Further evidence supporting the trihydrate formula will be presented later on.

The boundary CD (NH_4I–NH_4I_3). This boundary is of interest because the vector test shows that solid ammonium iodide separates negatively throughout the whole length from *D* to *C*. The critical region is the area between the boundary and lines drawn from *R* to *C* and from *R* to *D*, respectively.

The boundary CG ($NH_4I_3 \cdot 3H_2O$–NH_4I_3). The vector test shows that the anhydrous triiodide separates negatively along the whole boundary. There is a pronounced temperature maximum at *Q*. The critical region is the area enclosed by the boundary and straight lines drawn from *H* to *C* and from *H* to *G*, the whole giving a system like that shown in figure 3A. Test mixtures were found to depart from the boundary at the points required by the crystallization theory, and then to cut across the field of the hydrated triiodide,—thus failing to show the invariant arrests at *C*, *G*, or *K*, according to circumstances. For instance, in one experiment a mixture lying in the area *QHG* failed to give the arrest at *G* but did give the arrest at *K*, while in another experiment the mixture failed to give both these arrests, and crossed instead directly from the boundary *QG* to the boundary *KL*. Occurrences of this kind were not easy to interpret during the early stages of the investigation.

The Jänecke projection data make it possible to locate with considerable precision the position of the temperature maximum on this boundary, the estimate based upon the actual data being 7.0°C. and 64 per cent iodine in the total of ammonium iodide and iodine. The latter number again corresponds very closely to the iodine content of ammonium triiodide (63.7 per cent) and shows that the two coexisting solids are triiodides.

The "melting points" of the pure polyiodides. Each of the three polyiodides found in the present system melts incongruently when heated. The (stable) melting point—congruent or incongruent—of any solid compound appearing in a ternary diagram is always the point of highest temperature on the (stable) liquidus surface for that compound in the space model; this follows easily from the theory of crystallization in ternary systems if one considers the fact that the melting point of the pure compound (whether congruent or incongruent) must be the same as the end point of crystallization of a mixture the *total* composition of which is stoichiometrically identical with that of the compound. By pure compound is meant the solid free from any adhering liquid phase.

Accordingly, the compound $NH_4I_3 \cdot 3H_2O$ melts incongruently at the temperature (7.0°C.) corresponding to the dystectic Q,—the highest temperature anywhere on the liquidus surface of the trihydrate. As it melts, it gives liquid of the composition Q and solid of the composition R (figure 4), that is, solid NH_4I_3. The latter, in turn, melts at D (175°C.), giving liquid of composition D and solid NH_4I. However, the invariant point F (9.8°C.) is the highest temperature in the field of the pentaiodide; hence this compound melts incongruently at 9.8°C., giving liquid of the composition F and *two* solids, i.e., NH_4I_3 and iodine.

E. The indirect analysis of the solid polyiodides

Further work on the chemical identification of the polyiodides was done during the polythermal study in order to check the results obtained in the isothermal investigations. However, the usual method of analyzing liquid and wet solid residues was largely replaced by the alternate method involving the determination of crystallization paths. The latter method is simple experimentally, since it requires the sampling and analysis of only the liquid phase; but it suffers from the fact that in fields of limited area the crystallization paths are necessarily short and extrapolation is therefore uncertain. As was to be expected, therefore, the best results were obtained in the field of the hydrated triiodide, and the poorest in the field of the pentaiodide. The three polyiodide fields will be taken in order.

The NH_4I_3 *field.* Only crystallization paths were determined in this field; the data are collected in table 7. The paths (excepting Nos. 8 and 9) converge over a wide angle to a very satisfactory focus which is close enough to point R (figure 4) to show that the solid is NH_4I_3, thus confirming the isothermal extrapolations at 0°C. It is not deemed necessary to present a graph showing the crystallization paths in this case.

The $NH_4I_3 \cdot 3H_2O$ *field.* The crystallization paths in this field were in some instances supplemented with analyses of the wet solid residue. The data appear in table 8 and the extrapolations, numbered to accord with the table, in figure 6. With one exception, the extrapolated tie lines pass through the point corresponding to the formula $NH_4I_3 \cdot 3H_2O$, thus confirming the isothermal results at -15°C.

The pentaiodide field. The data are given in table 9 and the graph in figure 7. The crystallization paths (surveys 1 and 3) are necessarily very short, and little is to be expected from the method unless the analytical technique can be greatly improved. The greatest weight should therefore be given to the extrapolations through the wet solid residues, and these, though only two in number, are taken to indicate that the compound is probably a pentaiodide containing one molecule of water, i.e., $NH_4I_5 \cdot H_2O$. If this conclusion is correct, the compound is closely analogous to the hydrated higher polyiodide of potassium, $KI_7 \cdot H_2O$, reported by Grace (9).

F. Interpolated isothermals

Attention should be called to the fact (see the Jänecke projection) that the liquidus surfaces in the ice and $NH_4I_3 \cdot 3H_2O$ fields are comparatively flat in respect to the temperature axis (the other fields are steep). Accordingly, it was thought worthwhile to locate, at least with a moderate degree of accuracy, a number of contour isothermals in these two fields. This was done by carrying out several special thermal surveys—the details of

TABLE 7

Crystallization paths in the NH_4I_3 *field*

PATH NO.	LIQUID		TEMPERATURE
	NH_4I	I	
			°C.
1	36.5	52.4	
	36.5	48.8	25.0
	36.8	44.6	4.6
2	34.8	51.0	
	34.5	48.3	6.0
3	33.3	55.3	
	32.4	51.6	6.8
4	32.0	56.2	
	30.8	54.1	7.0
5	30.0	57.6	
	29.2	56.6	6.6
6	28.6	61.4	
	26.9	61.0	5.0
7	27.0	63.0	
	25.9	63.0	3.6
8	27.2	64.8	
	25.9	64.7	20.4
	25.0	64.5	2.4
9	26.0	67.0	
	24.0	67.3	7.4
10	24.0	69.0	
	22.8	69.5	12.3
11	24.2	70.4	
	22.0	71.6	

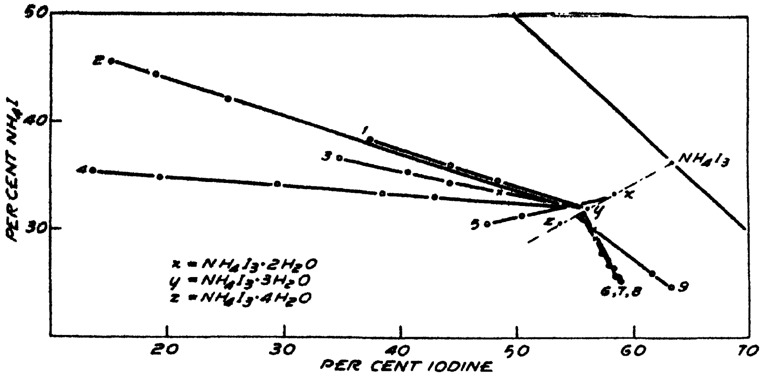

FIG. 6. Extrapolations for the $NH_4I_3·3H_2O$ field

TABLE 8

Crystallization paths in the $NH_4I_3·3H_2O$ *field*

PATH NO.	LIQUID		TEMPERATURE
	NH_4I	I	
			°C.
1	34.60	48.35	5.9
	36.02	44.40	4.4
	38.40	37.50	2.0
2	42.13	25.32	−2.6
	44.41	19.11	−5.6
	45.57	15.18	−8.4
3	34.45	44.26	3.9
	35.40	40.82	2.4
	36.62	34.83	0.2
(Wet solid..............	33.60	48.50)	
4	33.03	43.02	2.4
	33.40	38.47	0.2
	34.20	29.46	−3.1
	34.83	19.38	−8.4
	35.43	13.83	−12.1
5	31.30	50.45	4.8
	30.58	47.50	2.4
6	27.87	57.44	4.9
	26.80	58.00	2.7
	25.76	58.50	0.4
7	26.40	58.35	2.3
	25.43	58.75	0.2
(Wet solid..............	30.00	56.60)	
8	25.26	58.90	0.1
(Wet solid..............	29.24	56.80)	
9	26.00	61.70	3.3
	24.70	63.40	1.3

which need not be given—and combining the results with the data already available from tables 5 and 8. The final data for the various isothermals are collected in table 10; figure 8 shows the isothermals themselves.

The isothermals in the ice field are especially interesting, for if one takes a point on the ice–ammonium iodide side of the field and from it moves along the tie line leading to the iodine apex of the triangular diagram, one finds that the temperature *rises*. This means, of course, that iodine *raises* the freezing point of a solution of ammonium iodide in water. This elevation of the freezing point was observed almost fifty years ago by LeBlanc and Noyes (13; *cf.* also 14) (not with ammonium iodide solutions but with potassium iodide solutions, which behave similarly); and the fact that the freezing point was not lowered as expected was explained, it will be remembered, by postulating the formation of I_3^- ions in the solution.

TABLE 9

Indirect analysis in the pentaiodide field

SURVEY NO.	LIQUID*		WET SOLID	
	NH_4I	I	NH_4I	I
1	24.45	66.30		
	24.73	65.02	23.46	69.35
2	24.18	65.01	23.39	68.80
3	23.58	66.93		
	23.92	65.40		

* Temperatures not recorded in this field.

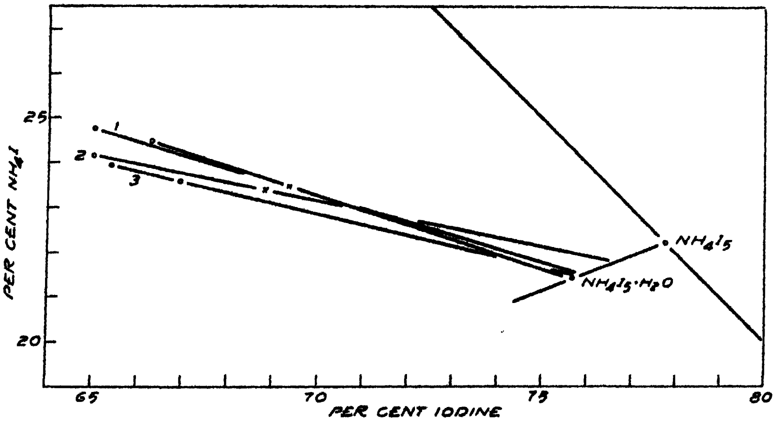

FIG. 7. Extrapolations for the pentaiodide field

Figure 8 also contains the isothermals in the field of the trihydrated triiodide, except that a short section of the −8°C. isothermal near the

TABLE 10

Interpolated isothermals

TEMPERATURE	ICE FIELD		$NH_4I_3 \cdot 3H_2O$ FIELD	
	NH_4I	I	NH_4I	I
°C.				
−24	51.5	0	54.4	5.6
	48.8	5.6	48.8	5.6
−20	46.4	0	54.6	7.1
	43.6	7.1	43.6	7.1
−16	40.7	0	54.6	9.5
	38.0	9.8	38.0	9.8
−12	34.0	0	54.0	12.0
	32.8	7.2	46.8	12.0
	31.6	13.8	35.4	13.1
			31.8	13.8
−8	25.8	0	52.8	16.1
	24.5	9.2	45.5	15.6
	23.8	22.3	34.9	20.0
	24.0	33.5	24.0	33.5
−4	15.0	0	50.2	22.3
	14.8	7.0	43.3	22.0
	15.0	15.0	38.9	24.5
			34.2	28.3
			25.6	44.7
			23.8	60.2
0	0	0	45.3	31.8
			40.4	32.0
			33.5	37.7
			29.0	44.7
			27.6	48.1
			25.6	58.7
			24.0	65.2
4			38.1	42.5
			36.6	43.0
			32.8	46.5
			31.1	49.5
			29.6	51.5
			27.6	57.7
			26.3	62.6

eutectic *L* (−8.3°C.) has been omitted because it cannot be shown satisfactorily in the drawing. The approximate position of the 25°C. isothermal has also been included; likewise the isothermal at 0°C.

It is apparent from the diagram (figure 8) that Miss Alrich's 0°C. isothermal is quite different from the one obtained in the polythermal study. It is now evident that she should have obtained the anhydrous triiodide along only a very short portion of the isothermal near the invariant *C*, that she should have found the hydrated triiodide along an extensive and strongly curving intermediate portion, and that she should have just missed the pentaiodide, in all probability. Actually, she missed the hydrated triiodide entirely.

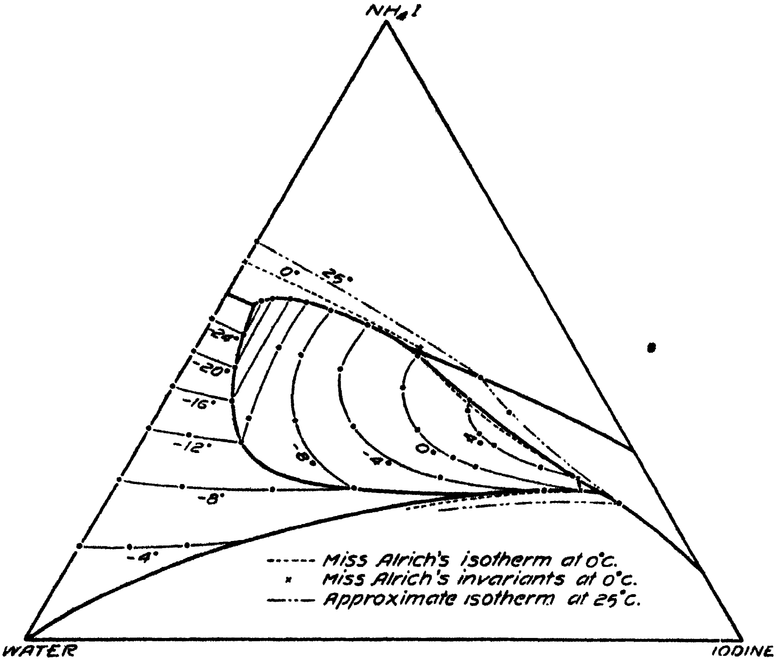
NH₄I
0°
25°
-24°
-20°
-16°
-12°
-8°
-4°
-8°
-4°
0°
------ Miss Alrich's isotherm at 0°C.
× Miss Alrich's invariants at 0°C.
—··— Approximate isotherm at 25°C.
WATER
IODINE

Fig. 8. Isothermals

However, if one recalls the trouble experienced in getting the hydrated triiodide to form even at −15°C., and the similar difficulty which confronted the polythermal work until inoculation was used, it is easy to see that Miss Alrich was dealing with metastable systems in the polyiodide region. The diagram shows clearly (*cf.* figure 8) that, allowing for small experimental discrepancies, the position of her isothermal is what it should be on the assumption of an extreme lag in the formation of the hydrated triiodide and little or no lag in the formation of the anhydrous triiodide or of the pentahydrate, an assumption which has plenty of experimental facts to support it. The 0°C. isothermal is not incorrect, but it does not represent the stable system.

Before this paper is concluded, the various polyiodides of ammonium which are formed in the presence of water will be compared briefly with those formed by the alkali metals. The work already accomplished in this laboratory and elsewhere, while in no single instance so complete as is the present study of the ammonium system, nevertheless indicates fairly conclusively that cesium and rubidium[3] form only unhydrated polyiodides. These are CsI_3, CsI_4, and RbI_3, respectively. On the other hand, potassium and sodium—and undoubtedly also lithium, which however has not been studied systematically—seem to form only hydrated polyiodides. In the case of potassium, for example, Grace has reported the compounds $KI_3 \cdot H_2O$ and $KI_7 \cdot H_2O$, and in a polythermal study now approaching completion in this laboratory, two additional solid forms have been discovered. Both of these new polyiodides are hydrated solids, and one is definitely known to be $KI_3 \cdot 2H_2O$. The system containing sodium iodide is also being investigated; and in this system three curiously complex and strongly hydrated polyiodides have been found. The ammonium system is the only one giving both hydrated and unhydrated polyiodides; it is therefore the intermediate case in the series cesium, rubidium, ammonium, potassium, sodium, and lithium.

SUMMARY

The more important results of this paper may be summarized as follows:

1. The temperature–composition diagram of the ternary system ammonium iodide–iodine–water has been completed. The diagram is restricted to solid–liquid systems in air at approximately normal pressure.

2. The solid phases are ice, NH_4I, iodine, NH_4I_3, $NH_4I_3 \cdot 3H_2O$, and probably a pentaiodide having the formula $NH_4I_5 \cdot H_2O$. Each of the polyiodide fields is incongruent.

3. Pure solid NH_4I_3 melts incongruently at 175°C., decomposing into binary liquid and solid NH_4I. Pure solid $NH_4I_3 \cdot 3H_2O$ melts incongruently at 7.0°C., decomposing into ternary liquid and solid NH_4I_3. The pure solid pentaiodide melts incongruently at 9.8°C., giving ternary liquid, solid NH_4I, and solid iodine.

4. A convenient graphical method of predicting the separation of solid phases along field boundaries has been described and applied to the general problem of crystallization from ternary melts.

5. The problem of suspended transformation has been considered. Of the three polyiodides, the trihydrated triiodide is by far the slowest to form.

6. As regards its tendency to form hydrated polyiodides, ammonium is

---

[3] Unpublished isothermal studies carried out in this laboratory show that RbI_3 (anhydrous) is the only solid polyiodide in the system rubidium iodide–iodine–water at 0° and 25°C.

the intermediate case in the series cesium, rubidium, ammonium, potassium, sodium, and lithium.

7. The polythermal diagram shown in this paper is the first for any ternary polyhalide system.

REFERENCES

(1) BANCROFT: The Phase Rule, p. 149. Journal of Physical Chemistry, Ithaca, New York (1897).
(2) BRIDGMAN: Proc. Am. Acad. Arts Sci. 52, 136 (1916–17).
(3) BRIGGS AND BALLARD: J. Phys. Chem. 44, 322 (1940).
(4) BRIGGS AND GEIGLE: J. Phys. Chem. 34, 2250 (1930).
(5) BRIGGS, GREENAWALD, AND LEONARD: J. Phys. Chem. 34, 1951 (1930).
(6) FOOTE AND AKERLOFF: Ind. Eng. Chem., Anal. Ed. 3, 389 (1931).
(7) FOOTE AND BRADLEY: J. Phys. Chem. 37, 29 (1933).
(8) GEER: J. Phys. Chem. 8, 357 (1904).
(9) GRACE: J. Chem. Soc. 1931, 594.
(10) GUTHRIE: Phil. Mag. [4] 49, 213 (1875).
(11) HARTLEY AND CAMPBELL: J. Chem. Soc. 93, 741 (1908).
(12) JOHNSON: J. Chem. Soc. 33, 397 (1878).
(13) LEBLANC AND NOYES: Z. physik. Chem. 6, 385 (1890).
(14) OSAKA: Z. physik. Chem. 38, 743 (1901).
(15) PARSONS AND WHITTEMORE: J. Am. Chem. Soc. 33, 1933 (1911).
(16) RIVETT AND PACKER: J. Chem. Soc. 1927, 1342.
(17) SMITH AND EASTLACK: J. Am. Chem. Soc. 38, 1500 (1916).
(18) VAN ALKEMADE, VAN RIJN: Z. physik. Chem. 11, 289 (1893).

POLYIODIDES OF POTASSIUM. II

THE TERNARY SYSTEM POTASSIUM IODIDE–IODINE–WATER

T. R. BRIGGS, K. D. G. CLACK, K. H. BALLARD, AND
W. A. SASSAMAN

Department of Chemistry, Cornell University, Ithaca, New York

Received July 24, 1939

The present paper—a companion to the one published several years ago on the binary system potassium iodide and iodine (3)—describes an isothermal and polythermal phase rule study of the system potassium iodide–iodine–water. This study, which has been in progress for several years, consists of two preliminary isothermal surveys—one at 25°C. by Mr. Sassaman and another at 0°C. by Mr. Ballard—followed by a much more detailed polythermal survey carried out for the most part by Mr. Clack, who employed the procedure already described in the paper on the system ammonium iodide–iodine–water (2). The investigation in all instances was confined to solid–liquid systems in air under approximately normal pressure.

PART I. ISOTHERMAL STUDIES

In conformity with the procedure adopted in the case of the ammonium iodide system, the isothermal studies were essentially exploratory in nature and preceded the work on the polythermal phase diagram. The experimental procedure has been described in the paper on the system cesium iodide–iodine–water (4).

The 25°C. isothermal

It will be recalled that as early as 1908 Foote and Chalker (9) made a brief phase rule investigation of the ternary system at 25°C. and reported finding three invariant solutions, saturated respectively with $KI–KI_3$, $KI_3–KI_7$, and KI_7–iodine. In 1911, however, Parsons and Whittemore (15), who published what was long accepted as being a sufficiently complete determination of the whole isothermal at 25°C. and who employed the Schreinemakers–Bancroft method of indirect analysis, failed to confirm the findings of Foote and Chalker, locating only one invariant solution, apparently saturated with potassium iodide and iodine. Parsons and Whittemore concluded, accordingly, that Foote and Chalker's polyiodides were non-existent, and this conclusion later (1930) received what seemed to be additional support from the work of Briggs and Geigle on the binary system potassium iodide and iodine, where it was demonstrated that no polyiodides—not even KI_3—separated from the anhydrous melts.

In 1931, however, the whole subject was reopened by Grace (10), who again took up the problem after pointing out that Parsons and Whittemore had not, as a matter of fact, made a sufficient number of solubility determinations in the critical region covering the Foote and Chalker invariants. Grace accordingly made a more careful study in that region, and, employing various phase rule procedures, concluded that three invariant solutions were really present in the ternary system at 25°C., as Foote and Chalker had claimed, but that these were saturated respectively with $KI–KI_3 \cdot H_2O$, $KI_3 \cdot H_2O–KI_7 \cdot H_2O$, and $KI_7 \cdot H_2O$–iodine in place of the unsolvated polyiodides assumed by Foote and Chalker. He then went on to suggest that although the polyiodides KI_3 and KI_7 do not exist as stable solids, they nevertheless can be formed in the presence of certain solvents in the form of solvated ternary compounds (*cf.* 8, 11, 14, 5).

However, a critical examination of Grace's extrapolation data, on which in part he based his formulas for the two polyiodides mentioned above, disclosed to us the fact—admitted by Grace himself—that these data were not satisfactorily convergent. Accordingly, we decided to begin the present work with a careful redetermination of the whole 25°C. isothermal,

TABLE 1

Potassium iodide–iodine–water at 25°C.

SERIAL NO.	LIQUID		WET SOLID		EXTRAPOLATED SOLID
	KI	I	KI	I	
1	60.15	0			KI
2	56.91	6.59	84.15	2.46	
3	46.56	26.76	82.13	8.97	
4	36.95	46.94	76.74	17.36	
5	32.54	57.05	70.84	24.64	
6	30.84	60.89	75.05	21.48	
7	30.12	61.97	65.10	30.90	
8	30.29	62.11	55.52	40.73	KI and $KI_3 \cdot H_2O$
9	29.86	62.45	39.99	54.84	
Average.........	30.0_8	62.2_8			
10	30.03	63.02	36.99	58.66	$KI_3 \cdot H_2O$
11	29.12	63.80	35.26	59.62	
12	28.90	64.18	36.20	59.29	
13	28.50	64.51	36.50	58.96	
14	27.33	66.42	35.58	59.89	
15	27.31	66.41	28.88	67.66	$KI_3 \cdot H_2O$ and $KI_7 \cdot H_2O$
16	27.24	66.47	26.77	69.89	
17	27.22	66.64	20.94	76.90	
18	27.19	66.53	22.39	73.90	
Average.........	27.2_4	66.5_1			
19	26.98	66.57	20.63	75.98	$KI_7 \cdot H_2O$
20	26.67	66.83	21.89	73.92	
21	26.22	67.31	20.62	75.98	
22	25.96	67.53	19.67	77.16	
23	25.80	67.71	19.90	76.86	
24	25.75	67.80	19.27	77.65	
25	25.72	67.74	16.11	80.70	$KI_7 \cdot H_2O$ and iodine
26	25.58	67.88	8.46	89.87	
27	25.61	67.67	14.90	81.67	
Average.........	25.6_4	67.7_6			
28	25.57	67.68	9.63	87.94	Iodine
29	25.28	67.26	10.52	86.29	
30	25.01	65.94	8.70	88.07	
31	24.89	57.03	6.71	88.42	
32	19.18	25.37	2.35	91.34	
33	10.87	10.49	1.31	89.63	
34	2.09	1.62			

for at the time we were admittedly prejudiced in favor of the work of Parsons and Whittemore, though recognizing its deficiencies. The redetermination resulted in a complete confirmation of Grace's main conclusions.

The data—compositions given in percentages by weight—appear in table 1 and the isothermal is shown in figure 1. For obvious reasons it is possible to show on this diagram only a few of the data in the region of the polyiodides; instead these are shown in figure 2, which gives the details of the Schreinemakers–Bancroft extrapolations in the latter region. The isothermal in figure 1 also shows the data of Parsons and Whittemore with the exception of their serial Nos. 8, 9 and 18,—the last being the supposed KI–iodine invariant.

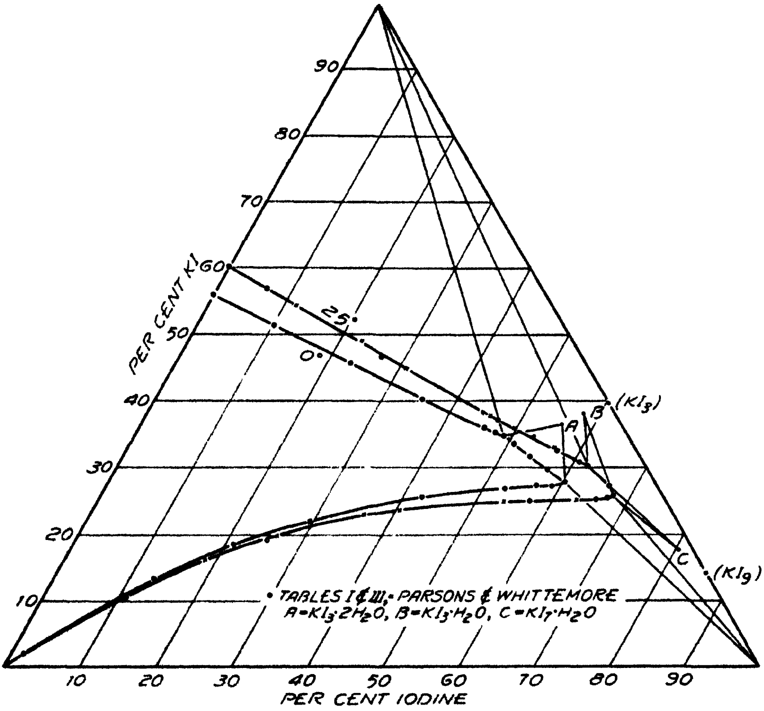

FIG. 1. Isothermals

It is evident from the second diagram that the extrapolation method is beset with difficulties because of the shortness of the polyiodide solubility curves and their general position in respect to the respective polyiodide compositions. Nevertheless, the extrapolations are reasonably conclusive,—especially as regards the first polyiodide (compound B in figure 1), where the tie lines indicate convergence at about the point (58.0 per cent iodine and 37.9 per cent potassium iodide) which corresponds to the formula $KI_3 \cdot H_2O$.

The other polyiodide (compound C in figure 1) was still more difficult to identify by the method. Only a narrow and slightly convergent band of tie lines was obtained; but this band definitely passes through the point (80.5 per cent iodine and 17.6 per cent potassium iodide) corresponding to the formula $KI_7 \cdot H_2O$. It also passes not far from the point (see figure 1) representing the anhydrous polyiodide KI_9, but there seems to be little reason for giving this possibility serious consideration. It is fairly certain that the compound is the monohydrate of KI_7, in agreement with the work of Grace.

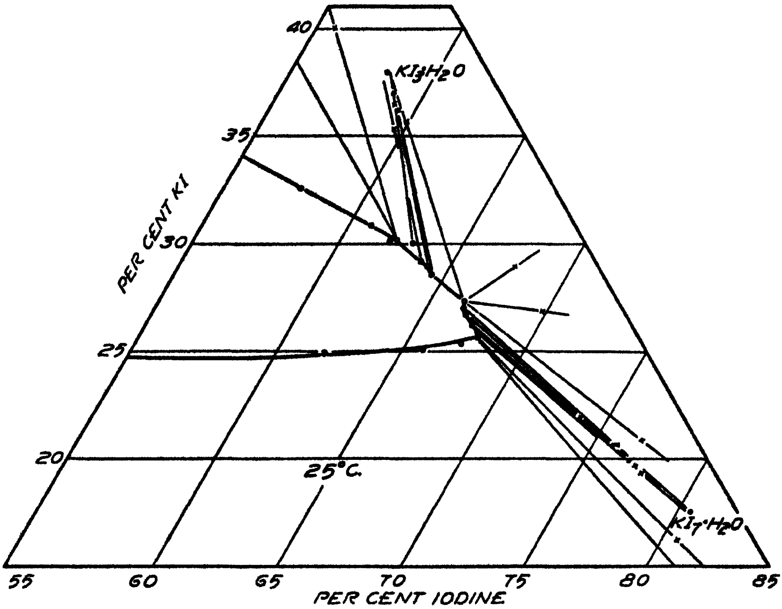

FIG. 2. Extrapolations in the region of the polyiodides at 25°C.

The various determinations of the invariant compositions have been assembled in table 2. The general agreement between Grace's determinations and those of Sassaman is good, except perhaps in the case of the invariant saturated with $KI_7 \cdot H_2O$–iodine. It may seem strange, however, to find invariants by Parsons and Whittemore included in the table—this of course is done only tentatively—in view of the undoubted reality of Grace's polyiodides. The value assigned to Parsons and Whittemore for the KI–$KI_3 \cdot H_2O$ invariant is the composition of the liquid phase in their serial No. 8. The wet solid residue in equilibrium with this solution was reported to contain 56.1 per cent iodine and 40.0 per cent potassium iodide, giving a tie line that did not pass as expected to the potassium iodide apex of their triangular diagram, but did intersect the potassium iodide–iodine side of the diagram *between* KI *and* KI_3. Parsons and Whittemore appear to have considered this determination erroneous—i.e., not representing a mixture in equilibrium—since the tie line for their serial No. 9 (which contained more iodine than No. 8) did pass to the potassium iodide apex. They therefore ignored No. 8; whereas it is possible that it was correct and was actually the invariant between KI and $KI_3 \cdot H_2O$. Note that the composition of the liquid phase is fairly close to the invariant composition as determined by Grace and by Sassaman, and much closer than the determination by Foote and Chalker.

TABLE 2

Invariant solutions at 25°C.

SOURCE	SOLIDS	KI	I
Foote and Chalker	KI and $KI_3 \cdot H_2O$	29.2	64.1
Grace		30.3	62.0
Sassaman (table 1)		30.1	62.3
Parsons and Whittemore (?)		29.7	62.8
Foote and Chalker	$KI_3 \cdot H_2O$ and $KI_7 \cdot H_2O$	27.1	66.8
Grace		27.3	66.1
Sassaman (table 1)		27.2	66.5
Foote and Chalker	$KI_7 \cdot H_2O$ and iodine	25.7	68.9
Grace		26.1	68.0
Sassaman (table 1)		25.6	67.8
Parsons and Whittemore (?)		26.0	68.1

The second invariant ($KI_7 \cdot H_2O$–iodine) ascribed tentatively to Parsons and Whittemore in table 2 is their serial No. 18. They supposed this to be saturated with potassium iodide and iodine; if this were true it would have had to be metastable in accordance with what we now know about the system. In proving that it was really an invariant, Parsons and Whittemore made only two independent analyses of wet solid residues, obtaining one tie line which passed through the iodine apex—in itself proving little—and a second which intersected the potassium iodide–iodine side of the triangular diagram, be it noted, *between* KI_7 *and iodine.* It is therefore quite possible that the invariant was really saturated with iodine and the hydrated heptaiodide instead of iodine and potassium iodide; note also the good agreement with Sassaman's and Grace's determinations, especially with that of Grace.

The 0°C. isothermal

Mr. Ballard's data are collected in table 3. The isothermal is shown in figure 1 and the details of the extrapolations appear in figure 3, plotted with rectangular coördinates. The extrapolations are definitely conclusive; convergence in the polyiodide field occurs close to the point (55.7 per cent

TABLE 3

Potassium iodide–iodine–water at 0°C.

SERIAL NO.	LIQUID		WET SOLID		EXTRAPOLATED SOLID
	KI	I	KI	I	
1	55.86	0			KI
2	51.43	10.21	78.17	4.42	
3	46.01	23.10	71.40	12.09	
4	40.34	35.23	68.78	18.36	
5	35.96	45.62	59.07	29.05	
6	35.20	47.50	59.05	30.30	
7	34.92	48.62	55.97	32.75	
8	35.04	48.83	43.08	46.31	KI and $KI_3 \cdot 2H_2O$
9	34.86	48.92	42.17	47.37	
10	34.49	48.93	41.57	47.66	
11	34.86	48.36	36.35	50.98	
Average.........	34.8_1	48.7_6			
12	34.27	49.39	36.01	54.12	$KI_3 \cdot 2H_2O$
13	33.51	50.75	34.91	53.03	
14	32.77	52.12	34.10	53.29	
15	31.64	53.77	33.33	54.58	
16	30.63	55.58	34.76	55.71	
17	29.60	57.18	32.03	56.61	
18	28.95	58.32	32.01	57.31	
19	28.20	59.60	35.27	56.31	
20	27.78	60.26	30.82	59.81	$KI_3 \cdot 2H_2O$ and iodine
21	27.76	60.40	32.81	60.24	
22	27.52	60.43	29.20	64.21	
23	27.40	60.30	25.69	66.48	
24	27.37	60.42	22.79	69.71	
25	27.44	60.25	14.11	79.75	
Average.........	27.5_5	60.3_4			
26	27.09	58.76	11.04	82.77	Iodine
27	27.19	56.79	13.53	78.58	
28	26.63	52.99	13.58	76.53	
29	25.36	42.28	9.05	79.10	
30	21.84	29.56	5.57	81.98	
31	18.40	21.12			
32	13.22	13.39			

iodine and 36.4 per cent potassium iodide) which corresponds to the formula $KI_3 \cdot 2H_2O$ (compound A in figure 1). The solid is certainly a *dihydrated* form of KI_3, a compound hitherto unreported in the literature. It is congruently soluble at this temperature.

PART II. THE POLYTHERMAL SYSTEM

A. The binary systems

The system iodine–water has been discussed in the paper on the ternary ammonium iodide system (2) and the diagram (in mole percentages, however) for the system potassium iodide–iodine will be found in the paper by Briggs and Geigle (3). In the latter system, the solid phases separating above the eutectic (80.8°C. and 15.7 per cent potassium iodide by weight) are potassium iodide and iodine, and no indication was found of the two liquid layer system which Fialkow (7) recently claimed to have observed just above the eutectic.

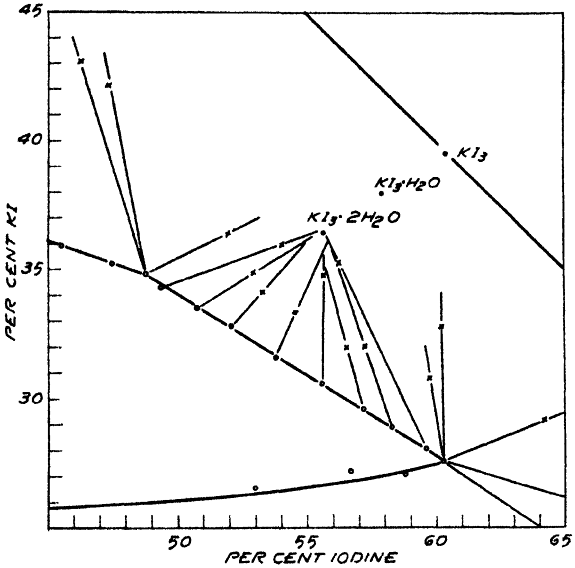

FIG. 3. Extrapolations in the region of the polyiodide at 0°C.

Complete data for the system potassium iodide–water are available (12). For the sake of convenience, the data needed in the present work have been assembled in table 4. According to the table, the eutectic between ice and potassium iodide lies at −23.02°C. and 52.2 per cent potassium iodide, but de Coppet's (6) temperature is −22.65°C., which is more consistent with the temperatures observed in the present investigation.

B. Procedure

The procedure was essentially the same as that described in the paper on the ternary ammonium iodide system (2). The cooling curves were obtained with extreme care, and inoculation with solid was employed throughout. Owing to the complexity of the system, the interpretation of many of the cooling curves was not easy and required constant use of the principles determining crystallization from ternary melts, of which principles a résumé will be found in the paper on the ternary ammonium iodide system (2). The phenomenon of departure from a field boundary line during cooling was very often observed and had to be given careful consideration.

TABLE 4

The binary system potassium iodide–water

TEMPERATURE	KI	TEMPERATURE	KI
Ice and solution		KI and solution	
°C.	*per cent*	*°C.*	*per cent*
−1.69	7.66	−20.0	52.75
−3.37	14.2	−15.0	53.6
−5.0	*ca.* 20.3	−10.0	54.5
−6.80	25.0	−5.0	55.3
−10.0	*ca.* 32.5	0	56.2
−10.35	33.25	5.0	56.9
−15.0	*ca.* 41.5	10.0	57.6
−17.5	45.35	15.0	58.2
−20.0	*ca.* 48.8	20.0	58.8
−23.02 E	52.2	25.0	59.5
		30.0	60.3
		40.0	61.3
		100	67.4

From *International Critical Tables* **4**, pp. 239, 259.

C. The ternary diagram

The temperature–composition data which were obtained from the cooling curves and from the analyses of the saturated liquid have been collected in table 5. Most of the data were obtained by Mr. Clack, but some additional measurements were made later—and entirely independently—by Messrs. J. L. Eaton and S. S. Hubard, to whom the authors are deeply indebted. In table 5, the serial numbers which represent determinations by Eaton and Hubard, respectively, are indicated by the letters E and H.

The triangular projection diagram is shown in figure 4, while figure 5 is an enlarged portion of the same diagram. Figure 6 shows the interesting part of the Jänecke projection on the potassium iodide–iodine plane. Most of the actual analyses appear as separate points in figures 5 and 6,

TABLE 5

Temperature–composition data

SERIAL NO.	POSITION ON DIAGRAM	TEMPERATURE	LIQUID	
			I	KI
		°C.		
1	AB	−22.7	8.77	48.42
2	AB	−23.0	15.62	45.99
3	AB	−23.3	16.63	45.43
4	B	−23.6	19.36	44.15
5	B	−23.6	19.62	44.08
6	B	−23.6	19.47	44.16
7	B	−23.7	19.39	44.11
8	BC	−17.6	26.90	41.49
9	BC	−12.1	35.14	39.09
10	BC	−5.6	42.96	36.66
11	C	1.2	48.81	34.96
12 E	C	0.4	48.55	35.00
13	CD	6.7	51.83	34.19
14 E	CD	7.0	52.35	34.05
15 H	CD	9.0	53.88	33.34
16	D	12.3	54.88	32.78
17	DE	15.2	56.25	32.47
18	DE	18.2	57.52	31.84
19	DE	20.0	58.67	31.51
20	DE	21.5	59.40	31.19
21	DE	23.9	60.77	30.60
22	DE	26.1	62.30	29.71
23	DE	28.5	64.68	28.50
24	DE	28.6	64.99	28.17
25	E	29.6	67.19	26.46
26	EF	31.0	67.49	26.59
27 H	EF	34.3	69.08	25.69
28	EF	37.3	70.60	24.54
29	F	38.0	70.93	24.34
30	FG	48.7	73.99	22.14
31	FG	63.3	78.21	19.22
32	SL	−1.5	5.96	7.41
33	SL	−2.8	9.87	12.34
34 H	SL	−3.6	15.57	15.04
35	SL	−5.9	27.35	21.26
36 E	SL	−8.0	34.90	23.75
37 H	SL	−8.6	37.34	24.70
38	SL	−12.4	45.62	26.97
39	SL	−15.6	49.12	27.75
40	SL	−18.6	51.38	28.45
41	SL	−18.9	51.51	28.35
42	L	−19.5	51.38	28.45

TABLE 5—*Continued*

SERIAL NO.	POSITION ON DIAGRAM	TEMPERATURE	LIQUID	
		°C.	I	KI
43	LK	−16.8	53.59	28.51
44	LK	−13.9	55.30	28.49
45	LK	−10.0	56.61	28.36
46	LK	−6.3	58.32	28.16
47	K	−5.2	58.83	28.21
48	K	−4.7	58.93	28.06
49	K	−4.6	59.08	28.16
50	K ?	−4.0	59.13	28.08
51 H	K	−5.0	58.72	28.25
52	KF	−1.0	60.06	27.93
53	KF	3.6	61.24	27.57
54	KF	6.4	61.71	27.46
55	KF	7.4	62.49	27.18
56	KF	11.2	63.54	26.89
57	KF	15.0	64.57	26.50
58	KF	21.9	66.03	25.95
59	KF	26.9	67.74	25.46
60	KF	27.4	67.80	25.40
61	BL	−23.2	21.07	43.17
62	BL	−22.3	24.24	41.25
63	BL	−20.2	36.75	34.47
64	BL	−19.9	38.08	33.91
65	BL	−19.6	38.94	33.42
66	BL	−19.3	44.68	31.10
67	BL	−19.0	44.92	30.82
68 E	CJ	0.4	50.50	33.95
69	CJ	1.3 ?	51.30	33.63
70 H	CJ	1.0	53.44	32.43
71 H	CJ	0.8	53.25	32.29
72	CJ	1.0	55.43	31.05
73	CJ	1.1	57.27	29.96
74	CJ	1.0	57.61	29.71
75	CJ	0.8	57.41	29.87
76	CJ	0.8	57.79	29.85
77	CJ	0.6	59.45	28.74
78	CJ	0.5	58.33	29.59
79	CJ	0.5	58.71	28.85
80	J	0.4	59.73	28.53
81	J	0.3	59.87	28.51
82	J	0.3	59.68	28.42
83	DH	10.8	56.54	31.53
84	DH	9.4	57.15	31.57
85	DH	9.0	58.50	30.38

TABLE 5—*Concluded*

SERIAL NO.	POSITION ON DIAGRAM	TEMPERATURE	LIQUID	
			I	KI
		°C.		
86	DH	8.9	58.37	30.69
87	DH	8.7	57.17	31.20
88	DH	8.5	57.60	31.04
89	DH	8.0	58.46	30.36
90	DH	8.0	58.29	30.66
91	DH	7.6	58.82	29.87
92	DH	7.5	58.59	30.29
93	DH	6.1	59.31	29.51
94	DH	5.3	59.85	28.98
95	H	3.0	60.29	28.49
96	KJ	−3.1	59.13	28.29
97	KJ	−0.7	59.48	28.33
98	KJ	−0.4	59.46	28.29
99	KJ	−0.4	59.36	28.43
100	JH	1.9	60.07	28.39
101	JH	2.1	60.10	28.40
102 E	HE	5.0	61.20	28.31
103	HE	15.1	63.42	27.90
104	HE	21.5	64.95	27.40
105	HE	29.5	66.89	26.63

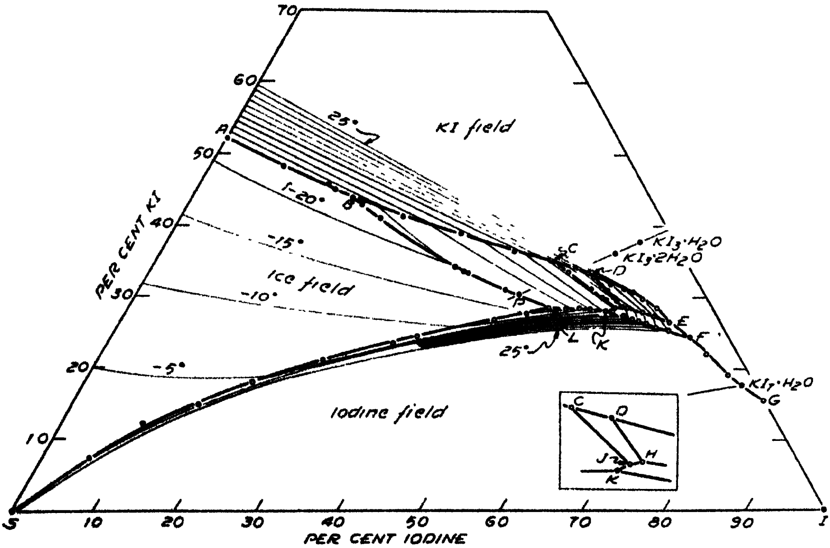

FIG. 4. Triangular projection diagram with contour isothermals up to 25°C.

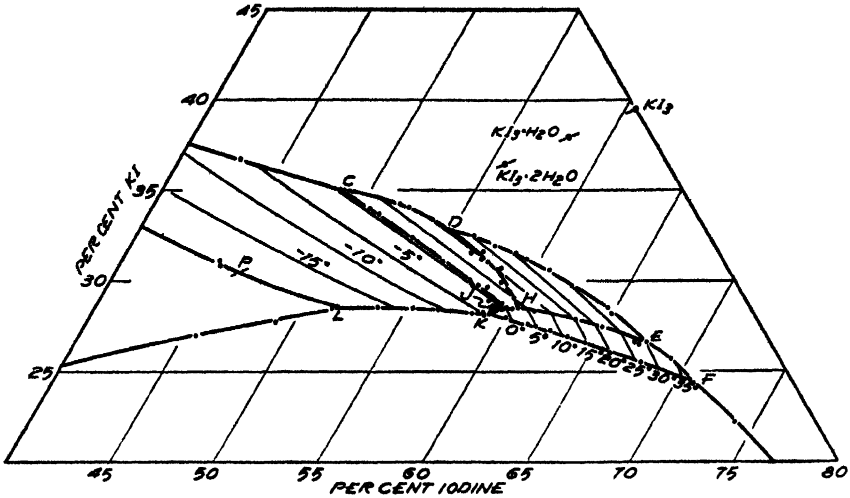

FIG. 5. Enlarged portion of the triangular projection diagram

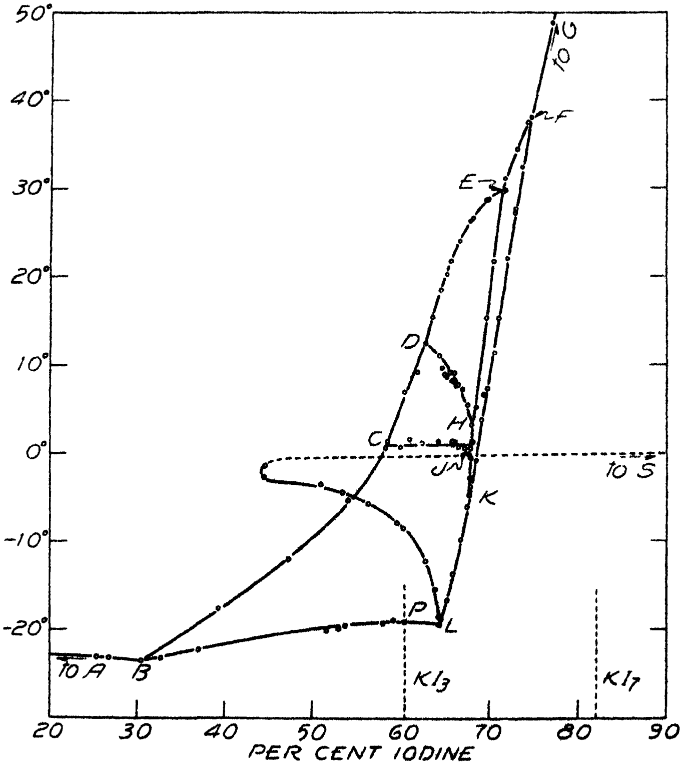

FIG. 6. Jänecke projection on the potassium iodide–iodine plane

and as many as possible in figure 4. The latter figure also shows the approximate position of a number of contour isothermals, beginning at 25°C. and passing downward in 5°C. steps; parts of these isothermals are likewise shown in figure 5. They will be discussed later.

The diagram is rather unusual. Although binary compounds are entirely absent, there are nevertheless no fewer than three ternary compounds —i.e., hydrated polyiodides—one of which—i.e., the dihydrated triiodide—exists in two polymorphic forms. If we include the ice, potassium iodide, and iodine, there are thus no less than seven distinct solid phases. Of the seven different fields appearing in the diagram, *DEHD* is the field for $KI_3 \cdot H_2O$, *KJHEFK* the field for KI_7H_2O, *BCJKLB* the field for alpha-$KI_3 \cdot 2H_2O$, and *CDHJC* the field for beta-$KI_3 \cdot 2H_2O$. The line *CJ* is apparently an isothermal transition boundary. Only two of the three-solid invariants—i.e., *B* and *L*—are ternary eutectics, while there appears to be a definite though slight dystectic temperature maximum on the *BL* boundary at *P*. The evidence supporting the polyiodide formulas will be presented later in detail (some of this evidence has been given already in connection with the isothermal studies), but it is well to point out here that the direction of temperature fall along the several ternary boundary lines (see the Jänecke projection) is experimentally in accord with the van Alkemade principle (1) applied on the basis of the formulas just given.

The ternary boundary lines

Both of the saturating solid phases separate positively along the boundaries *AB*, *BL*, *LK*, *KJ*, *JH*, *HE*, *FG* and (probably) *EF* during cooling. Negative separation of one solid (see reference 2, page 12) occurs along the other boundaries,—i.e., iodine along *KF* and practically all of *SL*, potassium iodide along *BC*, *CD*, and *DE*, monohydrated KI_3 along *DH*, and the beta-form of the dihydrated KI_3 along the transition boundary *CJ*. The critical areas, within which departure from the last-named boundaries will take place during cooling, may be readily determined by the reader on the basis of the principles explained in the paper on the ternary ammonium iodide system (2).

It was a comparatively easy matter to locate the first group of boundaries named in the last paragraph, since mixtures lying on either side of any one of these boundaries soon reached the boundary during cooling, and remained on it thereafter until an invariant arrest was obtained. It was only necessary, therefore, to note the boundary arrest on the cooling curve and to follow this with analyses of the liquid samples at appropriate temperature intervals.

The other boundary lines were not so easily determined. Since it is necessary to have plenty of the liquid phase present for sampling after a boundary has been reached, the original composition of the mixture being used for a survey should not be far removed, in general, from the boundary itself. In many cases, therefore, the original composition lay inside the critical area for the boundary and departure from the boundary took place at some point. Furthermore, these boundaries could be reached from one side only.

One or two examples of what actually happened may not be out of place. A test mixture was made up with extreme care to contain 65.5 per cent iodine, 25.5 per cent potassium iodide, and 9.0 per cent water. This mixture lies just below the boundary *KF* and within the critical area enclosed by *KF* and the straight lines drawn from *K* and *F*, respectively, to the point representing $KI_7 \cdot H_2O$. A graphical determination of the crystallization path with the aid of the phase diagram (figure 4) shows that the mixture should first give solid iodine on being cooled, then reach the *KF* boundary just below 15°C., then pass along the boundary towards *K*. At a point near 5°C., however, the path should leave the boundary, pass across the $KI_7 \cdot H_2O$ field (*JHEFK*), and arrive at the boundary *JH* at about 2°C. Thereafter, the path should reach *J* (first invariant arrest), then pass *via JK* and *KL* to *L*, the latter being the end point of crystallization.

The actual cooling curve confirmed most of these predictions. There was a definite though slight first arrest at 22°C. (separation of iodine). This was followed by a marked arrest at 13.2°C. (*KF* boundary arrest). There was next a very slight change in the slope of the cooling curve at about 5.5°C., which was indicative of departure from the *KF* boundary. This was followed by a definite boundary arrest at 1.9°C. (arrival at *JH*), and finally this was succeeded by a long but sluggish invariant arrest a little below 0°C. This was undoubtedly the arrest at *J*, which we have found always to be difficult to keep from undercooling. The cooling curve was not carried much beyond this arrest.

Further confirmation of these conclusions was obtained from three analyses of the liquid, made during the survey. The first (serial No. 55 in table 5) taken at 6.4°C. gave a point on the boundary *KF*. The second (serial No. 101 in table 5) taken at 1.9°C. gave a point on *JH* as predicted. The third (serial No. 100 in table 5) taken at −0.4°C. (temperature held constant for 15 min.) gave a point on *JK*.

Another survey began with a mixture containing 56.5 per cent iodine, 33.5 per cent potassium iodide, and 10.0 per cent water. At room temperature it still contained solid potassium iodide. The total composition lies in the critical area enclosed by the boundary *DE* and the straight lines drawn from *D* and *E*, respectively, to $KI_3 \cdot H_2O$. At the same time it also lies in a second critical area enclosed by the boundary *DH* and the lines drawn from *D* and *H*, respectively, to $KI_3 \cdot 2H_2O$. As a result, the crystallization path becomes extremely complex; it should begin by following the tie line from potassium iodide until it reaches the boundary *DE*; it should then proceed along *DE* toward *D*, leaving the boundary, however, and passing over to *DH* before *D* is reached. It should next move along *DH* in the direction of *H*; but before reaching *H*, it should leave *DH* and pass across the beta-$KI_3 \cdot 2H_2O$ field to the transition boundary *CJ*. The liquid cannot move along this boundary and must therefore remain at one point until the change to the alpha-form has been completed, after which it can pass across the alpha-$KI_3 \cdot 2H_2O$ field to the boundary *LK*.

The actual facts were as follows: The first arrest actually observed occurred at 17.5°C., the arrest on the *DE* boundary. This temperature agreed almost perfectly with the one predicted from the phase diagram. The next arrest occurred at 10°C., the point where the crystallization path met the boundary *DH* after leaving *DE* (the temperature at which departure took place was not apparent on the cooling curve). This temperature also agreed with the one predicted from the phase diagram. The third arrest which was observed was the long characteristic transition arrest on the *CJ* boundary, whereupon the survey was discontinued. Analyses of the liquid phase at the third arrest gave serial No. 76 in table 5,—a point on the *CJ* boundary in almost the exact position required by the theoretical crystallization path.

It is apparent from what has just been said that the boundaries *DH* and *CJ* were the most difficult to locate on the diagram, since many of the points on *DH* and all the points on *CJ* required different individual surveys. It was also not easy to determine the exact temperatures on *CJ*, the beta-alpha $KI_3 \cdot 2H_2O$ transition being rather sluggish and undercooling occurring easily. In the actual cooling curves, the *CJ* arrests rarely began above 0.3°C. and sometimes appeared 1 or 2°C. lower; but special experiments, made with a very small temperature differential between the test sample and the outside cooling bath, led us to believe that the true temperature of the transition is not far from 1°C.

When one reaches a point on the transition boundary *CJ*, a striking change in the solid phase begins at once to be apparent. Just above the boundary the liquid is freely mobile and appears to contain coarse granular crystals,—of the beta-form of $KI_3 \cdot 2H_2O$. At the boundary, however, the alpha-modification separates in the form of fine interlocking needles, producing immediately a felt-like structure which tends to immobilize the liquid, so that it becomes a difficult matter to withdraw a sample for analysis. At no other position on the diagram was so characteristic a change observed.

The invariant points

The invariant points have been assembled in table 6 for the sake of convenience. The values shown have been adopted after a critical examination of all the data and have been checked with the aid of special graphs formed by plotting separately the iodine and potassium iodide values of table 5 against the temperature. The temperatures given in the table are believed to be correct to within at least 0.5°C.

The "melting points" of the pure polyiodides

These are easily deduced from the phase diagram. All are incongruent. The hydrated heptaiodide melts at 38°C. (point *F*), where it decomposes into invariant liquid, solid potassium iodide, and solid iodine. In this connection it is interesting to note that this temperature—i.e., 38°C.—was long ago stated by Wells and Wheeler (16) to be the melting point of their "potassium triiodide." Since they give no analyses of their compound, it is not impossible that they really had the hydrated heptaiodide.

TABLE 6

Invariant points

POSITION ON DIAGRAM	TEMPERATURE	LIQUID		SOLID PHASES
		I	KI	
	°C.			
A	−22.7	0	52.2	Ice and KI
S	0	Trace	0	Ice and iodine
G	80.8	85.3	14.7	KI and iodine
B	−23.7	44.1	19.4	Ice, α-$KI_3 \cdot 2Aq$, and KI
C	*ca.* 1.0	48.7	35.0	KI, α-$KI_3 \cdot 2Aq$, and β-$KI_3 \cdot 2Aq$
D	12.3	54.9	32.8	KI, $KI_3 \cdot Aq$, and β-$KI_3 \cdot 2Aq$
E	30.0	67.4	26.5	$KI_3 \cdot Aq$, KI, and $KI_7 \cdot H_2O$
F	38.0	70.9	24.4	$KI_7 \cdot Aq$, KI, and iodine
H	3.0	60.3	28.5	β-$KI_3 \cdot 2Aq$, $KI_3 \cdot Aq$, and $KI_7 \cdot Aq$
J	*ca.* 1.0	59.8	28.4	α-$KI_3 \cdot 2Aq$, β-$KI_3 \cdot 2Aq$, and $KI_7 \cdot Aq$
K	−4.9	59.0	28.2	α-$KI_3 \cdot 2Aq$, $KI_7 \cdot Aq$, and iodine
L	−19.6	51.5	28.5	Ice, α-$KI_3 \cdot 2Aq$, and iodine

The monohydrated triiodide melts at 30°C.[1] (point *E*), where it decomposes into invariant liquid, solid potassium iodide, and solid hydrated heptaiodide. The beta-form of the dihydrated triiodide also melts incongruently,—at 12.3°C. (point *D*), where it decomposes into invariant solution, solid potassium iodide, and solid $KI_3 \cdot H_2O$. When the alpha-modification of the dihydrated triiodide is heated, it of course changes to the beta-form at about 1°C., a point on the *CJ* boundary. None of these predictions has been tested by direct experiment, owing to the difficulty of obtaining the respective polyiodides free from adhering liquid.

---

[1] Grace (J. Phys. Chem. 37, 347 (1933)) states that the compound $KI_3 \cdot H_2O$ melts at 31°C.

TABLE 7

Indirect analysis

SURVEY NO.	LIQUID		TEMPERATURE
	I	KI	
For $KI_3 \cdot H_2O$			
			°C.
1	57.70	32.02	
	57.60	31.04	8.5
2	59.74	30.61	
	59.93	29.87	9.7
	60.05	29.25	5.9
3	61.20	30.51	
	61.87	28.65	11.0
For β-$KI_3 \cdot 2H_2O$			
1	55.45	31.93	
	55.36	31.08	1.2
	55.43	31.05	1.0
2	57.55	31.06	
	58.04	29.65	1.3
3	55.60	32.25	
	55.65	31.02	
For $KI_7 \cdot H_2O$			
1	66.06	24.94	
	60.80	27.78	2.5
	59.91	28.20	0.1
2	66.62	25.21	
	62.12	27.66	9.3
	61.40	28.25	5.7
3	69.0*	24.5*	
	63.42	27.90	15.1
For α-$KI_3 \cdot 2H_2O$			
1	51.51	33.77	
	49.72	32.52	−6
Solid......................	53.35	34.90	−6
2	53.40	32.12	
	52.45	30.38	−10
Solid......................	54.38	33.90	−10

* Total composition of mixture as prepared.

TABLE 7—*Concluded*

SURVEY NO.	LIQUID		TEMPERATURE
	I	KI	
For α-$KI_3 \cdot 2H_2O$—*Cont.*			
			°C.
3	54.34	32.15	
	53.95	30.31	−7
Solid....................	54.90	34.19	−7
4	55.62	32.30	
	55.67	31.05	−3
	55.66	29.83	Not determined
Solid....................	55.42	33.75	Not determined
5	56.33	30.48	
	56.49	29.33	−4
Solid....................	55.92	33.33	−4
6	57.36	29.76	
	57.63	28.62	−5
Solid....................	56.45	32.81	−5

D. The indirect analysis of the solid polyiodides

The data on the indirect analysis of the various polyiodide phases—as obtained in the polythermal study—have been collected in table 7. Except as indicated in the table, the composition data refer to the liquid phase. The method of non-isothermal crystallization paths was relied upon exclusively for the first three solid phases,—i.e., $KI_3 \cdot H_2O$ in field *DEHD*, beta-$KI_3 \cdot 2H_2O$ in field *CDHJC*, and $KI_7 \cdot H_2O$ in field *KJHEFK*. The extrapolations are shown in figure 7. The results confirm the isothermal studies.

The details of the identification of the alpha-modification of $KI_3 \cdot 2H_2O$ are shown in figure 8. The crystallization paths in this case were supplemented with analyses of the wet solid residues, as indicated in table 7. The individual surveys shown in figure 8 are numbered to conform with the table.

As a matter of fact, the chemical identification of the alpha-modification of the dihydrated triiodide caused much trouble. At the beginning of the work on this solid Mr. Clack obtained a short crystallization path (in the field below *CJ* not far from survey 5 in figure 8) that pointed directly to the formula $KI_3 \cdot 3H_2O$, and another (near survey 2) that pointed between the latter and $KI_3 \cdot 2H_2O$. Believing that there was really a very slight temperature maximum (i.e., dystectic) on the boundary *CJ*, he therefore concluded, for the time being at least, that the solid was the trihydrated

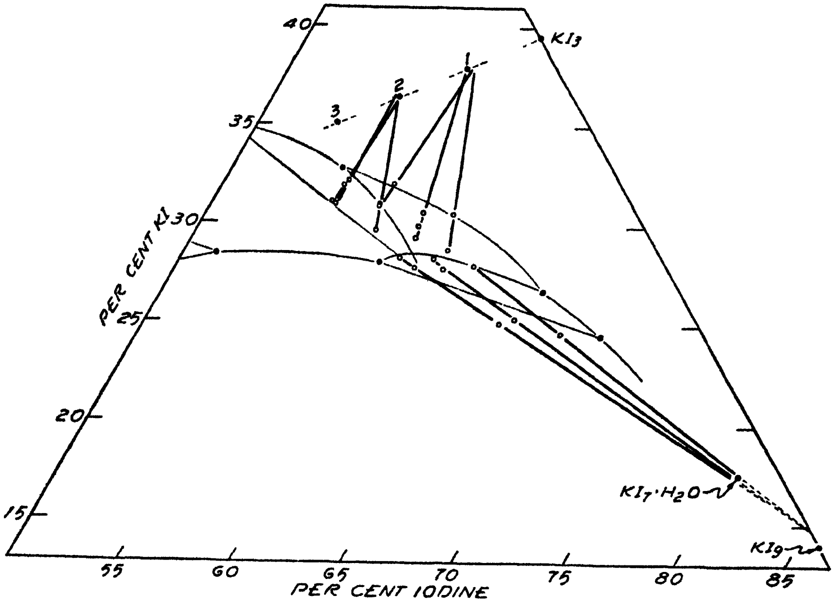

FIG. 7. Extrapolation diagram

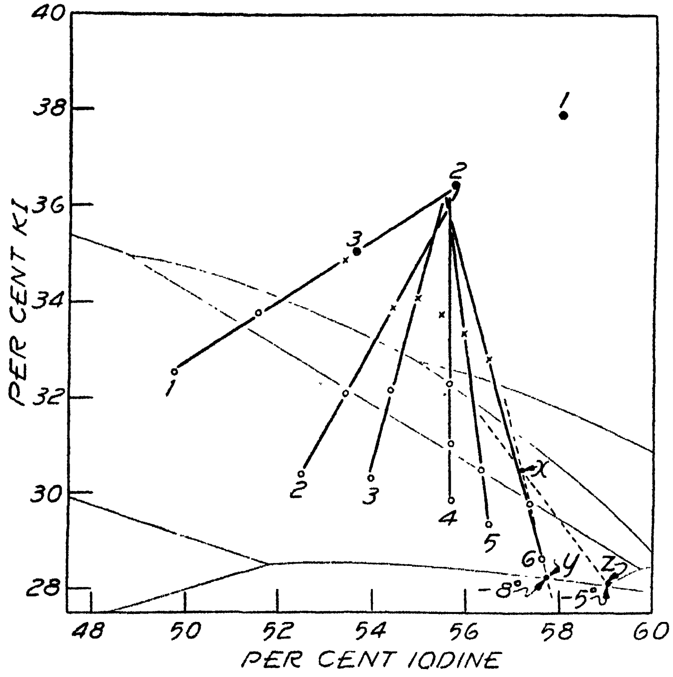

FIG. 8. Identification of the alpha-modification of $KI_3 \cdot 2H_2O$

triiodide,—that is to say, the potassium analog of the compound $NH_4I_3 \cdot 3H_2O$ found in the ammonium iodide system (2). He made no analyses of the wet solid residues, and as he was unable to complete the study in the time which remained at his disposal, the work was later continued by the senior author with the assistance of Mr. Eaton. Their data appear in table 7. The temperatures shown are only approximate.

The final separation of liquid and wet solid was accomplished by means of a special technique, made necessary because of the peculiar physical characteristics of the solid below the transition boundary *CJ*. The mixtures were cooled in a narrow tube and the felt-like mass of crystals was squeezed to the bottom of the tube by means of a closely fitting perforated platinum disc on the end of a plunger, previously brought to the proper temperature. By this procedure, most of the liquid phase could be easily removed through a filter tube. The solid residue was then further dried by pressing filter paper against the perforated metal plate. The procedure furnished a generous supply of fairly dry solid and avoided direct contact between the latter and the paper.

The results of the work—as plotted in figure 8—point definitely to the formula $KI_3 \cdot 2H_2O$ and not to $KI_3 \cdot 3H_2O$, though it is admitted that longer crystallization paths would have been desirable as well as paths on the other side of the KI_3–water tie line. However, the following special experiment seems to settle the question in favor of the dihydrate formula:

A homogeneous solution represented by point x in figure 8 was prepared and analyzed. A consideration of the theoretical crystallization path of this mixture on the phase diagram shows that it should give a third arrest at y if the solid between *CJ* and *LK* is $KI_3 \cdot 2H_2O$, but at z if the solid is $KI_3 \cdot 3H_2O$. By interpolation of the boundary data (table 5), y is found to be at -8°C., z at -5°C. Such a large difference should be easy to detect experimentally.

Two cooling curves were run with the mixture; three arrests were obtained as expected, the second being without question the characteristic arrest on the *CJ* boundary. The third arrest appeared at -8.0°C. in the first run and at -8.8°C. in the second where there was probably a little more undercooling. These results point conclusively to the dihydrate formula.

E. Interpolated isothermals

The isothermal contour lines shown in figures 4 and 5 were not located with the precision which was employed in the case of the ternary ammonium iodide system (2). The procedure actually followed was to determine by interpolation the desired points on the various boundary curves and to make the best guess possible concerning the rest. It seems quite certain, however, that the shape and position of the contour lines are substantially correct as shown on the diagrams. Note that in the ice field (*cf.* figure 4) the isothermals as drawn meet the condition that iodine raises the freezing points of potassium iodide solutions (*cf.* 13).

In concluding this paper, a few words will be said about the invariants interpolated on the phase diagram at 0° and 25°C., respectively, as compared with those found independently in the preliminary isothermal surveys. The comparison at 25°C. follows.

INVARIANT (25°C.)	INTERPOLATED		ISOTHERMAL	
	I	KI	I	KI
KI–$KI_3 \cdot H_2O$	61.7	30.1	62.3	30.1
$KI_3 \cdot H_2O$–$KI_7 \cdot H_2O$	66.1	27.1	66.5	27.2
$KI_7 \cdot H_2O$–iodine	67.3	25.6	67.8	25.6

It is, however, not so simple a matter to compare the invariants interpolated at 0°C. with those found in the isothermal study. For if one looks closely at the interpolated 0°C. contour lines in figures 4 and 5, it will be seen that the latter are not exactly like the isothermal in figures 1 and 3. The interpolated isothermal cuts across a small portion of the heptaiodide field, giving three invariant solutions instead of the two shown in the isothermal diagrams. The comparison, as far as it can be made, follows.

INVARIANT (0°C.)	INTERPOLATED		ISOTHERMAL	
	I	KI	I	KI
KI–$KI_3 \cdot 2H_2O$	48.2	35.1	48.8	34.8
$KI_3 \cdot 2H_2O$–$KI_7 \cdot H_2O$	59.8	28.4	Missing	
$KI_7 \cdot H_2O$–iodine	60.4	27.8	Missing	

The second invariant obtained in the isothermal studies at 0°C. (*cf.* figure 3) contained 60.3 per cent iodine and 27.6 per cent potassium iodide. The close agreement with the third interpolated invariant in the table just presented suggests that the two are one and the same, but inspection of the tie lines from the second invariant in figure 3 shows that the latter must have been the metastable invariant saturated with dihydrated triiodide and iodine. According to the polythermal phase diagram, this metastable invariant (for alpha-$KI_3 \cdot 2H_2O$ and iodine) should lie close to 60.6 per cent iodine and 27.9 per cent potassium iodide. It is thus certain that part of the 0°C. isothermal shown in figures 1 and 3 is metastable but nevertheless in substantial agreement with the polythermal system as shown in figures 4 and 5.

Little more remains to be said about the system at this time. The general results furnish a complete confirmation of Grace's thesis that all the polyiodides of potassium are solvated in the presence of water. The phase diagram which has resulted from this work should go far towards settling the long controversy over the reality of solid polyiodides of potassium; indeed as one views this controversy in retrospect, it seems most surprising that the phase diagram was not determined years ago. The deterrent appears to have been the belief that it would be very difficult, if not impossible experimentally, to set up the necessary conditions of equilibrium at the low temperatures required in much of the work; Parsons and Whittemore, as well as others, made reference to this matter. The difficulty appears to have been greatly overestimated.

SUMMARY

The results of this paper may be summarized briefly as follows:

1. The temperature–composition diagram of the ternary system potassium iodide–iodine–water has been determined in detail. The diagram is restricted to solid–liquid systems in air at approximately normal pressure.

2. The solid phases are ice, KI, iodine, $KI_3 \cdot H_2O$, $KI_7 \cdot H_2O$, and two polymorphic modifications of the compound $KI_3 \cdot 2H_2O$.

3. The previous work of Grace at 25°C. has been substantiated in all of its important features.

REFERENCES

(1) Bancroft: The Phase Rule, p. 149. Journal of Physical Chemistry, Ithaca, New York (1897).
(2) Briggs, Ballard, Miss Alrich, and Wikswo: J. Phys. Chem. **44**, 325 (1940).
(3) Briggs and Geigle: J. Phys. Chem. **34**, 2250 (1930).
(4) Briggs, Greenawald, and Leonard: J. Phys. Chem. **34**, 1951 (1930).
(5) Cremer and Duncan: J. Chem. Soc. **1933**, 181.
(6) de Coppet: Ann. chim. phys. [5] **30**, 417 (1883).
(7) Fialkow: Acta Physicochim. U. R. S. S. **3**, 711 (1935).
(8) Foote and Bradley: J. Phys. Chem. **36**, 673 (1932).
(9) Foote and Chalker: Am. Chem. J. **39**, 561 (1908).
(10) Grace: J. Chem. Soc. **1931**, 594.
(11) Grace: J. Phys. Chem. **37**, 347 (1933).
(12) *International Critical Tables*, Vol. III, p. 326; Vol. IV, pp. 239, 259. McGraw-Hill Book Company, New York (1928).
(13) LeBlanc and Noyes: Z. physik. Chem. **6**, 385 (1890).
(14) Martin: J. Chem. Soc. **1932**, 2641.
(15) Parsons and Whittemore: J. Am. Chem. Soc. **33**, 1933 (1911).
(16) Wells and Wheeler: Z. anorg. Chem. **1**, 442 (1892).

NOTE ON THE SYSTEM SODIUM IODIDE–WATER

T. R. BRIGGS AND W. F. GEIGLE

Department of Chemistry, Cornell University, Ithaca, New York

Received July 7, 1939

In the course of a phase rule study of the system sodium iodide–iodine–water, now nearing completion in this laboratory, we have had occasion to construct the temperature–composition diagram of the system sodium iodide–water. On assembling the available published data, however, we discovered that a few additional measurements were needed, especially at the lower temperatures, before the diagram could be drawn with the desired accuracy and completeness. A brief special investigation was accordingly carried out, the results of which are presented here in the form of a separate communication.[1]

As is well known, the solid phases encountered in the binary system are NaI, $NaI \cdot 2H_2O$, $NaI \cdot 5H_2O$, and ice. The solubilities of the anhydrous salt and dihydrate have been accurately determined over a wide range of temperatures by Kremers (8), de Coppet (2), Brønsted (1) (at 100°C.), Scott and Frazier (15) (at 25°C.), Scott and Durham (14), Hill, Wilson, and Bishop (4) (at 8°, 25°, and 40°C.), and Ricci (11) (at 25° and 40°C.). According to Scott and Durham the $NaI \cdot 2H_2O$–NaI transition temperature, as estimated from the point of intersection of the respective solubility curves, is 68.1°C.

We have been unable to find, however, more than two points on the solubility curve of the pentahydrate,—one of these having been determined by Étard (3) (51.5 per cent sodium iodide at -20°C.) and the other by de Coppet (2) (56.93 per cent sodium iodide at -15.2°C.). We have also been unable to find any exact determination of the pentahydrate–dihydrate transition temperature, though Panfilow (10) reports that it is about -10°C.

Freezing-point determinations up to moderate concentrations of sodium iodide have been made by Rüdorff (12), and these were later extended almost to the eutectic point by Jones and his associates (7). According to Meyerhoffer (9), the eutectic temperature is -31.5°C. and the eutectic composition is 39 per cent sodium iodide. It should be pointed out here, however, that the latter value is entirely inconsistent with the data of Jones and his coworkers, whose work was very carefully done.

Boiling-point determinations have been made by Schlamp (13), Johnston (6), and Jablczynski and Kon (5). Johnston's measurements are the most comprehensive, extending as they do to solutions containing up to 60 per cent sodium iodide. According to Kremers (8), the saturated solution boils at 141°C.

---

[1] The ternary system will be presented in a later paper.

EXPERIMENTAL

A number of carefully prepared mixtures of sodium iodide and water, designed so as to include the region of the pentahydrate, were subjected to thermal analysis in air-jacketed tubes held in a well-stirred cooling bath with a 10-degree temperature differential. The mixtures were agitated by means of a magnetic stirrer and all thermometers were especially calibrated by means of a number of standard fixed temperatures.

TABLE 1

Temperature arrests

SERIAL NO.	NaI	FIRST ARREST	SECOND ARREST
	per cent	°C.	°C.
1	18.7	−5.6	Not determined
2	37.2	−17.8	Not determined
3	41.9	−23.5	−31.7
4	44.2	−26.8	−31.2
5	46.5	−30.6	−31.5
6	49.0	−36.1	−31.6
7	53.3	−24.8 ?	−31.5
8	57.2	−17.3 ?	−31.8
9	61.0	−12.2	−31.8
10	64.0	−12.4	None
11	77.5	68.0	Not determined
12	82.4	68.0	Not determined

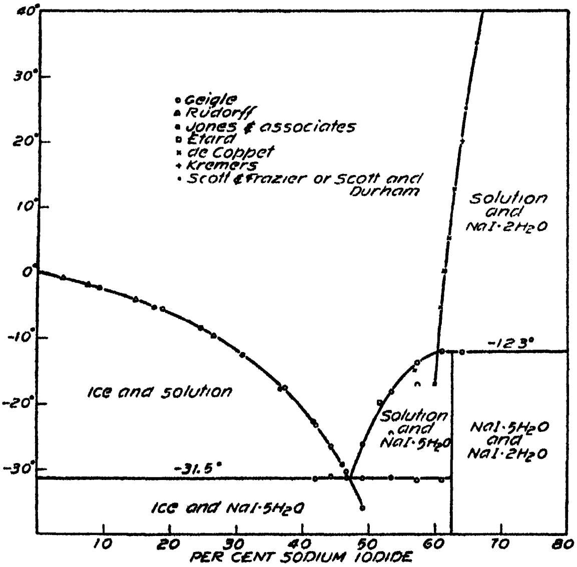

FIG. 1. Water and sodium iodide

The temperature arrests are presented in table 1. They have been designed as "first" and "second" arrests only as a matter of convenience in showing the order in which they were obtained.

These arrests (excepting Nos. 11 and 12) have been plotted in figure 1. Extreme undercooling with respect to the pentahydrate occurred in the case of Nos. 6, 7, and 8, so that the attempt to obtain points on the solubility curve of the pentahydrate was not successful. With No. 6, for example, the first arrest at −36.1°C. proved to be a point on the metastable extension of the ice line below the eutectic temperature, and the second arrest at −31.6°C. appeared only after the pentahydrate had actually begun to form. In the case of Nos. 7 and 8 the pentahydrate made its appearance before the eutectic temperature was reached; but there was still much undercooling, and the arrests (shown in figure 1 as half-circles) were indefinite and much too low. Accordingly, heating curves were run after each mixture had been cooled to the second (i.e., eutectic) arrest, with the following results (three points on the pentahydrate solubility curve):

TABLE 2

Boiling points of solutions of sodium iodide

NaI	BOILING POINT
per cent	°*C.*
37.2	104.8
44.2	107.0
53.3	113.0
57.2	117.4
64.0	121.6
70.0	131.8
75.0	142.0
76.2 (saturated)	142.4

SERIAL NO.	NaI	TEMPERATURE
	per cent	°*C.*
6	49.0	−26.5
7	53.3	−18.5
8	57.2	−14.0

According to figure 1, the eutectic point lies at −31.5°C. and 47.1 per cent sodium iodide. Meyerhoffer's value for the temperature is thus satisfactorily confirmed but not his value for the composition, which is found to be seriously in error, as had been suspected from the first. The pentahydrate-dihydrate transition temperature is found to be −12.3°C., at which point the solution contains 60.2 per cent sodium iodide. The dihydrate–anhydrous sodium iodide transition temperature (68.0°C.) is given by the "first" arrests of Nos. 11 and 12 in table 1; it is in good agreement with the value (68.1°C.) obtained by Scott and Durham. At this transition point the solution contains 74.8 per cent sodium iodide.

TABLE 3

Temperature–composition data

TEMPERATURE	NaI	SOURCE	TEMPERATURE	NaI	SOURCE
Solution and ice			Solution and vapor		
°C.	*per cent by weight*		*°C.*	*per cent by weight*	
−0.85	3.74	(12)	101.1	13.40	(6)
−1.9	7.48	(12)	102.4	24.03	(6)
−2.44	9.34	(7)	103.4	29.23	(6)
−4.25	14.59	(12)	104.8	35.30	(6)
−5.37	17.44	(7)	104.8	37.2	*
−5.6	18.7	*	106.7	41.38	(6)
−8.70	24.55	(7)	107.0	44.2	*
−9.75	26.50	(12)	108.3	45.41	(6)
−12.72	30.84	(7)	110.1	48.28	(6)
−17.8	37.2	*	111.6	50.72	(6)
−18.0	36.46	(7)	113.0	53.3	*
−23.0	41.55	(7)	113.3	53.31	(6)
−23.5	41.9	*	114.4	54.71	(6)
−26.8	44.2	*	116.2	57.64	(6)
−29.5	46.00	(7)	117.2	58.75	(6)
−30.6	46.5	*	117.4	57.2	*
−31.5 E	47.1	*	118.2	59.56	(6)
−36.1 m	49.0	*	118.6	60.31	(6)
Solution and $NaI \cdot 5Aq$			121.6	64.0	*
			131.8	70.0	*
−26.5	49.0	*	142.0	75.0	*
−20	51.5	(3)	142.4 S	76.2	*
−18.5	53.3	*	141 S	76.2	(8)
−15.2	56.93	(2)			
−14.0	57.2	*			
−12.3 U 2Aq	60.2	*			

* Briggs and Geigle; E, eutectic point; m, metastable; U, transition point; S, saturated.

A few determinations (probably accurate to ±0.5°C.) were also made in order to follow the boiling-point line to its point of saturation with the anhydrous salt. Precautions were taken to minimize superheating and to promote steady ebullition; the atmospheric pressure was about 745 mm. The results, which are fairly concordant with those of Johnston, are given in table 2.

In conclusion, the data which are now available for the construction of the freezing-point, boiling-point, and pentahydrate solubility curves have been assembled in table 3. All compositions are in percentages by weight.

REFERENCES

(1) Brønsted: Z. physik. Chem. **82**, 621 (1913).
(2) de Coppet: Ann. chim. phys. [5] **30**, 411 (1883).
(3) Étard: Ann. chim. phys. [7] **2**, 503 (1894).
(4) Hill, Wilson, and Bishop: J. Am. Chem. Soc. **55**, 521 (1933).
(5) Jablczynski and Kon: J. Chem. Soc. **123**, 2953 (1923).
(6) Johnston: Trans. Roy. Soc. Edinburgh **45** (2), 855 (1908).
(7) Jones, Getman, Bassett, McMaster, and Uhler: Carnegie Inst. Wash. Pub. No. 60, p. 35 (1907).
(8) Kremers: Pogg. Ann. **97**, 1 (1856).
(9) Meyerhoffer: Unpublished data given in Landolt-Börnstein *Tabellen*, 5th edition, p. 673. J. Springer, Berlin (1923).
(10) Panfilow: J. Russ. Phys. Chem. Soc. **25**, 264 (1893); *cf.* Chem. Zentr. [4] **5**, II, 910 (1893); Z. anorg. Chem. **5**, 490 (1894).
(11) Ricci: J. Am. Chem. Soc. **56**, 295 (1934).
(12) Rüdorff: Pogg. Ann. **116**, 55 (1862).
(13) Schlamp: Z. physik. Chem. **14**, 272 (1894).
(14) Scott and Durham: J. Phys. Chem. **34**, 1424 (1930).
(15) Scott and Frazier: J. Phys. Chem. **31**, 459 (1927).

THE PHYSICAL PROPERTIES OF THE TERNARY SYSTEM BUTYL ALCOHOL–ETHYL ACETATE–TOLUENE

E. E. LITKENHOUS, J. D. VAN ARSDALE, AND I. W. HUTCHISON, JR.

Chemical Engineering Laboratories, University of Louisville, Louisville, Kentucky

Received June 27, 1939

INTRODUCTION

This and two previous investigations (5, 6) were carried out to obtain physical data for use in chemical engineering design studies. The densities, viscosities, surface tensions, refractive indices, and boiling points of the ternary system butyl alcohol–ethyl acetate–toluene were determined and are reported in this paper.

EXPERIMENTAL

Materials

Normal c.p. butyl alcohol was treated as described in the paper of Ernst, Litkenhous, and Spanyer (5). The c.p. ethyl acetate was repeatedly distilled in a specially constructed long glass rectifying column, refluxed with phosphorus pentoxide for several hours (13), and finally redistilled. The toluene was purified by continued fractionation. Tests were made for aldehydes and acids before the materials were finally redistilled.

The physical properties of the purified materials were next determined as a check upon their purity before the preparation of both binary and ternary samples. These physical constants and a comparison with those of other investigators are listed in table 1.

TABLE 1

Physical constants of purified materials

MATERIAL	DENSITY	VISCOSITY	SURFACE TENSION	REFRACTIVE INDEX	BOILING POINT
					°C.
Butyl alcohol...	0.8075 (A)	0.02463 (A)	24.189 (A)	1.3981 (A)	117.7 (A)
	0.8080 (5)	0.02465 (5)	24.204 (5)	1.3981 (5)	117.69 (5)
	0.8080 (1)	0.02801 (10)	24.25 (15)	1.3974 (1)	117.71 (1)
	0.8083 (2)		24.16 (9)	1.4000 (3)	117.6 (11)
Ethyl acetate...	0.8933 (A)	0.00438 (A)	22.973 (A)	1.3715 (A)	77.1 (A)
	0.8935 (7)	0.00416 (8)	23.15 (9)	1.3704 (12)	77.15 (7)
	0.89852 (10)				77.1 (18)
Toluene....	0.8599 (A)	0.00551 (A)	27.541 (A)	1.4941 (A)	110.7 (A)
	0.8617 (16)		27.96 (9)	1.4936 (13)	110.7 (4)
	0.8654 (10)		28.58 (14)	1.4910 (12)	110.8 (17)

(A) Author's experimental values.

Preparation of samples

Sixty-six samples were then prepared, using weight increments of 10 per cent. The weight per cent composition of these samples is listed in table 2.

Apparatus

Apparatus identical with that used in the previous investigations (5, 6) was employed. A temperature of 25°C. ± 0.05° was maintained in the determination of density, viscosity, surface tension, and refractive index. All samples were kept in glass-stoppered bottles in a constant-temperature bath for 24 hr. before using.

DISCUSSION

The results of the experimental work are summarized in table 3. Both binoidal and triangular diagrams have been drawn for each property. The binoidal curves are plotted with the composition of the sample as abscissa against the particular property under consideration as the ordinate. The constant property lines on the triangular diagrams were prepared from the binoidal curves.

TABLE 2

Composition of samples

SAMPLE NUMBER	BUTYL ALCOHOL	ETHYL ACETATE	TOLUENE
	weight per cent	*weight per cent*	*weight per cent*
1	100		
2		100	
3			100
4		10	90
5		20	80
6		30	70
7		40	60
8		50	50
9		60	40
10		70	30
11		80	20
12		90	10
13	90		10
14	80		20
15	70		30
16	60		40
17	50		50
18	40		60
19	30		70
20	20		80
21	10		90
22	10	90	
23	20	80	
24	30	70	
25	40	60	
26	50	50	
27	60	40	
28	70	30	
29	80	20	
30	90	10	
31	80	10	10
32	70	10	20
33	60	10	30
34	50	10	40
35	40	10	50
36	30	10	60
37	20	10	70
38	10	10	80
39	70	20	10
40	60	20	20
41	50	20	30
42	40	20	40
43	30	20	50
44	20	20	60
45	10	20	70
46	60	30	10
47	50	30	20
48	40	30	30
49	30	30	40
50	20	30	50
51	10	30	60
52	50	40	10
53	40	40	20
54	30	40	30
55	20	40	40
56	10	40	50
57	40	50	10
58	30	50	20
59	20	50	30
60	10	50	40
61	30	60	10
62	20	60	20
63	10	60	30
64	20	70	10
65	10	70	20
66	10	80	10

Relative density

Figure 1 is a binoidal graph of the relative densities plotted against composition. The relative densities of all mixtures of ethyl acetate and toluene decrease as the per cent of butyl alcohol is increased (figure 1).

TABLE 3

Physical properties

SAMPLE NUMBER	BOILING POINT	DENSITY	VISCOSITY	REFRACTIVE INDEX	SURFACE TENSION
	°C.				
1	117.7	0.8075	0.02463	1.3981	24.189
2	77.1	0.8933	0.00438	1.3715	22.973
3	110.7	0.8599	0.00551	1.4941	27.541
4	104.6	0.8636	0.00534	1.4840	27.049
5	99.4	0.8666	0.00512	1.4709	26.530
6	94.6	0.8700	0.00506	1.4588	25.974
7	91.1	0.8727	0.00484	1.4463	25.424
8	87.8	0.8755	0.00482	1.4340	24.966
9	85.2	0.8786	0.00478	1.4211	24.512
10	82.8	0.8818	0.00455	1.4087	24.121
11	80.7	0.8851	0.00445	1.3968	23.762
12	78.8	0.8880	0.00428	1.3845	23.421
13	112.6	0.8112	0.02120	1.4072	24.376
14	109.2	0.8156	0.01730	1.4160	24.662
15	106.5	0.8211	0.01441	1.4248	24.983
16	104.4	0.8260	0.01199	1.4329	25.288
17	103.3	0.8307	0.00997	1.4428	25.588
18	103.0	0.8365	0.00840	1.4512	25.925
19	103.6	0.8421	0.00715	1.4611	26.336
20	104.8	0.8481	0.00635	1 4713	26.684
21	107.3	0.8537	0.00560	1.4829	27.095
22	79.2	0.8811	0.00480	1.3742	23.066
23	81.4	0.8714	0.00510	1.3770	23.126
24	83.9	0.8621	0.00578	1.3793	23.224
25	86.9	0.8531	0.00648	1.3823	23.305
26	90.4	0.8438	0.00790	1.3849	23.458
27	94.6	0.8348	0.00967	1.3875	23.528
28	98.5	0.8273	0.01165	1.3901	23.691
29	103.9	0.8199	0.01425	1.3930	23.865
30	110.0	0.8132	0.01815	1.3958	23.976
31	106.3	0.8188	0.01570	1.4050	24.296
32	104.0	0.8236	0.01350	1.4132	24.555
33	102.2	0.8293	0.01097	1.4222	24.842
34	100.8	0.8344	0.00908	1.4314	25.152
35	100.5	0.8399	0.00792	1.4408	25.467
36	100.6	0.8460	0.00694	1.4505	25.800
37	101.1	0.8518	0.00620	1.4603	26.238
38	102.3	0.8576	0.00563	1.4711	26.659
39	101.4	0.8260	0.01222	1.4021	24.121
40	99.7	0.8313	0.01022	1.4110	24.393
41	98.6	0.8368	0.00875	1.4199	24.673
42	97.8	0.8427	0.00755	1.4288	25.005
43	97.3	0.8482	0.00659	1.4391	25.328
44	97.3	0.8543	0.00594	1.4490	25.672
45	98.1	0.8601	0.00547	1.4600	26.089

TABLE 3—*Concluded*

SAMPLE NUMBER	BOILING POINT °C.	DENSITY	VISCOSITY	REFRACTIVE INDEX	SURFACE TENSION
46	97.3	0.8335	0.01005	1.4006	24.026
47	96.0	0.8395	0.00838	1.4087	24.278
48	95.2	0.8454	0.00737	1.4176	24.608
49	94.5	0.8512	0.00642	1.4264	24.907
50	94.2	0.8578	0.00592	1.4372	25.262
51	94.3	0.8639	0.00546	1.4477	25.553
52	93.2	0.8424	0.00809	1.3969	23.886
53	92.4	0.8490	0.00710	1.4062	24.153
54	91.8	0.8544	0.00633	1.4152	24.467
55	91.4	0.8609	0.00557	1.4246	24.775
56	91.3	0.8671	0.00520	1.4357	25.110
57	89.4	0.8511	0.00661	1.3943	23.731
58	88.8	0.8572	0.00600	1.4039	24.022
59	88.3	0.8631	0.00541	1.4127	24.310
60	88.1	0.8697	0.00511	1.4226	24.637
61	86.2	0.8600	0.00600	1.3919	23.604
62	85.8	0.8655	0.00540	1.4015	23.888
63	85.5	0.8723	0 00493	1.4109	24 168
64	83.1	0.8682	0.00516	1.3892	23.572
65	82.8	0.8755	0.00475	1.3887	23.834
66	80.8	0.8782	0.00468	1.3867	23.412

The slope of these curves indicates a slight decrease in volume upon mixing.

In the triangular diagram (figure 2) the constant density lines are practically parallel and slope generally in the direction of maximum per cent of ethyl acetate. This characteristic curvature is to be expected because of the change in volume when the different components are mixed.

Viscosity

The binoidal curves for viscosity (figure 3) show the effect of increasing percentages of ethyl acetate to butyl alcohol–toluene mixtures. The effect becomes less pronounced as increasing increments of ethyl acetate are added and is indicated by the closeness of the 60, 70, 80, and 90 per cent lines compared to the 10, 20, and 30 per cent lines.

In the triangular diagram (figure 4) showing constant viscosity lines, this effect is shown by the small change in viscosities as large increases in ethyl acetate are made. These lines do not have appreciable maxima, although the effect of additions of butyl alcohol is slightly in this direction.

Refractive index

The binoidal curves for refractive indices (figure 5) are practically straight-line functions of composition. The small amount of curvature present slopes similarly to the relative density curves.

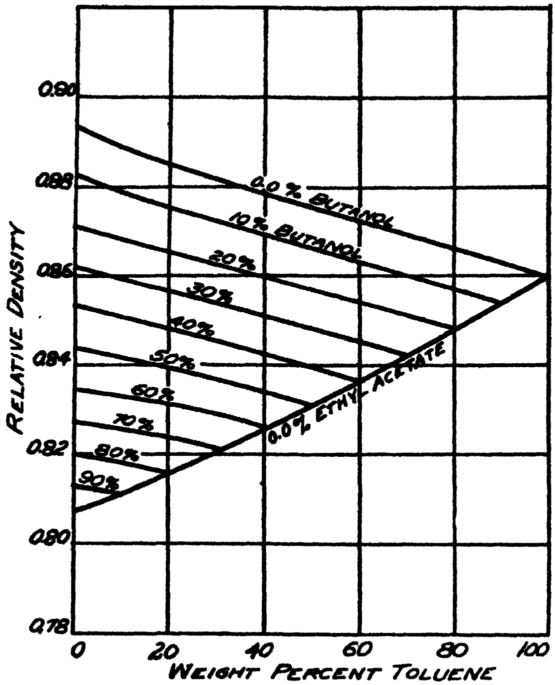

Fig. 1. Binoidal curves showing relative densities at 25°C.

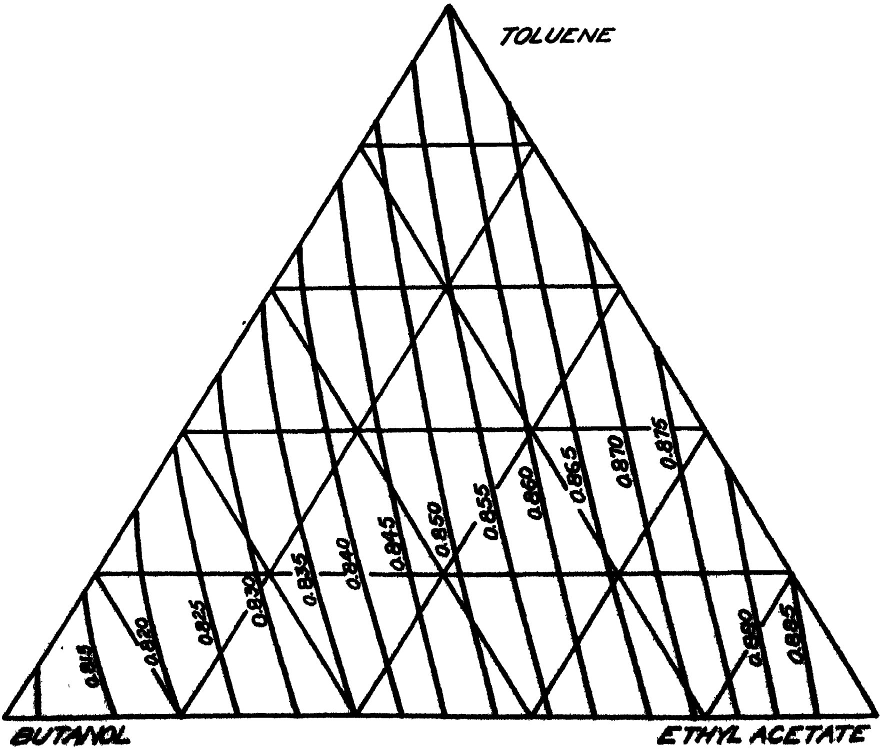

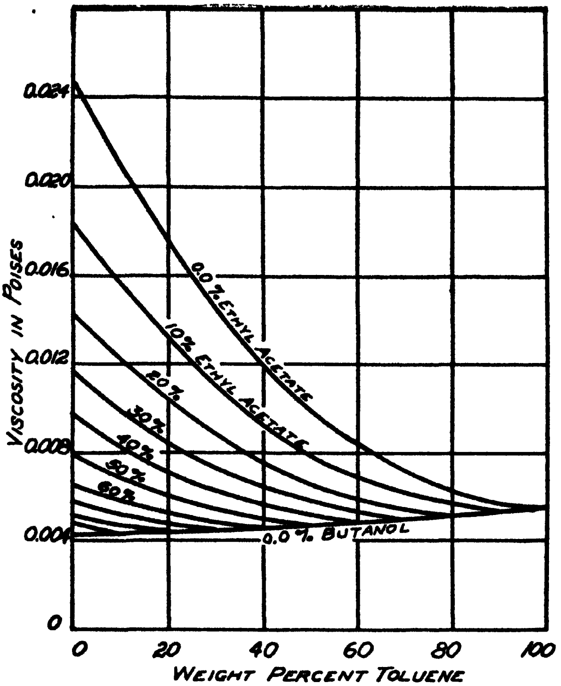

Fig. 3. Binoidal curves showing viscosities at 25°C.

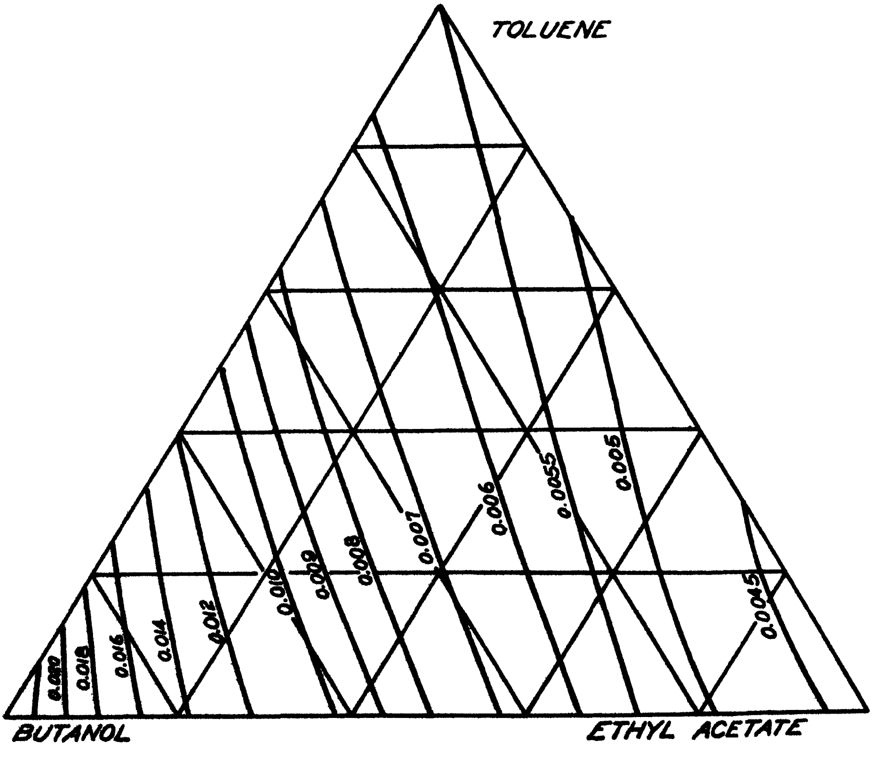

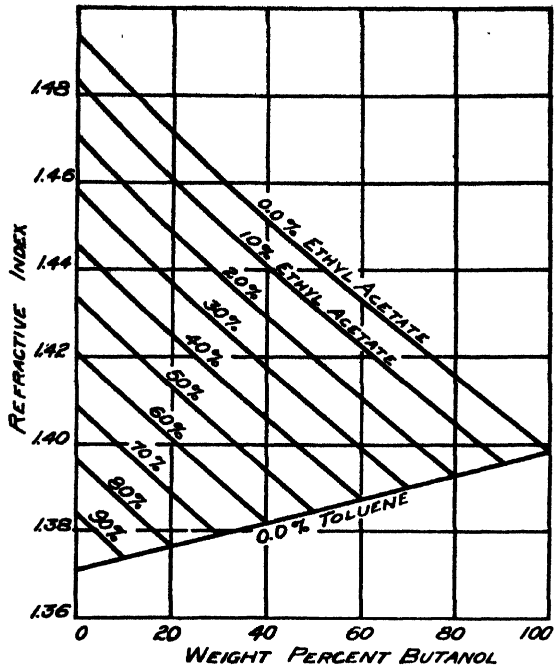

Fig. 5. Binoidal curves showing refractive indices at 25°C.

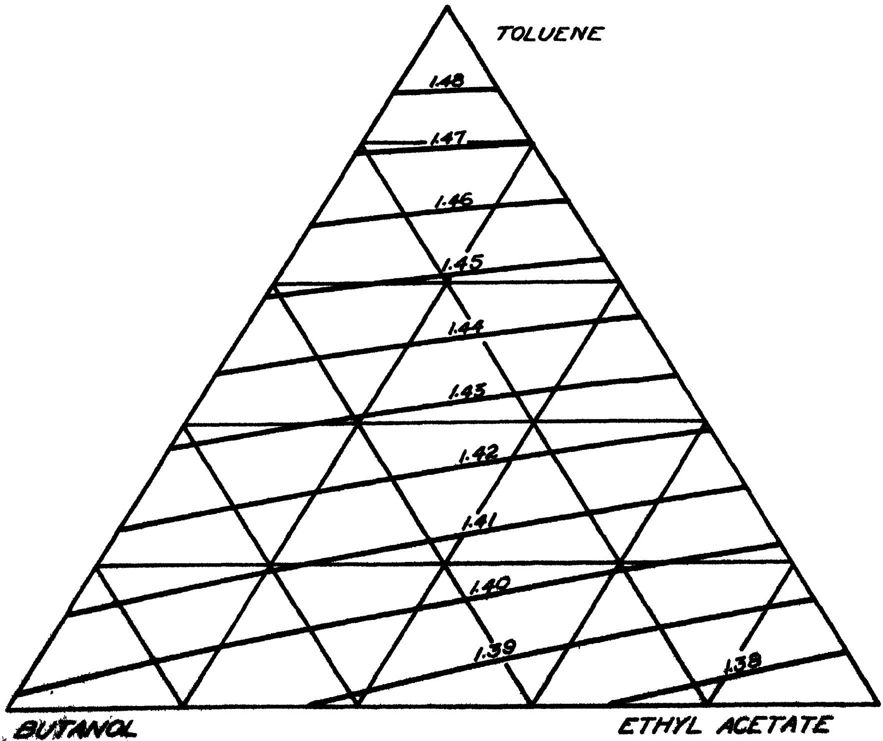

Fig. 6. Triangular diagram showing refractive indices at 25°C.

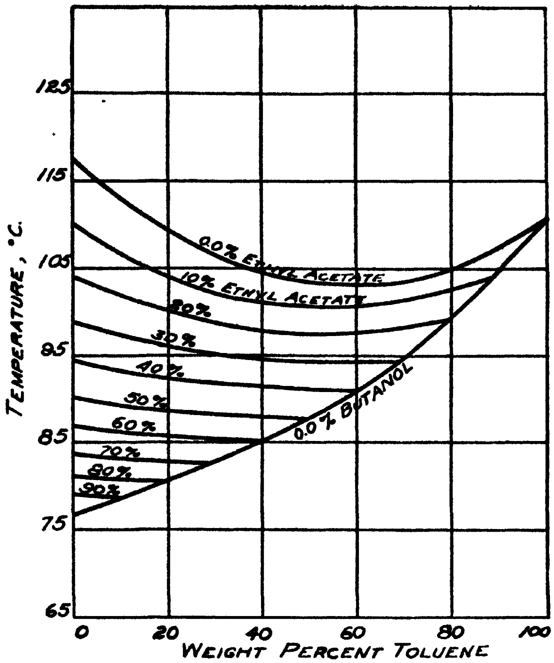

FIG. 7. Binoidal curves showing boiling points of butyl alcohol–ethyl acetate–toluene mixtures

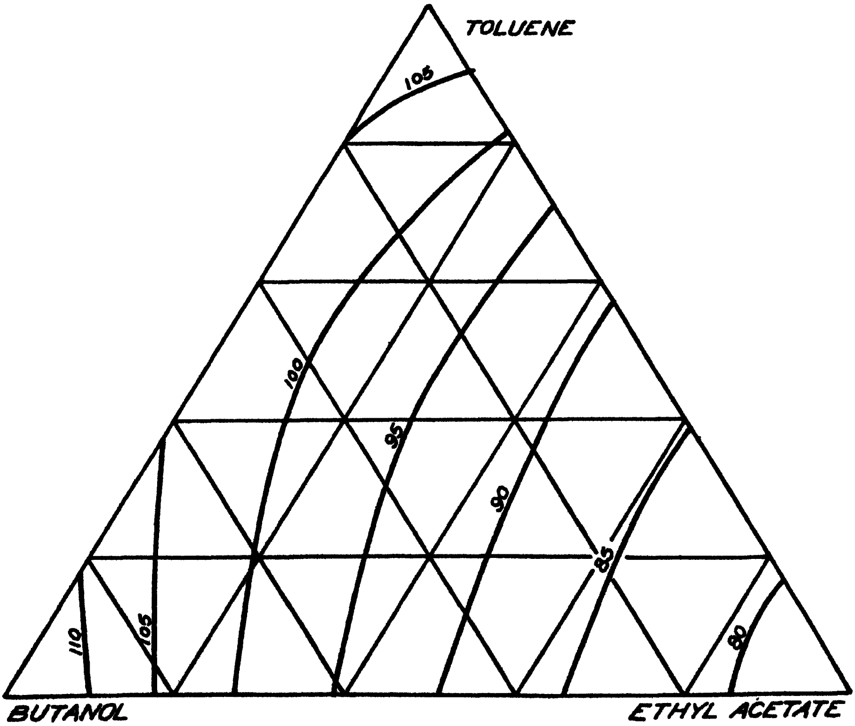

FIG. 8. Triangular diagram showing boiling points of butyl alcohol–ethyl

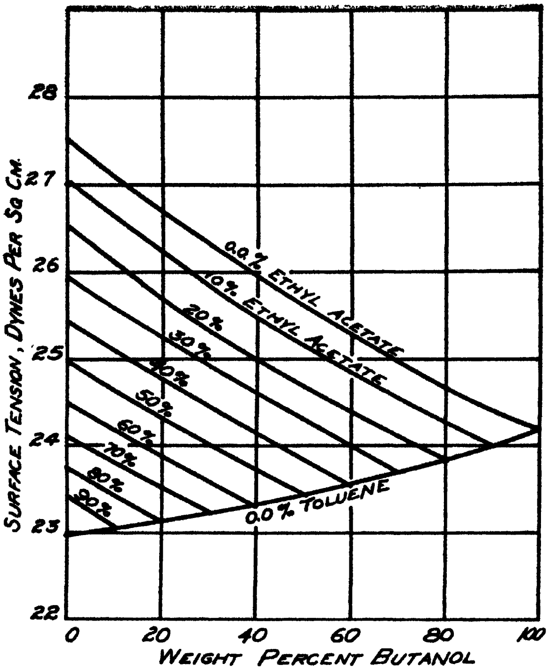

Fig. 9. Binoidal curves showing surface tensions at 25°C.

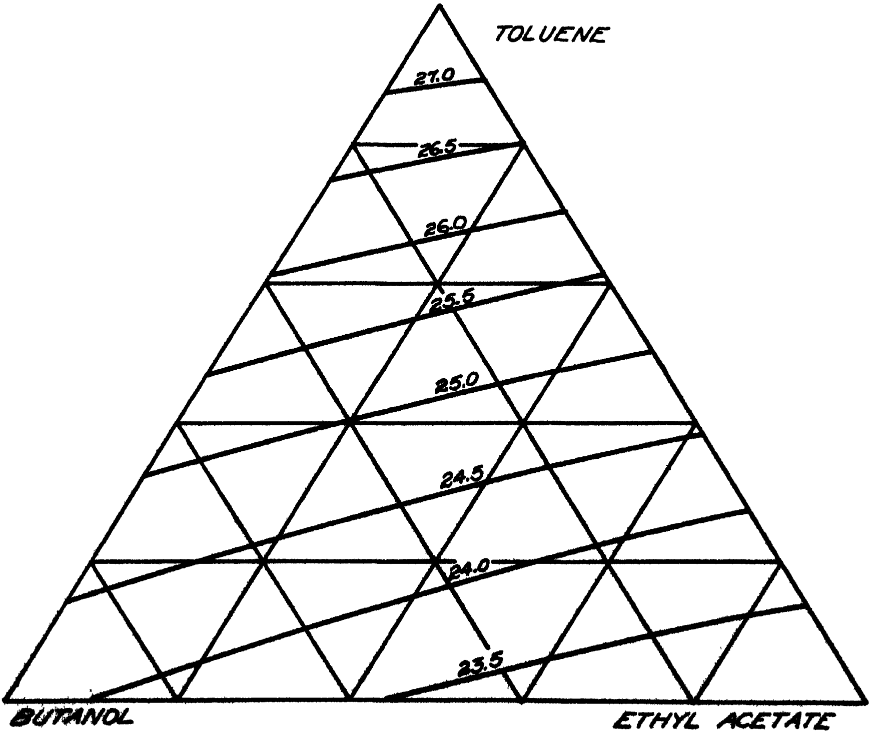

Fig. 10. Triangular diagram showing surface tensions at 25°C.

The effect of varying weights of butyl alcohol–ethyl acetate and toluene upon refractive indices is shown in figure 6. These lines are practically parallel, the increasing weight increments of all three components causing almost regular increases in refractive index values.

Boiling points

The boiling points of mixtures of butyl alcohol and toluene pass through a minimum at about 60 per cent toluene (figure 7). Increasing additions of ethyl acetate to this binary system cause the minimum to disappear when 40 per cent has been added. The curve for the toluene–ethyl acetate system shows neither maximum nor minimum as does the butyl alcohol–ethyl acetate system.

The triangular diagram (figure 8) showing compositions of mixtures of constant boiling point indicates that the minimum of the butyl alcohol–toluene mixtures at 60 per cent toluene has a boiling point of about 103°C. The effect of increasing additions of ethyl acetate to the butyl alcohol–toluene mixtures is to decrease continually the boiling points of the three-component system.

Surface tension

The binoidal curves for surface tension (figure 9) show slight curvature corresponding to those for refractive index. Increasing percentages of ethyl acetate to toluene–butyl alcohol mixtures tend to straighten the constant per cent ethyl acetate curves.

The triangular diagram for surface tension (figure 10) shows that this property is very regular, the addition of increasing weight increments of toluene effecting regular increases of surface tension values.

CONCLUSIONS

Densities, viscosities, refractive indices, boiling points, and surface tensions for the ternary system butyl alcohol–ethyl acetate–toluene have been determined. Both binoidal and triangular diagrams have been prepared for each property and are included in this paper.

REFERENCES

(1) Brunel, Crenshaw, and Tobin: J. Am. Chem. Soc. **43**, 566 (1921).
(2) Brunjes and Furnas: Ind. Eng. Chem. **27**, 396 (1935).
(3) Bushmakin, Begetova, and Kuchinskaya: Sintet. Kauchuk **4**, 8 (1936).
(4) Davis: Ind. Eng. Chem. **22**, 380 (1930).
(5) Ernst, Litkenhous, and Spanyer: J. Phys. Chem. **36**, 842 (1932).
(6) Ernst, Watkins, and Ruwe: J. Phys. Chem. **40**, 627 (1936).
(7) Furnas and Leighton: Ind. Eng. Chem. **29**, 709 (1937).
(8) Gill and Dexter: Ind. Eng. Chem. **26**, 881 (1934).
(9) Hennault-Roland and Lek: Bull. soc. chim. Belg. **40**, 177 (1931).
(10) *International Critical Tables:* Vols. III, IV, V, VII. McGraw-Hill Book Co., New York (1933).

(11) Kahlbaum: Z. physik. Chem. **26**, 577 (1898).
(12) Lange: *Handbook of Chemistry and Physics*, 2nd edition, p. 735. Handbook Publishers Inc., Sandusky, Ohio (1936).
(13) Mason and Washburn: J. Phys. Chem. **40**, 481 (1936).
(14) Richards and Coombs: J. Am. Chem. Soc. **37**, 1656 (1915).
(15) Richards and Mathews: J. Am. Chem. Soc. **30**, 8 (1908).
(16) Smith and Wojciechowski: Roczniki Chem. **16**, 104 (1937).
(17) Timmermans and Martin: J. chim. phys. **23**, 733 (1926).
(18) Wade and Merriman: J. Chem. Soc. **101**, 2438 (1912).

THE CONDUCTANCE OF SALTS IN MONOETHANOLAMINE

H. T. BRISCOE AND THEDFORD P. DIRKSE

Department of Chemistry, Indiana University, Bloomington, Indiana

Received July 24, 1939

Solutions in which monoethanolamine acts as the solvent have received very little theoretical consideration. Monoethanolamine is very viscous, it has a dielectric constant approximately half that of water, and it is a very good solvent for many salts. This study deals with the conductances of solutions of salts in this solvent. The equations to be tested include (*a*) the equation of Debye–Hückel for calculating activity coefficients, and (*b*) Onsager's conductance equation.

EXPERIMENTAL

The bridge used in this work was similar to the bridge recommended by Jones and Joseph (8). Every precaution they suggested was taken. All the leads were shielded to reduce capacitance, and a condenser was used to balance out capacitance that could not be eliminated by mechanical means. The average amount of this capacitance was 0.000005 microfarad. The frequency of the alternating current was 1250 cycles per second. Transformer oil was used in the constant-temperature bath to reduce stray capacitance between the leads of the cell. The temperature of the bath was maintained at 25°C. ± 0.015°, as measured by a Beckmann thermometer which was calibrated against a U. S. Bureau of Standards' thermometer.

The cell was made of Pyrex glass and was fitted with platinum electrodes. It was constructed according to the directions of Jones and Bollinger (6). The electrodes were not platinized, since the solutions used were dilute and alkaline (5). The cell constant was measured by using 0.01 demal potassium chloride which has a conductance of 0.00140877 mho, as determined by Jones and Bradshaw (7).

The salts were prepared according to the directions given by Dasher (2). The ethanolamine was purified by distillation. In the first distillation the middle fraction was directed into another distilling flask. This frac-

TABLE 1

Monomethylammonium picrate

$\Lambda_0 = 1724.14$; $K_1 = 0.4705 \times 10^{-6}$

$C \times 10^6$	Λ	$f_{\pm \text{exp.}}$	$f_{\pm \text{calc.}}$	$K_{\text{Onsager}} \times 10^{-6}$	$K_{\text{Ostwald}} \times 10^{-6}$	$K' \times 10^{-6}$	$K \times 10^{-6}$
1495	10.97	0.989	0.873	1546	0.06	0.06	0.05
252	36.90	0.992	0.946	260	0.11	0.11	0.11
59	83.05	0.994	0.973	62	0.14	0.14	0.14
19	189.47	0.995	0.985	21	0.25	0.25	0.25
7.6	381.58	0.995	0.990	9.8	0.47	0.47	0.47
2.5	600.00	0.997	0.994	3.8	0.46	0.46	0.46
0.9	888.88	0.998	0.997	1.8	0.49	0.49	0.49

TABLE 2

Dimethylammonium picrate

$\Lambda_0 = 757.57$; $K_1 = 5.611 \times 10^{-6}$

$C \times 10^6$	Λ	$f_{\pm \text{exp.}}$	$f_{\pm \text{calc.}}$	$K_{\text{Onsager}} \times 10^{-6}$	$K_{\text{Ostwald}} \times 10^{-6}$	$K' \times 10^{-6}$	$K \times 10^{-6}$
1394	19.08	0.979	0.877	1469	0.90	0.91	0.87
600	40.30	0.980	0.917	645	1.79	1.80	1.73
262	55.72	0.984	0.944	286	1.52	1.53	1.49
224	64.98	0.984	0.948	248	1.80	1.82	1.76
83	148.69	0.985	0.968	104	3.99	4.02	3.90
33	252.38	0.988	0.979	50	5.59	5.63	5.50
11	372.62	0.991	0.988	22	5.48	5.32	5.23
2	573.00	0.995	0.994	9	5.51	5.55	5.50

TABLE 3

Trimethylammonium picrate

$\Lambda_0 = 543.48$; $K_1 = 3.584 \times 10^{-6}$

$C \times 10^6$	Λ	$f_{\pm \text{exp.}}$	$f_{\pm \text{calc.}}$	$K_{\text{Onsager}} \times 10^{-6}$	$K_{\text{Ostwald}} \times 10^{-6}$	$K' \times 10^{-6}$	$K \times 10^{-6}$
953	28.85	0.975	0.897	1029	2.84	2.86	2.72
368	49.91	0.979	0.934	412	3.42	3.45	3.31
106	91.49	0.985	0.964	128	3.61	3.63	3.53
34	129.46	0.989	0.979	45	2.59	2.58	2.53
14	220.84	0.991	0.986	24	4.04	4.04	3.98
4	410.12	0.993	0.992	17	10.22	10.2	10.01

TABLE 4

Tetramethylammonium picrate

$\Lambda_0 = 2222.22$; $K_1 = 0.09145 \times 10^{-6}$

$C \times 10^6$	Λ	$f_{\pm \text{exp.}}$	$f_{\pm \text{calc.}}$	$K_{\text{Onsager}} \times 10^{-6}$	$K_{\text{Ostwald}} \times 10^{-6}$	$K' \times 10^{-6}$	$K \times 10^{-6}$
1256	15.52	0.989	0.883	1297	0.06	0.06	0.06
401	27.12	0.992	0.932	412	0.06	0.06	0.06
175	41.09	0.993	0.954	180	0.06	0.06	0.06
65	80.99	0.994	0.972	68	0.09	0.09	0.08
23	131.86	0.995	0.983	25	0.08	0.08	0.08
7	251.85	0.996	0.990	8	0.10	0.10	0.10
3	457.04	0.997	0.993	4	0.17	0.17	0.17

TABLE 5

Triisoamylammonium picrate

$\Lambda_0 = 1010.1;\ K_1 = 5.636 \times 10^{-7}$

$C \times 10^6$	Λ	$f_{\pm\text{exp.}}$	$f_{\pm\text{calc.}}$	$K_{\text{Onsager}} \times 10^{-6}$	$K_{\text{Ostwald}} \times 10^{-6}$	$K' \times 10^{-6}$	$K \times 10^{-6}$
1707	16.17	0.981	0.865	17860	4.44	4.48	4.31
667	29.20	0.984	0.913	7004	5.74	5.78	5.60
227	50.97	0.988	0.948	2423	6.10	6.13	5.98
87	82.74	0.990	0.967	954	6.36	6.38	6.26
30	119.96	0.993	0.980	342	4.80	4.81	4.75
9	291.97	0.994	0.989	135	11.27	11.30	11.17
3	602.59	0.995	0.993	55	29.28	29.37	29.08

TABLE 6

Monomethylammonium chloride

$\Lambda_0 = 221.24;\ K_1 = 6.538 \times 10^{-6}$

$C \times 10^6$	Λ	$f_{\pm\text{exp.}}$	$f_{\pm\text{calc.}}$	$K_{\text{Onsager}} \times 10^{-6}$	$K_{\text{Ostwald}} \times 10^{-6}$	$K' \times 10^{-6}$	$K \times 10^{-6}$
7466	7.23	0.946	0.738	8236	8.26	8.42	7.54
2388	12.44	0.960	0.842	2626	8.01	8.13	7.49
927	17.79	0.970	0.898	1033	6.53	6.60	6.21
290	30.25	0.978	0.941	341	6.33	6.36	6.08
108	44.08	0.984	0.964	137	5.414	5.43	5.27
45	74.33	0.986	0.976	114	7.79	7.82	7.61
16	98.28	0.990	0.985	29	5.79	5.81	5.70
13	112.69	0.990	0.987	27	7.07	7.07	6.94

TABLE 7

Dimethylammonium chloride

$\Lambda_0 = 373.13;\ K_1 = 12.64 \times 10^{-6}$

$C \times 10^6$	Λ	$f_{\pm\text{exp.}}$	$f_{\pm\text{calc.}}$	$K_{\text{Onsager}} \times 10^{-6}$	$K_{\text{Ostwald}} \times 10^{-6}$	$K' \times 10^{-6}$	$K \times 10^{-6}$
2641	25.63	0.953	0.835	2949	13.40	13.6	12.4
787	47.48	0.965	0.906	923	14.6	14.8	13.8
381	61.04	0.972	0.933	463	12.2	12.4	11.7
138	97.74	0.979	0.959	189	12.9	12.9	12.4
42	155.96	0.985	0.977	74	12.9	12.9	12.6
15	259.83	0.988	0.986	49	24.1	24.2	23.7

TABLE 8

Trimethylammonium chloride

$\Lambda_0 = 216.45;\ K_1 = 24.97 \times 10^{-6}$

$C \times 10^6$	Λ	$f_{\pm\text{exp.}}$	$f_{\pm\text{calc.}}$	$K_{\text{Onsager}} \times 10^{-6}$	$K_{\text{Ostwald}} \times 10^{-6}$	$K' \times 10^{-6}$	$K \times 10^{-6}$
4311	15.56	0.939	0.794	4889	24.1	24.6	21.8
1418	27.22	0.954	0.876	1673	25.7	24.7	22.5
508	47.17	0.963	0.923	664	31.1	31.4	29.2
216	63.16	0.972	0.949	310	26.7	26.4	24.9
69	88.21	0.981	0.971	117	19.5	19.6	18.9
24	132.79	0.986	0.982	64	24.4	24.4	23.8
16	126.88	0.989	0.985	40	13.8	13.8	13.5
8	208.74	0.990	0.990	242	242	225	221

tion was redistilled and fractionated again; only the middle fraction was collected. These distillations were conducted in an all-glass apparatus, and at no time did the ethanolamine come in contact with the air. The freezing point of the purified ethanolamine was 10.53°C. compared with 10.5°C., the value reported by the Carbide and Carbon Chemicals Corporation. The refractive index of the ethanolamine at 20°C. was found to be 1.45342 compared with 1.4539, the value reported by the Carbide

TABLE 9

Tetramethylammonium chloride

$\Lambda_0 = 45.05$; $K_1 = 150.3 \times 10^{-6}$

$C \times 10^6$	Λ	$f_{\pm\text{exp.}}$	$f_{\pm\text{calc.}}$	$K_{\text{Onsager}} \times 10^{-6}$	$K_{\text{Ostwald}} \times 10^{-6}$	$K' \times 10^{-6}$	$K \times 10^{-6}$
2750	11.27	0.911	0.832	3875	230	240	200
1180	14.07	0.934	0.886	1785	167	173	151
550	17.27	0.950	0.921	919	130	135	121
260	23.46	0.959	0.945	556	148	151	139
110	34.55	0.968	0.963	489	271	288	270
60	33.33	0.976	0.973	236	125	129	123
20	40.00	0.985	0.984	184	133	145	141

TABLE 10

Tetraisoamylammonium iodide

$\Lambda_0 = 617.28$; $K_1 = 7.117 \times 10^{-7}$

$C \times 10^6$	Λ	$f_{\pm\text{exp.}}$	$f_{\pm\text{calc.}}$	$K_{\text{Onsager}} \times 10^{-6}$	$K_{\text{Ostwald}} \times 10^{-6}$	$K' \times 10^{-6}$	$K \times 10^{-6}$
1245	11.00	0.983	0.883	12990	4.03	4.05	3 92
436	21.31	0.986	0.929	4589	5.39	5.41	5.27
162	38.43	0.988	0.956	1750	7.08	7.10	6.94
65	62.19	0.991	0.971	737	7.44	7.46	7.33
24	96.04	0.993	0.982	297	7.17	7.18	7.08
10	189.81	0.993	0.988	145	13.68	13.70	13.53

TABLE 11

Tetraisoamylammonium nitrate

$\Lambda_0 = 2272.7$; $K_1 = 1.01 \times 10^{-7}$

$C \times 10^6$	Λ	$f_{\pm\text{exp.}}$	$f_{\pm\text{calc.}}$	$K_{\text{Onsager}} \times 10^{-7}$	$K_{\text{Ostwald}} \times 10^{-7}$	$K' \times 10^{-7}$	$K \times 10^{-7}$
761	22.05	0.990	0.907	7844	0.72	0.72	0.71
546	26.55	0.991	0.921	5618	0.75	0.75	0.74
178	51.63	0.992	0.954	1841	0.94	0.94	0.93
64	84.98	0.994	0.972	676	0.93	0.94	0.93
24	145.51	0.995	0.982	265	1.08	1.08	1.07
9	229.12	0.996	0.989	107	1.08	1.08	1.07
5	352.05	0.996	0.991	63	1.53	1.53	1.52

and Carbon Chemicals Corporation. The dielectric constant at 25°C. was measured by V. E. Parker of this laboratory and found to be 37.72. W. C. Davis of this laboratory measured the viscosity of the ethanolamine at 25°C. and found it to be 0.19346 poise.

The solutions were made up by weight. A portion of the salt was weighed in a special flask. This flask was then filled with ethanolamine and reweighed. The cell was filled directly from this flask. The remaining solution was then diluted and the process repeated. Ground-glass joints were used throughout to prevent the solution from coming in direct contact with the air. The cell was washed out several times with the solution to be measured before a measurement was taken.

TABLE 12

Conductance of triisoamylammonium picrate

SOLVENT	$C \times 10^6$	Λ
D.K. = 26.04	120.8	12.42
79.8 per cent ethanolamine	46.51	19.35
20.2 per cent dioxane	22.55	31.04
	719.7	7.92
D.K. = 18.80	268.8	8.56
59.7 per cent ethanolamine	111.9	9.83
40.3 per cent dioxane	47.81	12.55
	20.41	68.59
	830.4	7.23
D.K. = 14.62	334.5	7.77
49.7 per cent ethanolamine	116.9	8.55
50.3 per cent dioxane	43.94	13.65
	17.60	17.05

RESULTS

Tables 1 to 12 show the experimental results. The concentration of the salt in equivalents per liter is represented by C; Λ is the equivalent conductance; $f_{\pm\,\text{exp.}}$ is the experimentally obtained activity coefficient as calculated by the method of Kraus and Fuoss (9), while $f_{\pm\,\text{calc.}}$ is the theoretical activity coefficient of the binary salt as a whole calculated by means of the Debye–Hückel equation (3):

$$\ln f_{\pm} = -z_{+}z_{-}\frac{\epsilon^3}{(DKT)^{3/2}}\sqrt{\frac{\pi N}{1000}\sum_i c_i z_i^2}$$

K_{Onsager} is the ionization constant calculated from Onsager's equation (11):

$$\Lambda_e = \Lambda_0 - \alpha\sqrt{C} - \frac{\Lambda_0 C}{K}$$

K_{Ostwald} is the ionization constant calculated from Ostwald's dilution law; K' is the stoichiometrical ionization constant; K is the thermodynamic ionization constant. The conductance at infinite dilution, Λ_0, and K_1, the experimental ionization constant, were obtained by using the method of Kraus and Fuoss (9).

According to D. Belcher (1), extrapolation may not give correct values of Λ_0 for weak electrolytes ($K \leqq 10^{-5}$). On this basis the values of Λ_0 for all the salts except the chlorides may be in error. For this reason the results for the chlorides only are given in graphical form (figure 1). The theoretical slope of the curve as given by the Onsager equation is also plotted for the chlorides.

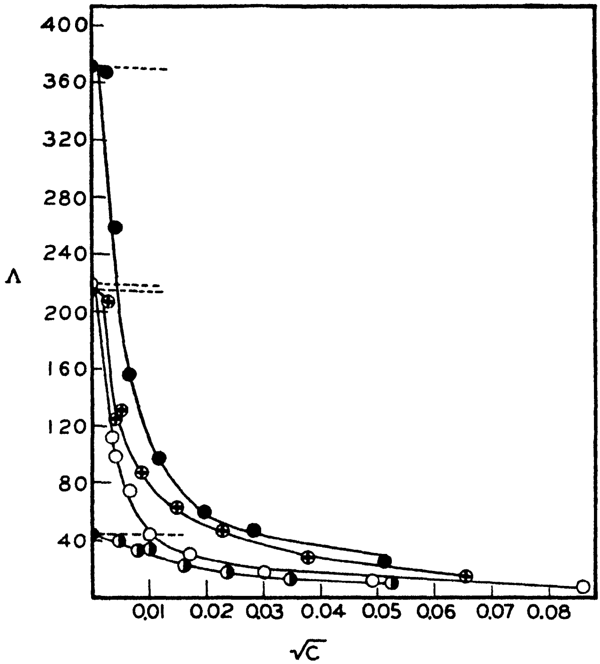

FIG. 1. Plot of $\sqrt{C}$ against Λ. ○, monomethylammonium chloride; ●, diethylammonium chloride; ⊕, trimethylammonium chloride; ◑, tetramethylammonium chloride.

DISCUSSION

Figure 1 shows that for each salt the experimental slope is much steeper than the Onsager slope. Only for tetramethylammonium chloride do the experimental and theoretical slopes approach each other. The fact that the conductances of all the solutions vary greatly with the concentration shows that these salts behave as weak electrolytes in monoethanolamine.

Walden and Birr (12) measured the conductances of substituted ammonium picrates and chlorides in acetonitrile. Their results show that in acetonitrile tetramethylammonium picrate behaves as a strong electrolyte in the dilute region. Wright, Murray-Rust, and Hartley (13) found that this salt behaved similarly in nitromethane. In monoethanolamine this same salt behaves as a weak electrolyte except at infinite dilution where its conductance is higher than that of the other salts. Walden and Birr's results vary considerably from the theoretical Onsager values. But in ethanolamine the same or similar salts all vary still more than in acetonitrile. For the chlorides, the experimental slope in monoethanolamine deviates from the theoretical Onsager slope about four times as much as in acetonitrile.

The differences in the behavior of these salts in acetonitrile and monoethanolamine may be explained in one or two ways. First, the differences may arise from differences in the extent to which ions are solvated in the two solvents. For all the salts studied, the ionization constants calculated according to Onsager's approximate equation decrease as the concentration decreases. This may be explained by solvation, which would cause some of the solvent to be used in solvating the ions, thus raising the concentration of the ions in the remaining solvent. This effect should diminish with increasing dilution. The chemical character and molecular structure of monoethanolamine strongly support the belief that it may strongly solvate ions.

In the second place, these differences may be explained by differences in some physical property of the solvents. The dielectric constant of acetonitrile is 36, and that of nitromethane is 37. These values are practically the same as that for monoethanolamine (37.72). If the apparent degree of dissociation depends solely upon the dielectric constant of the solvent, then the salts studied should behave similarly in these three solvents. The fact that this is not so indicates that the apparent degree of dissociation is not dependent entirely upon the dielectric constant of the solvent. An important physical difference in the three solvents is shown by their viscosities; the viscosity of monoethanolamine is thirty-two times as great as that of nitromethane and sixty-five times that of acetonitrile. Since increasing viscosity tends to decrease the mobilities of the ions and thus to decrease the conductance, the high viscosity of monoethanolamine may account for the fact that the salts here studied behave as weak electrolytes in monoethanolamine.

Kraus and Fuoss (10) found that tetraisoamylammonium nitrate is a strong electrolyte, but that triisoamylammonium picrate is a weak electrolyte when dissolved in ethylene dichloride and in mixtures of this solvent with benzene and dioxane. In monoethanolamine these two electrolytes show a difference only at infinite dilution. It may be that at dilutions other than infinite the high viscosity of monoethanolamine slows the mobilities of the ions down to about the same level, since the curves of all the salts studied are approximately the same.

The stoichiometrical ionization constants agree fairly well with the experimental ionization constants up to concentrations of about 1 × 10^{-3} equivalents per liter. The ionization constants calculated according to Ostwald's dilution law agree very well with the stoichiometrical ionization constants at all concentrations. Onsager's equation does not express accurately the ionization constants in these solutions. The values calculated from it do approach the experimental ionization constants as the dilution is increased, but only in one or two instances is there any agreement in the vicinity of infinite dilution. At very great dilutions, for some of the salts, the calculated ionization constants are greater than the experimental values. This is perhaps explained by the fact that at these high dilutions the conductance measurements cannot be made as accurately as in more concentrated solutions. The experimental value is only an approximate value. In some instances the ionization constant increases rather abruptly at certain concentrations.

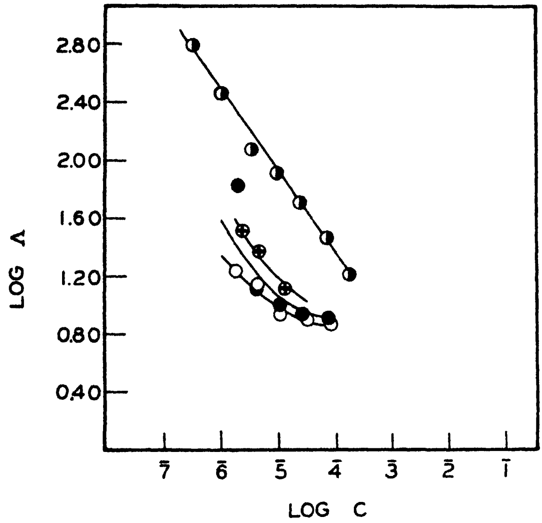

FIG. 2. Plot of log C against log Λ. ◑, dielectric constant = 37.72; ⊕, dielectric constant = 26.04; ●, dielectric constant = 18.80; ○, dielectric constant = 14.62.

In monoethanolamine the Debye-Hückel equation for the activity coefficient of a binary salt as a whole reduces to

$$\log f_{\pm} = -1.523\sqrt{C}$$

where C is the stoichiometric concentration. This equation assumes complete dissociation, since the stoichiometric concentration is substituted for the ionic concentration. Tables 1 to 11 show that for the solutions studied the experimental activity coefficients agree with the theoretical values up to a concentration of about 1×10^{-4} gram-equivalents per liter.

Table 12 and figure 2 show the results of the conductance measurements of triisoamylammonium picrate in solvents of different dielectric constants. The solvents were obtained by mixing monoethanolamine and dioxane in varying proportions. The percentages are given by weight. As the dielectric constant of the solvent decreases, the conductance at a definite concentration also decreases. This is to be expected, since a decrease in dielectric constant means greater electrical attraction between the ions. The curves in figure 2 show a tendency to flatten out as the concentration increases, and seem to approach a minimum. This is explained by means of the concept of triple ions as suggested by Fuoss and Kraus (4). It was hoped that it would be possible to extend the measurements to higher concentrations in order to determine at just which concentration the minimum appears. However, solutions of greater concentrations changed from an orange-yellow to a rather deep red color upon standing a few hours. This change of color probably indicates a reaction between the picrate and the ethanolamine. Thus, measurements in this range of concentration are, in all probability, in error. With dilute solutions such as those actually used, reproducible results were obtained for solutions over varying periods of time. This color change was also noticed in concentrated solutions of mixed solvents containing more than 60 per cent of ethanolamine. For this reason only measurements of the most dilute solutions are used.

SUMMARY

1. The salts studied behave as weak electrolytes in monoethanolamine as judged by the change in conductance with changing concentrations, but their conductances are high.

2. The Onsager equation does not give theoretical values for the conductances of these solutions which agree with the experimental values. The lack of agreement is the result, at least in part, of the failure of this equation to account fully for the viscosity effect.

3. The Debye–Hückel equation for activity coefficients agrees as well as could be expected with the experimental results for the solutions studied.

4. In dilute solutions the conductance of triisoamylammonium picrate decreases as the dielectric constant decreases and approaches a minimum with increasing concentration.

REFERENCES

(1) Belcher, D.: J. Am. Chem. Soc. **60**, 2744 (1938).
(2) Dasher, P.: Thesis, Indiana University, 1937.
(3) Debye, P., and Hückel, E.: Physik. Z. **24**, 185 (1923).
(4) Fuoss, R., and Kraus, C.: J. Am. Chem. Soc. **55**, 2387 (1933).
(5) Jones, G., and Bollinger, D.: J. Am. Chem. Soc. **57**, 280 (1935).
(6) Jones, G., and Bollinger, G.: J. Am. Chem. Soc. **53**, 411 (1931).
(7) Jones, G., and Bradshaw, B.: J. Am. Chem. Soc. **55**, 1780 (1933).
(8) Jones, G., and Joseph, R.: J. Am. Chem. Soc. **50**, 1049 (1928).
(9) Kraus, C., and Fuoss, R.: J. Am. Chem. Soc. **55**, 476 (1933); **57**, 488 (1935).
(10) Kraus, C., and Fuoss, R.: J. Am. Chem. Soc. **55**, 22 (1933).
(11) Onsager, L.: Physik. Z. **28**, 277 (1927).
(12) Walden, P., and Birr, E.: Z. physik. Chem. **A144**, 269 (1929).
(13) Wright, C., Murray-Rust, D., and Hartley, H.: J. Chem. Soc. **1931**, 199.

NEW BOOKS

An Introduction to the Principles of Physical Chemistry. By O. Maass and E. W. R. Steacie. Second edition. 15.5 x 23.5 cm.; ix + 395 pp.; 102 fig. New York: John Wiley and Sons, Inc., 1939. Price: $3.00.

The second edition of this text has been materially improved by the addition of new chapters on atomic structure, phase rule, and colloidal systems, and also by the rewriting, revision, and substantial extension of chapters dealing with chemical reactions, electrolytic dissociation, and electrochemistry. As in the first edition, the clarity of presentation is excellent. The inclusion of many new figures also constitutes a commendable addition and increases the value of the book as a text.

There can be no serious criticism of the scope of the topics presented. Although the content was limited to that which could be covered in about fifty lectures, the inclusion of a short chapter on crystalline state and crystal structure would probably have been justified. Possibly greater emphasis should have been given to determination of molecular weights in the chapter on the gaseous state. Also it might have been more logical to give the method for determination of molecular dissociation in this chapter than in the chapter on electrolytic dissociation near the end of the book. While the chapter on electrolytic dissociation has been somewhat expanded and improved in this edition, it would have been further improved by more rigorous and, in some instances, more detailed treatment.

On the whole, this new edition is an excellent book and will maintain its high place as a text for the students for whom it was written, namely, those who have had but limited experience in physics and mathematics.

F. E. Bartell.

Electromagnetics: A Discussion of Fundamentals. By Alfred O'Rahilly. xii + 884 pp. London, New York, and Toronto: Longmans, Green and Company, 1939. Cork, Ireland: Cork University Press, 1939. Price: $12.50.

Here is a book written with all the freshness and good-natured humorous combativeness that might be expected from one carrying the name of its author.

In the preface we have, summarized in sequence, the main theses, which are as follows: (*1*) The history of electromagnetic theory is rewritten. It is maintained that Maxwell's views, which were logically stated by Helmholtz and Duhem, are really off the main line of development. The ideas of Gauss and Weber are vindicated; the proposals of Lorentz and Riemann are claimed to supersede Maxwell's displacement-current. (*2*) In particular, the synthetic statement of the accepted "classical" electromagnetic theory is shown to be the force-formula published in 1898 by Liénard, who is still alive and active. (*3*) But it is also shown that the universally ignored alternative formula proposed by Ritz in 1908 is equally, and even more, successful.. The interest of this formula is that it is really and radically relativist,—in the proper acceptation of that much-abused word. Even if Ritz's theory is not accepted, it has at least the merit of proving the unsoundness of most of the arguments adduced in favor of the prevalent view. (*4*) Einstein's use of Voigt's transformation, generally known as the special theory of relativity, is subjected to fundamental criticisms, that is, as regards electromagnetics, for it is proposed to treat optics subsequently. In particular, Lorentz's "local time" and Minkowski's "space-time" are rejected. (*5*) Contemporary discussion of "the aether" is declared to be a mere logomachy, a waste of time. An important distinction is urged between the quantitative equations of physics and the "discourse" of physicists. (*6*) An elementary but radical exposition of the meaning of the symbols of physics is worked out. This is shown to have many practical and even philosophical consequences. It implies the rejection of Bergson's view of duration, of Bridgman's operational theory, and of Eddington's "bundles of pointer-readings." In fact, an attempt is made to sweep idealism and pseudo-mysticism completely out of physics; it is held that physical science is incapable of solving any philosophical problem. (*7*) The question of units and "dimensions," still the subject of controversy in scientific periodicals and of votes at international congresses, is treated in a simple but revolutionary manner. It is claimed that thereby an end is put to barren discussions which have now lasted over fifty years, and that there is no further excuse for electrotechnologists to continue talking nonsense.

The present reviewer has asserted on former occasions that there are three states of sophistication in physics. In the first, one accepts everything at face value and seeks to understand by the most primitive methods of intuition. In the second state, one sees that there is much that is illogical and even wrong in the condition of satisfaction of mind typified by the first state. He who lives in state No. 1 is the natural prey of the occupant of state No. 2, who can cut his arguments to pieces with infallible swords and knock away the foundations of almost everything upon which his brains rest for comfort. State No. 2 is the destructive state. Then there is state No. 3, in which, while one admits everything in state No. 2, one recognizes that there really was something to the ultimate doings of the denizen of state No. 1. The poor fellow in that state had said it all wrong, had sought much comfort in illusion and much tribulation in shadows, but did the right thing after all and used the tools which really mattered, even though one in state No. 2 could prove irrefutably that he did not know what he was doing.

Now the author of *Electromagnetics* is certainly not in state No. 1, and while he carries on the fight in a manner characteristic of a denizen of state No. 2, he obviously has the full appreciation of state No. 3. If the present reviewer had any criticism at all as regards much that is written, he would found it upon the following basis: Even the greatest minds, when controlled by the conventions of thought of their day, have on occasion built their intellectual structures in terms of very naïve pictures and of very vulnerable material. They have seen something which worked and have housed it in a structure characteristic of the mental architecture of the times. The structure and its attendant elements have indeed seemed to form an essential part of the whole scheme. Now in process of time many of these things have died, without having been actually killed, and with their sins unconfessed. Professor O'Rahilly seeks to exhume them for the purpose of holding an autopsy to discover the full enormity of their former wickedness. He then pieces them together and pumps enough life into them to enable them to be brought to public trial and to be disposed of legally by official execution.

Joking aside, however, Professor O'Rahilly is really to be congratulated upon a penetrating rediscussion of the fundamentals of this much discussed subject of electrodynamics. The present reviewer is heartily in sympathy with many of the main contentions of the book, and particularly with that to the effect that the working elements of the theory of restricted relativity have, in their essentials, nothing whatever to do with different frames of reference associated with observers traveling with different velocities. There would, in fact, be sense to a situation in which the Michelson-Morley experiment had given a positive result and in which the essential value of the restricted theory of relativity yet remained. Again, Professor O'Rahilly's objection to the garnishing of such concepts as electric and magnetic fields with such statements about them as attribute them to special states of the aether, etc., is an objection which, in the judgment of this reviewer, is well taken; and in spite of the somewhat facetious remarks above concerning the resuscitation and official execution of some of these bygone concepts, there is something to be said for such public execution, for the ghosts of these unhappy former courtiers of the throne of science still walk about the laboratories and, when they find a chance, will garb themselves in such alluring raiment as to tempt the unwary young investigator from the straight and narrow path of progress to the mental orgies of the materialistic era of Mid-Victorian times.

W. F. G. SWANN.

Thorpe's Dictionary of Applied Chemistry. By JOCELYN FIELD THORPE AND M. A. WHITELEY, assisted by eminent contributors. Fourth edition. Volume 1, A-acid to Bixin; xxvii + 703 pp. (1937). Volume 2, Black Ash to Chemical Analysis; xxiii + 711 pp. (1938). Volume 3, Chemical Calculations to Diffusion; xxiii + 608 pp. (1939). London, New York, Toronto: Longmans, Green and Company. Price: $25.00 per volume.

The statement in the preface to the first volume of this edition, that "It is intended to publish one volume yearly, the last volume containing a General Index and Glossary", has been thus far fulfilled. From the rapid advance of applied chemistry during the present century, it is not surprising to find that the material covered in these three volumes was completed on page 523 of the second volume in the previous (third) edition of 1927, although some of this material was included in the supplementary volumes of 1934 and 1935.

While the dictionary form has been preserved, more even than the third edition is the fourth a collection of monographs by authoritative authors; perhaps because of this, the work more and more covers the field of general chemistry, and includes very fully the applications of physical chemistry in industry.

The scope of this edition may be best illustrated by citing some examples of changes. The four-page article on "Colloids" in the third edition becomes a fifteen-page treatise, by Alexander King; "Coördination Compounds" does not appear in the third edition, but in this is represented by an excellently illustrated article of ten pages by Sir Gilbert Morgan and F. H. Burstall; Sir Gilbert Morgan also contributes twenty pages on "Diazo-compounds", as well as in conjunction with Dr. Glyn Rees Davies six pages on "Organic Antimonials" and sixteen pages on "Organic Arsenicals"; the "Organic Compounds of Bismuth" is given a too brief notice by

Dr. Challenger; "B_1 Vitamin" and "*l*-Ascorbic Acid" are discussed by Dr. Leslie J. Harris, "Androsterone" and "Testosterone" are given brief treatment by Dr. Kon, and a fuller paper on the "Sterones" is promised under "Hormones" in a later volume; five pages are devoted to R. P. Linstead's article on "Chlorophyll"; "Chemical Warfare" and "Chemical Warfare Defense" by J. Davidson Pratt are two other new topics treated in this edition; "Corrosion of Metals" is expanded from thirteen to thirty-two pages; "Anthraquinone" and "Anthraquinone Dyestuffs" occupy forty-two pages, the latter topic not appearing in the third edition, where the anthraquinone dyestuffs were described chiefly under their individual names; "Light Alloys" and "Atomic Structure" each receive six pages; in the third edition "Catalysis in Industrial Chemistry" was accorded two pages and that under the topic "Chemical Affinity"; in this edition it has been expanded to seven pages by Dr. Hilditch, but might well have been further enlarged; the excellent original article on the "Balance" by Professor Dittmar in the first edition of the book has been largely retained, but supplemented by sixteen pages from Dr. J. J. Manley, bringing the subject down to date, and including the microbalance; "Chemical Analysis," which covered one hundred and four pages in the earlier edition, now requires one hundred and seventy-one pages for treatment, is well arranged, and seems to be brought well up to the present.

This last article especially illustrates what is true of many of the longer papers,—a brief index or table of their contents is needed; while the materials are excellently classified, it demands too much time to determine in these longer papers just *how* they are classified, and whether a sought-for topic is treated under this topic, and if so just where. It is too long to wait for the general index in the last volume.

The authors are to be congratulated on the great improvement in this edition of an indispensable book.

JAS. LEWIS HOWE.

3. JUN. 19
LIBRAR

TRANSLUCENT FILMS OF ALUMINUM OXIDE

RICHARD E. VOLLRATH[1]

Norman Bridge Laboratory, California Institute of Technology, Pasadena, California

Received August 7, 1939

It is well known that a layer of aluminum oxide can be formed on a surface of aluminum by electrolytic oxidation (1). The aluminum is made the anode in an electrolytic cell with a cathode of some non-polarizing material, such as carbon, and an electrolyte consisting of an aqueous acid, such as oxalic acid. Layers of aluminum oxide of considerable thickness can be built up by continuing the electrolysis sufficiently long. The author during a search for a thin film to satisfy certain requirements attempted to make thin sheets of aluminum oxide by oxidizing aluminum foil electrolytically. It turned out to be possible to convert thin aluminum sheets into sheets of aluminum oxide (2).[2] The method of doing this is illustrated in the following description of a procedure by means of which sheets of aluminum oxide were prepared.

A piece of aluminum foil 0.002 cm. thick, 2 cm. wide, and 10 cm. long is fastened in a clamp constructed as shown in figure 1 (a). It consists of two strips, A and B, of ⅛-in. aluminum between which the foil is clamped by means of a screw holding the two strips together. The foil and a section of the clamp are immersed, as shown, in a 3 per cent aqueous solution of oxalic acid contained in a 1-liter battery jar or beaker. The clamp holding the foil is connected to the positive terminal of a 120-volt D.C. supply, while a carbon rod serves as the cathode. A rheostat or lamp bank is connected in series with the cell and the current adjusted to about 30 milliamperes. The actual voltage is not important but the current should not be too high, otherwise the foil may become overheated during the electrolysis. It turned out after a number of trials that alternating current could be used without making any difference in the results. Upon allowing the above current to flow for about 2 hr. the foil will become almost completely transparent and acquire a peculiar silky appearance. It is necessary that the foil be completely immersed in the electrolyte, that is, the clamp itself should be partly immersed as shown in figure 1. If the foil projects from the solution the portion at the air–electrolyte interface is soon converted into aluminum oxide, which extends as a band across the foil and, because it is an insulator, cuts off the current and stops the oxidation of the remaining parts of the foil. The aluminum foil treated in this manner when examined under the microscope appears to consist of a translucent glassy film in which a large number of minute irregular fragments of aluminum are dispersed. The silky appearance mentioned above is due to these minute fragments of aluminum. Apparently the progress of the oxidation causes small areas of aluminum in the foil to become completely surrounded by aluminum oxide, which, being an insulator, isolates these areas electrically so that they cannot be further oxidized.

---

[1] On leave from the University of Southern California, Los Angeles, California.

[2] During a discussion on electrolytic condensers Mott showed an audience aluminum oxide films, but gave no details of how they were made.

To overcome this difficulty the arrangement shown in figure 2 was adopted. In figure 2 the foil is held between 2 strips of aluminum, A and B, one of which is made long enough to permit placing it across the top of a battery jar or beaker as shown. The foil hangs down from this clamp and dips into the electrolyte which, again, is 3 per cent aqueous oxalic acid. At the beginning of a run the lower end of the foil is permitted to dip a few millimeters below the surface of the solution, which at the start is a few centimeters deep. The foil and the carbon rod serving as the cathode are connected in series with enough resistance to limit the current to about 2 milliamperes per square centimeter of foil surface. The ammeter A is in the circuit to permit this adjustment to be made. A short time after the current is started the section of the foil dipping below the surface of the electrolyte is converted into the oxide, as the transparency indicates. At

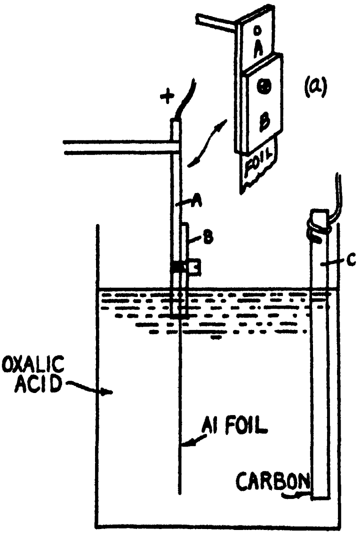

Fig. 1. Apparatus for oxidizing aluminum foil

this point a hissing noise due to heating develops in the region where the foil emerges from the electrolyte, and the current finally ceases because the oxide is a non-conductor. At this stage a 3 per cent solution of oxalic acid is allowed to flow into the cell from a reservoir whose liquid level is about 50 cm. above that in the cell. In figure 2 the reservoir is shown much lower in order to conserve space in the drawing. The rate of flow of the oxalic acid solution is adjusted by means of a stopcock until the electrolyte level in the cell rises just fast enough to permit the immersed portion of the foil to be completely oxidized. In this manner a piece of aluminum foil 0.002 cm. thick and 2 cm. wide was oxidized at the rate of about 2 cm. per hour. It was found possible to oxidize foils as thin as 0.0005 cm. Foils thinner than this can be oxidized, but it is very difficult to remove them from the electrolyte without tearing them. However, suitable mechanical means for lifting out the oxidized foils could be devised.

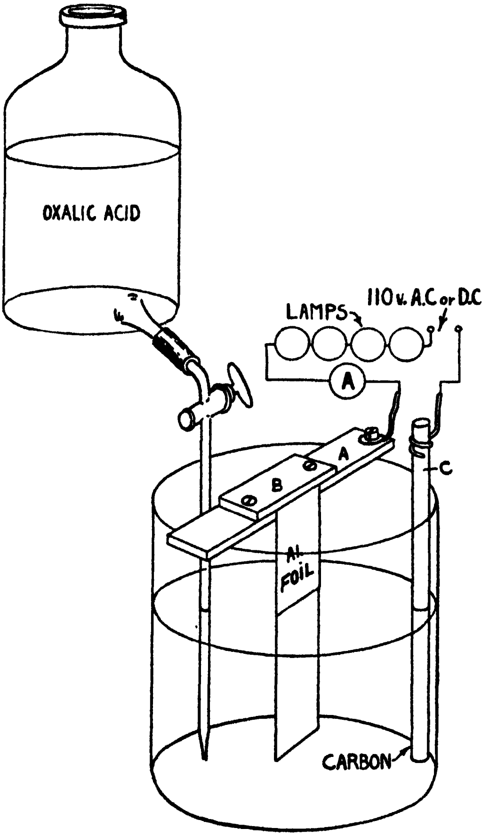

FIG. 2. Apparatus for oxidizing aluminum foil

The aluminum oxide foils prepared in this manner have considerable flexibility but break if bent too sharply. It is to be suspected that the lack of flexibility may be due to a survival of the crystalline structure in the original aluminum foil. In transparency these films resemble thin tissue paper or tracing paper. It is rather remarkable that every scratch or rolling mark on the aluminum foil is faithfully reproduced on the oxide film. The author has attempted to convert thin aluminum tubing into an equivalent oxide tube with the idea of using it as a diffusion thimble or semipermeable membrane, but so far without success. Further work is being carried out to determine the optical and electrical properties of the material.

REFERENCES

(1) GÜNTHER-SCHULZE: Z. Physik **3**, 349 (1920). This does not relate directly to the above work but contains many pertinent references.
(2) MOTT: Trans. Am. Electrochem. Soc. **5**, 162 (1904).

THE AZEOTROPIC SYSTEM ALCOHOL-WATER-BENZENE[1]

WALTER D. BONNER AND MAX B. WILLIAMS[2]
Department of Chemistry, University of Utah, Salt Lake City, Utah

Received July 7, 1939

Since ethanol, although miscible with water in all proportions, forms an azeotropic system of lower boiling point than either component, it is not possible to separate water and alcohol completely by fractionation. If, however, a sufficient quantity of benzene is added to aqueous alcohol, a complete separation of the water and alcohol can be effected by fractionation.

The mechanism of this separation is interesting. If sufficient benzene has been added, the system separates into two liquid phases. The lower, denser phase contains about equal amounts of water and alcohol with little benzene, while the upper phase contains benzene, alcohol, and little water. This heterogeneous system of three components and three phases has two degrees of freedom. If one fixes the pressure and the composition, the boiling point is thereby fixed, and the mixture boils at a constant temperature so long as two liquid phases are present. When one of the two liquid phases disappears, the boiling temperature will suddenly rise. If enough benzene has been added, all the water has been removed with the disappearance of the heterogeneous system, and what remains is a solution of alcohol and benzene. These two form a homogeneous azeotrope of minimum boiling point, and, if the solution now contains less than the azeotropic proportion of benzene, it can of course be separated by fractionation into the azeotrope and pure anhydrous alcohol. This method of separating water and alcohol is of considerable technical importance for the preparation of absolute alcohol, and has therefore been much studied. These studies, however, have all of them been made at pressures considerably above atmospheric, and no study seems to have been made at low pressures. We have therefore thought it worth while to carry out this investigation at pressures between 160 mm. and 960 mm.

---

[1] Contribution No. 55 from the Chemical Laboratories of the University of Utah.

[2] Present address: Department of Chemistry, Cornell University, Ithaca, New York.

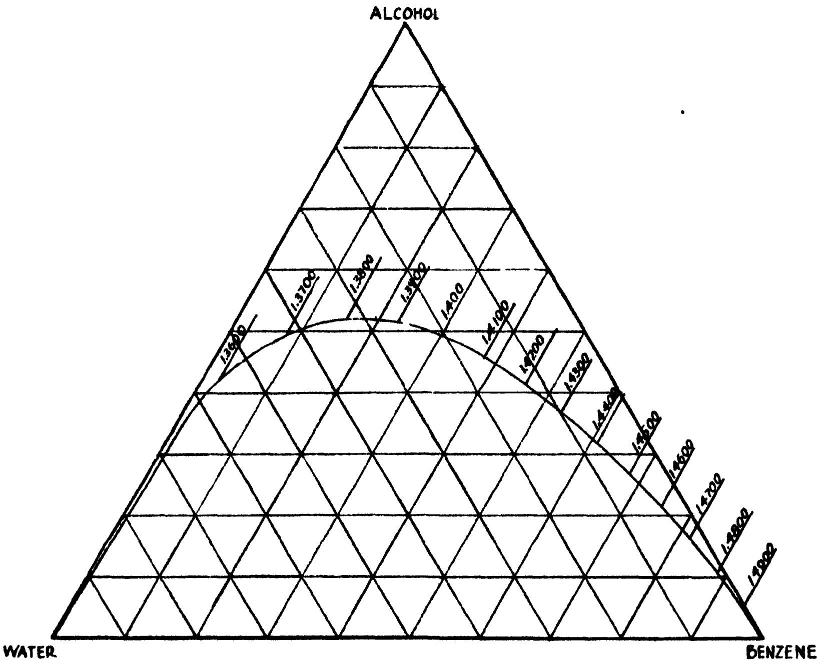

FIG. 1. Indices of refraction and compositions at the surface of separation of the system alcohol–water–benzene

The apparatus used was merely a distilling flask equipped with a fairly efficient fractionating column, a reflux condenser, a condenser for distillation, and a pressure control device for maintaining any predetermined constant pressure.

In working with systems such as this the greatest difficulty is frequently that of making satisfactory analyses. In 1926 Barbaudy (1) obtained data by means of which analyses of this heterogeneous system can readily be made. These data consist of the indices of refraction of a series of solutions of alcohol-water-benzene lying on the binodal curve of 25°C. From these we have plotted, on an 18″ x 24″ triangular diagram, the indices of refraction with equal increments on the binodal curve (see figure 1). The method of analysis is then very simple. The heterogeneous system is distilled, and the distillate is allowed to separate into two layers and to stand long enough at a constant temperature (25°C.) to insure that equilibrium has been established. This we do in a weight buret. The weight of the combined phases is determined, the phases are separated, and the separate weights determined. The index of refraction of each phase is then determined, in this work using an Abbé refractometer. These indices allow at once the two ends of the tie line between the consolute phases to be fixed, and the relative amounts of the two phases fixes the composition of the heterogeneous system.

In order to obtain reproducible results with our apparatus, we found that the following conditions must be maintained: The system must be allowed to reflux for a long time at the proper pressure, in order that the mixture in the distilling column may attain a constant distribution. The rate of distillation must be low, and the rate of reflux high. We used, as a desirable rate of distillation, ten drops per minute, and the ratio of reflux to distillation was fourteen. The reflux condenser must be maintained at a constant temperature. We used 14°C. ± 0.1°, merely because it was convenient and satisfactory.

In every case 100 g. of the alcohol-water-benzene mixture was used, and the volume of distillate taken for analysis was 15 ml. This was taken immediately after an initial 15 ml. had been distilled. The entire operation was conducted as follows: 19.2 g. of 95.57 per cent alcohol, 6.7 g. of redistilled water, and 74.1 g. of absolute benzene were weighed into a 125-ml. glass-stoppered flask. The mixture was shaken thoroughly, and transferred at once to the distilling flask. The flask was connected to the apparatus, and all stopcocks and ground-glass joints tested for leaks. The barometric pressure was accurately determined, the necessary temperature corrections made, and carbon dioxide under pressure introduced into the apparatus, or the apparatus evacuated, until the desired manometer reading was attained. Heat was then applied to the distilling flask, and, as the flask warmed up and boiling began, the manometer was constantly adjusted to the predetermined value. The manometer reading remained constant when the vapor reached the small reflux condenser at the top of the distilling column, and the mixture began to reflux. The mixture was allowed to reflux for 15 min., and then the stopcock at the top of the condensing system was opened full, and 5 ml. allowed to distil. Another 15 min. reflux and another 5 ml. distillation allowed any low-boiling components to excape from the system. The mixture was allowed to reflux from 3 to 9 hr., depending upon the pressure used, constant composition being reached more quickly at lower pressures.

TABLE 1

Refractive index and composition of upper and lower phases of the distillate

PRESSURE	REFRACTIVE INDEX (PHASE 1)	REFRACTIVE INDEX (PHASE 2)	PHASE 1			PHASE 2			BOILING TEMPERATURE
			H_2O	Alcohol	Benzene	H_2O	Alcohol	Benzene	
mm.			*per cent*	*per cent*	*per cent*	*per cent*	*per cent*	*per cent*	*°C.*
160	1.4758	1.3711	1.4	12.9	85.7	41.8	49.6	8.6	
460	1.4791	1.3656	1.1	11 1	87.8	48.6	46.5	4.9	51 8
660	1.4800	1.3640	1.0	10.6	88.4	50.6	45.4	4.0	61.0
760	1.4803	1.3637	1.0	10.4	88.6	51.0	45.1	3.9	64.5
860	1.4805	1 3631	0.95	10.25	88.7	51.9	44.6	3.5	67.8
960	1.4808	1.3625	0.9	10.1	89.0	52.7	44.1	3.2	70.9

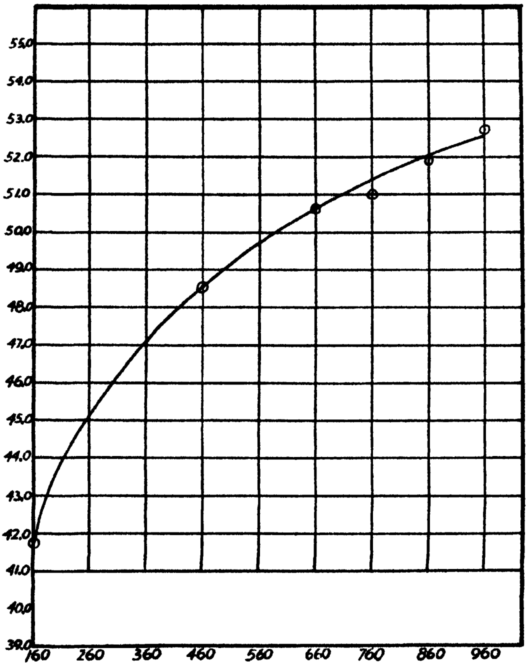

FIG. 2. Variation of percentage of water in the lower solution with pressure

At the end of the refluxing period, the stopcock at the top of the condenser was opened partially, to allow a distillation rate not faster than 10 drops per minute. When the distillation had been sufficient to rinse the condenser tube, the distillate was turned into a fresh receiver, by means of the three-way stopcock at the bottom of the condenser. When approximately 15 ml. had been collected, the apparatus was quickly disconnected, and the distillate poured without delay into a previously prepared weight buret. This was stoppered, weighed, and placed in a thermostat at a temperature of 25°C. (± 0.1°), where it was allowed to stay until the solution became perfectly clear. It was then removed from the bath, dried, and reweighed to check any loss by evaporation. The refractive indices of bottom and top layers were next determined, and, if desired, the separate weights of the two layers. The refractive indices were determined on at least three separate samples of each solution, and the temperature of the refractometer was maintained at 25°C. ± 0.1°. The limit of precision of our instrument is 0.0002 unit, and determinations of the refractive index of separate samples of the same layer should not differ by more than that. Table 1 shows the change of refractive index and the change of composition of the upper and lower phases of the distillate as the pressure changed from 160 mm. to 960 mm. It can be seen that most of the water is removed from the system in the lower phase. The percentage of water in this fraction drops rapidly as the pressure is lowered below about 600 mm., hence the efficiency of such a process for dehydrating alcohol must also decrease rapidly below this pressure. On the other hand, the rate of increase of water with increase of pressure becomes much smaller at pressures above atmospheric, so that the advantage due to increased pressure soon becomes slight. Figure 1 shows the surface of separation of the alcohol–water–benzene system at 25°C., with indices of refraction plotted on it. This is, we think, the most advantageous method yet devised for the analysis of these systems. Figure 2 shows the change of water content of the denser phase with change of pressure.

SUMMARY

This study shows that the effect of changing pressure on the water content of the heavier phase in heterogeneous systems of alcohol–water–benzene is greatest at low pressures, and that it becomes small and approximately constant at about one atmosphere pressure. It also shows the ready applicability of the method of Barbaudy to the analysis of such systems.

REFERENCE

(1) BARBAUDY: Bull. soc. chim. 39, 371 (1926).

A NOTE CONCERNING ION ADSORPTION BY PECTIN

GLENN H. JOSEPH

California Fruit Growers Exchange Research Department, Corona Laboratory,
Corona, California

Received July 24, 1939

During the past ten years the literature on pectin has been influenced to a large extent by the publications of Tarr and of Miss Spencer concerning the relations between acids and pectin in gel formation.

In 1929 and 1930 Miss Spencer published a series of papers dealing with the influence of sugar, salts, and acids on pectin gels. The third paper (2) of that series was devoted to a critical discussion of the 1923 data of Tarr (3). Miss Spencer used the data of Tarr to substantiate her contention that pectin carries a negative charge in solution due to adsorbed anions and to show that pectin does *not* possess a "buffer action" in acid solutions, as was claimed earlier by Tarr.

It has been felt in these laboratories that Miss Spencer erred mathematically in her interpretation of Tarr's data and that consequently her postulates were without suitable foundation. Since subsequent literature has failed to note the error we desire to call it to the attention of those working with pectin.

Tarr presented data showing the pH values of systems obtained by adding various volumes of 0.10 *N* acids to 100-ml. portions of distilled water and to the same volume of distilled water containing 1.0 g. of pectin. Curves of his data showed that the pH values of the systems containing pectin were higher than corresponding ones where pectin was absent, leading him to conclude that pectin was exhibiting "buffer action." Similar data have been obtained by us many times during the past decade.

Miss Spencer said, concerning Tarr's data relating to the pH of sulfuric acid systems, ". . . although the addition of 1 cc. of sulfuric acid to water resulted in an increase in acidity represented by 2.44 (5.50 − 3.06) points as against an increase of only 0.15 (4.21 − 4.06) points when pectin was present, *the next added increments*, 19 cc. in all, increased the pH value of water only 1.09 (3.06 − 1.97) points as against 1.92 (4.06 − 2.14) points when pectin was present. That is to say, after the added acid had disposed of some non-pectin influence in the pectin sol, presumably salt impurities, the presence of pectin, instead of "depressing" the dissociation of acid, increased the hydrogen-ion concentration."

The obvious error in the above reasoning centers around the subtraction of pH values and comparison of these differences as numerical entities. The logarithmic nature of pH values prevents such manipulations. The pH values should have been converted to the corresponding hydrogen-ion concentrations before Miss Spencer started her calculations. In the first instance related above, the "2.44 points" represents an increase in hydrogen-ion concentration of 8.7×10^{-4}, while in the second system, where pectin was present, the hydrogen ion increase is only 0.15×10^{-4}, due no doubt, in a small part, to the salt impurities, as pointed out by Miss Spencer. However, for the next 19 ml. of acid addition the hydrogen-ion concentration increased by 98.3×10^{-4} for water alone and by 71.6×10^{-4} when pectin was present, showing just the opposite from Miss Spencer's conclusion. Pectin *did* prevent the system from having the hydrogen-ion concentration it would have had in the absence of pectin, hence pectin *did* "buffer" the system as Tarr contended, although not necessarily by the mechanism he advanced.

In a similar manner it can be shown that in every acid system which Tarr discussed the pectin *decreased* the hydrogen-ion concentration. Thus it seems that Miss Spencer's theory of anion adsorption has rested on a false foundation, because, rather than adsorbing anions and leaving hydrogen ions free to decrease pH values as she concluded, we see that actually it was the hydrogen ions that were adsorbed by the pectin, thus *increasing* the pH. Tarr concluded that anions did not exert a noticeable effect on pectin gel formation.

We have data to show that the pH values of pectin–sugar–acid–water systems, in correct proportions for gel formation, go up from 0.06 to 0.15 of a pH unit as a result of actual gel formation (in the region of pH 2.9–3.5 as determined with a glass electrode). This indicates that a definite adsorption of hydrogen ions takes place during the process of pectin gel formation. This has been found true for both apple and citrus pectins.

The present conception of pectin structure is one of chain-like aggregates of anhydrogalacturonic acid residues bearing from three to ten times as many methylated carboxyls as free carboxyls. Preliminary work indicates that there are probably from 600 to 1200 of these residues in the molecular aggregate. The physicochemical nature of the pectin molecule is such that one need not assume anion adsorption to account for the fact that in cataphoresis pectin carries a negative charge.

The picture of gel formation need not be much different than the one so well presented by Kruyt (1) in 1930. When pectin is in the sol state it is stabilized by water layers, probably held to it by the electrical attraction of the pectin's negative charge and the unbalanced positive charge of the water dipoles. As sugar is added to the sol, the dehydrating influence of the sugar decreases the stability of the pectin by disturbing the water balance. When the sugar concentration gets up to 50 to 65 per cent, the dehydration of the pectin micells is sufficiently complete so that when an acid is added the hydrogen ions finish destabilization and a gel forms as a result of an unsuccessful attempt to precipitate.

There are a number of frequently overlooked pH changes which occur in aqueous sucrose–pectin–acid systems, especially in the region where gels can form. Data to be submitted in a later paper will show several of the individual factors affecting these pH changes and point out the importance of considering these factors when postulating a mechanism for gel formation. For instance, it will be shown that when sucrose is added to an acidified pectin sol the pH may decrease as much as 0.10 unit or in some cases may rise 0.20 pH higher than the original value, depending upon the pH region, the sucrose content, and upon whether or not gelation occurs. In the region of proper balance for gel formation, there is, in addition, a time factor which must be considered when making pH measurements.

REFERENCES

(1) Kruyt, H. R.: *Colloids, a Textbook*, 2nd edition, p. 200. John Wiley & Sons, Inc., New York (1930).

(2) Spencer, Gene: J. Phys. Chem. **34**, 410–17 (1930).

(3) Tarr, L. W.: Univ. of Delaware Agri. Expt. Sta. Bull. No. 134 (February, 1923).

PHOTOVOLTAIC CELLS WITH SILVER–SILVER BROMIDE ELECTRODES. III

Optical Sensitizing by Dyes[1]

S. E. SHEPPARD, W. VANSELOW, and G. P. HAPP

Kodak Research Laboratories, Eastman Kodak Company, Rochester, New York

Received July 24, 1939

In the previous papers of this series (6, 7) there have been described the photovoltaic phenomena observed with a cell of two silver–silver bromide electrodes, one exposed to light, the other kept dark; the electrodes were connected electrolytically, usually by a dilute potassium bromide solution, and externally either through a vacuum tube voltmeter or a three-stage amplification oscillograph. In the present investigation these instruments have been replaced by an Einthoven string-galvanometer. A detailed description of the apparatus and operation is being presented elsewhere.[2]

With this there have been studied the photovoltaic effects obtained when the silver bromide of the illuminated electrode is dyed with a sensitizing dye; the light incident might then have a spectral composition limited to that absorbed by the silver bromide alone, or to that absorbed by the adsorbed dye alone. Sensitizing dyes could be chosen whose light absorption (when adsorbed to silver halide) is well separated from that of silver bromide itself.

---

[1] Communication No. 742 from the Kodak Research Laboratories.

[2] In preparation.

The nature of the adsorbed dye layer at silver halide surfaces has been dealt with recently by Leermakers, Carroll, and Staud (3) and by Sheppard, Lambert, and Walker (5). Here it may be noted that the adsorption may be practically complete (irreversible) or incomplete (reversible), depending upon the number and position of solubilizing (polar) groups in the molecule. In the present investigation it was desirable to have a completely adsorbed dye and at such an adsorption density that optical shielding effects would not be present. The dye chosen,[3] 2,2′-diethyl-8-methylthiacarbocyanine bromide, of the following structure:

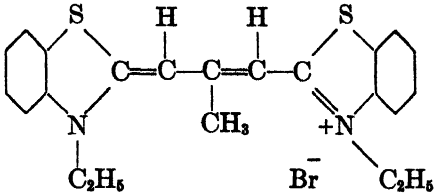

is satisfactory in these respects. The source of light was a mercury arc (Cooper Hewitt, quartz). It was operated at 150 volts potential drop across the terminals, and at 21.2 cm. distance from the front surface of the silver–silver bromide electrode.

The spectral distribution of the light from this source is largely discontinuous (4), with a relatively faint continuous background. In these experiments, *limited spectral regions* were isolated by the use of light filters of known transmissions. The filters used, their approximate spectral range, and the energy transmitted from the mercury arc to the photocell surface are given in the following tables. Table 1 refers to what are termed, inclusively, the first series of relevant experiments, and table 2 to the second series. There was no difference in principle between these, but several details were different, which will be noted as required. In addition, with *each* of the combinations in table 1 there was also present an infrared absorption filter, consisting of a cell of 1 cm. internal thickness filled with 5 per cent cupric chloride solution.

The investigations of Leermakers, Carroll, and Staud (3) have shown very definitely that the absorption spectrum of the dyed silver halide corresponds accurately to its spectral sensitivity. In figure 1 is shown the spectral reflectance curve for silver bromide dyed with dye IVb.

---

[3] Dye IV b; see reference 5.

TABLE 1

*Experiments in series I**

FILTER	SPECTRAL RANGE TRANSMISSION	ENERGY TRANSMITTED
		ergs per second per $mm.^2$
"Neutral" D1	Total	55.45
Wratten No. 61	Maximum 530 mμ	52.25
Wratten No. 61 plus D1	Same	12.80
Corning 986	Ultraviolet up to 400 mμ	50.25
Corning 986 plus D1	Same	1.71

* Cooper Hewitt lamp 10,474 was used.

TABLE 2

*Experiments in series II**

FILTER	SPECTRAL RANGE TRANSMISSION	ENERGY TRANSMITTED
		ergs per second per $mm.^2$
Wratten No. 16 cemented in optical B glass	*Cf.* figure 1	500
Wratten No. 16 plus Neutral D1 as required		150
Purple Corex "A" 986 (−1) (Corning Glass Co.)	*Cf.* figure 1	450

* Cooper Hewitt lamp 50,184 was used.

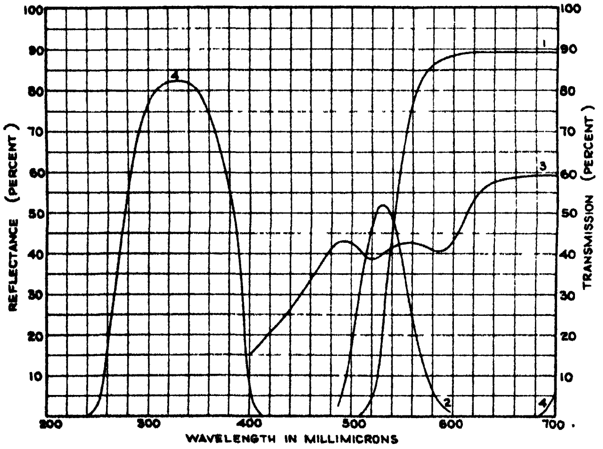

FIG. 1. Transmittances of Wratten filters No. 61 and No. 16 superposed on the reflectance curve. Curve 1, transmission of Wratten filter No. 16; curve 2, transmission of Wratten filter No. 61; curve 3, reflectance of silver bromide (in gelatin) sensitized with dye IVb, 1.00 mg. of dye per 100 cc. of emulsion; curve 4, transmission of Corning filter, Red Purple Corex "A" No. 986, thickness 5.02 mm.

The reflectance curve corresponds, inversely, to the absorption (and sensitizing). It will be seen that there are two well-marked absorption bands with maxima at 520 mμ and 590 mμ, respectively. In figure 1 are shown the transmittances of filters Wratten No. 61 (first series) and Wratten No. 16 superposed on the reflectance curve. Evidently in the first series the band at 520 mμ was fairly well isolated, there being little or no radiation shorter than 480 mμ, or longer than 580 mμ, while in the second series the band at 590 mμ was secured free from all radiation of less than 500 mμ, and with only a small amount at 520 mμ.

TABLE 3

Preparation of electrodes

OPERATION	SERIES I	SERIES II
Mechanical and heat treatment	Polished with 400-mesh carborundum paper	As in I
Annealing	Heated 2 hr. at 125°C., cooled slowly. Polished on wet MgO (Shamva)	Heated gradually over 8 hr. up to 525°C., cooled to room temperature. Polished as in I with carborundum paper. Annealed as in I. Polished as in I
Insulating, back face, etc.	Paraffin (Parowax)	As in I
Bromination	Electrolytic: paired electrodes as anode; Pt cathode, electrolyte 0.5 per cent KBr solution, 0.12 per cent HBr. Initial current 20 milliamperes over 2 x 100 mm.^{2} anode surface. p.d. = 0.8 volt. Time = 5.0 sec.	As in I
Thickness of AgBr layer	0.00025 mm.	0.00021 mm.
Aging	In water saturated with AgBr: (1) 7 days for undyed (2) few minutes for dyed	1 day in 0.001 *N* KBr solution saturated with AgBr
Dyeing time	4 days	Varied up to 4 days
Washing	Three changes of water saturated with AgBr in 3 days after dyeing	Three changes of 0.001 *N* KBr solution saturated with AgBr in 24 hr. following dyeing

Another experimental difference between series I and series II was in the preparation of the electrodes (see table 3). This subject has been rather fully discussed in Papers I and II (6, 7) and only some minor modifications will be mentioned here. A newer type of electrode was now employed, with the surface 100 sq. mm. in area, compared to 78.6 sq. mm., and mounted in solid brass leads (subsequently insulated) instead of glass tubes. The dye solution contained 0.0044 g. per liter of dye IVb and was saturated with silver bromide.

It may be noted that the period of aging was reduced to 1 day for the second series in accordance with findings of Kolthoff and O'Brien (2).

EXPERIMENTAL RESULTS

The photovoltaic effect is observed as a graph of potential difference (in volts) against time, taken from the (photographic) recorder connected with the Einthoven galvanometer. A typical record is shown in figure 2.

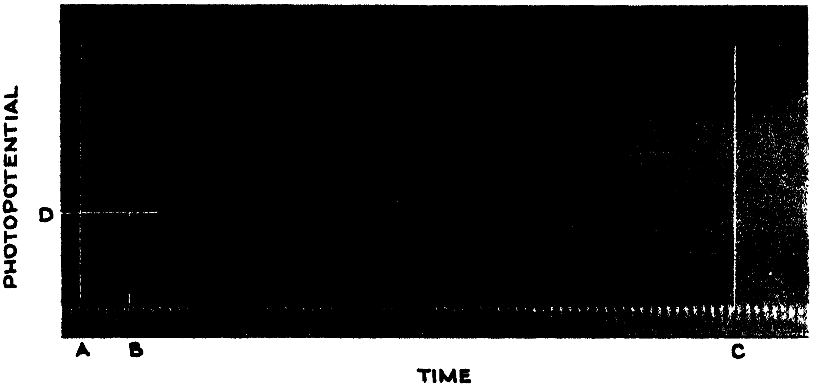

FIG. 2. Reproduction of record. 0, exposure starting time = zero or A. 00', zero potential line; D, maximum negative photopotential; AB, time to reach maximum negative photopotential = 0.09 sec.; AC, time to recross zero potential line = 1.23 sec.

As shown in the previous studies, there are two main phases in the production of a potential difference. There is an initial, inertia-less *negative* effect, which may attain its maximum (as negative potential difference) within 1 sec., when positivization follows, the potential difference becoming positive and then levelling off. It has been shown that the positivization can be reduced or eliminated by supplying sufficient halogen acceptor in the electrolyte.

Tables 4 and 5 for the first series show that, in the case of dyed silver bromide, the same phenomena appear *when the radiation is that absorbed by the adsorbed dye.*

Table 5 shows the same behavior, but, in addition, a phenomenon which will be noted again later, *viz.*, increasing sensitivity (magnitude of the negative response) as the concentration of soluble bromide of the electrolyte is decreased.

The next table (table 6) gives results obtained when the electrodes, both undyed and dyed, were illuminated with ultraviolet plus visible radiation, and also with ultraviolet alone. The ultraviolet radiation of experiment No. 3 was isolated by a Corning glass filter (Corex "A" 986 (−1)) of 5.02 mm. thickness, the transmission of which is shown in figure 1. The large "sensitization" which the dye has conferred with ultraviolet light is not optical sensitizing, since this radiation is strongly absorbed by silver bromide itself. It is to be attributed to the efficient *halogen-accepting* capacity of the dye. This has been demonstrated elsewhere in an investigation of the photolysis of dyed silver bromide by Sheppard, Lambert, and Walker (5). In that investigation it was found that these sensitizing dyes very readily form labile bromine addition compounds, which give up

TABLE 4

Series IA

NO.	MAXIMUM NEGATIVE RESPONSE		ELECTROLYTE*	RADIATION†
	Undyed	Dyed		
	volts	*volts*		*mμ*
1	0.0001	0.0025	0.1 *N* KBr	530
2	0.0002	0.0075	0.001 *N* KBr	530
3	0.0002	0.0070	0.001 *N* KBr 0.001 *N* $NaNO_2$	530
4	0.0010	0.0135	0.001 *N* KBr 0.01 *N* $NaNO_2$	530
5	0.0005	0.0080	0.001 *N* KBr 0.10 *N* $NaNO_2$	530

* The electrolyte was in each case saturated with respect to silver bromide.
† Radiation transmitted by Wratten filter No. 61 (*cf* figure 1).

TABLE 5

Series IB

NO.	MAXIMUM NEGATIVE RESPONSE		ELECTROLYTE	RADIATION
	Undyed	Dyed		
	volts	*volts*		*mμ*
1	0.002	0.0060	0.0001 *N* KBr 0.01 *N* $NaNO_2$	530
2	0.002	0.0075	0.0001 *N* KBr 0.10 *N* $NaNO_2$	530
3	0.0025	0.021	0.00001 *N* KBr 0.10 *N* $NaNO_2$	530

TABLE 6

Series IC

NO.	MAXIMUM NEGATIVE RESPONSE		ELECTROLYTE	RADIATION
	Undyed	Dyed		
	volts	*volts*		
1	0.001	0.0091	0.1 *N* KBr	Ultraviolet plus visible
2	0.000	0.0043	0.1 *N* KBr	Ultraviolet plus visible (at low intensity)
3	0.0008	0.0087	0.1 *N* KBr	Ultraviolet alone

TABLE 7

Experiments of series II with the dyed electrodes

ELECTRODES DYED	AVERAGE MAXIMUM NEGATIVE RESPONSE		AVERAGE TIME TO REACH MAXIMUM NEGATIVE POTENTIAL		AVERAGE TIME TO START POSITIVE ACTION		AVERAGE TIME TO RECROSS ZERO	
	No $NaNO_2$	0.01 *N* $NaNO_2$	No $NaNO_2$	0.01 *N* $NaNO_2$	No $NaNO_2$	0.01 *N* $NaNO_2$	No $NaNO_2$	0.01 *N* $NaNO_2$
	volts	*volts*	*seconds*	*seconds*	*seconds*	*seconds*	*seconds*	*seconds*
0	0.0003		0.49		No positive action in 6 sec.		No positive action in 6 sec.	
0		0.0005		0.31		Varied		Varied
minutes								
1	0.0068		0.07		0.07		1.70	
1		0.0131		0.05		0.05		1.68
5	0.0066		0.12		0.12		Approximately 2.38	
5		0.0137		0.06		0.06		Approximately 2
30	0.0077		0.12		0.12		Approximately 2.25	
30		0.0156		0.08		0.08		Approximately 2
hours								
3	0.0100		0.07		0.07		Not quite 0 at 6 sec.	
3		0.0175		0.06		0.06		Varied
24	0.0110		0.10		0.10		Varied	
24		0.0203		0.07		0.07		Not quite 0 at 6 sec.
days								
4	0.0130		0.08		0.08		Approximately 6	
4		0.0199		0.07		0.07		Approximately 6

bromine to more permanent halogen acceptors. In the study of the photolysis of silver bromide by ultraviolet or blue light it was also found that the sensitizing dyes acted as halogen acceptors.

The behavior of the silver–silver bromide electrode in light is, therefore, entirely consistent with the conclusions reached in the study of the photolysis.

These conclusions were fortified by the results of series II of experiments on the dyed electrodes, in which, as previously noted, some differences were made in the technique of preparing them. Furthermore, the electrodes were illuminated in the longer wave length band—maximum absorption at 560 mμ—by means of Wratten filter No. 16, with little or no radiation shorter than 520 mμ (*cf.* figure 1).

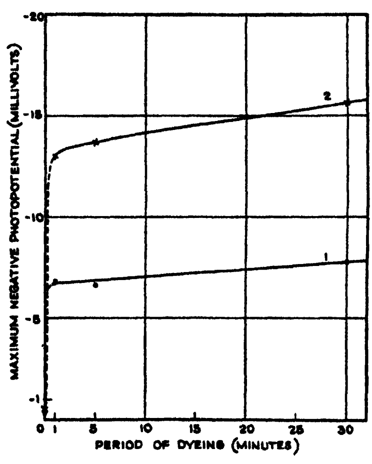

FIG. 3

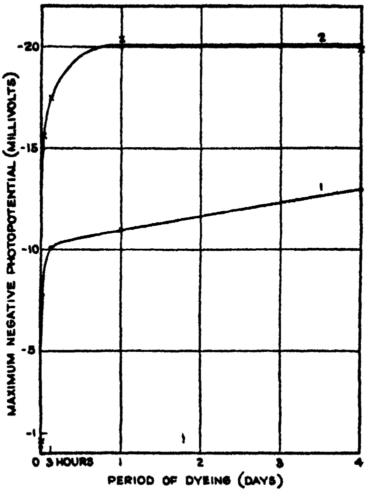

FIG. 4

FIG. 3. Relation of negative photopotential to time of dyeing. Curve 1, photocell electrolyte, 0.001 *N* potassium bromide saturated with silver bromide; curve 2, same with addition of 0.01 *N* sodium nitrite.

FIG. 4. Relation of negative photopotential to time of dyeing. Curve 1, photocell electrolyte, 0.001 *N* potassium bromide saturated with silver bromide; curve 2, same with addition of 0.01 *N* sodium nitrite.

Well-marked optical sensitizing of the negative or electronic photovoltaic effect was shown here also. The principal results are collected in table 7.

Two principal observations are resumed in the curves of figure 3 and figure 4. In figure 3 the maximum negative potential difference has been plotted against time in minutes of dyeing, i.e., the initial period. It is evident that there is an initial very rapid adsorption of the dye, followed by a much slower process which only increases the sensitivity very gradually. In figure 4, where the times of treatment in the dye bath have been extended to days, the same phenomenon is evident, with the difference that when a halogen acceptor, sodium nitrite, was included in the electrolyte, the sensitizing appeared to have approached saturation or equilibrium within 12 to 24 hr. From this it seems probable that the two phases of the dyeing process are (*i*) very rapid adsorption, as already observed in dyeing silver bromide sols, and (*ii*) a slower penetration of dye into fissures of the microcrystalline layer. This slower process continues to sensitize *in the absence of other halogen acceptor*, by furnishing more halogen acceptor for bromine produced by the primary *optical* sensitizing effect.

DISCUSSION

The previous investigation (6, 7) of the silver–silver bromide electrode in light absorbed by silver bromide had led to the following theory of the photovoltaic effect: The absorption of a quantum releases an electron from a bromide ion of the crystal, which becomes photoconducting. Such electrons can travel through the crystal, and, reaching the metallic silver base, tend to charge this negatively. The excess electron pressure is instantly revealed as a current through the circuit as the *negative* photopotential difference. The continuance of a current in this sense requires a compensatory process; this is considered to be (*a*) neutralization of Ag^+ ions in the dark electrode layer, (*b*) equivalent emigration of Br^- ions from the "dark" electrode into solution, and (*c*) transport of equivalent Br^- ions into the "light" electrode silver halide layer, thereby annulling any space charge due to Ag^+ ions left unbalanced by the displacement of photoelectrons. The entry of the photoelectrons into the subjacent silver metal consists, in the language of the quantum-mechanical "zone" model of semiconductors (10, 1), first, in raising an electron into the previously empty conductance band of the crystal, in which it is mobile, and then the "spilling over" of these electrons into the lower levels of the metallic silver.

The electrolytic section of the circuit described above accords with the observation that the magnitude of the negative potential difference is diminished as the concentration of bromide ion in solution is raised. Evidently higher bromide-ion concentration would lower the bromide-ion "solution tension" of the dark electrode, and thus reduce the current.

The genesis of the reverse positive current or potential difference in terms of the attack of bromine upon silver has already been explained (6, 7).

The reaction

$$Ag + \tfrac{1}{2} Br_2 = Ag^+Br^-$$

may be formulated (see figure 5) according to the Wagner model for such a corrosion reaction (8), *viz.*, as an "inverted electrolysis"; as though the system were an electric element with an E.M.F. corresponding to the free energy of the reaction, and in which the circuit is completed through an electronic conduction component of the corrosion layer, in this case silver bromide. Evidence in favor of this conception in the attack of halogens on silver has been presented by Wagner (9). Since it involves a reverse movement (reverse to the sense of the primary negative photovoltaic effect) of electrons outward from the (silver) metal through the silver bromide layer toward the bromine, in compensation of a migration of (silver) cations through the layer toward the bromine, it is evident that the E.M.F. generated should be, as actually found, opposed to the negative photovoltaic effect.

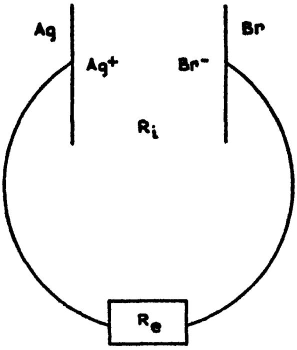

R_i = internal resistance of corrosion layer

R_e = external resistance through metal

FIG. 5

DYE-SENSITIZING OF PHOTOVOLTAIC EFFECT

The emission of electrons by the dyed silver bromide might be ascribed either directly to the dye, or as indirectly from bromide ions of the crystal activated by light-absorbing dye molecules. This has been discussed in recent papers on the photolysis (5), and reasons have been given in favor of some sort of "exciton" transmission from the dye molecule, with subsequent, rather than direct, electron liberation. The present investigation, while confirming the conclusions reached in the photolytic study, does not furnish definite evidence for or against the "direct emission" hypothesis for optical sensitizing.

The secondary sensitizing effect of dyes as halogen acceptors is well confirmed by the photovoltaic studies.

SUMMARY

1. An investigation has been made of the effect of an optically sensitizing (cyanine) dye on the photovoltaic effect with silver–silver bromide electrodes.

2. It was established that definite optical sensitizing of the primary negative, or photoelectronic, effect was effected. Light absorbed by the adsorbed dye,—and which is not absorbed by silver bromide itself,—produced relatively large (electronic) photocurrents.

3. At the same time, it was shown that the adsorbed dye acts as a halogen acceptor, diminishing the (reverse) positive effect, and this function occurs whether the active radiation is that absorbed by silver bromide or by the dye.

4. The results are in excellent agreement with those obtained in the study of the photolysis of dye-sensitized silver halide.

5. The results give further confirmation of the theory previously proposed by the authors for the photovoltaic effect with silver–silver halide electrodes. It is again shown that this effect can be analyzed into an initial photoelectronic effect, produced by photoelectrons released from the silver halide passing into the silver metal, and a relatively delayed chemical effect, *viz.*, the reaction of halogen with the silver. This latter process produces an E.M.F. opposing the primary effect.

6. The results, at present, do not permit a conclusion as to whether the electrons are initially released from the dye by absorption of light and recovered from bromide ions of the crystal (with release of bromine), or whether the dye merely transmits sufficient energy to the crystal to separate electrons and halogen.

REFERENCES

(1) CONDON, E. U.: Phys. Rev. **54**, 1089 (1938).
(2) KOLTHOFF, I. M., AND O'BRIEN, A. S.: J. Am. Chem. Soc. **61**, 3409, 3414 (1939).
(3) LEERMAKERS, J. A., CARROLL, B. H., AND STAUD, C. J.: J. Chem. Phys. **5**, 878 (1937).
(4) MCALISTER, E. D.: Smithsonian Inst. Pub. 3187, Vol. 87, No. 17, p. 9 (January 16, 1933).
(5) SHEPPARD, S. E., LAMBERT, R. H., AND WALKER, R. D.: J. Chem. Phys. **7**, 265, 426 (1939).
(6) SHEPPARD, S. E., VANSELOW, W., AND HALL, V. C.: J. Phys. Chem. **33**, 1403 (1929).
(7) VANSELOW, W., AND SHEPPARD, S. E.: J. Phys. Chem. **33**, 331 (1929).
(8) WAGNER, C.: Z. physik. Chem. **B21**, 25 (1933).
(9) WAGNER, C.: Z. physik. Chem. **B32**, 447 (1936).
(10) WILSON, A. H.: Proc. Roy. Soc. (London) **A133**, 458 (1931).

SILICIC ACID AS A PROTECTIVE COLLOID FOR MANGANESE DIOXIDE SOLS

FRED HAZEL

Department of Chemistry and Chemical Engineering, University of Pennsylvania, Philadelphia, Pennsylvania

Received August 15, 1939

Kruyt (10) reproduces data showing that silicic acid has no protective action when measured by the criterion of the gold number (17). Some evidence of the protective action of silica has been reported, however. Thus, clay suspensions are stabilized by addition of silica sols (14). Soil colloids of high silica: sesquioxide ratios, e.g., Sharkey soil colloid, are more stable toward electrolytes than those of low ratios, e.g., Norfolk soil colloid (12). It has been shown, also, that silica sols (prepared by acidifying sodium silicate with tartaric acid) have a protective influence on colloidal silver (2) and colloidal gold (3).

In the present study an investigation was made of the protective action of colloidal silicic acid for manganese dioxide sols.

PREPARATION OF SOLS

The silica sol was prepared by adding three volumes of a 1.6 per cent sodium silicate solution slowly, with stirring, to one volume of 2 normal hydrochloric acid. After aging for 48 hr. the mixture was dialyzed for 10 days in collodion membranes. The dialyzate had a silica concentration of 14.7 g. per liter and a pH of 4.8.

Colloidal manganese dioxide was prepared by a slight modification of a method recommended by Cuy (1). Three-fourths molar ammonium hydroxide was added dropwise at the rate of one drop every 10 sec. to $M/100$ potassium permanganate at 90°C. The sol was purified by dialyzing for 10 days with "Visking casing." The purified sol had a manganese dioxide concentration of 0.66 g. per liter and a pH of 6.0.

FLOCCULATION DATA

The protective action of colloidal silicic acid on manganese dioxide sols is illustrated by the data in table 1. Flocculation values, obtained by a method described previously (4), are given for the unprotected sol and for sols containing different amounts of silicic acid. The concentration of manganese dioxide, 0.013 g. per liter, was the same in all systems.

Two series of experiments were conducted in which the concentration of silica was kept constant at 2.9 g. per liter and the manganese dioxide concentration increased to 0.066 g. and 0.33 g. per liter, respectively. No coagulation was observed in either system at the end of 24 hr. in the presence of 60 millimoles of potassium chloride or of barium chloride.

TABLE 1

Protective action of colloidal silicic acid on manganese dioxide sols

SYSTEMS	FLOCCULATION VALUES IN MILLIMOLES PER LITER		
	KCl	$BaCl_2$	$Th(NO_3)_4$
MnO_2	5.6	0.044	0.002
MnO_2-SiO_2:			
0.12 g. SiO_2 per liter	60*	60*	
0.59 g. SiO_2 per liter	60†	60†	0.012
2.9 g. SiO_2 per liter	60†	60†	

* No coagulation at the end of 24 hr.

† Weak gels were formed in these systems over periods ranging from 48 hr. to 9 days.

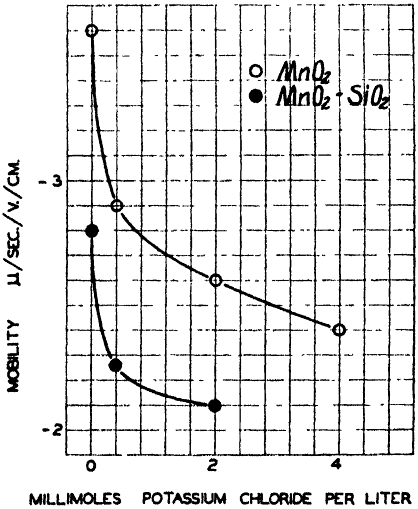

FIG. 1

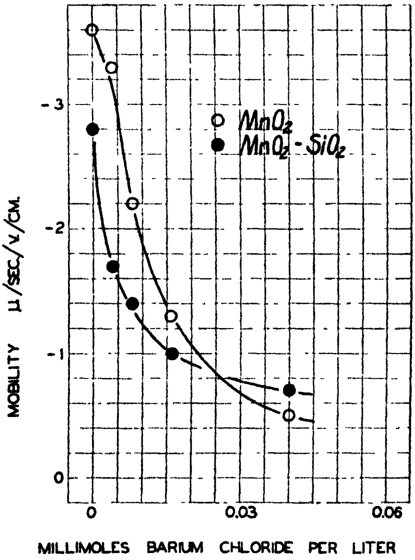

FIG. 2

MOBILITY STUDIES

Mobility measurements were made by an ultramicroscopic method. A velocity–depth curve was constructed and the value of the true mobility obtained from the area under the curve (16).

The following data are on manganese dioxide sols containing 0.013 g. of the dispersed substance per liter and on mixtures of manganese dioxide with colloidal silicic acid. The concentrations of manganese dioxide and silica in the mixtures were 0.013 g. and 0.59 g. per liter, respectively.

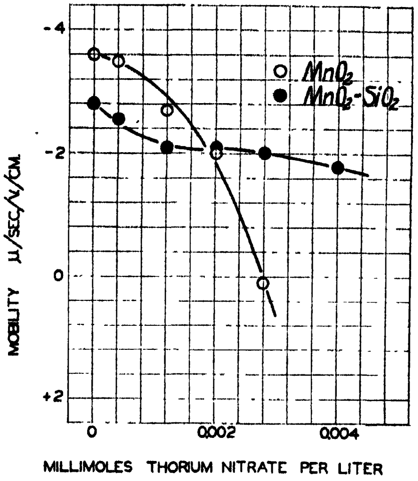

FIG. 3

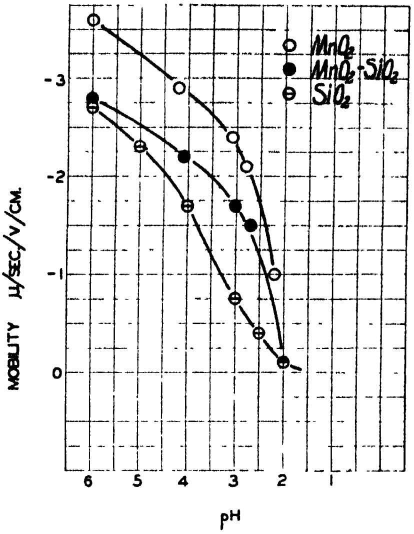

FIG. 4

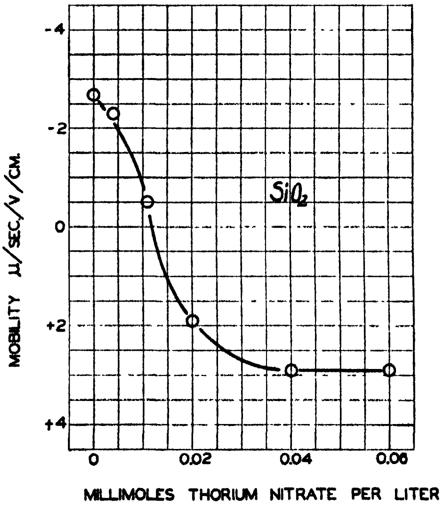

FIG. 5

The effects of potassium chloride, barium chloride, and thorium nitrate on particle mobility are shown in figures 1, 2, and 3. The mobility curves for the protected and unprotected systems demonstrate that the buffering effect of silicic acid is much greater with thorium nitrate than with the other two electrolytes.

Mobility data for the systems comprising the mixture and for the mixture itself are given in figure 4 in relation to hydrogen-ion activities. The acidities were adjusted with nitric acid. The mixture and the manganese dioxide coagulated at pH 3. The curve for colloidal silicic acid was obtained by a re-plot of the data from a previous study (5). Neither silicic acid (5, 9), manganese dioxide (6), nor the mixture[1] was recharged at the acidities investigated.

The mobility behavior of colloidal silicic acid with thorium nitrate is recorded in figure 5. The particles coagulated when their mobility was reduced to about 0.7 μ per second per volt per centimeter. Higher concentrations of thorium ions recharged the silica and yielded a stable sol.[2]

DISCUSSION

The critical potentials of potassium chloride, barium chloride, and thorium nitrate for the manganese dioxide sol used in preparing the mixtures were, in terms of mobilities, 2.4, 0.4, and 2.0 μ per second per volt per centimeter. The first and last of the electrolytes lowered the mobility of the particles in the mixture below their critical potentials for manganese dioxide without the precipitation of this substance occurring.

The critical mobilities of potassium chloride and barium chloride for silica sols of the same order of concentration as employed here have been determined to be less than 0.4 μ per second per volt per centimeter (5). The corresponding value for thorium nitrate is 0.7 μ per second per volt per centimeter. Since the critical potentials of the electrolytes are lower for silica and for mixtures of silica and manganese dioxide than for pure manganese dioxide, it seems plausible to assume that the stability of the particles in the mixtures is due to a silica covering established by adsorption.

For purposes of studying the state (5, 8) of the particles in the mixtures, a criterion was sought which would enable a rigid distinction to be made between the electrokinetic behaviors of colloidal silicic acid and of colloidal manganese dioxide comprising the mixtures. Sharp contrasts of kind were not found, however. Some of the parallel behaviors are summarized here. Thus, both systems were recharged by thorium ions but neither gave an irregular series.[3] Likewise, neither of these acidic oxides was recharged by hydrogen ions at a concentration corresponding to pH 1.5.[4]

---

[1] Mattson (13) has shown that soil colloids having a high silica:sesquioxide ratio are not recharged in acid solution.

[2] It has been pointed out that silicic acid sols are difficult to recharge (5). Many substances containing silica have been recharged, however. Among these is glass, for which data are available with thorium ions. White, Monaghan, and Urban (15) determined the isoelectric concentration to be of the order of $10^{-6}M$. In the present investigation an isoelectric concentration of $1.2 \times 10^{-5}M$ was found for a silicic acid sol containing 0.59 g. of silica per liter, while for a sol containing 0.12 g. per liter the concentration of thorium ions corresponding to zero mobility was slightly less than $4 \times 10^{-6}M$.

The fact that the particles in the mixtures were homogeneous with respect to migration velocity supports the conclusion that the silica and manganese dioxide were mutually adsorbed. It was found that addition of increments of colloidal silicic acid to the manganese dioxide sol progressively lowered the mobility of the particles until, at the composition corresponding to a silica content of 0.59 g. per liter, the particles had the same mobility as a pure silica sol of the same concentration. This result is comparable to that obtained on adding gelatin to a manganese dioxide sol (7), a case in which the idea of mutual adsorption is accepted.

TABLE 2

Sign of charge on the particles

CONCENTRATION OF THORIUM NITRATE	SIGN OF CHARGE ON THE PARTICLES
millimoles per liter	
0.0120	Negative*
0.0128	Negative* and positive*
0.0132	Negative* and positive*
0.0136	Positive
0.0140	Positive

* The velocity values were of varied magnitude in these cases.

The rule of homogeneous particle mobility was violated in certain of the systems containing electrolytes. Thus, in mixtures with potassium chloride in concentrations greater than 2 millimoles per liter, more than one mean mobility value was observed. A more pronounced anomaly was encountered with thorium nitrate over a very narrow range of concentrations in mixtures near the isoelectric point.[5] Migration of particles to both the anode and the cathode was observed. The results are shown in table 2.

SUMMARY

1. Silica sols increase the stability of colloidal manganese dioxide toward potassium chloride, barium chloride, and thorium nitrate.
2. The protective action has been explained on the basis of mutual adsorption.

---

[3] Concentrations to 60 millimoles per liter were used in an effort to coagulate the positive systems.

[4] Losenbeck (11) has reported the recharging of silica at hydrogen-ion concentrations between 10^{-3} and 10^{-2}. See, however, references 5 and 9.

[5] Precipitation occurred in these mixtures within 24 hr.

3. No protective action was observed with nitric acid as the added electrolyte.

4. Colloidal silicic acid is flocculated at low concentrations of thorium ions. The sol is recharged at concentrations of the order of 10^{-5} to 10^{-6} M.

5. Neither silica sols nor manganese dioxide sols yield an irregular series with thorium ions.

REFERENCES

(1) CUY: J. Phys. Chem. **25**, 415 (1921).
(2) DUMANSKII AND SHERSHNEV: J. Russ. Phys. Chem. Soc. **60**, 1593 (1928).
(3) DUMANSKII AND PUCHKOVSKII: J. Russ. Phys. Chem. Soc. **62**, 469 (1930).
(4) HAZEL AND SORUM: J. Am. Chem. Soc. **53**, 49 (1931).
(5) HAZEL: J. Phys. Chem. **42**, 409 (1938).
(6) HAZEL AND MCQUEEN: J. Phys. Chem. **37**, 553 (1933).
(7) HAZEL AND KING: J. Phys. Chem. **39**, 515 (1935).
(8) KOMAGATA: Electrochem. Lab., Tokyo, Bull. 348 (1933).
(9) KRESTINSKAYA AND NATANSON: Acta Physicochim. U.R.S.S. **7**, 915 (1937).
(10) KRUYT: *Colloids*. John Wiley and Sons, Inc., New York (1929).
(11) LOSENBECK: Kolloid-Beihefte **16**, 27 (1922).
(12) MATTSON: Soil Sci. **28**, 373 (1929).
(13) MATTSON: J. Am. Soc. Agron. **18**, 458 (1926).
(14) SMITH: J. Am. Chem. Soc. **42**, 460 (1920).
(15) WHITE, MONAGHAN, AND URBAN: J. Phys. Chem. **39**, 611 (1935).
(16) WILLEY AND HAZEL: J. Phys. Chem. **41**, 699 (1937).
(17) ZSIGMONDY: Z. anal. Chem. **40**, 697 (1901).

FREEZING POINTS IN MIXTURES OF STRONG ELECTROLYTES[1]

MERLE RANDALL AND BRUCE LONGTIN[2]

Department of Chemistry, University of California, Berkeley, California

Received August 15, 1939

Randall and Vietti (17; *cf.* also 9, 10, 16) have proposed a plot of $(1/z_+z_-)\log\gamma_\pm$ against the square root of the ionic strength[3] as a means

---

[1] Clerical assistance of the Works Progress Administration O. P. No. 665-08-3-144 is gratefully acknowledged.

[2] Shell Fellow in Chemistry.

[3] The notation in general is that of Lewis and Randall (6). The mean activity coefficient, $\gamma_\pm$, is defined as

$$\nu \ln \gamma_\pm = \nu_+ \ln \gamma_+ + \nu_- \ln \gamma_- \qquad (1)$$

where γ_+ is the activity coefficient and ν_+ is the number of the positive ions per of correlating activity coefficients in solutions of electrolytes. This plot has the advantage that the curves for different salts fall very closely together, at least at high dilution. The introduction of the factor z_+z_- serves to remove the wide divergences in the curves for different valence types, so that, for instance, the curve of barium chloride (2-1 type) is nearly the same as that of lanthanum nitrate (3-1 type). In the case of substances with only a few or inconsistent measurements this plot aids greatly in estimating a most probable curve. The z_+z factor is justified by the interionic attraction theory of Debye and Hückel (2, 1).

Randall and Cann (12; *cf.* 7) suggested a similar method of treating the freezing point lowering function for mixed electrolytes. They divided the function $j/m^{1/2}$ by the value of the limit which it approaches at infinite dilution, and plotted the result against the square root of the molality. They presented a typical curve for this plot. The present paper investigates the implications of their suggestion.

SOLVENT ACTIVITY IN A SOLUTION OF MIXED ELECTROLYTES

The theory of Debye and Hückel gives as a limiting law for the activity coefficient of the salt X_j in a dilute solution of mixed electrolytes,

$$\lim_{\mu \to 0} \log \gamma_{j\pm} = (Ad^{1/2})z_{j+}z_{j-}\mu^{1/2} \tag{3}$$

---

formal molecule of salt, while $\nu = \nu_+ + \nu_-$. The ionic strength, μ, is defined as $\frac{1}{2}\sum_i m_i z_i^2$, where m_i is the molality of the i^{th} kind of ion, and z_i is its valence.

The solution may be composed of the several binary salts X_j. The molality of positive ions yielded by the salt X_j is $\nu_{j+}m_j$ (where m_j is the molality of the salt) and that of the negative ions yielded by X_j is $\nu_{j-}m_j$. The ionic strength is then equal to

$$\frac{1}{2}\sum_j m_j(\nu_{j+}z_{j+}^2 + \nu_{j-}z_{j-}^2)$$

the summation now extending over the various salts, rather than over the individual ions. It is interesting to note that $\mu = \sum_j \mu_j$, where μ_j is the value which the ionic strength would have if only X_j were present at the molality m_j; ionic strengths are additive. Since the total positive valence, $\nu_{j+}z_{j+}$, of X_j must equal its total negative valence $\nu_{j-}z_{j-}$ (condition of electroneutrality), the factor $(\nu_{j+}z_{j+}^2 + \nu_{j-}z_{j-}^2)$ which enters into the ionic strength may also be written as $\nu_j z_{j+}z_{j-}$. Hence the ionic strength may also be written in the form

$$2\mu = \sum_j m_j \nu_j z_{j+} z_{j-} \tag{2}$$

in which $(Ad^{1/2})$ depends only on the nature of the solvent and on the temperature.[4,5] This equation is in agreement with the principle of ionic strength proposed by Lewis and Randall.[3]

The activity coefficient of the solvent may be obtained from those of the solutes as given by equation 3, by application of the Gibbs-Duhem (or partial molal) equation in the special form

$$-(1000/\mathrm{w}_1)\ \mathrm{d}\log(a_1/\mathrm{N}_1) = \sum_j \nu_j m_j\ \mathrm{d}\log\gamma_{j\pm} \tag{4}$$

the summation extending over all salts of the mixture.[6] The factor $(1000/\mathrm{w}_1)$, where w_1 is the molal weight of the solute, has the value 55.51 for aqueous solutions. The right-hand member becomes

$$(Ad^{1/2})\ \mathrm{d}\mu^{1/2}\ (\sum_j z_{j+} z_{j-} \nu_j m_j)$$

on substituting the value of log $\gamma_{i_\pm}$ from equation 3. The summation appearing here is simply twice the ionic strength, as is seen from equation 2. Hence equation 4 gives on integration

$$\lim_{\mu\to 0} -(1000/\mathrm{w}_1)\log(a_1/\mathrm{N}_1) = (Ad^{1/2}/3)\ 2\mu^{3/2} \tag{8}$$

---

[4] Randall and West (18) discuss equation 3 and give selected values of this constant for water as solvent at several temperatures.

[5] It is to be noted that Debye and Hückel used an ionic activity coefficient $\gamma_i = a_i/\mathrm{N}_i$ defined in terms of the mol fraction, N_i, of the ion X_i. For this mol fraction they used the symbol c_i, which has unfortunately been interpreted frequently to mean concentration. However, the definition in terms of mol fraction is essential if, as they state, the right-hand member of equation 3 is to represent the deviation of the solution from ideality. This follows since an ideal solution is one for which the activity is equal to the mol fraction (or in the case of aqueous solutions $55.51\mathrm{N}_i$, in order to make a_i approximate the molality; in this case $\gamma_i = a_i/55.51\mathrm{N}_i$). In the limit of high dilution it makes only formal difference which definition is used; hence we shall adhere to the original definition in terms of mol fraction as more convenient at higher concentrations.

[6] The Gibbs-Duhem equation itself is written for the solution of mixed electrolytes as

$$\mathrm{N}_1\ \mathrm{d}\log a_1 + \sum_i \mathrm{N}_i\ \mathrm{d}\log a_i = 0 \tag{5}$$

the summation extending over all ions. However, since $\mathrm{N}_1\,\mathrm{d}\ln\mathrm{N}_1 + \sum \mathrm{N}_i\ \mathrm{d}\ln\mathrm{N}_i$ must vanish identically as a result of the requirement that

$$\mathrm{N}_1 + \sum_i \mathrm{N}_i = 1 \tag{6}$$

equation 5 may be rewritten in the form

$$\mathrm{N}_1\ \mathrm{d}\log(a_1/\mathrm{N}_1) + \sum_i \mathrm{N}_i\ \mathrm{d}\log a_i/\mathrm{N}_i = 0 \tag{7}$$

Equation 4 results finally by taking into account the definition of ln $\gamma_{i_\pm}$ and the fact that $(1000/\mathrm{w}_i)\mathrm{N}_i/\mathrm{N}_1$ is equal to the sum of the molalities of the i^{th} kind of ion furnished by the various salts X_j.

This result may also be obtained directly from the theory of Debye and Hückel.

Equation 8 shows that the limit approached by the function [log $(a_1/\text{N}_1)]/\mu^{3/2}$ is independent of the nature of the solutes (provided they are all strong electrolytes). Thus we should expect this function to play a rôle in the estimation of solvent activities similar to that played by the function $(1/z_+z_-)\ \ln\ \gamma_\pm$ in the estimation of solute activities.

FREEZING POINT FUNCTION

In the limit of high dilution the activity of the solvent becomes sensibly equal to its mol fraction. By virtue of equation 6 the limiting value of ln a_1 may be shown to be that of

$$-\ln\left[1 + (\text{w}_1/1000) \sum_i m_i\right]$$

which is

$$-(\text{w}_1/1000) \sum_i m_i$$

In this expression $\sum_i m_i$ is the total ionic molality (i.e., the sum of the molalities of all the ions). Thus, as we should expect, the definition of the freezing point function j is to be generalized as[7]

$$j = 1 - \theta/(\lambda \sum_i m_i) \tag{9}$$

while the function h is defined as[3]

$$h = \frac{(1000/\text{w}_1) \ln a_1}{\sum_i m_i} + 1 \tag{10}$$

In these equations the usual expression, νm, for the total ionic molality is replaced by the expression $\sum_i m_i$, which may also be written $\sum_j \nu_j m_j$, in terms of the salt molalities. The definitions given in equations 9 and 10 must take this form in order that the functions h and j may approach zero at infinite dilution.

Combining equations 8 and 10, we find for the limiting value of the function h

$$\lim_{\mu \to 0} h \sum_i m_i = 2.303\ (Ad^{1/2}/3)\ 2\mu^{3/2} \tag{11}$$

---

[7] Here θ is the freezing point lowering and λ the molal lowering.

Equation 11 holds only at very high dilution. The expression log (a_1/N_1) contains terms which vary like μ^2 and higher powers of $\mu^{1/2}$ in addition to those given in equation 8, while a term

$$\sum_i m_i - (1000/\mathrm{w}_1) \ln \mathrm{N}_1$$

was dropped from equation 11 because it vanishes like μ^2. These terms are negligible as compared to the term in $\mu^{3/2}$ when μ is small. The function $j \sum_i m_i$ differs from $h \sum_i m_i$ only by terms (15) which also vanish like $(\sum_i m_i)^2$ and hence like μ^2. Thus equation 11 is also valid with j substituted for h.

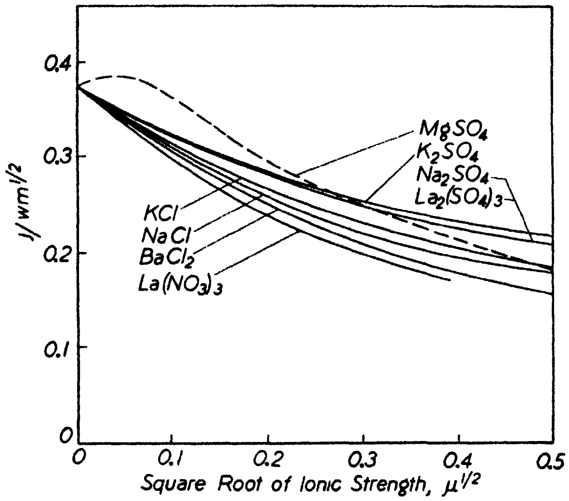

FIG. 1. Correlation of j functions for salts of various valence types

From these considerations it is evident that the function $j \sum_i m_i/2\mu^{3/2}$ (likewise $h \sum_i m_i/2\mu^{3/2}$) approaches the same limit (8), $2.303(Ad^{1/2}/3)$, for all types of solutions of strong electrolytes at high dilution. It is this function of the freezing point lowering which we should expect to be nearly the same for all solutions of strong electrolytes up to moderate ionic strengths. Curves of $j \sum_i m_i/2\mu^{3/2}$ versus $\mu^{1/2}$ are plotted in figure 1 for solutions of pure salts of several valence types.[8]

For a single pure salt the factor $\sum_i m_i/2\mu^{3/2}$ is identical with $1/wm^{1/2}$, where w is the valence factor tabulated by Randall and West (18), and m

---

[8] Taken from an unpublished summary of all the data on freezing point lowering.

is the molality of the salt. This follows since $\sum_i m_i$ reduces in this case to νm. Thus

$$\sum_i m_i/2\mu^{3/2} = \nu m \Big/ 2\left(\frac{\nu z_+ z_-}{2}\right)\left(\frac{\nu_+ z_+^2 + \nu_- z_-^2}{2}\right)^{1/2} m^{3/2}$$

$$= 1 \Big/ \left[z_+ z_- \left(\frac{\nu_+ z_+^2 + \nu_- z_-^2}{2}\right)^{1/2}\right] m^{1/2} \qquad (12)$$

in which the term in square brackets is w. Since the freezing point function is ordinarily tabulated in the form $j/m^{1/2}$ for electrolytes, it is only necessary to divide the tabulated values by the factor w in order to put them on the plot of figure 1. Since this factor ranges from unity for 1-1 type salts to 7.35 for the 1-3 and 10.62 for the 2-3 type salts, it is evident that this change of scale has brought the curves for the different valence types into superposition remarkably well up to moderately large values of μ, whereas otherwise they would be widely separated.

This form of plotting has the advantage that it brings the curves for salts of different valence types into close superposition. Thus it is possible to estimate the freezing point function for a salt of one valence type from that of a salt of different valence type. A single measurement of freezing point lowering (or a set of inconsistent data) may be located on the plot with the help of the theoretical valence factor. The complete curve may then be sketched in with considerable certainty by analogy to the curves for well-known substances. The method has the advantage of permitting the complete set of curves for substances of all valence types to be used in the estimation, rather than only curves for substances of the same valence type.

Values of the solvent activity (i.e., ln a_1) may be calculated directly from the estimated values of the freezing point function. It may also be desired to calculate the mean activity of the salt from these data. For this purpose the equation 6 of Randall and White (19) may be put in the form[3]

$$\ln a_\pm/m_\pm = -h - 2z_+z_- \int_0^m (h/wm^{1/2})\, d\mu^{1/2} \qquad (13)$$

$$\ln a_\pm/m_\pm = -j - 2z_+z_- \int_0^m (j/wm^{1/2})\, d\mu^{1/2}$$

$$+ 0.00057 \int_0^m \frac{\theta}{m}\, d\theta - 55.51 \int_0^m \frac{1}{m}\, d(2.303x) \qquad (14)$$

which is convenient for direct evaluation of the integrals from the plot of figure 1.

MIXED ELECTROLYTES

In a mixture of electrolytes, all of the same valence type, the factor $\sum_i m_i/2\mu_i^{3/2}$ reduces to $1/w(\sum_j m_j)^{1/2}$, where w is the common valence factor and $\sum_j m_j$ is the total molality of the salts. It thus has the same value that it would have for any one of the salts of this valence type at the same total molality (i.e., same ionic strength).

Hall and Harkins (3) measured the freezing point lowering of equimolal mixtures of potassium chloride and nitrate, and of sodium and potassium iodates, over a fairly wide range of concentrations, and found in each case that the freezing point lowering was substantially the mean of the freezing point lowering of the individual salts at the same total concentration. This leads readily to the conclusion that in these cases the function $j \sum_i m_i/2\mu_i^{3/2}$ for the equimolal mixture is the mean of those for the pure salts at the same ionic strength. Harkins and Roberts (4) found similar results with equimolal mixtures of sodium and potassium sulfates.

These results with pairs of salts of the same valence type are in close analogy with the findings of Randall and Breckenridge (11; see also 14 and 13) that the activity of a single electrolyte in a mixture varies approximately linearly with the molal proportions of the two salts at constant ionic strength. From these considerations we are led to suspect that $j \sum_i m_i/2\mu^{3/2}$ will vary approximately linearly with the molecular proportions of the salts in a mixture of different as well as like valence types.

The data of Hall and Harkins (3) and of Harkins and Roberts (4) for salts of the same valence type do not offer a serious test of the importance of the valence factor in $j \sum_i m_i/2\mu^{3/2}$, since that factor does not vary with varying proportions of the salts. The only freezing point data available for salts of mixed valence type appear to be those of LeBlanc and Noyes (5).[9] From these we have calculated the values of $j \sum_i m_i/2\mu^{1/2}$ for the mixtures of the nitrates of sodium, potassium, lead, and strontium.[10] These values are plotted in figure 2 against the square root of ionic strength, together with curves for the pure salts.[8] While the data are hardly sufficient for a complete test of our hypothesis, it is seen that in every case the experimental point for a mixture falls between the curves for the pure components at a position approximately proportional to the two salts in the mixture.

This property of the plot of $j \sum_i m_i/2\mu^{3/2}$ (likewise $h \sum_i m_i/2\mu^{3/2}$) *versus*

---

[9] The original data are given in mols per liter.

[10] The cases chosen are the only ones which could be considered free from complicating reactions.

$\mu^{1/2}$ permits the estimation of freezing points (and likewise solvent vapor pressures) of solutions of mixed electrolytes from data for solutions of the pure salts (or from data for other salts if necessary). It is also useful in interpreting freezing points of mixtures of electrolytes formed from solutions of a pure salt by chemical reaction.

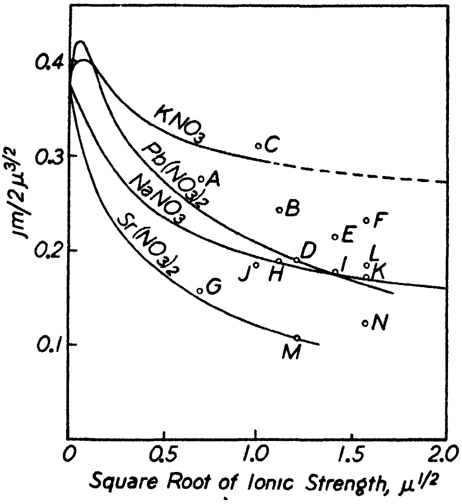

FIG. 2. Correlation of j functions for mixtures of some nitrates. Point A, 0.5 C potassium nitrate; point B, 0.5 C potassium nitrate and 0.25 C lead nitrate; point C, 1.0 C potassium nitrate; point D, 0.5 C lead nitrate; point E, 0.5 C potassium nitrate and 0.5 C lead nitrate; point F, 1.0 C potassium nitrate and 0.5 C lead nitrate; point G, 0.5 C sodium nitrate; point H, 0.5 C sodium nitrate and 0.25 C lead nitrate; point I, 0.5 C sodium nitrate and 0.5 C lead nitrate; point J, 1.0 C sodium nitrate; point K, 1.0 C sodium nitrate and 0.5 C lead nitrate; point L, 1.0 C potassium nitrate and 0.5 C strontium nitrate; point M, 0.5 C strontium nitrate; point N, 1.0 C sodium nitrate and 0.5 C strontium nitrate.

SUMMARY

1. The curves of $j/m^{1/2}$ for salts of different valence types may be brought into approximate superposition by dividing $j/m^{1/2}$ by a valence factor w. A plot of $j/wm^{1/2}$ *versus* the square root of the ionic strength permits convenient estimation of solvent (and solute) activities and freezing points for salt solutions for which data are lacking.

2. For solutions of mixed electrolytes the procedure is generalized by plotting the function $j\sum_i m_i/2\mu^{3/2}$ against the square root of the ionic strength, $\sum_i m_i$ being the total ionic molality. For this purpose the function j must be defined as $1 - \theta/\lambda\sum_i m_i$.

3. A like procedure may be employed with the function h, while a plot of the quotient of log solvent activity by $\mu^{3/2}$ against ionic strength should have similar properties.

REFERENCES

(1) Debye: Physik. Z. **25**, 97 (1924).
(2) Debye and Hückel: Physik. Z. **24**, 185 (1923).
(3) Hall and Harkins: J. Am. Chem. Soc. **38**, 2658 (1916).
(4) Harkins and Roberts: J. Am. Chem. Soc. **38**, 2676 (1916).
(5) LeBlanc and Noyes: Z. physik. Chem. **6**, 385 (1890).
(6) Lewis and Randall: *Thermodynamics and the Free Energy of Chemical Substances.* McGraw-Hill Book Company, Inc., New York (1923).
(7) Randall: J. Am. Chem. Soc. **38**, 788 (1916).
(8) Randall: J. Am. Chem. Soc. **48**, 2512 (1926).
(9) Randall: J. Chem. Education **8**, 1062 (1931).
(10) Randall: Am. Physics Teacher **7**, 292 (1939).
(11) Randall and Breckenridge: J. Am. Chem. Soc. **49**, 1435 (1927).
(12) Randall and Cann: J. Am. Chem. Soc. **50**, 347 (1928).
(13) Randall and Failey: Chem. Rev. **4**, 271, 285, 291 (1927).
(14) Randall and Langford: J. Am. Chem. Soc. **49**, 1445 (1927).
(15) Randall, Libby, and Longtin: J. Phys. Chem. **44**, 313 (1940).
(16) Randall and Shaw: J. Am. Chem. Soc. **57**, 427 (1935).
(17) Randall and Vietti: J. Am. Chem. Soc. **50**, 1526 (1928).
(18) Randall and West: To be published.
(19) Randall and White: J. Am. Chem. Soc. **48**, 2514 (1926).

THE PREPARATION OF FLUORESCENT CALCITE

GORTON R. FONDA

Research Laboratory, General Electric Company, Schenectady, New York

Received August 15, 1939

Certain specimens of natural calcite, such as those occurring at Franklin, New Jersey, show a rose fluorescence when excited by ultraviolet. According to Pringsheim (6), this is to be ascribed to the presence of manganese as activator. Such calcite is unique among natural phosphors, in that it has resulted from a sedimentation rather than from an igneous process. This distinction has stimulated attempts to produce it experimentally. Of several methods tried by the author, the most successful proved to be the precipitation of the carbonate in the presence of a manganese salt. The excitation of its fluorescence was stronger in the far ultraviolet in the neighborhood of the resonance line of mercury, 2536 Å., than in the near ultraviolet. The conditions for precipitation had to be so chosen that calcite crystallized out rather than aragonite, a fluorescent form of which could not be prepared.

The inability of a thermal treatment to form true fluorescent calcite was shown by tests in an atmosphere of carbon dioxide. When the fluorescent mineral, which is naturally white, was fired, a non-fluorescent product was obtained at all temperatures, darkened by decomposition of the manganese carbonate and liberation of manganese oxide. Thermal treatment of synthetic mixtures did nevertheless produce fluorescence when a mixture of calcium oxide or carbonate with less than 0.1 per cent of manganese oxide was fired under such conditions that a calcium oxide was formed which contained a small amount of carbonate. The brightest fluorescence resulted by introducing 0.005 per cent manganese as oxide to the carbonate and by firing at 1000°C. in an atmosphere of carbon dioxide for a period of 30 to 60 min. The resulting phosphor was a calcium oxide which still retained 1.5 to 10.0 molar per cent of calcium carbonate. Its phosphorescence was negligible.

Its characteristic rose fluorescence disappeared when the carbonate was completely decomposed by firing in air. It is, therefore, distinct from the oxide phosphor emitting red fluorescence, which can be prepared by firing at 1000°C. in air a mixture of calcium oxide or carbonate with manganese activator in the presence of a suitable flux. This latter phosphor is probably the fluorescent calcium oxide obtained by Nichols (5) in his studies on the fluorescence of calcite.

The rose fluorescence of the calcium oxide–carbonate phosphor disappeared also when the carbonate content was unduly increased by firing the phosphor in carbon dioxide at a temperature below 800°C. The upper limit of carbonate at which fluorescence could still be just barely perceived corresponded to about 50 molar per cent. In the absence of manganese, no fluorescence could be observed at any proportion of carbonate and oxide. The product is, therefore, not to be confused with those phosphors in which the introduction of a foreign salt of the same metal ion serves as activator (2). Furthermore, it is essentially different in composition from the natural mineral.

A successful synthesis of the natural fluorescent calcite was carried out by precipitating the carbonate from a mixture of calcium and manganese chlorides with a solution of ammonium carbonate at a temperature not too high. As the manganese content was increased, the fluorescence was found to rise to a peak and then to decrease. The optimum concentration for the solution of chlorides was at a composition of one atom of manganese to thirty of calcium. The other conditions favorable to a maximum intensity of fluorescence were (*1*) the use of dilute solutions containing 1.8 per cent of $CaCl_2 \cdot 6H_2O$ and 1.5 per cent of $(NH_4)_2CO_3 \cdot H_2O$, (*2*) a 50 per cent excess of ammonium carbonate, and (*3*) precipitation at about

70°C., followed by holding at room temperature for several weeks before filtering or, more effectively, by boiling for 10 min. Under these conditions the precipitate, whether wet or dry, had a fluorescence that was 30 per cent of that of natural calcite from Franklin, New Jersey, and was of the same rose color. Furthermore, its phosphorescence was similar in intensity and duration. It made no difference whether the carbonate solution was added to the chloride or *vice versa.*

The products were pure white in color. The diffraction patterns of some typical ones, obtained with MoK$_\alpha$ radiation through the courtesy of L. L. Wyman and E. T. Asp of this laboratory, are shown in figure 1. The unreflected beam, which is not shown in these patterns, lies to the left, and the angle of reflection becomes progressively greater as one passes from left to right. The limit at the right-hand side of the pattern represents a 90° reflection angle. In the absence of manganese, the pattern is identical with that of natural calcite, which crystallizes in the rhombohedral form. This is shown by a comparison of patterns c and d.

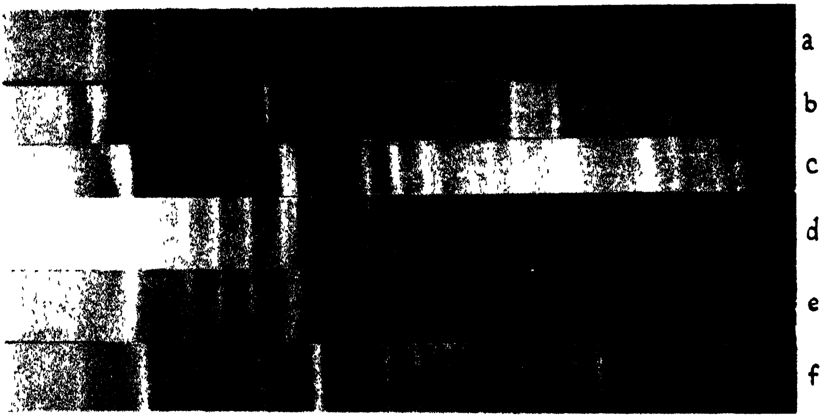

FIG. 1. Modified forms of calcium carbonate a, precipitated aragonite without manganese, b, natural aragonite; c, natural calcite; d, precipitated calcite without manganese; e, precipitated calcite with 16.6 molar per cent manganese; f, manganese carbonate.

When the calcite was precipitated in the presence of manganese, however, a contraction in the lattice parameter was observed, slight in the case of 3.3 molar per cent of manganese with reference to the calcium, the concentration which yielded the most intense fluorescence, but more pronounced at 16.6 molar per cent. At the latter concentration the contraction is in fact of sufficient magnitude to have a pronounced effect upon the position of the lines within the 90° reflection range covered by the diffraction patterns of figure 1. This is shown by a comparison of pattern d for the pure carbonate with pattern e for the carbonate with 16.6 molar per cent manganese. In the latter the same pattern of lines persists, but the lines are displaced toward the right to an extent that increases with the angle of reflection. This denotes that the crystalline structure is unaltered except for the reduction in lattice spacing. Fluorescence was still present at this higher concentration of manganese, though considerably reduced. A change in lattice size that results from the introduction of an activator element has also been observed in the case of zinc and cadmium silicate phosphors containing manganese (3). Such changes signify that the activator has adapted itself to the lattice of the basic material and that its atoms are substituted for occasional atoms of the base. In this case it is not surprising that manganese has been substituted for calcium, for the carbonates of both crystallize in the same form. The only difference is that the lattice of manganese carbonate, rhodochrosite, is constructed on a considerably smaller scale, because of the smaller size of manganese, the radius of whose ion measures 0.91 Å. as compared with 1.06 Å. for calcium. Its pattern is shown in figure 1f, taken of a precipitate formed by adding ammonium carbonate to a solution of manganese chloride. A comparison of f with d and e brings out the identity of lattice form and the increasing contraction in lattice spacing that accompanies the change from pure calcium carbonate to pure manganese carbonate. The effect of a foreign element on the lattice parameters of a double salt obtained by precipitation has also been observed by Averell and Walden (1) for the case of barium sulfate precipitated in the presence of permanganate ion.

No fluorescence could be observed in carbonates precipitated as calcite from solutions containing lead, copper, bismuth, or samarium as possible activators.

When the precipitation was carried out altogether at 100°C., there was formed in both dilute and concentrated solutions the allotropic orthorhombic form of aragonite. Its structure is shown in pattern a, identical with pattern b of the natural mineral, aragonite. This effect of temperature of precipitation in determining the crystalline character of the carbonate is in accord with the early observations of Rose, cited by Mellor (4), but seems to be not altogether in accord with the later experience of Adler, also cited by Mellor.

When the precipitation at 100°C. was carried out in the presence of 3.3 molar per cent manganese with reference to calcium, the product exhibited a pattern which was still identical with the aragonite pattern of a. It was non-fluorescent. With 16.6 molar per cent, however, a radical change appeared. The calcium carbonate, precipitated under the conditions for aragonite, was compelled by the presence of this larger amount of manganese carbonate to adapt itself to the "calcite" structure, so that the same pattern was obtained that resulted when the precipitation was carried out at lower temperatures under the conditions for yielding calcite in the presence of the same amount of manganese, as exhibited in pattern e. Both of these products emitted the same low red fluorescence, despite the difference in preparation. The formation of the "calcite" rather than the "aragonite" structure can therefore be accepted as the determining factor for the occurrence of fluorescence under activation by manganese.

Attempts to prepare fluorescent aragonite by precipitation failed also when lead, copper, and samarium were used as possible activators. Fluorescent aragonite does, nevertheless, occur in nature. A specimen from Girgenti, Sicily, examined by the author was unexcited by 2536 Å. but under 3650 Å. emitted a rose fluorescence.

REFERENCES

(1) Averell, P. R., and Walden, G. H., Jr.: J. Am. Chem. Soc. **59**, 906 (1937).
(2) Byler, W. H.: J. Am. Chem. Soc. **60**, 1247 (1938).
(3) Fonda, G. R.: J. Phys. Chem. **43**, 561 (1939).
(4) Mellor, J. W.: *A Comprehensive Treatise on Inorganic and Theoretical Chemistry*, Vol. III, p. 818. Longmans, Green and Company, London (1923).
(5) Nichols, E. L., Howes, H. L., and Wilber, D. T.: *Cathodo Luminescence and the Luminescence of Incandescent Solids*, p. 23. Carnegie Institution, Washington, (1928).
(6) Pringsheim, P.: *Fluorescenz und Phosphorescenz*, p. 312. Julius Springer, Berlin, (1928).

THE COPPER SULFATE-SODIUM SILICATE REACTION

HAROLD V. ANDERSON and FRANK P. HOCHGESANG[1]
Department of Chemistry, Lehigh University, Bethlehem, Pennsylvania

Received June 20, 1939

INTRODUCTION

When solutions of copper sulfate and sodium silicate are mixed a blue-green precipitate forms. This precipitate is of varying composition (4) and may or may not be gelatinous depending upon the $CuO:SiO_2$ ratio of the initial solutions. The precipitate or gel may be boiled; or the dried material may be heated at 100°C., without turning black. Neville and Oswald (6) have shown that a copper hydroxide suspension does turn black upon boiling but that gelatin will stabilize and protect this precipitate. Because of this fact Weiser (9) suggests that the precipitate obtained upon mixing copper sulfate and sodium silicate solutions may be blue copper hydroxide stabilized by hydrous silica. It is the purpose of this investigation to establish the composition of this precipitate with the aid of x-ray powder analysis.

---

[1] William L. Heim Research Fellow, 1937-39.

PREPARATION AND ANALYSIS

The materials were precipitated by mixing $M/10$ copper sulfate and $M/10$ sodium metasilicate solutions in varying proportions. The majority of the precipitations were carried out at the boiling point, but a few were made at room temperature. The principal difference detectable by x-rays in the products obtained by precipitation at various temperatures appears to be one of particle size only. The materials to be discussed here will be those obtained by precipitation from boiling solutions, since the larger particle size is more satisfactory for x-ray analysis. After mixing, the solutions and precipitates were maintained at the boiling temperature for 10 to 15 min., washed by decantation, transferred to a filter, and washed again. They were then dried to constant weight in an oven at 65–70°C. The results of a chemical analysis of these materials are tabulated in table 1.

TABLE 1

Results of chemical analysis

VOLUME OF $M/10$ $CuSO_4$ TO $M/10$ Na_2SiO_3	TOTAL			WEIGHT LOSS ON IGNITION	TOTAL*
	CuO	SO_3	SiO_2		
	per cent	*per cent*	*per cent*	*per cent*	*per cent*
2 to 1	65.29	16.63	1.12	33.03	99.4
1 to 1	59.48	14.93	9.94	29.99	99.4
1 to 2	48.30	0.97	35.65	14.57	98.5

* Above total equals CuO plus SiO_2 plus weight loss on ignition.

X-ray spectrograms were obtained of all the materials. The patterns were taken using copper K_α radiation (0.001 in. nickel foil filter) obtained from a Philips Metalix tube operated at 38 kilovolts and 14 milliamperes. The exposure time was 10 hr. in a previously calibrated cylindrical camera of 59.10 mm. radius. The samples to be analyzed were ground in an agate mortar, pasted on a hair with a little petroleum jelly, and rotated during exposure. Also, pinhole patterns were taken of all the materials in order to follow variations in particle size.

DISCUSSION

The wet precipitates varied from those which were easily filtered to those which came down in a voluminous, gelatinous mass, while the color varied from a pale greenish blue to deep blue. These properties were found to be in direct order with increasing silica content and with decreasing particle size, as shown by the pinhole patterns. With the exception of those precipitates which contain a relatively large amount of silica, i.e., those made using more than one volume of $M/10$ sodium silicate to one of $M/10$ copper sulfate, the materials are definitely crystalline. Also, all the materials prepared exhibit the same basic diffraction pattern. Even in the dense background scattering which appears on the patterns of the essentially non-crystalline materials, one can easily find weak lines corresponding to the strongest lines of the crystalline materials.

Diffraction patterns of a great variety of known materials were obtained in an effort to establish the identity of this unknown material which is common to all the precipitates. That the material is not blue copper hydroxide is quite evident by reference to figure 1. This figure shows typical patterns of the unknown material with comparison patterns of blue copper hydroxide (stabilized by the addition of gelatin), the rare copper silicate mineral dioptase, and the more common mineral chrysocolla. Mineralogical literature (2) records several analyses of dioptase which show conclusively that it is $CuSiO_3 \cdot H_2O$. Chrysocolla is thought to be the dihydrate, but it occurs in nature intimately mixed with impurities so that its composition is not certain.[2] It is improbable that anhydrous copper silicate can exist as such. Upon heating either dioptase or chrysocolla to a temperature at which water is given off (*ca.* 500°C.) the samples decrepitate, decomposing completely into cupric oxide and the α-quartz modification of silicon dioxide.

Posnjak and Tunell (7) investigated with considerable thoroughness the system cupric oxide-sulfur trioxide-water. Among their results they recorded powder x-ray diffraction data for several of their basic copper sulfates, the identities of which are conclusively established. Table 2 records their data for several of these compounds and compares them with those obtained for the precipitated "copper silicates." Both the relative intensities of the lines and the interplanar spacings agree very well.[3] The unknown crystalline material present in all the prepared precipitates is thus shown to be a mixture of the basic sulfates $4CuO \cdot SO_3 \cdot 3H_2O$ and $3CuO \cdot SO_3 \cdot 2H_2O$.

Chemical analysis of the prepared materials supports the fact that they consist of a basic copper sulfate plus some other amorphous material, presumably hydrous silica. Attempts to calculate the original analysis

---

[2] Chemical analyses made on the mineral samples from which the x-ray patterns were obtained (figure 1) agreed well with the analysis recorded by Doelter (2).

[3] The slight discrepancies are accounted for by the fact that Posnjak and Tunell obtained their data using molybdenum radiation and General Electric cassettes, whereas the data recorded in column 1 of table 2 were recorded in a cylindrical camera using copper radiation.

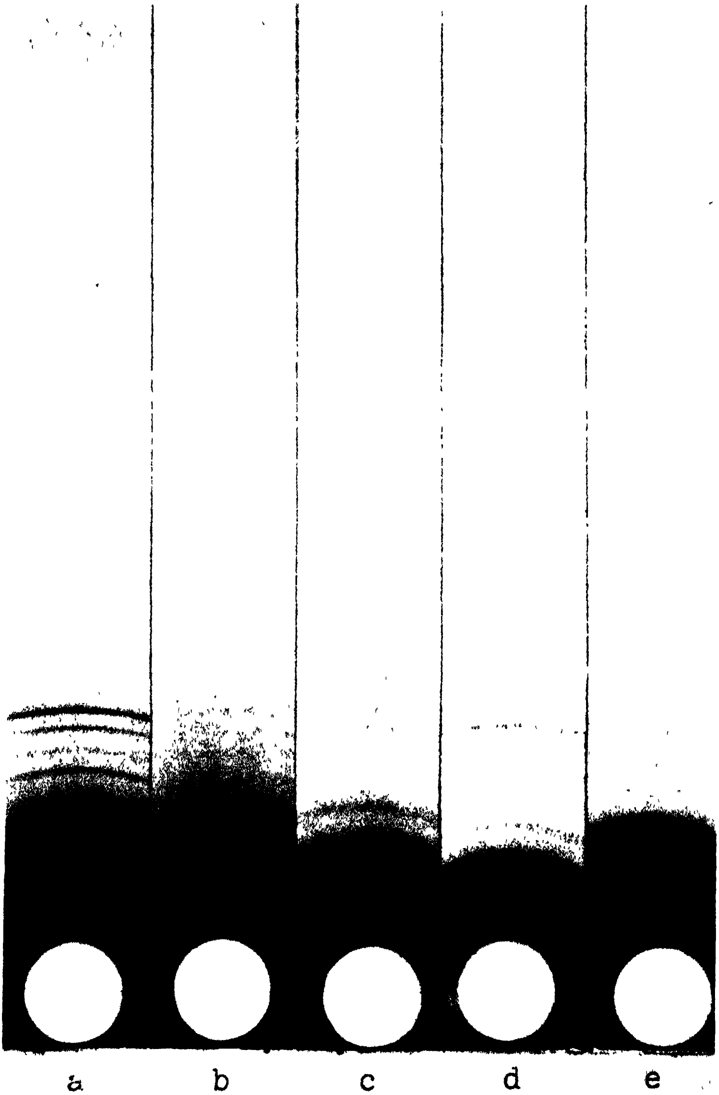

FIG. 1. Diffraction patterns taken in a cylindrical powder camera, using copper radiation. a, typical pattern obtained when equal, or excess, volumes of copper sulfate were used in precipitation; b, typical pattern obtained from materials of higher silica content; c, blue cupric hydroxide; d, dioptase; e, chrysocolla.

to mole ratios of CuO, SiO_2, SO_3, and H_2O which were very nearly whole numbers ended in failure. However, if the silica is subtracted from the original analysis and the resulting composition recalculated to 100 per cent, then table 3 shows that the mole ratios for some of the compounds are

TABLE 2

Diffraction pattern data

UNKNOWN MATERIAL		$4CuO \cdot SO_3 \cdot 3H_2O$*		$3CuO\ SO_3\ 2H_2O$*	
$I_{est.}$	Spacings	$I_{est.}$	Spacings	$I_{est.}$	Spacings
	Å.		Å.		Å.
4	6.5	7	6.20		
2	5.9			5	5.83
8	5.36	7	5.25	4	5.35
1	4.99			7	4.80
1	4.33				
10	3.90	9	3.83		
0.5	3.52			7	3.58
5	3.20	4	3.14	1	3.31
3	2.92	2	2.88	2	3.07
3	2.79			3	2.99
5	2.68	7	2.65	2	2.73
2	2.60	1	2.58	4	2.67
10	2.52	10	2.49	9	2.55
1	2.45	1	2.44	1	2.48
2	2.38	1	2.36	2	2.42
2	2.28	2	2.26	1	2.37
3	2.19	3	2.17	1	2.31
1	2.14	1	2.12	1	2.25
2	2.08	2	2 06	10	2.12
2	2.02	1	2.00	1	2.06
2	1.962	2	1.95	1	2 01
		1	1.88	1	1.94
2	1.818	1	1.81	1	1.83
6	1.744	5	1.73	1	1.81
1	1.712	1	1.70	5	1.63
2	1.672	1	1.66	1	1.56
1	1.633	2	1.62	1	1.55
2	1.596	1	1.59	7	1.50
3	1.561	2	1.56	1	1.48
2	1.534	2	1.53	2	1.44
2	1.500	3	1.50	2	1.39
2	1.463	1	1.46	2	1.31
2	1.432	1	1.42	3	1.28
3	1.409	2	1.39	1	1.24
1	1.369			1	1.21
1	1.336	1	1.33	1	1.19
3	1.311	2	1.31	1	1.16
2	1.288	1	1.28	2	1.10
1	1.143			1	1.06
0.5	1.095				
0.5	1.083				
0.5	1.073				
1	1.058				
0.5	0.999				
1	0.978				
0.5	0.906				

* Columns 2 and 3 reproduce the data recorded by Posnjak and Tunell (7).

very nearly whole numbers. The values used here as equal to the water content were obtained by subtracting the per cent of sulfur trioxide from the weight loss on ignition. It is highly probable that some water would be held rather tenaciously by hydrous silica, resisting the original drying at 70°C., thereby making the values recorded in table 3 too high. Samples made from solutions containing more silica than $1CuO:1SiO_2$ apparently do not contain enough sulfate sulfur to make it possible for them to combine all the cupric oxide as basic sulfate.

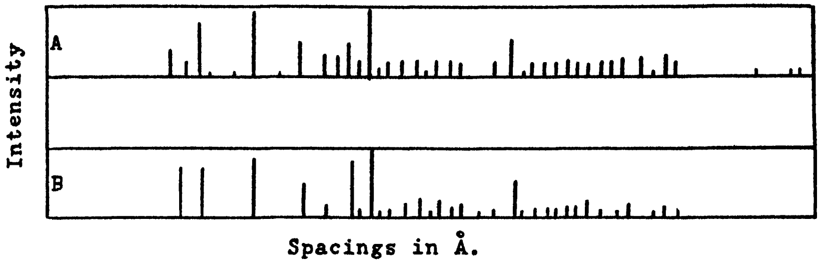

FIG. 1b. A, copper sulfate–sodium silicate reaction; B, brochantite, $4CuO \cdot SO_3 \cdot 3H_2O$ (by Posnjak and Tunell).

TABLE 3

Mole ratios

Analysis, as in table 1, recalculated to 100 per cent after subtracting the SiO_2 from the total as found

VOLUMES OF $M/10$ $CuSO_4$ TO $M/10$ Na_2SiO_3 USED IN PREPARATION	MOLE RATIOS		
	CuO	SO_3	H_2O
2 to 1	4.00	1.01	4.44
1 to 1	4.00	1.00	4.47
1 to 2	4.00	0.08	4.97
P & T calculated*............. ..	4	1	3
P & T found....................	4.00	1.01	3.15

* P & T are the values of Posnjak and Tunell for $4 CuO \cdot SO_3 \cdot 3 H_2O$.

Attempts to recalculate the original analysis subtracting sulfur trioxide (instead of silicon dioxide as in table 3) showed a constantly varying ratio of $CuO:SiO_2$ which approximated whole numbers in only one case. The sample made from one part of sulfate plus two parts of silicate showed a $1:1:1\frac{1}{2}$ ratio of $CuO:SiO_2:H_2O$, but the few lines obtained on the x-ray pattern agreed with those of the basic copper sulfate and not the monohydrate of copper silicate.

While igniting the materials in a porcelain crucible over a Bunsen burner a yellow "center" was found to develop in many cases, especially in those precipitates of high sulfate content. This same yellow material was found when copper sulfate pentahydrate was heated at 600–650°C. for a short time. Binder (1) reported finding such a compound and ascribed to it the formula $SO_3 \cdot 2CuO$. Comparison of the spacings of this material with those given by Hanawalt, Rinn, and Frevel (3) for anhydrous cupric sulfate finds very little agreement, showing that the yellow compound is apparently not anhydrous cupric sulfate. All the prepared materials completely break down into cupric oxide and α-quartz upon heating to constant weight over a Bunsen burner.

Basic copper sulfates readily form upon the addition of alkali to dilute solutions of copper sulfate (8). Thus the condition of alkalinity brought about by hydrolysis of a sodium silicate solution favors the formation of a basic sulfate. Also, hydrous silica is not necessary to stabilize or protect the complex sulfate, for equal volumes of $M/10$ copper sulfate and $M/10$ sodium oxide ($M/5$ sodium hydroxide) solutions upon mixing yield a precipitate which is identical in every respect with the "copper silicate" precipitates.

The silicate ion in aqueous solution is protected by a hydrated shell (8) which would tend to make it inactive. Also, upon the least provocation, such as slight acidity, hydrous silica is thrown out of solution. Several stoichiometrically possible equations may be written for the copper sulfate–sodium silicate reaction which will account for the products. If we write for the reaction the following equation:

$$4CuSO_4 + 2Na_2SiO_3 + 6H_2O \rightarrow 4CuO \cdot SO_3 \cdot 3H_2O + 2H_2SiO_3 + 2Na_2SO_4 + H_2SO_4$$

then silicic acid itself may be one of the products. Also, acid is generated by the reaction, thereby supplying the condition necessary to throw down silica gel from any excess sodium silicate which may be present. If hydrous silica does accompany the basic copper sulfate precipitate, no matter what the process by which it is formed, it would account for the excessive background scattering present on the diffraction patterns.

SUMMARY

1. $M/10$ copper sulfate and sodium silicate solutions mixed at the boiling point yield characteristic precipitates. These precipitates vary from light bluish green to deep blue in color and from crystalline to colloidal in size as the concentration varies from excess sulfate to excess silicate, respectively.

2. These prepared materials were shown by means of x-ray analysis, supported by chemical analysis, to consist of basic copper sulfate, $4CuO \cdot SO_3 \cdot 3H_2O$, or a mixture of this compound with $3CuO \cdot SO_3 \cdot 2H_2O$.

Also, all these materials were found to occlude varying amounts of an amorphous material, essentially silica.

3. Hydrous silica is not necessary for the stabilization of the complex compounds.

4. Reasons are discussed to explain the formation of such a compound rather than the copper silicate to be expected in such a reaction.

The authors are indebted to Dr. Harvey A. Neville, Head of the Department of Chemistry and Chemical Engineering of Lehigh University, for his valuable criticism of their paper.

REFERENCES

(1) BINDER: Ann. chim. **5**, 337–409 (1936).
(2) DOELTER: *Handbuch der Mineralchemie*, Vol. II, pp. 775–9. Theodor Steinkopff, Dresden and Leipzig (1914).
(3) HANAWALT, RINN, AND FREVEL: Ind. Eng. Chem., Anal. Ed. **10**, 457 (1938).
(4) JORDIS AND HENNIS: J. prakt. Chem. [2] **77**, 238–61 (1908).
(5) MELLOR: *Treatise on Inorganic and Theoretical Chemistry*, Vol. III, p. 261. Longmans, Green and Co., London (1923).
(6) NEVILLE AND OSWALD: J. Phys. Chem. **35**, 60–72 (1931).
(7) POSNJAK AND TUNELL: Am. J. Sci. [5] **18**, 1–34 (1929).
(8) STERICKER: Chem. Met. Eng. **25**, 61 (1921).
(9) WEISER: *Inorganic Colloid Chemistry*, Vol. III, p. 369. John Wiley and Sons, Inc., New York (1938).

CONVERGENCE OF TIE LINES IN TERNARY LIQUID SYSTEMS

IRVIN BACHMAN

U. S. Industrial Chemicals, Inc., Fairfield, Maryland

Received June 20, 1939

Tie lines connecting compositions of conjugate solutions on ternary liquid diagrams appear to converge to a point on the extension of the base of the triangle. Tarasenkov and Paul'sen (2) have attempted to locate this point mathematically by writing an equation for tie lines, but these authors failed to take into account the fact that compositions on a ternary chart must be translated to the rectangular system of coördinates before substituting such compositions in the equation. These authors, moreover, concluded that tie lines converge to a common point.

The mathematical method of the present article corrects the error made by Tarasenkov and Paul'sen and presents data to show that tie lines for less concentrated solutions have no common focal point.

Referring to figure 1, we observe that any point, such as P_1, representing a ternary mixture of components A, B, and C, may be located on a

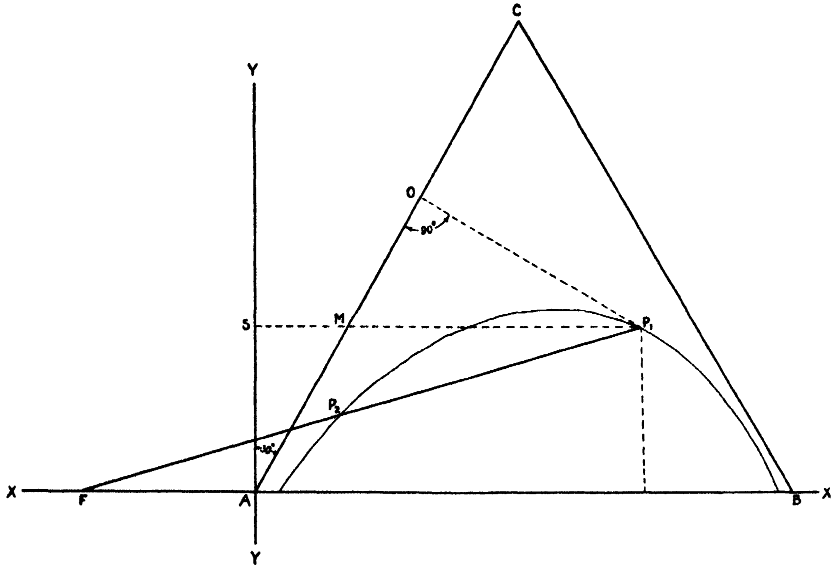

Fig. 1. Location of ternary compositions on rectangular coördinates

TABLE 1

Points of intersection of tie lines with extended base of triangle

1*		2		3		4		5		6		7		8	
Abscissa distance	Average *C*	Abscissa distance	Average *C*	Abscissa distance	Average *C*	Abscissa distance	Average *C*	Abscissa distance	Average *C*	Abscissa distance	Average *C*	Abscissa distance	Average *C*	Abscissa distance	Average *C*
3.5	14.8	14.5	24.9	1.6	16.5	0.4	23.3	3.7	2.4	19.5	3.8	95.9	22.3	5.7	5.9
7.3	28.3	14.5	29.6	4.4	25.6	1.1	28.3	8 1	9.6	24.3	10.8	95.8	33.9	5.1	6.9
6.6	32.2	15.1	33.7	4.4	31.5	0.8	38.1	10.2	16.1	29.2	15.9	105.0	44.4	9.8	17.2
6.7	33.0	14.1	36.8	5.5	34.4			13.4	35.1	31.3	17.8	112.7	49.6	9.9	20.2
9.4	33.9	13.5	37.7					13.7	37.1	33.7	22.4	104.8	55.3	9.8	20.5
6.2	33.8	11.8	37.2					14.3	41.9	33.3	30.9	117.2	58.4	11.8	25.5
								15.7	43.9	31.8	36.4			11.6	25.8
								12.4	48.4	32.5	38.0			12.1	27.2
								13.7	49.9					11.5	33.0
														11.5	34.8
														12.0	36.4
														12.0	36.5
														11.8	36.7

---

* The numbers refer to the system numbers of table 2.

system of rectangular coördinates of which the x-axis is an extension of the base of the ternary diagram and the y-axis passes through vertex A.

The ordinate of P_1, or y_1, is identical with its content of component C. The abscissa of P_1, or x_1, is given by the line SP_1. From the geometry of the figure it is evident that

$$SP_1 = SM + MP_1$$

$$= \frac{\sqrt{3}C_1}{3} + \frac{2B_1}{\sqrt{3}}$$

where C_1 and B_1 are the C and B content, respectively, of the point P_1. Consequently,

$$x_1 = \frac{(C_1 + 2B_1)}{\sqrt{3}}$$

TABLE 2

Systems investigated

SYSTEM NUMBER	TEMPERATURE	SYSTEM	REFERENCE
	°C.		
1	20	Benzene–alcohol–water	(2)
2	25	Benzene–alcohol–water	(3)
3	20	Toluene–alcohol–water	(2)
4	25	Cyclohexane–alcohol–water	(2)
5	25	Benzene–acetic acid–water	(1)
6	25	Chloroform–acetic acid–water	(5)
7	25	Acetone–chloroform–water	(1)
8	25	Benzene–alcohol–water	(4)

The general equation of a straight line passing through two points is

$$\frac{y - y_2}{x - x_2} = \frac{y_1 - y_2}{x_1 - x_2}$$

Letting $y = 0$ to obtain the intercept of the line upon the x-axis, we have

$$x(y_1 - y_2) = x_2y_1 - y_2x_1$$

If, now, we substitute in this equation the coördinates of the points P_1 and P_2 we obtain the abscissa of the point where the extended tie line crosses the x-axis. This expression reduces to

$$x_P = \frac{2(C_1B_2 - C_2B_1)}{\sqrt{3}(C_1 - C_2)}$$

The above equation has been applied to data taken from the literature for ternary liquid systems. Table 1 gives the distances thus calculated under the columns headed "abscissa distances".

In columns adjacent to the abscissa values of table 1 the corresponding values of the average concentrations of the consolute components are given (average $C = (C_1 + C_2)/2$). With increasing concentrations the value of average C approaches the per cent C at the critical point.

The abscissa distances in the upper part of table 1, corresponding to tie lines for the less concentrated solutions closer to the base of the ternary diagram, are definitely not constant. The abscissa distances in the lower part of table 1, applying to the more concentrated solutions, show less variation, yet even in this region there is considerable deviation from constancy. These findings are in line with D. B. Hand's (1) empirical equation, which holds for concentrated ternary mixtures but falls down for those mixtures very dilute with respect to either component A or component B. For several of the systems investigated a graph of abscissa distance *versus* concentration of the consolute component shows a trend of the abscissa values toward a maximum point.

REFERENCES

(1) HAND, D. B.: J. Phys. Chem. **34**, 1961 (1930).
(2) TARASENKOV, D. N., AND PAUL'SEN, I. A.: J. Gen. Chem. (U. S. S. R.) **8**, 76–82 (1938).
(3) TAYLOR, S. F.: J. Phys. Chem. **1**, 461 (1897).
(4) VARTERESSIAN, K. A., AND FENSKE, M. R.: Ind. Eng. Chem. **28**, 928 (1936).
(5) WRIGHT, C. R. A., THOMPSON, C., AND LEON, J. T.: Proc. Roy. Soc. (London) **49**, 174 (1891).

THE EFFECT OF VARIATION IN IONIC STRENGTH AND TEMPERATURE ON THE APPARENT DISSOCIATION CONSTANTS OF THIRTY SUBSTITUTED BARBITURIC ACIDS

M. E. KRAHL

The Lilly Research Laboratories, Indianapolis, Indiana, and the Marine Biological Laboratory, Woods Hole, Massachusetts

Received August 30, 1939

Although it has long been known from the work of Wood (12) that barbituric acid and certain of its mono- and di-substituted derivatives behave in aqueous solution as weak acids, little attention has been devoted to the determination of the degree of electrolytic dissociation of these substances in solutions of varying salt content and temperature. Such data are now of biochemical interest for two reasons:

First, as pointed out by Michaelis (9) for 5,5-diethylbarbituric acid, the disubstituted barbituric acids and their salts may be used as buffers to cover the range from pH 6 to pH 9, where the number of other substances available for buffers is relatively small.

Secondly, the di- and tri-substituted barbituric acids are now widely used as hypnotic agents in medicine and physiology, and as such become partially dissociated in physiological media into hydrogen ions and barbiturate anions. From the preliminary experiments of Clowes and Keltch (3) it appears that certain of the barbituric acids penetrate living cells more readily as undissociated molecules than as anions. During a more extensive investigation of the factors bearing on the penetration and anesthetic action of these substances (4), it became necessary to determine, with some accuracy, to what degree each of a large number of barbituric acids would dissociate when dissolved in sea water. The present study was undertaken in an effort to provide data to meet this need and, at the same time, to provide data and equations from which the approximate degree of ionization of any of the commonly used barbituric acids could be calculated for solutions of any salt content and temperature within the biological range of interest.

THEORETICAL

In aqueous solution at constant temperature the dissociation of a monobasic acid, HA, may be expressed as the reaction

$$\mathrm{HA(aq.)} \rightleftarrows \mathrm{H}^+ + \mathrm{A}^- \qquad (1)$$

for which the equilibrium expression is the equation

$$\mathrm{p}K' = \mathrm{pH} - \log \frac{[\mathrm{A}^-]}{[\mathrm{HA}]} \qquad (2)$$

In equation 2, $[\mathrm{A}^-]$ and $[\mathrm{HA}]$ are the molar concentrations of anion and undissociated acid molecule respectively; pH is equal[1] to $\log \frac{1}{a_{\mathrm{H}^+}}$; $\mathrm{p}K'$, the negative logarithm of the apparent dissociation constant, is related to the true thermodynamic dissociation constant, K, by the equation

$$\mathrm{p}K' = \mathrm{p}K + \log \frac{\gamma_{\mathrm{A}^-}}{\gamma_{\mathrm{HA}}} \qquad (3)$$

For salt concentrations and temperatures in the physiological range it is assumed that γ_{HA}, the activity coefficient of the undissociated molecules, may be taken as unity. Under the same conditions γ_{A^-}, the activity coefficient of the monovalent anion, is dependent on the ion content and temperature of the solution, according to the modified Debye-Hückel (5) equation:

---

[1] pH, rather than paH, is used here to represent $\log \frac{1}{a_{\mathrm{H}^+}}$ for the reasons discussed by Clark (2, footnote pp. 479–81).

$$-\log \gamma_{A^-} = \frac{A\sqrt{\mu}}{1 + Ba\sqrt{\mu}} \qquad (4)$$

In equation 4, A and B are independent of the acid used and are dependent on the dielectric constant and the temperature of the solution; a is an empirical constant which depends on the nature of the anion.[2] The ionic strength, μ, of a solution is defined as one-half the sum of the products of the concentration of each ion present in the solution multiplied by the square of its valence.[3]

According to Lewis and Randall (7, page 294), the thermodynamic dissociation constant, K, for reaction 1 is related to the standard free energy change, ΔF^0, and the absolute temperature, T, by the equation:

$$\Delta F^0 = -RT \ln K \qquad (5)$$

where R is the gas constant having a value of 1.9864 calories per degree. Equation 5 may be put into the following form, which is more favorable for use here:

$$\Delta F^0 = 2.3RT\,\mathrm{p}K \qquad (6)$$

ΔF^0 varies with temperature (7, page 172), according to the equation

$$\frac{\mathrm{d}(\Delta F^0)}{\mathrm{d}T} = -\Delta S^0 \qquad (7)$$

In equation 7, ΔS^0 is the entropy change for reaction 1 under the same standard conditions as those for which K is determined. The numerical value of ΔS^0 is the slope of the line obtained by plotting experimental values of ΔF^0 against T. For the purpose of the present discussion ΔS^0 may be regarded as independent of the salt content of the solution.

---

[2] Values of A and B, along with a discussion of the significance of a, are given by Clark (2, p. 500).

[3] Both γ and μ were originally defined for molal concentrations, which are expressed in terms of grams of solute per 1000 grams of solvent. The highest concentration of total salt (sodium chloride) used in the present experiments was 2 molar. From the specific gravity of a 2 molar sodium chloride solution, it may be calculated that at this concentration of sodium chloride the substitution of molar for molal concentrations results in a value for $\sqrt{\mu}$ which is about 3 per cent too high. This error, however, affects the value of $-\log \gamma_{A^-}$ by less than 0.01 unit, and may be disregarded for the purposes of the present paper.

By integration of equation 7 and combination with equations 3 and 6, the following equation may be derived:

$$\mathrm{p}K'_T = \frac{\Delta F^0_{T_0} - \Delta S^0(T - T_0)}{2.3RT} + \log \gamma_{A^-} \qquad (8)$$

This means that, for a given acid, the apparent dissociation constant, K'_T at the temperature T, for any ionic strength can be calculated after the entropy change, ΔS^0, the standard free energy change, $\Delta F^0_{T_0}$ at any temperature T_0, and the activity coefficient of the anion, γ_{A^-}, at the temperature T, are known.[4]

EXPERIMENTAL METHODS AND MATERIALS

The following cell was used for the electrometric measurements:

$$\begin{array}{cccc} & \text{barbiturate} & & \\ \text{Hg : HgCl, KCl (satd.) :} & \text{solution} & \text{: glass :} & \text{HCl(0.1}N\text{) : Pt} \\ & \text{or} & & \text{quinhydrone} \\ & \text{standard} & & \\ & \text{phthalate} & & \end{array}$$

All components were in thermal equilibrium at each of the temperatures stated. The glass electrode system was standardized at 25°C. with a 0.05 *M* potassium hydrogen phthalate buffer to which a pH value of 4.00 was assigned (8). The glass electrode system used was equipped with a temperature compensator to take account of the changes in potential of the quinhydrone and calomel half-cells with temperature. Potentiometric readings were made to ± 0.01 pH unit with an overall error not greater than ± 0.03 pH unit.

The sodium salts of the barbituric acids were dried over calcium chloride or concentrated sulfuric acid. For each experiment, the desired barbiturate sodium salt was dissolved in freshly distilled water of low carbon dioxide content to give a stock solution of twice the final strength to be used. To a 5-ml. aliquot of this stock solution the volume of 0.02 *N* hydrochloric acid required to give the desired final $\frac{[A^-]}{[HA]}$ ratio and the volume of 5 M sodium chloride required to give the desired final salt concentration were added. The total volume was in every case made up to 10 ml. The pH values of the resulting solutions were then immediately determined. The corresponding pK' values were then calculated from equation 2.

---

[4] Harned and Embree (6) and Shedlovsky and MacInnes (11) have pointed out that the dissociation constants of many monobasic acids have a maximum value at some one temperature. As shown in the experimental part of this paper, the temperature range employed for the present measurements is apparently so far removed from the optimum temperature for the barbituric acids that the presence of any such optimum may be disregarded.

The method of treatment used in the present paper assumes that ΔH for equation 1 is independent of temperature. Although adequate for the present purpose, this assumption is only a first approximation and may be in part responsible for the fact that the ΔS values here obtained are lower than those summarized for other monobasic acids by Pitzer (10).

For each substituted barbituric acid, pK' values were determined at $\frac{[A^-]}{[HA]}$ ratios of 3, 1, and 0.33, five independent potentiometric readings being made for each solution. In every case, the pK' value obtained with any given acid at any given $\frac{[A^-]}{[HA]}$ ratio agreed, within ± 0.03 unit, with the arithmetic mean of the three pK' values.

In this paper the substituted barbituric acids are named according to the convention employed in *Chemical Abstracts*.[5] For example, according to this system, the following compound:

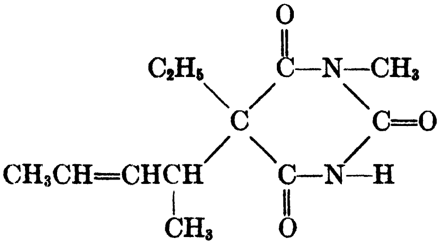

would be named 5-ethyl-1-methyl-5-(α-methylbutenyl-2)barbituric acid.

The substituted barbituric acids having hydrogens attached to both nitrogens of the ring behave as monobasic acids in the physiological pH range, the ionization of the second hydrogen not being significant below pH 10.

RESULTS

Effect of variation in ionic strength

The pK' values, as experimentally determined at 25°C., for one trisubstituted and twenty-nine disubstituted barbituric acids are given in table 1. For each acid, measurements were made at six levels of ionic strength. The disubstituted acids are listed in order as derivatives of

---

[5] Many of the compounds listed in table 1 are sold under their trade-marked names, which can be readily found in the formula index of *Chemical Abstracts* by the use of the empirical formulas of table 1.

Seventeen of the barbituric acids used in the present investigation were supplied through the kindness of Mr. H. A. Shonle, of this laboratory. The other acids were purchased in the open market. All of the acids used had been purified by recrystallization to constant melting point. The author wishes to thank Miss A. K. Keltch for her help in the purification of a number of these compounds.

TABLE 1

pK' values of substituted barbituric acids at 25°C. for solutions of varying ionic strength

The total molar barbiturate concentration for each acid is equivalent to the lowest value of μ given for that acid

BARBITURIC ACID	μ	pK'
5,5-Diethylbarbituric acid, $C_8H_{12}N_2O_3$, M. W. = 184	0.002	7.90
	0.04	7.82
	0.16	7.74
	0.70	7.62
	1.20	7.59
	2.00	7.56
5-Ethyl-5-isopropylbarbituric acid, $C_9H_{14}N_2O_3$, M. W. = 198	0.002	7.98
	0.04	7.92
	0.16	7.86
	0.70	7.77
	1.20	7.70
	2.00	7.65
5-Ethyl-5-butylbarbituric acid, $C_{10}H_{16}N_2O_3$, M. W. = 212	0.002	7.92
	0.04	7.82
	0.16	7.74
	0.70	7.63
	1.20	7.59
	2.00	7.55
5-Amyl-5-ethylbarbituric acid, $C_{11}H_{18}N_2O_3$, M. W. = 226	0.001	7.93
	0.04	7.86
	0.16	7.79
	0.70	7.69
	1.20	7.63
	2.00	7.60
5-Isoamyl-5-ethylbarbituric acid, $C_{11}H_{18}N_2O_3$, M. W. = 226	0.002	7.92
	0.04	7.83
	0.16	7.75
	0.70	7.65
	1.20	7.59
	2.00	7.53
5-Ethyl-5-(α-methylbutyl)barbituric acid, $C_{11}H_{18}N_2O_3$, M. W. = 226	0.002	8.07
	0.04	8.01
	0.16	7.96
	0.70	7.88
	1.20	7.83
	2.00	7.80
5-Ethyl-5-(α-ethylpropyl)barbituric acid, $C_{11}H_{18}N_2O_3$, M. W. = 226	0.001	8.00
	0.04	7.90
	0.16	7.86
	0.70	7.75
	1.20	7.68
	2.00	7.65

TABLE 1—*Continued*

BARBITURIC ACID	μ	pK'
5-Ethyl-5-(α-methylbutenyl-2)barbituric acid, $C_{11}H_{16}N_2O_3$, M. W. = 224	0.002	7.99
	0.04	7.90
	0.16	7.83
	0.70	7.74
	1.20	7.68
	2.00	7.65
5-Cyclopentyl-5-ethylbarbituric acid, $C_{11}H_{16}N_2O_3$, M. W. = 224	0.001	8.08
	0.04	7.99
	0.16	7.91
	0.70	7.85
	1.20	7.80
	2.00	7.77
5-Ethyl-5-piperidylbarbituric acid, $C_{11}H_{17}N_3O_3$, M. W. = 239	0.001	7.71
	0.04	7.61
	0.16	7.51
	0.70	7.43
	1.20	7.35
	2.00	7.30
5-Ethyl-5-hexylbarbituric acid, $C_{12}H_{20}N_2O_3$, M. W. = 240	0.001	7.78
	0.04	7.71
	0.16	7.62
	0.70	7.53
	1.20	7.50
	2.00	7.46
5-(α,γ-Dimethylbutyl)-5-ethylbarbituric acid, $C_{12}H_{20}N_2O_3$, M. W. = 240	0.002	8.14
	0.04	8.04
	0.16	7.96
	0.70	7.85
	1.20	7.80
	2.00	7.77
5-Ethyl-5-phenylbarbituric acid, $C_{12}H_{12}N_2O_3$, M. W. = 232	0.002	7.40
	0.04	7.32
	0.16	7.24
	0.70	7.14
	1.20	7.09
	2.00	7.05
5-Ethyl-5-cyclohexenylbarbituric acid, $C_{12}H_{16}N_2O_3$, M. W. = 236	0.002	7.49
	0.04	7.41
	0.16	7.36
	0.70	7.23
	1.20	7.19
	2.00	7.15

TABLE 1—*Continued*

BARBITURIC ACID	μ	pK'
5-Ethyl-5-(β-ethylhexyl)barbituric acid, $C_{14}H_{24}N_2O_3$, M. W. = 268	0.001	7.87
	0.04	7.79
	0.16	7.70
	0.70	7.61
5-Ethyl-5-(β-phenylethyl)barbituric acid, $C_{14}H_{16}N_2O_3$, M. W. = 260	0.001	7.91
	0.04	7.81
	0.16	7.70
	0.70	7.61
	1.20	7.54
	2.00	7.50
5,5-Diallylbarbituric acid, $C_{10}H_{12}N_2O_3$, M. W. = 208	0.002	7.78
	0.04	7.69
	0.16	7.61
	0.70	7.49
	1.20	7.45
	2.00	7.41
5-Allyl-5-isopropylbarbituric acid, $C_{10}H_{14}N_2O_3$, M. W. = 210	0.002	7.90
	0.04	7.80
	0.16	7.72
	0.70	7.60
	1.20	7.55
	2.00	7.51
5-Allyl-5-isobutylbarbituric acid, $C_{11}H_{16}N_2O_3$, M. W. = 224	0.002	7.66
	0.04	7.60
	0.16	7.50
	0.70	7.41
	1.20	7.40
	2.00	7.37
5-Allyl-5-(α-methylbutyl)barbituric acid, $C_{12}H_{18}N_2O_3$, M. W. = 238	0.002	8.06
	0.04	7.97
	0.16	7.90
	0.70	7.78
	1.20	7.72
	2.00	7.67
5-Allyl-5-benzylbarbituric acid, $C_{14}H_{14}N_2O_3$, M. W. = 258	0.002	7.20
	0.04	7.12
	0.16	7.05
	0.70	6.94
	1.20	6.88
	2.00	6.85

TABLE 1—*Continued*

BARBITURIC ACID	μ	pK'
5-(β-Methylallyl)-5-propylbarbituric acid, $C_{11}H_{16}N_2O_3$, M. W. = 224	0.002	7.81
	0.04	7.72
	0.16	7.61
	0.70	7.52
	1.20	7.47
	2.00	7.41
5-Isobutyl-5-(β-methylallyl)barbituric acid, $C_{12}H_{18}N_2O_3$, M. W. = 238	0.002	7.79
	0.04	7.70
	0.16	7.61
	0.70	7.49
	1.20	7.42
	2.00	7.38
5-(α-Methylbutyl)-5-(β-methylallyl)barbituric acid, $C_{13}H_{20}N_2O_3$, M. W. = 252	0.002	7.97
	0.04	7.88
	0.16	7.78
	0.70	7.67
	1.20	7.59
	2.00	7.58
5-(β-Bromoallyl)-5-isopropylbarbituric acid, $C_{10}H_{13}BrN_2O_3$, M. W. = 289	0.002	7.72
	0.04	7.62
	0.16	7.54
	0.70	7.46
	1.20	7.41
	2.00	7.39
5-(β-Bromoallyl)-5-(α-methylpropyl)barbituric acid, $C_{11}H_{15}BrN_2O_3$, M. W. = 303	0.002	7.71
	0.04	7.62
	0.16	7.55
	0.70	7.47
	1.20	7.42
	2.00	7.39
5-(β-Bromoallyl)-5-(α-ethylpropyl)barbituric acid, $C_{12}H_{17}BrN_2O_3$, M. W. = 317	0.002	7.70
	0.04	7.60
	0.16	7.53
	0.70	7.45
	1.20	7.40
	2.00	7.37
5-Benzyl-5-isopropylbarbituric acid, $C_{14}H_{16}N_2O_3$, M. W. = 260	0.002	7.99
	0.04	7.89
	0.16	7.78
	0.70	7.68
	1.20	7.64
	2.00	7.61

TABLE 1—*Concluded*

BARBITURIC ACID	μ	pK'
5-Benzyl-5-butylbarbituric acid, $C_{15}H_{18}N_2O_3$, M. W. = 274	0.002	7.89
	0.04	7.80
	0.16	7.73
	0.70	7.62
	1.20	7.56
	2.00	7.52
5-Cyclohexenyl-1,5-dimethylbarbituric acid, $C_{12}H_{16}N_2O_3$, M. W. = 236	0.002	8.32
	0.04	8.25
	0.16	8.18
	0.70	8.10
	1.20	8.05
	2.00	8.01

TABLE 2

pK and ΔF^0 values at 25°C. for substituted barbituric acids as calculated from the data of table 1 according to equations 3, 4, and 6

BARBITURIC ACID	a	pK	$K \times 10^8$	ΔF^0
	cm. × 10^8			*calories per mole*
5-Allyl-5-benzyl-	2.0	7.21	6.2	9,829
5-Ethyl-5-phenyl-	2.0	7.41	3.9	10,102
5-Ethyl-5-cyclohexenyl-	2.3	7.50	3.1	10,224
5-Allyl-5-isobutyl-	2.7	7.68	2.1	10,470
5-(β-Bromoallyl)-5-(α-ethylpropyl)-	2.5	7.70	2.0	10,497
5-(β-Bromoallyl)-5-(α-methylpropyl)-	2.5	7.71	1.9	10,510
5-Ethyl-5-piperidyl-	1.5	7.71	1.9	10,510
5-(β-Bromoallyl)-5-isopropyl-	2.3	7.72	1.9	10,524
5-Ethyl-5-hexyl-	2.5	7.79	1.6	10,620
5-Isobutyl-5-(β-methylallyl)-	1.5	7.79	1.6	10,620
5,5-Diallyl-	1.7	7.79	1.6	10,620
5-(β-Methylallyl)-5-propyl-	1.5	7.82	1.5	10,660
5-Ethyl-5-(β-ethylhexyl)-	1.7	7.89	1.3	10,756
5-Ethyl-5-(β-phenylethyl)-	1.5	7.90	1.3	10,770
5,5-Diethyl-	2.0	7.91	1.2	10,784
5-Allyl-5-isopropyl-	1.5	7.91	1.2	10,784
5-Benzyl-5-butyl-	1.7	7.91	1.2	10,784
5-Ethyl-5-butyl-	2.0	7.92	1.2	10,797
5-Isoamyl-5-ethyl-	1.5	7.94	1.2	10,824
5-Amyl-5-ethyl-	2.3	7.95	1.1	10,838
5-(α-Methylbutyl)-5-(β-methylallyl)-	1.5	7.98	1.0	10,878
5-Benzyl-5-isopropyl-	1.5	7.99	1.0	10,892
5-Ethyl-5-(α-methylbutenyl-2)-	2.0	8.00	1.0	10,906
5-Ethyl-5-isopropyl-	2.5	8.01	1.0	10,920
5-Ethyl-5-(α-ethylpropyl)-	2.0	8.01	1.0	10,920
5-Allyl-5-(α-methylbutyl)-	1.5	8.08	0.8	11,015
5-Cyclopentyl-5-ethyl-	2.5	8.09	0.8	11,029
5-Ethyl-5-(α-methylbutyl)-	2.7	8.11	0.8	11,056
5-(α, γ-Dimethylbutyl)-5-ethyl-	1.7	8.14	0.7	11,097
5-Cyclohexenyl-1,5-dimethyl-	2.5	8.34	0.5	11,370

5-ethyl-, 5-allyl-, 5-(β-methylallyl)-, 5-(β-bromoallyl)-, and 5-benzylbarbituric acids.

From the pK' values presented in table 1 the pK value for each substituted barbituric acid was calculated from equations 3 and 4. By empirical trial that value of a which resulted in the best agreement between the pK values obtained from the pK' values at various ionic strengths was chosen. The pK values so obtained are listed in table 2 in the order of increasing pK.

Having established a value of pK for each substituted barbituric acid, corrected pK' values for all ionic strengths up to $\mu = 2.00$ were calculated from equations 3 and 4. The agreement between the measured and corrected pK' values for four representative barbituric acids is illustrated by figure 1. A similar degree of agreement between observed and calculated values was found for the other twenty-six acids used. The circles, which have a size corresponding to an experimental error of ± 0.02 pH unit, represent the experimentally determined pK' values. Within the error of the present experimental methods, the variation of pK' with ionic strength for each of the thirty substituted barbituric acids listed in table 2 is correctly described by equations 3 and 4.

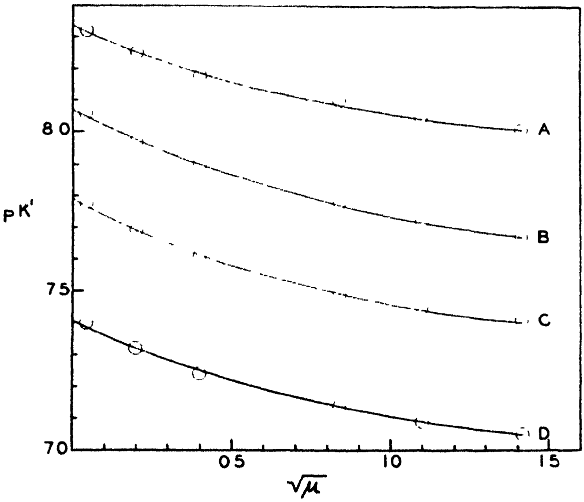

FIG. 1. Observed and calculated pK' values at 25°C. A, 5-cyclohexenyl-1,5-dimethylbarbituric acid; B, 5-allyl-5-(α-methylbutyl)barbituric acid; C, 5,5-diallylbarbituric acid; D, 5-ethyl-5-phenylbarbituric acid. The circles represent the experimental values; the solid curves the values calculated from equations 3 and 4.

Effect of variations in temperature

The pK' values for 5-isoamyl-5-ethylbarbituric acid were determined at six temperatures and three levels of ionic strength. From these pK'

values, the value of pK at each temperature was calculated by the method described in the previous section. The value of the standard free energy change, ΔF^0, at each temperature was then calculated according to equation 6. The results are given in table 3.

It was found that the increase of ΔF^0 with temperature was relatively small, corresponding to an entropy change, ΔS^0, of −3.1 calories per degree.[4]

TABLE 3

pK′ and pK values for 5-isoamyl-5-ethylbarbituric acid at temperatures from 15°C. to 40°C. in solutions of varying ionic strength

All measurements were made with a total barbiturate concentration of 0.002 M and an anion/molecule ratio of 1

t	T	μ	MEASURED pK'	CALCULATED $-\log \gamma_{A^-}$	pK		ΔF^0
°C.	*°A.*						*calories per mole*
15	288	0.002	8.17	0.02	8.19	8.19	10,790
		0.16	8.00	0.17	8.17		
		0.70	7.91	0.29	8.20		
20	293	0.002	8.04	0.02	8.06	8.06	10,803
		0.16	7.87	0.17	8.04		
		0.70	7.78	0.30	8.08		
25	298	0.002	7.92	0.02	7.94	7.94	10,824
		0.16	7.75	0.17	7.92		
		0.70	7.65	0.30	7.95		
30	303	0.002	7.80	0.02	7.82	7.82	10,839
		0.16	7.64	0.17	7.81		
		0.70	7.52	0.30	7.82		
35	308	0.002	7.69	0.02	7.71	7.70	10,849
		0.16	7.52	0.17	7.69		
		0.70	7.40	0.31	7.71		
40	313	0.002	7.58	0.02	7.60	7.59	10,868
		0.16	7.40	0.17	7.57		
		0.70	7.28	0.31	7.59		

After substitution of this value of ΔS^0, equation 8 becomes, for 5-isoamyl-5-ethylbarbituric acid:

$$\mathrm{p}K'_T = \frac{\Delta F^0_{T_0} + 3.1(T - T_0)}{2.3RT} + \log \gamma_{A^-} \qquad (9)$$

Corrected pK' values for 5-isoamyl-5-ethylbarbituric acid at all temperatures from 15°C. to 40°C. and three levels of ionic strength were then calculated from equation 9 and plotted in figure 2, using the ΔF^0 value for 25°C. The circles, which have a diameter corresponding to an experimental error of ±0.02 pH unit, represent the experimentally determined pK' values. From the agreement between the experimental points and the calculated curve it may be concluded that the variation in pK' with temperature and ionic strength for 5-isoamyl-5-ethylbarbituric acid is correctly described by equation 9, within the limits of error of the present experimental methods.

From a consideration of the magnitude of ΔS^0 for 5-isoamyl-5-ethylbarbituric acid, it appears that equation 9 may possibly be used, without further experiment, for the approximate calculation of pK' values for all

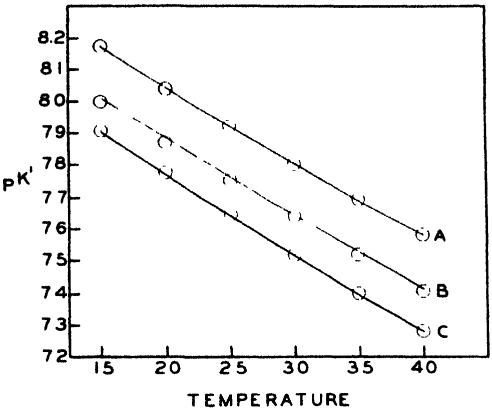

FIG. 2. Observed and calculated pK' values at temperatures from 15°C. to 40°C. for 5-isoamyl-5-ethylbarbituric acid. The circles represent the experimental values; the solid curves the values calculated from equation 9. For curve A, $\mu = 0.002$; for curve B, $\mu = 0.16$; for curve C, $\mu = 0.70$.

of the substituted barbituric acids listed in table 2. The reasons for this statement are as follows:

First, if the term

$$-\frac{\Delta S^0(T - T_0)}{2.3RT}$$

in equation 8 is neglected in the calculation of corrected pK' values for 5-isoamyl-5-ethylbarbituric acid, it is found that, with $\mu = 0.7$, the values of pK' for 15°C. and 40°C. are 7.93 and 7.25, respectively, as compared with the corrected values of 7.90 and 7.28 which were obtained with $\Delta S^0 = -3.1$. Thus, in the range of temperature and ionic strength of interest to biologists, the maximum error introduced by setting $\Delta S^0 = 0$ is only +0.03 pK' unit at 15°C. and −0.03 pK' unit at 40°C.

Secondly, it is likely that the differences between the ΔS^0 values for the thirty closely related acids listed in table 2 are small. The variation from the mean value of ΔS^0 is almost certainly less than ±100 per cent. Since a variation of ±100 per cent in the value of ΔS^0 for 5-isoamyl-5-ethylbarbituric acid produces, as shown above, a maximum error of only ±0.03 pK' unit over a 25°C. temperature range, it may reasonably be assumed that the use of equation 9 for all of the substituted barbituric acids listed in table 2 will yield pK' values, for any temperature and ionic strength in the physiological range, which are very close to the true values which would be found by experiment.

To facilitate the calculation of pK' values by this means, the ΔF^0 values at 25°C. for thirty substituted barbituric acids are listed in the last column of table 2. The values are given to five figures, although only three figures are significant, with the understanding that the calculated pK' values are to be rounded off to the nearest 0.01 unit; the data suggest that the difference between such calculated values and the experimental values will be usually not larger than ±0.03 unit and, in any case, not larger than ±0.05 unit.

Comparison of previously determined pK′ values with pK′ values in this paper

Of the barbituric acids employed for the present measurements, 5,5-diethylbarbituric acid is the only one for which pK' values have been previously obtained.

For this substance, Wood (12) in 1906, from conductivity measurements, obtained a pK' at 25°C. of 7.43 with $\mu = 0.16$. The value calculated from equation 9 is 7.77. Michaelis (9), with the hydrogen electrode, obtained a pK' of 7.82 at 25°C. with $\mu = 0.07$. The value calculated from equation 9 is 7.82. Britton and Robinson (1), also with the hydrogen electrode, obtained pK' values from 7.92 to 7.98 at 18°C. with $\mu = 0.04$. The value calculated from equation 9 is 7.98. This close agreement between observed and calculated pK' values for 5,5-diethylbarbituric acid serves as an independent confirmation of the validity of equation 9.

SUMMARY

1. By means of glass electrode pH measurements, the effects of variation in sodium chloride concentration on the pK' values of thirty substituted barbituric acids have been determined at 25°C. With concentrations of sodium chloride up to 2 molar, the relation between pK' and the ionic strength is approximately expressed by one form of the Debye-Hückel equation. By means of this equation, pK values at 25°C. have been calculated for all of the acids employed.

2. The effects of variation in temperature on the pK' and pK values of 5-isoamyl-5-ethylbarbituric acid have been determined at temperatures between 15°C. and 40°C., and the values of the standard free energy change, ΔF^0, have been calculated. For this acid in this temperature range the relation between ΔF^0 and temperature is expressed by the usual

thermodynamic equations, in which ΔS^0, the standard entropy change, has a value of -3.1 calories per degree.

3. It has been shown that, by means of the experimental data here presented and an equation derived for this purpose, the approximate pK' values of the thirty substituted barbituric acids can be calculated for any ionic strength and any temperature within the physiological range.

REFERENCES

(1) Britton, H. T. S., and Robinson, R. A.: J. Chem. Soc. **1931,** 1456.
(2) Clark, W. M.: *The Determination of Hydrogen Ions,* 3rd edition. The Williams & Wilkins Company, Baltimore (1928).
(3) Clowes, G. H. A., and Keltch, A. K.: Proc. Soc. Exptl. Biol. Med. **29,** 312 (1931).
(4) Clowes, G. H. A., Keltch, A. K., and Krahl, M. E.: J. Pharmacol., March, 1940, in press.
(5) Debye, P., and Hückel, E.: Physik. Z. **24,** 185 (1923).
(6) Harned, H. S., and Embree, N. D.: J. Am. Chem. Soc. **56,** 1050 (1934).
(7) Lewis, G. N., and Randall, M.: *Thermodynamics and the Free Energy of Chemical Substances.* McGraw-Hill Book Company, Inc., New York (1923).
(8) McInnes, D. A., Belcher, D., and Shedlovsky, T.: J. Am. Chem. Soc. **60,** 1094 (1938).
(9) Michaelis, L.: J. Biol. Chem. **87,** 33 (1930).
(10) Pitzer, K. S.: J. Am. Chem. Soc. **59,** 2365 (1937).
(11) Shedlovsky, T., and MacInnes, D. A.: J. Am. Chem. Soc. **57,** 1705 (1935).
(12) Wood, J. K.: J. Chem. Soc. **89,** 1831 (1906).

ON THE THEORY OF GALVANIC CELLS SUBJECT TO FIELDS OF FORCE. I

The Gravitational Field[1]

F. O. KOENIG and S. W. GRINNELL[2]

Department of Chemistry, Stanford University, California

Received June 27, 1939

I. INTRODUCTION

Objects

Our object in this paper is to obtain in general and exact form the thermodynamic laws of galvanic cells subject to external gravitational fields. In attaining this object we shall make use of a thermodynamic theorem deduced recently by one of us (8) and called the "condition for quasi-reversible conduction" or "qrc. condition." We shall accordingly use the terminology and mathematical notation given previously (8) throughout the present paper. This paper is, however, not only a sequel to the earlier paper (8) but is also intended as a preparation for a later paper reporting experiments on "gravity cells" that have been in progress at Stanford University for a number of years.

---

[1] The contents of this paper are taken largely from the dissertation submitted by S. W. Grinnell to the Faculty of Stanford University in partial fulfillment of the requirements for the degree of Doctor of Philosophy, 1938.

[2] Shell Research Fellow, Stanford University, 1937–38.

Relation to previous work

Effects of gravity upon E.M.F. have been previously investigated both experimentally and theoretically by Des Coudres (1, 3) and by Tolman (11). A brief review of the experimental work of these authors has recently been given by MacInnes (9). The present study is an attempt to generalize and purify the theoretical deductions of Des Coudres and Tolman. Details concerning the work of these authors in relation to the present study are given in section IV below.

II. THE GENERAL CASE

Description of the cell

We shall consider a cell in which both the gravitational potential φ and the mole fractions N_i may vary throughout the solution in any way whatever compatible with instantaneous fulfillment of (*i*) the conditions of hydrostatic and thermal equilibrium:

$$\text{grad}\, P = -\rho\, \text{grad}\, \varphi \tag{1}$$

$$\text{grad}\, T = 0 \tag{2}$$

and (*ii*) the conditions of electrochemical equilibrium between the electrodes α, α' and the adjacent layers of solution β, β' (*cf.* 8, equations 12, 15):

$$\sum_r \nu_r \mu_r^{\beta} = \sum_q \nu_q \mu_q^{\alpha} + \mu_{\text{El}^-}^{\alpha} \tag{3}$$

$$\sum_{r'} \nu_{r'} \mu_{r'}^{\beta'} = \sum_{q'} \nu_{q'} \mu_{q'}^{\alpha'} + \mu_{\text{El}^-}^{\alpha'} \tag{4}$$

We shall furthermore, as in reference 8, assume electrodes and solution to consist of mutually insoluble materials. Finally we shall suppose that the electrodes are relatively thin and so arranged that φ and therefore P may without appreciable error be regarded as constant throughout each electrode. This allows us to write without appreciable error

$$\varphi^{\alpha} = \varphi^{\beta} = \bar{\varphi} \tag{5}$$

$$\varphi^{\alpha'} = \varphi^{\beta'} = \bar{\varphi}' \tag{6}$$

$$P^{\alpha} = P^{\beta} = \bar{P} \tag{7}$$

$$P^{\alpha'} = P^{\beta'} = \bar{P}' \tag{8}$$

Formulae for the potentials of the components in a gravitational field

For the purposes in hand we need the following general formulae: For the potentials μ_{el} and μ_{nt} of the electrolyte and neutral components, respectively, of a subphase in a gravitational field it is true that

$$\mu_{el} = \tau_{el} + M_{el}\varphi \tag{9}$$

$$\mu_{nt} = \tau_{nt} + M_{nt}\varphi \tag{10}$$

where τ_{el}, τ_{nt} are functions of P, T, and composition independent of φ, and M_{el}, M_{nt} are the molar weights (first pointed out by Gibbs (4); for a simple proof see reference 7). If, as will be assumed throughout, the electrolyte components in a given subphase are at each instant in dissociative equilibrium with the charged components, it is evidently always correct to write for the potential of any *charged or neutral* component i

$$\mu_i = \tau_i + M_i\varphi + z_iF\psi \tag{11}$$

where τ_i is a function of P, T, and composition independent of φ, and ψ is a function of the electrochemical state[3] of the subphase called the electric potential. We note that for neutral components the term in ψ disappears because z_i is zero. It is often convenient to expand τ_i in the form

$$\tau_i = \tau_i^0 + RT \log N_i + RT \log f_i \tag{12}$$

where τ_i^0 is a function only of P and T, N_i is the mole fraction of i, and f_i is a function of P, T, and composition called the activity coefficient. The potential μ_i may then be written as

$$\mu_i = \tau_i^0 + RT \log N_i + RT \log f_i + M_i\varphi + z_iF\psi \tag{13}$$

The function ψ is thermodynamically indeterminate and so are, for charged components, the functions τ_i and f_i. From equations 11 and 13 the following theorems, needed later, are readily evident. If λ_i are a set of scalars such that

$$\sum_i z_i\lambda_i = 0 \tag{14}$$

then, although for such of the components i as are charged the μ_i are functions of the *electrochemical* state, it is nevertheless true that

$$\sum_i \lambda_i\mu_i = \text{a function of the } \textit{chemical} \text{ state and the } \lambda_i \tag{15}$$

---

[3] For the exact definition of "electrochemical state" and "chemical state" in the sense used in this paper, see reference 8, equations 7, 8.

Furthermore, although for such of the components i as are charged the τ_i and f_i are thermodynamically *indeterminate* functions of P, T, and composition, it is nevertheless true that

$$\sum_i \lambda_i \tau_i = \text{a thermodynamically } \textit{determinate} \text{ function of } P,\ T, \text{ and composition and the } \lambda_i \tag{16}$$

$$\sum_i \lambda_i \log f_i = \text{a thermodynamically } \textit{determinate} \text{ function of } P,\ T, \text{ and composition and the } \lambda_i \tag{17}$$

Equations 11 to 17 are the obvious extensions to the case of systems in a gravitational field of the considerations of Guggenheim (5) concerning electrochemical potentials and the electric potential of a phase interior.

Calculation of the E.M.F. *as a function of chemical state and configuration*

The E.M.F. may now be calculated by the same method as that leading to equations 106 and 109 in reference 8. The E.M.F. is always given by

$$E^{\alpha\alpha'} = \frac{1}{F}\left(\mu^{\alpha'}_{\mathrm{El}^-} - \mu^{\alpha}_{\mathrm{El}^-}\right) \tag{18}$$

By virtue of the equilibrium conditions, equations 3 and 4, this becomes

$$E^{\alpha\alpha'} = \frac{1}{F}\left[\sum_q \nu_q \mu^{\alpha}_q - \sum_{q'} \nu_{q'} \mu^{\alpha'}_{q'} + \sum_{r'} \nu_{r'} \mu^{\beta'}_{r'} - \sum_r \nu_r \mu^{\beta}_r\right] \tag{19}$$

Recalling from reference 8 that the subscripts q, q' refer to electrolyte and neutral components, we note that the sums $\sum_q \nu_q \mu^{\alpha}_q$ and $\sum_{q'} \nu_{q'} \mu^{\alpha'}_{q'}$ are functions of the *chemical* states at α and α', respectively. The subscripts r, r', however, refer to charged and neutral components with (*cf.* reference 8, equations 10, 14)

$$\sum_r z_r \nu_r = -1 \tag{20}$$

$$\sum_{r'} z_{r'} \nu_{r'} = -1 \tag{21}$$

and therefore the sums $\sum_r \nu_r \mu^{\beta}_r$ and $\sum_{r'} \nu_{r'} \mu^{\beta'}_{r'}$ are functions of the *electrochemical* states at β and β', respectively. We can nevertheless express the *difference*

$$\sum_{r'} \nu_{r'} \mu^{\beta'}_{r'} - \sum_r \nu_r \mu^{\beta}_r \tag{22}$$

as a function of the *chemical* state at every point of the solution, and of the configuration. For this purpose we have recourse to reference 8, equation 104

$$\sum_{r'} \nu_{r'} \mu^{\beta'}_{r'} = \sum_{r'} \nu_{r'} \mu^{\beta}_{r'} + \int_V \vec{J} \cdot \sum_{r'} \nu_{r'} \operatorname{grad} \mu_{r'} \, \delta V \tag{23}$$

the deduction of which by means of Gauss's theorem and the definition of the specific electrolytic current vector $\vec{J}$ (8, equations 36 to 38) applies unchanged to the present case. We obtain for the difference 22

$$\sum_{r'} \nu_{r'} \mu_{r'}^{\beta'} - \sum_{r} \nu_r \mu_r^{\beta} = \sum_{r'} \nu_{r'} \mu_{r'}^{\beta} - \sum_{r} \nu_r \mu_r^{\beta} + \int_V \vec{J} \cdot \sum_{r'} \nu_{r'} \operatorname{grad} \mu_{r'} \delta V \tag{24}$$

Now from equations 20, 21 we have

$$\sum_{r'} z_{r'} \nu_{r'} - \sum_{r} z_r \nu_r = 0 \tag{25}$$

and therefore equations 14 and 15 show that the difference

$$\sum_{r'} \nu_{r'} \mu_{r'}^{\beta} - \sum_{r} \nu_r \mu_r^{\beta} \tag{26}$$

which occurs on the right side of equation 24, is a function of the chemical state at β. It remains to show that the integral

$$\int_V \vec{J} \cdot \sum_{r'} \nu_{r'} \operatorname{grad} \mu_{r'} \delta V \tag{27}$$

is a function of chemical state and configuration. For this purpose we introduce the qrc. condition in the form of equation 73, in reference 8: namely,

$$\int_V \vec{J} \cdot \sum_{i} \frac{t_i}{z_i} \operatorname{grad} \mu_i \delta V = 0 \tag{28}$$

and are therefore enabled to write

$$\int_V \vec{J} \cdot \sum_{r'} \nu_{r'} \operatorname{grad} \mu_{r'} \delta V = \int_V \vec{J} \cdot \left(\sum_{r'} \nu_{r'} \operatorname{grad} \mu_{r'} + \sum_{i} \frac{t_i}{z_i} \operatorname{grad} \mu_i \right) \delta V \tag{29}$$

Since: (*i*) the vector $\vec{J}$ at any point is fixed by the chemical state at all points of the solution and by the configuration (8, auxiliary assumption 5), (*ii*) the transport numbers t_i at any point are functions of the pressure, the temperature, and the composition at that point (8, auxiliary assumption 4), (*iii*) according to reference 8, equation 87, we have

$$\sum_{i} z_i \frac{t_i}{z_i} = 1 \tag{30}$$

so that, by equation 21,

$$\sum_{r'} z_{r'} \nu_{r'} + \sum_{i} z_i \frac{t_i}{z_i} = 0 \tag{31}$$

it is evident from equations 14 and 15 that the integral on the right of equation 29 is a function of the chemical state at every point of the solution and of the configuration. From equations 19, 24, and 29 we therefore obtain for the E.M.F. as a function of chemical state and configuration

$$E^{\alpha\alpha'} = \frac{1}{F}\left[\sum_q \nu_q \mu_q^{\alpha} - \sum_{q'} \nu_{q'} \mu_{q'}^{\alpha'} + \sum_{r'} \nu_{r'} \mu_{r'}^{\beta} - \sum_r \nu_r \mu_r^{\beta} + \int_V \vec{J}\cdot\left(\sum_{r'} \nu_{r'} \operatorname{grad} \mu_{r'} + \sum_i \frac{t_i}{\bar{z}_i} \operatorname{grad} \mu_i\right)\delta V\right] \quad (32)$$

which corresponds to equation 106 in reference 8. As an alternative to equation 23 we can of course use

$$\sum_r \nu_r \mu_r^{\beta} = \sum_r \nu_r \mu_r^{\beta'} - \int_V \vec{J}\cdot\sum_r \nu_r \operatorname{grad} \mu_r \delta V \quad (33)$$

which yields for the E.M.F.

$$E^{\alpha\alpha'} = \frac{1}{F}\left[\sum_q \nu_q \mu_q^{\alpha} - \sum_{q'} \nu_{q'} \mu_{q'}^{\alpha'} + \sum_{r'} \nu_{r'} \mu_{r'}^{\beta'} - \sum_r \nu_r \mu_r^{\beta'} + \int_V \vec{J}\cdot\left(\sum_r \nu_r \operatorname{grad} \mu_r + \sum_i \frac{t_i}{\bar{z}_i} \operatorname{grad} \mu_i\right)\delta V\right] \quad (34)$$

corresponding to equation 109 in reference 8.

In the special case that the solution is simply connected and chemically lamellar we use instead of equations 23 and 33 the equations

$$\sum_{r'} \nu_{r'} \mu_{r'}^{\beta'} = \sum_{r'} \nu_{r'} \mu_{r'}^{\beta} + \int_C \sum_{r'} \nu_{r'} \operatorname{grad} \mu_{r'}\cdot\delta\vec{s} \quad (35)$$

$$\sum_r \nu_r \mu_r^{\beta} = \sum_r \nu_r \mu_r^{\beta'} - \int_C \sum_r \nu_r \operatorname{grad} \mu_r\cdot\delta\vec{s} \quad (36)$$

where C is any path through the solution from β to β'. The corresponding form of the qrc. condition is that of equation 77 in reference 8: namely,

$$\int_C \sum_i \frac{t_i}{\bar{z}_i} \operatorname{grad} \mu_i\cdot\delta\vec{s} = 0 \quad (37)$$

For the E.M.F. we thus obtain instead of equations 32 and 34 the simpler equations

$$E^{\alpha\alpha'} = \frac{1}{F}\left[\sum_q \nu_q \mu_q^{\alpha} - \sum_{q'} \nu_{q'} \mu_{q'}^{\alpha'} + \sum_{r'} \nu_{r'} \mu_{r'}^{\beta} - \sum_r \nu_r \mu_r^{\beta} + \int_C \left(\sum_{r'} \nu_{r'} \operatorname{grad} \mu_{r'} + \sum_i \frac{t_i}{\bar{z}_i} \operatorname{grad} \mu_i\right)\cdot\delta\vec{s}\right] \quad (38)$$

$$E^{\alpha\alpha'} = \frac{1}{F}\left[\sum_q \nu_q \mu_q^{\alpha} - \sum_{q'} \nu_{q'} \mu_{q'}^{\alpha'} + \sum_{r'} \nu_{r'} \mu_{r'}^{\beta'} - \sum_r \nu_r \mu_r^{\beta'} + \int_C \left(\sum_r \nu_r \operatorname{grad} \mu_r + \sum_i \frac{t_i}{\bar{z}_i} \operatorname{grad} \mu_i\right)\cdot\delta\vec{s}\right] \quad (39)$$

which correspond to equations 132 and 133, respectively, in reference 8.

The special case grad $\varphi = 0$

In this case φ and P are both constant throughout the cell. We should therefore expect the general formulae obtained above to reduce to formulae for cells with liquid–liquid junctions of the type obtained in reference 8. In order to show this we write for the electrolyte and neutral components q, q', in accordance with equations 9, 10,

$$\mu_q = \tau_q + M_q\varphi \tag{40}$$

$$\mu_{q'} = \tau_{q'} + M_{q'}\varphi \tag{41}$$

and for the charged and neutral components r, r', i, in accordance with equation 11

$$\mu_r = \tau_r + M_r\varphi + z_rF\psi \tag{42}$$

$$\mu_{r'} = \tau_{r'} + M_{r'}\varphi + z_{r'}F\psi \tag{43}$$

$$\mu_i = \tau_i + M_i\varphi + z_iF\psi \tag{44}$$

On substitution of equations 40 to 44 into equation 34 the terms in ψ cancel because of equations 25 and 31, and we obtain, since φ is constant,

$$\begin{aligned} E^{\alpha\alpha'} = \frac{1}{F}\Bigg[&\sum_q \nu_q\tau_q^\alpha - \sum_{q'} \nu_{q'}\tau_{q'}^{\alpha'} + \sum_{r'} \nu_{r'}\tau_{r'}^\beta - \sum_r \nu_r\tau_r^\beta \\ &+ \int_C \vec{J}\cdot\left(\sum_{r'} \nu_{r'} \operatorname{grad} \tau_{r'} + \sum_i \frac{t_i}{\bar{z}_i} \operatorname{grad} \tau_i\right)\delta V\Bigg] \\ &+ \frac{\varphi}{F}\left[\sum_q \nu_qM_q - \sum_{q'} \nu_{q'}M_{q'} + \sum_{r'} \nu_{r'}M_{r'} - \sum_r \nu_rM_r\right] \end{aligned} \tag{45}$$

Conservation of mass in the electrode processes requires that

$$\sum_q \nu_qM_q - \sum_{q'} \nu_{q'}M_{q'} + \sum_{r'} \nu_{r'}M_{r'} - \sum_r \nu_rM_r = 0 \tag{46}$$

and therefore the term in φ disappears from equation 45. Furthermore, for given electrode materials the τ_q^α are in general functions of $\bar{P}$ and T, and the $\tau_{q'}^{\alpha'}$ functions of $\bar{P}'$ and T. When, as is here the case, P is constant throughout, we may therefore set

$$\sum_q \nu_q\tau_q^\alpha - \sum_{q'} \nu_{q'}\tau_{q'}^{\alpha'} = B(P, T) \tag{47}$$

Equation 45 accordingly reduces to

$$\begin{aligned} E^{\alpha\alpha'} = \frac{1}{F}\Bigg[&B(P, T) + \sum_{r'} \nu_{r'}\tau_{r'} - \sum_r \nu_r\tau_r \\ &+ \int_V \vec{J}\cdot\left(\sum_{r'} \nu_{r'} \operatorname{grad} \tau_{r'} + \sum_i \frac{t_i}{\bar{z}_i} \operatorname{grad} \tau_i\right)\delta V\Bigg] \end{aligned} \tag{48}$$

in which the terms in τ_r, $\tau_{r'}$, τ_i evidently constitute a thermodynamically determinate function of the pressure and temperature of the system, the composition of the solution at every point, and the configuration. Equation 48 is therefore a general formula for a cell with liquid–liquid junction uncomplicated by gravitational effects. That it is equivalent to the equations obtained in reference 8 for the case in which not only grad φ but also φ itself is zero is readily verified by substituting equations 40 to 44 without the terms in φ into equations 106 and 85 of reference 8.

We point out that the deduction of equation 48 constitutes an exact theoretical proof of the intuitively obvious fact that in the absence of a *gravitational field* the E.M.F. of any galvanic cell becomes independent of the *gravitational potential.* It is of interest that in this proof the law of the conservation of mass plays a part very similar to that which it plays in the proof that the equilibrium constant is independent of the gravitational potential (*cf.* 6).

The electric potential difference produced in a solution by a gravitational field

In order to combat misunderstanding of a type still prevalent, we shall calculate as a function of chemical state and configuration the difference of electric potential in the solution, $\psi^{\beta} - \psi^{\beta'}$. Since grad T is zero, we obtain from equation 13

$$\text{grad}\,\mu_i = \left(\frac{\partial \tau_i^0}{\partial P}\right)_T \text{grad}\,P + RT\,\text{grad}\log N_i f_i + M_i\,\text{grad}\,\varphi + z_i F\,\text{grad}\,\psi \quad (49)$$

We may set

$$\left(\frac{\partial \tau_i^0}{\partial P}\right)_T = V_i^0 \quad (50)$$

and regard V_i^0 as the partial molar volume of i at infinite dilution. By virtue of equations 1 and 50 equation 49 becomes

$$\text{grad}\,\mu_i = RT\,\text{grad}\log N_i f_i + (M_i - V_i^0\rho)\,\text{grad}\,\varphi + z_i F\,\text{grad}\,\psi \quad (51)$$

Substituting equation 51 into the qrc. condition in the form of equation 28 and taking account of equation 30 we obtain

$$\int_V \vec{J}\cdot\sum_i \frac{t_i}{z_i}\,[RT\,\text{grad}\log N_i f_i + (M_i - V_i^0\rho)\,\text{grad}\,\varphi]\,\delta V + F\int_V \vec{J}\cdot\text{grad}\,\psi\,\delta V = 0 \quad (52)$$

According to the deduction of equation 117 in reference 8, we have

$$\int_V \vec{J}\cdot\text{grad}\,\psi\,\delta V = \psi^{\beta'} - \psi^{\beta} \quad (53)$$

Equations 52 and 53 give for the electric potential difference in question

$$\psi^{\beta} - \psi^{\beta'} = \frac{1}{F}\int_V \vec{J}\cdot\sum_i \frac{t_i}{\bar{z}_i}[RT \text{ grad} \log N_i f_i + (M_i - V_i^0 \rho) \text{ grad } \varphi]\delta V \quad (54)$$

If the solution is simply connected and chemically lamellar we use equations 51 and 37 and obtain instead of equation 54 the simpler equation

$$\psi^{\beta} - \psi^{\beta'} = \frac{1}{F}\int_C \sum_i \frac{t_i}{\bar{z}_i}[RT \text{ grad} \log N_i f_i + (M_i - V_i^0 \rho) \text{ grad } \varphi]\cdot\delta\vec{s} \quad (55)$$

When grad φ is zero, equations 54 and 55 reduce respectively to equations 119 and 135 of reference 8 for the potential difference of liquid–liquid junctions. It is thus evident from the manner in which the f_i occur in equations 54 and 55 that the potential difference in a solution subject to a gravitational field is thermodynamically indeterminate, just as is the potential difference due to a liquid-liquid junction. This is, moreover, true even if the composition of the solution as measured by the mole fractions is constant throughout, for in that case the f_i still vary throughout the solution because of the gradient of pressure. When the grad N_i are zero, equations 54 and 55 may be put into more compact form as follows: We define the partial molar volume V_i by the equation

$$V_i = \left(\frac{\partial \tau_i}{\partial P}\right)_{T, \text{comp.}} \quad (56)$$

where the subscript "comp." denotes constancy of the mole fractions. We note that for charged components the V_i so defined are thermodynamically indeterminate. When grad $N_i = 0$ we have, from equations 12, 50, 56, and 1,

$$\begin{aligned} \text{grad} \log f_i &= \frac{1}{RT}(\text{grad } \tau_i - \text{grad } \tau_i^0) \\ &= \frac{1}{RT}\left[\left(\frac{\partial \tau_i}{\partial P}\right)_{T, \text{comp.}} - \left(\frac{\partial \tau_i^0}{\partial P}\right)_T\right] \text{grad } P \\ &= \frac{V_i^0 - V_i}{RT} \rho \text{ grad } \varphi \end{aligned} \quad (57)$$

Substitution of equation 57 into equations 54 and 55 yields for the case grad $N_i = 0$

$$\psi^{\beta} - \psi^{\beta'} = \frac{1}{F}\int_V \vec{J}\cdot\sum_i \frac{t_i}{\bar{z}_i}(M_i - V_i\rho) \text{ grad } \varphi\delta V \quad (58)$$

$$\psi^{\beta} - \psi^{\beta'} = \frac{1}{F}\int_C \sum_i \frac{t_i}{\bar{z}_i}(M_i - V_i\rho) \text{ grad } \varphi\cdot\delta\vec{s} \quad (59)$$

These expressions are thermodynamically indeterminate, owing to the V_i. We conclude that the electric potential difference produced in a solution by a gravitational field is a concept just as meaningless experimentally as is the electric potential difference due to a liquid–liquid junction.

III. SOME SPECIAL CASES OF EXPERIMENTAL INTEREST

Two restrictions and their consequence

The cases of greatest experimental interest are evidently included within the following two restrictions: (*i*) the solution is simply connected and chemically lamellar; (*ii*) the two electrodes consist of the same materials.

Owing to restriction (*i*) we need consider only equations 38 and 39. Since restriction (*ii*) means that the components q and q' are identical, and likewise the components r and r', the equations in question both reduce to

$$E^{\alpha\alpha'} = \frac{1}{F}\left[\sum_q \nu_q(\mu_q^{\alpha} - \mu_q^{\alpha'}) + \int_C \left(\sum_r \nu_r \operatorname{grad}\mu_r + \sum_i \frac{t_i}{\bar{z}_i}\operatorname{grad}\mu_i\right)\cdot\delta\vec{s}\right] \tag{60}$$

In order to apply this equation to the special cases described below it is expedient to transform it as follows: We substitute equation 40 and obtain

$$E^{\alpha\alpha'} = -\frac{1}{F}\left[\sum_q \nu_q M_q \Delta\varphi + \sum_q \nu_q(\tau_q^{\alpha'} - \tau_q^{\alpha}) - \int_C \left(\sum_r \nu_r \operatorname{grad}\mu_r + \sum_i \frac{t_i}{\bar{z}_i}\operatorname{grad}\mu_i\right)\cdot\delta\vec{s}\right] \tag{61}$$

where $\Delta\varphi$ is defined as

$$\Delta\varphi = \bar{\varphi}' - \bar{\varphi} \tag{62}$$

Since we have assumed electrodes and solution to be mutually insoluble, we may take the total number of moles, n_q of any component q of an electrode to be independent of the pressure of the electrode. We therefore have

$$\begin{aligned}\tau_q^{\alpha'} - \tau_q^{\alpha} &= \tau_q(\bar{P}', T, n_q) - \tau_q(\bar{P}, T, n_q) \\ &= \int_{\bar{P}}^{\bar{P}'} \left(\frac{\partial \tau_q}{\partial P}\right)_{T,n_q} \mathrm{d}P \\ &= \int_{\bar{P}}^{\bar{P}'} V_q \,\mathrm{d}P \end{aligned} \tag{63}$$

where V_q is the partial molar volume of q in the electrode and is of course thermodynamically determinate, because the q are electrolyte or neutral components. Substitution of equation 63 into equation 61 gives the desired result.

$$E^{\alpha\alpha'} = -\frac{1}{F}\left[\sum_q \nu_q M_q \Delta\varphi + \int_P^{\bar{P}'} \sum_q \nu_q V_q \, \mathrm{d}P \right.$$

$$\left. - \int_C \left(\sum_r \nu_r \operatorname{grad} \mu_r + \sum_i \frac{t_i}{\bar{z}_i} \operatorname{grad} \mu_i\right) \cdot \delta\vec{s} \right. \qquad (64)$$

Three special cases

The following three special cases appear to be of experimental interest: *Case* 1: the gradients of the mole fractions in the solution are zero. *Case* 2: the solution is in sedimentation equilibrium. *Case* 3: a cell with solution originally in sedimentation equilibrium has been rapidly transported to a region in which grad φ is zero, the temperature of the cell and the volume and shape of the solution having been kept constant.

Case 1 is that of the "gravity cells" that have been studied by Des Coudres and by Tolman; it is, moreover, the only case which has been experimentally realized hitherto. Opposing the experimental realization of case 2 and therefore of case 3 are serious practical difficulties, especially the prevention of convection and mixing over the long periods of time required for sedimentation under available gravitational or centrifugal fields.

Theory of case 1

From equation 11 we have

$$\operatorname{grad} \mu_i = \operatorname{grad} \tau_i + M_i \operatorname{grad} \varphi + z_i F \operatorname{grad} \psi \qquad (65)$$

Since grad T and the grad N_i are zero, we have, from equation 56,

$$\operatorname{grad} \tau_i = V_i \operatorname{grad} P \qquad (66)$$

From equations 65, 66, and 1, we obtain

$$\operatorname{grad} \mu_i = \left(V_i - \frac{M_i}{\rho}\right) \operatorname{grad} P + z_i F \operatorname{grad} \psi \qquad (67)$$

and therefore, of course,

$$\operatorname{grad} \mu_r = \left(V_r - \frac{M_r}{\rho}\right) \operatorname{grad} P + z_r F \operatorname{grad} \psi \qquad (68)$$

Substituting equations 67 and 68 into the integral in equation 64 and noting that the terms in ψ cancel because of equations 20 and 30, we obtain

$$-\int_C \left(\sum_r \nu_r \operatorname{grad} \mu_r + \sum_i \frac{t_i}{\bar{z}_i} \operatorname{grad} \mu_i\right) \cdot \delta\vec{s}$$

$$= \int_C \left[\sum_r \nu_r \left(\frac{M_r}{\rho} - V_r\right) + \sum_i \frac{t_i}{\bar{z}_i}\left(\frac{M_i}{\rho} - V_i\right)\right] \operatorname{grad} P \cdot \delta\vec{s} \qquad (69)$$

Since at constant T and N_i the quantities V_r, V_i, t_i, and ρ are functions only of P, the line integral on the right becomes a definite integral between the limits $\bar{P}$ and $\bar{P}'$, so that

$$-\int_C \left(\sum_r \nu_r \operatorname{grad} \mu_r + \sum_i \frac{t_i}{\bar{z}_i} \operatorname{grad} \mu_i\right)\cdot\delta\vec{s} = \int_{\bar{P}}^{\bar{P}'} \left[\sum_r \nu_r \left(\frac{M_r}{\rho} - V_r\right) + \sum_i \frac{t_i}{\bar{z}_i}\left(\frac{M_i}{\rho} - V_i\right)\right] \mathrm{d}P \qquad (70)$$

Substitution of equation 70 into equation 64 gives

$$E^{aa'} = -\frac{1}{F}\left\{\sum_q \nu_q M_q \Delta\varphi + \int_{\bar{P}}^{\bar{P}'} \left[\sum_q \nu_q V_q + \sum_r \nu_r \left(\frac{M_r}{\rho} - V_r\right) + \sum_i \frac{t_i}{\bar{z}_i}\left(\frac{M_i}{\rho} - V_i\right)\right] \mathrm{d}P\right\} \qquad (71)$$

From equations 20, 30, 14, 16, and 56 it is evident that the linear combination of the functions V_r, V_i in equations 69, 70, and 71 is thermodynamically determinate. Equation 71 is the exact law for case 1.

The integral in equation 71 can in general be evaluated only approximately. A convenient approximation consists in regarding V_q, V_i, V_r, and t_i, at constant T and N_i, as independent of P. This permits us to replace V_q, V_i, V_r, t_i, and also ρ by their values at the same temperature and composition but zero pressure, which will be indicated by the superscript *. Equation 71 then integrates to

$$E^{aa'} = -\frac{1}{F}\left\{\sum_q \nu_q M_q \Delta\varphi + \left[\sum_q \nu_q V_q^* + \sum_r \nu_r \left(\frac{M_r}{\rho^*} - V_r^*\right) + \sum_i \frac{t_i^*}{\bar{z}_i}\left(\frac{M_i}{\rho^*} - V_i^*\right)\right] \Delta P\right\} \qquad (72)$$

where ΔP is defined as

$$\Delta P = \bar{P}' - \bar{P} \qquad (73)$$

An equation more suitable than equation 72 for comparison with experiment is obtained if ΔP is eliminated in favor of $\Delta\varphi$. Since the solution is regarded as incompressible, the relation between ΔP and $\Delta\varphi$ is

$$\Delta P = -\rho^* \Delta\varphi \qquad (74)$$

The desired equation is therefore

$$E^{aa'} = -\frac{\Delta\varphi}{F}\left[\sum_q \nu_q (M_q - \rho^* V_q^*) - \sum_r \nu_r (M_r - \rho^* V_r^*) - \sum_i \frac{t_i^*}{\bar{z}_i}(M_i - \rho^* V_i^*)\right] \qquad (75)$$

We shall apply equation 75 to three special types of electrode equilibrium to be known as A, B, and C, respectively.

Electrode equilibrium A is that of the system

Me | solution of a single salt of Me in a non-electrolyte solvent

The chemical equation for this equilibrium, written according to equation 9 in reference 8, is

$$-\frac{1}{z_+}\,\mathrm{Me}^{(+)} = -\frac{1}{z_+}\,\mathrm{Me} + \mathrm{El}^- \tag{76}$$

where $\mathrm{Me}^{(+)}$ is the formula of the ion of the metal Me, and z_+ is the valence of this ion. Equation 75 then yields, by a series of obvious transformations,

$$E^{\alpha\alpha'} = \frac{\Delta\varphi}{z_+F}\left[M_{\mathrm{Me}} - \rho^* V^*_{\mathrm{Me}} - \frac{t^*_-}{b_+}(M_s - \rho^* V^*_s)\right] \tag{77}$$

where t^*_- is the Hittorf number at zero pressure of the solute anion, s refers to the solute salt, and b_+ is the number of moles of $\mathrm{Me}^{(+)}$ per mole of salt.

Electrode equilibrium B is that of the system

Ag | AgCl | solution of a single chloride in a non-electrolyte solvent

The chemical equation for this equilibrium is to be written in the form

$$\mathrm{Cl}^- = \mathrm{AgCl} - \mathrm{Ag} + \mathrm{El}^- \tag{78}$$

Equation 75 then yields, by a series of obvious transformations,

$$E^{\alpha\alpha'} = -\frac{\Delta\varphi}{F}\left[M_{\mathrm{Cl}} - \rho^*(V^*_{\mathrm{AgCl}} - V^*_{\mathrm{Ag}}) - \frac{t^*_+}{z_+}(M_s - \rho^* V^*_s)\right] \tag{79}$$

where t^*_+ and z_+ are, respectively, the Hittorf number at zero pressure and the valence of the solute cation, and s refers to the solute salt.

Electrode equilibrium C is that of the system

Pt | solution of iodine and an excess of a single iodide in a non-electrolyte solvent

In this case we may describe the electrochemically active components by two alternative sets of chemical formulae: namely, (*i*) I^-, I_3^-, El^-, or (*ii*) I^-, I_2, El^-. The corresponding chemical equations for the electrode equilibrium are in description (*i*)

$$\frac{3}{2}\,\mathrm{I}^- - \frac{1}{2}\,\mathrm{I}_3^- = \mathrm{El}^- \tag{80}$$

and in description (*ii*)

$$\mathrm{I}^- - \frac{1}{2}\,\mathrm{I}_2 = \mathrm{El}^- \tag{81}$$

Equation 75 yields, by a series of obvious transformations, for description (*i*)

$$E^{\alpha\alpha'} = -\frac{\Delta\varphi}{z_+F}\left[\left(\frac{1}{2} + t^*_{I_3^-}\right)(M_{s'} - \rho^* V^*_{s'}) - \left(\frac{1}{2} + t^*_+ + t^*_{I_3^-}\right)(M_s - \rho^* V^*_s)\right] \quad (82)$$

and for description (*ii*)

$$E^{\alpha\alpha'} = -\frac{\Delta\varphi}{F}\left[\left(\frac{1}{2} + t^*_{I_2}\right)(M_{I_2} - \rho^* V^*_{I_2}) - \frac{t^*_+}{z_+}(M_s - \rho^* V^*_s)\right] \quad (83)$$

in which t^*_+ and z_+ are, respectively, the Hittorf number at zero pressure and the valence of the solute cation, and the subscripts s and s' refer, respectively, to the iodide and triiodide salt. If the excess of iodide over triiodide (or iodine) is sufficiently great, $t^*_{I_3^-}$ (or $t^*_{I_2}$) may be neglected and equations 82 and 83 become respectively

$$E^{\alpha\alpha'} = -\frac{\Delta\varphi}{z_+F}\left[\frac{1}{2}(M_{s'} - \rho^* V^*_{s'}) - \left(\frac{1}{2} + t^*_+\right)(M_s - \rho^* V^*_s)\right] \quad (84)$$

$$E^{\alpha\alpha'} = -\frac{\Delta\varphi}{F}\left[\frac{1}{2}(M_{I_2} - \rho^* V_{I_2}) - \frac{t^*_+}{z_+}(M_s - \rho^* V^*_s)\right] \quad (85)$$

Inspection of the two descriptions readily shows the transformation connecting equations 82, 84 with equations 83, 85 to be

$$t^{*(i)}_+ = t^{*(ii)}_+ \quad (86)$$

$$t^{*(i)}_{I^-} = t^{*(ii)}_{I^-} - t^{*(ii)}_{I_2} \quad (87)$$

$$t^{*(i)}_{I_3^-} = t^{*(ii)}_{I_2} \quad (88)$$

$$M_{s'} - M_s = z_+ M_{I_2} \quad (89)$$

$$V^*_{s'} - V^*_s = z_+ V^*_{I_2} \quad (90)$$

Theory of case 2

This case is characterized by the equilibrium conditions

$$\text{grad } \mu_i = 0 \quad (91)$$

$$\text{grad } \mu_r = 0 \quad (92)$$

Equation 64 therefore reduces to

$$E^{\alpha\alpha'} = -\frac{1}{F}\sum_q \nu_q\left(M_q\Delta\varphi + \int_{\bar{P}}^{\bar{P}'} V_q \mathrm{d}P\right) \quad (93)$$

which is the exact law for case 2.

Taking V_q to be independent of P, we may integrate equation 93 and obtain the approximate formula

$$E^{\alpha\alpha'} = -\frac{1}{F}\sum_q \nu_q(M_q\Delta\varphi + V_q^*\Delta P) \tag{94}$$

where the asterisk as before indicates zero pressure.

In order to eliminate ΔP from equation 94 we write, in accord with equation 1,

$$\begin{aligned} \Delta P &= -\int_C \rho \operatorname{grad} \varphi\cdot\delta\vec{s} \\ &= -[\rho]\Delta\varphi \end{aligned} \tag{95}$$

where $[\rho]$ is in general merely a suitable mean value of the density of the solution. It is readily shown that for the only two cases of practical interest,—namely, (*i*) a cylindrical cell with the electrodes at the ends, in a uniform gravitational field, and (*ii*) an annularly sectorial cell with the electrodes at the ends, in a centrifugal field,—the quantity $[\rho]$ is exactly given by

$$[\rho] = \frac{M}{V} \tag{96}$$

where M is the total mass and V the total volume of the solution in sedimentation equilibrium. From equations 94 and 95 we obtain

$$E^{\alpha\alpha'} = -\frac{\Delta\varphi}{F}\sum_q \nu_q(M_q - [\rho]V_q^*) \tag{97}$$

For electrode equilibrium A, equation 97 gives

$$E^{\alpha\alpha'} = \frac{\Delta\varphi}{z_+F}(M_{\mathrm{Me}} - [\rho]\,V_{\mathrm{Me}}^*) \tag{98}$$

For electrode equilibrium B, equation 97 gives

$$E^{\alpha\alpha'} = -\frac{\Delta\varphi}{F}[M_{\mathrm{Cl}} - [\rho](V_{\mathrm{AgCl}}^* - V_{\mathrm{Ag}}^*)] \tag{99}$$

For electrode equilibrium C we obtain without approximations from the exact equation 93, since components q are absent,

$$E^{\alpha\alpha'} = 0 \tag{100}$$

Theory of case 3

In this case φ and P are constant throughout, so that we obtain from equation 64

$$E^{\alpha\alpha'} = \int_C \left(\sum_r \nu_r \operatorname{grad}\mu_r + \sum_i \frac{t_i}{z_i}\operatorname{grad}\mu_i\right)\cdot\delta\vec{s} \tag{101}$$

and from equation 13

$$\operatorname{grad} \mu_i = RT \operatorname{grad} \log N_i f_i + z_i F \operatorname{grad} \psi \tag{102}$$

$$\operatorname{grad} \mu_r = RT \operatorname{grad} \log N_r f_r + z_r F \operatorname{grad} \psi \tag{103}$$

On substitution of equations 102, 103 into equation 101 the terms in ψ cancel and we obtain

$$E^{\alpha\alpha'} = \frac{RT}{F} \int_C \left(\sum_r \nu_r \operatorname{grad} \log N_r f_r + \sum_i \frac{t_i}{z_i} \operatorname{grad} \log N_i f_i \right) \cdot \delta \vec{s} \tag{104}$$

In order to relate this equation to the sedimentation equilibrium from which the cell is derived, we mark quantities referring to this sedimentation equilibrium with the superscript e and deduce from equations 91, 92, and 51

$$RT \operatorname{grad} \log N_i^e f_i^e + (M_i - \rho^e V_i^{0e}) \operatorname{grad} \varphi^e + z_i F \operatorname{grad} \psi^e = 0 \tag{105}$$

$$RT \operatorname{grad} \log N_r^e f_r^e + (M_r - \rho^e V_r^{0e}) \operatorname{grad} \varphi^e + z_r F \operatorname{grad} \psi^e = 0 \tag{106}$$

whence we obtain, since the terms in ψ^e cancel,

$$\begin{aligned} &\frac{RT}{F} \int_C \left(\sum_r \nu_r \operatorname{grad} \log N_r^e f_r^e + \sum_i \frac{t_i}{z_i} \operatorname{grad} \log N_i^e f_i^e \right) \cdot \delta \vec{s} \\ &+ \frac{1}{F} \int_C \left[\sum_r \nu_r (M_r - \rho^e V_r^{0e}) + \sum_i \frac{t_i}{z_i} (M_i - \rho^e V_i^{0e}) \right] \operatorname{grad} \varphi^e \cdot \delta \vec{s} = 0 \end{aligned} \tag{107}$$

Subtraction of equation 107 from equation 104 gives

$$\begin{aligned} E^{\alpha\alpha'} = &\frac{RT}{F} \int_C \left(\sum_r \nu_r \operatorname{grad} \log \frac{N_r f_r}{N_r^e f_r^e} + \sum_i \frac{t_i}{z_i} \operatorname{grad} \log \frac{N_i f_i}{N_i^e f_i^e} \right) \cdot \delta \vec{s} \\ &- \frac{1}{F} \int_C \sum_r \nu_r (M_r - \rho^e V_r^{0e}) + \sum_i \frac{t_i}{z_i} [M_i - \rho^e V_i^{0e}] \operatorname{grad} \varphi^e \cdot \delta \vec{s} \end{aligned} \tag{108}$$

This is the exact law for case 3.

For an approximate evaluation of the integrals in equation 108, it is convenient to regard V_i, V_r as independent not only of pressure but also of composition. According to this approximation we have

$$V_i = V_i^0 = V_i^{0e} = V_i^{0*} \tag{109}$$

where V_i^{0*} is the partial molar volume at infinite dilution and zero pressure. The approximation furthermore permits us to regard the solution as incompressible and therefore to neglect the elastic displacement within the solution on passing from sedimentation equilibrium to the state $\operatorname{grad} \varphi = 0$. This means that at each point of the solution

$$N_i^e = N_i \tag{110}$$

Finally since, in general, from equations 12, 50, 56,

$$\left(\frac{\partial \log f_i}{\partial P}\right)_{T,\,\text{comp.}} = \frac{V_i - V_i^0}{RT} \tag{111}$$

it is evident from equations 109 and 110 that we also have at each point of the solution

$$f_i^e = f_i \tag{112}$$

On substitution of equations 109, 110, and 112 (along with similar equations for the components r) into equation 108, the first integral vanishes and the second integral can be evaluated to give

$$E^{\alpha\alpha'} = -\frac{\Delta\varphi^e}{F}\left[\sum_r \nu_r(M_r - [\rho^e]V_r^{0*}) + \sum_i \frac{[t_i]}{\bar{z}_i}(M_i - [\rho^e]V_i^{0*})\right] \tag{113}$$

in which $[\rho^e]$ has exactly the same significance as $[\rho]$ in equations 95, 96, 97 for case 2, and the $[t_i]$ are suitable mean values of the transport numbers.

For electrode equilibrium A, equation 113 gives

$$E^{\alpha\alpha'} = \frac{\Delta\varphi^e}{z_+ b_+ F}[t_-](M_s - [\rho^e]V_s^{0*}) \tag{114}$$

For electrode equilibrium B, equation 113 gives

$$E^{\alpha\alpha'} = -\frac{\Delta\varphi^e}{z_+ F}[t_+](M_s - [\rho^e]V_s^{0*}) \tag{115}$$

For electrode equilibrium C, equation 113 gives, in terms of components I^-, I_3^-,

$$E^{\alpha\alpha'} = \frac{\Delta\varphi^e}{z_+ F}\left[\left(\frac{1}{2} + [t_{I_3^-}]\right)(M_{s'} - [\rho^e]V_{s'}^{0*}) - \left(\frac{1}{2} + [t_+] + [t_{I_3^-}]\right)(M_s - [\rho^e]V_s^{0*})\right] \tag{116}$$

or alternatively, in terms of components I^-, I_2,

$$E^{\alpha\alpha'} = \frac{\Delta\varphi^e}{F}\left[\left(\frac{1}{2} + [t_{I_2}]\right)(M_{I_2} - [\rho^e]V_{I_2}^{0*}) - \frac{[t_+]}{z_+}(M_s - [\rho^e]V_s^{0*})\right] \tag{117}$$

in which $[t_{I_3^-}]$ and $[t_{I_2}]$ become negligible if the excess of iodide is large.

An approximate relation connecting cases 1, 2, and 3

The following considerations apply to the cylindrical cell with electrodes at the ends in a uniform gravitational field such as that near the earth, and to the annularly sectorial cell with electrodes at the ends in a centrifugal field. In the case of the cylindrical cell, the gravitational field is applied by placing the cell parallel to the field and may always be effectively removed by placing the cell perpendicular to the field. In the case of the sectorial cell, the field is of course applied and removed by starting and stopping rotation. We shall assume the cell contents to be so nearly incompressible and the cell container to be so nearly rigid that the changes in volume and shape of the solution and the electrodes on applying or removing the field are negligible. Let the cell be initially filled with a uniform solution and a steady gravitational field applied. We then have case 1 and the E.M.F. is very nearly that given by equation 75. Now let the gravitational field act until the solution has practically reached sedimentation equilibrium. We then have case 2 and the E.M.F. is very nearly that given by equation 97. Finally let the field be removed. We then have case 3 and the E.M.F. is very nearly that given by equation 113. Under the circumstances we have the relations

$$\Delta\varphi_{\text{Case 1}} = \Delta\varphi_{\text{Case 2}} = \Delta\varphi^{e}_{\text{Case 3}} \tag{118}$$

$$\rho_{\text{Case 1}} = [\rho]_{\text{Case 2}} = [\rho^{e}]_{\text{Case 3}} \tag{119}$$

We also have, at least to a first approximation,

$$V^{*}_{i_{\text{Case 1}}} \sim V^{0*}_{i_{\text{Case 3}}} \tag{120}$$

$$t^{*}_{i_{\text{Case 1}}} \sim [t_i]_{\text{Case 3}} \tag{121}$$

Comparison of the three equations 75, 97, and 113 therefore yields the result that

$$E^{\alpha\alpha'}_{\text{Case 1}} - E^{\alpha\alpha'}_{\text{Case 2}} + E^{\alpha\alpha'}_{\text{Case 3}} \sim 0 \tag{122}$$

This approximate relation holds for any type of electrode equilibrium. In particular for electrode equilibrium C, moreover, equation 122 simplifies to

$$E^{\alpha\alpha'}_{\text{Case 1}} + E^{\alpha\alpha'}_{\text{Case 3}} \sim 0 \tag{123}$$

owing to the exact equation 100.

IV. CONCLUDING REMARKS

On the relation between "gravity cells" and cells with liquid–liquid junctions

By a "gravity cell" we mean the type of cell considered under case 1 above. *Physically* the relation between "gravity cells" and cells with liquid–liquid junctions consists in the fact that in both cases the solution is subject to diffusion. In the foregoing we have arrived at a general theory of galvanic cells which includes both "gravity cells" and cells with liquid–liquid junctions as special cases. From this theory it is evident that *analytically* the relation between "gravity cells" and cells with liquid–

liquid junctions expresses itself in the fact that in both cases the calculation of the E.M.F. as a function of chemical state and configuration depends upon the qrc. condition. It is the qrc. condition which in both cases causes transport numbers to appear in the equations for the E.M.F. In reference 8 it was proved that the qrc. condition is invariant under a change of the convention required to fix the numerical values of the transport numbers at each point of a given solution. It follows that, whenever the solvent is a non-electrolyte, one may set its transport number equal to zero and thus obtain exact equations involving the *Hittorf* numbers of the other components. The Hittorf numbers are thus *sufficient but not necessary* for an exact theory of "gravity cells" as well as of cells with liquid–liquid junctions.

On previous theoretical work

Des Coudres published his researches on galvanic cells subject to gravitational (or centrifugal) fields in two papers appearing in 1893 (1) and 1896 (3), respectively. In his first paper Des Coudres studies the cells

Cd amalgam | solution of Cd chloride or iodide | Cd amalgam

the electrode equilibrium of which is of our type A. He points out the possibility of the physical situations designated by us as cases 1, 2, and 3, and derives equations for the corresponding E.M.F's. by calculation of the work done on reversible flow of electricity through the cell. Except for slight differences of notation, these equations of Des Coudres are identical with the equations which would result from our approximate equations 77, 98, and 114 on dropping the terms $\rho^*V^*_{\mathrm{Me}}$, $\rho^*V^*_s$, $[\rho]V^*_{\mathrm{Me}}$, and $[\rho^e]\ V^{0*}_s$. The absence of these terms is due to Des Coudres's failure, in reference 1, to take into account the work due to "buoyancy forces" in the solution. In his second paper (3) Des Coudres, at the suggestion of Nernst, corrects this error. With the theory thus improved he studies, in addition to the cadmium amalgam cells mentioned above, also the cells

Hg | HgCl | solution of a single chloride | HgCl | Hg

the electrode equilibrium of which is of our type B (with mercury instead of silver). In reference 3 Des Coudres confines his attention to case 1 (i.e., to the "gravity cell"), for which he obtains equations essentially identical with our equations 77 and 79. These equations he verifies experimentally.

It is worth mentioning that Des Coudres in 1895 (2) was the first to obtain the differential equation for rate of sedimentation in a gravitational field and to solve it approximately. From his solution he was able to show that the rate is much too small to interfere with the measurement of the E.M.F. of "gravity cells" in the earth's field.

Following Des Coudres the only work of importance has been that of

Tolman, who in 1910–11 (11) published a very thorough experimental and theoretical study of "gravity cells" with electrodes Pt | I^-, I_2 (i.e., case 1, electrode equilibrium C). Tolman was the first to deduce what is essentially equation 85 above. He did this by two methods, of which the first is a thermodynamic one similar to that of Des Coudres, and the second combines a thermodynamic calculation of the contribution of the electrodes to the E.M.F. with a kinetic calculation of the contribution of the solution, after the manner of Nernst (10) for cells with liquid–liquid junctions. By virtue of this derivation Tolman is in fact the first to point out the fundamental similarity between "gravity cells" and cells with liquid–liquid junctions. Tolman gives a careful account of the approximations involved in equation 85.

V. SUMMARY

With the help of the condition for quasi-reversible conduction (8), general equations are deduced which express the E.M.F. of a galvanic cell subject to arbitrary gradients of the gravitational potential and of the mole fractions, as a function of the chemical state at every point and of the configuration (equations 32, 34, 38, 39). It is shown that, when the gravitational field strength is zero, these equations reduce to the general equations for cells with liquid–liquid junctions (equation 48), whence the E.M.F. becomes independent of the gravitational potential. The electric potential difference in a solution subject to a gravitational field is calculated as a function of chemical state and configuration (equations 54, 55, 58, 59) and is shown to be thermodynamically indeterminate. From the general equations the laws for certain special types of cell of experimental interest are deduced in detail (equations 71, 75, 77, 79, 82 to 85, 93 to 100, 108, 113 to 117, 122, 123). Previous theoretical work on galvanic cells subject to gravitational fields is reviewed.

REFERENCES

(1) Des Coudres, T.: Wied. Ann. **49**, 284 (1893).
(2) Des Coudres, T.: Wied. Ann. **55**, 213 (1895).
(3) Des Coudres, T.: Wied Ann. **57**, 232 (1896).
(4) Gibbs, J. W.: *The Collected Works of J. Willard Gibbs, etc.* Vol. I, pp. 144–7. Longmans, Green and Co., New York, London, Toronto (1928).
(5) Guggenheim, E. A.: J. Phys. Chem. **33**, 842 (1929); **34**, 1540 (1930).
(6) Guggenheim, E. A.: *Modern Thermodynamics by the Methods of Willard Gibbs*, p. 158. Methuen, London (1933).
(7) Koenig, F. O.: J. Phys. Chem. **40**, 373 (1936).
(8) Koenig, F. O.: J. Phys. Chem. **44**, 101 (1940).
(9) MacInnes, D. A.: *The Principles of Electrochemistry*, pp. 174–80. Reinhold Publishing Corporation, New York (1939).
(10) Nernst, W.: Z. physik. Chem. **2**, 613 (1888).
(11) Tolman, R. C.: Proc. Am. Acad. Art. Sci. **46**, 109 (1910); J. Am. Chem. Soc. **33**, 121 (1911).

THE SPECIFIC HEATS OF SOME AQUEOUS SODIUM AND POTASSIUM CHLORIDE SOLUTIONS AT SEVERAL TEMPERATURES. I

C. B. HESS AND BRUCE E. GRAMKEE

Department of Chemistry, University of Rochester, Rochester, New York

Received May 10, 1939

The need of precise specific heat data of aqueous salt solutions in the field of thermochemistry has been recognized for many years. Within the past twenty years it has been shown that such data are of perhaps greater value in the field of thermodynamics, and more recently they have been shown to be of value in checking recent theoretical deductions concerning the electrical nature of aqueous solutions. Several years ago a start was made with the two simple salts sodium chloride and potassium chloride at the temperatures 15°, 25°, 35°, and 45°C. This paper will have for its object the description of the apparatus[1] used and the presentation of the results obtained in this research.

APPARATUS

The apparatus was a modification of that used by Richards and Gucker (4), who applied adiabatic calorimetry to the electrical twin method first invented by Joule (2) and later improved by Pfaundler (3), and who first developed the substitution method of comparing specific heats. On carefully studying their apparatus the following improvements suggested themselves: (*1*) a closed calorimeter, (*2*) thermels completely covered,[2] (*3*) stirring a little more positive and geared, and (*4*) a vacuum jar instead of a dead air space. The apparatus was nearly completed when a paper appeared by Gucker (1) describing a modified twin calorimeter incorporating the first three points just mentioned, but since his set-up is somewhat different from the present one, a full description of the apparatus appears to be desirable.

The apparatus consists mainly of two Dewar flasks[3] as calorimeters (A and B) suspended in a water jacket. Figure 1 shows the whole set-up and the top and side views of one of the calorimeters in some detail.

Calorimeters

Since a closed calorimeter was desired, some suitable method had to be found to fasten the glass Dewar flask (H) to the heavy cast-brass (silver-

---

[1] Recently some results (6), which were precise to 0.01 per cent, were obtained with a modified form of this apparatus.

[2] This point was suggested in an interview with Dr. W. P. White.

[3] Obtained from Manning, Bowman and Co., Meriden, Connecticut.

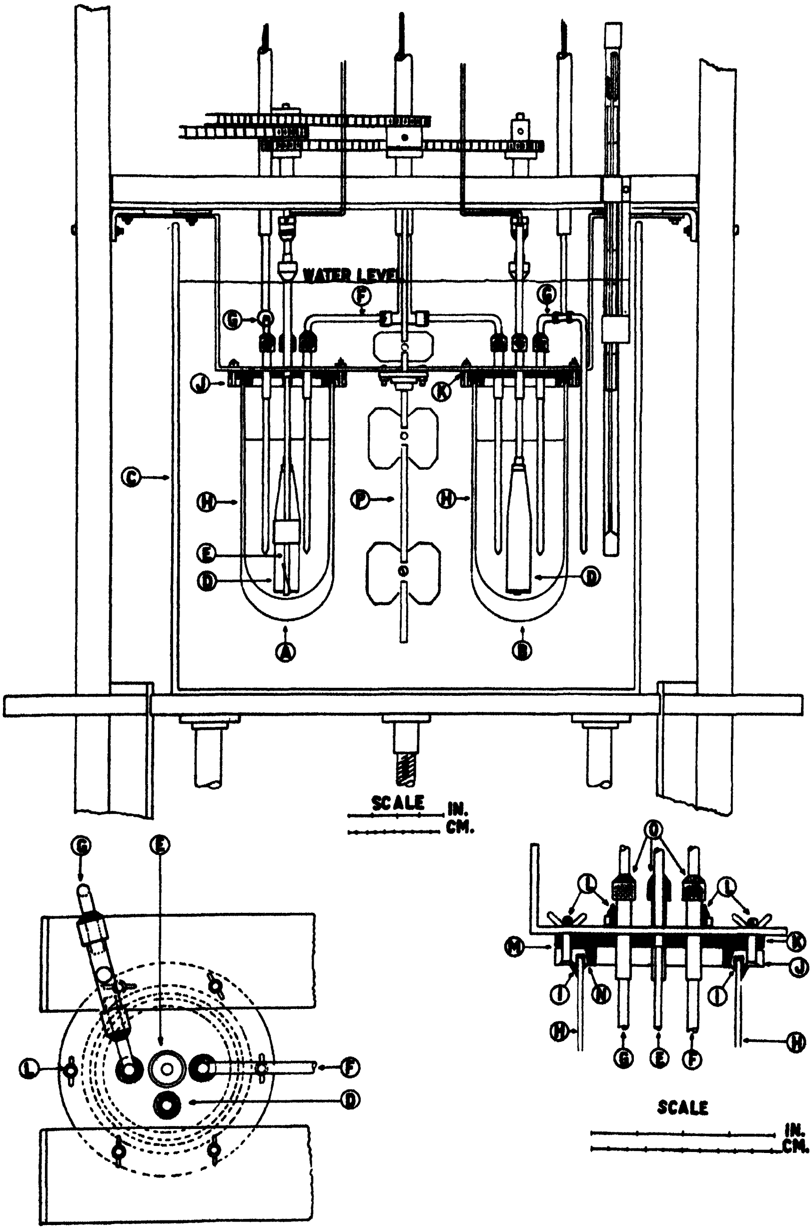

Fig. 1. The calorimeter

plated) ring[4] (J, in figure 1). A mixture of litharge and glycerol (I) was first tried, but invariably the flask broke when the assembled apparatus was heated to 35° to 40°C., thus indicating a rigidity too great for the purpose in hand. deKhotinsky cement was then used and proved successful. It was necessary, however, to provide some additional support (not shown) for the Dewar, because the cement softened a little at 45°C. and there was danger that the flask would become detached from the ring. The Dewar flasks had a capacity of about 1 liter. The volume of solution used was very nearly 700 cc.; the air space above the solution was about 250 cc.

The annular ring (J) was fastened to the heavy cast-brass cap (K) above it by six bolts fitted with wing nuts (L). A very gradual and accurately machined tapered joint is shown at N. Before assembling the apparatus this tapered joint was given a final careful grinding with fine rouge. This joint has worked satisfactorily throughout this research. The heavy brass cap was fitted with four sleeves (three are shown in figure 1), brazed to the cap. Three of the sleeves were provided with packing boxes (O) which were water-tight; through two of these sleeves passed two thermels (to be described later) and through the other passed the heater (described below). The fourth sleeve was somewhat longer than the others and carried the calorimeter stirrer; it was centrally located in the cap and calorimeter. The top of the fourth sleeve carried a little cup in which was placed a small amount of oil to provide a seal (to be described more fully below).

Both the annular ring and cap with its sleeves were heavily plated with silver before the calorimeters were assembled. The flasks were chosen from a considerable number because of similar heat leaks.

Calorimeter heaters

The two calorimeters were heated by means of two electric heaters (D). These heaters should have nearly the same resistance and heat capacity; they should be rugged and as nearly lagless as possible; they should furthermore be permanent, since the failure of a heater *may* entail the construction of a new heater and also the restandardization of the apparatus. Heaters meeting these requirements in a satisfactory way were constructed as follows: The requisite length of nichrome ribbon (1/32 in. x 0.004 in.) was wound bifilar on a slotted strip of mica, and the ends of the ribbon were soldered to copper wire (No. 18 B. & S. gauge). The resistances were adjusted to ±0.2 per cent by the usual method. Thin protecting pieces of mica were tied with thread to the slotted strip and the whole was then slipped into the case of the heater. The case was then flattened in a vise and closed with a small amount of solder. The case,[5] which was of thin copper, chromium-plated, had been previously fitted at its upper end with a special packing box similar to (but considerably smaller than) those used on the three sleeves of the calorimeter cap; a glass tube (Pyrex) was also fitted into this packing box and made water-tight by the application of a small amount of litharge and glycerol and, after this had dried, several coats of waterproof varnish were applied to this surface. The copper leads passed through this Pyrex tube and could be connected separately or in series with the leads of the duplicate heater and with the 110 D.C. current supply. The heaters were designed to heat 700 g. of water 2°C. in 6 min., using 1.4 amperes.

---

[4] Valuable suggestions concerning the construction of the ring and cap were obtained from Professor Farrington Daniels.

Calorimeter stirrers

These stirrers (E) were two-bladed, were made of brass (chromium-plated), and were fitted into fibre tubing at their upper ends to prevent undue heat leakage and friction. At the point where the stirrer shaft emerged from the stirrer sleeve there was placed an inverted cap which dipped into the small amount of oil forming the oil seal. Both stirrers were run at 75 R.P.M. through sprockets mounted on ball bearings and connected by a chain drive to the drive shaft (not shown in figure 1).

Thermels

The thermels were three in number and were constructed of copper-Constantan according to the recommendations of White (7). The main thermel (F) was made in two opposable sections of twelve junctions each, from No. 35 d.s.c. copper wire and No. 30 Constantan (Advance) tested for thermoelectric homogeneity by White's method. It had a total resistance of 140 ohms.

The two smaller thermels (G) were each made in two opposable sections of four junctions each, using No. 40 d.s.c. copper wire and No. 31 d.s.c. Constantan wire tested as above mentioned. The resistance of the small thermels was 72.5 ohms.

The thermel cases were of Pyrex glass and were joined by an inverted tee fitted with packing boxes. The leads were brought out the top of the tee and encased in rubber tubing to protect them from moisture and damage through handling.

The main thermel or the two small ones (in series) could be connected at will to the high-sensitivity Leeds and Northrup galvanometer. The instrument was ballasted for critical damping and found to have no appreciable zero drift, other than that caused by changing room temperature. The sensitivity of the main thermel was about 0.00029° per millimeter on a scale about 4 meters from the galvanometer, while that of the smaller thermels in series was about 0.00087° per millimeter.

---

[5] These cases were those used in the construction of the Cenco Lagless Knife Type Heaters and were supplied by the Central Scientific Company.

The galvanometer, thermel circuits, and energy circuits were protected by a complete equipotential shield according to the recommendation of White and proved satisfactory in every way.

Jacket, etc.

The jacket consisted of a round copper tank (C), 18 in. x 20 in., heated by Cenco lagless knife type heaters of approximately 2300 watts capacity. A suitable variable resistance was placed in series with one of the heaters to enable a fine adjustment of heat during a run under adiabatic conditions. Two elongated 40-watt bulbs, one of which had a variable resistance in series with it, were used especially in holding the jacket to the desired temperature during the "fore" and "aft" periods. A three-bladed propeller stirrer (P), rotated at 300 R.P.M. through a chain drive, agitated the water vigorously. The jacket was provided with a cooling coil and electric pump for circulating ice water through it, to obtain temperatures below that of the room.

The jacket was placed on a platform which could be raised or lowered by a suitable mechanical device. This arrangement made it possible to fasten the calorimeters rigidly to the upright posts; this proved satisfactory in every way. Three sides and the top of the supporting framework were built solid, thus aiding the attainment of temperature constancy in the set-up.

A Beckmann thermometer was inserted in the jacket and served to determine the temperature *interval* (2°C.). This thermometer could be read and raised or lowered from the operator's seat. It was of course necessary to reset the thermometer at each temperature. Another thermometer of precision grade, having a range of 0° to 50°C. and having been carefully compared with one of similar range standardized by the Bureau of Standards, served to determine the average temperature of the run to ±0.02°C.

MATERIALS, CONSTANTS, ETC.

The salts used in this work were anhydrous C. P. samples thoroughly dried[6] in an oven at 130°C. The water used was the laboratory supply of freshly distilled water.

The molality of a given solution was calculated from the weight of the water and the weight of the salt added, using the international atomic weights for 1939. The water in the flask was weighed to 0.01 g., while the added salt was weighed in milligrams except in the case of the more dilute solutions, where it was weighed to a tenth of a milligram.

---

[6] Richards and Hall (5) have apparently shown that sodium chloride so treated contains 0.07 per cent water.

Because of the pronounced heat of solution in the more concentrated solutions it was necessary to prepare solutions of approximately the desired molality in glass-stoppered bottles. A portion of the prepared solution was then weighed into the solution calorimeter. The molality was determined by evaporating a sample to dryness and heating the residue to 130°C.

Calibrated weights were used throughout. The weights of water were reduced to weights *in vacuo.*

The specific heats of water used in the calculations were obtained from the *International Critical Tables;* at 15°, 25°, 35°, and 45°C. the values are 1.0000, 0.9979, 0.9974, and 0.9976, respectively.

EXPERIMENTAL METHOD

Method of standardization

This method was identical with the method first used by Gucker (1). It may be likened to determining the sensitivity of a chemical balance In the calorimetric analog, a definite weight of water (W_0) is always put into the tare calorimeter while varying weights (W_1) of water are put into the solution calorimeter; on heating the two with similar heaters under adiabatic conditions over a range of 2°C. the deflections of the galvanometer are carefully noted. The uncorrected weight of water always used in the tare calorimeter was 700.00 g., while for the solution calorimeter the weights of water were 705.00, 700.00, and 692.00 g. Two sets of standardizations were necessary because one of the Dewar flasks broke after one month of service; the data, at the temperatures 15°, 25°, 35°, and 45°C., are found in table 1. In the second set of standardizations no runs were made with 700.00 g. (uncorrected) in the solution calorimeter, since it was found that the data of the first set gave a straight line on plotting and there was no reason to suspect that the second set would act differently.

The values of table 1 are given at the approximate mean temperatures of the determinations; the actual mean temperatures were 15.07°, 25.14°, 35.13°, and 44.95°C. A simple calculation shows that no appreciable error is introduced in doing this.

Experimental procedure

For the actual measurement of specific heat, freshly distilled water was cooled to 10–12°C., and 700.00 g. (uncorrected) weighed into the tare calorimeter. The calorimeter was immediately put in its proper place and the wing nuts tightened snugly. Cooled distilled water was likewise weighed into the solution calorimeter and the proper weight of salt added. The solution calorimeter was put in place and the wing nuts tightened. The jacket, cooled to a little below 14°C., was next raised into position. Cold water was added to bring the level of the jacket to the position shown in figure 1. Then, with stirrers operating, the jacket was made ready for the determination by heating to the proper temperature.

The two calorimeters were then heated to the same temperature and to the temperature of the jacket. The temperatures of the calorimeters were adjusted to within 0.0006°C. of each other and to within 0.001°C. of the temperature of the jacket.

About 10 min. after the initial temperature adjustments, readings of the galvanometer deflections were made every 2 min. for 10 min. Then the run was started by closing the switches to the calorimeter and the jacket heaters. The rise in the temperature of the water jacket was noted on the Beckmann thermometer; when this thermometer indicated that a rise of nearly 2°C. had occurred, the current was turned off. About 8 min. were then allowed to insure thermal homogeneity in each calorimeter before the galvanometer deflection was read again. After this the readings were repeated at 2-min. intervals for an "after" period of 10 min., to make sure that a steady state had been reached.

TABLE 1

Water standardization data

DEWAR FLASKS	WEIGHT OF WATER (IN VACUO)	APPROXIMATE MEAN TEMPERATURE			
		15°C.	25°C.	35°C.	45°C.
	grams				
A-B	705.74	+3.93	+4.33	+4.95	+4.56
		+3.70	+4.14	+4.71	+4.00
		+3.78	+4.40	+4.90	+4.05
A-B	700.74	+0.90	+1.03	+1.65	+0.96
		+1.02	+1.30	+1.88	+1.13
A-B	692.73	−3.21	−3.60	−3.22	−3.53
		−3.45	−3.27	−2.89	−3.60
		−3.39	−3.26	−2.95	−3.41
A-C	705.74	+4.20	+4.52	+4.88	+4.25
		+3.88	+4.23	+4.79	+4.27
		+4.02	+4.27	+4.91	+4.34
A-C	692.43	−2.96	−3.02	−2.49	−3.16
		−2.86	−2.95	−2.55	−3.16

During the heating period, the thermels which register the difference in temperature between the calorimeters and bath were connected to the galvanometer, and observations of the scale were made continuously. By occasional slight adjustment of the heating currents, the temperature of the bath was kept to within ±0.008°C. of that of the calorimeters (which themselves seldom differed by more than 0.009°C.). Better agreement was obtained in the "fore" and "aft" periods, and in this way heat transfer between the calorimeters and their surroundings was made practically negligible. When a determination was finished, the apparatus was heated adiabatically (to avoid condensation effects, etc.) to the temperature desired for the next run, thus making it possible to use the same sample of solution for determinations at 15°, 25°, 35°, and 45°C.

TABLE 2

A complete record of a typical determination

August 19, 1929; run Q-2; 0.300 molal potassium chloride; approximate temperature, 35°C.

	TARE	SOLUTION
Calorimeter + contents..	2255.94 g.	2224.50 g. KCl = 15.768 g.
Calorimeter.	1555.94 g.	1503.73 g.
Contents.................	700.00 g. (water)	720.77 g. (solution) 15.77 g. (KCl) 705.00 g. (water)

TIME OF READING	DIFFERENCE	GALVANOMETER READINGS DEFLECTION	CHANGE	TIME FACTOR	TREND
7:18.0		−0.30			
20.0		−0.30			
22.0		−0.34			
24.0	10	−0.36	−0.10 (fore)	7/10	−0.07 (fore)
26.0		−0.40			
28.0		−0.40			
	14		+2.40 (experiment)		
42.0		+2.00			
44.0		+1.98			
46.0		+1.98			
48.0	10	+1.96	−0.08 (aft)	7/10	−0.06 (aft)
50.0		+1.90			
52.0		+1.92			

$\Delta G = +2.40 - (-0.13) = +2.53$ cm.

(Corrected 2°C.) $\Delta G = +2.52$ cm.

Final temperature, 3.910°; initial temperature, 1.910°; rise (uncorrected), 2.000°; rise (corrected), 2.012°

Initial temperature of bath, 34.17°C.; mean temperature, 35.18°C.

A typical experiment

The log of one of the runs employing the Dewar flasks A–C is given in table 2. The average value of ΔG obtained in two runs was +2.53 cm.

TABLE 3

Specific heats of sodium and potassium chloride solutions: summary of experimental results

MOLALITY OF SALT		15°C.		25°C.		35°C.		45°C.	
NaCl	KCl	ΔG	Specific heat	ΔG	Specific heat	ΔG	Specific heat	ΔG	Specific heat
0.01000		+2.12, 3, 7	0.9994	+2.51, 3, 11	0.9971	+3.01, 3, 9	0.9966	+2.44*, 2, 11	0.9974
0.0500		+2.33, 3, 4	0.9962	+2 92, 2, 4	0.9943	+3.33, 3, 4	0.9937	+3.13*, 2, 3	0.9954
0.0700		+2.10, 2, 2	0.9944	+2.73, 2, 10	0.9928	+3.27, 2, 3	0.9923	+2.87*, 2, 2	0.9936
0.1000		+1.85, 2, 0	0.9920	+2.43, 2, 0	0.9903	+2.95, 2, 3	0.9899	+2.78*, 2, 4	0.9916
0.300		+1.37, 2, 4	0.9766	+2.43, 2, 5	0.9762	+3.20, 2, 1	0.9763	+2.97, 2, 4	0.9779
0.713		+1.12, 1, -	0.9493	+2.40, 2, 2	0.9501	+3.65, 2, 2	0.9512	+3.22, 2, 8	0.9518
1.033		−0.54, 1, -	0.9299	+1.18, 1, -	0.9319	+2.59, 1, -	0 9335	+2.45, 1, -	0.9347
	0.01000	+1.26, 1, -	0.9991	+1.35, 1, -	0.9968	+1.95, 1, -	0.9964	+1.39, 1, -	0.9967
	0.0500	+1.34, 2, 4	0.9949	+1.52, 2, 1	0.9929	+2.20, 2, 1	0.9927	+1.58, 2, 5	0.9928
	0.0700	+1.52, 2, 5	0.9925	+1.81, 2, 2	0.9908	+2.50, 2, 2	0.9906	+1.98, 2, 4	0.9910
	0.1000	+1.51, 2, 3	0.9897	+1.86, 2, 2	0.9881	+2.58, 2, 1	0.9880	+1.98, 2, 2	0.9881
	0.300	+1.02, 2, 4	0.9704	+1.62, 2, 4	0.9695	+2.53, 2, 1	0.9699	+1.99, 2, 3	0.9702
	0.699	+0.38, 2, 1	0.9341	+0.54, 2, 1	0.9342	+1.68, 2, 0	0.9351	+1.29, 2, 2	0.9358
	1.027	+3.81, 2, 4	0.9082	+5.28, 1, -	0.9090	+6.75, 1, -	0.9105	+6.43, 1, -	0.9112

* When the apparent molal heat capacities were plotted at 45°C., a distinct minimum was obtained. It is established by the points which are marked. They deviate from the linear portion of the curve by 0.1 per cent. Although this is greater than the experimental error, no reason could be found for these anomalous results. In a later research this range of concentration was studied more carefully. It is planned to present the results of this investigation in the following paper.

(see table 3); from the graph obtained in the water standardization, the weight of water which at 35°C. gives this deflection is 701.64 g. (*in vacuo*). The weight of solution, corrected to the vacuum standard, is 721.52 g., so that the specific heat of the solution referred to water is equal to 701.64 ÷ 721.52 = 0.9724; the specific heat of the solution is thus 0.9724 × 0.9974 = 0.9699.

EXPERIMENTAL RESULTS

In table 3 will be found a summary of the results obtained with the two salts, sodium chloride and potassium chloride, at 15°, 25°, 35°, and 45°C. The first column gives the molality of the salt. Under ΔG will be found (in general) three figures separated by commas; the first is the average deflection of the galvanometer in centimeters, the second gives the number of determinations made, while the third gives the average deviation from the mean in hundredths of a centimeter; thus for 0.0500 molal sodium chloride at 35°C. three runs were made whose average deviation was 0.04 cm., as may be seen from the three figures 3.35, 3.27, and 3.36. Under the column headed "specific heat" will be found the specific heats of the solutions in 15°C. calories (see the section headed "Materials, constants, etc." for the values of the specific heat of water used in these calculations).

DISCUSSION OF RESULTS

The determinations at the lower concentrations of sodium chloride were made first, thus less perfect technique is the most plausible explanation for the larger deviations from the mean noted in these runs; but even if these are included in a calculation of the average deviation for all the runs a value of 0.032 cm. is obtained, distributed as follows: 0.028, 0.035, 0.023, and 0.040 cm. at the respective temperatures 15°, 25°, 35°, and 45°C. This average value, 0.03 cm., corresponds to nearly 0.06 g. of water, as an inspection of table 1 will show; since 700 g. of water is involved in each determination the precision of measurement is seen to be a little better than 0.1 part per mille.

Of all of the runs only two have been omitted from table 3, since the results were definitely out of line with the others made under similar conditions; one of these was at 45°C. and 0.01 molal sodium chloride, the other was at 25°C. and 0.05 molal sodium chloride.

Roughly, the first third of the runs (as listed in table 3) was made with the Dewar flasks A–B. An uncalibrated Beckmann thermometer was used to measure the rise in temperature in these runs, so there may be in some instances an uncertainty of several hundredths of a centimeter in the ΔG values, which may be reduced somewhat because the same thermometer was used in the corresponding water standardizations. The last two thirds of the runs were made with Dewar flasks A–C. In these runs a

Beckmann thermometer which had been carefully compared with one standardized by the Bureau of Standards was employed; the corrections for a 2°C. rise in temperature varied from +0.009 to +0.018°. No correction was made for the varying amount of mercury in the bulb of the thermometer at the different temperatures, but calculations of the magnitude of this correction have been made. A rough average value of ΔG for all of the runs (2.4 cm.) was employed, and it was found that at 15°, 25°, 35°, and 45°C. the final effect on the specific heat on the percentage basis was −0.001, +0.001, +0.002, and +0.004, respectively. It is evident that such corrections are unnecessary in this research.

Some of the runs were made at average temperatures somewhat removed from the nominal values given in table 3; the greatest difference in these two temperatures was 0.22°C., while the average for all the runs was slightly less than 0.1°C., distributed as follows: 0.06°, 0.13°, 0.13°, and 0.08° at the respective temperatures 15°, 25°, 35°, and 45°C. An average value of the temperature coefficient of the specific heat was used to calculate the effect of this error on 1 molal potassium chloride solution at 45°C.; it was found that the specific heat of this solution was changed by 0.002 per cent for a 0.2°C. change in temperature. Therefore no effort was made to correct any of the specific heat values to the rounded temperatures listed, but it is apparent that as the precision of measurement is increased it will become necessary to do so.

The concentrations of the solutions were made with the precision indicated, which was considerably higher than was necessary, as may easily be seen by inspecting table 3.

The weights of water and solution were not corrected for evaporation losses, nor was any correction applied for the different heat input required in the two calorimeters, owing to the different weights of water vaporized during a run. A calculation of this effect was made, using the best data available, but only the result will be given here. For a 1 molal solution at 45°C. it was found that the solution calorimeter would lose at the most 1.75 mg. of water by evaporation, while the tare calorimeter would lose 0.05 mg. more. This weight of water would require about 0.025 calorie for its vaporization, but since the total heat absorbed by the solutions was about 1400 calories, it is seen that such a correction would be superfluous in the present research.

Because of lack of time the present authors were unable to complete the calculations. Therefore empirical equations for the apparent molal heat capacities of these solutions, as well as a discussion of the results, will be found in the following paper, but it may be said here that the specific heats at 25°C. compare favorably with results which are believed to be precise to 0.01 per cent.

SUMMARY

1. A modified twin calorimeter is described in some detail.

2. Specific heats are presented for sodium chloride and potassium chloride solutions at four temperatures. The concentration of the solutions ranged from 0.01 to 1.0 molal.

This research was carried out at the suggestion of and under the direction of Professor Arthur A. Sunier; grateful acknowledgment is here made of his assistance.

REFERENCES

(1) Gucker: J. Am. Chem. Soc. **50**, 1005 (1928).
(2) Joule: Mem. Proc. Manchester Lit. Phil. Soc. (2) 559 (read 1845); Scientific Papers **1**, 192 (Taylor and Francis, London (1884)).
(3) Pfaundler: Sitzsber. Akad. Wiss. Wien **59**, 2145 (1869).
(4) Richards and Gucker: J. Am. Chem. Soc. **47**, 1876 (1925).
(5) Richards and Hall: J. Am. Chem. Soc. **51**, 707 (1929).
(6) White, C. M.: J. Am. Chem. Soc. **58**, 1615, 1620 (1936).
(7) White, W. P.: J. Am. Chem. Soc. **36**, 2292 (1924).

THE SPECIFIC HEATS OF SOME AQUEOUS SODIUM AND POTASSIUM CHLORIDE SOLUTIONS AT SEVERAL TEMPERATURES. II

CHESTER M. WHITE

Department of Chemistry, University of Rochester, Rochester, New York

Received May 10, 1939

In recent years precise specific heats for aqueous salt solutions have been determined principally from 18° to 25°C., although results have been reported at a few higher and lower temperatures. Apparently no attempt has been made to investigate thoroughly the region from 35° to 45°C. This temperature range is particularly interesting, since the specific heat of water is known to pass through a minimum at 38°C. Furthermore, earlier work (9) in this laboratory on sodium chloride solutions seemed to show a departure from the usual linear relation for Φ at 45°C., while the results at 35°C. were definitely linear. It therefore seemed advisable to study the specific heat of dilute sodium chloride solutions at several temperatures in this range. In this paper new measurements are reported at 35°, 38°, 41°, and 45°C. for sodium chloride solutions which varied in concentration from 0.01 to 0.20 molal, and the data of Hess and Gramkee (9) are discussed in considerable detail.

APPARATUS AND MATERIALS

The apparatus used previously (9) was set up in a more suitable laboratory and a few minor changes were made; somewhat better results were obtained under these conditions. The calorimeter stirrers were run at a higher rate of speed (138 R.P.M.). Several coatings of Bakelite varnish were found to make the deKhotinsky seal between the annular ring and the Dewar jar more permanent at 45°C. The top of the annular ring was coated with a thin layer of stopcock grease to insure a water-tight ground joint.

The leakage constants (k = degrees per minute per degree) and the heat of stirring (w = degrees per minute) were determined by obtaining the rate of heating under two thermal heads. With the larger value of k it was difficult to measure the small fraction of the total heat due to stirring. However, the heat of stirring is probably the same in the two units because of the method of operating the stirrers. The approximate heat capacity of a calorimeter unit was determined by the electrical method. The values, which are given in table 1, are the average of several experiments.

TABLE 1

Constants of the apparatus

TEMPERATURE RANGE	SOLUTION k	TARE k	TARE w	HEAT CAPACITY
°C.				*calories per degree*
28–34	0.0021	0.0013	0.00007	102

The solutions were made from Baker's C.P. sodium chloride, which was not further purified, but was dried for several days at 120°C. The solutions were prepared as described in the preceding paper.

PROCEDURE

The only change in the method was to lengthen the "fore" and "aft" periods to 14 min. The value of ΔG was determined graphically from a plot of the galvanometer deflections; this procedure was sufficiently precise in the present case. In the standardization of the calorimeter 700.00 g. of water was always placed in the tare, while the solution calorimeter contained 705, 710, and 715 g. (uncorrected) of water. Several determinations were made with each of these weights of water in the solution calorimeter. The averaged points are plotted for the four temperatures in figure 1. The radii of the circles are proportional to the average deviation of the runs. Probably the error of the standardization runs is about ±0.01 per cent. The equivalent weights of water for the salt runs were obtained from this plot. At frequent intervals during the course of the research a standardization run was made to insure constancy of the apparatus.

The Beckmann thermometer, which was used to measure the temperature rise in all of the determinations, was carefully compared with a thermometer standardized by the Bureau of Standards, and suitable corrections were applied. The temperature rise was also corrected for the varying amounts of mercury in the bulb at the different temperatures; the magnitude of this correction is briefly discussed in the preceding paper.

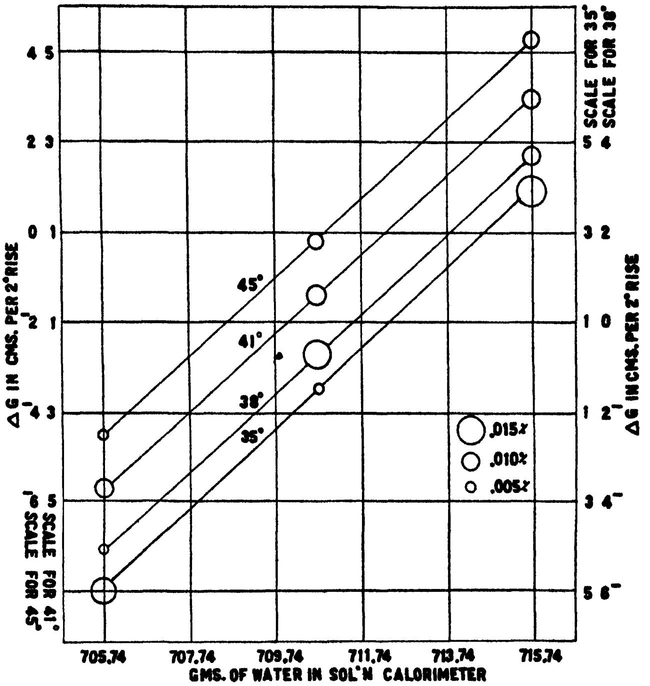

FIG. 1. Plot of water standardization data

RESULTS

In table 2 the data for the sodium chloride solutions are summarized at 35°, 38°, 41°, and 45°C. The first column records the molality and also the weights (*in vacuo*) of the salt and water with which the solution calorimeter was charged. The second column gives the nominal temperature, since the specific heat changes only slightly with the temperature. The third and fourth columns record the ΔG values, which are the average of three determinations (except at 0.01 molal where four runs were averaged) and the average deviation, respectively. The average deviation for all runs is 0.06 cm., which is equivalent to a change of 0.01 per cent in the specific heat. The fifth column gives the specific heat in

TABLE 2

Summary of results for sodium chloride solutions

MOLALITY	TEMPERATURE	ΔG	AVERAGE DEVIATION	SPECIFIC HEAT	Φ	Φ (CALCULATED)
	°C.	cm.	cm.	cal.$_{15°}$ per degree per gram		
0.00999 (salt, 0.416 g.; water, 712.75 g.)	35	1.19	0.07	0.9967	−12.8	−17.5
	38	0.85	0.08	0.9966	−24.8	−19.6
	41	1.22	0.04	0.9966	−22.8	−19.7
	45	1.49	0.07	0.9968	−24.7	−18.7
0.03283 (salt, 1.371 g.; water, 713.49 g.)	35	1.58	0.07	0.9950	−14.6	−16.7
	38	1.35	0.09	0.9950	−15.8	−18.1
	41	1.84	0.11	0.9950	−14.3	−17.9
	45	1.87	0.14	0.9952	−14.0	−17.1
0.04994 (salt, 2.081 g.; water, 712.75 g.)	35	0.69	0.04	0.9935	−19.2	−16.2
	38	0.41	0.05	0.9935	−19.6	−17.3
	41	0.79	0.02	0.9936	−18.4	−16.9
	45	1.03	0.06	0.9938	−18.6	−16.2
0.06993 (salt, 2.917 g.; water, 713.75 g.)	35	1.35	0.07	0.9923	−14.4	−15.8
	38	1.13	0.01	0.9922	−16.9	−16.5
	41	1.56	0.02	0.9923	−15.6	−15.9
	45	1.85	0.01	0.9925	−14.9	−15.4
0.09989 (salt, 4.178 g.; water, 713.75 g.)	35	1.19	0.07	0.9904	−12.7	−15.2
	38	1.03	0.04	0.9902	−14.0	−15.6
	41	1.51	0.04	0.9904	−11.8	−14.8
	45	1.64	0.02	0.9905	−13.6	−14.4
0.1299 (salt, 5.418 g.; water, 713.75 g.)	35	0.86	0.10	0.9879	−15.6	−14.7
	38	0.65	0.06	0.9879	−15.2	−14.7
	41	1.00	0.05	0.9879	−15.5	−13.7
	45	1.28	0.08	0.9881	−15.5	−13.5
0.1598 (salt, 6.668 g.; water, 713.75 g.)	35	0.61	0.04	0.9858	−15.1	−14.3
	38	0.36	0.04	0.9857	−15.4	−14.0
	41	0.96	0.06	0.9861	−12.9	−12.8
	45	1.34	0.03	0.9866	−11.5	−12.8
0.2000 (salt, 8.347 g.; water, 714.75 g.)	35	1.28	0.08	0.9832	−13.4	−13.8
	38	1.25	0.05	0.9834	−12.6	−13.1
	41	1.70	0.02	0.9836	−11.3	−11.7
	45	1.84	0.03	0.9837	−12.2	−11.8

15°C. calories. The specific heat of water was taken as 0.9974 at 35°, 38°, and 41°C., and as 0.9976 at 45°C.

The calculations of Φ were based on the average specific heat values carried to five significant figures; they were then rounded to 0.1 calorie and are given in column six. This rounding process accounts for the occurrence in several instances of different values of Φ when the specific heat is the same at the temperatures 35°, 38°, and 41°C. The calculated Φ values given in the last column were obtained from empirical equations derived from the specific heats (carried to five significant figures), in turn obtained from the individual values of ΔG.

TREATMENT AND DISCUSSION OF RESULTS

Empirical equations were derived for the apparent molal heat capacities by the method of least squares. A given error in the specific heat produces a large percentage error in Φ in dilute solution, but the error rapidly diminishes as the concentration increases (see dotted lines in figure 2). For this reason it is advisable to weight the Φ values in proportion to the concentration before the least squares procedure is applied. Since ΔC_p is defined as $m\Phi$, the weighting may be accomplished by fitting the data expressed as ΔC_p to an empirical equation of the form:

$$\Delta C_p = A'm + B'm^{3/2} + \dots$$

In order to test the procedure the precise results of Randall and Rossini (18) with sodium chloride at 25°C. were treated by this method. Since their Φ values when plotted against $m^{1/2}$ showed a slight but definite curvature, it seemed advisable to fit the data to a parabolic[1] as well as a linear equation. The following equations were obtained:

$$\Phi = -23.36 + 13.28m^{1/2} + 0.50m$$

$$\Phi = -23.95 + 14.41m$$

The probable errors of a single observation from the empirical equations are approximately 0.005 per cent (parabolic) and 0.007 per cent (linear). A curve was constructed from the rounded values of Randall and Rossini, and the probable error of each observation from this curve was found to be about 0.01 per cent. The parabolic equation seems to fit the data

---

[1] Recently Gucker, Ford, and Moser (3) have found that a parabolic equation is necessary to represent adequately their apparent heat capacity data on aqueous solutions of glycine and glycolamide; the form of their equation is

$$\Phi = \Phi^0 + am + bm^2$$

the constants being obtained by a least squares procedure. A similar form of equation was used by Gucker, Pickard, and Planck (4) in connection with heat capacities of sucrose solutions.

more closely than the curve which Randall and Rossini drew. Thus the slope becomes a function of the concentration. Other investigators (5, 27) have shown from heats of dilution that the slope of the curve for sodium chloride is not constant but varies with the concentration.

The present results (table 2) were fitted to linear equations. The constants for the Φ equations are summarized in table 3 for the four temperatures. Also the slopes (B_1) of the corresponding partial molal heat capacity equations are given in the last column of table 3. The two slopes differ by a factor of 3/2. The intercepts for both equations are identical. Plots of the individual runs show no deviations from these equations which are substantially greater than ±0.01 per cent. Also the probable error of a single determination for each equation calculates to ±0.01 per cent.

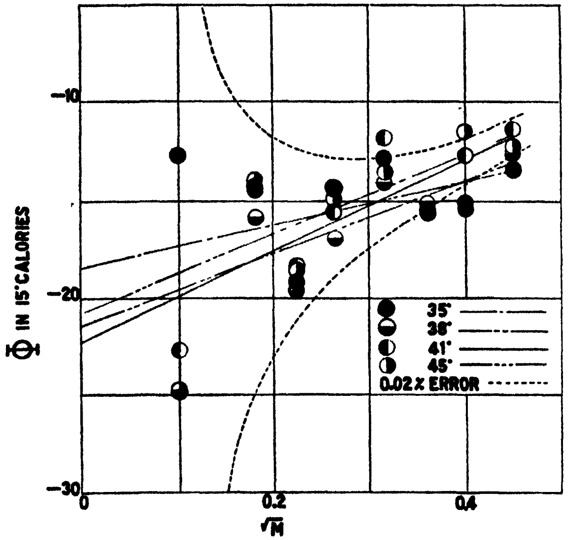

FIG. 2. Plots of the apparent molal heat capacities for sodium chloride solutions

TABLE 3

Constants for the heat capacity equations

TEMPERATURE	A Φ^0 or $\bar{C}^0_{p_2}$	B $d\Phi/dm^{1/2}$	B_1 $d\bar{C}_{p_2}/dm^{1/2}$
°C.			
35	−18.61	+10.83	+16.25
38	−21.42	+18.56	+27.84
41	−22.01	+22.96	+34.44
45	−20.67	+19.81	+29.72

Therefore the equations adequately represent the data. At 45°C. and in the range of concentration up to 0.30 molal the results of Hess and Gramkee indicate a minimum in the Φ *versus* $m^{1/2}$ curve (see figure 3). The present results give a linear equation throughout the range of concentration studied; it has not been possible to ascertain, with certainty, the reason for this discrepancy.

Since the uncertainty in the standardization runs is estimated at ±0.01 per cent, the precision of the heat capacities is placed at ±0.02 per cent. In figure 2 the average values of the apparent molal heat capacities are plotted at the four temperatures. The dotted lines indicate an error of ±0.02 per cent from the 41°C. curve. From this plot it is evident that the four equations as well as the averaged points are almost entirely contained within the dotted lines. These results tend to prove that the apparent molal heat capacities for these dilute solutions remain constant from 35° to 45°C. The precision of the apparatus is not sufficient to resolve the individual Φ curves (if linear) in this range. If there were a transition from a linear curve to one with a minimum, the precision should be sufficient to indicate it.

TABLE 4

*Constants for the heat capacity equations**

Derived from Hess and Gramkee's data

TEMPERATURE	SODIUM CHLORIDE SOLUTIONS				POTASSIUM CHLORIDE SOLUTIONS			
	A Φ^0 or $\bar{C}^0_{p_2}$	B $d\Phi/dm^{1/2}$	B_1 $d\bar{C}_{p_2}/dm^{1/2}$	Probable error	A Φ^0 or $\bar{C}^0_{p_2}$	B $d\Phi/dm^{1/2}$	B_1 $d\bar{C}_{p_2}/dm^{1/2}$	Probable error
°*C.*				*per cent*				*per cent*
15	−27.19	+13.48	+20.22	0.02	−34.18	+12.08	+18.12	0.02
25	−21.46	+11.80	+17.77	0.02	−29.14	+9.85	+14.77	0.02
35	−19.76	+12.28	+18.42	0.01	−24.91	+7.53	+11.30	0.03
45					−24.39	+7.64	+11.46	0.02

* The author wishes to thank Mr. Joseph T. Anderson for the valuable aid which he rendered in connection with the least squares calculations.

TREATMENT AND DISCUSSION OF THE RESULTS OF THE PRECEDING PAPER

In the preceding paper, Hess and Gramkee presented specific heats for sodium chloride and potassium chloride solutions at several temperatures. Their results (except those for sodium chloride at 45°C.) were treated in the same manner as described above. The constants for the empirical (linear) equations for both the apparent and partial molal heat capacities are found in table 4. The probable error of a single determination is given for each temperature.

Plots of the Φ values for sodium chloride and potassium chloride at

15°, 35°, and 45°C. are shown with the corresponding linear equations in figures 3 and 4, respectively, while in figure 5 the 25°C. results for both salts are plotted along with the linear equations. Two runs at 0.01 molal sodium chloride and 25°C. do not appear on figure 5, since they fall off the plot. In figures 4 and 5 results of other investigators are also shown. Omitting the data for sodium chloride at 45°C., there are in all three determinations which deviate from the linear equations by more than 0.04 per cent, while in the case of potassium chloride there are twelve such deviations. The probable errors, recorded in table 4, show on the average about 0.02 per cent. In view of the precision claimed for the specific heat measurements the linear equations adequately represent the data.

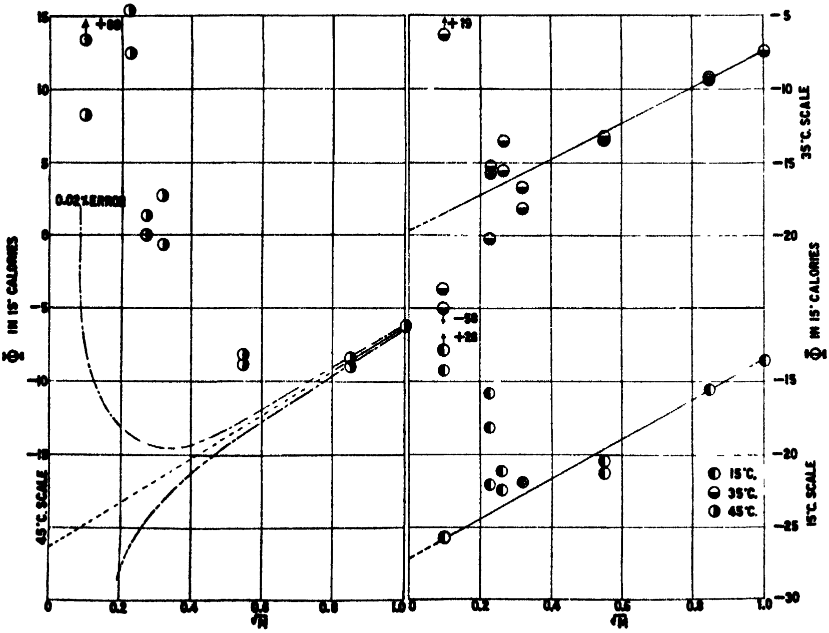

FIG. 3. Plot of Hess and Gramkee's Φ values for sodium chloride solutions at 15°, 35°, and 45°C.

After considering the heat capacity data of the various workers on sodium chloride solutions, it was thought that the $\Phi - \Phi^{0'}$ values which Young and Machin (27) obtained from dilution work constituted the most precise values of the slope at the present time, and that the results of Randall and Rossini (18) based on direct measurements offered the most precise values of Φ itself. By combining the results of these two investigations in a suitable manner, it has been possible to arrive at a series of precise values of Φ with which to compare the present results at 25°C.

In dilute solution Young and Machin have employed the empirical equations of Young and Groenier (26), which were based entirely on the precise dilution work of Gulbransen and Robinson (5). The latter investigators believed that the probable error in their $\Phi - \Phi^0$ values amounted to 10 per cent. Since Young and Machin's results in dilute solution were dependent on their data, it would seem reasonable to assume the same magnitude of error in their $\Phi - \Phi^0$ values up to $m^{1/2} = 0.46$. A constant percentage error in $\Phi - \Phi^0$ implies a corresponding percentage error in the specific heat which varies with the concentration; thus a 10 per cent error in $\Phi - \Phi^0$ changes the specific heat by 0.00011 per cent at 0.01 molal, while at 0.25 molal a change of 0.026 per cent is produced. Randall and Rossini claim a precision of 0.01 per cent over the entire

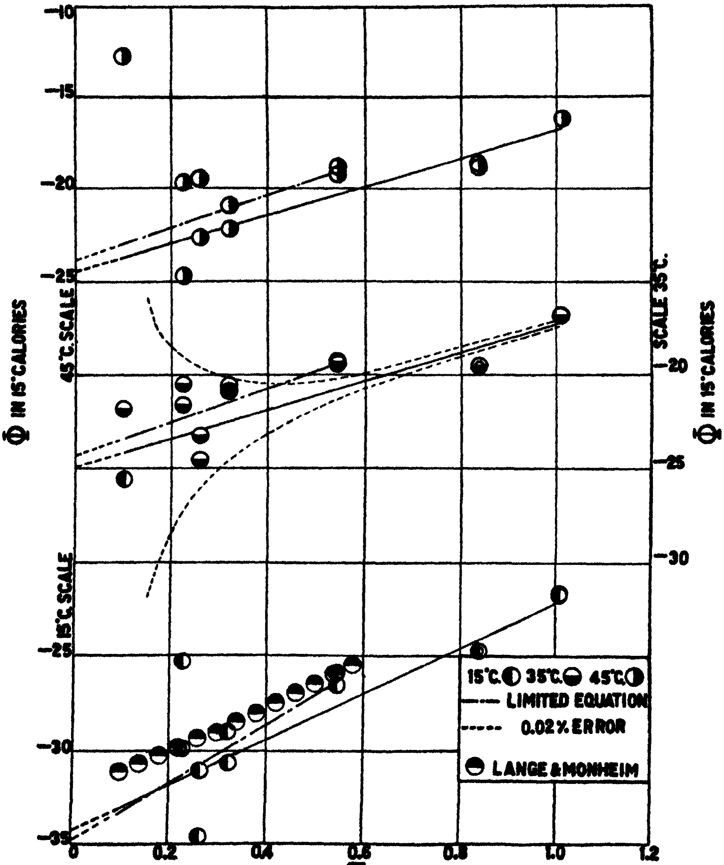

FIG. 4. Plot of Hess and Gramkee's Φ values for potassium chloride solutions at 15°, 35°, and 45°C. and the values of Lange and Monheim at 15°C.

concentration range. To combine these two pieces of data a value of $\Phi - \Phi^0$ was selected from Young and Machin's data at which the precision was believed to be equal to 0.01 per cent. This value (4.40) of $\Phi - \Phi^0$ was equated to the value of Φ computed from the empirical linear equation of Randall and Rossini's data at the same concentration; the resulting value of Φ^0 when combined with the $\Phi - \Phi^0$ values computed from Young and Machin's data leads to the values of Φ given in table 5 and plotted in figure 5, and in this section will be referred to as reference data and curve, respectively. A definite degree of curvatuve is exhibited in the plot of these Φ values. The dotted lines on either side of the curve correspond to a 10 per cent error in the Φ values. Randall and Rossini's linear equation, given above, is also plotted in figure 5 up to $m^{1/2} = 0.6$, and 0.01 per cent error curves are drawn on either side of this straight line. It will be noted that the two sets of dotted lines either cross or become tangent at $m^{1/2} = 0.457$, at which concentration the precision of the direct and indirect measurements is thought to be the same.

TABLE 5

Calculated values of the apparent molal heat capacity of sodium chloride solutions

$m^{1/2}$	Φ	$m^{1/2}$	Φ	$m^{1/2}$	Φ
0.0	−21.76	0.4	−18.03	0.7	−14.19
0.1	−20.98	0.457	−17.36	0.8	−12.73
0.2	−20.10	0.5	−16.84	0.9	−11.20
0.3	−19.12	0.6	−15.57	1.0	−9.63

Possibly the Φ values of table 5 may require a slight temperature correction to make them strictly comparable with 25°C. data, since the $\Phi - \Phi^0$ values computed from Young and Machin's data apply at 18.75°C. It is generally believed that $d\Phi/dm^{1/2}$ either is independent of or changes but slightly with the temperature. Theoretical considerations indicate that the slope of the reference curve at 1.0 molal, for example, would be altered by 0.4 calorie in correcting the data to 25°C. The Φ values of table 5 were recalculated with this correction applied, and the *D* curve in figure 5 shows the percentage difference on the specific heat basis between the corrected and the uncorrected curves. The *R* curve indicates the difference in specific heat between the original reference curve and a second curve whose intercept has been decreased by 0.2 calorie; this curve also indicates the difference between any two Φ curves differing by 0.2 of a calorie throughout.

The *Q* curve in figure 5 shows the percentage difference on the specific heat basis between the curve of Randall and Rossini and the reference curve, and it is quite clear that the results by these two methods agree excellently. It should be noted that the two intercepts and the Φ values at 1.0 molal are in very good agreement. When this agreement is considered in connection with the *R* and *D* curves, further assurance is obtained that $d\Phi/dm^{1/2}$ is either independent of or changes but slightly with temperature. If the difference between Randall and Rossini's and the corrected reference curves is desired, the algebraic sum of the *D* and *Q* curves must be used. The effect of lowering the reference curve intercept by 0.2 of a calorie is shown by curve *Q*′. The parabolic equation given above for Randall and Rossini's data developed by the method of least squares (yielding a probable error of 0.005 per cent) when combined with the dilution data according to the procedure outlined above gave a Φ^0 value of -21.81 and the percentage difference curve falls slightly above curve *Q*; this agreement gives added weight to the correctness of the method outlined above.

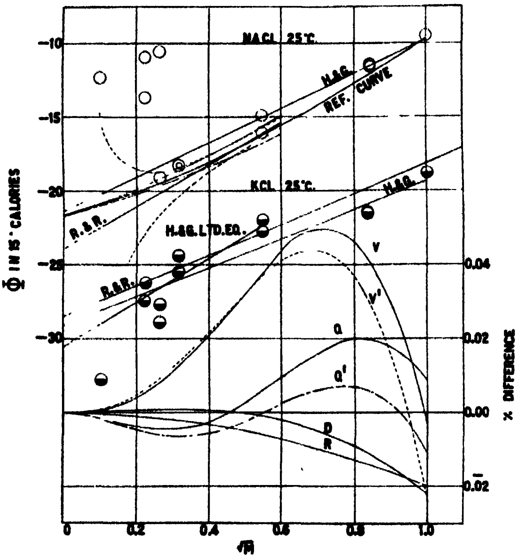

FIG. 5. Comparison of Hess and Gramkee's Φ values for sodium chloride and potassium chloride solutions at 25°C. with those of some other investigators.

In figure 5 the data of Hess and Gramkee at 25°C. are plotted except for the two values of Φ, -66.8 and $+12.8$, at 0.01 molal which did not fall on the plot. The linear empirical equation is also graphed in figure 5. The *V* curve indicates the difference between the reference curve and the linear equation of Hess and Gramkee. The agreement between the two curves is about that indicated by the probable error given in table 4. It should be noted that the intercept and the 1.0 molal value of Φ agree well with the results of other investigators. The *V*′ curve shows the difference between the corrected reference curve and that of Hess and Gramkee, or the sum of curves V and D.

Gulbransen and Robinson have derived a linear equation for Φ by combining their own results with the heat capacity of the solid salt and heat of solution data; their equation is

$$\Phi = -21.90 + 10.5m^{1/2}$$

Combining their value of the slope with the appropriate Φ value from Randall and Rossini in the same manner as described in connection with Young and Machin's work, the following equation was obtained:

$$\Phi = -22.19 + 10.5m^{1/2}$$

Both intercepts are in good agreement with those of Randall and Rossini and the reference work. These equations, valid only to 0.4 molal, deviate at the highest concentration by 0.002 per cent and 0.01 per cent from the reference values, respectively.

Lipsett, Johnson, and Maas (16) have reported specific heats at 20° and 25°C. from their integral heat of solution data and the heat capacity of the solid salt. A linear equation was obtained by the least squares procedure for their 25°C. data (to 1.09 molal); the equation is

$$\Phi = -19.59 + 10.72m^{1/2}$$

The probable error of a single observation from the equation is 0.005 per cent. The average deviation of this equation from the reference Φ values is 0.06 per cent. By means of E.M.F. measurements, Harned and Nims (8) have arrived at Φ values which are in fair agreement with results of other methods up to 0.2 molal but deviate considerably at higher concentrations.

In figure 5 the data of Hess and Gramkee for potassium chloride are plotted along with a straight line through Randall and Rossini's rounded values. The average deviation of the empirical equation from Randall and Rossini's rounded values amounts to 0.036 per cent. Since the determinations at the two highest concentrations show rather large deviations from Randall and Rossini, four linear equations were calculated by the least squares procedure in which the heat capacities at the two highest concentrations were eliminated. The modified equation at 25°C. shows a deviation of only 0.008 per cent from Randall and Rossini's data. The constants for these limited equations (valid to 0.3 molal) are given in table 6, and the equations are plotted in figures 4 and 5. The potassium chloride equations (table 4) at 35° and 45°C. differ by 0.02 per cent at 0.25 molal, while the limited equations differ by less than 0.01 per cent. These results tend to prove that the Φ values for the potassium chloride solusions, like the results for sodium chloride solutions, remain constant over this temperature and concentration range.

Lange and Monheim (13, 14) have reported Φ values at 18.75°C. for potassium chloride solutions from a combination of the temperature coefficient of the integral heat of dilution and the heat capacity of solid salt. Their most recent Φ values were corrected to 15°C. by the temperature coefficient of table 4; the resulting Φ values are plotted in figure 4. The precision of their data is considered to be better than that of Hess and Gramkee. The average deviations of the limited and complete equations from Lange and Monheim's data are 0.008 per cent and 0.02 per cent, respectively.

Other data which did not seem to be sufficiently precise to be discussed here are as follows: the earlier work on sodium chloride and potassium chloride solutions given in the *International Critical Tables* (10), the work of Urban (23), the results of Clews (1) on potassium chloride solutions at several temperatures, and the results of D'Ans and Tollert (2) on sodium chloride and potassium chloride solutions at various temperatures and concentrations above 1 molal.

TABLE 6

Constants for the potassium chloride apparent heat capacity equations valid to 0.3 molal

TEMPERATURE	*A*	*B*
°*C.*		
15	−34.67	+15.30
25	−30.59	+15.01
35	−24.31	+9.07
45	−23.91	+8.89

THEORETICAL SLOPE AND OTHER CONSIDERATIONS

It is generally recognized that dilution data yield the most precise value of the limiting slope ($d\bar{C}_{p_2}/dm^{1/2}$), but since such data are available only at 15° and 25°C. it was thought desirable to calculate the theoretical slopes for a uni-univalent electrolyte from the Debye-Hückel theory at the higher temperatures and compare them with those given in tables 3 and 4, which apparently are the only values in the literature. Values of dV/dT were computed from data given in the *International Critical Tables*, while the Wyman equation (25) supplied the values of dD/dT and d^2D/dT^2. These calculations, carried out by the procedure of La Mer and Cowperthwaite (11), yielded the following results: 15, 16, 17, and 18 at 35°, 38°, 41°, and 45°C., respectively. Any differences between the experimental and theoretical slopes may be accounted for by the probable errors of the experimental results. At 15° and 25°C. the calculations yielded, for the values of the slope, 14 and 13, respectively, which are recorded here for the sake of completeness.

The values of Φ^0 at 25°C. for the individual ions K^+, Na^+, and Cl^- were calculated (assuming the value for K^+ equals that of Cl^-) and found to be −14.6, −6.9, and −14.6, respectively. These values are in good agreement with those given by Pitzer (17) and Rossini (21). The value of Φ^0 for Ba^{++}, computed from earlier data (24), was found to be −44.3.

The temperature coefficient $d\Phi/dT$ at or near room temperature has been assumed by Rossini (21) to be constant for all uni-univalent electrolytes from the most dilute solution to 2.5 molal, and the value employed by him is 0.3 calorie per mole per degree per degree Centigrade. The present results for a 20°C. interval (15° to 35°C.) lead to the value of $d\Phi/dT$ for sodium chloride of 0.3 calorie from 0.1 to 1.0 molal, while for potassium chloride the value was 0.3 calorie, with a variation of ±0.1 calorie. Both sodium chloride and potassium chloride show a zero temperature coefficient from 35° to 45°C. This statement may not be strictly true above 0.2 molal. By inspection of table 4 it is seen that $d\Phi^0/dT$ is positive and of such a magnitude as to be in line with the discussion just given for $d\Phi/dT$.

RELATIVE PARTIAL MOLAL HEAT CONTENTS FOR SODIUM CHLORIDE AND POTASSIUM CHLORIDE SOLUTIONS

Since values of $\bar{C}_{p_2} - \bar{C}^0_{p_2}$ may easily be calculated from data given in table 4 at several temperatures, the Person–Kirchoff relation has been used to compute the relative partial molal heat contents ($\bar{L}_2$) of sodium chloride and potassium chloride solutions at several temperatures from known values of $\bar{L}_2$ at 25° and 18°C., respectively. For sodium chloride solutions at 25°C. Robinson (19), Young and Vogel (29), and Gulbransen and Robinson have reported values of $\bar{L}_2$. Recently Young and Machin have presented data from which $\bar{L}_2$ values can be obtained. They coupled their experimental data in concentrated solutions with the very precise results of Gulbransen and Robinson in dilute solution. In order to calculate $\bar{L}_2$ the S values were plotted against $m^{1/2}$ and the resulting curve was integrated graphically to provide the integral heats of dilution (ΔH_∞). Below 0.15 molal the empirical equation of Young and Groenier (26) was integrated analytically to give the ΔH_∞ values. The $\bar{L}_2$ values at 25°C. were calculated by Rossini's equation (20):

$$\bar{L}_2 = \Delta H_\infty - \frac{Sm^{1/2}}{2}$$

The 25°C. curve in figure 6 was constructed from these values. The $\bar{L}_2$ values at the other temperatures were calculated from these results at 25°C. and the heat capacity data in table 4 by means of the Person–Kirchoff relation.

The necessary heat capacity data were calculated at various concentrations from the linear least squares equations. The average value of $\bar{C}_{p_2} - \bar{C}^0_{p_2}$ was used in the calculations. For the 45°C. values the empirical equation of Hess and Gramkee at 35°C. was used, since it has been shown that the Φ values are independent of temperature to 0.2 molal. The values above 0.2 molal have been enclosed in brackets, since there may be some doubt as to their precision. The results of these calculations are summarized in table 7 and shown graphically in figure 6.

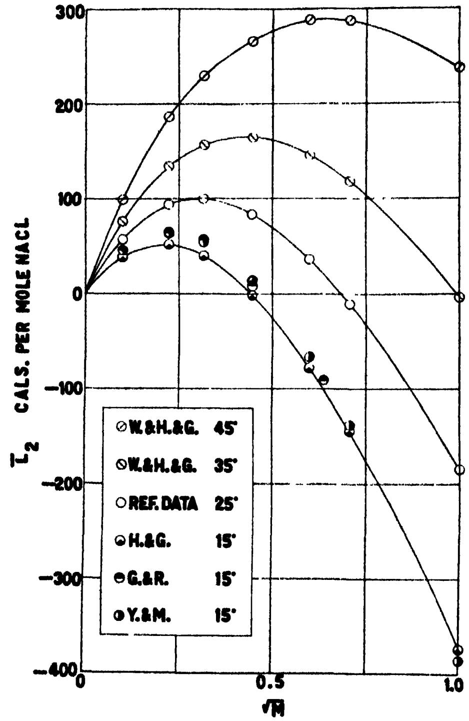

FIG. 6. Curves of calculated $\bar{L}_2$ values for sodium chloride at several temperatures compared with the results of other investigators.

The same procedure which was applied to the results of Young and Machin at 25°C. was employed on their data at 12.5°C. These values at 12.5°C. were corrected to 15°C. by their temperature coefficients; they are given in table 7 and are plotted in figure 6. The $\bar{L}_2$ values of Gulbransen and Robinson at 15°C. are also plotted in figure 6. The calculated values of $\bar{L}_2$ at 15°C. are in good agreement with the work of Young and Machin and Gulbransen and Robinson, showing an average deviation of 11 and 8 calories, respectively.

The results of Harned and Nims as recalculated by Harned and Hecker

(7) are not shown in figure 6. They are in satisfactory agreement with the other data below 0.2 molal; but differences of more than 150 calories are found at 35° and 40°C. (not shown in table 7). An error of 35 calories may exist in their $\bar{L}_2$ values at 1.0 molal because of the uncertainty in dE/dT. Errors of this magnitude are not unusual in comparing E.M.F. and calorimetric data (15). Recently the results of Harned and Nims have been subjected to a second calculation by Harned and Cook (6). The precision of their $\bar{L}_2$ values does not appear to be sufficiently improved to warrant inclusion in table 7 and figure 6.

Rossini (20) has made a critical study of heat of dilution data published prior to 1930 and has presented $\bar{L}_2$ for sodium chloride and potassium chloride at 18°C. in 18° calories. His values for sodium chloride solutions have been calculated to 15°C. by the linear equations of Hess and Gramkee. These results may be said to be in satisfactory agreement with the corresponding data in table 7. Also the $\bar{L}_2$ values at 25°C., which Saxton and Smith (22) computed from Rossini's values at 18°C., are in good agreement with the corresponding values in table 7. These results have not been plotted, since it was felt that they would complicate figure 6. $\bar{L}_2$ values could also be obtained from the data of Lipsett, Johnson, and Maas at 20° and 25°C.; however, these calculations were not made, as it seemed desirable to compare their results on the Φ basis.

TABLE 7

$\bar{L}_2$ values for aqueous sodium chloride solutions at several temperatures

MOLALITY	VALUES OF $\bar{L}_2$				
	15°C. (Y. & M.)	15°C.	25°C. Reference data	35°C.	45°C.
0.01	45.5	38.6	57.6	75.7	99
0.05	64.1	51.6	94.0	134	186
0.10	54.9	40.0	100	157	230
0.20	14.1	−1.3	83.5	164	267
0.36	−65.8	−77.4	36.4	145	(289)
0.50	−138	−144	−10.4	118	(288)
1 00	−387	−375	−185	−4.4	(236)

Values of $\bar{L}_2$ for potassium chloride solutions at 15°, 25°, 35°, and 45°C. were calculated from Rossini's $\bar{L}_2$ values at 18°C., using the partial molal heat capacity equations of Hess and Gramkee and the Person-Kirchoff relation. No attempt was made to correct the results to 15° calories, since the magnitude of the correction was so small. The calculated values and the reference data at 18°C. are recorded in table 8 and plotted in figure 7. Some difficulty was experienced in drawing a smooth curve through the reference data at 18°C., since the values of $\bar{L}_2$ at 0.20, 0.36, and 0.50 molal fell on a straight line.

Recently Young and Seligman (28) have presented empirical S equations at 12.5° and 25°C. for potassium chloride solutions. These equations

TABLE 8

L_2 values for aqueous potassium chloride solutions at several temperatures

MOLALITY	VALUES OF $\bar{L}_2$				
	15°C.	18°C. Reference data	25°C.	35°C.	45°C.
0.01	44	49	61	74	85
0.05	53	64	90	119	144
0.10	46	62	98	139	175
0.20	16	38	90	148	199
0.36	−74	−44	25	103	171
0.50	−140	−105	−24	68	149
1.00	−355	−306	−191	−61	53

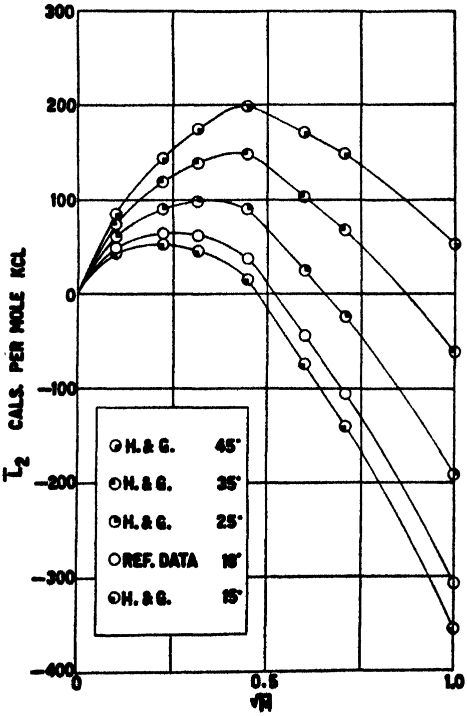

FIG. 7. Curves of calculated L_2 values for potassium chloride at several temperatures

are valid to about 0.1 mole per liter and were derived from the experimental data of Lange and Leighton (12). Following the same procedure which was used above to calculate $\bar{L}_2$ values from the data of Young and

Machin, $\bar{L}_2$ values at 12.5° and 25°C. were obtained from the S equations. The results at 12.5°C. were brought to 15°C. in the usual way. At 15°C. the calculated $\bar{L}_2$ values at 0.01 and 0.05 mole per liter are 41.4 and 51.6 calories, respectively. At 25°C. the $\bar{L}_2$ values at 0.01, 0.05, and 0.10 moles per liter are 52.9, 85.4, and 89.0 calories, respectively. The results at 15°C. seem to be in slightly better agreement with the data of table 8 than the values at 25°C.

The data of Lange and Monheim would also yield values of $\bar{L}_2$ at 12.5° and 25°C. for potassium chloride solutions; however, the necessary calculations were not performed, since it seemed desirable to compare the results on the Φ basis (see figure 4).

A comparison of figures 6 and 7 will show that the sodium chloride and potassium chloride family of $\bar{L}_2$ curves are quite similar in shape. An inspection of tables 7 and 8 will show that the corresponding values of $\bar{L}_2$ for the two salts show fairly close agreement in dilute solution but deviate considerably at higher concentrations. The differences increase as the temperature is raised. The deviations in the two series of curves can be traced to differences in the values of $\bar{C}_{p_2} - \bar{C}^0_{p_2}$ for the two salts, as shown by the values of $d\Phi/dm^{1/2}$ given in table 4.

SUMMARY

1. The twin adiabatic calorimeter method was used to investigate the heat capacities of aqueous sodium chloride solutions at 35°, 38°, 41°, and 45°C. from 0.01 to 0.2 molal with a precision of 0.02 per cent.

2. The apparent molal heat capacities follow a linear relation at the four temperatures when plotted against $m^{1/2}$. It is shown that the earlier results of Hess and Gramkee at 15°, 25°, and 35°C. for sodium chloride solutions and at 15°, 25°, 35°, and 45°C. for potassium chloride solutions follow the same relationship from 0.01 to 1.0 molal. Empirical equations, derived by the method of least squares, are presented for all data.

3. Agreement of the present results and those of Hess and Gramkee with earlier specific heats (where comparable) is found to be satisfactory. Hess and Gramkee's data for sodium chloride at 25°C. are compared with a reference Φ curve constructed (by an apparently new method) from indirect dilution measurements and direct specific heats, and satisfactory agreement is obtained.

4. The experimental slopes are compared with the Debye–Hückel slopes and some other theoretical considerations are given.

5. The Person–Kirchoff equation is used to calculate relative partial molal heat contents for sodium chloride and potassium chloride solutions at several temperatures; where comparable, there is fair agreement among the various sets of data.

The author is very grateful to Professor Arthur A. Sunier for his helpful advice during the investigation and for his assistance in the preparation of the paper.

REFERENCES

(1) CLEWS: Proc. Phys. Soc. (London) **48,** 95 (1936).
(2) D'ANS AND TOLLERT: Z. Elektrochem. **43,** 81 (1937).
(3) GUCKER, FORD, AND MOSER: J. Phys. Chem. **43,** 153 (1939).
(4) GUCKER, PICKARD, AND PLANCK: J. Am. Chem. Soc. **61,** 459 (1939).
(5) GULBRANSEN AND ROBINSON: J. Am. Chem. Soc. **56,** 2637 (1934).
(6) HARNED AND COOK: J. Am. Chem. Soc. **61,** 495 (1939).
(7) HARNED AND HECKER: J. Am. Chem. Soc. **55,** 4838 (1933).
(8) HARNED AND NIMS: J. Am. Chem. Soc. **54,** 423 (1932).
(9) HESS AND GRAMKEE: J. Phys. Chem. **44,** 483 (1940).
(10) *International Critical Tables.* McGraw-Hill Book Co., New York (1928).
(11) LAMER AND COWPERTHWAITE: J. Am. Chem. Soc. **55,** 1004 (1933).
(12) LANGE AND LEIGHTON: Z. Elektrochem. **34,** 566 (1928).
(13) LANGE AND MONHEIM: Z. Elektrochem. **35,** 29 (1929).
(14) LANGE AND MONHEIM: Z. physik. Chem. **A150,** 349 (1930).
(15) LANGE, MONHEIM, AND ROBINSON: J. Am. Chem. Soc. **55,** 4733 (1933).
(16) LIPSETT, JOHNSON, AND MAAS: J. Am. Chem. Soc. **49,** 1940 (1927).
(17) PITZER, J. Am. Chem. Soc. **59,** 2365 (1937).
(18) RANDALL AND ROSSINI: J. Am. Chem. Soc. **51,** 323 (1929).
(19) ROBINSON: J. Am. Chem. Soc. **54,** 1311 (1932).
(20) ROSSINI: Bur. Standards J. Research **6,** 791 (1931).
(21) ROSSINI: Bur. Standards J. Research **7,** 47 (1931).
(22) SAXTON AND SMITH: J. Am. Chem. Soc. **54,** 2626 (1932).
(23) URBAN: J. Phys. Chem. **36,** 1108 (1932).
(24) WHITE: J. Am. Chem. Soc. **58,** 1615 (1936).
(25) WYMAN: Phys. Rev. **35,** 623 (1930).
(26) YOUNG AND GROENIER: J. Am. Chem. Soc. **58,** 187 (1936).
(27) YOUNG AND MACHIN: J. Am. Chem. Soc. **58,** 2254 (1936).
(28) YOUNG AND SELIGMAN: J. Am. Chem. Soc. **60,** 2379 (1938).
(29) YOUNG AND VOGEL: J. Am. Chem. Soc. **54,** 3030 (1932).

X-RAY STUDIES OF CRYSTALLITE ORIENTATION IN CELLULOSE FIBERS. III

FIBER STRUCTURES FROM COAGULATED CELLULOSE[1]

WAYNE A. SISSON

Boyce Thompson Institute for Plant Research, Inc., Yonkers, New York

Received August 30, 1939

It is well known that crystallite orientation may be closely correlated with the physical, chemical, and optical properties of cellulose fibers. The laws which govern the production of crystallite orientation in synthetic fibers, therefore, are not only of theoretical interest but also of practical importance. For example, the tensile strength and elongation of rayon fibers may change several hundred per cent as the orientation is varied from a random to a parallel orientation. The usual method of increasing orientation in rayons is by stretching. This produces an alignment of the major (*b*) axes of the cellulose crystallites parallel to the direction of stretching. The cellulose crystallite also possesses a secondary or minor orienting tendency, as shown by the fact that a minor axis [101] of the crystallite is oriented parallel to the direction of shrinkage when swollen cellulose is dehydrated (3).

It is the purpose of the present paper to extend the previous investigations on the orientation behavior of the native cellulose crystallite (2, 3) to that of the hydrate cellulose crystallite which exists in fibers produced from coagulated cellulose, to study separately and collectively the factors which affect the production of orientation, and to formulate into a rule the general orientation behavior of cellulose. The paper is divided into four parts: (*a*) the effect of shrinkage produced by dehydration, (*b*) the effect of mechanical deformation, (*c*) discussion of the combined effects of shrinkage and deformation in producing the various types of orientation, and (*d*) citation of the orientation found in Cellophane and rayons as an application of the above factors.

MATERIALS AND METHODS

The majority of samples examined were prepared either from alcohol–benzene-extracted and Kiered cotton or from commercial wood pulp which was dispersed and coagulated from viscose solutions as recommended by Snell (5). The general orientation behavior was also checked on cellulose coagulated from cuprammonium, quaternary ammonium hydroxide, and phosphoric acid, and also on cellulose regenerated from the acetate and nitrate derivatives. After subjecting the hydrate cellulose thus formed to various restricted conditions during drying, the final dried samples were examined with x-rays as described in the earlier publications (2, 3, 4). The Cellophane and rayon samples examined were of the usual commercial variety.

---

[1] Presented before the Division of Cellulose Chemistry at the Ninety-third Meeting of the American Chemical Society, held at Chapel Hill, North Carolina, April 12–15, 1937. This paper is a contribution from the Cellulose Department of the Chemical Foundation, located at the Boyce Thompson Institute for Plant Research, Inc., Yonkers, New York.

Since the present investigation represents a large number of individual experiments performed under varying conditions over a period of several years, space does not permit a detailed description of each; only a few experiments are described and a summary of the results is given. The terms for the various types of orientation (random, uniplanar, selective uniplanar, uniaxial, and biaxial) are used as defined in the earlier paper (3). Instead of representing the results with stereographic projections, however, they are illustrated by drawings of the unit cell (figure 1 A). The orientation of the unit cell is located by the *b*-axis (direction of cellulose chain) and the 101 plane which is shaded in the drawing. The minor axis [101] is perpendicular to the 101 plane. The x-ray diagram of hydrate or mercerized cellulose is represented in figure 1 B. The concentric rings of increasing diameter in the diagram are the 101, 10$\bar{1}$, and 002 diffraction lines, respectively.

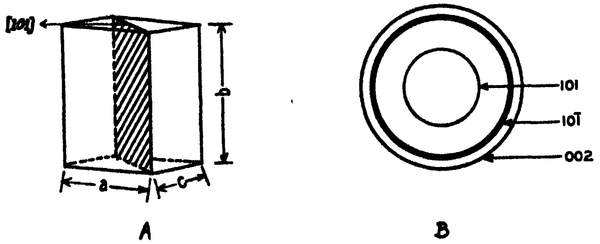

FIG. 1. Schematic representation of unit cell (A) and x-ray diagram (B) of hydrate cellulose (see text for explanation).

SHRINKAGE

Coagulated cellulose, when first formed, is usually in a highly swollen condition. The present observations would indicate that the equilibrium condition of a swollen sample is random orientation. Upon dehydration, produced either by chemical reagents, or by drying, considerable shrinkage in volume takes place, and, simultaneously with this shrinkage, orientation is produced. The type of orientation is apparently governed by the direction of shrinkage, and the degree of orientation by the degree or percentage of that shrinkage. The x-ray results on shrinkage are summarized in figure 2.

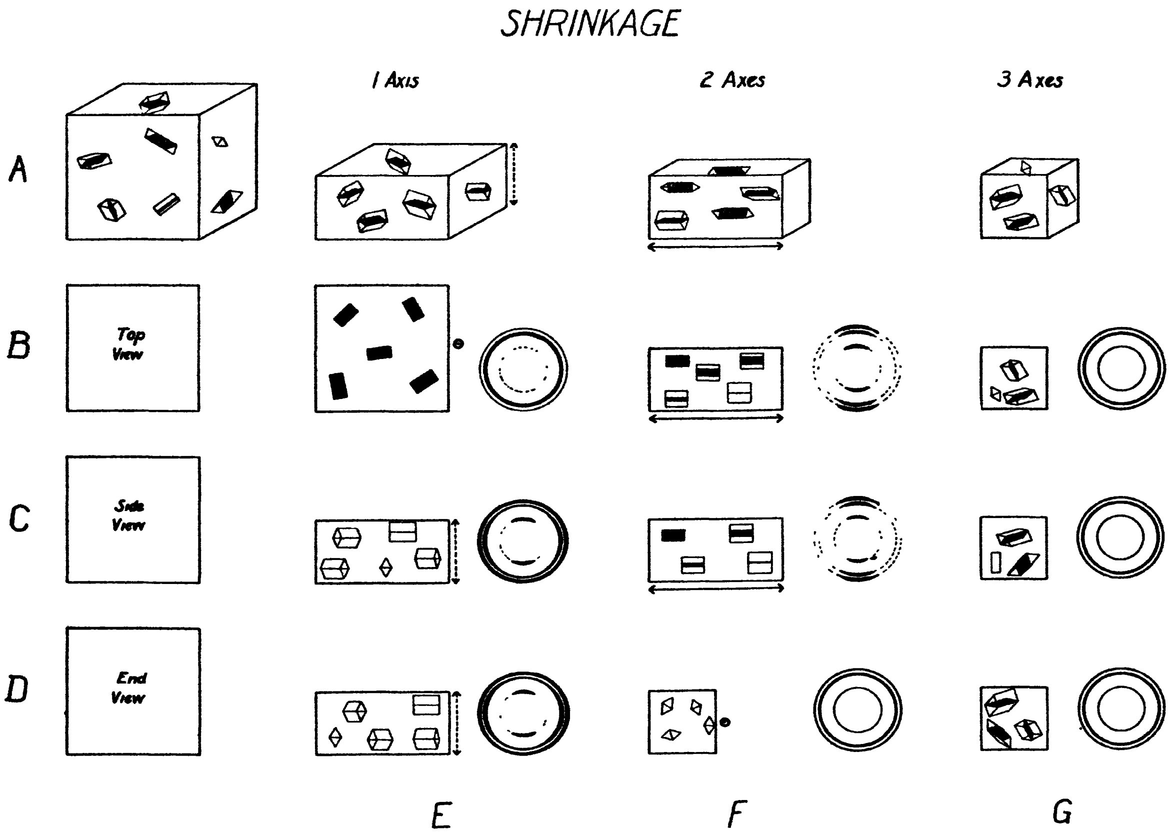

FIG. 2. Schematic representation of type of orientation and corresponding x-ray diagrams obtained when swollen hydrate cellulose shrinks along various axes (see text for explanation).

In figure 2A, a cube of swollen coagulated cellulose having random orientation is diagrammatically represented in the upper left-hand corner. The types of orientation obtained when the cube shrinks along different axes are represented diagrammatically in the vertical columns E, F, and G. The corresponding x-ray diagrams are shown with the sketches. The horizontal columns A, B, C, and D show the orientation and x-ray diagrams when viewed from different positions. Arrows indicate the direction of fiber axes; solid lines represent major axes (orientation of *b*-axes of unit cell), while dotted lines represent minor axes (orientation of perpendiculars to 101 plane of unit cell). Thus, figure 2BE refers to the orientation produced by shrinkage in one direction when viewed from the top (axis of shrinkage).

If the cube shrinks along one axis (figure 2AE), the 101 planes are oriented perpendicular to the direction of shrinkage, but there is random arrangement of the *b*-axes about this direction. When viewed from the top (figure 2BE), the 101 planes are parallel to the top surface.[2] Since diffraction is possible from the 101 planes only when they form an angle of 6° with the x-ray beam, these planes are not in a diffracting position, hence the 101 line is absent in the diffraction pattern. The $10\bar{1}$ planes, which form an angle of slightly less than 90° to the 101, are in a diffracting position and an intense $10\bar{1}$ line is present showing random orientation. When viewed from the side (figure 2CE) the 101 planes, being parallel to the top surface, are now in a diffracting position, as evidenced by two meridian reflections in the x-ray diagram (minor fiber axis parallel to shrinkage axis). The $10\bar{1}$ and 002 planes diffract only when the unit cells are approximately end-on. Since the $10\bar{1}$ and 101 planes intersect at an angle of less than 90°, the $10\bar{1}$ planes thus diffract near the equator in four positions which merge to form two equatorial arcs. The 002 planes behave in a similar manner, with the exception that the 002 arcs are much broader. The end view (figure 2 DE) is the same as the side. As in the previous paper (3), the type of orientation resulting from shrinkage along one axis will be referred to as a selective uniplanar orientation, because the only limitation imposed is that the 101 planes be oriented parallel to a plane (surface) which is perpendicular to the direction of shrinkage.

If shrinkage takes place in two directions[3] (figure 2AF), the *b*-axes of the unit cells are oriented parallel to the axis which did not shrink, but the unit cells have random orientation around their *b*-axes. When viewed from the top (figure 2 BF), the 101, 10$\bar{1}$, and 002 planes all diffract, giving equatorial reflections (fiber axis parallel to direction which did not shrink). The same orientation is present when viewed from the side (figure 2 CF). When viewed from the end (figure 2 DF), the direction is parallel to the *b*-axes of the unit cells (fiber axis), and the 101, 10$\bar{1}$, and 002 planes all diffract, showing a random orientation. This type of orientation resulting from shrinkage along two axes will be referred to as a uniaxial orientation, because the only limitation imposed is that the *b*-axes of the unit cell be oriented parallel to an axis (fiber axis).

---

[2] In drawing the x-ray diagrams the x-ray beam is assumed to pass through the sample in the same relative position as the direction of view. The diagrams are drawn with a considerable deviation from the preferred type, since a large deviation was found in all of the experimentally prepared samples.

[3] In referring to shrinkage along two axes it is implied that shrinkage also takes place at all angles in a plane containing these two axes, which are located at 90° to each other.

If shrinkage takes place in all directions (figure 2 AG), the unit cells are oriented in all directions, and there is random orientation when viewed from any direction.

DEFORMATION

Another property of swollen coagulated cellulose is that it can be deformed, either by tension or pressure, to produce preferred orientation. Figure 3 summarizes the results obtained by elongation and contraction.

In figure 3 a cube of swollen material, showing random orientation, is represented diagrammatically in the upper left-hand corner. If the cube is elongated along one axis and allowed to contract only along one axis (figure 3 AE), then the *b*-axes of the unit cells are oriented parallel to the axis of elongation and the 101 planes perpendicular to the axis of shrinkage. When viewed from the top (figure 3 BE), the *b*-axes are oriented parallel in a horizontal direction (fiber axis), while the 101 planes are parallel to the top surface. As a result, the 101 planes are not in a diffraction position; the 10$\bar{1}$ and 002 planes, however, do diffract, each giving two equatorial reflections. When viewed from the side (figure 3 CE), the 101 planes diffract, giving two equatorial reflections, while the 10$\bar{1}$ planes are not in a diffracting position. When viewed from the end (figure 3 DE), the 101 planes diffract at the meridian (minor axis); the 10$\bar{1}$ planes diffract at the equator, and the 002 diffract in four positions, two of which merge with the result that two broad equatorial arcs are formed. This type of orientation, produced by shrinkage on one axis and elongation on one axis, will be referred to as biaxial or selective uniaxial orientation, because the *b*-axes of the unit cells are oriented parallel to an axis (major fiber axis) and the 101 planes are oriented parallel to a plane containing the major axis (minor fiber axis perpendicular to plane).

If the cube is elongated along one axis, and contracted along two axes (figure 3 AF), then the *b*-axes of the unit cell are oriented parallel to the axis of elongation (fiber axis), with the 101 planes rotated at random around the *b*-axes. This type of uniaxial orientation is the same as that obtained by shrinkage along two axes (figure 2 AF). When viewed from the top (figure 3 BF) or side (figure 3 CF), all three planes diffract to give

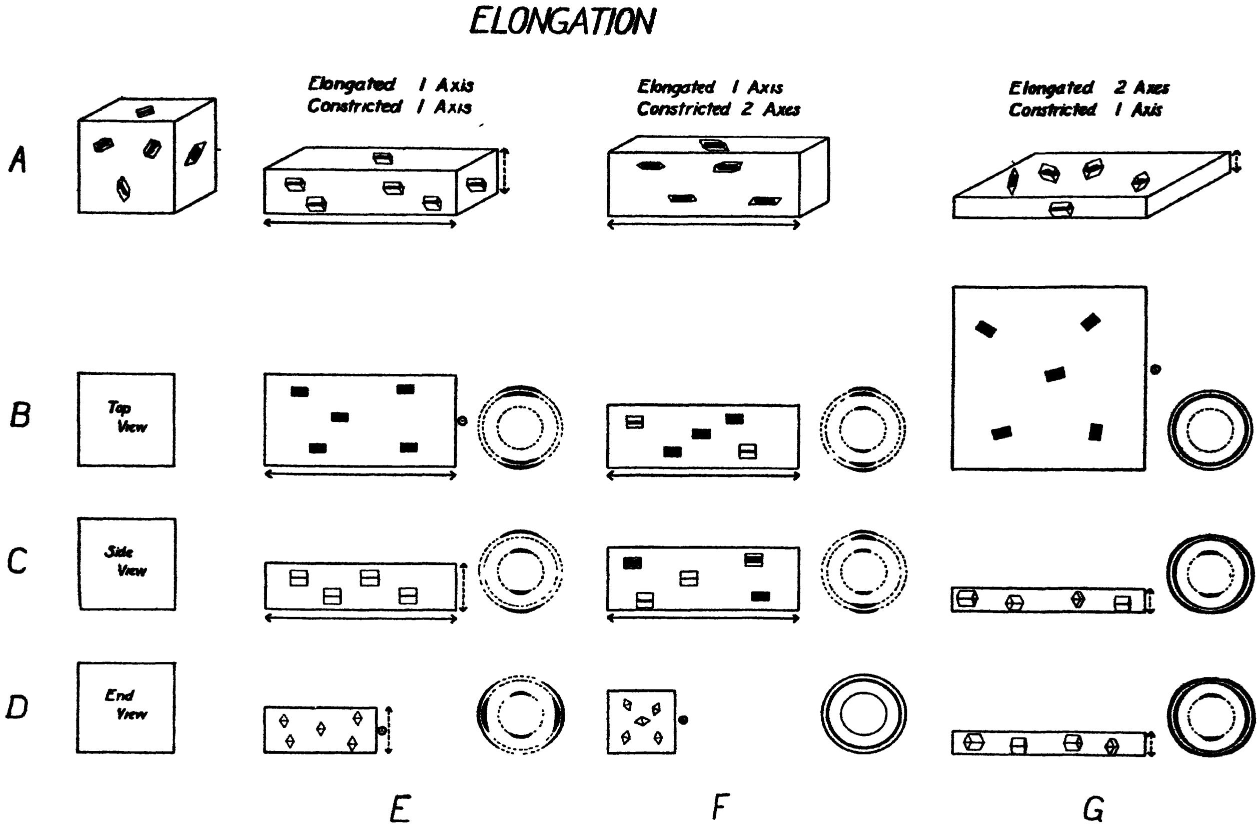

FIG. 3. Schematic representation of type of orientation and corresponding x-ray diagram obtained when swollen hydrate cellulose is deformed along various axes (see text for explanation).

equatorial reflections; when viewed end-on, all planes diffract to give a random orientation.

If the cube is elongated in two directions and contracted along a third axis (figure 3 AG), the same type of selective uniplanar orientation is obtained as when shrinkage occurs along one axis (figure 2 AE); the 101 planes are oriented perpendicular to the axis of contraction with the *b*-axes oriented at random in a plane perpendicular to the axis of contraction.

DISCUSSION

The results obtained by either shrinkage or elongation are summarized in figure 4. A random orientation is obtained in the swollen condition or by shrinkage (S) along three axes; uniaxial orientation by shrinkage along two axes, or by elongation (E) on one axis and shrinkage along two; uniplanar orientation by shrinkage along one axis, or by elongation on two axes and shrinkage along one; and biaxial orientation by shrinkage along one axis and elongation along one axis.

It is difficult to evaluate separately the effect of shrinkage and deformation, since the two always act collectively in producing a dry sample necessary for x-ray diffraction analysis. The most tangible factor which may be correlated with the production of orientation appears to be the relative change in sample dimensions. In terms of dimensional changes, the following general conclusion may be drawn: Whenever there is a relative increase in dimension of a sample in one direction, the *b*-axes of the unit cell tend to orient parallel to that direction; if there is a relative decrease in dimension in one direction, the 101 planes are oriented perpendicular to that direction. The degree of orientation in each case is proportional to the relative change in dimensions of the sample. If one cares to think in terms of the cellulose chain instead of the unit cell, the cellulose chain tends to orient parallel to the direction of increase, while the hydroxyl groups of the glucose unit tend to rotate in the direction of decrease.

All four types of orientation have been produced experimentally: random orientation by permitting a sample to dry while supported on a blotter or mercury; uniaxial by stretching a fiber or allowing it to dry with ends fixed; uniplanar by pressing or allowing a film to dry on a glass plate so that it shrinks only in thickness; and biaxial by rolling or pressing a sample in a groove, so as to elongate along one axis and shrink along one axis. The experimental conditions necessary for the production of these different types of orientation have been given in greater detail in an earlier paper (3). In each sample there is a rather wide deviation from its preferred type of orientation.

After a given type of orientation is formed, it is possible in some instances to change from one type to another. For example, if a uniplanar sample

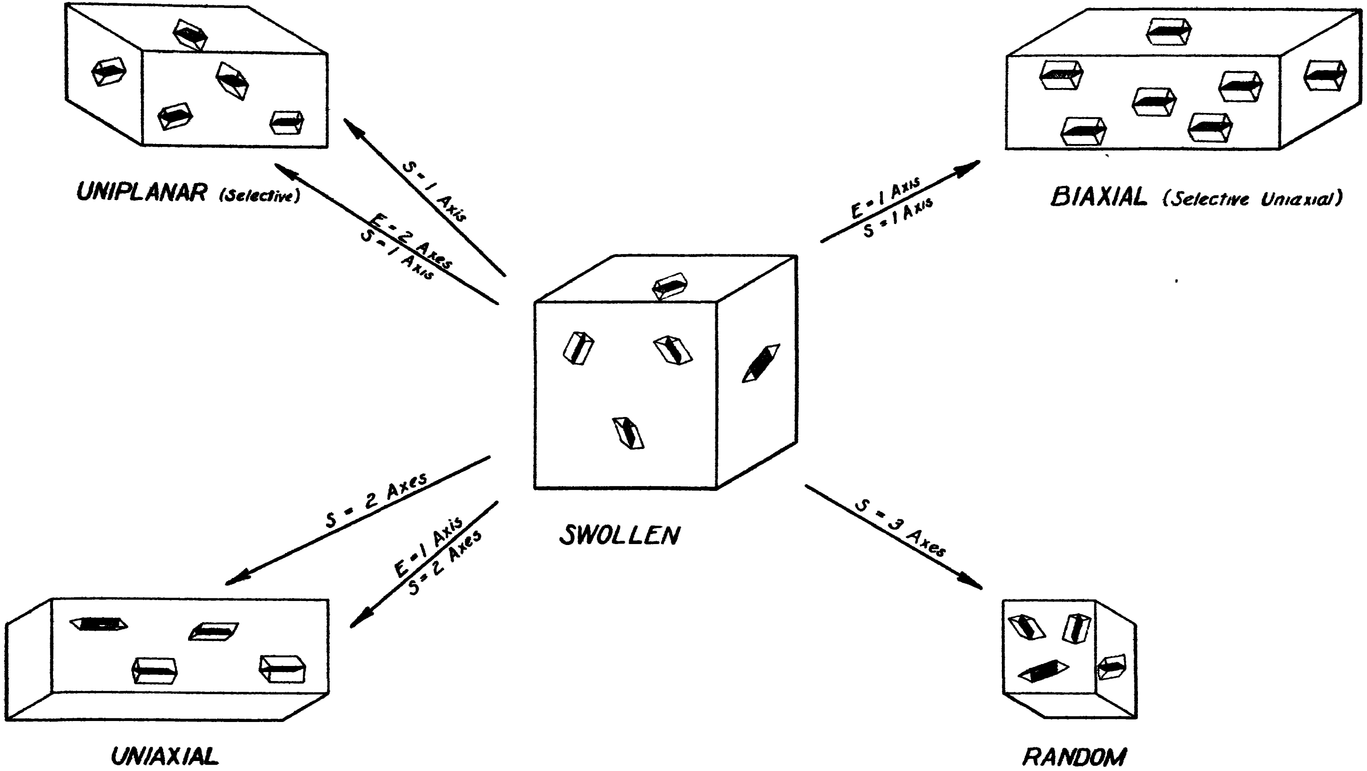

FIG. 4. Schematic representation of various types of orientation and how they may be obtained from swollen cellulose (see text for explanation).

is stretched (perpendicular to fiber axis) it is changed first into an imperfect biaxial and eventually into a uniaxial orientation. If uniaxial or biaxial oriented samples are pressed (perpendicular to fiber axis), they are changed into a uniplanar orientation.

Preliminary results indicate that certain general laws of swelling are closely related to the above general laws of shrinkage and deformation. It is obvious, however, that a distinction must be made between inter- and intra-crystalline swelling or shrinkage. In reswollen samples where only intercrystalline swelling is involved, shrinkage or deformation may not produce the same quantitative effect as in freshly coagulated samples. These and related factors pertaining to the mechanism of cellulose orientation are being investigated further.

APPLICATIONS

The present discussion of the orientation found in industrial samples produced from coagulated cellulose will be limited to Cellophane and viscose rayons.

Cellophane

If the x-ray beam is passed perpendicular to the surface of Cellophane, the 101 line is missing, while the $10\bar{1}$ and the 002 show a random orientation. With the beam parallel to the plane of the sheet, the 101 line now appears as two strong intensity maxima, and the $10\bar{1}$ as two weaker intensity maxima at right angles to the 101, while the 002 shows two broad intensity maxima in the same quadrants as the $10\bar{1}$. This type of pattern, as previously pointed out, is typical of a selective uniplanar orientation (figure 2 AE or 3 AG), which may be produced either by shrinkage along one axis or by elongation along two and shrinkage along one. This selective orientation may be anticipated, since the principal shrinkage takes place perpendicular to the sheet in the usual commercial method of producing Cellophane.

In sheets of commercial Cellophane, the above type of orientation is often found in a modified form. For example, the selective orientation of the 101 plane may be less perfect, or there may be a preferred orientation of the *b*-axes in the plane of the sheet. Figure 5A is the x-ray diagram made near the edge of a sheet of Cellophane, with the beam perpendicular to the flat surface. The 101 line is missing, but the $10\bar{1}$ line does not have a completely random orientation. This condition is typical of a uniplanar orientation with a slight tendency toward a biaxial orientation, and it probably originated during the production of the sheet by an equivalent shrinkage or elongation along an axis lying in the plane of the Cellophane sheet.

The existing type of orientation can be modified also by deformation in the dry condition. Figure 5 B is the x-ray diagram (beam perpendicular to surface) of the same sample as figure 5 A after 10 per cent elongation, produced by stretching a strip of the Cellophane. The 101 now appears as a faint arc, and the 10$\bar{1}$ is more sharply oriented,—the orientation is beginning to change to a uniaxial orientation. After 30 per cent elongation (figure 5 C), all lines are present as sharp intensity maxima,—the orientation is uniaxial. If the sample is treated with steam and allowed to shrink, the orientation does not completely reverse itself. There is a "hysteresis effect" with the uniaxial orientation tending to be more pronounced on the return curve. By repeating the process of stretching and relaxing, it is possible to change the orientation without the usual corresponding change in dimensions of the sample.

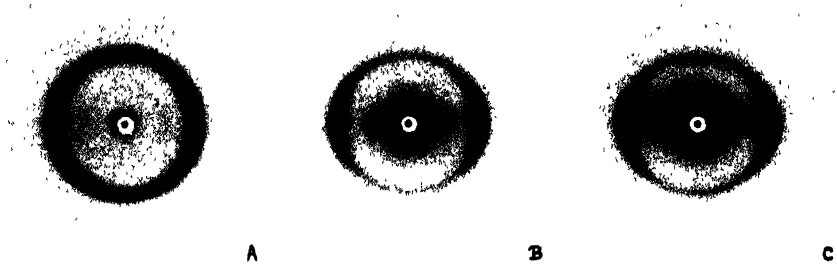

FIG. 5. X-ray diagrams of Cellophane with x-ray beam perpendicular to sheet: A, unstretched; B, stretched 10 per cent; C, after stretching 30 per cent.

Rayons

In the industrial production of rayons, deformation is usually followed by or produced simultaneously with shrinkage; the two factors either reinforce or oppose each other, thus complicating the situation and making it difficult to evaluate the factors which influence the production of orientation. Many workers have assumed that the orientation present in unstretched rayon filaments is produced before coagulation, while the viscose is passing through the spinnerette, and that the rôle of the coagulating agent is primarily to "fix" the orientation already present. Although orientation may be produced in the spinnerette, the present results indicate that the degree and type of shrinkage is the more important factor in producing the final orientation in the dried filament. The composition and length of spinning bath, rate of spinning, and filament diameter all have a pronounced influence, but here, too, the orientation can be correlated to a certain degree with the change in dimensions of the fiber during the coagulating and drying process. In figure 6 there is represented diagrammatically the cross section (figure 6 AD), orientation (figure 6 BD), and the x-ray diagram (figure 6 CD) of a swollen rayon fiber. Al-

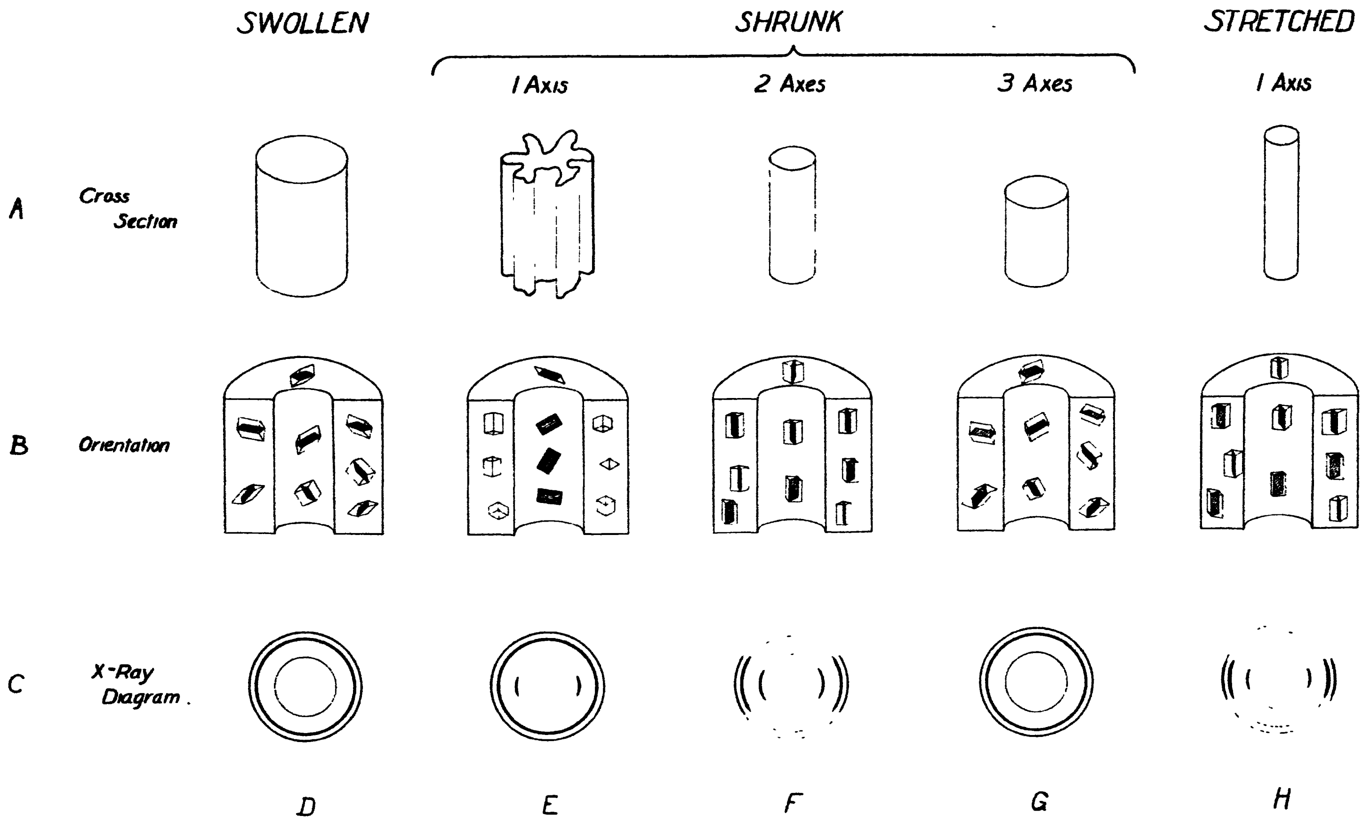

FIG. 6. Schematic representation of cross section, type of orientation, and x-ray diagram obtained when rayon filaments shrink along various axes (see text for explanation).

though shrinkage along one axis[4] could occur either in the longitudinal, tangential, or radial direction, only the latter possibility will be considered. Figure 6 AE represents the probable effect of shrinkage only in the radial direction. Since the circumference of the fiber does not change, the cross section could assume any shape between the serrated type (figure 6 AE) and a flat ribbon-like type. As pointed out in a previous section, radial shrinkage should produce a selective uniplanar orientation with the 101 planes parallel to the filament surface and the *b*-axes randomly arranged in a plane parallel to the surface. With the x-ray beam perpendicular to the fiber axis, the 101 line should exist as equatorial reflections and the $10\bar{1}$ as a random orientation (figure 6 CE).

In the case of shrinkage along two axes, there are also three possibilities, only one of which is represented,—shrinkage in the radial and tangential direction (figure 6 AF). This produces a uniaxial orientation with the *b*-axes parallel to the fiber axis; all three planes diffract as intensity maxima on the equator (figure 6 CF).

Shrinkage along three axes (figure 6 AB) can occur in only one way to produce a random orientation.

In the case of elongation, there is only one direction in which a rayon fiber can be stretched,—in the direction of the fiber axis, which tends to produce a uniaxial orientation parallel to the fiber axis (figure 6 AH). In practice, however, any combination of the seven shrinkage possibilities may have begun to occur or may be in the process of occurring while elongation is taking place, giving a large number of possibilities, the detailed discussion of which space does not permit.

Each type of orientation illustrated in figure 6 has been produced experimentally. Figure 7 A is the x-ray diagram of a viscose fiber spun and allowed to dry without tension. All of the diffraction lines show a random orientation. Figure 7 B is a fiber spun under the same conditions, with the exception that the ends of the fiber were fastened to a support immediately after coagulation so that longitudinal shrinkage was prohibited. The 101 diffraction line shows some orientation, while the $10\bar{1}$ and 002 have a random orientation. In figure 7 C the fiber was stretched and allowed to dry under tension. All of the x-ray lines exist as equatorial arcs indicating a uniaxial orientation.

The two latter types of orientation described above may be identified in samples of commercial rayons,—the second (figure 7 B) in older types, and the third (figure 7 C) in modern viscose fibers. The x-ray diagram of a viscose rayon (older type, 1928) is shown in figure 8 A. The 101 line exists as a much shorter arc than either the 10$\bar{1}$ or the 002 line. This type of diagram, which is similar to that of figure 7 B, can be interpreted on the basis of a selective uniplanar orientation, which would result if the fibers were spun without tension, and if, during the formation of the filament, shrinkage were confined largely to the radial direction (figure 6 AE). For a selective uniplanar orientation, the 101 planes would be parallel to the filament surface and hence in a diffracting position only in the side section of the fiber. As a result the 101 lines would exist as equatorial reflections. The 10$\bar{1}$ planes, on the other hand, would be in a diffracting position only at the front and back of the fiber, and since the *b*-axes are arranged at random in the surface, the 10$\bar{1}$ line has a random orientation.

---

[4] In rayons also, shrinkage will be considered in terms of a small cube located at any section of the fiber. Thus, in shrinkage along one axis in the radial direction, all the shrinkage axes of the cubes would point inward toward the center of the fiber similar to the spokes of a wheel.

If this interpretation is correct, the orientation in the surface of an unstretched rayon filament is similar to that in the surface of a Cellophane sheet and it should be possible to synthesize the same type of x-ray diagram by rotating a strip of Cellophane. Figure 8 B is the x-ray diagram of a sheet of Cellophane having a selective uniplanar orientation, as shown diagrammatically in figure 8 F, with the x-ray beam parallel to the plane of the sheet. The 101 planes, being parallel to the surface, diffract strongly as intensity maxima on the equator, the 10$\bar{1}$ faintly on the meridian. Figure 8 C is the x-ray diagram with the beam perpendicular to the plane of the Cellophane sheet. The 101 plane is not in a diffracting position, but the 10$\bar{1}$ plane is in a diffracting position giving a random orientation (figure 8 G). If, therefore, this sheet of Cellophane is rotated during exposure, statistically it should pass through all the angles to the x-ray beam at which sections of the rayon wall are oriented. Figure 8 D is the x-ray diagram of the sheet rotated through 360° on a goniometer during exposure. The rotation diagram is almost identical with that of the viscose fiber (figure 8 A). Radial shrinkage of the rayon is also indicated by the photomicrograph of the rayon filament (figure 8 H), which shows a serrated cross

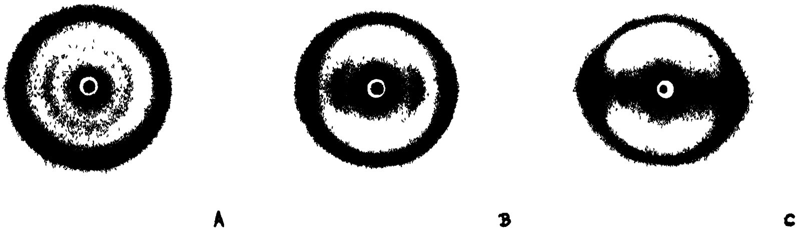

FIG. 7. X-ray diagrams of viscose fibers spun under various conditions: A, allowed to shrink freely, B, not allowed to shrink in length; C, stretched and dried under tension.

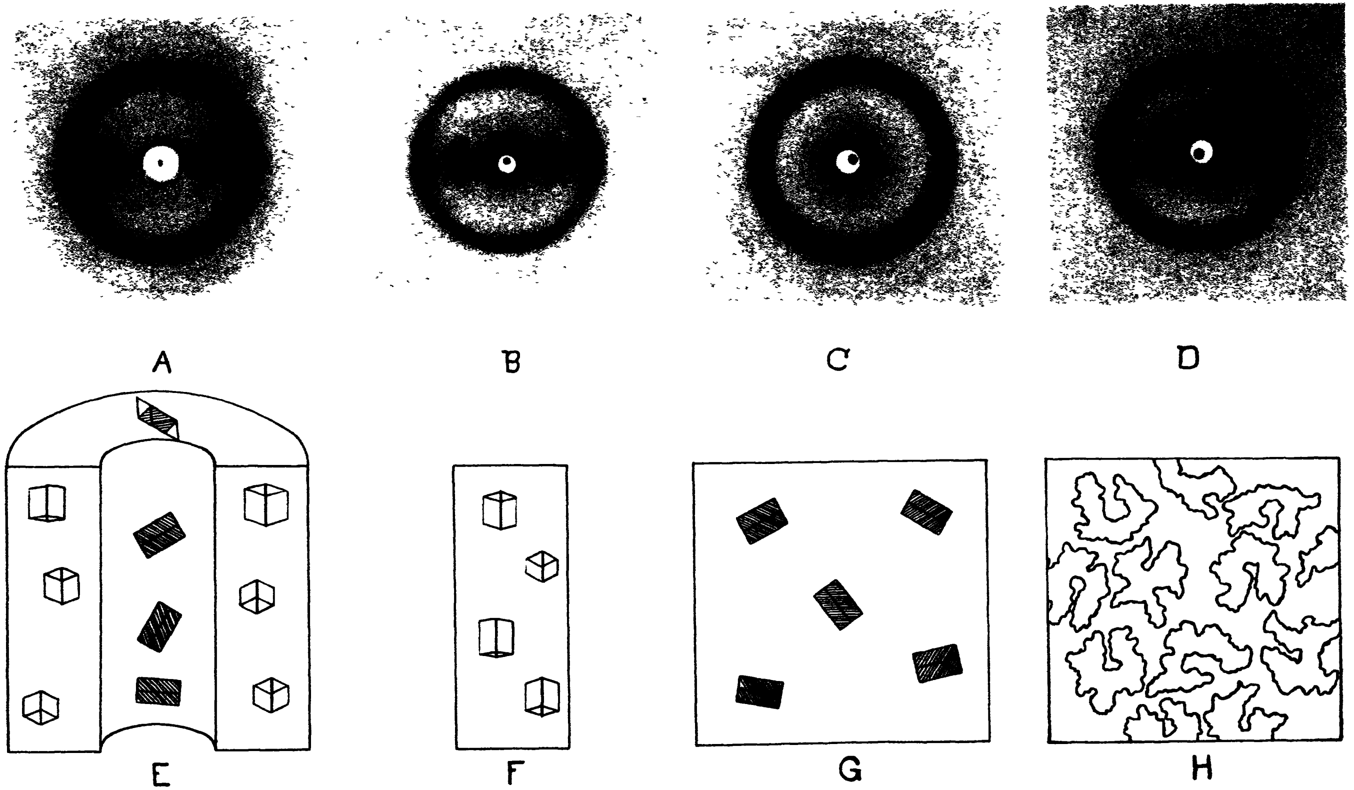

FIG. 8. X-ray diagrams, photomicrographs of cross sections, and schematic representation of orientation in rayons and Cellophane (see text for explanation).

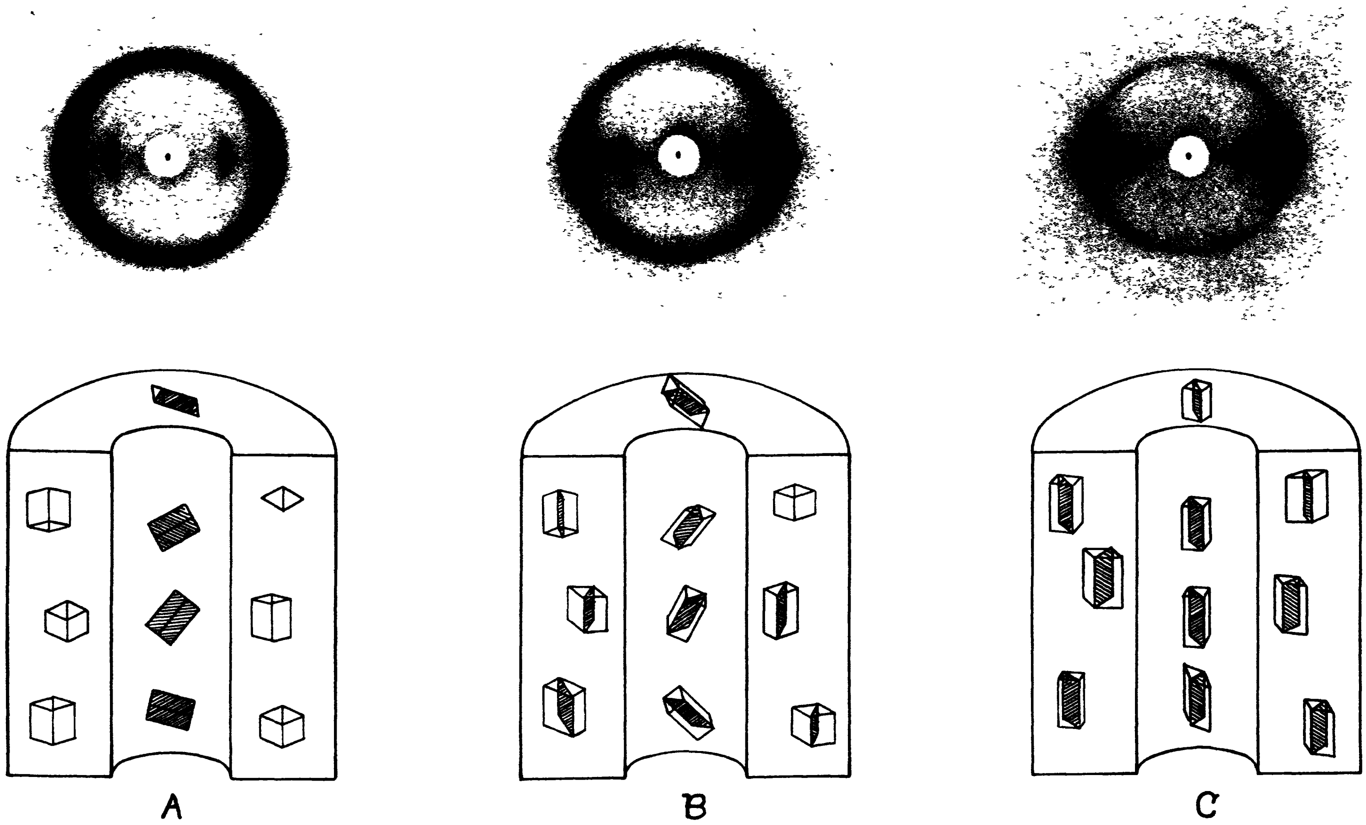

FIG. 9. X-ray diagrams and schematic representation of orientation in three rayon fibers possessing different types of orientation (see text for further explanation).

section. A roll of Cellophane also gives the type of diagram shown in figure 8D.

To the writer's knowledge, this type of orientation has not, heretofore, been recognized in rayons. On the basis of optical studies it has been interpreted erroneously as being due to a more highly oriented skin, produced by hydrodynamical friction set up by the viscose solution as it flows through the jet orifice (1). With polarized light, however, it is difficult to distinguish between a uniaxial and a selective uniplanar orientation in the surface of a rayon filament, and since earlier workers were aware of only two types of orientation (random and parallel), produced by either hydrodynamical friction or the "draft" to which the filament was subjected, it is logical that the optically different surface should be interpreted as being due to a more parallel orientation in the skin, rather than to a selective orientation.

When rayon filaments showing selective orientation are moistened and slowly stretched, the selective orientation is gradually changed to a uniaxial orientation. A diagrammatical representation of this change in orientation and the corresponding x-ray diagrams are shown in figure 9. Figure 9A represents the x-ray diagram and orientation, respectively, of a rayon fiber showing selective orientation. Figure 9B represents an imperfect uniaxial orientation after the fiber has been subjected to about 35 per cent elongation; while figure 9C represents a more perfect uniaxial orientation obtained after stretching 60 per cent. The orientation shown in figure 9A is representative of the average viscose rayon of ten years ago and figure 9B of the average present-day rayon, while figure 9C is typical of the highly stretched special rayons. Most cuprammonium rayons have an orientation approaching that of figure 9C.

SUMMARY

Earlier investigations regarding the orienting properties of native cellulose in both natural fibers and in synthetic fibers made from bacterial cellulose membranes have been extended to hydrate cellulose in synthetic fibers produced from cellulose coagulated from various solutions.

The hydrate cellulose crystallite possesses a major orienting tendency with reference to the *b*-axis, and a minor or selective orienting tendency with reference to the 101 plane. Orientation of these axes may be produced either by shrinkage or by elongation of the sample. Whenever there is a relative increase in dimension of a sample in one direction, the *b*-axes of the unit cell tend to orient parallel to that direction; if there is a relative decrease in dimension in one direction, the 101 planes are oriented perpendicular to that direction. The degree of orientation in each case is proportional to the relative change in dimensions of the sample.

In films such as Cellophane, the x-ray diagram shows a selective uni-

planar orientation of the 101 plane if, upon drying, the swollen film is allowed to shrink only normal to the plane of the film. Likewise rayon fibers, especially viscose, if spun without tension, show a similar selective orientation with reference to the fiber surface.

In both films and fibers, selective orientation of the 101 plane is destroyed by stretching, which produces a uniaxial orientation of the *b*-axis (axis of cellulose chains) parallel to the direction of stretching.

REFERENCES

(1) PRESTON, J. M.: J. Soc. Chem. Ind. **50**, 199T (1931).
(2) SISSON, W. A.: Ind. Eng. Chem. **27**, 51 (1935).
(3) SISSON, W. A.: J. Phys. Chem. **40**, 343 (1936).
(4) SISSON, W. A., AND CLARK, G. L.: Ind. Eng. Chem., Anal. Ed. **5**, 296 (1933).
(5) SNELL, F. D.: Ind. Eng. Chem. **17**, 198 (1925).

NEW BOOKS

Explosions- und Verbrennungs-vorgänge in Gasen. By WILHELM JOST. 16.5 x 24.5 cm.; viii and 608 pp. Berlin: Julius Springer, 1939. Price: 49.50 RM.

Prof. Jost addresses this fine book primarily to German readers, but it will be a most useful addition to the book of Lewis and von Elbe, the U. S. A. Commercial Gas Association's handbook *Combustion*, Laffitte's recent memoir, and Methuen's modest *Chemical Monograph*. (The second and third of these are not mentioned in an almost perfect bibliography.) In so brief a notice, it is easier to enumerate gaps than to particularize in congratulations. Moreover the references almost make good the textual omissions, and there is a subject index of some eighteen hundred entries.

The book is illustrated with hundreds of diagrams, and the odophotographs are excellent; but there are no shadow photographs, and the pictorial photographs are meagre and badly chosen,—a fault that might easily be remedied in a further edition, which also might well expand the too brief chapter 6 into an account of the flames of gas-heated furnaces, and mention Argand, father of all "diffusion-flames," from whose burner, as modified by Frankland, Bunsen's was by one step derived. The modernist trend of the book could indeed be indicated no better than by the omission of Argand, Frankland, Clerk, and Beyling from the long list of seven hundred authors, or by the one mention of Bunsen as compared with the numerous references to Bodenstein or to Semenoff. Another edition might also, despite the superficial limits imposed by the title, say something of the propagation of flames through dusts and sprays. After all, what could be a better introduction to "burning back" than the travelling zone of combustion in a test tube filled with ammonium dichromate or with a mixture of iron filings and sulfur dust, or, for that matter, in a squib?

A chapter on aerodynamics, expanding chapter 4, would be useful, too, in generalizing on the growth of a flame, or of flames, in an explosive medium. One of the innumerable spiral motions in nature, the "spin" of detonation, to which the author gives many pages, would then fall into place as an example among many of how flame travels, with least energy expense, as one fluid through another. "Turbulence", too, would then be generally explained as a crumpling of the streamlined isobars, and the disturbance of the flame front in wide tubes, to which a great deal of attention is given, would follow as one of many corollaries.

OLIVER C. DE C. ELLIS.

Technische Adsorptionstoffe in der Kontaktkatalyse. By FRANZ KRCZIL. xxxi + 726 pp. Leipzig: Akademische Verlagsgesellschaft, 1938. Price: 40 RM.

This volume is a storehouse of information concerning a large number of catalysts of the more porous type used in a great variety of heterogeneous reactions. After a brief introductory chapter the book is divided into three parts.

Part I discusses the many types of surface-active catalysts which have been and are being used in chemical processes. Single contact agents, mixed agents containing two substances, and mixed agents containing more than two substances are considered in that order. All types of active carbon, silicious materials, silica gels, alumina, and hydrated aluminum oxides of various kinds are among the single surface-active substances considered. Mixtures of these together with metals, metallic oxides, as well as non-metallic oxides are discussed as mixed contact agents. Methods of preparation of the catalyst are often briefly given. Part II concerns the use of these adsorption types of catalysts in a number of inorganic reactions such as oxidations, reductions, decompositions, and a variety of syntheses. The third section, and this occupies roughly two-thirds of the book, treats of the many uses of these adsorption catalysts in the wide range of catalytic reactions covered by the field of organic chemistry.

The factual material covered by this book is remarkably complete. The author makes no attempt to consider theories of contact catalysis, since he is interested in presenting as fully as possible all of the experimental results as well as the industrial procedures in this field. References are made to patent literature as well as to the usual journal sources. A separate section of the index is devoted to listing the patents on the subject from all countries. All chemists interested in contact catalysis will find Dr. Krczil's book an important reference work in the field. The completeness of the index makes the work particularly valuable to industrial laboratories.

L. H. REYERSON.

Applied Mathematics in Chemical Engineering. By T. K. SHERWOOD AND C. F. REED. New York: McGraw-Hill Book Company, Inc., 1939. Price: $4.00.

This is the book that many people have been waiting a long time to see. It represents the ideal combination of the talents of a mathematician and an engineer to make mathematics a really useful tool rather than an abstract mental exercise. Although its title might imply that its usefulness is limited to chemical engineering, such is not the case. Anyone engaged in constructive scientific or technical work will find a great deal of valuable material here, even though the bulk of the examples are taken from the field of chemical engineering. Even those who have spent years in adapting the instruments of mathematics to their particular needs will find many useful suggestions here for solutions and approximation. Many teachers of graduate students will find it ideal as a supplementary text in courses which include the use of mathematical treatments. As a matter of fact, a graduate course based largely on this book would be very valuable for chemists, physicists, and engineers.

The scope of the work can best be indicated by citing the chapter headings, which are as follows: (1) Integration and Differentiation; (2) The Use of Differential Equations; (3) Solution of Ordinary Differential Equations; (4) Applications of

Partial Differential; (5) Infinite Series; (6) Partial Differential Equations; (7) Numerical Analysis; (8) Graphical Treatment of Chemical Engineering Processes; (9) Theory of Errors and Precision of Measurements.

C. C. FURNAS.

Ferromagnetismus. By R. BECKER AND W. DÖRING. 25 x 17 cm.; viii + 440 pp. Berlin: J. Springer, 1939. Price: unbound, 39 RM.; bound, 42.60 RM.

In the investigation of ferromagnetism there are two groups of questions to be considered: the first is concerned, broadly speaking, with the occurrence of intrinsic spontaneous magnetization, and its magnitude and temperature variation, and the second with the details of the variation with field of the bulk magnetization and with various secondary effects. This book deals mainly with the second group.

There are six sections. The first two deal briefly but illuminatingly with fundamental principles and with the general theory of ferromagnetism. The third section, more than a third of the whole book, deals with magnetization processes in ferromagnetics and the factors controlling them. An excellent opening chapter introduces questions connected with crystal, strain, and field energy, describes boundary movement and gradual change of direction of magnetization in spontaneously magnetized regions, and indicates the part they play in the course of magnetization. These topics are discussed in detail in subsequent chapters with reference to initial permeability, coercivity, high frequency permeability, and magnetic after effects. The thermal, electrical, and strain effects accompanying magnetization are then considered, and also the peculiar effects of a magnetic field on elastic properties and on the damping of mechanical oscillations. The final section, which deals with magnetic materials in relation to technological applications, opens with an account of precipitation processes in alloys and their effect on magnetic properties. Technological requirements for different purposes are clearly set forth, and the properties of a large number of both commercial and laboratory alloys are discussed in the light of the general theoretical outlook.

From the point of view of a specialist the book is particularly useful for the remarkably comprehensive theoretical treatment, much of which is here published for the first time, of the interrelations between magnetization and strain, both applied and internal. The formal completeness in this one direction does, however, to some extent distort the impression given of ferromagnetism as a whole. None the less, the general parts of the book give good surveys of the present position, and show a wide appreciative knowledge of relevant work, though the selection of references to the literature sometimes seems rather arbitrary. The three hundred and nineteen diagrams, with explanatory captions, are an admirable feature. The table of contents makes the general plan clear, but the index is very inadequate.

The book at once takes its place as a valuable contribution to the literature of magnetism. It will be of great interest, however, not only to magneticians, but also to all those concerned with the properties of metals and alloys.

EDMUND C. STONER.

Reine Metalle. Edited by A. E. VAN ARKEL. 24 x 16 cm.; vii + 574 pp. Berlin: Julius Springer, 1939. Price: unbound, 48 RM.; bound, 49.80 RM.

The increased interest in the metallic state which has been so conspicuous in recent years has called for a more complete knowledge of the properties of pure metals. Absolute purity being unattainable, and the removal of traces of foreign elements from several of the metals being very difficult, it is important to know what degree of purification has been reached in each instance, and how products of high quality may be obtained. The present monograph, in which twenty workers of several countries have collaborated, does more than this, as it includes under each metal a full account of such physical and mechanical properties as have been determined with sufficient accuracy, although not always on material of identical purity. This part of the work has been exceedingly well done, and will be found invaluable by metallurgists and by physicists who are working on the properties of metals.

The monograph is weaker on the chemical side. When a preparation is described by an author as, say, 99.97 per cent pure, the statement cannot be accepted without close examination. It is necessary to know the methods of analysis which were used, and the degree of care which was taken to ensure that no impurities were overlooked. With products of such a degree of purity, a direct analytical determination of the principal metal is of no value. It must always be estimated by difference, and any omission to determine an impurity which is actually present leads to a fictitiously high value for the purity. It is only rarely that a satisfactorily full analysis is made. The task has been greatly aided by the recent development of quantitative spectrographic analysis, but even this is limited by the difficulty of preparing standards containing known small quantities of impurities. Also, some of the non-metallic impurities are overlooked by this method, while hydrogen, nitrogen, and oxygen, which may profoundly influence the properties of a metal, are rarely looked for. The problem of "blanks" is the most important factor in such analyses. This side of the subject is rather scantily treated in the present work, in which the statements of authors as to the purity of their metals are accepted rather at their face value, and the difficulties of analysis are not fully treated.

A most interesting, and at first sight surprising, fact is the very high degree of purity of certain metals now produced industrially. It would be quite impracticable to prepare aluminum in the laboratory of such high purity as the metal electrolytically refined by the A.F.C. process, described here by Gadeau, which contains less than 0.01 per cent of foreign elements. The cost of such a metal is not greatly above that of the commercial product, which has itself steadily risen in quality in recent years. Several other metals, including magnesium, zinc, and cadmium, have reached a similar stage in their industrial preparation.

The situation is different in regard to metals of high melting point. No industrial variety of iron is pure enough for exact research, and tedious laboratory methods have to be used for its purification. The editor of this book, who is now Professor at Leyden, has been particularly associated with a method for the preparation of the more refractory metals, such as tungsten, thorium, and zirconium, by the thermal dissociation of their halogen compounds; this process has been found to be widely applicable, and to lend itself well to the production of single crystals. The physical properties of tungsten, in spite of its refractory character, are better known than those of almost any other metal, its importance to the electric lamp industry, with its many well-equipped physical laboratories, being responsible for this.

There are still some metals which are hardly obtainable in a satisfactory state for modern research, and in some instances, such as that of beryllium, minute traces of difficulty removable impurities hamper the investigator. The accounts written and collected by Dr. van Arkel are of the highest value, and this well-printed volume should receive a cordial welcome.

C. H. DESCH.

Principles of Mineral Dressing. By A. M. GAUDIN. First edition. 554 pp. New York: McGraw-Hill Book Company, Inc., 1939. Price: $5.00.

This is an excellent classroom text, thoroughly modern, which lays emphasis on principles and minimizes machine descriptions, details of practice, and discussion of auxiliary operations. It comes from the pen of the Professor of Mineral Dressing of the Massachusetts Institute of Technology, who has had some years of experience in teaching this rapidly growing subject. A number of the author's own sketches and drawings add to the clarity of the exposition. The unique chapter on liberation is illustrated with some of the finest drawings and photographs ever assembled on this important and often neglected subject. Many types of locked particles are pictured. A fine set of flow sheets appears in the very first chapter, serving to tie the whole subject together as an introduction and to create a desire to study the individual unit processes mentioned in the flow sheets. Gravity concentration on tables has been very happily called "flowing film concentration," thus creating an immediate picture of the mechanism of the process. Scientific principles are well described, and the mathematics is within easy reach of students. Excellent bibliographies at the end of each chapter lead one to the more professional papers and to further detail. The very name of the book shows that dressing of ores is only a part of its subject matter and that both coal washing and the dressing of other industrial minerals are included. The book is useful.

OLIVER C. RALSTON.

Lectures on Osmosis. By F. A. H. SCHREINEMAKERS. 16 x 25 cm.; 45 figures; x + 266 pp. New York: Nordemann Publishing Company, 1938. Price: $7.00.

This book presents a summary of the extensive theoretical and practical researches on osmosis carried out in the University of Leyden by Dr. Schreinemakers and his associates. The treatment embraces a great diversity of systems, ranging from simple systems of binary liquids and a single membrane to highly complex liquid systems involving two or more membranes. Paths representing possible diffusion behavior of each of the components were developed for each of the systems. The various types of concentration changes which might occur during diffusion are given detailed treatment, but no consideration is given to the mechanism of osmosis or to osmotic pressures which might attend the process of diffusion.

The experimental systems treated include those with aqueous solutions of salts such as sodium chloride, ammonium chloride, or sodium carbonate, of acids such as oxalic, tartaric, succinic, salicylic, phthalic or boric, with membranes such as cellophane, parchment paper, pigs' bladder, or pigs' omentum. In addition to these systems for which data are given a large number of imaginary systems were treated in detail. Included in the factors considered were the number and the concentration of the components in the liquids, the presence of hydrous or anhydrous solid phases, the pressure and volume variability, the elasticity of the walls, and the selectivity of the membranes. Each of the different factors was treated as an "osmotic complex," and the different diffusion possibilities were referred to as "diffusion types."

The justification for such an extensive and detailed treatment of such a diversity of imaginary systems can come only through the fact that the osmotic systems were considered to have permeable, not semipermeable, membranes. Equilibrium conditions would not exist at any stage of the process of diffusion, and hence thermodynamic treatment could not be employed in the prediction of the diffusion paths of these systems. The main value of the book is that it depicts the multitudinous variety of conditions which may prevail in experiments on diffusion through membranes. It serves to impress upon one the various changes which may occur in an osmotic system during the process of osmosis. One can, however, have no assurance that any designated "diffusion type" will apply to a given experimental osmotic system.

The price of the book, which seems high, perhaps indicates that it is anticipated that the use of the book will be limited largely to those having an active interest in this rather specialized subject.

F. E. Bartell.

Colloid Chemistry (A Textbook). By Harry Boyer Weiser. viii + 428 pp. New York: John Wiley and Sons, Inc., 1939. Price: (cloth) $4.00.

The purpose of this book by the well-known investigator and author in the field of colloid chemistry is, in his own words, "to acquaint the student with the foundations of colloid chemistry and with the rôle that the classical experiments have played in the development of the modern theories and applications of the subject; to formulate systematically and to correlate critically the theories underlying colloid chemical behavior; and to illustrate the widely diversified applications of the principles of colloid chemistry in such fields as the industrial arts, agriculture, and biology."

The general plan of the book is as follows: After a short introductory chapter, the first section of seven chapters deals in the conventional way with adsorption. The next section of ten chapters deals with the sols, only the last chapter of this section being devoted exclusively to the hydrophilic sols. Shorter sections on gels, emulsions and foams, aerosols and solid sols follow. The last part of the book deals with the "Applications of Colloid Chemical Principles to Contact Catalysis, Dyeing, and Clay." In addition there are indices of authors and subjects.

The value of this otherwise very readable and instructive book is unfortunately somewhat diminished by too short a treatment or by complete omission of many newer developments, e.g., in the field of hydrophilic sols. The selection of the references is another point, in which improvements could be made in a second edition.

Weiser's book will be a valuable aid to students seeking an introduction to the field of colloids. Its clarity, didactic skill, and simplicity (with an occasional tendency to oversimplify) will be extremely helpful to the newcomer in the field in acquiring much well-balanced basic information.

Karl Sollner.

27. JUN. 1940
LIBRARY

THE INHIBITING ACTION OF MINUTE AMOUNTS OF SODIUM HEXAMETAPHOSPHATE ON THE PRECIPITATION OF CALCIUM CARBONATE FROM AMMONIACAL SOLUTIONS. I[1,2]

QUANTITATIVE STUDIES OF THE INHIBITION PROCESS

R. F. REITEMEIER[3] AND T. F. BUEHRER

Department of Agricultural Chemistry and Soils, University of Arizona, Tucson, Arizona

Received August 24, 1939

The fact that polymerized metaphosphates can inhibit as well as entirely prevent the precipitation of calcium carbonate has been applied on an industrial scale in the conditioning of boiler water, in flotation, in the removal of calcareous incrustations, in the stabilization of sols, and in other processes. These applications have, in the main, been developed by Hall (4). In those processes in which the water is completely softened, Hall[4] states that the metaphosphate must be added in the proportion of "... 4 formula-weights of sodium metaphosphate to 1 formula-weight of calcium at a pH of 8.5, but 7 formula-weights of sodium metaphosphate were required for this amount of calcium when the pH value was 10." The calcium is assumed to be present in the form of a stable complex from which it cannot be precipitated either as the carbonate or as an insoluble soap. The exact composition of this complex has not yet been definitely established.

A more recent application of sodium metaphosphate has been made by Rosenstein (11) for the prevention of calcium carbonate deposition from irrigation water when anhydrous ammonia is introduced as a source of nitrogen for growing crops. It was discovered that the precipitation of calcium carbonate can be prevented by an extraordinarily minute con-

---

[1] This paper is part of a dissertation submitted by R. F. Reitemeier to the Graduate College of the University of Arizona in partial fulfillment of the requirements for the degree of Doctor of Philosophy, which was conferred June 1, 1938. A more detailed account of this investigation, including the results of later work, is soon to appear in a Technical Bulletin of the Arizona Agricultural Experiment Station.

[2] Presented before the Division of Physical and Inorganic Chemistry at the Ninety-sixth Meeting of the American Chemical Society, held in Milwaukee, Wisconsin, September, 1938.

[3] Holder of the Shell Chemical Company Fellowship, 1936–38. Present address: U. S. Regional Salinity Laboratory, Riverside, California.

[4] Hall: U. S. patent 1,956,515 (April 24, 1934), page 5.

centration of metaphosphate, of the order of one part per million by weight. Rosenstein (11) states, for example, that when ammonia in an amount sufficient to produce a concentration of 75 p.p.m. NH_3 was added to a water containing 120 p.p.m. of calcium, the precipitation of calcium carbonate could be prevented entirely by the addition of sodium metaphosphate in an amount sufficient to bring its concentration to 0.75 p.p.m. In this case the water is not softened, as it is in the instances cited above, since the metaphosphate concentration represents only an extremely small fraction of the amount necessary to convert the calcium into the complex ion.[5]

The most striking characteristic of this phenomenon is the minuteness of the concentration of metaphosphate which is capable of preventing precipitation. No attempt has apparently been made to explain the mechanism of this process. A quantitative study of the factors affecting it was therefore made, the results of which will be presented in this paper.

THEORETICAL CONSIDERATIONS

The precipitation of calcium carbonate can be represented by the equation:

$$Ca^{++} + HCO_3^- + OH^- = CaCO_3 + H_2O$$

This reaction is actually a summation of three simpler reactions, and its equilibrium constant is of the order of 10^{12}. Hence the precipitation would be expected to approach completion even in the presence of a minute concentration of metaphosphate, since under these conditions the conversion of the calcium into the stable ionic complex, as is the case in water softening, must be negligibly small. The effect of the metaphosphate therefore appears to be largely an indirect one. Theoretically, however, it should be possible to introduce into the above equation the metaphosphate ion or molecule involved in the mechanism so it may adequately represent the inhibition process.

This intriguing phenomenon at once suggests a number of problems for investigation: Does the metaphosphate affect the *extent* to which the reaction proceeds or primarily its rate? What is the magnitude of the effect at different concentrations of the reactants? Do other phosphates, genetically related to the metaphosphates, as well as other similar inorganic salts, exhibit a similar property? Does the presence of neutral salts influence the effectiveness of metaphosphate as an inhibiting agent? Is the high specificity of the metaphosphate related to the chemical nature of the reactants or to that of the reaction products?

---

[5] Since this manuscript was first written, the use of hexametaphosphate in these low concentrations for the prevention of calcium carbonate deposits from industrial waters, as well as their disintegration after having been deposited, has been described (see Hatch and Rice: Ind. Eng. Chem. **31**, 51–7 (1939); Rice and Partridge: Ind. Eng. Chem. **31**, 58–63 (1939)).

The quantitative evidence, both analytical and physicochemical, which was obtained in carefully controlled experiments in which these factors were systematically varied, will now be presented. The results of these studies are of interest not only from an academic but also from an industrial point of view.

PREPARATION OF MATERIALS

The calcium bicarbonate stock solution was prepared by the action of carbon dioxide on a suspension of pure calcium carbonate, the latter having been precipitated from solutions containing recrystallized calcium chloride and ammonium carbonate, respectively. This solution was diluted with distilled water, before addition of the desired reagents, to give the calcium bicarbonate concentration desired.

Standard ammonia solutions, of approximately 1 *N* concentration, were prepared by dilution of reagent grade ammonium hydroxide, and standardized against 0.1 *N* hydrochloric acid.

Sodium metaphosphate may be obtained in various crystalline forms or as an amorphous glass, according to the conditions of preparation. All of these forms exhibit more or less polymerization when dissolved in water, the extent depending upon the method of preparation. On this account it seemed desirable to use both the amorphous and one of the definite crystalline forms for purposes of comparison. The so-called hexametaphosphate, known as "Graham's salt" (3), was prepared as follows: Twice-recrystallized monosodium dihydrogen orthophosphate was fused in a platinum dish at about 640°C., and held at that temperature for 15 min. It was then quickly chilled, ground, and used without further purification.

The crystalline form was prepared according to the method of Beans and Kiehl (1) and twice recrystallized from aqueous solution by the addition of ethanol, according to the method used by Hill (7). In this paper we shall use the term "hexametaphosphate" in referring to the amorphous form of sodium metaphosphate, realizing that the extent of its polymerization is variable and that the term probably does not represent the exact nature of this salt. Because of a similar uncertainty in regard to the crystalline modification, we shall designate this form as "soluble crystalline sodium metaphosphate."

Tetrasodium pyrophosphate was prepared by the ignition of recrystallized disodium monohydrogen orthophosphate, in a platinum dish, after which it was recrystallized from the aqueous solution by means of ethanol.

The other inorganic salts which were tested for their effectiveness as inhibiting agents, such as certain borates, nitrates, and vanadates, were of reagent grade and not further purified.

EXPERIMENTAL RESULTS

A. Effect of varying the ammonia concentration

Since ammonia provides the alkalinity for the precipitation of calcium carbonate, it seemed of interest to carry out a series of experiments in which its concentration was varied, in order to determine (*1*) its effect on the actual amount of calcium carbonate precipitated, and (*2*) its effect on the concentration of metaphosphate required for complete prevention of precipitation.

In the first series, the reaction mixtures were prepared by adding different volumes of the stock ammonia solution to a constant volume of stock calcium bicarbonate solution and diluting the mixtures in all cases to a final volume of 100 cc. One such series was allowed to stand 1 hr.; the other, 6 days. After standing the desired length of time, the carbonate precipitates formed were collected on filter paper and analyzed for total calcium. The results are shown in figure 1(A).

The two curves show that the amount of calcium carbonate formed varies as the ammonia concentration, but not linearly. The time factor is evidently of great importance. After 6 days, the amount of calcium carbonate precipitated was about double the amount which formed during the first hour. The 6-day curve approaches a limiting value, which approximates the solubility of calcium carbonate under these conditions. The amount of calcium carbonate precipitated after standing 1 hr. was found to be a linear function of the pH of the solution. As the ammonia concentration was increased from 200 to 2000 p.p.m., the pH increased from 9.8 to 10.8. The fact that time is so important in this process and that precipitation is relatively slow suggests that supersaturation may occur in the precipitation of calcium carbonate even from such dilute solutions.

In the second experiment sodium hexametaphosphate was added to the reaction mixtures before the addition of ammonia. Four series of mixtures were prepared, each with the same amount of calcium bicarbonate but with a concentration of ammonia which, though increasing from series to series, was held constant within each series. After 1 hr. the precipitates were analyzed for calcium with results shown in figure 1(B).

Several significant conclusions can be drawn from these graphs. First, the amount of calcium carbonate precipitated in the absence of the metaphosphate increases only about 95 per cent as the ammonia concentration is increased 1100 per cent. This result agrees with those presented in figure 1(A) and is consistent with the low degree of dissociation of ammonium hydroxide. Secondly, an increase in metaphosphate concentration results in a gradual diminution of the amount precipitated, up to the concentration beyond which no calcium carbonate formation can be detected. This limiting concentration we have chosen to call the "threshold inhibition value." Near this point the amount of carbonate precipitate formed is very small and therefore the analytical determination of calcium is relatively inaccurate. The actual threshold value is obtained by prolonging the curve until it intersects the x-axis. Thirdly, while the threshold inhibition value increases with the ammonia concentration, the increase is very slight. Thus, an increase of 1100 per cent in the ammonia concentration caused an increase in the threshold concentration of only 53 per cent. In the presence of the metaphosphate the relative efficiency of ammonia in effecting precipitation by virtue of its alkalinity decreases with increasing concentration of metaphosphate.

B. Effect of varying the calcium concentration

In this case the procedure was the same as in the foregoing experiment, except that the ammonia concentration was held constant and the calcium bicarbonate and metaphosphate concentrations were varied. The results are shown in figure 1(C).

The curves show that calcium ion, accompanied by an equivalent amount of bicarbonate ion, exerts a pronounced effect on the reaction. In the absence of metaphosphate, a fourfold increase in calcium concentration brings about a tenfold increase in the amount of calcium carbonate precipitated. The effect of varying the calcium concentration on the threshold inhibition value is even more pronounced. A fourfold increase in the former, from 25 to 100 p.p.m., increases the metaphosphate requirement from 0.1 to 12.0 p.p.m., a one hundred and twentyfold increase. The present investigation indicates that the calcium bicarbonate concentration may be the most important single factor which affects the inhibition of calcium carbonate precipitation.

C. Effect of ammonium ion

Since ammonium ion reduces the dissociation of ammonium hydroxide, an increase in the initial concentration of ammonium ion should cause a marked decrease in the threshold metaphosphate requirement, if the reaction as shown by the equation proceeds as written in the presence of metaphosphate. Using the same procedure as before, but keeping the calcium bicarbonate and ammonia concentrations as well as the ammonium-ion concentration in each of four series of determinations constant, the amount of calcium carbonate precipitated in the presence of increasing concentrations of metaphosphate was determined. The results are shown in figure 1(D).

With no ammonium chloride present, the threshold metaphosphate

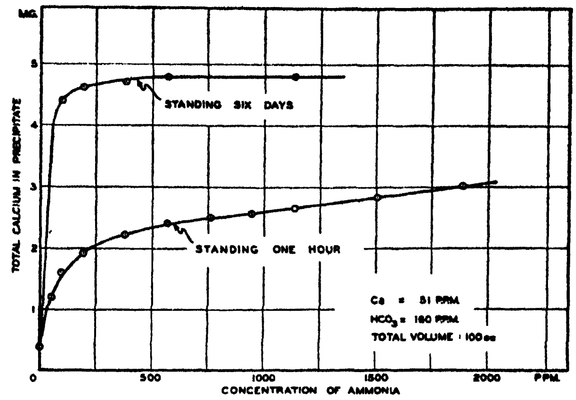

[A] EFFECT OF AMMONIA WITHOUT METAPHOSPHATE

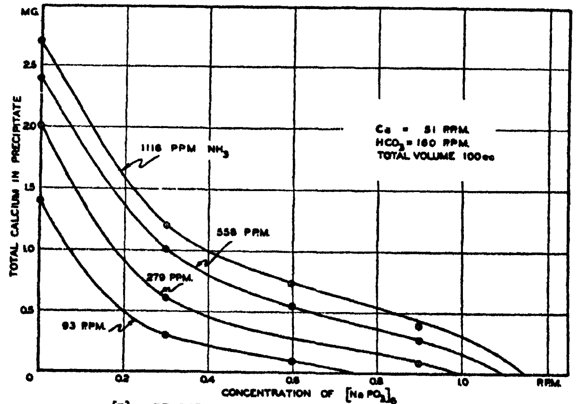

[B] EFFECT OF AMMONIA WITH METAPHOSPHATE

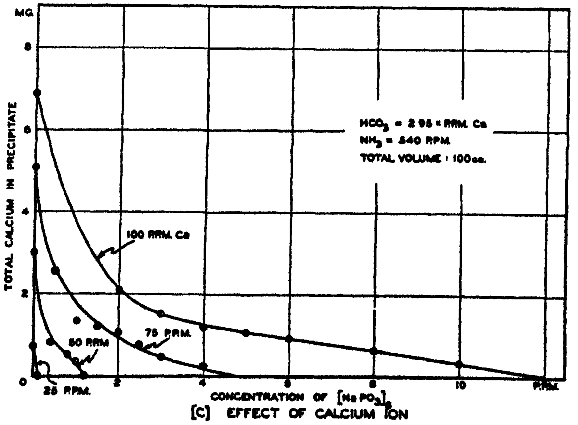

[C] EFFECT OF CALCIUM ION

Fig. 1. Effect of varying the concentrations of the individual reacting components on the precipitation of calcium carbonate.

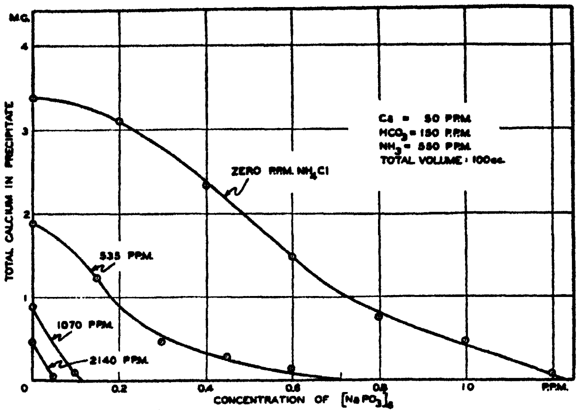

[D] THE EFFECT OF AMMONIUM CHLORIDE

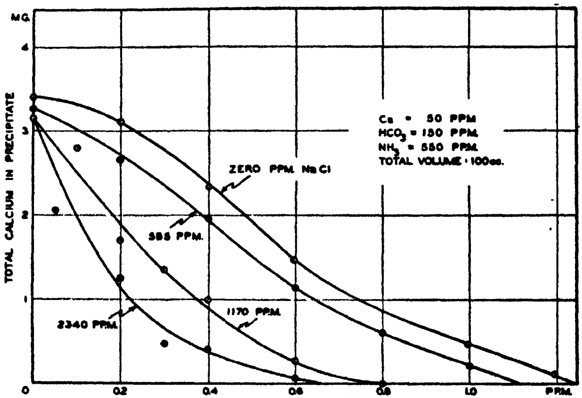

[E] EFFECT OF SODIUM CHLORIDE

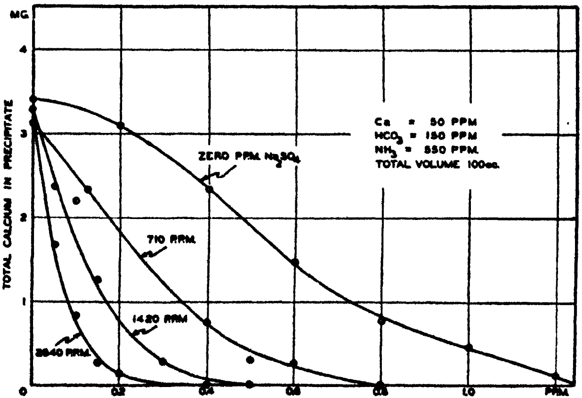

[F] EFFECT OF SODIUM SULFATE

FIG. 1—*Concluded*

requirement was 1.17 p.p.m., while in the presence of 2140 p.p.m. ammonium chloride (0.04 *N*), it was reduced to 0.05 p.p.m., that is, about twenty-threefold. The fact that calcium carbonate is appreciably soluble in ammonium chloride solution is well known; however, in this case free ammonia present to the extent of 550 p.p.m. would reduce such solvent action considerably. The increase in effectiveness of metaphosphate may be attributed in part to a reversal of the precipitation equilibrium as a result of a reduction in the dissociation of the ammonia.

D. Effect of neutral salts

When hexametaphosphate is used to inhibit precipitation of calcium carbonate from natural waters, it has been found that a lower concentration of metaphosphate is required than in the case of pure calcium bicarbonate solution, which suggests that the neutral salts usually present in the water may affect the process. To investigate this effect, sodium chloride and sodium sulfate were chosen as typical of the neutral salts present in such waters. Four series of determinations were made. The calcium bicarbonate and ammonia concentrations were the same as used in previous experiments, but sodium chloride and sodium sulfate were used in progressively increasing amounts so that the concentrations of Cl^- and SO_4^{--} ranged from 0 to 0.04 *N*. After 1 hr. the calcium in the precipitates was determined. The results are shown in figure 1(E, F).

Increasing the salt concentration causes a comparatively slight decrease in the amount of calcium carbonate precipitated, but a much greater decrease in the concentration of metaphosphate required for complete prevention of precipitation. For example, addition of sodium sulfate to produce a concentration of 0.04 *N* reduces the threshold requirement of hexametaphosphate from 1.25 p.p.m. to about 0.3 p.p.m., whereas sodium chloride at a concentration of 0.04 *N* reduces it to about 0.65 p.p.m.

The nature of this neutral-salt effect is not entirely obvious. These salts may conceivably affect the activity of the ammonia so as to lower the pH perceptibly and thus reduce the precipitation. To secure evidence on this point, pH measurements were made on ammonia solutions which contained 560 p.p.m. ammonia and to which the respective neutral salts had been added to give chloride and sulfate concentrations of the same range as used in the foregoing experiments. The data obtained with the glass electrode are assembled in table 1.

The above data show that instead of the pH being lowered by the presence of neutral salts, a definite *increase* occurs, the effect of sulfate being more pronounced than that of chloride ion. Since the differences in pH are scarcely significant, however, so far as the precipitation of calcium carbonate is concerned, the neutral salts must in some manner influence the activity or behavior of the calcium or bicarbonate ions. The effect may consist in a reduced activity of one or both of them, or, on the other hand, an increase in the solubility of calcium carbonate under these conditions. That sodium chloride and sodium sulfate increase the solubility of calcium carbonate is well known. Kohlschütter and Egg (8) found that the presence of potassium chloride and sodium chloride caused fewer crystals to form when a current of air was passed through a calcium bicarbonate solution. Stumper (12) found that sodium chloride and sodium sulfate inhibit the thermal decomposition of calcium bicarbonate, the effect of the sulfate being about three times that of the chloride. While these evidences point to a possible reduction in activity of calcium and/or bicarbonate ions, these neutral salts may affect the dissociation or depolymerization of the hexametaphosphate, favoring the formation of an ionic or molecular species which is highly specific in its inhibiting action.

TABLE 1

Effect of neutral salts on the alkalinity of ammonia solutions

Ammonia concentration = 560 p.p.m. NH_3

CONCENTRATION OF Na_2SO_4	CONCENTRATION OF NaCl	pH
N	*N*	
0	0	10.16
0.0104	0	10.55
0.0209	0	10.79
0.0417	0	10.86
0	0.0141	10.55
0	0.0282	10.61
0	0.0564	10.62

E. Variation of the threshold value with the time

The importance of the time factor in the precipitation of calcium carbonate was illustrated in figure 1(A). Since the precipitation experiments presented in figure 1(B to F) involved a reaction period of 1 hr., several experiments were designed to determine the specific effect of time on the threshold inhibition value. For this purpose the conductance method offered the most sensitive means of following the precipitation process over an extended period of time, since precipitation of calcium carbonate would result in a diminution of the conductance due to the removal of ions.

A glass-stoppered conductivity cell of 63-ml. capacity was employed. Appropriate volumes of calcium bicarbonate, sodium hexametaphosphate, and ammonia solutions, all at 25°C., were pipetted into the cell in the order just mentioned and diluted in each case to 63 ml. with conductivity water. The results of a series of studies with different concentrations of the metaphosphate are presented in figure 2.

These curves show clearly that precipitation proceeds through three stages, which are modified somewhat according to the metaphosphate concentration. First, there is a sharp increase in the conductance; secondly, the conductance reaches a maximum value at which it may remain for a considerable length of time; and thirdly, there is a decrease in the conductance, the rate of which depends on the metaphosphate concentration.

The initial rise in the conductance curves was found, from studies on two-component systems, to be due to the reaction between ammonium hydroxide and carbonic acid. In relation to the precipitation reaction it evidently represents the time required for a sufficient concentration of carbonate ions to be formed to saturate the solution with calcium carbonate and thus allow precipitation to proceed. The comparative slowness of this process is apparently due to the slow rate of hydration and neutralization of carbon dioxide (9). When sodium hydroxide is used instead of ammonia in the precipitation reaction, no such initial rise in the conductance curve occurs. This result is in accord with the interpretation given by Hammett (5). When ammonia is used, the reaction with carbon dioxide produces primarily bicarbonate ion, whereas with sodium hy-

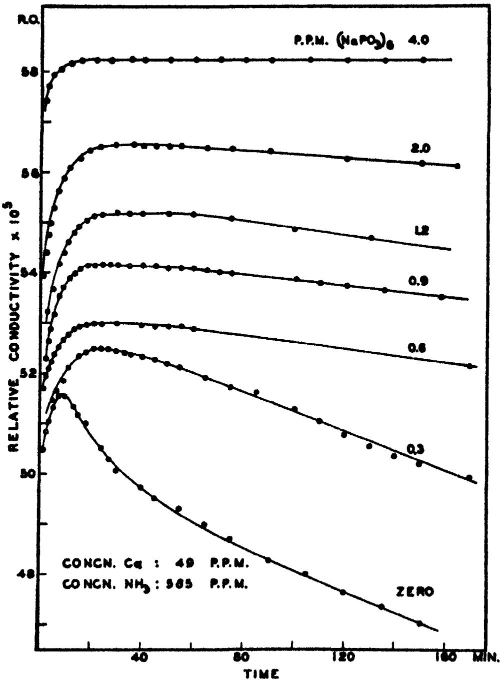

FIG. 2. Variation of the threshold value with the time

droxide, carbonate ion is formed. The rate of the latter reaction being proportional to the square of the hydroxyl-ion concentration, it is evident that the formation of carbonate ion is much more rapid in the presence of sodium hydroxide than of ammonia.

Another significant fact is shown by the curves of figure 2, namely, that an increase in metaphosphate concentration prolongs the time during which the conductance remains at its maximum value. This effect is shown in table 2. As the concentration of metaphosphate increases, a longer period of time is required for the system to reach the point where calcium carbonate begins to precipitate from the solution. After precipitation has begun, its rate is fairly constant, depending upon the metaphosphate concentration.

TABLE 2

Effect of sodium hexametaphosphate on the period during which the conductance was at a maximum

CONCENTRATION OF $(NaPO_3)_6$	ESTIMATED PERIOD OF MAXIMUM CONDUCTANCE
p.p.m.	*minutes*
0	2
0.3	6
0.9	25
1.2	40
2.0	55
4.0	>150

These results indicate three significant aspects of the inhibition process: first, the presence of the metaphosphate lengthens the time required for precipitation to commence; secondly, after precipitation has begun, the metaphosphate diminishes the rate of the reaction; and thirdly, if sufficient metaphosphate is present, precipitation is entirely prevented.

Reference has already been made to the fact that the inhibition mechanism might involve an effect of metaphosphate on the conversion of bicarbonate to carbonate ion. Evidently, if the metaphosphate exhibits the same order of effectiveness in systems containing carbonate ions initially, this step in the mechanism might be definitely eliminated. A conductance study similar to the above was accordingly made, in which calcium chloride and sodium carbonate were substituted for calcium bicarbonate and ammonia. The results are shown graphically in figure 3.

Except for the absence of the initial rise in conductance, the same general effects were observed. Sodium hexametaphosphate appears to be as effective in systems containing a high initial concentration of carbonate ions as in bicarbonate solutions having a high potential supply of carbonate ions. It is therefore concluded that the inhibiting action of metaphosphate does not consist of a retardation of the conversion of bicarbonate to carbonate ions.

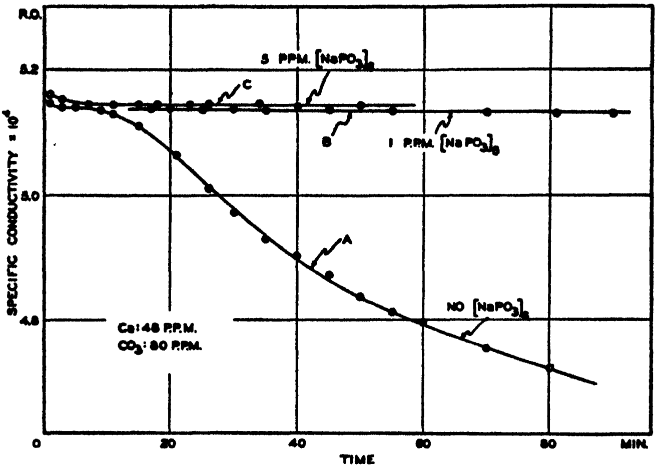

FIG. 3. Effect of sodium hexametaphosphate on the precipitation of calcium carbonate from calcium chloride–sodium carbonate mixtures.

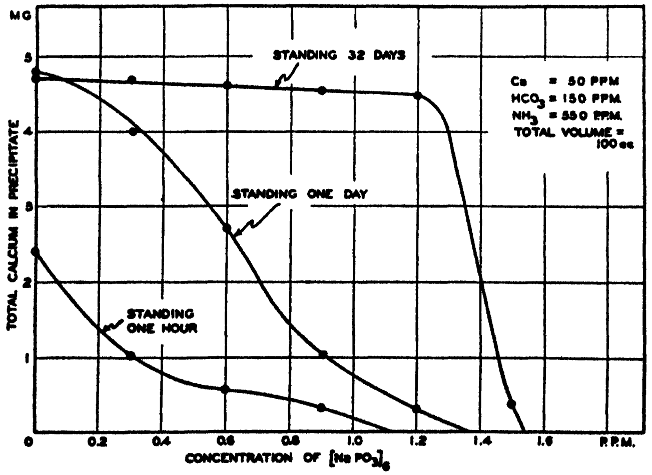

FIG. 4. Effect of time on the precipitation of calcium carbonate in the presence of sodium hexametaphosphate.

The effect of time on the inhibition process was likewise studied by way of precipitation experiments. Three series of mixtures containing constant amounts of the reactants were prepared and allowed to stand for different periods of time: namely, 1 hr., 1 day, and 32 days, all at room temperature. The precipitates were analyzed for calcium as before, with the results shown in figure 4.

The maximum amount of calcium that could be precipitated in the absence of metaphosphate was 5 mg. It will be noted that about 4.8 mg. of calcium, representing 96 per cent of the total calcium present, had been precipitated both at the end of 1 day and after 32 days; the amount thus remaining in solution is equivalent to the solubility of calcium carbonate under these conditions.

As the time of standing increases, the efficiency of metaphosphate decreases; thus, in 1 hr. 11 per cent of the total calcium precipitated in the presence of 0.6 p.p.m. of metaphosphate, while at the end of 1 day and 32 days, respectively, this concentration had permitted 2.7 mg. (54 per cent) and 4.6 mg. (92 per cent) of the calcium to precipitate. The threshold requirement does not, however, show so marked an increase; for the three periods of time, the threshold values were 1.1, 1.35, and 1.5 p.p.m. of metaphosphate, respectively.

It will be noted that as the time allowed for precipitation was increased, the shape of the area under the curve approached that of a rectangle. The respective areas represent a summation of the amounts of precipitate formed in the mixtures to which had been added varying amounts of metaphosphate from zero to the threshold concentration, and during the period of time chosen for the respective experiments. The magnitudes of the areas give a quantitative indication of the extent to which the time element enters into the process and the extent to which the inhibition is permanent.

When measured with a planimeter, the three areas, when referred to the area under the 1-hr. curve as unity, are to each other as 1:3.47:7.25. An increase of only 36 per cent in the threshold value thus increased the total precipitation, as determined from the areas, by 625 per cent. Only 3.8 per cent of the total precipitation occurring during the 31-day interval occurred at metaphosphate concentrations higher than the threshold inhibition value required for complete prevention of precipitation on 1 day's standing. These facts indicate that the inhibition is a permanent effect under the conditions in these experiments. For the system under consideration, it appears safe to assume that there is a permanent threshold value of approximately 1.5 p.p.m. of metaphosphate, beyond which no calcium carbonate will precipitate regardless of the length of time allowed for precipitation to take place.

F. Comparison of various phosphates as inhibiting agents

The close genetic relationship between the ortho-, meta-, and pyrophosphates suggested that the structure, polymerization, and chemical nature of the phosphate molecule might determine in large measure its ability to inhibit calcium carbonate precipitation. It was therefore thought that a knowledge of their relative efficiencies as inhibiting agents under similar experimental conditions might afford evidence as to the mechanism of the inhibition process.

By means of the technique previously described, the relative effectiveness of hexametaphosphate, tetrasodium pyrophosphate, and primary sodium orthophosphate was determined. The precipitates were analyzed for calcium after standing for 2 days. The data are plotted in figure 5, the "concentrations of phosphate" along the axis of abscissae having been calculated to indicate the actual concentration of the respective phosphates on a weight basis.

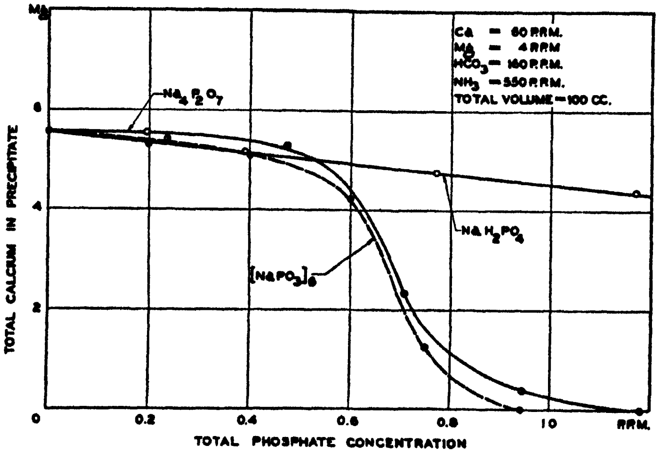

FIG. 5. Inhibiting action of various phosphates

The meta- and pyro-phosphate curves exhibit a striking similarity in shape and in magnitude of the threshold inhibition value at the calcium concentration here used, namely, 60 p.p.m. These results are in agreement with those of Hartung (6), who worked with calcium solutions at ordinary concentrations. He concluded that the meta- and pyro-phosphates were about equally effective in the stabilization of a water softened by the lime–soda process. Quoting Hartung's statement: ". . . waters with high calcium concentrations are not so easily (if at all)[6] stabilized by tetra-sodium pyrophosphate."

The orthophosphate curve is a straight line of gentle slope with no evidence of any definite threshold value. In the latter case it was observed that a precipitate of calcium phosphate was formed at the higher phosphate concentrations, which appears to offset the inhibiting effect of the orthophosphate. Nevertheless, the orthophosphate is capable of reducing the precipitation of calcium carbonate to a limited extent and within a limited range of conditions.

---

[6] The parentheses are Hartung's.

Similar experiments with the crystalline sodium metaphosphate indicated that it was practically without effect. The close similarity in behavior of the pyrophosphate and hexametaphosphate suggests that the inhibition mechanism may be similar, if not identical, in the two cases. From a study of these two phosphates in connection with the softening of water, Gilmore (2) concluded that both are effective, but that the latter is superior to the former. Since the metaphosphate is genetically related to the pyrophosphate,—by way of $Na_2H_2P_2O_7$ which forms as an intermediate product in the original decomposition of the primary phosphate,—and since it is also formed in the re-hydration of the metaphosphate, it is reasonable to assume that some intermediate form of pyrophosphate, or possibly a more complex phosphate,[7] is responsible for the inhibition in the two cases.

It has been found by Partridge (10) that the conditions of preparation of the glassy hexametaphosphate, such as the time and temperature at which the melt is held in the fused state, may modify the effectiveness of the product as an inhibiting agent. A metaphosphate glass, which he prepared "by dehydration and fusion of monosodium orthophosphate at 650°C., for 15 hours, followed by quenching between steel plates," was found to possess an inhibiting power similar to that which we have reported for hexametaphosphate in this paper. However, a more active product was obtained by holding the melt at 1000°C. for 2 hr. Hence he concludes that the temperature of preparation is of primary importance in the manufacture of an actively inhibiting product.

G. Behavior of other inorganic salts as inhibiting agents

The action of the various phosphates illustrated in the foregoing experiments led to the question whether analogous salts of other elements possess a similar property. Inhibition experiments were accordingly carried out with the following salts: sodium tetraborate, ammonium metavanadate, sodium metavanadate, fused sodium metavanadate, sodium orthovanadate, fused sodium orthovanadate, sodium metaborate, dipotassium dihydrogen antimonate, sodium bismuthate, sodium arsenite, disodium orthoarsenate, potassium nitrate, and fused potassium nitrate. (It is recognized that fusion of the vanadates and nitrates results in partial decomposition.) However, of the fourteen salts studied, none was found to inhibit measurably the precipitation of calcium carbonate. In nearly all cases the concentration of the particular salt was carried to a value as high as 20 p.p.m. without noticeable effect. Although most of these salts can form an analogous series of ortho, meta, and pyro salts, they do not possess the ability to inhibit calcium carbonate precipitation. Even the transformation to an amorphous or glassy form does not impart to them this peculiar property. It therefore appears to be a highly specific characteristic of the inorganic salts containing phosphorus in the pentavalent form.

---

[7] A somewhat more reasonable possibility to account for this behavior is suggested by Terrey (13), quoting several authors who attribute it to tri- and tetrapolyphosphates which may be formed in the original fusion process, depending upon the conditions. The action of such phosphates was not, however, considered in the present investigation.

DISCUSSION

The data presented in this paper demonstrate conclusively that the molecularly hydrated phosphates,—sodium hexametaphosphate and sodium pyrophosphate,—in their ionic or polymerized molecular forms are able, in minute concentrations, not only to retard but also to prevent entirely the precipitation of calcium carbonate from ammoniacal solutions. The possibility of permanent prevention of such precipitation, demonstrated by way of long-time inhibition experiments, indicates the existence of an extraordinarily stable system. The evidence obtained by varying the concentration of individual reactants indicates that calcium bicarbonate is the most important constituent involved in the mechanism, and hence implies a close relationship between the phosphate and either calcium or bicarbonate ion. Since the use of metaphosphates in water softening involves the removal of calcium, it is very unlikely that bicarbonate ion plays an important part in the mechanism. In the light of these findings, the authors are inclined to postulate a mechanism involving first, the primary precipitation reaction and secondly, an inhibition reaction which involves the meta- or pyro-phosphate. Varying the concentrations of ammonia, ammonium ion, and of neutral salts like sodium chloride and sodium sulfate affects only the primary precipitation reaction in the conventional manner. Variations in calcium bicarbonate concentration, however, affect the inhibition process and thus have a more pronounced effect on the quantitative results.

The mechanism is, however, complicated by certain physical factors which are concerned in the formation of the calcium carbonate crystal. These have been subjected to an intensive study, the results of which will be presented in a subsequent paper.

SUMMARY

1. Glassy sodium hexametaphosphate, at extremely low concentrations of the order of 1 p.p.m. (10^{-6} molal), is found to prevent the precipitation of calcium carbonate from solutions containing 200 p.p.m. of calcium

bicarbonate (10^{-3} molal) and 550 p.p.m. of ammonia (0.03 molal). Crystalline sodium metaphosphate is relatively ineffective under similar conditions. At low calcium concentrations pyrophosphates are as effective as metaphosphates; orthophosphates exhibit a slight ability to inhibit precipitation, but it is limited by the precipitation of an orthophosphate of calcium. No other analogous inorganic salts, similar to the phosphates, possess this property. It is highly specific of the molecularly dehydrated phosphates only.

2. The threshold concentration of hexametaphosphate required to prevent precipitation increases with the ammonia concentration as well as with that of calcium bicarbonate, but to a much greater extent with the latter. Ammonium salts and neutral sodium salts increase the effectiveness of the metaphosphate; this indicates an indirect effect on the activities of calcium ion, bicarbonate ion, and ammonium hydroxide.

3. At such low concentrations the metaphosphate retards precipitation and, if present in sufficient amount, will prevent it permanently. The evidence points to the existence of a highly stable inhibition system, possibly involving calcium ions.

We desire herewith to express our thanks to the Shell Chemical Company of San Francisco, California, for their support of this research by way of a fellowship; to Dr. Ludwig Rosenstein, who suggested the problem and manifested much interest in its progress; and to Mr. W. T. McGeorge, Chemist of the Arizona Agricultural Experiment Station, for his interest and support.

REFERENCES

(1) Beans, H. T., and Kiehl, S. J.: J. Am. Chem. Soc. **49**, 1978–91 (1927).
(2) Gilmore, B. H.: Ind. Eng. Chem. **29**, 584–90 (1937).
(3) Graham, T.: Phil. Trans. **123**, 253 (1833).
(4) Hall, R. E.: U. S. patents 1,956,515 (1934); 1,965,339 (1934); 2,035,652 (1936); 2,087,089 (1937); reissue 19,719 (1935).
(5) Hammett, L. P.: *Solutions of Electrolytes*, 2nd edition, pp. 91–2. McGraw-Hill Book Company, New York (1936).
(6) Hartung, H. O.: Water Works & Sewerage **86**, 56–60 (1939).
(7) Hill, T. M.: Dissertation, Columbia University, New York, 1925.
(8) Kohlschütter, V., and Egg, C.: Helv. Chim. Acta **8**, 470–90 (1925).
(9) McBain, J. W.: Trans. Chem. Soc. (London) **1912**, 814.
(10) Partridge, E. P.: Personal communication.
(11) Rosenstein, L.: U. S. patents 2,038,316 (1936); reissue 20,360 (1937); reissue 20,754 (1938).
(12) Stumper, R.: Z. anorg. allgem. Chem. **204**, 367–77 (1932).
(13) Terrey, H.: Annual Reports on Progress in Chemistry **34**, 121 (1938).

THE INHIBITING ACTION OF MINUTE AMOUNTS OF SODIUM HEXAMETAPHOSPHATE ON THE PRECIPITATION OF CALCIUM CARBONATE FROM AMMONIACAL SOLUTIONS. II[1]

Mechanism of the Process, with Special Reference to the Formation of Calcium Carbonate Crystals

T. F. BUEHRER AND R. F. REITEMEIER

Department of Agricultural Chemistry and Soils, University of Arizona, Tucson, Arizona

Received August 24, 1939

In a previous paper by the authors (14) it was shown that the inhibiting effect of metaphosphates on the precipitation of calcium carbonate manifests itself as either a retardation of precipitation or its complete prevention, depending upon the properties of the reacting components present in the solution, primarily those of calcium bicarbonate and sodium hexametaphosphate. Chemical studies designed to explain the mechanism of this process have shown definitely that it is not due to some mysterious interaction between metaphosphate and bicarbonate ion, or carbonate ion, or the ammonia. Nor does it affect the possible interactions between these constituents. The minuteness of the concentration of metaphosphate which is effective in this process would appear to eliminate complex formation between calcium ion and the hexametaphosphate as a possible explanation, since only an extremely small amount of it is necessary to prevent precipitation completely. The quantitative evidence obtained in these studies has proved, moreover, that the primary precipitation reaction, represented by the simple equation

$$Ca^{++} + HCO_3^- + OH^- = CaCO_3(s) + H_2O$$

is not affected by traces of hexametaphosphate.

The only other plausible basis for explaining the mechanism must be sought either in the effect of hexametaphosphate on the nature of the solid phase which separates out, or in the conditions attending the crystallization process. Preliminary experiments had shown that, when calcium carbonate was precipitated from calcium bicarbonate by the addition of ammonia, the crystals formed rapidly, did not adhere to the walls of the vessel, and settled readily. If, however, the same precipitation was carried out in the presence of one part per million or less of hexametaphosphate, that is, below the level necessary completely to prevent precipitation, there was no immediate precipitation but, after standing several hours, clear, brittle crystals were formed which adhered firmly to the sides and bottom of the precipitating vessel. Microscopically these crystals were strikingly different from the well-known calcite rhombs. It was concluded that the metaphosphate must in some manner interfere with the crystallization process.

---

[1] Presented before the Division of Physical and Inorganic Chemistry at the Ninety-sixth Meeting of the American Chemical Society, held at Milwaukee, Wisconsin, September, 1938. See footnote to Paper I of this series for additional information.

The problem resolves itself into two questions: (*1*) Does the metaphosphate stabilize calcium carbonate particles of colloidal dimensions and prevent them from aggregating into macroscopic particles, or (*2*) does it interfere with the subsequent growth of the crystal from nuclei that were formed in the normal manner? The present paper sets forth a study of these two questions.

ULTRAMICROSCOPIC STUDIES

Preliminary experiments indicated that calcium carbonate suspensions formed in the presence of metaphosphate did not show the Tyndall effect. More conclusive quantitative evidence was secured with the slit ultramicroscope, on mixtures containing 50 p.p.m. of calcium, 155 p.p.m. of bicarbonate ion, 560 p.p.m. of ammonia, and sodium hexametaphosphate in concentrations varying from 0 to 5 p.p.m. The preparation of the compounds used in making up these solutions has been described in the preceding paper (14). These solutions had been prepared from water doubly distilled from alkaline permanganate. The ammonia was redistilled over calcium hydroxide into cooled conductivity water. The mixtures were allowed to stand 1 hr. The density of particle distribution was determined for each mixture by the method of rhythmic counting. An 8-mm. objective and a 10× ocular were used in all of the measurements.

The results obtained are assembled in table 1.

The data in table 1 show that the metaphosphate does not increase or stabilize the particles of colloidal dimensions, since the number of particles in the mixtures in which precipitation was entirely prevented did not differ significantly from that of the "blanks" on the original solution. It might be pointed out that the precipitation of calcium carbonate which occurred in the mixtures containing up to 1.2 p.p.m. of metaphosphate resulted from coprecipitation with the suspended impurities present initially in all of the mixtures. Photomicrographic evidence has shown that, in the presence of metaphosphate at a concentration so low that the inhibition is not complete, the calcium carbonate crystals will form on any kind of suspended impurity that may be present in the solution. Under such circumstances many of the initially suspended particles might be deposited, with the obvious result that the ultramicroscopic count would be lowered.

An independent experiment was designed to determine the "life" of a colloidal calcium carbonate particle if its existence were possible. For this purpose a sample of a calcium bicarbonate–ammonia mixture without metaphosphate was placed in the ultramicroscope cell and observed for a few minutes. It was found that the number of particles observable under these conditions increased to a maximum in about 5 min. and then began to decrease. This observation proves that the existence of such a colloidal state is very transitory and that the particles grow rapidly to macroscopic dimensions.

TABLE 1

Density of particle distribution in the precipitation of calcium carbonate as indicated by rhythmical counts with the ultramicroscope

CONCENTRATIONS OF CONSTITUENTS				RESULTS OF 100 COUNTS		AVERAGE NUMBER PER COUNT
Ca^{++}	HCO_3^-	NH_3	$(NaPO_3)_6$	T.F.B.*	R.F.R.†	
p.p.m.	*p.p.m.*	*p.p.m.*	*p.p.m.*			
				24	26; 15	0.21
50	155			22	14	0.18
			5	63	80	0.72
		560		27	38	0.31
				27	33	
50	155	560	5	47	54	0.50
50	155	560	4	60	79	0.70
50	155	560	3	54	44	0.49
50	155	560	2	67	61	0.64
50	155	560	1.5	74	51	0.63
50	155	560	1.2	47	39	0.43
50	155	560	0.9	19	24	0.22
50	155	560	0.6	22	24	0.21
50	155	560	0.3	24	16	0.20
50	155	560	0.0	21	20	0.21

* T. F. Buehrer.

† R. F. Reitemeier.

With respect to the theory of colloid stabilization the foregoing results indicate definitely the absence of any such stabilized colloidal calcium carbonate particles. If such a process occurred, it would enormously increase the colloidal content of the suspension, a condition easily detectable with the ultramicroscope. The very slight increase in the count may be accounted for in terms of the deposition of the precipitate on the suspended particles as rapidly as it is formed.

It is of course possible that there might be particles too small to be visible even under the ultramicroscope. Even if the existence of such colloidal particles were demonstrable, it is still problematical whether hexametaphosphate could stabilize such particles. Gortikov and Malinovskaya (5) found calcite and aragonite to be positively charged. Hence the negative metaphosphate ion would *coagulate* rather than stabilize them. On the other hand, Chwala (1) has demonstrated the use of sodium pyrophosphate as a peptizing agent. The experimental evidence here presented has convinced the authors that the theory of colloid stabilization, to account for inhibition by metaphosphates, is not tenable.

PHOTOMICROGRAPHIC STUDIES ON CALCIUM CARBONATE PRECIPITATED UNDER DIFFERENT CONDITIONS

It is recognized that the formation of crystal nuclei and the subsequent growth of the crystal are two distinct phenomena. The foregoing experiments demonstrated that metaphosphates do not influence the rate of nuclei formation. Hence it was thought that the inhibition manifested itself as an abnormal or deranged crystallization process, in which either the growth of the crystal may be retarded or the form or habit of the crystals may be markedly changed. Preliminary microscopic examination of the firmly adherent crystals, above referred to, showed them to be very different in appearance from the typical calcite rhombs obtained under ordinary conditions of precipitation.

The typical crystalline forms of calcium carbonate,—namely, calcite, aragonite, and μ-calcium carbonate,—are well known (8). It is possible, however, for these modifications to assume a great variety of crystal habits (4). Kohlschütter and his coworkers (10, 11) have shown that the crystal habit of a substance may be markedly influenced by the presence of colloidally dispersed material in the solution in which the precipitation took place. They found, for example, that certain dyes, gelatin, agar, and other substances produced what they termed "somatoid" forms of calcium carbonate. France and his associates (2, 3, 9) demonstrated a similar effect in their work on the crystallization of copper sulfate, certain alums, and other highly soluble salts. A series of experiments was accordingly designed, which closely paralleled the inhibition experiments of the preceding paper (14) and in which changes in crystal form could be recorded in the form of photomicrographs.

Procedure for obtaining photomicrographs

To mixtures containing 50 p.p.m. of calcium and 150 p.p.m. of bicarbonate, varying amounts of the respective phosphates were added, and an amount of ammonia solution subsequently added such that when the total volume was in each case brought to 100 ml. with distilled water, the final ammonia concentration would in all cases be 550 p.p.m. of ammonia. The mixtures were allowed to stand undisturbed for a definite period of time, after which the supernatant liquid was decanted to terminate the reaction. The crystals were then washed and, if loosely adherent, transferred to a microscope slide by means of a medicine dropper. In cases where the crystals adhere firmly to the beaker, and it seemed unwise to break them while removing them with a spatula, they were photographed directly in the bottom of the beaker. A uniform magnification of 300 diameters was employed throughout. The photomicrographs so obtained will be presented in figures 1, 2, 4, 5, 6, 7, 8, 9, and 10.

Calcium carbonate precipitates from the system $Ca(HCO_3)_2$–$(NaPO_3)_6$–NH_3 *after 4 hr.* (*see figure 1*)

The effect of the hexametaphosphate on the crystal habit is at once apparent. With no metaphosphate present, typical rhombs of calcite are obtained. In the presence of metaphosphate at concentrations of 0.3 to 0.6 p.p.m., the rhombs are fewer in number and larger in size, many of them showing various degrees of distortion. At 0.9 p.p.m. the original rhombic form has entirely disappeared, and only grotesquely deformed masses of somewhat smaller size remain. At 1.2 p.p.m., corresponding to the "threshold value" for this system as found in the preceding paper (14), only a few crystals were obtained, of about the size of normal rhombs but without definite form. Above this concentration no crystals whatever were obtained, i.e., precipitation was entirely prevented. These results are in striking accord with those found in the inhibition experiments, based on the analytical determination of the amount of calcium precipitated under like conditions.

Calcium carbonate precipitates from the system $Ca(HCO_3)_2$–$(NaPO_3)_6$–NH_3 *after 2 days* (*see figure 2*)

Figure 2 illustrates the effect of time on the extent of deformation that may occur. The crystals are much larger in size, fewer in number, and much more distorted. In some the deformation has just begun to appear in the form of a roughening at the edges; in others there is complete distortion. The size of the normal rhombs, obtained in the absence of metaphosphate, does not change on standing. Beyond 1.5 p.p.m., no crystals whatever were obtained.

The change in size of the crystals precipitated from a solution of calcium bicarbonate and also from a natural water, as the metaphosphate concentration is increased, is shown graphically in figure 3. The natural water, included in the study because of its unusual interest, came from a well near Goleta, California. Among many such waters studied by Rosenstein and his coworkers, the Goleta water proved to be exceptional in its behavior, requiring an extraordinarily high concentration of metaphosphate to inhibit precipitation. This behavior is probably due in part

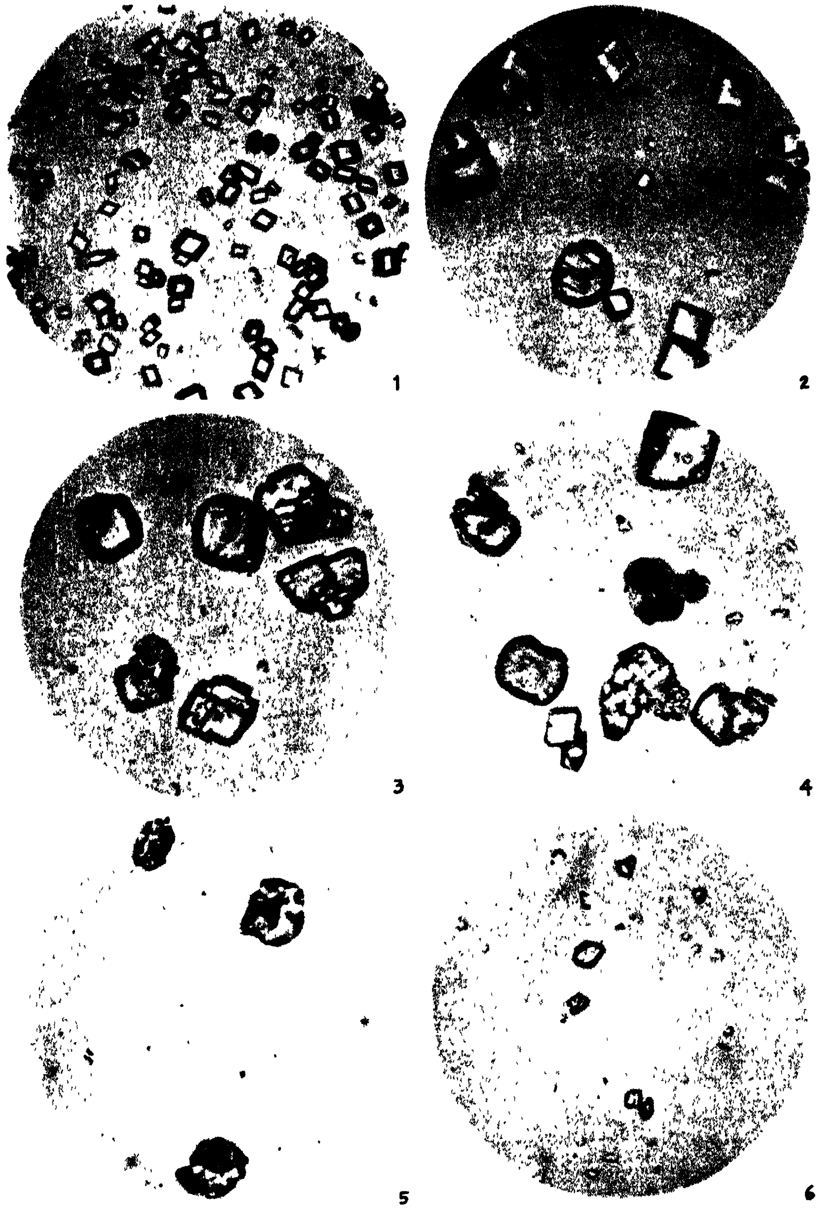

FIG. 1. Calcium carbonate precipitates from the system $Ca(HCO_3)_2$–$(NaPO_3)_6$–NH_3 after 4 hr. Amount of $(NaPO_3)_6$: 1, none; 2, 0.3 p.p.m.; 3, 0.6 p.p.m.; 4, 0.6 p.p.m. (other portion of field); 5, 0.9 p.p.m.; 6, 1.2 p.p.m.

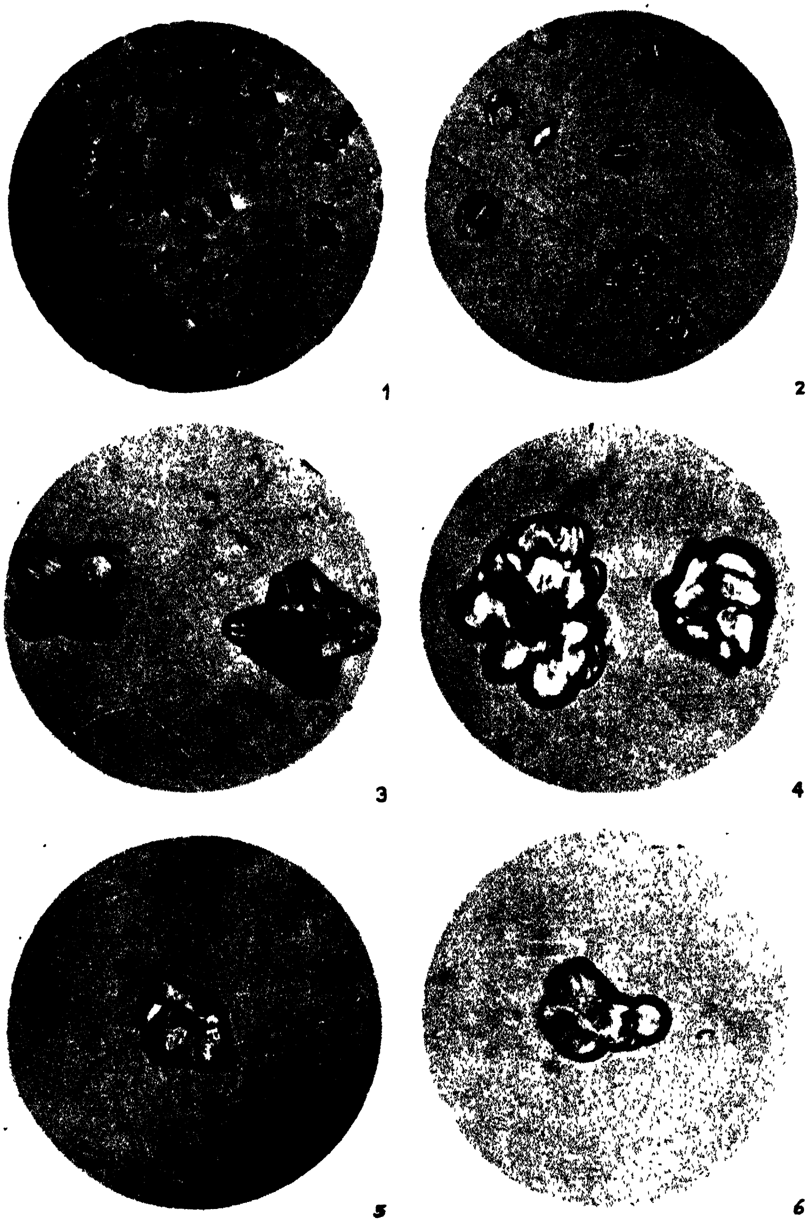

Fig. 2. Calcium carbonate precipitates from the system $Ca(HCO_3)_2$-$(NaPO_3)_6$-NH_3 after 2 days. Amount of $(NaPO_3)_6$: 1, none; 2, 0.3 p.p.m.; 3, 0.6 p.p.m.; 4, 0.9 p.p.m.; 5, 1.2 p.p.m.; 6, 1.5 p.p.m.

to an unusually high concentration of calcium (216 p.p.m.) and magnesium (80 p.p.m.).

It will be observed that the mean diameter of the particle increases with the concentration of metaphosphate to a maximum at a "threshold value" of about 1 p.p.m., thereafter decreasing sharply in the direction of a point where no precipitate whatever would be obtained. The size of the crystals appears to depend upon two factors: (*1*) the extent of the inhibition at any given metaphosphate concentration, and (*2*) the actual supply of calcium and carbonate ions which are available for precipitation. There are apparently two steps in this process. The inhibition process requires that the crystals become progressively larger as the metaphosphate concentration increases. This tendency is counteracted by a decrease in the supply of calcium and phosphate ions which is, in turn, controlled by the metaphosphate concentration. In other words, by *retarding* precipitation the inhibition process causes larger crystals to form, and by eventually *preventing* precipitation it reduces the quantity of precipitate which can form.

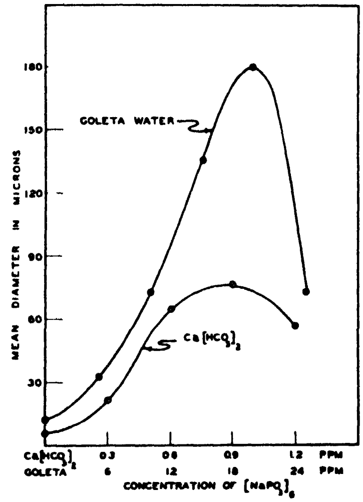

FIG. 3. Mean diameter of calcium carbonate crystals as a function of metaphosphate concentration in solutions from which they were precipitated.

Calcium carbonate precipitates from the system $Ca(HCO_3)_2$-$(NaPO_3)_6$-NH_3 *after 32 days (see figure 4)*

Figure 4 shows the enormous size and the extraordinary degree of distortion which the crystals can attain on long standing. It is significant to note that typical rhombs obtained in the absence of metaphosphate remained unchanged in form and were only slightly smaller in average size at the end of this period. Rough measurements of the areas of the distorted particle in No. 2 and the average dimensions of those in No. 1 indicated a volume ratio of the order of 10,000:1, a change brought about by a concentration of only 0.9 p.p.m. of hexametaphosphate. The actual diameter of the distorted crystal here shown was about 0.2 mm.

Calcium carbonate precipitates from the system $Ca(HCO_3)_2$-$Na_4P_2O_7$-NH_3 *after 4 hr.* (*see figure 5*)

The effect of pyrophosphate is similar to that of the metaphosphate, involving a progressively increasing distortion of the crystals (see figure 5). At 0.3 p.p.m., one finds typical nodular growths on the faces of the rhombs. At 0.45 p.p.m., the original rhombic form has entirely disappeared.

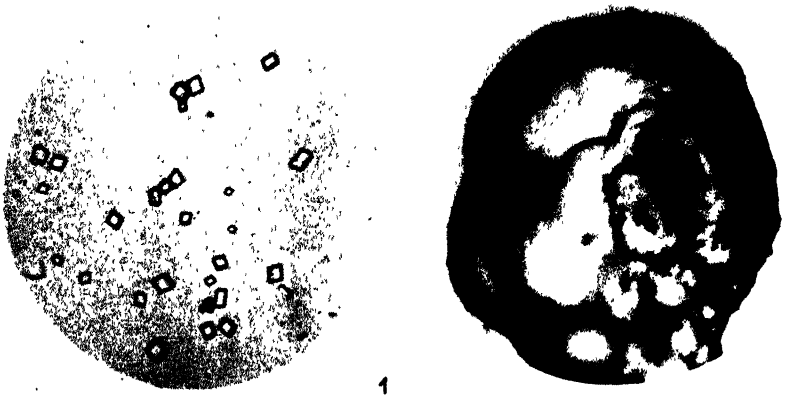

FIG. 4. Calcium carbonate precipitates from the system $Ca(HCO_3)_2$-$(NaPO_3)_6$-NH_3 after standing 32 days. 1, no $(NaPO_3)_6$; 2, 0.9 p.p.m. $(NaPO_3)_6$.

Calcium carbonate precipitates from the system $Ca(HCO_3)_2$-NaH_2PO_4-NH_3 (*see figure 6*)

It was shown in the preceding paper (14) that orthophosphates do not inhibit the precipitation of calcium carbonate in the same sense as do the corresponding meta and pyro salts. The photomicrographs of figure 6 substantiate this observation. At a concentration of 0.3 p.p.m., the rhombs are still unchanged. At 0.9 p.p.m., which is approximately the threshold value for the other phosphates, there is still considerable precipitation, but it will be noted that another species of crystal has made its appearance, which is probably an orthophosphate of calcium.

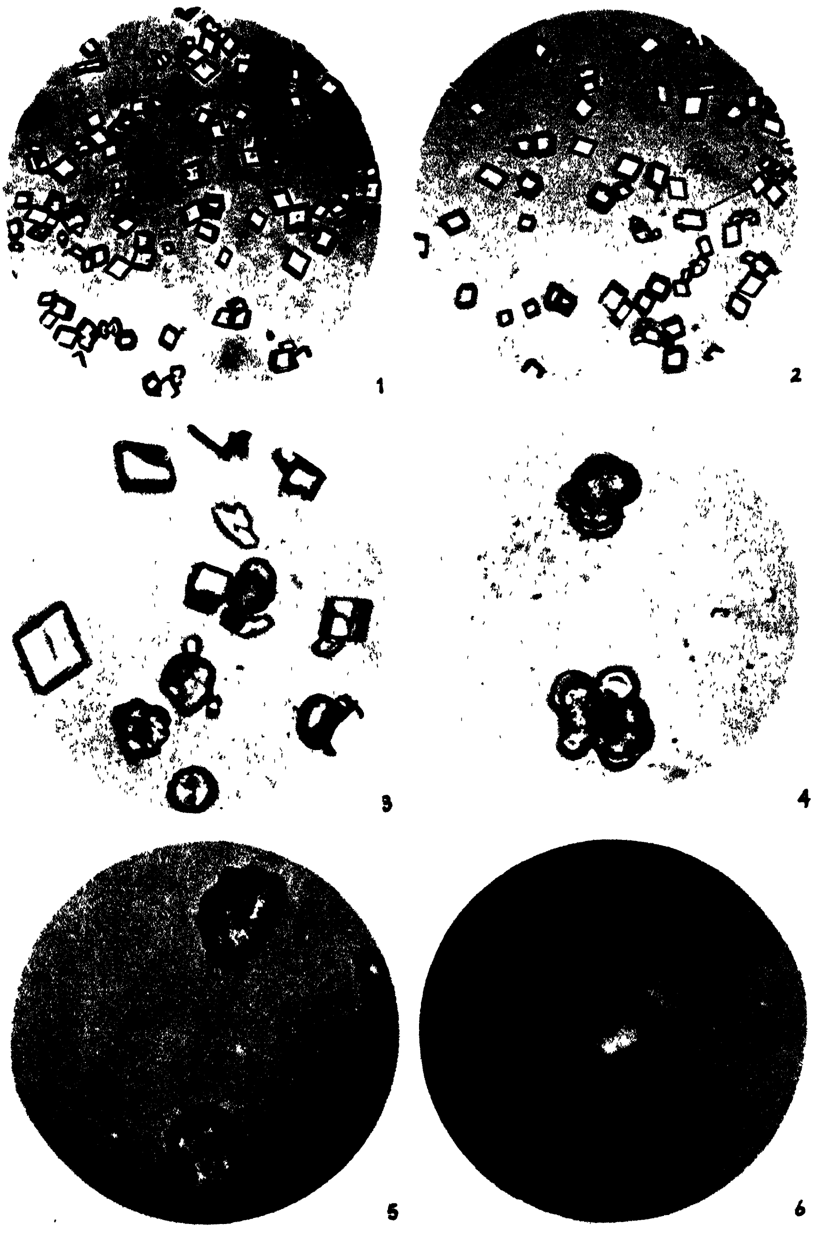

Fig. 5. Calcium carbonate precipitates from the system $Ca(HCO_3)_2$ $Na_4P_2O_7$–NH_3 after 4 hr. Amount of $Na_4P_2O_7$: 1, none; 2, 0.1 p.p.m.; 3, 0.3 p.p.m.; 4, 0.45 p.p.m.; 5, 0.6 p.p.m.; 6, 0.75 p.p.m.

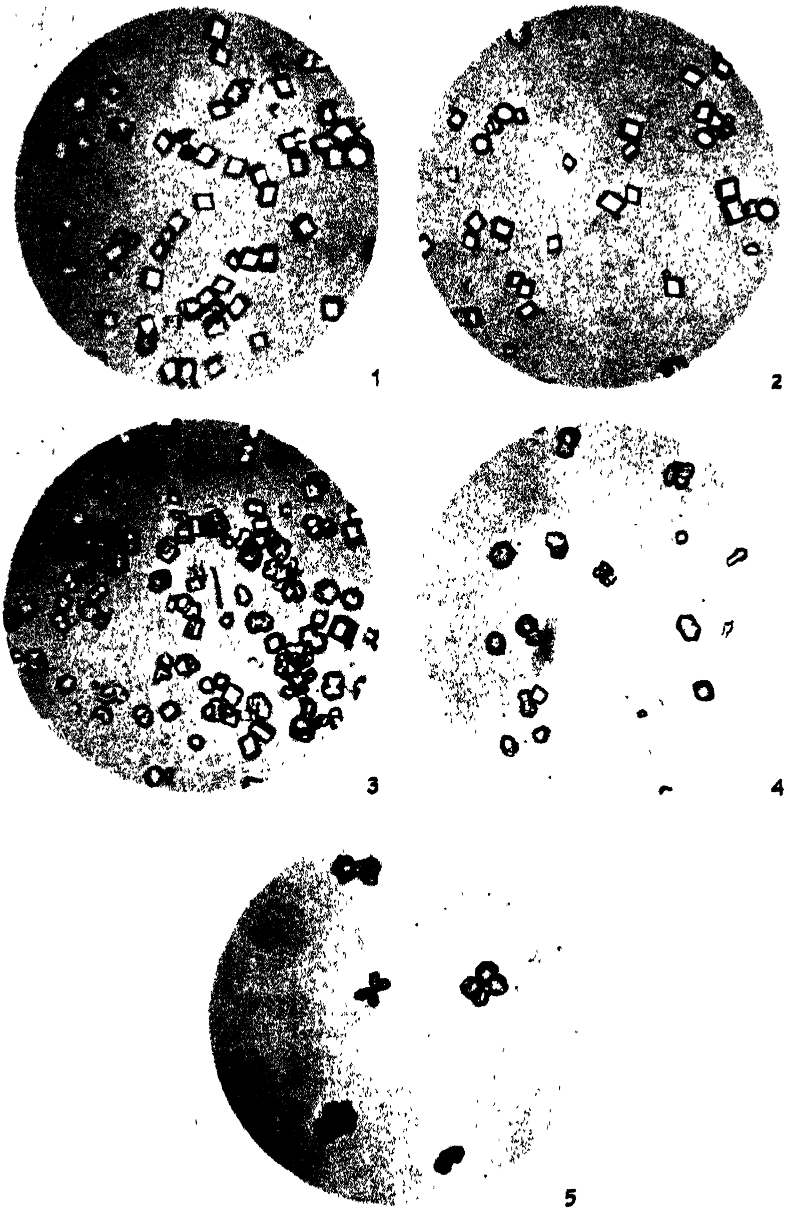

FIG. 6. Calcium carbonate precipitates from the system $Ca(HCO_3)_2$-NaH_2PO_4-NH_3. Amount of NaH_2PO_4: 1, none; 2, 0.3 p.p.m.; 3, 0.9 p.p.m.; 4, 1.2 p.p.m.; 5, 2.0 p.p.m.

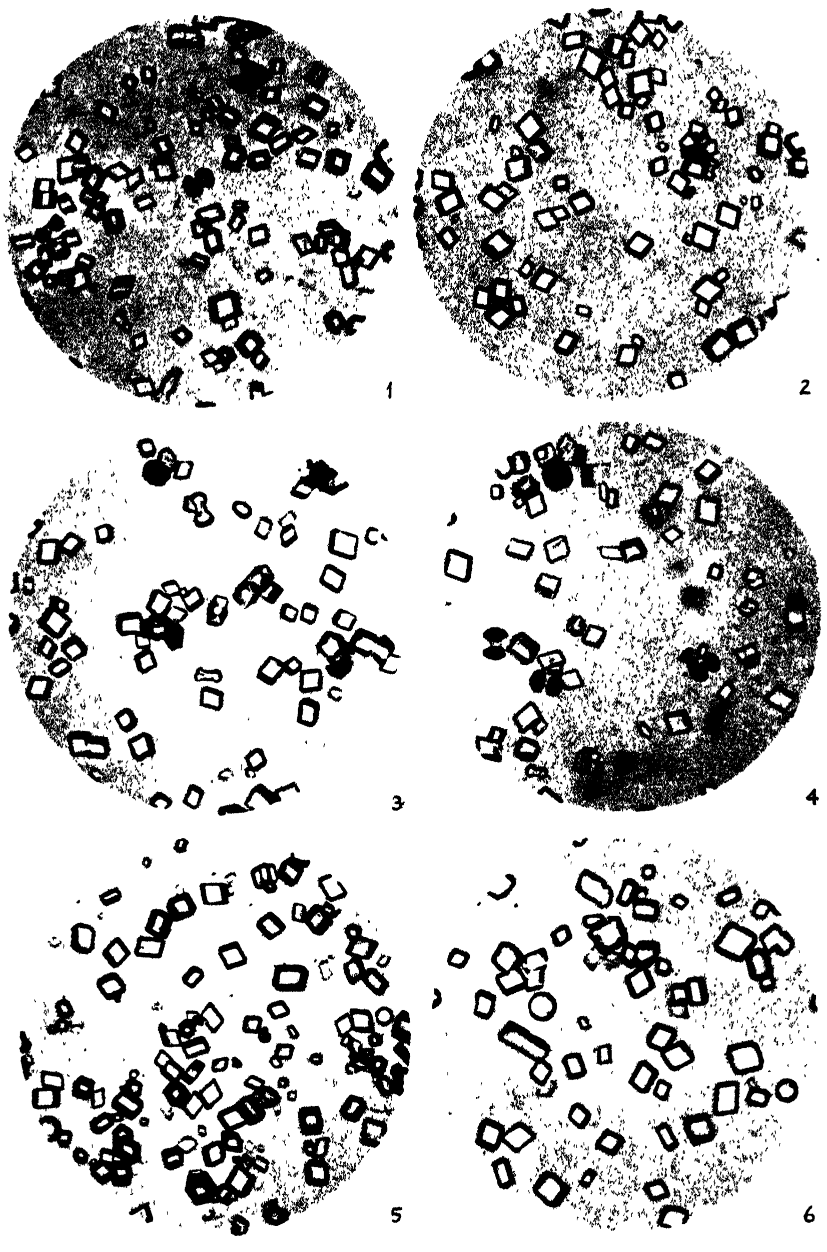

FIG. 7. Calcium carbonate precipitates from the system $Ca(HCO_3)_2$-$NaPO_3$ (crystalline)-NH_3. Amount of $NaPO_3$ (crystalline): 1, none; 2, 0.5 p.p.m.; 3, 1.0 p.p.m.; 4, 1.5 p.p.m.; 5, 4.0 p.p.m.; 6, 10 p.p.m.

Calcium carbonate precipitates from the system $Ca(HCO_3)_2$-$NaPO_3$ *(crystalline)*-NH_3 *(see figure 7)*

The crystalline sodium metaphosphate, sometimes referred to as "soluble trisodium metaphosphate," had been prepared by slow crystallization of the melt at 450°C. Analytical determination of calcium in the precipitates had shown that this salt is ineffective as an inhibitor of calcium carbonate precipitation. Figure 7 confirms this finding, since there is neither a distortion of the crystals nor an appreciable change in size up to the relatively high concentration of 10 p.p.m.

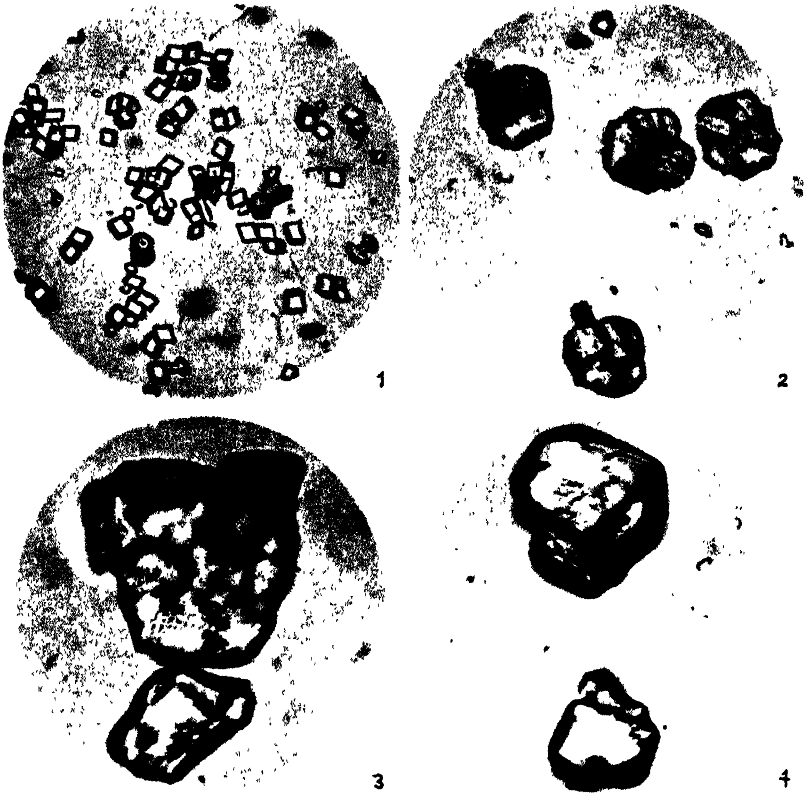

FIG. 8. Calcium carbonate precipitates from the system $Ca(HCO_3)_2$-$NaPO_3$ (crystalline) in 2 *N* KOH-NH_3. Amount of $NaPO_3$ (crystalline): 1, none; 2, 0.5 p.p m.; 3, 1.0 p.p.m.; 4, 1.5 p.p.m.

Calcium carbonate precipitates from the system $Ca(HCO_3)_2$-$NaPO_3$ *(crystalline) in* KOH-NH_3

The experiments illustrated in figures 7 and 8 were suggested by Rosenstein (15), who writes: "Our experiments have shown that this (soluble, crystalline) trimetaphosphate is ineffective as an inhibitor of calcium carbonate precipitation but becomes just as effective as the hexametaphosphate if it is first dissolved in dilute potassium hydroxide solution." In the present instance the crystalline metaphosphate, before being added to the calcium bicarbonate solution was made alkaline to the extent of 2 *N* with potassium hydroxide.

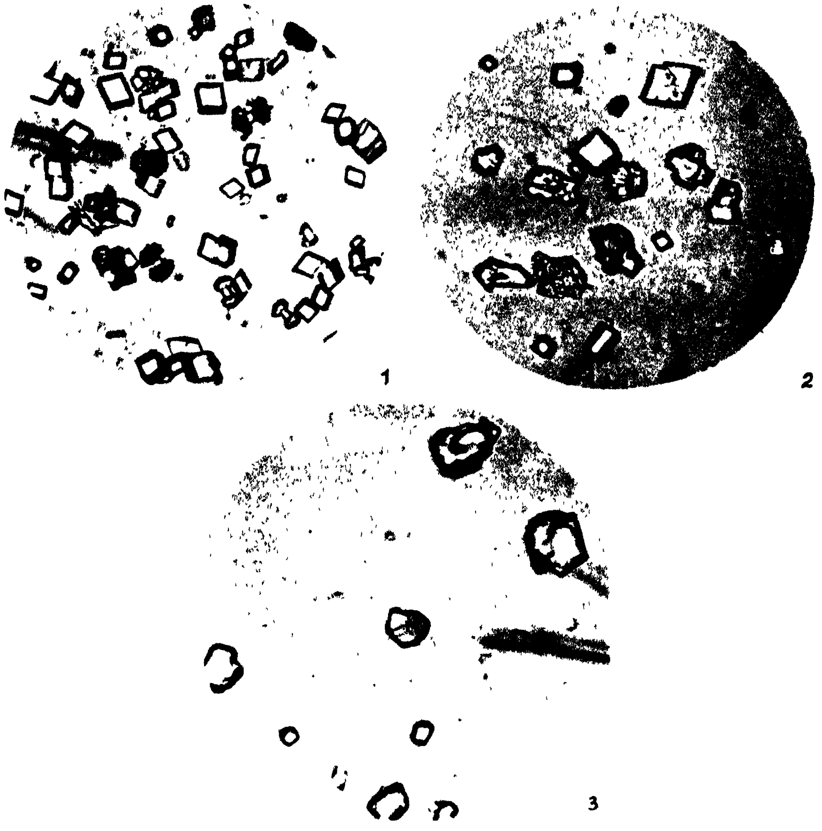

FIG. 9. Calcium carbonate precipitates from the system $Ca(HCO_3)_2$–$(NaPO_3)_6$ in 2 *N* KOH–NH_3 after 4 hr. Amount of $(NaPO_3)_6$: 1, none, 2, 0.3 p.p.m., 3, 0.6 p.p.m.

The photomicrographs show that in the presence of potassium hydroxide the characteristic crystal abnormalities manifest themselves. At a concentration of the metaphosphate as low as 0.5 p.p.m., the normal calcite rhombs are entirely absent, and in their places we again find fewer, larger, and grossly distorted crystals. The size reached a maximum at 1.0 p.p.m., and beyond 1.5 p.p.m. no precipitate whatever was formed. These results suggest that the potassium hydroxide may have acted to convert the crystalline metaphosphate into the hexa-modification or to some active intermediate form.

The question now arises: Would potassium hydroxide affect the inhibiting efficiency of the hexametaphosphate? The results of a similar experiment to prove this point are shown in figure 9.

Calcium carbonate precipitates from the system $Ca(HCO_3)_2$–$(NaPO_3)_6$ *in 2 N* KOH-NH_3

It appears that the base actually increased the efficiency of the hexametaphosphate (see figure 9). This result is the more striking because the high alkalinity would increase the concentration of carbonate ions and *thus favor precipitation.* The crystals show the same tendency to become distorted. The threshold concentration was found to be 0.8 p.p.m., as compared with 1.2 p.p.m. without the potassium hydroxide. It is possible that the base in some manner affects the polymerization of the hexametaphosphate to produce a more reactive phosphate.

Calcium carbonate precipitates from the system $Ca(HCO_3)_2$ NaCl–NH_3 *(see figure 10)*

Although as a rule calcium carbonate is more soluble in solutions of neutral salts than it is in pure water, it was expected that the extent of precipitation would be decreased, even in the absence of metaphosphate. The effect of a salt such as sodium chloride on the crystal habit is not readily predictable, although Marc and Wenk (12) found that sodium chloride and other simple neutral salts have a marked effect upon the formation of alum crystals from their saturated solutions. In the present experiment, where the sodium chloride concentration was carried through an extended range from 0 to about 12,000 p.p.m. (0.2 *N*), there is only a slight increase in the size of the crystals, while at the same time a progressive replacement of the calcite rhombs by the dumbbell-shaped aragonite crystals occurs. It is evident, therefore, that inhibition of the type which characterizes the metaphosphates does not occur even in the presence of high concentrations of the ordinary neutral salts. It is merely a change from one allotropic modification to another, probably due in part to a change in the activity of the ions involved in the precipitation.

X-RAY POWDER SPECTROGRAMS OF VARIOUS CARBONATES

The foregoing experiments raised the question as to whether the distorted crystals represented a fundamentally different crystal modification of calcium carbonate when precipitated in the presence of metaphosphate. To obtain evidence on this point, x-ray powder spectrograms of the precipitates, prepared in the presence as well as absence of metaphosphate, were obtained and these in turn were compared with the patterns yielded

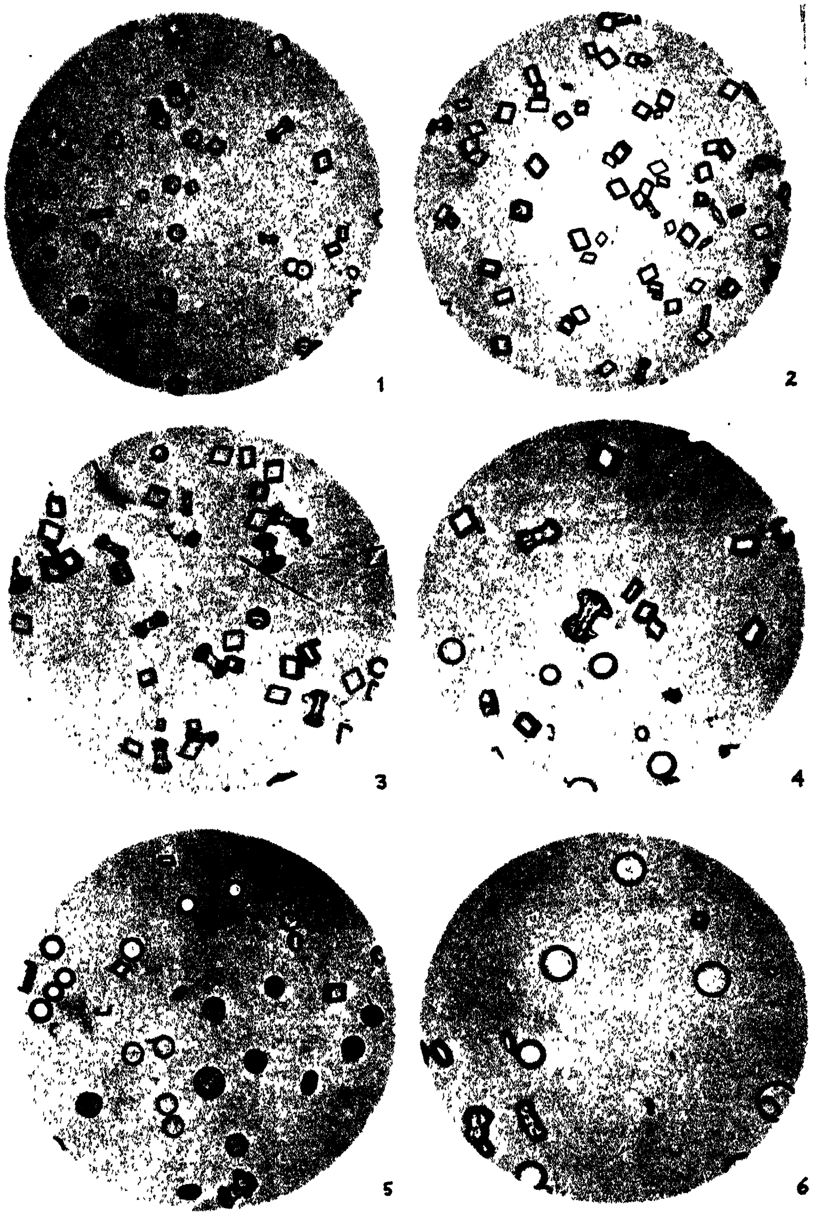

FIG. 10. Calcium carbonate precipitates from the system $Ca(HCO_3)_2$-NaCl-NH_3 after 6 hr. Amount of NaCl: 1, none; 2, 1480 p.p.m., 3, 2970 p.p m.; 4, 6430 p p.m.; 5, 8500 p.p.m.; 6, 11,780 p.p.m.

by pure calcite and aragonite. The spectrograms were found in all cases to be identical with that of calcite. Thus, although the metaphosphate causes considerable distortion of the crystals, so that they exhibit no external signs of a definite structure, they are, nevertheless, true calcite. In natural waters, where magnesium may be present in considerable amounts, there is a tendency for magnesium carbonate to precipitate out also; under those conditions calcium carbonate often precipitates in the form of aragonite.

RATIO OF CALCIUM TO PHOSPHORUS IN THE CALCIUM CARBONATE PRECIPITATES

The foregoing photomicrographic studies have shown that the inhibitory effect of metaphosphates consists in part of a retardation of the crystallization of calcite, and, in addition, an extensive derangement of the normal growth of the crystal lattice. It seems necessary to assume that the metaphosphate has in some manner entered the lattice or has been adsorbed on the surface of the crystal. The latter view has been taken by Rosenstein (15) and by Hatch and Rice (7). It seemed of considerable interest to determine the order of magnitude of the ratio of Ca:P, and to ascertain how it changes as the metaphosphate concentration is increased. While the x-ray diffraction method indicates the nature of the crystals which were formed, it does not offer an answer to the question as to a possible combination of the metaphosphate with the calcium carbonate.

To secure quantitative evidence on this point, four sets of precipitation mixtures were prepared, each set consisting of eight mixtures in which the concentration of metaphosphate was varied from 0 to 1.5 p.p.m. The concentration of calcium was 50 p.p.m., of bicarbonate 150 p.p.m., and of ammonia 567 p.p.m. These concentrations were the same in all of the mixtures, and the total volume was kept constant at 400 cc. The four series of mixtures were allowed to stand 3, 21, 76, and 420 hr., respectively. At the end of these time intervals, the precipitates were filtered off, dissolved in hydrochloric acid, and warmed on the water bath for 10 hr. to hydrate the meta- to the ortho-phosphate. The solutions were then analyzed for calcium and phosphate, respectively. The results are shown graphically in figures 11, 12, and 13.

Figure 11 shows the amounts of calcium precipitated as a function of metaphosphate concentration and of time of standing. It will be seen that the curves so obtained correspond closely to those of figure 4 of the preceding paper (14).

Two significant relationships are evident from figure 12. First, the amount of phosphorus associated with the precipitated calcium carbonate increases with the concentration of metaphosphate up to a maximum which in all cases occurs at or near a concentration of 0.6 p.p.m., beyond which point the curves show a sharp drop. Below this concentration the curves have the characteristics of a typical adsorption isotherm. Apparently the metaphosphate is adsorbed by the precipitate in increasing amounts until this limiting concentration is reached, beyond which the amount adsorbed decreases. This decrease beyond the maximum is merely incidental, since the amount of precipitate that separates out decreases with increasing metaphosphate concentration. The amount of calcium precipitated decreases more rapidly than the amount of phosphate adsorbed increases, hence the molecular ratio of the two constituents decreases rapidly up to the metaphosphate concentration of 0.6 p.p.m.

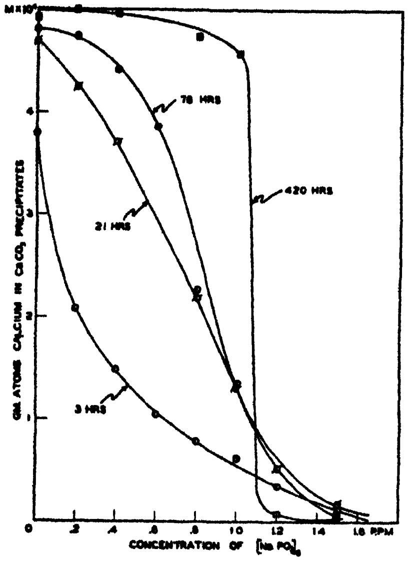

FIG. 11

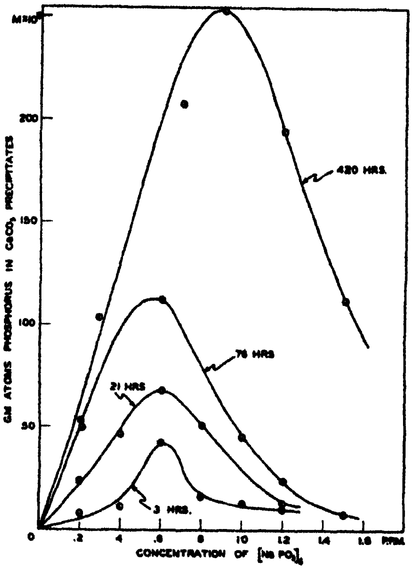

FIG. 12

FIG. 11. Calcium content of calcium carbonate precipitates
FIG. 12. Phosphorus content of calcium carbonate precipitates

Another point of interest shown by figure 12 is the phenomenal increase in the amount of phosphorus adsorbed as the time of standing is increased. This is the more striking in view of the photomicrographic evidence, which indicated that, as the time of standing was increased, the number of extraordinarily large particles as well as their size increased at the expense of the smaller ones. Such a process should result in a markedly decreased surface and hence decreased adsorption.

In figure 13 the atomic ratios of calcium to phosphorus are plotted against the metaphosphate concentration. The ratio decreases sharply and tends to level out to a constant value beyond a metaphosphate concentration of 0.6 p.p.m. Because of the inherent limitations of the semimicro analytical method used, the curves do not converge to, or become precisely superimposable at, a particular value of the ratio. There is no apparent trend, however, since the points lie above and below a mean value of the ratio, which at the "threshold inhibition value" of 1.0 p.p.m. was about 320. The deviations of the curves from this limiting value are within limits of error of the analytical methods.

The magnitude of this ratio, in spite of its apparent constancy, does not justify the conclusion that a definite compound is formed between the metaphosphate and calcium carbonate. The phenomenon rather indicates adsorption on the surfaces of the calcium carbonate particles, which in turn is responsible for the subsequent abnormal growth of the crystal. The constancy of the ratio, which is remarkable in view of the extended period of time through which the experiment was carried, is probably to some extent fortuitous. The experiments do show, however, that the effect of the metaphosphate is not altogether an indirect one, as, for example, by affecting the activity of the reacting components in some manner, but a direct effect upon the calcium carbonate precipitate itself at the time of its formation.

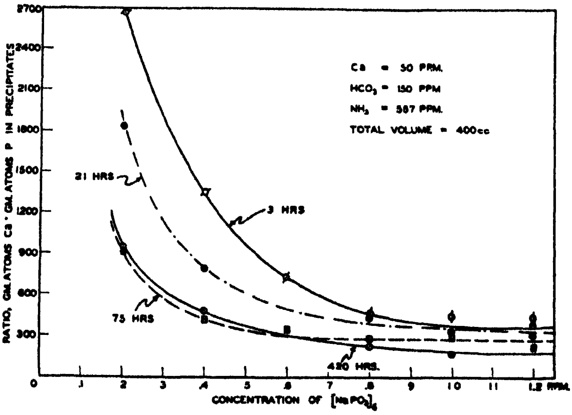

FIG. 13. Molal ratio of calcium to phosphorus in calcium carbonate precipitates

DISCUSSION

The evidence presented in the preceding paper (14), as well as in the experiments just described, makes it possible to deduce a tentative mechanism for the inhibition process. It has been shown that the inhibition may be either partial or complete, depending upon the metaphosphate concentration. When the latter exceeds considerably the "threshold" concentration, there is a relatively permanent postponement of the precipitation. Such an inhibition as well as complete prevention of precipitation takes place in the solution phase, notwithstanding the high degree of alkalinity on account of the free ammonia, together with a sufficient concentration of calcium and bicarbonate ions to favor precipitation. Such behavior cannot be justifiably attributed to complex formation between calcium and metaphosphate, in view of the extraordinarily small formula-weight ratio of metaphosphate to calcium, namely, 1:1000. This conclusion is also consistent with the fact that under such conditions the calcium is almost quantitatively titratable with soap solution. For the complete softening of boiler-feed water, on the other hand, Hall (6) finds that the corresponding Ca:$NaPO_3$ ratio must be at least 1:4 at pH 8.5 and 1:7 at pH 10. He attributes the softening action to the formation of a complex, the composition of which apparently varies with the pH value.

Since in the present case complex formation occurs to a negligible extent, we must conclude that the action is largely an indirect one, involving either a stable electrostatic attraction between calcium and metaphosphate ion or a marked decrease in the activity of calcium ion due to the presence of the metaphosphate.

Whatever the effect of the metaphosphate may be upon calcium ion in completely preventing precipitation of calcium carbonate, the experimental evidence regarding its inhibiting effect within the range of the threshold concentration of 1 p.p.m. points definitely to an interference in the growth of the calcium carbonate crystals. It was found that under these conditions the growth of the crystals was greatly retarded and the crystals formed were fewer in number, larger in size, and more or less distorted. The rate of deposition of the carbonate is approximately inversely proportional to the metaphosphate concentration.

It is generally conceded that the formation of crystal nuclei and the subsequent growth of the crystal are entirely distinct phenomena. While certain investigators have been inclined to consider the effect of the metaphosphate to be one of stabilizing a supersaturated solution of calcium carbonate and thus preventing precipitation, the very fact that crystals do form argues against such a possibility. It was found, moreover, on the basis of ultramicroscopic observations that calcium carbonate does not exist in colloidal dispersion, or, if it does, its existence in that state is very transitory. Hence we are led to the conclusion that the metaphosphate does not interfere with the normally rapid transition from nuclear through colloidal to macroscopic dimensions, but that it retards the subsequent growth of the crystals.

The experimental evidence indicates fairly definitely what occurs during this retarded process of crystal growth. First, it is found by analysis that the metaphosphate actually enters the lattice or is adsorbed on the surfaces of the crystals. The greatest amount of phosphorus was found in those crystals which exhibited the greatest degree of distortion. Secondly, the abnormal growths usually make their appearance on the faces and apices of the normal calcite rhombs first formed. This finding is in accord with the view of Pauling (13), who states that such an effect will usually manifest itself first at the apices of a crystal lattice, which are the points of greatest instability and reactivity. Evidently the metaphosphate is adsorbed by the crystals and thereafter the normal process of crystal growth is deranged.

Similar abnormalities in the process of crystallization as well as in the form of the crystal obtained have been encountered by other workers. Marc and Wenk (12) were among the first to observe the effect of small amounts of a foreign adsorbable substance in preventing the crystallization of potassium sulfate from its saturated solution even after long standing. They showed, further, that such foreign substances did not prevent crystals from dissolving in their own unsaturated solution. In the light of their findings it seems reasonable to conclude that any nuclei or submicroscopic crystals of calcium carbonate are readily dissolved because they have a higher solubility than the large crystals, and because their solubility is not influenced by the metaphosphate. The larger crystals thus grow at the expense of the small ones, but their growth is retarded and their shape distorted, owing to the presence of the metaphosphate.

Keenen and France (9) explain the effect of gelatin and certain dyes on the rate of growth of potassium alum crystals by assuming that the foreign substance is adsorbed by the crystals "... in areas of different concentration, corresponding to the different fields of force existing at the various crystal faces. Those faces having alternate planes of like ions exhibit much greater adsorbing power than those with a checkerboard arrangement of positive and negative ions." Such a mechanism may serve to explain the exaggerated growths from certain faces of the calcium carbonate crystals as shown in figure 2 (2 and 3). This behavior is also consistent with the nature of the "etch-figures" used by the mineralogist in determining the symmetry of a crystal. In this case the action of the solvent begins at certain points and proceeds with greater rapidity in certain directions than in others; in addition, it may produce different figures on certain faces and leave others entirely unaffected.

A strikingly similar type of abnormality in the case of calcium carbonate crystals was found by Kohlschütter and Egg (10, 11). They obtained such distorted crystals, which they called "somatoids," in the presence of various colloidal sols and dye solutions. They concluded that such somatoid forms result from the adsorption of foreign substances present in solution upon the crystals of calcium carbonate during the period of their precipitation.

In the present case we have an example of derangement of crystal growth by reason of the adsorption of a substance which is not colloidally dispersed but in true solution, and, furthermore, is present in an exceedingly small concentration. These facts, together with the observation that inorganic salts of other elements, similar to sodium metaphosphate, and other simple salts like sodium chloride, even when present at high concentration, are entirely without such inhibiting action, indicate that the action of sodium metaphosphate is highly specific.

SUMMARY

1. Ultramicroscopic studies have been made on solutions in which calcium carbonate was formed by precipitation in the presence of progressively increasing concentrations of sodium hexametaphosphate. The results indicate conclusively that calcium carbonate does not go into the colloidal state nor is such a state stabilized by the presence of the metaphosphate.

2. Photomicrographic studies indicate that the metaphosphate promotes the formation of larger, fewer, and grossly distorted crystals in place of the typical rhombs of calcite. It was found that the meta-, pyro- and ortho-phosphates possess in varying degrees this ability to hinder the process of crystallization.

3. The soluble crystalline sodium metaphosphate does not possess the property of inhibiting the precipitation of calcium carbonate, but acquires it in the presence of potassium hydroxide.

4. Neutral salts such as sodium chloride promote the transformation of calcite to aragonite rather than to the abnormal somatoid forms. This may be a simple solubility effect.

5. X-ray powder spectrograms have shown that the distorted crystals obtained in the presence of these phosphates are true calcite, although their exterior surfaces may show complete absence of typical polyhedral faces.

6. Chemical studies of the precipitates indicate that the metaphosphate is adsorbed by the calcium carbonate in amounts such that the Ca:P ratio attains a constant value of approximately 300 in the presence of metaphosphate concentrations greater than 0.6 p.p.m., which is the concentration at which the adsorption reaches a maximum.

7. The mechanism of the inhibition process is conceived to involve primarily a restricted or deranged crystallization due to the adsorption of the metaphosphate on the crystal faces.

The authors desire to acknowledge with thanks the assistance and encouragement of the Shell Chemical Company, which sponsored this research, and the kindness of the General Electric X-Ray Corporation of

Chicago, Illinois, and of Dr. D. H. Reynolds in particular, in making the powder spectrograms of the various carbonate and phosphate samples obtained in this study.

REFERENCES

(1) Chwala, A.: Kolloid-Beihefte **31**, 222 (1930).
(2) Eckert, T. S., and France, W. G.: J. Phys. Chem. **31**, 877-81 (1927).
(3) Eckert, T. S., and France, W. G.: J. Am. Ceram. Soc. **10**, 579-91 (1927).
(4) Goldschmidt, A.: *Atlas der Kristallformen*, Volume II, p. 5. Carl Winters, Heidelberg (1913).
(5) Gortikov, V. M., and Malinovskaya, N. P.: Colloid J. (U. S. S. R.) **2**, 429-33 (1936).
(6) Hall, R. E.: U. S. patent 1,956,515 (April 24, 1934), p. 5.
(7) Hatch, G. B., and Rice, Owen: Ind. Eng. Chem. **31**, 51-7 (1939).
(8) Johnston, J., Merwin, H. E., and Williamson, E. D.: Am. J. Sci. [4] **41**, 473-512 (1916).
(9) Keenen, P. G., and France, W. G.: J. Am. Ceram. Soc. **10**, 821-7 (1927).
(10) Kohlschütter, V., and Egg, C.: Helv. Chim. Acta **8**, 470-90 (1925).
(11) Kohlschütter, V., and Egg, C.: Helv. Chim. Acta **8**, 697-703 (1925).
(12) Marc, R., and Wenk, W.: Z. physik. Chem. **68**, 104 (1909).
(13) Pauling, L.: Personal communication.
(14) Reitemeier, R. F., and Buehrer, T. F.: J. Phys. Chem. **44**, 535 (1940).
(15) Rosenstein, L.: Private communication.

A SENSITIVE STATIC VAPOR PRESSURE APPARATUS[1]

RAY CALVIN CHANDLER[2]

Department of Plant Nutrition, University of California, Berkeley, California

Received June 27, 1939

The vapor of an aqueous solution under its own vapor pressure in a closed system approximates the behavior of an ideal gas. Such a system is constantly in equilibrium, capable of rapid reversible adjustments to variation in temperature, pressure, and concentration. A satisfactory static vapor pressure apparatus is very desirable for the calculation of thermodynamic functions in the study of solutions. Hitherto the use of this method has been limited by the difficulties involved in the preparation of experimental solutions which were sufficiently free from residual gases and uniform in concentration so that measurements of high accuracy could be obtained. Furthermore, colloidal solutions preclude the use of extremes of heat or cold in freeing the solutions from gases as practiced in the treatment of true solutions. A study on colloidal solutions presented the need for a highly sensitive vapor pressure method not limited by these difficulties. There is general need for such apparatus, both directly and as an adjunct to other methods now employed in thermodynamic studies. The possibilities of the vapor pressure method have been shown by Frazer and Lovelace and coworkers (1, 2, 3, 4, 5, 6) in their application of the Rayleigh manometer to the study of true solutions. The description of a new practical apparatus is herewith presented.

---

[1] This paper constitutes a portion of a thesis submitted by the author to the Graduate Division of the University of California in partial fulfillment of the requirements for the degree of Doctor of Philosophy, December, 1937.

[2] Present address: Department of Botany, University of Arizona, Tucson, Arizona.

DESCRIPTION

The static vapor pressure apparatus consists essentially of a U-tube manometer, the upper limbs terminating in solution bulbs immersed in a constant-temperature bath. The lower part of the differential manometer contains a liquid piston which actuates a mirror suitably arranged to measure changes in the level of the liquid with a sensitivity corresponding to a change in vapor pressure of less than 10^{-4} mm. of mercury. A convenient efficient method for evacuating the system as a whole and then separating the two sides of the manometer into two systems completes the plan of the apparatus.

The differential manometer (figure 1), mounted in the insulated case (d), consists of two upright limbs of 15-mm. tubing which are expanded into 7-cm. tubing at the bases. It contains a liquid piston of dibutyl phthalate, an ester of low vapor pressure whose properties have been described by Hickman (7) and Hickman and Sanford (8). Its specific gravity was found to be 1.0422 at 25°C. The entire manometer is mounted in an insulated case (d) having a transparent face. The case is pivoted at the level of the liquid surface (q), so that the solution bulbs may be agitated vigorously with minimum disturbance of mirror A. External to the manometer case (d) the high-vacuum line contains the following: a flexible glass coil (j) which allows the necessary movement for agitation of solutions and calibration of the manometer; the mercury seal No. 2 (i) utilized in evacuation; and the McLeod gauge (h) for measuring residual gas pressure. The high vacuum then connects (n) with the diffusion pump. Accessory connections (e) for preliminary evacuation of the solution bulbs and the connection (f) to the helium tank are shown. The automatic control (g) of seal No. 2 is driven by the backing pump and provides for periodic exposure of the manometer system to high vacuum. Near the level of the surface of the liquid piston in the base of the right-hand limb of the manometer a plane glass window is sealed. This window and assembly (figure 2,a) consist of the plane window (a^3)

and a semicircular glass shield (a^4) supporting a mirror (a^1) and bulb (a^2). The bulb rests upon the surface of the liquid piston and actuates the mirror (a^1), hereafter called mirror A. A second one, mirror B, is fixed stationary in the manometer case (figure 4) in such way that it, too, reflects illuminated scale No. 1 side by side with its reflection from mirror A, as seen by the observer. The reading of mirror A indicates the change of level of the liquid piston, while mirror B enables one to set the manometer accurately in position for readings. Reference to figures 1, 2, 3, and 4 shows the relationships between the parts described.

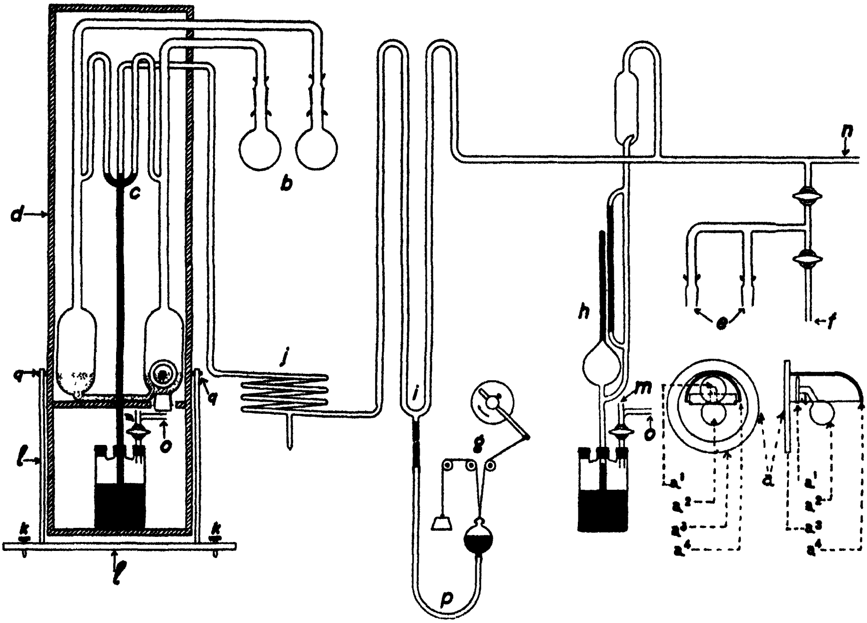

FIG. 1. Vapor pressure apparatus. a, detail of window and mounting of mirror; a^1, mirror; a^2, bulb; a^3, window; a^4, shield; b, solution bulbs; c, seal No. 1; d, manometer case; e, outside connections; f, to helium tank; g, automatic seal control; h, McLeod gauge; i, seal No. 2; j, flexible glass coil; k, levelling screws; l, supporting base of manometer case; m, to atmosphere; n, to high vacuum; o, to house vacuum; p, flexible rubber tubing; q, pivot point.

Since long-continued evacuation is necessary, the usual freezing-out trap is omitted from the system. The presence of mercury vapor requires a special mirror for which optically plane, aluminum-faced mirrors proved satisfactory.

The removal of dissolved gases from all parts of the system, including the liquid piston as well as the experimental solutions, and the maintenance of uniform concentration throughout the solutions present difficulties inherent in the static method. A preliminary evacuation of the apparatus for 3 weeks or more may be necessary and must be continued until no pressure develops in the apparatus when the highly evacuated systems are separated by closing seal No. 1.

When experimental solutions were to be introduced, the non-polar gas helium was admitted into the system momentarily. During evacuation the solutions were agitated by rocking the pivoted manometer case by motor-driven apparatus. Frazer, Lovelace, and Taylor (6) described a "rapid expansion" method for the final removal of gases from boiled true solutions. In dealing with natural or artificial colloidal solutions extremes of temperature must be avoided. The effective removal of residual gases at ordinary temperatures was facilitated by use of an automatic control of seal No. 2, which greatly improved the method and rate for attaining equilibrium between liquid and vapor phase.

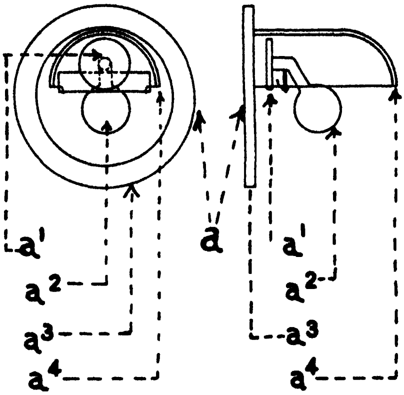

FIG. 2. Detail of window and mounting supporting mirror A. a, assembly of parts; a^1, mirror A; a^2, bulb actuating mirror; a^3, window; a^4, shield.

Further improvement in technique was introduced by use of gas-free solutes, such as fused potassium chloride, in small tubes which were evacuated and sealed with mercury while hot. These gas-free solute charges may be suspended inside the system above the solutions and introduced when desired. Two or more concentrations may thus be studied by one evacuation. The tendency of the mirror to become clouded by dibutyl phthalate when no experimental solutions are present may be prevented by use of a small cooling coil about the dibutyl phthalate on the mirror side of the manometer.

An extra set of bulbs and outside connections (e) to the vacuum system permit a preliminary evacuation of solutions. At the beginning of an experiment an atmosphere of helium is admitted to the system (at f), the solution bulbs and solute charges quickly transferred to the manometer, and the ground-glass joints sealed with picein wax. The solutions are kept near 0°C. and continuously agitated while evacuation proceeds. After 1 or 2 hr. direct evacuation the automatic valve control (g) of seal No. 2, driven by the backing pump of the high-vacuum system, opens this valve every 4 min. for a few seconds, permitting a rapid expansion of the gases evolved from the experimental solutions periodically into the outer part of the system, which is directly connected to the vacuum pump continuously. Preliminary readings may be made in 36 hr.; accurate readings require a week. With the solutions at 0°C. the water loss amounts to about 15 g. per bulb before the removal of residual gases is sufficiently complete. The progress of evacuation must be carefully followed by use of the McLeod gauge.

When the residual gas pressure (rgp) has been reduced to approximately 2×10^{-4} mm. of mercury, does not accumulate to exceed 10^{-3} mm. after 4 hr. agitation, and the temperature has been constant to 0.001°C. for 36 hr., readings may be obtained as follows: With seal No. 1 open and the vacuum system operating at maximum efficiency, the manometer is opened to the vacuum system by means of the automatic seal No. 2 briefly until the desired residual gas pressure is attained. Then seal No. 1 is closed and the solutions agitated for 90 min. The manometer is then fixed firmly and its position noted by mirror B. After 10 min., readings may be made from mirror A as often as desired over a period of an hour or more. A constant set of readings indicates a stable equilibrium, which is the "pressure reading". Seal No. 1 is then opened, and after a few minutes a series of constant readings indicates the "zero reading" or null point. The vapor pressure reading may be calculated as indicated below.

CALIBRATION

The manometer is calibrated by measuring the change in level of the liquid supporting the bulb which actuates mirror A as the manometer is rotated about the point of rest on the left-hand levelling screws. The vertical plane of the manometer may be maintained in its place by aid of mirror B. The flow of the liquid, as the manometer is rotated, changes the angle of mirror A and the reading of scale No. 1 in mirror A (by a telescope, figure 3). Simultaneously this angular rotation of the manometer is measured by using the entire length of the manometer case as a long lever (figure 4) to actuate mirror C, which has a short lever and is supported by a fixed fulcrum. The angular rotation of mirror C is measured by illuminated scale No. 2, which is read by a telescope trained on mirror C.

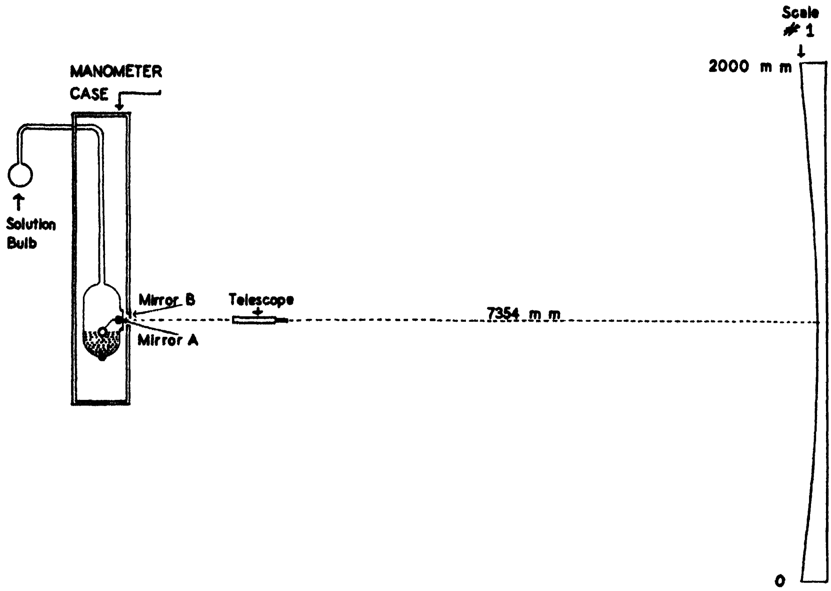

FIG. 3. Side view of manometer showing relative positions of manometer, scale No. 1, mirror A, mirror B, and solution bulbs.

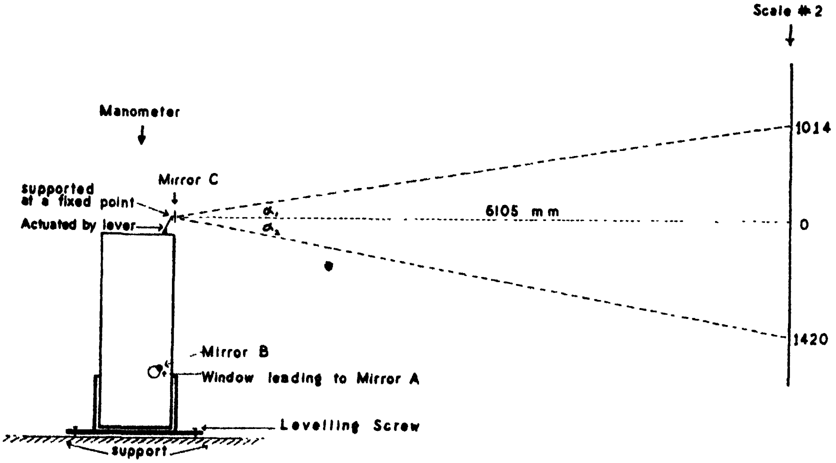

FIG. 4. Front view of manometer case showing relative positions of manometer case, mirrors A, B, and C, and illuminated scale No. 2.

Figure 4 illustrates the readings for three points on scale No. 2. For any angle measured on scale No. 2 the change in level of the liquid piston may be measured by the angle *cbc′* (figure 5), which is also equal to angle β_1, the angular rotation of the manometer. For the small angles involved

$$\tan cbc' = \sin cbc'$$

$$= \frac{\text{length short lever}}{\text{length long lever}} \times \tan \tfrac{1}{2}\alpha$$

from which the value y for the change in level may be calculated. By plotting the curve for a number of points the equation for the circle upon which all points (x, y) lie may be determined and scale values tabulated. An equal and opposite change occurs in the other limb of the manometer, and the data obtained, when dibutyl phthalate with a density of 1.0422 at 25°C. is used, may be transformed into millimeters of mercury by the factor

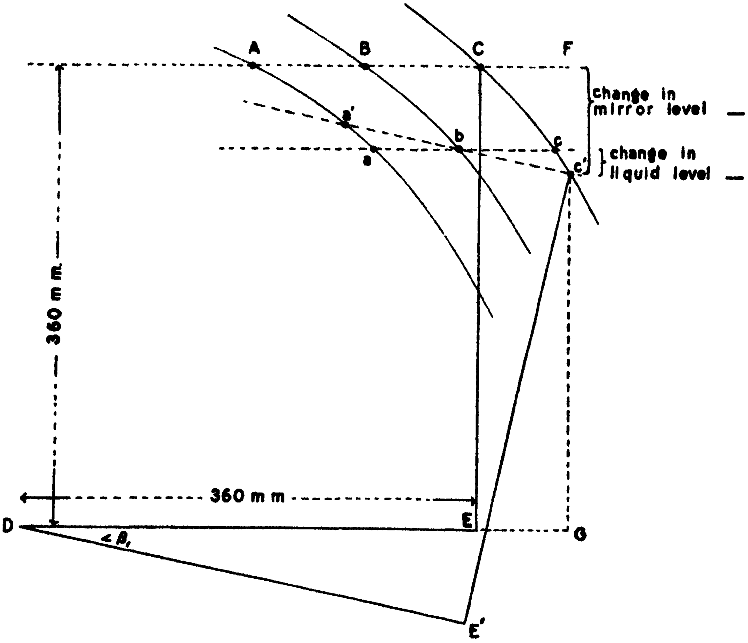

FIG. 5. Diagram showing effect of rotation of manometer about point D upon the reading of scale No. 1 and the change in liquid level. A and C, midpoints in manometer limbs at surface of liquid piston; B, midpoint between points A and C; $a'bc'$, position of ABC after rotation if flow did not occur; abc, position of ABC after rotation due to gravity; Fc', change in position of mirror A; cc', change in level of liquid piston.

$$\frac{2 \times 1.0422}{13.5955} = 0.1533$$

A check on the apparatus may be made by comparison with data obtained by others. Potassium chloride solutions indicated vapor pressure depressions 0.6 per cent greater than those reported by Frazer, Lovelace, and Sease (5). Further test of the equational curve was made by measurements of the vapor pressure lowering of the same potassium chloride solution at opposite ends of scale No. 1 (see table 1).

TABLE 1

Vapor pressure measurement at different portions of scale No. 1 on the same potassium chloride solution

UPPER HALF OF SCALE	LOWER HALF OF SCALE
mm. Hg	*mm.* Hg
0.0612	0.0605
0.0617	0.0613
0.0614	0.0606
0.0616	0.0597
0.0610	0.0626
0.0617	0.0630
0.0614	0.0613

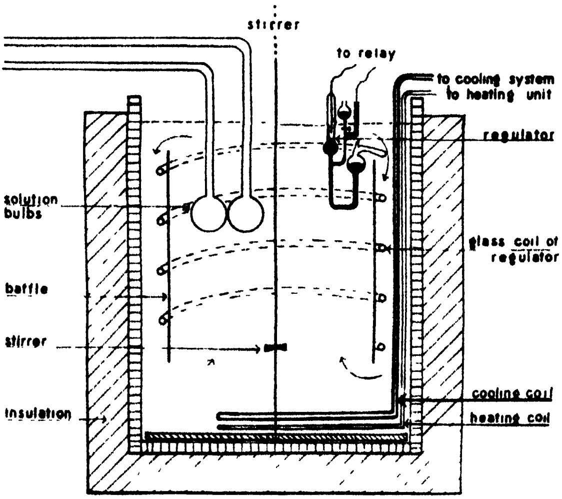

Fig. 6. Detail of bath and thermoregulator

TEMPERATURE CONTROL

The bath is controlled by an all-glass mercury–toluene regulator, as illustrated in figure 6. A gentle vibrator attached to it prevents the sticking of mercury in the capillary, and no visible change can be observed in Beckmann readings at 20°C. Uniformity of temperature change

TABLE 2

Vapor pressure lowering of potassium chloride solutions at 20°C.

CONSECUTIVE SCALE READINGS ON SCALE NO. 1 IN MILLIMETERS				
(a) Solutions agitated 3 hr.; then read each minute			(b) Solutions agitated 1.5 hr.; then read after 8 hr.	
1828	1800	1790	1858	1857
1822	1798	1790	1858	1858
1821	1794	1790	1856	1858
1819	1794	1790	1858	1858
1818	1794	1790	1858	1858
1814	1792	1790	1858	1859
1810	1791	1792	1857	1858
1810	1790	1790	1857	1857
1808	1790	1790	1857	1857
1808	1790	1790	1857	1858
1808	1790	1790	1857	1858
1805	1790	1790	1856	1857
1802	1790	1790	1856	1858
1802	1790	1790	1856	1858
1802	1790	1790	1857	1858
1800	1788	1790	1857	
1800	1788	1790		
1800	1788			
y_2 = 1790 = 0.8685 y_1 (zero) = 850 = $\underline{0.4678}$ 0.4007 0.4007 × 0.1533 = 0.0614 mm. Hg			y_2 = 1858 = 0.8940 y_1 (zero) = 899 = $\underline{0.4912}$ 0.4028 0.4028 × 0.1533 = 0.0617 mm. Hg	

TABLE 3

Data on a gelatin solution

Solution agitated 125 min.; time of readings of scale No. 1 in minutes as indicated by figures in parentheses; gelatin solution in right-hand bulb and distilled water in left-hand bulb

CONSECUTIVE READINGS ON SCALE NO. 1 IN MILLIMETERS					
1040	1029	1030	1027	1029	1029
(10) 1033	1030	1029	1028	1027	1030
(20) 1029	1030	1029	1028	1027	1030
(30) 1029	1030	1028	1028	1027	1029
1029	1029	1027	1029	1028	1029
1029	1030	1027	1028	1028	(65) 1029

y_2 = 1048 = 0.5603

y_1 (zero) = 1029 = $\underline{0.5519}$

0.0084 × 0.1533 = 0.0013 mm. Hg

in the two bulbs as well as constancy of temperature must be considered. These are accomplished by efficient stirring and circulation of the water and proximity of the bulbs to each other. With care, errors due to temperature changes may be kept within the sensitivity of the instrument. The base of the manometer was maintained at 25°C. ± 0.1°.

VAPOR PRESSURE TECHNIQUE

When the proper degree of evacuation and temperature control have been attained, the essential features for securing equilibrium measurements were, first, thorough agitation of the solutions, which hastens equilibrium between liquid and vapor phases and, secondly, time for readjustment of liquid surfaces following agitation.

Data were obtained in the following manner: When the proper degree of evacuation had been secured (2×10^{-4} mm. residual gas pressure), the two systems were separated by seal No. 1 and agitated for 90 min., then set in a fixed position (by aid of mirror B) and observed at intervals of 1 min. for a suitable length of time, about 90 min. Inspection of the data showed that equilibrium was reached in about 30 min. following agitation. When a series of readings remained constant, showing that no interfering conditions disturbed the equilibrium, the pressure reading and the subsequent zero reading or null point reading could be made. The permanence of the equilibria was tested at times for longer periods (see readings below). Table 2 gives representative data for the vapor pressure lowering of a potassium chloride solution at 20°C.

The usefulness of the apparatus in measuring very small depressions may be illustrated by the data on a 3.6 per cent gelatin solution, given in table 3.

In the foregoing examples consecutive scale readings (millimeters on scale No. 1) are given. Values for the equilibrium pressure (y_2) and the null point (y_1) are calculated from the equation.

These representative measurements have been selected from a large number made during the progress of experimental work and illustrate the usefulness of the instrument for a wide range of application where vapor pressure measurements are desirable.

REFERENCES

(1) Frazer, J. C., and Lovelace, B. F.: J. Am. Chem. Soc. **36**, 2439 (1914).

(2) Frazer, J. C., Lovelace, B. F., and Balke, W. H.: J. Am. Chem. Soc. **45**, 2930 (1923).

(3) Frazer, J. C., Lovelace, B. F., and Miller, E.: J. Am. Chem. Soc. **38**, 515 (1916).

(4) Frazer, J. C., Lovelace, B. F., and Rogers, T. H.: J. Am. Chem. Soc. **42**, 1793 (1920).

(5) Frazer, J. C., Lovelace, B. F., and Sease, V. B.: J. Am. Chem. Soc. **43**, 102 (1921).

(6) Frazer, J. C., Lovelace, B. F., and Taylor, R. K.: J. Phys. Chem. **30**, 1669 (1926).

(7) Hickman, K. C. D.: J. Franklin Inst. **221**, 383 (1936).

(8) Hickman, K. C. D., and Sanford, C. R.: J. Phys. Chem. **34**, 637 (1930).

PARTICLE SIZE DETERMINATION OF COLLOIDAL SYSTEMS BY THE SUPERCENTRIFUGE[1]

E. A. HAUSER AND H. K. SCHACHMAN

Department of Chemical Engineering, Massachusetts Institute of Technology, Cambridge, Massachusetts

Received September 20, 1939

The possibility of determining particle size or particle size distribution in colloidal systems must today be considered a problem of utmost importance to the colloid chemist. Desirable as this information is, its attainment is in many cases only approximated, unless highly involved or costly methods are employed. This paper outlines a method whereby it is believed that particle size determinations of colloidal systems can be simply and accurately obtained.

First let us briefly examine the limitations of the most outstanding methods now in use. A simple convenient optical method is the direct count of reflection disks in the slit ultramicroscope. From this number and the specific gravity and concentration of the substance in suspension, it is a simple matter to evaluate the size of the particles. The method is strictly accurate only as long as monodisperse systems are being examined, and even then only a well-trained observer will be able to obtain reliable results. These limitations rule out exact determinations in most colloidal systems, which rarely are monodisperse.

Methods involving kinetics and mechanics such as measurements of sedimentation rates when applied to colloidal systems are vitiated by Brownian movement and adhesion effects. Also, unless gravity is replaced by forces of higher magnitude they are extremely time-consuming. The Svedberg (6) and his collaborators were the first to apply Odén's work on sedimentation in an extremely strong centrifugal field. McBain (4), Beams (1), and others have also contributed much in this direction. These ultracentrifugal methods possess a high degree of accuracy and are valuable for many purposes. However, machines of the Svedberg type are expensive both in initial cost and in operation and are, therefore, available only to a few laboratories in the entire world. McBain's ultracentrifuges of the spinning-top type (opaque as well as transparent) are reasonably priced and simple to operate. However, they too are of extremely small capacity and do not permit a more or less continuous production of reasonable quantities of individual fractions.

Lenoir (3) extended Svedberg's principles to apply to the supercentrifuge manufactured by The Sharples Corporation of Philadelphia, Pennsylvania. Hauser and Reed (2), continuing this work, systematically developed a method of obtaining particle size distribution by the use of the supercentrifuge. This method overcame the limitations of availability and cost of equipment and permitted particle size determinations to be performed simultaneously with a reasonable degree of fractionation. The mathematics of this method, however, still are tedious and extremely involved.

---

[1] Presented before the Division of Colloid Chemistry at the Ninety-eighth Meeting of the American Chemical Society, held in Boston, Massachusetts, September, 1939.

Because the factors of availability, price, and continuous fractionation even in highly colloidal systems are of such importance, it was felt that a method of particle size determination, by means of the supercentrifuge, which presented no real mathematical difficulties nor time-consuming operations would be of real value.

THEORY UNDERLYING USE OF THE SUPERCENTRIFUGE

Although it is well known that few colloidal systems consist of spherical particles, mathematical evaluation taking account of shape is as yet beyond our abilities. To permit evaluation of all systems the standard of an "equivalent spherical diameter" (e.s.d.) was set up. The e.s.d. of a particle is an arbitrary dimension equal to the diameter of a sphere which sediments at the same rate as the particle under consideration. This convention permits solution of the mathematical problems and gives relative values as long as due cognizance of morphological considerations is taken.

Prior to a mathematical analysis of the problem, a logical analysis should be of value in outlining the variables to be encountered. Since the particles in suspension generally are denser than the dispersion medium they will settle towards the walls of the centrifuge bowl under the influence of the centrifugal force. The three major controlling factors for any sedimentation are the density difference between the disperse and continuous parts of the system, the magnitude of the gravitational or centrifugal force applied, and the kind and magnitude of any other forces applied. (Hauser and Reed, applying Stokes' law for falling bodies and Newton's law for viscous flow have already solved the problem involving these factors in the sedimentation equation.) In addition, large particles will be thrown out on the liner sooner than would small particles, and, consequently, the large particles will settle at the bottom of the bowl and the small ones at the top.

Turning from general considerations to a closer examination of a particle as it passes through the bowl, it is apparent that the path must be completely described by two velocity vectors of the particle, one parallel to and one perpendicular to the axis of rotation of the bowl. Also, if external conditions such as type and rate of feed, temperature, angular velocity, etc., are maintained constant, the point at which a particle hits the wall will be a function of the point of departure and the size of the particle. Coming back to a mathematical viewpoint, $Y = f(D, X_0)$, where Y is the distance up from the bottom of the bowl at which the particle settles, D is the equivalent spherical diameter of the particle, and X_0 is the distance from the axis of rotation at which sedimentation started (figure 1).

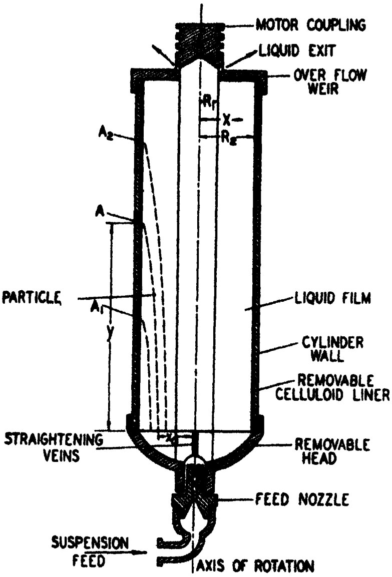

FIG. 1. Path of particles in the bowl of a Sharples supercentrifuge

THE EVALUATION OF D AS A FUNCTION OF X AND Y

As a result of previous work done on a similar centrifuge, the assumption can be made that streamline flow is in effect with the streamlines parallel to the axis of rotation. Obviously there are some slight errors in that assumption, owing to end effects at the bottom and top of the bowl. The possibility of turbulent flow at the very bottom of the bowl, due to the speed of input through the small entrance nozzle, is eliminated by taking the entrance plane a small distance above the nozzle. This seems permissible because the turbulent region is probably confined to the space in which the straightening vanes act.

If the suspensions used throughout all the work on the centrifuge are sufficiently dilute so that they can be considered truly viscous fluids obeying Newton's law of viscous flow, we obtain, by following the derivation of the velocity equation as given by Lamb, an equation for the velocity of any streamline *parallel* to the axis of rotation. By the derivation of Odén, using Stokes' law for falling bodies, an equation for the velocity component *perpendicular* to the axis of rotation is obtained. Now, the two velocity components can be combined to find D as a function of X_0 and Y.

$$\frac{dY}{dX} = \frac{\frac{dY}{dt}}{\frac{dX}{dt}} = \frac{\frac{Q_{\text{min.}}K}{60\pi\,(R_2^2 - R_1^2)}\left[R_1^2 \ln \frac{X}{R_2} + \frac{R_2^2 - X^2}{2}\right]}{\frac{\omega^2 X D^2 \Delta\rho}{18\eta}} \tag{1}$$

At constant values of $Q_{\text{min.}}$, η, $\Delta\rho$, and ω and integrating between the limits $X = X_0$, $Y = 0$ and $X = R_2$, $Y = Y$ the desired equation is obtained.

$$Y = \frac{18\eta Q_{\text{min.}}K}{60\pi(R_2^2 - R_1^2)D^2\Delta\rho\omega^2} \left[-\frac{R_1^2}{2}\left(\ln \frac{R_2}{X_0}\right)^2 + \frac{R_2^2}{2}\ln\frac{R_2}{X_0} + \frac{X_0^2 - R_2^2}{4}\right] \tag{2}$$

where Y = the distance from the bottom of the bowl at which the particle strikes,
X = the distance from the axis of rotation at which the particle starts,
D = the equivalent spherical diameter of the particle,
K = a constant, depending on the dimensions of the bowl (1.109),
η = the viscosity of the dispersion fluid in poises,
$Q_{\text{min.}}$ = the rate of flow of the suspension in cubic centimeters per minute,
$\Delta\rho$ = the difference in density between the disperse and the continuous phases,
R_1 = the distance of the overflow weir from the axis of rotation in centimeters,
R_2 = the radius of the bowl less that of the liner in centimeters,
t = time,
X_0 = the distance from the axis of rotation at which the particle starts, and
ω = the angular velocity of the bowl in radians per second.

While the above equation fulfills the task of obtaining Y as a function of X_0 and D, simple determinations of particle size are still impossible, since the equation is implicit in X_0 and therefore has no exact solution.

DEVELOPMENT OF THE FINAL EQUATION

If the conditions be imposed that the system under consideration be well defined (particle sizes covering but a small range) and that passage through the centrifuge be at an appropriate rate, the alignment of particles will approach a continuous distribution from large particles at low values of Y to small particles at high values of Y. Thus, contrary to the first assumptions, at a given point on the bowl there is essentially but one particle size or, conversely, a particle at a given value of Y could have started only from a unique value of X_0. Hence the further limitations have permitted the elimination of D as an independent variable, so that $Y = f(X_0)$ holds with but negligible error. In the transformation of equation 2 to the form $Y = f(X_0)$ it is important to note that $Q_{\text{min.}}$ must be proportional to D^2, a fact which is of considerable value in the fractionation procedure.

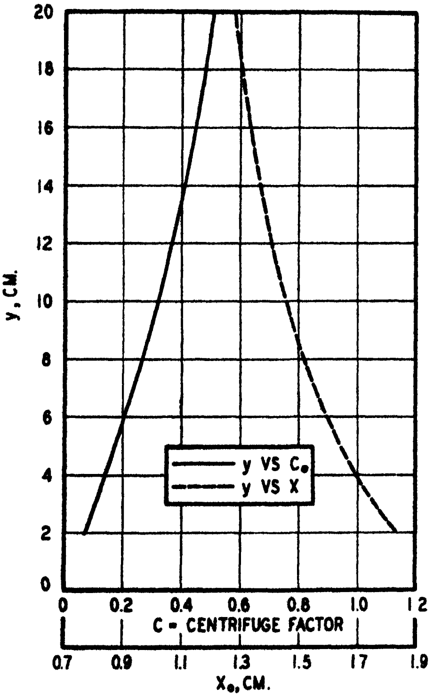

FIG. 2

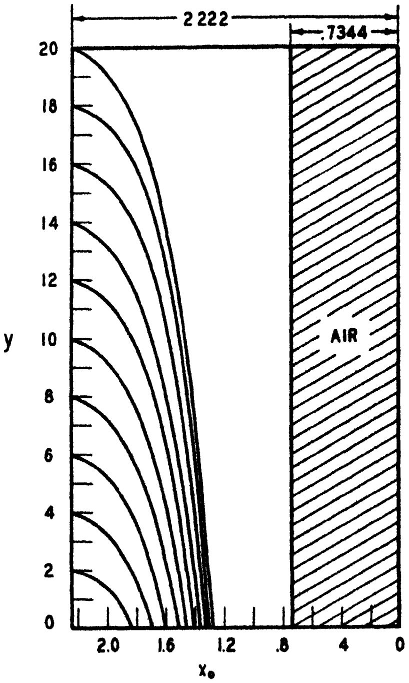

FIG. 3

FIG. 2. Plot of C against Y

FIG. 3. Showing the paths of the various particles in the bowl and the relationship between X_0 and Y

Justification of this new equation is found in the work of Reed (5). He found that the slope of the cumulative weight per cent curve was directly proportional to the square of the diameter of the particle and inversely proportional to the rate of flow of the suspension. Furthermore, if the fractionation is carried out so as to conform to the limitations imposed,—a well-defined range of particles and uniformity of the material sedimented on the liner,— the slope of this curve is constant. Therefore, we have

$$Q_{\text{min.}} = aD^2 \tag{3}$$

a being a constant.

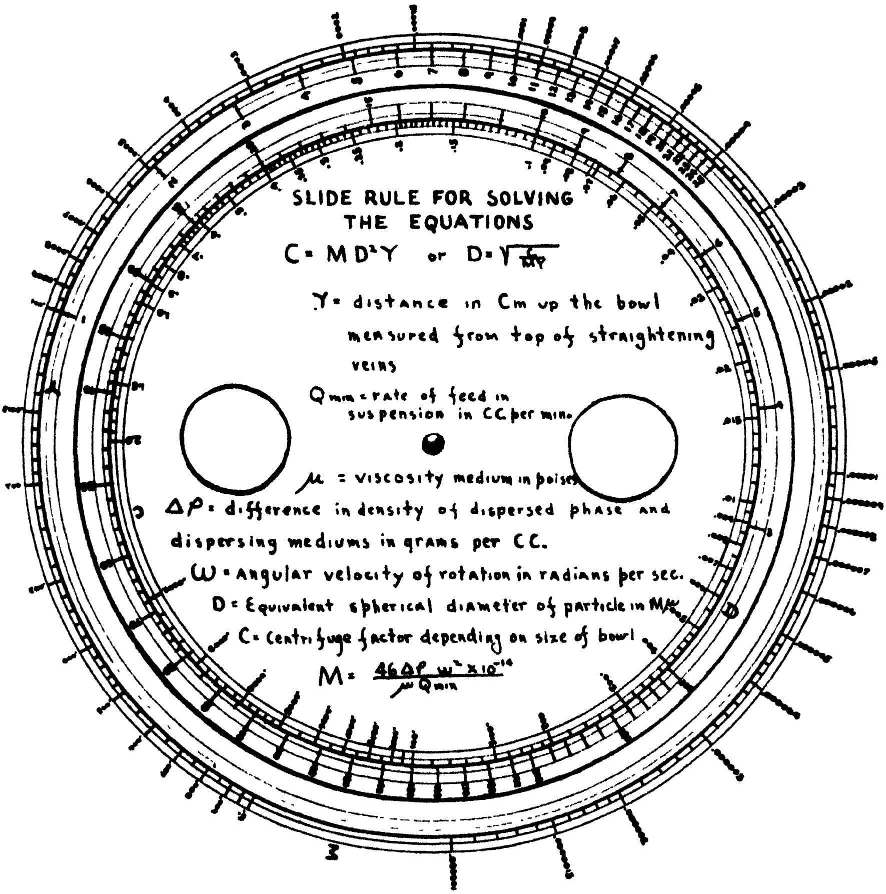
SLIDE RULE FOR SOLVING
THE EQUATIONS
C = MD²Y or D = √(C/MY)
Y = distance in Cm up the bowl measured from top of straightening veins
Qmin = rate of feed in suspension in CC per min.
μ = viscosity medium in poises
Δρ = difference in density of dispersed phase and dispersing mediums in grams per CC.
ω = Angular velocity of rotation in radians per sec.
D = Equivalent spherical diameter of particle in Mμ
C = Centrifuge factor depending on size of bowl
M = 46Δρ ω² × 10⁻¹⁴ / μ Qmin

FIG. 4. Circular slide rule for solving the equations $C = MD^2Y$ or $D = \sqrt{C/MY}$

Since X_0 depends only on Y, the quantity in brackets of equation 2 can be assigned numerical values for all values of Y. This quantity has been called C and a plot of C *versus* Y made (figure 2). Figure 3 has been constructed to show the paths of the various particles in the bowl and the relationship between X_0 and Y.

Calling the product of all the other constants in equation 2 $1/M$ (modulus of sedimentation), a final simple equation is reached:

$$Y = C/MD^2 \tag{4}$$

or, since D is what is desired,

$$D = \sqrt{C/MY} \tag{5}$$

To facilitate the solution of this equation, an alignment chart in the form of a circular slide rule has been constructed (figure 4), with the aid of which particle sizes can be calculated in a few minutes by anyone.

SAMPLE CALCULATIONS

To illustrate the method the particle size of a fraction from a bentonite suspension will be calculated. Data on the fractionation are as follows: temperature of suspension = 72°F.; $\eta = 0.00953$ poise; $\omega = 51{,}500$ R.P.M. = 5390 radians per second; density of bentonite = 2.78; $\Delta\rho = 1.78$ g. per cubic centimeter; $Q_{\text{min.}} = 41.75$ cc. per minute.

(*A*) The first step is to calculate M, the modulus of sedimentation for the run.

$$M = \frac{46\Delta\rho\omega^2 10^{-14}}{\eta Q_{\text{min.}}} = \frac{46 \times 5390^2 \times 1.78 \times 10^{-14}}{0.00953 \times 41.75}$$

$$M = 0.0000597$$

(*B*) The next step is to pick a value of Y at which we desire to obtain the size of the particle. $Y = 2$ is chosen.

(*C*) Picking Y fixes X_0 and C. The value of C is read off the graph of C *versus* Y (figure 2). It is 0.072.

(*D*) The slide rule is now used to find D. The value of C (innermost scale) is brought opposite the value of M (outermost scale). The pointer is now moved to the value of Y on the second outer scale and the value of D read off opposite it on the second inner scale. It is found to be 24.6 millimicrons. To avoid mistakes in reading the slide rule it is advisable to have the two sets of scales on the slide rule drawn in two distinctly different colors.

(*E*) For particle sizes of this fraction at other points the process is repeated, utilizing the desired values of Y.

FRACTIONATION PROCEDURE

Inasmuch as the derivation of the final equation was made possible only by a number of assumptions, it is necessary to carry out the actual experimental work carefully so that all these are valid. The layer of material sedimented out must not be too thick and must be of uniform depth for the entire length of the liner. The suspension fed into the centrifuge should contain only a limited range of particle sizes.

To secure these conditions the fractionations are carried out in two stages. First, a run is made under appropriate conditions of concentration and rate of flow. Extreme care as to constancy of flow and speed of rotation and to thickness of sedimented layer is not required in this first run. The bottom portion of this layer is rejected, since the first run is made with a polydisperse system and all the particles larger in size than called for by the calculation will deposit in the layer closest to the bottom of the bowl. The rest is redispersed and rerun. During the rerun all possible precautions are taken in regard to the points mentioned above. The very bottom portion of the sedimented layer (for example, a strip of 1 cm. height) is again rejected, as a precautionary measure. The rest is divided into the requisite number of fractions.

If the amount of suspended material is very great in the range being sedimented, it is advisable to rerun the effluent liquor, adding the additional sediment of that secured in the first run before going through with the redispersion and so forth.

To get still finer fractions the effluent liquor is now run through the centrifuge at a slower rate and the above procedure repeated at this new rate of flow. By suitably varying rotational speed and rate of input of suspension any desired degree of separation can be secured and calculations made as to the size of the particles so obtained.

The authors wish to express their sincere thanks to Professor R. D. Douglas of the Department of Mathematics of the Massachusetts Institute of Technology for his valuable advice and assistance.

Their thanks are also due to Mr. L. L. Baral of the Department of Chemical Engineering for his assistance in the preparation of this paper.

They also wish to express their appreciation to The Sharples Corporation of Philadelphia, Pennsylvania, for putting a steam-driven supercentrifuge at their disposal to make this work possible.

REFERENCES

(1) BEAMS, J. W.: Rev. Sci. Instruments **6**, 299 (1935).

(2) HAUSER, E. A., AND REED, C. A.: J. Phys. Chem. **40**, 1169 (1936).

(3) LENOIR, W. F.: Master's Thesis, Department of Chemical Engineering, Massachusetts Institute of Technology, 1936.

(4) MCBAIN, J. W., AND O'SULLIVAN, C. M.: J. Am. Chem. Soc. **57**, 2631 (1935).

(5) REED, C. E.: Doctor of Science Thesis, Department of Chemical Engineering, Massachusetts Institute of Technology, 1937.

(6) SVEDBERG, THE: Ind. Eng. Chem., Anal. Ed. **10**, 113 (1938). This paper is an up-to-date summary of Svedberg's work and contains also an excellent summary of the literature.

CYBOTAXIS AT INTERFACES

T. H. HAZLEHURST AND HARVEY A. NEVILLE

William H. Chandler Chemistry Laboratory, Lehigh University,
Bethlehem, Pennsylvania

Received September 30, 1939

Evidence for the existence of structural groups in liquids is provided by numerous investigations and was reviewed by Stewart (5), who referred to the phenomenon as *cybotaxis* and to these molecular swarms as *cybotactic* groups. The report of a more recent symposium on "Molecular Forces in Pure Liquids and Solutions" (6) shows general acceptance of some degree of orderliness in the structure of liquids although disagreement as to details.

Differing views of the nature of cybotaxis range from that of Bernal (1), who merely assumes statistical swarms of vaguely ordered molecules, to that of Irany (4), in which a liquid is considered as two separate phases, the one consisting of two-dimensional sheets of highly ordered molecules enclosing in its interstitial spaces the other phase which is completely disordered or gaseous. The present paper follows the approach of Frenkel (2), who pictures a liquid as composed of molecules so closely spaced that they are never even approximately gaseous and are occasionally grouped into swarms approaching crystallinity. These swarms are assumed to possess a certain shape and rigidity, but their existence is transitory and their surfaces merge imperceptibly into the surrounding completely disorganized liquid.

THE EFFECT OF INTERFACES

A cybotactic group is analogous to a crystal in equilibrium with its melt. Its surfaces are being constantly eroded to produce disordered liquid, while new cybotactic groups are constantly being formed. Since there is no single molecule or group of molecules sufficiently distinguished in structure or properties, there is no unique point capable of serving as an enduring nucleus for cybotactic groups. If some point or region of unique properties is provided which can act as a permanent and permanently fixed nucleus or anchorage for cybotactic groups, these may become stronger and more persistent, approaching the orderliness and stability of crystals. Such a region is provided by an interface of any type, for the nature of an interface necessitates that the forces active there are different from those in the interior of either of the adjacent phases. It is, therefore, logical to expect that interfaces which offer permanent location of directed forces will stabilize normally fugitive cybotactic groups.

Naturally the intrinsic stability of cybotactic groups will depend upon the properties of the liquid molecules themselves. Completely isotropic molecules, such as those in the so-called monatomic liquids, will form cybotactic groups of far less stability than those formed by anisotropic molecules. The energy required to disperse cybotactic groups may be regarded as analogous to a heat of fusion. All cybotactic groups are subject to vibrational motions similar to those in crystals and this agitation may be sufficient to destroy the grouping, but when directed forces are chiefly responsible for the preservation of the group, its dispersion will depend to a greater extent upon the rotational movements of the constituent molecules. Obviously, linear or plate-like molecules which orient in favored patterns will have a lower rate of rotation and will meet a greater frictional resistance than will those of spherical form. An extreme example of the spherical molecule is provided by helium, in which the directed forces are so weak that the discontinuity of its liquid–solid transformation is uncertain. At the other extreme, certain elongated molecules with polar groups at the ends or middle have directive forces so strongly developed that they are able to form a separate phase of liquid crystals.

LIQUID GAS INTERFACE

While the cybotactic groups throughout the bulk of an ordinary liquid will have only a fleeting existence, the coherent and quasi-crystalline nature of liquid surfaces is fairly well established. Among the effects to be expected at liquid surfaces as a result of this structure are (*1*) that not every molecule striking the surface from the vapor phase condenses and (*2*) the formation of primary "rolling drops" of the liquid upon its own surface. Actually only a small fraction of the impinging vapor molecules condenses, as expressed by the "accommodation coefficient." In an earlier paper (3) the authors presented a table of critical heights as a measure of the tendency of liquids to form rolling drops and showed that this property, and hence the stability of the liquid film, is proportional to the anistropy of the molecules concerned. By extending these measurements to solutions it was demonstrated that these surface films are not only resistant to rupture but have a definite structure, for the surface film of the drop and that of the bulk liquid must very nearly match or rolling drops will not form.

As illustrated in figure 1 and discussed below, the stability of an air bubble at a liquid-liquid interface is conditioned by cybotaxis in the lower liquid at the liquid-gas (bubble) and liquid–liquid interfaces.

LIQUID–LIQUID INTERFACE

The structure of the surface at a liquid–gas interface is determined almost entirely by the nature of the liquid; the liquid structure at the boundary between condensed phases (liquid–liquid or liquid–solid) depends upon both phases. At such interfaces the cybotactic condition will be more pronounced than at free surfaces.

Experiments analogous to those for rolling drops at free liquid surfaces (6) were performed at liquid-liquid interfaces, using drops of either liquid or bubbles of air. For example, water was dropped downward upon water through lighter liquids such as benzene, kerosene, and Nujol, and upward upon water through the denser liquids carbon disulfide, carbon tetrachloride, etc. The other liquid in each pair was likewise dropped upward or downward upon itself through the water layer. The stability of air bubbles at both sides of each water-organic liquid interface was tested by injecting a bubble from a fine glass tube below the boundary of the bulk liquids and also below this same interface inverted by anchoring some of the lighter liquid at the bottom of the vessel. When water is the lighter liquid, a sufficient quantity can be attached directly to the floor of the glass vessel under the organic liquid (e.g., carbon tetrachloride); when the organic liquid is the less dense, a large globule of it can be held under water by adhesion to mercury. This is illustrated photographically in figure 1a for benzene retaining a bubble of air under water and by the diagram in figure 2. An air bubble will not pause at the other liquid-liquid interface in figure 1a,—that is, in passing upward from water to benzene. In figure 1b a bubble is shown stably held by carbon tetrachloride under water. When this interface is inverted, the air bubble passes through it immediately. Typical experimental results for air bubbles and liquid drops at liquid-liquid interfaces are listed in table 1.

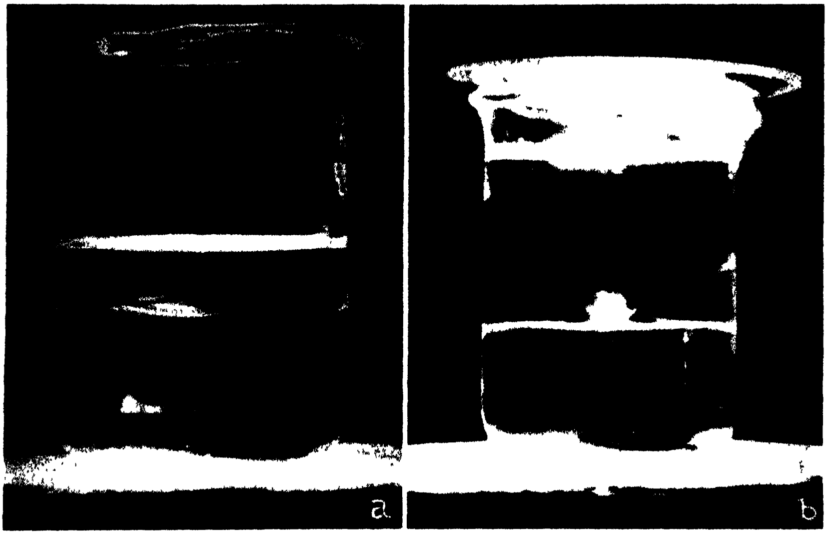

FIG. 1. Air bubble in (a) benzene and (b) carbon tetrachloride at interfaces with water.

It might be argued that these results could be anticipated or explained by the principles of preferential wetting or spreading coefficients. For example, benzene has a positive spreading coefficient on water and should displace water at a water–air interface or preferentially wet a bubble of

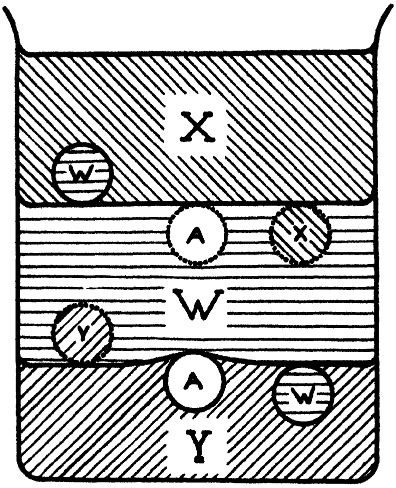

FIG. 2. Stability of bubbles and drops at liquid–liquid interfaces. A = air; W = water; X and Y = organic liquids. Solid outlines indicate stability; broken outlines indicate instability.

TABLE 1

Stability of bubbles and drops at liquid–liquid interfaces

LIQUID PAIR*	AIR BUBBLES		DROPS OF OTHER LIQUID	
	W† side	O side	W side	O side
Water–benzene	U†	S	s	s
Water–petroleum ether	U	S	s	S
Water–kerosene	U	S	s	s
Water–isoamyl alcohol	U	S	s	S
Water–Nujol	U	S	U	S
Carbon tetrachloride–water	U	S	U	S
Carbon disulfide–water	s	S	U	S
Nitrobenzene–water	U	S	s	s
Methylene iodide–water	U	S	U	s
6 *N* Ammonium acetate–benzene	S	S	S	s
6 *N* Sodium acetate–benzene	U	S	s	s
6 *N* Ammonium hydroxide–benzene	U	S	s	s
6 *N* Acetic acid–benzene	S	S	S	s
Carbon tetrachloride–6 *N* ammonium acetate	s	S	S	s

* The denser liquid in each pair is listed first.

† W = water; O = organic liquid; U = unstable; S = stable; s = slightly stable.

air. However, paraffin oil (Nujol), carbon disulfide, and methylene iodide have negative spreading coefficients, while that of carbon tetrachloride is doubtful. It would, therefore, not be expected that these liquids could displace or cover water at the water–air boundary, yet they will retain an air bubble at their interfaces with water permanently, as will those liquids which have positive spreading coefficients.

From the experimental data, and as represented in the diagrams, it may be stated as a general conclusion that at water–organic liquid interfaces an air bubble will penetrate the interface readily from the water side but not from the side of the organic liquid. Likewise, drops of the organic liquid will usually break through this interface at once or in a few seconds from the water side, but water drops are generally retained at the interface for a longer time or indefinitely on the opposite side. As indicated above, these results cannot be predicted directly from surface energy relationships, but are apparently conditioned by the degree of cybotaxis on the two sides of liquid–liquid interfaces. If this viewpoint is significant, a liquid–liquid interface should be considered not merely as a boundary plane of negligible thickness, but rather as a structure having two sides which differ in character and in extension into the two bulk phases.

As a general rule, the stability of liquid drops at a liquid–liquid interface is at best less than that of air bubbles, which may persist there for several days. It may be suggested as a tentative explanation of this difference that the cybotactic condition in the film between the bubbles and the upper liquid is strengthened by having gas on one side and a condensed phase on the other side. If the film has condensed phases on both sides, the simultaneous action of strong forces from opposite directions might result in a smaller net directive influence, whereas a strongly unbalanced force would be more effective in inducing and maintaining cybotaxis.

It will be noted from the data in table 1 that certain aqueous solutions, such as those of ammonium acetate and acetic acid in moderate concentration, exhibit the cybotactic behavior of an organic liquid. Other solutes, including common mineral acids, bases, and salts, in equivalent concentrations do not appreciably increase the cybotactic condition of water. Extensive investigation of cybotaxis in solutions has not been undertaken.

It should be emphasized that the bubbles or drops which are retained at a liquid–liquid interface are not in contact with the two liquids simultaneously but are completely surrounded by that liquid phase in which they rest. The bubble or drop is a slightly distorted sphere and its contour is continuous. The photographs are somewhat misleading in this respect, owing to reflection and refraction. Excellent evidence for the continuity of the film of the lower organic liquid around air bubbles is provided by the transport of a quantity of this lower liquid to the top surface of the water when the bubbles are enlarged sufficiently to cause them to break away from the lower liquid by their buoyancy. By blowing a stream of air through the lower organic liquid (e.g., carbon tetrachloride) the latter can be efficiently pumped to the top of the water. Of course, the carbon tetrachloride drops back through the water after releasing the air bubbles except for the quantity which can be supported as a disc upon the water surface. This process of circulation provides a convenient means for bringing about intimate contact between two immiscible liquids if the lower liquid is sufficiently cybotactic. This effect does not obtain when water is the lower liquid.

It occurred to the authors that the pumping of carbon tetrachloride to the surface of water by means of air bubbles is analogous to the Frasch method for mining sulfur and involves the same principle. An experiment was performed in which air was bubbled through molten sulfur under a glycerol-water solution at about 125°C. Small air bubbles were quite stable in the sulfur phase at the liquid-liquid interface, and large bubbles lifted a surrounding mass of sulfur to the top of the aqueous phase where it released the air and could be recovered by some simple means. This experiment provides a demonstration of the operation of the Frasch process suitable for laboratory or lecture.

It follows from the experimental results discussed above that if factors other than cybotaxis are eliminated, a water-in-oil emulsion will be more stable than the conjugate system. In the absence of an emulsifying agent there is no reason to conclude from purely energetic considerations that the one or the other system would be more stable, since the interfacial tension is identical in the two systems and the difference in density is likewise a common factor. A difference in stability of the two conjugate emulsions may, however, be predicted if the drops of one liquid penetrate films of the other liquid less readily as a result of cybotaxis in the liquid which constitutes the external phase. By analogy with this reasoning it follows that an emulsifying agent will stabilize that system in which it is preferentially in the external phase,—a general principle which has been arrived at from other considerations and which has experimental support.

LIQUID–SOLID INTERFACES

At the surface of a solid the directive forces are stronger than at a liquid surface, for it is just this surplus which induces the solid state. It is therefore to be expected that cybotactic effects will be most evident in liquids where they are in contact with a solid. Furthermore, it may be reasoned that the extent of tactoid formation will be greatest adjacent to "active centers" of the solid surface—at edges, corners, extra-lattice crystal units—and will thus be favored by irregular, anisotropic particles rather than by spherical forms. Thixotropic phenomena may be explained as resulting when cybotactic groups extend sufficiently as spines or tentacles from active centers on neighboring particles to form bridges of quasi-crystalline material which will offer resistance to lateral shear. A more extended discussion of thixotropy from this viewpoint will be offered in a subsequent paper.

DUAL LIQUID CONTACT

In contrast to the conclusion relative to bubbles and drops held at a liquid–liquid interface, it appears that solid particles of some materials may rest in contact with both liquids simultaneously at such an interface. The stabilization of emulsions by certain solid powders is conditioned by the equilibrium of surface forces in this dual wetting.

When a bead of glass, fused borax, or sodium hydroxide is dropped upon a liquid–liquid interface from the side of the organic liquid, it is arrested momentarily in the organic liquid before breaking through the interface, and then drops to a stable position in contact with both liquids. The contrast of this condition with the behavior of a liquid drop is shown in figure 3 for solid sodium hydroxide and for a drop of its concentrated solution. That the solid pellet is in contact with the underlying layer of water is indicated by the visible solution lines or schlieren as the denser solution flows down through the water. The absence of these lines below the drop of solution at the same interface proves that the drop is not in contact with the water but is entirely surrounded by the organic liquid. When it does break through the interface it goes at once and as a whole into the water phase.

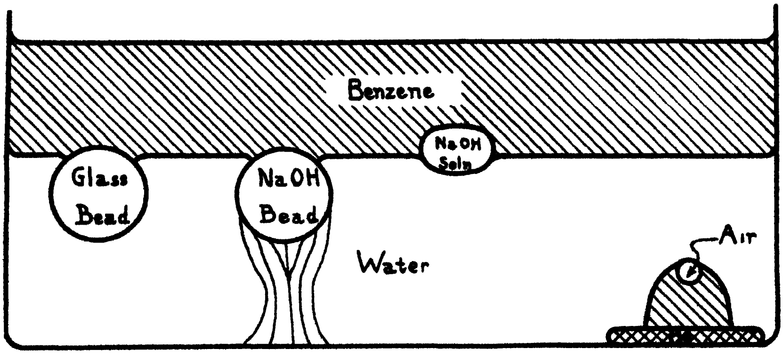

FIG. 3. Dual liquid contact. Glass bead and sodium hydroxide bead stable in dual contact; sodium hydroxide bead dissolving. Drop of sodium hydroxide solution and air bubble not in contact with water.

It is obviously impossible for a liquid drop to preserve a recognizable outline after breaking through an interface if the drop is miscible with the liquid into which it enters. However, if it is immiscible with both liquids, it may exhibit two stages of rest,—the first due to cybotaxis and the second to an equilibrium of surface forces with the drop in contact with both liquids. Mercury droplets if sufficiently small will hang indefinitely at liquid–liquid interfaces. The size of the drop is a factor since, if it is too large, the strong pull of gravity causes the upper liquid to neck off, and the drop, surrounded by a shell of the upper liquid, falls before it has had time to penetrate the cybotactic film. In this manner globules of lighter organic liquid may be carried down through water and retained at the bottom of a vessel, as illustrated for benzene in figure 1a.

By using the system water–aniline–kerosene, which forms three layers in that order (when the last two are mutually saturated), large density differences were avoided. It is possible to hang quite large drops of water at the aniline–kerosene interface if the proper technique is employed. If the water drop is allowed to fall freely onto the interface it goes through at once, because the interfacial tension between aniline and kerosene is very low and even a small force is capable of causing the kerosene to neck off. Each water drop is then quite clearly surrounded by a rather thick shell of kerosene as it falls through the aniline, and this kerosene subsequently streams upward. If, however, the water drop, while still adhering to the glass capillary, is carefully manipulated at the interface so as to break the kerosene film and bring the drop into contact with both aniline and kerosene, it will hang indefinitely at the interface and may be enlarged at any time by adding more water through an inserted capillary. Definite proof that the hanging drop is in contact with the aniline phase is provided by dissolving in the water a dyestuff (National safranine 8B) which is soluble in water and in aniline but insoluble in kerosene. The hanging purple drop loses all of its color to the aniline.

It may be concluded that liquid drops may rest at liquid–liquid interfaces in defiance of gravity for either of two reasons: (*1*) because they fail to penetrate the cybotactic layer or (*2*) because the three interfacial tensions have values which permit equilibrium, that is, none is greater than the sum of the other two. The first effect is operative in all cases to some degree but is impermanent; the second is operative only when (*a*) the drop is immiscible with both liquid layers and (*b*) the interfacial tensions satisfy the above condition.

In this respect liquid drops and solid beads exhibit the same behavior. Bubbles of gas appear to be exceptional in the matter of dual liquid contact. All experiments designed to show that bubbles were in contact with both liquids gave negative results. For example, a bubble of ammonia is stable without contraction under kerosene covered by water. If bubbles could exist in contact with both liquid phases the condition governing the equilibrium of interfacial tensions should be satisfied, but bubbles of air will be retained below the interfaces in both spreading and non-spreading liquids when water is the upper liquid. Theoretically, from surface energy relations, an air bubble should be stable at a Nujol–water interface in contact with both liquids and, it is to be emphasized, the same condition should obtain regardless of whether the bubble is introduced from the water side or the Nujol side of the interface. Actually, as recorded in table 1, the bubble is stable only as a result of cybotaxis in the organic liquid.

SUMMARY

Molecular swarms or cybotactic groups in the bulk of liquids have only a transitory existence for lack of an anchorage or directive influence. This is provided by an interface of any type and here the cybotactic effects will be stronger and more persistent, possibly approaching the orderliness and stability of crystals.

Cybotaxis at liquid–air interfaces accounts for the existence of primary rolling drops, and "critical heights" for different liquids provide a relative measure of this effect.

Analogous experiments are made at liquid–liquid interfaces with drops of either liquid or bubbles of air. The stability of a bubble at a liquid–liquid interface depends upon cybotaxis in the lower liquid. In general, at water–oil interfaces an air bubble will break through from the water side but not from the oil side; oil drops will break through from the water side, but usually water drops will not from the oil side.

If factors other than cybotaxis are eliminated, a water-in-oil emulsion is more stable than the conjugate system. By analogy with cybotaxis, it follows that an emulsifying agent will stabilize that system in which it is preferentially in the external phase.

In thixotropic systems cybotactic groups extend as spines or tentacles from active spots on neighboring particles and form bridges of quasi-crystalline character which offer resistance to lateral shear.

Drops of an immiscible liquid or solid particles may rest at a liquid–liquid interface in contact with both liquids if equilibrium conditions of interfacial energies are satisfied. Dual liquid contact is apparently not possible for bubbles of gas.

REFERENCES

(1) Bernal: Trans. Faraday Soc. **33**, 27 (1937).
(2) Frenkel: Trans. Faraday Soc. **33**, 58 (1937).
(3) Hazlehurst and Neville: J. Phys. Chem. **41**, 1205 (1937).
(4) Irany: J. Am. Chem. Soc. **61**, 1436 (1939).
(5) Stewart: Phys. Rev. **29**, 919 (1927); **30**, 232 (1927); Chem. Rev. **6**, 483 (1929).
(6) Symposium: Trans. Faraday Soc. **33**, 1–283 (1937).

THE PHOTOCHEMICAL OXIDATION OF OXALIC ACID SENSITIZED BY FERRIC ION[1]

ROBERT LIVINGSTON

School of Chemistry, University of Minnesota, Minneapolis, Minnesota

Received September 30, 1939

It has been shown by Allmand and Webb (2) that the photochemical oxidation of oxalic acid by ferric ion,

$$2Fe^{+++} + C_2O_4^{--} = 2Fe^{++} + 2CO_2$$

requires approximately two quanta for each molecule of oxalic acid oxidized. It was also shown qualitatively by the same authors[2] that carbon dioxide is formed, though no measurable amount of ferrous ion is produced, when a ferric oxalate solution is illuminated in the presence of oxygen. This result led them to the very plausible surmise that the photochemical process is not inhibited by oxygen, as had been erroneously suggested by several earlier workers, but that the ferrous ion, formed photochemically, is rapidly reoxidized by oxygen. Apparently without further evidence, this process has been cited in a well-known monograph on photochemistry (6) as a typical example of the "oxygen-carrier" type of photosensitization. While there can be no legitimate doubt that such processes occur, a search of the literature failed to reveal any simple case for which the mechanism had been reasonably established.

The experiments presented here were performed in the hope that this reaction would prove to be a simple example of the "carrier" type of photosensitization. While this expectation has not been realized in its simplest form, the results of Allmand and Webb (2) on the reaction in the absence of oxygen have been fully confirmed, and furthermore it has been shown that the presence of oxygen doubles the quantum yield, one molecule of oxalic acid being oxidized for each quantum absorbed. Since this latter result was somewhat unexpected, it was tested and confirmed by the use of an entirely independent analytical method.

EXPERIMENTAL PROCEDURE

Materials

The potassium ferric oxalate [$K_3Fe(C_2O_4)_3$] was prepared according to the method of Biltz (4). The procedure described by Leighton and Forbes (14) was followed in the preparation of the uranyl sulfate. The oxalic acid was twice recrystallized. All other reagents were of "analytical" grade and were used without further purification. Conductivity water was used in preparing all solutions.

---

[1] This work was made possible by a grant from the Graduate School of the University of Minnesota.

[2] A somewhat similar result had been reported previously by Jodblauer (7).

Analytical methods

Oxalate was determined with standard potassium permanganate solution by the usual method (11). Carbon dioxide was determined by absorbing it in standard 0.010 *N* barium hydroxide and titrating the resulting solution with standard hydrochloric acid to a phenolphthalein end point, taking care to prevent contamination by the carbon dioxide of the air (10). Ferric ion was determined with standard titanium trichloride solution in the absence of oxygen (9). Calibrated volumetric burets were used in all titrations, a microburet being used in those experiments where the titrating volume was small. Samples were measured with pipets, care being taken to see that the irradiated and "blank" solutions were at the same temperature when the samples were withdrawn.

Apparatus

The light source was a water-cooled, quartz-capillary mercury arc of the atmospheric pressure type described by Langer and Meggers (13). It was operated at 60 or 70 volts and 4 or 5 amperes. Glass color filters were used to isolate the desired spectral regions.

Energy measurements were made with a Moll large-surface thermopyle and a Leeds and Northrup HS galvanometer, provided with a suitable shunt and series resistance. To reduce the uncertainty due to corrections, the thermopyle was used and calibrated without its reflecting horn and window. The second window of the reaction cell was placed directly in front of the thermopyle and satisfactorily eliminated drifting due to air currents. The galvanometer–thermopyle system was calibrated with a United States Bureau of Standards radiation standard lamp, following the explicit directions furnished with the lamp. The calibration was repeated at intervals during the course of the experiments.

The reaction cell (figure 1) which was used in the final series of experiments was a Pyrex cylinder with plane parallel ends. It was about 5 cm. long and had a volume of about 25 cc. It was provided with a neck and ground-glass tubulated stopper (O) and had a bent capillary tube (I) attached at the bottom. These tubes served for filling and emptying the cell and as gas inlets and outlets. In all of the experiments the solutions were stirred by a steady slow stream of small bubbles of oxygen, nitrogen, or carbon dioxide, which was forced in at I. When nitrogen or carbon dioxide was used, a water trap or capillary leak was attached to O to prevent the diffusion of air back to the solution. In those experiments where the gas was analyzed, the tube (O) was connected to the absorption system.

The entire system was attached rigidly to an optical bench. In figure 2, A represents the arc, which was suspended in a water-filled copper box provided with a quartz window, Q. To eliminate the effect of stray light, the diaphragms D_1 and D_2 were used, and the cells, C, and thermopyle, T, were enclosed in a large blackened box. The glass color filter, F, was placed outside of this box. The reaction vessel, C_1, and a vessel of similar dimensions, C_2, which was kept full of water, were attached to a metal carriage. This could be operated from outside of the box so as to bring either C_1 or C_2 into the light beam. A glass condensing lens, L, and a shutter, S, completed the optical system.

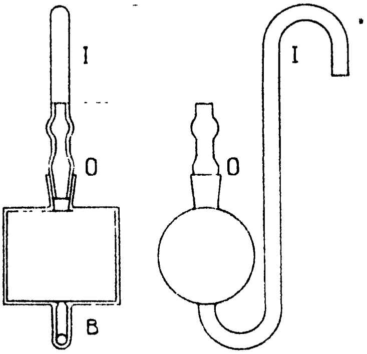

FIG. 1. The reaction cell

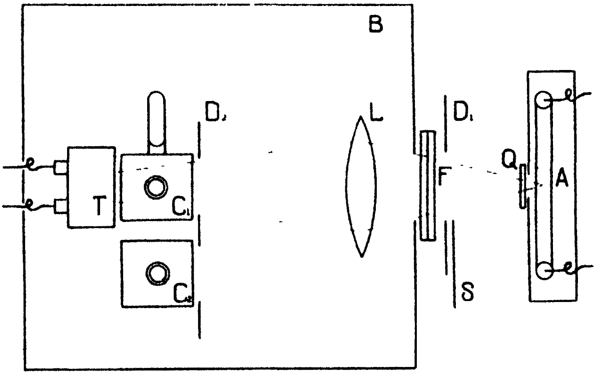

FIG. 2. Diagram of the apparatus

The experiments were run at room temperature, which varied from 23° to 34°C. These temperatures are listed in the tables.

Routine procedure and computations

Coincident with each experiment, one or more blank analyses were performed, using samples which had the same volume as the reacting solution and which, except for exposure to light, had been treated in the same way. The number of molecules which had reacted photochemically was computed in the usual way from the blank titre, the change in titre, the concentration of the blank, and the volume of the reacting solution.

During the course of each experiment, the galvanometer deflection corresponding to the light transmitted by the reaction cell as well as that transmitted by the water cell was observed at 30-min. intervals. The total time of irradiation for a single experiment was from 1 to 4 hr. In computing the energy absorbed by the reactants, allowance was made for the (slight) difference in transmission of the two cells, when they were both filled with water, and for the (4.5 per cent) loss due to reflection at the second window of the reaction cell. This reflection loss was computed by means of Fresnel's formula, assuming that the light was perpendicularly incident upon the window. A series of measurements made with the uranyl oxalate actinometer of Leighton and Forbes (14) indicated that the energy measurements were too small by 2.8 per cent. This discrepancy was probably due to the use of an inhomogeneous light beam and a surface thermopyle (15). This correction was applied to all of the quantum yield measurements. The uranyl actinometer was also used to check all variations in procedure (incldiung the carbon dioxide method of analysis).

RESULTS

The experiments which are summarized in table 1 were performed in the absence of oxygen, the extent of the reaction being determined by titration with titanium trichloride. The solution used in these experiments was similar to that used by Allmand and Webb (2) in the majority of their experiments. It was 0.020 *M* in respect to potassium ferric oxalate and 0.100 *M* in respect to sodium oxalate. The duration of each experiment was 3 hr. A compound Jena-glass filter, which isolated the mercury lines at λ 4360 Å., was used. The intensities of the absorbed light, which are given in column four, are average values. The percentages of reaction, listed in column five, are given in terms of ferric ion reduced. The quantum yields, which are recorded in the sixth column, were computed by dividing the number of molecules of oxalate oxidized by the total number of quanta absorbed in the solution. The values given in the last column have been corrected for the internal filter action of the complex ferrous oxalate, using the extinction coefficients given by Allmand and Webb (2) and making allowance for the gradual change in the composition of the reacting mixture.[3]

---

[3] This latter effect was taken into account by the use of the following formula:

$$\frac{\phi_{\text{corrected}}}{\phi} = \frac{k_1 - k_2}{k_1} - \frac{k_2 C^0}{k_1(C^0 - C)} \ln C/C^0$$

where k_2 and k_1 are, respectively, the extinction coefficients of the complex ferrous and ferric oxalates, and C^0 and C are, respectively, the initial and final concentrations of the ferric oxalate.

The average of the corrected values of the quantum yield is 0.44 ± 0.02, where the uncertainty is expressed as the average error of a single determination. The corresponding value expressed in terms of ferric ion reduced is 0.87 ± 0.04, which is in excellent agreement with the value of 0.89, obtained by Allmand and Webb (2) for the same solution and wave length.

Experiments 1 to 4 of table 2 demonstrate that oxalic acid is oxidized in the presence of oxygen, although under these conditions no detectable amount of ferrous iron is formed. In all of the experiments summarized in table 2, the oxalate concentration was determined with standard permanganate. The light filter used in the first four experiments was a Corning Blue-purple Ultra, which transmits several of the mercury arc lines. For the present optical system and absorbing solution, the average wave length of the absorbed light was estimated to be 4000 Å. In experiments 5 and 6, a compound Jena filter, transmitting 4360 Å., was used; and in experiments 7 to 9 a Corning Violet Ultra filter, which transmits chiefly the lines at 3660 Å. Since in these experiments no ferrous oxalate was formed, it was unnecessary to make any correction for internal filter action.

TABLE 1

Reduction of ferric ion by oxalate in the absence of oxygen

(1) EXPERIMENT NO.	(2) CARBON DIOXIDE	(3) t	(4) $I_{\text{abs.}} \times 10^{-18}$	(5) PER CENT OF REACTION (Fe^{+++})	(6) $\phi = \frac{M_{C_2O_4^{--}}}{h\nu}$	(7) $\phi_{\text{corrected}}$
	bubbles per second	°*C.*	*quanta per second*			
1	5	24	3.1	10	0.38	0.43
2	5	23	2.9	9	0.385	0.43
3	5	23	2.1	7	0.39	0.43
4	5*	29	1.6	5	0.39	0.43
5	5*	29	1.8	5	0.365	0.39
6	1*	32	1.7	6	0.445	0.48
7	1*	34	1.5	5.5	0.44	0.47
8	1*	34	1.9	5.5	0.38	0.41
Average......................................						0.44 ± 0.02

* In these experiments the carbon dioxide was passed through a dilute solution of titanium trichloride before being admitted to the reaction vessel.

The quantum yields obtained in these experiments are twice as great as those obtained in the absence of oxygen. In table 3 the average values corresponding to λ 4360 Å. and to λ 3660 Å. are recorded for both the direct and the sensitized reactions, and are compared to the values published by Allmand and Webb (2) and by Allmand and Young (3). Since these authors expressed their quantum yields in terms of moles of ferric ion reduced, their values have been divided by 2, to reduce them to the same basis as those given in this paper. It is interesting to note that the yields of the sensitized oxidation and of the direct reduction of ferric iron appear to be the same function of wave length. This indicates that the increase of efficiency with decreasing wave length is determined by the primary process and is not merely the result of an error in applying the correction for the internal filter action of the ferrous compound.

TABLE 2

Oxidation of oxalic acid sensitized by ferric ion

EXPERIMENT NO.	DURATION	λ	OXYGEN	t	$I_{abs.} \times 10^{-16}$	PER CENT OF REACTION ($C_2O_4^{--}$)	$\phi = \frac{M_{C_2O_4^{--}}}{h}$
	minutes	*Å.*	*bubbles per second*	*°C.*	*quanta per second*		
1	180	4000	10	26	2.3	1.4	0.92
2	180	4000	3	27	3.0	1.4	0.90
3	180	4000	0.1	27	2.1	0.5	0.49
4	180	4000	0*	26	2.1	0.05	0.05
5	180	4360	10	28	2.2	1.1	0.94
6	180	4360	10	28	2.2	1.0	0.87
7	360	3660	10	28	0.7	0.7	1.10
8	360	3660	10	28	0.7	0.9	1.31
9	360	3660	10	29	0.7	0.7	1.02

* Stirred with carbon dioxide, but no special precautions were taken to exclude traces of air.

TABLE 3

Comparison of average values of the quantum yield

λ	REACTION IN THE PRESENCE OF OXYGEN	REACTION IN THE ABSENCE OF OXYGEN		
		Livingston	Allmand and Webb (2)	Allmand and Young (3)
Å.				
4360	0.90 ±0.04	0.44 ±0.02	0.445	0.405
3660	1.14 ±0.11		0.58	0.525

Allmand and Webb (2) did not observe any reaction when they illuminated their reaction mixture with light of λ 5790 Å. Since the absorption of ferric oxalate solutions is very small in this region, it was thought worth while to test the effect of red light, which is strongly absorbed. The reaction mixture, while stirred with oxygen, was illuminated with a 500-watt projection lamp through a Jena RG1 filter. In no case was there any detectable reaction. If there is any reaction produced by red light, its quantum yield is certainly less than 0.05.

Since the twofold difference between the quantum yields of the reactions occurring in the presence and in the absence of oxygen was somewhat unexpected, the following experiments were performed to confirm the result. Carbon dioxide-free gas was bubbled through the reaction mixture and was then passed into dilute standard barium hydroxide solution. The amount of carbon dioxide produced by the oxidation of oxalic acid could thus be determined by analysis of the absorbent. Since either oxygen or oxygen-free nitrogen can be used, this method is obviously applicable to the study of either the direct or the sensitized oxidation. In using this method of analysis, it was found necessary to observe several precautions. To obtain an efficient removal of the carbon dioxide, it was necessary to use an acidified reaction mixture[4] and to continue the flow of gas for at least 15 min. after the illumination. It was of course necessary to take extreme care to free the incoming nitrogen, or oxygen, from traces of carbon dioxide and to avoid contamination by carbon dioxide of the air. The carbon dioxide absorption vessel, which was a narrow cylinder with a sintered-glass gas injector, was shown to be efficient in taking up the carbon dioxide by using a second absorption vessel and analyzing its contents separately.

No direct test was made for the presence of carbon monoxide in these gases; however, the fact that the potassium permanganate titre remains unchanged when the mixture is illuminated and titrated in the absence of oxygen, proves that if carbon monoxide is formed its amount is very small compared to that of the carbon dioxide.[5]

The results of these experiments are summarized in table 4. The solutions used in experiments 1 and 4 were 0.020 M, 0.0193 M, and 0.0962 M in respect to sulfuric acid, potassium ferric oxalate, and sodium oxalate. In experiments 5 to 13 the concentrations, given in the same order, were 0.0198 M, 0.0198 M, and 0.0990 M. The duration of each experiment was 60 min., except in the case of experiment 13 which was continued for 68 min. To obtain a conveniently rapid reaction, a Corning Blue-purple Ultra filter was used. In computing the quantum yield, the average wave length was estimated to be 4000 Å. (compare the first four experiments of table 2). No attempt was made to correct the quantum yields of experiments 11 to 13 for the absorption of light by ferrous oxalate, and the values tabulated for these experiments are, therefore, probably 10 or 15 per cent too small. The per cent completion of the reactions (column 4) is given in terms of the concentration of oxalate. The quantum yields ($\phi_{\text{titration}}$, given in column 6) were determined by titration of the reaction mixtures at the end of the experiments. The titrations were made with potassium permanganate in experiments 1 to 4 and with titanium trichloride in experiments 11 to 13. The quantum yields based upon the carbon dioxide determinations are given in column 7.

---

[4] A comparison of the experiments listed in table 4 with those in table 2 shows that the dilute acid used has no specific effect on the reaction. This is in agreement with the results of Allmand and Webb (2).

[5] A separate attempt was made to detect the presence of carbon monoxide in the reaction products by passing oxygen-free carbon dioxide through the reaction mixture and collecting this gas in a nitrometer. Since the carbon dioxide used in these experiments was not entirely free from nitrogen, the results were somewhat uncertain. However, they did demonstrate that if any carbon monoxide is formed under these conditions, its amount is less than one-third of that of the carbon dioxide produced.

TABLE 4

Confirmation of the previous results by direct analysis of the carbon dioxide formed in the reaction

(1) EXPERIMENT NO.	(2) GAS	(3) t	(4) PER CENT OF REACTION ($C_2O_4^{--}$)	(5) $I_{abs.} \times 10^{-17}$	(6) $\phi_{\text{titration}}$	(7) ϕ_{CO_2}
	bubbles per second	°*C.*		*quanta per second*		
1	2 (oxygen)	27	2.6	1.9	0.82	0.67
2	2 (oxygen)	28	2.3	1.8	0.78	0.65
3	2 (oxygen)	28	2.4	1.7	0.86	0.80
4	2 (oxygen)	29	2.3	1.9	0.72	0.78
5	1 (oxygen)	29	2.2	1.7		0.80
6	2 (oxygen)	29	1.5	1.1		0.82
7	2 (oxygen)	28	1.9	1.6		0.71
8	2 (oxygen)	28	0.8	1.5		0.92
9	2 (oxygen)	28	2.2	1.6		0.85
10	2 (oxygen)	30	2.6	2.0		0.79
Average..................................					0.80 ±0.05	0.78 ±0.07
11	1 (nitrogen)*	30	1.3	2.4	0.33	0.45
12	1 (nitrogen)*	30	1.3	1.8	0.43	0.36
13	1 (nitrogen)*	31	0.9	1.5	0.39	0.39
Average..................................					0.38 ±0.04	0.40 ±0.03

* Purified with chromous chloride solution (19).

These measurements fully confirm the conclusions based upon the comparison of the results given in tables 1 and 2. The quantum yield, expressed in terms of moles of oxalate oxidized, is approximately 0.5 when the oxidizing agent is ferric iron, but is twice as great when the iron salt acts as a sensitizer and the oxidizing agent is oxygen.

In 1928 Kornfeld and Mencke (12) published an account of certain experiments on the photochemical reduction of ferric ion by oxalate ion, which were in disagreement with the earlier work of Lemoine (16). The experiments of Allmand and Webb (2) and of Allmand and Young (3), as well as those presented in this paper, are in direct contradiction to the claims of Kornfeld and Mencke (12). Believing that their results might have been due to the nature of the solutions which they used, we performed a number of experiments using a wide variety of solutions. Although we did obtain rather erratic results with some of these solutions, particularly those which were obviously colloidal, we were unable to realize anything even approaching the results reported by Kornfeld and Mencke (12).

DISCUSSION

Probably the simplest mechanism which could be postulated for the sensitized reaction is one in which the photochemical reduction of ferric ion,

$$Fe^{+++} + \tfrac{1}{2}\, C_2O_4^{--} + h\nu \longrightarrow Fe^{++} + CO_2$$

is compensated by a rapid thermal oxidation of ferrous ion[6]

$$4Fe^{++} + 4H^+ + O_2 \longrightarrow 4Fe^{+++} + 2H_2O$$

However, this mechanism must be rejected, since it predicts that the quantum yield of the reaction is the same in the presence and in the absence of oxygen.

An obvious way to avoid this difficulty would be to assume that the thermal oxidation of ferrous ion induces[7] the oxidation of oxalate ion with an induction factor of $\tfrac{1}{2}$. This possibility was tested directly by studying the oxidation of ferrous ion by oxygen, in the dark and in the presence of an excess of oxalate ion. In none of these tests was there any detectable (induced) oxidation of oxalate ion. Furthermore, these experiments, while neither very extensive nor accurate, indicated that the direct oxidation of ferrous ion is too slow to account for the low concentration of ferrous ion which is observed at the photochemical steady state.[8]

Since for these reasons both the simple "carrier-action" mechanism and its first modification must be rejected, it appears very probable that the reaction follows a more complex mechanism in which the thermal oxidation of ferrous ion is in some way coupled to the photochemical reduction of ferric ion. The following statement is a generalized description of such a mechanism: The primary photochemical act consists of (or is immediately followed by) an electron transfer from an oxalate ion to a ferric ion. The partially reduced oxalate ion formed in this way disappears, in the absence of oxygen, by a bimolecular process yielding carbon dioxide and ordinary oxalate ion. In the presence of oxygen, it is rapidly oxidized to carbon dioxide and induces the oxidation of ferrous ion (with an induction factor of unity). The partially oxidized oxalate may undergo these reactions either as the free ion ($C_2O_4^-$ or HC_2O_4) or as part of an iron-containing complex. Any mechanism which had these characteristics would predict a quantum yield of ½ for the direct oxidation by ferric ion and of 1.0 for the sensitized reaction in which oxygen is the oxidizing agent. This general mechanism may be formulated in a number of possible ways. One such detailed scheme is presented in the following paragraph.

---

[6] Compare reference 6.

[7] For a simple discussion of induced reactions, see Bray (5) or Kolthoff and Livingston (8).

[8] This conclusion is in interesting agreement with the results of Lipmann (18) on the corresponding system containing ferric ion and pyruvic acid.

It has been fairly well established (2) that ferric iron in the presence of an excess of oxalate is present as the complex ion, $[Fe(C_2O_4)_3]^{---}$. We shall assume that the absorption of a photon by this complex results in the transfer of an electron from an oxalate ion to the ferric ion and a rearrangement of the several ions which make up the complex. We shall assume, furthermore, that this new ion is moderately stable, and designate it by the symbol X^{---}.[9]

$$[Fe(C_2O_4)_3]^{---} + h\nu \rightarrow X^{---} \tag{1}$$

In the absence of oxygen this ion disappears by the bimolecular process

$$2X^{---} \rightarrow 2[Fe(C_2O_4)_2]^{--} + C_2O_4^{--} + 2CO_2 \tag{2}$$

but in a solution saturated with oxygen the following reaction is favored:

$$X^{---} + H_2O + O_2 \rightarrow\rightarrow [Fe(C_2O_4)_2]^- + 2CO_2 + OH^- + HO_2^- \tag{3}$$

The dioxalato ferric complex then takes up a third oxalate ion, and the peroxide ion decomposes either bimolecularly,

$$2HO_2^- \rightarrow 2OH^- + O_2$$

or more probably by some less direct path. While it is scarcely profitable, in our present state of incomplete knowledge of the system, to discuss the postulated steps in detail, it may be worth mentioning that step 3 is probably complex. It may consist of several consecutive steps, or it may possibly be an example of the type of mechanism recently proposed by Szent-Gyorgi (20).[10] Further quantitative work on this and on related systems is necessary before we can arrive at any definite conclusions about the detailed mechanism.

---

[9] Another, perhaps equally probable assumption, is that the complex immediately dissociates

$$X^{---} \rightarrow Fe(C_2O_4)_2^{--} + C_2O_4^-$$

and that it is the free ion, $C_2O_4^-$, which undergoes the subsequent reaction. There is reasonably good evidence for the existence of this ion (1), and there appears to be no valid reason for rejecting this type of mechanism.

[10] The statement in this reference that oxalic acid is rapidly oxidized by ferric ion in the dark is incorrect.

SUMMARY

1. The results of Allmand and Webb (2) and of Allmand and Young (3) on the photolysis of ferric oxalate by monochromatic light at room temperature have been confirmed quantitatively.

2. The corresponding iron-sensitized oxidation has been shown to have a quantum yield of approximately unity, twice as great as the yield of the photolysis.

3. These results have been checked by an independent experimental method.

4. It has been shown that the absorption of red light by the system does not induce the reaction.

5. A series of semi-quantitative experiments, performed in the dark, has demonstrated that the thermal oxidation of ferrous ion by oxygen does not induce the oxidation of oxalate ion.

6. A brief discussion of the more probable mechanisms is included.

In conclusion I should like to express my thanks to Mr. William Horowitz and Mr. George Rashka, who performed the majority of the experiments reported here, and to Dr. Foster Riecke for his kindness in reading and criticising the manuscript.

REFERENCES

(1) Abel, Jockisch, and Larisch: Z. Elektrochem. **43**, 629 (1937).
(2) Allmand and Webb: J. Chem. Soc. **1929**, 1518.
(3) Allmand and Young: J. Chem. Soc. **1931**, 3079.
(4) Biltz: *Laboratory Methods of Inorganic Chemistry*, translated by Hall and Blanchard, p. 153. John Wiley and Sons, Inc., New York (1928).
(5) Bray and Ramsay: J. Am. Chem. Soc. **55**, 2279 (1933).
(6) Griffith and McKeown: *Photoprocesses*, p. 613. Longmans, Green and Company, New York (1929).
(7) Jodblauer: Z. physik. Chem. **59**, 516 (1907).
(8) Kolthoff and Livingston: Ind. Eng. Chem., Anal. Ed. **7**, 209 (1935).
(9) Kolthoff and Menzel: *Die Massanalyse*, Vol. II, pp. 555–6. J. Springer, Berlin (1931).
(10) Kolthoff and Sandell: *Textbook of Quantitative Inorganic Analysis*, pp. 510, 525. The MacMillan Company, New York (1936).
(11) Reference 10, pp. 563–5.
(12) Kornfeld and Mencke: Z. Elektrochem. **34**, 598 (1928).
(13) Langer and Meggers: J. Research Natl. Bur. Standards **4**, 711 (1930).
(14) Leighton and Forbes: J. Am. Chem. Soc. **52**, 3139 (1930).
(15) Leighton and Leighton: J. Phys. Chem. **36**, 1882 (1932).
(16) Lemoine: Compt. rend. **121**, 817 (1895).
(17) Lind and Livingston: J. Am. Chem. Soc. **54**, 94 (1932).
(18) Lipmann: Skand. Arch. Physiol. **76**, 186 (1937).
(19) Stone: Ind. Eng. Chem., Anal. Ed. **8**, 188 (1936).
(20) Szent-Gyorgi: Z. physiol. Chem. **254**, 147 (1938).

FIGURES IN THIN LAYERS OF GREASE AND VISCOUS LIQUIDS

W. D. KUMLER

College of Pharmacy, University of California, San Francisco, California

Received September 30, 1939

Many chemists have observed that the grease on a vacuum desiccator usually becomes opaque when air enters the evacuated vessel. Some time ago, when some high-vacuum stopcock grease was used on a desiccator, it was observed that, instead of the usual smudge, large figures of great beauty (figure 1) were formed in the grease when the pressure was released. Since we found nothing in the literature on the subject, an investigation of the nature of these figures was undertaken.

The grease was made according to Birch's method (2), by taking the residue that was left after distilling yellow petrolatum at a pressure of 10^{-3} to 10^{-4} mm. of mercury and at a bath temperature of 300° to 320°C.

This petrolatum residue is not only a good high-vacuum stopcock grease but also an excellent material for use on a vacuum desiccator. Figure 1 is a photograph taken by reflected light of the figures formed in this grease on a Pyrex desiccator. The largest figures were about 1 cm. long.

The kind of glass from which the desiccator is made does not affect the figures, for similar figures were formed on Pyrex and on soft-glass desiccators. The kind of grease, however, does affect them. Six greases ordinarily used in greasing an automobile were obtained from a service station and the characteristic figures were obtained with the three most viscous greases. The other three gave only a translucent smudge.

The figures disappear when the desiccator is reëvacuated and are distorted or destroyed when the top is slid on the base. Turning the desiccator top when the two surfaces are in contact either before or after the vessel is evacuated does not change the direction or shape of the figures that are subsequently formed when air enters the desiccator. The figures have the same general configuration when observed from either the top or the bottom.

When air is allowed to enter the desiccator slowly, small spots forming in the grease are first observed. The spots then seem to push out branches which grow into the completed figures. The spots form at some distance from the edges of the ground surfaces. Only rarely does a branch from one figure extend into another figure.

The fact that the figures did not extend to the edges of the ground surface suggested that the vacuum as such had no effect on the figures but that the resulting pressure was the important factor. If that was the case, then the figures should be formed by the mechanical application and release of pressure. To test this the grease was placed between two glass plates about 1 in. square and the plates were squeezed together in a vise made for the purpose. Upon releasing the pressure the characteristic figures were obtained. The figures were likewise obtained when two pieces of celluloid were treated in the same way. The necessary conditions for the formation of the figures appear to be two reasonably smooth surfaces, a substance of the proper viscosity and stickiness, and the application and subsequent release of pressure.

Although the general appearance of the figures is similar to that of some crystals, the evidence indicates that they are definitely not crystalline but, on the contrary, that the figures are holes in the grease. First, the photographs (figures 1 to 8) show that the edges of the figures are curved and not straight, as would be expected for crystals. Second, the figures are invariably dark under crossed Nicols (figures 3, 6, 7), even when the grease itself is anisotropic. Third, it was found possible to separate the plates without disturbing the general pattern of the figures that previously had been formed thereon. An examination under the microscope revealed that the figures were places where the grease did not make a continuous medium from one plate to the other. By rubbing a pointed instrument on the glass where the figures appeared it was found that a thin film of grease was still on the glass in these areas, so that apparently grease pulls away from grease and not grease from glass during the formation of the figures.

There is a possibility that the figures may result from trapped air, which upon application of pressure decreases in volume or dissolves in the grease and then reappears upon release of the pressure to form the figures. To investigate this possibility an apparatus was constructed from a filter flask by which the operations of putting the greased plates together, applying pressure, and then releasing it could all be carried out in a vacuum. Several experiments were carried out at a pressure of 0.01 to 0.02 mm. of mercury and in each case the characteristic figures were obtained; this rules out the possibility that trapped air is responsible for their formation.

With the petrolatum residue grease the field was almost entirely dark when viewed under crossed Nicols, both without and with pressure being applied to the plates[1]. However, if pressure is applied and then released so that figures are formed, then the figures are dark and the grease relatively bright (figure 3). This we interpret as indicating that under these circumstances an orientation of the molecules occurs, which gives an anisotropic character to the grease in mass. The individual molecules may be anisometric, but under most conditions they are oriented at random so that the individual effects neutralize one another. When pressure is applied and then released, an orientation occurs which makes the grease anisotropic as a whole.

---

[1] The vise used consisted of two blocks of wood held together at the four corners with bolts and nuts. There was a ¾-in. hole through the center of both blocks. With this arrangement pressure could be applied to the plates and the whole arrangement could be placed on the stage of a polarizing microscope for observation either while the pressure was applied or later when it was released. Lead washers were used between the glass and the wood. The glass plates have to be thick, otherwise they will bend and not produce the desired pressure within the ¾-in. hole where the figures are to be observed. Glass ⅛ in. thick was satisfactory.

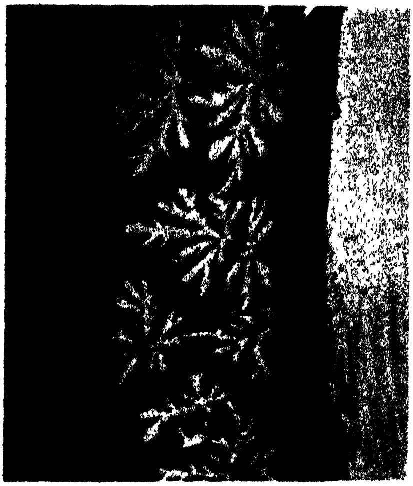

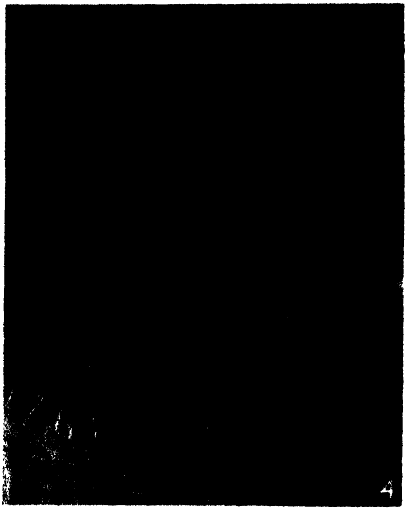

FIG. 1. Petrolatum residue on a Pyrex desiccator; taken by reflected light
FIG. 2. Petrolatum residue; Nicols parallel
FIG. 3. Petrolatum residue; Nicols crossed
FIG. 4. Polymerized butene; Nicols parallel

The thickness of the films was determined by placing a weighed amount of grease between the plates and applying pressure until the figures formed when the pressure was released. The diameter of the circular disc into which the grease was squeezed was then measured. Knowing the density of the grease, the diameter of the disc, and the weight of the grease, the thickness of the disc or films could be calculated. With petrolatum residue grease the films had a thickness of from 2500 to 6500 Ångström units.

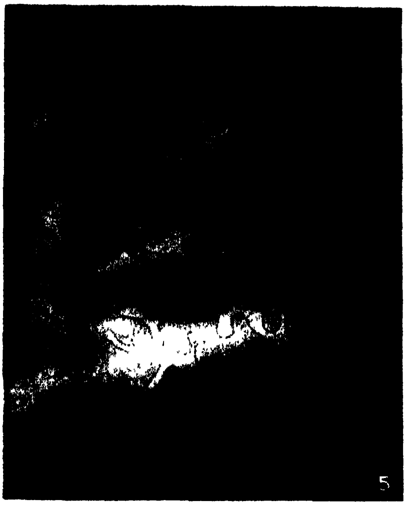
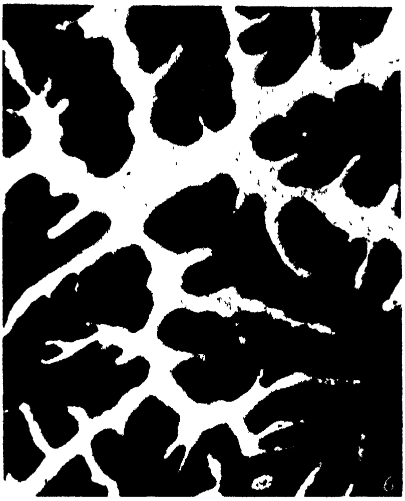

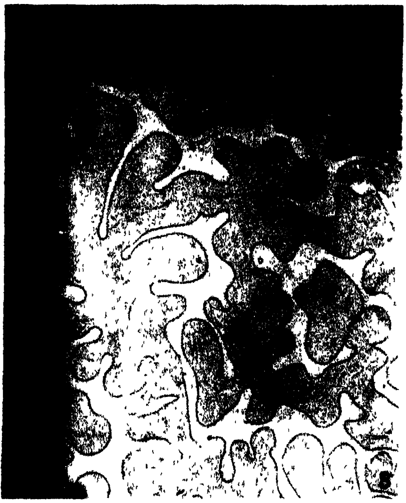

Fig. 5. Polymerized glycerol; Nicols parallel
Fig. 6. Ammonium oleate; Nicols crossed
Fig. 7. Aluminum stearate-vaseline; Nicols crossed
Fig. 8. Triton S.A.E. 70; Nicols parallel

It was discovered that, by repeated application and release of pressure on the plates, the grease could be squeezed out thin enough so that interference colors would form in the figures themselves. This phenomenon not only substantiates the previous conclusion that the figures are holes but it also confirms the order of magnitude of the above determination of the thickness of the film. To give interference figures the distance between surfaces must be of the order of magnitude of a wave length of visible light (4000 to 8000 Å.); this compares favorably with the thickness of 2500 to 6500 Å. previously determined by an entirely different method.

It is apparent that the plates must spring apart when the pressure is released, because the substance makes a continuous medium (a disc of a certain diameter, both faces of which are in contact with the glass plates) between the plates while the pressure is applied and in only a small part of this area does the substance touch both plates when the pressure is released and the figures are formed. Hence the plates must be farther apart after figure formation.

It does not seem to make any difference how long the pressure is applied before it is released, for the figures formed on a desiccator that had been evacuated for 3 weeks.

Since the materials thus far studied were all petrolatum greases it seemed desirable to try other substances that differed chemically from these greases. Materials that gave figures include ammonium oleate, oleic acid, *n*-butyl stearate, lanolin, benzoinated lard, triethanolamine, non-crystalline glucose, glycerol, polymerized glycerol, concentrated sulfuric acid, polymerized butene, and three lubricants made from the following materials: glycerol–water–sodium alginate, castor oil–carnauba wax, and aluminum stearate–vaseline. Thus the figures are formed in a wide variety of chemical substances from the very polar water-soluble substances such as glycerol, triethanolamine, and concentrated sulfuric acid to the non-polar hydrocarbons such as the petrolatum residue. There appears to be no correlation between ability to form the figures and ability to form hydrogen bonds.

Some of the compounds that give the figures, such as ammonium oleate, form liquid crystals. The conditions favorable to the formation of liquid crystals have been defined by Bernal and Crowfoot (1) as follows: First, the molecule must be anisometric and rod- or lath-shaped; second, it must contain not more than one highly polar group and may contain additional mildly polar groups. Ammonium oleate shows birefringence, which is a property common to all liquid crystals and is the property most commonly used in identifying the state. The polymerized butene possibly has rod-shaped molecules, but it lacks the polar group. This substance showed no evidence of birefringence, the field being entirely dark with crossed Nicols. Polymerized glycerol likewise gave no evidence of birefringence. In this case, although the possibility of rod-shaped molecules and dipoles is present, the even distribution of polar groups throughout the molecule would prevent any regular arrangement in one or two coördinate directions,—a condition which is characteristic of liquid crystals. Some of the other materials that show birefringence, such as lanolin, benzoinated lard, castor oil–carnauba wax, and aluminum stearate–vaseline, do so not because they are in the liquid crystalline state, but because soft anisotropic solid crystals are present in these substances.

Compounds such as glycerol, sulfuric acid, and triethanolamine, which do not have the molecular characteristics favorable to liquid crystal formation and give no evidence of such formation, give the figures. There seems to be no parallel between compounds that form the figures and compounds that form liquid crystals.

The viscosity and a less well-defined property, the "stickiness" of the substance, are the only properties thus far observed to be connected with the formation of the figures. The substances that give the most elaborate figures are viscous and sticky, such as the petrolatum residue (figures 1, 2, 3) and the polymerized butene (figure 4). The effect of viscosity can be noticed by examining the figures given by materials made up of molecules of the same type but of different size. For instance, a free-flowing petroleum oil (Triton S.A.E. 70) gives figures (figure 8) without any apparent symmetry which lose their original shape a few minutes after they are formed. The petrolatum residue gives figures of a high degree of symmetry that retain their original shape for several months. A hard grease made mostly of paraffin gives figures that lack symmetry and have the appearance of cracks. Their shape is very much the same as that of the figures in figure 7, which is a picture of a hard aluminum stearate–vaseline grease. Thus three substances similar in regard to the type of molecules but varying in the size of the molecules and in viscosity give figures that are different.

The effect of viscosity was investigated also by observing the type of figures that were formed when the vise was immersed in carbon dioxide snow. With some substances, such as the petrolatum residue, the shape of the figures was changed very markedly at the low temperature; with others, such as glycerol, the effect was less noticeable.

Figures 2 to 8 are photomicrographs of 12×. They were all taken of the various substances when placed on glass plates which were squeezed together in the special vise. Figures 2 and 3 are of the same figures, the only difference being that in figure 2 the Nicols were parallel, while in figure 3 they were crossed. Not enough substances have been investigated to show what value the figures may have as a means of analysis. However, the possibility that they may have some use in this connection is evident.

The cause of the formation of the figures is a question of much interest.

The fact that the petrolatum residue gives a bright field under crossed Nicols after the figures are formed (figure 3), although the field is dark before they are formed, indicates that some kind of orientation takes place during their formation. Ammonium oleate shows the same effect, although in this case the material is visible under crossed Nicols before figure formation but there is a marked increase in brightness after figure formation, indicating additional orientation. These are the only two cases in which this effect was noticed. With the other substances the brightness of the field under crossed Nicols did not change after figure formation, so that any orientation occurring in these cases was not sufficient to give rise to birefringence.

The greases and liquids act as if they were in an unstable state when squeezed out into a thin film. When the pressure is released they tend to assume a more stable condition, which involves bunching up with the resulting formation of the figures. This might be thought of as a kind of surface tension effect, such as gives rise to the formation of drops. Another view is that the molecules are squeezed out of their normal shape or out of their normal orientation with respect to one another. When the pressure is released they assume their more normal orientation and the figures result.

The general shape of the figures might be worthy of a mathematical investigation. Also, it would be interesting to study the figures formed when the plates were made of other transparent substances such as quartz, mica, and various resins.

SUMMARY

Figures are formed in greases or liquids of the proper viscosity when the substance is placed between smooth plates and pressure is applied and subsequently released. The figures are holes in the material, and their shape depends upon the viscosity and composition of the material used. The figures are formed in a wide variety of chemical compounds, including the very polar and the very non-polar. There is no parallel between compounds that form the figures and compounds that form liquid crystals. The viscosity and "stickiness" of the material were the only properties that were observed to be associated with ability to form the figures.

I wish to express my appreciation to Dr. Frank M. Goyan for several helpful discussions during the course of this work.

REFERENCES

(1) Bernal and Crowfoot: Trans. Faraday Soc. **29**, 1032 (1933).
(2) Birch: Nature **122**, 729 (1928).

MOLAL VOLUMES OF SOLUTES. IV

OTTO REDLICH

Department of Chemistry, State College of Washington, Pullman, Washington

Received October 3, 1939

The relationship between the apparent molal volume of a strong electrolyte and the concentration has been represented by Masson (37) and Geffcken (8, 9) through the empirical rule

$$\phi = \phi^0 + k'c^{1/2} \tag{1}$$

where ϕ is the apparent molal volume and c is the concentration in moles per liter. From the definition of the apparent molal volume

$$V = n_1 v_1^0 + n_2 \phi \tag{2}$$

where V is the volume of the solution, n_1 and n_2 are the number of moles of solvent and solute, respectively, and v_1^0 is the molal volume of the solvent, the relation follows between apparent molal volume and specific gravity:

$$\phi = \frac{w_2}{s^0} - \frac{1000}{c} \cdot \frac{s - s^0}{s^0} \tag{3}$$

(w_2 is the molal weight of the solute; s and s^0 are the specific gravities of the solution and solvent, respectively.)

A formula similar to equation 1 has been derived from the Debye–Hückel theory in the first papers of this series (41, 43, 44). According to this theory the free energy, F, of the solution of a strong electrolyte is given in the limit of low concentrations by[1]

$$F = n_1 F_1^0 + n_2[\bar{F}_2^0 + \nu RT \ln m - K(D, T)w^{3/2}c^{1/2}] \tag{4}$$

where F_1^0 and $\bar{F}_2^0$ are the partial molal free energies of solvent and solute, respectively, in the reference states; D is the dielectric constant of the solvent; m is the molality; K is a function of D and T given by the Debye–Hückel theory; $w = \frac{1}{2}\Sigma\nu_i z_i^2$; ν_i is the number of ions of species i formed by one molecule of the electrolyte; $\nu = \Sigma\nu_i$; and z_i = valence.

Applying a well-known thermodynamical relation we obtain

$$\left(\frac{\partial F}{\partial P}\right)_{T,m} = V = n_1 v_1^0 + n_2\left[\bar{v}_2^0 + k\left(D, T, \frac{dD}{dP}, \beta\right) w^{3/2} c^{1/2}\right] \tag{5}$$

---

[1] Bachem (2) expressed the opinion that in the logarithmic term of the following formula c should be used rather than m. As this term follows from the laws of the perfect dilute solution, we cannot see any basis for this opinion (*cf.* Lewis and Randall (36)).

where β is the compressibility of the solvent. The function k is given by

$$k = R\left(\frac{2\epsilon^2}{Db}\right)^{3/2}\left(\frac{\pi N}{1000T}\right)^{1/2}\left(\frac{1}{D}\frac{\mathrm{d}D}{\mathrm{d}P} - \frac{\beta}{3}\right) \tag{6}$$

where R is the gas constant in cc.-atmos., ϵ is the electric charge of a univalent ion, b is Boltzmann's constant, N is Avogadro's constant, and the pressure is in atmospheres.

Comparing equations 2 and 5 we have

$$\phi = \phi^0 + kw^{3/2}c^{1/2} \tag{7}$$

Although similar to Masson's rule (equation 1), this theoretical formula has an entirely different meaning. While the empirical rule is claimed to represent the data over a considerable concentration range, formula 7 cannot be expected to be more than a limiting law for low concentrations. This fact was stressed as early as 1931 (43, 44). But there is another important point. The empirical rule has always been used with different coefficients for different electrolytes; the theoretical equation, however, postulates a single coefficient k, common to all electrolytes and dependent only on the temperature and the nature of the solvent.

Although we believed that the experimental material available in 1931 was sufficient to confirm equation 7 (44), various objections have since been raised. These objections, summarized by Stewart (49) (*cf.* 50), concern (*a*) the question as to whether the square-root law is characteristic of electrolytes alone or applies to non-electrolytes as well, (*b*) the experimental proof with improved data, and (*c*) the valence factor.

A thorough discussion of all objections seems desirable, as formula 7 was derived from the theory of Debye and Hückel by means of thermodynamics alone. Any failure of equation 7 would indicate therefore the invalidity of the theory.

NON-ELECTROLYTES

A linear relationship at low concentrations between molal volumes (or some other properties like the logarithms of the activity coefficients, molal heat contents, and capacities) and the *square root* of the concentration is characteristic of *strong electrolytes* alone. According to extensive investigations by Hildebrand (23, 24, 25), Scatchard (46), Guggenheim, London, Kratky and other authors, deviations from the laws of the perfect solution are to be represented by *first-power terms* in the case of *non-electrolytes.* This holds true even for strong dipoles (32).

Contrary to some earlier statements, very accurate data for sucrose (42) and urea (22) give evidence for the linear relationship between the apparent molal volumes and the first power of the concentration. Some amino acids, though strong dipoles, are characterized by a linear relationship to the first power, while the corresponding salts obey a square-root relation (5).

A comparison of the plots given in the two papers quoted above (42, 22) can hardly leave any doubt as to the validity of the linear relationship to the concentration. However, a still more significant criterion of general applicability may be indicated. We have for apparent molal volumes (and similar properties):

$$\text{Electrolytes: } \left(\frac{d\phi}{dc^{1/2}}\right)_{c=0} \text{ finite, therefore } \left(\frac{d\phi}{dc}\right)_{c=0} = \infty \qquad (8)$$

$$\text{Non-electrolytes: } \left(\frac{d\phi}{dc}\right)_{c=0} \text{ finite, therefore } \left(\frac{d\phi}{dc^{1/2}}\right)_{c=0} = 0 \qquad (9)$$

The curves representing the apparent molal volumes of sucrose and urea are in striking accord with relation 9.

Relation 8 explains, by the way, why some early and promising attempts to develop the deviations from the laws of the perfect solution in a Taylor series with respect to c (27, 38) *could not* succeed in the case of strong electrolytes. The only condition of convergence, that all differential quotients be finite, is not satisfied.

TEST OF EQUATION 7

Some questions arising in an experimental test of equation 7 were discussed in 1931 (44). From the data given by Baxter and Wallace (4), by far the most accurate then available, the values

$$k = 2.8 \ (0°\text{C.}); \quad k = 1.7 \ (25°\text{C.}); \quad k = 1.5 \ (50°\text{C.}) \qquad (10)$$

were derived for aqueous solutions.

Only data of outstanding accuracy may be used for a decisive test. Such data have been published by Geffcken, Beckmann, Kruis, and Price (11, 12, 13, 14, 34), by Gibson (15), and by Wirth (52). From the results obtained by Jones and his collaborators (28, 29, 31) the figures given for ionic strengths higher than 0.02 have been included in the following diagrams. Prang's data (40) are not quite as precise as Wirth's, although the same method was used.[2]

---

[2] An additional confirmation of equation 7, however, may be seen in Prang's results. That Prang's valence factor for uni-divalent salts does not agree with Geffcken's figure is explained by the fact that he calculates molal volumes while Geffcken uses equivalent volumes. One must not, as Prang does, assume the polarizability for long waves to be independent of pressure in the case of a dipole liquid like water. In fact, the correct order of magnitude of Prang's figure for k is caused by a numerical error only. The formula given by Prang for the apparent molal volumes applies actually to the partial molal volumes, the coefficients differing by the factor 2/3.

The following discussion is not claimed to comprise all pertinent material. The author believes, however, that the data used furnish an appropriate basis for a conclusive test of equation 7 and for a numerical value of *k* at 25°C. and, moreover, that a discussion of any number of less accurate data would be of little value in testing equation 7.

In figure 1 the quantity $\phi - \phi^0$ of a few uni-univalent salts is plotted against $c^{1/2}$. This diagram agrees exactly with what we would expect: namely, a common limiting slope, excellently defined by each series of measurements, and individual deviations from the limiting tangent increasing with increasing concentration.

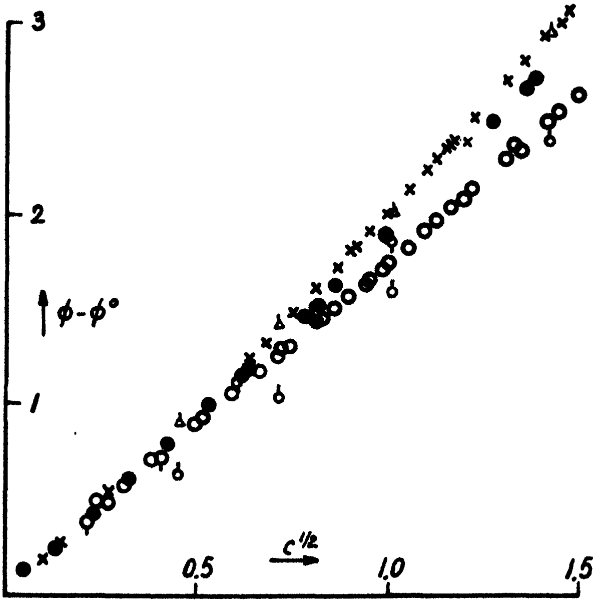

FIG. 1. Apparent molal volumes of uni-univalent salts

	Geffcken	Jones	Wirth
KCl	×	△	....
NaCl	●	....	....
KBr	....	♂	♀
NaBr	○	....	....

Table 1 contains the values of ϕ^0, in part considerably different from the figures of previous authors. These values have been used in plotting figures 1 and 2.

Wirth (52) has already pointed out the inconsistency of the ϕ^0 values to be derived for these salts. The value $\phi^0(\text{KBr}) = 33.71$, which we find from the figures of Jones and Bickford (28), would eliminate the discrepancy between chlorides and bromides but the discrepancy between these salts and the sulfates would still remain.

The discrepancy exceeds considerably the uncertainty of the extrapolations involved. There must be a systematic error which we are unable to locate in some of the experimental data.

The value

$$k = 1.86 \pm 0.02 \quad (25°\text{C.}) \qquad (11)$$

has been derived from the data represented in figure 1.

The molal volumes of ammonium nitrate are less suitable for determining the value of k, since ammonium salts behave somewhat irregularly (*cf.* 47). However, even in this case the limiting slope has been confirmed (12, 14).

Batuecas (3) did not extend his determinations of the densities of sodium and potassium chloride at 0°C. to very low concentrations. According to his figures a provisional value $k = 2.4$ for 0°C. may be assumed.

TABLE 1

Molal volumes at infinite dilution

KCl. . . .	26 81	KBr . .	33.97	K_2SO_4	32.44	$SrCl_2$	17.94
NaCl	16.61	NaBr .	23.48	Na_2SO_4 . . .	11.64		
K − Na. . .	10.20		10.49		10.40		

THEORETICAL VALUE OF THE COEFFICIENT

Using Falckenberg's (7) value for dD/dP we had calculated (43), according to equation 6,

$$k = 1.8 \pm 0.6 \quad (16°\text{C.}) \qquad (12)$$

This value agrees with equation 11.

Gucker (18), however, pointed out that more recent determinations of the dielectric constant of water at high pressures by Kyropoulos (35) should be used, resulting in the value

$$k = 2.53 \quad (20°\text{C.}) \qquad (13)$$

The discrepancy between this figure and all others cannot be satisfactorily explained. From Falckenberg's determination at 200 atmospheres the value $(1/D)dD/dP = 46 \times 10^{-6}$ atmos.$^{-1}$ is obtained. The results of Kyropoulos, who gives smoothed values in intervals of 500 atmospheres up to 3000 atmospheres, can be represented by

$$D = 80.79(1 + 59.2 \times 10^{-6}P - 3.28 \times 10^{-9}P^2 - 1.61 \times 10^{-12}P^3 + 0.42 \times 10^{-15}P^4) \qquad (14)$$

so that $(1/D)dD/dP = 59.2 \times 10^{-6}$ at atmospheric pressure.

The assumption that the measurements of both authors are correct gives an inflexion point between 200 and 500 atmospheres,—a result perhaps not implausible in the case of a liquid as abnormal as water. However, using a somewhat indirect but fairly probable method we can invalidate this assumption.

The contraction caused by the electric charges of the ions in the limit of infinite dilution, the "electrostriction," has been found by Drude and Nernst (6) to be proportional to $(1/D^2)\mathrm{d}D/\mathrm{d}P$.[3] Kritschewsky (33) has shown that the electrostriction may be made responsible for practically the entire variation of the limiting values, $\bar{v}_2^0$, of the molal volumes with increasing pressure. One may therefore expect $\bar{v}_2^0$, at different pressures, to be a linear function of $(1/D^2)\mathrm{d}D/\mathrm{d}P$; this has been confirmed by Kritschewsky in the cases of sodium chloride and potassium sulfate on the basis of Kyropoulos' results.[4]

The whole set of Kyropoulos' data must therefore be considered inconsistent with the other figures. Only new experimental work is likely to bring about a final decision.

POLYVALENT ELECTROLYTES

The values of $\phi - \phi^0$ for strontium chloride, sodium sulfate, and potassium sulfate are represented in figure 2. The dashed straight line indicates the slope resulting from equations 7 and 11 with $w = 3$.

The limiting slope of the strontium chloride curve agrees precisely with the predicted value. The experimental material for the two sulfates is somewhat scanty at high dilutions, so that no definite conclusion can be drawn.

The molal volumes of lanthanum chloride, computed from data of Jones and Bickford (28), can be represented by a straight line in a $c^{1/2}$ plot with the slope $6^{3/2} \times 0.79$ between $c = 0.025$ and $c = 1$. It is possible, however, that the molal volume curve turns below $c = 0.025$, as Jones and Bickford found that deviations of the conductivity persisted to still lower concentrations. The available density data do not give any hint of this turn.

NON-AQUEOUS SOLUTIONS

The discussion of non-aqueous solutions is restricted by the fact that adequate data for both $\mathrm{d}D/\mathrm{d}P$ and densities are available only in the case of methyl alcohol. Some results obtained by Vosburgh, Connell, and Butler (51) are represented in figure 3. The agreement with the theoretical

---

[3] The electrostriction can be deduced from the common formula of the electric energy of a charged sphere in the same way as formula 5, which represents, indeed, nothing else but the dependence of the electrostriction on concentration (*cf.* Gross (17)).

[4] Values of $\bar{v}_2^0$ obtained by means of the $c^{1/2}$ relationship should be used instead of the values given by Adams (1). In addition, we find minor differences from Kritschewsky's values of $(1/D^2)\mathrm{d}D/\mathrm{d}P$ when using formula 14. But the general conclusion is not altered by these modifications.

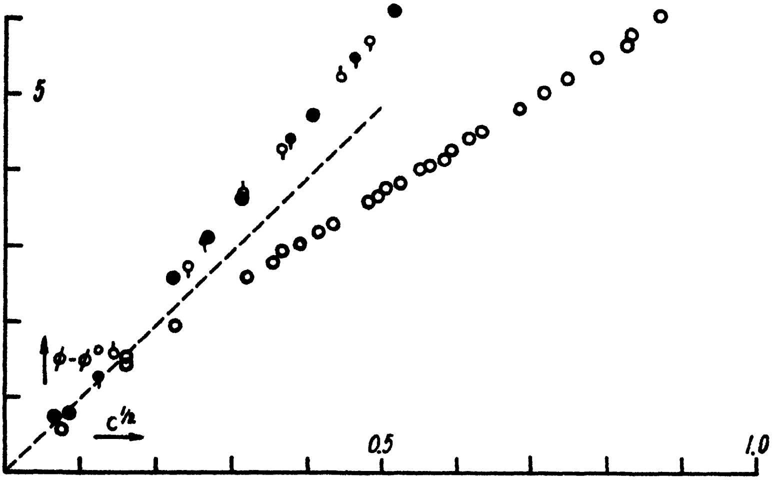

FIG. 2. Apparent molal volumes of uni-divalent salts

	Geffcken	Gibson	Jones	Wirth
K_2SO_4			♁	♀
Na_2SO_4	●	⧭		
$SrCl_2$	○			

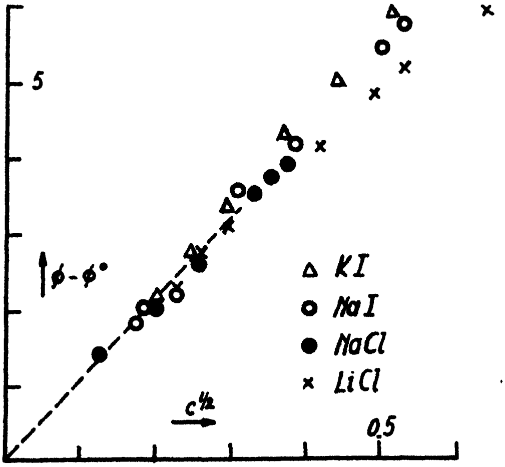

FIG. 3. Apparent molal volumes of uni-univalent salts in methyl alcoholic solution

slope, based on Falckenberg's (7) measurements and indicated by a dashed line, is very satisfactory. The results of Jones and Fornwalt (30) on ammonium chloride and potassium iodide also agree fairly well with the theoretical equation. Stark and Gilbert (48) did not extend their determinations to very low concentrations.

APPLICATIONS

The interpolation of specific gravities of dilute solutions of strong electrolytes and particularly the extrapolation should be carried out according to the theoretical formula 7.

A relation between s and c may be obtained by eliminating ϕ from equations 3 and 7. We omitted to state this relation in our first papers, because we wished equation 7 to be considered as a limiting law only. A corresponding formula, given by Root (45), has been used by several authors with individual coefficients consistent with Masson's rule rather than with the theoretical equation. Nevertheless it has proved useful for interpolation in many instances.

A correct representation of the apparent molal volumes is given by the series

$$\phi = \phi^0 + kw^{3/2}c^{1/2} - \frac{\beta}{s^0}c - \frac{\gamma}{s^0}c^2 - \cdots \tag{16}$$

We obtain from equations 3 and 16

$$1000(s - s^0) = \alpha c - s^0kw^{3/2}c^{3/2} + \beta c^2 + \gamma c^3 + \cdots \tag{17}$$

where

$$\alpha = \mathrm{W}_2 - \phi^0 s^0 \tag{18}$$

The value

$$s^0k = 1.85 \tag{19}$$

should be used for aqueous solutions at 25°C.

The number of individual constants $\alpha, \beta, \gamma \cdots$ required in equation 17 depends on the nature of the electrolyte, the range, and the precision desired. In many cases the term βc^2 will be sufficient.

The following method is likely to be the most convenient for determining the coefficients α, β, γ of equation 17.[5] The quantity

$$\frac{1000}{c}(s - s^0) - s^0kc^{1/2} = \alpha + \beta c + \gamma c^2 + \cdots \tag{20}$$

is computed from experimental data and equation 19. This quantity can in almost any case easily be plotted against c with the precision required. If the experimental points may be connected by a straight line, the constants α and β are immediately given. In the case of a distinct curvature, three points of a smoothed curve are used for calculating α, β, and γ. The specific gravities should be recalculated from the resulting formula for all experimental points, and minor adjustments of the coefficients should be carried out if systematic deviations occurred.

---

[5] A similar method has been devised already by Gucker (20); *cf.* also Gibson (16).

The quotient $(s - s^0)/c$ loses little accuracy in an extrapolation to zero concentration according to equation 20. Up to a certain concentration the differences $s - s^0$ are found, therefore, with higher precision by extrapolation than by direct measurement. Numerous series of measurements have been extended far below that limit.

The limit is determined by the probable error of the numerical value of k; for aqueous solutions at 25°C. the limits are as follows:

$$\begin{aligned} wc &= 0.03 \text{ if the accuracy of } s \text{ equals } 10^{-7} \\ &= 0.1 \text{ if the accuracy of } s \text{ equals } 10^{-6} \\ &= 0.6 \text{ if the accuracy of } s \text{ equals } 10^{-5} \end{aligned}$$

There is no use in extending measurements *much* below these limits (say to one-tenth of the limit concentration).

On the other hand, measurements should be extended at least to these limits to furnish the best possible basis for determining the numerical value of k as well as individual deviations from the limiting law.

Many authors, early and recent, have attempted to investigate molecular changes occurring in solutions by discussing volume changes. This aim has often been frustrated by the interfering effect of the electrical interaction between ions. Geffcken and Price (14) succeeded in splitting the two effects in the case of the second dissociation of sulfuric acid and of the hydrolysis of sodium carbonate. A similar application was made by Hoather and Goodeve (26) in a discussion of the molal volumes of sulfuric and sulfurous acids.

Gucker (18, 19) and Geffcken (10) derived a square-root formula of the apparent molal compressibility. The experimental data then available were hardly sufficient. In the meantime this formula has been confirmed by measurements carried out with the aid of ultrasonic waves (2, 39).

A similar formula has been deduced and discussed by Gucker for the apparent molal expansibility.

SUMMARY

The difference between Masson's empirical rule and the square-root relation between molal volumes and concentration derived from the theory of Debye and Hückel is stressed. The latter is verified by means of the available data for aqueous and non-aqueous solutions. The value $k = 1.86 \pm 0.02$ is derived for aqueous solutions at 25°C.

The molal volumes of non-electrolytes in dilute solutions depend linearly on the first power of the concentration.

The theoretical formula should be used as a limiting law only and with a common coefficient varying only with the temperature and the solvent.

A formula for interpolating and extrapolating molal volumes is indicated. Below a certain limiting concentration densities are determined by means of extrapolation better than by direct measurement.

REFERENCES

(1) Adams, L. H.: J. Am. Chem. Soc. **53**, 3769 (1931); **54**, 2229 (1932).
(2) Bachem, Ch.: Z. Physik **101**, 541 (1936).
(3) Batuecas, T.: Z. physik. Chem. **A182**, 167 (1938).
(4) Baxter, G. P., and Wallace, C. C.: J. Am. Chem. Soc. **38**, 70 (1916).
(5) Cohn, E. J., *et al.*: J. Am. Chem. Soc. **57**, 637 (1935); **58**, 415 (1936).
(6) Drude, P., and Nernst, W.: Z. physik. Chem. **15**, 79 (1894).
(7) Falckenberg, G.: Ann. Physik [4] **61**, 145 (1920).
(8) Geffcken, W.: Naturwissenschaften **19**, 321 (1931).
(9) Geffcken, W.: Z. physik. Chem. **A155**, 1 (1931).
(10) Geffcken, W.: Z. physik. Chem. **A167**, 240 (1933).
(11) Geffcken, W., Beckmann, Ch., and Kruis, A.: Z. physik. Chem. **B20**, 398 (1933).
(12) Geffcken, W., and Kruis, A.: Z. physik. Chem. **B23**, 175 (1933).
(13) Geffcken, W., Kruis, A., and Solana, L.: Z. physik. Chem. **B35**, 317 (1937).
(14) Geffcken, W., and Price, D.: Z. physik. Chem. **B26**, 81 (1933).
(15) Gibson, R. E.: J. Phys. Chem. **31**, 496 (1927).
(16) Gibson, R. E.: J. Phys. Chem. **38**, 319 (1934).
(17) Gross, Ph.: Z. Elektrochem. **37**, 711 (1931).
(18) Gucker, F. T., Jr.: Chem. Rev. **13**, 111 (1933).
(19) Gucker, F. T., Jr.: J. Am. Chem. Soc. **55**, 2709 (1933).
(20) Gucker, F. T., Jr.: J. Phys. Chem. **38**, 307 (1934).
(21) Gucker, F. T., Jr.: J. Am. Chem. Soc. **56**, 1017 (1934).
(22) Gucker, F. T., Jr., Gage, F. W., and Moser, Ch. E.: J. Am. Chem. Soc. **60**, 2583 (1938).
(23) Hildebrand, J. H.: J. Am. Chem. Soc. **57**, 66 (1929).
(24) Hildebrand, J. H.: *Solubility of Non-electrolytes.* American Chemical Society Monograph No. 57. Reinhold Publishing Corporation, New York (1936).
(25) Hildebrand, J. H., and Wood, S. E.: J. Chem. Phys. **1**, 817 (1933).
(26) Hoather, R. C., and Goodeve, C. F.: Trans. Faraday Soc. **30**, 630 (1934).
(27) Jahn, H.: Z. physik. Chem. **37**, 490 (1901); **41**, 257 (1902).
(28) Jones, G., and Bickford, Ch. F.: J. Am. Chem. Soc. **56**, 602 (1934).
(29) Jones, G., and Christian, S. M.: J. Am. Chem. Soc. **59**, 484 (1937).
(30) Jones, G., and Fornwalt, H. J.: J. Am. Chem. Soc. **57**, 2041 (1935).
(31) Jones, G., and Ray, W. A.: J. Am. Chem. Soc. **59**, 187 (1937).
(32) Kirkwood, J.: J. Chem. Phys. **2**, 351 (1934).
(33) Kritschewsky, I. R.: Acta Physicochim. U.R.S.S. **8**, 181 (1938).
(34) Kruis, A.: Z. physik. Chem. **B34**, 1 (1936).
(35) Kyropoulos, S.: Z. Physik **40**, 507 (1926).
(36) Lewis, G. N., and Randall, M.: *Thermodynamics and the Free Energy of Chemical Substances*, Chap. XIX, XX. McGraw-Hill Book Company, Inc., New York (1923).

(37) MASSON, D. O.: Phil. Mag. [7] **8**, 218 (1929).
(38) NERNST, W.: Z. physik. Chem. **38**, 487 (1901).
(39) PASSYNSKI, A.: Acta Physicochim. U.R.S.S. **8**, 385 (1938).
(40) PRANG, W.: Ann. Physik [5] **31**, 681 (1938).
(41) REDLICH, O.: Naturwissenschaften **19**, 251 (1931).
(42) REDLICH, O., AND KLINGER, H.: Sitzber. Akad. Wiss. Wien IIb, **143**, 489 (1934) or Monatsh. **65**, 137 (1934). Data from PLATO, F., DOMKE, J., AND HASTINGS, H.: Wiss. Abhandl. Normaleichungskommission (J. Springer, Berlin (1900)).
(43) REDLICH, O., AND ROSENFELD, P.: Z. physik. Chem. **A155**, 65 (1931).
(44) REDLICH, O., AND ROSENFELD, P.: Z. Elektrochem. **37**, 705 (1931).
(45) ROOT, W. C.: J. Am. Chem. Soc. **55**, 850 (1933).
(46) SCATCHARD, G.: Chem. Rev. **8**, 321 (1931); Trans. Faraday Soc. **33**, 161 (1937).
(47) SCATCHARD, G., AND PRENTISS, S. S.: J. Am. Chem. Soc. **54**, 2696 (1932).
(48) STARK, J. B., AND GILBERT, E. C.: J. Am. Chem. Soc. **59**, 1818 (1937).
(49) STEWART, G. S.: Trans. Faraday Soc. **33**, 238 (1937).
(50) STEWART, G. S.: J. Chem. Phys. **7**, 381 (1939).
(51) VOSBURGH, W. C., CONNELL, L. C., AND BUTLER, J. A. V.: J. Chem. Soc. **1933**, 933.
(52) WIRTH, H. E.: J. Am. Chem. Soc. **59**, 2549 (1937).

THE TERNARY SYSTEMS ETHYLENE GLYCOL–POTASSIUM CARBONATE–WATER AND DIOXANE–POTASSIUM CARBONATE–WATER

KENNETH A. KOBE AND JOSEPH P. STONG, JR.

Department of Chemical Engineering, University of Washington, Seattle, Washington

Received October 3, 1939

The study of ternary systems of water-miscible organic liquids, salts, and water was initiated by Frankforter and Frary (2), who studied methanol, ethanol, and 1-propanol and various salts and reported that potassium carbonate was the only salt that would salt out methanol, while many salts salt out ethanol. Frankforter and Cohen (1) studied acetone and several salts, and Frankforter and Temple (3) studied some of the higher alcohols. Further work has been done since 1930 by Ginnings and Chen (4), who used 2-propanol and various salts at 25°C.; by Ginnings and Robbins (7), who used tertiary butyl alcohol (2-methyl-2-propanol); by Ginnings, Herring, and Webb (6), who used 1-butanol; and by Ginnings and Dies (5), who used allyl alcohol. Ginnings and coworkers developed mathematical relationships for the equilibrium curve.

This work was started to study the salting-out effect on the dihydric alcohol ethylene glycol and its dehydration product dioxane. Both compounds are miscible with water in all proportions.

EXPERIMENTAL

Ethylene glycol could not be salted out from its aqueous solution by potassium carbonate. Eleven solutions were made up, varying in known weight composition from pure water to pure glycol; each was then shaken with a small excess of solid anhydrous potassium carbonate until saturated. The potassium carbonate in a weighed sample was titrated, and the composition of the liquid phase was determined by a materials balance.

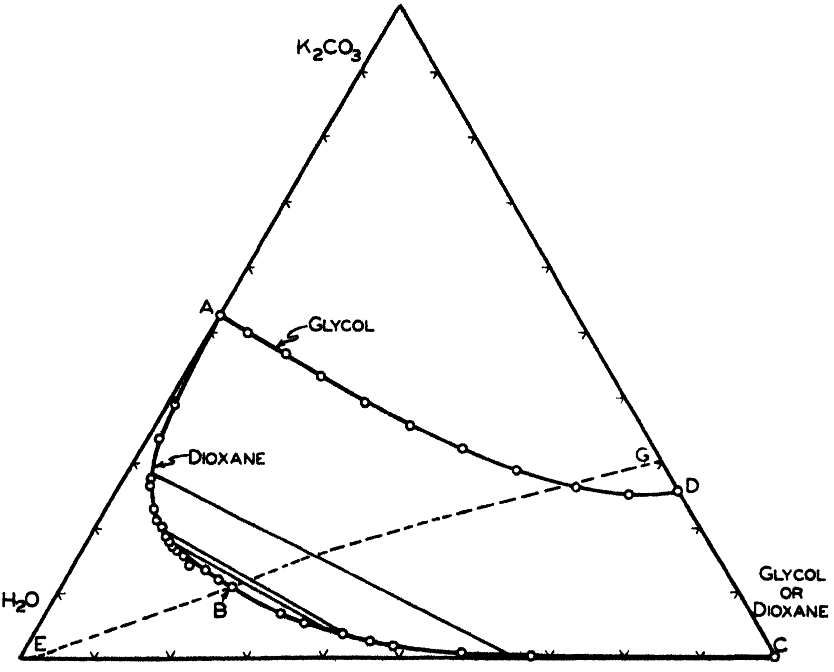

FIG. 1. The systems ethylene glycol–potassium carbonate–water and dioxane–potassium carbonate–water.

The dioxane was found to be salted out of water solution by potassium carbonate. The synthetic method was used to determine the phase relationships. A few milliliters of concentrated potassium carbonate solution of known density and composition was placed in an oil sample bottle, and dioxane was delivered from a buret until two layers formed. Water was delivered to the mixture from a buret until the mixture just became homogeneous. The weight composition of this solution was calculated from the known volumes and densities and represented a single point on the equilibrium curve. Additional dioxane was added to this homogeneous solution, and the procedure was repeated to give additional points. Phenolphthalein was used to assist in determining the

TABLE 1

The system ethylene glycol-potassium carbonate-water

COMPOSITION AT 25°C.			COMPOSITION AT 40°C.		
Glycol	Potassium carbonate	Water	Glycol	Potassium carbonate	Water
weight per cent	*weight per cent*	*weight per cent*	*weight per cent*	*weight per cent*	*weight per cent*
0	52.8	47.2	0	53.9	46.1
5.5	50.0	44.5	5.4	50.9	43.7
11.8	46.2	42.0			
18.4	43.0	38.6	17.8	44.7	37.5
26.1	38.7	35.2			
33.9	35.7	30.4	33.6	36.3	30.1
42.5	32.1	25.4	41.7	33.5	24.8
51.5	28.8	19.7	51.5	28.8	19.7
60.4	26.2	13.4			
68.2	24.8	7.0	67.7	25.4	6.9
74.4	25.6	0	73.5	26.5	0

TABLE 2

The system dioxane-potassium carbonate-water

Representative points selected from a large number of experimental values

COMPOSITION AT 0°C.			COMPOSITION AT 25°C.			COMPOSITION AT 40°C.		
Dioxane	Potassium carbonate	Water	Dioxane	Potassium carbonate	Water	Dioxane	Potassium carbonate	Water
weight per cent	*weight per cent*	*weight per cent*	*weight per cent*	*weight per cent*	*weight per cent*	*weight per cent*	*weight per cent*	*weight per cent*
0	51.7	48.3	0	52.8	47.2	0	53.9	46.1
0.56	40.64	58.8	0.9	39.0	60.1	1.0	39.7	59.3
1.06	37.6	61.34	1.7	33.7	64.6	2.5	30.0	67.5
2.1	32.0	65.9	3.7	27.5	68.8	4.1	25.3	70.6
5.0	25.7	69.3	6.2	22.9	70.9	5.7	22.6	71.7
8.8	21.0	70.2	10.9	17.6	71.5	9.1	19.0	71.9
11.0	18.9	70.1	13.9	15.5	70.6	14.2	15.1	70.7
16.5	14.5	69.0	22.5	10.8	66.7	22.6	10.6	66.8
20.2	12.3	67.5	31.0	6.8	62.2	26.4	8.7	64.9
23.3	10.6	66.1	41.12	3.22	55.66	32.67	5.96	61.37
25.0	9.8	65.2	48.38	1.66	49.96	44.12	2.54	53.34
27.9	8.3	63.8	58.44	0.31	41.25	58.44	0.31	41.25
35.8	4.8	59.4	67.59	0.21	32.2	67.59	0.21	32.2
100	0	0	100	0	0	100	0	0

presence of two phases, as it is soluble in the dioxane-rich phase. Several tie lines were determined by analyzing solutions containing two liquid layers. From these the conjugate line was determined and the plait point found as the intersections of the equilibrium curve and the conjugate line.

RESULTS

The data at 25°C. are shown in figure 1. The equilibrium curve for glycol is shown by line *AD*; that for dioxane by *ABC*, for which the conjugate line is *EBG* showing the plait point at *B*. The data for glycol at 25° and 40°C. are given in table 1; for dioxane at 0°, 25°, and 40°C. in table 2.

The equation for the equilibrium curve for dioxane–potassium carbonate–water was determined:

$$\text{Water-rich layer, } AB: \qquad y = -0.35 + 60.2(10)^{-0.042x}$$

$$\text{Dioxane-rich layer, } BC: \qquad y = 100 - 45.7x^{0.22}$$

y = weight per cent of dioxane; x = weight per cent of potassium carbonate.

The effect of temperature is very slight, as the various isotherms practically coincide. The only change with temperature is the increased solubility of the potassium carbonate in water with a corresponding shift upward of the water-rich layer.

SALTING-OUT EFFECTS

The theory of salting out is not well understood, and no theory has been advanced which will account for all the phenomena involved. Thirty-one salts were qualitatively tested to determine whether or not they would salt out glycol and dioxane. A saturated aqueous solution of the salt was made, the non-electrolyte was added dropwise, and the formation of two immiscible layers was noted. None of the salts salted out ethylene glycol from its aqueous solution. Dioxane was salted out by the following: sodium hydroxide, sodium chloride, sodium carbonate, sodium sulfate, sodium acetate, ammonium chloride, ammonium sulfate, potassium carbonate, potassium fluoride, potassium formate, potassium acetate, lithium bromide, lithium acetate, calcium chloride, strontium chloride, and strontium chlorate.

SUMMARY

1. Solubilities in the system ethylene glycol–potassium carbonate–water at 25° and 40°C. have been determined. The liquid phase remains homogeneous for all compositions.
2. Solubilities in the system dioxane–potassium carbonate–water at 0°, 25°, and 40°C. have been determined. Two liquid phases are formed in this system.
3. Of thirty-one electrolytes tried, none would salt out ethylene glycol but sixteen salted out dioxane.

REFERENCES

(1) Frankforter and Cohen: J. Am. Chem. Soc. **36**, 1103–34 (1914).
(2) Frankforter and Frary: J. Phys. Chem. **17**, 402–73 (1913).
(3) Frankforter and Temple: J. Am. Chem. Soc. **37**, 2697–716 (1915).
(4) Ginnings and Chen: J. Am. Chem. Soc. **52**, 2282–6 (1930).
(5) Ginnings and Dies: J. Am. Chem. Soc. **57**, 1038–40 (1935).
(6) Ginnings, Herring, and Webb: J. Am. Chem. Soc. **55**, 875–8 (1933).
(7) Ginnings and Robbins: J. Am. Chem. Soc. **53**, 3765–9 (1931).

SOLID POLYIODIDES OF RUBIDIUM[1]

H. W. FOOTE and MICHAEL FLEISCHER

Department of Chemistry, Yale University, New Haven, Connecticut

Received June 20, 1939

Rubidium triiodide was first prepared by Wells and Wheeler (9). Solubility results in water solutions at 25°C. by Foote and Chalker (5) and freezing point measurements by Briggs and Patterson (2) on rubidium iodide–iodine mixtures show that this is the only binary polyiodide of rubidium at temperatures of 25°C. or above. However, the work of Abegg and Hamburger (1) by the solubility method with benzene as solvent indicated the existence of three compounds which they believed to be RbI_3, RbI_7, and RbI_9. In the light of the results obtained in this laboratory on the polyiodides of potassium (3) and cesium (4), it seemed likely that the two higher polyiodides of rubidium reported by Abegg and Hamburger were actually ternary compounds containing benzene of crystallization. We have therefore studied the systems rubidium iodide–iodine–benzene and rubidium iodide–iodine–toluene at 6° and 25°C.

The experimental procedure and the purification of materials have been described (3). Rubidium iodide was prepared from a pure sample of the nitrate by fusion in platinum with oxalic acid and subsequent evaporation with excess hydriodic acid. The material was twice recrystallized as the triiodide, and was converted to the iodide by gentle heating.

The system rubidium iodide–iodine–toluene proved to be very simple (see table 1). No solvated compounds exist, as shown by closed-tube tests on residues, and both the iodide and triiodide are insoluble in the solvent, so that the composition of all residues could be calculated from the known original charges and the analytically determined iodine concentration in the solution. As found by the earlier workers by other methods, the triiodide is the only stable binary compound. The average of the six results on rubidium triiodide is 54.51 per cent available iodine, in excellent agreement with the theoretical value, 54.45 per cent.

---

[1] This article is based on a thesis presented by Michael Fleischer to the Faculty of the Graduate School of Yale University in partial fulfillment of the requirements for the degree of Doctor of Philosophy, June, 1933.

Qualitative tests at the iodine end of the system rubidium iodide–iodine–benzene showed that the residues were solvated. The system proved to be rather perplexing and a large number of determinations was carried out. Considerable trouble was caused by persistent metastable equilibria. It was found necessary to grind the solids very fine, and to shake the bottles vigorously before placing them in the thermostat. The solubility results show that there are four points of constant solution composition with varying solid phase composition at each temperature; three compounds are present, two of which are solvated. The results at both temperatures are given in table 2. All compositions are in weight per cent.

TABLE 1

The system rubidium iodide–iodine–toluene

SERIAL NO.	IODINE IN SOLUTION	AVAILABLE IODINE IN RESIDUE	SOLID PHASES PRESENT
		$t = 6°C.$	
	weight per cent	*weight per cent*	
1	0.19	9.18	RbI and RbI_3
2	0.21	49.95	
3	0.76	54.57	RbI_3
4	1.02	54.49	
5	7.03	54.47	
6	10.19	60.69	RbI_3 and I_2
7	10.33	90.33	
		$t = 25°C.$	
8	0.39	7.91	RbI and RbI_3
9	0.41	48.74	
10	0.40	49.33	
11	1.83	54.54	RbI_3
12	14.90	55.10	
13	15.07	53.90	
14	15.40	62.85	RbI_3 and I_2
15	15.46	93.77	

As indicated in table 2, three different methods were used to obtain the compositions of the solid residues in different parts of the system. When

TABLE 2

The system rubidium iodide-iodine-benzene

SERIAL NO.	IODINE IN SOLUTION	SOLID RESIDUE			METHOD OF DETERMINING COMPOSITION OF RESIDUE	SOLIDS PRESENT
		RbI	Available iodine	Benzene		
				t = 6°C.		
	weight per cent	*weight per cent*	*weight per cent*	*weight per cent*		
1	0.17	91.56	8.44	0.0	a*	RbI and RbI$_3$
2	0.18	50.93	49.07	0.0	a	
3	0.61	46.00	54.00	0.0	a	RbI$_3$
4	3.71	45.65	54.35	0.0	a	
5	4.08	26.1	57.6	16.3	b	RbI$_3$ and RbI$_7$·4C$_6$H$_6$
6	4.07	22.1	58.2	19.7	b	
7	4.24	16.82	62.93	20.25	c	RbI$_7$·4C$_6$H$_6$
8	4.49	16.87	62.50	20.63	c	
9	4.99	16.23	62.46	21.31	c	
10	5.34	15.80	60.86	23.34	c	
11	5.70	15.79	62.83	21.38	c	
12	5.75	15.90	59.18	24.92	c	
13	5.97	16.27	60.47	23.24	c	
14	6.92	16.18	61.63	22.19	c	
15	6.98	16.1	60.3	23.6	b	RbI$_7$·4C$_6$H$_6$ and RbI$_8$·4C$_6$H$_6$
16	7.00	15.4	61.4	23.2	b	
17	6.98	15.0	62.9	22.1	b	
18	7.17	14.43	65.89	19.68	c	RbI$_8$·4C$_6$H$_6$
19	7.58	13.27	62.26	24.47	c	
20	7.88	13.32	62.82	23.86	c	
21	7.95	13.90	66.76	19.34	c	
22	8.15	13.55	64.83	21.62	c	
23	8.53	14.13	63.22	22.65	c	
24	8.72	14.8	63.5	21.7	b	RbI$_8$·4C$_6$H$_6$ and I$_2$
25	8.71	12.0	70.3	17.7	b	
26	8.69	8.8	78.2	13.0	b	
				t = 25°C.		
27	0.37	91.93	8.07	0.0	a	RbI and RbI$_3$
28	0.36	50.13	49.87	0.0	a	
29	0.38	46.66	53.34	0.0	a	
30	0.99	45.49	54.51	0.0	a	RbI$_3$
31	6.05	45.70	54.30	0.0	a	
32	8.06	45.76	54.24	0.0	a	

* a, residue unsolvated, composition calculated as in toluene system; b, composition of residue calculated algebraically; c, composition of residue determined by analysis.

TABLE 2—*Concluded*

SERIAL NO.	IODINE IN SOLUTION	SOLID RESIDUE			METHOD OF DETERMINING COMPOSITION OF RESIDUE	SOLIDS PRESENT
		RbI	Available iodine	Benzene		
				t = 25°C.—*Continued*		
	weight per cent	*weight per cent*	*weight per cent*	*weight per cent*		
33	9.19	41.3	55.1	3.6	b	RbI_3 and $RbI_7 \cdot 4C_6H_6$
34	9.13	16.8	59.1	24.1	b	
35	9.68	15.69	63.91	20.40	c	$RbI_7 \cdot 4C_6H_6$
36	9.79	16.59	64.60	19.81	c	
37	10.04	15.55	61.54	22.91	c	
38	10.92	16.2	60.0	23.8	b	$RbI_7 \cdot 4C_6H_6$ and $RbI_9 \cdot 4C_6H_6$
39	10.88	15.2	62.4	22.4	b	
40	11.61	13.92	66.86	19.22	c	$RbI_9 \cdot 4C_6H_6$
41	12.85	14.18	66.34	19.48	c	
42	13.44	14.11	64.78	21.11	c	
43	13.65	13.94	64.85	21.21	c	
44	14.13	12.7	68.6	18.7	b	$RbI_9 \cdot 4C_6H_6$ and I_2
45	14.15	10.4	74.2	15.4	b	
46	14.31	3.2	92.1	4.7	b	

the residue was unsolvated, the composition of the residue was calculated as in the toluene system. When two solid phases, one or both of which was solvated, were present, the composition of the solid residue was calculated algebraically. When the solid residue consisted of one of the ternary compounds, it was analyzed for available iodine and for rubidium iodide, after being dried between filter papers.

The solubility data in table 2 show that three compounds are present at each temperature. The presence of rubidium triiodide is shown by the results, the average of the five runs in which it was the solid phase being 54.28 per cent available iodine in the residue (theoretical value, 54.45 per cent).

The molecular composition of the ternary compound lower in iodine, as determined from the analyses in table 2, is given in table 3(A). Since the solid analyzed always contained free iodine derived from the evaporation of mother liquor, the molecular ratios are always high for available iodine. The results in table 3(A) indicate that the formula of the ternary compound is $RbI \cdot 6I \cdot 4C_6H_6$. However, it is apparent that if the ratio $RbI:C_6H_6$ in the solid phase is known, the composition of the solid phase can be calculated as in the toluene system. Such a calculation has been carried out for each experiment in which the compound was present, assuming the ratio $RbI:C_6H_6$ to be 1:4. The results of this calculation, given in table 3(B), confirm the formula above, the ratio I:RbI being, as expected, much closer to 6 than the ratio derived from the direct analyses.

The molecular composition, calculated from the analyses in table 2, of the ternary compound higher in iodine is given in table 4(A). From the analyses, the ratio I:RbI appears at first glance to be 8:1. However, it must be remembered that the solutions from which the solid was removed for analysis were high in iodine content, so that even a small amount of evaporating mother liquor would deposit considerable free iodine. Allowing for the fact that the analyses are to be expected to show an excess of iodine, the formula of the compound would appear to be $RbI\cdot 7I\cdot 4C_6H_6$. If the ratio $RbI:C_6H_6$ is taken as 1:4 and the composition of the residue is calculated, the results given in table 4(B) are obtained. These confirm the formula above with I:RbI = 7:1. Thus, the two ternary compounds have the formulas $RbI\cdot 6I\cdot 4C_6H_6$ and $RbI\cdot 7I\cdot 4C_6H_6$, differing by one atom of iodine. No ternary compounds with analogous formulas have been reported in the literature, but we have obtained a very unstable compound $KSCN\cdot 6I\cdot 4C_6H_6$ (6). It is rather interesting to note that the compounds $CsI\cdot 9I\cdot 2C_6H_6$, $KI\cdot 8I\cdot 3C_6H_6$, and $RbI\cdot 7I\cdot 4C_6H_6$

TABLE 3

Composition of ternary compound lower in iodine

SERIAL NO.	(A) MOLECULAR RATIOS FROM ANALYSES IN TABLE 2			(B) RESIDUE CALCULATED ASSUMING $RbI:C_6H_6 = 1:4$		
	RbI :	Available iodine :	C_6H_6	RbI	Available iodine	Ratio I:RbI
				weight per cent	*weight per cent*	
7	1.0	6.26	3.27	16.22	59.91	6.18
8	1.0	6.20	3.33	16.34	59.62	6.10
9	1.0	6.44	3.57	16.38	59.53	6 08
10	1.0	6.44	4.02	15.74	59.53	6.33
11	1.0	6.66	3.68	16.33	59.64	6.11
12	1.0	6.22	4.27	16.57	59.05	5.96
13	1.0	6.22	3.89	17.07	57.82	5.67
14	1.0	6.37	3.73	16.91	58.23	5.76
35	1.0	6.82	3.54	15.93	60.65	6.37
36	1.0	6.52	3.08	16.43	59.40	6.05
37	1.0	6.62	4.01	16.09	60.23	6.26
Average...	1.0	6.43	3.67	16.36	59.42	6.08
Theoretical for $RbI\cdot 6I\cdot 4C_6H_6$				16.50	59.18	6.00

differ by having one atom of iodine less and one molecule of benzene more, in order.

Recently Grace (8) published a study of the system rubidium iodide–iodine–benzene at 25°C. He also found two solvated compounds, but gave their compositions as $RbI \cdot 6I \cdot 2C_6H_6$ and $RbI \cdot 8I \cdot 2C_6H_6$. It seems probable that the discrepancy in benzene content is due to the different methods used by Grace and by us to prepare the solids for analysis. His method consisted in placing the material in an isoteniscope and pumping off slowly until the dissociation pressure of the compound, determined in a preliminary experiment, was reached. Grace's results therefore give a lower limit to the benzene content. Our own method consisted in drying the solid between filter papers until decomposition had just begun, as told by a lightening of the color of the compound, then analyzing immediately. Our results should also give a lower limit to the benzene content, but it seems likely that Grace's material had lost more benzene of constitution than had ours before analysis. It is difficult to decide the correct degree of solvation for such compounds, which are removed from solutions in volatile solvents and which lose their solvent of crystallization so readily. Our formulas are based on twenty-one analyses of the two compounds; Grace's formulas on four.

TABLE 4

Composition of ternary compound higher in iodine

SERIAL NO.	(A) MOLECULAR RATIOS FROM ANALYSES IN TABLE 2			(B) RESIDUE CALCULATED ASSUMING $RbI:C_6H_6 = 1:4$		
	RbI :	Available iodine :	C_6H_6	RbI	Available iodine	Ratio I:RbI
				weight per cent	*weight per cent*	
18	1.0	7.64	3.71	14.68	63.73	7.27
19	1.0	7.85	5.02	14.65	63.80	7.29
20	1.0	7.89	5.28	15.04	62.84	6.99
21	1.0	7.95	3.74	14.89	63.12	7.09
22	1.0	8.01	4.34	14.68	63.73	7.27
23	1.0	7.48	4.36	15.13	62.70	6.92
40	1.0	8.04	3.75	14.52	64.14	7.39
41	1.0	7.83	3.74	14.83	63.37	7.16
42	1.0	7.68	4.07	14.60	63.94	7.33
43	1.0	7.78	4.14	14.78	63.49	7.19
Average...	1.0	7.82	4.22	14.78	63.49	7.19
Theoretical for $RbI \cdot 7I \cdot 4C_6H_6$............				15.02	62.87	7.00

The ratio I:RbI found by Grace for the ternary compound higher in iodine was 8, which is in excellent agreement with our analyses of the same compound. Nevertheless, as we have pointed out, this ratio appears incorrect, because of contamination of the sample with free iodine deposited by evaporating solvent. At 25°C. the compound is stable only in contact with solutions containing over 11 per cent by weight of iodine, and it is impossible to dry the solution without contamination. The data in table 4(B) indicate also that the higher ternary compound has the ratio I:RbI = 7, not 8.

The dissociation pressure of rubidium triiodide has been obtained from the solubility results at 6° and 25°C. by the method previously explained (4). The values of c/c_0 for both solvents at both temperatures are given in table 5. The agreement is within the error of the solubility determinations.

TABLE 5

Showing the ratio c/c_0 at 6° and 25°C. for both solvents

SOLIDS PRESENT	IODINE IN SOLUTION	IODINE IN SOLUTION	c/c_0
Toluene; t = 6°C.			
	weight per cent	*mole per cent*	
I_2 and RbI_3	10.26	3.98 (c_0)	
RbI_3 and RbI	0.20	0.0727 (c)	0.0182
Benzene; t = 6°C.			
I_2 and $RbI_9 \cdot 4C_6H_6$	8.71	2.85 (c_0)	
RbI_3 and RbI	0.175	0.0539 (c)	0.0189
Toluene; t = 25°C.			
I_2 and RbI_3	15.43	6.21 (c_0)	
RbI_3 and RbI	0.40	0.146 (c)	0.0234
Benzene; t = 25°C.			
I_2 and $RbI_9 \cdot 4C_6H_6$	14.20	4.84 (c_0)	
RbI_3 and RbI	0.37	0.114 (c)	0.0236

From these values of c/c_0 the dissociation pressure of rubidium triiodide is calculated to be 0.00101 and 0.00736 mm. at 6° and 25°C., respectively, and the heat of dissociation is −17.2 kg.-cal. In these calculations the vapor pressure of iodine has been assumed to be 0.0546 and 0.313 mm. at 6° and 25°C., respectively. These vapor pressures were obtained by interpolation from the *International Critical Tables.* The values would be changed slightly if we had used the "best" values for the vapor pressure of iodine, 0.0556 and 0.309 mm. at 6° and 25°C., recently given by Gillespie and Fraser (7). The older values were used so that the dissociation pressures calculated would be consistent with those given in our earlier papers.

SUMMARY

The systems rubidium iodide–iodine–toluene and rubidium iodide–iodine–benzene have been studied at 6° and 25°C. The binary compound rubidium triiodide is the only compound stable at both temperatures in the toluene system. In the benzene system two ternary polyiodides, $RbI \cdot 6I \cdot 4C_6H_6$ and $RbI \cdot 7I \cdot 4C_6H_6$, are stable phases at both temperatures. The dissociation pressure of rubidium triiodide at both temperatures has been calculated from the solubility results.

REFERENCES

(1) Abegg and Hamburger: Z. anorg. Chem. **50**, 403 (1906).
(2) Briggs and Patterson: J. Phys. Chem. **36**, 2621 (1932).
(3) Foote and Bradley: J. Phys. Chem. **36**, 673 (1932).
(4) Foote, Bradley, and Fleischer: J. Phys. Chem. **37**, 21 (1933).
(5) Foote and Chalker: Am. Chem. J. **39**, 561 (1908).
(6) Foote and Fleischer: Unpublished data.
(7) Gillespie and Fraser: J. Am. Chem. Soc. **58**, 2260 (1936).
(8) Grace: J. Phys. Chem. **37**, 437 (1933).
(9) Wells and Wheeler: Am. J. Sci. **44**, 43 (1892).

ADDITION COMPOUNDS OF IODINE WITH ALKALI BROMIDES AND THIOCYANATES[1]

H. W. FOOTE and MICHAEL FLEISCHER

Department of Chemistry, Yale University, New Haven, Connecticut

Received June 20, 1939

Addition compounds of iodine with the iodides of potassium (4), ammonium (5), rubidium (7), and cesium (6) have been studied in this laboratory by the solubility method. It seemed desirable to extend our work to study the addition of iodine to alkali bromides and thiocyanates in order to widen our knowledge of the stability relations of this type of addition compound. We used benzene and toluene as solvents, since our previous work had shown that only binary polyiodides are formed with toluene as solvent, but that there are a number of solvated ternary compounds composed of an iodide, iodine, and benzene.

---

[1] This article is taken in part from a dissertation submitted by Michael Fleischer to the Faculty of the Graduate School of Yale University in partial fulfillment of the requirements for the degree of Doctor of Philosophy, June, 1933.

The experimental procedure used and the method of purification of the iodine, benzene, and toluene have been described (4). The bromides were recrystallized from water solution and dried at 105°C. Their purity was checked by determination of the bromide content by precipitation of silver bromide. The thiocyanates were recrystallized from water solution and dried over phosphorus pentoxide. Analyses by titration with standard silver nitrate solution gave results close to the theoretical values for the thiocyanate content of each salt.

ADDITION OF IODINE TO ALKALI BROMIDES

The only addition compound of the alkali bromides and iodine reported in the literature is $CsBrI_2$, prepared by Wells (9) by crystallization from water or alcohol solutions. Attempts to prepare analogous compounds with potassium bromide and rubidium bromide failed (10). The cesium compound was also obtained by Cremer and Duncan (3). The only equilibrium study on such systems was made by the latter workers, who studied the system potassium bromide–iodine–carbon tetrachloride at 25°C. and found that no compounds were formed.

TABLE 1

The system rubidium bromide–iodine–benzene at 6°C.

IODINE IN SOLUTION	IODINE IN RESIDUE	SOLIDS PRESENT
weight per cent	*weight per cent*	
8.67	10.77	RbBr and I_2
8.70	48.23	
8.74	94.03	

We have studied the systems sodium bromide–iodine–benzene, potassium bromide–iodine–benzene, rubidium bromide–iodine–benzene, thallous bromide–iodine–benzene, cesium bromide–iodine–benzene, and cesium bromide–iodine–toluene at 6°C. The system with thallous bromide was included because thallous iodide adds iodine to form two higher iodides, Tl_6I_8 and TlI_3 (1). No compounds were found in any of the systems except the two systems containing cesium bromide. The data for the four other systems are essentially identical and only that for the rubidium bromide system will be given (see table 1). These results show clearly that no compounds are formed.

In these systems and in the two cesium bromide systems given in table 2, the composition of the solid residue was calculated in each case from the known original mixture and the analytically determined concentration of iodine in the solution after equilibrium had been reached, as qualitative tests showed that no solvated phases were present and that the bromides were insoluble in the solvents. The results show clearly that only one compound, $CsBrI_2$, is stable in both systems. The average of the five results in which the pure compound was present is 54.48 per cent iodine; the theoretical value is 54.41 per cent. No ternary compound containing benzene was formed, although such a compound was found in the system cesium iodide–iodine–benzene (6).

TABLE 2

The system cesium bromide–iodine–solvent

SERIAL NO.	IODINE IN SOLUTION	IODINE IN RESIDUE	SOLIDS PRESENT
Toluene; $t = 6°C.$			
	weight per cent	*weight per cent*	
1	0.99	24.20	CsBr and $CsBrI_2$
2	0.97	47.48	
3	1.51	54.27	$CsBrI_2$
4	9.63	54.71	
5	10.41	63.53	$CsBrI_2$ and I_2
6	10.31	86.93	
Benzene; $t = 6°C.$			
7	0.83	24.82	CsBr and $CsBrI_2$
8	0.81	47.32	
9	1.43	54.18	$CsBrI_2$
10	5.82	54.37	
11	7.74	54.86	
12	8.67	64.61	$CsBrI_2$ and I_2
13	8.71	93.08	

TABLE 3

Showing the ratio c/c_0 in toluene and in benzene

SOLIDS PRESENT	IODINE IN SOLUTION	IODINE IN SOLUTION	c/c_0
Toluene; $t = 6°C.$			
	weight per cent	*mole per cent*	
I_2 and $CsBrI_2$	10.36	4.026 (c_0)	
$CsBrI_2$ and CsBr	0.98	0.358 (c)	0.0889
Benzene; $t = 6°C.$			
I_2 and $CsBrI_2$	8.69	2.845 (c_0)	
$CsBrI_2$ and CsBr	0.82	0.254 (c)	0.0892

The dissociation pressure of $CsBrI_2$ at 6°C. has been calculated from these results by the method previously explained (6). The values of c/c_0 for both solvents are given in table 3. From the average of these values of c/c_0, the dissociation pressure of $CsBrI_2$ at 6°C. is calculated to be 0.00486 mm., taking the vapor pressure of iodine at 6°C. to be 0.0546 mm.[2]

ADDITION OF IODINE TO ALKALI THIOCYANATES

The remarkable similarities in the behavior of thiocyanates to that of iodides, bromides, and chlorides have often been pointed out in the past. Iodides and thiocyanates, especially, have been found to behave in almost the same fashion towards many reagents, a striking example being the formation of addition compounds with sulfur dioxide by both iodides and thiocyanates (8). Some years ago, in this laboratory, Dr. Joseph Fleischer observed that aqueous solutions of thiocyanates were remarkably good solvents for iodine. The solutions were not stable, however, as a slow reaction gave free sulfur, some thiosulfate, and other products. This reaction is well known and has been studied (2) for dilute iodine solutions, but, as far as we know, there is no mention in the literature of the fact that the solubility of iodine in thiocyanate solutions is of the same order of magnitude as its solubility in iodide solutions.

It seemed probable that the alkali thiocyanates would form addition compounds with iodine similar to those formed by the alkali iodides. The reaction mentioned above precludes the study of such compounds in aqueous solution, but it was thought possible that the reaction would be sufficiently slow in non-aqueous solvents to allow solubility equilibrium to be reached before the side reaction had used up much iodine and thiocyanate. Accordingly, we have studied the systems sodium thiocyanate–iodine–toluene, sodium thiocyanate–iodine–benzene, potassium thiocyanate–iodine–toluene, potassium thiocyanate–iodine–benzene, ammonium thiocyanate–iodine–toluene, and ammonium thiocyanate–iodine–benzene at 6°C.

The extent to which the side reaction was consuming iodine was determined for each system by making up mixtures such that the solution was nearly, but not quite, saturated with iodine, rotating for 4 days in the thermostat, and analyzing the solution for iodine. In every case, there was a deficiency of iodine. In the four systems with potassium thiocyanate and sodium thiocyanate, from 2 to 3 per cent of the total iodine had been used by the side reaction; in the two systems with ammonium thiocyanate about 8 per cent of the iodine had reacted with the thiocyanate. The results obtained are therefore subject to some uncertainty. However, the results showed clearly that no compounds were formed in any of the six systems studied, excepting the system potassium thiocyanate–iodine–benzene.

---

[2] By interpolation of the data in the *International Critical Tables*.

The data obtained in the five other systems are essentially identical and need not be given in detail, the data given below for the system potassium thiocyanate–iodine–toluene being typical of all five. It is evident that there is no compound formation in this system.

TABLE 4

The system potassium thiocyanate–iodine–toluene at 6°C.

IODINE IN SOLUTION	IODINE IN RESIDUE*	SOLID PHASES PRESENT
weight per cent	*weight per cent*	
10.21	38.50	KSCN and I_2
10.29	63.97	
10.18	92.48	

* Calculated from the amount of iodine originally added and the analytically determined concentration of iodine in the solution. The results have not been corrected for the iodine used by the reaction with thiocyanate.

TABLE 5

The system potassium thiocyanate–iodine–benzene at 6°C.

SERIAL NO.	IODINE IN SOLUTION	SOLID RESIDUE			METHOD OF DETERMINING COMPOSITION OF RESIDUE	SOLID PHASES PRESENT
		KSCN	I_2	C_6H_6		
	weight per cent	*weight per cent*	*weight per cent*	*weight per cent*		
1	7.34	100.0	0.0	0.0	a*	KSCN
2	8.15	78.63	15.16	6.21	b	KSCN and ternary compound
3	7.93	27.89	51.14	20.97	b	
4	8.11	22.74	54.79	22.47	b	
5	7.91	12.86	61.80	25.34	b	
6	8.30	8.47	65.78	25.75	c	Ternary compound
7	8.45	8.12	63.61	28.27	c	
8	8.59	7.83	64.09	28.08	c	
9	8.70	7.67	67.67	24.66	b	Ternary compound and I_2
10	8.69	6.60	72.24	21.16	b	

* a, Residue unsolvated, composition calculated as in toluene system; b, composition of residue obtained by algebraic extrapolation; c, composition of residue obtained by analysis.

Qualitative tests showed that the solid residues at the iodine-rich end of the system potassium thiocyanate–iodine–benzene were solvated. As shown by the results in table 5, a ternary compound is formed in this system. It resembles those formed by the alkali iodides, but is much less stable. At a temperature below room temperature and estimated to be approximately 12°C. it melts incongruently and loses both iodine and benzene very rapidly. This increased the difficulty of analyzing the compound, as samples for analysis had to be dried and weighed extremely rapidly.

The residues from Nos. 6, 7, and 8 were analyzed for available iodine by titration with thiosulfate solution, and for potassium thiocyanate by evaporating with sulfuric acid and igniting to potassium sulfate in a current of ammonia gas. The molecular composition of the ternary compound from the analyses is as follows:

TABLE 6

Compound formation of RX compounds with iodine at 6°C. in the presence of benzene

R	X = I	X = SCN	X = Br
Na	None	None	None
K......	No binary compound $KI \cdot 8I \cdot 3C_6H_6$	No binary compound $KSCN \cdot 6I \cdot 4C_6H_6$	None
NH_4...	NH_4I_3 No ternary compound	None	None
Rb.....	RbI_3 $RbI \cdot 6I \cdot 4C_6H_6$ $RbI \cdot 7I \cdot 4C_6H_6$		None
Cs.....	CsI_3; CsI_4 $CsI \cdot 9I \cdot 2C_6H_6$		$CsBrI_2$ No ternary compound
Tl.....	Tl_6I_8; TlI_3 No ternary compound		None

SERIAL NO.	COMPOSITION OF TERNARY COMPOUND
6	$KSCN:5.95I:3.79C_6H_6$
7	$KSCN:6.00I:4.33C_6H_6$
8	$KSCN:6.27I:4.46C_6H_6$

Assuming that the ratio $KSCN:C_6H_6$ in the residue is 1:4, the composition of the residue in each of these three experiments has been calculated from the original charges and the analytically determined iodine concentration in the solution, with the following results:

SERIAL NO.	KSCN	I_2	RATIO I:KSCN
	weight per cent	*weight per cent*	
6	8.28	65.11	6.01
7	8.27	65.16	6.03
8	8.25	65.24	6.06

These results confirm the probable formula derived from the analyses. The compound $KSCN \cdot 6I \cdot 4C_6H_6$ is analogous to $RbI \cdot 6I \cdot 4C_6H_6$, found by us (7) to be one of two ternary compounds of rubidium iodide, iodine, and benzene. It is improbable that the error due to the side reaction could be large enough to cause much error in the formula determined, although the experiments in which both potassium thiocyanate and the ternary compound were present (Nos. 2 to 5) show much more variation than usual in the determined iodine concentration in the solution.

Table 6 gives a comparison of the results obtained with iodides, bromides, and thiocyanates at 6°C. It seems safe to predict that rubidium thiocyanate and cesium thiocyanate will form ternary compounds with iodine and benzene, and that cesium thiocyanate will probably form a binary compound with iodine. It is also possible that thallous thiocyanate will form addition compounds with iodine.

SUMMARY

A study at 6°C. of systems composed of an alkali bromide (or thiocyanate), iodine, and benzene (or toluene) has shown that sodium bromide, potassium bromide, ammonium bromide, thallous bromide, sodium thiocyanate, and ammonium thiocyanate form no compounds with iodine. Cesium bromide adds iodine to form $CsBrI_2$, and potassium thiocyanate forms the solvated ternary compound $KSCN \cdot 6I \cdot 4C_6H_6$. The dissociation pressure of $CsBrI_2$ at 6°C. has been calculated from the solubility results.

REFERENCES

(1) Abegg and Maitland: Z. anorg. Chem. **50**, 403 (1906).
(2) Angelescu and Popescu: Z. physik. Chem. **A156**, 258 (1931).
(3) Cremer and Duncan: J. Chem. Soc. **1931**, 1857, 2243.
(4) Foote and Bradley: J. Phys. Chem. **37**, 673 (1933).
(5) Foote and Bradley: J. Phys. Chem. **37**, 29 (1933).
(6) Foote, Bradley, and Fleischer: J. Phys. Chem. **37**, 21 (1933).
(7) Foote and Fleischer: Unpublished data.
(8) Foote and Fleischer, J.: J. Am. Chem. Soc. **53**, 1752 (1931); **54**, 3902 (1932).
(9) Wells: Am. J. Sci. **43**, 17 (1892).
(10) Wells and Wheeler: Am. J. Sci. **43**, 475 (1892).

THE IODIDES OF SOME POLYVALENT METALS[1]

H. W. FOOTE AND MICHAEL FLEISCHER

Department of Chemistry, Yale University, New Haven, Connecticut

Received June 20, 1939

The methods which have been used in this laboratory to study the addition compounds of alkali iodides and iodine (2, 3) are equally applicable to the study of the iodides of polyvalent metals. From a phase rule standpoint, the relations are the same in both cases and, furthermore, are not changed if the starting material is a metal rather than an iodide. The study of systems composed of a metal, iodine, and a solvent in which the metal and its iodides are insoluble but which dissolves iodine, is an extraordinarily simple and accurate method of determining the stability conditions of metal iodides.

We have studied the iodides of iron, copper, silver, and thallium, at 6°C., using toluene and benzene as solvents. The experimental procedure and the methods used to purify iodine and the solvents have been described (2, 3). Equilibrium was reached very rapidly in these systems, but a period of 5 days was always allowed before analyzing. As qualitative tests showed that the solid residues were not solvated and that the iodides were insoluble in the solvents used, the composition of the solid residues was calculated from the known original composition and the analytically determined concentration of iodine in the solution after equilibrium had been reached.

THE IODIDE OF IRON

The well-known fact that in water solution ferric iodide is unstable and decomposes into the ferrous compound and free iodine does not prove that a solid ferric iodide does not exist and that it could not be prepared in a non-ionizing solvent. It has been shown (4) that when a mixture of iron and iodine is heated to a high temperature, pure ferrous iodide is formed and the excess iodine is volatilized. Ferric iodide is therefore unstable at high temperatures, but there has been no systematic study of iron iodides at low temperatures.

The results obtained by us in the systems iron–iodine–toluene and iron–iodine–benzene at 6°C. are summarized in table 1. The iron used was a pure sample of finely divided metal which had been prepared from iron carbonyl. We are indebted to Dr. Oskar Baudisch for the gift of this material.

---

[1] This article is based upon a thesis presented by Michael Fleischer to the Faculty of the Graduate School of Yale University in partial fulfillment of the requirements for the degree of Doctor of Philosophy, June, 1933.

The results in table 1 show clearly that ferrous iodide (iodine content 81.94 per cent) is the only stable binary iodide of iron at 6°C. Ferric iodide can not be prepared at 6°C. or above. As no iodine could be detected in the solution when the solid was a mixture of iron and ferrous iodide, the dissociation pressure of ferrous iodide at 6°C. must be very low.

THE IODIDE OF COPPER

Solid cupric iodide has never been prepared, but polyiodides of copper have been reported by Jörgensen (5) and by Walker and Dover (9). A study of the freezing points of mixtures of iodine and cuprous iodide by Kremann and Borjanovics (6) gave no evidence of compound formation, but there has been no systematic study at low temperatures. We have therefore studied the systems copper-iodine-toluene and copper-iodine-benzene at 6°C. Table 2 gives the data obtained for the system with benzene; those for the toluene system are in complete accord and are omitted for brevity.

TABLE 1

The systems iron–iodine–toluene and iron–iodine–benzene

IODINE IN SOLUTION	TOTAL IODINE IN RESIDUE	SOLIDS PRESENT
Toluene; t = 6°C.		
weight per cent	*weight per cent*	
0.0	50.00	Fe and FeI_2
1.31	81.50	FeI_2
10.06	81.67	
10.46	82.91	FeI_2 and I_2
10.30	90.82	
Benzene; t = 6°C.		
1.11	81.41	FeI_2
6.98	82.28	
8.81	87.62	FeI_2 and I_2
8.81	95.44	

The results show clearly that cuprous iodide (iodine content 66.63 per cent) is the only stable binary copper iodide at 6°C. and that cupric iodide can not be prepared at 6°C. or above. It seems probable that the compounds analyzed by Jörgensen and by Walker and Dover were mechanical mixtures. As no iodine could be detected in the solution when the solid was a mixture of copper and cuprous iodide, the dissociation pressure of cuprous iodide must be very low at 6°C.

THE IODIDE OF SILVER

As it seemed possible that silver might form polyiodides like those of the alkali metals, the systems silver iodide–iodine–toluene and silver iodide–iodine–benzene were studied at 6°C. Schmidt (8) reported the preparation of silver triiodide, AgI_3, by the addition of silver nitrate to a concentrated solution of iodine in potassium iodide. Our results show that he was undoubtedly dealing with a mixture of silver iodide and iodine. The data for the benzene system are given in table 3; those for the toluene system are similar and so are omitted.

TABLE 2

The system copper–iodine–benzene at 6°C.

IODINE IN SOLUTION	TOTAL IODINE IN RESIDUE	SOLIDS PRESENT
weight per cent	*weight per cent*	
0.0	55.00	Cu and CuI
3.05	65.99	CuI
7.79	66.20	
8.53	69.40	CuI and I_2
8.61	91.57	

TABLE 3

The system silver iodide–iodine–benzene at 6°C.

IODINE IN SOLUTION	AVAILABLE IODINE IN RESIDUE	SOLIDS PRESENT
weight per cent	*weight per cent*	
7.46	0.0	AgI
8.71	12.13	AgI and I_2
8.68	96.62	

THE IODIDES OF THALLIUM

Thallous salts are in many ways rather similar to the correspondind salts of the alkali metals. It seemed possible that thallous iodide woulg react with iodine to form polyiodides, so the systems thallous iodide–iodine–toluene and thallous iodide–iodine–benzene were studied at 6°C. While there is considerable evidence for the existence of two higher iodides (7), the only systematic work is that of Abegg and Maitland (1), who used the solubility method with carbon disulfide as solvent at 25°C. They found the compounds TlI_3 and Tl_6I_8 or $TlI_3 \cdot 5TlI$. Thallous iodide was prepared by mixing equivalent amounts of pure thallous carbonate and potassium iodide solutions, washing the precipitate thoroughly, and drying at 105°C. The results obtained are given in table 4.

The average of the four results on the higher iodide is 43.28 per cent available iodine; TlI_3 requires 43.38 per cent. The lower iodide was present in Nos. 3 to 7 and 17 to 22. The composition of the residue shows

TABLE 4

The systems thallous iodide–iodine–toluene and thallous iodide–iodine–benzene

SERIAL NO.	IODINE IN SOLUTION	AVAILABLE IODINE IN RESIDUE	SOLIDS PRESENT
		Toluene; $t = 6°C.$	
	weight per cent	*weight per cent*	
1	0.043	2.67	TlI and Tl_6I_8
2	0.045	8.66	
3	0.17	11.33	Tl_6I_8
4	0.74	11.87	
5	1.51	12.28	
6	1.75	12.30	
7	1.81	12.35	
8	2.29	14.91	Tl_6I_8 and TlI_3
9	2.27	25.02	
10	2.27	39.27	
11	2.97	43.47	TlI_3
12	9.40	43.66	
13	10.17	49.26	TlI_3 and I_2
14	10.07	95.14	
		Benzene; $t = 6°C.$	
15	0.038	2.98	TlI and TlI_3
16	0.038	10.00	
17	0.18	11.32	Tl_6I_8
18	0.36	11.44	
19	0.75	11.76	
20	1.40	11.93	
21	1.43	11.82	
22	1.57	11.95	
23	1.97	12.27	Tl_6I_8 and TlI_3
24	1.99	39.88	
25	3.07	42.76	TlI_3
26	8.27	43.23	
27	8.66	49.93	TlI_3 and I_2
28	8.60	94.12	

good agreement with the formula Tl_6I_8 (available iodine, 11.32 per cent) only when the solution was very low in iodine content (Nos. 3, 17, 18). The other results are all high, the excess iodine in the residue being roughly proportional to the concentration of iodine in the solution. This may be due to adsorption of iodine by the compound. These results confirm the work of Abegg and Maitland (1) at 25°C.

The dissociation pressures of the two compounds at 6°C. have been calculated by the method previously described (3). The values of c/c_0 calculated from the results in the two solvents are in good agreement. Using the averages of these values, and taking the vapor pressure of iodine at 6°C. to be 0.0546 mm.[2], the dissociation pressures of TlI_3 and Tl_6I_8 are 0.0116 and 0.00022 mm., respectively, at 6°C. Unfortunately, the work of Abegg and Maitland at 25°C. is given in terms of volumes, and the densities of their solutions are not known, so that dissociation pressures can not be calculated from their data.

TABLE 5

Showing the ratio c/c_0 for both periodides in benzene and in toluene

SOLIDS PRESENT	IODINE IN SOLUTION	IODINE IN SOLUTION	c/c_0
Benzene; t = 6°C.			
	weight per cent	*mole per cent*	
TlI_3 and I_2	8.63	2.95 (c_0)	
Tl_6I_8 and TlI_3	1.98	0.618 (c)	0.209
TlI and Tl_6I_8	0.038	0.0118 (c)	0.00398
Toluene; t = 6°C.			
TlI_3 and I_2	10.12	3.92 (c_0)	
Tl_6I_8 and TlI_3	2.28	0.839 (c)	0.214
TlI and Tl_6I_8	0.044	0.016 (c)	0.00407

SUMMARY

The iodides of iron, copper, silver, and thallium have been studied by the solubility method at 6°C., using toluene and benzene as solvents. Ferric iodide, cupric iodide, and silver triiodide have been found not to exist at this temperature. Thallium forms two higher iodides, Tl_6I_8 and TlI_3. Their dissociation pressures at 6°C. have been calculated from the solubility results.

REFERENCES

(1) Abegg and Maitland: Z. anorg. Chem. **49**, 341 (1906).
(2) Foote and Bradley: J. Phys. Chem. **36**, 673 (1932).

---

[2] By interpolation of the data in the *International Critical Tables.*

(3) Foote, Bradley, and Fleischer: J. Phys. Chem. 37, 21 (1933).
(4) Jackson and Derby: Am. Chem. J. 24, 16 (1900).
(5) Jörgensen: J. prakt. Chem. 2, 347 (1870).
(6) Kremann and Borjanovics: Monatsh. 36, 923 (1915).
(7) Mellor: *Comprehensive Treatise on Theoretical and Inorganic Chemistry*, Vol V, p. 460. Longmans, Green and Company, London (1924).
(8) Schmidt: Z. anorg. Chem. 9, 432 (1895).
(9) Walker and Dover: J. Chem. Soc. 87, 1584 (1905).

THE COEFFICIENT OF THIXOTROPY OF SUSPENSIONS OF CARBON BLACK IN MINERAL OIL

J. E. ARNOLD AND C. F. GOODEVE

The Sir William Ramsay and Ralph Forster Laboratories of Chemistry, University College, London, England

Received February 6, 1939

I. INTRODUCTION

It is well known that certain classes of fluids do not obey the ordinary Newtonian laws of flow in that their viscosity is dependent on the rate of shear. Fluids possessing such non-Newtonian viscosity at constant temperature may be divided into three main classes: (*a*) those showing a reversible *decrease* of viscosity with increasing rate of shear, a phenomenon which has been called "thixotropy" by Freundlich (1); (*b*) those showing a reversible *increase* of viscosity with increasing rate of shear; and (*c*) those showing irreversible viscosity changes. Colloidal dispersions commonly show non-Newtonian behavior and especially that of type *a*. Extreme cases of thixotropy are those in which a more or less rigid gel is made fluid by mechanical agitation and again sets to a gel on standing.

Goodeve and Whitfield (4) among others (5, 8, 10) have recently shown that if a thixotropic fluid is subjected to a uniform and steady shear rate, σ, the apparent viscosity, η, generally follows the empirical equation

$$\eta = \eta_0 + \frac{\theta}{\sigma} = \frac{F_T}{\sigma} \tag{1}$$

where η_0 and θ are constants and F_T is the force per unit area. If the apparent viscosity is plotted against the reciprocal rate of shear, $1/\sigma$, a straight line is obtained, the slope of which, θ, is called (4) the "coefficient of thixotropy." As deviations from this equation are sometimes found to occur at low shear rates, the values of the coefficient are taken from the "limiting slope of the apparent viscosity–reciprocal shear rate curve as the shear rate approaches a high value." A critical examination (2) of the application of equation 1 has shown that the two terms on the right represent independent parts of the apparent viscosity,—a Newtonian and a thixotropic part. η_0 has been called (4) the "residual viscosity."

The object of the present work was to investigate the effect of concentration of dispersed phase, temperature, and degree of dispersion on the coefficient of thixotropy of a simple colloidal suspension (carbon black in non-polar paraffin), using a new form of apparatus.

II. DESCRIPTION OF THE THIXOVISCOMETER

Any type of viscometer in which the sample is subjected to a uniform and continuous shear, the rate of which may be conveniently altered over a wide range, may be used to measure thixotropy. A new type of instrument has been developed fulfilling these requirements and has been called a "thixoviscometer." This has been used for the present work. A subsequent model, differing in some details, has been described in a recent paper (3), to which the reader is referred for a critical examination of the design.

The instrument is shown in figure 1. A heavy triangular base X, to which is bolted at right angles a length of T-section casting, Y, forms the framework of the apparatus. A gramophone motor R, of the synchronous type, operating on 50-cycle A.C. mains, is mounted on the casting Y as shown and is capable of being swung out sideways to facilitate the interchange of gear wheels on the motor spindle. The whole motor unit may be locked in position by the thumb screw L. A hollow aluminum cone B, of semi-angle 22.5°, is attached coaxially at its base to a spindle, which is set in ball bearings mounted in a casting, C, bolted to Y. An accurately cut gear wheel G is placed on the lower end of the spindle and this engages with the gear system operated by the motor. It is thus possible, using a range of different gear wheels and employing either single or double reduction gearing, to rotate the outer cone B at a large number of different speeds.

Suspended coaxially inside the cone B is a solid aluminum conical frustum A of the same angle as B, whose upper and under surfaces are cut away as shown. The dimensions of this frustum are given in figure 2. A thermometer, T, of the Anschütz type is placed inside a hollow brass stem attached coaxially to A, and the whole unit is suspended by a steel wire from the torsion head H so that it hangs inside B. The torsion head may be moved in a horizontal plane in two directions at right angles by means of the screws SS′ in order that the inner cone A may be adjusted until it hangs coaxially with B, the whole instrument, of course, having first been levelled. A mirror M, attached to the thermometer stem and used in conjunction with a lamp and circular scale, is used to measure the deflection of the inner cone resulting from the torque transmitted to it when a liquid is placed in the cone B and the motor switched on. The whole of the shaded part of the apparatus, together with the inner cone, can be moved vertically up or down by means of the screw head V, the position being read on the head scale, *h*, on the tube F.

The length of the suspension wire, W, is adjusted so that, when the head scale reading is zero, the inner cone is just in contact with the inner surface of the outer cone B and a light twisting motion of the fingers applied to the upper surface of the inner cone just fails to move it. On raising the inner cone by screwing up through one small scale division, the same finger motion should just cause the inner cone to rotate. This method of setting the zero position has been found very satisfactory.

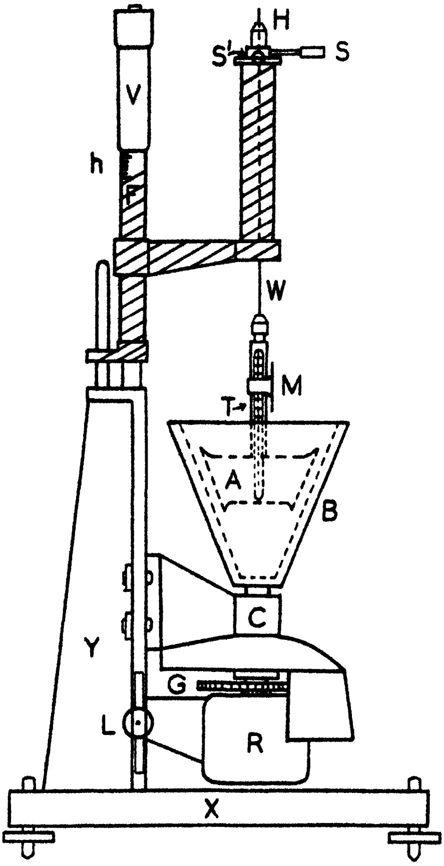

FIG. 1. An instrument for the measurement of thixotropy in absolute units

This instrument possesses sundry advantages over that described by Goodeve and Whitfield (4), among which may be mentioned the quantity of material required for a measurement, the greater accuracy due to the optical system, and the larger range of viscosities measurable, as the cone speeds can be varied and the suspension wires interchanged. The advantages to be obtained by the use of cones rather than cylinders have been pointed out by one of the present authors (3).

III. CALIBRATION OF THIXOVISCOMETER AND CALCULATION OF SHEAR RATE

The instrument is most conveniently calibrated using a Newtonian oil whose viscosity, η, has been accurately determined at a temperature T°C. in a standard viscometer of the Ostwald type. Deflections, α, are obtained for the complete range of head scale readings, h, at constant outer cone speed, Ω, in R.P.M., the zero position of the inner cone being first adjusted as described and the temperature of the oil being maintained constant at T°C. throughout. From these data, a value for a factor P (which contains the torsion constant of the wire, the distance between the conical surfaces, and factors relating to the geometry of the suspended frustum) may be deduced from the relation

$$\eta = \frac{P \cdot \alpha}{\Omega} \tag{2}$$

The apparent viscosity, η, of any non-Newtonian fluid is defined as the viscosity of the Newtonian liquid which would, at the same setting, h, and cone speed, Ω, give the same deflection, α.

The question now arises—is this apparent viscosity as measured equal to a quantity which may be described as the "elemental" viscosity and defined as the ratio of stress to shear rate for an *element* of volume? In other words, is the apparent viscosity a property only of the fluid and independent of the apparatus? The following considerations show that it is.

Let us first consider the case of *coaxial cylinders*. If we take a thin layer of liquid of thickness δL formed by two planes perpendicular to the axis of the cylinders, the moment, δM, on any ring of liquid of radius r is given by

$$\delta M = A \cdot r \cdot F = 2\pi r \cdot \delta L \cdot r \cdot F \tag{3}$$

where A is the surface area of the ring and F the force on the ring per unit area of surface. This equation is, of course, independent of the nature of the liquid. A Newtonian viscosity, η_N, is defined by the equation

$$F_N = \eta_N \cdot \sigma \tag{4}$$

The rate of shear, σ, can be written $r \frac{d\omega}{dr}$, where ω is the angular velocity of the ring of liquid under consideration. Substituting for F in equation 3 we have, for a Newtonian liquid,

$$\frac{\delta M_N}{2\pi \cdot \delta L} \cdot \frac{1}{r^3} \cdot dr = \eta_N \cdot d\omega \tag{5}$$

As δM_N is, in the steady state, the same for a ring of any radius, we may integrate this equation between the limits $r = r_i$, the radius of the inner cylinder, and $r = r_e$, that of the outer:

$$\frac{\delta M_N}{4\pi \cdot \delta L}\left(\frac{1}{r_i^2} - \frac{1}{r_e^2}\right) = \eta_N \omega_e \tag{6}$$

ω_e being the angular velocity of the outer cylinder.

If, on the other hand, we substitute in equation 3 the value of F for a thixotropic fluid, given by equation 1, and integrate the resultant equation between the same limits as above, we obtain

$$\frac{\delta M_T}{4\pi \cdot \delta L}\left(\frac{1}{r_i^2} - \frac{1}{r_e^2}\right) = \eta_0 \omega_e + \theta \ln \frac{r_e}{r_i} \tag{7}$$

This equation describes the behavior, in a coaxial cylinder type of viscometer, of a liquid obeying equation 1 and is essentially the same as that derived by Reiner and Riwlin (7). We thus have two equations (6 and 7), valid respectively for Newtonian and thixotropic fluids under the same experimental conditions, and it is clear that calibration with a Newtonian liquid implies that $\delta M_N = \delta M_T$. We see that, for this to be the case,

$$\eta = \eta_0 + \frac{\theta}{\omega_e} \cdot \ln \frac{r_e}{r_i} \tag{8}$$

i.e., a non-Newtonian liquid will give a scale deflection corresponding to a Newtonian viscosity, η, given numerically by equation 8. If we let d be the separation between the cylinders (i.e., $r_e - r_i$), it may be shown (e.g., using log. tables) that the logarithmic factor is equal to $\dfrac{d}{r_i + \frac{1}{2}d}$ within a maximum error of 0.1 per cent for the greatest value of d/r_i (5/31.6) which was used. Therefore

$$\eta = \eta_0 + \frac{\theta}{\omega_e} \cdot \frac{d}{(r_i + \frac{1}{2}d)} \tag{9}$$

The term $\dfrac{d}{\omega_e(r_i + \frac{1}{2}d)}$ has the dimensions of a reciprocal shear rate, and if the apparent viscosity, η, is plotted against this term, a straight line should be obtained, the slope of which is θ. *Conversely, if we find experimentally that the plot of η against $\dfrac{d}{\omega_e(r_i + \frac{1}{2}d)}$ is a straight line, we know that the viscosity of an element of volume is given by equation 1.*

We may now proceed to a consideration of the *coaxial cone* instrument in a similar manner. It should, however, first be pointed out that the flow of the fluid in such an instrument is not only in the form of coaxial conical laminae, but must also have a vertical component arising from the centrifugal force. This component can contribute no rotational force to the suspended inner cone, but may have a slight effect on the thixotropic viscosity. It has been calculated that, for the order of shear rates used and viscosities measured in this work, the magnitude of this component, even at the greatest value of d used, is quite negligible compared with the horizontal viscous force.

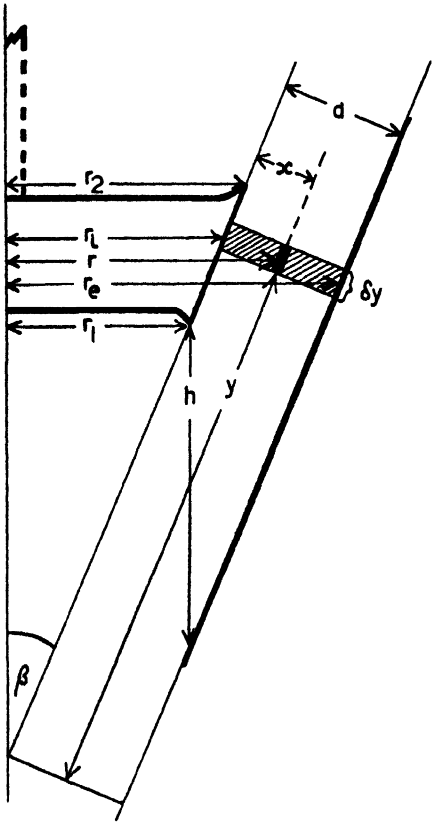

FIG. 2. A section of the inner cone showing its dimensions (all to scale, except that the distance d as shown is relatively four times greater than the largest value used). The actual dimensions were $r_1 = 27.0$ mm., $r_2 = 35.4$ mm., $\beta = 22.5°$.

If, as before, we take a thin layer of liquid of thickness δy (represented in section by the shaded area in figure 2), the moment, δM, on the surface of the "conical ring" of radius r (represented in section by the short thick line) will be given by (*cf.* equation 3)

$$\delta M = 2\pi r \cdot \delta y \cdot r \cdot F \tag{10}$$

(the force F is normal to the plane of the paper). If we now substitute the value of F for a thixotropic fluid, given by equation 1, we obtain

$$\delta M_T = 2\pi r^2 \cdot \delta y \left(\eta_0 \cdot r \cdot \frac{d\omega}{dx} + \theta \right) \tag{11}$$

x being as shown in figure 2. It may be seen from the figure that

$$r = x \cos \beta + y \sin \beta \tag{12}$$

and since y is constant irrespective of the value of x, equation 11 becomes

$$\frac{\delta M_T}{2\pi \cdot \delta y} \cdot \frac{1}{r^3} = \eta_0 \cdot \cos \beta \cdot \frac{d\omega}{dr} + \frac{\theta}{r} \tag{13}$$

Integrating with respect to r between limits r_i and r_e (*cf.* equation 7),

$$\frac{\delta M_T}{4\pi \cdot \delta y} \left(\frac{1}{r_i^2} - \frac{1}{r_e^2} \right) = \eta_0 \cdot \cos \beta \cdot \omega_e + \theta \ln \frac{r_e}{r_i} \tag{14}$$

where r_i and r_e are as shown and ω_e is the angular velocity of the outer cone.

If we now substitute $\delta y = \delta r_i \operatorname{cosec} \beta$, equation 14 may be integrated over the length of the cone to give the total moment,

$$M_T = 4\pi \cdot \cot \beta \int_{r_1}^{r_2} \left[\eta_0 \omega_e + \theta \sec \beta \cdot \ln \frac{r_e}{r_i} \right] \frac{r_i^2 r_e^2}{r_e^2 - r_i^2} \cdot dr_i \tag{15}$$

where r_1 and r_2 are the lower and upper radii, respectively, of the suspended frustum.

Replacing r_e by $(r_i + d')$ (where $d' = d \cos \beta$, d being as shown in figure 2 and itself $= h \sin \beta$) and the logarithmic factor by $\dfrac{d'}{r_i + \dfrac{d'}{2}}$, expanding, and neglecting terms of order $\left(\dfrac{d}{r_i}\right)^3$ and higher, gives

$$M_T = \frac{2\pi \cot \beta}{d'} \int_{r_1}^{r_2} [\eta_0 \omega_e (r_i^3 + \tfrac{3}{2} d' r_i^2 + \tfrac{1}{4} d'^2 r_i) + \theta \sec \beta (d' r_i^2 + d'^2 r_i)]\, dr_i \tag{16}$$

from which we may at once write down the corresponding value of M_N for a Newtonian liquid; thus,

$$M_N = \frac{2\pi \cot \beta}{d'} \int_{r_1}^{r_2} \eta \cdot \omega_e (r_i^3 + \tfrac{3}{2} d' r_i^2 + \tfrac{1}{4} d'^2 r_i)\, dr_i \tag{17}$$

As before, calibration with a Newtonian liquid implies that $M_N = M_T$. Equating 16 and 17 and integrating, gives

$$\eta = \eta_0 + \frac{\theta \sec \beta}{\omega_e} \cdot \frac{[\tfrac{1}{3} d' r_i^3 + \tfrac{1}{2} d'^2 r_i^2]_{r_1}^{r_2}}{[\tfrac{1}{4} r_i^4 + \tfrac{1}{2} d' r_i^3 + \tfrac{1}{8} d'^2 r_i^2]_{r_1}^{r_2}} \tag{18}$$

which may be written

$$\eta = \eta_0 + \theta \cdot \frac{d}{\omega_e \cdot r_m} = \eta_0 + \frac{\theta}{\sigma_m} \tag{19}$$

r_m, which is a function only of d, is obtained by comparing equations 18 and 19 and, when expanded as far as the first power of d, gives

$$r_m = \frac{3}{4}\left(\frac{r_2^4 - r_1^4}{r_2^3 - r_1^3}\right) + \frac{3}{2}d \cos \beta \left\{1 - \frac{3}{4}\frac{(r_2^2 - r_1^2)(r_2^4 - r_1^4)}{(r_2^3 - r_1^3)^2}\right\} \tag{20}$$

This equation may be applied to the coaxial cone instrument for any given set of geometrical dimensions.

For a coaxial cylinder instrument, $\beta = 0°$ and $r_1 = r_2 = r_i$, where r_i is the radius of the inner cylinder. If these values are substituted in equation 20 (the terms in round brackets must first be factorized in order to avoid indeterminates) r_m becomes equal to $(r_i + \frac{1}{2}d)$, which agrees with the result obtained for cylinders in equation 9.

For the present instrument, $\beta = 22.5°$; $r_1 = 27.0$ mm.; $r_2 = 35.4$ mm. and, substituting these values in equation 20, we find

$$r_m = 31.6 + 0.48d \tag{21}$$

The number 31.6 represents a radius of the suspended frustum slightly greater than its mean radius, and if we let $r_0 = 31.6$ we may rewrite equation 19 as

$$\eta = \eta_0 + \frac{\theta}{\omega_e} \cdot \frac{d}{(r_0 + 0.48d)} \tag{22}$$

This final equation corresponds exactly with equation 9, which was deduced for coaxial cylinders. As for the corresponding term in equation 9, the term

$$\frac{d}{\omega_e(r_0 + 0.48d)}$$

has the dimensions of a reciprocal shear rate and, if the apparent viscosity of a non-Newtonian fluid obeying equation 1 is plotted against this term, a straight line will be obtained, having a slope θ. Hence the value for the reciprocal shear rate which has been taken throughout this work is given by

$$\frac{1}{\sigma} = \frac{d}{\omega_e} \cdot \frac{1}{(r_0 + 0.48d)} \tag{23}$$

(In the above treatment, no account has been taken of the difference between the "end effects" with Newtonian and non-Newtonian fluids. This is small (3) when the separation between the cones is small, as in the experimental work described below.)

It is to be concluded from this theoretical treatment that values of the apparent viscosity obtained at small separations with this instrument describe the ratio of stress to shear rate for an element of volume of a fluid obeying equation 1, as is the case for carbon black suspensions. This is confirmed experimentally by the fact that the values of the apparent viscosity and of the coefficient of thixotropy are independent of the method of altering the shear rate (by altering ω or d; see sections V and VI C). A special test of one of the carbon suspensions in an apparatus having cones of semi-angle 11.5° gave the same values as for the present apparatus.

For convenience, equation 23 may be rewritten

$$\frac{1}{\sigma} = \frac{60d}{2\pi\Omega} \cdot \frac{1}{(r_0 + 0.48d)} = \frac{1}{\Omega \cdot Q} \tag{24}$$

where Ω is the speed of the outer cone in revolutions per minute, and $Q = f(d) = f(h)$. Values of Q corresponding to each head scale reading, h, are shown in figure 3.

IV. PREPARATION OF CARBON BLACK SUSPENSIONS

The carbon black used for this work was of the grade used in the manufacture of newspaper printing ink. The suspending medium was "liquid paraffin B.P.", $d_{18°} = 0.88$ g. per cc., viscosity (18°C.) = 2.5 poises. Measurements of its dielectric constant showed that its molecules were effectively non-polar, and spectroscopic examination showed that only a very small amount of cyclic aromatic hydrocarbon was present. Absence of an iodine value showed that it was completely saturated.

In order to standardize conditions, the carbon black was first heated for 2 hr. in an evacuated flask placed in a water bath, thus removing adsorbed water and gases. It was then weighed with the flask still evacuated and the calculated volume of liquid paraffin to make a suspension of the required concentration (by weight) was introduced into the still evacuated flask. After thoroughly shaking, the mixture was transferred to a single roller mill of the type used by paint manufacturers[1] and milled until homogeneous, when it was then ready for use. (See, however, section VI B.)

V. EXPERIMENTAL PROCEDURE

The thixoviscometer was first adjusted as described in section II and the scale reading when the inner cone was at rest in air noted. The carbon black suspension was then placed in the outer cone and the suspended cone lowered into it until the separation between the cones was as small as practicable. It was then possible to alter the rate of shear either (*a*) by rotating the outer cone at a constant speed and varying the separation between the cones by means of the screw head (method 1), or (*b*) by keeping the cone separation constant and small and varying the angular velocity of the outer cone by means of the system of gears (method 2). The available range was 0.08 to 8 radians per second. In either case the outer cone was allowed to rotate until a steady deflection was obtained before commencing to take readings. In the case of the more concentrated suspensions, it was found convenient to leave the instrument running overnight in order to attain the initial steady state before commencing to vary the shear rate. The steady state for subsequent readings was attained in a few minutes. Except where stated otherwise, all readings were taken at 18°C. The apparent viscosities were then calculated using equation 2 and plotted against reciprocal shear rate, calculated from equation 24. For a given suspension, the slopes of the curves obtained by both of the above methods have been found to agree quite well (see table 1).

---

[1] Supplied by S. Smith, Ltd., Manchester, England.

VI. EXPERIMENTAL RESULTS

A. Preliminary experiments (series A)

Mixtures containing 4, 5, 6, 7, and 9 per cent by weight of carbon black were prepared separately, and each was milled to as nearly the same degree as possible by keeping the setting of the mill constant throughout. The results obtained for each of these suspensions show that θ is a marked function of the concentration of carbon black. The values of θ and η_0 are given in table 1.

B. Effect of milling

It is important in standardizing the procedure to study the effect of successive millings on the same suspension, and accordingly a 6 per cent mixture was prepared for this purpose. This mixture is not very homogeneous before milling, since it contains large and irregular aggregates of carbon black. Measurements for such a mixture were not attempted, as it is probable that the non-homogeneity would render them quite irreproducible. The mixture was therefore milled very lightly in the single roller mill until thoroughly mixed, placed in the thixoviscometer, and a series of readings taken. It was then removed, remilled more heavily, and a further series of readings taken. This process was repeated, giving the suspension successively heavier millings, until at a fourth milling the "shearing plate" was hard down upon the roller. A final fifth milling was then given.

The results are shown in figure 3,—the deflection α being plotted against the head scale reading h. The values of the factor P (equation 2) and Q (equation 24) for each head scale reading are also shown. The derived apparent viscosity-reciprocal shear rate curves are shown in figure 4. It is seen from these two figures that the values of the deflection and of the apparent viscosity increase with milling until the third milling, after which they are effectively constant. Also, the coefficient of thixotropy, θ, increases to a constant value. This means that it is possible, with a given milling apparatus, to mill a suspension to constant thixotropy.

During the course of the millings, horizontal ridges were observed in the issuing mixtures,—a phenomenon well known to the printing ink and paint manufacturer. The more thixotropic the mixture, the more pronounced were the ridges.

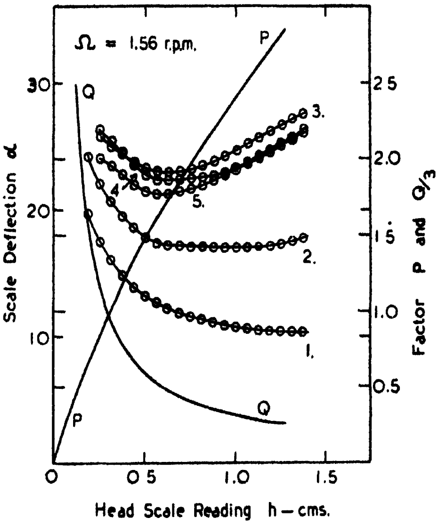

FIG. 3

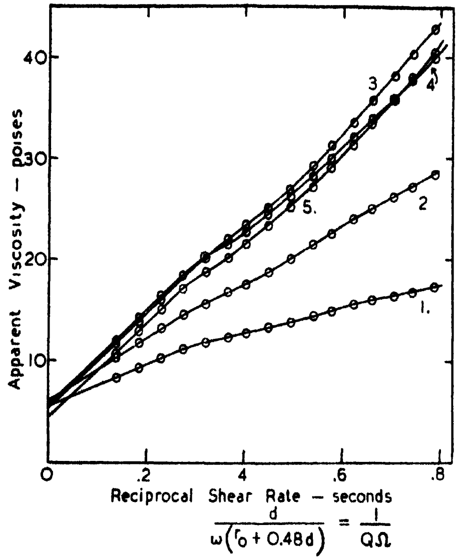

FIG. 4

FIG. 3. Observations on a suspension (6 per cent carbon) subjected to successive millings (curves 1 to 5). The apparent viscosity is obtained by multiplying the deflection α by the value of P for the same head scale reading and dividing by the number of revolutions per minute, Ω. Likewise, the shear rate corresponding to any head scale reading is the product of Q and Ω.

FIG. 4. Results derived from those shown in figure 3

C. *Effect of concentration*

For experiments subsequent to the preliminary ones the following procedure was adopted: A 7 per cent mixture was prepared in the usual manner and milled to maximum thixotropy. Its carbon black content was checked by analysis (repeated washings with petroleum ether and weighing), and its viscosity measured at a number of rates of shear, varied by methods 1 and 2. The required quantity by weight of paraffin was added to reduce the concentration to 6.5 per cent, the mixture milled, its carbon content again checked by analysis, and the measurements re-

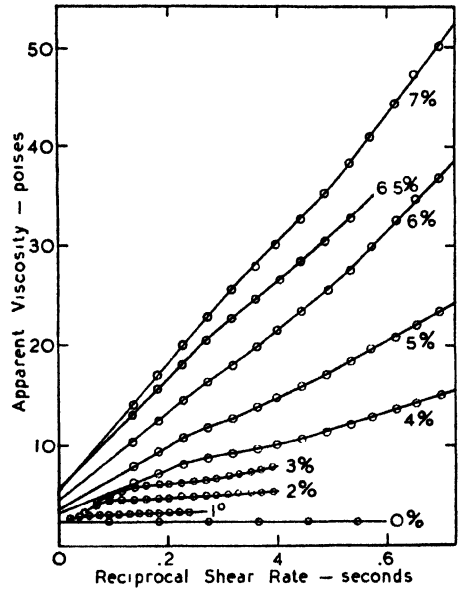

Fig. 5. Results for suspensions of various concentrations

TABLE 1

Values of the residual viscosity and the coefficient of thixotropy for series A, B, and C

CONCENTRATION OF CARBON BLACK	PRELIMINARY SERIES SERIES A		SERIES B				SERIES C	
	Method 1		Method 1		Method 2		Method 1	
	θ	η_0	θ	η_0	θ	η_0	θ	η_0
per cent by weight	*dynes per cm.²*	*poises*	*dynes per cm.²*	*poises*	*dynes per cm.²*	*poises*	*dynes per cm.²*	*poises*
9	163	13.7						
7	70	5.5	63	5.2	65	7.0	62	6.8
6.5			52	5.8	52	5.8		
6	46	4.5	45	4.1	41	5.5	45	4.1
5	21	6.5	30.5	3.5	28	4.9	30.5	3.5
4	18.5	5.2	21	3.1	18.5	4.2	21	3.0
0	$\theta = 0$; $\eta = 2.5$ poises							

peated. The mixture was then diluted successively to various lower concentrations, using the same procedure. The results obtained are shown in figure 5, and the derived values of η_0 and θ are given in table 1 (series B).

A new 7 per cent suspension was prepared 3 months later and the series of measurements described above repeated, using the same procedure. A new sample of the liquid paraffin was used. The values of η_0 and θ for this series (C) are also given in table 1.

It will be seen from this table that, except for the preliminary series (A), the reproducibility of the measurements is good. (In series A the suspensions were not milled to constant thixotropy and their composition was not so accurately controlled.) This shows that it is possible to make accurate quantitative measurements on colloidal systems, provided that the procedure is standardized.

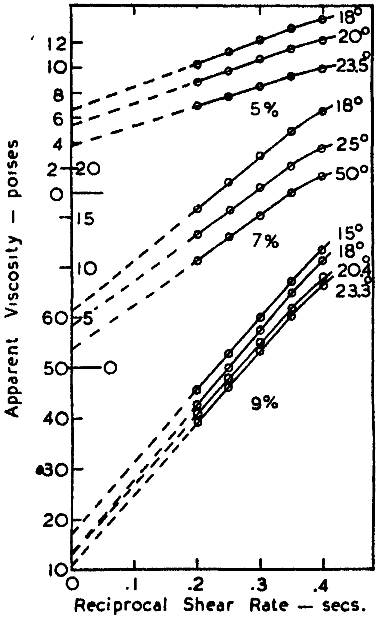

FIG. 6. The effect of temperature

It will be observed from figure 5 that the curves for concentrations less than 4 per cent do not follow equation 1 over an appreciable range of shear rates. No values of θ or η_0 have therefore been calculated. These curves are discussed in section VII F.

D. Effect of temperature

In each of the three series of measurements already described, the temperature of the suspensions was maintained constant at 18°C. For the 5, 7, and 9 per cent suspensions (series A), values of θ have been obtained at other temperatures in order to see whether the coefficient is altered. The outer cone containing the suspension was heated with a Bunsen burner and allowed to stand until a steady temperature was attained. It was necessary only to obtain four or five points to establish the slope of the $\eta-\frac{1}{\sigma}$ curve; the cone separations could be altered and the corresponding scale deflections noted before any appreciable temperature drop occurred (even when the temperature was considerably in excess of that of the room). The curves in figure 6 show the results obtained. It may be seen from the figure that increase in temperature decreases the apparent viscosity by an amount which is practically independent of rate of shear. The *fractional* rates of change of the residual viscosity and of the coefficient of thixotropy with temperature are shown in table 2, together with that of the oil medium. It is seen from the table that the temperature coefficient of the residual viscosity is of the same order of magnitude as that of the oil, whereas for the coefficient of thixotropy the effect of temperature is many times less. The temperature coefficients, being differences, are subject to a higher limit of error than the individual observations.

TABLE 2

Temperature coefficients of the residual viscosity and the coefficient of thixotropy

CONCENTRATION	$\frac{d\eta_0}{\eta_0 dT}$	$\frac{d\theta}{\theta dT}$
per cent		
9	−0.041	−0.0047
7	−0.057	−0.0032
5	−0.11	−0.02
0	−0.074	

VII. DISCUSSION

A. The structure of carbon black suspensions

It is now generally agreed that the phenomenon of thixotropy involves a breaking down and a subsequent reforming of some type of structure. Opinions differ, however, as to the precise nature of this structure. Some investigators favor a non-contact structure held together by long-range forces of the van der Waals' type between the colloidal particles. Others postulate the formation of a "scaffolding" structure, in which the particles are actually in contact. In the case of carbon black there is considerable evidence for the second type. Carbon black particles are plate-like with strong valence forces around the edges. Therefore they have the possibility of building up large structures enmeshing considerable quantities of the suspending medium. Such a structure might be likened in this case to a "house of cards."

McDowell and Usher (6) have found that a 1 per cent carbon black suspension in non-conducting organic solvents conducts the electric current when allowed to stand, but ceases to do so on shaking. The phenomenon is apparently indefinitely reversible (the observations of McDowell and Usher have been qualitatively confirmed by the present authors). The conductivity of such suspensions could only be explained by direct contact between the particles, chain-like structures being formed and thus providing a series of continuous paths from one electrode to the other.

A structure involving direct contact is shown to be extremely likely by measurements made on the bulk density of the carbon black. When carbon black particles were allowed to settle out of the air, they occupied a volume corresponding to a density of 0.075 g. per cubic centimeter. As ordinarily obtained, carbon black has a concentration two to three times this value. In the dry bulk condition each carbon black particle must be touching other particles at a number of points. It would seem, therefore, that in liquid suspensions (density about 1) in which the concentration is 7.5 weight per cent or higher, the particles are forced into touching one another at many points,—there is not room for them to be separated. As the dry particles, even when allowed to settle out of air, are somewhat compressed by gravitational forces, touching of particles is to be expected at concentrations somewhat lower than 7.5 per cent.

B. Effect of milling

The particles of carbon black in a non-milled mixture are in the form of large and irregular aggregates of ultimate plate-like particles. These ultimate particles, the size of which varies to some degree with the grade of carbon black, are extremely small, probably smaller than those of any other known pigment. Recent measurements (9) suggest that the value is about 0.06 μ. As the force breaking up the aggregates in milling decreases as the square of the diameter, it is unlikely that they are ever resolved to ultimate particles. The fact that the suspensions can be milled to constant thixotropy indicates either that the milling is unable to break down the particles any further, or simply that further breakdown does not alter the values of the apparent viscosity and thixotropy.

The increase in viscosity and thixotropy with milling is probably associated with the fact that the actual number of particles able to build up a structure has increased. On a number of occasions suspensions several months old were reëxamined, and it was found that the coefficient of thixotropy had decreased by 10 to 20 per cent. Remilling brought the coefficient back to its former value.

C. The residual viscosity

The residual viscosity is that at infinite shear rate, i.e., when the thixotropic effect is absent. It may be seen from tables 1 and 2 that it is somewhat greater than the viscosity of the medium and its temperature coefficient is of the same order of magnitude. It is well known from hydrodynamical considerations that independent solid particles increase the viscosity by an amount proportional to their volume concentration. The proportionality constant increases with the anisometry of the particles. The viscosity is Newtonian, and the particles act through the dispersion medium. The observed values of the residual viscosity and of the temperature coefficients can be completely accounted for by this hydrodynamical mechanism.

D. The impulse theory of thixotropy

It has recently been shown by one of the authors (2) that the resistance to flow of a non-Newtonian fluid can be divided up into two parts, operating by different mechanisms. The first part is "Newtonian," that is, the force is proportional to the rate of flow, or the viscosity coefficient is constant. The second part is thixotropic, that is, the force is approximately constant, independent of the rate of shear. This thixotropic behavior has been explained by considering the impulses conveyed from a moving layer to a non-moving layer by interference of the colloidal particles. It is seen in section VII A that the particles of carbon black have a marked tendency to link together. When a shearing force is applied to the system, the link between a fast and a slower moving particle will be stretched and a force will be applied to the latter. When a critical point is reached, the link will break. The slower moving particle will thus have experienced a force for a definite period of time, i.e., it will have received an *impulse*. After the link has broken, the faster moving particle will pass on to form a link with another slower moving particle and the whole process will be repeated. It has been shown that the value of each impulse is *inversely proportional* to the shear rate, while the number of impulses is *proportional* to the shear rate. The total force, which is the product of the impulse value and the rate of impulses, is therefore a constant, independent of the shear rate, and the apparent viscosity, which is F/σ, decreases with increasing shear rate. The theory gives a quantitative description of the phenomenon of thixotropy and shows the conditions under which it is to be expected.

E. Relation between coefficient of thixotropy and concentration of carbon black

It is possible to deduce from the impulse theory the relation to be expected between the coefficient of thixotropy and the concentration. The rate of formation of links, or the number of impulses per second, given by *one* particle will be proportional to the concentration of particles in the layer passing over it. The number of particles receiving impulses from the passing layer will also be proportional to the concentration. The total number of impulses per second between the layers is therefore proportional to the square of the concentration.

That this is the case for the system carbon black–non-polar paraffin may be seen from figure 7, in which the logarithm of the coefficient of thixotropy taken from table 1 is plotted against the logarithm of the concentration. It is seen that between concentrations of 4 and 7 per cent, inclusive, the coefficient is proportional to the square of the concentration, but rises more rapidly at higher concentrations. The values at lower concentrations are rather indefinite, and at the higher concentrations agreement is not to be expected, in view of the fact that the particles are crowded very closely together. It would appear, therefore, that the impulse theory in its present state of development can explain the relation between θ and concentration.

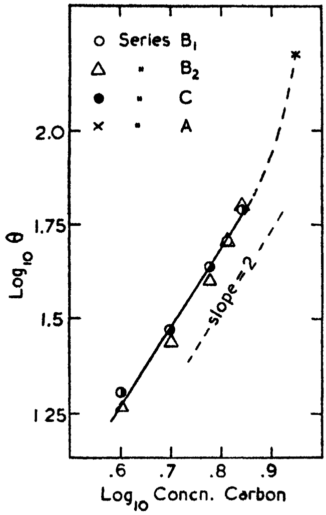

FIG. 7. Showing that the coefficient of thixotropy is proportional to the square of the concentration. (Points for series B_1 and C in most cases coincide.)

F. Low concentrations

If the concentration of the suspended particles is low, a continuous structure of links throughout the fluid (in an unsheared state) will not be possible. It is probable that isolated groups or aggregates of linked particles are formed, the size of which is limited by the low thermal diffusion. Shearing slowly will result first of all in these aggregates being orientated in the usual way and very little breaking of links will occur.

When the shear rate becomes sufficiently high, however, these links will be broken as before, and a decrease in viscosity will result. Such a suspension will therefore behave very nearly as a Newtonian liquid until high shear rates are attained, when the η–$\frac{1}{\sigma}$ curve will drop sharply. This is what happens for concentrations of 3 per cent carbon and less, as may be seen from figure 5. Apparently the 4 per cent curve represents a transition type before normal thixotropy is shown. A slight irregularity appears in all of the curves.

At low concentrations we therefore have two characteristic viscosity values for a given suspension,—the residual viscosity and the limiting viscosity at low shearing stresses. de Waele and Dinnis (11) have observed similar "high and low shearing stress mobilities" in work with cellulose nitrate sols.

G. The temperature coefficient

The low value of the temperature coefficient of thixotropy compared with that of viscosity is to be expected from the "impulse theory." A process in which the links between particles are broken and reformed by a shearing motion does not depend upon thermal energy and is therefore independent of temperature. In the full treatment of the theory (2) it is shown that in a case where the heat of formation is not too large compared with kT, the life of the links will be governed by thermal energy; the viscosity is then Newtonian and strongly temperature-dependent. High values of the link energy lead to high viscosities. In colloidal solutions, however, there are generally fewer links per unit volume and a structure by which energy can be concentrated on each link. In these cases links are broken only by the shear; the viscosity is thixotropic and independent of temperature.

The results for carbon black suspensions described in section VI D indicate that the impulse theory may be applied to this system and that the link energy is great compared with kT. It may be of the order of magnitude of a carbon–carbon bond in graphite.

SUMMARY

An instrument for the measurement of anomalous viscosity has been described, together with its calibration and mode of use. An analysis has been made of the flow of thixotropic fluids, and it is shown that true elemental viscosities may be measured in absolute units. Suspensions of carbon black in liquid paraffin have been studied, and it has been found possible to mill them to give constant and reproducible results. It has been found that over the range 4 to 7 per cent carbon black, the value of the coefficient of thixotropy, θ, increases as the square of the concentration.

Temperature has been shown to have little effect on θ over a fairly wide range but the normal large effect on the residual viscosity. The results have been interpreted in terms of the "impulse theory" of thixotropy.

The authors desire to record their indebtedness to Mr. A. C. Stevenson, of this College, for his valuable advice, and criticism of the mathematical treatment in section III.

REFERENCES

(1) Freundlich, H.: *Thixotropy.* Hermann et Cie, Paris (1935).
(2) Goodeve, C. F.: Trans. Faraday Soc. **35**, 342 (1939).
(3) Goodeve, C. F.: J. Sci. Instruments **16**, 19 (1939).
(4) Goodeve, C. F., and Whitfield, G. W.: Trans. Faraday Soc. **34**, 511 (1938).
(5) Kuhn, W.: Z. physik. Chem. **A161**, 1 (1932).
(6) McDowell, C. M., and Usher, F. L.: Proc. Roy. Soc. (London) **A131**, 573 (1931).
(7) Reiner, M., and Riwlin, R.: Kolloid Z. **43**, 1 (1927).
(8) Rossi, C.: Gazz. chim. ital. **67**, 691, 751 (1937); **68**, 3 (1938).
(9) Sweitzer, C. W.: Official Digest, Federation of Paint and Production Clubs, February, 1935; and Messrs. Binney & Smith & Ashby, Ltd., London.
(10) Szegvari, A.: Z. physik. Chem. **108**, 175 (1924).
(11) de Waele, A., and Dinnis, G.: Physics **7**, 426 (1936).

MIXED COPPER-CHROMIUM OXIDE HYDROGENATION CATALYSTS

V. N. IPATIEFF, B. B. CORSON, AND J. D. KURBATOV

Research Laboratories, Universal Oil Products Company, Riverside, Illinois

Received October 3, 1939

INTRODUCTION

It has been shown (7) that pure copper does not hydrogenate benzene at ordinary pressure at 225°C., but that the presence of certain impurities enables it to do so. It was thirty years ago that the senior author discovered this promoter action in hydrogenation (5, 9). Pure copper is able to hydrogenate benzene only under superatmospheric pressure.

This paper describes a series of coprecipitated copper–chromium oxide catalysts whose activities were evaluated by the hydrogenation of benzene and of isopentene at ordinary and superatmospheric pressures. Under the test conditions both of the pure components—copper and chromium oxide—were inactive, but as chromium oxide was added to copper the activity rose abruptly to a maximum at 5 per cent of oxide, and then fell with continued addition. Incidentally, catalytic activity in these copper–chromium oxide catalysts was accompanied by pyrophoricity, although there is no simple relationship between these two characteristics[1] (2).

We propose to call this composition of maximum activity the *eucoactic* composition. It will be interesting in the future to study the dependence of the eucoactic composition upon the type of unsaturation and upon the operating conditions. Another problem for future study concerns poisoning and heat deactivation as a function of chemical composition.

Adkins (1, 4) and Calingaert (3) have previously described a number of copper–chromium oxide catalysts, with and without calcium, barium, strontium, and magnesium as stabilizers, but they used a much higher concentration of chromium oxide than would be recommended on the basis of this work.

This paper describes for the first time the hydrogenation of isopentene (trimethylethylene) with pure copper. Sabatier (15, 16) was unable to hydrogenate this olefin with copper and made the generalization that only those olefins which contained the $=CH_2$ group could be hydrogenated in the presence of copper. Kistiakowsky (11, 12) has hydrogenated isopentene over copper, but his catalyst was prepared from the commercial granular oxide, which doubtless contained impurities.[2]

Pure copper (containing about 0.001 per cent of nickel) does not hydrogenate isopentene at ordinary pressure in 10 sec. at 75°C., but it does so to the extent of 6 per cent in 14 sec. at 100°C. and 85 per cent in 20 sec. at 225°C. Under 125 atmospheres of hydrogen at 100°C., hydrogenation is complete.

The effect of small amounts of chromium oxide is remarkable. Copper requires a temperature of 225°C. to hydrogenate isopentene to the extent of 55 per cent in 10 sec., whereas copper containing 0.1 per cent of chromium oxide shows the same activity at 75°C. Thus, the presence of 1 mole of chromium oxide in 2500 atoms of copper lowers the temperature requirement 150°C., although chromium oxide alone has no hydrogenating ability, even at 350°C. under 150 atmospheres of hydrogen.

However, even the best of the copper–chromium oxide catalysts is weak when compared with supported nickel (6), which hydrogenates benzene to the extent of 100 per cent in 1 sec. at 50°C. and ordinary pressure, whereas the eucoactic copper–chromium oxide catalyst is completely inactive under these conditions and hydrogenates benzene to the extent of only 16 per cent at 225°C. in 90 sec.

---

[1] In some unpublished work we found very active copper–nickel and copper–cobalt catalysts to be non-pyrophoric, whereas much less active copper–chromium oxide catalysts were very pyrophoric.

[2] Considerable work has been done in the past on the catalytic properties of copper, but the source of the copper was usually the commercial granular oxide, which contains catalytically significant amounts of nickel, iron oxide, alumina, magnesia, silica, and other impurities, and with this complicated system it is impossible to learn anything about the catalytic properties of copper itself.

Mixed copper-chromium oxide catalysts are even more susceptible to activation by traces of nickel than is copper alone. For instance, copper containing not more than 0.001 per cent of nickel does not hydrogenate benzene at ordinary pressure and 225°C. in 90 sec. and the presence of 0.005 per cent of nickel raises the hydrogenation to 4 per cent. On the other hand, the hydrogenating activity of the 95 per cent copper–5 per cent chromium oxide is raised from 16 per cent to 24 per cent by the addition of 0.005 per cent of nickel.

Another example of this amplifier effect is the following: The addition of 0.2 per cent of nickel raises the hydrogenating activity of copper from 0 to 19 (per cent hydrogenation of benzene at ordinary pressure and 225°C. in a contact time of 12 sec.), whereas the same addition of nickel raises the activity of the 95 per cent copper–5 per cent chromium oxide catalyst from 2 to 62.

The promotion of copper by nickel and cobalt, and the poisoning of copper by bismuth, cadmium, lead, mercury, and tin, will be described in a subsequent paper.

In view of the importance of small amounts of impurities and the difficulty of detecting these traces by the usual qualitative tests, a serious doubt arises as to the reliability of much of the data in the field of catalysis.

EXPERIMENTAL

Apparatus and procedure for hydrogenation at atmospheric pressure; calculation

The apparatus was essentially the same as previously described (7), except that the hydrogen-purification train was as follows: copper gauze in a silica tube at 500°C., lead acetate solution, potassium hydroxide solution, anhydrous calcium chloride, ascarite, and activated alumina. After several months' operation the inlet tube of the lead acetate wash bottle had blackened, indicating a trace of hydrogen sulfide in the electrolytic hydrogen.

In the benzene tests the hydrocarbon saturator was thermostated at 25.0°C. ± 0.1°, and the hydrogen–benzene ratio of the gas issuing from the saturator averaged 7. The free space of the reduced catalyst was determined by adding water to the charged tube.

In the hydrogenation of isopentene, the saturator was packed in ice, and the hydrogen–isopentene ratio of the exit gas averaged 3, the vapor pressure of the sample of isopentene being 184 mm. of mercury at 0°C.

Blank experiments made under the conditions of the tests, by passing hydrogen–benzene and hydrogen–isopentene mixtures through a tube filled with glass balls, showed that the apparatus was non-catalytic.

The method of calculating the results was the same as previously described.

Preparation of materials

Benzene. C.P. benzene was purified by repeated washing with concentrated sulfuric acid, followed by washing with caustic soda and water; it was then distilled through a Podbielniak column (reflux ratio, 20), collecting the middle third of the distillate.

Isopentene. Isopentene was prepared by dehydrating dimethylethylcarbinol over activated alumina at 427°C. After separating the water layer, the dehydration product was distilled through a Podbielniak column (reflux ratio, 20) and the middle third of the distillate was collected (b.p., 35–37°C. at 747 mm.; bromine number, 225; n_D^{20}, 1.3848). According to its refractive index the olefin mixture contained about 75 per cent of trimethylethylene and 25 per cent of *as*-methylethylethylene.

Catalysts. The catalysts were prepared by coprecipitating basic copper carbonate and chromium hydroxide from the corresponding nitrates by ammonium carbonate, followed by drying, granulation, decomposition, and reduction. The compositions of the reduced catalysts were checked by analysis. The catalysts containing a known amount of nickel were made by adding the calculated amount of dilute nickel nitrate solution to freshly precipitated copper or copper–chromium catalysts and stirring the mixture to a homogeneous slurry, the mixture being then processed as usual. The reagents were of the highest "reagent" purity; they were examined spectroscopically, as were also the final catalysts.

Reduction of catalysts

Granular 6- to 10-mesh oxide catalyst was charged to a 14-mm. I.D. glass tube and hydrogen was passed for 20 hr. at 225°C. The length of the catalyst bed averaged 35 cm. in the benzene tests and 18 cm. in the isopentene tests; the hydrogen rate was 2000 cc. per hour in the former case and 1000 cc. per hour in the latter. After reduction, the tube was tapped to compact the catalyst bed, the shrinkage averaging 20 per cent. Practically all of the copper oxide was reduced, even in the presence of chromium oxide, as evidenced by the water produced. For example, the catalysts containing 99.9, 68.2, and 11.3 per cent of copper (the remainder being chromium oxide) produced 97, 98, and 96 per cent, respectively, of the theoretical amount of water.

Analysis of liquid catalysate

The composition of the liquid catalysate was estimated from its refractive index. The composition–index curve for isopentane–isopentene was plotted from the following data: weight per cent of isopentane, 0.0, 31.8, 65.2, 100.0; n_D^{20}, 1.3848, 1.3747, 1.3645, 1.3545. The isopentane was prepared by the hydrogenation of the original isopentene with supported nickel (6) at room temperature under 100 atmospheres of hydrogen. The hydrogenated product was stable to a nitrating mixture and showed a bromine number of 0.1.

TABLE 1

Hydrogenation of benzene over copper-chromium oxide catalysts

Conditions of hydrogenation: 225°C.; 90 sec. contact time; ratio of H_2 to C_6H_6 = 7; atmospheric pressure

Cr_2O_3	MOLES OF Cr_2O_3 TO ATOMS OF Cu	HYDROGENATION OF BENZENE
weight per cent		*weight per cent*
0	0	0
0.1	0.0004	3
0.5	0.002	13
1.0	0.004	13
5	0.02	16
10	0.05	14
25	0.1	8
50	0.4	4
75	1.3	2
90	3.7	1
99	41	0
100	∞	0

Hydrogenation of benzene at atmospheric pressure

The data in table 1 show that the most active hydrogenating catalyst of the copper–chromium oxide series, for the experimental conditions used, contains 95 per cent of copper and 5 per cent of chromium oxide.

The pyrophoric characteristics of the used catalysts ran roughly parallel to their activities, the first one (table 1) being non-pyrophoric, the next one pyrophoric, the next three very pyrophoric, the next three less pyrophoric, and the last four non-pyrophoric.

The colors of the used catalysts, given in the order in which they occur in table 1, were S, S–B, B, B, Bl–B, Bl–B, Bl–B, Bl–B, Bl, G, G, and G (S, B, Bl, and G denoting salmon, brown, black, and green, respectively).

In one experiment with pure copper (0.001 per cent of nickel), hydrogen and benzene were passed simultaneously over the granulated oxide at 225°C. It was thought that the reduced copper might be sufficiently active *in statu nascendi* to hydrogenate benzene, but this was not so. The hydrocarbon catalysate was unchanged benzene (n_D^{20}, 1.5014).

Promoting effect of nickel on copper and copper–chromium oxide catalysts

The data in table 2 illustrate the promoting effect of nickel on copper and copper–chromium oxide catalysts, as measured by their ability to hydrogenate benzene.

TABLE 2

Promoting effect of nickel on copper and copper–chromium oxide catalysts

Conditions of hydrogenation: 225°C.; ratio of H_2 to C_6H_6 = 7; atmospheric pressure

Cr_2O_3	Ni	HYDROGENATION OF BENZENE	CONTACT TIME
weight per cent	*weight per cent*	*weight per cent*	*seconds*
0	0.001	0	90
0	0.005	4	90
5	0.001	16	90
5	0.005	24	90
0	0.2	19	12
5	0.001	2	12
5	0.2	62	12

TABLE 3

Hydrogenation of isopentene over copper–chromium oxide catalysts

Conditions of hydrogenation: 75°C.; 10 sec. contact time; ratio of H_2 to C_5H_{10} = 3; atmospheric pressure

Cr_2O_3	HYDROGENATION OF ISOPENTENE	Cr_2O_3	HYDROGENATION OF ISOPENTENE
weight per cent	*weight per cent*	*weight per cent*	*weight per cent*
0	0	25	85
0.05	46	50	66
0.1	51	75	40
1.0	79	100	0
2.5	96		

Hydrogenation of isopentene at atmospheric pressure

The data in table 3 were obtained with copper–chromium oxide catalysts which contained about 0.003 per cent of nickel, and experiments were not made with catalysts containing 0.001 per cent of nickel, as was done in the case of benzene.

A preliminary survey showed that it was impossible to differentiate between these catalysts at 100°C. and contact times which were practical for the apparatus. At this temperature all the catalysts in the series, except pure copper and pure chromium oxide, were about equally active, as shown by the following data: per cent chromium oxide in catalyst, 0, 0.05, 0.1, 1, 2.5, 25, 50, 75, 100; per cent hydrogenation of isopentene, 6, 98, 90, 98, 100, 100, 98, 100, 0; contact time in seconds at 100°C., 14, 12, 9, 17, 7, 15, 8, 20, 13.

Effect of temperature

An exploratory run was made at ordinary pressure on the effect of temperature. At the conclusion of the run the temperature was brought back to the original value and the activity of the catalyst was found to be unchanged. In a contact time of 90 sec. the 95 per cent copper–5 per cent chromium oxide mixture hydrogenated benzene to the extent of 16, 9, 2, and 0 per cent at 225°, 200°, 175°, and 150°C., respectively.

Hydrogenation of ethylene at atmospheric pressure

An attempt was made to evaluate the copper–chromium oxide series of catalysts by the hydrogenation of ethylene at 25°C. and ordinary pressure, but the results were erratic. The catalysts were probably deactivated by oxygen (14).

Inactivity of pressure-reduced copper

Copper which had been precipitated by hydrogen under pressure (8, 10) was unable to hydrogenate ethylene in 70 sec. at 225°C. and ordinary pressure with a hydrogen–ethylene ratio of 5.5, whereas copper prepared from the basic carbonate hydrogenated ethylene completely under these conditions, and also in 26 sec. at 100°C.

Superatmospheric hydrogenation of benzene

The apparatus was an 850-cc. rotating Ipatieff bomb which was equipped with a glass liner. The charge was 50 cc. of benzene, 20 g. of reduced catalyst, and 100 atmospheres of hydrogen. The time of rotation was 12 hr. Blank runs made in the absence of catalyst showed that the bomb was non-catalytic under the conditions of the experiments.

Although it was impossible to differentiate between these catalysts at 350°C., it was possible to do so at lower temperatures, and the peak of the activity curve was in the vicinity of 5 to 25 per cent of chromium oxide (table 4). Perhaps the eucoactic composition was displaced at superatmospheric pressure toward higher chromium oxide concentrations, but the data are incomplete on this point.

Superatmospheric hydrogenation of isopentene and ethylene

Isopentene was completely hydrogenated by pure copper in 12 hr. at 100°C. under 125 atmospheres of hydrogen, and by all the mixed copper–

chromium oxide catalysts, including the 1 per cent copper–99 per cent chromium oxide mixture, but it was not hydrogenated by chromium oxide itself at 100°C., or even at 350°C., in 12 hr.

TABLE 4

Superatmospheric hydrogenation of benzene at different temperatures

Cr_2O_3	HYDROGENATION AT DIFFERENT TEMPERATURES			
	150°C.	200°C.	250°C.	350°C.
weight per cent	*weight per cent*	*weight per cent*	*weight per cent*	*weight per cent*
0	1	0	19	90
0.1	2	26	81	100
5	7	39	100	100
25	6	30	90	99
50	6	17	83	99
75	1	17	86	100
90	0	5	38	100
99	0	0	0	2
100	0	0	0	0

TABLE 5

Deactivation of reduced copper by heat

Conditions of hydrogenation test: 225°C.; ratio of H_2 to C_6H_6 = 7; atmospheric pressure

DEACTIVATION TEMPERATURE	CONTACT TIME	ACTIVITY*	ACTIVITY EXTRAPOLATED TO 150 SEC. CONTACT TIME
°C.	*seconds*		
225	52	20	54
	104	36	
	125	46	
400	53	12	36
	103	23	
	126	32	
500	58	0	2
	110	2	
	135	2	

* Per cent hydrogenation of benzene under the conditions of the test.

Pure copper prepared from the basic carbonate hydrogenated ethylene to the extent of 100 per cent in less than half an hour at 200°C., starting with an initial ethylene partial pressure at room temperature of 35 atmospheres and 65 atmospheres of hydrogen, but pure copper, prepared by reduction of copper ions under pressure, hydrogenated ethylene to the extent of only 20 per cent in 12 hr. at 200°C.

Heat-deactivation of copper catalyst

A 200.4-g. sample of granular (6- to 10-mesh) copper oxide (Kahlbaum-Schering, für Analyse), which contained 0.1 per cent of nickel and smaller amounts of other impurities, was reduced at 225°C. for 60 hr. with a hydrogen rate of 2000 cc. per hour, 44.5 g. of water being produced. The reduced catalyst was cooled in hydrogen and divided into three samples which were treated as follows:

The first sample was heated 15 hr. in hydrogen at 225°C. and then tested with benzene at 225°C. in the usual manner. The second sample was heated 10 hr. in hydrogen at 400°C., cooled in hydrogen during 5 hr. to 225°C., and tested with benzene at 225°C. The third sample was heated 10 hr. in hydrogen at 500°C., cooled in hydrogen during 5 hr. to 225°C., and tested with benzene at 225°C. The only variable was the temperature at which the reduced catalyst was heated just before being tested for hydrogenating activity. The activities (per cent hydrogenations of benzene) are given in table 5. The relative activities for the catalysts treated at 225°C., 400°C., and 500°C. are 27, 18, and 1, respectively.

SUMMARY

1. The hydrogenating activities of copper–chromium oxide catalysts have been evaluated by the hydrogenation of benzene and isopentene at atmospheric and superatmospheric pressures.

2. As chromium oxide is added to copper, the hydrogenating activity of the mixture rises abruptly to a maximum at about 5 per cent of chromium oxide, and then falls with continued addition of chromium oxide.

3. This optimum concentration has been named the *eucoactic* concentration.

4. Copper is very susceptible to activation by traces of nickel, and the 95 per cent copper–5 per cent chromium oxide is even more susceptible.

The authors express their thanks to Mr. W. J. Cerveny for much of the experimental work, and to Dr. W. C. Pierce of the University of Chicago for spectroscopic analyses.

REFERENCES

(1) ADKINS AND CONNOR: J. Am. Chem. Soc. **53**, 1091 (1931).
(2) ARMSTRONG AND HILDITCH: Proc. Roy. Soc. (London) **99**, 490 (1921).
(3) CALINGAERT AND EDGAR: Ind. Eng. Chem. **26**, 878 (1934).
(4) CONNOR, FALKERS, AND ADKINS: J. Am. Chem. Soc. **54**, 1138 (1932).
(5) IPATIEFF: Ber. **42**, 2090 (1909).
(6) IPATIEFF AND CORSON: Ind. Eng. Chem. **30**, 1039 (1938).
(7) IPATIEFF, CORSON, AND KURBATOV: J. Phys. Chem. **43**, 589 (1939).
(8) IPATIEFF AND IPATIEFF: Ber. **62**, 386 (1929).

(9) Ipatieff and Matov: J. Russ. Phys. Chem. Soc. **44**, 1695 (1912); Ber. **45**, 3205 (1912).
(10) Ipatieff and Werchowsky: Ber. **42**, 2078 (1909).
(11) Kistiakowsky, Romeyn, Ruhoff, Smith, and Vaughan: J. Am. Chem. Soc. **57**, 65 (1935).
(12) Kistiakowsky, Ruhoff, Smith, and Vaughan: J. Am. Chem. Soc. **58**, 137 (1936).
(13) Pease and Purdum: J. Am. Chem. Soc. **47**, 1435 (1925).
(14) Russell and Ghering: J. Am. Chem. Soc. **57**, 2544 (1935).
(15) Sabatier: 50th Congr. soc. sav., J. offic., p. 3628, April 11, 1912.
(16) Sabatier and Senderens: Compt. rend. **134**, 1127 (1902).

NEW BOOKS

Theoretical Electrochemistry. By N. C. McKenna. 469 pp. New York: D. Van Nostrand Company, Inc., 1939. Price: $5.50.

This is a modern, quite up-to-date text on theoretical electrochemistry which is well balanced with regard to theory, experimental technique, and results. The author distinguishes between irreversible and reversible (or free energy) properties of solutions of electrolytes and he discusses these on the basis of the theory of Debye and Hückel and its more recent extensions. Due credit is given to the work of Onsager, MacInnes, and many other workers. The second part of the book is devoted to the thermodynamics of reversible cells and the theories of the galvanic cell. A chapter on "irreversible electrode processes" and one on "ions in solution" are included, in which recent views on these important subjects have been given in a satisfactory way. The author states in the preface that the book is not comprehensive. However, a more detailed discussion of electrolytes in non-aqueous solution would have been desirable. Also a discussion of membrane potentials in general and of the glass electrode in particular might have been anticipated in a book of this nature.

The first eleven chapters are so good that the monograph could be recommended unreservedly, were it not for the fact that the last three chapters, dealing with ionic equilibria, the hydrolysis of salts, and neutralization and the theory of indicators, are decidedly bad. These chapters are classical in nature, and they give so many details of older work based on the theory of Arrhenius that one wonders why the author has not modernized these topics and condensed them. For example, to write the acid-base equilibrium of an acid salt (equation 561 on page 379) in terms of concentrations of undissociated salts is objectionable. The abscissa of figure 96 (page 399) is incorrect. So is the statement on page 400 that an amino acid shows complete acid and base dissociation at the isoelectric point. Several mistakes are found on page 421. It is a serious omission that the glass electrode is not mentioned on page 426 for the measurement of the pH of ferric salts. The calculation of the percentage dissociation of rosolic acid at various pH values is incorrect. On page 437 it is stated that the pH at which the indicator is half dissociated is called the titration exponent; this is never done. The discussion on page 439 of the change of pH close to the end point is confusing and very bad. Also incorrect is the statement on page 431 of the behavior of an acidified solution of the sodium salt of *p*-nitrophenol. Probably the author had in mind phenylnitromethane.

The discussions on pages 450 and 451 also need drastic revision. It is hoped that the author will revise the three last chapters considerably when a new edition is prepared.

I. M. KOLTHOFF.

Volumetric and Phase Behavior of Hydrocarbons. By BRUCE H. SAGE AND WILLIAM N. LACEY. 294 pp.; 188 fig. Stanford University, California: Stanford University Press, 1939. Price: $5.00.

Much of the data presented in this volume is the well-known work of the authors carried out as "Research Project 37" of the American Petroleum Institute.

The authors state, "It is the purpose of this volume to set out for consideration the fundamental principles and some of the facts relating to that type of hydrocarbon behavior which does not involve chemical reactions or changes in the molecular species present. The treatment is also limited to cases characterized by the absence of solid phases. The portion of the subject thus chosen for discussion finds application in the process of petroleum and natural gas production and transportation, of natural gasoline manufacture, and of certain parts of petroleum refining." The subject has been developed "in a logical manner, without assuming that the reader has made intensive studies of physical chemistry."

All who are familiar with the compilations of physical data used by petroleum engineers will appreciate the value of the work of Sage and Lacey. As the authors have noted, "The quantitative application of scientific principles in petroleum technology has been retarded by the surprising scarcity of determinations of the necessary constants." Much of the physical data now used by petroleum engineers has been determined since 1920, much of it since 1930. The work presented by Sage and Lacey, largely their own, is of the greatest value to petroleum engineers.

The use of liquid propane in refinery operations, the separation and recovery of low-boiling hydrocarbons from gas mixtures, and the recovery of so-called "distillate" by retrograde condensation from high-pressure natural gas, in the field, need only be mentioned to indicate the very practical value and interest of the work of Sage and Lacey. The volume contains abundant data, shown mostly by diagrams or figures, of the phase behavior of low-boiling hydrocarbon systems. The phase behavior of such systems, indicated by the well-known volume of Kuenen, *Verdampfung und Verflüssigung von Gemischen* (1906), has been experimentally determined for many gas-liquid systems by Sage and Lacey. This little volume is a gem of clear exposition and explanation.

B. T. BROOKS.

Quantitative Biological Spectroscopy. By ELMER S. MILLER. 21.3 x 27.3 cm.; 213 pp.; 121 fig. Minneapolis: Burgess Publishing Company, 1939. Price: $3.50.

This is a preliminary, mimeographed edition of a text used by the author in a course dealing with the applications of spectroscopy to biological problems, which is given in the Department of Botany to advanced students in the biological sciences. The author is well known for his outstanding work in the measurement of absorption coefficients of compounds having biological importance and in the application of photoelectric spectrophotometry to quantitative chemical analysis of such materials.

The unique and most useful feature of this book, from the viewpoint of the physical chemist, is the detailed discussion of spectroscopic apparatus, particularly that used in photoelectric spectrophotometry. The characteristics of specific types of equipment on the market are discussed and procedures and precautions in the use of the apparatus are made clear, so that anyone intending to work in this field will know exactly what equipment he can get, how to set it up, and how to use it.

Even those familiar with the technique will find it profitable to study the author's very practical recommendations.

In addition to the technical information, there are several chapters showing how spectroscopy has become an important tool in the study of vitamins, cytochrome, hemoglobin, and lipids. Of especial interest is the summary of recent researches on lipid metabolism by the author and his associates. Another noteworthy chapter is that dealing with the quantitative spectroscopic analysis of binary and ternary systems. The discussion is illustrated by data taken from the author's publications.

However, this book shows too plainly that it was finished in a hurry. Mistakes in spelling and grammar are too common. An occasional definition or explanation is not exact or complete enough to be of value to one who is not already familiar with the subject. These faults will no doubt be corrected in the next edition.

JOSEPH VALASEK.

The Raman Effect. By JAMES H. HIBBEN. 6 x 9 in.; 544 pp. New York: Reinhold Publishing Corporation, 1939. Price: $11.00.

The remarkable development in the study of Raman spectra of all types of substances since the discovery of this phenomenon by Sir V. Raman in 1928 can best be seen in the tremendous growth of the literature of this subject. The present volume gives one thousand nine hundred and eighty-seven references, compiled in two bibliographies which are arranged alphabetically. The second or supplementary bibliography (two hundred and thirty papers) is not used in the text proper, but it brings the subject up to date. It is evident that the routine labor of systematizing and compiling this scientific material is a major effort, requiring great accuracy and perseverance. The author is to be congratulated on the execution of such a time-consuming task. By the same token it is also obvious that the scientific community owes Dr. Hibben a vote of thanks for having undertaken this arduous labor. Workers in the special field of Raman spectrography owe a particular debt to the author, since the present volume is the only comprehensive compilation in English of this interesting field of research.

The volume is divided into three parts. Part I gives a general discussion of the Raman effect in practice and theory and includes six chapters dealing with such topics as the nature of the Raman effect, the experimental methods used, the definition of terms employed, vibration and rotation of polyatomic molecules, the general theory of infrared absorption spectra and the Raman effect, the determination of Raman frequencies and factors which modify the vibrational and rotational spectra. The material is presented in a rather descriptive, narrative, non-mathematical style and should help the student to understand other more theoretical treatments. For the sake of simplification the author has employed a novel method of presentation by eliminating (in chapters IV to VI) most of the names of the scientific workers responsible for the development of the subject.

Parts II and III are a compilation of the existing information on this subject of Raman lines, divided into organic compounds (Part II, Chapters 7 to 19) and inorganic compounds (Part III, Chapters 20 to 29). The material is arranged very systematically, and ninety-three tables and seventy-two figures help greatly in the presentation of the large amount of information contained in the book. It will be evident to anyone reading this treatise that a still much larger effort is before us for further improving and completing our knowledge of molecular structure by the use of this interesting phenomenon. In spite of the large number of scientific publications enumerated in the present volume, a great deal of work still lies ahead. In this sense the book contains hundreds of suggestions for further research.

The book does not possess the usual type of index. Besides the two bibliographies mentioned there is an "index of compounds," which gives a complete tabulation of Raman work up to the present time. A further section called "numerical index" is a helpful aid for cross reference. The printing of the volume is done with care and the tables are neatly arranged, but the draftsmanship of the figures could be better. Scientific libraries, physicists, and chemists interested in the general field of molecular structure will need this compendium in their work.

GEO. GLOCKLER.

Molecular Spectra and Molecule Structure. I. Diatomic Molecules. By GERHARD HERZBERG. 6 x 9 in.; xviii + 592 pp. New York: Prentice-Hall, Inc., 1939. Price: $6.50.

This book is the English translation of the German version; according to the author a number of additions have been made and in several places the text has been improved to cover more recent developments. The table containing the molecular constants for the normal state of diatomic molecules has been revised to date (July, 1939).

All workers in this country interested in band spectroscopy and the structure of molecules will welcome this volume as presenting this intricate field of physics and chemistry in their own language, with a clarity of style and a forceful directness which cannot be surpassed. Similar books have been written, but the present volume portrays the subject with just the right balance between theory and experimental material to make its perusal a distinct pleasure. Every chemist and physicist and all students interested in these branches of physical science will want to own this work. Beginning students will have to read appropriate texts in wave mechanics in order to follow the presentation, for the author has wisely refrained from extraneous mathematical derivations which would only serve to confuse the issues involved in any given discussion. After a short résumé of the elements of atomic structure in the first chapter, the remaining chapters (2 to 8) cover the following topics: Observed molecular spectra and their representation by empirical formulae; rotation and vibration of diatomic molecules, interpretation of infrared and Raman spectra; general discussion of electronic states and electronic transitions and their finer details; building-up principle, electron configurations, and valence; continuous and diffuse molecular spectra, dissociation and predissociation and, finally, examples, results, and applications. The last three chapters (6 to 8) will be of special interest to the chemist, for there is presented the modern picture of valency theory, at least in its beginnings, and several applications to other chemical topics, such as free radicals and photochemistry, are touched upon. However, the important function of this review is perhaps to stress the fact that the chemist must know some band spectroscopy if he would understand the modern approach to his own science.

The book contains thirty-eight tables and one hundred and eighty-one illustrations. They really are works of art. The draftmanship is superb. The whole makeup of the volume is most excellent. The reviewer considers it a privilege to have had the opportunity of reading this book.

GEO. GLOCKLER.

27. AUG. 194
LIBRAR

THE QUATERNARY SYSTEM ACETIC ACID-CHLOROFORM-ACETONE-WATER AT 25°C.

A. V. BRANCKER, T. G. HUNTER, AND A. W. NASH

Department of Oil Engineering and Refining, The University of Birmingham, Birmingham, England

Received July 12, 1939

Equilibrium in liquid mixtures has been studied for a large number of ternary systems, but no detailed study of a quaternary system such as will be considered in this paper has, so far as we are aware, been reported.

The choice of liquids to be used was based on the ease of purification and analysis, the particular system studied being composed of acetone, acetic acid, chloroform, and water at a temperature of 25°C.

PURIFICATION OF THE FOUR COMPONENTS

Pure glacial acetic acid crystals were prepared by equilibrium melting, and the resultant acid was freed from water by distillation with the addition of ethylene dichloride. The ethylene dichloride was found to be stable in boiling acetic acid solution, no chlorine derivatives being formed.

Analar acetone was dried over calcium chloride, filtered, and fractionated. The fraction distilling at 56.0°C. at 760 mm. was employed.

Distilled water was treated with solid barium hydroxide, filtered, and redistilled.

Analar chloroform was fractionated and the fraction boiling at 61.1°C. at 760 mm. was employed.

All solutions were stored in clean dry Winchester bottles, fitted with soda lime tubes and hand pumps for transfer of reagents. Air in the storage bottles was previously displaced by nitrogen.

METHODS OF ANALYSIS

1. Chloroform

A method was developed for the estimation of chloroform, based upon the formation of potassium chloride by treatment with alcoholic potassium hydroxide, the potassium chloride formed being titrated with silver nitrate.

About 5 ml. of chloride-free normal alcoholic potassium hydroxide was weighed in a small stoppered glass tube. A few drops of chloroform were added and the reweighed tube dropped into a flask containing 40 to 50 ml. of normal alcoholic potassium hydroxide.

The solution was then refluxed under two double-surface condensers in series, down which trickled alcoholic potassium hydroxide. The reaction was found to be complete within 15 min. The solution was then cooled to 0°C., filtered, and washed with alcohol previously saturated with potassium chlorate at room temperature. The potassium chloride was dissolved in chloride-free water, the solution made up to 100 ml., and aliquot parts taken for titration with silver nitrate.

2. *Acetone*

For the estimation of this component a modification of Messingers' (1) method was used. It is based on the formation of iodoform by the addition of iodine to an alkaline solution of acetone. The excess iodine is liberated by acid, and titrated with sodium thiosulfate.

About 10 ml. of water was weighed in a glass-stoppered bottle, ten drops of acetone were added, and the mixture was reweighed and made up to 200 ml. A 25-ml. portion of this acetone solution was then pipetted into a conical flask containing 25 ml. of normal caustic soda. Twenty-five milliliters of decinormal iodine was run in slowly, the liquid in the flask being gently agitated.

The flask was stoppered and allowed to stand at room temperature until the yellow iodoform settled out, and the supernatant liquid was perfectly clear. The clear solution was then neutralized with 2 *N* sulfuric acid. To avoid using excess acid, this was run in until the solution was just brown due to liberated iodine. The brown color was then discharged with decinormal sodium thiosulfate. A few more drops of acid were added, which again darkened the solution, and the titration was continued. Proceeding in this way it was possible to restrict the excess acid to not more than one drop. Towards the end of the titration starch indicator was added, the end point being sharp. Inconsistent results were obtained only when insufficient time had been allowed for the complete formation of the iodoform. By waiting until the iodoform settled, leaving the supernatant liquid perfectly clear, complete iodoform formation was assured.

3. *Acetic acid*

The acetic acid was estimated by titration with barium hydroxide free from carbon dioxide. In view of the low concentration of acetic acid encountered in certain parts of the work it was found essential to employ an indicator, the pH range of which included the pH of the reaction, found by calculation and electrometric titration to be about 7.5 for the concentrations used. From a comparison of determined and calculated titration curves it was clear that a suitable indicator should have a pH range from 6 to 8.

Titrations were then made using different indicators of this range. The indicator under test was added to 10 ml. of a buffer solution of pH = 7.5 and titration made to this color standard. By this method bromothymol blue was found to be the most suitable indicator for the titration.

DETERMINATION OF TERNARY CURVES AND TIE LINES

Known weights of chloroform and acetone were run into a small glass bottle which was then attached to a buret containing water and immersed in a thermostat at 25°C. Water was run into the bottle until the solution became slightly opalescent. The solution was then allowed to attain the temperature of the thermostat, and the addition of water was continued until turbid.

TABLE 1

Ternary isotherm data for the system acetone–chloroform–water at 25°C.

ACETONE	CHLOROFORM	WATER
weight per cent	*weight per cent*	*weight per cent*
	99.2	0.2
18.8	80.0	1.2
28.5	70.0	1.5
42.3	55.2	2.5
52.0	43.4	4.6
57.3	35.4	7.3
60.5	28.5	11.0
60.0	22.0	18.0
59.2	17.8	23.0
58.5	14.5	27.0
56.6	11.0	32.4
55.6	10.0	34.4
54.0	8.6	37.4
53.2	8.0	38.8
51.6	7.0	41.4
49.0	5.6	45.4
42.6	3.2	54.2
35.5	2.3	62.2
26.0	1.5	72.5
15.5	1.0	83.5
	0.6	99.4

The volume of water added was recorded, the buret temperature read, and the titer in milliliters converted into grams. In this manner one half of the isotherm was obtained. Known weights of acetone and water were then run into a dry bottle and the solution titrated in the same way with chloroform to give the remainder of the isotherm.

TABLE 2

Ternary isotherm data for the system acetic acid–chloroform–water at 25°C.

ACETIC ACID	CHLOROFORM	WATER
weight per cent	*weight per cent*	*weight per cent*
	99.2	0.8
8.7	90.0	1.3
17.8	80.0	2.2
26.0	70.0	4.0
29.0	65.0	6.0
32.1	60.0	7.9
35.0	55.0	10.0
41.1	45.0	14.0
43.5	40.0	16.5
46.0	35.0	19.0
49.7	25.0	25.3
50.6	20.0	29.4
50.0	15.0	35.0
47.6	10.0	42.4
43.6	6.4	50.0
36.5	3.5	60.0
34.6	1.9	63.5
24.9	1.6	73.5
18.8	1.2	80.0
9.2	0.8	90.0
	0.6	99.4

TABLE 3

Ternary tie line data for the system acetic acid–chloroform–water at 25°C.

COMPONENTS	INITIAL MIXTURE	TOP LAYER	BOTTOM LAYER
	weight per cent	*weight per cent*	*weight per cent*
Acetic acid	10.0	17.4	4.1
Chloroform	50.0	1.1	95.0
Water	40.0	81.5	0.9
Acetic acid	23.5	34.1	10.8
Chloroform	40.0	2.6	87.8 *
Water	36.5	63.3	1.4
Acetic acid	34.0	44.5	17.9
Chloroform	35.0	7.0	80.0
Water	31.0	48.5	2.1
Acetic acid	37.0	49.5	22.6
Chloroform	41.0	12.4	74.4
Water	22.0	38.1	3.0

* See table 9.

The equilibrium data for the acetone–chloroform–water system are given in table 1. The data so found agreed closely with those given by Hand (2) for this system.

TABLE 4

Ternary tie line data for the system acetone–chloroform–water at 25°C.

COMPONENTS	INITIAL MIXTURE	TOP LAYER	BOTTOM LAYER
	weight per cent	*weight per cent*	*weight per cent*
Acetone	6.0	3.0	9.0
Chloroform	44.0	1.0	90.0
Water	50.0	96.0	1.0
Acetone	17.0	8.3	23.7
Chloroform	43.0	1.2	75.0
Water	40.0	90.5	1.3
Acetone	24.0	13.5	32.0
Chloroform	38.0	1.5	66.4 *
Water	38.0	85.0	1.6
Acetone	29.0	17.4	38.0
Chloroform	33.0	1.6	60.0
Water	38.0	81.0	2.0
Acetone	34.0	22.1	42.5
Chloroform	33.0	1.8	55.0
Water	33.0	76.1	2.5
Acetone	35.0	25.5	42.6
Chloroform	31.0	1.5	55.0
Water	34.0	73.0	2.4
Acetone	44.0	31.9	50.5
Chloroform	30.0	2.1	45.0
Water	26.0	66.0	4.5
Acetone	50.0	44.5	57.0
Chloroform	20.0	4.5	35.0
Water	30.0	51.0	8.0

* See table 8.

The equilibrium data for the system acetic acid–water–chloroform were determined in an exactly similar way and are given in table 2. This system has been previously studied by Wright (3) and Hand (2), whose results are closely coincident with the present data.

For the determination of tie lines, known quantities of the three liquids acetone–chloroform–water or acetic acid–chloroform–water such as would form two layers were placed in a small glass-stoppered bottle. This bottle was immersed in the thermostat at 25°C. for about 30 min., removed, dried, and placed in an insulated tube at 25°C. The tube was fitted to a shaking machine and agitated for 2 hr. The glass bottle was then reimmersed in the thermostat until both layers when viewed in a cone of light were clear.

Samples for analysis were withdrawn from each layer by means of a glass tube drawn into a very fine capillary and fitted with a rubber teat. The top-layer sample, usually about 0.5 g., was weighed in a small glass-stoppered tube and the whole dropped into water. The resultant solution was made up to a convenient volume, and aliquot parts taken for analysis of acetone and acetic acid.

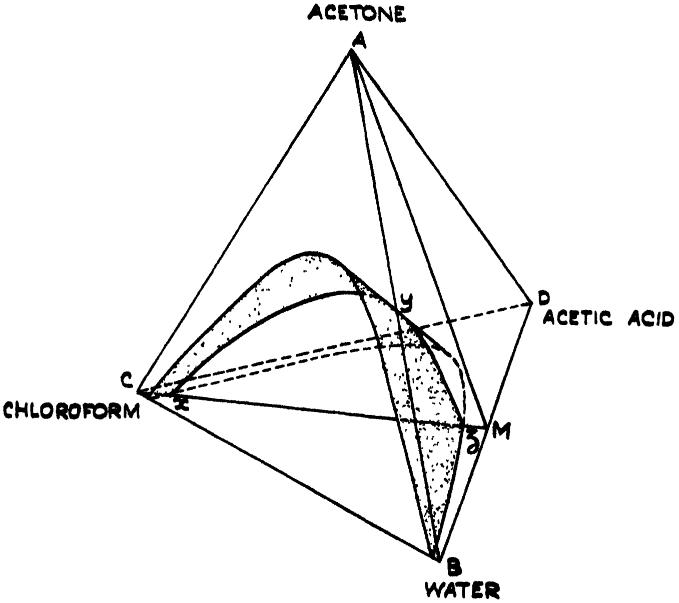

FIG. 1. Schematic representation of the quaternary system by a regular tetrahedron

For chloroform determination in both top and bottom layers the small tube was dropped into alcoholic potash. As samples from the bottom layers contained most of the chloroform, it was necessary to dissolve the bottom layer in acetic acid when analyzing for acetone, and in neutral alcohol when analyzing for acetic acid.

The total weights of the two layers were ascertained, and from these values, together with the concentrations of the three components in each layer as determined by analysis, the total weight of each component in the two-layer system was calculated. If these calculated weights differed by more than ± 4.0 per cent from the weights of the three liquids originally taken, the results were discarded. The average experimental error in the data obtained was ± 0.9 per cent.

Tie line data for the two systems are given in tables 3 and 4.

TABLE 5

Quaternary isotherm data for the system acetone–acetic acid–chloroform–water at 25°C.

ACETONE	CHLOROFORM	MIXTURE: 30 PER CENT ACETIC ACID AND 70 PER CENT WATER
weight per cent	*weight per cent*	*weight per cent*
	98.5	1.5
40.0	56.4	3.6
49.2	43.8	7.0
54.4	32.0	13.6
54.2	26.8	19.0
53.0	23.5	23.5
51.0	21.0	28.0
45.7	16.1	38.2
41.0	13.0	46.0
32.9	8.1	59.0
22.7	4.2	73.1
13.5	2.5	84.0
	1.9	98.1

TABLE 6

Quaternary isotherm data for the system acetone–acetic acid–chloroform–water at 25°C.

ACETONE	CHLOROFORM	MIXTURE: 40 PER CENT ACETIC ACID AND 60 PER CENT WATER
weight per cent	*weight per cent*	*weight per cent*
	98.6	1.4
14.1	83.4	2.5
39.7	54.3	6.0
46.3	43.1	10.6
47.7	36.6	15.7
47.4	31.6	21.0
45.7	27.0	27.3
42.8	22.8	34.4
38.0	18.6	43.4
31.1	13.9	55.0
18.7	7.7	73.6
10.2	6.3	83.5
	4.4	95.6

QUATERNARY EQUILIBRIUM CURVES

In figure 1 a schematic representation of the quaternary system is given in the usual manner by a regular tetrahedron. In all figures in this paper where solid models are illustrated schematic representation has been used,

TABLE 7

Quaternary isotherm data for the system acetone-acetic acid-chloroform-water at 25°C.

ACETONE	CHLOROFORM	MIXTURE: 66.7 PER CENT ACETIC ACID AND 33.3 PER CENT WATER
weight per cent	*weight per cent*	*weight per cent*
	97.4	2.6
4.7	91.9	3.4
16.2	79.8	4.0
26.0	66.4	7.6
31.8	54.7	13.5
31.5	47.9	20.6
29.0	42.5	28.5
23.0	38.4	38.6
14.5	34.2	51.3
6.1	27.9	66.0
	26.5	73.5

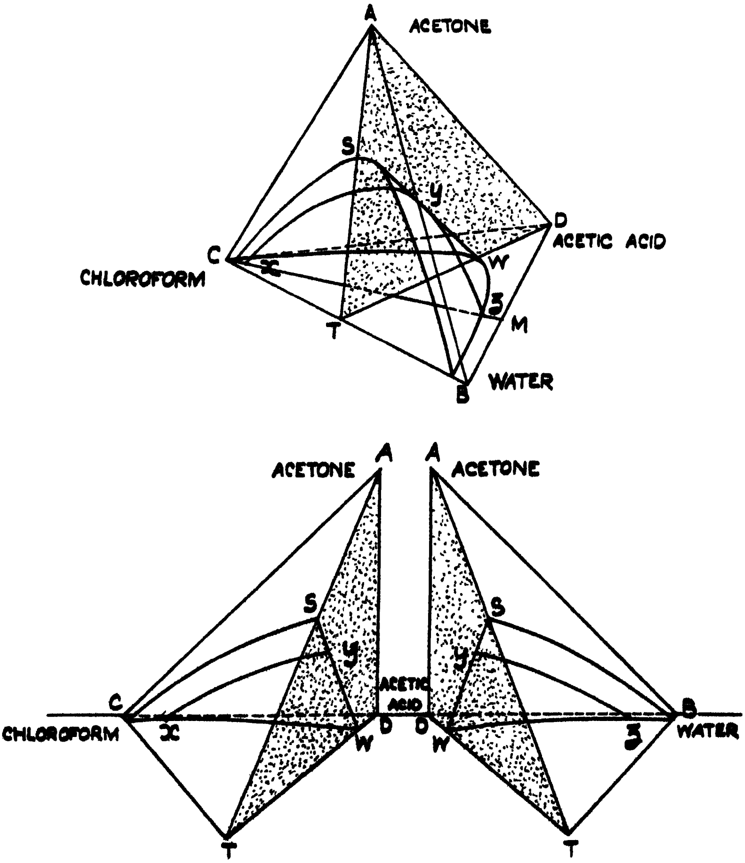

FIG. 2. The tetrahedron sectioned through the perpendicular plane *ATD*

that is, such figures are not exactly quantitative. All the remaining figures, however, are quantitative. The two ternary equilibrium curves for acetone–chloroform–water and acetic acid–chloroform–water lie on two triangular faces of the tetrahedron. By joining the two ternary isotherms a hollow figure or frustum is obtained inside the tetrahedron, as shown in figure 1; this frustum should define the heterogeneous region.

From the chloroform apex C of the tetrahedron in figure 1 a line is drawn on the base of the figure to a point M on the side of the triangular base opposite the chloroform apex. This point M represents a mixture of acetic acid and water in a known ratio. From M a line MA is drawn to the acetone apex. This construction gives an isosceles triangle CMA, where $CM = MA$. The intersection of the plane CMA with the quaternary equilibrium surface gives a quaternary equilibrium curve xyz, shown in figure 1, where x and z are the points of intersection of CM with the acetic acid–chloroform–water isotherm.

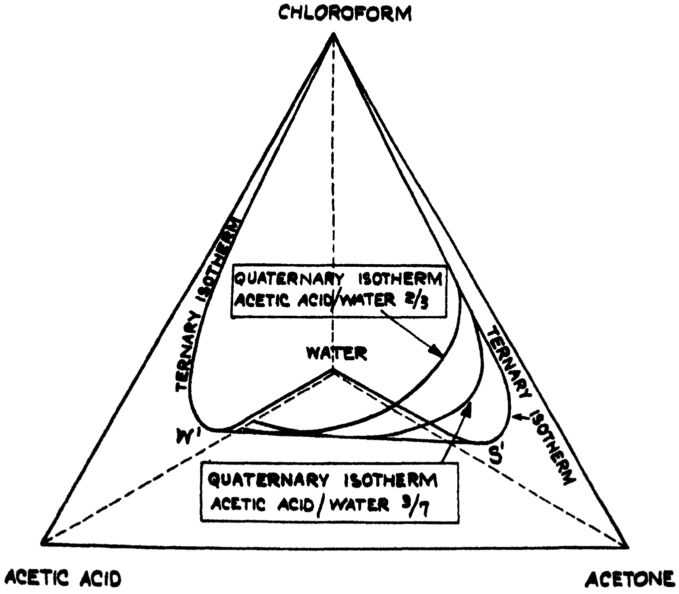

FIG. 3. The tetrahedron projected orthogonally on to the acetic acid-acetone-chloroform base

A number of acetic acid–water mixtures were prepared whose composition could be represented by points M, M_1 and M_2, etc. The quaternary equilibrium curve in each triangular plane CM_nA was then determined by titrating known acetone–chloroform mixtures with the prepared acetic acid–water mixtures M, M_1 and M_2. Equilibrium data obtained in this way for three quaternary isotherms are given in tables 5, 6, and 7.

The quaternary equilibrium data were plotted on equilateral triangles, as for a ternary system acetone–chloroform–mixture M_n. The actual equilibrium curves as *xyz* in figure 1, however, are situated on triangles which are not equilateral, but isosceles. It is a simple matter of geometrical manipulation to transfer the curves from the equilateral triangle to the isosceles triangle CM_nP. The curves so obtained are then true quaternary equilibrium curves as they exist in the tetrahedron. In figure 2 the tetrahedron has been sectioned through the perpendicular plane *ATD*. The section through *ATD* cuts the acetone–chloroform–water and the acetic acid–chloroform–water isotherms at the points *S* and *W*, respectively, and cuts the quaternary isotherm *xyz* for the acetone–chloroform–mixture *M* system at the point *y*. By drawing the triangular plane *ATD* separate from the tetrahedron and locating on it geometrically the points *S*, *y*, and *W*, the shape of the equilibrium surface can be obtained from the curve *SyW*. Four parallel sections through the tetrahedron were taken and the curves of section plotted. In each case the curve of section was found to be a straight line.

In figure 3 the tetrahedron has been projected orthogonally on to the acetic acid–acetone–chloroform base. Both of the determined isothermal ternary curves are shown in the figure, together with two of the isothermal quaternary curves. A projection with the tetrahedron in this position gives the shape of the equilibrium surface, and it will be seen that the quaternary isotherms touch the straight line *S′W′*, which is the projection profile of the equilibrium surface.

The frustum inside the tetrahedron as illustrated in figure 1 therefore represents the heterogeneous region for the quaternary system at 25°C.

QUATERNARY TIE LINES

Any point inside the quaternary equilibrium surface is in the heterogeneous region and represents a mixture of composition such that it forms two layers. The composition of the two layers can be represented by two points on the equilibrium surface in positions such that a straight line can be drawn through them and through the point representing the composition of the original mixture separating into two layers. The line so obtained is a quaternary tie line.

It was found that a quaternary tie line was situated on the line of intersection of two planes, each of which had for its base line a ternary tie line in the two different ternary systems. This is shown in figure 4, where *DEF* and *AGH* are the two planes, *MN* and *KL* are ternary tie lines, and *OP* is the quaternary tie line on the line of intersection *IJ* of the two planes. The quaternary tie line *OP* contained on *IJ* terminates at the quaternary equilibrium surface.

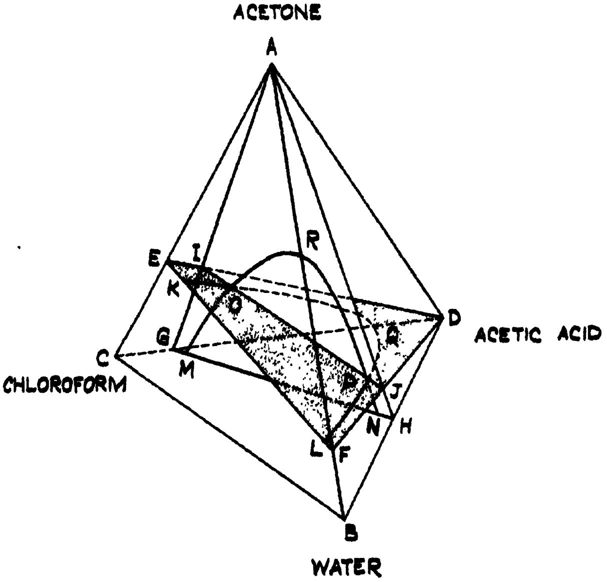
ACETONE
A
R
E
I
K
O
D
ACETIC ACID
Q
G
C
CHLOROFORM
M
P
J
N
H
L
F
B
WATER

Fig. 4

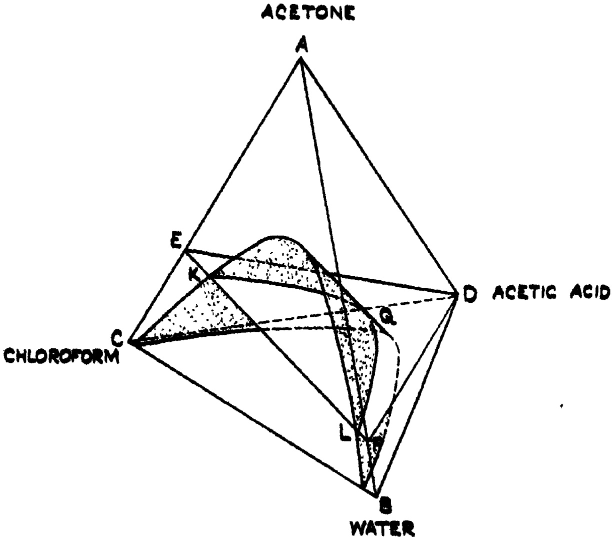
ACETONE
A
E
K
D
ACETIC ACID
Q
C
CHLOROFORM
L
B
WATER

Fig. 5

A number of such coplanar tie lines, or tie lines on the same plane, would by terminating at the equilibrium surface form a curve, such as *KQL* or *MRN* in figure 4.

These curves are also formed by the intersection of the tie line planes with the equilibrium surface as is clearly shown in figure 5, where the curve *KQL* is formed by the intersection of the tie line plane *DEF* with the equilibrium surface.

Mixtures of the four components acetic acid, chloroform, acetone, and water were prepared of composition such that two phases were formed at 25°C. Further these mixtures were so chosen that their composition could be indicated by points on a triangular plane having for its base line a ternary tie line. From the predetermined ternary tie lines two tie lines were selected, one in the acetone–chloroform–water system and the other in the acetic acid–chloroform–water system. The composition of mixtures such as would fall on these two tie line planes and also in the heterogeneous region were then calculated, and these mixtures were used in the experimental determination of quaternary tie lines. In this way two series of coplanar quaternary tie lines were obtained. Experimental data for the two series of tie lines are given in tables 8 and 9.

TABLE 8

*Quaternary tie line data for the system acetone–acetic acid–chloroform–water at 25°C. Initial mixtures all lie in the plane of the ternary tie line marked * in table 4*

COMPONENTS	INITIAL MIXTURE	TOP LAYER	BOTTOM LAYER
	weight per cent	*weight per cent*	*weight per cent*
Acetone	21.6	11.2	31.6
Acetic acid	9.3	15.3	3.3
Chloroform	32.8	1.8	63.5
Water	36.3	71.7	1.6
Acetone	19.2	9.3	29.2
Acetic acid	19.6	29.9	8.7
Chloroform	29.6	3.7	58.8
Water	31.6	57.1	3.3
Acetone	19.2	10.8	25.8
Acetic acid	26.6	38.2	16.2
Chloroform	30.6	9.8	51.8
Water	23.6	41.2	6.2
Acetone	18.0	13.6	22.8
Acetic acid	32.0	39.0	24.1
Chloroform	30.0	19.1	42.5
Water	20.0	28.3	10.6

As was done for the ternary tie lines, any experiment giving an error in the weight balance of any component greater than ± 4.0 per cent was rejected. The average experimental error was ± 1.0 per cent.

In figure 6 *DE′F′* and *A′G′H′* are orthogonal projections of the tie line planes *DEF* and *AGH*. These two tie line planes intersect to give the line of intersection *IJ* in figure 4. In figure 6 the points *I′* and *J′* give the projection of the line of intersection, and this line therefore contains in its length the projection of a quaternary tie line.

TABLE 9

Quaternary tie line data at 25°C.

Initial mixtures all lie in the plane of the tie line marked * in table 3

COMPONENTS	INITIAL MIXTURE	TOP LAYER	BOTTOM LAYER
	weight per cent	*weight per cent*	*weight per cent*
Acetic acid	19.6	32.8	9.6
Acetone	8.5	4.6	11.8
Chloroform	43.5	3.1	76.8
Water	28.4	59.5	1.8
Acetic acid	20.0	31.6	9.6
Acetone	14.4	7.5	20.3
Chloroform	37.4	3.5	67.3
Water	28.2	57.4	2.8
Acetic acid	18.0	30.4	9.2
Acetone	21.2	10.9	28.9
Chloroform	35.0	3.9	57.9
Water	25.8	54.8	4.0
Acetic acid	17.6	28.8	9.6
Acetone	27.2	15.4	36.8
Chloroform	28.1	4.4	47.3
Water	27.1	51.4	6.3
Acetic acid	16.0	24.2	11.2
Acetone	36.7	24.4	44.3
Chloroform	21.7	6.9	30.8
Water	25.6	44.5	13.7

In this manner it is possible to obtain a series of lines each containing in its length the projection of a quaternary tie line. These lines in themselves however give no indication of the position occupied in their length by the projected tie lines. This position can only be defined by the projection of the curve *KQL* of figures 4 and 5.

In figure 7 the projection of actual lines of intersection of a single acetone–chloroform–water tie line plane with a series of acetic acid–

chloroform–water tie line planes are shown as broken lines. Projections of the corresponding quaternary tie lines are shown as full lines coincident

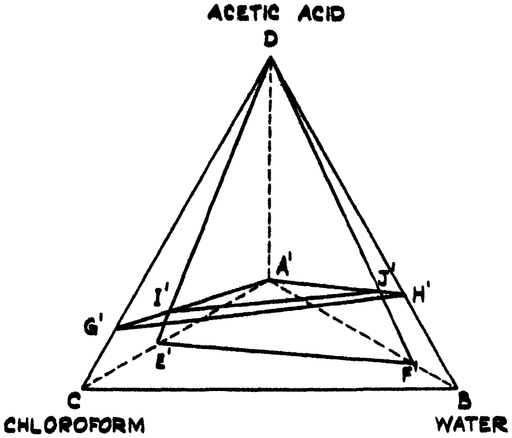

FIG. 6

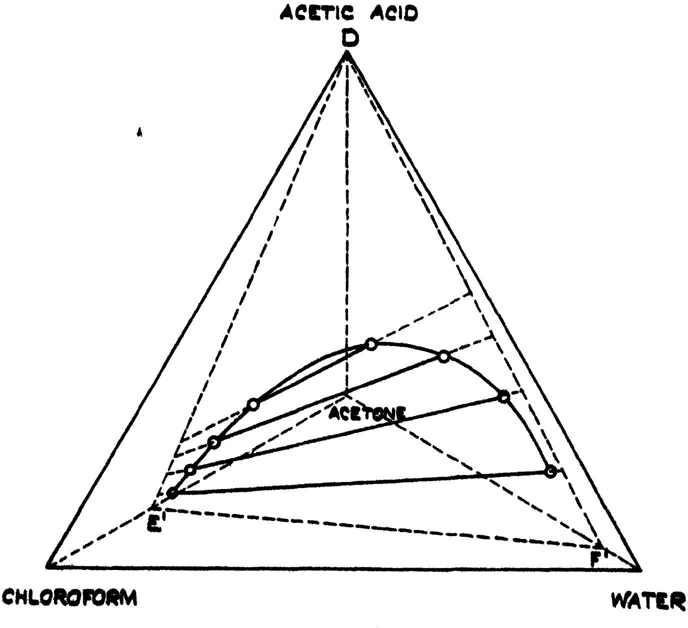

FIG. 7

of course with the projected lines of intersection, but only occupying a portion of their length. The curve joining the terminal points of the projected tie lines is the projection of the quaternary tie line curve *KQL* of figures 4 and 5. The projection of such quaternary tie line curves can be easily obtained by geometrical construction without actually knowing the quaternary tie lines.

In figure 8 *ATD* is a triangular plane in the tetrahedron perpendicular to the base. *S* and *W* are points of intersection of this plane with the acetone–chloroform–water and acetic acid–chloroform–water isotherms, respectively. *U* is the intersection of plane *ATD* with the ternary tie line *KL*, and *UD* is the intersection of the plane *ATD* with the tie line plane *EFD*.

SQW is the intersection of the quaternary equilibrium surface with the plane *ATD*. In this particular case *SQW* is a straight line but as a general case its contour, curved or straight, would be known from the method of triangular section applied earlier (*cf.* figure 2).

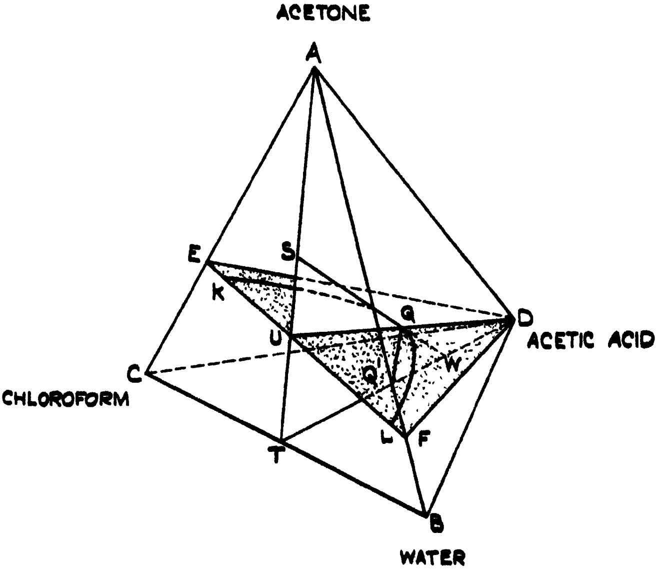

Fig. 8

Point *Q* lies on the quaternary tie line curve and can be located from the intersection of *UD* and *SW*. *Q'* is the orthogonal projection of *Q* on to the base of the tetrahedron. As *ATD* is a perpendicular plane, *Q'* must be on *TD*.

A series of planes similar to *ATD* would in this manner give a series of points similar to *Q* and a corresponding series of projected points similar to *Q'*, which would define the projection of such a quaternary tie line curve.

It is possible to obtain such a curve in the *EFD* plane by titration where the three components are (*1*) acetic acid, (*2*) the acetone–chloroform mixture represented by point *E* (figure 8), and (*3*) the acetone–water mixture represented by point F (figure 8). This is unnecessary, however, as it is easily calculated by the above construction.

It has been shown that in this quaternary system of mixed liquids a knowledge of the tie lines in the two heterogeneous ternary systems, together with a knowledge of the shape of the equilibrium surface, enables the quaternary tie lines to be located.

THE COMPLETE QUATERNARY SYSTEM

The complete quaternary system acetic acid–chloroform–acetone–water at 25°C. is illustrated in figure 9. The two ternary isotherms acetone–chloroform–water and acetic acid–chloroform–water define the heterogeneous region on two sides of the tetrahedron. The points of intersection of the ternary isotherms and triangular shaped planes perpendicular to both the acetone–chloroform–water and the acetic acid–chloroform–water triangles when joined by straight lines outline a frustum which defines the heterogeneous region.

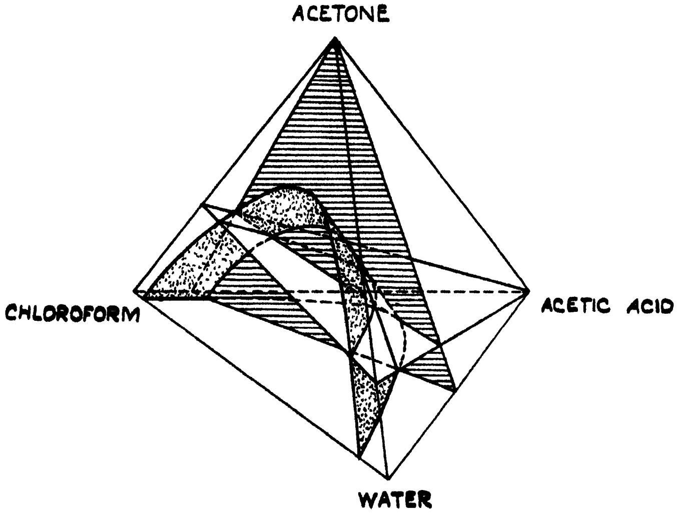

Fig. 9. The complete quaternary system acetic acid-chloroform-acetone-water at 25°C.

One tie line in each of the two heterogeneous ternary systems is shown in figure 9. The planes passing through each of these tie lines and the opposite apex of the tetrahedron intersect to give a quaternary tie line whose two terminal points lie on the quaternary equilibrium surface.

REFERENCES

(1) Goodwin, L. F.: J. Am. Chem. Soc. **42**, 39 (1920).
(2) Hand, D. B.: J. Phys. Chem. **34**, 1961 (1930).
(3) Wright, C. R. A.: Proc. Roy. Soc. (London) **49**, 183 (1891); **50**, 375 (1892).

THE DERIVATION OF THE EQUILIBRIUM CONDITIONS IN PHYSICAL CHEMISTRY ON THE BASIS OF THE WORK PRINCIPLE

J. N. BRØNSTED

University Institute of Physical Chemistry, Copenhagen, Denmark

Received November 13, 1939

I. INTRODUCTION. THE ENERGETIC BASIS

In some previous publications (3) an attempt has been made to revise the fundamental concepts of energetics and to formulate the fundamental laws of thermodynamics on the basis of new points of view. It is the concept of heat evolution and the relation between heat and work as advanced by classical thermodynamics which has particularly called for criticism and necessitated a revision of the accepted theories. As an introduction to the present paper it will be necessary to delineate briefly certain of the elementary considerations which have contributed particularly to this altered orientation.

It should be observed first that traditional thermodynamics does not seem to recognize the fundamental difference between the problems of defining, on the one hand, amounts of heat *communicated*, i.e., added to or removed from a system through thermal conduction or radiation, and, on the other hand, heat *produced* or *consumed* within the boundary of the system itself.

In traditional thermodynamics heat communicated is defined and determined by means of calorimetric methods which are at any rate self-consistent. As regards heat produced or consumed, no general definition exists to separate it from heat communicated. The practical determination of heat evolution imitates the methods employed in the determination of heat communicated, the temperature change at the process, irrespective of its reversibility, being introduced as an indicator and a measure of the heat involved. This procedure, however, completely lacks a theoretical foundation, and leads in a great measure to contradiction with the fundamental principle, recognized and made use of also in classical thermodynamics, that heat is a form of energy the production and consumption of which demands an energetic equivalent.

A simple example will illustrate this assertion. If by means of a weight falling through a certain distance an ideal gas of pressure p is compressed from the volume v to $v - dv$, it is claimed by classical thermodynamics that, owing to the rise in temperature, an evolution of heat takes place, which in the case considered has the value pdv. This well-known interpretation of the compression process, however, entirely overlooks the fact that on compression the gaseous system, i.e., the gas + the surrounding vacuum, has received an amount of work *pdv*, exactly equal to the loss of work accompanying the transport of the weight. Accordingly, if the energy principle has to be maintained, no room will be left for the additional production of energy such as the pretended evolution of heat would imply.

On the other hand, when an ideal gas expands irreversibly, the classical theory postulates the evolution of heat to be zero, because of the rise in temperature being zero. This interpretation cannot be maintained either, since the irreversible expansion, exactly as the irreversible fall of a weight from a higher to a lower position or the irreversible flow of electric charges from higher to lower potential, is accompanied by a loss of work and therefore, if the energy principle is to be fulfilled, must evolve heat.

With this lack of clarity in the traditional conception of heat evolution, obviously a corresponding lack of clarity as to the concept of work is closely connected. In the first place, on account of the straight phenomenologic analogy between the various basic processes, it is not permissible to confine the concept of work to processes of a mechanical nature. This is well recognized in the classical treatment, as shown by its introduction of an electric work term as an energetic concept. Exclusion of chemical, thermal, and other kinds of work, however, does not only mean incompleteness and awkwardness in the treatment, but unavoidably leads to contradiction. In the second place, as clearly illustrated by the above example, one finds in classical thermodynamics a fatal uncertainty as regards the purely elementary enumeration of the individual members of work taking part in a process.

It is under the impression of these and similar decisive weaknesses in the classical conception, regarding which further information is to be found in the papers quoted above, that a rationalized exposition of the fundamental problems of thermodynamics has been attempted. As an essential part of such an exposition it has proved necessary first to analyze more closely the nature of the fundamental energetic entities and of the elementary components in which the changes occurring in nature can be schematically divided. For this purpose the concepts of quantity and intensity or potential already used by earlier authors have proved suitable, the sense of these concepts appearing particularly clearly through introducing the idea of the *basic energetic process.*

By this term is meant transport or displacement of energetic quantities, in the first place entropy, volume, chemical substance, and electricity, between states which may be characterized by their energetic potentials, i.e., temperature, pressure, chemical and electrical potential. To such a process, as a logical extension of the existing mechanical concept of work, there must quite generally be coördinated a *loss of work*, given as the product of the amount of quantity transported and the difference between the corresponding potentials in the two states:

$$\delta A = (P_1 - P_2)\delta K \tag{1}$$

This loss of work is said to take place within the system which contains the quantities transported. In particular we may write for the thermal loss of work:

$$\delta A = (T_1 - T_2)\delta S \tag{2}$$

T being the temperature and S the entropy.[1]

The basic processes described here are necessary constituents of all natural changes. The changes consisting of basic processes alone are reversible changes. The fundamental law governing such changes is the *work principle*, which postulates that the total loss of work involved in the reversible process is zero:

$$\Sigma\delta A = 0 \tag{3}$$

This equation, which emphasizes the perfect symmetry with which all basic processes enter in the process, offers a simple and exhaustive description of the reversible phenomena in nature and does not in any way lead to contradiction.

In the irreversible changes, in addition to the basic processes, an evolution of heat will take place. Now the work principle is no longer valid, since a positive loss of work will occur in the system, which, irrespective of the nature of the basic processes, is equal to the heat produced:

$$\Sigma\delta A = \delta Q \tag{4}$$

This heat, which we shall call the *energetic heat evolution*, and which obviously satisfies an extended equivalence principle dealing with work in a general sense, is defined as the heat communication of the system on reversible reproduction of the irreversible process considered. It is related to the entropy formed simultaneously through the general equation:

$$\delta Q = T\delta S \tag{5}$$

The theory is thus in conformity with the classical assertion that entropy increases in all irreversible processes in an adiabatically isolated system.

As the summary of the above considerations it may thus be maintained that all natural processes are characterized by the fact that either the loss of work is zero (equation 3), in which case the process is reversible, or else the loss of work is positive and equal to the evolution of heat (equation 4), in which case the process is irreversible. Processes in which loss of work and evolution of heat are negative are not possible according to this theory.

---

[1] As emphasized by Callendar (4) and also in the first of the papers mentioned in reference 3, Carnot's conception of the "motive power of heat" (5) is in agreement with this expression if the term "calorique" with which he operates is identified with entropy. The expression is also to a certain extent in conformity with Zeuner's (7) conception of the function of the heat engine.

It is the object of the present paper to show how the various equilibrium equations in thermodynamics and physical chemistry can be derived on the basis given here. Since every transformation occurring through a state of equilibrium is a reversible process, it is the work principle upon which these calculations should be based. This method is not only theoretically unassailable, but, on account of the perspicuity of the work principle, also possesses a considerable didactic significance.

For the application of the work principle in a given case it is necessary that the reversible character of the change in question should be ascertained. We shall begin our exposition by proving the reversibility of certain groups of processes of particular significance for our purpose.

II. THE WORK THEOREM FOR INFINITESIMALLY DIVERGING SYSTEMS

In this and the following sections we shall suppose the systems in question to be constituted exclusively by the independently variable quantities, entropy, volume, and chemical components.

We shall consider two systems, I and II, homogeneous with respect to quantity and potential and so constituted that a certain fraction of I contains the quantities:

$$S, V, n_1, n_2 \cdots\cdots\cdots \tag{6}$$

and a certain fraction of II the quantities:

$$S + \mathrm{d}S, V + \mathrm{d}V, n_1 + \mathrm{d}n_1, n_2 + \mathrm{d}n_2, \cdots\cdot \tag{7}$$

The quantities indicated, which define the systems completely, are measured in reservoirs each communicating only a single quantity.

The potentials, corresponding to the quantities given by expressions 6 and 7, are

$$T, p, \mu_1, \mu_2 \cdots\cdots\cdots\cdot \tag{8}$$

and

$$T + \mathrm{d}T, p + \mathrm{d}p, \mu_1 + \mathrm{d}\mu_1, \mu_2 + \mathrm{d}\mu_2, \cdots \tag{9}$$

respectively. The two systems are supposed completely miscible.

We now consider a process completely cut off from the surroundings and consisting in the transference from I to II of the fraction of I given by expression 6. The transference is supposed to be differential, which means that the amount transferred is so small in comparison to the total amount of the two systems that the changes in potential resulting from the transference are negligible compared to the potential differences already existing.

It is easy to see, then, that *such a transference is a reversible process.* As a matter of fact, on account of the complete miscibility which, as mentioned before, is presupposed, the amount presented by expression 6 after being isolated from I and then brought into contact with II will dissolve spontaneously in this system, while reversely the amount presented by expression 7 after being isolated from II and brought into contact with I will spontaneously dissolve in this phase. Since these two spontaneous processes are opposite with respect to direction and only infinitesimally different from each other, they deviate only infinitesimally from truly reversible processes.

This important result now permits the application of the work principle to the process of transfer defined above. According to the work principle the total work lost in the process is zero. For each kind of work the loss is obtained by multiplying the quantity appearing in expression 6 by the corresponding difference in potential appearing from expressions 8 and 9. Thus the equation

$$\delta A = -S\,\mathrm{d}T + V\,\mathrm{d}p - \bar{n}_1\,\mathrm{d}\mu_1 - n_2\,\mathrm{d}\mu_2 - \cdots\cdots = 0 \qquad (10)$$

is obtained as an expression of the *work theorem for infinitesimally diverging systems.*

The total loss of work being zero means in the present case that it is small compared to the individual work terms entering in the equation, or at any rate to some of them. The contents of equation 10 may therefore be expressed in a quite unambiguous way by:

$$\frac{\Sigma K_i P_i}{\Sigma |K_i P_i|} \ll 1 \qquad (11)$$

where the denominator indicates the sum of the numerical values of all work terms involved.

Actually this equation can be taken as a characterization of the reversible process. Since the natural processes are never completely reversible, but are always accompanied by a certain net loss of work, the question of the definition of reversibility must be that of the definition of the deviation from reversibility, i.e., of the irreversibility. It would be possible to introduce the absolute loss of work as a measure of the irreversibility, but it would no doubt be more rational to use the loss of work in proportion to the total work involved. It is this conception which is the basis of the reversibility principle established above and mathematically formulated in equation 11.

It should be carefully noted that the theorem concerning the zero value of the transference work applies only to fractional amounts having the composition of the systems with respect to all quantities. In special cases one obtains simplified expressions. If, for instance, the temperature and pressure differences between systems I and II are zero, equation 10 is reduced to the following form:

$$\delta A = -n_1\,\mathrm{d}\mu_1 - n_2\,\mathrm{d}\mu_2 - \cdots = 0 \tag{12}$$

an expression the validity of which for two components has been demonstrated by the author in an earlier publication (2; *cf.* 1). From the expression given there for the differential transport of a mixture of mole fraction a from its own solution to a mixture of mole fraction x, one obtains in the case of ideal miscibility conditions the expression:

$$\frac{\mathrm{d}A}{\mathrm{d}x} = RT\,\frac{a - x}{x(1 - x)}$$

which shows that when $a - x$ is small, A changes proportionally to the square of the difference in concentration. This expresses the validity of equation 12 in the special case under consideration.

It will be of interest finally to compare the work theorem for infinitesimally diverging systems with the fundamental Gibbs equation for the potential variations of a homogeneous system (6). Like equation 10 the Gibbs equation expresses that the sum $\Sigma K_i\,\mathrm{d}P_i$ is zero. But the treatment of Gibbs does not interpret this sum as representing the transference work considered here or any other work whatsoever. In Gibbs' treatment the equation expresses the correlation between the potential changes generated in the system through the addition of arbitrary infinitesimal amounts of quantity or through intrinsic irreversible changes. It is possible, of course, as an alternative procedure, to base our considerations upon the Gibbs equation and establish its character as a work expression under the assumption of reversibility. Through this method, however, one will to a certain extent conceal the fundamental idea on which our exposition is based, and which it is the special purpose of this paper to emphasize and elucidate.

III. THE HETEROGENEOUS EQUILIBRIUM

The work theorem, which in the previous section has been shown to hold for infinitesimally diverging systems, forms the immediate basis for the derivation of all formulas in physical chemistry for heterogeneous and homogeneous equilibria.

We shall first consider the simple two-phase equilibrium in a one-component system. We imagine the two phases in equilibrium with each other in a system I, where the potentials are T, p, and μ, and in another system II, where the potentials are $T + \mathrm{d}T$, $p + \mathrm{d}p$, and $\mu + \mathrm{d}\mu$. The quantities in a certain section of phase A in system I are

$$S_A\,,\ V_A\,,\ n_A \tag{13}$$

and in a certain section of phase B in the same system

$$S_B\,,\ V_B\,,\ n_B \tag{14}$$

In system II the corresponding quantities are

$$S_A + dS_A\,,\ V_A + dV_A\,,\ n_A + dn_A \tag{15}$$

and

$$S_B + dS_B\,,\ V_B + dV_B\,,\ n_B + dn_B \tag{16}$$

respectively.

We now pass a fraction of system I A, given by expression 13, differentially from I A to II A, and a fraction of II B, given by expression 16, differentially from II B to I B. Since systems I and II are differing only infinitesimally from each other, the loss of work involved in each of these processes will be zero according to the work theorem. Disregarding members which are small of second order we can thus write for the total loss of work associated with the transport:

$$-(S_A - S_B)\,dT + (V_A - V_B)\,dp - (n_A - n_B)\,d\mu = 0 \tag{17}$$

This is the general expression, valid for the two-phase equilibrium, i.e., for the changes in potential caused by arbitrary changes of the state of equilibrium. The usual expression, which contains only the potentials T and p, is obtained by putting $n_A = n_B = 1$. Equation 17 is then reduced to:

$$-(S_A - S_B)\,dT + (V_A - V_B)\,dp = 0 \tag{18}$$

the quantities involved now referring to unit amount of substance. Equation 18 may also be written:

$$\left(\frac{\delta p}{\delta T}\right)_{\mathrm{Eq}} = \frac{S_A - S_B}{V_A - V_B} \tag{19}$$

index "Eq" referring to the equilibrium condition.

Equation 18 is identical with the vapor pressure formula of Clapeyron and the William Thomson equation for the dependence of the melting point on pressure. It is brought into formal agreement with these equations by introducing $T(S_A - S_B) = q$, i.e., the heat of evaporation or fusion.

In a quite similar manner one derives from equation 17 ·

$$(S_A - S_B)\,dT + (n_A - n_B)\,d\mu = 0 \tag{20}$$

where the quantities are those contained in the unit of volume, and

$$(n_A - n_B)\,d\mu - (V_A - V_B)\,dp = 0 \tag{21}$$

where the quantities are those associated with unit amount of entropy.

The general two-phase equilibrium expression for systems containing two chemical components is deduced analogously to equation 17. The amounts S_A, V_A, n_{1A}, n_{2A} are transferred from system I to system II, and the amounts S_B, V_B, n_{1B}, n_{2B} are transferred in the opposite direction, the net process being a transport of: $S_A - S_B$, $V_A - V_B$, $n_{1A} - n_{1B}$, $n_{2A} - n_{2B}$ from I to II. On the basis of the work principle for infinitesimally diverging systems we put the transference work equal to zero. Hence,

$$(S_B - S_A)\,dT - (V_B - V_A)\,dp + (n_{1B} - n_{1A})\,d\mu_1 + (n_{2B} - n_{2A})\,d\mu_2 = 0 \qquad (22)$$

an equation which is symmetrical with respect to all quantities and potentials involved. In the special case of $n_{2B} = n_{2A} = 1$ the quantities involved will be those associated with unit amount of the second chemical component. The last term in equation 22 then disappears. Further simplification into the equilibrium expressions usually employed in physical chemistry, containing only two variable potentials, is obtained by putting one of the remaining potential differences equal to zero.

Thus, if one wishes to determine the equilibrium at constant temperature, one puts $dT = 0$, obtaining

$$-(V_B - V_A)\,dp + (n_{1B} - n_{1A})\,d\mu_1 = 0 \qquad (23)$$

or

$$\left(\frac{\delta\mu_1}{\delta p}\right)_{\mathrm{Eq},T} = \frac{V_B - V_A}{n_{1B} - n_{1A}} \qquad (24)$$

while for constant pressure

$$(S_B - S_A)\,dT + (n_{1B} - n_{1A})\,d\mu_1 = 0 \qquad (25)$$

or

$$\left(\frac{\delta\mu_1}{\delta T}\right)_{\mathrm{Eq},p} = -\frac{S_B - S_A}{n_{1B} - n_{1A}} \qquad (26)$$

From the general equations 22 to 26, thus deduced on the basis of the work principle, all the equations and qualitative laws concerning physicochemical equilibria are derivable by simple transformations with or without introduction of special equations of state for vapors and solutions. For example, the laws on the osmotic pressure, on vapor pressure lowering and freezing point depression, the influence of temperature and pressure on the solubility of solid substances, Konowalow's rule of the composition of liquids and saturated vapors, the laws of electromotive force, etc.

The law on the freezing point depression, for instance, is obtained by introducing in equation 26 the following equations:

$$n_{1B} = 0$$

$$n_{1A} = n_1$$

$$\left(\frac{\delta\mu_1}{\delta T}\right)_{Eq.,p} = \left(\frac{\delta\mu_1}{\delta T}\right)_{n_1,p} + \left(\frac{\delta\mu_1}{\delta n_1}\right)_{T,p}\left(\frac{\delta n_1}{\delta T}\right)_{Eq.,p}$$

$$\left(\frac{\delta\mu_1}{\delta T}\right)_{n_1,p} = -s_1$$

$$S_A = s_2 + n_1 s_1$$

$$T(S_B - s_2) = q$$

and the gas law expression

$$\left(\frac{\delta\mu_1}{\delta n_1}\right)_{T,p} = \frac{RT}{n_1}$$

where s_1 and s_2 are the differential entropy in the liquid mixture for 1 g. of the first and second chemical component, respectively, and q the melting heat appearing in the freezing point equation:

$$\mathrm{d}T = -\frac{RT^2\,\mathrm{d}n_1}{q}$$

i.e., the differential heat of dissolution for 1 g. of the second component in the solid state at the existing equilibrium.

IV. THE HOMOGENEOUS EQUILIBRIUM

The law of "chemical mass action" in its usual formulation deals with concepts and unities which are of molecular–theoretical origin. Moreover it is valid only for systems of particular simplicity. The main law for homogeneous equilibria is therefore essentially different in character from the purely energetic laws with which we have been concerned in the previous sections.

As a basis of the traditional mass action expression, valid at constant temperature and pressure, there exists, however, an expression of a purely energetic character, which may be termed the "energetic mass action law." In order to derive this general law we shall consider a reversible basic process, consisting in the transport of quantity between two homogeneous systems I and II. While in the case of the processes considered in the previous sections the fraction transported had the same composition as the system from which it was taken, we are here dealing with the transport of an assemblage of quantities, the composition of which differs from that of the communicating systems, and which in general, therefore, can only be conducted reversibly if coupled to another working system, for instance, a work reservoir.

It is essential to note that this transport at the same time as being defined by the initial and final states of the quantities transported generally may be effected in a number of different ways, owing to the fact that the chemical systems between which the transport takes place are themselves describable in terms of a number of freely selected components.

Let us suppose that a homogeneous system, in addition to entropy, volume, and some material substances which need not be specified, is constituted by a chemical system A, containing the components A_1, $A_2 \cdots\cdot$ in the amounts ν_{A_1}, $\nu_{A_2} \cdots\cdot$, and let us further suppose that the same homogeneous system may just as well be made up of the quantities mentioned above, if a B system, containing the components B_1, $B_2 \cdots\cdot$ in the amounts ν_{B_1}, $\nu_{B_2} \cdots\cdot$ be substituted for the A system. Between the two systems A and B the stoichiometric relation

$$\nu_{A_1}A_1 + \nu_{A_2}A_2 + \rightleftarrows \nu_{B_1}B_1 + \nu_{B_2}B_2 + \cdots \tag{27}$$

must then hold true, where no condition is imposed upon the figures ν beyond that implied by this stoichiometric relation. It should be noticed in particular that the components chosen need not be "chemical individuals."

If systems I and II are characterized by such an alternative possibility of constitution, the transference of system A from I to II will be chemically equivalent to the corresponding transference of system B. If entropy and volume do not participate in the transport, the total loss of work will only be of chemical nature and consequently, if the two systems differ only infinitesimally from each other, the potential in I, being $d\mu$ higher than the potential in II, will be expressible as:

$$\delta A_A = -\nu_{A_1}\, d\mu_{A_1} - \nu_{A_2}\, d\mu_{A_2} - \cdots\cdot = -\Sigma\nu_{A_1}\, d\mu_{A_1} \tag{28}$$

and

$$\delta A_B = -\nu_{B_1}\, d\mu_{B_1} - \nu_{B_2}\, d\mu_{B_2} - \cdots\cdot = -\Sigma\nu_{B_1}\, d\mu_{B_1} \tag{29}$$

for the transport of system A and system B, respectively.

Now according to the work principle the loss of work associated with reversible processes depends only upon the initial and final states of the system involved. Hence:

$$-\Sigma\nu_{A_1}\, d\mu_{A_1} + \Sigma\nu_{B_1}\, d\mu_{B_1} = 0 \tag{30}$$

By integration or by direct application of the work principle to systems with final potential differences, one obtains

$$-\Sigma\nu_{A_1}\mu_{A_1} + \Sigma\nu_{B_1}\mu_{B_1} = I \tag{31}$$

I being a constant the value of which depends on the zero states chosen for the chemical potentials. By adequate choice of these the constant will be zero, and we may write:

$$-\Sigma\nu_{A_1}\mu_{A_1} + \Sigma\nu_{B_1}\mu_{B_1} = 0 \tag{32}$$

Putting

$$\Sigma\nu_{A_1}\mu_{A_1} = \mu_A \tag{33}$$

and

$$\Sigma\nu_{B_1}\mu_{B_1} = \mu_B \tag{34}$$

the last equation simplifies into

$$-\mu_A + \mu_B = 0 \tag{35}$$

Equations 30, 31, 32, and 35 are equivalent expressions for the *energetic mass action law.* It should be emphasized in particular that this law, as appears from the deduction, is not confined to changes at constant temperature and pressure, but is of a quite general character.

In order to derive the usual mass action law from equations 30 to 35 one should first introduce molecular unities, thus changing the figures ν into integers and scheme 27 into the ordinary chemical reaction scheme. Further—as a condition for the validity of the usual mass action law—the gas laws must be introduced, for instance in the form

$$\mu_{A_1} = \mu_{A_1(0)} + RT \ln x_{A_1} \tag{36}$$

where μ_{A_1} and x_{A_1} are corresponding values for the molar chemical potential and mole fraction of component A_1 in a system maintained at constant temperature T and constant pressure. As appears from equation 36, the magnitude $\mu_{A_1(0)}$ formally equals the potential of A_1 for $x_{A_1} = 1$ at the same temperature and pressure. The equation indicates how the potential of a molecular component depends upon its concentration under ideal conditions at constant temperature and pressure.

By summation over all the components involved equation 36, on application of equations 33 and 34, gives

$$\mu_{A_0} - \mu_{B_0} - (\mu_A - \mu_B) = RT \ln K_x \tag{37}$$

where

$$K_x = \frac{x_{B_1}^{\nu_{B1}}\, x_{B_2}^{\nu_{B2}} \cdots}{x_{A_1}^{\nu_{A1}}\, x_{A_2}^{\nu_{A2}} \cdots} \tag{38}$$

Introducing the energetic equilibrium condition 35 in this expression we finally obtain

$$\mu_{A_0} - \mu_{B_0} = RT \ln (K_x)_{Eq} \tag{39}$$

$(K_x)_{\mathrm{Eq}}$ being the value of K_x in the state of equilibrium. As appears from equation 39, $(K_x)_{\mathrm{Eq}}$ is constant under the given temperature and pressure conditions, which is an expression for the traditional mass action law.

By this law evidently a structure definition is implied for the homogeneous mixture which has not been required in the case of the energetic expressions established previously. The chemical "composition" as given by the figures ν in these expressions was defined from a purely energetic standpoint as the amounts of given components necessary for making up the system in question, and this definition was implicitly supposed not to lead to any kind of ambiguity. The possibility of the same system being constructed from different components A and B led to the energetic mass action law. The traditional mass action law, on the other hand, is based upon the possibility of a logical discrimination between these component systems within the mixture itself, and upon a detailed structure determination based upon this possibility.

In such a case the two reciprocal systems A and B cannot under all conditions yield identical mixtures. Starting from either A or B there may be formed mixtures which alter their properties by time, indicating chemical instability. At an arbitrary stage of this transformation definite amounts of components from both systems will be required for the construction of the mixture, the intrinsic composition of which is defined exactly through these amounts. Supposing such a homogeneous change of state to take place, a new energetic variable, which is the *degree of reaction*, will come into the calculation.

It is only when considering this intrinsic composition of the homogeneous system that the influence of temperature and pressure makes itself noticed. The energetic mass action law as represented by equations 30 to 35 obviously does not reflect such influence.

The effect of temperature upon the equilibrium constant may be obtained by differentiation of equation 39 with respect to temperature. This gives the well-known equation

$$H_{\mathrm{B}_0} - H_{\mathrm{A}_0} = RT^2\left(\frac{\delta \ln K_x}{\delta T}\right)_{\mathrm{Eq},p} \tag{40}$$

H being the heat function, while differentiation with respect to pressure gives

$$V_{\mathrm{A}_0} - V_{\mathrm{B}_0} = RT\left(\frac{\delta \ln K_x}{\delta p}\right)_{\mathrm{Eq},T} \tag{41}$$

The lack of symmetry displayed by these expressions is due to the unsymmetrical manner in which T and p enter in the gas law equation (equation 36).

Equations equivalent with these, but containing entropy and volume of the reactants in the equilibrium mixture itself, are obtained by introducing the new variable, the degree of reaction. We shall write for μ_A and μ_B, given by equations 33 and 34,

$$d\mu_A = \left(\frac{\delta\mu_A}{\delta T}\right)_{p,\alpha} dT + \left(\frac{\delta\mu_A}{\delta p}\right)_{T,\alpha} dp + \left(\frac{\delta\mu_A}{\delta\alpha}\right)_{T,p} \delta\alpha \tag{42}$$

and

$$d\mu_B = \left(\frac{\delta\mu_B}{\delta T}\right)_{p,\alpha} dT + \left(\frac{\delta\mu_B}{\delta p}\right)_{T,\alpha} dp + \left(\frac{\delta\mu_B}{\delta\alpha}\right)_{T,p} \delta\alpha \tag{43}$$

whence

$$-d\mu_A + d\mu_B = (S_A - S_B)\,dT - (V_A - V_B)\,dp - \left[\left(\frac{\delta\mu_A}{\delta\alpha}\right)_{T,p} - \left(\frac{\delta\mu_B}{\delta\alpha}\right)_{T,p}\right] d\alpha \tag{44}$$

or by introduction of equation 36

$$-d\mu_A + d\mu_B = (S_A - S_B)\,dT - (V_A - V_B)\,dp + RT\left(\frac{\delta \ln K_x}{\delta\alpha}\right)_{T,p} d\alpha \tag{45}$$

Now supposing the system to be in a state of equilibrium, i.e., $-d\mu_A + d\mu_B = 0$, the influence of temperature on this state is calculated from equation 45 by introducing $dp = 0$, and

$$\left(\frac{\delta \ln K_x}{\delta T}\right)_{\text{Eq},p} = \left(\frac{\delta \ln K_x}{\delta T}\right)_{p,\alpha} + \left(\frac{\delta \ln K_x}{\delta\alpha}\right)_{T,p}\left(\frac{\delta\alpha}{\delta T}\right)_{\text{Eq},p} \tag{46}$$

where the first term on the right-hand side is zero. One then obtains

$$-(S_A - S_B) = RT\left(\frac{\delta \ln K_x}{\delta T}\right)_{\text{Eq},p} \tag{47}$$

In a similar manner one obtains at constant temperature

$$V_A - V_B = RT\left(\frac{\delta \ln K_x}{\delta p}\right)_{\text{Eq},T} \tag{48}$$

That equation 47 is identical with equation 40 follows from the gas law expression (expression 36), since this by differentiation with respect to temperature gives

$$-S_{A_1} = -S_{A_{1(0)}} + R \ln x_{A_1} \tag{49}$$

That equation 48 is identical with equation 41 is seen in a similar manner, equation 36 on differentiation with respect to pressure giving

$$V_{A_1} = V_{A_{1(0)}} \tag{50}$$

As seen by comparing equations 43 and 44, the quantities S_{A_1} and V_{A_1} are defined by the relations

$$-\left(\frac{\delta\mu_{A_1}}{\delta T}\right)_{\alpha,p} = S_{A_1} \tag{51}$$

and

$$\left(\frac{\delta\mu_{A_1}}{\delta p}\right)_{\alpha,T} = V_{A_1} \tag{52}$$

thus being the symbols for entropy and volume in mixtures at constant α. On the other hand $S_{A_1,\text{Eq}}$ and $V_{A_1,\text{Eq}}$ given by

$$-\left(\frac{\delta\mu_{A_1}}{\delta T}\right)_{\text{Eq},p} = S_{A_1,\text{Eq}} \tag{53}$$

and

$$\left(\frac{\delta\mu_{A_1}}{\delta p}\right)_{\text{Eq},T} = V_{A_1,\text{Eq}} \tag{54}$$

represent the differential quantities at equilibrium.

V. SUMMARY

1. The assumption of traditional thermodynamics that heat can be produced or consumed in reversible processes is caused by an incomplete analysis of the basic phenomena associated with such processes.
2. The fundamental law for all reversible processes is the work principle $\Sigma\delta A = 0$, indicating that the total work expended or lost in a reversible process is zero.
3. Since the reversible process is a change through states of equilibrium, the work principle, valid for such processes, can be made the basis for the deduction of all expressions of physicochemical equilibria.
4. The differential transport of a fraction of a homogeneous system from a certain state into another deviating infinitesimally from the first is a reversible process. The work associated with it is therefore zero. This is called the *work theorem for infinitesimally diverging systems.*
5. On the basis thus given a detailed deduction of some important equilibrium equations in physical chemistry has been presented.

REFERENCES

(1) Bjerrum, N.: Z. physik. Chem. **104,** 411 (1923).
(2) Brønsted, J. N.: *Affinity Studies* III, p. 2. Copenhagen (1908).
(3) Brønsted, J. N.: Kgl. Danske Videnskab. Selskab Math.-fys. Medd. **15,** No. 4 (1937); **16,** No. 10 (1939); Phil. Mag. (1939).
(4) Callendar, H. L.: Proc. Roy. Soc. (London) **23,** 153 (1910-11).
(5) Carnot, S.: *Reflexions sur la puissance motrice du feu* (1824).
(6) Gibbs, W.: *Collected Works,* Vol. I, p. 88 (1928).
(7) Zeuner, C.: *Grundzüge der mechanischen Wärmetheorie* (1877).

BRØNSTED'S CRITICISM OF CLASSICAL THERMODYNAMICS

F. H. MacDOUGALL

School of Chemistry, University of Minnesota, Minneapolis, Minnesota

Received February 16, 1940

Having had an opportunity of reading the preceding paper by Professor Brønsted on "The Derivation of the Equilibrium Conditions in Physical Chemistry on the Basis of the Work Principle", I feel that some reply should be made to his adverse criticisms of the concepts and methods of "traditional" thermodynamics. Professor Brønsted asserts that the concepts of traditional thermodynamics are characterized by a lack of clarity, that they result in incompleteness and awkwardness of treatment, and that they unavoidably lead to contradiction. In my opinion, such conclusions can result only from a complete misunderstanding of the concepts employed in traditional thermodynamics.

As might be expected, difficulty arises in connection with the concepts of heat and work. It is an unfortunate fact that most chemists and physicists, in thermodynamic discussions, often make use of expressions, borrowed perhaps from other fields of science, which are inaccurate or misleading if they are regarded as thermodynamic statements. The familiar remark that work done against frictional forces is converted into heat is an example of a misleading phrase. In classical thermodynamics, no attempt is made, nor is it considered useful, to subdivide the energy of a body into various forms such as the kinetic energy of translation and of rotation of the molecules and the kinetic and potential energies of atomic vibrations, although this procedure is highly desirable when studying the body from the standpoint of kinetic theory and statistical mechanics.

When two systems A and B are in contact, there may be a transfer of energy from one system to the other in one or more ways. For example, matter (containing energy) may pass from A to B or energy unaccompanied by matter may flow from A to B. In the latter case we speak of a transfer of heat or of work or of both, depending on the nature and the observed behavior of the two systems. If the transfer of energy from A to B is due solely to the fact that the temperature of A is higher (even infinitesimally higher) than that of B, then we say that energy in the form of heat has passed from A to B. Strictly speaking, it is only in the moment of its passing from A to B that the energy being transferred is called heat. We do not say that the energy was heat while it was in the system A nor that it is heat after it is added to the energy originally in B.

Similarly, if a set of weights on a piston brings about a compression of a gas, we say that the weights and the piston have done mechanical work on the gas or that energy has been transferred from the weights and piston to the gas in the form of work. We should not, however, say that the amount of work in the gas has been increased and that the amount of work possessed by the weights and the piston has been diminished, unless we are prepared to give the term "work" some new meaning. In the same way, it is not allowed to speak of the quantity of heat in a system, unless some additional, properly defined significance is given to the term "heat".

Professor Brønsted states that "traditional thermodynamics does not seem to recognize the fundamental difference between the problems of defining, on the one hand, amounts of heat *communicated*, i.e., added to or removed from a system through thermal conduction or radiation, and, on the other hand, heat *produced* or *consumed* within the boundary of the system itself." In view of the sense in which traditional thermodynamics uses the term "heat", the criticism of Professor Brønsted seems pointless. In traditional thermodynamics, changes in the properties of a system seem to be adequately described in terms of such well-defined properties as the energy, entropy, free energy, etc. of the system.

Professor Brønsted also remarks that "when an ideal gas expands irreversibly (into a vacuum?), the classical theory postulates the evolution of heat to be zero, because of the rise in temperature being zero. This interpretation cannot be maintained either, since the irreversible expansion . . . is accompanied by a loss of work and therefore, if the energy principle is to be fulfilled, must evolve heat." To this we must reply that the classical "theory" does not postulate the evolution of heat to be zero because the temperature change is zero but because no heat is observed to flow from the system to the surroundings. Moreover, if the system loses work, as Professor Brønsted asserts, then he is certainly not using the term "work" in the traditional sense. In the familiar statement of the energy principle, $dU = Q - W$, the heat and work terms must be defined in the traditional manner.

To illustrate Professor Brønsted's misunderstanding of the language of traditional thermodynamics, we may discuss his description of the compression of gas. "If by means of a weight falling through a certain distance an ideal gas of pressure p is compressed from the volume v to $v - dv$, it is claimed by classical thermodynamics that, owing to the rise in temperature, an evolution of heat takes place, which in the case considered has the value pdv. This well-known interpretation of the compression process, however, entirely overlooks the fact that on compression the gaseous system, i.e., the gas + the surrounding vacuum, has received an amount of work pdv, exactly equal to the loss of work accompanying the transport of the weight. Accordingly, if the energy principle has to be maintained, no room will be left for the additional production of energy such as the pretended evolution of heat would imply." The process described by Professor Brønsted is evidently supposed to be carried out adiabatically, so that it is simply not true that classical thermodynamics would claim that an evolution of heat had taken place. On the contrary, it would maintain that the evolution of heat was zero. It would describe the process by saying that a certain amount of energy was transferred from the weight to the gaseous system in the form of mechanical work, with the result that, at the conclusion of the process, the energy of the weight was decreased by the amount of pdv and the *energy* of the gas was increased by an equal amount. That the temperature of the gas rose during the process is merely a consequence of the relation between the energy and temperature of an ideal gas. If the compression of the gas had been carried out isothermally, then traditional and even modern thermodynamics would observe an evolution of heat, i.e., a flow of energy in the form of heat from the gas to the surroundings.

I submit that the meanings I have assigned to the terms "heat" and "work" are those employed by such masters of classical or traditional thermodynamics as Gibbs and Planck, and I deny that these terms as defined by them are characterized by lack of clarity or that they lead to inconsistencies or contradictions. Lack of clarity and contradictions appear only when Professor Brønsted, while ostensibly describing a process in classical or traditional language, uses the terms "heat" and "work" with meanings not recognized by classical thermodynamicists.

It is of course Professor Brønsted's privilege to assign to the terms he uses whatever meanings he considers to be most useful or advisable. It must be left to his readers to decide for themselves whether or not his proposed "work principle" and his derivation of a number of important physicochemical relations represent a thermodynamic method which is superior in any way to what I suppose he would call the traditional or classical method.

THE DIELECTRIC PROPERTIES OF THE SYSTEM GELATIN-WATER. II

HUGO FRICKE AND EDWARD PARKER

Walter B. James Laboratory for Biophysics, The Biological Laboratory, Cold Spring Harbor, Long Island, New York

Received September 20, 1939

In a recent paper, we described some of the polarizability properties exhibited by the system gelatin–water (2). These properties are essentially the same for the sol and the gel state and may be summarized as follows: Over the whole range of frequencies of 0.5 to nearly 10^5 kilocycles, for which measurements have been made, the dielectric constant increases as the frequency decreases, reaching values many times higher than that of water, at low frequencies, in systems of moderately high gelatin contents. The change in dielectric constant is associated with energy absorption. The variation of the dielectric constant and conductance increments with frequency can be represented rather closely by a power of the frequency law.

Orientation polarization of the gelatin appears to be of negligible importance for the polarizability of the gelatin–water system. The essential polarizability mechanism, which is present generally in dispersed systems (1), is believed to be concerted orientation of the polymolecular layer of loosely bound water molecules at the internal surfaces, an effect probably of the same nature as that underlying the polarizability rise observed in many dipolar solids near their melting points. Anomalous dispersion of a similar character may be found in adsorption films of other dipolar substances.

Our earlier work on gelatin dealt with systems of fairly high water contents. For our understanding of the underlying polarization process, observations on systems of lower water contents are desirable and such observations are reported in this paper.

EXPERIMENTAL PROCEDURE

The gelatin was the purified product of the Eastman Kodak Company. This gelatin contains about 13 per cent water. The gelatin content was determined as the weight obtained after heating at 90°C. for 2 days.

The change in internal structure, produced by a temporary exposure of the system gelatin–water to a higher temperature, affects (increases, if the heat treatment is not too intense) the polarizability of the system. The effect of the heating is irreversible, at least in a practical sense, when the temperature used is over 70°C. (approximately). It is important to recognize this in the present work, since we are unable to prepare homogeneous gelatin gels of low water contents except by the use of higher temperatures, and therefore the dielectric properties of these systems depend on the method of preparation used. Examples of this will be given below. We have made no systematic study of the effect of heating on the dielectric properties of gelatin, but we shall in the following limit ourselves to show observations on systems prepared under certain specified conditions.

In order to prepare a gel for measurement, finely cut gelatin was placed in the electrolytic cell, and the appropriate amount of water was added, whereafter the cell was sealed off and exposed to a suitable high temperature until perfect homogeneity was obtained. The gels were tested for homogeneity by determining the dry weight of different small portions of each.

The electrolytic cells were similar to those described earlier (1, 3). It is advantageous to use cells of different design, according to the gelatin concentration and range of frequencies studied. At low frequencies and at low gelatin concentration the electrode separation should be comparatively high to reduce the influence of electrode polarization. At high frequencies and at high gelatin concentration, cells with small electrode separation are required to avoid errors resulting from stray capacity.

All measurements were carried out at 21.0°C.

EXPERIMENTAL RESULTS

Figures 1A and 1B record results obtained on aged systems of different concentrations. The gelatin concentration is given as grams of gelatin per 100 grams of the system. The dielectric constant ϵ and conductivity increment κ^d are represented as functions of frequency, in a double logarithmic graph; the value κ^d is the difference between the conductivity κ at the frequency ω under consideration and at very low frequencies. The values ϵ and κ are defined by representing the complex impedance Z of a 1-cm. cube of the gelatin as

$$Z = \left(\kappa + j\,\frac{10\epsilon}{36\pi}\,\omega\right)^{-1}$$

The points representing κ^d lie closely on a straight line for each particular system. The points representing ϵ lie on a straight line for the systems of lower concentration, while a straight-line representation is obtained for all the systems tested, if, instead of using ϵ, we represent the increment in dielectric constant

$$\Delta\epsilon = \epsilon(\omega) - \epsilon(2\omega)$$

Thus, within the range of frequencies tested, the dielectric observations can be represented by the relations:

$$\Delta\epsilon \sim \omega^{-X}$$
$$\kappa^d \sim \omega^{Y}$$

The same type of relation was found for the systems of lower gelatin concentrations studied earlier (2).

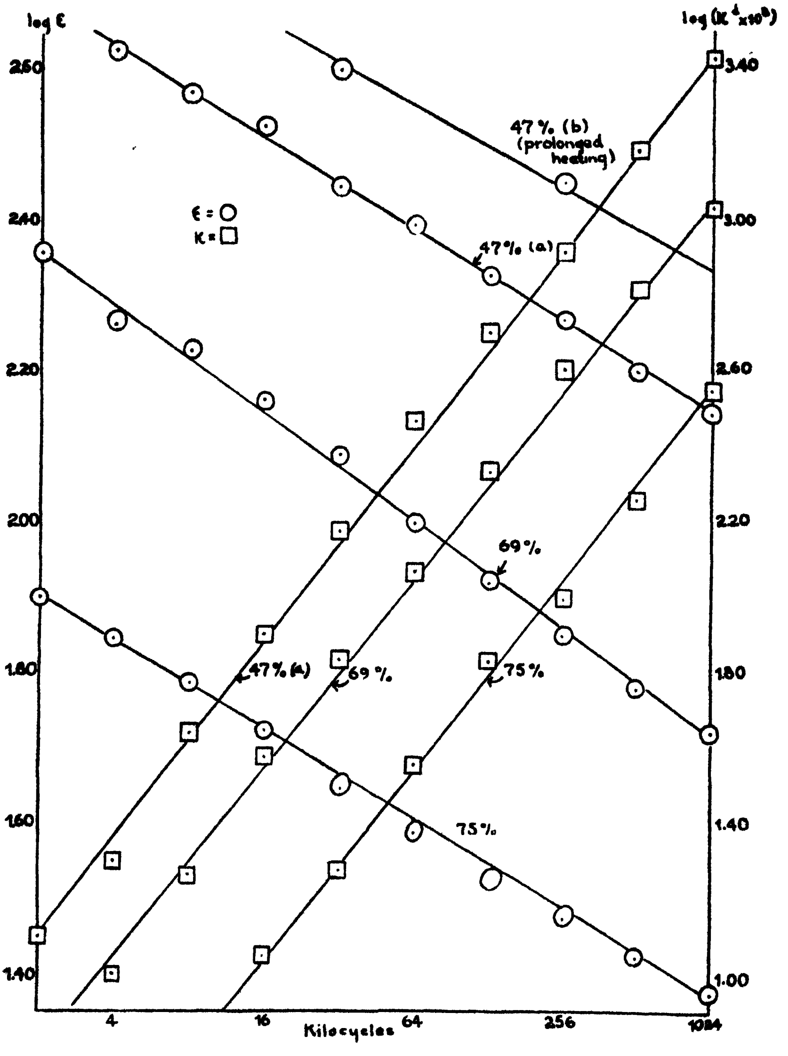

FIG. 1A. The dielectric constant ε (○) and conductance increment κ^d (□) as functions of frequency for aged gelatin systems of different concentrations. $[(\kappa^d = \kappa(\omega) - \kappa(0))]$. (1a) 47 g. gelatin per 100 grams; gelatin and water heated at 95°C. for 45 min. (1b) 47 g. gelatin per 100 grams; dried[1] gelatin and water heated at 95°C. for 89 hr. (2) 69 g. gelatin per 100 grams; gelatin and water heated at 95°C. for 18 hr. (3) 75.9 g. gelatin per 100 grams; gelatin and water heated at 95°C. for 45 hr.

---

[1] Original gelatin heated at 100°C. for 48 hr.

The values of X and Y show no apparent dependence on gelatin concentration. However, a small degree of dependence would be difficult to detect because of the lack of complete reproducibility of the results ob-

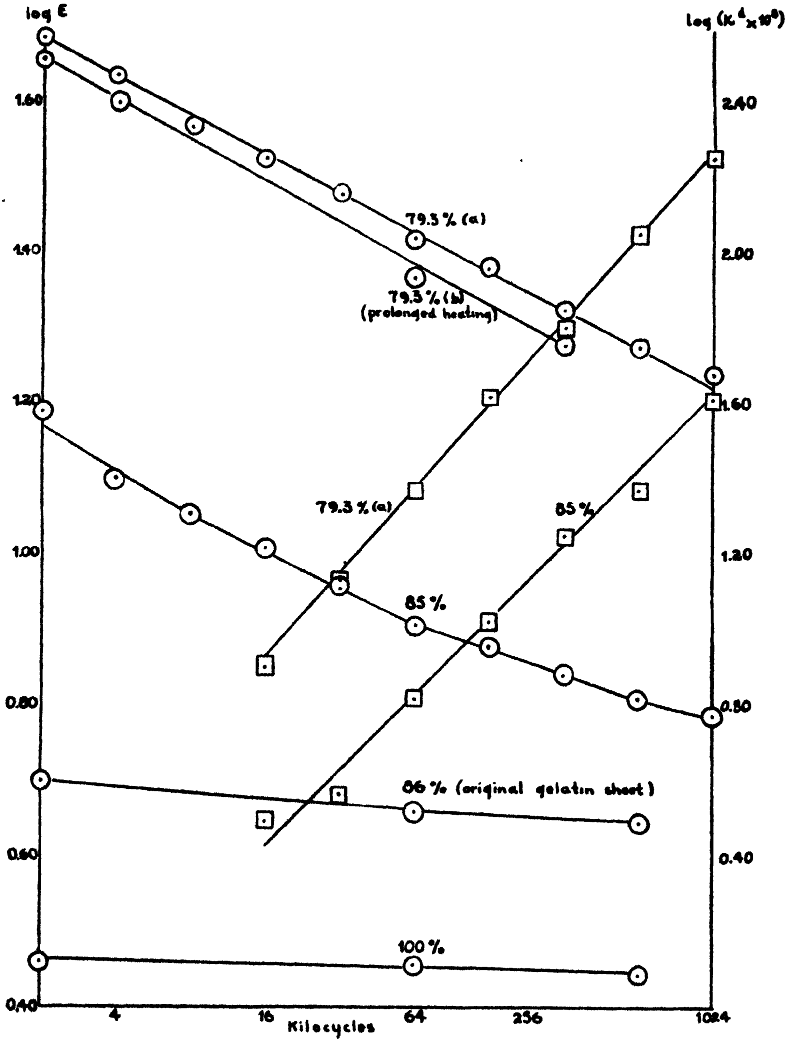

FIG. 1B. The dielectric constant ϵ (○) and conductance increment κ^d (□) as functions of frequency for aged gelatin systems of different concentrations. [$\kappa^d = \kappa(\omega) - \kappa(0)$]. (1a) 79.3 g. gelatin per 100 grams; gelatin and water heated at 95°C. for 14 hr. (1b) 79.3 g. gelatin per 100 grams; gelatin and water heated at 95°C. for 127 hr. (2) 85 g. gelatin per 100 grams; dried gelatin and water heated at 95°C. for 72 hr. (3) 86 g. gelatin per 100 grams; original gelatin sheet. (4) 100 g. gelatin per 100 grams; dried by heating at 100°C. for 48 hr.

tained for gels prepared at different times. This is shown in figures 1A and 1B by small irregular differences in the slope of the curves for the different systems represented. This lack of reproducibility seems to result, in part at least, from differences between different samples of the original gelatin.

The values of X for the systems shown in figures 1A and 1B lie around $X = 0.20$, while the values of Y lie around $Y = 0.80$. The values of X are lower and the values of Y higher than the values obtained for the gelatin used in our earlier work.

The dielectric constant of dried gelatin is nearly independent of frequency. The value at 512 kilocycles is $\epsilon = 2.68$, corresponding to a refractive index of 1.63. This value agrees quite closely with the refractive index observed in the optical region.

Figures 1A and 1B show a few examples of the way in which the dielectric properties of the gelatin systems depend on the heat treatments to which they have been exposed. In figure 1A the lower dielectric constant curve for 47 per cent gelatin is for a system prepared by heating the original gelatin with water at 95°C. for 45 min. The upper curve is for a system prepared by heating dried gelatin with water at 95°C. for 89 hr. This system remained fluid for more than 2 weeks and was measured in this state. The slope of the curves is the same for the two systems, within the limits of reproducibility, but the dielectric constant values of the more highly heated system are about 50 per cent higher than those of the less highly heated system. Figure 1B shows two series of experiments on 79.3 per cent gelatin. The upper curve is for a system prepared by heating at 95°C. for 41 hr.; the lower curve is for the same system after it had been exposed to this same temperature for an additional 86 hr. The effect of this prolonged heating is a decrease in the polarizability of the system.

The effect of heating on the dielectric properties of gelatin is particularly well brought out by the measurements on the original gelatin sheet, which are included in figure 1B. At the time these measurements were made, the gelatin had taken up a small amount of water in addition to that which it contained originally, and the water content was 14 per cent. Although, therefore, this sheet has nearly the same composition as the 85 per cent gelatin gel, which had undergone the regular prolonged heating, the polarizability of the sheet is very much smaller than that of the heated system.

A few words should be said about the dielectric properties exhibited by gelatin systems during the period of internal change following a temporary exposure to high temperature. If we plot instantaneous values of $\Delta\epsilon$ and κ^d against frequency in the double logarithmic scale of figures 1A and 1B, at different times during the transition period, a series of (approximately) straight lines is obtained, which move downward with time at a steadily decreasing rate. No systematic change in the slope of these lines with the aging of the systems could be seen, although small irregular changes were found in some cases.

Transitions involving a change from the sol to the gel state show no particular indication of this change in these dielectric graphs.

Within certain limits, the more intense the heat treatment, the higher the initial values of dielectric constant and absorption. The dielectric properties are reversible if the temperature is kept below 70°C. (approximately). With higher temperatures the heat treatment produces a permanent increase in the dielectric constant and absorption values, as far as can be judged from observations extending over a few weeks.

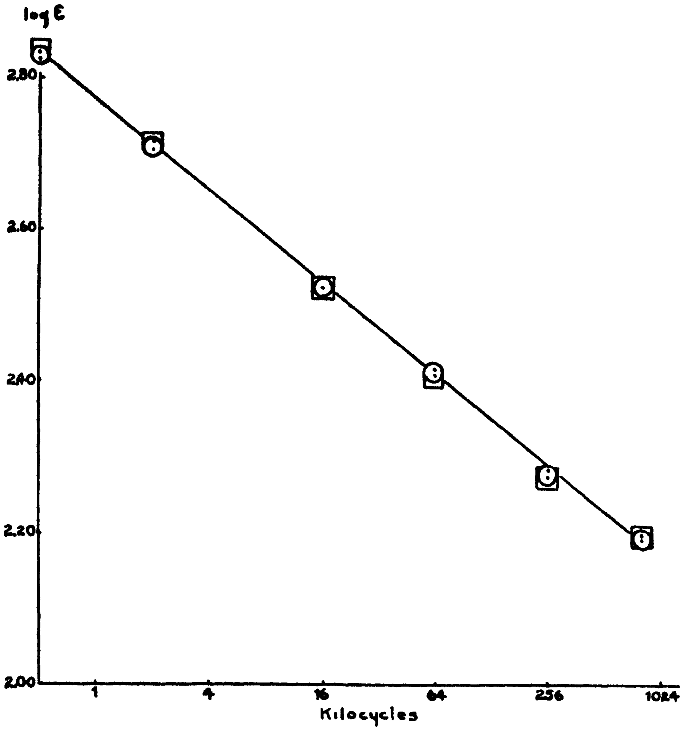

FIG. 2. The dielectric constant of 10 per cent gelatin heated at 78°C. for 17 hr. Observations made 2 hr. (○) and 7 hr. (□) after return to room temperature. During the first series of observations the system was in the sol state. The second series of observations were taken after gelatination had set in.

The correlation between the polarizability and the mechanical properties of the gelatin systems should be remarked upon. With increasing heat treatment, the gelatin becomes increasingly softer (finally passing into the sol state) and the polarizability increases correspondingly. With aging, the gelatin becomes harder and the polarizability decreases. The irreversible increase in polarizability resulting from intense heat treatment is bound up with a permanent increase in the degree of softness of the gelatin, and with sufficient exposure to high temperature the gelatin loses its power to gel and remains indefinitely in the sol state.

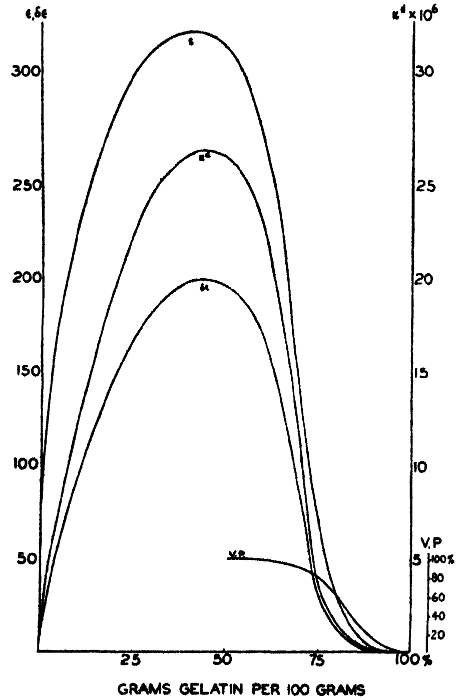

FIG. 3. The dielectric constant ϵ at 16 kilocycles, the dielectric constant increment $\delta\epsilon$ [$\delta\epsilon = \epsilon$ (16 kilocycles) $-$ ϵ (1024 kilocycles)] and conductance increment κ^d at 16 kilocycles [κ^d (16 kilocycles) $=$ κ (16 kilocycles) $-$ κ (0)] of the gelatin systems in figures 1A and 1B, represented as functions of gelatin concentration. The curve marked V.P. represents the pressure of water vapor over gelatin gels, according to measurements by Katz (4).

As just stated, our measurements so far show no distinctive features in the dielectric properties of gelatin sols as compared to the gels. Observations on sols were shown in our earlier paper (2). This work dealt with reversible systems, which were not exposed to temperatures over 50°C. The work was limited, therefore, to sols of low concentration and the measurements could be carried out over a rather narrow range of high frequencies only, owing to the error from electrode polarization present at lower frequencies. By heating to higher temperatures, sols of higher concentration can be prepared and it is possible to extend the measurements to lower frequencies. The results of dielectric constant observations on a 10 per cent gelatin sol are recorded in figure 2. The system was prepared by heating gelatin and water at 78°C. for 17 hr. One series of observations was carried out 2 hr. after the gelatin was returned to room temperature, at which time the system was still in the sol state. No observable difference in dielectric properties was found 5 hr. later, at which time gelatination had set in.

In figure 3 dielectric characteristics of some of the systems of figures 1A and 1B are represented as functions of gelatin concentration. The qualities shown are ϵ and κ^d at 16 kilocycles and the dispersion in dielectric constant as represented by $\delta\epsilon = \epsilon$ (16 kilocycles) $- \epsilon$ (1024 kilocycles). In addition to the data for the systems of figures 1A and 1B we have included in figure 3 the results of measurements on aged gels of lower concentration, prepared by dissolving gelatin in water at 50°C.

Even though the form of the curves of figure 3 depends to a great extent on the procedure used in preparing the gels, the curves exhibit certain general features which should be remarked upon. The addition of small quantities of water to gelatin—up to 10 to 20 per cent water—causes hardly any change in the dielectric properties. As more water is added the dispersion becomes rapidly more pronounced and reaches its highest value at about 45 per cent gelatin, whereafter the polarizability decreases with further addition of water. The small dielectric effect of the first addition of water to gelatin may be explained by the strong binding of this water by the gelatin. For comparison, we have shown in figure 3 the water vapor pressure over the gels, according to measurements by Katz (4).

DISCUSSION

We remarked above upon the correlation exhibited between the polarizability of a gelatin system and its mechanical properties, as the system is changed internally by a temporary exposure to high temperature. A more consistent relation is obtained by comparing the polarizability to the intermolecular forces, as represented by the volume of the system. Heat treatment results in expansion and increased polarizability. Aging results in contraction and decreased polarizability (for systems of low gelatin concentration the volume change is generally considered to result from a change in the forces between the gelatin and the water, i.e., it is supposed to represent the change in hydration). This relation gives also an explanation of the effect of acid and base on the polarizability of gelatin.

When the pH is changed from the isoelectric point, whether to higher or lower values, the gelatin expands and the polarizability increases.

The existence of a correlation of this type is indicative of orientation polarization. Because of the zwitter-ion character of the gelatin molecule, its moment may be high, and therefore it might appear likely that we are dealing with orientation of the gelatin molecule. The dielectric effect of adding water to gelatin would result, then, partly because the water increases the moment of the gelatin molecule and partly because the water loosens the forces between the gelatin molecules, thus facilitating the orientation of the gelatin molecules in the field.

In considering this hypothesis, we should keep in mind that the dielectric properties of the gelatin sol are essentially the same as those of the gel and, as regards the form of the dispersion curve and the high polarizability values reached at lower frequencies, these properties are of a type shown by dipolar systems in the solid rather than in the fluid state.[2] Obviously, therefore, the essential underlying dielectric mechanism is the same in the sol as in the gel and, if this mechanism is orientation polarization of the gelatin, the state of affairs in the sol must be wholly different from that found in simple solutions of dipolar substances, such as amino acids, whose dispersion properties can be, in the main, described by Debye's theory. Furthermore, since the polarizability of the gel is only slightly smaller than that of the sol, we should have to accept that there is no great change in the binding forces between the gelatin molecules as we pass from the gel to the sol state.

These considerations raise some doubt that orientation of the gelatin molecules can be responsible for the dielectric properties of the gelatin systems, and this doubt is increased in view of the fact that dielectric properties similar to those found for gelatin are observed when water is added to other high-molecular substances, such as cellulose or starch, whose molecules are not zwitter ions and can not be expected to be distinguished by particularly high moments (1). This indicates that the high polarizability of the gelatin systems is not conditioned by the possibly high moment of the gelatin molecule.

In our earlier paper (2) we discussed evidence indicating that the dispersion in gelatin and other high-molecular systems is a property of the water molecules at the internal surfaces. This hypothesis is supported by the observation that dispersion of a similar character is found much more strongly in more coarsely dispersed systems. The systems investigated include a number of different suspensions and colloids, and a sufficiently extensive study has been made to justify us in concluding that dispersion of the type found in gelatin is a general property of dispersed systems containing water as the dispersion medium (1). By studying the dielectric properties of suspensions as functions of particle size and volume concentration, it was possible to show that the dispersion is a surface effect and to obtain evidence that the region in which the dispersion resides lies in the water and is of multimolecular dimension.

---

[2] The dispersion in solids is often studied by measuring the anomalous charging current. Generally this is found to vary with time according to $i \sim t^{-m}$. From this it follows, theoretically, that the dielectric constant, as obtained from observation in an alternating field, varies inversely as a power of the frequency with an exponent equal to $1 - m$.

For the case of systems so highly dispersed as gelatin, the depth of the highly polarizable region would have to be much smaller than it is for suspensions. From the value of the gelatin concentration (45 per cent gelatin) at which the polarizability of the gelatin is a maximum it would appear that the layer is of the order of five water molecules thick. The small dielectric effect produced by adding as much as 10 to 20 per cent water to gelatin indicates that the strongly bound water molecules directly at the gelatin surface are without importance for the high polarizability of this layer, but that the effective water molecules are at some small distance from the gelatin. These molecules may differ from those in the bulk of the water only by an increased orientation with respect to the gelatin surface.

The simplest explanation of the decrease in polarizability which takes place when gelatin ages or when the pH is changed toward the isoelectric point is to assume a decrease in internal surface while the highly polarizable water layer at the remaining part of the internal surface is not greatly changed. This may not be a wholly correct picture. The aggregation which takes place in these processes may be caused not by direct forces between the gelatin molecules but by a kind of interlocking effect between the water layers of the different gelatin molecules. On this conception, the decrease in polarizability and associated contraction in volume should be connected with the increased rigidity of these interlocking water layers. We may hope that a more extensive dielectric study of gelatin will lead to a clearer understanding of the exact rôle played by these water layers in structural changes of the system.

SUMMARY

In continuation of earlier work (2), dielectric constant and electric conductance measurements were carried out on the system gelatin–water in the range of high gelatin concentrations (47 to 100 per cent gelatin) between 2 and 1024 kilocycles. The dielectric constant of dried gelatin is low and nearly independent of frequency ($\epsilon = 2.68$ at 512 kilocycles). The addition of water results in increased polarizability and strong anom-

alous dispersion which reaches its maximum value at approximately 45 per cent gelatin. At this concentration ϵ = *ca.* 500 at 2 kilocycles. The addition of the first 10 to 20 per cent of strongly bound water has little effect on the dielectric properties of the gelatin. The dispersion in dielectric constant and in conductance varies with frequency according to a power of the frequency law, as found earlier for systems of lower gelatin concentration.

The internal change produced in the gelatin–water system by a temporary exposure to high temperature results in increased polarizability, which is practically reversible only if the temperature used is not over 70°C. (approximately). Under the conditions studied, no distinctive features could be seen in the dielectric properties of the sols as compared to the gels. The change in polarizability resulting from heat treatment or from a change in pH runs parallel to the change in internal forces as represented by the change in volume. Contraction is associated with decreased polarizability, expansion with increased polarizability.

Anomalous dispersion, similar in character to that in gelatin, is found generally in dispersed systems containing water as the dispersion medium (suspensions, colloids, high-molecular solutions) (1) and appears to be a property of the polymolecular layer of loosely bound water at the internal surfaces. Dispersion connected with orientation polarization of the gelatin is, if present, not sufficiently pronounced to be detected in the presence of this greater effect, under the experimental conditions so far studied.

REFERENCES

(1) Fricke and Curtis: J. Phys. Chem. **41**, 729 (1937).
(2) Fricke and Jacobson: J. Phys. Chem. **43**, 781 (1939).
(3) Fricke and Parts: J. Phys. Chem. **42**, 1171 (1938).
(4) Katz: Kolloidchem. Beihefte **9**, 1 (1917).

CATALYTIC HYDROLYSIS OF CHLOROBENZENE IN THE VAPOR PHASE

ARTHUR A. VERNON[1] AND FRANCIS X. THOMPSON[2]

Department of Chemistry, Rhode Island State College, Kingston, Rhode Island

Received September 30, 1939

Owing to its commercial importance, the catalytic hydrolysis of chlorobenzene has been the subject of several patents. Jenkins and Norris (5) described a method of recirculating steam and chlorobenzene over silica gel at 550°C. They also found that passage of the vapors over copper shavings helped to maintain the catalytic activity of silica gel impregnated with metals. Lloyd and Kennedy (6) and Rittler (8) reported the formation of phenol from steam and chlorobenzene vapor by the use of silica gel and aluminum hydrosilicates. Groggins (4) describes the Raschig process for the formation of phenol from chlorobenzene and steam, using silica gel as a catalyst. The hydrochloric acid produced is used to chlorinate benzene by a regenerative process. He (3) also states that in pilot plant operations high yields of phenol have been obtained using silica gel as a catalyst. Bertsch (1) used catalysts with strong base-exchange properties for the same reaction, while Steingroener and Zellman (9) found that small additions of inorganic salts increased the catalytic activity of zinc oxide and aluminum oxide for the reaction. They found that the ratio of steam to hydrocarbon halide was important, and Lloyd and Kennedy (7) showed that an excess of steam increased the yield when catalysts such as silica gel, bauxite, and oxides of certain metals were used. Chalkey (2) steam-distilled chlorobenzene over silica gel and oxides of titanium, tungsten, zirconium, and aluminum. The highest yield of phenol was 68.5 per cent of the amount hydrolyzed when silica gel at 500°C. was the catalyst. Tishchenko, Gutner, Faerman, and Shchigelshaya (10) found that the most favorable temperature for hydrolysis of chlorobenzene was 500–600°C., using chlorides of calcium, strontium, barium, magnesium, and copper on silica gel.

In the course of some work on catalysis, it was desired to carry out experiments on hydrolysis in the vapor phase. The data obtained when chlorobenzene was used are presented in this paper.

---

[1] **Present address:** Department of Chemistry, Northeastern University, Boston, Massachusetts.

[2] **Present address:** Department of Chemistry, Seton Hall College, Newark, New Jersey.

EXPERIMENTAL

Material

The catalyst supports were silica gel of 8 to 12 mesh prepared by the Davison Chemical Company, activated alumina of 8 to 12 mesh supplied by the Aluminum Ore Company, and carborundum No. 8 furnished by the Carborundum Company. All chemicals used in the preparation of the catalysts were of C.P. grade. The chlorobenzene was used as obtained from the Eastman Kodak Company.

TABLE 1

Catalytic hydrolysis of chlorobenzene

CATALYST	TEMPERATURE	SPACE VELOCITY			YIELD OF PHENOL	CHLOROBENZENE HYDROLYZED	YIELD ON BASIS OF AMOUNT OF CHLOROBENZENE HYDROLYZED
		Steam	Chlorobenzene	Ratio			
	°C.				*per cent*	*per cent*	*per cent*
Al_2O_3 (alfrax).........	440	23,380	269	86.8	2.2	5.6	38.5
	510	24,965	499	50.0	1.0	3.72	27.0
	575	25,260	368	68.7	4.1	16.6	24.6
$Cu(NO_3)_2$ on SiO_2....	510	24,965	598	41.7	1.9	9.5	20.0
Cu_2Cl_2 on SiO_2	510	27,705	188	147.3	10.1	27.0	40.0
$SnVO_3$ on SiO_2 ...	440	24,350	844	28.8	0.8	2.0	40.0
	510	27,705	507	54.8	3.1	5.6	55.2

Catalysts

The oxide catalysts used were zinc oxide, nickel oxide, molybdenum trioxide, and titanium oxide on silica gel, as well as tungsten trioxide on alfrax, and magnesium oxide on silicon carbide. The salts tested were tin vanadate, cadmium phosphate, copper phosphate, copper nitrate, copper sulfate, and cuprous chloride on silica gel. Granular copper, a copper-cobalt mixture, silica gel, and alfrax were also tried.

Method

Water and chlorobenzene were introduced into a heated silica tube containing the catalyst. The exit gases passed through a water-cooled condenser and then through an absorption bottle containing standard potassium hydroxide. The amount of hydrolysis was determined from the hydrochloric acid produced, and the phenol by the iodophenol method.

Results

With the experimental set-up used the space velocities were necessarily high. Expressed as liters of gas at the reaction temperature per liter of catalyst per hour, the space velocity of chlorobenzene was varied between 25 and 5000, while the ratio of water to chlorobenzene at the different space velocities was varied between 10 and 150. The lowest temperature at which any activity was evidenced was 400°C. The highest temperature which could be used was 575°C., and at this temperature much carbonization was evident. The yield was favored by an increase of the water–chlorobenzene ratio and by a decrease in the space velocity with the ratio constant.

In the temperature range and space velocity variation given above the only catalysts besides silica gel which gave any more than 0.1 per cent of phenol were alfrax, copper nitrate on silica gel, cuprous chloride on silica gel, and tin vanadate on silica gel. Typical results for these catalysts are given in table 1.

Discussion

Under the conditions shown in table 1, silica gel gave a maximum yield of about 10 per cent phenol and a yield of about 60 to 70 per cent based on the amount hydrolyzed. The copper compounds which decompose do not give as good activity as cuprous chloride; this was substantiated by experiments with copper oxide and copper sulfate on silica gel. The per cent of hydrolyzed chlorobenzene which goes to phenol is as important as the per cent hydrolyzed. With aluminum oxide as the catalyst the per cent of chlorobenzene hydrolyzed increases with temperature, but the phenol yield does not increase proportionally.

Tin vanadate has not been reported before as a catalyst for this reaction. It seems to give a lower side reaction than many other substances and might bear further investigation. Data on space velocities are very scant in the literature, and from these results it is evident that they must be low to obtain a reasonable yield per pass.

SUMMARY

Experiments with a number of unreported catalysts for the hydrolysis of chlorobenzene have been made, and of these tin vanadate on silica gel has been found to be the best. Data on space velocities are presented which have not been reported in the literature before, and it is concluded that they must be fairly low for reasonable yields.

REFERENCES

(1) **Bertsch**: U. S. patent 1,966,281 (1931).
(2) **Chalkey**: J. Am. Chem. Soc. 51, 2489 (1929).

(3) GROGGINS: *Unit Processes in Organic Synthesis*, p. 630. McGraw-Hill Book Company, New York (1938).
(4) Reference 3, pp. 631–2.
(5) JENKINS AND NORRIS: U. S. patents 1,950,359 (1934) and 1,844,710 (1932).
(6) LLOYD AND KENNEDY: U. S. patent 1,735,327 (1929).
(7) LLOYD AND KENNEDY: U. S. patent 1,849,844 (1932).
(8) RITTLER: U. S. patent 1,936,567 (1933).
(9) STEINGROENER AND ZELLMAN: U. S. patent 1,961,834 (1931).
(10) TISHCHENKO, GUTNER, FAERMAN, AND SHCHIGELSHAYA: J. Applied Chem. (U. S. S. R.) 8, 685–94 (1935).

BOILING POINT RELATIONSHIPS AMONG ALIPHATIC HYDROCARBONS[1]

GUSTAV EGLOFF, J. SHERMAN, AND R. B. DULL

Research Laboratories, Universal Oil Products Company, Chicago, Illinois

Received October 3, 1939

INTRODUCTION

The boiling points of the paraffin, olefin, and acetylene hydrocarbons have recently been collated (3)[2] and evaluated critically. A correlation of the data, as dependent upon molecular structure, becomes important in order that its consistency may be checked and that boiling points for those compounds where data are lacking may be calculated with the same order of accuracy as the experimental data.

In 1842 Kopp (5) announced that in any homologous series the boiling point rises 18° for the addition of each methylene group to the molecule, but he soon recognized that the increase in boiling point became less with increasing size of the molecule; since then many attempts have been made to correlate the data. Each of these efforts need not be individually considered here. However, in order to show the diverse forms of boiling point equations used, a representative list is given in table 1.

Each of the equations given in table 1 has certain disadvantages which need not be considered in detail. In general, it may be said that the early workers frequently expressed the boiling point as a function only of the molecular weight, and consequently all isomers would have the same calculated boiling point. The data of this early period were too limited and unreliable to justify more elaborate formulae to calculate the boiling points of organic compounds.

---

[1] Presented before the Division of Physical and Inorganic Chemistry at the Ninety-eighth Meeting of the American Chemical Society, held in Boston, Massachusetts, September 11–15, 1939.

[2] The boiling point data in this paper are taken from reference 3.

Burnop (2) and Kinney (4) have calculated the boiling point of a compound in a manner analogous to the calculation of the molecular weight from the atomic weights,—i.e., they assign certain "boiling point numbers" to the different atoms such that the boiling point is a function of this additive variable. Unfortunately, the boiling points are not sensitive functions of the "boiling point numbers."

In the present study of thirty-one aliphatic series, a set of equations has been found which reproduce the data to within their experimental limits.

TABLE 1

Boiling point equations

EQUATION*	AUTHOR	YEAR
$\Delta = 18°$	Kopp (5)	1842
$T = AM^b$	Walker (8)	1894
$T = A\sqrt{M + B}$	Boggio-Lera (1)	1899
$T_{n+1} - T_n = \frac{144.86}{T_n^{0.0148\sqrt{T_n}}}$	Young (9)	1905
$T = a \log (bn + c) + 70/2^n$	Plummer (6)	1916
Quantity $M \log_{10} T + 8.0\sqrt{M}$ is additive.	Burnop (2)	1938
$T = 230.14\sqrt[3]{N} - 543$, where N is additive.	Kinney (4)	1938

* M = molecular weight; n = number of carbon atoms; T = boiling point in °K.; Δ = difference in boiling point between two successive compounds in an homologous series; a, A, b, B, c, N = empirical constants.

THE EMPIRICAL EQUATION

It has been pointed out by Wakeman (7) and others that the curves showing the dependence of boiling point upon the number of carbon atoms are very nearly parallel for various homologous series. If an equation for any one series can be found, then a satisfactory equation for any other will differ from this one only by an additive constant. The equation to use will be derived from the boiling point data of the normal paraffins, since these are the most reliable and include more compounds than any other series.

A plot of the boiling points against the number of carbon atoms of linear, logarithmic, and other scales suggests that an equation[3] of the following form will represent the dependence of T on n:

$$T = a \log (n + b) + k \tag{1}$$

---

[3] T is the boiling point and n the number of carbon atoms in the molecule. a, b, and k are the empirical constants to be evaluated. In this study T is expressed in

For convenience, ordinary Briggsian logarithms will be used.

Equation 1 may be expressed in several equivalent forms. The constant k can be incorporated into the logarithmic term, so that

$$T = a' \log (b'n + k') \tag{2}$$

the old constants being related to the new by the equations

$$a = a' \tag{2a}$$

$$b = k'/b' \tag{2b}$$

$$k = a' \log b' \tag{2c}$$

The boiling point may also be expressed as a function of the molecular weight, rather than as a function of the number of carbon atoms, as shown by equation 3.

$$T = a'' \log (M + b'') + k'' \tag{3}$$

M = the molecular weight. For paraffins

$$M = n\text{C} + (2n + 2)\text{H}$$

where C and H represent the atomic weights of carbon and hydrogen, respectively.

$$a = a''$$

$$k = a'' \log (\text{C} + 2\text{H}) + k''$$

$$b = \frac{b'' + 2\text{H}}{\text{C} + 2\text{H}} \text{ for paraffins}$$

$$= b''/(\text{C} + 2\text{H}) \text{ for olefins with one double bond, and}$$

$$= \frac{b'' - 2\text{H}}{\text{C} + 2\text{H}} \text{ for monoacetylenes, etc.}$$

In the present study equation 1 is used in preference to equations 2 and 3, because the parameters a and b can be kept constant for all of the thirty-one homologous series, only k varying from series to series.

EVALUATION OF THE CONSTANTS

The constants a, b, and k in equation 1 were evaluated by the method of least squares from the boiling points of the normal alkanes from ethane to nonadecane inclusive. The resulting equation 4 is

$$T = 745.42 \log (n + 4.4) - 416.31 \tag{4}$$

The agreement between the calculated and observed values is shown in table 2. Methane, the first member of the series, is inserted to indicate

---

degrees Kelvin. A shift to the Centigrade scale would merely change the constant k by 273.1°.

that its calculated boiling point is in marked disagreement with the experimental value.

The remarkably close agreement between the observed and calculated boiling points indicates the consistency of the data. The average deviation between the calculated and observed boiling points for the eighteen compounds from ethane through nonadecane ($C_{19}H_{40}$) is 0.40°. From butane to dodecane the mean deviation is only 0.05°. This is even smaller than the probable error of the data, and may therefore be fortuitous to some extent.

TABLE 2

Normal alkanes

$T = 745.42 \log (n + 4.4) - 416.31$

NAME OF COMPOUND	NUMBER OF CARBON ATOMS	T (OBSERVED)	T (CALCULATED)	ΔT
		°K.	°K.	°K.
(Methane)	(1)	(111.55)	(129.63)	(−18.08)
Ethane	2	184.6	184.6	0.0
Propane	3	230.9	231.6	−0.7
Butane	4	272.6	272.7	−0.1
Pentane	5	309.08	309.08	0.0
Hexane	6	341.88	341 80	+0.08
Heptane	7	371.53	371.52	+0.01
Octane	8	398.88	398.75	+0.13
Nonane	9	423.83	423.85	−0.02
Decane	10	447.1	447.2	−0.1
Undecane	11	468.9	468.9	0.0
Dodecane	12	489.3	489.3	0.0
Tridecane	13	507	508.4	−1.4
Tetradecane	14	524	526.5	−2.5
Pentadecane	15	543.6	543.6	0.0
Hexadecane	16	560.6	559.9	+0.7
Heptadecane	17	576	575.4	+0.6
Octadecane	18	590.0	590.2	−0.2
Nonadecane	19	603.1	604.3	−1.2

The constants 745.42 and 4.4 for a and b, respectively, in equation 1 are used in all the equations covering the other thirty homologous series of the aliphatic hydrocarbons, i.e., equation 5 is used where k is a constant to be determined for each series.

$$T = 745.42 \log (n + 4.4) + k \qquad (5)$$

The detailed data of the thirty other homologous series are shown in tables 3 to 32, inclusive. In many tables the first entry is given in parentheses, which signifies that the particular hydrocarbon was not considered in the evaluation of k but was inserted to show the limits of validity of the formula.

TABLE 3

2-Methylalkanes

$T = 745.42 \log (n + 4.4) - 424.51$

NAME OF COMPOUND	NUMBER OF CARBON ATOMS	T (OBSERVED)	T (CALCULATED)	ΔT
		°K.	°K.	°K.
(2-Methylpropane)	(4)	(260.9)	(264.5)	(−3.6)
2-Methylbutane	5	300.93	300.88	+0.5
2-Methylpentane	6	333.43	333.59	−0.16
2-Methylhexane	7	363.23	363.32	−0.09
2-Methylheptane	8	390.3	390.4	−0.1
2-Methyloctane	9	416.1	415.7	+0.4
2-Methylnonane	10	439.9	439.0	+0.9
2-Methylheptadecane	18	586	588.5	−2.5

TABLE 4

3-Methylalkanes

$T = 745.42 \log (n + 4.4) - 422.88$

NAME OF COMPOUND	NUMBER OF CARBON ATOMS	T (OBSERVED)	T (CALCULATED)	ΔT
		°K.	°K.	°K.
3-Methylpentane	6	336.43	335.23	+1.20
3-Methylhexane	7	364.9	364.95	0.0
3-Methylheptane	8	392.18	392.18	0.0
3-Methyloctane	9	417.3	417.28	0.0
3-Methylnonane	10	440.9	440.58	+0.3

TABLE 5

4-Methylalkanes

$T = 745.42 \log (n + 4.4) - 424.59$

NAME OF COMPOUND	NUMBER OF CARBON ATOMS	T (OBSERVED)	T (CALCULATED)	ΔT
		°K.	°K.	°K.
(4-Methylheptane)	(8)	(381.1)	(390.5)	(−9.4)
4-Methyloctane	9	415.59	415.57	+0.02
4-Methylnonane	10	438.8	438.9	−0.1

A summary of all the results given in tables 2 to 32, inclusive, is given in table 33. In this table the name of each series is given in column 1, the value of constant k in column 2, the average deviation between calculated and observed boiling points in column 3, and finally the difference

TABLE 6

2-Ethylalkanes

$$T = 745.42 \log (n + 4.4) - 423.01$$

NAME OF COMPOUND	NUMBER OF CARBON ATOMS	T (OBSERVED)	T (CALCULATED)	ΔT
		°K.	°K.	°K.
3-Ethylpentane	7	366.4	364.8	+1.6
3-Ethylhexane	8	392.0	392.0	0.0
3-Ethylheptane	9	416.2	417.2	−1.0
3-Ethyloctadecane	20	614	611.2	+3

TABLE 7

2,2-Dimethylalkanes

$$T = 745.42 \log (n + 4.4) - 435.34$$

NAME OF COMPOUND	NUMBER OF CARBON ATOMS	T (OBSERVED)	T (CALCULATED)	ΔT
		°K.	°K.	°K.
(2,2-Dimethylpropane)	(5)	(282.58)	(290.05)	(−7.47)
2,2-Dimethylbutane	6	322.83	322.77	+0.06
2,2-Dimethylpentane	7	352.43	352.49	−0.06
2,2-Dimethylhexane	8	380.1	379.72	+0.4

TABLE 8

2,3-Dimethylalkanes

$$T = 745.42 \log (n + 4.4) - 425.88$$

NAME OF COMPOUND	NUMBER OF CARBON ATOMS	T (OBSERVED)	T (CALCULATED)	ΔT
		°K.	°K.	°K.
2,3-Dimethylbutane	6	331.18	332.23	−1.05
2,3-Dimethylpentane	7	362.93	361.95	+0.98
2,3-Dimethylhexane	8	388.93	389.18	−0.25
2,3-Dimethylheptane	9	413.7	414.28	−0.6

TABLE 9

2,4-Dimethylalkanes

$$T = 745.42 \log (n + 4.4) - 431.31$$

NAME OF COMPOUND	NUMBER OF CARBON ATOMS	T (OBSERVED)	T (CALCULATED)	ΔT
		°K.	°K.	°K.
(2,4-Dimethylpentane)	(7)	(353.6)	(356.5)	(−2.9)
2,4-Dimethylhexane	8	384	383.8	+0.2
2,4-Dimethylheptane	9	408.9	408.9	0.0

between k for the normal paraffins and k for each of the other homologous series.

TABLE 10

2,5-Dimethylalkanes

$T = 745.42 \log (n + 4.4) - 431.91$

NAME OF COMPOUND	NUMBER OF CARBON ATOMS	T (OBSERVED)	T (CALCULATED)	ΔT
		°K.	°K.	°K.
2,5-Dimethylhexane	8	382.4	383.2	−0.8
2,5-Dimethylheptane	9	408.9	408.3	+0.6
2,5-Dimethyloctane	10	429	431.5	−2

TABLE 11

2,6-Dimethylalkanes

$T = 745.42 \log (n + 4.4) - 431.10$

NAME OF COMPOUND	NUMBER OF CARBON ATOMS	T (OBSERVED)	T (CALCULATED)	ΔT
		°K.	°K.	°K.
2,6-Dimethylheptane	9	407.6	409.1	−1.5
2,6-Dimethyloctane	10	433	432.4	+1

TABLE 12

3,3-Dimethylalkanes

$T = 745 \log (n + 4.4) - 430.10$

NAME OF COMPOUND	NUMBER OF CARBON ATOMS	T (OBSERVED)	T (CALCULATED)	ΔT
		°K.	°K.	°K.
3,3-Dimethylpentane	7	359.1	357.7	+1.4
3,3-Dimethylhexane	8	384	384.9	−1
3,3-Dimethylheptane	9	410.6	410.1	+0.5

TABLE 13

Miscellaneous dimethylalkanes

NAME OF COMPOUND	NUMBER OF CARBON ATOMS	T (OBSERVED)	T (CALCULATED)	ΔT
		°K.	°K.	°K.
2,7-Dimethyloctane	10	432.79	432.79	0.0
3,6-Dimethyloctane	10	433	433.0	0
7,8-Dimethyltetradecane	16	541.6	541.6	0.0

The mean deviation between the observed and calculated boiling points for the one hundred forty-three hydrocarbons tabulated in the thirty-one tables is 0.7°. This is the magnitude of the probable error of the data, and so the correlation of the boiling points with structure presented here may be considered to be satisfactory.

From equation 5, the difference in boiling points between two successive members of an homologous series is given by the equation

$$T_{n+1} - T_n = 745.42 \log \left(\frac{n + 5.4}{n + 4.4}\right)$$

TABLE 14

1-Alkene series

$T = 745.42 \log (n + 4.4) - 421.91$

NAME OF COMPOUND	NUMBER OF CARBON ATOMS	T (OBSERVED)	T (CALCULATED)	ΔT
		°K.	°K.	°K.
(Ethene)	(2)	(170.7)	(179.0)	(−8.3)
1-Propene	3	226.1	226.0	+0.1
1-Butene	4	267.0	267.1	−0.1
1-Pentene	5	303.3	303.4	−0.1
1-Hexene	6	336.48	336.20	+0.28
1-Heptene	7	366.2	365.9	+0.3
1-Octene	8	393.5	393.2	+0.3
1-Nonene	9	418.4	418.3	+0.1
1-Decene	10	443.5	441.6	+1.9
1-Dodecene	12	486	484.7	+1

TABLE 15

cis-2-Alkene series

$T = 745.42 \log (n + 4.4) - 416.31$

NAME OF COMPOUND	NUMBER OF CARBON ATOMS	T (OBSERVED)	T (CALCULATED)	ΔT
		°K.	°K.	°K.
(*cis*-2-Butene)	(4)	(276.86)	(272.67)	(+4.19)
cis-2-Pentene	5	309.6	309.1	+0.5
cis-2-Hexene	6	342	341.8	+0.2
cis-2-Heptene	7	372.1	371.5	+0.6
cis-2-Octene	8	398.6	398.7	−0.1
cis-2-Nonene	9	421.6	423.9	−2.3

This difference is dependent only upon n, the number of carbon atoms per molecule of the lowest boiling compound, and is independent of the particular series considered.

The dependence of the boiling points upon the structure of molecules containing a given number of carbon atoms is shown in the right-hand column of table 33, where the values of the constant k are given relative to k for the normal alkanes. These relative values of k signify the difference in boiling point between a given compound and the corresponding normal paraffin.

TABLE 16

trans-2-Alkene series

$T = 745.42 \log (n + 4.4) - 416.61$

NAME OF COMPOUND	NUMBER OF CARBON ATOMS	T (OBSERVED)	T (CALCULATED)	ΔT
		°K.	°K.	°K.
trans-2-Pentene	5	308.98	308.78	+0.2
trans-2-Hexene	6	341.2	341.5	−0.3
trans-2-Heptene	7	371.3	371.2	+0.1

TABLE 17

2-Methyl-1-alkene series

$T = 745.42 \log (n + 4.4) - 422.81$

NAME OF COMPOUND	NUMBER OF CARBON ATOMS	T (OBSERVED)	T (CALCULATED)	ΔT
		°K.	°K.	°K.
2-Methyl-1-propene	4	266.5	266.2	+0.3
2-Methyl-1-butene	5	304	302.6	+1
2-Methyl-1-pentene	6	334.9	335.3	−0.4
2-Methyl-1-hexene	7	364	365.0	−1
2-Methyl-1-heptene	8	392.4	392.3	+0.1
2-Methyl-1-octene	9	416	417.4	−1

TABLE 18

3-Methyl-1-alkene series

$T = 745.42 \log (n + 4.4) - 431.07$

NAME OF COMPOUND	NUMBER OF CARBON ATOMS	T (OBSERVED)	T (CALCULATED)	ΔT
		°K.	°K.	°K.
3-Methyl-1-butene	5	294.3	294.4	−0.1
3-Methyl-1-pentene	6	326.7	327.0	−0.3
3-Methyl-1-hexene	7	357.0	356.8	+0.2
3-Methyl-1-heptene	8	384.1	383.2	+0.9
3-Methyl-1-octene	9	409.7	409.1	+0.6

Of the four alkane series listed in table 33 in which there is only one branched chain—namely, the 2-methyl-, 3-methyl-, 4-methyl-, and 3-ethyl-alkanes—it may be noted that the boiling point lowering relative to the normal alkanes is of the same order of magnitude in each case, ranging from 6.57° for the 3-methylalkane to 8.28° for the 4-methylalkanes.

TABLE 19

4-Methyl-1-alkene series

$T = 745.42 \log (n + 4.4) - 428.21$

NAME OF COMPOUND	NUMBER OF CARBON ATOMS	T (OBSERVED)	T (CALCULATED)	ΔT
		°K.	°K.	°K.
4-Methyl-1-pentene	6	328.4	329.9	−1.5
4-Methyl-1-hexene	7	360.1	359.6	+0.5
4-Methyl-1-heptene	8	385.9	386.9	−1.0

TABLE 20

2-Methyl-2-alkene series

$T = 745.42 \log (n + 4.4) - 419.21$

NAME OF COMPOUND	NUMBER OF CARBON ATOMS	T (OBSERVED)	T (CALCULATED)	ΔT
		°K.	°K.	°K.
2-Methyl-2-butene	5	308	306.2	+2
2-Methyl-2-pentene	6	339.1	338.9	+0.2
2-Methyl-2-hexene	7	368.2	368.6	−0.4
2-Methyl-2-heptene	8	395.7	395.9	−0.2
2-Methyl-2-octene	9	419.3	422.0	−2.7

TABLE 21

2,3-Dimethyl-1-alkene series

$T = 745.42 \log (n + 4.4) - 431.11$

NAME OF COMPOUND	NUMBER OF CARBON ATOMS	T (OBSERVED)	T (CALCULATED)	ΔT
		°K.	°K.	°K.
2,3-Dimethyl-1-butene	6	327.1	327.0	+0.1
2,3-Dimethyl-1-pentene	7	357.0	356.7	+0.3
2,3-Dimethyl-1-hexene	8	383.6	384.0	−0.4

TABLE 22

2,4-Dimethyl-1-alkene series

$T = 745.42 \log (n + 4.4) - 431.60$

NAME OF COMPOUND	NUMBER OF CARBON ATOMS	T (OBSERVED)	T (CALCULATED)	ΔT
		°K.	°K.	°K.
2,4-Dimethyl-1-pentene	7	354.2	356.2	−2.0
2,4-Dimethyl-1-hexene	8	384.2	383.5	+0.7

The boiling points of paraffins containing two methyl side chains in the molecule which are not attached to the same carbon atom in the penultimate position along the main chain or to adjacent carbon atoms is inde-

TABLE 23

2,6-Dimethyl-2-alkene series

$T = 745.42 \log (n + 4.4) - 427.86$

NAME OF COMPOUND	NUMBER OF CARBON ATOMS	T (OBSERVED)	T (CALCULATED)	ΔT
		°K.	°K.	°K.
2,6-Dimethyl-2-heptene........	9	412.0	412.3	−0.3
2,6-Dimethyl-2-octene.... ..	10	436	435.6	+0.4

TABLE 24

3,3-Dimethyl-1-alkene series

$T = 745.42 \log (n + 4.4) - 437.71$

NAME OF COMPOUND	NUMBER OF CARBON ATOMS	T (OBSERVED)	T (CALCULATED)	ΔT
		°K.	°K.	°K.
3,3-Dimethyl-1-pentene........	7	350	350.1	0
3,3-Dimethyl-1-hexene	8	378.0	377.4	+0.6
3,3-Dimethyl-1-heptene... ..	9	401.9	402.5	−0.6

TABLE 25

4,4-Dimethyl-1-alkene series

$T = 745.42 \log (n + 4.4) - 435.41$

NAME OF COMPOUND	NUMBER OF CARBON ATOMS	T (OBSERVED)	T (CALCULATED)	ΔT
		°K.	°K.	°K.
(4,4-Dimethyl-1-pentene)......	(7)	(345.48)	(352.42)	(−6.94)
4,4-Dimethyl-1-hexene........	8	380.3	379.7	+0.6
4,4-Dimethyl-1-heptene.... ...	9	404.2	404.8	−0.6

TABLE 26

2,3-Dimethyl-2-alkene series

$T = 745.42 \log (n + 4.4) - 422.11$

NAME OF COMPOUND	NUMBER OF CARBON ATOMS	T (OBSERVED)	T (CALCULATED)	ΔT
		°K.	°K.	°K.
2,3-Dimethyl-2-pentene.	7	365.1	365.7	−0.6
2,3-Dimethyl-2-hexene...	8	393.3	393.0	+0.3
2,3-Dimethyl-2-heptene	9	418.6	418.1	+0.5

pendent of the relative position of these methyls, as is evidenced by *k* remaining approximately constant for these series. For 2,2-dimethylalkanes the boiling points are about 4° lower than for the corresponding members of the other dimethylalkanes.

TABLE 27

2,4-Dimethyl-2-alkene series

$T = 745.42 \log (n + 4.4) - 432$

NAME OF COMPOUND	NUMBER OF CARBON ATOMS	T (OBSERVED)	T (CALCULATED)	ΔT
		°K.	°K.	°K.
2,4-Dimethyl-2-pentene	7	356	356	0
2,4-Dimethyl-2-hexene	8	383	383	0
2,4-Dimethyl-2-heptene	9	408	408	0

TABLE 28

2,5-Dimethyl-2-alkene series

$T = 745.42 \log (n + 4.4) - 429.66$

NAME OF COMPOUND	NUMBER OF CARBON ATOMS	T (OBSERVED)	T (CALCULATED)	ΔT
		°K.	°K.	°K.
2,5-Dimethyl-2-hexene	8	385.4	385.4	0.0
2,5-Dimethyl-2-heptene	9	411	410.6	+0.4
2,5-Dimethyl-2-octene	10	435	433.9	+1.1

TABLE 29

Miscellaneous dimethylalkenes

NAME OF COMPOUND	NUMBER OF CARBON ATOMS	T (OBSERVED)	T (CALCULATED)	ΔT
		°K.	°K.	°K.
2,5-Dimethyl-1-hexene	8	384.7	384.7	0.0
2,6-Dimethyl-1-heptene	9	408.4	408.4	0.0
3,4-Dimethyl-1-hexene	8	378	378.0	0
3,5-Dimethyl-1-hexene	8	378.5	378.5	0.0
3,7-Dimethyl-1-octene	10	427	427.0	0

TABLE 30

1,2-Alkadiene series

$T = 745.42 \log (n + 4.4) - 407.75$

NAME OF COMPOUND	NUMBER OF CARBON ATOMS	T (OBSERVED)	T (CALCULATED)	ΔT
		°K.	°K.	°K.
Propadiene	3	238.79	240.19	−1.40
1,2-Butadiene	4	283.4	281.7	+1.7
1,2-Pentadiene	5	317.8	317.6	+0.2
1,2-Hexadiene	6	351.5	350.4	+1.1
1,2-Heptadiene	7	378	380.1	−2

The introduction of a double bond in the molecule affects the boiling point quite markedly. In the straight-chain molecules, a double bond in the terminal position lowers the boiling point (relative to the normal alkane) by 5° to 6°. A double bond in the 2-position (*cis*- and *trans*-2-alkenes) lowers the boiling point less than 0.5°.

TABLE 31

$C{=}C{-}(C)_x{-}C{=}C$ *series*

$T = 745.42 \log (n + 4.4) - 424.89$

NAME OF COMPOUND	NUMBER OF CARBON ATOMS	T (OBSERVED)	T (CALCULATED)	ΔT
		°K.	°K.	°K.
1,2-Propadiene	3	238.79	223.05	+15.74
1,3-Butadiene	4	268.38	264.09	+4.29
1,4-Pentadiene	5	302.6	300.5	+2.1
1,5-Hexadiene	6	332.70	333.22	−0.52
1,7-Octadiene	8	390.6	390.2	+0.4
1,8-Nonadiene	9	415.9	415.3	+0.6
1,9-Decadiene	10	443	438.6	+4
1,11-Dodecadiene	12	480	480.7	−0.7

TABLE 32

1-Alkyne series

$T = 745.42 \log (n + 4.4) - 413.81$

NAME OF COMPOUND	NUMBER OF CARBON ATOMS	T (OBSERVED)	T (CALCULATED)	ΔT
		°K.	°K.	°K.
Ethyne	2	189.5	187.1	+2.4
1-Propyne	3	245.6	234.1	+11.5
1-Butyne	4	281.0	275.2	+5.8
1-Pentyne	5	312.4	311.6	+0.8
1-Hexyne	6	344.0	344.3	−0.3
1-Heptyne	7	373	374.0	−1
1-Octyne	8	400.9	401.3	−0.4
1-Nonyne	9	424	426.4	−2
1-Undecyne	11	473	472.0	+1

For molecules containing one side chain, the difference between the boiling points of the olefin and the corresponding paraffin depends upon the relative positions of the double bond and the side chain. If the side chain is attached to one of the carbons forming the double bond, the boiling point of the olefin is higher than that of the paraffin. The 2-methyl-1-alkenes boil approximately 1.7° higher than the 2-methylalkanes, and the 2-methyl-2-alkenes boil about 5.3° higher than the 2-methylalkanes. On the other hand, if the side chain is attached to a carbon atom

TABLE 33

Values of the constant k for various hydrocarbon series

SERIES	k	MEAN DEVIATION	$k - k_{\text{normal alkanes}}$
	Alkanes		
Alkane	−416.31	0.40	0.0
2-Methylalkane	−424.51	0.36	−8.20
3-Methylalkane	−422.88	0.30	−6.57
4-Methylalkane	−424.59	0.06	−8.28
3-Ethylalkane	−423.01	0.50	−6.70
2,2-Dimethylalkane	−435.34	0.17	−19.03
2,3-Dimethylalkane	−425.88	0.72	−9.57
2,4-Dimethylalkane	−431.30	0.98	−15.00
2,5-Dimethylalkane	−431.90	1.13	−15.60
2,6-Dimethylalkane	−431.11	1.25	−14.80
2,7-Dimethylalkane	−430.67		−14.38
3,3-Dimethylalkane	−430.10	0.97	−13.79
3,6-Dimethylalkane	−430.46		−14.15
7,8-Dimethylalkane	−434.62		−18.31
	Alkenes		
1-Alkene	−421.91	0.46	−5.60
cis-2-Alkene	−416.31	0.70	0.00
trans-2-Alkene	−416.61	0.20	−0.30
2-Methyl-1-alkene	−422.81	1.30	−6.50
3-Methyl-1-alkene	−431.07	0.42	−14.76
4-Methyl-1-alkene	−428.21	1.00	−11.90
2-Methyl-2-alkene	−419.21	1.10	−2.92
2,3-Dimethyl-1-alkene	−431.11	0.27	−14.80
2,4-Dimethyl-1-alkene	−431.64	0.90	−15.33
2,5-Dimethyl-1-alkene	−430.40		−14.09
2,6-Dimethyl-1-alkene	−431.80		−15.49
3,3-Dimethyl-1-alkene	−437.71	0.40	−21.40
3,4-Dimethyl-1-alkene	−428.76		−12.45
3,5-Dimethyl-1-alkene	−436.56		−20.25
3,7-Dimethyl-1-alkene	−436.46		−20.15
4,4-Dimethyl-1-alkene	−435.41	0.60	−19.10
2,3-Dimethyl-2-alkene	−422.11	0.50	−5.80
2,4-Dimethyl-2-alkene	−432	1.0	−16
2,5-Dimethyl-2-alkene	−429.66	0.33	−13.35
2,6-Dimethyl-2-alkene	−427.86		−11.55
1,2-Alkadiene	−407.75	1.28	+8.56
$C{=}C{-}(C)_x{-}C{=}C$	−424.89	1.7	−8.54
	Alkyne		
1-Alkyne	−413.81	1.7	+2.50

at least one removed from the double bond, the boiling point of the olefin is less than that of the corresponding paraffin. For example, the 3-methyl-1-alkenes boil 8.2° lower than the 3-methylalkanes, and the 4-methyl-1-alkenes boil about 3.6° lower than the corresponding alkanes.

In the 2,3-dimethyl-2-alkene series, where both side chains are attached to the carbon atoms forming the double bond, the boiling point is 3.8° higher than that of the corresponding alkane, whereas in the 2,3-dimethyl-1-alkenes, where one of the side chains is attached to a carbon atom one removed from the double bond, the boiling point is 5.2° lower than that of the corresponding paraffin. When the double bond is in the 1-position and a methyl group is attached to a double-bonded carbon atom, i.e., in the 2-position, the boiling point is independent of the position of the other methyl group except when that group is in the 3-position, and is the same as that of the corresponding dimethylalkane. Thus, isomers of the n,n'-dimethylalkane series ($n + 1 \neq n'$ and $n' = 2$) and of the $2,n'$-dimethyl-1-alkene series have the same boiling points within experimental error. In the case of the $3,n'$-dimethyl-1-alkene group ($n' > 3$) the boiling point is independent of n' and all isomers boil at the same temperature, except members of the 3,4-dimethyl-1-alkene series. This exception is identical with that for the dimethylalkane series. The above rule does not apply to the dimethyl-m-alkene series with $m > 1$.

The effect of two adjacent double bonds in the molecule is shown by the boiling points of the 1,2-alkadienes being 8.6° higher than for the normal alkanes, and furthermore in table 31. In this table it may be noted that the difference between observed and calculated boiling points is large in the case of 1,2-propadiene and gradually decreases as the distance between double bonds increases. For 1,5-hexadiene and higher members of the series the difference is negligible. The large deviation between the observed and the calculated boiling points of 1,9-decadiene is probably due to experimental error.

The presence of a triple bond in the terminal position raises the boiling point relative to the normal alkanes about 2.5°.

The boiling point can be correlated with other physical properties, such as the molal volume and the mole refraction. Studies along this line are being made and will be reported at a later date.

SUMMARY

The boiling points of thirty-one homologous series of aliphatic hydrocarbons have been correlated by means of the equation

$$T = a \log (n + b) + k$$

the mean deviation between calculated and observed values being only 0.7° for the one hundred forty-three hydrocarbons considered.

In this equation k varies from series to series while a and b remain constant. The constants a and b were evaluated from the data of normal alkanes, the values being 745.42 and 4.4, respectively. The values for k were calculated for each series and the results reported.

Generalizations are given concerning the effect of the structures of the hydrocarbons of the different series on their boiling points.

REFERENCES

(1) Boggio-Lera, E.: Gazz. chim. ital. **29**, I, 441 (1899).
(2) Burnop, V. C. E.: J. Chem. Soc. **1938**, 826.
(3) Egloff, G.: *The Physical Constants of Hydrocarbons. Volume 1. Paraffins, Olefins, and Acetylenes.* Reinhold Publishing Corporation, New York (1939).
(4) Kinney, C. R.: J. Am. Chem. Soc. **60**, 3032 (1938).
(5) Kopp, H.: Ann. **41**, 79, 86, 169 (1842).
(6) Plummer, H. C.: Phil. Mag. [6] **32**, 371 (1916).
(7) Wakeman, R. L.: Rec. trav. chim. **53**, 832 (1934).
(8) Walker, J.: J. Chem. Soc. **65**, 193 (1894).
(9) Young, S.: Phil. Mag. **9**, 1 (1905).

LIGHT SCATTERING IN NORMAL HUMAN DENTINE[1]

The Calculation of Absorption and Scattering Constants

RICHARD S. MANLY,[2] JOHN F. BONNER, and HAROLD C. HODGE

Department of Biochemistry and Pharmacology, School of Medicine and Dentistry, University of Rochester, Rochester, New York

Received June 20, 1939

INTRODUCTION

In the transmission of light by opal glass and gelatin suspensions, the relatively coarse particles cause considerable light scattering in comparison with the absorption. Bloch and Renwick (1) found that the data are described empirically by an equation of the form

$$\log \frac{I_0}{I} = at^b \qquad (1)$$

where I_0 and I represent the intensities of the original and transmitted beam, respectively, a is the absorption coefficient, t is the thickness in centimeters, and b is an empirically chosen constant. From theoretical considerations, Channon, Renwick, and Storr (2) showed that the magnitudes of the coefficients of absorption and scattering may be calculated from an exponential series

---

[1] This work was supported in part by a grant from the Carnegie Foundation of New York.

[2] Present address: Chemical Division, Procter and Gamble Company, Ivorydale, Ohio.

$$\frac{I_0}{I} = Pe^{\lambda t} + Qe^{-\lambda t} \tag{2}$$

where P, Q, and λ are constants.

In order to evaluate the constants P, Q, and λ, and from these to obtain the coefficients of scattering (x) and absorption (k), Channon, Renwick, and Storr simplified Schuster's equation (reference 8, page 4, equation 12) for the intensity of emergent radiation through a foggy atmosphere. For ease of computation we have rewritten their equation (reference 2, page 228, equation 3) in the following form

$$\frac{I_0}{I} = \frac{(\lambda + k)^2 e^{\sqrt{k(k+s)}\,t} - (\lambda - k)^2 e^{-\sqrt{k(k+s)}\,t}}{4k\sqrt{k(k+s)}} \tag{3}$$

It is apparent that this expression has a form parallel to that of equation 2, and we can therefore write:

$$P = \frac{(\lambda + k)^2}{4\lambda k} \tag{4}$$

$$Q = -\frac{(\lambda - k)^2}{4\lambda k} \tag{5}$$

$$\lambda = \sqrt{k(k+s)} \tag{6}$$

In order to solve the equations for k and s, numerical values for P and Q are first obtained from equation 2 by assuming different values of λ, until optimum agreement with the data is obtained. By equation 4, k may be calculated from λ and P, and by equation 6, s may be calculated from λ and k. These values for k and s are dependent on assumptions of scattering by small particles (of molecular magnitude). Ryde and Cooper (7) and Silberstein (9) have derived comparable equations in which k and s values for scattering by large particles have been calculated. The latter equations give the same k and s constants as the former.

Although the scattering surfaces in dentine are cylindrical and not comparable directly to the particles in opal glass, nevertheless the transparency of normal dentine may be described by equation 1. Constants of absorption and scattering in dentine have been calculated from equation 3. The absorption constant of normal dentine is found to be comparable in magnitude to that of opal glass, while the scattering constant is about three times greater. The scattering is about three hundred times as important as absorption in decreasing the fraction of light transmitted by normal dentine.

EXPERIMENTAL

Materials

Five teeth having large areas of normal, unmodified dentine were ground roughly planoparallel to a thickness of about 2 mm. The transmission of light was measured in reproducible locations in the dentine and thickness determined at these areas, using a special ball-point micrometer. The slabs were then ground to successive thicknesses of approximately 1.0, 0.5, 0.2, and 0.1 mm. and remeasured in the same locations after grinding.

Apparatus

A galvanometer (Leeds and Northrup, sensitivity 0.003 milliampere per millimeter) was wired directly to a photocell (Weston, blocking layer) mounted on a 5 × microscope ocular by adhesive tape. A potentiometer was shunted across the galvanometer circuit to permit measurement of widely differing light intensities with the same accuracy.

Procedure

For a determination the section was covered with a few drops of water and a cover glass superimposed. The microscope without substage condenser was focussed, using a 4-mm. objective and illumination from a ribbon filament lamp adjusted to give approximately parallel light. The ocular of the microscope was replaced by the ocular with the photocell, the shunt resistance adjusted, and the reading and shunt resistance recorded. Without disturbing the lighting adjustment, a blank reading was made with the section pushed aside.

RESULTS

In figure 1 the optical densities per unit thickness are plotted as ordinates against the thicknesses of the tooth sections. With decreasing thickness, especially under 0.5 mm., there is a rapid increase in density per unit thickness. Obviously Lambert's law does not apply; however, the solid line, $\log I_0/I = at^{0.43}$, fits the data closely. The probable error of the constant a is 3.8 per cent, as calculated from the deviations in each tooth separately. The average deviation for I_0/I values in a given measurement is about 5 per cent; this may be ascribed to variation in relocating the area measured. This small error includes the biological variation within the tissue and indicates that the method is sufficiently accurate for comparison of histological changes in dental tissues of similar thicknesses. It is evident that normal dentine is a very uniform substance, since the variations from tooth to tooth are no greater than the experimental errors.

For normal dentine, the values for the scattering and absorption coefficients were calculated by the procedure outlined above. From the experimental values in figure 2, a preliminary curve (not shown) was drawn by inspection. Constants were obtained for equation 2 by successive approximation in the following manner: Values of λ between 0.2 and 1.0 were assumed and substituted in the equation; two sets of corresponding values for I_0/I and t, read from the preliminary curve, were also substituted, and the resulting pair of simultaneous equations was solved for P and Q. The solutions were tested graphically by comparison with the data. The best agreement was obtained when $\lambda = 0.50 \pm 0.05$, in which case, $P = 5$ and $Q = -4$. Solution by means of equations 4 and 6 gave a coefficient of absorption of 0.03 and a coefficient of scattering of 9.0 for normal dentine. The large variation in the optical density

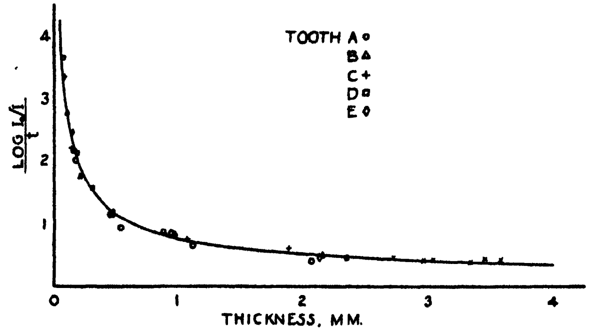

FIG. 1. Plot of optical densities per unit thickness against the thicknesses of the normal tooth sections

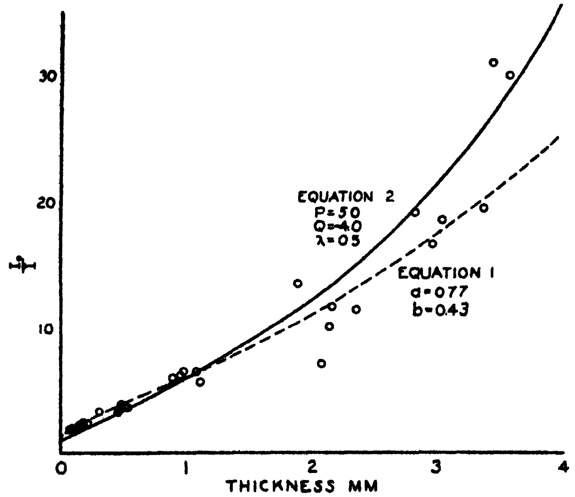

FIG. 2. Plot of I_0/I against the thickness of normal dentine

per unit thickness (figure 1) can be explained by the fact that the scattering coefficient is about three hundred times the absorption coefficient.

An attempt was made to correlate the data for a few areas of "transparent dentine" which represent pathologically changed tissues. The wide scatter of points at each thickness may be attributed to the variability in the extent of transformation from normal to transparent dentine. In figure 3 a dotted line has been drawn through the points of maximum transparency, representing the areas of greatest possible transformation. The dotted line, however, does not fulfil the theoretical condition of passing through 1.0 at zero thickness, because of reflections from the first and second surfaces of the tooth section. From the first surface about 2 per cent of the light is lost, while from the second a larger amount is rejected, depending upon the extent of scattering within the slab. To eliminate the error due to surface reflections, a solid curve computed from equation 2 has been drawn parallel to the dotted line. From the solid curve the values obtained for P, Q, and λ are 1.6, -0.6, and 0.13, respectively, giving a coefficient of scattering of 0.5 and a coefficient of absorption of 0.03 for dentine of "maximum" transparency.

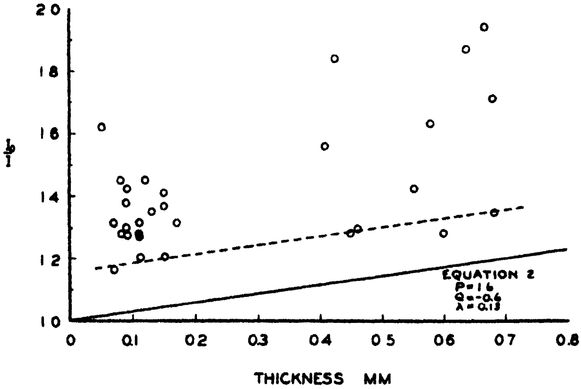

FIG. 3. Plot of I_0/I against the thickness of transparent dentine

DISCUSSION

The curves obtained from the equation of Channon, Renwick, and Storr (equation 2) and from the empirical formula (equation 1) are both shown in figure 1 for comparison with the data. Either describes about equally well the relation between opacity and thickness. This finding is in agreement with the results of Channon, Renwick, and Storr (2), who found that the empirical relation held over the entire range of their measurements on opal glass. The scattering coefficient of opal glass lies between those of normal and transparent dentine, but the absorption coefficients of the three substances are similar.

SUBSTANCE	ABSORPTION COEFFICIENT	SCATTERING COEFFICIENT
Normal dentine	0.03	9.0
Transparent dentine	0.03	0.5
Opal glass (2)	0.0566	3.350

The large amount of scattering in normal dentine is due to the tubular structure. In normal dentine a calcified matrix (n_D = 1.56) (5) surrounds minute tubules which contain an aqueous medium (n_D = approx. 1.3) and probably Tomes' fibers, which are hollow, pipe-like structures filled with liquid. The large difference between the refractive indices of the matrix and of the tubular fluid gives rise to the opacity of normal dentine. Experimental proof of this mechanism has been obtained by successively filling the tubules with media of increasing refractive indices (6). An increasing transparency was found with media of n_D from 1.3 to 1.56, and a decreasing transparency above 1.56. When the refractive indices of the matrix and of the tubule contents were the same, the transparency thus produced was maximal.

Any calcification of the tubules should decrease the scattering coefficient by tending to equalize the refractive indices of the matrix and tubules. In transparent dentine a deposition of calcific material in the tubules has been shown to occur (3, 4), and for this reason the constants derived from the curve in figure 3 are of especial interest. The absorption coefficient is practically the same as that of normal dentine, as would be expected. In contrast, the scattering coefficient is markedly decreased for transparent dentine. Although the amount of scattering is about one-twentieth that of normal dentine, the scattering coefficient is still sixteen times the absorption coefficient. A considerable scattering remains in transparent dentine, apparently either (*1*) because a layer of less refractive substance remains in the calcified tubules, or (*2*) because the tubules are not completely filled with calcific material.

SUMMARY

1. The empirical equation of Bloch and Renwick has been found to hold for the relation between transparency and thickness of normal dentine.

2. Absorption and scattering constants were calculated from the theoretical relation of Channon, Renwick, and Storr. The coefficient of scattering (9.0) for normal dentine is about three hundred times the absorption coefficient (0.03).

3. In transparent dentine, which has partially calcified tubules and

consequently less scattering surface, the scattering coefficient is one-twentieth that of normal dentine; the absorption constant, however, is not changed.

The authors acknowledge the assistance of Dr. J. Stuart Campbell and Dr. Brian O'Brien of the College of Arts and Science of the University of Rochester.

REFERENCES

(1) Bloch, O., and Renwick, F. F.: Phot. J. **56**, 49 (1916).
(2) Channon, H. J., Renwick, F. F., and Storr, B. V.: Proc. Roy. Soc. (London) **A94**, 222 (1917-18).
(3) Fish, E. W.: *An Experimental Investigation of Enamel, Dentine and the Dental Pulp*, p. 84. John Bale, Sons, and Danielson, Ltd., London (1933).
(4) Furrer, B.: Inaugural Dissertation, "Die Verkalkungszonen bei ber Denticaries," Zurich, 1922.
(5) Manly, R. S.: J. Am. Chem. Soc. **60**, 2884 (1939).
(6) Manly, R. S., and Simmons, E. J.: Unpublished data.
(7) Ryde, J. W., and Cooper, B. S.: Proc. Roy. Soc. (London) **A131**, 451 (1931).
(8) Schuster, A.: Astrophys. J. **21**, 1 (1905).
(9) Silberstein, L.: Phil. Mag. [7] **4**, 1291 (1927).

THE PRECIPITATION OF SILVER CHROMATE[1]

ANDREW VAN HOOK

Department of Chemical Engineering, University of Idaho, Moscow, Idaho

Received August 7, 1939

INTRODUCTION

In a recent contribution (24) to the theory of Liesegang ring formation, the necessity is pointed out for kinetic data on the formation of the banding precipitate. There is some information available in the literature (2, 5, 6, 7, 8) on the precipitation of silver chromate in gelatin medium, but none of it has been analyzed kinetically, and all represents the formation from equivalent concentrations of the forming ions. The situation when the ions are present in non-stoichiometric amounts is of primary importance for the complete interpretation of the Liesegang phenomenon in mind (23). For this ultimate purpose a kinetic study of the precipitation of silver chromate has been undertaken.

---

[1] Presented before the Division of Colloid Chemistry at the Ninety-eighth Meeting of the American Chemical Society, held in Boston, Massachusetts, September, 1939.

Part I deals with the precipitation in aqueous medium with equivalent concentrations of reactants; part II covers the case of non-equivalent ratios. These results will be extended to the gelatin medium in part III and presented in another paper.

METHODS

The course of reaction was followed by means of the silver electrode as described by Bolam (2). The comparison electrolyte was usually 0.01 *M* silver nitrate. Silver-ion concentrations were calculated from observed E.M.F.'s, employing the activity coefficients given by Kielland's modification (12) of Lewis and Randall's standard table. E.M.F.'s were read to the nearest 0.5 millivolt, and in some cases even closer. Supplementary results (15) were obtained conductimetrically but the potentiometric method is preferred because it is unique for silver-ion concentration and is independent of other ions confronted (4).

It is known that the pH of the environment exerts a marked effect on the precipitation of silver chromate from gelatin medium (7). The pH of the unbuffered mixed solutions as used in this work was between 5.8 and 6.0; in this range some of the eccentricities reported in the above reference are avoided. Much of the preliminary work was done at room temperature, but the results presented were obtained at 25°C. All reacting solutions were stirred well in excess of the threshold rate.

The effect of the addition of crystal seeds to the reacting system has supplied important interpretive results. The stock slurry used throughout the work was completely aged, and contained 6.7×10^{-5} moles of silver chromate per milliliter. By direct count[2] it contained 10^8 to 10^9 particles per milliliter, while the seed density calculated from the observed size (as spheres with major dimensions of 2 to 3 μ) is 0.3×10^9. Upon dilution of this stock slurry to an extent obtained in the experiments, no alteration could be observed during a period well in excess of the time consumed in an ordinary run.

Most of the exploratory work was done at concentrations equivalent to an ion product of 50×10^{-12}. At higher concentrations (200×10^{-12} and above) the reaction is too fast and adsorption effects become strong, while at lower values (10×10^{-12} and below) the reactions are too slow.

DATA

Part I

There has been considerable work done on the rates of crystallization of both soluble and insoluble solutes from solution (9, 21, 27), and in most of these experiments the precipitating material is formed without excess of the forming ions. The precipitation velocity can be represented as some function of the supersaturation, and the curve usually consists of a relatively flat induction period, followed by a rapidly decreasing portion. These two parts may be associated with the crystal nuclei formation and growth, respectively. Silver chromate is entirely normal in this respect (2, 5, 6, 7, 8, figure 1).[3]

---

[2] Courtesy of A. L. Anderson of the Department of Geology of the University of Idaho.

Figure 1 represents the precipitation of silver chromate from supersaturated aqueous solutions, the initial concentrations being designated as the value of the ion product, $H^0 = [Ag^+]^2[CrO_4^{--}]$, at zero time. The termination of the induction period is quite sharp and could usually be ascertained within 1 min. from inspection of the data. In other cases it is readily obtained by back extrapolation of the growth curve.

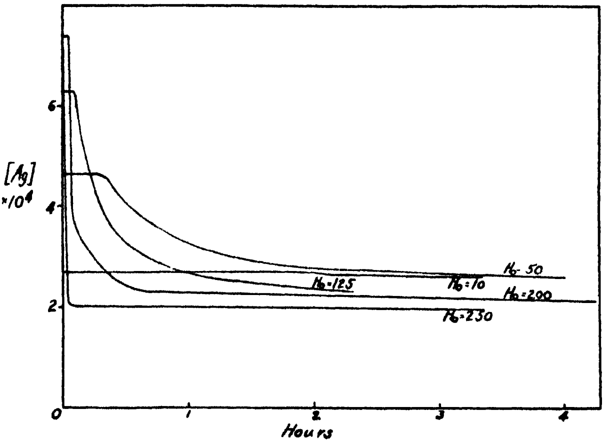

Fig. 1. Adjustment of silver chromate aqueous solutions

The progressive addition of seeds, at a definite H^0, continuously diminishes the length of the induction period and also accelerates the velocity during the main part of the curve. Figure 2 illustrates this. The effect of a constant quantity of inoculating seeds on the induction period as the initial concentration is changed is demonstrated in table 1.

Part II

All of the few papers published (11, 14, 17, 18) on the rate of precipitation of difficultly soluble materials from non-stoichiometric proportions of reactants are agreed on the induction period (J) being some function of the ion product. Jensen, working with calcium fluoride, represents the relation between J and H^0 as an empirical hyperbolic formula which reduces to JH^0 = constant over a considerable range (25). Odén's relation, for strontium sulfate and thallous chloride, in the nomenclature of this paper is $J^{\alpha}H^0$ = constant, where $\alpha > 3$. Kurbatov states that non-equivalent amounts of precipitating agents discourage new centers of crystallization; this is in harmony with the above type of equations.

---

[3] W. M. Fischer (Z. Anorg. Chem. **145**, 311 (1925); **153**, 62 (1926)) in two papers on the "Mechanism of Separation of Salts from Supersaturated Solutions" presents data of the type given here, but only for equivalent concentrations, over a much narrower range, and only for the induction period. The small induction periods (20 sec. at $H^0 = 50$) observed turbidimetrically vitiate, in the writer's opinion, the quantitative analysis attempted.

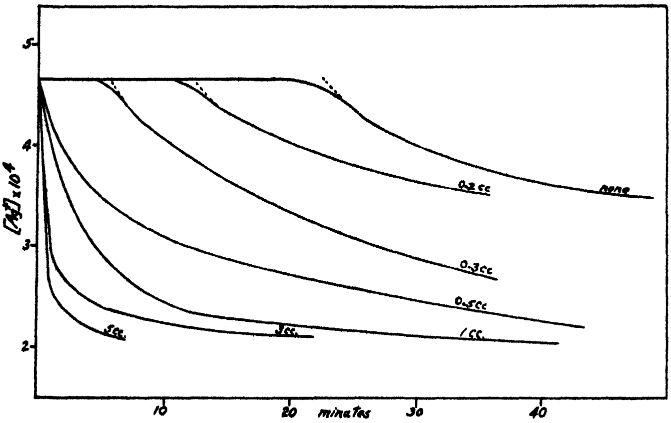

FIG. 2. Adjustment of silver chromate solutions in the presence of seeds. $H^0 = 50 \times 10^{-12}$ cc. of stock seed slurry added to 50 cc. of reaction volume.

TABLE 1

Effect of a constant quantity of inoculating seeds on the induction period as the initial concentration is changed

0.25 cc. of stock seed slurry added to 50 cc. of total reaction volume

H_0	J	$J(H_0 - K_{SP})$	H_0	J	$J(H_0 - K_{SP})$
	minutes			*minutes*	
25	16.5	346	100	4.5	432
50	9.3	427	125	3.5	426
75	5.8	412	150	3	438

The induction period for silver chromate, at a certain initial ion product value, remains unchanged when the concentrations of the reacting ions are varied, within reasonable limits. For $H^0 = 50$ and 75×10^{-12}, these limits of the ratio

$$\frac{\text{Equivalents AgNO}_3}{\text{Equivalents K}_2\text{CrO}_4} = R$$

are between 10 and 1/100, and between 10 and 1/50, respectively. Below the lower values the termination of the induction period is indefinite, and the seed generation curve is not as flat as previously. These effects become more pronounced at higher concentrations,– at $H^0 = 150$ the in-

TABLE 2

Induction period; non-stoichiometric ratio of reactants

RATIO R	VALUES OF J IN MINUTES			
	$H^0 = 50$	$H^0 = 75$	$H^0 = 100$	$H^0 = 150$
10:1	*ca.* 24	*ca.* 16	10.5	*ca.* 5
6:1	21			
5:1		15	10	6.5
3:1	19			
1:1	22	15	11	6.5
1:2	24		10	5.5
1:5	21.5	16	10.5	3.5
1:10	21	15 5		*ca.* 2
1:25	20		*ca.* 5	?
1:50	23	14	?	
1:100	*ca.* 23	?		

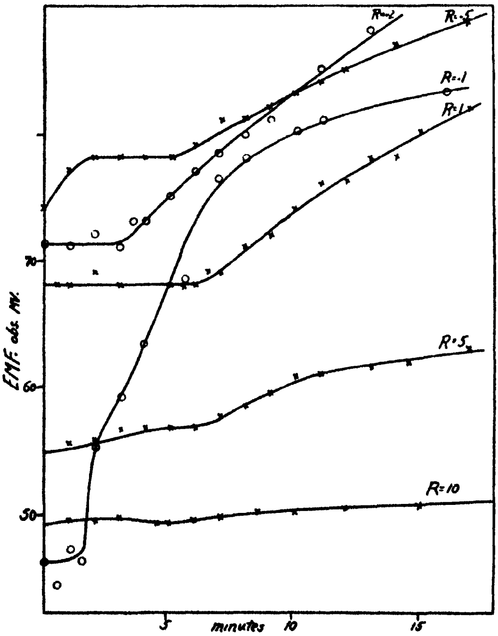

FIG. 3. Progress of non-stoichiometric reactions. $H^0 = 150 \times 10^{-12}$; no added seeds. $R = 0.1$, ordinate diminished by 40 millivolts; $R = 0.2$, ordinate diminished by 10 millivolts.

duction period becomes shortened and indefinite at $R = 1/5$. This behavior is illustrated in table 2 and figure 3. As R is made greater than 1, the percentage change in silver-ion concentration during reaction becomes smaller, and a ratio of 10 to 1 is about the maximum feasible to measure.

When R is varied over the range from 10 to 0.02, the results during the growth period are regular only for low initial concentrations (up to $H^0 = 50$). As H^0 is increased and R altered from 1, irregularities become pronounced. With excess chromate ion the curves tend to type b in figure 4, while with excess silver ion a waviness and pause is all that can be detected experimentally. These irregularities are direct evidence of what may variously be called adsorption, aggregation (17, 18), aging (13), ripening, etc. They are all undoubtedly manifestations of the same fundamental process, the operation of which obscures the primary rate of crystal growth.

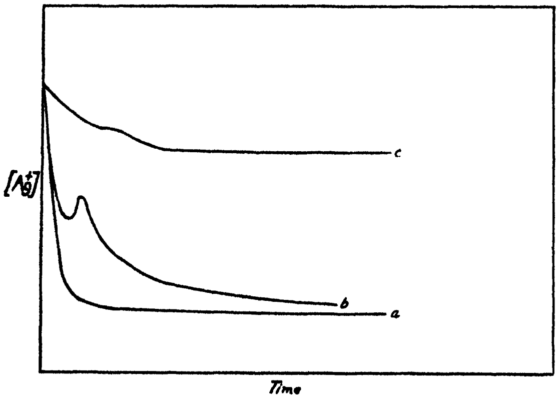

FIG. 4. Course of reaction at high concentrations. Curve a, $R = 1$; curve b, $R \ll 1$; curve c, $R \gg 1$.

DISCUSSION

Part I

The velocity equations which are found to represent the data of part I best are a first-order reaction for nuclei generation, followed by a second-order growth of each of these nuclei. The concentration is interpreted best in terms of supersaturation of silver chromate, $S = C - C_{\text{sat.}}$, where the C's are expressed as ion products and may be considered as proportional to the actual silver chromate concentration in the sense of the mass action law. In this same sense equation 1 is identical with von Weimarn's equation for the velocity of nuclei formation. The equations are:

$$\frac{dn}{dt} = k_1 S = k_1'(H - K_{SP}) \tag{1}$$

and

$$-\frac{dS_2}{dt} = k_2 n S^2 \qquad (2)$$

It is not improbable that a nucleus is, on the average, a conglomerate of a minimum number of molecules, and therefore

$$dn = -k_3 dS_1 \qquad (3)$$

The subscripts 1 and 2 designate the contributions of seed generation and growth, respectively, while n is the seed density.

The observed velocity of reaction will be the sum of the velocities of the two parts:

$$\frac{dS}{dt} = -\left(\frac{dS_1}{dt} + \frac{dS_2}{dt}\right) = \frac{k_1}{k_3} S + k_2 n S^2 \qquad (4)$$

(*a*) *Induction period.* The two parts of this equation were established independently. Experimentally each nuclei generation period is a zero-order reaction, but the change in induction period with initial concentration of reactants, with or without added seeds, is defined by a first-order change. For, if

$$\frac{-dS_1}{dt} = \frac{k_1}{k_3} S$$

$$-\int_{S_0}^{S_J} \frac{dS_1}{S} = \int_0^J \frac{k_1}{k_3} dt$$

$$\ln \frac{S_0}{S_J} = \frac{k_1}{k_3} J$$

Since S does not change materially during the induction period, we may approximate:

$$S_J = S_0 - \alpha$$

$$\ln \frac{S_0}{S_0 - \alpha} \simeq \ln\left(1 + \frac{\alpha}{S_0}\right) \approx \frac{\alpha}{S_0} = \frac{k_1}{k_3} J$$

$$S_0 J = (H_0 - K_{SP}) J = \text{const.}$$

Tables 3 and 1 approve this result.

When varying amounts of seeds are added at a given beginning concentration we may write, from equation 1,

$$\int_A^{n_J} dn = k_1 \int_0^J S\, dt$$

Since S remains practically unchanged during the induction period, and since n_J will be essentially a constant,

$$n_J - A = k_1 S_0 J$$

The family of curves in figure 5, whose empirical equation is

$$J = \frac{1050 \times 10^{-12}}{50}\left(1 - \frac{\text{ml. seeds}}{0.42}\right)$$

TABLE 3

Induction periods

$H^0 \times 10^{12}$	J	$(H^0 - K_{SP}) \times 10^{12}$
	minutes	
200	*ca.* 2	392
150	6.5	945
125	9	1090
100	11	1055
75	15	1065
50	22	1010
30	35	910
22	*ca.* 65	1170
20	67	1070
10	*ca.* 120	720
Average.		1050

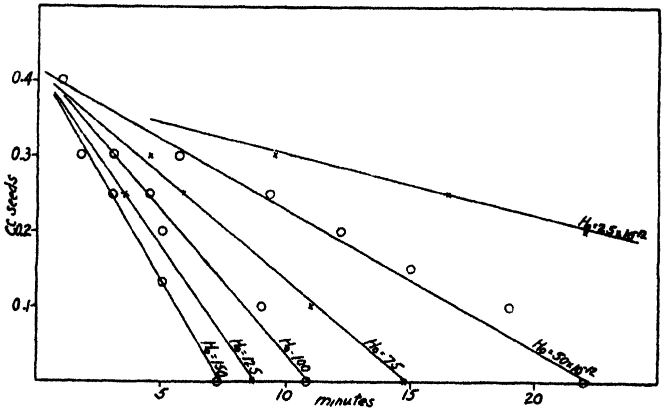

FIG. 5. Induction period *versus* cubic centimeters of stock seed slurry added per 50 cc. of reaction volume.

confirms this. Comparing these equations we may estimate the value of k_1 as 10^{15} to 10^{16}, the dimensions being the number of nuclei per cubic centimeter per minute per (unit ion product $- K_{SP}$). The best observations at $H^0 = 50$ indicate that the total decrease in silver-ion concentration over the induction period is of the order of 0.05×10^{-4} mole per liter. From this we may estimate $k_3 = 10^{14}$ to 10^{15} nuclei per mole of silver chromate. The reciprocal times the Avogadro number is tantamount to 10^8 to 10^9 molecules per seed crystal, which amounts to a spherical seed about 1 mμ in diameter. While this order of size is far in excess of that usually conceived as composing the elementary seed, it is interesting to note that it is the limiting size observed as necessary to promote crystallization from metastable solutions (1, 17, 18).

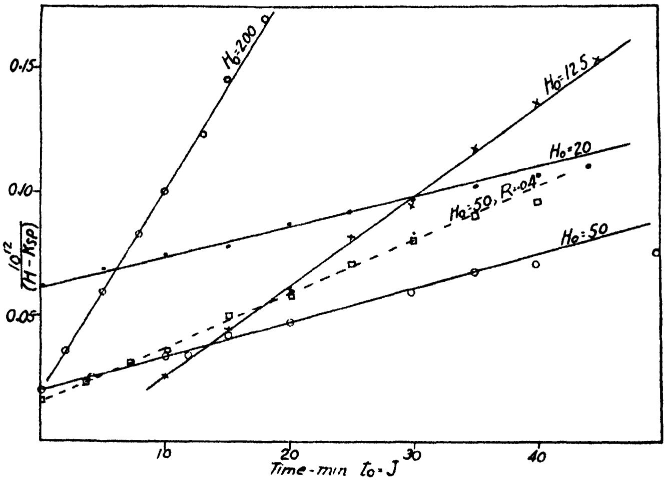

FIG. 6. Bimolecularity of growth period. No added seeds

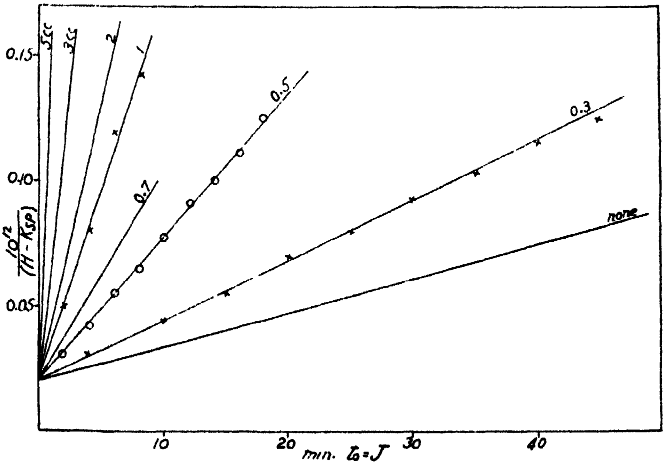

FIG. 7. Bimolecularity of growth period. $H^0 = 50 \times 10^{-12}$. Seeds added, cubic centimeters of stock slurry per 50 cc. of reaction volume.

(*b*) *Growth period.* Preliminary calculations suggested an approximate bimolecular mechanism in terms of the supersaturation as already defined. The bimolecularity is better the higher the initial concentration, and the greater the amount of added seeds. These behaviors are illustrated in figures 6 and 7. The reason for the deviations is unquestionably the effect of the number of seeds formed during reaction.[4] If the correct velocity expression for the growth portion of the curves is

$$\frac{-dS_2}{dt} = k_2 n S^2$$

and the seed density is large and constant, then the integrated curve is

$$\frac{1}{t}\left(\frac{1}{S} - \frac{1}{S^0}\right) = k_2 A$$

The left-hand side of this equation is the slope of the early part of the curves, and figure 8 demonstrates that it is linear in terms of added seeds.

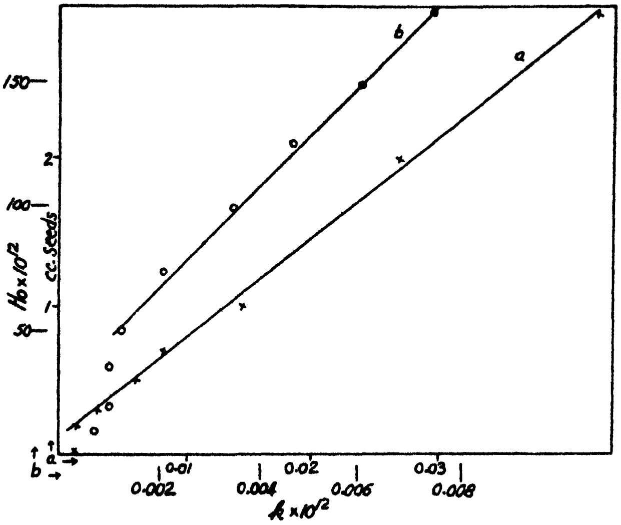

FIG. 8. (a) Bimolecular velocity constant *versus* cubic centimeters of stock seed slurry added per 50 cc. of reaction volume. (b) Bimolecular velocity constant *versus* initial concentration; no added seeds. Units of k are (unit ion product)$^{-1}$ (min.)$^{-1}$.

When A is zero or small, the effect of the seed generation factor can not be neglected. In this case it is best to express n as an implied function[5] of t (17, 18, 19, 20, 22, 26):

$$n = A + kSt$$

The complete differential equation describing the entire course of precipitation is then

$$\frac{-dS}{dt} = \frac{k_1}{k_2} S + k_2 A S^2 + k k_2 t S^3$$

---

[4] Campbell and Campbell's drifting unimolecular constants for barium succinate may be due to the same cause.

[5] The correct form of the expression $n = f(S, t)$ is not available or obvious. As n increases, aggregation and adsorption effects become pronounced.

This equation, and its approximation when $n = A + kS^0t$, are Ricatti type equations which can not be solved in finite terms; and the series integration is too cumbersome for practical use. If a further approximation in the form of

$$\frac{-\mathrm{d}S_2}{\mathrm{d}t} = k_2AS^2 + kk_2S^0tS^2$$

is made, the solution is

$$\frac{1}{t}\left(\frac{1}{S} - \frac{1}{S^0}\right) = k_2\left(A + \frac{kS^0t}{2}\right)$$

Qualitatively this correction will improve the constancy of the velocity constants in the latter part of the reactions, especially when A is small. This equation also demands an increase in value of the apparent bimolecular rate constant as the initial concentration is increased. This increase is roughly linear above $H^0 = 50$, according to curve b of figure 8. Quantitatively the equation is not exact, but this is to be expected in the light of its very approximate nature. It gives a fairly good half-life test over the range $H^0 = 10$ to 200.

Part II

The data of part II have been treated in the same way as already done for part I. In general, the same equations hold, but their range of validity is decreased as the ratio of reactant ions is altered from 1.

(*a*) *Induction period.* From table 2 it is concluded that the product S^0J remains equal to 1050×10^{-12} for reasonable values of R and values of S^0 up to 100, but begins to decrease thereafter. Apparently excess chromate ion exerts more of a disturbing effect than does excess silver ion, and this is to be expected with such a divalent anion. The operation of these adsorption factors also explains the wavy nature of the many curves obtained of types b and c in figure 4, and the fact that in some cases (figure 3, 5/1) a silver-ion concentration less than that permitted by the solubility product principle was observed. It also means that we can not expect very direct or clean-cut kinetic results for the growth period when H^0 is high and/or R very different from 1.

(*b*) *Growth period.* As anticipated, the rate of growth curves do not agree well with the foregoing analysis. It is surprising though, that the growth remains bimolecular in terms of S throughout a considerable portion of the growth period for values of H^0 up to 50×10^{-12}. The dashed line in figure 6, which is for the case $H^0 = 50$ with $R = 1/25$, is typical of the ranges $H^0 = 10$ to 50 and $R = 10$ to 0.02. The increase in the bimolecular velocity constant as R changes, for initial concentrations up to $H^0 = 50$, is displayed in figure 9. At higher initial concentrations a bimolecular constant increases rapidly as reaction proceeds, and more so the further from 1 the value of R. These cases have been considered empirically according to the general equation,

$$\frac{-dS_2}{dt} = kS^n$$

and the trend is to smaller values of n as H^0 increases, and to increasing values of k for a certain value of n as R deviates from unity. No general quantitative behavior has been detected.

A factor contributing to these increasing values of k and to the eccentric behaviors at higher concentrations is the fact that the chromate-ion concentration employed is one calculated from the observed silver-ion concentration decrease. While the Paneth–Fajans adsorption rule indicates that Ag^+ and CrO_4^{--} ions will be the principal ones adsorbed, it is not certain that the attending ions do not exert an effect. In the range where bimolecularity exists it is found experimentally that the addition of 5 to 10 times excess potassium nitrate does not disturb the velocity constants, while at higher concentrations large excesses cause further irregularities in the curves. Generally (16), adsorbed materials decrease the rate of crystallization, but this was found not always to be the case. Gapon (10) finds similar behavior with more soluble materials. However, at the high concentrations where this effect was observed, the adjustment of the Ag^+ and CrO_4^{--} solutions is undoubtedly controlled by adsorption rather than by simple crystal building. The deviations from a rather well-behaved bimolecular reaction strongly suggest that adsorption in-

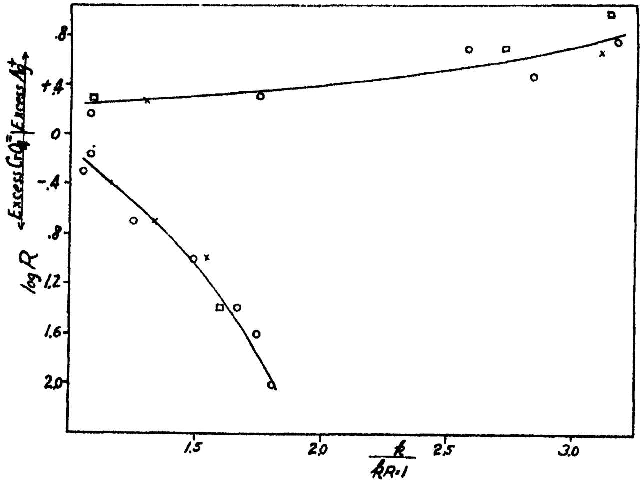

FIG. 9. Bimolecular velocity constant; non-stoichiometric ratio of reactants. ○, $H^0 = 50$; □, $H^0 = 25$; ×, $H^0 = 10$.

troduces disorder into an otherwise orderly mechanism. Such actions would explain why Campbell and Campbell (3) did not find a maximum in the rate of crystallization from supersaturated solutions.

It is expected that the simple expressions will be valid over a much larger range in gelatin medium, and therefore they may be applicable to the Liesegang ring problem already mentioned. Further analysis of the data available will be delayed until that time.

SUMMARY AND CONCLUSIONS

1. When silver chromate is formed from equivalent amounts of silver nitrate and potassium chromate in aqueous solution, the rate of adjustment of the solution may be represented as a two-step process: first, a unimolecular induction period during which the principal action is the generation of crystal nuclei; second, a bimolecular growth of these nuclei.
2. From non-equivalent solutions the velocity expressions are valid only over a narrow range. The deviations become more serious the greater the excess of either one of the reactants.
3. The complete velocity equation is not amenable to a simple treatment.
4. Adsorption, aggregation, etc., become pronounced at high supersaturations and high non-equivalence.
5. It is expected that the simple expressions will apply over a much larger range in gelatin medium.

REFERENCES

(1) Balarew, D.: Kolloid-Beihefte **50**, 1 (1939).
(2) Bolam, T. R.: Trans. Faraday Soc. **22**, 151, 162 (1926); **26**, 133 (1930); **29**, 864 (1933).
(3) Campbell, A. N., and Campbell, A. J. R.: Trans. Faraday Soc. **33**, 299 (1937).
(4) Cann, J. Y., and Mueller, G. B.: J. Am. Chem. Soc. **57**, 2525 (1935).
(5) Desai, B. N., and Nabar, G. M.: Trans. Faraday Soc. **28**, 449 (1932).
(6) Desai, B. N., *et al.*: J. Indian Chem. Soc. **11**, 45, 59 (1934).
(7) Desai, B. N., *et al.*: Proc. Indian Acad. Sci. **4A**, 468 (1936).
(8) Dhar, N. R., and collaborators: J. Phys. Chem. **28**, 41 (1924); Kolloid-Z. **34**, 270 (1924); Trans. Faraday Soc. **23**, 23 (1927).
(9) Freundlich, H.: *Kapillarchemie*, Vol. I, p. 456. Akademische Verlagsgesellschaft, Leipzig (1930).
(10) Gapon, E. N.: J. Russ. Phys. Chem. Soc. **61**, 1729, 2319 (1929); Ukrain. Khem. Zhur. **4**, 161, 505 (1929); Chem. Abstracts **24**, 2366, 5204, 5583 (1930); **25**, 5339 (1931).
(11) Jensen, A. T.: Z. physik. Chem. **A180**, 93 (1927).
(12) Kielland, J.: J. Am. Chem. Soc. **59**, 1677 (1937).
(13) Kolthoff, I. M.: J. Am. Chem. Soc. 1934 to date.
(14) Kurbatov, V.: Z. Krist. **77**, 164 (1931).
(15) Larkam, W.: Thesis, B. S. in Chemical Engineering, University of Idaho, 1939.
(16) Marc, R.: Z. physik. Chem. **61**, 385 (1908); **67**, 470 (1909); **68**, 104 (1909); **73**, 685 (1910).
(17) Odén, S.: Arkiv Kemi, Mineral. Geol. **9**, No. 23 (1925).

(18) Odén, S., and Werner, D.: Arkiv Kemi, Mineral. Geol. **9**, No. 32 (1926).
(19) Stranski, I. N.: Physik. Z. **36**, 393 (1935).
(20) Stranski, I. N.: In Jellinek's *Lehrbuch*, Vol. V, p. 870. Stuttgart (1937).
(21) Thiessen, P. A.: In Eucken-Jakob's *Der Chemie-Ingenieur*, Vol. I, Part 3, p. 170. Leipzig (1933).
(22) Thiessen, P. A., and Triebel, E.: Z. anorg. Chem. **179**, 267 (1929).
(23) Van Hook, A.: J. Phys. Chem. **42**, 1191 (1938).
(24) Van Hook, A.: J. Phys. Chem. **42**, 1201 (1938).
(25) Van Hook, A.: Northwest Sci. **13**, 45 (1939).
(26) Volmer, M.: Z. physik. Chem. **119**, 277 (1926); **125**, 151, 236 (1927); *Kinetik der Phasenbildung*, T. Steinkopff, Dresden (1939).
(27) von Weimarn, P. P.: Chem. Rev. **2**, 217 (1925).

INTERMICELLAR HOLE AND TUBE SYSTEM IN FIBER STRUCTURE[1]

H. MARK

Canadian International Paper Company, Hawkesbury, Ontario, Canada

Received June 3, 1939

I. INTRODUCTION

Combined chemical and physical investigations of various high-polymeric substances have led to the conviction that they are built up of very long chain-like molecules (3, 14, 27, 48, 68, 98, 100, 101). All kinds of information could be obtained regarding the average length of these chains, its distribution over the individual molecules, and its change by different chemical or physical treatment. In connection with these results the question was put forward (36, 37, 43, 50, 51, 63, 65) as to how the mechanical and optical properties of fibers and films consisting of high-molecular substances may be explained by the molecular picture of their fine structure. The first attempts to tackle this problem led to two divergent suggestions, which we can regard as extreme opposing points of view from which we may visualize our problem.

One can start with the idea that the crystallized regions which have been found by x-ray analysis,—the so-called *micellae,*—have the form of longish rod-like crystals with more or less regular surfaces and are arranged in the fibers or films similarly to the bricks in a wall. Figure 1a explains schematically this conception, which we might call the extreme micellar structure. It involves a very distinct difference between the space inside the crystal lattice (a, b) and outside of it (c, d); intramolecular and intermolecular volumes are to be clearly distinguished. Intramolecular swelling would mean that the penetrating molecules enter the crystalline ranges and are divided homogeneously over the whole material. Intermolecular swelling means that only the spaces (c, d) between the small crystals are accessible to the swelling agent, the inner structure (a, b) of the micelle itself remaining unchanged (45).

---

[1] Presented at the ninety-seventh meeting of the American Chemical Society, held in Baltimore, Maryland, April, 1939.

The other extreme possibility with regard to the structure of a high-molecular material is to assume that there is no formation of defined

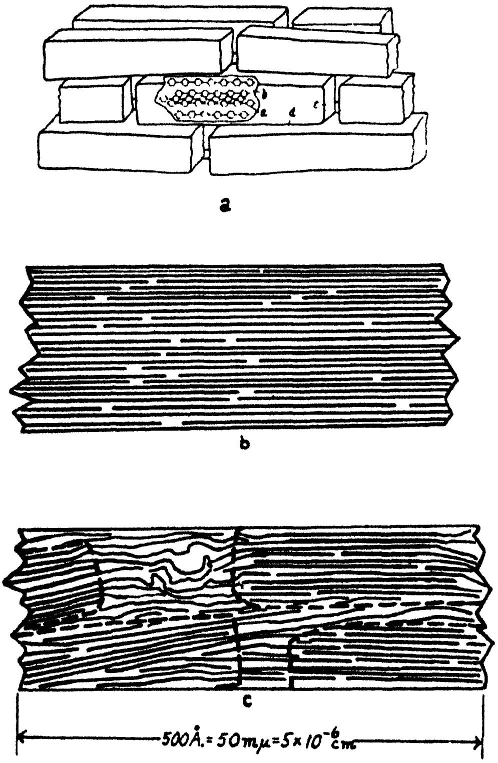

FIG. 1. Representation of the possible structures of high-molecular substances

micellae at all, the long main-valence chains forming a more or less compact mass in which it is impossible to point out certain regions of higher orientation. Figure 1b gives a sketch of this other extreme point of view, which might be called an extreme chain structure. This conception was brought forward by Astbury (3) and Staudinger (101).

In recent years new experimental evidence necessitated the abandonment of these two preliminary pictures and the working out of more detailed ideas as to the fine structure of high-polymeric substances in the solid stage.

In the following a short report of some experiments carried out since 1932 at the First Chemical Institute of the University of Vienna will be given; the aim was to learn something about the intermicellar spaces in natural and synthetic fibers. Figure 1c shows schematically the result, which may be regarded as lying between the two extreme conceptions represented in figures 1a and 1b.

The method used for this purpose was x-ray analysis, which has already given much valuable information about the crystallized portion of cellulosic samples. It may be justifiable to regard the study of this crystallized portion as more or less completed, and a recent very careful investigation by S. T. Gross and G. L. Clark (29) seems to have settled the last doubtful questions in this field.

As a result of a long series of scientific work started in 1918 (1, 3, 10, 29, 39, 40, 42, 46, 62, 76, 77, 81, 83, 84, 85, 89, 93, 94, 100) we can put forward certain lattices for the micellae of the native and mercerized cellulose which imply definite coördinates for all atoms in the elementary cell and describe the relative positions of the glucose residues and the main-valence chains in a more or less quantitative manner. But this picture excludes entirely the *non-crystallized* portion of the samples, and another series of publications has pointed out with increasing emphasis that this part which has escaped to date the direct attack of the x-ray method may also be of considerable interest, especially for the technical properties of the fibers (2, 8, 11, 15, 21, 28, 32, 36, 37, 38, 43, 51, 53, 54, 55, 60, 62, 66, 69, 70, 81, 97). Therefore the question was acute as to whether it would not be possible to get experimental evidence regarding the amorphous portion by making suitable x-ray investigations.

Two possibilities seem to offer themselves for tackling this problem: namely, (*A*) the direct x-ray analysis of the amorphous material in the fibers, and (*B*) the introduction of minute crystals in the intermicellar holes and their observation with x-rays. Let us consider these two ways and refer briefly to the results.

II. THE NON-CRYSTALLIZED PORTION OF CELLULOSE

A. X-ray study of the non-crystallized portion of cellulose

Although the x-ray method refers mainly to crystallized or semi-crystallized materials, its applicability has been lately extended to the study of the structure of liquids and amorphous solids. Following the ideas of Prins and Debye (16, 17, 49, 64, 90) a number of investigators have satisfactorily cleared up the structure of the liquid state by measuring the scattered x-ray radiation under different deviation angles (47, 49, 56, 64, 78, 87, 88, 91, 99, 102, 103, 104, 106, 108).

While crystals give the well-known sharp spot- or ring-diagrams, which indicate a high-molecular order in the samples investigated, liquids give diffused rings which show roughly that there is a certain order inside the investigated material but that it is distinctly inferior to the degree of orientation in crystals. But it turned out that the angular distribution of the scattered intensity furnished enough information to paint a picture of the molecular arrangement of liquids. From the point of view of experimental method, it was necessary to follow the *whole intensity curve* point by point and not to confine the measurements to the deviation angle of the intensive peaks. Hence the study of the liquids means to measure and discuss carefully and quantitatively the intensity of the diffused scattered radiation and not merely the deviation angles of the interference spots (16, 17, 90, 91).

If one attempts to apply this method to the diagrams of cellulose fibers, the first question will be whether enough diffused radiation can be observed to indicate that amorphous portions of considerable percentage are present.

A first and rough orientation about the problem in question showed that, in fact, practically all x-ray diagrams of natural and synthetic fibers show considerable blackening of the background even when one works with carefully filtered radiation and excludes altogether the scattering from other solid or gaseous material. This fact encouraged us to follow the way just briefly outlined here and to put forward for the investigation the following questions: (*1*) How large is the amorphous amount in different fibers? (*2*) Can its percentage be changed by mechanical or chemical treatment? (*3*) What do the diagrams show about the structure of the amorphous portions? We shall consider these three questions separately:

(*1*) Figure 2 shows the diagrams of three cellulosic samples, hemp, ramie, and a highly stretched viscose rayon yarn. In all three cases the same amount of matter (in grams) has been irradiated with filtered radiation. In fact, it can be seen quite clearly that the intensity of the interference spots is practically identical. Yet the amount of diffuse scattered radiation is entirely different. A similar effect is given in figure 3. Figure 3a shows a fiber spun from a viscose solution under certain stretching devices. One sees a clear fiber diagram but observes at the same time an appreciable amount of diffuse scattered radiation. If the fiber is swollen and extended about 60 per cent, it gives the diagram shown in figure 3b. One observes that the orientation of crystallized portions of the filament has slightly improved and at the same time the general background of the picture has decreased. If one stretches again to about 120 per cent elongation one gets the diagram in figure 3c, which shows another increase of the intensity of the interference spots and a decrease of the general blackening of the picture.

Another set of diagrams is shown in figure 4. A thread of cellulose hydrate was photographed (a), then extended in the swollen state and again photographed, after drying (b). One observes that the stretching increases slightly the orientation of the micellae and at the same time decreases very distinctly the general background of the diagram. The two other diagrams (c and d) show the same effect for ethylcellulose. This behavior reminds one very much of the well-known phenomenon

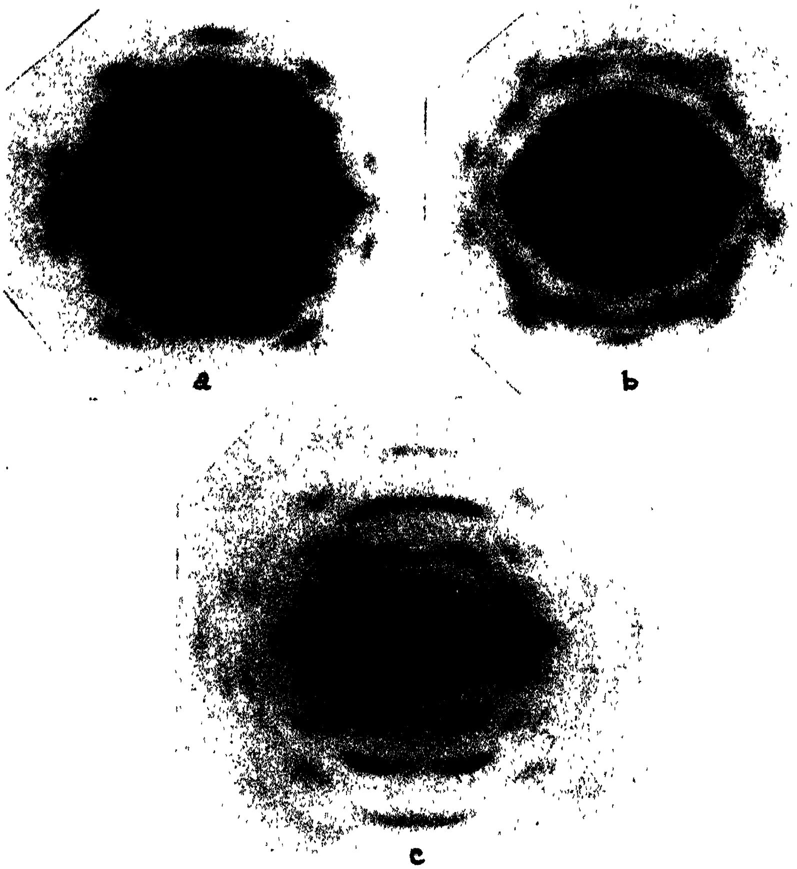

FIG. 2. X-ray diagrams of (a) a raw native hemp fiber, (b) a filament of refined native ramie, and (c) a highly oriented viscose rayon yarn.

which one gets when stretching rubber. As I. R. Katz (44, 45, 82) first observed, unstretched rubber gives the diagram of a liquid, while stretched rubber gives a distinct fiber diagram.

Figure 5a shows the monochromatic x-ray diagrams of unstretched rubber. Figure 5b represents a partially stretched sample, which shows very clearly the interference spots and at the same time the amorphous halo. Figure 5c was obtained from very much stretched rubber, while the sample together with the slit was rotated around the incident beam. One obtains a normal crystal powder diagram.

In the case of native cellulose it is not possible to swell a fiber so much with water that it does not give any interference spots at all, but if one applies stronger swelling agents, such as phosphoric acid, calcium rhodanide, or quaternary ammonium bases, one can convert the fiber diagram practically into the diagram of a liquid.

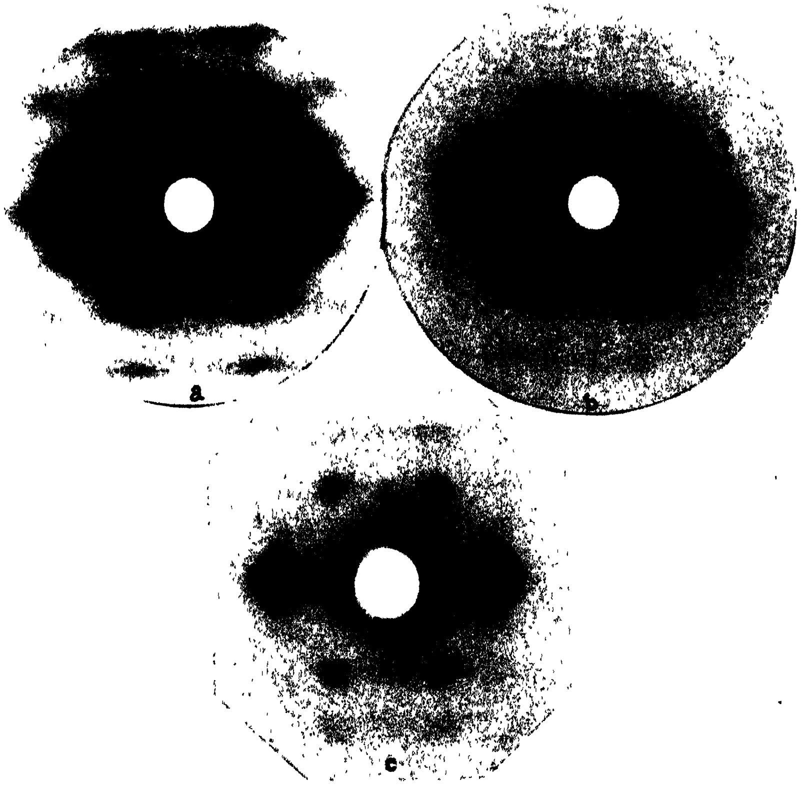

FIG. 3 X-ray diagrams of (a) a fiber spun from a viscose solution under certain stretching devices, (b) a swollen fiber extended about 60 per cent, and (c) a fiber stretched to about 100 per cent elongation.

Figure 6a shows a picture of the x-ray diagram of liquid water. Figure 6b is a diagram of a highly swollen cellulose filament which can be stretched and furnishes after the swelling the fiber diagrams shown in figures 6c and 6d.

All these experiments show us that beneath the crystallized portions each cellulose filament contains an appreciable amount of amorphous, or at least badly oriented, material. To estimate this amount careful intensity measurements must be carried out. It has already been mentioned that we have a rather complete knowledge of the cellulose lattice, owing to the recent work of G. L. Clark and his collaborators (29, 93, 100). This enables us to construct an ideal diagram of a fiber which consists of up to 100 per cent of crystallized cellulose. For this purpose we have to combine the different factors which together build up the intensity of an x-ray diagram.

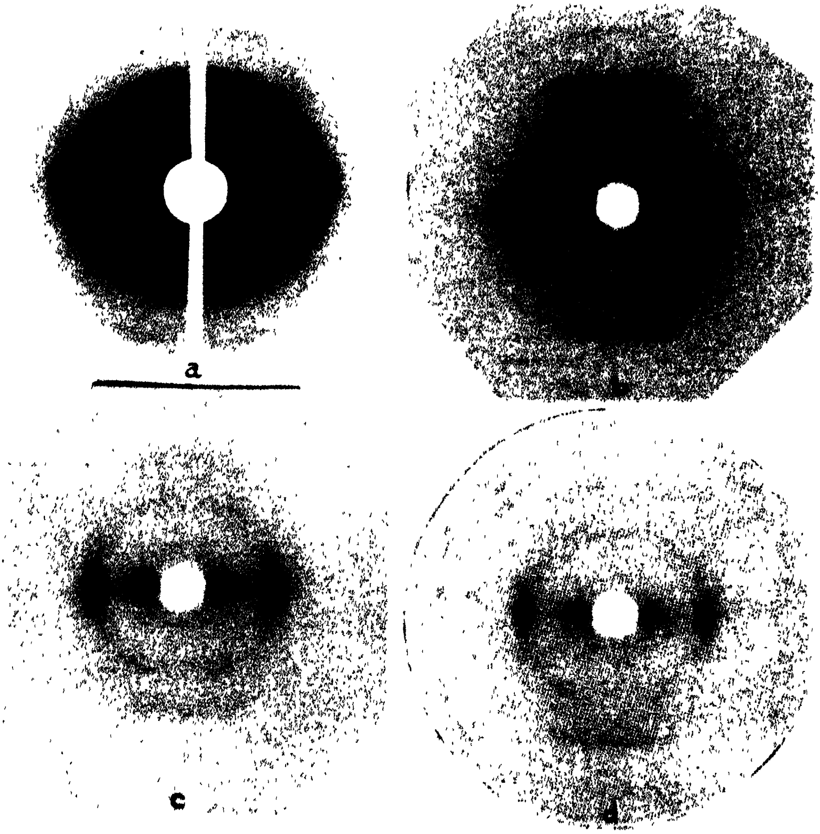

FIG. 4. X-ray diagrams of (a) a thread of cellulose hydrate, (b) the same after swelling and drying, (c) a thread of ethylcellulose before stretching, and (d) a thread of ethylcellulose after stretching.

Figure 7 shows how this has to be done in the case of cellulose. Figure 7a gives the intensities of the different reflections listed in table 1. The deviation angles are taken from the cellulose model which was recently and finally proved by G. L. Clark, and all intensity factors,—namely, the Lorentz, Debye, polarization, and frequency factors. Figure 7b shows the atomic form factor, which for the present case was taken as an average between the values of this factor for oxygen and for carbon.

The superposition of the two parts of figure 7 gives what we could call the "theoretical diagram of ideal crystallized cellulose." It is shown in figure 8b, while figure 8a gives the intensity distribution which one gets experimentally. The difference between the two can be seen very clearly.

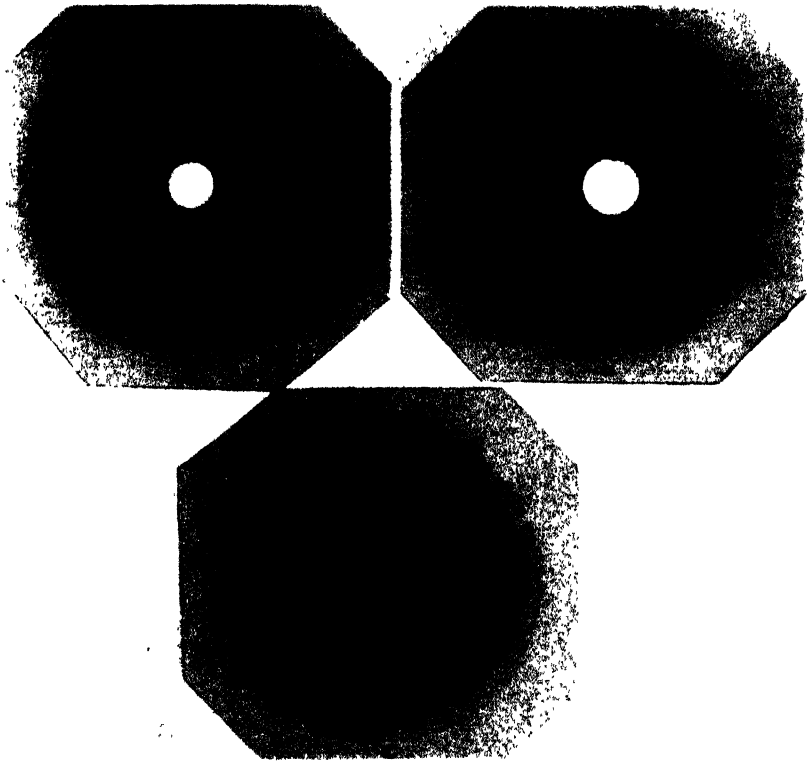

FIG. 5. Monochromatic x-ray diagrams of (a) unstretched rubber, (b) a partially stretched rubber, and (c) a highly stretched rubber.

There is much more diffuse scattered radiation in the actual sample than in the ideal diagram. The same effect is shown in figure 9, where one sees the original photoregistration curve of a native cellulose fiber. One observes distinctly the high amount of diffuse scattered radiation in the immediate neighborhood of the direct x-ray beam. The evaluation of these diagrams leads to the conclusion that in all natural and artificial cellulose filaments an appreciable amount of the total matter is present not in crystallized but in a more or less amorphous form.

(2) During these studies it turned out that in a normally settled viscose filament only about 40 per cent of the fiber is crystallized and 60 per cent amorphous, while at the end of the stretching about 70 per cent is crystallized and the rest amorphous. This shows us that even in the case of apparently good x-ray diagrams a large amount of the material which forms a sample is not in its crystallized state.

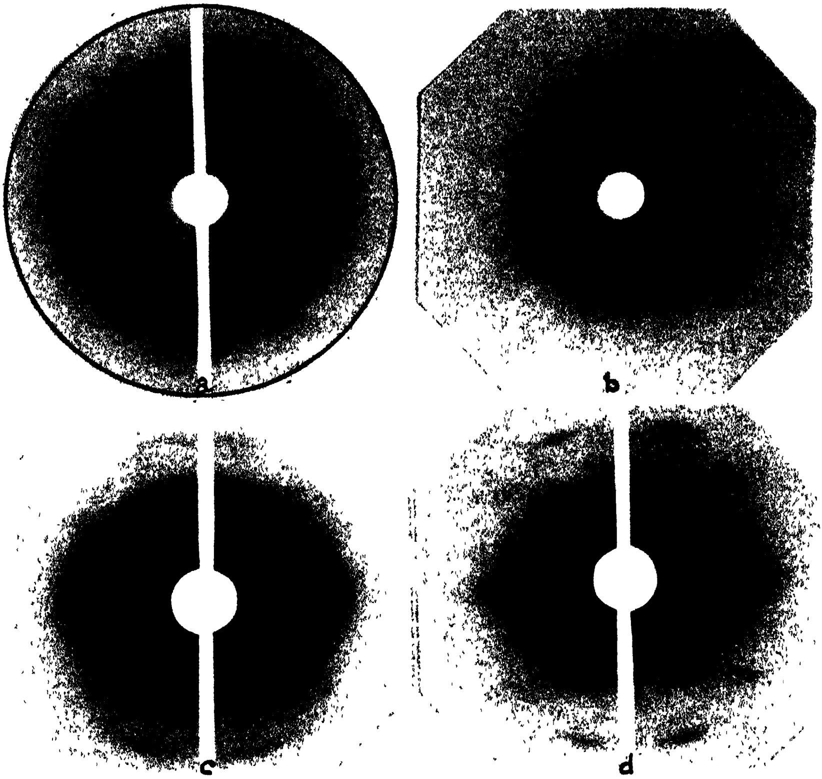

FIG. 6. X-ray diagrams of (a) liquid water, (b) a highly swollen cellulose filament, and (c) and (d) the highly swollen cellulose filament after stretching.

At the same time these experiments show that a cellulose thread undergoes a similar process during stretching to that which a rubber sample does. It suffers a partial conversion of the amorphous state into the crystallized. Of course, this change is not as reversible as with rubber and very much less pronounced, but it was observed by several authors (27, 36, 37, 38, 52, 53, 54, 67, 97, 98) and there can be no doubt that mechanical and chemical treatment changes the relative amounts of the crystallized and amorphous part in a cellulose sample. This effect appears to a greater degree in cellulose derivatives than in cellulose itself, appar-

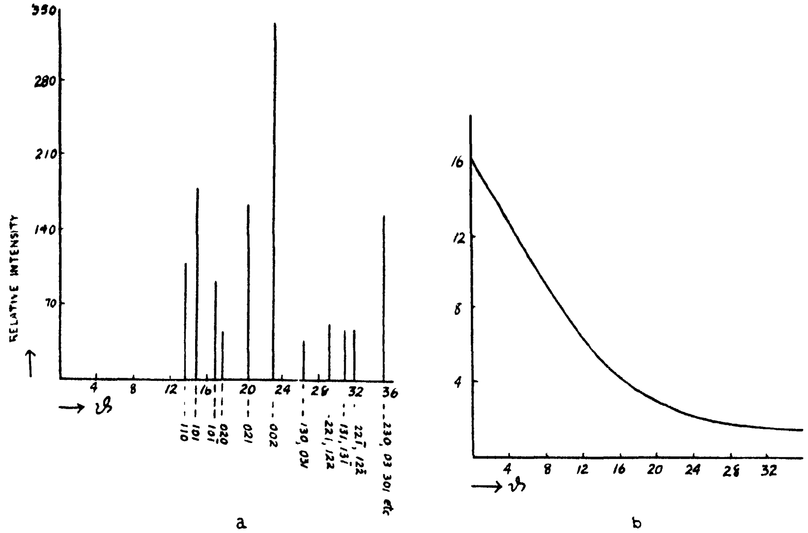

Fig. 7. (a) Relative intensities of the main interference lines of native cellulose as listed in table 1 (b) Atomic form factor for the cellulose reflections.

TABLE 1

List of interferences of native cellulose

INTERFERENCE	$\frac{4}{\lambda^2}\sin^2\frac{\vartheta}{2}$	ϑ	INDICES	INTENSITY
I_1	0.0245	13° 40′	110	7
A_1	0.0284	14° 55′	101	83
A_2	0.0348	16° 30′	101	57
II_0	0.0384	17° 30′	020	7
II_1	0.0540	20° 40′	021	82
A_4	0.0660	22° 50′	002	360
III_1	0.100	26° 0′	130 031	5
II_3	0.106	29° 10′	221 122	10
III_2	0.116	30° 30′	131 131	5
II_4	0.122	31° 10′	221 121	10
A_8 I_5 III_3	0.149	34° 40′	230 103 301 002 310 311	40

ently owing to the fact that the forces between the main-valence chains are not so strong when the hydroxyl groups are covered by esterification.

The increased strength of an oriented fiber and its improved water resistance may be due to a certain extent to this shift from the amorphous, easily swelling amount toward the more rigid crystallized portion.

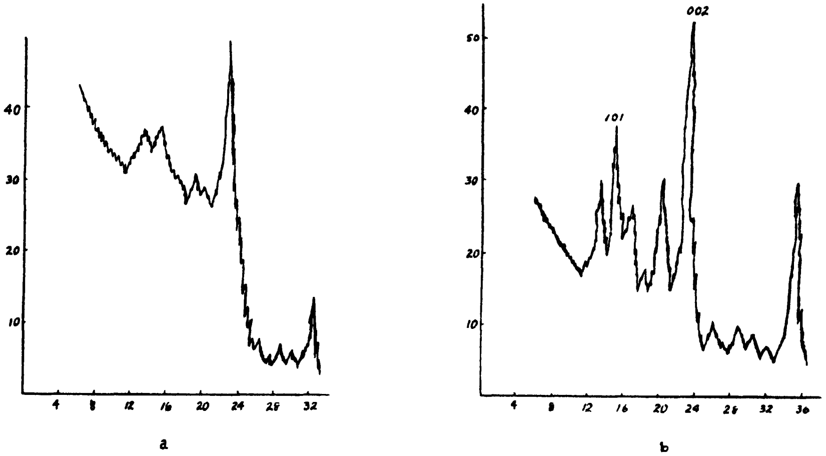

FIG. 8. (a) Experimental intensity distribution; (b) superposition of figures 7a and 7b

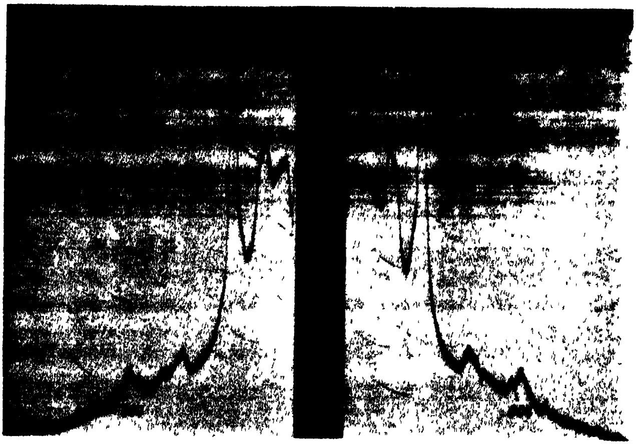

FIG. 9. Original photoregistration curve of a native cellulose fiber

(3) To get some information on the structure of this amorphous fiber portion we have to look at the intensity distribution which remains when we subtract from the total intensity the crystallized scattered radiation. Then we have to evaluate this residual diagram in the same way as one evaluates the diagrams of liquids built up of long-chain molecules. If one

does this, one finds that the chains in the amorphous portions do not lie around entirely unordered but form bundles approximately parallel to the fiber axis which give rise to no sharp interference spots because the chains are not oriented enough. We can compare the crystallized micellae and the non-crystallized portions if we consider a bundle of well-shaped pencils on one side and a bundle of shapeless tree branches on the other. In both cases we have rod-like longish sticks, but in the former case they fit perfectly together and build up a regular building, while in the latter they give just a rough construction full of holes and intermediate spaces.

If we generalize this point of view we may say that the mechanical behavior of a substance which is built up from long-chain molecules is determined by two different tendencies of the chains: (*1*) the tendency of crystallization under the influence of molecular forces, and (*2*) the tendency of the kinetic (statistical) rolling or curling up of the main-valence chains. If the chains are relatively stiff and the forces between them large, then the first tendency predominates and one gets *rigid*, *strong*, and *inelastic* fibers. Hemp, silk, and the so-called Lilienfeld rayon approach this extreme case to a certain extent. When, on the other hand, the chains are very flexible and their mutual forces small, the statistical effect of entangling predominates and one gets *soft* materials with *high rubber-like elasticity* and *peculiar thermoelastic properties*. Representative of such substances are natural rubber and chain-like polymerization products of hydrocarbons, such as Vistanex or other polyisobutylenes.

It seems that all intermediate stages between these two extreme cases are realized in nature and can be obtained technically. If one wants, for instance, to get a sample of stiffer, less elastic, and stronger rubber, one can either just stretch it and produce rubber crystals or one can incorporate into the unstretched material certain crystallized fillers such as carbon black and zinc oxide. In both cases a certain amount of crystallized material is formed in the sample, which shifts the properties of the resulting fiber toward the first case.

The information which x-ray analysis gives about the ratio of crystallized and amorphous matter in cellulose fibers shows that one can compare a cellulose fiber in certain respects to a rubber sample filled with carbon black or zinc oxide. The cellulose micellae represent the crystallized particles in the rubber and are the stiff and rigid part of the construction. The amorphous intermicellar amounts, on the other hand, contain a certain rubber-like elasticity, owing to the fact that these parts of the main-valence chains are more or less flexible and hence give rise to a certain amount of statistical elasticity of long flexible chain molecules (30, 31, (57, 71, 72, 73, 74, 75, 79, 86, 107). The tenacity and strength are located in the crystals; the elasticity and extensibility in the amorphous portions.

Although this picture has a certain amount of probabilities in itself, one must be extremely suspicious of any assumption which is not proven experimentally, and hence every possible way to check the ideas just brought forward must be welcomed and looked into.

One consequence of the picture just developed is the fact that the amorphous portions of a cellulosic fiber should have a *higher energy content* than the crystallized ones. They may be regarded as being highly distorted crystallized lattices in which the single atoms are shifted to a considerable degree out of their normal equilibrium positions. It has been shown by several investigators that lattice distortions can be experimentally detected by anomalous x-ray intensities and by anomalous heats of combustion (12, 23, 24, 25, 26, 33, 34, 54). As an example, some measurements carried out by Fricke and his collaborators are shown in table 2. They investigated two kinds of iron powder, one having normal properties and the other being in a very unstable state. Table 2 shows that the heat of combustion of the unstable, pyrophoric iron powder is considerably higher than that of the normal one and that the intensities of the x-ray reflections are smaller in the case of the distorted lattices than in the case of the undistorted. Table 3 shows some measurements which have been carried out in the course of the present investigations. The heat of combustion of several cellulosic fibers has been measured in a highly sensitive combustion calorimeter. One sees that native cellulose and unstretched viscose thread have heats of combustion of about 4200 calories per gram. Stretching in the swollen state decreases this value to 4186, this being distinctly outside the limits of error which the method includes. This result indicates that the increase of crystallized portions which is created during the stretching is due to the fact that the forces between the chains bring the different atoms in positions of their minimum potential energy. It is very interesting to see that stretching in the dry or insufficiently swollen state produces the reverse effect. This is due to the fact that such stretch-

TABLE 2

Energy content and x-ray intensity of iron powder

	PYROPHORIC IRON POWDER	NORMAL IRON POWDER
Heat of combustion, in kg-cal. per mole	23.72 23.73	22.29 22.40
Intensity of the reflectories 110, 211, and 220	241 252 238	247 297 321
Average shift of atoms from equilibrium position, in Å	0.050 0.089 0.039	0.032

ing does not influence the orientation of the molecules (as x-ray diagrams show) but apparently creates a number of fine slits and crevasses in the fiber, which loosen up the inner structure and as a consequence give an increase of the heat of combustion. In this way the calorimeter measurements corroborate the results of the x-ray analysis, and support our view of the rôle which the amorphous portions of the fiber are playing.

B. The introduction of minute crystals in the intermicellar spaces and their observation with x-rays

The x-ray method gives us another possibility of measuring the size and shape of the crystallized areas by observing the angular width of the x-ray interference spots. Already ten years ago this method was applied (12, 13, 34, 35, 39, 41, 58, 82, 95) and the following results were obtained: Native and regenerated cellulose is built up of micellae which have an average width of around 50 Å. and which are longer than about 600 Å. Similar observations could be made with rubber and other high-polymeric substances.

TABLE 3

Energy content and diffuse scattered radiation of some cellulose samples

CELLULOSE	HEAT OF COMBUSTION	INTENSITY RATIO BETWEEN REGULARLY AND DIFFUSE SCATTERED RADIATION
	calories per gram	
Native cellulose (ramie fiber)	4200 ± 6	1
Unstretched cellulose filament from viscose	4205 ± 7	0.42
Cellulose filament from viscose stretched 50 per cent in swollen state	4192 ± 5	0.61
Cellulose filament from viscose stretched 100 per cent in swollen state	4186 ± 6	0.74
Cellulose filament from viscose stretched 50 per cent in dry state	4238 ± 4	0.48

Recently an independent possibility of determining the average width of crystallized portions was worked out (22, 52, 54, 68) on the following basis: The larger the spacings (d) of a lattice, the smaller will be the angle (ϑ) under which a certain x-ray wave length is reflected. The well-known reflection law of Bragg

$$n\lambda = 2\,d\sin\vartheta$$

$$\lambda = \text{wave length of x-rays applied}$$

shows very clearly that the lattice constant d and the sine of the deviation angle ϑ are inverse to each other. Lattices with large meshes give small patterns, lattices with small meshes large ones.

In a filament which is built up of highly orientated longish micellae this over-molecular structure builds up something like an irregular lattice, the average constant of which would be the breadth of the crystallized areas. As this width is of the order of magnitude of 50 Å., this lattice is a very coarse one and hence the interference pattern which it produces will appear in the immediate neighborhood of the primary beam. It was therefore attractive to study the intensity distribution of fiber diagrams in the very neighborhood of the direct x-ray beam and to see whether this intensity indicates some scattering due to an over-lattice built up by the micellular structure in the fiber. An easy calculation shows that the maximum of intensity has to be expected at a deviation angle of about 1°. Already the first orientation showed that, in fact, the intensity distribution of cellulose diagrams in the immediate neighborhood of the direct beam shows the appearance of a more or less strong blackening, which indicates the existence of a structure as just discussed.

One can increase this effect very distinctly if one adopts an idea which was first used by Frey-Wyssling during his investigations of the morphological structure of natural fibers (21, 22). This is the introduction of minute crystals of heavy metals in the interior of the fiber. If one impregnates a filament with a solution of gold or platinum salts and then precipitates the metal in a suitable form the crystal x-ray diagram of the cellulose is not changed. This means that the heavy metal atoms are not able to penetrate the highly oriented and tightly packed inner micellar spaces, but that they were just deposited between the micellae. It is easy to understand that the presence of thin layers of particles of high atomic weight increases the scattering power of these intermolecular lamellae and hence reinforces the diffraction scattering effect of the over-lattice which we have just visualized.

As a matter of fact, careful intensity measurements of scattered radiation near the primary beam carried out by O. Kratky (52, 54) show that the incorporation of heavy metals gives a very remarkable additional scattering under small deviation angles, which can not be reasonably explained unless we assume that the heavy metal is distributed in fine lamellar sheets with an average distance of about 50 Å. from each other. This would be easily understood if we assume that the micellae exhibit this average width when they are oriented parallel to the axis of the fiber. Figure 10 shows the intensity distribution in the immediate neighborhood of the primary beam. It exhibits a broad maximum at an angle of deviation of about 1°.

We may say that this independent method leads to the same results as the direct measurement of the micellar dimensions and authorizes us to trust to a certain extent to the picture of long-shaped crystallized micellae which are more or less combined by amorphous interspaces.

Another possibility of getting further information regarding the intermicellar hole and tube spaces in a fiber was shown by Frey-Wyssling (21, 22) following the deposition of small crystals in the intermicellar spaces. These minute particles of gold or platinum fill in these spaces to

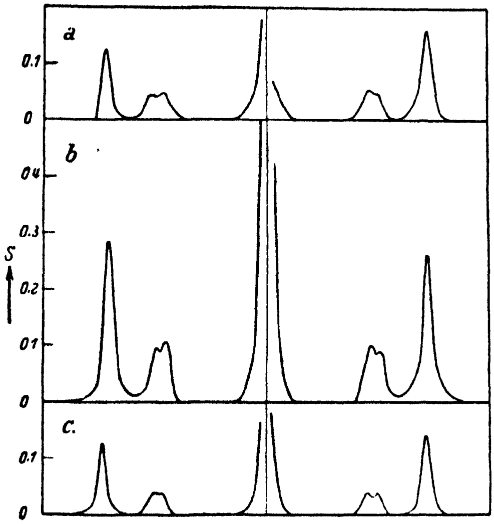

FIG. 10

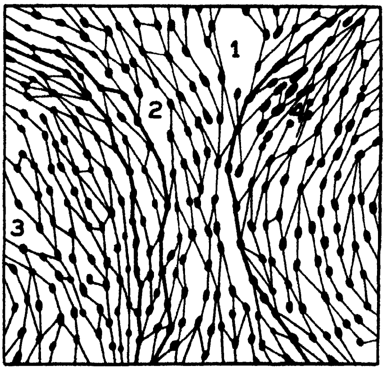

FIG. 11

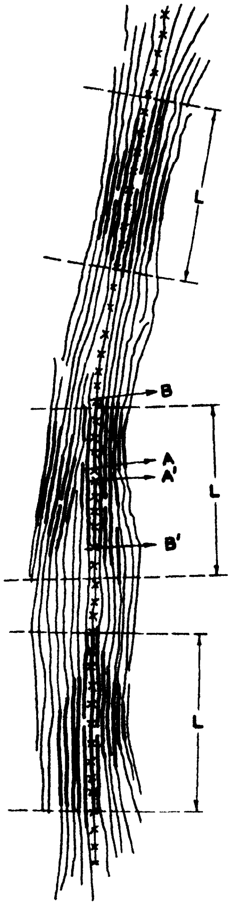

FIG. 12

FIG. 10. Intensity distribution in the immediate neighborhood of the primary beam

FIG. 11. The lines represent the crystals; the dots show the amorphous areas

FIG. 12. Main-valence chains going through more than one micella

a more or less complete degree and exhibit in this way something like a negative of the fiber, the study of which may contribute to the knowledge of the over-molecular and over-micellar structure of natural and artificial threads.

Earlier work of Böhm, Berkmann, and Zocher (9) was continued during the last few years by Frey-Wyssling, Kratky, Mark, and Schossberger (21, 22, 53, 105) and yielded the following results: If one impregnates ramie with gold, silver, or platinum crystals one finds that a certain part of them may still be observed in the ultramicroscope. They are of a longish shape and lie parallel to the fiber axis. Their mutual distance is of the order of magnitude of the wave length of light, that is, about 5000 Å. These large particles seem to be secondary particles composed of more minute crystals, which can be detected by observing the width of the interferences given by the incorporated metal. The primary crystals are of about spherical shape with average diameter around 100 Å. Figure 11 gives a picture of these results and shows that we have to assume a rather coarse system of wide slits and holes. The diameter as well as the mutual distance of these holes is on the average about one hundredfold the width of the single micellae. These large holes seem to be of the shape of a lens with a diameter of about 200 Å. and a length of about 1000 Å.

Kratky and Frey-Wyssling (21, 22, 52, 54) point out that these hollow spaces in the fibers may play an important rôle in a biological as well as in a technical respect, but it must be pointed out that as far as our present knowledge goes there is no indication of strict rules regarding their shape and relative position. It seems, moreover, that these depend to a very high degree on the type of fiber which one is investigating and very much more of them are, for instance, observable in a non-oriented rayon thread than in an oriented one. Also, the average size and shape of the minute metal crystals inside the fiber depend to a high degree on the nature of the investigated filament. We are far from having enough evidence to understand the formation of this coarse structure of a thread and to link it with the production of the investigated sample, but we may assume that such large holes are certainly present and that they may play an important rôle regarding the behavior of the fibers, and there is good reason for the hope of getting more information about them by applying more carefully the methods which have just been described.

III. MAIN-VALENCE CHAINS AND MICELLAE

The methods described, together with the determination of end groups, studies with the ultracentrifuge, and osmotic and viscosity measurements, have pointed to the conclusion that the principal valence chains in native cellulose reach a degree of polymerization of at least 2000. If the chains are assumed to be stiff, they would have a length of 1.5 μ and a diameter[2] of about 7 Å. (3, 10, 11, 29, 82, 100). If they are considered to be wound into a ball, the diameter of same would be about 100 Å. It has been well established experimentally that most technical treatments of native cellulose cause a certain amount of degradation. Several different investigators agree that in the precipitated material of technical threads and films consisting of cellulose, the degree of polymerization lies between 150 and 500.

---

[2] This means that their length would be about two thousand times their diameter.

A rough classification can be established so that it may be stated that samples which consist mainly of chains with a degree of polymerization of less than 200 may be expected to show rather poor technical properties, such as tenacity, elasticity, and pliability. An increasing degree of polymerization is accompanied by rapid improvement in the quality, until at a chain length above 300 there seems to be no further direct influence on the tensile strength of the material. In order to explain these observations more fully, it is useful first to consider the cellulose sample as built up from chains of infinite length into an ideal material. In order to tear this fiber or film, it is necessary to rupture all the single chains contained in a given cross section. It is possible to estimate the energy required to do this, if the tensile strength of the principal valence bond is known.

The modulus so calculated is 800 kg. per square millimeter. It is an interesting fact that Meyer and Lotmar (80, 82) have measured very carefully the modulus of elasticity for different fibers and have actually found several specimens which gave values corresponding very closely to the figures for an ideal sample of infinite chain length. It is not quite easy to understand why chains of finite length should have properties so closely in agreement with an ideal cellulose built up of infinitely long molecules. Every chain in the real sample must have an end somewhere and obviously this point should be a potentially weak spot where a break may take place without a rupture of the primary-valence chain itself.

This paradoxical situation is explained diagrammatically in figure 12 (52). Considering the two molecule ends, A and A′, it is apparent that if they are not inside of a crystallized region in the material, under the influence of a stress, they might be separated from each other quite easily, inasmuch as they are held together only by weak intermolecular forces. The work required to separate them would be small, and consequently the tensile strength of the sample should be low. On the other hand, when the ends of the two molecules lie inside of a crystallized region of one micella, then they are kept in their positions not only by the forces between A and A′, but also in addition by the van der Waals' forces along the two lengths AB and A′B′. In order to separate the two molecules, it is necessary to pull them out of the lattice and to overcome all the forces along the length with which they are held inside of the crystallized region. If the parts of the main-valence chains which belong to the micella are long enough, then the total energy required to pull them out of this range will be great, because the two ends of the chains are entirely concealed in the center of the micella and do not form on this account a potentially weak spot for the rupture of the filament. The line of chains which is designated in figure 12 by small crosses behaves, therefore, like a single main-valence chain of infinite length, just as Meyer and Lotmar (80) have discovered in their investigation. These crystallized regions in the total structure have the effect of strengthening the fibers by covering up the chain ends inside of the solid structure. In this way, the micellae in the cellulose may play a rôle similar to that of carbon black particles in rubber, which pick up the loose ends of the rubber hydrocarbon chains on their surfaces and thus fortify the structure, which might otherwise be potentially very weak.

The structure depicted in figure 12 is in a sense, therefore, a combination of the two extreme points of view above described as the extreme micellar and the extreme chain structures. According to this working hypothesis, there are crystallized ranges but they are not clearly separated from each other by a distinct micellar surface. The chains are of considerable length, and hence pass through several micellae and cement them together. This picture indicates that with increasing chain lengths the probability of finding the chain ends inside of one crystallized region or another increases, and at the same time the length of the track along which one chain must be pulled in order to separate it from its neighbors also increases. This may, at least in a qualitative way, explain the above-mentioned relationship between chain length and tenacity: namely, that above a certain degree of polymerization the chain length no longer has a measurable influence on the tensile strength. The chain ends are distributed at random in the micellae and their effect in producing potentially weak spots is rendered negligible by the crystallizing forces. It is clear that if the length of the chains approaches the length of micellae, it will frequently occur that the end of a chain will coincide with the end of a micella, with the result that the tensile strength of the sample will be determined by the weak secondary-valence forces.

It may now be concluded that the crystallized portions of the material are the reinforcing backbone of the structure, while the unordered regions may be regarded as the weak spots. If a film is soaked in water, the x-ray evidence shows that there is no change in the crystallized regions and that the water penetrates only the amorphous material which is built up by the fringes of the micellae (28). If chain ends occur, as they frequently do, in these swollen areas, then tensile strength will be a very sensitive function of swelling. The wet strength of cellulose fibers depends, therefore, to a large degree upon the average length of the chains, for the longer the chains are, the larger the amount of crystallized material and the smaller the chance of chain ends occurring in the unordered network of the fringes. From this point of view, instead of distinguishing between intermicellar and intramicellar swelling, it is better to speak of entrance of water into the fringes or into the crystallized regions or micellae themselves (21, 22, 28, 52, 54, 68.)

This conception of cellulose structure indicates that the *physical properties*—tenacity, elasticity, etc.,—are functionally related to the amount of crystalline material, while the *reactivity* of the fiber,—swelling, drying, ease of chemical reactions, etc.,— is to be associated with the amorphous parts. The relative frequency and the length of the micellae depend upon the average chain length; hence this in turn determines in large measure both physical and chemical properties.

In order to understand the mechanical behavior of systems of high molecular weight, it is not sufficient to believe that more or less extended and tightly constructed elongated particles are present. Nor is it sufficient to assume that homogeneously dispersed long-chain molecules undergo the flow of plastic deformation. It is necessary to visualize a *mixture of both*, a combination of crystallized ranges with many chain ends emerging from their surface so that they are imbedded in an amorphous movable medium formed by the flexible fringes.

The total behavior of the system is influenced by the following: (*a*) the relative amounts of crystallized and amorphous fractions; (*b*) the ratio between the average length of the main-valence chains and the average length of the crystallized regions; and (*c*) the flexibility of the fringes and their sensitivity to swelling and chemical reactions.

IV. SUMMARY

To summarize briefly the present ideas about the structure of a cellulosic fiber, figure 13 may serve as a rough illustration. This figure is drawn with the assumption that we would have at our disposal a microscope, the amplification of which could be changed step by step, always increasing by a factor of 10, to the point where 1 Å. would be 1 cm.[3]

When we first look at the fiber with the highest amplification we have at our disposal, we get the first picture of figure 13. In this we see the atoms and the glucose unit as the last chemical element of the investigated material. Now we switch to the next amplification, which is ten times less, and means that 1 mμ (or 10 Å.) is equal to the length of 1 cm. In this picture we see the elementary cell of the cellulosic crystals and the main-valence chains which form the backbone of the fiber structure. The next switch brings us an amplification of 1 to 1,000,000, 1 cm. in the picture being 100 Å. in the fiber. We now see the crystallized portions of the fiber, the micellae, and between them the amorphous parts which we have especially discussed in this paper. Another decrease of the amplification of our microscope gives us the fourth picture. Here we have the network of crystallized portions (parallel lines) being combined and linked together by the flexible amorphous regions (circles). We see also that irregular holes are present, the same as have been described on the previous pages.

---

[3] This means an amplification of from 1 to 100 million.

Up to now we have been far outside of the region of a microscope operating with visible light and have confined ourselves to the region of x-rays. The next picture with amplification of 10,000 shows us those structural units which are at the utmost range of the microscopic technique, the fibrils on which considerable important work has been done in recent years (3, 4, 5, 6, 7, 18, 19, 20, 21, 22, 92, 96, 97, 98).

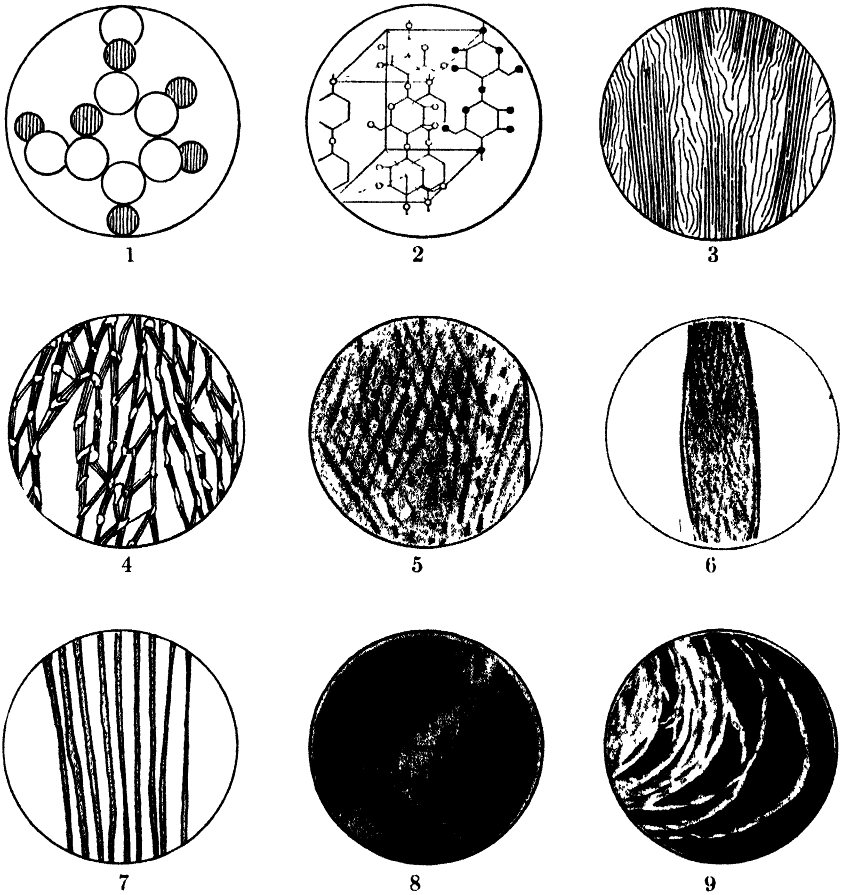

FIG. 13. Structure of a cellulosic fiber. 1, glucose unit, white circles = carbon atoms; other circles = oxygen atoms. 2, elementary cell; glucose chains. 3, micellae and amorphous areas. 4, network of crystallized and amorphous regions. 5, fibrillar structure. 6, single fiber. 7, group of fibers. 8, single yarn 9, skein of rayon yarn.

Again another step toward smaller amplification shows us a single cotton fiber with its characteristic cell-wall structure. We have now reached an amplification of 1 to 1000 and are well inside the region of microscopical visibility. Hence the next two pictures give us information on the rough structure of the single fibers and the yarn, revealing inhomogeneities in cross sections and diameter. Finally, the last picture shows the normal aspect of a yarn without any microscopical aid.

We may be authorized to say that the above picture of a cellulosic fiber seems to be not too far from the truth and that it can be regarded at least as a reasonable starting point for further and better work.

It is a pleasant duty for me to express my sincerest gratitude to Dr. C. B. Thorne, Technical Director, and to Mr. S. Wang, Manager of Laboratories, of the Canadian International Paper Company, who have been so kind as to enable me to present this paper.

REFERENCES

(1) Andress, R. K.: Z. physik. Chem. **B2**, 380 (1929).

(2) Astbury, W. T.: Trans. Faraday Soc. **28**, 232 (1932); **29**, 193 (1933).

(3) Astbury, W. T.: *Fundamentals of Fibre Structure*, p. 77 ff. Oxford University Press, London (1933).

(4) Bailey, A. J.: Ind. Eng. Chem., Anal. Ed. **8**, 52, 389 (1936).

(5) Bailey, A. J.: Ind. Eng. Chem. **30**, 40 (1938).

(6) Bailey, I. W., and Kerr, T.: J. Arnold Arboretum **16**, 273 (1935); **18**, 261 (1937).

(7) Bailey, I. W., and Vestal, M. R.: J. Arnold Arboretum **18**, 185, 196 (1937).

(8) Bass, S. L., and Kauppi, T. A.: Ind. Eng. Chem. **29**, 679 (1937).

(9) Böhm, I., Berkmann, S., and Zocher, H.: Z. physik. Chem. **124**, 83 (1926).

(10) Bragg, W. H., and Bragg, W. L.: *X-rays and Crystal Structure*. G. Bell and Sons, London (1933).

(11) Breuer, F., Kratky, O., and Saito, G.: Kolloid-Z. **80**, 139 (1937).

(12) Brill, R.: Z. Physik **105**, 378 (1937).

(13) Brill, R., and Pelzer, H.: Z. Krist. **72**, 398 (1929).

(14) Conaway, R. F.: Ind. Eng. Chem. **30**, 516 (1938).

(15) de Boer, I. H.: Trans. Faraday Soc. **31**, 10, 28 (1935).

(16) Debye, P.: Physik. Z. **31**, 384 (1930).

(17) Debye, P., and Menke, H.: Physik. Z. **31**, 797 (1930).

(18) Farr, W. K.: J. Applied Phys. **8**, 228 (1937).

(19) Farr, W. K., and Eckerson, S. H.: Contrib. Boyce Thompson Inst. **6**, 189, 309, 315 (1934); **10**, 71 (1938).

(20) Farr, W. K., and Sisson, Wayne A.: Contrib. Boyce Thompson Inst. **6**, 315 (1934).

(21) Frey-Wyssling, A.: Kolloid-Z. **85**, 148 (1938).

(22) Frey-Wyssling, A.: Protoplasma **25**, 262 (1936); **26**, 75 (1936); **27**, 372, 563 (1937).

(23) Fricke, R., and Gwinner, E.: Z. physik. Chem. **A183**, 165 (1938).

(24) Fricke, R., Lohrmann, O., and Eolf, W.: Z. physik. Chem. **B37**, 60 (1937).

(25) Fricke, R., and Meyer, F. R.: Z. physik. Chem. **A183**, 177 (1938).

(26) Fricke, R., Schnabel, R., and Beck, K.: Z. Elektrochem. **42**, 881 (1936).

(27) Gehman, S. D., and Field, J. E.: Ind. Eng. Chem. **30**, 1031 (1938).

(28) Gerngross, O., Hermann, K., and Abitz, W.: Biochem. Z. **228**, 499 (1930).
(29) Gross, S. T., and Clark, G. L.: Z. Krist. **A99**, 357 (1938).
(30) Guth, E., and Mark, H.: Monatsh. **65**, 93 (1934).
(31) Guth, E., and Mark, H.: Naturwissenschaften **25**, 353 (1937).
(32) Guth, E., and Rogowin, S.: Sitzber. Akad. Wiss. Wien Math.-naturw. Klasse **145**, 531 (1936).
(33) Heisenberg, E.: Cellulosechem. **12**, 159 (1931).
(34) Hengstenberg, I., and Mark, H.: Z. Physik **61**, 442 (1930).
(35) Hengstenberg, I., and Mark, H.: Z. Krist. **69**, 271 (1928).
(36) Hermans, P. H.: Kolloid-Z. **81**, 143, 300 (1937).
(37) Hermans, P. H.: Kolloid-Z. **82**, 58; **83**, 71 (1938).
(38) Hermans, P. H.: Rec. trav. chim. **58**, 1 (1939); Kolloid-Z. **86**, 107 (1939).
(39) Herzog, R. O.: Svensk Papperstidn. **231**, No. 8 (1927).
(40) Herzog, R. O., and Jancke, W.: Z. Physik **3**, 196 (1920).
(41) Herzog, R. O., and Krueger, D.: Z. physik. Chem. **34**, 466 (1926).
(42) Hess, K.: Papier-Fabr. **32**, 61 (1939); **37**, 25 (1939).
(43) Houwink, R.: Trans. Faraday Soc. **31**, 127 (1935).
(44) Katz, J. R.: *X-ray Investigations of Colloids*. Urban and Schwarzenberg, Berlin (1935).
(45) Katz, J. R.: In K. Hess' *Die Chemie der Zellulose und ihrer Begleiter*, p. 605 ff. Akademische Verlagsgesellschaft, Leipzig (1928).
(46) Katz, J. R., and Mark, H.: Z. physik. Chem. **115**, 385 (1925).
(47) Katzoff, S.: J. Chem. Phys. **2**, 84 (1934).
(48) Kraemer, E. O.: Ind. Eng. Chem. **30**, 1200 (1938).
(49) Kratky, O.: Physik. Z. **34**, 482 (1933).
(50) Kratky, O.: Kolloid-Z. **70**, 14 (1935).
(51) Kratky, O.: Kolloid-Z. **80**, 139 (1937).
(52) Kratky, O.: Holz **56**, 149 (1938).
(53) Kratky, O., and Mark, H.: Z. physik. Chem. **B36**, 129 (1937).
(54) Kratky, O., and Mark, H.: Papier-Fabr. **38**, 345 (1938).
(55) Kratky, O., and Platzek, P.: Kolloid-Z. **84**, 268 (1938).
(56) Krishnamurti, B. E.: Indian J. Phys. **2**, 355 (1928); **4**, 449 (1930).
(57) Kuhn, W.: Kolloid-Z. **76**, 258 (1934); Naturwissenschaften **24**, 346 (1936).
(58) Laue, M. von: Z. Krist. **64**, 115 (1926).
(59) Levi, G. R., and Rossi, G.: Gazz. chim. ital. **68**, 570, 576 (1938).
(60) Lieser, Th.: Kolloid-Z. **84**, 234 (1937).
(61) Ludtke, H.: Cellulosechem. **13**, 169, 191 (1932); **14**, 1 (1933).
(62) Mark, H.: Ber. **59**, 2982 (1926).
(63) Mark, H.: Melliand Textilber. **10**, 695 (1929).
(64) Mark, H.: Z. Physik **54**, 505 (1929).
(65) Mark, H.: Kunstseide **12**, 219 (1930).
(66) Mark, H.: Papier-Fabr. **30**, 197 (1930).
(67) Mark, H.: Rayon Record **1932**, 498.
(68) Mark, H.: *Physik und Chemie der Cellulose*, p. 159. J. Springer, Berlin (1932).
(69) Mark, H.: Trans. Faraday Soc. **29**, 6 (1933).
(70) Mark, H.: Ergeb. techn. Roentgenkunde **4**, 75 (1934).
(71) Mark, H.: Congr. intern. quím. pura aplicada, 9th Congr., Madrid, **1934**, Vol. 6, p. 197.
(72) Mark, H.: Nature **144**, 313 (1939).
(73) Mark, H.: Trans. Faraday Soc. **32**, 311 (1936).
(74) Mark, H.: Oesterr. Chem.-Ztg. **40**, No. 13 (1937).

(75) Mark, H.: *Der feste Körper*, p. 65. S. Hirzel, Leipzig (1938).
(76) Mark, H., and Meyer, K. H.: Z. physik. Chem. **B2**, 115 (1929).
(77) Mark, H., and v. Susich, G.: Z. physik. Chem. **B4**, 431 (1929).
(78) Meyer, K. H.: Ann. Physik **5**, 701 (1930).
(79) Meyer, K. H., and Ferri, C.: Helv. Chim. Acta **18**, 570 (1935).
(80) Meyer, K. H., and Lotmar, W.: Helv. Chim. Acta **19**, 68 (1935).
(81) Meyer, K. H., and Mark, H.: Ber. **61**, 593 (1928).
(82) Meyer, K. H., and Mark, H.: *Der Aufbau der hochpolymeren organischen Substanzen*, p. 115. Akademische Verlagsgesellschaft, Leipzig (1930).
(83) Meyer, K. H., and Mark, H.: Z. physik. Chem. **B35**, 83 (1937).
(84) Meyer, K. H., and Misch, L.: Helv. Chim. Acta **20**, 232 (1937).
(85) Meyer, K. H., Misch, L., and Badenhuizen, N. P.: Helv. Chim. Acta **22**, 59 (1939).
(86) Meyer, K. H., v. Susich, G., and Valkó, E.: Kolloid-Z. **59**, 208 (1932).
(87) Muller, A.: Nature **129**, 436 (1932).
(88) Pierce, W. C.: J. Chem. Phys. **3**, 252 (1935).
(89) Polanyi, M.: Naturwissenschaften **15**, 288 (1921).
(90) Prins, J. A.: Physica **6**, 305 (1926).
(91) Rehaag, H., and Stuart, H. A.: Physik. Z. **38**, 1027 (1937).
(92) Ritter, G. J.: Ind. Eng. Chem. **17**, 1194 (1925).
(93) Sauter, E.: Z. physik. Chem. **B35**, 83 (1937).
(94) Scherrer, P.: Göttinger Nachrichten **1918**, p. 18.
(95) Scherrer, P.: In R. Zsigmondy's *Kolloidchemie*, Vierte Auflage, p. 409. O. Spamer, Leipzig (1920).
(96) Seifriz, W., Hock, C. W., and Morehead, F. F.: Papers read before the Division of Cellulose Chemistry at the Ninety-seventh Meeting of the American Chemical Society, held in Baltimore, Maryland, April 6, 1939.
(97) Sisson, W. A.: J. Phys. Chem. **40**, 343 (1936); **43**, 687 (1939).
(98) Sisson, W. A.: Ind. Eng. Chem. **27**, 51 (1935); **30**, 530 (1938); Contrib. Boyce Thompson Inst. **8**, 389 (1937); **9**, 239, 381 (1938); **10**, 113 (1938).
(99) Sogani, C. M.: Indian J. Phys. **2**, 97 (1928).
(100) Sponsler, L. O., and Dore, H. W.: Colloid Symposium Monograph **3**, 174 (1926).
(101) Staudinger, H.: Holz **1**, 259 (1938); Ber. **70**, 2502 (1937); Melliand Textilber. **18**, 681 (1937).
(102) Stewart, G. W.: Phys. Rev. **30**, 232 (1927).
(103) Stewart, G. W.: Phys. Rev. **31**, 174; **32**, 153 (1928).
(104) Stewart, G. W.: Phys. Rev. **37**, 9 (1931).
(105) Thiessen, P. A.: Angew. Chem. **51**, 170 (1938).
(106) Wilson, D. A., and Ost, E.: J. Chem. Phys. **2**, 231 (1934).
(107) Woehlisch, E.: Z. Biol. **85**, 406 (1927); **87**, 353, 364 (1928); Kolloid-Z. **89**, 239 (1939).
(108) Zernike, F., and Prins, J. A.: Z. Physik **41**, 184 (1927).

References added in proof

Since this paper was written a number of articles have appeared containing further contributions to the subject under discussion. The most important of these are the following:

Clark, G. L.: Ind. Eng. Chem. **31**, 1397 (1939).
Farr, W. K., and Sisson, W. A.: Contrib. Boyce Thompson Inst. **10**, 127 (1939).

Gehman, L. D., and Field, J. E.: J. Applied Chem. **10**, 564 (1939).
Hermans, P. H.: Kolloid-Z. **89**, 344 (1939).
Hermans, P. H., and de Booys, J.: Kolloid-Z. **88**, 73 (1939).
Hermans, P. H., Kratky, O., and Platzek, P.: Kolloid-Z. **86**, 245 (1939).
Kratky, O., and Platzek, P.: Kolloid-Z. **88**, 78 (1939).
Preston, G. D.: Nature **142**, 569 (1938).
Sisson, W. A.: Chem. Rev. **26**, 187 (1940).
Warren, B. E.: Chem. Rev. **26**, 237 (1940).

HEVEA LATEX: EFFECT OF PROTEINS AND ELECTROLYTES ON COLLOIDAL BEHAVIOR[1]

A. R. KEMP AND W. G. STRAITIFF

Bell Telephone Laboratories, New York, New York

Received December 22, 1939

It is generally recognized that the protein adsorbed on the rubber particles in Hevea latex plays a predominant rôle in connection with stability and coagulation phenomena. Although the function of proteins as protective substances in colloidal dispersions is well known, very little exact information is available regarding the mechanism of their protective action.

Different latices containing protein have been found to differ markedly in colloidal stability. For example, Hevea latex is coagulated by the addition of protein coagulants, whereas *Balata* (*Mimusops globosa*) and *Funtumia elastica* latices also contain protein but are not coagulated by the addition of electrolytes or acids. On the other hand, latex from the *Manihot glaciovii* behaves towards coagulants like latex from the Hevea.

One might postulate that the proteins present in Hevea and Manihot latices differ from those in Balata or Funtumia, or that other substances are present in the more stable latices which offer additional protective action. In this connection Daniel, Freundlich, and Söllner (4) and Kemp (7) have recognized protective substances in Abiurana and Balata latices which when added to Hevea latex prevent its coagulation with acids or salts. Latex from the *Ficus elastica* behaves differently from the other latices above mentioned. It gives a negative test for protein and is flocculated but not coagulated with acids and salts.

The influence of crystalloidal serum substances in aiding coagulation was discussed by Henri (6) in his classical investigations of Hevea latex. He found that diluted ammonia-preserved latex which had been exhaustively dialyzed flocculated but did not readily coagulate upon addition of acids or alcohol. Dekker (5) also noted that the coagulation of dialyzed latex with acids was incomplete. On the other hand, Beadle and Stevens (1), Stevens and Rowe (15), and Noble (9) all observed that ammonia-preserved latex reacted normally towards acid after dialysis.

---

[1] Presented before the Division of Colloid Chemistry at the Ninety-eighth Meeting of the American Chemical Society, held in Boston, Massachusetts, September 11-15, 1939.

Henri (6) showed that the latex particles in dialyzed latex are negatively charged and coagulate upon the addition of various metal salts. He also showed in a qualitative manner that the addition of various salts to dialyzed latex increases its tendency to coagulate upon addition of alcohol.

The present investigation was undertaken to show the effect of electrolytes on the colloidal stability of latex in a quantitative manner and to relate these findings with the stability characteristics of separate protein fractions contained in the latex. In this way it was hoped that the mechanism of coagulation and the fundamental factors effecting latex stabilization could be more completely elucidated.

In this investigation direct recourse was had to fresh latex from the Hevea and other species through the courtesy of the Division of Plant Exploration and Introduction, Bureau of Plant Industry, of the U. S. Department of Agriculture, which maintains a garden tract near Coconut Grove, Florida, containing various rubber-bearing trees and shrubs.

ISOLATION AND IDENTIFICATION OF PROTEINS IN LATEX

Bishop (2) isolated three protein fractions from fresh latex serum obtained by freezing the latex to coagulate and separate the rubber particles. Protein A was separated by adding acetic acid to adjust the serum to a pH of 4.5. Protein B was isolated by saturating the filtrate from protein A with sodium chloride, and protein C was precipitated by heating the saturated sodium chloride solution on the steam bath. Bondy and Freundlich (3) separated two protein fractions, designated A and B, from centrifuged and filtered ammonia-preserved latex serum by addition of ammonium sulfate.

In the present investigation the Bondy and Freundlich procedure was followed, except that the latex was filtered through filter cel on filter paper in a Büchner funnel. A special technique was employed which made it possible to filter either undiluted ammonia-preserved or fresh latex without recourse to the use of a centrifuge. The filtered serum was dialyzed against distilled water, using a cellophane membrane to remove coloring matter and crystalloids before precipitating the proteins.

Separation of protein A

Saturated ammonium sulfate solution was added with stirring to an equal volume of the dialyzed serum at a pH of 6.5. After 2 hr. precipitation was complete and the supernatant liquor was decanted. The precipitate was dissolved on the filter in dilute ammonia water of pH 8.5 and reprecipitated twice. The material was then dissolved in dilute ammonia water, dialyzed simply for 48 hr. in the presence of toluene, and electrodialyzed under a potential gradient of 36 volts per centimeter for 8 hr. During this time the proteinic material precipitated as a light brown flocculent precipitate which settled to the bottom of the cell. Precipitating apparently was complete, as the supernatant liquid gave a negative biuret reaction.

Separation of protein B

The filtrate from protein A was saturated with ammonium sulfate at room temperature. The precipitation was complete after 48 hr., and the light brown precipitate was redissolved on the filter in a dilute ammonium sulfate solution and reprecipitated twice. Final purification was accomplished through simple dialysis and electrodialysis. Electrodialysis brought about the precipitation of protein B, as was the case with protein A.

Separation of protein C

The filtrate from protein B was subjected to simple dialysis until practically free of ammonium sulfate. It was then heated on the steam bath; when the temperature reached 60°C. precipitation took place and was practically complete within 20 min.

It was considered possible that protein C was a heat-denatured product of protein B which had not been removed by the salting-out process. In order that this doubt might be removed, separate aqueous solutions of proteins A and B with a minimum of salt present were prepared. When these solutions were heated to 60°C. and maintained at that temperature for some time, precipitation did not take place. Furthermore, aqueous solutions of protein C did not show evidence of precipitation after long periods of dialysis, as did proteins A and B. There was also a difference in the stability of the unprotected protein hydrosols towards bacteria. Protein B hydrosol was strongly attacked by bacteria within 24 hr., while hydrosols of proteins A and C were not attacked for several days.

Identification of proteins

The protein fractions were freed from electrolytes by electrodialysis as was done by Bondy and Freundlich. Bishop, on the other hand, simply dialyzed proteins A and B and washed protein C in warm water. The nitrogen contents of these protein fractions found by different investigators are given in table 1. It is seen that agreement is good between our results and those of Bondy and Freundlich; however, we do not agree with Bishop's results in the case of the nitrogen content of fresh latex proteins. In our work the latex was collected in Pyrex glass tubes and filtered immediately in an atmosphere of nitrogen in the presence of toluene. The proteins were then quickly precipitated. It is believed that these precautions largely prevented bacterial attack on the complex proteins.

Chemical analysis of protein A from ammoniated latex gave the following results: carbon, 50.67 per cent; hydrogen, 7.25 per cent; nitrogen, 13.4 per cent; sulfur, 0.55 per cent; ash, 1.4 per cent; oxygen by difference, 26.73 per cent. The protein A from fresh latex was found to contain 1.32 per cent sulfur and 2.26 per cent ash. The lower content of nitrogen in the proteins from fresh latex as compared with those from ammoniated latex is evidence that the proteins in fresh latex are highly conjugated. The higher sulfur and ash content of protein from fresh latex also confirms this view. It appears from these and other observations that ammonia reacts with the complex proteins in fresh latex. The proteins are conjugated glycoproteins, and this also in part accounts for their low nitrogen content.

TABLE 1

Nitrogen content of protein fractions

	NITROGEN BY KJELDAHL IN		
	Protein A	Protein B	Protein C
	per cent	*per cent*	*per cent*
Bishop (2) (fresh latex)	14.0-15.1	14.5-15.4	16.4-16.9
Bondy and Freundlich (3) (ammoniated latex)	13.8	15.2	
Present investigation (ammoniated latex)	13.4	14.8	14.0
Present investigation (fresh latex)	12.7	11.8	

Phospholipids, soaps, and other colloids are present in latex which might be carried down with the protein and be difficult to remove. These observations are recited to point out that the proteins separated from latex cannot be considered as pure substances of uniform composition but are probably mixtures which are sometimes called complexes. Their predominant protein characteristics, however, are not greatly altered by the presence of other colloidal bodies.

Color and precipitation reactions of the proteins are shown in table 2. These tests show the true proteinic nature of the fractions and serve to identify them as conjugated glycoproteins. This confirms the work of Spence and Kratz (13), who placed the insoluble protein in crude Hevea rubber in the same classification. Proteins from ammonia-preserved latex fail to show the ninhydrin test, whereas proteins from fresh latex show a positive ninhydrin reaction. It is well known that the alpha amino group next to a carboxyl group which gives the ninhydrin reaction is easily split off, especially by alkali treatment. Bishop (2) observed negative Molisch reactions with all three proteins from fresh latex; this result is confirmed. Molisch tests in the case of proteins from ammoniated latex, however, are positive. Bondy and Freundlich (3) obtained positive Millon's tests for proteins A and B, whereas our Millon's tests were negative for all three proteins from both fresh and ammoniated latex. The results of this investigation show that the proteins in fresh latex are changed as a result of standing in the presence of ammonia.

TABLE 2

Reactions of rubber latex proteins

REACTIONS	PROTEIN A	PROTEIN B	PROTEIN C
Color reactions:			
Biuret	+	+	+
Ninhydrin	− (a)	− (a)	− (a)
Xanthoproteic	+	+	+
Millon's	−	−	−
Hopkins-Cole	+	+	+
Molisch	+ (b)	+ (b)	+ (b)
Fehling's	+	+	+
Precipitation reactions:			
Nitric acid (Heller)	+	+	−
Lead acetate	+	+	+
Mercuric acetate	+	+	+
Copper sulfate	+	+	+
Picric acid	+	+	+
Tungstic acid	+	+	−
Dichromic acid	+	+	−
Aluminum sulfate	+	+	−
Calcium acetate	+	+	−

(a) Test positive in the case of proteins from fresh latex.

(b) Test negative in the case of proteins from fresh latex.

EFFECT OF SALTS ON THE COAGULATION OF PROTEINS

A study of the colloidal behavior of the different proteins should test the validity of the protein theory and aid in determining which proteins are important as far as the colloidal properties of the rubber particles are concerned. An attempt was therefore made to determine the effect of salts on the stability of each protein hydrosol towards coagulants. A comparison of the properties of the protein hydrosols with the properties of normal and dialyzed latex is shown in table 3. Protein hydrosols A and B were prepared by dissolving the freshly precipitated proteins in a small amount of water and dialyzing the resulting solution until free of ammonium sulfate. The protein hydrosol C was prepared by simple dialysis followed by electrodialysis of latex serum in order to precipitate completely proteins A and B which were filtered off, leaving protein C in solution. The negative sign in table 3 means that precipitation of the proteins did not readily take place.

It was not possible to show in table 3 the relative effect of different salts on the coagulation of the proteins. A divalent salt such as barium chloride was found to be more effective than a monovalent salt such as sodium chloride. In some cases the addition of a small amount of barium chloride brought about the coagulation of proteins A and B without the necessity of adding a coagulant. In addition, there was a difference in the coagulating power of the organic coagulants,—acetone, for example, being much more effective than alcohols. In order to obtain comparable results the amount of coagulant added was that necessary to show rapid coagulation in the presence of salt.

TABLE 3

Effect of salts on coagulation of protein hydrosols and latex

pH of protein hydrosols = 6.5 to 7

COAGULATING CONDITIONS	SODIUM CHLORIDE CONTENT	PROTEIN A	PROTEIN B	PROTEIN C	LATEX
	per cent				
Dilute acetic acid..	1.0	+	+	−	+ (a)
	0.05	−	−	−	− (b)
	0.0	−	−	−	− (c)
Methyl alcohol (40 to 60 per cent)	1.0	+	+	+	+
	0.05	−	+	−	+
	0.0	−	−	−	−
Acetone (10 to 20 per cent)	1 0	+	+	+	+
	0.05	−	+	−	+
	0.0	−	−	−	−
Heating at 75°C.	1.0	+	−	+	+
	0.05	−	−	+	−
	0.0	−	−	+	−

(a) Normal ammoniated latex, pH = 10.4.

(b) Normal ammoniated latex exhaustively dialyzed and 0.05 per cent sodium chloride added. Flocculation took place in the isoelectric region.

(c) Normal ammoniated latex exhaustively dialyzed with no added sodium chloride. Flocculation took place in the isoelectric region.

These observations show that the hydrosols of all three proteins are subject to a "salt effect," which acts in the direction of increasing the instability of the hydrosols upon heating and in the presence of the usual latex coagulants. The experiments also show that latex is readily coagulated by acids if salts are present and the hydrogen-ion concentration approaches the isoelectric range of proteins A and B. Bondy and Freundlich (3) found the isoelectric point of protein A to be 4.5 and that of protein B to be 3.9. Addition of organic coagulants results in the coagulation of all three proteins in the presence of salts. As the salt content is reduced, more coagulant is required. In the absence of salts no coagulation occurred at a pH of 6.5 to 7.0. Heat coagulation of normal latex appears to be primarily due to protein A, since protein B is not heat-coagulated and protein C is not readily coagulated with heat in the presence of salts. The heat coagulation of latex may be greatly accelerated by the addition of a small quantity of salt, as would be expected in view of the effect of salt in the coagulation of protein A. The resistance of dialyzed latex towards heat coagulation, while protein C readily coagulates, indicates either that this protein is not adsorbed on the rubber particle or that its coagulation is not sufficiently strong to bring about coagulation of latex. It was therefore concluded that the colloidal properties of normal ammoniated latex are principally governed by proteins A and B.

CHANGES IN LATEX ON DIALYSIS

In dialyzing ammoniated latex in the simple dialyzer shown in figure 1 distilled water was passed through the apparatus continuously at the rate of 5 gallons per day. A nitrogen pressure of 6 cm. of mercury prevented dilution for the first 48 hr., while 3 cm. of pressure was sufficient thereafter. The tendency for the latex to foam prevented a continuous passage of nitrogen through the system until dialysis had proceeded for 72 hr. The latex at this time was almost pure white and behaved normally towards latex coagulants.

When dialysis was continued for 24 hr. longer, latex cream formed on the membranes and a sample of the uncreamed latex showed increased resistance towards coagulation by alcohol and organic acid. It was not, however, completely stable towards the addition of acid to a pH of about 5 over long periods of standing or when vigorously agitated. The coagulum which formed was very spongy and closely resembled fresh latex coagulum. The rapid addition of a larger amount of acid yielded a stable acid latex. Acetone coagulated this partially dialyzed latex with practically the same ease as the undialyzed latex.

At the end of an additional 72-hr. period of dialysis the latex had creamed to such an extent that continued dialysis was not feasible. The latex was very stable towards immediate coagulation by organic acids at a pH of about 5, as compared with the ammoniated latex, and when made strongly acid did not coagulate or undergo putrefaction after standing several weeks. The mechanical stability of latex as measured by flocculation upon agitation is greatly decreased by dialysis. On the other hand, the addition of ammonia or strong acids to dialyzed latex restores its mechanical stability.

The creaming of latex on membranes during dialysis has been given attention by Stevens, Dyer, and Rowe (14), who suggested that the creaming was caused by ionic movement which carried the particles to the membrane. It was observed in the present investigation that creaming of the latex particles on the membranes always took place when dialysis had progressed sufficiently to lower the pH of the latex within the vicinity of the neutral point. The dialyzed cream on redispersion in distilled water recreams in a short period. However, upon the addition of a small amount of acid or alkali it forms a stable dispersion. It has been noted that creaming on the membrane does not occur when the latex is exhaustively dialyzed against dilute ammonia water having a pH of about 10.5. When the ammonia is then removed by dialysis against distilled water, creaming does not occur. Dialysis of ammoniated latex against distilled water quickly removes the ammonia, reducing the pH, which in turn reduces the

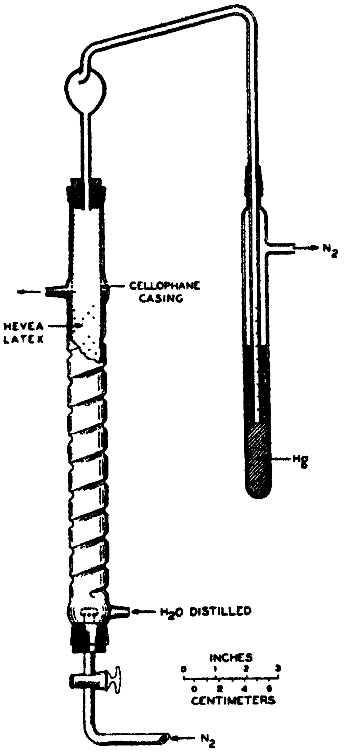

FIG. 1. Simple dialyzer

electrical charge on the particles before the electrolytes have been removed. Under these conditions the particles readily cream.

Effect of dialysis on serum proteins

Filtered normal ammoniated latex serum protected by several drops of toluene was dialyzed against distilled water between cellophane membranes in the convertible dialyzer shown in figure 2. After 2 days' dialysis the serum became almost colorless, and at the end of 5 days protein had started to precipitate and collect on the membranes. New membranes were placed in the apparatus, and dialysis was continued with a constant flow of distilled water to the end of 12 days. During this time protein continued to precipitate and the serum became very turbid, while the membranes were covered with films of protein. If dialysis is conducted against ammonia water of pH of 10.5 for example, no coagulation of proteins will occur. It appears that coagulation of protein A results from the reduction of the pH to an unstable range before salts have been removed.

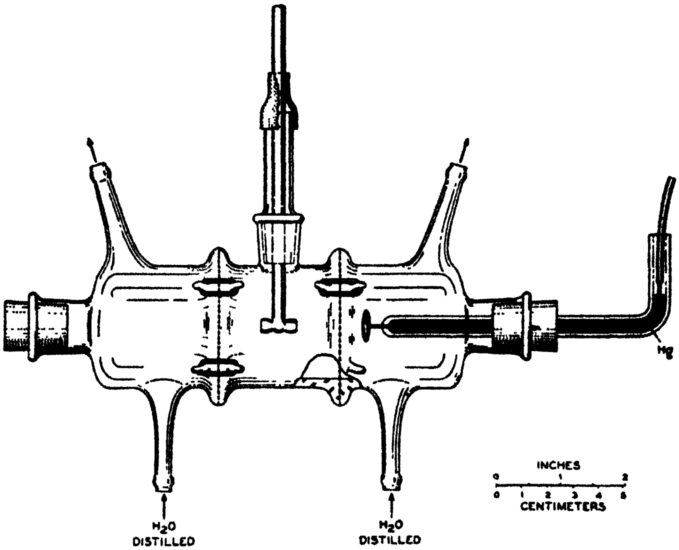

FIG. 2. Convertible dialyzer

In order to determine which protein had separated upon exhaustive dialysis, a sample of the filtered dialyzed serum was mixed with an equal volume of a saturated ammonium sulfate solution. After standing 24 hr. a small amount of a colorless flocculent material separated. This was isolated; upon being redispersed in a small amount of distilled water it immediately redissolved, and the solution gave negative protein tests.

The half-saturated serum from the above was completely saturated by the addition of solid ammonium sulfate. Precipitation took place immediately, and after standing 24 hr. a considerable amount of protein B precipitated. These experiments show that simple dialysis brings about the complete precipitation of protein A, while having very little effect on protein B. Tests also showed that protein C remained unprecipitated upon dialysis.

TABLE 4

Coagulation characteristics of Hevea latex

COAGULATING CONDITIONS	FRESH LATEX	FILTERED* FRESH LATEX	DIALYZED† FRESH LATEX	NORMAL AMMONIATED LATEX	DIALYZED AMMONIATED LATEX
Dilute acetic acid‡	+ Slow§; 1–2 hr.	− Very slow§	−	+	−
Dilute acetic acid and salt‡	+ Fast¶	+ Fast	+ Fast	+	+
Methyl alcohol (40–60 per cent)	+	−	−	+	−
Methyl alcohol (20–40 per cent) and salt	+	+	+	+	+
Heating at 75°C.	+ Slow	− Very slow	− Very slow	− Slow	− Very slow
Heating at 75°C. in the presence of salt	+ Fast	+ Fast	+ Fast	+ Fast	+ Fast

[*] Latex filtered through filter cel, rubber-washed, and redispersed in distilled water.

[†] Latex exhaustively dialyzed.

[‡] Acid added until pH was approximately 5.

[§] Slow is 0.5 hr. to 2 hr.; very slow is 2 to 8 hr.

[¶] Fast is less than 0.5 hr.

Effect of dialysis on the coagulation of latex

A comparison of the colloidal properties of normal and dialyzed latex demonstrated that the "salt effect" is prevalent in normal ammoniated latex. The coagulating properties of normal and salt-free latices are given in table 4. In these experiments an attempt has been made to correlate the observations with those made on the proteins shown in table 3 to determine which of the proteins are responsible for the colloidal behavior of the rubber particles.

The slow coagulation of fresh latex in comparison with ammonia-preserved latex may be explained on the basis that the proteins in fresh latex are different chemically from those in ammoniated latex. Coagulation experiments on fresh latex proteins A and B showed that they were more stable than proteins A and B from ammoniated latex.

If freshly tapped latex is quickly coagulated by adding alcohol to 40 per cent concentration, filtering the serum, and raising the alcohol concentration of the clear serum to 80 per cent, a precipitate is formed. When this precipitate is separated, dried, and added to dilute ammonia-preserved latex it prevents coagulation by acetic acid. This protective substance has a proteinic character and appears to be similar to the protective substance separated from Balata latex.

Changes in latex composition upon dialysis

Of the crystalloidal substances removed by dialysis, the ash constituents, consisting mainly of alkali and alkaline-earth phosphates, are almost completely eliminated. The total solids of exhaustively dialyzed fresh and ammoniated latex have been found to contain from 0.06 to 0.11 per cent ash, which was found to be largely phosphorus pentoxide. Rhodes and Bishop (12) found that latex contains a phosphatide in such a quantity as would account for this ash, since this substance is probably not removed by dialysis. Water-soluble organic crystalloids such as l-methylinositol, which is present in latex to the extent of 1 to 2 per cent, would be completely removed by dialysis.

Fresh latex and ammoniated latex lose nitrogenous substances upon dialysis. These substances consist in part at least of salts of amino acids, several of which have already been identified as being present in latex. The decrease in nitrogen content upon dialysis depends upon the particular latex studied. A sample of freshly tapped latex lost 22 per cent of its nitrogen, whereas two samples of ammonia-preserved latex showed losses of 36 to 39 per cent when dialyzed exhaustively.

Most of the coloring matter in the serum is removed by dialysis, which results in the latex becoming milky white. It was found that the serum of filtered freshly tapped latex is colorless but turns brown quickly upon exposure to air. Some lots of ammonia-preserved latex have a deep brown-colored serum, while others are light brown in color.

The total diffusible material on the total solid basis has been found to range from 8.2 per cent in the case of freshly tapped latex to 9.5 in the case of latex from the same source after 1 per cent ammonia had been added and it had stood for 2 months. The diffusate is a brown, transparent, brittle, gummy substance and is very hygroscopic.

The rate of removal of dialyzable substances from a sample of normal ammonia-preserved latex when dialyzed in the simple dialyzer is shown in figure 3. It is seen that dialysis is practically complete after 5 days. In this experiment the dialysis was made against ammonia water of pH 10.5 and the dialyzate was replaced periodically. The diffusate was determined by drying to constant weight.

EFFECT OF SALTS ON ALCOHOL COAGULATION OF DIALYZED LATEX

It has been shown that washed filtered fresh latex, dialyzed fresh latex, and dialyzed ammoniated latex at a pH of about 7 resist the coagulating action of alcohol to a greater extent than was the case with normal ammoniated latex. Although coagulation in the absence of salt can be accomplished by the addition of a considerable quantity of alcohol, it was definitely established that added salts of different types materially reduced the amount of coagulant. This conforms to the previous observations that a reduced salt content in the protein hydrosol greatly increases its stability. Since some salts have a greater effect than others, an attempt was made to determine the variations quantitatively. Methyl alcohol was chosen as the coagulant, and the technique developed for this purpose was as follows: The dialyzed latex of pH 7.4 was prepared by dialyzing normal ammoniated latex for 10 days against ammonia water of a pH of 10, followed by 4 days against distilled water. The latex after dialysis was adjusted to a total solids content of 15 per cent by the addition of distilled water. In the case where the pH was 5.4, acetic acid was added to the dialyzed latex. A sample of this latex was mixed with an equal volume of the salt solution of known molality, and the amount of alcohol necessary for coagulation was determined. This was done by first obtaining the approximate volume of alcohol which would coagulate the latex in 2 to 3 min. with mild agitation, followed by gradually increasing the amount of alcohol until coagulation was complete after 1 min. Coagula-

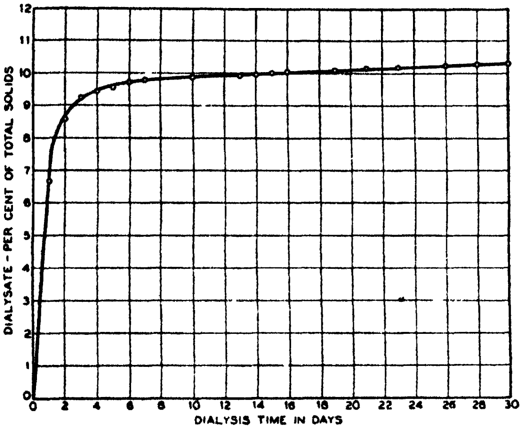

FIG. 3. Rate of dialysis of ammoniated latex

TABLE 5

Effect of salts on alcohol coagulation of dialyzed latex

SALT	SALT CONCENTRATION		ALCOHOL REQUIRED FOR COAGULATION	
	pH 5.4	pH 7.4	pH 5.4	pH 7.4
	moles	*moles*	*per cent by volume*	*per cent by volume*
KCl	0.0000	0.0000	38	95
	0.0025	0.0068	23	73
	0.0100	0.0096	18	66
	0.0200	0.0137	15	63
		0.0205		61
		0.0274		57
		0.0342		54
		0.0475		47
$BaCl_2$	0.0000	0.0000	38	95
	0.0012	0.0004	15	55
	0.0025	0.0012	11	30
	0.0050	0.0021	8	20
	0.0100	0.0029	6	15
		0.0067		13
		0.0104		11
		0.0475		0
$AlCl_3$		0.0000		95
		0.0004		62
		0.0008		49
		0.0016		48
		0.0030		78
		0.0047		84

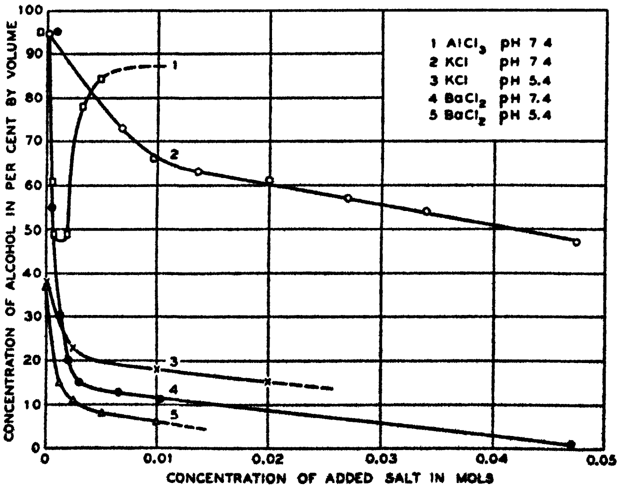

FIG. 4. Effect of salts on alcohol coagulation of dialyzed latex

tion was called complete when the alcoholic serum no longer gave indications of milkiness when rotated in an inclined test tube. The results of the experiments are given in table 5 and plotted in figure 4.

The steepness of the initial part of each curve indicates that the alcohol coagulation of latex does not result simply from the dehydration of the adsorbed proteins, as generally believed. The aluminum chloride curve is unique, as it shows that small amounts of this salt behaved normally in respect to other salts, but at higher concentrations it shows very little effect. The other curves show a gradual slope towards the abscissa, the barium chloride curve striking it at a molality of 0.475, while at the same molality of potassium chloride a concentration of 47 per cent by volume of methyl alcohol was required for coagulation. The greater coagulating

TABLE 6

Effect of salts on alcohol coagulation of dialyzed acid latex at 2.5 pH

SALT	SALT CONCENTRATION	ALCOHOL REQUIRED FOR COAGULATION	REMARKS
	moles	*per cent by volume*	
KCl	0. -0.1	>95	Stable alcosol
	0.1-0.4	>95	Slight coagulation
	0.5	92	
	0.6	77	
	0.7	63	
	0.8	47	
	0.9	32	
	1.0	17	
	1.11	0	
K_2SO_4	0.0	>95	Stable alcosol
	0.0025	>95	Slight coagulation
	0.005	79	
	0.010	53	
	0.013	41	
	0.015	30	
	0.020	17	
	0.025	12	
	0.030	7	
	0.040	0	
$BaCl_2$	0.0	>95	Stable alcosol
	0.01-0.05	>95	Slight coagulation
	0.10-0.20	>95	Slight coagulation and flocculation
	0.30	77	
	0.40	47	
	0.50	13	
	0.55	0	

power of divalent as compared with monovalent metal salts confirms the results of Henri (6). The abnormal behavior of aluminum chloride may possibly be related to its hydrolysis, which changes the pH of the solution. The cause of this effect, however, is not clear.

A study was made of the effect of potassium chloride, barium chloride, and potassium sulfate on the coagulation of dialyzed latex adjusted to a pH of 2.5 by the addition of formic acid. In the case of potassium sulfate the coagulation was not as sharp and complete as in the case of the other salts, making it necessary to approach the coagulation point very carefully by a very gradual increase in alcohol. Part of the latex at this end point was flocculated and the remainder coagulated, so it was necessary to determine the point where the flocculation was no longer increased by further addition of alcohol. The results are given in table 6 and plotted in figure 5.

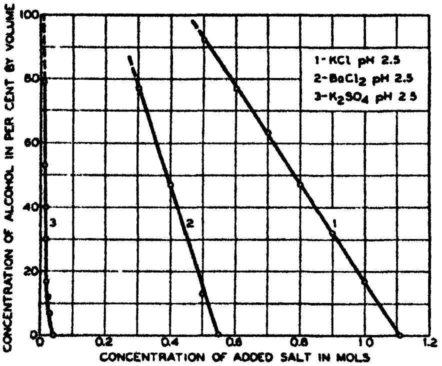

FIG. 5

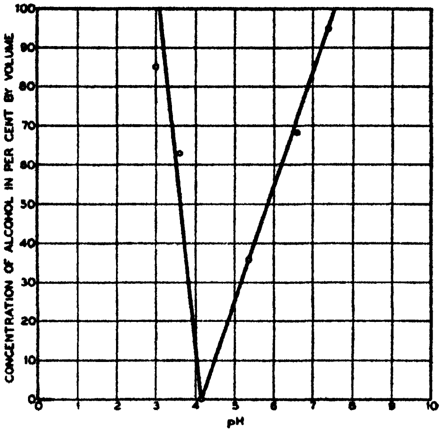

FIG. 6

FIG. 5. Effect of salts on alcohol coagulation of dialyzed latex

FIG. 6. Effect of pH on alcohol coagulation of dialyzed latex

The maximum effect of salt on coagulation is shown in the case of barium chloride at a pH of 5.4 and 7.4, which is on the alkaline side of the isoelectric point, and by potassium sulfate at a pH of 2.5, on the acid side. Barium chloride at a pH of 2.5 is approximately twice as effective as potassium chloride at the same pH, indicating that the chloride ions in the barium chloride are involved primarily and that the barium ions do not enter into the coagulation phenomena. On the other hand, at a pH of 7.4 it is the barium or positive ions which effect coagulation. These data show that the divalent positive ions are more effective than monovalent positive ions when the pH is on the alkaline side of the isoelectric point, and that the divalent negative ions are more effective than the monovalent ions when the latex is on the acid side of the isoelectric state of the particles.

A study was made of the effect of pH on the amount of alcohol required for coagulation of 7.5 per cent dialyzed latex. These results have been plotted in figure 6, and show that alcohol coagulation depends on the magnitude of the charge on the latex particles. The maximum sensitivity to coagulation is seen to be at the isoelectric point of the latex particles, which in turn is controlled by the isoelectric points of the adsorbed proteins on the particles. Evidence in favor of the conclusion that both protein A and protein B are adsorbed on the rubber particles was obtained by a

TABLE 7

Effect of pH on stability of dialyzed latex

pH OF LATEX	IMMEDIATELY UPON DILUTION	AFTER 8 MIN. AGITATION
1.75	Completely dispersed	Partly coagulated; serum very turbulent
2.00	Very slightly flocculated into very small flocculi	Partly coagulated; serum very turbulent
2.50	Very slightly flocculated into very small flocculi	Partly coagulated; serum very turbulent
2.75	Very slightly flocculated into very small flocculi	Partly coagulated; serum very turbulent
3.00	Partly flocculated into very small flocculi	Partly coagulated; serum very turbulent
3.50	Partly flocculated into small flocculi	Largely coagulated; serum cloudy
3.60*	Partly flocculated into small flocculi	Largely coagulated; serum cloudy
3.70	Partly flocculated into small flocculi	Largely coagulated; serum cloudy
3.80	Almost completely flocculated into large flocculi	Largely coagulated; serum cloudy
3.90	Almost completely flocculated into large flocculi	Almost completely coagulated; serum slightly cloudy
4.00	Almost completely flocculated into large flocculi	Almost completely coagulated; serum very slightly cloudy
4.15	Completely flocculated into large flocculi	Completely coagulated after 2 min. agitation
4.30	Almost completely flocculated into large flocculi	Almost completely coagulated; serum cloudy
4.40	Partly flocculated into small flocculi	Largely coagulated; serum very cloudy
4.55	Very slightly flocculated into very small flocculi	Partly coagulated; serum very cloudy
4.70*	Completely dispersed	Very slightly flocculated; serum very turbulent
4.90	Completely dispersed	Completely dispersed

* Addition of a little sodium chloride brought about sharp coagulation.

careful study of the changes in the colloidal stability of a diluted dialyzed latex at various pH intervals between 1.75 and 4.9. The experimental procedure consisted in diluting 0.05 cc. of a 29 per cent total solids dialyzed latex with 3 cc. of distilled water having a definite pH, and observing the state of the rubber particles immediately upon dilution and after 3 min. agitation. It was found that maximum instability was reached at a pH of 4.15, which is approximately half-way between the isoelectric points of the two proteins. When the pH was varied to either side of this point, a definite trend towards increased stability was noted. This was more pronounced when the pH was increased rather than when it was decreased, as is seen in table 7. The pH determinations were made with a Beckmann pH meter, using a glass electrode.

Twiss (16) has given 4.2 as the isoelectric point of dialyzed latex, determined by studying the electrophoretic movement of latex particles under various pH conditions under a microscope. He therefore showed that there is a reversal of charge on the latex particles at a pH of 4.2, whereas the present work shows that latex has its minimum stability at a pH of 4.15. The agreement of these separate investigations using different methods is excellent and leads to the conclusion that the isoelectric point of latex particles lies at a pH between 4.15 and 4.2.

DISCUSSION

It has been shown in confirmation of the finding of other investigators that the rubber particles are stabilized in ammoniated latex by complex conjugated proteins. It appears that two of the three proteins present are primarily responsible for the colloidal behavior of the rubber particles. The mechanism by which they function in this capacity is intimately associated with the electrical charge they induce on the surfaces of the rubber particles. The way in which native soluble proteins of the type similar to the rubber proteins become charged and exist in aqueous solution as proteinic anions and cations may be explained on an ampholytic basis. The two rubber proteins A and B are ampholytes, as they respond to reversible precipitation by changes in the hydrogen-ion concentration of the dispersion medium. This property has been accounted for in the case of other native soluble proteins on the basis that such proteins are polybasic acids and polyacidic bases. This would imply that the rubber proteins contain in their molecular structure a number of the amino acid residues of the basic and acid type. The presence of these free amino and carboxyl groups results in the so-called zwitter-ion effect, which is useful in explaining the mechanism of coagulation. The actual existence of these groups in rubber proteins has been shown by Midgley, Henne, and Renoll (8). This insight on the amphoteric nature of the rubber proteins as applied to the proteinic sheath on the rubber particle is of fundamental importance. The adsorbed protein layer on the particles, which may be continuous or discontinuous, scatters on the surface of the rubber particles numerous positive and negative charges. When the pH of the serum is on the alkaline side of the isoelectric point of the proteins, protons are lost and the surface of the particle contains a majority of negatively charged carboxyl groups; the magnitude of the charge on the particle depends on the pH of the solution. If the pH of the serum is on the acid side of the isoelectric point, the majority of the charges are positive and the rubber particle is positively charged. The particle becomes isoelectric when the pH of the solution is midway between the isoelectric points of the adsorbed proteins on the particles, which has been shown to be at a pH of 4.15.

Normal ammoniated latex has been shown to exhibit a "salt effect," which is due not only to the original salts present but to those formed by neutralization in the process of coagulation. This "salt effect" has a wider application than the explanation of the properties of a well-dialyzed latex. It explains the additional stability of any latex in which the salt content has been lowered to within the neighborhood of 0.1 per cent or lower. There are many different ways in which this may be accomplished: for example, repeated filtration with intermittent washing and repeated centrifuging result in latices which exhibit additional stability towards coagulating agents.

Pauli (10, 11) showed that the complete removal of electrolytes resulted in greatly increased stability of albumin towards coagulating influences. Apparently no one has satisfactorily explained the mechanism of this "salt effect." As a matter of fact, this effect has not been widely recognized.

The experiments described in this paper on the effect of salts in the coagulation of latex with alcohol bring out many interesting points. The generally accepted idea that the coagulation of latex and proteins with alcohol is solely a dehydration phenomena must be questioned, since it has been shown that the nature and quantity of the salts present and the pH of the solution are controlling factors in the amount of alcohol required for coagulation.

Salts have their greatest effect in coagulating latex near the isoelectric state of the adsorbed proteins. This is probably because under this condition the latex particles are weakly charged and become easily discharged by bombardment of ions of opposite charge. A highly charged latex particle, on the other hand, would not be so readily discharged to the isoelectric state by ionic bombardment. The effect of adding divalent ions of opposite charge to the particles would be expected to neutralize the charge on collision more effectively than a monovalent ion. This would explain why barium chloride is more effective than potassium chloride in the coagulation of negatively charged latex particles, and why potassium sulfate is more effective than potassium chloride in the coagulation of positively charged latex particles.

Alcohol coagulation in the presence of salts, however, may be influenced by other factors, such as salt formation directly with the protein whereby the protein becomes less soluble. The well-known precipitation of proteins with heavy-metal salts is a case in point. The addition of alcohol to a protein hydrosol would be expected to influence its hydration, and it might reduce the overall charge by reducing its ionizing power. The greatest stability of the rubber proteins would be expected in water free from electrolytes and dehydrating influences and at a pH furthest removed from its isoelectric point. This appears to be confirmed by this investigation. As the concentration of water is reduced by addition of alcohol, the amphoteric nature of the protein would be less pronounced and its electrical charge reduced.

Latex immediately after tapping does not coagulate for some time after adding acetic acid, whereas instant coagulation occurs in the case of the ammonia-preserved product. This difference appears to be due to the increase in the salt content of the ammonia-preserved product and to a greater protective power of the fresh latex protein, which is partly destroyed by bacterial action and by reaction with ammonia on standing. In spontaneous coagulation the protective power of the proteins and associated substances apparently is destroyed by extensive bacterial action under pH conditions favorable for bacterial activity and for coagulation. It is known that native protein sols frequently become much more sensitive towards the effect of electrolytes when subjected to various treatments which change their nature. The effect of bacteria and ammonia on fresh latex is a case in point.

The complexity of the colloid chemistry of the proteins and their function as protective coatings on dispersed particles is well illustrated in the present investigation. Progress in this field has been slow, since it is very difficult to control the numerous variables which enter into experiments with proteins. Knowledge is very incomplete concerning the molecular structure of proteins, and it is well recognized that the preparation of proteins of uniform composition and properties offers the greatest difficulty.

Further work in determining the effect of salts on the colloidal stability of the numerous types of proteins found in nature may be found very useful. It is well known that the solubility of certain types of proteins, such as the globulins, is increased in the presence of neutral salts.

In colloid systems the electrical charges on the dispersed particles appear to be of fundamental importance to their stability. Maximum stability exists when either the positive or the negative charge is predominantly high. A wider recognition of this view should be helpful in future studies of factors which influence the stability of such systems.

SUMMARY

1. Three protein fractions have been isolated from fresh and ammoniated latex serum. The usual color and precipitation reactions have been carried out and place these proteins in the classification of conjugated glycoproteins. Proteins from fresh latex differ in composition from and are less sensitive to coagulating influences than the proteins from ammonia-preserved latex.

2. Coagulation tests using latex coagulants were performed on the protein hydrosols. It was found that as the concentration of electrolytes decreased coagulation of the proteins was inhibited, whereas coagulation readily took place when salts were present in sufficient concentration.

3. Normal ammoniated latex has been subjected to extensive dialytic treatment in specially constructed apparatus. As the ash content of the total solids from the latex approached a value of 0.1 per cent, the mechanical stability decreased and the chemical stability increased. Addition of excess acid or alkali to dialyzed latex yielded stable latices which were highly resistant to spontaneous coagulation.

4. Quantitative coagulation studies, using methyl alcohol and salts of varying types and made on dialyzed latex adjusted to various pH conditions, show that small amounts of a dissolved salt greatly aid coagulation. Considerable variation in the effectiveness of different salts was found. In acid latex of pH 2.5 the charge on the latex particles was reversed from negative to positive and the salt effect was shown to be different from that experienced in the case where the pH was on the negative side of the isoelectric point.

5. The amount of alcohol required to coagulate dialyzed latex depends on the pH of the latex. It is shown that the amount of alcohol required for coagulation increases on each side of the isoelectric point, which was determined to be at a pH of 4.15.

6. The protective mechanism of proteins has been discussed on the basis of the electrical charges induced on the surface of the latex particles by the presence of the protein layer. The zwitter-ion effect induced by the presence of free amino and carboxyl groups in the rubber proteins is of fundamental importance in determining the colloidal characteristics of latex.

The fresh latex from the Hevea and some of the other types of latices mentioned in this paper were obtained from the Department of Agriculture through the U. S. Plant Introduction Garden, Coconut Grove, Florida. The authors wish to express their appreciation for the assistance and coöperation of the Department.

REFERENCES

(1) **Beadle, C., and Stevens, H. P.**: Kolloid-Z. **13**, 211 (1913).
(2) **Bishop, R. O.**: Malayan Agr. J. **15**, 27 (1927).

(3) Bondy, C., and Freundlich, H.: Compt. rend. trav. lab. Carlsberg, Sér. chim. **22**, 89–98 (1938); Rubber Age **44**, 377 (1938).
(4) Daniel, F. K., Freundlich, H., and Söllner, K.: Trans. Faraday Soc. **32**, 1570 (1936).
(5) Dekker, P.: Comm. Delft **1**, 27 (1916).
(6) Henri, V.: Caoutchouc & la gutta-percha **3**, 510 (1906).
(7) Kemp, A. R.: Proceedings of the Rubber Technology Conference, London, 1938, pp. 68–79: India Rubber World **99**, 41 (1938).
(8) Midgley, T., Henne, A. L., and Renoll, M. W.: J. Am. Chem. Soc. **59**, 2501 (1937).
(9) Noble, R.: Proceedings of the Rubber Technology Conference, London, 1938, pp. 131–50.
(10) Pauli, Wo.: Ann. Rev. Biochem. **3**, 118 (1934).
(11) Pauli, Wo., and Valko, E.: *Kolloidchemie der Eiweisskörper.* Theodor Steinkopff, Dresden and Leipzig (1933).
(12) Rhodes, E., and Bishop, R. O.: J. Rubber Research Inst. Malaya **2**, 124 (1930).
(13) Spence, D., and Kratz, G. O.: Kolloid-Z. **14**, 262 (1914).
(14) Stevens, H. P., Dyer, J. W. W., and Rowe, J. W.: J. Soc. Chem. Ind. **56**, 397T (1937).
(15) Stevens, H. P., and Rowe, J. W.: J. Soc. Chem. Ind. **58**, 116 (1939).
(16) Twiss, D. F.: Trans. Inst. Rubber Ind. **6**, 419 (1931).

THE LIQUID STATE OF THE ELEMENTS

WILLIAM HUME-ROTHERY

The Old Chemistry Department, The University Museum, Oxford, England

Received January 8, 1940

I

In recent years much attention has been paid to the structure of liquids, both theoretically and by the application of x-ray diffraction methods. Most of this work has been concerned with the liquid state near the melting point of the substances concerned, and the general conclusion has been that at these temperatures the liquid state possesses a structure of a dynamic nature bearing some resemblance to the crystal structure of the same substance. The phenomena associated with the critical temperature and pressure show that at the higher temperatures there is no sharp distinction between the liquid and the gaseous states, although at the lower temperatures the difference is well marked. In the present paper we shall examine the ranges of existence of the liquid state of the elements, and discuss the data in a general way. Any really quantitative treatment of the subject must of course involve a knowledge of the complete equations of state of the different elements, and the necessary data are generally lacking. For a preliminary treatment we shall examine the boiling points at the pressures 760 and 7.6 mm., and ignore the very slight change in melting point with pressure in this range.

The experimental data used are discussed in the appendix. Great care is needed before boiling point data are used for critical comparison, and in general the possible errors are much greater than those given in collected tables or in summaries of papers.

II

We may first define the *liquid range*, L_p, as the difference between the melting point and the boiling point at the pressure p. At a given pressure, the boiling point represents the maximum temperature at which a substance can exist in a condensed state. We may therefore define the *solid ratio*, S_p, and the *liquid ratio*, F_p, at a pressure p, by the relations

$$S_p = \frac{\text{Absolute melting point at pressure } p}{\text{Absolute boiling point at pressure } p} = \frac{(T_m)_p}{(T_b)_p}$$

$$F_p = \frac{\text{Liquid range at pressure } p}{\text{Absolute boiling point at pressure } p} = \frac{F_p}{(T_b)_p}$$

so that $S_p + F_p = 1$. The values of S and F thus give the fractions of the temperature range of the condensed state occupied by the solid and liquid states, respectively.

Table 1 shows the boiling points, melting points, liquid ranges, and liquid ratios of the elements of Groups I A and II A and of the first two elements in Groups III A and IV A. The elements of the first short period have abnormally high melting points and boiling points. For the remaining alkali metals, the liquid ranges are of the same order, while the liquid ratios are surprisingly constant, the values of F_{760} lying between 0.67 and 0.69. At 760 mm., therefore, the liquid state occupies about two-thirds of the total condensed range, while at 7.6 mm. the liquid state still occupies about one-half of the condensed range. For lithium the values of the liquid range and liquid ratio are somewhat higher.

For the alkaline-earth metals the position is quite different. Beryllium has an abnormally high boiling point and melting point, and its liquid range is greater than that of lithium at high pressures, but smaller at low pressures. Its liquid ratio is, however, smaller than those of the alkali metals at all pressures. Magnesium, calcium, and strontium have liquid ranges of the same order, which are smaller than those of the preceding alkali metals, and their liquid ratios are approximately constant, and very much less than those of the alkali metals. The values of F_{760} lie between 0.331 and 0.363, so that at 760 mm. the liquid state occupies roughly one-third of the total condensed range, while at 7.6 mm. the $F_{7.6}$ values are less than 0.1, and the liquid occupies less than one-tenth of the condensed range. The values for barium are somewhat higher than those for the remaining alkaline earths, and the reason for this is discussed later.

In Group III data are available only for aluminum, whose boiling point and liquid range are very much greater than those of magnesium. The liquid ratios of aluminum are, however, approximately equal to those of the alkali metals, the liquid again occupying about two-thirds of the total condensed range at 760 mm. Boiling point data are not available for the remaining elements of Group III.

TABLE 1

Boiling points, melting points, liquid ranges, and liquid ratios of lithium, sodium, potassium, and other elements

METAL	MELTING POINT	BOILING POINT		LIQUID RANGE		LIQUID RATIO	
		760 mm.	7.6 mm.	L_{760}	$L_{7.6}$	F_{760}	$F_{7.6}$
	°K.	°K.	°K.	°K	°K.		
Li	452	1599	1142	1147	690	0.717	0.604
Na	370.5	1156	810	785	439	0.679	0.542
K	336.6	1035	703	698	366	0.674	0.521
Rb	311.5	969?		657?		0.678?	
		986?		674?		0.684?	
Cs	299	943?	632	644?	333	0.683	0.527
		977?		678?		0.694	
Be	1551	3243	2086	1692	535	0.522	0.257
Mg	923	1380	994	457	71	0.331	0.071
Ca	1124	1712	1238	588	114	0.343	0.092
Sr	1044	1639	1153	595	109	0.363	0.095
Ba	977	1880	1285	903	308	0.480	0.240
B	2500?						
Al	932	2543	1945	1611	1013	0.634	0.520
C	3845						
Si	1694	2628	2093	934	399	0.355	0.191

In Group IV data are available only for silicon, and it will be seen that on passing from aluminum to silicon the liquid range and liquid ratio change in the same way as on passing from sodium to magnesium. Both boiling point and melting point increase, but the change in melting point is much the greater, so that the liquid range falls, and the liquid ratios approximate to those of the alkaline earths. It should also be noted that, although exact data are not yet available for the boiling point of carbon, it is almost certain that the liquid range and liquid ratio are relatively small, since marked volatilization occurs at the melting point.

From the above survey it can be seen that if we regard the change solid → liquid → gas as involving an increasing destruction of an ordered state, the general effect of increasing valence is to preserve the ordered state to higher temperatures. But as regards the existence of the liquid phase, this effect is not continuous, but shows an alternation on passing from one group to the next. Groups I and III give high liquid ratios and liquid ranges greater than those required by smooth curves, while Groups II and IV give small liquid ratios and liquid ranges below a smooth curve, except in the cases of beryllium and barium. In general, therefore, we may say that for these elements the liquid state is favored by odd valences.

We may next consider copper, silver, and gold, and the elements immediately following them in the Periodic Table. These are distinguished from the elements of the A subgroups by a sharp fall in both boiling point and melting point on passing from Group I to Group II; the reason for this is discussed later. For the first three groups, the liquid ranges show the same alternation as in the elements of the A groups. There is first a sharp fall in the liquid range on passing from the elements of Group I B (copper, silver, and gold) to those of Group II B (zinc, cadmium, and mercury). This is followed by an enormous rise in the liquid range on passing to Group III B (gallium, indium, and thallium), in the same way that the liquid range increases so markedly on passing from magnesium to aluminum in the second period.[1] In the case of mercury, the very low melting point results in an abnormally high liquid ratio, but for the remaining elements of Groups I B, II B, and III B, the liquid ratios show the same alternations as those of the A subgroups, the ratios being low for Group II, and higher for Groups I and III. In general, therefore, we may say that for the elements of these three subgroups, the liquid state is again favored by odd valences. The data are given in table 2.

For the elements of Group IV B, the position is less simple. Data are not available for germanium,[2] although its boiling point is probably above 1700°C. The comparatively high melting point (960°C.) naturally lowers the liquid ratio. After germanium a remarkable change takes place. The boiling points of tin and lead remain very high, but the melting points fall to comparatively low values, so that the liquid range is greatly increased. This change between the third and fourth periods is shown also in the elements of Groups V and VI. In Group V the first three members,—nitrogen, phosphorus, and arsenic,—have small or zero liquid ranges at the pressures with which we are concerned, but on passing to antimony the liquid range L_{760} is of the order 1000°C., while for bismuth

---

[1] The boiling point of indium is not known, but is undoubtedly very high, since the metal is described as comparatively non-volatile at 1450°C.

[2] The melting point of germanium is 960°C., and the metal is not appreciably volatile at 1500°C. The liquid range is therefore certainly more than 800°C.

L_{760} is as great as 1289°C. In Group VI, on passing from oxygen to selenium, the liquid range increases gradually, the values of L_{760} being 35°, 324°, and 468°C. for oxygen, sulfur, and selenium, respectively, and there is then a marked increase on passing to tellurium, for which L_{760} = 938°C. For the elements of Groups IV, V, and VI, therefore, the liquid state is greatly favored on passing from the third to the fourth and later periods. In Group VII, however, the liquid range always remains very small, although the range of the condensed state (solid or liquid) increases

TABLE 2

Melting points, boiling points, liquid ranges, and liquid ratios of copper, silver, gold, and other elements

METAL	MELTING POINT	BOILING POINT		LIQUID RANGE		LIQUID RATIO	
		760 mm.	7.6 mm	L_{760}	$L_{7.6}$	F_{760}	$F_{7.6}$
	°K.	°K.	°K.	°K.	°K.		
Cu	1356	2610	1881	1254	525	0.480	0.279
Ag	1233.5	2424	1808	1190	574	0.491	0.317
Au	1336	2983	2100?	1647	764	0.552	0.359
Zn	692	1180	844	488	152	0.414	0.180
Cd	594	1040	774	446	180	0.429	0.233
Hg	234.2	630	449	396	215	0.629	0.479
Ca	302.8	2300	1695	1997	1392	0.868	0.821
In	429.4	>>1720		>1300		>0.75	
Tl	430	1730	1255	1300	825	0.751	0.657
Ge	1231						
Sn	505	2635	1726	2130	1221	0.808	0.707
Pb	600	1965	1404	1365	804	0.694	0.573
N	63	77	Sublimes	14		0.182	
P	317	554	415	237	98	0.427	0.236
As	Sublimes	903					
Sb	903	1910		1007		0.527	
Bi	544	1833		1289		0.703	
O	55	90	61	35	6	0.389	0.098
S	393	718	507	325	114	0.453	0.225
Se	493	961		468		0.487	
Te	725	1663		938		0.564	
F	50	85.2		35.2		0.413	
Cl	171	238.4	Sublimes	67		0.281	
Br	265.7	331.8	Sublimes	66		0.199	
I	387	457	Sublimes	70		0.153	

with increase in the number of the period. Thus iodine as a solid is stable above the boiling points of the other halogens.

III

In the process of condensation the free atoms of a metallic vapor combine to form the liquid, and if the latter is regarded as held together by electrons, we may reasonably expect some relation between the ionization potentials of the free atoms and the boiling point phenomena. A simple relation can only be expected in the case of the alkali metals, for which the ions are very small and there is only one electron per atom. In these metals the interactions of the cores or ions will be relatively small, and the cohesion of the liquid will be due essentially to the valence electrons. In the solid, where the atoms are close together, the single normal electronic state of the valence electron of the free atom is broadened out into a band of allowed levels, but, since there is only one electron per atom, the most stable condition is that with the electrons entirely (or almost entirely) in *s* states, as in the free atoms. With elements of higher valence this is no longer the case. Thus with magnesium, the free atom contains a complete subgroup of two electrons in *s* states, but in solid magnesium the work of Skinner (19) shows that the most stable condition is that with some electrons in *p* states. Since the interatomic distances in liquid metals are not greatly different from those in solids, we may reasonably expect similar considerations to apply, so that with metals of valence greater than one, the electronic states in the free atoms and in the liquid metal will probably not be the same. With copper, silver, and gold, at the distances concerned in solids and liquids, there is appreciable interaction between the outermost electrons of the cores or ions, so that the position is much more complicated than for the alkali metals, and it is for the latter alone that we may expect a simple relation.

Let V be the ionization potential of the valence electron of an alkali metal, N the principal quantum number of the valence electron, $T_{b_{760}}$ the boiling point, and m the atomic weight. If then we plot log N^2V against log $\frac{T_b}{mN^2}$, we obtain a straight line as shown in figure 1. Further, the gradient of this straight line is -3, so that

$$T_{b_{760}} = \frac{mC}{N^4V^3}$$

or

$$\frac{T_bN^4V^3}{m} = C$$

The values of C for the different alkali metals are as follows:

METAL	$C \times 10^{-4}$	METAL	$C \times 10^{-4}$
Lithium	57.02	Rubidium	50.98* 51.87†
Sodium	54.54	Cesium	53.56* 55.50‡
Potassium	54.68		

* These values are calculated from the boiling point data of Ruff and Johannsson (18).

† This value for rubidium is from the review by Eucken (4).

‡ This value for cesium is from the work of Langmuir and Taylor (14).

The only really accurate data are for sodium and potassium, and for these, C is constant to within the limits of accuracy of the experimental data.

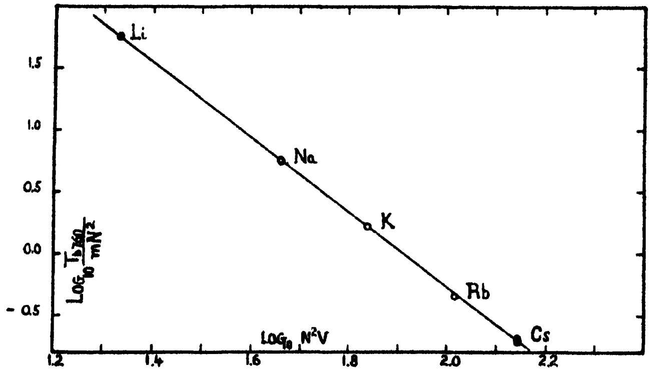

FIG. 1. Plot of $\log_{10}\frac{T_{b760}}{mN^2}$ against $\log_{10}N^2V$ for the alkali metals

For cesium the boiling point is 943°K. according to the work of Ruff and Johannsson (18) and 977°K. according to the vapor pressure work of Langmuir and Taylor (4), who used an indirect positive-ion method. The corresponding values of C lie on opposite sides of the value for sodium, and a more accurate direct determination is desirable. For rubidium no accurate data are yet available. The boiling point (969°K.) given by Ruff and Johannsson (18) is almost certainly too low, and the slightly higher value (986°) given by Eucken (4) is from incomplete vapor pressure work. For lithium the value of C is 5 per cent higher than for sodium, and this difference is probably genuine, although the boiling point is unfortunately not well established, since, apart from experimental errors, the value (1599°K.) involves an extrapolation of 250° from vapor pressure measurements at lower temperatures, and the presence of diatomic molecules makes this uncertain. In general, therefore, except for lithium the above relation is in good agreement with the facts.

It is natural to look for relations between the energy constants of vaporization and the ionization potentials of the valence electrons in a series of elements such as sodium, magnesium, aluminum, and silicon, and a relation has been found in the following way: It is well known that the vapor pressures of liquid metals can often be expressed over wide ranges by empirical equations of the type

$$\ln p = -\frac{a}{T} + b$$

In many papers it is assumed that the constant a is equal to λ/R, where λ is the latent heat of evaporation. Actually this is not true, and the constant a involves not only λ/R, but other factors such as the difference in specific heats of the gaseous and liquid phases, the departure from the ideal gas laws, dissociation or association equilibrium in the gaseous phase, etc. In so far as the vapor pressures are accurately expressed by the above type of equation, the constant g is of course in some ways a definite characteristic of the liquid. Eucken (4) has tabulated the most probable values of $L_s = Ra$ for different metals, some of his figures being given in table 3. For the series sodium to silicon we now find that simple relations exist between the constants L_s and the ionization potentials (V) of the free atoms. These may be summarized by saying that L_s is directly proportional to $f(V)$, where the function $f(V)$ has the following values:

TABLE 3

Most probable values of $L_s = Ra$ for different metals

METAL	$L_s = Ra$	BOILING POINT*
Sodium	23,400	1156
Magnesium	32,000	1380
Aluminum	69,600	2543
Silicon	72,600	2628
Gold	82,300	2983
Mercury	14,100	630
Thallium	39,700	1730
Lead	42,700	1965
Bismuth	41,100	1833

* From tables 1 and 2.

For sodium: $$f(V) = \frac{V_1}{1}$$

For magnesium:
$$f(V) = \frac{V_1 + V_2}{3}$$

For aluminum and silicon:
$$f(V) = \frac{V_1 + V_2 + V_3}{3}$$

where V_1, V_2, and V_3 are the first three ionization potentials of the elements concerned. This relation is shown graphically in figure 2, and holds within the limits of accuracy of the values of L_s. This figure also serves to illustrate the second characteristic of the series: namely, that L_s increases rapidly with increasing valence from sodium to aluminum and then becomes practically constant, the values for aluminum and silicon differing by only 3000.

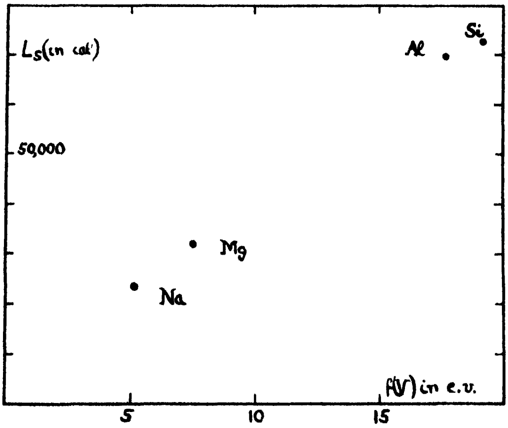

FIG. 2. Plot of L_s in calories against $f(V)$ in electron volts

In the series gold, mercury, thallium, lead, and bismuth, the core interaction results in a very high value of L_s for gold, but for the remaining elements it will be seen that L_s becomes practically constant at thallium, so that, as in the series sodium–magnesium–aluminum–silicon, L_s reaches its limiting value at Group III.

IV

In considering the data described above, it is necessary first to understand the difference between the elements of the A and B subgroups. In the A subgroup metals at the beginning of each period, the ions are very small compared with the interatomic distances in solid and liquid metals, and the cohesive forces in the liquid and solid states may be regarded as due essentially to the valence electrons. In the transition elements, and also in copper, silver, and gold, the ions are relatively much larger, and, at the interatomic distances in solid and liquid metals, the electron clouds of the ions overlap appreciably. It is now generally recognized that in these elements part of the cohesion is due to outermost electrons of the ions, the nature of this cohesion being regarded as due to "core interaction," van der Waals forces, or covalent bond formation (Pauling). At the end of the transition process, when the outermost shell of the ion contains a group of eighteen electrons, the ion contracts rapidly with increasing atomic number, so that at each step the cohesion becomes due more to the valence electrons and less to the electrons of the ions. It is for this reason, presumably, that in copper, silver, and gold the melting points and boiling points are much higher than those for the succeeding Group II elements zinc, cadmium, and mercury, whereas in the A subgroups the opposite is the case.

The boiling point is the temperature at which the liquid and solid are in equilibrium, and the process of condensation of a metallic vapor may be looked upon as one in which the electronic structure of the free atom breaks down and is replaced by the modified valence electron structure of the liquid. On general principles we should, therefore, expect the vapor phase to be favored by a stable electronic grouping of the free atom, and this is clearly what is required in order to explain the alternating valence effects described in the preceding section. In Groups I and III the free atoms have a single unpaired electron with a comparatively low ionization potential, as can be seen from table 4, and hence the tendency for the atoms to combine is great, and the liquid state is favored. In Group II the valence electrons form a complete subgroup of two *s* electrons, and the stability of the gas is favored. We can therefore understand why the liquid state of the elements of Group II is less stable than would be expected from the properties of the liquids of the elements in Groups I and III. In the B subgroup elements, the stabilities of liquid copper, silver, and gold are favored in addition by the core interaction, which diminishes

TABLE 4

Ionization potentials of free atoms in Groups I and III

ELEMENT	FIRST IONIZATION POTENTIAL	ELEMENT	FIRST IONIZATION POTENTIAL
Lithium	5.37	Potassium	4.32
Beryllium	9.28	Calcium	6.09
Sodium	5.12	Rubidium	4.16
Magnesium	7.61	Strontium	5.67
Aluminum	5.96	Cesium	3.87
Silicon	8.12	Barium	5.19

rapidly as the ion contracts on passing to the later elements, but the relative stabilities of the liquids zinc and gallium, cadmium and indium, and mercury and thallium, are quite parallel to those of magnesium and aluminum.

In Group IV the boiling points and L_e values of the elements, so far as they have been determined, are not much greater than those of the preceding elements of Group III, so that, in so far as the gas–liquid equilibrium is concerned, there is little change in passing from Group III to Group IV. For carbon and silicon this can be partly understood when it is remembered that, although the normal states of the atoms contain two unpaired electrons, the vapors contain polyatomic molecules. In so far as the atomic attraction is satisfied by the formation of molecules, less is available for the liquid cohesion, and the vapor state is therefore favored. For tin and lead, however, the vapors are monatomic, and a further explanation is required (see page 18).

On passing from Group III A to Group IV A the liquid range is lowered, owing to a rise in melting point, showing that the solid becomes more stable when there are four electrons per atom. This point is dealt with later, as well as the low melting points of the B subgroup elements of Groups III and IV.

V

The fact that the upper limit (i.e., the boiling point) of the liquid phase is relatively so much higher for the metals of odd valence, suggests that the cohesive forces in liquid metals resemble those of covalent or electron-pair bonds, so that the orbital model of Pauling (16), although incomplete for solid metals, may be much more valid for the liquid state. To understand the nature of the condensation process further, we have to consider the characteristic property of the liquid,—namely, a constant volume irrespective of shape. We may suggest tentatively that one condition for a liquid is that each atom (or molecule) is bound to three neighbors, but not in general to more than three. If each atom is bound only to two neighbors, zigzag chains may be formed, but a third bond is necessary to hold the chains together, and a fourth bond is necessary to form a stable solid lattice, unless long-range or strongly directive forces are imagined.[3]

In support of this hypothesis we may point to the remarkable increase in the range and stability of the liquid state on reaching Group III, where there are three electrons per atom able to form three covalent bonds.

---

[3] We may illustrate this point by considering two chains of atoms, A_1, A_2 . . ., B_1, B_2 . . . of which A_1 and B_1 are joined by a bond. In this case A_6 and B_6

$$\begin{array}{l} A_1\text{—}A_2\text{—}A_3\text{—}A_4\text{—}A_5\text{—}A_6 \\ | \\ B_1\text{—}B_2\text{—}B_3\text{—}B_4\text{—}B_5\text{—}B_6 \end{array}$$

will only be stabilised vertically if the bonds have very great directional strength.

The increased stability of the liquid state of the Group III elements is shown both by the great rise in boiling point and by the marked increase in the latent heat of evaporation. The increase in the range and stability of the liquid state between Groups II and III is one of the most striking features of the relations between the properties of the elements and their positions in the Periodic Table, and clearly suggests that the essential factor which stabilizes a liquid has come into play at Group III. From this point of view we should regard the changes taking place on heating a solid as involving first, a general increase in the amplitude of the vibrations, and then, as the melting point is approached, a breaking of bonds until only four bonds per molecule remain, after which transformation will occur to the liquid, which requires only three bonds per molecule. We may note also that our hypothesis would lead us to expect the phenomena associated with the critical point, since at sufficiently high pressures a gas molecule will have three neighbors within its zone of attraction, and the difference between a gas and a liquid may vanish for this reason.

TABLE 5

Melting points

ELEMENT	MELTING POINT	ELEMENT	MELTING POINT	ELEMENT	MELTING POINT	ELEMENT	MELTING POINT	ELEMENT	MELTING POINT
Li	452	Na.. .	371	K . . .	337	Rb..	312	Cs.	299
Be.. . .	1551	Mg .	923	Ca ..	1124	St	1044	Ba.	977
B.. . . .	2500?	Al . .	932	Sc. .	1670	Yt .		La	1099
C.......	3845	Si.....	2093	Ti .. .	2073	Zr	2200	Hg..	2500

VI

In contrast to the boiling point phenomena, the melting points of the A subgroup elements show their greatest increase between Groups I and II, as can be seen from table 5. Aluminum is clearly anomalous, but in general the melting points increase by a factor of 3 or 4 on passing from Group I A to the following element in Group II A, and then continue to increase less rapidly. We may conclude, therefore, that the essential factor which stabilizes a liquid is greatly favored when there are three or more electrons per atom, but that, up to Group IV A, the solid shows a continually increasing stability, the greatest increase being between Groups I and II.

VII

In the alkali metals there is only one electron per atom, and if we assume that the electrons in the liquid, as in the solid, occupy *s* states only, there will only be one bond per atom and one single *s* orbital. This bond is, however, independent of direction and is therefore well suited for liquid cohesion. Using the Pauling model, therefore, we shall regard the liquid alkali metals as involving only one bond per atom resonating between different neighbors so as to hold the liquid together.

On passing to the alkaline earths we have two electrons per atom, and since the *s* and *p* states overlap in the solid (see page 813) we shall assume that four orbitals are now available for bond formation. We suggest that it is this fact which is partly responsible for the marked increase in stability of the *solid* phase (i.e., the rise in melting point) on passing from Group I to Group II. In the later groups (III and IV) those four orbitals are still available, and the continual rise in melting point is the result of the continually increasing numbers of electrons in these four orbitals. The point which we wish to emphasize is that, whereas the valence increases continuously, the passage from Group I A to Group II A produces the change from one orbital to four orbitals, this last number then remaining constant.[4]

VIII

The general principles underlying the liquid elements may now be summarized as follows:

1. On passing from Group I A to II A, the solid state increases greatly in stability, partly owing to the general effect of higher valence, and partly owing to the increase in the number of orbitals available for bond formation and the very strong nature of the *s-p* bonds. The boiling point does not rise to such a marked extent, because the free atoms of the Group II elements with their completed outer group of two *s* electrons are very stable, and so the gaseous phase is favored. We have noted previously that the boiling point of barium is higher than those for the remaining alkaline-earth metals, while its melting point is lower. It has been shown in a former paper (12) that when the atomic and ionic radii of the metals are compared, the ion of barium is larger than would be expected from the values for the remaining alkaline-earth elements. This was regarded as due to the approaching internal rearrangement taking place in the rare-earth group, and it is possibly this fact which accounts for the anomalous behavior of barium.

2. On passing from Group II A to III A the melting point still increases, owing to the general valence effect, aluminum being anomalous (see below). The boiling point and heat of vaporization increase enormously, since in Group III A there are three electrons to form the three bonds characteristic of a liquid.

---

[4] In the long periods the process is of course complicated by the later introduction of the *d* orbitals.

3. In the first and second short periods, on passing to Group IV, the melting point continues to increase, owing to the general valence effect. The boiling point does not increase to the same extent, partly because the gaseous phase is favored by the formation of stable molecules, and, if our hypothesis is accepted, partly because only three bonds per atom are required for the liquid, and little is gained by having more than three electrons, unless these introduce new orbitals, as in the case of the transition elements. This explanation also applies to the approximate constancy of the boiling points and of the L_s values of the series thallium–lead–bismuth.

4. The transitional elements have high melting and boiling points, owing to cohesion involving *s*, *p*, and *d* orbitals which are very stable.

5. In the first and second short periods, and in the series arsenic → bromine in the third period, the liquid phase in Groups V, VI, and VII almost vanishes, owing to the formation of very stable molecules in the gaseous state and sometimes also of molecular crystals of the solid.

6. In Groups III B and IV B indium, tin, thallium, and lead have low melting points, owing to incomplete ionization in the solid state, as shown by the interatomic distances. The anomalous melting point of aluminum is probably due to the same cause. The high boiling points suggest that these elements are fully ionized in the liquid. This interpretation implies that the subgroup of two *s* valence electrons is sufficiently stable to be preserved unchanged in the solid, but that it breaks down in the liquid. In germanium, on the other hand, the crystal structure resembles that of silicon, and the subgroup may be regarded as breaking down in both solid and liquid. This, of course, is in agreement with the chemistry of the elements, the divalent salts of germanium being much less stable than those of tin or lead.

7. In Groups V and VI the remarkable change in the stability of the liquid phase on passing from arsenic to antimony, and from selenium to tellurium, corresponds with a diminishing tendency to form large molecules in the gaseous phase. Thus phosphorus and arsenic form P_4 and P_2, and As_4 and As_2 molecules, respectively, while sulfur and selenium form S_8, S_6, S_2, Se_8, Se_6, and Se_2 molecules, respectively. Tellurium, on the other hand, forms only Te_2 molecules, while antimony vapor near the boiling point is said to consist mainly of Sb_2 molecules with some of Sb_4, and bismuth vapor at the boiling point is a mixture of Bi_2 molecules and single atoms. We may say, therefore, that in phosphorus, arsenic, sulfur, and selenium, the liquid phase is restricted because the attractive forces of the atoms in the gaseous phase are satisfied by the formation of large stable molecules, so that little attraction is left to form a liquid. Antimony is an intermediate case, and it is interesting to note that, according to the data given in table 4, the liquid range and liquid ratio for antimony are distinctly less than those for bismuth.

8. The characteristics of the B group elements which remain to be considered are the abnormal properties of gallium and mercury. In contrast to indium and thallium, the interatomic distances in solid gallium indicate that the atoms are fully ionized, and this, of course, is in agreement with the chemistry of the Group III elements, which indicates that the stability of the univalent Ga^+, In^+, and Tl^+ compounds increases with increasing atomic number. This would, at first sight, lead one to expect a metal of high melting point, in contradiction to what is found. A possible explanation lies in the tendency of the B group elements to crystallize according to the $(8 - N)$ rule, where N is the number of the group. This rule would require gallium to crystallize so that each atom had five close neighbors. The actual structure is sometimes described as corresponding to the deformation of a structure with five neighbors, but the deformation is considerable, and results in each atom having one close neighbor at 2.44 Å., two at 2.71 Å., two at 2.74 Å., and two at 2.80 Å. The existence of one close neighbor to each atom has been taken to indicate the existence of Ga_2 molecules in the solid, while another interpretation regards the structure as a layer structure in which each atom has six neighbors in its layer (at distances from 2.71 to 2.80 Å.), the layers being bound together by the single close bond at 2.44 Å. The low thermal stability of the solid is in marked contrast to the great stability of liquid gallium, which behaves as a normal trivalent liquid. The instability of the solid may perhaps be due to the opposition of various factors. A structure in which each atom has five neighbors is not one which favors close packing of atoms, so that the tendency to satisfy the $(8 - N)$ rule may be regarded as opposed by geometrical considerations. In indium and thallium, the stability of the subgroup of two *s* valence electrons is sufficiently great for this subgroup to persist in the solid, and the crystal structures are normal, or slightly modified, close-packed structures.[5] In gallium the stability of the subgroup is not sufficient for this, so that we may perhaps regard the instability of the gallium structure as due to a failure to satisfy any one definite tendency.

The properties of mercury are very curious, since its boiling point, melting point, and latent heat of evaporation are all abnormally low. The vapor is known to be monatomic, and, since Trouton's constant for the entropy of vaporization at the boiling point is normal, the abnormal properties cannot be ascribed to the existence of Hg_2 molecules in the liquid. The relative instability of the solid and liquid may suggest that only the one *s* orbital is involved in the cohesion, and in this connection it is interesting to note that the L_s value for mercury given on page 815 is roughly one-third of those for thallium and lead, just as the value for sodium is one-third of those for aluminum and silicon.

---

[5] The crystal structure of indium is face-centered tetragonal, but the axial ratio is nearly unity, so that the structure is only a slightly deformed modification of the face-centered cube.

The author must express his gratitude to Professor C. N. Hinshelwood for laboratory accommodation and for many other facilities for research.

REFERENCES

(1) Bauer and Brunner: Helv. Chim. Acta **17**, 958 (1934).
(2) Claussen: J. Am. Chem. Soc. **56**, 615 (1934).
(3) Coleman and Egerton: Phil. Trans. Roy. Soc. **A234**, 177 (1935).
(4) Eucken: Metallwirtschaft **15**, 65 (1936).
(5) Fischer: Z. anorg. Chem. **219**, 367 (1934).
(6) Fischer, Brünger, and Grieneisen: Z. anorg. Chem. **231**, 54 (1937).
(7) Gordon: J. Chem. Phys. **4**, 100 (1936).
(8) Harteck: Z. physik. Chem. **134**, 1 (1928).
(9) Hartmann and Schneider: Z. anorg. Chem. **180**, 275 (1929).
(10) Heycock and Lamplough: Proc. Chem. Soc. **28**, 3 (1912).
(11) Hoffmann and Schulze: Z. Metallkunde **27**, 155 (1935).
(12) Hume-Rothery and Raynor: Phil. Mag. [7] **26**, 129 (1938).
(13) Kohlmeyer: Metall u. Erz **29**, 105 (1932).[6]
(14) Langmuir and Taylor: Phys. Rev. **51**, 760 (1937).
(15) Leitgebel: Z. anorg. Chem. **202**, 305 (1931).
(16) Pauling: *The Nature of the Chemical Bond.* Cornell University Press, Ithaca, New York (1939).
(17) Ruff and Bergdahl: Z. anorg. Chem. **106**, 76 (1919).
(18) Ruff and Johannsson: Ber. **38**, 3601 (1905).
(19) Skinner: Phys. Rev. **45**, 370 (1934).

APPENDIX

The boiling data given in the tables have been selected as follows:

Alkali metals. For sodium and potassium the direct measurements of Heycock and Lamplough (10) appear preferable to values deduced from vapor pressure measurements, since the pyrometry of Heycock was of a very high standard. For lithium we used the value given by Gordon (7) in his analysis of the vapor pressure data of Hartmann and Schneider (9). The data for rubidium and cesium have been discussed previously (page 814).

Alkaline-earth metals, aluminum, and silicon. For beryllium, aluminum, and silicon the data are taken from the work of Bauer and Brunner (1), while for the remaining alkaline-earth metals the data are from the work of Hartmann and Schneider (9).

B group elements. The data of Bauer and Brunner (1) have been used for copper, gold, zinc, tin, and lead. For silver the data are taken from the work of Fischer (5). For cadmium the work of Leitgebel (15) appears the most reliable for the normal boiling point; the boiling point at 7.6 mm. has been estimated graphically from a log $p/(1/T)$ graph of the results of Ruff and Bergdahl (17) which are not very consistent. The data for mercury are from the *International Critical Tables.* For gallium, Harteck (8) has estimated the boiling point from experiments at low pressures, but this involves a very long extrapolation and the values are only approximate.

---

[6] We have not been able to consult the original, and the value 1918°K. for antimony referred to in the appendix is from the Landolt-Börnstein *Tabellen.*

For thallium the normal boiling point is from the work of Leitgebel (15), while the value at 7.6 mm. is calculated from the equation of Coleman and Egerton (3). For antimony the normal boiling point is placed at 1910°K. on the basis of the values 1908°K. of Leitgebel (15) and 1918°K. of Kohlmeyer (13). For bismuth the value given is that of Leitgebel (15).

For sulfur, bromine, chlorine, and iodine the data are taken from the *International Critical Tables*, graphical methods being used where necessary. For fluorine the work of Claussen (2) is used, and the values for selenium and tellurium are from the Landolt-Börnstein *Tabellen*.

The melting point data are more securely established, and call for little comment, except that the melting points of calcium, strontium, and barium are taken from the work of Hoffmann and Schulze (11), and the value for scandium from the work of Fischer, Brünger, and Grieneisen (6).

RADIOACTIVE STANDARDS[1]

A series of radioactive standards is being prepared under the direction of the Committee on Standards of Radioactivity of the National Research Council. These standards will be deposited at the National Bureau of Standards in Washington, D. C., to be issued as working standards to investigators who may desire them.

The standards under preparation at present are:

(*1*) Radium standards: (*a*) 100-cc. solutions sealed in 200-cc. Pyrex flasks containing 10^{-9} and 10^{-11} g. of radium, to be used as emanation standards either directly or by subdilution. (*b*) 5-cc. solutions sealed in Pyrex ampoules containing 0.1, 0.2, 0.5, 1.0, 2.0, 5.0, 10, 20, 50, and 100 micrograms of radium to be used as gamma-ray standards.

(*2*) Thorium standards: Sealed ampoules containing sublimed thorium chloride. These may be used in preparing standard thorium solutions. Directions for use will be furnished with the standards.

(*3*) Standard rock samples: Twelve rock samples, ground to pass a 40-mesh screen and be retained on a 100-mesh screen, are available in 100-g. portions. These samples will be analyzed for radium and thorium and are intended for use as working standards to check methods used in extraction of radon and thoron from rock samples.

All samples will be analyzed at a number of laboratories equipped to make such measurements, and ultimately certificates will be issued by the National Bureau of Standards. This work is in progress but will require considerable time for its completion, so that final figures are available only for a part of the samples at the present time.

Accurate knowledge of the radioactive content of the materials of the earth's crust is of primary importance in many phases of geology, geophysics, and cosmology. Reliable radioactive standards are also essential in studies of radium and thorium poisoning and in biological and medical investigations using the technique of radioactive indicators, or internal artificial radioactivity therapy. For the latter purposes calibrated standard sources of β-rays will be made available.

---

[1] This work is being supported in part by a grant from the American Philosophical Society to the Massachusetts Institute of Technology.

It is hoped that the standards which have been prepared by the Committee will provide all workers in these fields with a common basis for comparison of measurements and also improve the accuracy of all measurements of this type. It is likely that they will have other applications, and the Committee would appreciate hearing from interested persons who may desire similar standards for their work. The Committee is also glad to coöperate as far as possible in aiding investigators to use these standards to the best advantage and welcomes specific inquiries regarding their use. It is urged that any suggestions regarding other desirable radioactive standards, not at present available, be submitted promptly to the Committee. In particular, it will facilitate the work of the Committee if those laboratories and individuals which can make use of these standards will advise the Committee of their probable requirements.

Communications may be addressed to the Chairman, Professor Robley D. Evans, Department of Physics, Massachusetts Institute of Technology, Cambridge, Massachusetts.

L. F. Curtiss
Clark Goodman
Alois F. Kovarik
S. C. Lind
C. S. Piggot
Robley D. Evans

NEW BOOKS

M. K. S. Units and Dimensions and a Proposed M. K. O. S. System. By G. E. M. Jauncey and A. S. Langsdorf. viii + 62 pp. New York: The Macmillan Company, 1940. Price: $1.00.

This interesting and instructive brochure can be best described by quoting the authors' foreword. "The International Electrotechnical Commission (I.E.C.), meeting at Scheveningen in June, 1935, adopted the meter, kilogram, and second as the basic units of length, mass, and time, this action becoming effective in January, 1940.

The purposes of this little book are: to acquaint electrical engineers, physicists, and teachers and students of electrical engineering and physics with the properties of the new meter-kilogram-second (M. K. S.) system of basic units; to describe methods for changing from one set of basic units to another; to give reasons for the adoption of the ohm as the fourth basic unit (a question left open by the I.E.C. in 1935); to describe a proposed M. K. O. S. system of basic units; and to discuss the difference between magnetic flux density (B) and magnetic field strength (H)."

F. H. MacDougall.

Thermodynamics and Chemistry. By F. H. MacDougall. Third edition. 6 x 9 in.; ix + 491 pp.; 53 tables. New York: John Wiley and Sons, Inc., 1939. Price: $5.00.

The new edition brings up to date MacDougall's well-known text on *Thermodynamics and Chemistry.* The principal portion of the book derives the usual equations based on the first and second laws and indicates clearly their application to chemical problems. The symbolism has been changed to correspond in general with the prevailing American practice. The treatment of the phase rule and various relationships at phase boundaries is particularly complete. The Debye-Hückel theory for electrolytes is derived and discussed in a clear concise fashion.

In many cases the numerical data quoted are not the most accurate available. While this matter is not important to the student learning general principles, it detracts considerably from the usefulness of the book to research workers. The tables of data toward the back of the book appear to be much better in this respect than the rest of the text; however, the electrode E.M.F. values are not consistent with the standard free energy values. This situation should be kept in mind by those proposing to use the book for these purposes. Although a few typographical errors were noticed, they were mostly of a sort not likely to lead to confusion. The non-integral values listed for the symmetry number, σ, in table XL on page 469 must be erroneous. The correct value is 2 for both chlorine and bromine, since isotopes are considered identical for this purpose.

The treatment of the third law in a book of this type is a problem. Since a very considerable fraction of the free energy values now available have been obtained from third law calculations, this subject must be given an important place. On the other hand, the third law cannot be used with perfect accuracy in practice unless one understands its basis in quantum statistics. MacDougall's general plan for considering the third law along with a brief discussion of statistical mechanics is excellent. However, a concise statement of the types of situation leading to failure of the third law would have been an improvement. In this chapter, and at some other points, more explicit indication of the importance and relationship of the individual topics would assist the reader.

This book should be most valuable to the student learning thermodynamics. The numerous problems are notable from this point of view. Although certain disadvantages have been mentioned, this work should prove an aid also to the research worker in chemical thermodynamics.

KENNETH S. PITZER.

Einführung in die technische Fliesskunde. By G. W. SCOTT BLAIR. 6 x 9 in.; viii + 132 pp. Dresden and Leipzig: Theodor Steinkopff, 1939. Price: unbound, 6 RM.; bound, 6.75 RM.

This is a translation by H. Kauffmann of the author's *Introduction to Industrial Rheology,* published in this country by Blakiston's Sons and Company. In so brief a work an author cannot be expected to cover the details of his subject, but in an introduction the general reader has a right to expect a modicum of well-established facts upon which are built laws which have been found acceptable. The reader however should expect more, and the technical reader, more perhaps than any other, should look for the illumination of facts and laws by means of a clear theoretical development. The author has chosen to treat briefly of nearly two hundred and fifty recent monographs on rheology, with the result that clarity is often lost. The book will serve well as a review of recent work, particularly on plasticity, and rather better than as an introduction to the science.

The translator has changed the Poiseuille law to the "Hagen-Poiseuille law." Poiseuille published his first paper on the circulation of the blood ten years before Hagen's paper and then worked steadily on that subject and published a series of papers up to 1847. The name "Hagen-Poiseuille," like Gay-Lussac-Charles, is clumsy. Furthermore, it is impracticable to do historical justice in a name. Newton and Stokes and others antedate Poiseuille and have a greater claim than Hagen.

EUGENE C. BINGHAM.

The Nature of the Chemical Bond. By LINUS PAULING. 6 x 9 in.; xiv + 429 pp.; 60 figures. Ithaca, New York: Cornell University Press, 1939. Price: $4.50.

This is a clearly written survey of the nature of chemical bonding as seen from the viewpoint of the atomic orbital method. It is in this method that the wave mechanics connects most easily and naturally with the traditional ideas of chemists on the nature of chemical bonds and with the Lewis theory. Hence the presentation will have wide appeal and usefulness among chemists.

The book is mainly a review of the author's work on chemical bonding, with special emphasis on the study of bond distances in molecules and crystals, and on the use of the resonance concept in explaining bond structure, bond distances, and bond energies. Although based on quantum-mechanical ideas, the treatment is remarkably non-mathematical.

After an introductory chapter on "Resonance and the Chemical Bond" comes a chapter on ionic character and electronegativity, based largely on a study of bond energies. This subject is peculiarly difficult to treat quantitatively, but the author has made great progress by his pioneer work and stimulating new ideas, which are further usefully developed in the book. Nevertheless, in the reviewer's opinion, much probably remains to be done before the subject will be in a wholly satisfactory state.

Some specific criticisms may here be in order. The reviewer has shown theoretically (*cf.* equation 41 of a paper[1] quoted by the author on page 66) that if one adopts with the author the postulate of the additivity of covalent bonds, then the amount of ionic character Q in a partially polar bond varies according to an equation of the type:

$$Q = \tfrac{1}{3}(x_A - x_B) - (x_A - x_B)^3/48 \tag{1}$$

The x's refer to the electronegativities of the atoms A and B forming the bond.

The author, however, on page 69 gives

$$Q = 1 - e^{-1/4(x_A - x_B)^2} \tag{2}$$

which conflicts with equation 1 in making Q vary nearly with $(x_A - x_B)^2$ instead of with $(x_A - x_B)$ for small values of $x_A - x_B$ (compare the figure on page 80). Hence some of the author's Q values and derived conclusions are questionable. Thus for C≡N in R—C≡N, where the bond moment indicates about 57 per cent ionic character (*cf.* page 75), equation 2 gives only 18 per cent, while equation 1 gives 47 per cent.

To be sure, equation 2 fits well the values 5, 11, and 17 per cent for Q for HI, HBr, and HCl deducible from observed bond moments, μ, if with the author one assumes $\mu = Qer$ (r = internuclear distance). But it has been pointed out (*loc. cit.*,[1] pages 584–5) that μ must in general contain a large "homopolar dipole" contribution μ_h, here of polarity H^-X^+, so that $\mu = Qer - \mu_h$, making the true Q's much larger than those just given, and in agreement with equation 1 rather than equation 2.

A related matter is the conflict between the large observed μ's of the C—I, C—Br, C—Cl bonds and the small Q values (nearly zero for C—I) predicted by the electronegativity scale. The author suggests (page 69) that these effects may be due to an unsymmetrical distribution of the electrons,—referring presumably to the homopolar dipole and related contributions,—so that the Q's may still be as calculated. Unfortunately, the homopolar dipole terms are of polarity C^-X^+, whereas the bond moments are of polarity C^+X^- beyond much question. There seems to be no escape from the conclusion that all the C—X bonds have strong ionic character with the halogens negative. This indicates that the electronegativity values for the halogens require alteration, and that the electronegativity scale is less consistent and well founded than one might have hoped. There are also other indications of this: for example, the apparent absence of ionic resonance energy in the C≡N bond in spite of its high polarity (footnote on page 124).

---

[1] R. S. Mulliken: J. Chem. Phys. 3, 573 (1935). This paper gives (insofar as the additivity postulate is valid) a theoretical justification of the basis of the x scale.

Chapter IV deals with the forms of bond orbitals and their relations to bond strengths and bond angles, and the magnetic criteria of bond type. Chapters IV and VI contain a stimulating discussion of the structure and properties of aromatic and other molecules involving resonance among several valence-bond structures. The author gives many ingenious interpretations. In the "quantitative treatment" here (pages 137-9), the large corrections in the observed resonance energies to allow for shrinkage and stretching of bonds accompanying resonance, discussed by Lennard-Jones, might well have been mentioned.

Chapter V is a thorough discussion of interatomic distances and their interpretation. Chapter VII contains interesting ideas on the structure of molecules with partial double-bond character. Chapter VIII is on one-electron and three-electron bonds, including a section on semiquinones and related substances. Chapter IX is an excellent survey of the hydrogen bond problem. Chapter X deals very thoroughly with the sizes of ions and the structure of ionic crystals. Chapter XI treats "the metallic bond" rather briefly and unconventionally but interestingly. Chapter XII contains concluding remarks on resonance and its future applications.

As was mentioned above, the book is written from the atomic orbital (AO) viewpoint. The alternative molecular orbital (MO) point of view is not discussed at all, aside from mention without explanation on pages 138-9. Thus the unfamiliar reader will be likely to suppose that the viewpoint presented is the only possible one. This result could have been avoided by a few prefatory paragraphs concerning the MO method.

Most authorities would feel that for a deeper understanding of the electronic structures of molecules a knowledge of both methods is necessary, and that for many problems the MO method is the simpler and more intelligible. For example, in problems such as that of partial ionic character, or the structure of benzene or of metals, or one-electron and three-electron bonds, where the AO method requires the concept of resonance among several valence-bond structures, the MO method allows one to think in terms of a single structure. Thus one sees that "resonance" does not have the clear-cut structural significance which exclusive use of the AO viewpoint tends to assign to it.

Nevertheless, the use of the AO viewpoint makes for maximum availability of the book, especially among chemists, and the book is a landmark in the history of valence theory. In its perusal most readers will probably share the reviewer's experience of encountering a wealth of important and interesting facts and ideas.

ROBERT S. MULLIKEN.

The Cyclotron. By W. B. MANN. 92 pp. New York: Chemical Publishing Company, 1940. Price: $1.50.

This timely little volume, with a brief introduction by Lawrence, treats the following subjects: magnetic resonance acceleration; cyclotron vacuum chambers and magnets; higher frequency supply and ion source; electrostatic and magnetic focusing; adjustment of the cyclotrons. It contains a brief section on well-selected applications.

S. C. LIND.

Abridged Scientific Publications from the Kodak Research Laboratories, Vol. XX. 273 pp. Rochester, New York: Eastman Kodak Company, 1939.

This book contain abstracts of forty-four papers published during 1938.

Rheological Memoirs. Edited by EUGENE C. BINGHAM. Vol. I, No. 1, January, 1940. Published in Easton, Pennsylvania. Price: $2.00 per volume. *Experimental Investigations upon the Flow of Liquids in Tubes of Very Small Diameter.* By J. M. L. POISEUILLE. Translated by Winslow H. Henschel from the Memoirs of the Royal Academy of Sciences of the Institute of France Sci. Math. & Phys., Vol. IX, Paris, 1846.

This is the first of a series of classical papers in the subject of rheology which Professor Bingham, the well-known authority in this field, prepares to make available through reprinting and translation into English under the auspices of the Publication Committee of the Society of Rheology. Subscription may also be placed through the American Institute of Physics, 175 Fifth Avenue, New York.

S. C. LIND.

The Physics and Chemistry of Surfaces. By N. K. ADAM. Second edition. 6 x 9 in.; x + 402 pp. Oxford University Press. Price: $7.50.

This edition of Professor Adam's well-known book has been largely rewritten without materially changing the plan of the book. A new chapter has been added on electrical phenomena at surfaces, which rather completely covers the many phases of this subject.

The first part of the book is perhaps its best, if there can be said to be any best. Here the author draws on the great reservoir of knowledge obtained in his own laboratory, to elucidate the behavior of substances on liquid surfaces. This he does without detracting in any way from the important work of other investigators. In the chapter on adsorption on liquid surfaces, the author presents essentially the analytical proof of Gibbs for the adsorption equation and in addition the beautiful new proof due to Guggenheim. The section on the general properties of solid surfaces presents many interesting concepts and leads up to an excellent discussion of spreading films and lubrication. In considering adsorption on the solid surface and catalysis, the modern concepts are all presented, but the chapter on the whole seems a little too compressed. The last chapter, which follows the one on electrical phenomena at interfaces, presents the problem of the measurement of surface tension.

This volume is a distinct improvement over the first edition, in that it covers the subject more completely. It is an important addition to the literature on the subject of surface phenomena and will be welcomed by all workers in the field. The book is well printed and presents a nice appearance.

L. H. REYERSON.

Kurzes Lehrbuch der physikalischen Chemie. Heft 2. By K. JELLINEK. 24.5 x 16 cm.; xii + 292 pp. Deventer (Holland): N. V. Uitgevers-Maatschappij A. E. Kluwer, 1939. Price: Fl. 7.50.

The second part of Jellinek's *Short Textbook of Physical Chemistry* treats the subjects electrochemistry, the phase rule, colloid chemistry, and chemical kinetics. In the opening chapter on electrochemistry the author deals faithfully with electroconductance, giving clear and adequate accounts of G. N. Lewis's thermodynamic theory of stronger electrolytes, the methods of determining activity coefficients, and the kinetic theory of Debye and Hückel for dilute solutions of electrolytes. Electrode potentials are discussed, and many applications of this quantity to other physicochemical determinations are explained in detail. Ionization and neutralization curves are discussed and the essential significance of these curves elaborated. Indicators are considered and both the qualitative and quantitative theories of color change examined. Finally an account is given in this section of the chemical equilibria in molten salts.

The phase rule is dealt with in connection with systems of one and two components, and this is followed by a full treatment of phase boundary relationships, including non-electrical phase boundary phenomena and also the phenomena at electrified boundaries (electroendosmosis, adsorption potential, and electrokinetic potential). In this section colloids are considered as systems of enormous surface. The final section of the book is devoted to chemical kinetics. Here reactions up to the fourth order are considered and modern ideas of chemical kinetics are applied to both homogeneous and heterogeneous reactions. A discussion of irreversible potential, including such phenomena as passivity, overvoltage, and decomposition voltage, is developed in the final section.

The material included in this very erudite book is presented with remarkable clarity and in a logical manner. The book is, without any doubt, one which will commend itself to students of physical chemistry. The value to students is greatly enhanced by the large number (102) of numerical examples which are given in the text with the solutions worked out in sufficient detail to enable even a backward student to understand the method. The lack of an index is to be deplored, despite the presence of a paginated contents table.

This book is one which can safely be recommended to students of physical chemistry.

James F. Spencer.

Introduction to Atomic Physics. By Henry Semat. 6 x 8.5 in.; xv + 360 pp.; 34 fig. New York: Farrar and Rinehardt. Price: $3.50.

This volume contains one hundred and twenty-seven items concerning our present-day knowledge of matter and radiation. The first chapter gives a few introductory remarks on the modern theory of electricity and magnetism, while the remaining chapters (II to VII) cover the following topics: elementary charged particles, electromagnetic radiation, waves and particles, the hydrogen atom, atomic spectra, and electron distribution and the nucleus. The author has succeeded in encompassing the whole field of atomic physics in an exceedingly small space, with the result that the individual topics are condensed into very few pages. Not a word is wasted. If one considers that nearly every one of the hundreds of items mentioned could easily be expanded into a good-sized book, one can realize the fount of information contained in the volume before us. The extent of the field covered necessitated extreme brevity in the presentation of the material. However, some important developments as, for example, Rutherford's experiments on the scattering of alpha particles are given more space, and in this respect the author has chosen with great care and wisdom the important topics on which modern atomic physics rests. Nuclear physics is dealt with adequately, considering the fact that the aim of the book is to introduce students of physics and chemistry into this particular branch of physics. The short treatment involved in so many of the topics should give the teacher ample opportunity for expanding the material in his lectures. The book certainly should form a valuable guide and frame-work for the section of physics which it aims to develop. The style and presentation are very lucid, and not only beginning students but also the reader who already has a good background of modern physics and chemistry will enjoy reading the book in order to review the topics given.

Geo. Glockler.

The Physical Examination of Metals. Vol. I. Optical Methods. First edition. By BRUCE CHALMERS. 176 pp. New York: Longmans, Green and Company, 1939. Price: $4.00.

The author makes no claim to have prepared a complete treatise on this subject; however, he has illustrated well all of the fundamental optical methods used for metals. The book is not a treatment of optical metallography alone, as the title might imply, but covers all optical methods which might be used for many materials other than metals.

From Chapter I, the introduction, we get an idea of the properties of light, the visible spectrum, and the electromagnetic spectrum. In Chapter II, "Geometrical Optics," may be mentioned such subjects as measurement of reflectivity, fluorescence, and the optical properties of thin films.

Two chapters are devoted to the subject of wave optics. In the first, "Interference," we find parallel and inclined plate systems and the Michelson interferometer discussed with such applications as Newton's rings, measurement of elastic moduli, precision extensometer, dilatometers, micro-topography, micro-interferometer, colors of oxide films, etc. The second chapter, "Diffraction," treats of diffraction by edge, slit, and wire; diffraction grating, measurement of mesh; measurement of size of powder; and resolving power of microscope, touching upon ultraviolet microscopy.

In Chapter V, "Polarized Light," the most important applications seem to be in the determination of microstructure and the presence and nature of inclusions. The book closes with a discussion of sources of light, with some reference to radiation pyrometry, spectrographic analysis, and photography.

One need not be an atomic physicist to be able to read the book. A layman or the average scientist can profit considerably by studying this volume and applying the fundamental concepts of light to his own problems so as to extend his particular branch of science. The author points the way for the use of many of these methods in practice. The book is written systematically in a clear and concise manner and is well indexed. Dr. Chalmers has accomplished a good job and is to be congratulated.

RALPH L. DOWDELL.

Statistical Thermodynamics. By R. H. FOWLER AND E. GUGGENHEIM. London: Cambridge University Press, 1939.

To readers of Professor Fowler's treatise, *Statistical Mechanics,* this work will need neither introduction nor recommendation, since in essentials it is a revised version of the most important portions of the earlier treatise. In scope it is roughly that of *Statistical Mechanics,* with the exclusion of the astrophysical problems and with the inclusion of much new material particularly of chemical interest. Even though it does not altogether supersede its predecessor, the present work will undoubtedly find even greater favor and usefulness as a reference source.

The changed title may seem a little misleading, particularly to American readers, since it suggests that the book covers both statistical mechanics and thermodynamics. This is true only insofar as statistical methods are used for the computation of thermodynamic functions, but thermodynamic arguments *per se* are not used. To the present reviewer it seems a little regrettable that a short treatment of the mathematical structure of thermodynamic equations was not included, as it would have materially enhanced the pedagogic features of the book. But this is only a very minor point.

The approach to statistical mechanics through the so-called "Darwin-Fowler method" has been somewhat simplified, and the reader will probably need some preliminary acquaintance with wave mechanics in order to follow it successfully, but on the whole it makes distinctly easier reading than in the earlier editions.

It would be impossible to indicate in any detail the many additions and revisions which have been made in the material over the second edition of *Statistical Mechanics*, and it will probably suffice to point out only the major items.

The important chapter on "Chemical Equilibria, Evaporation and Nernst's Theorem" has been considerably simplified and promises to be much more useful than formerly. The systematic discussion of chemical constants and their collection into easily accessible formulas will be especially appreciated.

A new chapter on "Grand Partition Functions" does much to clarify the nature of the choice of the unit system in statistical mechanics.

For the problems of physical chemistry, the chapters on liquids, electrolytic solutions, and surface layers are probably among the most important. They include much new material from the literature, and are thoroughly up to date. To the reviewer's knowledge the discussion of the present status of the theory of the liquid state is the best obtainable anywhere.

The discussion of the order–disorder theory of lattice imperfections, which formerly occupied a minor place, has been expanded into a long chapter and gives a particularly interesting discussion of the various methods of attack which have been used in this field. In view of its recent successful applications to a number of problems, there is every reason to believe that this theory will become of increasing importance in the near future.

The reviewer is painfully aware of the inadequacy of a review in covering even the essentials of a book of this character. It is all too rarely that the scientific literature is graced by a work of such wide scope, and yet one in which the material has been so well digested. It is not presumptuous to recommend this book above all others to the serious reader, for it has no competitors in its own field.

E. L. HILL.

Rutherford (being the Life and Letters of the Right Honorable Lord Rutherford). By A. S. EVE. 450 pp. New York: The Macmillan Company, 1939. Price: $5.00.

The shock which the world felt in October, 1937, at the death of Rutherford, the greatest experimental physicist of modern times, inevitably left the feeling that something besides his monumental work should survive,—be left in living memory of the noble spirit and the great soul that were his. No one who ever came within the charmed circle of his magnetic personality could forget the experience. To those who were not so fortunate, the present letters will be the next best substitute. By their skillful selection and arrangement they almost reproduce the living Rutherford.

The scientific world is indebted to Lady Rutherford for the preservation and selection and to Professor Eve for the reproduction of the letters which carry Rutherford in a natural transition from his early boyhood in New Zealand to a glorious climax in Cambridge.

But let no one think it is possible to separate his work and his personality. If anyone ever lived his work every hour of the day, every day in the year, it was Rutherford. It breathed in everything he said or wrote or did.

And to those who have lived through the development of radioactivity, these letters are a delightful review of its entire history. They furnish the personal touch of great ideas in the making. So intimately was Rutherford associated with each step and so skillfully has Professor Eve supplied the essential connections that nothing is lacking to complete the story from atomic disintegration through the radioactive families, the displacement law, the nucleus, artificial disruption, the neutron, artificial radioactivity, and even the prediction of fission.

Many snatches of delicious humor are scattered through the four hundred pages. The indescribable picture of Rutherford in the early days at Montreal sitting before the electroscope with a pair of round cuffs prominently in view, borrowed for the picture from one of the students. His own sense of humor frequently comes to light. Jacques Loeb, whom he met in California, he describes as a "worse enthusiast than I am." On hearing a student from another university claiming his professor had stolen his ideas without giving due credit, he admonished, "Well, it never does to quarrel with your Mother's milk." Again his delightful arraignment of a colleague, the Professor of Philosophy, "When you come to think of it, Alexander, all that you have said and all you have written during the last thirty years—what does it amount to? Hot air! Hot air!" And Alexander's reply accusing Rutherford of being a noble savage and advising him to continue so.

Rutherford always delighted in twitting chemists and poking sly fun at chemistry. The tables were turned when in 1908 he was awarded the Nobel Prize in Chemistry. In his address of acceptance he said he had "dealt with many rapid transformations, but the quickest he had met was his own transformation in one moment from a physicist to a chemist."

During the World War and again in his later years, he devoted much time to public service; he organized a national institute for the acquisition and distribution of radium for therapeutic use; he was adviser on industrial problems of first importance to the empire; he injected new life into the meetings of the Royal Society and as its president rendered it invaluable service by his distinguished leadership.

Rutherford's ashes lie beneath the flagstones of Westminster Abbey, in exalted company, close beside Newton, Faraday, Maxwell, and Kelvin. But somewhere in freer space and outdoor air, in Cambridge or Manchester, in Montreal or New Zealand, should rise a nobler monument in memory of the greatest experimenter and interpreter of physical phenomena of all time.

S. C. LIND.

Some Problems in Adsorption. By J. K. ROBERTS. x + 120 pp. London: Cambridge University Press; New York: The Macmillan Company, 1939. Price: $2.00.

This book is one of a series of Cambridge Physical Tracts, the aim of which is to provide authoritative accounts of subjects of topical interest by those actively engaged in research.

Generally speaking, this book deals with the development of new experimental and theoretical methods for the study of adsorption of gases on solids. Dr. Roberts has conclusively shown that the accommodation coefficient of helium or neon may be used as a measure of the extent to which metallic surfaces, particularly tungsten, are covered with adsorbed layers of gases. Dr. Roberts and coworkers have confined themselves to simple systems where the composition of the substrate is definitely known and which can be reproduced and kept free from impurities. The results indicate in a very striking manner the difference between adsorption on a perfectly clean surface and on one already coated with a film of impurities, as will be the case in most adsorbing materials as ordinarily prepared. Professor Roberts has also developed a new technique for the experimental study of heats of adsorption and the extent to which adsorption occurs on a clean surface by using the adsorbing wire as a calorimeter.

The mathematical theory of the heat of adsorption with interaction between the adsorbed particles has been worked out in detail for both mobile and immobile films.

This research has been particularly fruitful in providing experimental evidence which is reliable enough to be useful in testing such proposed theories.

The tract is really a collection of the various recent publications of Dr. Roberts and coworkers in the Laboratory of Colloid Science at Cambridge, together with a complete set of references to related works.

The reviewer considers Dr. Roberts' work to be the most significant fundamental research on adsorption in progress at the present time. This book should be read by every one who is interested in the problem of adsorption.

A. B. VAN CLEAVE.

Casein and its Industrial Applications. By EDWIN SUTERMEISTER AND FREDERICK L. BROWNE. Second edition. 405 pp. New York: Reinhold Publishing Corporation, 1939. Price: $6.50.

Rapidly increasing use of casein in American industry, coupled with many important technical developments in its production, made it desirable to rewrite this monograph. One or the other of the authors, sometimes with collaboration, has written seven of the thirteen chapters. The other six have been contributed by experts in their respective fields. There has been a rearrangement of chapters which makes the presentation of the subject more logical. Chapter I—"Casein in Milk and its Isolation"—is new and is a better opening chapter than the one on the "Organic Chemistry of Casein" which introduced the first edition. The chapters on casein in food and casein in medicine, of the first edition, have been combined into one and a new chapter on casein in leather has been added, with the result that this edition is much improved.

Those interested in the subject will find that the material of the earlier edition has been considerably expanded. They will also welcome the more extensive citations to the literature, including references to many patents. It is the opinion of the reviewer that this edition will be found to be a good deal more useful than the earlier one. The printing is good and the illustrations are well chosen. It can be recommended to those interested in this important protein.

L. H. REYERSON.

ERRATA

Volume 44, Number 2, February, 1940

Page 211: The sentence beginning in line 25 should read as follows: "The molecular weight of D_2O was taken as 1.1117 times that of ordinary water."

Page 257: The last line in column 2 of table 1 should be 1.0938 instead of 0.9938.

LIBRARY

GAS IMPERFECTION. I

Experimental Determination of Second Virial Coefficients for Seven Unsaturated Aliphatic Hydrocarbons

EDWIN E. ROPER[1]

Department of Chemistry, Harvard University, Cambridge, Massachusetts

Received January 3, 1940

Gas imperfection data provide information for the correct calculation of many thermodynamic quantities when such accuracy is required that the approximation $pV = RT$ cannot be employed. Considerable data are available for high pressures, but the low-pressure range has received comparatively little attention. There has been some work done on low-pressure data of state for molecular compounds (e.g., 8, 9, 16, 22, 33) and for the elementary gases utilized in gas thermometry (12). Recent theoretical work (4, 10, 13, 17) in quantum and statistical mechanics has given rise to methods whereby the second virial and its temperature coefficient may be calculated, providing the law of molecular force is known; however, for complex polymolecular compounds the subject is not in an advanced stage.

A gas imperfection study has been undertaken over a temperature range for seven hydrocarbons: namely, ethene, propene, propadiene, 2-methylpropene, 1-butene, *trans*-2-butene, and *cis*-2-butene. This provides an unusually interesting group, since it contains members of an homologous series four of which are isomers, two being of a simple *cis–trans* type.

EXPERIMENTAL PART

The method of gas density measurement at 0°C. developed for the evaluation of atomic weights was extended so that a range of −80° to +80°C. could be covered. This method consists in filling an evacuated globe of known internal volume with the gas under measured conditions of pressure and temperature, the mass of the contained gas being determined by the difference in weight of the evacuated and filled globe, making use of an almost identical counterpoise in the weighing process. The four quantities involved in the determination, v, p, T, and m, which are, respectively, the specific internal volume of the globe in cubic centimeters, the pressure in millimeters of mercury, the temperature in °K., and the mass of the contained gas in grams, are capable of being measured with high accuracy. References (1, 2, 25, 34, 35) should be consulted for details of technique for a temperature of 0°C.

---

[1] Present address: Stanolind Oil and Gas Company, Tulsa, Oklahoma.

Four different globes of Pyrex glass were utilized, with special stopcocks sealed to two of them. These special cocks had provision for exhausting a small bulb on the bottom end of the barrel (see S6, figure 1), so that the force of the atmosphere tended to seat the plug at all times; this type proved advantageous when compared with a plain type. The internal volume of each globe was found from the weight (to milligrams) of the contained water, at least two determinations being carried out, generally at two different temperatures for each filling. The internal volume was known to ± 0.002 per cent or better. The external volumes were ascertained by weighing in water and in air.[2] For each globe, an almost identical counterpoise was constructed. The variation of the internal volume of the globes with pressure was taken from the experimental values on Pyrex globes of Baxter and Butler (3) of these Laboratories; the globes used in this work were very similar to theirs. The varia-

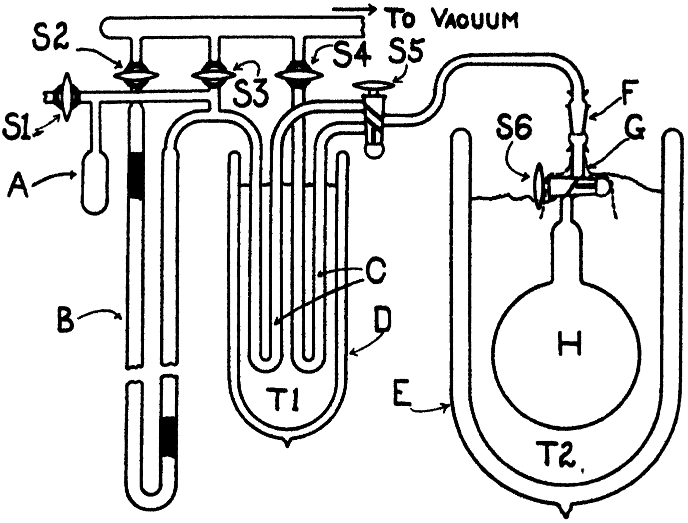

Fig. 1. Schematic representation of apparatus for determination of gas molal volumes over a temperature range. The apparatus may be exhausted through cock S3. The globe H may be exhausted *via* S4-S5 without disturbing the contents of the main line. Gas may be added or withdrawn through S1. The traps C must always be as cold as, and preferably somewhat colder than, globe H, otherwise mercury vapor will condense in H if it is below room temperature. The globe is shown in position in an ice bath, the aluminum sheet G serving to keep the bore of cock S6 at the temperature of the bath, since it was not considered advisable to immerse S6 in the bath fluids.

[2] Dr. A. Q. Butler kindly allowed the use of apparatus for weighing in water.

tion in the internal volume of the globes with temperature was calculated, employing the results of Buffington and Latimer (6) on the coefficient of expansion of Pyrex glass. Determinations made in the temperature range 0° to 30°C. agreed sufficiently well with the calculated values to indicate that no appreciable error would be introduced by such a calculation. The largest correction in the globe volumes which needed to be made for the p–V–T data for the pressure effect was 0.007 per cent and for the temperature effect 0.08 per cent. One of the globes had a nominal volume of 284 cc. and the three others *ca.* 520 cc.

Weighings of the difference between globe and counterpoise were made on an analytical balance to 0.01 mg., using the method of swings to ascertain the no-load rest-point, the balance sensitivity, and the load rest-point at the time of performing *each* weighing. All weighings, made with a standardized set of weights (26), were converted to a vacuum basis. As a general rule, the weights of the globes could be checked to ± 0.02 mg., so that the weight of the contained gas was known to ± 0.04 mg., corresponding to a mean error of ± 0.006 per cent.

A 4-liter Dewar jug, the contents being vigorously stirred, was used as a container for a constant-temperature bath. Temperature control was maintained by a bimetallic strip thermoregulator (modified) in conjunction with an FG-57 Thyratron tube and heating coil immersed in the bath liquid. Cooling was furnished by a mechanical refrigeration unit (see reference 31 for a description of the cooling cycle), or by dry ice for the lowest temperatures. The temperature of the cryostat could be held to around 0.02°C., and of the thermostat to somewhat better than this, for the short periods necessary for one determination. The temperature variation leads to an accuracy of about ±0.005 per cent. The measurements at 0°C. were made in the Dewar containing washed ice (28).

A 25-ohm, coiled-filament type (24) platinum resistance thermometer was used for ascertaining the temperatures of the various constant-temperature baths, the thermometer coil resistance being obtained by means of an oil-thermostated, Mueller type, calibrated Wheatstone bridge. This thermometer and accessory apparatus and the details of standardization and of temperature scale establishment have been mentioned in previous papers (21, 28, 29, 31). For the standardization the temperatures of the fixed points above 0°C. were taken as specified by the International Temperature Scale (7) and for below 0°C. as determined by Heuse and Otto (11). The temperature measurements bracketed the pressure determination and were recorded to 0.001°, the mean obtained and then rounded off to the nearest hundredth. The absolute accuracy is about 0.01° in the range −100° to +100°C., owing to the uncertainty existing in the thermodynamic temperature of the ice point, which was taken herein to be 273.16°K. (32).

The pressure was determined to ± 0.03 mm. (± 0.06 mm. for pressures greater than 950 mm.) on an absolute manometer of 15-mm. inside diameter Pyrex tubing, with a high-grade cathetometer. Meniscus corrections (14) were determined for each observation. The final results are expressed in international millimeters (7) (int. mm.) of mercury. The above tolerance leads to a mean calculated precision of ± 0.008 per cent.

The hydrocarbon gases had been prepared by Professor Kistiakowsky and his coworkers of these Laboratories for their study of the heats of hydrogenation (18, 19, 20). Considerable data exist concerning their high purity (18, 19, 20, 21, 36). The ethene was dried and de-aerated by simple bulb-to-bulb distillations, while the remaining six hydrocarbons were rendered perfectly anhydrous by a physical process (27). The gases ethene, propene, propadiene, and ultimately 2-methylpropene were stored as such and the remaining substances were stored as liquid phase, in all-Pyrex-glass containers fitted with internal break-off seals operated by an external electromagnet. In view of the instability of liquid 2-methylpropene (30), a freshly distilled sample was employed for the determination.

High-vacuum technique was used in all operations, with special care taken to remove,—and then to avoid contamination with thereafter,—air, water, and stopcock grease. The gas was admitted to the apparatus through cock S1 (figure 1), the storage container serving as a temporary reservoir for the excess material. By the proper manipulation of cocks S1, S3, S4, S5, and S6 and through the application of refrigerant about tube A, the apparatus could be exhausted, the desired gas pressure built up, and the globe removed from the line or emptied of its contents without any loss of gas to the atmosphere. Thermal equilibrium of the globe contents was rapidly established; pressure readings were recorded 10 to 30 min. after equilibrium was attained.

Adsorption and precondensation might be presumed to exist in the interior of the globes, since in some cases an almost saturated gas was contained therein. If such effects are present, they were undetectable with the present apparatus. Others (16, 22) have deduced that adsorption is not significant in such cases. The ratio of surface to volume in certain of the globes was different, but no difference could be found in the molal volumes determined in different globes. The effect of pressure was found to be within the experimental error, that is, the second virial coefficient was not a function of the pressure. These two effects are strong evidence that adsorption was not an appreciable factor. Indications from another project, on the density of the saturated vapors of the butenes determined by means of a gas density balance, were that such effects were negligibly small.

TREATMENT OF RESULTS

The equation of state applied is the virial form of Kamerlingh Onnes (10, 17)

$$pV = RT + \frac{\theta}{V} + \frac{\iota}{V^2} + \frac{\kappa}{V^4} + \cdots \tag{1}$$

where θ, ι, κ, . . . are termed the second, third, fourth, . . . virial coefficients, respectively, and are temperature-dependent only, the dependence generally being expressed by an equation of the form

$$\theta = f + \frac{g}{T} + \frac{h}{T^2} + \frac{i}{T^4} + \cdots \tag{2}$$

A preliminary analysis of the data indicated that the use of the second virial only would be sufficient to express the results to the requisite precision. This is equivalent to considering pair-interaction only in the theoretical treatment, the effect of a neighboring molecule upon the original pair-interaction being taken as insignificant. A least-square solution for an equation employing both second and third virials for *trans*-2-butene, as an example of a molecule exhibiting large imperfection in which instance the third virial might be expected to become relatively important, showed that about the same correspondence of the equation with the observed results was obtained as when the second virial only was considered. Three constants in the temperature coefficient of the second virial were used, so that the complete equation of state as used herein becomes

$$pV = RT + \theta/V = RT + \frac{f}{V} + \frac{g}{VT} + \frac{h}{VT^2} \tag{3}$$

This nomenclature has been employed in order to avoid any possible confusion with the second virial coefficient B in the equation

$$pV = RT + Bp \tag{4}$$

The collected data of m, p, v, and T were transformed into p, V, T by the use of 1937 international atomic weights (C = 12.010; H = 1.0078). The values of fundamental constants used were: T_0 = 273.16°K. (32), and V_0 (the molal volume of a perfect gas at N. T. P.) = 22.414 dm.^{3} (5). The units for the equation of state are therefore cubic decimeters, degrees Kelvin, and international millimeters; the value of the gas constant R on this basis becomes 62.362 dm.^{3} × mm. Hg per degree per mole. Values of θ were calculated from the equation

$$\theta = pV^2 - RTV \tag{5}$$

θ being in the resulting units of mm. Hg × dm.^{6} per mole.[2] The difference between 1 liter and 1 cubic decimeter being about one part in thirty thou-

TABLE 1

Molal volume data

T	p	V OBSERVED MOLAL VOLUME	PER CENT DIFFERENCE IN V (CALCULATED − OBSERVED)
		Ethene	
°*K.*	*int. mm.*	*dm.*^{3}	*per cent*
343.11	1072.1	19.848	−0.017
343.10	438.36	48.663	+0.067 (D)*
273.16	759.87	22.246	−0.016
273.16	443.13	38.260	+0.018
223.24	721.08	19.053	−0.017
223.23	465.82	29.632	−0.006
198.78	760.14	15.987	0.000
Mean of seven			±0.020
Mean of six			±0.012
		Propene	
343.12	833.38	25.416	−0.018
308.18	1104.0	17.077	+0.005
273.16	831.51	20.066	−0.038
273.16	790.96	21.105	+0.019
273.16	758.90	22.020	−0.004
273.16	378.89	44.522	+0.032
226.99	752.07	18.169	−0.042
223.21	550.95	24.582	+0.004
Mean			±0.020
		Propadiene	
343.15	836.29	25.325	−0.003
273.16	1038.9	15.937	+0.053
273.16	762.64	21.884	+0.023
273.16	341.09	49.323	+0.356 (D)
237.16	692.31	20.728	−0.011
222.66	334.80	40.751	−0.033
Mean of six			±0.080
Mean of five			±0.025
		2-Methylpropene	
333.15	838.03	24.272	+0.078
273.16	850.72	19.172	−0.121
273.16	575.31	28.783	−0.122
243.29	244.26	60.900	+0.062
Mean			±0.095

* (D) = discarded value.

TABLE 1—*Concluded*

T	p	V OBSERVED MOLAL VOLUME	PER CENT DIFFERENCE IN V (CALCULATED − OBSERVED)
		1-Butene	
°*K.*	*int. mm.*	*dm.*^{3}	*per cent*
333.17	689.80	29.604	+0.078
294.26	656.79	27.254	−0.035
273.16	851.48	19.178	−0.216
273.16	776.45	21.115	−0.198
243.38	191.80	77.926	+0.055
Mean			±0 116
		***trans*-2-Butene**	
333.15	829.92	24.476	−0.056
333.15	717.65	28.344	+0.129
308.17	839.59	22.204	−0.042
308.17	739.83	25.302	−0.068
308.17	577.09	32.622	−0.024
273.16	723.59	22.557	+0.170
273.16	717.77	22.667	+0.523 (D)
273.16	665.54	24.649	+0.013
273.16	692.37	23.659	−0.002
273.16	604.19	27.264	−0.034
273.16	492.35	33.690	−0.074
250.92	258.86	59.297	+0.001
243.30	166.21	90.039	+0.006
Mean of thirteen			±0.088
Mean of twelve			±0.052
		***cis*-2-Butene**	
343.10	756.90	27.756	+0.075
333.14	689.12	29.579	+0.111
308.17	822.36	22.694	−0.007
273.16	629.29	26.064	+0.147
273.16	638.76	25.697	+0.015
273.16	577.49	28.566	−0.111
273.16	577.69	28.591	−0.236
259.94	353.09	44.815	+0.000
250.93	236.91	64.785	+0.079
Mean			±0.087

sand (5), the difference between dm.^{3} and liters may be neglected for the majority of purposes. A least-squares method applied to the θ–T data gave the values of the constants f, g, and h. A comparison made between the values of θ (calculated) and θ (observed) revealed any widely erratic value; in such an instance the erratic value was withdrawn from the least-square summation and a new set of constants obtained. Such a withdrawal was necessary thrice in a total of fifty-two determinations. An analytical method has been adopted to show the type of deviations occurring in the observed and calculated molal volumes (table 1), and a graphical presentation to illustrate the correspondence in θ (figures 2 to 7, inclusive). It will be noticed that as the individual substance studied becomes more complex, the deviation increases; it is possible that this

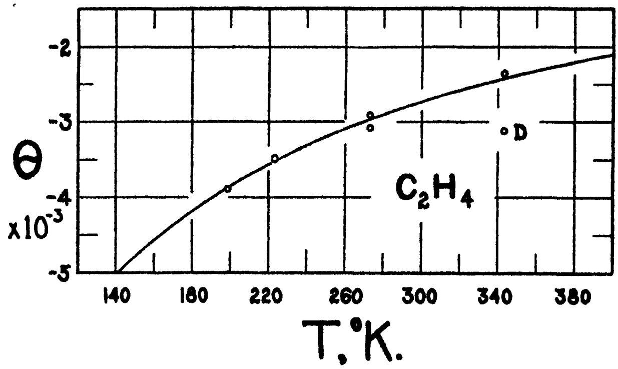

FIG. 2. Second virial of ethene as a function of temperature. The points represent the experimentally determined values and the continuous line the course of the developed equation. The point marked with a D was withdrawn from the first least-squares summation as being an erratic value, the equation as represented by the line not taking the erratic point into consideration.

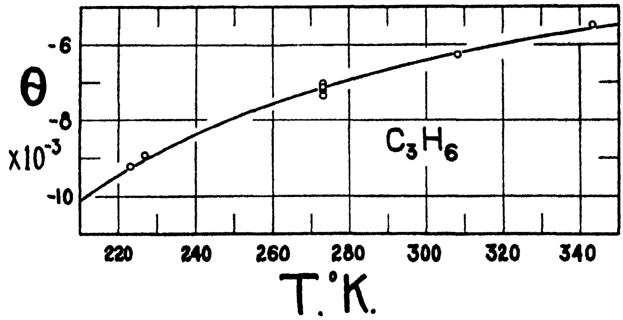

FIG. 3. Second virial of propene as a function of temperature

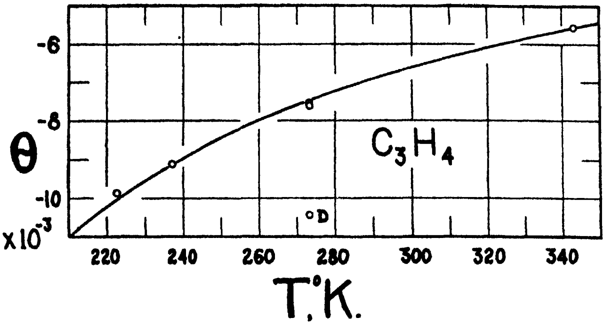

FIG. 4. Second virial of propadiene as a function of temperature The point marked with a D was discarded when deriving the equation represented by the line.

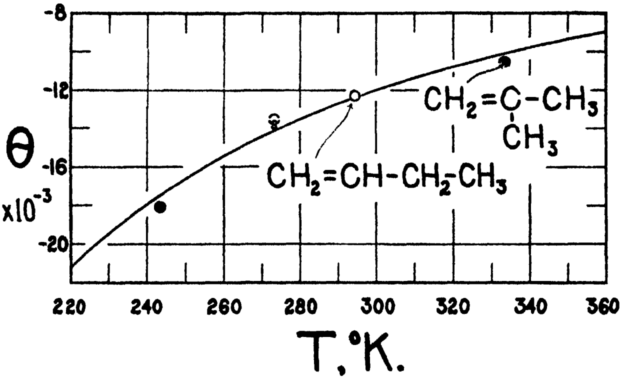

FIG. 5. Second virials of 2-methylpropene and of 1-butene as functions of temperature. The smaller circles represent the values for 2-methylpropene and the larger those for 1-butene. The line represents both virials within the accuracy with which they can be shown on this graph.

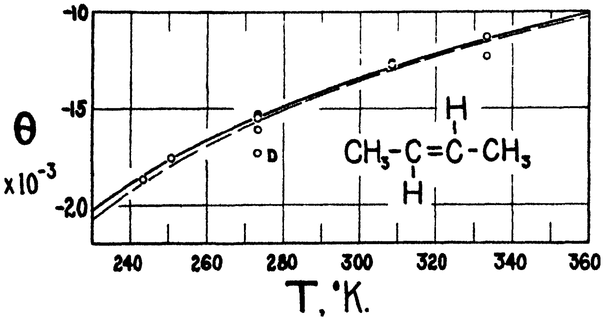

FIG. 6. Second virial of *trans*-2-butene as a function of temperature. The dotted line represents the course of the first equation derived, utilizing all points. The full line represents the second equation derived, when the point marked D was discarded.

may be attributed to impurities. The higher hydrocarbons are more difficult to obtain in a pure state. An analogous behavior was observed in the vapor pressure data (21); this reference should be consulted for a discussion of the possibility of a slight fractionation effect when transferring gas in the apparatus, due to the use of refrigerants. Todd and Parks' (36) estimate of the impurities in the three butenes (portions of the identical samples here employed) from the pre-melting heat capacity data was of the order of about 0.1 mole per cent. The mean calculated precision is ± 0.02 per cent, the sum of the precisions in measuring v, m, T, and p in the molal volume. It will be noticed in table 1 that the molal volume of the simpler hydrocarbons has been determined to this precision. In figures 2 to 7, inclusive, the temperature coefficient of the second virials

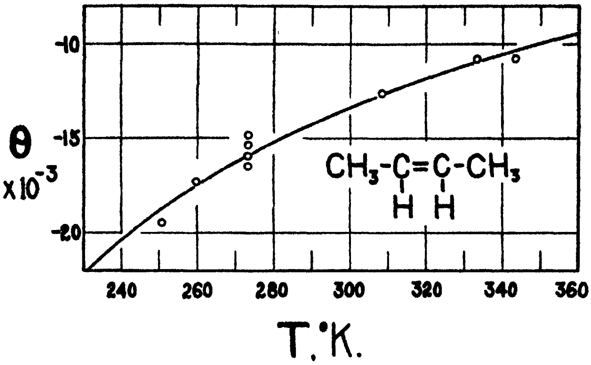

FIG. 7. Second virial of *cis*-2-butene as a function of the temperature. It would have been desirable to plot the data of figure 6 on this sheet, but the result of so doing is confusing.

TABLE 2

Second virial temperature coefficient equation constants

$$\theta = f + \frac{g}{T} + \frac{h}{T^2}$$

HYDROCARBON	f	$g \times 10^{-3}$	$h \times 10^{-7}$	TEMPERATURE RANGE
				°K.
Ethene	+72.	−953.58	−3.3855	199 to 343
Propene	−2906.	−6.81	−31.360	223 to 343
Propadiene	−2164.	−114.7	−36.509	223 to 343
2-Methylpropene	−1953.	+62.16	−93.500	243 to 333
1-Butene	−1802.	+57.86	−93.867	243 to 333
trans-2-Butene	−3630.	+10.69	−88.72	243 to 333
cis-2-Butene	−771.	+33.65	−113.69	251 to 343

is shown plotted, the course of the developed equation being indicated by a line. In table 2 are given the constants, derived by least squares, for expressing the second virial coefficient as a function of the temperature.

DISCUSSION

The second virial is the difference between two very large numbers, as is evident from equation 5, so that even though the molal volumes have been determined with high precision, the relative error in θ will be appreciable. It can be seen from table 1 that the equation of state represents the behavior very satisfactorily. There is very little data in the literature with which a comparison can be made. The normal densities of ethene (25) and of propene (1) have been carefully determined in the interests of the atomic weight of carbon; table 3 shows a comparison with the data obtained in this research. Eucken and Parts (9) have determined the second virial for ethene over approximately the same range as was taken in this work. The two sets of data are not in agreement at the lower temperatures, the difference being outside the limit of experimental error.

TABLE 3

Molal volume at N. T. P. of ethene and of propene

HYDROCARBON	MOLAL VOLUME AT 0°C. AND 1 ATMOSPHERE IN LITERS		
	This research	Others	Difference
			per cent
Ethene	22.236	22.257* (15, 25)	−0.09
		22.245† (34)	−0.04
Propene	21.984	21.973 (1)	+0.05

* The maximum accurate value recorded in the literature.

† The minimum value recorded.

For closely related compounds, such as the three pairs propene–propadiene, 2-methylpropene–1-butene and the *cis*–*trans*-2-butenes, the second virials and the temperature coefficients are similar. The similarity is most marked in the second-mentioned pair, for which the virials are indistinguishable within the experimental error over a temperature range of 100°. The difference between the two geometric isomers is slight but apparent, while comparatively large differences exist between propene and propadiene. It should be noted that these differences are quite closely related to the differences in the normal boiling points (21) of the six compounds concerned. This subject will be treated in greater detail in a later paper.

SUMMARY

A modified method of gas density determination is applied in order to obtain second virial temperature coefficients for ethene, propene, propadiene, 2-methylpropene, 1-butene, *trans*-2-butene, and *cis*-2-butene. The temperature range covered is from *ca.* 340°K. to the normal boiling point, with the exception of ethene for which the lowest temperature is 199°K. The original data of p–V–T are given. A comparison between the molal volumes calculated from the developed equations of state with those experimentally observed indicates a mean deviation of ± 0.06 per cent. The second virial coefficients in an Onnes type equation of state were computed and the temperature coefficient equation constants evaluated by a least-squares method. Graphs of the observed and calculated second virials over a temperature range are given.

I wish to thank Professor Arthur B. Lamb for his advice and for apparatus and material placed at my disposal. Professor George B. Kistiakowsky and coworkers very kindly made available the hydrocarbon samples.

REFERENCES

(1) Batuecas: J. chim. phys. **31**, 65, 165 (1934).
(2) Baxter and Starkweather: Proc. Natl. Acad. Sci. U. S. **15**, 441 (1929).
(3) Baxter and Butler: Unpublished results.
(4) Beth and Uhlenbeck: Physica **4**, 915 (1937).
(5) Birge: Phys. Rev. Suppl. **1**, 1 (1929).
(6) Buffington and Latimer: J. Am. Chem. Soc. **48**, 2305 (1926).
(7) Burgess: Bur. Standards J. Research **1**, 635 (1928).
(8) Cooper and Maass: Can. J. Research **4**, 283, 495 (1931).
(9) Eucken and Parts: Z. physik. Chem. **B20**, 184 (1933).
(10) Fowler: *Statistical Mechanics*, 2nd edition. University Press, Cambridge (1936).
(11) Heuse and Otto: Ann. Physik **9**, 486 (1931); **14**, 181, 185 (1932).
(12) Holborn and Otto: Z. Physik **33**, 1 (1925).
(13) Hirschfelder and Roseveare: J. Phys. Chem. **43**, 15 (1939).
(14) *International Critical Tables*, Vol. I, p. 70. McGraw-Hill Book Company, Inc., New York (1926).
(15) *International Critical Tables*, Vol. III, p. 3. McGraw-Hill Book Company, Inc., New York (1928).
(16) Johnston and Weimer: J. Am. Chem. Soc. **56**, 625 (1934).
(17) Kennard: *Kinetic Theory of Gases*. McGraw-Hill Book Company, Inc., New York (1938).
(18) Kistiakowsky, Romeyn, Ruhoff, Smith, and Vaughan: J. Am. Chem. Soc. **57**, 65 (1935).
(19) Kistiakowsky, Ruhoff, Smith, and Vaughan: J. Am. Chem. Soc. **57**, 876 (1935).
(20) Kistiakowsky, Ruhoff, Smith, and Vaughan: J. Am. Chem. Soc. **58**, 146 (1936).

(21) **Lamb and Roper**: J. Am. Chem. Soc. **62**, 806 (1940).
(22) **Long and Gulbransen**: J. Am. Chem. Soc. **58**, 203 (1936).
(23) **Margenau**: J. Chem. Phys. **6**, 896 (1938).
(24) **Meyers**: Bur. Standards J. Research **9**, 807 (1932).
(25) **Moles, Toral, and Escribano**: Compt. rend. **207**, 1044 (1938).
(26) **Richards**: J. Am. Chem. Soc. **22**, 144 (1900).
(27) **Roper**: Ind. Eng. Chem., Anal. Ed. **9**, 414 (1937).
(28) **Roper**: J. Am. Chem. Soc. **60**, 866 (1938).
(29) **Roper**: J. Am. Chem. Soc. **60**, 1693 (1938).
(30) **Roper**: J. Am. Chem. Soc. **60**, 2699 (1938).
(31) **Roper**: Ind. Eng. Chem., Anal. Ed. **12**, 113 (1940).
(32) **Roebuck**: Phys. Rev. **50**, 370 (1936).
(33) **Schäfer**: Z. physik. Chem. **B36**, 85 (1937).
(34) **Stahrfoss**: J. chim. phys. **16**, 175 (1918).
(35) **Starkweather**: Ph.D. Thesis, Harvard University, 1925.
(36) **Todd and Parks**: J. Am. Chem. Soc. **58**, 134 (1936).

STUDIES ON SILICIC ACID GELS. X

THE TIME OF SET OF GEL MIXTURES CONTAINING HIGH CONCENTRATIONS OF MINERAL ACIDS

CHARLES B. HURD AND RAYMOND W. BARCLAY

Department of Chemistry, Union College, Schenectady, New York

Received December 27, 1939

INTRODUCTION

It has been shown (4) that silicic acid gel mixtures show minimum time of set with pH slightly above 7. Mixtures containing a high concentration of strong acids also set rapidly (3). The optimum limits for setting have been published (11), and also the curve for time of set against acid concentration (8).

Former studies have shown that the time of set of slightly acid mixtures and the hydrogen-ion concentration follow a linear relation (10). The effect of temperature was shown by a value of about 17,000 cal. for the energy of activation.

In this paper are given the results of a study of the highly acid gel mixtures, in particular, of the effect of pH and temperature on time of set.

EXPERIMENTAL

The technique used has been described in previous papers in this series. The solution of sodium silicate prepared by diluting "E" brand silicate, from the Philadelphia Quartz Company, titrated 1.28 normal with standard hydrochloric acid, using methyl orange. The pH was measured with a quinhydrone indicator, using a bright platinum wire (7). Time of set was measured by the tilted-rod method (9).

EXPERIMENTAL RESULTS

To conserve space, data are not tabulated, but are plotted in figure 1. A constant concentration of silicate was used; the hydrochloric or sulfuric acid concentrations were varied. To give one example, the concentrations for the point on the 38.2°C. curve in figure 1 for pH = 0 are, in gram-moles per liter: SiO_2, 0.67; NaCl, 0.40; and HCl, 1.65.

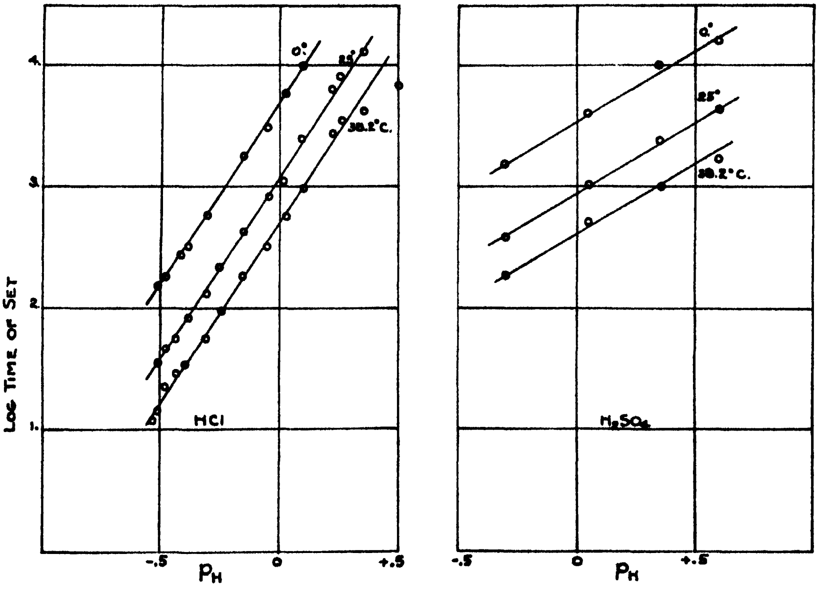

FIG. 1. Relation between logarithm of time of set and pH for silicic acid gels containing hydrochloric or sulfuric acid at different temperatures.

From figure 1 new curves were constructed, showing the relation between the logarithm of the time of set and the reciprocal of the absolute temperature. The data picked off the curves of figure 1 are given in table 1 and are plotted in figure 2.

As previously explained (9), the slope of the curves of figure 2 multiplied by 2.30R gives the energy of activation. For gel mixtures containing hydrochloric acid, the energy of activation is about 11,000 cal., and for those containing sulfuric acid about 9000 cal. for these highly acid mixtures.

Gel mixtures containing hydrochloric acid became more yellow as the

TABLE 1

The logarithm of the time of set of gel mixtures containing hydrochloric or sulfuric acid as a function of pH and temperature

pH	LOG TIME		
	At 0.0°C.	At 25.0°C.	At 38.2°C.
	Hydrochloric acid gels		
+0.02	3.780	3.061	2.744
−0.16	3.232	2.626	2.250
−0.31	2.751	2.121	1.740
−0.43	2.428	1.756	1.462
−0.51	2.176	1.532	1.146
	Sulfuric acid gels		
0.96		4.007	3.586
0.60	4.204	3.644	3.220
0.34	4.008	3.391	3.000
0.05	3.601	3.033	2.703
−0.31	3.179	2.578	2.263

These values are shown in figure 2 for the gels containing hydrochloric or sulfuric acid.

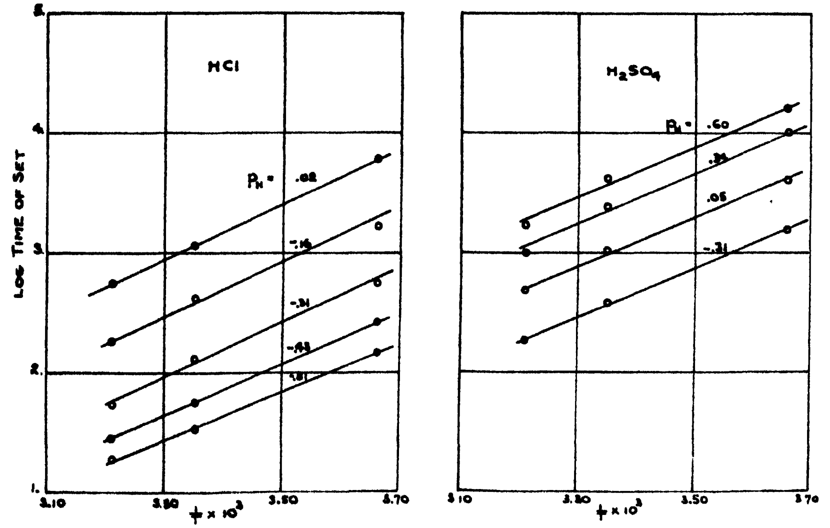

FIG. 2. Relation between logarithm of time of set and reciprocal temperature in highly acid gels.

acid concentration increased. Those containing sulfuric acid were white and turbid.

The quinhydrone apparatus gave steady and reproducible results up to pH = −0.5 for hydrochloric acid mixtures and to pH ≠ −0.3 for sulfuric acid mixtures. With higher acid concentrations variable results were obtained.

At 0°C. a precipitate of sodium chloride appeared with higher acid concentrations. It did no harm.

Drift of pH, so troublesome with mixtures containing strong acids in the pH range 3.0 to 6.0, as already noted (6), caused little trouble at pH = 0. At higher pH values increasing drift was noted. The pH always showed an increase.

DISCUSSION

Briefly, the curves of figure 1 appear linear within experimental error. Even if the pH values here from quinhydrone are not really absolute, they are relative. They show a linear relation. Note here, however, that the time of set increases with increase of pH, while with mixtures containing the strong acids, from pH 3.0 to 6.0, the time of set decreases with a pH increase (6). Figure 1 shows that a change of pH causes more change in time of set with gels containing hydrochloric acid than with those containing sulfuric acid.

The energies of activation,—11,000 and 9,000 cal.,—must be in error by less than 10 per cent. These highly acid mixtures show lower energies of activation than those with pH 3.0 to 6.0; therefore, temperature has less effect on the time of set of the former.

In the least acid of these highly acid mixtures, a small pH drift was noted, always an increase. This disagrees with Batchelor's (1) results, but agrees with those of Hanks and Weintraub (2) and with former results from this laboratory (6).

This small drift of pH agrees with the theory explained by Hurd, Frederick, and Haynes (6), namely, that during condensation the silicic acid becomes successively weaker. The drift seemed larger here than one would expect.

Formerly, in theories for a mechanism of setting of the gel, much mention has been made of the dehydrating effect of substances present. In refutation, Hurd and Carver (5) offered the failure of glycerol to accelerate setting. In the present paper, note that mixtures containing sulfuric acid at pH = −0.31, for example, set more slowly than those with hydrochloric acid.

The end product with gels containing sulfuric acid is white and milky. Possibly in the final gel the dehydrating power of sulfuric acid changes the state of the water bound or contained in the gel.

SUMMARY

The effect of pH and temperature upon the time of set of very acid gels prepared from sodium silicate and either hydrochloric acid or sulfuric acid has been studied.

For the range pH = +0.5 to −0.5, there is a linear relation between logarithm of time of set and the pH. In contrast to the analogous relation at pH = 3. to 6., the time of set increases with increase of pH.

A rise of temperature decreases the time of set for these highly acid gels, as is the case in the pH range 3.0 to 6.0. With these highly acid gels the energy of activation is 11,000 or 9,000 cal., respectively, for gels containing hydrochloric or sulfuric acid.

In spite of the greater dehydrating power of the sulfuric acid, gel mixtures containing it set somewhat more slowly than those containing hydrochloric acid. The first-named gels are milky; those containing hydrochloric acid are clear and yellow in color.

REFERENCES

(1) Batchelor, H. W.: J. Phys. Chem. **42**, 575 (1938).
(2) Hanks, J. H., and Weintraub, R. L.: J. Phys. Chem. **41**, 583 (1937).
(3) Holmes, H. N.: J. Phys. Chem. **22**, 510 (1918).
(4) Hurd, C. B.: Chem. Rev. **22**, 403 (1938).
(5) Hurd, C. B., and Carver, D. H.: J. Phys. Chem. **37**, 321 (1933).
(6) Hurd, C. B., Frederick, K. J., and Haynes, C. R.: J. Phys Chem. **42**, 85 (1938).
(7) Hurd, C. B., and Griffeth, R. L.: J. Phys. Chem. **39**, 1155 (1935)
(8) Hurd, C. B., and Letteron, H. A.: J. Phys. Chem. **36**, 604 (1932).
(9) Hurd, C. B., and Miller, P. S.: J. Phys. Chem. **36**, 2194 (1932).
(10) Hurd, C. B., Raymond, C. L., and Miller, P. S.: J. Phys. Chem. **38**, 663 (1934).
(11) Ray, R. C., and Ganguli, P. B.: J. Phys. Chem. **34**, 352 (1930).

THE YELLOW AND RED ZINC SILICATE PHOSPHORS

GORTON R. FONDA

Research Laboratory, General Electric Company, Schenectady, New York

Received November 16, 1939

Zinc orthosilicate, activated with manganese, emits a fluorescence which lies in the green. The reaction leading to its formation is catalyzed by several foreign salts. All of them prevent the attainment of normal brightness and in that respect they are undesirable. In another respect, however, they have a unique value in that they facilitate the formation at a low temperature of a zinc silicate which fluoresces yellow. The most effective of these salts are the chlorides. In a study of the results produced by them and of the spectral distribution of the phosphors formed (2), it was found that the fluorescence shifted from yellow to the normal green as the reaction was accelerated by increasing the concentration of the chloride. This change in color was accompanied by an increase in brightness. The yellow silicate was regarded therefore as the product of an incomplete reaction.

Recent tests have yielded more definite information as to its constitution. It was found that the yellow silicate might be formed even in the absence of a catalyst but only at an exceedingly slow rate. In the presence of any neutral chloride, however, the yellow phosphor was formed in a rapid reaction at 850°C. It was even formed at a moderate speed by introducing the manganese activator as the chloride, instead of the more usual nitrate or oxide. Potassium chloride proved to be the best catalyst.

The further observation was then made that the yellow silicate prepared at 850°C. is identical with that obtained by fusion and fairly rapid cooling, a method used successfully by Gruhl (5). Gruhl prepared also a zinc silicate fluorescing red. The distinctive emission of both the yellow and the red silicate he ascribed to the occurrence of allotropic forms of zinc silicate. The present experiments, however,—both those at 850°C. and those at a fusion temperature,—make it evident that it is the existence of the phosphors as amorphous complexes which accounts for the peculiarities in their emission. The features of their preparation and the character of their x-ray diffraction patterns are described below. From these the conclusion was formed that the yellow phosphor is essentially an amorphous complex of zinc oxide and silica in the orthosilicate proportions, and that the red phosphor is an amorphous complex of zinc oxide with an amount of silica in excess of the orthosilicate proportions. This is in contrast to the normal phosphor fluorescing green, which is crystalline zinc orthosilicate.

ZINC SILICATE FLUORESCING YELLOW

Preparation at 850°C.

A zinc silicate phosphor is generally prepared by firing a mixture of zinc oxide, silica, and manganese at a temperature of 1000–1300°C. Its fluorescence is green, regardless of proportions and particle size of ingredients, and of time of firing. It is always crystallized in the form of the orthosilicate, Zn_2SiO_4. This is the only known compound and its composition is made up of 2 moles of zinc oxide to 1 mole of silica. When a mixture of these oxides at this proportion is fired at 850°C., a temperature at which the reaction is extremely sluggish, no other product can be obtained under any conditions than the crystalline one fluorescing green. It is invariably the same, both with and without catalysts and with either fine or coarse ingredients. Even at so short a time of firing that the first appearance of fluorescence is just dimly observable, the peak of fluorescence still lies in the green whenever the ingredients are in the orthosilicate proportions. It is only when either zinc oxide or silica is in excess that the peak of fluorescence shifts to the yellow.

The use of a catalyst reduces the time of reaction from hours to minutes and almost doubles the intensity of the ultimate fluorescence obtainable. The halides are the most active catalysts. The chlorides of cadmium and zinc have already been mentioned. Still more effective are the potassium, sodium, and calcium chlorides and potassium fluoride. Their activity increases with their concentration. The yellow silicate can be formed only by limiting their concentration, for at too high a value only the green silicate is formed. It is necessary also to limit the time of reaction, for, if it is unduly prolonged, the yellow silicate passes over into the more normal green. Potassium chloride yielded the best quality of yellow phosphor and was used at a concentration of 15 per cent with a firing period of 40 min. Chlorides are solvents for zinc silicate, and their catalytic activity can therefore be regarded as due to a removal of the silicate shell that forms as a barrier between reacting oxide particles. The chloride does not enter into the constitution of the phosphor, for it could be dissolved out completely after the firing without altering the properties except to raise slightly the intensity of fluorescence.

Although the yellow phosphor could be obtained with an excess of zinc oxide, the reaction in that case was sluggish and the brightness attainable was low. An excess of silica yielded a much better product. The most favorable proportions lay between 2 to 4 moles of silica to 1 mole of zinc oxide.

The fineness of the silica used was important. When the reactive mixture was prepared from a colloidal gel formed from a solution of zinc and manganese nitrates in ethyl silicate, the speed of the reaction was increased and most of the product formed consisted of the crystalline green silicate. It was only by a radical decrease in firing temperature or in catalyst concentration that the pure yellow silicate could be formed, and then only at a reduced intensity of fluorescence.

The strongest fluorescence of the yellow phosphor, amounting to 45 per cent of the standard green zinc silicate, was obtained by using a mixture of precipitated zinc oxide either with precipitated silica or with ground quartz. The optimum concentration of manganese lay in the range of 0.4 to 1.2 per cent. An increase to 2.5 per cent lowered the brightness but did not shift the color of the fluorescence. The spectral distribution of several of these phosphors was photographed by H. Huthsteiner of this laboratory. It is shown in figure 1.

X-ray diffraction patterns of the products involved were obtained through the courtesy of L. L. Wyman and E. T. Asp of this laboratory.

They showed that the yellow silicate is entirely distinct from the green. Patterns of typical products are shown in figure 2. Pattern (a) is that of the pure orthosilicate, Zn_2SiO_4, and is the same for the synthetic product as for natural willemite, except for the slight distortion produced in the lattice by the presence of more or less manganese (2). Pattern (b) is that for a product obtained by firing at 1300°C. a mixture of 1 mole of zinc oxide and 2 moles of silica with 0.6 per cent of manganese. Its fluorescence is, of course, green. Despite the presence in it of 3 moles of silica to 1 mole of the orthosilicate, its pattern is identical with pattern (a) except that two weak lines of silica appear. This is made evident by comparison with (c), the pattern of pure silica which had been fired likewise at 1300°C. The same silica pattern was also obtained by firing at 850°C. It is the pattern of cristobalite. Washburn and Navias have shown that this is the crystalline form into which amorphous silica or quartz is first converted by heating, regardless of the temperature employed (6). It is noteworthy that the lines of the orthosilicate should predominate so strongly in pattern (b) despite the presence of such a large excess of silica,—3 moles of the latter to 1 mole of the former. The relative weakness of the silica lines is due to the lower atomic number of silicon as compared with that of zinc. When this same mixture was fired at 850°C. under conditions to yield the green phosphor, its pattern was found to be identical with (b).

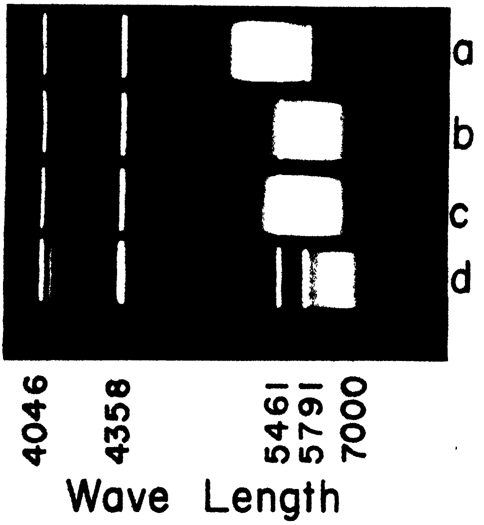

FIG. 1. Spectral distribution of fluorescence of zinc silicate phosphors. (a) Green phosphor, prepared at 1530°C. by slow cooling; (b) yellow phosphor, prepared at 850°C. with potassium chloride; (c) yellow phosphor, prepared at 1530°C. by rapid cooling; (d) red phosphor, prepared at 1530°C. by quenching.

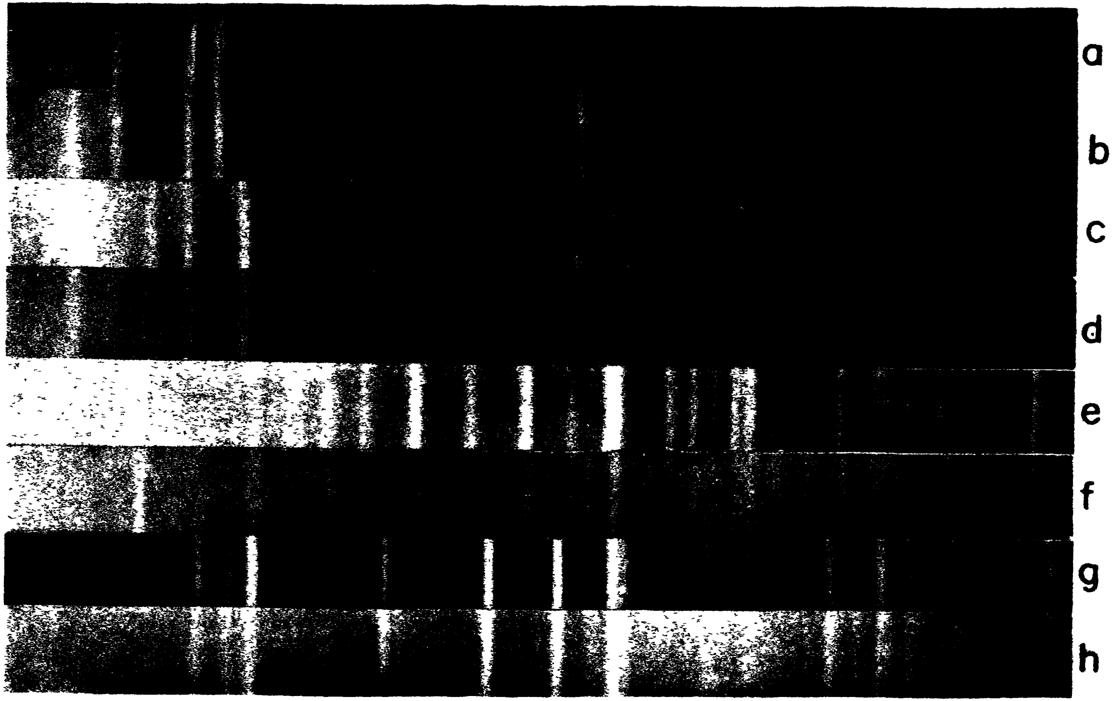

FIG. 2. X-ray diffraction patterns of zinc silicate phosphors emitting green and yellow fluorescence. (a) Zn_2SiO_4 + 0.6 per cent Mn, prepared by firing at 1300°C.; (b) $Zn_2SiO_4 \cdot 3SiO_2$ + 0.6 per cent Mn, prepared by firing at 1300°C.; (c) cristobalite; prepared by firing amorphous silica at 850°C. or 1300°C.; (d) $Zn_2SiO_4 \cdot 3SiO_2$ + 0.6 per cent Mn, prepared by firing a mixture of zinc oxide and amorphous silica with potassium chloride at 850°C.; (e) quartz; (f) $Zn_2SiO_4 \cdot 3SiO_2$ + 0.6 per cent Mn, prepared by firing a mixture of zinc oxide and powdered quartz with potassium chloride at 850°C.; (g) ZnO; (h) $ZnSiO_4 \cdot ZnO$ + 0.6 per cent Mn, prepared by firing a mixture of zinc oxide and amorphous silica with potassium chloride at 850°C.

Pattern (d) is that of the same mixture of 1 mole of zinc oxide with 2 moles of precipitated silica which had been fired at 850°C. with potassium chloride to yield the yellow phosphor. The potassium chloride was washed out before the diffraction pattern was taken. The noteworthy feature is that its pattern is identical with that of cristobalite, as shown by comparison of (d) with (c), with no alteration in spacing and with no evidence of either zinc oxide or zinc silicate. There is, however, considerable diffuse scattering present on the film, and this is of necessity to be ascribed to a zinc compound of very fine particle size.

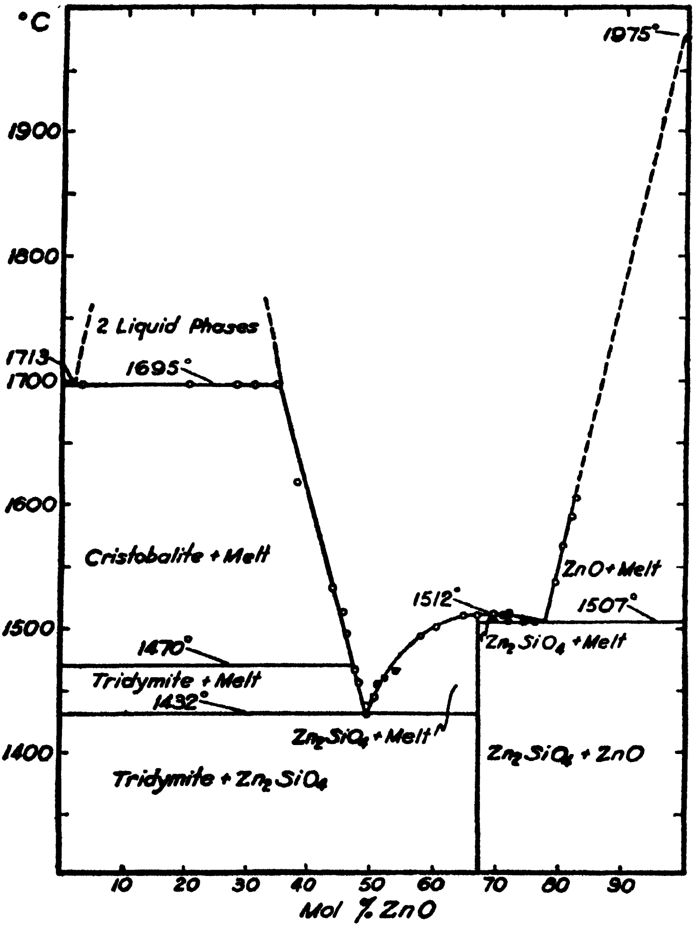

FIG. 3. Phase diagram for the system zinc oxide-silica (from Bunting (1)).

When a mixture having the same proportions was made up with powdered quartz rather than with precipitated silica, the same yellow phosphor was formed, but the pattern was radically different. It is shown in figure

2(f). Again there is considerable diffuse scattering and an absence of lines pertaining to any zinc compound, but the crystalline pattern is in this case that of quartz, as brought out by comparison with (e). When quartz alone was fired at 850°C. for as long a period as 14 hr. the quartz pattern was still retained.

Thus it is found that the same yellow phosphor is formed in the presence of an excess of silica, whether the silica be present as cristobalite or as quartz, and that the x-ray pattern shows no lines of any zinc compound, although the presence of any in a crystallized form would yield a predominating pattern of lines. The direct conclusion is that the silicate is present as an amorphous complex of zinc oxide and silica in the orthosilicate proportions. Such a complex is the only possible source of fluorescence emission, for products obtained by firing zinc oxide or silica alone with manganese and potassium chloride were non-fluorescent.

When the same yellow phosphor was prepared by firing similarly a mixture containing an excess of zinc oxide, its pattern showed only the lines of zinc oxide, as is seen by a comparison of (g) and (h) in figure 2.

This phosphor has the same spectral emissivity as the "zinc meso-disilicate" which was reported by Randall (4) and for which the peak of fluorescence lay at 6030 Å. It seems probable that the two have the same constitution.

Fusion preparations

The materials were fused in a covered platinum crucible heated by a blast lamp in a Hempel furnace, consisting of a series of concentric cylinders so arranged that the hot combustion gases passed downward over the outside of the crucible. This secures both uniformity and intensity of heating. The temperature of the crucible was held at 1530°C. for 5 min.

Gruhl's method of varying the speed at which the crucible was cooled was followed. Under slow cooling the resulting phosphor at all compositions emitted green fluorescence and exhibited the diffraction patterns characteristic of zinc orthosilicate, such as shown in figure 1 (a and b). The yellow phosphor was obtained when the fused mass was cooled fairly rapidly, such as by removal of the crucible from the hot furnace to cool in the open air. A temperature drop to 1100°C. occurred in about 5 sec.

The yellow phosphor could be obtained at all proportions of zinc oxide and silica, including an excess of either one. The highest intensity resulted from the use of a mixture of 1 mole of each, with 0.4 to 1.2 per cent of manganese. Its fluorescence was 66 per cent of that of the normal green silicate. The spectral distribution of fluorescence is shown in figure 1 (c).

In the case of an excess of silica, the diffraction pattern was identical with that of figure 2 (c), showing no lines but those of cristobalite. There was, however, a strong background of diffuse scattering. The result was the same whether the mixture was made up from powdered quartz or from precipitated silica. Each of these forms of silica yielded cristobalite when heated alone at 1530°C. for 5 min.

The same pattern made up of diffuse scattering with lines of cristobalite persisted when the phosphor was prepared from a mixture having the orthosilicate proportions and even when the green orthosilicate phosphor itself was given the same thermal treatment. There is evidently some decomposition at the temperature of fusion. Measurements on changes in weight showed that there is a slight evaporation of zinc.

When the phosphor was prepared from a mixture containing a small excess of zinc oxide, the diffraction pattern was made up mainly of diffuse scattering with a few broken lines which included some of zinc oxide and some of cristobalite, indicating again the presence of both constituents in the liquid melt. The character of their lines denoted that there was very little crystalline material present.

When zinc oxide or silica alone was fired at 1530°C. with 1 per cent of manganese, the resulting product was devoid of fluorescence.

The direct conclusion is therefore the same as from the tests at 850°C.: namely, that the fluorescence of the yellow phosphor is emitted by zinc silicate and that this silicate is in the form of an amorphous complex of zinc oxide and silica in the orthosilicate proportions.

In the absence of any excess zinc oxide, the phosphorescence decay of the yellow phosphor is of the same character as that of the green phosphor. The presence of excess zinc oxide, however, in either the green or the yellow phosphor serves to accelerate greatly the second stage of decay (3).

ZINC SILICATE FLUORESCING RED

In the case of preparations at 850°C. there were occasional small particles fluorescing red, insufficient in amount for examination. By fusion at 1530°C., however, the entire product could be converted into a red phosphor by extremely rapid cooling, sufficient to reduce the temperature to 1100°C. in about 1 sec. This was secured either by quenching in water or else by extinguishing the gas of the blast-lamp so that the crucible was suddenly subjected to a blast of cool compressed air. It was impossible to obtain the red phosphor from mixtures having the proportions of the orthosilicate or containing excess zinc oxide. In these cases, only the yellow phosphor resulted. The red could be obtained only from mixtures which included 1 mole or more of silica in excess of that demanded by the orthosilicate proportions,—a significant feature. The intensity of fluorescence was only 5 per cent or less of that emitted by the standard green silicate. Its spectral distribution, as shown in figure 1 (d), has a peak at about 6700 Å.; the cut-off at about 7100 Å. is due to lack of sensitivity of the emulsion.

Randall (4) has measured and discussed the spectral distribution of fluorescence emitted at 90°K. by various manganese halides as well as by phosphors containing manganese and has attempted to relate the fluorescence of the latter to that of the pure manganese salts. Several of the phosphors emit fluorescence whose peak lies at about the same location as does the fluorescence from the manganese salts, namely, 5925–6360 Å. The fluorescence of others measured by him lies at shorter wave lengths. From the Randall viewpoint, the fluorescence of the red zinc silicate phosphor would seem to be anomalous, for its peak lies at about 6700 Å.,—longer in wave length than that of the pure manganese salts. Such differences are significant, but they cannot properly be evaluated except as considered with reference to the excitation frequency. A characteristic essential in the emission of all solid phosphors is that the peak of their fluorescence should be at a longer wave length than that of the exciting radiation. Some of the energy of an excited electron is dissipated as emission in the infrared by means of the proximity of other ions contiguous to the parent ion of the excited electron. The energy emitted within the visible range is therefore reduced so that the fluorescence is displaced to longer wave lengths. The extent of the displacement depends upon the magnitude of the energy interchanges between the excited electron and the lattice. So far as an electron excited from a manganese atom is concerned, these interchanges are just as prevalent in a pure manganese salt as in the compound of any other metal whose manganese content is limited to that of an impurity. The variation of such losses with the nature of the compound gives rise to a variable dissipation of excited energy and hence to the differences in fluorescence color found in diverse phosphors all of which contain the same activator.

The diffraction patterns of the red phosphor always showed strong diffuse scattering. With 3 moles of excess silica, a few faint lines of cristobalite appeared, which were the same in number and location whether the silica was introduced in the precipitated form or as quartz. The most favorable mixture contained 1 mole of excess silica. With this mixture, whether the silica was present in the precipitated form or as powdered quartz, there were not even the faintest lines observable on the films. The essential source of the fluorescence therefore is an amorphous complex of zinc oxide with an amount of silica in excess of that required for the orthosilicate proportions.

Gruhl's pattern for the red phosphor is best disclosed in the *Handbuch der Physik* (5). It shows only four lines, and these cannot be identified as pertaining to any of the substances involved in the reaction. His assumption that they denote an allotropic form of zinc silicate could not be justified by our own work. It seems apparent that they are the lines of some chance impurity.

REVIEW

The conclusion has already been stated that the yellow phosphor is an amorphous complex of zinc oxide and silica in the orthosilicate proportions. The grounds for this are as follows:

1. Zinc silicate is the source of fluorescence. A phosphor could not be obtained from zinc oxide or silica alone.

2. The diffraction patterns show strong diffuse scattering, characteristic of the presence of amorphous material. The only lines present are those of zinc oxide or of silica, depending upon which is in excess. The spacings of these lines are unaltered from those of the pure oxides. If the silicate had entered into solid solution with either of the oxides, their crystal lattices would have been expanded or contracted and the positions of the lines would have been correspondingly altered. Furthermore, the product prepared at 850°C. has the same fluorescence characteristics whether the pattern exhibits the lines of cristobalite or those of quartz. The presence in the phosphor of these crystallized forms of silica or of zinc oxide is therefore purely incidental.

3. Rapidity in cooling the flux is a condition favorable for retaining it in the amorphous condition and for preventing crystallization. On the basis of the diffraction patterns, it is plain that silica can crystallize more readily from the flux than can zinc silicate. The choice of a rate of cooling which allows the silica to crystallize and not the silicate is an essential condition for obtaining the yellow phosphor. When both crystallize, the green phosphor results; when neither crystallizes, the red phosphor.

4. In preparations at 850°C. an essential feature in the formation of the yellow phosphor is a limitation that will prevent the agglomeration into crystalline form of the amorphous complex of zinc oxide and silica that results from the initial reaction between those ingredients. This is partly attained by the presence of some neutral material, such as an excess of silica or of zinc oxide, capable of acting as a physical barrier to an agglomeration into crystals. In addition, however, the reaction itself must be retarded. The green crystalline phosphor rather than the yellow phosphor always results if the reaction is allowed to proceed too far,—whether this be attained by adding an excess of catalyst, by using too fine oxides, or by allowing an increase in temperature or too long a time of reaction.

5. Confirmatory evidence was furnished by Dr. Louis Navias of this laboratory, who examined with the polarizing microscope the phosphors prepared by fusion. The green phosphor he found to be altogether anisotropic and optically positive. Its refractive index approximated 1.710, which is characteristic of crystalline Zn_2SiO_4. The yellow phosphor, on the other hand, was somewhat anomalous. It appeared to be anisotropic, less so when zinc oxide was in excess than when silica was in excess. Under

rotation of the polarized beam there was only a poor and shaded extinction, denoting a mixture of amorphous and crystalline material. Its refractive index was less than 1.710.

The red phosphor, as prepared by fusion, appears definitely to be an amorphous complex of 1 mole of zinc oxide with about 1 mole of silica, an amount which is in excess of that in the orthosilicate. This is on the basis of the following direct evidence: (*1*) As in the case of the yellow phosphor, it cannot be formed from zinc oxide or silica alone. In contrast to the yellow, it cannot be formed in zinc orthosilicate proportions but only in the presence of an excess of silica. (*2*) As is evident from the phase diagram of the zinc oxide–silica system published by Bunting (1) and reproduced in figure 3, zinc orthosilicate with 1 mole of excess silica forms a eutectic, melting at 1432°C. When such a mixture is cooled suddenly from a temperature of 1530°C., there is therefore good opportunity for obtaining it in the amorphous condition. The complete absence of lines in its diffraction pattern and the presence of strong continuous radiation bear witness that this was accomplished. It is not surprising that a few cristobalite lines should appear when the phosphor contained 2 moles of excess silica, for at this composition some crystals of cristobalite would be in stable equilibrium with the liquid at 1530°C. (*3*) Dr. Navias found that the red phosphor containing 1 mole of excess silica was completely isotropic. The particles were not clear glass but were definitely in the amorphous state. Their refractive index was much below 1.710.

REFERENCES

(1) Bunting, L. N.: Bur. Standards J. Research **4**, 134 (1930).
(2) Fonda, G. R.: J. Phys. Chem. **43**, 561 (1939).
(3) Fonda, G. R.: J. Applied Phys. **10**, 408 (1939).
(4) Randall, J. T.: Proc. Roy. Soc. (London) **170**, 290 (1939).
(5) Schleede, A., and Gruhl, A.: Z. Elektrochem. **29**, 411 (1923); *cf. Handbuch der Physik* **23**, 571 (1926) and Leverenz, H. W., U. S. patent 2,129,096 (1938)
(6) Washburn, E. W., and Navias, Louis: J. Am. Ceram. Soc. **5**, 565 (1922).

SUGAR ALCOHOLS. XXI

A Study of the Effect of the Anhydrides of Sorbitol on the Dissociation Constant of Boric Acid

FREDERICK K. BELL, C. JELLEFF CARR, AND JOHN C. KRANTZ, JR.

Department of Pharmacology, School of Medicine, University of Maryland, Baltimore, Maryland

Received November 2, 1939

INTRODUCTION

In a previous communication (4) two of the authors (C. J. C. and J. C. K., Jr.) with Oakley studied the effect of the anhydrides of mannitol upon the dissociation constant of boric acid. Later the extraordinary potentiation of the dissociation constant of boric acid produced by α-mannitan was reported (1). Since sorbitan and isosorbide, the mono- and di-anhydrides, respectively, of sorbitol, were available for metabolic study, it was decided to determine the effect of these two compounds upon the titration curve of boric acid and to compare this with the influence of sorbitol.

MATERIALS AND METHOD

The boric acid was of buffer quality. The sorbitol was the C.P. compound generously supplied by the Atlas Powder Company of Wilmington, Delaware. Likewise the sorbitan was supplied by the Atlas Powder Company, which obtained it as a by-product in the electrolytic reduction of glucose. The recrystallized compound melted at 112°C. Its specific rotation, $[\alpha]_D^{26°}$, was $-24.5°$ (H_2O; $C = 10$). The isosorbide was prepared for study by Dr. Wilton C. Harden of the firm of Hynson, Westcott, and Dunning of Baltimore. It was prepared by Fauconnier's method (2) of preparing isomannide from mannitol. The recrystallized compound melted at 60°C. Its specific rotation, $[\alpha]_D^{26°}$ was $+ 46.5°$ (H_2O; $C = 10$). The crystalline dibenzoate analyzed 101 per cent upon saponification.

Solutions of the various compounds studied contained 4 g. of the compound in 100 cc. of 0.1 molar boric acid. Stronger concentrations were employed for conductivity measurements. To 10-cc. portions of this was added 0.1 normal sodium hydroxide in quantities varying from 1 cc. to 11 cc. Immediately after the addition of the alkali the pH of the solution was determined electrometrically at 25°C. ± 0.5°, using the Wilson type hydrogen electrode (6).

The following formulas indicate the supposed structural relationship existing among the compounds.

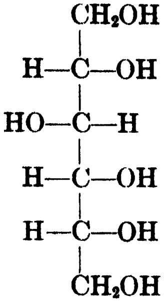

d-Sorbitol

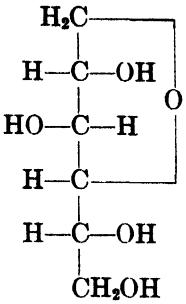

1,4-Anhydrosorbitol
Sorbitan

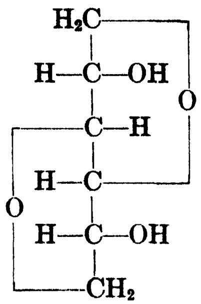

1,4,3,6-Dianhydro-sorbitol
Isosorbide

TABLE 1

Specific conductivities

Aqueous solutions at 25°C.; cell constant = 0.1417

SOLUTION	SPECIFIC CONDUCTIVITY
	mhos
0.5 *M* H_3BO_3	30.5×10^{-6}
0 5 *M* H_3BO_3 + 0.2 *M* sorbitol (Pfanstiehl)	415×10^{-6}
0.5 *M* H_3BO_3 + 0 2 *M* sorbitol (Atlas)	396×10^{-6}
0.5 *M* H_3BO_3 + 0.2 *M* sorbitan	122×10^{-6}
0.5 *M* H_3BO_3 + 0.2 *M* isosorbide (Atlas)	43.3×10^{-6}

The results of the pH measurements are set forth in figure 1.

The specific conductivities of the polyol–boric acid complexes are shown in table 1.

In figure 2 a comparison of the effect of dilution upon the sorbitan–boric acid complex and the corresponding α-mannitan complex is shown.

DISCUSSION

The data in figure 1 show that the titration curve of the sorbitol–boric acid complex is practically the same as that previously reported for the two hexahydric alcohols mannitol and dulcitol. The curve for the isosorbide–boric acid complex coincides with that obtained employing the isomannide–boric acid complex. This suggests that there are not two hydroxyl groups linked to the same side of adjacent carbon atoms within the molecule and bespeaks a structure similar to that of isomannide, namely, 1,4,3,6-dianhydrosorbitol. This assumption is further substantiated by the specific conductivity values of the isosorbide–boric acid complex of 43.3

$\times 10^{-6}$ mhos. The value obtained by van Romburgh and van der Berg (5) is 34.4×10^{-6} mhos for the isomannide complex in the same concentrations.

The titration curve of the sorbitan–boric acid complex shows approximately the same downward displacement as does the dulcitan–boric acid complex and not the strong displacement produced by the α-mannitan–boric acid complex. This compound, therefore, does not possess the structure of the Fischer and Zach (3) crystalline sorbitan, which is the 3,6-anhydrosorbitol with two hydroxyl groups linked to the same side of adjacent carbon atoms, similar to the α-mannitan structure. The degree of downward displacement of the titration curve and the conductivity measurements shown in figure 2 bespeak the 1,4-anhydrosorbitol structure for this compound, i.e., an anhydride without two hydroxyl groups linked to the same side of adjacent carbon atoms.

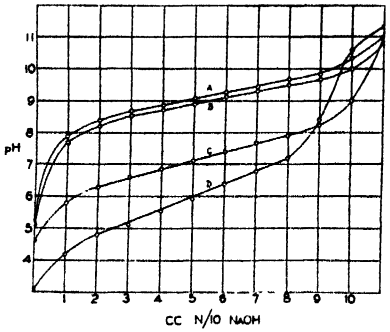

FIG. 1

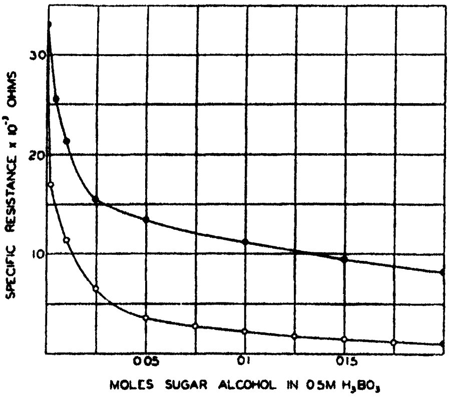

FIG. 2

FIG. 1. Effect of isosorbide, sorbitan, and sorbitol upon the dissociation constant of boric acid. Curve A, M/10 boric acid + 4 per cent of isosorbide; curve B, M/10 boric acid; curve C, M/10 boric acid + 4 per cent of sorbitan; curve D, M/10 boric acid + 4 per cent of sorbitol.

FIG. 2. Comparison of the effects of dilution upon the sorbitan–boric acid complex and the α-mannitan–boric acid complex. ○, α-mannitan; ●, sorbitan.

SUMMARY

1. The downward displacement of the titration curve of boric acid in the presence of sorbitol, sorbitan, and isosorbide has been determined. Conductivity measurements are also included.

2. These data suggest a 1,4-anhydro structure for sorbitan and a 1,4,3,6-anhydro structure for isosorbide.

REFERENCES

(1) **Bell, K. K., Carr, C. J., Evans, W. E., Jr., and Krantz, J. C., Jr.**: J. Phys. Chem. **42**, 507 (1938).
(2) **Fauconnier, A.**: Bull. soc. chim. **41**, 119 (1884).
(3) **Fischer, E., and Zach, K.**: Ber. **45**, 456 (1912).
(4) **Krantz, J. C., Jr., Oakley, M., and Carr, C. J.**: J. Phys. Chem. **20**, 151 (1936).
(5) **van Romburgh, G., and van der Berg, J. H. N.**: Proc. Acad. Sci. Amsterdam **25**, 335 (1922).
(6) **Wilson, J. A.**: Ind. Eng. Chem. **17**, 74 (1925).

THE QUANTUM YIELDS OF SOME DYE-SENSITIZED PHOTOÖXIDATIONS

FRANK HURD AND ROBERT LIVINGSTON

School of Chemistry, Institute of Technology, University of Minnesota, Minneapolis, Minnesota

Received January 18, 1940

The photosensitization of oxidation–reduction reactions by dyes has been extensively studied. Since 1910 about fifty papers have appeared on this or closely related subjects. However, relatively little quantitative work has been reported. This lack of quantitative information has seriously handicapped the establishment, upon a sound basis, of a theory or mechanism of these reactions, as is demonstrated by the fact that at least four mutually inconsistent theories have been proposed in the recent literature.

Since these reactions have important biological analogs and are not without intrinsic interest, it appeared to the authors that they were worthy of a careful quantitative study from the physicochemical viewpoint. The present paper reports the results of a series of determinations of the quantum yields of photoöxidations of several reducing agents sensitized by various dyes. The results of a detailed investigation of one of these systems,—solutions of eosin and potassium iodide,—will be published shortly.

EXPERIMENTAL PROCEDURE

Materials

The rose bengal, phenosafranine, and safranine T were Grübler preparations. The fluorescein was a Kahlbaum product. The neutral red was a product of the National Aniline and Chemical Company. The indigosulfonates and one sample of methylene blue were LaMotte indicators.

The second sample of methylene blue was a zinc-free product of the du Pont Company, prepared for biological use. These dyes were used without further purification. The eosin was purified by precipitating it with dilute hydrochloric acid, washing it, dissolving it with an equivalent amount of base, and crystallizing it from the resulting solution. All other reagents were of analytical grade and were used without further purification. Conductivity water was used in preparing all solutions.

Analytical methods

Oxalate was determined with standard 0.01 *N* potassium permanganate, following the standard procedure. In a few cases where the dye caused an erratic consumption of potassium permanganate, the oxalate was precipitated as calcium oxalate, filtered off, washed, dissolved in acid, and then titrated with potassium permanganate (reference 10, page 325). Solutions of thiosulfate, arsenite, and those containing both iodide and arsenite were titrated with a standard iodine solution (reference 10, pages 590–6). In certain experiments, particularly those with eosin, the end point was determined by the polarized-electrode method of Faulk and Bowden (5). Iodine formed in arsenite-free solutions of iodide was titrated with standard thiosulfate.

A calibrated microburet was used in all of these titrations, except in the oxalate determinations, where a weight buret was used.

Apparatus

The light source was a water-cooled quartz-capillary mercury arc of the atmospheric pressure type (4, 11, 14). Glass color filters were used to isolate the desired spectral regions.

Energy measurements were made with a Moll surface thermopyle and a Leeds and Northrup galvanometer, provided with a suitable shunt and series resistance. The galvanometer thermopyle system was calibrated with a radiation standard lamp from the United States Bureau of Standards, following the explicit directions furnished with the lamp. These calibrations were checked with the uranyl oxalate actinometer of Leighton and Forbes (12).

Two different optical systems were used in these measurements. The system used in the final series of measurements, which includes all of the experiments using I^- and AsO_2^- as acceptors, was similar to that described by Livingston (15). In the experiments in which either oxalic acid or thiosulfate was used as the acceptor, a spherical reaction cell of about 4-ml. capacity was used. This cell, like the cylindrical cell used in the other series of measurements, was fitted with a gas inlet tube in the bottom, by means of which oxygen could be forced into the solution through a sintered-glass plate. A large glass condensing lens was used to bring the light to focus at the center of the cell. A surface thermopyle was placed directly behind the cell and intercepted all of the emergent light. The whole system was mounted rigidly on an optical bench. The cell was protected from stray light and was so arranged that it could be moved in or out of the light beam in a reproducible manner (8). While the use of this sytem resulted in a high intensity of absorbed light (quanta per second per milliliter of solution), it had the disadvantage that the distribution of intensity in the cell was far from uniform.

The experiments on methylene blue were performed separately by a different method.[1] The light sources used in these experiments were a 200-watt projection lamp and a 500-watt carbon arc. The rates of the reactions were followed manometrically, using a standard Warburg respiration apparatus. The energy absorbed was not measured directly, but the quantum yields were estimated by comparison with certain convenient known reactions.

Routine procedure and computations

Coincident with each experiment, two blank analyses were made, using samples which had the same volume as the reacting solution. The first of these titrations was made at the beginning of the run; the second, at the conclusion. The dark reactions were negligible in all of the experiments reported here. The number of molecules which reacted photochemically was computed in the usual way:—from the blank titre, the change in titre, the concentration of the blank, and the volume of the reacting solution.

During the course of each experiment, galvanometer deflections, corresponding to the light transmitted by the reaction cell as well as that transmitted by the water cell, were observed at 15-min. intervals. The total time of irradiation for a single experiment was from 0.5 to 3 hr. Comparison with the uranyl oxalate actinometer (12) showed that the measurements of the absorbed energy were correct within 3 or 4 per cent when the cylindrical cell was used but were about 42 per cent low when the spherical cell and strongly convergent light were used.

EXPERIMENTAL RESULTS AND CONCLUSIONS

The quantum yields of the photoöxidation of I^-, using several dyes as sensitizers, are listed in table 1. All of these experiments were performed with the cylindrical cell and slightly convergent beam of light. Oxygen was passed through the cell at the rate of 30 bubbles per minute. A monohydrogen phosphate–dihydrogen phosphate buffer was used in all of these experiments, the total phosphate concentration being kept constant at 0.005 *M*. In addition to the dye, potassium iodide, and buffer, a small amount of sodium metarsenite was added to each solution. The sodium metarsenite prevented the formation of detectable concentrations of I_3^-, which would have interfered with the measurements by absorbing light.[2] Monochromatic filtered light was used in all of these experiments, except the one with rose bengal and the 0.05 *M* potassium iodide run with eosin. In these two cases, the light source was a 1000-watt projection lamp, provided with a cupric sulfate solution filter. In the experiment with fluorescein, the wave length of the light was 3650 Å. In the third experiment with indigotetrasulfonate, light of λ 5780 Å. was used. In all of the other experiments, light of λ 5460 Å. was used. The quantum yields are expressed as moles of iodide ion oxidized per Einstein absorbed.

---

[1] These experiments were performed in the Jones Chemical Laboratory of the University of Chicago by R. Livingston while he was a holder of a Lalor Fellowship. The apparatus used was kindly placed at his disposal by Professor J. Franck.

TABLE 1

The photoöxidation of iodide

DYE	INITIAL MOLARITY			$I_{abs.}$	pH	ϕ QUANTUM YIELD
	Dye	I^-	$NaAsO_2$			
	M	*M*	*M*	$\frac{ergs}{ml.\ sec.} \times 10^{-3}$		
Fluorescein	5×10^{-5}	0.4	4×10^{-4}	0.65	7	0.055
Eosin	5×10^{-5}	0.05	5×10^{-3}	3.7	7	0.011
	2×10^{-5}	1.00	5×10^{-4}	1.4	6.7	0.29
	2×10^{-5}	3.00	1×10^{-3}	1.9	6.8	1.05
Rose bengal	1×10^{-6}	0.05	5×10^{-3}	2.9	7	0.021
Neutral red	5×10^{-6}	1.00	5×10^{-4}	10.0	6.7	0.11
	5×10^{-6}	1.00	5×10^{-4}	2.3	6.7	0.13
Phenosafranine	5×10^{-6}	0.50	3×10^{-4}	0.83	7.0	0.036
	1×10^{-5}	1.00	4×10^{-4}	2.74	6.6	0.10
	5×10^{-6}	1.00	4×10^{-4}	1.82	6.3	0.18
Safranine T	5×10^{-6}	1.00	3×10^{-4}	1.6	6.9	0.15
Indigodisulfonate	8×10^{-6}	0.05	4×10^{-4}	0.8	6.1	0.0014
	8×10^{-6}	1.00	4×10^{-4}	0.96	6.8	0.0035
Indigotetrasulfonate	7×10^{-6}	0.50	3×10^{-4}	1.01	7.0	0.011
	7×10^{-6}	0.50	3×10^{-4}	0.88	7.2	0.011
	7×10^{-6}	1.00	4×10^{-4}	1.00	6.7	0.068

The results of a few experiments on the photoöxidation of $S_2O_3^{--}$ and of $C_2O_4^{--}$ are listed in table 2. All of these experiments were performed at a pH of approximately 7. Oxygen was bubbled slowly through the solutions during their irradiation. The light filter used transmitted both λ 5460 and λ 5780 Å. Since the spherical cell and strongly convergent beam of light were used in these experiments, the tabulated intensities

---

[2] I_3^- could act either as an internal filter (18) or as a photosensitizer (2).

(column 4) are spatial average values. The quantum yields are expressed as moles of reducing agents oxidized per Einstein absorbed. The upper limits of the quantum yields in the oxalate experiments were determined by the error of the potassium permanganate titration; there is no evidence that these reactions proceed with detectable speeds.

The value for the upper limit of the quantum yield of the photoöxidation of oxalate sensitized by methylene blue is 0.0005. This value is an estimate based upon a comparison with the ferric-sensitized oxidation of oxalate, making a semi-quantitative allowance for the difference in absorption of the incident light. The dye concentration in these experiments was $10^{-5}M$. Two different samples of methylene blue were used in preparing the solutions. Experiments were performed with 0.2 M oxalic acid, with 0.8 M oxalic acid, and with a solution which contained both sodium oxalate and oxalic acid at concentrations of 0.10 M and 0.01 M, respectively. The yield in all of these measurements was less than the error of measurement. However, in one experiment in which a solution (0.8 M oxalic acid) was irradiated with light in the near ultraviolet (radiation from a 500-watt carbon arc filtered by Pyrex and a Corning # 597 filter), a slow reaction was observed. By comparison with the ferric–oxalate reaction, under the same conditions of illumination, the quantum yield of this reaction was estimated to be 0.005. However, even this result should be considered as an upper limit, since no special precautions were taken to obtain reagents and water free from heavy-metal ions. The observed reaction may have been due entirely to a trace of iron. It must be mentioned that these results on methylene blue are in direct contradiction to those reported by Levaillant (13). We were also unable to confirm his claim that an air-free solution containing oxalic acid and methylene blue is rapidly bleached by exposure to visible light. Indeed, a

TABLE 2

The photoöxidation of thiosulfate and of oxalate

DYE	INITIAL MOLARITY		$I_{\text{abs.}}$ (AVERAGE)	ϕ QUANTUM YIELD
	Dye	Acceptor		
	M		$\frac{ergs}{ml.\ sec.} \times 10^{-3}$	
Eosin. . . .	5×10^{-5}	0.05 M $Na_2S_2O_3$	2.7	0.11
Rose bengal.	1×10^{-6}	0.003 N $Na_2C_2O_4$ + 0.097 N $H_2C_2O_4$	14	<0.003
Neutral red .	5×10^{-6}	0.05 M $Na_2S_2O_3$	2.1	0.03
	5×10^{-6}	0.003 N $Na_2C_2O_4$ + 0.097 N $H_2C_2O_4$	14	<0.003
Phenosafranine.	5×10^{-6}	0.003 N $Na_2C_2O_4$ + 0.097 N $H_2C_2O_4$	14	0.003

sealed tube containing this solution was not appreciably faded by being exposed to direct daylight for several months. These contradictions are difficult to explain unless we assume that the solutions used by Levaillant (13) contained some iron salt as an impurity.

The photoöxidation of allylthiourea, in acetone or methyl alcohol, is sensitized by eosin and by methylene blue. Using the Warburg apparatus and an intense source of white light, these reactions were compared to the corresponding reaction with chlorophyll (6) as a sensitizer. The comparison indicated that the quantum yields of both of these reactions are of the order of magnitude of unity. Under the conditions of the experiment, the oxidation sensitized by methylene blue was accompanied by an irreversible bleaching of the dye.

Table 3 summarizes the quantum yields of dye-sensitized photoöxidations in which oxygen is the oxidizing agent. In addition to the measurements reported here, it includes the results of several earlier experiments, in some of which the sensitizers were naturally occurring pigments. The numbers following the trade names of the dyes (column 1) are the serial numbers of the *Colour Index*. In all cases, the quantum yield listed is the largest reported for the particular system. Values followed by the symbol *m* are the maximum yields which are attained at high concentrations of the acceptor. Where the measurements were not sufficiently extensive to permit the determination of the maximum, the tabulated value of the quantum yield is followed by the corresponding molarity of the acceptor.

Values of the fluorescence yield of the dyestuffs in dilute solutions in the pure solvents are listed in the second column. The numerical values in the column are taken from the literature. The four dyes marked "slight" show a noticeable though weak fluorescence when illuminated with an intense, sharply focussed beam of white light. The two marked "none?" do not produce any visible fluorescence under these conditions.

It is noteworthy that, in all cases which have been studied over a sufficiently wide range, the quantum yields approach unity at high concentrations of the substrate. However, it would be misleading to generalize upon these results without considering certain characteristics of the data upon which they are based. The quantum yields for the photoöxidation of allylthiourea (6, 7) are not computed upon the same basis as those for the photoöxidation of iodide (17, 18). The yields in the first case are equal to the number of moles of oxygen consumed per Einstein absorbed; but in the second case, to the number of moles of iodide ion oxidized per Einstein absorbed. To express the quantum yields of the iodide-ion reaction in terms of the moles of oxygen, it would be necessary to decrease the present values by a factor of 4. Except for Gaffron's (6) finding, that 1.5 moles of oxygen are used for each mole of allylthiourea present when the reaction is allowed to go practically to completion, nothing is known

TABLE 3

Summary of the quantum yields of dye-sensitized photoöxidations

DYE	FLUORESCENCE YIELD (a)	ACCEPTOR			
		Allylthiourea (b)	Oxalic acid (c)	$S_2O_3^{--}$ (c)	I^- (c)
Ethyl chlorophyllide	0.08	1.0 *m* (6)			
Porphyrin	∽0.1 (9)	1.0 *m* (6, 7)			
Acid rhodamine(d)	<0.8 (17)				1.0 *m* (17)
Fluorescein (766)	0.8 (3)		− (1)		1.0 *m* (17)
Eosin (768)	0.2 (3)	+		0.11 (0.05 *M*)†	1.0 *m**
Rose bengal (777)	0.02 (16)		<0.003 (0.05 *M*)†		0.14 (0.1 *M*)(18)
Neutral red (825)	Slight		<0.003 (0.05 *M*)†	0.03 (0.05 *M*)†	0.13 (1.0 *M*)*
Phenosafranine (840)	Slight		<0.003 (0 05 *M*)†		0 18 (1.0 *M*)*
Safranine T (841)	Slight				0.15 (1.0 *M*)*
Methylene blue (922)	Slight	+	<0 0005 (0.8 *M*)		
Indigodisulfonate (1180)	None ?				0.004 (1.0 *M*)*
Indigotetrasulfonate (1181)	None ?				0.007 (1.0 *M*)*

(a) These are maximum fluorescence yields observed in dilute solution.

(b) Solvent: acetone or methanol. Yield based upon moles of oxygen absorbed.

(c) Solvent: water. Yield based upon moles of acceptor oxidized.

(d) This is a sulfonation product of rhodamine G.

* Table 1.

† Table 2.

(−) Little or no reaction.

(+) Rapid reaction.

of the stoichiometry of the oxidation of this substance. The reported (7) maximum yield for the photoöxidation of allylthiourea sensitized by mesoporphyrin is 1.10. While the stoichiometry of the iodide oxidation is definite and simple, there is some uncertainty about the maximum value of the quantum yield. In a series of careful measurements with solutions of $2 \times 10^{-5}M$ eosin and varying concentrations of potassium iodide, Hurd and Livingston[3] found that the quantum yield reached a value of 1.18 in 4.0 M potassium iodide and was apparently still increasing with the iodide concentration. Using fluorescein solutions and white light, Schneider (17) found that the quantum yield increased to value of unity at 0.3 M potassium iodide, remained constant to 0.5 M potassium iodide, and then increased rapidly as the potassium iodide concentration was further increased. Working with rhodamine, he found that the behavior depended upon the type of illumination. With red light, the quantum yield reached a flat maximum of unity at 1.5 M potassium iodide and remained constant to 3.0 M (the highest concentration used). In white light the yield increased steadily in this range, (apparently) reaching a value greater than 2 in 2.5 M potassium iodide. He suggested that all of the observed values greater than unity are due to the autocatalytic (i.e., sensitizing) effect of I_3^-. While this explanation of his results seems quite probable, it has not been tested quantitatively, and should not be regarded as proven. It is very unlikely that this explanation can be applied to the results of Hurd and Livingston.

While "non-fluorescent" dyes are poor sensitizers, there appears to be no relation between sensitizing action and fluorescent efficiency of dyes, once the latter has attained a value of 1 per cent or more. Although this lack of parallelism is contradictory to a view once held tenaciously by several investigators, it is consistent with modern theories of the fluorescence phenomena of complex molecules.

SUMMARY

Quantum yields have been determined of the photoöxidation of iodide ion by fluorescein, eosin, rose bengal, neutral red, phenosafranine, safranine T, indigodisulfonate, and indigotetrasulfonate, and of the photoöxidation of thiosulfate ion by eosin and neutral red. It has been shown that, within the limits of experimental error, there is no photosensitized oxidation of oxalic acid in the presence of rose bengal, neutral red, phenosafranine, or methylene blue. A few observations on the sensitizing action of eosin and of methylene blue on the photoöxidation of allylthiourea, in acetone and methanol solutions, are described.

A table is presented summarizing the results of these measurements and

---

[3] Details of this study will be published later.

of the other quantum yield determinations of dye-sensitized oxidations which are available in the literature. A brief discussion of these results and of the data upon which they are based is included.

REFERENCES

(1) BACON: Phillipine J. Sci. **5**, 281 (1910).
(2) BERTHOUD: Trans. Faraday Soc. **21**, 554 (1925).
(3) BOWEN: Trans. Faraday Soc. **35**, 15 (1939).
(4) FORBES AND HARRISON: J. Am. Chem. Soc. **47**, 2449 (1925).
(5) FOULK AND BOWDEN: J. Am. Chem. Soc. **48**, 2045 (1926).
(6) GAFFRON: Ber. **60**, 755 (1927).
(7) GAFFRON: Biochem. Z. **264**, 251 (1933).
(8) HURD: Ph. D. Thesis, University of Minnesota, 1939.
(9) KAUTSKY: Ber. **68**, 152 (1935).
(10) KOLTHOFF AND SANDELL: *A Textbook of Quantitative Inorganic Analysis*. The Macmillan Company, New York (1936).
(11) LANGER AND MEGGERS: Bur. Standards J. Research **4**, 711 (1930).
(12) LEIGHTON AND FORBES: J. Am. Chem. Soc. **52**, 3139 (1930).
(13) LEVAILLANT: Compt. rend. **177**, 398 (1923).
(14) LIND AND LIVINGSTON: J. Am. Chem. Soc. **54**, 94 (1932).
(15) LIVINGSTON: J. Phys. Chem. **44**, 601 (1940).
(16) PRINGSHEIM: Trans. Faraday Soc. **35**, 29 (1939).
(17) SCHNEIDER: Z. physik. Chem. **B28**, 311 (1935).
(18) SPEALMAN AND BLUM: University of California Publications in Physiology **8**, 147 (1937).

THE REACTION OF FORMALDEHYDE WITH AMINO ACIDS: X-RAY DIFFRACTION PATTERNS[1]

ALLAN K. SMITH AND PHILIP HANDLER

U. S. Regional Soybean Industrial Products Laboratory,[2] Urbana, Illinois

AND

J. N. MRGUDICH

William A. Noyes Chemical Laboratory, University of Illinois, Urbana, Illinois

Received November 29, 1939

In a previous publication (12) data were presented which showed the amount of formaldehyde which combines with soybean protein, casein, and zein under various experimental conditions. A procedure for preparing dispersions of these proteins in the presence of formaldehyde was outlined, and data relative to the influence of hydrogen-ion concentration on such dispersions were also presented.

The type of linkage involved in the reaction between amino acids or proteins and formaldehyde is problematical. It is known that aldehydes react in a neutral or alkaline solution with amines to form Schiff's bases of the general structure, RCH═NR′. Consequently, when Sørensen found that certain amino acids could be titrated in the presence of formaldehyde to a fairly sharp end point, he assigned to the reaction product the general structure,

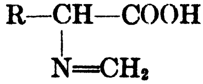

$$\begin{array}{l}\mathrm{R{-}CH{-}COOH} \\ \quad\ \ |\\ \quad\ \mathrm{N{=}CH_2}\end{array}$$

which concept was supported by the supposed structure of the products prepared from asparagine and formaldehyde. Since most proteins contain free amino groups, as determined by the Van Slyke procedure, the methylene-imino linkage has been suggested to describe analogously the protein–formaldehyde combination.

Actually, little or no evidence exists for assigning such a structure to the reaction products formed between formaldehyde and amino acids or proteins. A review of the literature shows that the reaction of monoamino acids with formaldehyde gives products too unstable to be readily separated from solution. Most investigators (1, 5, 9, 10) of this subject have used salts, primarily alkaline-earth salts, or esters of the amino acids in order to obtain stable reaction products. However, with these more stable compounds there has been no agreement as to the nature of the linkage involved in the reaction.

---

[1] Presented before the Division of Physical and Inorganic Chemistry at the Ninety-eighth Meeting of the American Chemical Society, held in Boston, Massachusetts, September 11-15, 1939.

[2] A coöperative organization participated in by the Bureau of Agricultural Chemistry and Engineering and the Bureau of Plant Industry of the United States Department of Agriculture, and the Agricultural Experiment Stations of the North Centra-States of Illinois, Indiana, Iowa, Kansas, Michigan, Minnesota, Missouri, Nebraska, North Dakota, Ohio, South Dakota, and Wisconsin.

Several investigators who directed their efforts toward explaining the nature of the reaction between proteins and formaldehyde, made use of x-ray diffraction methods. Clark and Shenk (3, 4) examined egg albumin, gelatin, zein, and several of the fibrous proteins; Brother and McKinney (2) investigated commercial casein and soybean protein plastic materials; and Highberger and Kersten (6, 7) reported studies on collagen. For the non-fibrous proteins the x-ray diffraction pattern usually consists of two halos, one at approximately 4.9 Å., which is said to represent the backbone structure of the protein, and the other at approximately 10 Å., which represents the side chains. The x-ray diffraction patterns of formaldehyde-treated proteins show the same two halos as are observed with the untreated proteins; and, in addition, if the reaction is carried out in an alkaline medium, several new interference patterns are sometimes observed, chief among which are two strong rings representing spacings at approximately 3.9 and 2.6 Å. It has been shown that the latter spacings are also characteristic of paraformaldehyde. Therefore, if any new diffraction lines result from the formaldehyde treatment of the proteins, they might be obscured by diffraction lines resulting from the presence of paraformaldehyde.

The present research is a continuation of the work presented in a previous publication, but is concerned primarily with the nature of the reaction between formaldehyde and amino acids. Arginine, lysine, and histidine were chosen as the amino acids for this investigation, since they contribute the basic groups of the intact protein molecule.

HEXONE BASES AND FORMALDEHYDE

The free bases arginine and lysine were prepared according to the procedure of Vickery and Leavenworth (14, 15), and the free base histidine by the method of Pyman (11). The formaldehyde derivatives of the amino acids were prepared by dissolving the free bases in a small amount of water, adding an excess of 37 per cent formaldehyde (C.P. grade), and precipitating the reaction product with alcohol. The precipitation was assisted by cooling in a refrigerator for several hours.

The amino acid-formaldehyde products were analyzed for carbon, hydrogen, and nitrogen (Kjeldahl), and the results compared with the formulas heretofore assigned to this reaction. The analytical results, the specific rotations in water, and the decomposition temperatures of the products are recorded in table 1. Inspection of these data would seem to indicate that the formaldehyde reacted with the hexone bases, although the analyses do not coincide with any of the structures,—namely, the methyleneimino, methylol, or heterocyclic,—which have been described in the

TABLE 1

Data on formaldehyde derivatives of the hexone bases

AMINO ACID	$[\alpha]_D^{23°}$ IN WATER		MELTING POINT		ANALYSIS OF FORMALDEHYDE DERIVATIVE			MOLECULAR WEIGHT OF AMINO ACID	EMPIRICAL FORMULA WEIGHT OF FORMALDEHYDE DERIVATIVE†	FORMULA WEIGHT ASSUMING FOLLOWING STRUCTURES		
	Amino acid*	Formaldehyde derivative	Amino acid	Formaldehyde derivative	N	C	H			Methylol	Heterocyclic ring	Methylene-imino linkage
			°C.	°C.	per cent	per cent	per cent					
l-(+)-Lysine	+13.7	+1.6 (pH = 8.0)	224 (dec.)	113 (dec.)	13.09	53.53	9.0	146.1	214	206.1	218.1 290.2	170.1
l-(−)-Histidine	−39.1	−138 (pH = 7.3)	265 (dec.)	187 (dec.)	20.68	48.04	5.72	155.1	203	184.0	227	167.0
l-(+)-Arginine	+12.0	+57.4 (pH = 7.5)	238 (dec.)	123 (dec.)	23.20	40.62	7.55	174.1	241	234.3	246	198.2

* Data for the amino acids at the same pH values as the formaldehyde derivatives.

† Calculated from their nitrogen content.

literature for this reaction. The calculations showed that the methylene-imino linkage, which has been most generally accepted for this reaction, was further from agreement with the analytical results than the other postulated structures.

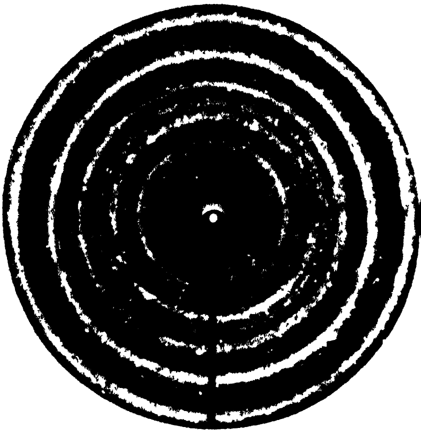

1

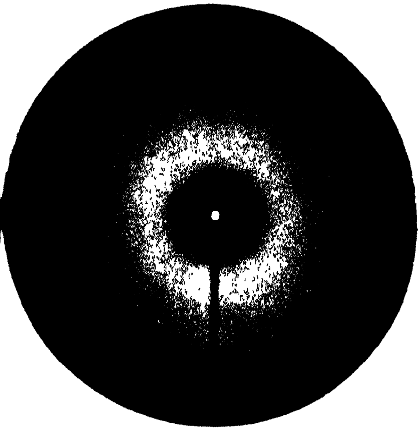

2

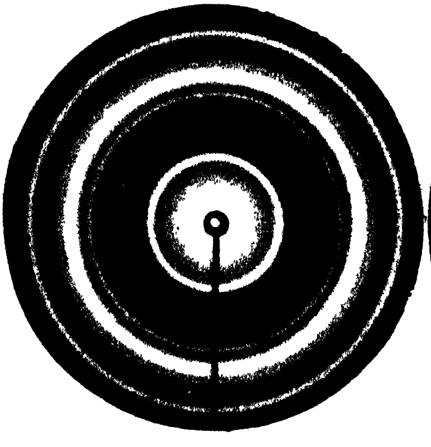

3

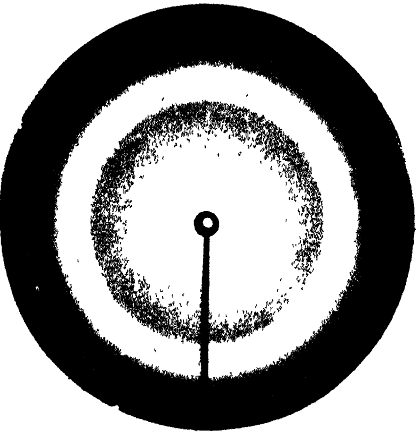

4

Fig. 1. Arginine (free)
Fig. 2. Arginine formaldehyde
Fig. 3. Lysine (free)
Fig. 4. Lysine-formaldehyde (partial reaction)

The reaction of formaldehyde with the diamino acids was investigated further by means of x-ray diffraction patterns of the free bases and of their formaldehyde derivatives. The Hull, Debye, and Scherrer powder technique, employing filtered Cu K_α radiation was followed, using a 5-cm. sample-to-film distance in photographing the diffraction patterns. A more detailed description of the equipment and method employed has been published recently by Tuckey, Ruehe, and Clark (13). The diffraction patterns are reproduced in figures 1 to 8.

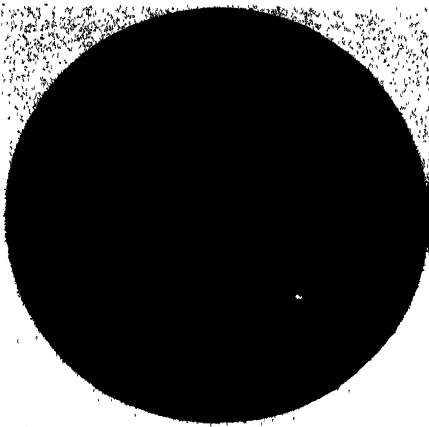

5

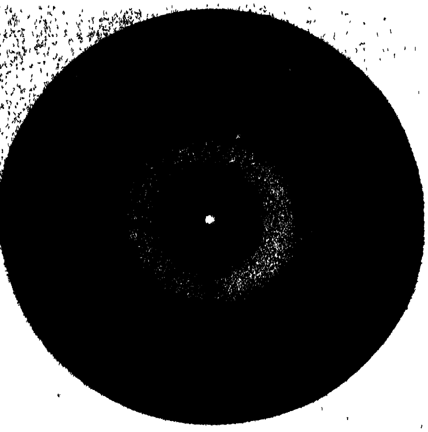

6

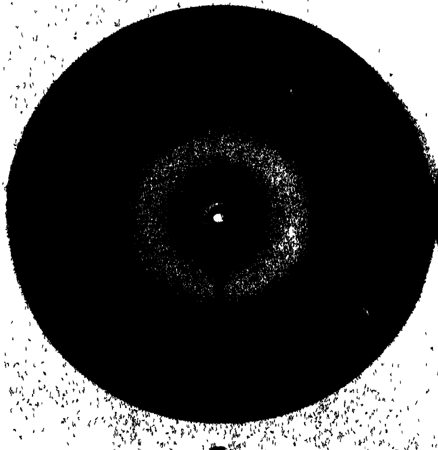

7

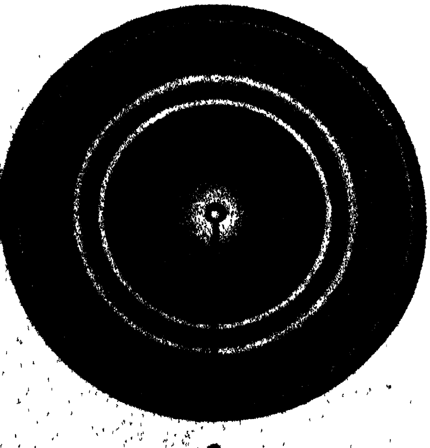

8

Fig. 5. Lysine–formaldehyde (complete reaction)
Fig. 6. Histidine (free)
Fig. 7. Histidine–formaldehyde (freshly precipitated)
Fig. 8. Histidine–formaldehyde (aged)

It may be seen from these diffraction patterns that the free bases lysine, arginine, and histidine (figures 1, 3, and 6) are highly crystalline materials, as is also the histidine–formaldehyde product (figure 8), but the formaldehyde derivatives of lysine and arginine (figures 2 and 5) give patterns of the type normally exhibited by amorphous materials. Photographs of the latter type, diffuse rings, are usually assumed to result from crystals too small to serve as efficient diffraction units or from distortion of the crystal lattice. For the lysine–formaldehyde and arginine–formaldehyde products the distorted lattice is the more acceptable explanation.

Figure 4 is a diffraction pattern of a lysine–formaldehyde product in which the reaction between the lysine and formaldehyde appears to be incomplete. In comparing this pattern with that of lysine (figure 3), it is observed that the shorter spacings in both diffraction patterns are the same, but that the three inner rings, long spacings, of the lysine are absent in the partially reacted product. It is expected that this diffraction pattern will be useful in studying the mechanism of the lysine–formaldehyde reaction; this phase of the problem will be continued in a subsequent paper.

It was found, in following the method described in this paper for the preparation of histidine–formaldehyde, that aging of this material is a factor in its crystallinity. A diffraction pattern of histidine–formaldehyde taken soon after its preparation contained only two rings, one of which is too weak to reproduce well. This pattern is reproduced in figure 7, but the same histidine–formaldehyde photographed after three months' time gave the pattern shown in figure 8. On the other hand, reëxamination of the lysine formaldehyde and arginine–formaldehyde products after several months' aging gave the same results as for the freshly prepared material.

A comparison of the diffraction pattern of the histidine–formaldehyde with the diffraction pattern of paraformaldehyde showed the absence of paraformaldehyde in this photograph.

Highberger and Kersten (6, 7) and Jordan-Lloyd (8) in their investigations of the tanning of leather made x-ray diffraction patterns of collagen before and after treatment with tanning agents and obtained results which are somewhat analogous to those observed for the formaldehyde treatment of lysine and arginine. Collagen does not give sharp diffraction lines; nevertheless, Highberger and Kersten (6) observed a pronounced blurring of both its diffraction bands when tanned with chrome and vegetable tans. Later they observed (7) a blurring or disappearance of the 10-Å. spacing, owing to quinone tanning, but no change was observed in either spacing when tanned with formaldehyde or with 4, 4′-dihydroxydiphenyldimethylmethanemonosulfonic acid (Syntan).

CONCLUSIONS AND SUMMARY

It is thus observed from the preceding data that the histidine–formaldehyde product is highly crystalline, while the formaldehyde derivatives of lysine and arginine are amorphous products. Although it is impossible at the present time to define the nature of the linkages involved on any of the amino acids when reacting with formaldehyde, it seems possible that, in the instance of the lysine and arginine derivatives, a condensation or polymerization has taken place with the formaldehyde serving as a cross linkage between the amino groups of the diamino acids.

REFERENCES

(1) Bergman, M.: Z. physik. Chem. **145**, 194 (1925).
(2) Brother, G. H., and McKinney, L. L.: Ind. Eng. Chem. **30**, 1236 (1938).
(3) Clark, G. L., and Shenk, J. H.: Radiology **28**, 58 (1937).
(4) Clark, G. L., and Shenk, J. H.: Radiology **28**, 357 (1937).
(5) Franzen, H., and Tellmer, E.: J. prakt. Chem. **95**, 299 (1917).
(6) Highberger, J. H., and Kersten, H. J.: J. Am. Leather Chem. Assoc. **33**, 16 (1938).
(7) Highberger, J. H., and Kersten, H. J.: J. Am. Leather Chem. Assoc. **33**, 289 (1938).
(8) Jordan-Lloyd, D.: J. Intern. Soc. Leather Trades' Chem. **19**, 336 (1935).
(9) Krause, H.: J. Chem. Soc., Abstracts **114**, 1156 (1918).
(10) Levene, P. A., and Schormüller, A.: J. Biol. Chem. **105**, 547 (1934).
(11) Pyman, F. L.: J. Chem. Soc. **109**, 186 (1916).
(12) Smith, A. K., Max, H., and Handler, P.: J. Phys. Chem. **43**, 347 (1939).
(13) Tuckey, S. L., Ruehe, H. A., and Clark, G. L.: J. Dairy Sci. **21**, 767 (1938).
(14) Vickery, H. B., and Leavenworth, C. S.: J. Biol. Chem. **76**, 437 (1928).
(15) Vickery, H. B., and Leavenworth, C. S.: J. Biol. Chem. **76**, 701 (1928).

THE EFFECTS OF CERTAIN SALTS ON THE DISSOCIATION OF ALANINE. II

Experiments on Cells without Liquid-junction Potentials[1]

A. C. BATCHELDER and CARL L. A. SCHMIDT

The Division of Biochemistry, University of California Medical School, Berkeley, California

Received November 16, 1939

In a previous communication (1) the effects of certain salt mixtures on the dissociation of glycine and alanine were described. The experiments served to answer the question as to whether or not the effect of a salt mixture is equal to the sum of the effects of the individual salts. Since the measurements of the electromotive forces of the cells used involved liquid junctions, the experiments are of questionable value with regard

---

[1] The authors were aided by grants from the Research Board of the University of California and from Eli Lilly and Company. They are also indebted to the Cyrus M. Warren Fund of the American Academy of Arts and Sciences for the loan of the Type K potentiometer.

to the quantitative determination of the effects of single salts on the ionization of amino acids. Formulas for the calculation of liquid-junction potentials are accurate only for solutions at high dilutions or under certain specialized conditions. At higher salt concentrations, the liquid-junction potential cannot be calculated without extrathermodynamic assumptions. Measurements of the electromotive forces of any cells that involve salt bridges must be regarded as of limited quantitative value. This is especially true when the salt concentration on one side of the salt bridge is varied between wide limits. Only in very special cases where it is likely that the sum of the two liquid-junction potentials approaches a zero value may such cells yield quantitative results. These conditions were not fulfilled in our previous experiments.

In the present work a method for the determination of electromotive forces that is free from these objections has been employed. The calculations have, therefore, involved no consequential extrathermodynamic assumptions.

The electromotive forces of cells of the following types were measured:

$$H_2(Pt) \mid \text{amino acid } (m_T), \text{NaOH or HCl } (m_B \text{ or } m_A), \text{MCl } (m_s) \mid AgCl \mid Ag \quad (1)$$

where the concentrations m_B, m_A, and m_T of the sodium hydroxide' hydrochloric acid, and the amino acid, respectively, were maintained constant, while the concentration m_s of the salt, MCl, was varied from an ionic strength of 0.0 to 2.3. Potassium chloride, sodium chloride, lithium chloride, and barium chloride were employed for the salt.

The cells in which the solutions were placed for the electromotive force measurements were of the usual H-shaped type. The silver-silver chloride electrode was placed in one arm of the cell and the hydrogen electrode in the other. The hydrogen entered the cell at the bottom of the arm which contained the hydrogen electrode. The two arms of the cell were connected by a glass stopcock. When partially closed, it reduced the diffusion of any silver into the arm of the cell that contained the hydrogen electrode.

The silver and silver chloride were deposited, according to Harned's (6) second method, on a 1.5-in. spiral of 26-gauge platinum wire, which was sealed into the end of a piece of glass tubing. After electrolysis, the electrodes were soaked overnight in distilled water and, before use, were well soaked in a sample of the solution in which they were to be used. Electrical contact with the potentiometer was made by means of a mercury cup. For testing the preparation of these electrodes and the general technique used, the electromotive forces of cells of the following types were measured:

$$H_2(Pt) \mid HCl\ (m) \mid AgCl \mid Ag$$

The results of Harned's (7) very accurate measurements of the electromotive forces of similar cells were plotted on a large-scale graph that could be read to the nearest 0.1 millivolt and to ±0.00005 unit of concentration. Illustrative values for the voltages observed with the present electrodes and those obtained from the graph for the same acid concentration are given in table 1.

The preparation of the hydrogen electrodes and the measurement of the potentials were essentially the same as described in the previous paper. The preparation of the amino acid solutions was likewise essentially the same. Vacuum technique was not used in the preparation of the solutions. Contact with air was minimized. The solutions were prepared with hot, freshly distilled water and, after cooling, the volumes were adjusted. All weighings were corrected to *in vacuo* and all pipets and flasks were calibrated by weight. All reagents used were purified within the limits of analytical accuracy.

TABLE 1

Comparison between the present values and the values obtained by Harned in solutions of hydrochloric acid

m_{HCl}	PRESENT VALUE	HARNED'S VALUE
	volts	*volts*
0.003578	0.51479	0.5147
0.01123	0.45887	0.4587
0.06289	0.37489	0.3748

CALCULATION OF RESULTS

The electromotive force, E, of cell 1 is related to the hydrogen-ion and chloride-ion concentrations by the thermodynamic equation:

$$E = E^0 - y \log m_{H^+} m_{Cl^-} \gamma_{H^+} \gamma_{Cl^-} \qquad (2)$$

where the γ's refer to the activity coefficients denoted by the subscripts, E^0 is the electromotive force of the cell at unit activities of hydrogen and chloride ion, and $y = 2.3026\, RT/F$. Solution of equation 2 for $-\log m_{H^+}$, and letting

$$(\gamma_{H^+} \gamma_{Cl^-})^{1/2} = \gamma_{HCl}$$

gives

$$-\log m_{H^+} = \frac{E - E^0}{y} + \log m_{Cl^-} + 2 \log \gamma_{HCl} \qquad (3)$$

Equation 3 was used for all calculations of the hydrogen-ion concentration in the following experimental work.

The value of 0.22239 volt (10) was used for E^0 at 25.0°C. The values of the other constants have been taken from Birge's compilation (2).

The values of γ_{HCl} in the solutions that were used in cell 1 are not available. Therefore the assumption that the values are the same in these solutions and in solutions of the inorganic salt only, at the same total ionic strength, has been made. This assumption is obviously not valid throughout the whole possible range of concentrations of the amino acid and the salt, but the concentration of the amino acid is sufficiently low to make any error from this assumption negligible.

That portion of the amino acid that was present in the isoelectric condition has not been included in the calculations of the ionic strength. All other ionic species in the solutions have been included in the summation.

The values of γ_{HCl} that were obtained from the literature were plotted against the square root of the ionic strength on a large-scale graph. The values that were necessary for the calculations were then read from a smooth curve that was drawn through these points. The values of γ_{HCl} in barium chloride solutions were taken from Harned and Mason (14), Harned and Robinson (16), and four values from Randall and Breckenridge (25). The values of γ_{HCl} in lithium chloride solutions were obtained from Harned and Copson (9). The values of γ_{HCl} in sodium chloride and potassium chloride solutions were taken from Harned and Murphy (15) and Harned (8). The data of Harned and coworkers were obtained with cells containing 0.01 *M* hydrochloric acid and the particular salt. However, it has been shown by Harned (8; 26, page 804) that the activity coefficient of hydrochloric acid in salt solutions is independent of the acid concentration below about 0.1 *M* and dependent only on the ionic strength of the solution.

In the present work the solutions were prepared on a molarity basis, while the data of Harned and coworkers are given on a molality basis. Equations relating the molarity and molality of the salt solutions were calculated by the method of least squares from the density data given in *International Critical Tables* (17). The density data of Dalton and Schmidt (5) indicate that the densities of the pure salt solutions may be used with sufficient accuracy for the present purpose. The equations that were used for the conversion, m_s being the molality and c_s the molarity of the salt, are:

For barium chloride, $m_s = 1.0031c_s + 0.0278c_s^2 + 0.00427c_s^3$

For lithium chloride, $m_s = 1.0023c_s + 0.0187c_s^2 + 0.00080c_s^3$

For sodium chloride, $m_s = 1.0026c_s + 0.0182c_s^2 + 0.00115c_s^3$

For potassium chloride, $m_s = 1.0029c_s + 0.0279c_s^2 + 0.00196c_s^3$

The ionic strength, as defined by Lewis and Randall (20), was calculated next. The value of γ_{HCl} in each of the experimental solutions was then read from the graphs described previously. These and other necessary values were substituted in equation 3, solution of which enables m_{H^+}

to be evaluated. The hydrogen-ion molarity was calculated from the molality by application of the ratio c_s/m_s. The various constants were calculated from the hydrogen-ion molarity as described below.

A. Alanine: acidic solutions

The effects of neutral salts on the ("classical") constant, that is, formulated on the basis of the ionization of the amino acid involving the hydroxyl ion, were determined. The equilibrium involving the hydroxyl ion is

$$H_2O + NH_3^+CH(CH_3)COO^- \rightleftarrows OH^- + NH_3^+CH(CH_3)COOH \qquad (4)$$

and the apparent constant is defined by

$$-\log k_b' = -\log c_{OH^-} + \log N_{H_2O} - \log \frac{c_{R^+}}{c_{R^{+-}}} \qquad (5)$$

where N_{H_2O} is the mole fraction of water. In all but the more concentrated solutions, N_{H_2O} may be taken as unity.

It was more convenient, in practice, to calculate $-\log (k_b' N_{H_2O})$, for reasons that will be given later. This term is related to the experimental data by

$$-\log (k_b' N_{H_2O}) = -\log c_{OH^-} - \log \frac{c_{R^+}}{c_{R^{+-}}} \qquad (6)$$

The hydrogen-ion concentration in each of the solutions was calculated from the observed electromotive force by means of equation 3. The hydroxyl-ion concentration was calculated by use of the relation

$$m_{OH^-} m_{H^+} K_{\gamma(s)} = K_w \qquad (7)$$

in which K_w is the ionization constant of water and $K_{\gamma(s)}$ is equal to $\frac{\gamma_{H^+}\gamma_{OH^-}}{a_{H_2O}}$, where a_{H_2O} is the activity of water in the particular salt solution. Values for the term $K_{\gamma(s)}$ were taken from the data of Harned and coworkers and plotted against the square root of the ionic strength on a large-scale graph. Values necessary for the present calculations were taken from a smooth curve drawn through these points. For the values of $K_{\gamma(s)}$ in solutions of sodium chloride the data of Harned and Mannweiler (13) were employed. Similar values in potassium chloride solutions were taken from Harned and Hamer (12), values in lithium chloride solutions from Harned and Copson (9), and values in barium chloride solutions from Harned and Mason (14). The value of 1.008×10^{-14} (11) was used for K_w.

The hydroxyl-ion molality that was obtained from equation 7 was converted to molarity in the manner that was described for the hydrogen-ion concentration.

The ratio in equation 6 was evaluated by the following relations, which were obtained upon consideration of the electrical neutrality of the solutions:

$$c_{R^+} = c_A - c_{H^+}$$

$$c_{R^{+-}} = c_T - c_{R^+} \qquad (8)$$

where c_A is the added concentration of hydrochloric acid and c_T is the total amino acid concentration. Equations 7 and 8 give all of the values that are necessary for the evaluation of equation 6. The experimental data are represented graphically in figures 1 and 2. The points are experimental. The curves are theoretical.

The thermodynamic equilibrium constant for equation 4 is given by

$$k_b = \frac{\alpha_{R^+}\alpha_{OH^-}}{\alpha_{H_2O}\alpha_{R^{+-}}} \qquad (9)$$

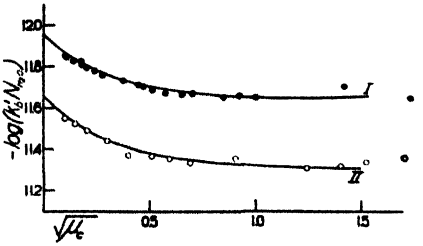

FIG. 1

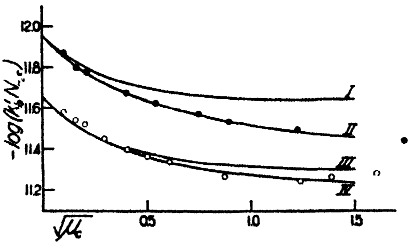

FIG. 2

FIG. 1. The effects of sodium chloride and potassium chloride on $-\log k'_b$ of alanine. ● = potassium chloride; ○ = sodium chloride. Note: 0.3 unit has been added to each value for potassium chloride for the purpose of separating the curves.

FIG. 2. The effects of lithium chloride and barium chloride on $-\log k'_b$ of alanine. ● = lithium chloride; ○ = barium chloride. Note: 0.3 unit has been added to each value for lithium chloride for the purpose of separating the curves.

where the α's refer to the activity denoted by the subscript. By introducing the term $\alpha = \gamma c$ into equation 9, the following relation between $k'_bN_{H_2O}$ and k_b is obtained:

$$k'_bN_{H_2O} = k_b\,\frac{\gamma_{R^{+-}}}{\gamma_{OH^-}\gamma_{R^+}}\,\alpha_{H_2O} \qquad (10)$$

or, in logarithmic form,

$$-\log(k'_bN_{H_2O}) = -\log k_b - \log\gamma_{R^{+-}} + \log\gamma_{OH^-} + \log\gamma_{R^+} - \log\alpha_{H_2O} \qquad (11)$$

By keeping the term N_{H_2O} on the left-hand side of the equation, the necessity for the theoretical calculation of the activity coefficient of water has been avoided. This equation, after combination with the Debye-Hückel equation

$$-\log \gamma_i = \frac{0.504 z^2 \sqrt{\mu_c}}{1 + 0.328 a' \sqrt{\mu_c}} \tag{12}$$

(where γ_i is the activity coefficient of the i^{th} ion, z is the valence of the ion, a' is the "collision diameter," expressed in Angström units, and μ_c is the ionic strength) and Kirkwood's (19) equation[2]

$$-\log \gamma_{\mathrm{R}^{+-}} = 0.125 \frac{R^2 \mu_c}{a} \cdot \frac{1}{1 + 0.328 a \sqrt{\mu_c} + 0.036 a^2 \mu_c + 0.018 \frac{b^3 \mu_c}{a}} \tag{13}$$

(where a represents the closest distance of approach of the salt ions to the zwitter ion, a value comparable to a' in equation 12, b is the radius of the zwitter ion, and R is the dipole distance) was used for the calculation of curves I and II in figure 1 and curves I and III in figure 2.

TABLE 2

Values for a and a′ used in figures 1 and 2

SALTS	a	a'
Sodium chloride (curve II, figure 1) in Å.	4.2	3.4
Potassium chloride (curve I, figure 1) in Å..	3.8	4.0
Lithium chloride (curve I, figure 2) in Å	4.9	4.0
Barium chloride (curve III, figure 2) in Å.....	4.2	3.6

The value of $\alpha_{\mathrm{H_2O}}$ in solutions of sodium chloride, potassium chloride, and lithium chloride was taken from the data of Pearce and Nelson (23). The values of $\alpha_{\mathrm{H_2O}}$ in barium chloride solutions were obtained from Perreu (24).

The value of 4.0 Å., corresponding to a dipole moment of 19.1×10^{-18} E.S.U., was used for R in equation 13. The value of 3.08 Å. (4) was employed for b.

The values that were used for a and a' in equations 12 and 13 are shown in table 2. The term a in the expression for γ_{OH^-} has been assumed to be equal to a' in the term for γ_{R^+}. Although this equality is open to question if a' is taken to represent an actual physical dimension of the ion, it is doubtful that the theory on which equation 12 is based is sufficiently rigorous to demand differentiation between these two values.

Curves I and III in figure 2 fall somewhat above the experimental points. The curves could be lowered by using lower values for a', smaller values for R, or higher values for a. The term a' presumably represents the sum of the radii of the alanine anion or hydroxyl ion and the salt ions, and a

---

[2] Equation 13 was obtained by the introduction of the proper constants and employing the assumption that the center of the alanine molecule coincides geometrically with the center of the dipole.

represents the sum of the radii of the zwitter ion and the salt ions. It is not probable that a and a' would differ greatly in value. Therefore, any increase in the value of a should require a proportional increase in the value of a'. The net effect of any such increase in the values of both a and a' is a shift of the theoretical curve in a direction opposite to that desired. In consideration of the ionic dimensions that have been obtained from x-ray data (22) and apparent molal volumes (18), it does not appear that a and a' should have values significantly lower than those that have been employed. The present value of R has been retained because of the agreement in figure 1 and in later figures.

The addition of a "salting-out" term, $B\mu_c$, to equation 11 will not produce the desired agreement between the theoretical and experimental values. However, if a term, $-C\sqrt{\mu_c}$, is added to the right-hand side of equation 11, where C is an arbitrary constant, the desired result is obtained. The resultant equation is

$$-\log (k_b' N_{\mathrm{H_2O}}) = -\log k_b - \log \gamma_{\mathrm{R}^{+-}} + \log \gamma_{\mathrm{OH}^-} + \log \gamma_{\mathrm{R}^+} - \log \alpha_{\mathrm{H_2O}} - C\sqrt{\mu_c} \quad (11a)$$

Curves II and IV in figure 2 have been calculated by this equation. The terms for the activity coefficients were evaluated by equations 12 and 13, using the values that are given above for the various dimensions. Curve II in figure 1 has also been calculated by this equation. The values of C obtained for the curves are: curve II and curve IV (figure 2), 0.127 and 0.042, respectively; curve II (figure 1), 0.0273.

At present, the term $C\sqrt{\mu_c}$ cannot be justifiably considered as anything more than empirical. It may represent a correction term that is necessary because of the particular values chosen in equations 12 and 13. It may be an indication that additional terms in the infinite series, of which equation 13 is the first member, should have been employed to account for lack of symmetry in the location of the dipole of the alanine molecule (see 19). Because of the introduction, at high salt concentrations, of factors that are not accounted for by equations 11 and 12, further attempts at refinement of the calculations would be of doubtful significance.

The dissociation of alanine in acidic solutions, according to Brönsted's (3) definition of acids and bases, is represented by the equation

$$\mathrm{NH_3^+CH(CH_3)COOH} \rightleftarrows \mathrm{H^+} + \mathrm{NH_3^+CH(CH_3)COO^-} \quad (14)$$

The "apparent" constant for this equilibrium is defined by

$$K_1' = \frac{c_{\mathrm{H}^+} c_{\mathrm{R}^{+-}}}{c_{\mathrm{R}^+}}$$

where the c's refer to the concentration of the ionic species denoted by the subscript. In its logarithmic form, the constant is defined by

$$-\log K_1' = -\log c_{H^+} - \log \frac{c_{R^{+-}}}{c_{R^+}} \tag{15}$$

The values for $-\log c_{H^+}$ in each of the salt solutions were obtained from equation 3. The ratio in equation 15 was evaluated with the aid of equation 8. The same experimental data were employed for the calculation of both $-\log k_b'$ and $-\log K_1'$.

The variations of $-\log K_1'$ in solutions of sodium chloride, potassium chloride, barium chloride, and lithium chloride are shown in figures 3 and 4.

The thermodynamic equilibrium constant for equation 14 is defined by

$$K_1 = \frac{\alpha_{R^{+-}} \alpha_{H^+}}{\alpha_{R^+}} \tag{16}$$

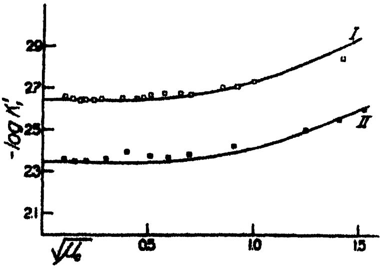

FIG. 3

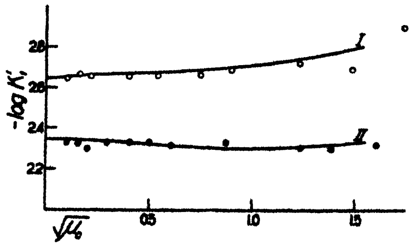

FIG. 4

FIG. 3. The effects of sodium chloride and potassium chloride on $-\log K_1'$ of alanine. Curve I, □ = potassium chloride; curve II, ■ = sodium chloride. Note: 0.3 unit has been added to each value for potassium chloride for the purpose of separating the curves.

FIG. 4. The effects of lithium chloride and barium chloride on $-\log K_1'$ of alanine. Curve I, ○ = lithium chloride; curve II, ● = barium chloride. Note: 0.3 unit has been added to each value for lithium chloride for the purpose of separating the curves.

Introduction of the expression $\alpha = \gamma c$ into equation 16 leads to the relation, expressed in its logarithmic form, between K_1' and K_1:

$$-\log K_1' = -\log K_1 - \log \gamma_{R^+} + \log \gamma_{H^+} + \log \gamma_{R^{+-}} \tag{17}$$

For the theoretical calculations, equations 12 and 13 were introduced into equation 17. A term, $B\mu_c$, was added to the right-hand side of equation 16 for the calculation of the curves in figures 3 and 4. In addition, the term $C\sqrt{\mu_c}$, that was used for the calculation of curves II and IV in figure 2, was retained. The complete equation, omitting introduction of equations 12 and 13 for brevity, that was used for the calculation of the theoretical curves in figures 3 and 4 is

$$-\log K_1' = -\log K_1 + \log \gamma_{R^{+-}} + C\sqrt{\mu_c} + B\mu_c \tag{18}$$

The terms for γ_{R^+} and γ_{H^+} have disappeared, because the assumption has been made that they are equal. The values for the constants in the calculation of $\gamma_{R^{+-}}$ were the same as those given in table 2. The values that were employed for C and B are given in table 3.

B. *Alanine: basic solutions*

On the basis of Brönsted's (3) definition of acids and bases, the ionization of alanine in alkaline solutions is represented by

$$NH_3^+CH(CH_3)COO^- \rightleftarrows H^+ + NH_2CH(CH_3)COO^- \tag{19}$$

The apparent constant for this equilibrium, in its logarithmic form, is defined by

$$-\log K_2' = -\log c_{H^+} - \log \frac{c_{R^-}}{c_{R^{+-}}} \tag{20}$$

TABLE 3

Values for C and B employed in figures 3 and 4

SALTS	*C*	*B*
Sodium chloride (curve II, figure 3)	0.0273	0.195
Potassium chloride (curve I, figure 3)	0.0	0.213
Lithium chloride (curve I, figure 4)	0.127	0.0582
Barium chloride (curve II, figure 4)	0.042	0.0662

Values for $-\log c_{H^+}$ were obtained from equation 3 when applied to cells of the type indicated in equation 1. The ratio in equation 20 was evaluated by the following:

$$c_{R^-} = c_B - c_{OH^-}$$

$$c_{R^{+-}} = c_T - c_{R^-} \tag{21}$$

where c_T is the total concentration of amino acid, c_B is the added concentration of sodium hydroxide, and the remaining c's refer to the species denoted by the subscript. The hydroxyl-ion concentration was calculated in the manner previously described.

The variation of $-\log K_2'$ in solutions of potassium chloride, lithium chloride, sodium chloride, and barium chloride is shown in figure 5. The points are experimental and the curves are theoretical.

The corresponding constant which involves the hydroxyl ion in the equilibrium

$$H_2O + NH_2CH(CH_3)COO^- \rightleftarrows OH^- + NH_3^+CH(CH_3)COO^- \tag{22}$$

is defined by

$$K'_B = \frac{c_{OH^-} c_{R^{+-}}}{N_{H_2O} c_{R^-}} \tag{23}$$

For convenience, the term $-\log (K'_B N_{H_2O})$ has been calculated from the experimental data. The logarithmic expression for this is

$$-\log (K'_B N_{H_2O}) = -\log c_{OH^-} - \log \frac{c_{R^{+-}}}{c_{R^-}} \tag{24}$$

The same experimental data that were obtained in connection with $-\log K'_2$ were used. $-\log c_{OH^-}$ was calculated from the hydrogen-ion concentration in the manner previously described. The ratio in equation 24 was evaluated by means of equation 21.

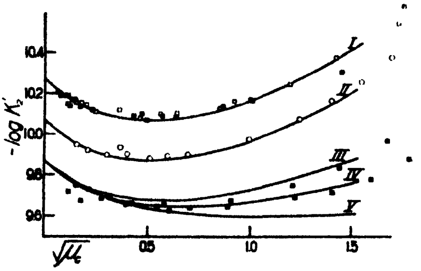

FIG. 5

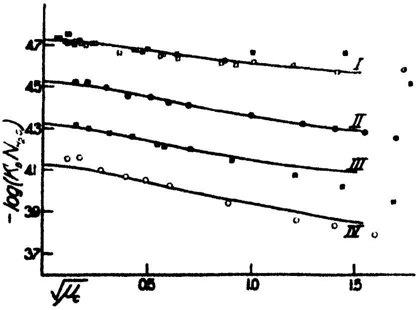

FIG. 6

FIG. 5. The effects of sodium chloride, potassium chloride, lithium chloride, and barium chloride on $-\log K'_2$ of alanine. ■ = sodium chloride; ○ = lithium chloride; □◩ = potassium chloride; ▣ = barium chloride. Note: 0.2 and 0.4 unit, respectively, has been added to each value for sodium chloride and potassium chloride for the purpose of separating the curves.

FIG. 6. The effects of sodium chloride, potassium chloride, lithium chloride, and barium chloride on $-\log K'_B$ of alanine. ● = sodium chloride; ■ = lithium chloride; □◩ = potassium chloride; ○ = barium chloride. Note: 0.2, 0.4, and 0.6 units, respectively, have been added to the values for lithium chloride, sodium chloride, and potassium chloride for the purpose of separating the curves.

The variation of $-\log K'_B$ in the salt solutions is shown graphically in figure 6. The points are experimental and the curves are theoretical. The thermodynamic constants, K_2 and K_B, are defined by

$$K_2 = \frac{a_{H^+} a_{R^-}}{a_{R^{+-}}} \tag{25}$$

$$K_B = \frac{a_{OH^-} a_{R^{+-}}}{a_{H_2O} a_{R^-}} \tag{26}$$

By introducing the expression $a = \gamma c$, converting to logarithmic form, and rearranging, the following relations between the thermodynamic and apparent constants are obtained:

$$-\log K_2' = -\log K_2 - \log \gamma_{\mathrm{R}^{+-}} + \log \gamma_{\mathrm{H}^+} + \log \gamma_{\mathrm{R}^-} \qquad (27)$$

$$-\log K_B' = -\log K_B + \log \gamma_{\mathrm{R}^{+-}} + \log \gamma_{\mathrm{OH}^-} - \log \gamma_{\mathrm{R}^-} - \log \alpha_{\mathrm{H_2O}} \qquad (28)$$

Addition of the term $-C\sqrt{\mu_c}$ to equations 28 and $-C\sqrt{\mu_c}$ and $B\mu_c$ to equation 27 gives the expressions

$$-\log K_2' = -\log K_2 - \log \gamma_{\mathrm{R}^{+-}} + \log \gamma_{\mathrm{H}^+} + \log \gamma_{\mathrm{R}^-} + C\sqrt{\mu_c} + B\mu_c \qquad (29)$$

$$-\log K_B' = -\log K_B + \log \gamma_{\mathrm{R}^{+-}} - \log \alpha_{\mathrm{H_2O}} - C\sqrt{\mu_c} \qquad (30)$$

The approximation that γ_{R^-} is equal to γ_{H^+} has been made. Curves I, II, III, and IV in figure 5 were calculated by equation 29. The curves in figure 6 were calculated by equation 30. The activity coefficients in equations 29 and 30 were calculated by means of equations 12 and 13. Curve V in figure 5 was calculated by equation 30, the term $B\mu_c$ being omitted.

In all of the calculations for equations 29 and 30, R of equation 13 has been taken equal to 4.0 Å. and b equal to 3.08 Å. The values of a' in the expressions for γ_{H^+}, γ_{OH^-}, and γ_{R^-} were assumed to be equal. The values that were used for the remaining constants in equations 12 and 13, after introduction of these equations into equations 29 and 30, are given in table 4.

TABLE 4

Values used for a, a′, B, and C for potassium chloride, sodium chloride, lithium chloride, and barium chloride

SALTS	a	a′	B	C
	Å.	Å.		
Potassium chloride	3.8	4.0	0.213	0.0
Sodium chloride	4.2	3.4	0.195	0.0273
Lithium chloride	4.9	4.0	0.104	0.0733
Barium chloride	4.2	3.6	0.0662	0.042

In all of the theoretical calculations for the curves in figures 1 to 6, the values of 2.345 and 9.870 have been employed for $-\log K_1$ and $-\log K_2$, respectively. These are in excellent agreement with the values of 2.340 and 9.870 that have been reported by Nims and Smith (21). This agreement provides a check on the methods of extrapolation as well as on the accuracy of the data.

The complete data are on file in the Library of the University of California.

SUMMARY

1. By the use of cells without liquid-junction potentials, the effects of certain salt mixtures on the dissociation of alanine in acid and alkaline solutions have been determined.

2. A comparison has been made between the curves obtained by plotting the data and those obtained from theoretical considerations.

3. Certain factors that are not accounted for by the theoretical equations have been discussed.

REFERENCES

(1) Batchelder, A. C., and Schmidt, C. L. A.: J. Phys. Chem. **43**, 1121 (1939).
(2) Birge, R. T.: Phys. Rev. Supplement **1**, 1 (1929).
(3) Brönsted, J. N.: Rec. trav. chim. **42**, 718 (1923).
(4) Cohn, E. J., McMeekin, T. L., Edsall, J. T., and Blanchard, M. H.: J. Am. Chem. Soc. **56**, 784 (1934).
(5) Dalton, J. B., and Schmidt, C. L. A.: J. Biol. Chem. **103**, 549 (1933).
(6) Harned, H. S.: J. Am. Chem. Soc. **51**, 416 (1929).
(7) Harned, H. S.: J. Am. Chem. Soc. **54**, 1350 (1932).
(8) Harned, H. S.: J. Am. Chem. Soc. **48**, 326 (1926).
(9) Harned, H. S., and Copson, H. R.: J. Am. Chem. Soc. **55**, 2206 (1933).
(10) Harned, H. S., and Ehlers, R. W.: J. Am. Chem. Soc. **55**, 652 (1933).
(11) Harned, H. S., and Hamer, W. J.: J. Am. Chem. Soc. **55**, 2194 (1933).
(12) Harned, H. S., and Hamer, W. J.: J. Am. Chem. Soc. **55**, 2204 (1933).
(13) Harned, H. S., and Mannweiler, G. E.: J. Am. Chem. Soc. **57**, 1873 (1935).
(14) Harned, H. S., and Mason, C. M.: J. Am. Chem. Soc. **54**, 3112 (1932).
(15) Harned, H. S., and Murphy, G. M.: J. Am. Chem. Soc. **53**, 8 (1931).
(16) Harned, H. S., and Robinson, R. A.: J. Am. Chem. Soc. **50**, 3157 (1928).
(17) *International Critical Tables:* Vol. III. McGraw-Hill Book Company, Inc., New York (1929).
(18) *Internationale Tabellen zur Bestimmung von Kristallstrukturen,* Vol. 2, p. 610; edited by C. Hermann. Gebrüder Borntraeger, Berlin (1935).
(19) Kirkwood, J. G.: J. Chem. Phys. **2**, 351 (1934).
(20) Lewis, G. N., and Randall, M.: *Thermodynamics and the Free Energy of Chemical Substances.* McGraw-Hill Book Company, Inc., New York and London (1923).
(21) Nims, L. F., and Smith, E. R. B.: J. Biol. Chem. **101**, 401 (1933).
(22) Pauling, L.: J. Am. Chem. Soc. **50**, 1036 (1928).
(23) Pearce, J. N., and Nelson, A. F.: J. Am. Chem. Soc. **54**, 3544 (1932).
(24) Perreu, J.: Compt. rend. **200**, 1588 (1935).
(25) Randall, M., and Breckenridge, G. F.: J. Am. Chem. Soc. **49**, 1435 (1927).
(26) Taylor, H. S.: *A Treatise on Physical Chemistry,* 2nd edition. D. Van Nostrand Company, New York (1931).

THE EFFECTS OF CERTAIN SALTS ON THE DISSOCIATION OF ASPARTIC ACID, ARGININE, AND ORNITHINE[1]

A. C. BATCHELDER AND CARL L. A. SCHMIDT

Division of Biochemistry, University of California Medical School, Berkeley, California

Received November 16, 1939

The present experiments dealing with the effects of salts on the dissociation of aspartic acid, arginine, and ornithine were carried out with the same technique as described in the previous paper (1). These amino acids were chosen since one, aspartic acid, represents the group of dicarboxylic amino acids, while the other two are representative of the predominantly basic amino acids.

CALCULATION OF RESULTS

A. *Aspartic acid:* K'_1 *and* K'_2

The equilibria

$$\mathrm{HOOCCH_2CHNH_3^+COOH} \rightleftarrows \mathrm{H^+} + \mathrm{HOOCCH_2CHNH_3^+COO^-} \tag{1}$$

$$\mathrm{HOOCCH_2CHNH_3^+COO^-} \rightleftarrows \mathrm{H^+} + \mathrm{^-OOCCH_2CHNH_3^+COO^-} \tag{2}$$

are described by the apparent constants K'_1 and K'_2, respectively. These constants are defined by

$$K'_1 = \frac{c_{\mathrm{R}^{+-}} c_{\mathrm{H}^+}}{c_{\mathrm{R}^+}} \tag{3}$$

$$K'_2 = \frac{c_{\mathrm{R}^-} c_{\mathrm{H}^+}}{c_{\mathrm{R}}} \tag{4}$$

Actually the zwitter ion and the cation are in equilibrium between the various possible structures. The charges have been placed on particular groups for convenience only. The constants are therefore over-all constants, obtained by considering the total concentration of the various species of ions, each species being differentiated by the net electrical charge and not by the spatial location of the charge.

The above two constants are "overlapping" (4). Therefore they have been calculated from the experimental data by an adaptation of the method suggested by Neuberger (7).

In two solutions of aspartic acid that have different pH values, the amino acid will exist in the three forms that are given in equations 1 and 2, provided the pH of both solutions is such that the concentration of the divalent anion is negligible. Or, in mathematical terms,

---

[1] The authors were aided by a grant from the Research Board of the University of California and by Eli Lilly and Company. They are indebted to the Cyrus M. Warren Fund of the American Academy of Arts and Sciences for the loan of the Type K potentiometer.

$$c_{\mathrm{R}^+_\alpha} + c_{\mathrm{R}^{+-}_\alpha} + c_{\mathrm{R}^-_\alpha} = c_{T_\alpha} \tag{5}$$

$$c_{\mathrm{R}^+_\beta} + c_{\mathrm{R}^{+-}_\beta} + c_{\mathrm{R}^-_\beta} = c_{T_\beta} \tag{6}$$

where c_{R^+}, $c_{\mathrm{R}^{+-}}$, and c_{R^-} refer to the concentrations of the aspartic acid cation, zwitter ion, and monovalent anion, respectively. c_T indicates the total concentration of the aspartic acid, regardless of form. The subscript α refers to the first solution and β to the second. The divalent anion of aspartic acid need not be considered, since $-\log K_3$ is about 6.0 units greater than $-\log K_2$.

In the present experiments, solution α was made up by adding hydrochloric acid to isoelectric aspartic acid, and solution β by adding sodium hydroxide. The following are therefore obtained upon consideration of the electrical neutrality of the solutions:

$$c_A = c_{\mathrm{R}^+_\alpha} + c_{\mathrm{H}^+_\alpha} - c_{\mathrm{R}^-_\alpha} \tag{7}$$

$$c_B = c_{\mathrm{R}^-_\beta} - c_{\mathrm{H}^+_\beta} - c_{\mathrm{R}^+_\beta} \tag{8}$$

where c_A and c_B refer to the added concentration of hydrochloric acid and sodium hydroxide, respectively, and c_{H^+} indicates the hydrogen-ion concentration.

If both solutions have been brought to the same value of the ionic strength by the addition of the same neutral salt to each,

$$K_1' = \frac{c_{\mathrm{R}^{+-}_\alpha} c_{\mathrm{H}^+_\alpha}}{c_{\mathrm{R}^+_\alpha}} = \frac{c_{\mathrm{R}^{+-}_\beta} c_{\mathrm{H}^+_\beta}}{c_{\mathrm{R}^+_\beta}} \tag{9}$$

$$K_2' = \frac{c_{\mathrm{R}^-_\alpha} c_{\mathrm{H}^+_\alpha}}{c_{\mathrm{R}^{+-}_\alpha}} = \frac{c_{\mathrm{R}^-_\beta} c_{\mathrm{H}^+_\beta}}{c_{\mathrm{R}^{+-}_\beta}} \tag{10}$$

Division of equations 5 and 6 by $c_{\mathrm{R}^{+-}_\alpha}$ and $c_{\mathrm{R}^{+-}_\beta}$, respectively, gives the following:

$$\frac{c_{\mathrm{R}^+_\alpha}}{c_{\mathrm{R}^{+-}_\alpha}} + \frac{c_{\mathrm{R}^{+-}_\alpha}}{c_{\mathrm{R}^{+-}_\alpha}} + \frac{c_{\mathrm{R}^-_\alpha}}{c_{\mathrm{R}^{+-}_\alpha}} = \frac{c_{T_\alpha}}{c_{\mathrm{R}^{+-}_\alpha}} \tag{11}$$

$$\frac{c_{\mathrm{R}^+_\beta}}{c_{\mathrm{R}^{+-}_\beta}} + \frac{c_{\mathrm{R}^{+-}_\beta}}{c_{\mathrm{R}^{+-}_\beta}} + \frac{c_{\mathrm{R}^-_\beta}}{c_{\mathrm{R}^{+-}_\beta}} = \frac{c_{T_\beta}}{c_{\mathrm{R}^{+-}_\beta}} \tag{12}$$

By combination with equations 9 and 10, the ratios in the left-hand sides of equations 11 and 12 may be expressed in terms of hydrogen-ion concentration and the apparent constants. After performing this substitution and rearranging, the following equations are obtained:

$$\frac{(c_{\mathrm{H}^+_\alpha})^2 + c_{\mathrm{H}^+_\alpha}K'_1 + K'_1K'_2}{c_{\mathrm{H}^+_\alpha}K'_1} = \frac{c_{T_\alpha}}{c_{\mathrm{R}^{+-}_\alpha}} \tag{13}$$

$$\frac{(c_{\mathrm{H}^+_\beta})^2 + c_{\mathrm{H}^+_\beta}K'_1 + K'_1K'_2}{c_{\mathrm{H}^+_\beta}K'_1} = \frac{c_{T_\beta}}{c_{\mathrm{R}^{+-}_\beta}} \tag{14}$$

Analogous operations on equations 7 and 8 result in two additional equations that are similar to equations 13 and 14. Combination of these four equations results in the following pair of equations:

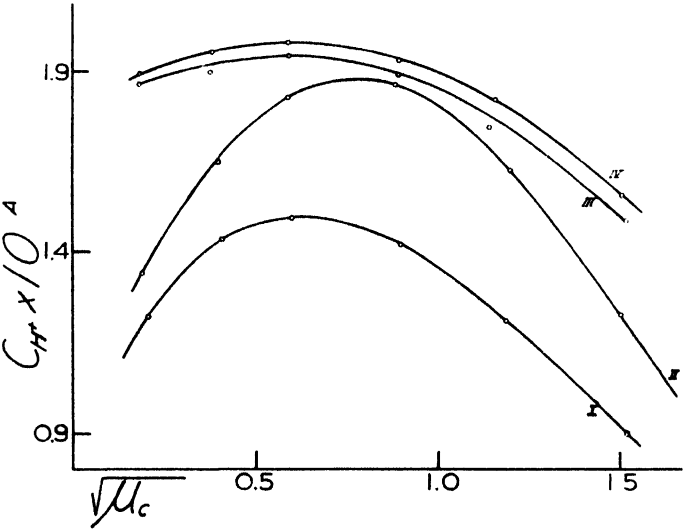

FIG. 1 The effects of varying amounts of sodium chloride and potassium chloride on the hydrogen-ion concentration of partially neutralized solutions of aspartic acid. Curve I, potassium chloride, $A = -4$; curve II, sodium chloride, $A = -4$; curve III, potassium chloride, $A = -3$; curve IV, sodium chloride, $A = -3$ Note: 0.3×10^{-4} units have been subtracted from the experimental values for curve II to place the curve on the graph.

$$\frac{c_{T_\alpha}}{c_A - c_{\mathrm{H}^+_\alpha}} = \frac{(c_{\mathrm{H}^+_\alpha})^2 + K'_1c_{\mathrm{H}^+_\alpha} + K'_1K'_2}{(c_{\mathrm{H}^+_\alpha})^2 - K'_1K'_2} \tag{15}$$

$$\frac{c_{T_\beta}}{c_B + c_{\mathrm{H}^+_\beta}} = \frac{(c_{\mathrm{H}^+_\beta})^2 + K'_1c_{\mathrm{H}^+_\beta} + K'_1K'_2}{K'_1K'_2 - (c_{\mathrm{H}^+_\beta})^2} \tag{16}$$

These equations were applied to the experimental data in the following manner: Two series of solutions, α and β, were prepared. The same salt was employed in both series. The hydrogen-ion concentration of each solution was determined. These values were plotted on a large-scale graph against the square root of the ionic strength, and a smooth curve was drawn through the points. This graph is shown in figure 1. The hydrogen-ion concentration of both series at several values of the ionic strength was then obtained from the graph. Several pairs of values for c_{H^+} at equal values of the ionic strength were thus obtained. The values of the two constants at each of these several values of the ionic strength were then calculated from the hydrogen-ion concentration by equations 15 and 16.

The effects of potassium chloride and sodium chloride on the $-\log K_1'$ of aspartic acid are shown in figure 2. The points are experimental, and the curves have been drawn to fit the points.

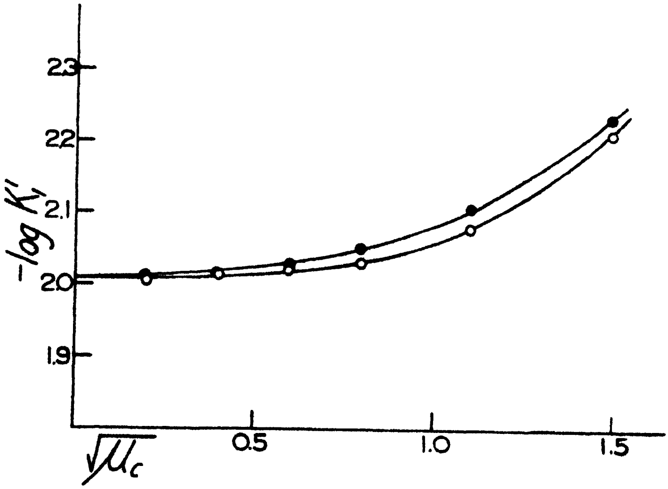

FIG. 2. The effects of varying amounts of sodium chloride and potassium chloride on $-\log K_1'$ of aspartic acid. ● = sodium chloride; ○ = potassium chloride.

No attempt has been made to calculate the theoretical curves for the effects of salts on the $-\log K_1'$ of aspartic acid. Because of the assumptions involved in its derivation, Kirkwood's equation (see reference 19 of the preceding paper (1)) for the activity coefficients of zwitter ions is not so adaptable to aspartic acid as it is to alanine. If, as the simplest case possible, the activity coefficient of aspartic acid is equal to unity, and the activity coefficient of the aspartic acid cation equals that of the hydrogen ion, the resultant theoretical curve will be a horizontal line whose origin on the ordinate corresponds with the origin of the experimental curve. Any decrease of $\gamma_{R^{+-}}$ from unity will give the curve a negative slope. Any departure from $\gamma_{R^+} = \gamma_{H^+}$ will give a negative slope if $\gamma_{R^+} > \gamma_{H^+}$, and a positive slope if $\gamma_{R^+} < \gamma_{H^+}$. The exact shape of the theoretically calculated curve would depend on the functions describing the γ's. The general shape of the curve is similar to those in figure 3 of the preceding paper (1). The theoretical equation has the form

$$-\log K_1' = -\log K_1 + f(\mu_c) + f'(\sqrt{\mu_c}) + B\mu_c \tag{17}$$

where the functions of the ionic strength and the square root of the ionic strength of (μ_c) and $f'(\sqrt{\mu_c})$ represent the theoretical expressions for the activity coefficients, and $B\mu_c$ is the "salting-out" term. This type of curve, if $f(\mu_c) = f'(\sqrt{\mu_c}) = 0$, will approximately fit the experimental data. If $f'(\sqrt{\mu_c}) > 0$, equation 17 will describe the experimental data exactly.

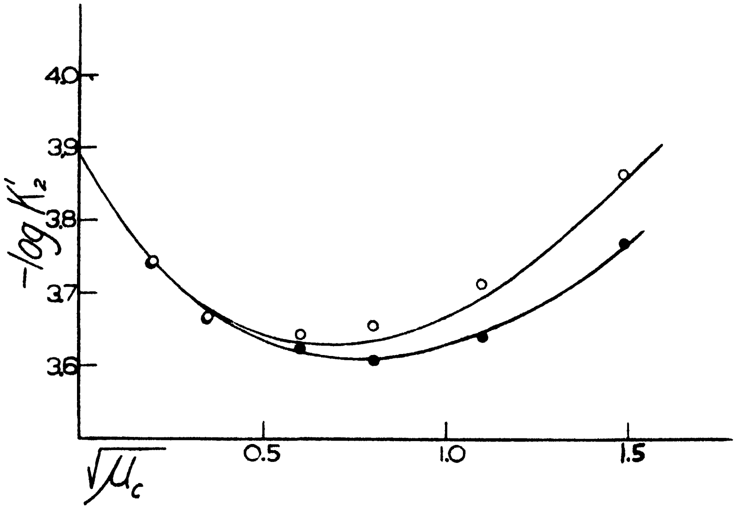

FIG. 3. The effects of sodium chloride and potassium chloride on $-\log K_2'$ of aspartic acid. ● = sodium chloride; ○ = potassium chloride.

The effects of sodium chloride and potassium chloride on the $-\log K_2'$ of aspartic acid are shown in figure 3.

Equation 29 (reference 1) will describe the present curves. If $\gamma_{\mathrm{R}^{+-}}$ is taken as equal to unity at all concentrations, equation 12 (reference 1) is introduced for γ_{R^-} and γ_{H^+}, $C = 0$, and a' in this equation is equal to 4.0 Å., the following modification of equation 29 (reference 1) is obtained:

$$-\log K_2' = -\log K_2 + \frac{1.008\sqrt{\mu_c}}{1 + 1.312\sqrt{\mu_c}} + B\mu_c \tag{18}$$

This semi-empirical equation provides a means to fit the experimental results mathematically. The curves in figure 3 were calculated by equation 18. The values of the constants B and $-\log K_2$ were determined from the experimental points. B for the potassium chloride curve has a value of 0.208 and B for the sodium chloride curve has a value of 0.168. $-\log K_2$ has a value of 3.895.

In its logarithmic form, K_3' of aspartic acid is defined by

$$-\log K_3' = -\log c_{\mathrm{H}^+} - \log \frac{c_{\mathrm{R}^{--}}}{c_{\mathrm{R}^-}} \tag{19}$$

It applies to the equilibrium:

$$^-\mathrm{OOCCH_2CHNH_3^+COO^-} \rightleftarrows {}^-\mathrm{OOCCH_2CHNH_2COO^-} + \mathrm{H^+} \tag{20}$$

In making up the experimental solutions, approximately 1.5 moles of sodium hydroxide were added to each mole of aspartic acid. In consideration of this fact and the electrical neutrality of the solution, the ratio in equation 19 may be evaluated by

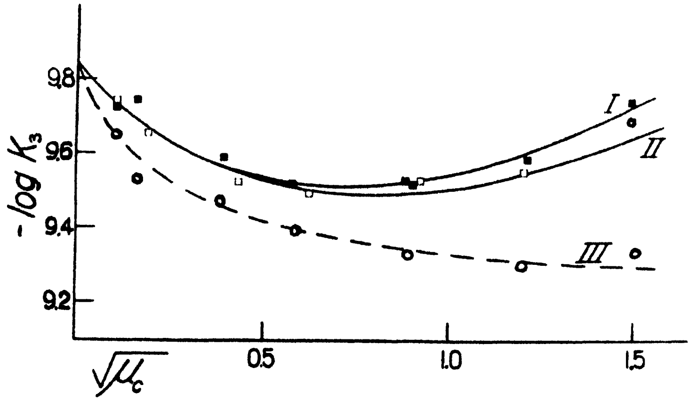

FIG. 4. The effects of sodium chloride, potassium chloride, and barium chloride on $-\log K_3'$ of aspartic acid. ■ = potassium chloride; □ = sodium chloride; ○ = barium chloride.

$$c_{\mathrm{R}^{--}} = c_B - c_T - c_{\mathrm{OH}^-}$$

$$c_{\mathrm{R}^-} = 2c_T - c_B - c_{\mathrm{OH}^-} \tag{21}$$

where c_B is the added concentration of sodium hydroxide, c_T is the total concentration of aspartic acid, and the remaining c's refer to the concentration of the species denoted by the subscript. $-\log c_{\mathrm{H}^+}$ in each of the solutions was calculated by means of equation 3 (reference 1). c_{OH^-} was evaluated in the manner described in the preceding paper (1).

The experimental results are shown graphically in figure 4.

By reasoning that is identical with that followed in obtaining equations 17 and 27 (preceding paper (1)), the following relation between $-\log K_3'$ and $-\log K_3$ of aspartic acid is obtained:

$$-\log K_3' = -\log K_3 + \log \gamma_{\mathrm{R}^{--}} + \log \gamma_{\mathrm{H}^+} - \log \gamma_{\mathrm{R}^-} + B\mu_c \quad (22)$$

The "salting-out" term has been added. If equation 12 (reference 1) is introduced for the activity coefficients, letting a' for R^- and R^{--} equal 4.8 Å., and a' for H^+ equal 3.0 Å., equation 22 will not fit the data even approximately. The limiting slope calculated in this manner is considerably greater than that indicated by the experimental data. Simms (10) suggested a modification of the Debye-Hückel equation to apply to the case of divalent ions with widely separated charges of like sign. For the present case, his equation may be written

$$-\log \gamma_{\mathrm{R}^{--}} = \frac{0.504z^x\sqrt{\mu_c}}{1 + 0.328a'\sqrt{\mu_c}} \quad (23)$$

where x is an empirically determined constant, the value of which lies between 1.0 and 2.0. Introduction of equations 12 (reference 1) and 23 into equation 22, and inclusion of the values for a', gives

$$\begin{aligned}-\log K_3' = -\log K_3 &- \frac{0.504(2^x)\sqrt{\mu_c}}{1 + 1.574\sqrt{\mu_c}} \\ &- \frac{0.504\sqrt{\mu_c}}{1 + 0.984\sqrt{\mu_c}} + \frac{0.504\sqrt{\mu_c}}{1 + 1.574\sqrt{\mu_c}} + B\mu_c \quad (24)\end{aligned}$$

Curves I and II in figure 4 were calculated with the aid of equation 24. The constants were determined from the experimental data. The following values were obtained: $-\log K_3'$, 9.842; x, 1.23. For curve I, $B = 0.220$ and for curve II, $B = 0.185$.

The displacement of curve III may be explained by the formation of complexes of the type noted by Cannan and Kibrick (2). Their equation (equation 4, page 2316, bottom of first column) has been applied to the present case. Using their values for C_1 and C_2 for succinic acid, the correction to be applied to curve III for complex formation is calculated to be 0.46 unit at $\mu_c = 1.5$. This correction superimposes curve III on curve I at this concentration. If it is assumed, in agreement with Cannan and Kibrick, that addition of potassium chloride to the solution of aspartic acid does not result in the formation of complexes, the calculated correction for complex formation in the present case is of the correct magnitude.

B. Arginine

The effects of sodium chloride and lithium chloride on $-\log K_1'$ and $-\log K_2'$ of arginine have been determined. $-\log K_1'$ is defined by

$$-\log K_1' = -\log c_{H^+} - \log \frac{c_{R^+}}{c_{R^{++}}} \tag{25}$$

The equation applies to the equilibrium:

$$NH_3^+C(=NH)NH(CH_2)_3CHNH_3^+COOH \rightleftarrows NH_3^+C(=NH)NH(CH_2)_3CHNH_3^+COO^- + H^+ \tag{26}$$

$-\log K_2'$ is defined by

$$-\log K_2' = -\log c_{H^+} - \log \frac{c_{R^{+-}}}{c_{R^+}} \tag{27}$$

It applies to the equilibrium:

$$NH_3^+C(=NH)NH(CH_2)_3CHNH_3^+COO^- \rightleftarrows NH_3^+C(=NH)NH(CH_2)_3CHNH_2COO^- + H^+ \tag{28}$$

As in the case of aspartic acid, the spatial location of the charges in the chemical formulas on any group is a matter of convenience only. It does not imply the non-existence of other isomeric forms in the solution.

Arginine monohydrochloride was used in the present experiments. The ratio in equation 25 was evaluated by

$$\begin{aligned} c_{R^{++}} &= c_A - c_{H^+} \\ c_{R^+} &= c_T - c_{R^{++}} \end{aligned} \tag{29}$$

and the ratio in equation 27 was evaluated by

$$\begin{aligned} c_{R^{+-}} &= c_B - c_{OH^-} \\ c_{R^+} &= c_T - c_{R^{+-}} \end{aligned} \tag{30}$$

where c_B and c_A are, respectively, the added concentrations of sodium hydroxide and hydrochloric acid, and the other symbols have their previous significance. A separate series of solutions was used for each constant. Equations 29 and 30 and the values for $-\log c_{H^+}$ that were obtained from equation 3 (reference 1) provided all the values necessary for the evaluation of equations 25 and 27. c_{OH^-} was evaluated in the manner previously described.

The results of these experiments are shown graphically in figures 5 and 6.

In order to evaluate the ionic strength of the first three solutions of the series for $-\log K_1'$, it was necessary to know the hydrogen-ion concentration. This, in turn, could not be evaluated without knowledge of the value of the ionic strength. A rough value of the hydrogen-ion concentration was therefore calculated, employing the assumption that $c_{R^{++}} = c_A$. With this approximate value of the hydrogen-ion concentration, it was

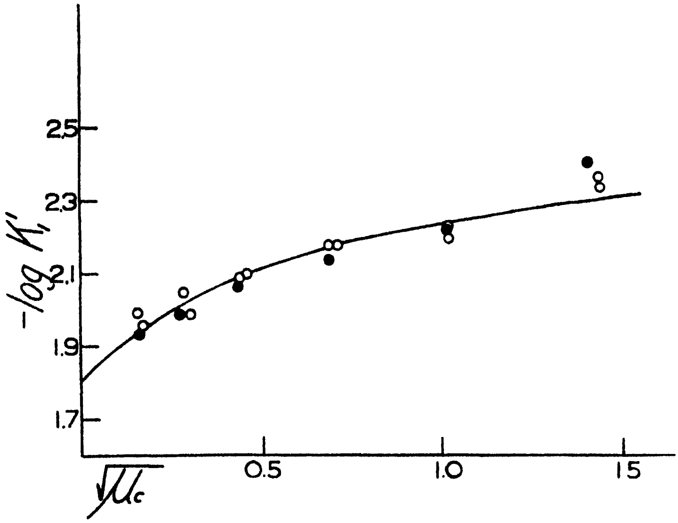

FIG. 5. The effects of sodium chloride and lithium chloride on $-\log K'_1$ of arginine. ● = sodium chloride; ○ = lithium chloride.

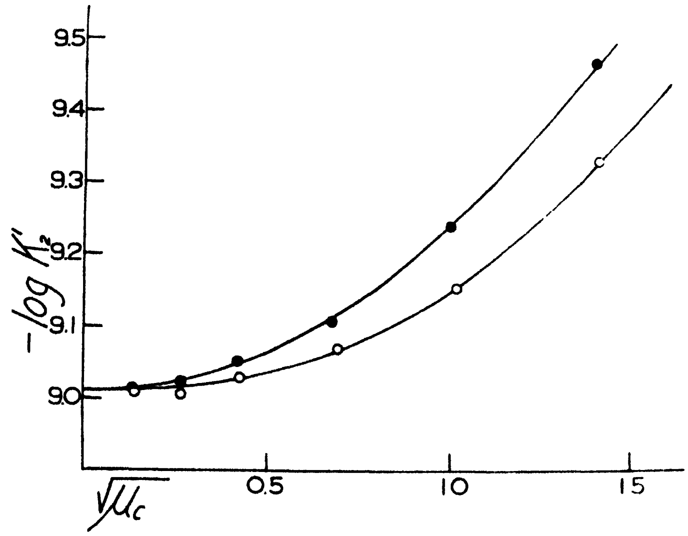

FIG. 6. The effects of sodium chloride and lithium chloride on $-\log K'_2$ of arginine. ● = sodium chloride; ○ = lithium chloride.

then possible to evaluate $c_{R^{++}}$ with sufficient accuracy to obtain a true value of the ionic strength. This true value was employed for the calculation of the actual hydrogen-ion concentration. In the remaining members of this series, the salt contributes such a large portion of the ionic strength that this approximation was unnecessary.

The relation between $-\log K_1'$ and $-\log K_1$ is given by the equation

$$-\log K_1' = -\log K_1 + \log \gamma_{R^+} + \log \gamma_{H^+} - \log \gamma_{R^{++}} \qquad (31)$$

where K_1 is the thermodynamic equilibrium constant for equation 26. Upon introduction of equation 12 (reference 1) into equation 31, and letting a' equal 4.0 Å. in all cases, the following equation is obtained:

$$-\log K_1' = -\log K_1 + \frac{1.008\sqrt{\mu_c}}{1 + 1.312\sqrt{\mu_c}} \qquad (32)$$

The curve given in figure 5 was calculated by this equation, using a value of 1.807 for $-\log K_1$. If Simms' equation is employed, the limiting slope will be decreased. The experimental accuracy of the present experiments has been limited by the magnitude of the term c_{H^+} in equation 29. It is not believed that the accuracy of the experimental data warrants this additional refinement of the theoretical calculations.

The curves shown in figure 6 have been drawn to fit the experimental data.

It was not considered feasible to investigate the effects of salts on $-\log K_3'$ of arginine. The high alkalinity of the solutions increases the effects of experimental deviations to such an extent that the experiments lose all significance.

C. Ornithine

Ornithine ionizes according to the following equations:

$$NH_3^+(CH_2)_3CHNH_3^+COOH \rightleftarrows NH_3^+(CH_2)_3CHNH_3^+COO^- + H^+ \qquad (33)$$

$$NH_3^+(CH_2)_3CHNH_3^+COO^- \rightleftarrows NH_2(CH_2)_3CHNH_3^+COO^- + H^+ \qquad (34)$$

$$NH_2(CH_2)_3CHNH_3^+COO^- \rightleftarrows NH_2(CH_2)_3CHNH_2COO^- + H^+ \qquad (35)$$

The apparent constants for these equilibria are defined by

$$-\log K_1' = -\log c_{H^+} - \log \frac{c_{R^+}}{c_{R^{++}}} \qquad (36)$$

$$-\log K_2' = -\log c_{H^+} - \log \frac{c_{R^{+-}}}{c_{R^+}} \qquad (37)$$

$$-\log K_3' = -\log c_{H^+} - \log \frac{c_{R^-}}{c_{R^{+-}}} \qquad (38)$$

Schmidt, Kirk, and Schmidt (8, 5) found that the values for $-\log K_2'$ and $-\log K_3'$ are 8.65 and 10.77, respectively. The difference between the two values is 2.12. Simms (9) has shown that for malonic acid, whose constants differ by 2.59 units, the true constants may be taken as identical with the "titration constants." He has also shown that in the case of succinic acid, whose constants differ by 1.42 units, the titration constants and the true constants differ by 0.02 unit. Ornithine is, therefore, a borderline case. In the present calculations it is assumed that no correction need be applied for "overlapping," i.e., that the constants obtained by the following method of calculation are the true constants.

The following equations were used to evaluate the ratios in equations 36, 37, and 38:

$$c_{\mathrm{R}^{++}} = c_T - c_B - c_{\mathrm{H}^+}$$

$$c_{\mathrm{R}^+} = c_B + c_{\mathrm{H}^+} \tag{39}$$

$$c_{\mathrm{R}^+} = 2c_T - c_B$$

$$c_{\mathrm{R}^{+-}} = c_B - c_T \tag{40}$$

$$c_{\mathrm{R}^-} = c_B - c_{\mathrm{OH}^-} - 2c_T$$

$$c_{\mathrm{R}^{+-}} = 3c_T - c_B + c_{\mathrm{OH}^-} \tag{41}$$

where the symbols have their previous significance. The equations are obtained upon consideration of the electrical neutrality of the solutions and the fact that ornithine dihydrochloride was employed in the experiments.

The solutions used for determining the changes in $-\log K_1'$, $-\log K_2'$, and $-\log K_3'$, respectively, were prepared by adding 0.5, 1.5, and 2.5 moles of sodium hydroxide to each mole of ornithine dihydrochloride.

$-\log c_{\mathrm{H}^+}$ in equations 36, 37, and 38 was obtained from equation 3 (reference 1). c_{OH^-} was evaluated in the manner previously described.

The effects of sodium chloride on the three constants are shown in figure 7. The curves have been moved to a common point of origin by addition or subtraction of the amount stated in the caption.

The relation between $-\log K_1'$ and $-\log K_1$ of ornithine is given by equation 31. Curve I in figure 7 was calculated with the aid of the following equation:

$$-\log K_1' = -\log K_1 + \frac{1.008\sqrt{\mu_c}}{1 + 1.312\sqrt{\mu_c}} + B\mu_c \tag{42}$$

which was obtained by the addition of the term $B\mu_c$ to equation 32. $B = 0.0564$ and $-\log K_1 = 1.705$.

Curve II of figure 7 was calculated according to the empirical equation

$$-\log K_2' = -\log K_2 + B\mu_c \tag{43}$$

where $B = 0.235$. Considerations similar to those that were discussed in connection with the theoretical calculation of the effects of salts on $-\log K_1'$ of aspartic acid apply to the present case.

The relation between $-\log K_3'$ and $-\log K_3$ of ornithine is given by

$$-\log K_3' = -\log K_3 + \log \gamma_{H^+} + \log \gamma_{R^-} - \log \gamma_{R^{+-}} \tag{44}$$

Curve III of figure 7 has been calculated by the semi-empirical equation

$$-\log K_3' = -\log K_3 - \frac{1.008\sqrt{\mu_c}}{1 + 1.312\sqrt{\mu_c}} + B\mu_c \tag{45}$$

which is obtained by introducing equation 12 (reference 1) into equation 44, adding the "salting-out" term, letting a' equal 4.0 Å., and employing

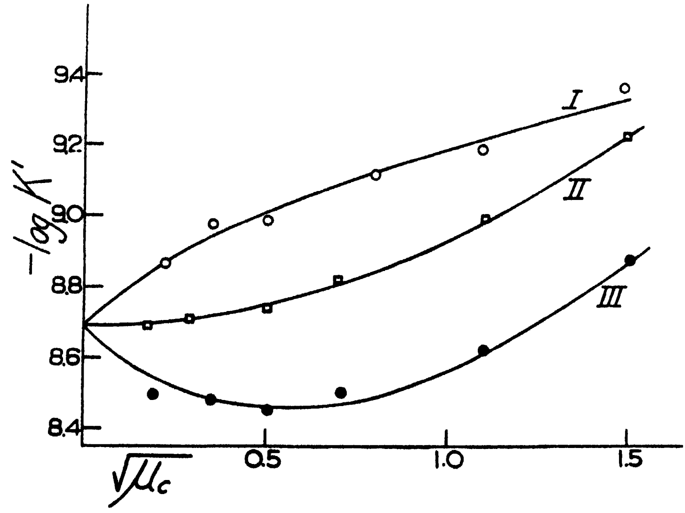

FIG. 7. The effects of sodium chloride on the ionization of ornithine. ○ = $-\log K_1'$. 6.985 units have been added to all values. □ = $-\log K_2'$. ● = $-\log K_3'$. 2.065 units have been subtracted from all values. Note: the curves are calculated.

the approximation that $\gamma_{R^{+-}} = 1.0$. The values of 0.302 and 10.755 have been obtained for B and $-\log K_3'$, respectively.

DISCUSSION

The effects of salts on the ionization of amino acids have been explained in the same manner as the effects of salts on the ionization or activity coefficients of other electrolytes. At low salt concentrations, the form of the curves showing the changes in the values of the apparent dissociation constants has been correctly predicted on the basis of the theory of interionic attraction. Because the activity coefficient of the electrically neutral portion of the amino acid and the "salting-out" term are proportional to the first power of the ionic strength, the chief factors that determine the shape of the curves at low salt concentrations are the activity coefficients of the other ionic species that are involved in the ionization equilibrium. In common with certain other electrolytes, it has been necessary to use a "salting-out" constant to obtain agreement between the experimental and the calculated values at higher salt concentrations. At higher values of the ionic strength, the activity coefficient of the zwitterionic portion of the amino acid plays a relatively more important part in determining the course of the theoretical curve. However, the theoretical uncertainties at these higher salt concentrations and the introduction of the "salting-out" term make accurate evaluation of the constants in Kirkwood's equation difficult.

In solvents of low dielectric constant, the effects of the electrostatic forces are increased and the effects of the non-electrostatic forces tend to disappear. In order to estimate the relative importance of these forces in determining the effects of salts on the ionization of amino acids, it would be of interest to determine the effects of salts in solvents with lower dielectric constants than that of water.

On the assumption that none but electrostatic forces determine the effects of salts on the ionization of proteins as well as amino acids, the following method may be employed to obtain a limiting equation relating the pH of an ampholyte solution to the salt concentration.

Each of the steps in the ionization of proteins and amino acids can be represented by the following general equation:

$$\mathrm{AH}_n^+ \rightleftarrows \mathrm{AH}_m^+ + \mathrm{H}^+ \qquad (46)$$

where A represents the isoelectric ampholyte. The value of n is greater than that of m by unity.

The thermodynamic equilibrium constant is given by

$$K = \frac{\alpha_{\mathrm{AH}_m^+}\alpha_{\mathrm{H}^+}}{\alpha_{\mathrm{AH}_n^+}} = \frac{c_{\mathrm{AH}_m^+}c_{\mathrm{H}^+}}{c_{\mathrm{AH}_n^+}} \cdot \frac{\gamma_{\mathrm{AH}_m^+}\gamma_{\mathrm{H}^+}}{\gamma_{\mathrm{AH}_n^+}} \qquad (47)$$

Under the restriction that the value of the ratio $\frac{c_{\mathrm{AH}_m^+}}{c_{\mathrm{AH}_n^+}}$ is constant, and incorporating its value with that of K,

$$-\log c_{\mathrm{H}^+}\gamma_{\mathrm{H}^+} = -\log \alpha_{\mathrm{H}^+} = -\log K - \log \gamma_{\mathrm{AH}_n^+} + \log \gamma_{\mathrm{AH}_m^+} \qquad (48)$$

Since

$$-\log \gamma_{\mathrm{AH}_n^+} = 0.5n^2\sqrt{\mu};\ -\log \gamma_{\mathrm{AH}_m^+} = 0.5m^2\sqrt{\mu};\ -\log \gamma_{\mathrm{H}^+} = 0.5\sqrt{\mu} \qquad (49)$$

$$-\log \alpha_{\mathrm{H}^+} = -\log K + (n^2 - m^2)0.5\sqrt{\mu} \qquad (50)$$

Or, since $n - m = 1$,

$$-\log \alpha_{\mathrm{H}^+} = -\log K + (m + n)0.5\sqrt{\mu} \qquad (51)$$

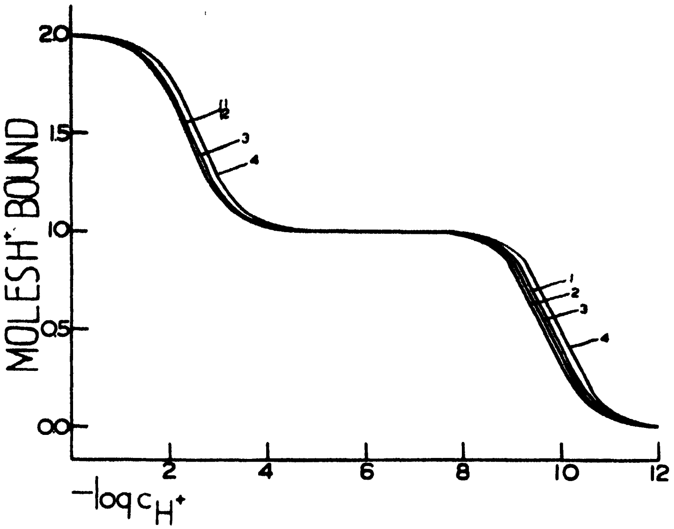

FIG. 8. The dissociation curves of alanine in solutions of sodium chloride. Curve 1 = infinite dilution; curve 2 = 0.5 *M* sodium chloride; curve 3 = 1.0 *M* sodium chloride; curve 4 = 1.5 *M* sodium chloride.

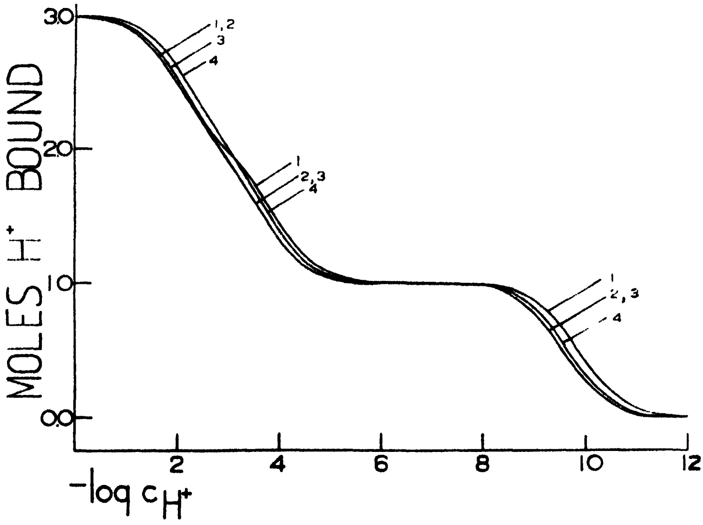

FIG. 9. The dissociation curves of aspartic acid in solutions of sodium chloride. Curve 1 = infinite dilution; curve 2 = 0.5 *M* sodium chloride; curve 3 = 1.0 *M* sodium chloride; curve 4 = 1.5 *M* sodium chloride.

$$-\log c_{H^+} = -\log K + (m + n - 1)0.5\sqrt{\mu} \qquad (52)$$

Equations 51 and 52 are limiting equations. In a more detailed treatment it would be necessary to account for the finite size of the ions, the spatial location of the electrical charges on the ions, and any specific effects of the salt.

When these equations are applied to the ionization of proteins, $m + n - 1$ will approximately equal $m + n$, except possibly in certain limited pH regions immediately on either side of the isoelectric point. The limiting slope of the $-\log c_{H^+} : \sqrt{\mu}$ curve will differ only slightly from the limiting slope of the $-\log a_{H^+} : \sqrt{\mu}$ curve, provided the pH of the solution does not approximate too closely that of the isoelectric point of the protein. It is therefore possible to compare the dissociation curves of proteins, in the presence of salts, that have been obtained by measurements of $-\log a_{H^+}$ with the present results that have been obtained by measurement of $-\log c_{H^+}$.

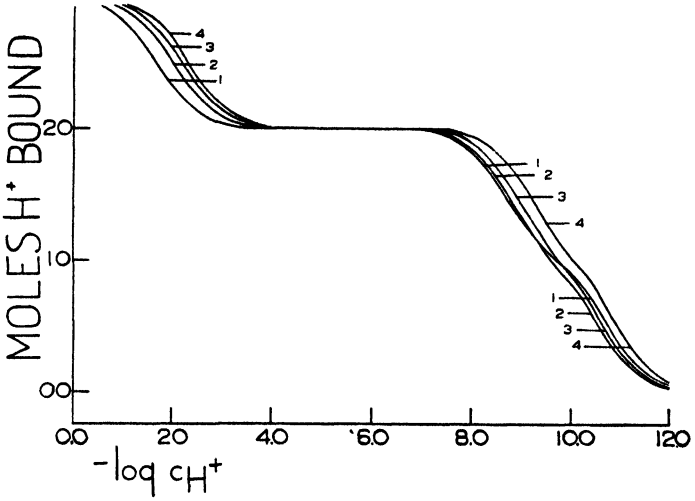

FIG. 10. The dissociation curves of ornithine in solutions of sodium chloride Curve 1 = infinite dilution; curve 2 = 0.5 *M* sodium chloride; curve 3 = 1.0 *M* sodium chloride; curve 4 = 1.5 *M* sodium chloride.

According to equation 51, addition of salts to a protein solution will cause an increase in the pH of the solution if the initial pH was less than that of the isoelectric point and a decrease in pH if the initial pH was greater than that of the isoelectric point. Results in accord with this have been observed on various occasions (11, 6, 12, 3).

Sufficient data have been obtained to enable the calculation of the dissociation curves of alanine, aspartic acid, and ornithine in salt solutions. The dissociation curves of these amino acids in sodium chloride solutions are shown in figures 8, 9, and 10. The constants from which the curves were calculated were obtained from the graphs given previously. The "titration constants" were calculated, when necessary, from the dissociation constants by the method of Simms (9). The dissociation curves were calculated by the method outlined by Greenstein (4).

The differences between the dissociation curves at infinite dilution and those in 0.5 *M* sodium chloride solution are all qualitatively predicted by equation 52. Lack of quantitative agreement at this and higher concentrations is due to the fact that the equation is applicable to only the more dilute solutions.

At all points on the dissociation curves, except where *n* has a value of unity, the effects of salts in low concentrations correspond qualitatively to the effects of salts on the dissociation curves of proteins. It could not be anticipated that the similarity would be quantitative, because of the structural differences between amino acids and proteins. Where $n = 1.0$, the dissociation of the amino acids is not appreciably affected by salts at concentrations less than 0.5 *M*. The lack of similarity between the effects of salts on this one step in the ionization of the amino acids and the effects of salts on the dissociation of proteins is readily explained by the greater number of ionizable groups in the protein molecule and the overlapping of the dissociation constants.

The complete data are on file in the Library of the University of California.

SUMMARY

1. By the use of cells without liquid-junction potentials, the effects of certain salt mixtures on the dissociation of aspartic acid, arginine, and ornithine in acid and alkaline solutions have been determined.

2. A comparison has been made between the curves obtained by plotting the data and those obtained from theoretical considerations.

3. Certain factors that are not accounted for by the theoretical equations have been discussed.

4. A comparison has been made of the effects of salts on the ionization of amino acids and proteins.

REFERENCES

(1) Batchelder, A. C., and Schmidt, C. L. A.: J. Phys. Chem. **44**, 880 (1940).
(2) Cannan, R. K., and Kibrick, A.: J. Am. Chem. Soc. **60**, 2314 (1938).
(3) Cohn, E. J., Green, A. A., and Blanchard, M. H.: J. Am. Chem. Soc. **59**, 509 (1937).
(4) Greenstein, J. P.: J. Biol. Chem. **93**, 479 (1931).
(5) Kirk, P. L., and Schmidt, C. L. A.: University of California Publications in Physiology **7**, 57 (1929).

(6) KONDO, K.: Compt. rend. trav. lab. Carlsberg **15**, No. 8 (1925).
(7) NEUBERGER, A.: Biochem. J. **30**, 2085 (1936).
(8) SCHMIDT, W., KIRK, P. L., AND SCHMIDT, C. L. A.: J. Biol. Chem. **81**, 249 (1929).
(9) SIMMS, H. S.: J. Am. Chem. Soc. **48**, 1239 (1926).
(10) SIMMS, H. S.: J. Phys. Chem. **32**, 1121 (1929).
(11) SØRENSEN, S. P. L.: Compt. rend. trav. lab. Carlsberg **12**, 1 (1915–17).
(12) SØRENSEN, S. P. L., LINDERSTRÖM-LANG, K., AND LUND, E.: J. Gen. Physiol. **8**, 543 (1926).

EQUILIBRIA IN THE SYSTEMS Na_2O–SiO_2–H_2O AND Na_2O–Al_2O_3–H_2O AT 25°C.

J. W. SPRAUER[1] AND D. W. PEARCE

Department of Chemistry, Purdue University, Lafayette, Indiana

Received October 24, 1939

As a preliminary to a study of certain regions of the four-component system Na_2O–SiO_2–Al_2O_3–H_2O at 25°C. some confirmatory work on the three-component systems Na_2O–Al_2O_3–H_2O and Na_2O–SiO_2–H_2O seemed advisable. The system Na_2O–Al_2O_3–H_2O has been investigated by Goudriaan (3) and by Fricke and Jucaitis (2) at 30°C. The present work on this system was carried only to the point necessary to confirm the results of the latter investigators, allowing for the 5° difference in temperature. The system Na_2O–SiO_2–H_2O has been investigated by Harman (4). The results presented at this time differ in several important respects from those reported by that investigator.

MATERIALS

Three materials were used for the preparation of the solutions: $Al_2O_3 \cdot 3\,H_2O$, $Na_2O \cdot SiO_2 \cdot 9\,H_2O$, and a solution (*ca.* 50 per cent) of sodium hydroxide.

The alumina trihydrate was prepared by slow hydrolysis of C.P. sodium aluminate solutions, filtered off, rapidly washed with cold water on a suction filter, and dried in a steam chest. One such preparation gave 35.3 per cent loss on ignition (theoretical, 34.65 per cent H_2O) and contained less than 0.2 per cent sodium oxide.

The hydrated sodium metasilicate was prepared by water recrystallization of the C.P. salt, was filtered with exclusion of carbon dioxide under a rubber hood fitted over the suction filter (the air being drawn through a soda-lime tube), washed with alcohol, and sucked dry. Analysis showed 21.65 per cent Na_2O (theoretical, 21.81 per cent) and 21.7 per cent SiO_2 (theoretical, 21.13 per cent).

---

[1] This article is part of a thesis presented by J. W. Sprauer to the Graduate School of Purdue University in partial fulfillment of the requirements for the degree of Master of Science.

The concentrated sodium hydroxide solution was made as nearly carbon dioxide-free as possible by dissolving C.P. pellets in an equal weight of water and decanting after long settling. One such solution contained 0.19 per cent sodium carbonate. In a few instances more concentrated solutions were prepared by vacuum concentration on the steam plate and decantation after settling.

PROCEDURE

Supersaturated solutions were stirred through mercury seals in glass equilibrium flasks contained in a thermostat. Solution samples were withdrawn at bath temperature from a side arm on the flask through a fritted-glass plug filter by means of gentle suction and were transferred to stoppered weighing bottles; crystal samples with adhering mother liquor were drawn into sampling tubes and transferred to weighing bottles. In some cases "residue" samples were rapidly centrifuged at room temperature, and excess solution was decanted.

The well-known procedure of determining composition of the solid phase by "residue" lines was not in all cases adequate in the study of the silicate system. The method of using a "tracer," i.e., a reference component present in small proportion only in the solution phase, was found reasonably satisfactory. Sodium iodide was employed for this purpose. In three instances the solids were crystallized from a solution containing iodide; in all other cases the iodide was added about an hour before sampling.

In general, attainment of approximate equilibrium was judged by analytical checks of better than 1 per cent accuracy on samples taken at an interval of about 1 week. Equilibrium was usually reached about 1 month after crystallization, although the aluminate solutions frequently required a longer time. The time required for spontaneous crystallization was decreased by seeding with the equilibrium solid when it was definitely known.

ANALYTICAL METHODS

SiO_2 was determined (5) by double dehydration with hydrochloric acid, long ignition, and volatilization with hydrofluoric acid; Na_2O was determined (5) as sodium zinc uranyl acetate (it was previously ascertained that aluminum, in its maximum concentration encountered, did not interfere in the presence of an optimum concentration of hydrochloric acid); Al_2O_3 was determined (5) with 8-hydroxyquinoline. Iodide was determined (6) by oxidation to iodate with chlorine, removal of excess chlorine by boiling, reduction to iodine with iodide, and titration with thiosulfate.

RESULTS AND DISCUSSION

The data obtained are presented in tables 1, 2, and 3. The data of table 1, dealing with the determination of solid phase composition by the "tracer" method, are not equilibrium values, as will be evident upon reference to the method of preparation.

TABLE 1

Composition of the solid phase in the system Na_2O-SiO_2-H_2O

NO.	SOLUTION			RESIDUE			SOLID PHASE CALCULATED MOLAR RATIO		
	Na_2O	SiO_2	I	Na_2O	SiO_2	I	Na_2O :	SiO_2 :	H_2O
	per cent	*per cent*	*per cent*	*per cent*	*per cent*	*per cent*			
15	27.2	1.55	0.266	31.4	11.3	0.146	3.1 :	2 :	11.6
16	33.0	0.34	0.310	34.9	12.1	0.131	3.4 :	2 :	13.7
17	27.2	1.62	0.431	31.8	10.8	0.238	3.3 :	2 :	12.3
18	33.2	0.36	0.410	35.2	11.5	0.197	3.3 :	2 :	12.7
19	37.1	0.38	0.188	37.0	12.1	0.256	2.9 :	2 :	10.1
20	26.4	2.07	0.300	30.9	11.9	0.167	2.91 :	2 :	10.8
21	27.9	1.01	0.366	32.8	14.2	0.155	2.96 :	2 :	11.1
22	41.0	0.34	0.248	43.9	13.5	0.136	3.1 :	2 :	5.2
23	35.4	1.60	0.210	41.4	17.1	0.112	2.7 :	2 :	3.3
24	26.1	2.29	0.366	28.1	16.3	0.178	0.98 :	1 :	4.5
25	20.7	2.39	0.390	24.4	16.8	0.149	1.08 :	1 :	6.12

Notes: 15 and 16: residue from samples No. 10 and 13; sodium iodide added and centrifuged.

17, 18, and 19: residue from samples No. 10, 13, and 14 at room temperature for 2 weeks, sodium iodide added and centrifuged.

20 and 21: sodium iodide in supersaturated solution; crystallized by seeding at 25°C., analyses after 3 days.

22 and 23: spontaneously crystallized at room temperature with occasional shaking for several weeks; sodium iodide added.

24: sodium iodide in supersaturated solution; spontaneously crystallized at room temperature; analyses after 3 days.

25: residue from sample No. 5 at room temperature for several weeks, sodium iodide added and centrifuged.

Assuming the iodide present only in the solution phase and uniformly distributed, one may calculate the solid phase composition reported in the last three columns of table 1. Such a calculation is subject to cumulative error and is strongly dependent upon the iodide analyses. The proportion of water in the crystal, since it is determined by difference, is especially subject to error. However, the method is felt to be superior to the determination of composition by the intersection of "tie lines."

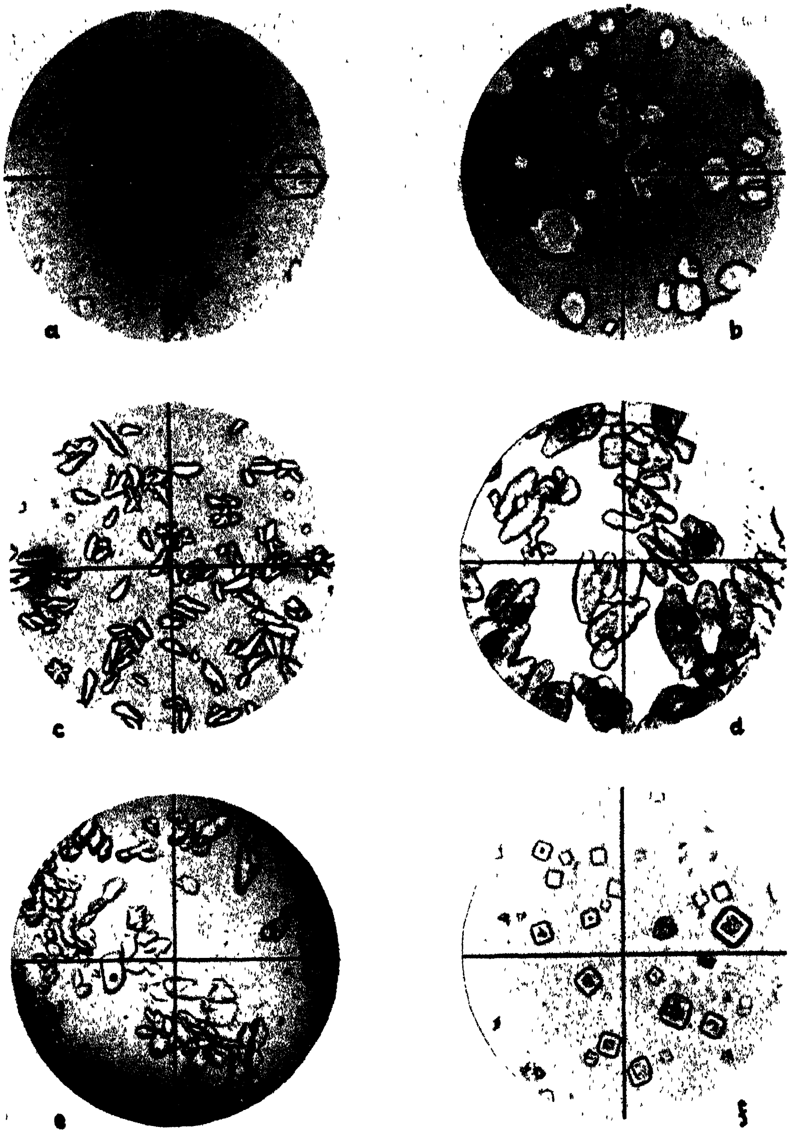

FIG. 1. Photomicrographs. a, lower hydrate of $3Na_2O \cdot 2SiO_2$, analysis No. 22; b, $Na_2O \cdot SiO_2 . 6H_2O$, aged crystals; c, freshly precipitated $Na_2O \cdot SiO_2 \cdot 6H_2O$; d, spontaneously crystallized $3Na_2O \cdot 2SiO_2 \cdot 11H_2O$, aged; e, seeded $3Na_2O \cdot 2SiO_2 \cdot 11H_2O$, analysis No. 9B before seeding with $Na_2O \cdot SiO_2 \cdot 6H_2O$; f, $Na_2O \cdot Al_2O_3 \cdot 2.5H_2O$.

The assumption of uniform distribution of iodide is dependent upon the efficiency of mixing in the cases in which iodide was added after crystallization. If there were solution containing no iodide trapped within the crystal, the $Na_2O:SiO_2$ and $H_2O:SiO_2$ ratios of the calculated composition would be high, since the solution in all cases was relatively poor in silica. When iodide was added before crystallization, this would not be the case; therefore, such values should be given added weight. The distribution of iodide would be more nearly uniform in the case of large, well-formed crystals.

The determination of the composition of $3Na_2O \cdot 2SiO_2 \cdot 11H_2O$ by the intersection of "tie lines" would have been impossible without greatly increasing the analytical accuracy and without growing larger, well-formed crystals by controlled seeding. However, the calculated composition by the "tracer" method is reasonably well represented by the formula given. Analyses No. 20 and 21 should be given added weight, both because iodide was added before crystallization and because the crystallization was effected by seeding. Photomicrographs of fairly characteristic crystals of $3Na_2O \cdot 2SiO_2 \cdot 11H_2O$ are shown in figure 1, d and e. This is the formula give by Morey (7) and mentioned in a footnote by Baker, Woodward, and Pabst (1), who reported crystallographic data on sodium metasilicate penta-, hexa-, octa-, and nona-hydrates. It presumably is the "crystalline sodium pyrosilicate hydrate" of Waddell (9).

Analyses No. 22 and 23 show evidence of lower hydrates of this salt. A photomicrograph of the No. 22 crystals is shown in figure 1, a. The crystals of No. 23 were, unfortunately, not photographed, but were distinctly different from any of the others, being in the form of thick needles.

The sodium metasilicate hexa- and nona-hydrates are well known. However, the characteristic habit of the hexahydrate observed in this study bore little resemblance to the triangular plates in the photographs by Vail (8), who summarizes the early work on this system, or to those of Baker, Woodward, and Pabst. The observed habit is well illustrated by figure 1, b.

Analysis No. 24 shows evidence of a lower hydrate of metasilicate obtained in one attempt to crystallize $3Na_2O \cdot 2SiO_2 \cdot 11H_2O$ spontaneously. The crystals were of indistinguishable form. On the basis of only one analysis, identification with either the pentahydrate of Baker, Woodward, and Pabst or the tetrahydrate of Vail would be unjustified. It is thought to be metastable at 25°C., though the solution falls fairly close to the solubility curve.

The reproducibility of equilibrium data may be judged by the separate determinations of the invariant points of tables 2 and 3. The differences are at least of the order of maximum estimated analytical error and presumably of the order of error in attainment of equilibria.

The data obtained in this study and the results of Harman are compared graphically in figure 2. Our region of stability of sodium metasilicate hexahydrate cannot be metastable with respect to the nonahydrate, since the seeding with nonahydrate of any solution in this region merely resulted in the dissolving of the seed. Harman did not experimentally establish univariant points but obtained them by intersection of the solubility curves, whereas most conclusive in regard to the accuracy of the present

TABLE 2

Equilibria in the system Na_2O–SiO_2–H_2O *at 25°C.*

NO.	COMPOSITION OF SOLUTION		SOLID PHASE
	Na_2O	SiO_2	
	per cent	*per cent*	
1	9.65	10.1	$Na_2O\cdot SiO_2\cdot 9H_2O$
2	8.69	2.93	$Na_2O\cdot SiO_2\cdot 9H_2O$
3	17.8	1.46	$Na_2O\cdot SiO_2\cdot 9H_2O$
4A	21.06*	2.03*	$Na_2O\cdot SiO_2\cdot 9H_2O + Na_2O\cdot SiO_2\cdot 6H_2O$
4B	21.03*	1.98*	$Na_2O\cdot SiO_2\cdot 9H_2O + Na_2O\cdot SiO_2\cdot 6H_2O$
5	20.6	2.18	$Na_2O\cdot SiO_2\cdot 6H_2O$ (metastable)
6	21.8	1.97	$Na_2O\cdot SiO_2\cdot 6H_2O$ (metastable)
7	22.9	1.98	$Na_2O\cdot SiO_2\cdot 6H_2O$ (metastable)
8	24.2	2.04	$Na_2O\cdot SiO_2\cdot 6H_2O$ (metastable)
9A	25.7*	1.83*	$Na_2O\cdot SiO_2\cdot 6H_2O + 3Na_2O\cdot 2SiO_2\cdot 11H_2O$
9B	25.9*	1.87*	$Na_2O\cdot SiO_2\cdot 6H_2O + 3Na_2O\cdot 2SiO_2\cdot 11H_2O$
10	27.2	1.55	$3Na_2O\cdot 2SiO_2\cdot 11H_2O$
11	27.8	1.23	$3Na_2O\cdot 2SiO_2\cdot 11H_2O$
12	28.9	0.75	$3Na_2O\cdot 2SiO_2\cdot 11H_2O$
13	33.0	0.34	$3Na_2O\cdot 2SiO_2\cdot 11H_2O$
14	36.7	0.30	$3Na_2O\cdot 2SiO_2\cdot 11H_2O$

* Determinations on separate equilibrium preparations.

TABLE 3

Equilibria in the system Na_2O–Al_2O_3–H_2O *at 25°C.*

NO.	SOLUTION		RESIDUE		SOLID PHASE
	Na_2O	Al_2O_3	Na_2O	Al_2O_3	
	per cent	*per cent*	*per cent*	*per cent*	
26	38.5	0.65			$Na_2O\cdot Al_2O_3\cdot 2\cdot 5H_2O$ + "Trisodium aluminate"‡
27	36.0	0.97	35.0	9.80	$Na_2O\cdot Al_2O_3\cdot 2.5H_2O$
28	28.8	2.16	29.0	11.14	$Na_2O\cdot Al_2O_3\cdot 2.5H_2O$
29	26.0	6.05			$Na_2O\cdot Al_2O_3\cdot 2.5H_2O$
30	21.1	15.5	25.2	29.5	$Na_2O\cdot Al_2O_3\cdot 2.5H_2O$
31A	20.9†	23.6†			$Na_2O\cdot Al_2O_3\cdot 2.5H_2O + Al_2O_3\cdot 3H_2O$
31B	20.1	23.4			$Na_2O\cdot Al_2O_3\cdot 2.5H_2O + Al_2O_3\cdot 3H_2O$
32	18.6	9.7			$Al_2O_3\cdot 3H_2O$

† Three weeks in thermostat as compared to about 7 weeks for 31B. Determinations on separate preparations.

‡ Reported by Fricke and Jucaitis (2) as $3Na_2O\cdot Al_2O_3\cdot 6H_2O$.

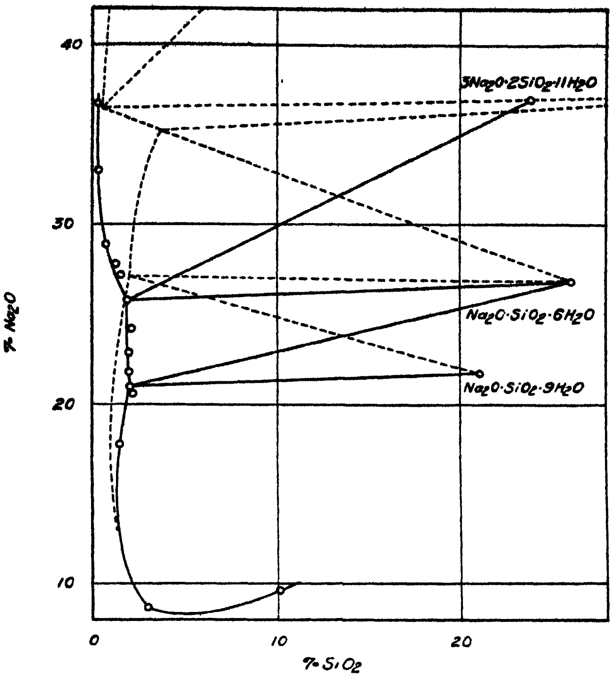

FIG. 2. The system Na_2O–SiO_2–H_2O at 25°C. ——, present work; - - -, Harman

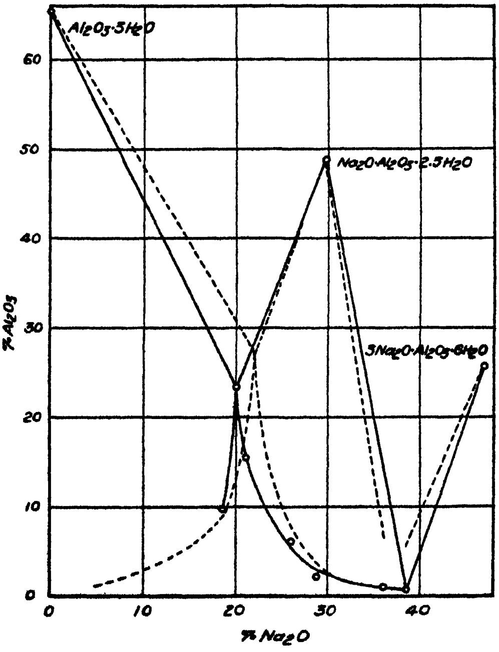

FIG. 3. **The system Na_2O–Al_2O_3–H_2O. ——, present work at 25°C.; - - -, Fricke and Jucaitis at 30°C.**

work in this respect is the reproducibility of the univariant point $Na_2O \cdot SiO_2 \cdot 6H_2O$–$Na_2O \cdot SiO_2 \cdot 9H_2O$ as indicated by analyses No. 4A and 4B, table 2.

Harman's reported region of stability of $Na_2O \cdot SiO_2 \cdot 6H_2O$ might possibly be a metastable extension of our equilibrium curve. No attempt was made to follow the metastable curve.

In figure 3 the present data on the sodium aluminate system are compared with that of Fricke and Jucaitis (2). The crystalline habits of the two aluminates were identical with the photomicrographs which illustrate the paper of these investigators (*cf.* figure 1, f). No attempt was made to check the composition of the high-soda aluminate. Microscopic identification of the two spontaneously crystallized aluminates established the univariant point.

SUMMARY

1. The system Na_2O–SiO_2–H_2O has been investigated at 25°C. from the ratio $Na_2O:SiO_2$ equal to 1:1 up to 36 per cent Na_2O by weight.

2. The phase diagram shows, in several places, marked differences from that derived from the work of previous investigators. In particular is the field of stability of $Na_2O \cdot SiO_2 \cdot 6H_2O$ at lower Na_2O concentrations than reported by Harman.

3. Evidence for the compound $3Na_2O \cdot 2SiO_2 \cdot (11?)H_2O$ at stable equilibrium is presented; lower hydrates may exist at somewhat higher temperatures and concentrations.

4. Some data on the system Na_2O–Al_2O_3–H_2O at 25°C. are presented.

We wish to acknowledge gratefully the valuable help given to us from time to time by Professor R. F. Newton of this laboratory.

REFERENCES

(1) Baker, Woodward, and Pabst: Am. Mineral. **18**, 206 (1933).
(2) Fricke and Jucaitis: Z. anorg. allgem. Chem. **191**, 129 (1930).
Jucaitis: Z. anorg. allgem. Chem. **220**, 257 (1934).
(3) Goudriaan: Proc. Acad. Sci. Amsterdam **23**, 129 (1920); Rec. trav. chim. **41**, 82 (1922).
(4) Harman: J. Phys. Chem. **31**, 511 (1927).
(5) Hillebrand and Lundell: *Applied Inorganic Analysis*, pp. 116, 522, 540. John Wiley and Sons, Inc., New York (1929).
(6) Kolthoff and Sandell: *Textbook of Quantitative Inorganic Analysis*, p. 599. The Macmillan Company, New York (1936).
(7) Morey: U. S. patent 1,948,730 (February 27, 1934).
(8) Vail: *Soluble Silicates in Industry*, p. 58. Chemical Catalog Company, Inc., New York (1928).
(9) Waddell: U. S. patent 1,953,840 (April 3, 1934).

THE ACTIVITY OF THE CONSTITUENTS IN MIXTURES OF *n*-BUTYL ALCOHOL AND WATER AT 30°C.

MERLE RANDALL AND HEINZ P. WEBER

Department of Chemistry, University of California, Berkeley, California

Received December 22, 1939

The partial vapor pressures of the constituents in binary mixtures of *n*-butyl alcohol and water were measured by a modification of the method of Winkelmann (6), which consists in passing a measured amount of inert gas,—in this case air,—through a solution, removing the absorbed vapors, and determining their weight and composition.

The glass contact tower A (figure 1), 1.8 cm. inside diameter by 100 cm. high, as measured between the entrance openings B and C for liquid and gas, respectively, was packed with shoe-eyelets (5) from a point 5 cm. below C to a height of 6 cm. above B. After passing through the calibrated wet-gas meter D, air was dried in the calcium chloride tower E, and passed through the soda-lime tower F and the bubbling tower G, which contained about 250 ml. of the same *n*-butyl alcohol–water solution as was circulated through the contact tower. After leaving A, the saturated air passed through the preheater H (resistance wire wound around the glass tube), where it was slightly heated to prevent any condensation, to the trap I, which was a U-shaped glass tube, the entrance leg having an internal diameter of 3 cm. and the bulb a capacity of approximately 50 ml. The *n*-butyl alcohol and water were condensed out of the air in the trap by means of a saturated solution of carbon dioxide in methyl alcohol, contained in the Dewar vessel J. Most of the water collected in the enlarged section where the ice adhered to the walls in large needles, while the larger portion of the *n*-butyl alcohol collected in the bulb. The air then passed to the house vacuum line, its pressure being measured by the manometer K and controlled by the manostat L.

The aqueous *n*-butyl alcohol was stored in the feed tank M (a 5-gallon tin can), which was equipped with a gauge glass Q, thermometer P, heater R, stirrer N, and toluene thermoregulator O (± 0.01°C.). It passed through the feed regulator S and a liquid trap T, and was collected by the sump tank U, from which it was returned to the feed tank by a small rotary pump V. Neoprene tubing was used to make the few necessary glass–metal and glass–glass connections.

The *n*-butyl alcohol was dehydrated by refluxing with benzene and removing the water layer from the distillate. After preliminary removal of the benzene, the *n*-butyl-alcohol-rich layer was fractionated in a 22-plate (approximately) column, the fraction between 117.40° and 117.45°C. being used for these experiments.

Samples were analyzed with the aid of a Zeiss–Raleigh interferometer (1) (cell 5 mm. long) kept in the same thermostated room (at 30°C. ± 0.1°) as that containing the vapor pressure apparatus.

The solution of a previous run was diluted slightly. After circulation through the contact tower at 50 or 60 ml. per minute without air flow and when temperature equilibrium was established, a sample was withdrawn and analyzed interferometrically. The flow of air was then adjusted to approximately 5 liters per hour, which was far below the safe maximum rate which was determined by preliminary tests. After approximately 80 liters of air had passed, the air stream was discontinued, and the trap was disconnected and closed with neoprene dams. After reaching room temperature, it was weighed, *n*-butyl alcohol was added to obtain a homogeneous solution, the trap was again weighed, and the contents were analyzed.

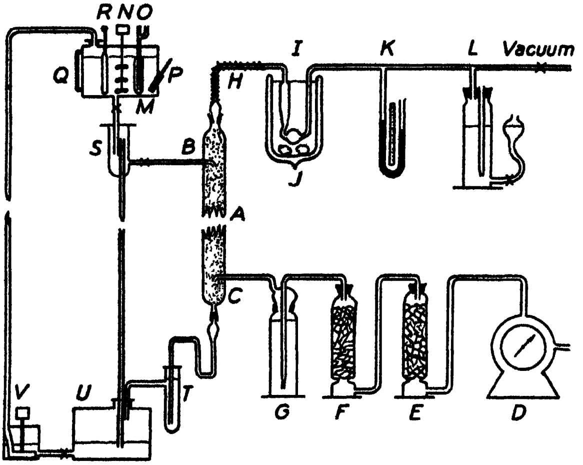

FIG. 1. Apparatus for measuring partial pressures of constituents in volatile mixtures

The results are given in table 1, where the first column gives the mol fraction of *n*-butyl alcohol in the solution in the tower, the second the dry-air volume in liters, the third the pressure at the top of the tower (which is the barometric height less the reading on the manometer K), the fourth the weight of condensed vapor, the fifth the average mol fraction of the condensate, the sixth the mol fraction of *n*-butyl alcohol in air at 1 atm. total pressure (designated p_1), the seventh the mol fraction of water in air at 1 atm. (designated p_2), and the eighth and ninth the activities of *n*-butyl alcohol and water, respectively.

If we assume that the gaseous solution is perfect, then the activity of *n*-butyl alcohol in the solution is given by the expression p_1/p_1^0, where p_1^0

is the mol fraction of the pure n-butyl alcohol at 30°C. in air at 1 atm. total pressure. Actually, p_1^0 was taken equal to the vapor pressure of n-butyl alcohol at 30°C. from the *International Critical Tables* (3). This procedure is justified by the fact that the measured values of p_1 shown in figure 2 extrapolated satisfactorily to the assumed value of p_1^0. Similarly (3) we have the values of the activity of water, a_2, shown in figure 2 and given in the last column of table 1. The solid curves of the activity shown in figure 2 were drawn through the experimental points, the circles on the curve being at the concentration of the mol fraction of water in the two conjugate liquid phases. The broken curves representing the activities of n-butyl alcohol and water were estimated with the aid of the expression (4)

TABLE 1

Activities of n-butyl alcohol and water

N_1 (SOLUTION)	V (DRY AIR)	P (IN TOWER)	WEIGHT OF CONDENSATE	N_1 (CONDENSATE)	$p_1 \times 10^3$	$p_2 \times 10^3$	a_1	a_2
	liters	*mm.*	*grams*					
0.9468*	87.666	743.5	4.0724	0.5512	12.539	10.211	0.999	0.234
0.9115*	81.013	744.0	3.9402	0.4294	11.882	15.789	0.949	0.377
0.8816	76.613	747.1	3.8610	0.3631	11.329	19.868	0.905	0.475
0.8455	85.696	751.0	4.5062	0.3198	11.026	23.447	0.880	0.560
0.8190	87.933	747.7	4.7882	0.2897	10.737	26.618	0.866	0.635
0.8048	81.477	746.6	4.5128	0.2756	10.461	28.224	0.857	0.674
0.7805	78.867	745.8	4.4397	0.2558	10.197	30.434	0.835	0.726
0.7553	71.164	745.1	4.046	0.2408	10.184	32.145	0.814	0.769
0.7338	90.759	744.4	5.260	0.2336	10.171	33.421	0.812	0.798
0.7105	50.548	745.7	3.001	0.2245	10.171	35.132	0.811	0.839
0.6885	83.069	744.8	4.879	0.2148	9.803	35.842	0.782	0.856
0.6680	97.714	744.2	5.838	0.2088	9.776	37.053	0.780	0.884
0.6420	64.963	742.8	3.897	0.2012	9.592	38.092	0.765	0.909
0.6195	72.535	748.1	4.380	0.1970	9.539	38.882	0.761	0.928
0.5965	74.980	749.0	4.545	0.1919	9.421	39.671	0.752	0.947
0.0076	81.418	744.2	3.803	0.1000	4.605	41.447	0.368	0.990

* Preliminary measurement.

$$\frac{N_1}{P_1}\left(\frac{\partial p_1}{\partial N_1}\right)_{P,T} = \frac{N_2}{P_2}\left(\frac{\partial p_2}{\partial N_2}\right)_{P,T} \tag{1}$$

There are two experimental measurements of the activity of n-butyl alcohol and water by Butler, Thomson, and Maclennan (2) at 25°C., which are shown as double circles in figure 2. The agreement with our measurements is excellent. The partial mol of heat of dilution of the constituents is small.

The agreement between the calculated and experimental values of the slopes is shown in table 2, where the symbols represent quantities already discussed.

We wish to thank Dr. Bruce Longtin for many valuable suggestions and Mr. Beppino Fontana and Mr. William Twitchell for the use of their fractionating columns.

Clerical and mechanical assistance of the Works Progress Administration is also gratefully acknowledged (O.P. No. 665-08-3-144).

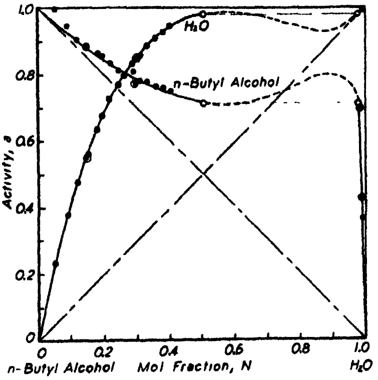

FIG. 2. Activities of the constituents in *n*-butyl alcohol–water mixtures at 30°C.

TABLE 2

Slope of the fugacity of water versus mol fraction curve

N_1	$p_1 \times 10^3$	$p_2 \times 10^3$	$\frac{\partial p_1}{\partial N_1} \times 10^3$	$\frac{\partial p_2}{\partial N_2} \times 10^3$ (CALCULATED)	$\frac{\partial p_2}{\partial N_2} \times 10^3$ (EXPERIMENTAL)
0.6	9.41	39.5	4.74	29.9	31.1
0.7	9.86	35.6	5.79	48.9	50.7
0.8	10.52	31.3	7.36	89.0	90.8
0.9	11.39	17.37	10.00	151.2	148.8
0.99	12.44	2.24	12.50	222.3	217.3

REFERENCES

(1) ADAMS: J. Am. Chem. Soc. **37**, 1181 (1915).
(2) BUTLER, THOMSON, AND MACLENNAN: J. Chem. Soc. **1933**, 674.
(3) *International Critical Tables*, Vol. III. McGraw-Hill Book Company, New York (1928).
(4) LEWIS AND RANDALL: *Thermodynamics and the Free Energy of Chemical Substances*. McGraw-Hill Book Company, New York (1923).
(5) RANDALL AND WEBB: Ind. Eng. Chem. **31**, 227 (1939).
(6) WINKELMANN: Ann. Physik [3] **39**, 99 (1890).

STUDIES ON AGING AND COPRECIPITATION. XXXIII

THE THERMAL AGING OF IMPERFECT BARIUM SULFATE

I. M. KOLTHOFF

School of Chemistry, Institute of Technology, University of Minnesota, Minneapolis, Minnesota

AND

W. M. MACNEVIN

Department of Chemistry, The Ohio State University, Columbus, Ohio

Received November 29, 1939

The purpose of this paper is to present data on the effects associated with the thermal aging of barium sulfate precipitates and to establish an hypothesis as to the probable mechanism involved. The term "thermal aging" is used in a collective sense, involving any permanent structural or dimensional or other change occurring in a precipitate when it is subjected to various temperatures. The method followed in this study was to prepare samples of barium sulfate which were both physically and chemically imperfect and to study changes in their physical and chemical character after various heat treatments. The thermal effects were studied by measuring the loss in weight on heating, by determining the specific surface of the heated products by adsorption of wool violet and water and by chromate exchange, by measuring the sedimentation volume, by determining the extractability of impurities, and by observation under the microscope.

PREPARATION OF BARIUM SULFATE

Product C_1: Forty grams of C.P. barium chloride dihydrate was dissolved in 240 ml. of water at room temperature. This solution was added over a period of 1.5 min. to a vigorously stirred solution of 24 g. of anhydrous sodium sulfate in the same volume of water (the sulfate was about 3 per cent in excess of the amount of barium). The suspension was quickly transferred to 250-ml. bottles, and centrifuged for 5 min. The supernatant liquid was immediately poured off, 150 ml. of water was added, and the bottles were shaken mechanically until the precipitates were well suspended, after which the suspension was centrifuged again. The supernatant liquid was discarded and the above washing process repeated eight times, after which no visible turbidity was obtained in a test for sulfate in the supernatant liquid. The age of the precipitate at this time was 46 min. The precipitate was now washed twice with 50 per cent ethanol, once with 95 per cent ethanol, and twice with absolute ethanol. To remove the alcohol, air was sucked through, and the precipitate was placed in an oven at 50°C. for 4 hr. and finally kept in a desiccator over sulfuric acid. Several batches of the above precipitate were prepared and thoroughly mixed.

Product C_2: This was prepared in a similar manner, except that the washing with water required 4 hr. before the treatment with alcohol. Consequently product C_2 was more aged than C_1 and had a smaller specific surface.

LOSS IN WEIGHT ON HEATING

In the following experiments about 5-g. samples of barium sulfate C_1 and C_2 were heated in a platinum crucible at various temperatures for a given period of time. The barium sulfate rested loosely in a heap in the bottom third of the crucible. After each period of heating the residue was cooled in a desiccator over concentrated sulfuric acid and weighed. The losses in weight are given in table 1.

TABLE 1

Losses in weight of barium sulfate products C_1 and C_2 on heating

TEMPERATURE	LOSS IN WEIGHT OF PRODUCT C_1 WHEN HEATED		TEMPERATURE OF HEATING	LOSS IN WEIGHT OF PRODUCT C_2 WHEN HEATED		
	1 hour	24 hours		1 hour	24 hours	80 hours
°C.	mg. per gram	mg. per gram	°C.	mg. per gram	mg. per gram	mg. per gram
100	0.04	1.36	100	0.2		
210	2.64		247	2.34		
310	8.14	10.7	300	3.60	4.40	9.6
395	10.98	16.9	380	5.32		
520	20.08	20.5	400	7.3	11.4	12.04
680	20.2		500	11.20	11.22	11.6
825	20.9		600	12.40	12.48	
1020	25.0		810	12.48	14.04	14.44
1210	28.7		970	14.44	14.5	
			1020	14.44	14.45	

By the following experiments it is shown that the loss in weight upon heating to temperatures of 700°C. are to be attributed to an escape of water. Samples of about 0.4 to 0.5 g. of the original air-dry product C_1 were heated in a micro combustion tube for 1 hr. at 580°C. with a slow current of dried air passing through. A micro adsorption tube filled with magnesium perchlorate and weighed to the nearest 2 micrograms was attached to the combustion tube. The losses in weight of the samples corresponded to those given in table 1 at temperatures between 570° and 680°C. and were equal to the gains in weight of the adsorption tube. Condensed water was observed at the exit of the combustion tube during the heating. Moreover, samples of barium sulfate were heated under similar conditions and the escaping gas passed through 1 ml. of water.

The pH of the water was unchanged and no chloride or sulfate was detectable.

The experiments were repeated with samples of product C_2 and corresponding results were obtained.

Upon longer periods of heating at 810°C. (table 1; see figure 1) or upon short periods of heating at higher temperatures an increased loss in weight was noticed. As the samples of barium sulfate used were not pure and contained occluded sodium chloride and sulfate in addition to water, it was thought that the additional losses in weight obtained at temperatures above 800°C. might be attributed to the volatilization of sodium chloride. This was proved to be true by the following experiments: One-gram samples of product C_2 were heated in a platinum boat which was contained in a quartz tube through which passed a stream of dry air. A micro water adsorption tube weighed to the nearest 2 γ was attached to the end of the quartz tube. The gains in weight of the adsorption tube were 12.08 mg. after heating for 1 hr. at 800°C. and 12.11 mg. after heating for 1 hr. at 1000°C., whereas the losses in weight of the precipitate were 12.3 mg. and 14.1 mg., respectively. Hence, the difference between the latter two figures is not caused by an escape of water after the precipitate had been heated to 800°C. The results reported in table 3 show that the additional loss in weight obtained at temperatures above 800°C. is to be attributed to a volatilization of occluded sodium chloride. Chloride was determined by dissolving the samples of barium sulfate in concentrated sulfuric acid, followed by distillation of the hydrochloric acid, which was collected in water. The chloride was precipitated, filtered on a Jena micro filtering tube, and weighed as silver chloride to the nearest 2 γ. Sodium was

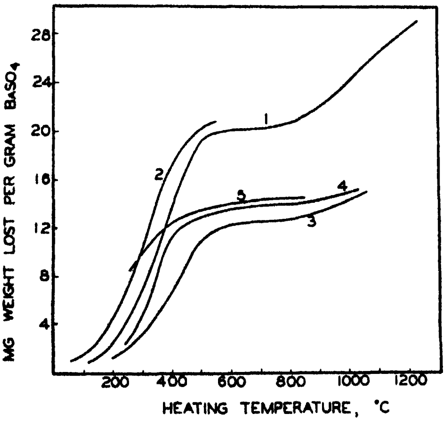

FIG. 1. Loss in weight of products C_1 and C_2 on heating. Curve 1, product C_1 1 hr.; curve 2, product C_1, 24 hr.; curve 3, product C_2, 1 hr.; curve 4, product C_2, 24 hr.; curve 5, product C_2, 80 hr.

determined by dissolving the samples in concentrated sulfuric acid and reprecipitating the barium sulfate with water. After filtration the barium sulfate was redissolved and reprecipitated. The combined filtrates were evaporated to dryness in platinum and the sodium determined in the residue as sodium zinc uranyl acetate. The amounts of chloride and sodium found are expressed in table 2 as sodium chloride. Evidently the greatest part of the occluded sodium is present in the form of sodium sulfate.

TABLE 2

Chloride and sodium contents and total losses in weight of samples (C_2) after heating for 1 hr. at specified temperatures

TEMPERATURE OF HEATING	LOSS IN WEIGHT	CHLORIDE CONTENT EXPRESSED AS NaCl	SODIUM CONTENT EXPRESSED AS NaCl	TOTAL LOSS IN WEIGHT MINUS LOSS IN WATER	DECREASE OF CHLORIDE CONTENT EXPRESSED AS NaCl	DECREASE OF SODIUM CONTENT EXPRESSED AS NaCl
°C.	*per cent*	*per cent*	*per cent*	*per cent*	*per cent*	*per cent*
		0.22	0.89			
600	1.24	0.21	0.88	0.0	0.0	0.0
800	1.26	0.17	0.82	0.02	0.04	0.06
1000	1.44	0.04	0.68	0.20	0.18	0.20

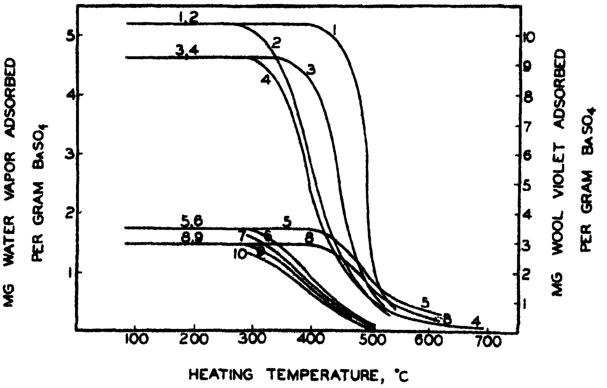

FIG. 2. Adsorption of water vapor and of wool violet by the heated products C_1 and C_2

	SUBSTANCE ADSORBED	PRODUCT	TIME
			hours
Curve 1	Wool violet	C_1	1
Curve 2	Wool violet	C_1	24
Curve 3	Water	C_1	1
Curve 4	Water	C_1	24
Curve 5	Wool violet	C_2	1
Curve 6	Wool violet	C_2	24
Curve 7	Wool violet	C_2	80
Curve 8	Water	C_2	1
Curve 9	Water	C_2	24
Curve 10	Water	C_2	80

The last three columns in table 2 show that the difference between the total loss in weight and the loss in water after heating for 1 hr. at 1000°C. is equal to the loss caused by the volatilization of sodium chloride.

TABLE 3

Specific surface: adsorption of water and wool violet

Period of heating in hours ..		1	24	1	24	1	24
PRODUCT	TEMPERATURE OF HEATING	GAIN IN WEIGHT (RELATIVE VAPOR TENSION = 0.57)		WOOL VIOLET ADSORBED		SPECIFIC SURFACE	
	°C.	*mg. per gram*		*mg. per gram*		*$M.^2$ per gram*	
C_1 . .	100	4 4	4.7	10.2		9.7	
	210	4.6	4.9	10.3	10.3	9.8	9.8
	310	4.6	4.6	10.2	10.0	9.7	9.5
	395	4.3	2.5	10.5	5.7	10.1	5.5
	520	0.54	0.46	1.1	0.75	1.06	0.7
	680	0.08	a*	(a)†	a	a	a
	825	<0.1	a	(a)	a	a	a
	1020	a	a	(a)	a	a	a
	1210	a	a	(a)	a	a	a

Period of heating in hours		1	24	80	1	24	80
PRODUCT	TEMPERATURE	GAIN IN WEIGHT (RELATIVE VAPOR TENSION = 0.57)			WOOL VIOLET ADSORBED		
	°C.	*mg. per gram*			*mg. per gram*		
C_2.	100	1.48			3.52		
	247	1.48			3 53		
	300	1.48	1.48	1.48	3.50	3.50	3.15
	380	1.48			3.54		
	400	1.48	0.72	0.64	3.54	1.76	1.52
	500	0.7	0.06	0.04	1.62	0.11	0.09
	600	0.24	0.02		0.60	0.05	a
	810	0.06	a	a	a	a	a
	970	a	a	a	a	a	a
	1020	a	a	a	a	a	a

* a = too small to be determined.

† (a) = not determined.

SPECIFIC SURFACE AFTER HEATING

Adsorption of water vapor

The heated products were placed in a hygrostat over deliquescent sodium bromide dihydrate (relative vapor tension = 0.57) until constant weight was obtained. The water taken up at this humidity was readily given off again over concentrated sulfuric acid. Qualitatively the behavior of product C_2 was found to be comparable to that of C_1, although the former had a specific surface which was only about one-third of that of product C_1. The results are summarized in table 3 (see figure 2).

Adsorption of wool violet

The specific surface was determined by the wool violet method described in a previous paper (3). The amounts of dye adsorbed were compared with those obtained with a product of known specific surface. A suitable amount (0.1 to 0.2 g.) of barium sulfate was shaken with 25 ml. of a wool violet solution containing 0.5 g. of dye per liter. After centrifuging, the dye content was determined in the clear supernatant liquid. The results obtained with product C_1 are given in table 3 (see also figure 2).

Exchange with chromate ion

From the exchange between chromate and sulfate ions in the surface of barium sulfate it is possible to calculate the specific surface of the latter (1). Upon shaking 0.4 g. of the original unheated sample (C_1) of barium sulfate with 50 ml. of an aqueous solution which was 0.001 molar in both sodium chromate and sulfate, the percentages of chromate removed were 22.7, 26.6, 31.2, and 53.0 after 20 min., 60 min., 180 min., and 21 hr., respectively. Extrapolation to a zero time of shaking yields an exchange in the surface corresponding to a removal of 28.7 per cent of chromate, and a specific surface of 5.75×10^{19} sulfate ions per gram of barium sulfate. This figure is in good agreement with the specific surface of 5.1×10^{19} barium ions per gram calculated from the adsorption of wool violet (table 3). In the following experiments 0.4-g. samples of the heated barium sulfate (C_1) were shaken for 3 hr. and 20 hr. with 50-ml. samples of the above chromate–sulfate solution, and the supernatant liquids after centrifuging were analyzed for chromate. By a linear extrapolation to a zero time of shaking the amount of chromate exchanged in the surface was found, and from this and the composition of the solution the specific surface

TABLE 4

Speed of exchange with chromate (product C_1): specific surface of barium sulfate

TEMPERATURE OF HEATING	TIME OF HEATING	CHROMATE REMOVED			SPECIFIC SURFACE $SO_4^{--} \times 10^{-19}$ PER GRAM OF $BaSO_4$	SPECIFIC SURFACE $Ba^{++} \times 10^{-19}$ FROM DYE ADSORPTION
		After shaking for 3 hr.	After shaking for 20 hr.	Extrapolated to zero time		
°C.	*hours*	*per cent*	*per cent*	*per cent*		
		32.4	53.0	28.7	5.8	5.1
100	24	30.8	46.5	27.9	5.5	
200	24	29.7	42.8	27.5	5.9	5.1
300	1	30.6	45.0	28.0	6.3	5.1
300	24	26.4	34.5	24.8	5.3	5.0
400	1	27.3	38.5	25.5	5.5	5.2
400	24	18.0	22.0	17.5	3.3	2.85
500	1	4.5	7.0	4.1	0.63	0.55
500	24	3.5	5.0	3.0	0.45	0.37

was calculated. The linear extrapolation gives only approximate values of the surface exchange, as the products were fairly imperfect. However, the order of magnitude of the calculated specific surface should be correct. The results are given in table 4. The speed of penetration of the chromate into the sulfate gives an indication of the degree of perfection of the product (4). The slope of the lines giving the percentage of chromate removed with time of shaking is given in figure 3. It is seen that the products are hardly perfected when heated for 1 hr. to temperatures of 400°C. When they are heated for 24 hr. at 300°C. the slope of the line becomes slightly less, which may be due to a difficulty in breaking up the agglomerated particles. The decreased slope of the lines obtained with the products heated for 24 hr. at 400°C. and for 1 hr. or longer at 500°C. is due mainly to a decrease of the specific surface as a result of sintering. No conclusive indication is obtained from these experiments that the precipitates perfect themselves at temperatures of 500°C.

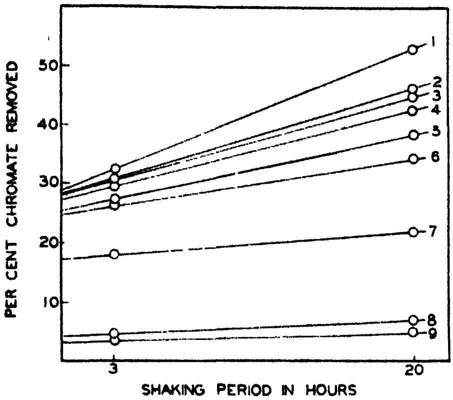

FIG. 3. Removal of chromate from solution by heated products

	TREATMENT OF BARIUM SULFATE (C_1)	
	Temperature	Time
	°C.	*hours*
Curve 1 (original)		
Curve 2	100	24
Curve 3	300	1
Curve 4	200	24
Curve 5	400	1
Curve 6	300	24
Curve 7	400	24
Curve 8	500	1
Curve 9	500	24

SEDIMENTATION VOLUME (PRODUCT C_1)

One-gram samples of the heated products were shaken for 24 hr. with 25 ml. of distilled water. After centrifuging, the pH was determined in the supernatant liquid with the glass electrode and found to be equal to 5.5 ± 0.3 in the extracts of all of the heated products (100–1200°C.). The precipitates were transferred to 15-ml. graduated conical centrifuge tubes and centrifuged slowly (800 R.P.M.) for 5 min. The volume of the precipitates was read and the tubes were centrifuged for another 5 min. When the second reading differed from the first, a third centrifuge treatment for 5 min. was given. Duplicates were run in each case with agreement as good as the reading of the precipitate volumes (0.02 ml.). The results are given in table 5. The sedimentation volumes of the first four products undoubtedly would have been greater if aging during the 24 hr. of shaking with water had been prevented.

TABLE 5

Sedimentation volume (product C_1)

HEATING OF BARIUM SULFATE		SEDIMENTATION VOLUME	HEATING OF BARIUM SULFATE		SEDIMENTATION VOLUME
Temperature	Time		Temperature	Time	
°C.	*hours*	*ml.*	*°C.*	*hours*	*ml.*
		0.90	500	1	0.45
100	1	0.92	680	1	0.38
300	1	0.90	825	1	0.33
400	1	0.91	1020	1	0.33
400	24	0.63	1210	1	0.33

EXTRACTABILITY OF OCCLUDED CHLORIDE AND SODIUM (PRODUCT C_2)

The extraction experiments were carried out with a Soxhlet apparatus, using 5-g. samples. The extraction was allowed to run for 2 hr., during which time the liquid filled the chamber twenty-two times. Extractions were also run for 10 hr., but the amounts of chloride and sodium extracted never exceeded 2 per cent of those extracted after 2 hr. The extracts were diluted to 250 ml., and the chloride and sodium were determined in aliquot portions. The original sample contained 0.22 per cent of chloride (expressed as sodium chloride) and 0.88 per cent of sodium (expressed as sodium chloride). From the results in table 6 it is evident that about one-half of the occluded sodium and chloride is extracted from the unheated product. This has to be attributed mainly to an aging (recrystallization) of the barium sulfate during the extraction. After heating for 1 hr. at 1000°C. only 0.03 per cent of chloride was extracted and only 75 per cent of the total amount of sodium which was present in the original precipitate. The reason is that at 1000°C. practically all of the occluded chloride volatilizes in the form of sodium chloride (see also table 2). After heating for 1 hr. at 800°C. only 0.05 per cent of chloride was found to have volatilized (table 2), whereas the remaining chloride and sodium (the latter partly as chloride and partly as sulfate) was completely extractable (table 6).

MICROPHOTOGRAPHS

Microphotographs were made of samples of C_1 and C_2 after heating for various periods at different temperatures. Some of the results are given in figures 4, 5, 6, and 7. The photographs of the samples which had been heated to 500°C. show agglomerates containing a great number of primary particles. Vigorous mechanical shaking with water or with aqueous solutions of wool violet or sodium citrate caused complete disintegration of the agglomerates, but on standing the particles formed aggregates. After heating to temperatures below 500°C. the size of the individual primary particles was too small to allow their microscopic measurement. The growth of the primary particles and the development of the crystals became very pronounced at temperatures above 680°C. After heating for 1 hr. at 810°C. the individual crystals had a size of the order of 10 microns, and after heating to 1210°C. of 40 to 90 microns. The beautiful development of the rhombohedron faces is shown by the photograph in figure 7.

TABLE 6

Extractability of chloride and sodium after heating for 1 hr. at specified temperatures

Product C_2, containing 0.22 per cent Cl^- (as NaCl) and 0.88 per cent Na^+ (as NaCl)

Temperature of heating, in °C.		600	800	1000
Chloride extracted in per cent (as NaCl)	0.082	0.083	0.17	0.03
Sodium extracted in per cent (as NaCl)	0.46	0.45	0.81	0.66

DISCUSSION

1. The water which was slowly given off upon heating the imperfect samples of barium sulfate at temperatures below 400°C. and more rapidly at higher temperatures is not *adsorbed* water but *occluded* water (table 1). The heated products took up water again when placed at relative water vapor tensions of 0.6 to 1.0, but this water was rapidly lost when the samples were placed over concentrated sulfuric acid at room temperature or when they were heated at 100°C. One might attribute this behavior to the fact that the original samples of the barium sulfate had a porous character and that the capillaries in the inside were difficultly wetted after the heat treatment. In order to disprove this assumption the following experiments were made: Products heated for 1 hr. at 100°C. and at 480°C., respectively, were shaken vigorously for 1 hr. with 25 ml. of 0.001 molar barium chloride solution in water, after which they were washed in the

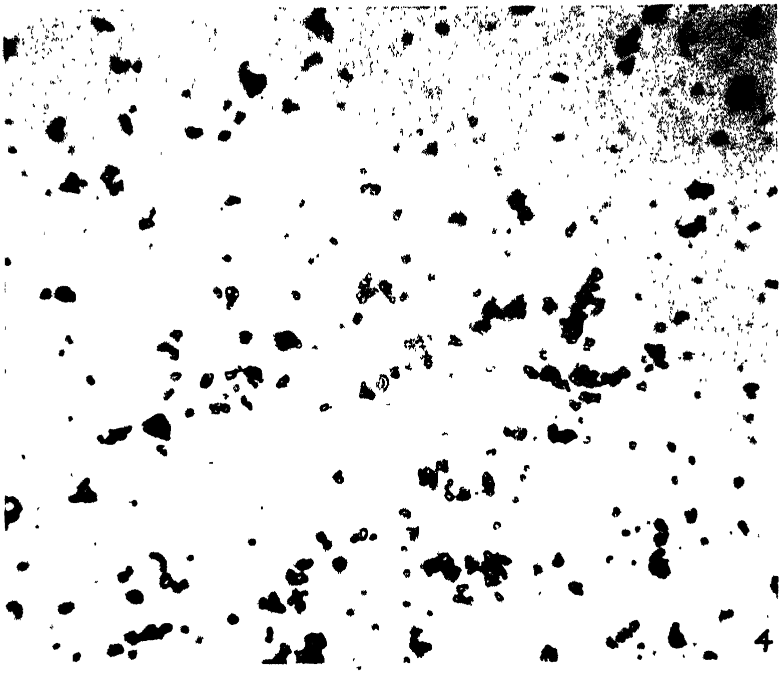

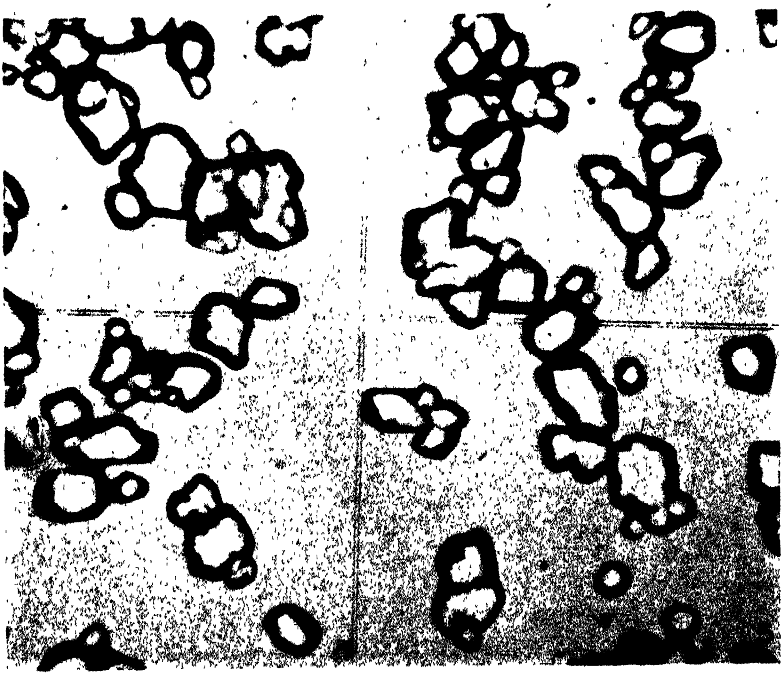

FIG. 4. Product C_1 after 1 hr. at 520°C. Magnification = 1000 ×
FIG. 5. Product C_1 after 1 hr. at 680°C. Magnification = 1000 ×

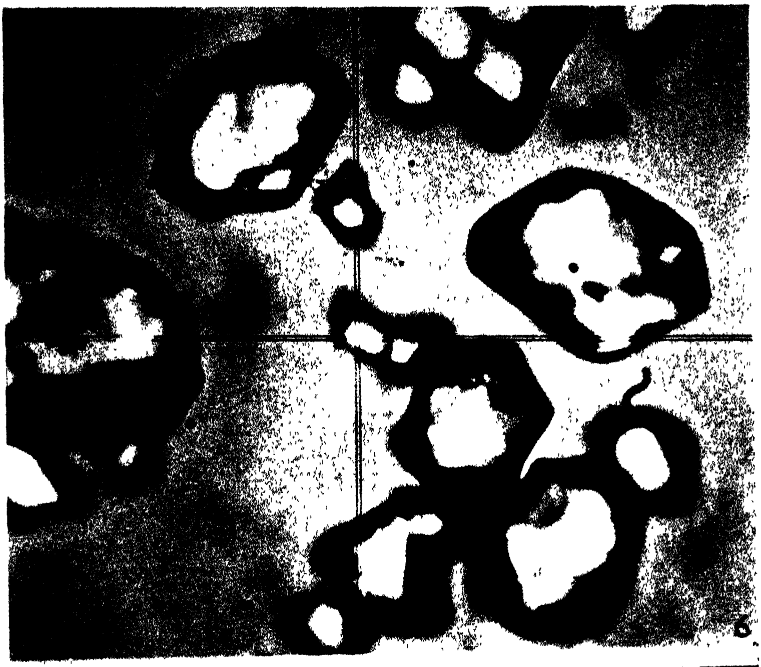

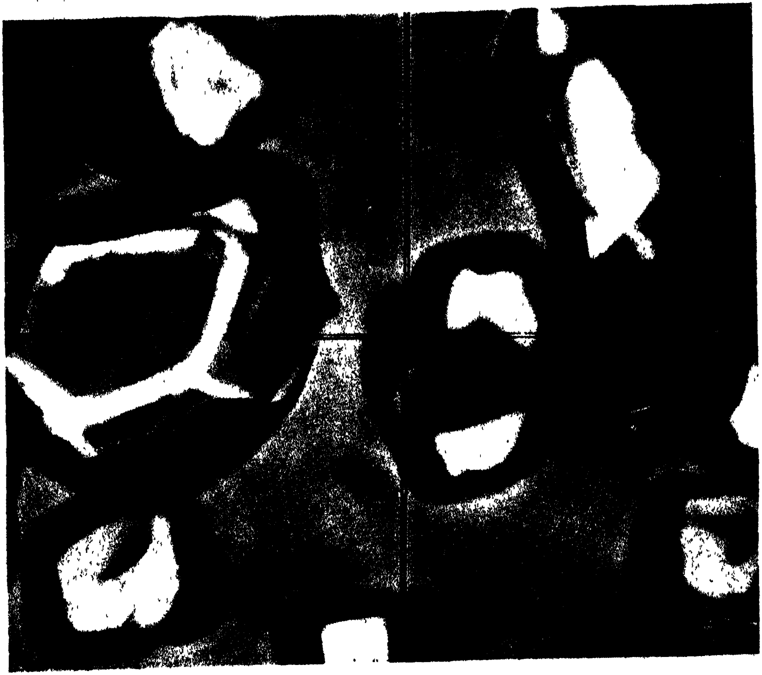

FIG. 6. Product C_1 after 1 hr. at 1020°C. Magnification = 1000 ×
FIG. 7. Product C_1 after 1 hr. at 1210°C. Magnification = 1000 ×

centrifuge until free from chloride, filtered, and made air-dry. They were then subjected to a heat treatment as described in table 1. The product, dried at 100°C., gave a loss-in-weight curve comparable to that of the original product, except that the losses in weight were less than found with the unheated product, as the specific surface had decreased by about 40 per cent, owing to aging in the barium chloride solution. The product which had been heated for 1 hr. at 480°C. did not lose in weight after the treatment with barium chloride and reheating to 480°C. for 1 hr. From work carried out with more perfect products of barium sulfate it was also concluded (2) that the above loss in weight upon heating is due to occluded water. From a practical point of view it is of interest to conclude that the amount of occluded water in these imperfect and impure products is given off quantitatively when the products are heated for 1 hr. at temperatures between 500° and 800°C. Upon heating for longer periods of time at 800°C., or for shorter periods at higher temperatures, occluded sodium chloride is also removed by volatilization.

2. The water taken up by a dry product over deliquescent sodium bromide dihydrate (relative vapor tension = 0.57) is reversibly adsorbed. Adsorption equilibrium is attained within 12 hr. From the results given in tables 1 and 3 it is seen that the amounts of water adsorbed at a relative water vapor tension of 0.57 are strictly proportional to the specific surface. Taking the average of the ratios of the number of milligrams of water and milligrams of wool violet adsorbed we find from the results in tables 1 and 3 that 1 mg. of water is adsorbed per 2.1 mg. of wool violet. Working with an entirely different product, Bushey and Kolthoff (2) found 1 mg. of water adsorbed for 2.0 mg. of wool violet. In a previous paper (3) it has been reported that an adsorption of 1 mg. of wool violet per 1 g. of barium sulfate corresponds to a specific surface of 4.8×10^{18} barium ions and of 0.95 M.^{2} per gram and an average particle size of 1.38 microns. Hence the specific surface of product C_1 corresponds to 49×10^{18} barium ions or 9.7 M.^{2} per gram, and to an average particle size of 0.14 micron. The corresponding figures of product C_2 are about 2.9 times smaller and the average particle size 2.9 times greater.

From the above we find that, at a relative vapor tension of 0.57, 1 mg. of water or 3.4×10^{19} molecules of water are adsorbed per 1.01×10^{19} barium ions in the surface of barium sulfate. Approximately, then, three molecules of water are adsorbed per molecule of barium sulfate in the surface, which would correspond to a trimolecular layer of water.

The thickness of the adsorbed layer seems to depend upon the relative vapor tension. Thus we found at a relative vapor tension of 0.85 that the amount of water taken up was 3.5 times greater than that adsorbed at a vapor tension of 0.57. At the higher vapor tension it took several days before equilibrium was attained, and an aging of highly dispersed and imperfect barium sulfate might occur in that period of time.

Upon heating the samples of barium sulfate for 24 hr. at 500°C. the specific surface was found to decrease by ten to thirty times (table 3). In spite of this pronounced thermal aging the surprising result was found that the amount of water taken up at the vapor tension of 0.85 was 100 times as great as that taken up at the vapor tension of 0.56. This striking result is attributed by us to a condensation of water in the capillaries of the sintered particles (500°C.) at a vapor tension of 0.85, whereas no such condensation occurred at a vapor tension of 0.57. More work should be done to substantiate this conclusion.

Incidentally, it may be mentioned that the *specific surface of barium sulfate can be calculated from the amount of water adsorbed at a vapor tension of 0.57*. The product of barium sulfate is dried at 100°C. or at room temperature over concentrated sulfuric acid until constant weight is attained and then placed over deliquescent sodium bromide dihydrate until constant weight is reached (1 day). One milligram of adsorbed water corresponds to a specific surface of 10×10^{18} barium ions, or of 2.0 $M.^2$ per gram, and an average particle size of 0.66 micron.

Preliminary experiments have also been made on the adsorption of ethanol by barium sulfate. Unheated and heated samples of product C_1 were placed over absolute ethanol. The amounts of alcohol taken up were unusually large and greatly dependent upon the temperature of the room. However, when the samples were placed in a hygrostat over deliquescent $CaCl_2 \cdot 3C_2H_5OH$ the amounts of alcohol adsorbed seemed to be proportional to the specific surface and were found to be less than the amounts of water adsorbed at a water vapor tension of 0.56. For example, under the above conditions, 1 g. of product C_1 adsorbed 2.52 mg. of ethanol and 4.5 mg. of water per gram.

3. Thermal aging of the samples of barium sulfate used was found to be extremely slow at 300°C. After 24 hr. of heating at this temperature the specific surface of the products remained unchanged, but after 80 hr. of heating of sample C_2 a slight decrease was noticed. Even at 400°C. no change of the specific surface was noticed after 1 hr. of heating, but after 24 hr. of heating, a distinct decrease was found. At 500°C. the aging was already very pronounced after 1 hr. of heating. But after 24 hr. of heating at 500°C. the specific surface of product C_2 decreased to one-tenth of its original value. Apparently the occluded water has no effect upon the speed of aging. After 1 hr. of heating at 500°C. practically all of the occluded water had been removed, but a very pronounced decrease of the specific surface occurred upon further heating.

It is evident from the results in table 5 that the thermal aging, as indicated by the decrease of the specific surface, is accompanied by a decrease of the sedimentation volume.

The various experiments described do not show conclusively exactly what is happening during the thermal aging. The microscopic observations indicate that at temperatures below 600°C. a cementing of the particles in the agglomerates occurs by sintering, without being accompanied by a perfection (recrystallization) of the sintered primary particles. These sintered agglomerates have a loose porous structure. Upon heating at temperatures of 700°C. and above, a rapid recrystallization occurs and the individual crystals grow with increasing temperature, a final state being reached within 1 hr. of heating. There is no conclusive evidence to show that the development of the larger crystals is a result of the fact that the tiny imperfect particles have a larger vapor tension than the larger crystals. We believe that the recrystallization of the sintered particles to larger, more perfect and compact individual crystals is a result of the thermal mobility of the ions in the barium sulfate at higher temperatures. The emanation experiments of Hahn and coworkers (1) show conclusively that the "loosening temperature" (relaxation temperature) of barium sulfate is about 770°C. (1043° Abs.), corresponding to about one-half of its absolute melting point (1853° Abs.) (5).

The above interpretation is substantiated by the following observations: It has been mentioned that the sintered agglomerates formed at 500°C. absorb large quantities of water at a relative vapor tension of 0.85, indicating their porous structure. Moreover, it should be mentioned that after heating to 600°C. the occluded sodium and chloride could not be extracted, whereas the extraction became complete after heating for 1 hr. at 800°C. (table 6). At the latter temperature complete recrystallization had occurred and the foreign material was eliminated from the more perfect lattice. The complete volatilization of occluded sodium chloride at temperatures higher than 800°C. is no indication of recrystallization.

Finally, we wish to emphasize that the conclusions drawn should not be generalized, as it is anticipated that the kind and amount of thermal aging will greatly depend upon the physical and chemical purity and the size of the particles of the precipitate used.

SUMMARY

1. Imperfect products of barium sulfate slowly lost occluded water when heated to temperatures between 200° and 400°C. When heated for 1 hr. at 500°C. practically all of the occluded water was removed.

2. The removal of occluded water upon heating at temperatures below 400°C. was not accompanied by thermal aging. The presence of occluded water was shown to have no effect upon the speed of thermal aging.

3. Barium sulfate, dried either at room temperature over concentrated sulfuric acid or at 100°C., adsorbed water at a relative vapor tension of 0.57. The amount of water adsorbed corresponds to a layer three molecules thick. Use of this fact can be made in the determination of the specific surface of barium sulfate.

4. At a relative vapor tension of 0.85 the amount of water taken up was about 3.5 times that adsorbed at a vapor tension of 0.56. Upon thermal aging of barium sulfate at 500°C. the amount of water taken up at a vapor tension of 0.85 became abnormally great. This is attributed to condensation of water in the capillaries of the sintered particles.

5. Occluded sodium chloride was completely removed by volatilization at temperatures above 800°C.

6. Occluded sodium chloride could be completely extracted with water after heating the barium sulfate for 1 hr. at 800°C.

7. Thermal aging, as indicated by a decrease of the specific surface, did not occur after heating for 24 hr. at 300°C. or for 1 hr. at 400°C. After longer periods of heating at 400°C. a slow decrease of the specific surface was found. At 500°C. a marked aging was found after 1 hr. of heating, the surface decreasing greatly upon longer periods of heating. This aging is attributed to a sintering of the primary particles in the agglomerates without being accompanied by internal recrystallization.

8. The aging became very rapid upon heating at temperatures above 700°C., a final state being reached after 1 hr. Well-developed individual crystals were formed, the size of which increased with increasing temperature. The development of these crystals is attributed to the combined effects of sintering and internal recrystallization (thermal mobility), the latter being responsible for the extrusion of foreign materials which do not fit into the lattice.

This work was started with the aid of a grant assigned to one of us by the Graduate School of the University of Minnesota in the summer of 1936. The experimental study was later continued in the Department of Chemistry of The Ohio State University.

REFERENCES

(1) Hahn, O., and Keim, R.: Z. anorg. allgem. Chem. **206**, 398 (1932).
(2) Kolthoff, I. M., and Bushey, A. S.: Bull. soc. chim. Belg. **47**, 689 (1938).
(3) Kolthoff, I. M., and MacNevin, W. M.: J. Am. Chem. Soc. **59**, 1639 (1937).
(4) Kolthoff, I. M., and Noponen, G. E.: J. Am. Chem. Soc. **60**, 499, 505 (1938).
(5) Tammann, G., and Sworykin, A.: Z. anorg. allgem. Chem. **176**, 46 (1928).

PHOTOVOLTAIC BEHAVIOR OF PURE SILVER BROMIDE

HERBERT L. SANDERS[1] AND I. M. KOLTHOFF

School of Chemistry, Institute of Technology, University of Minneapolis, Minneapolis, Minnesota

Received October 24, 1939

Although photovoltaic effects at a large number of electrode systems have been studied, the silver halide system is of particular interest for the light such investigations may shed on the mechanism of photosensitivity.

Previous work in this field (3, 6, 7) has not succeeded in producing very concordant results. The electrodes used were invariably of the silver–silver halide type, in which a metallic silver electrode is coated with a porous layer of the silver halide. The potential changes at such electrodes, upon illumination, have been found to depend largely on the thickness and structure of the silver halide coating. Both negative and positive changes have been observed, usually the former for the first moment of illumination, followed by a change to the latter type with continued irradiation.

It was felt by the present authors that the general lack of agreement amongst previous workers was connected with the metallic nature of these electrodes. Such silver–silver halide systems act primarily as simple metallic silver electrodes, and are therefore susceptible to complicating oxidation–reduction effects from the products of reaction. If the potential changes at pure silver halide surfaces could be studied in the absence of any metal phase, the results obtained might conceivably be less obscure.

A previous paper (4) has shown that membranes of pure silver halides alter their potential with changes in silver-ion or halide-ion activities in the surrounding solution. Further, these changes in potential follow the well-known Nernst equation over very wide ranges. In other words, the surface of a pure silver halide in contact with a solution behaves electromotively like a simple silver electrode towards changes in silver-ion or halide-ion activities. Unlike a silver electrode, however, the presence of mild oxidizing or reducing substances has no effect on the potentials of the halide.

Later work by the junior author (5) has extended these results to the case of silver thiocyanate and thallous iodide as well.

For the purposes of this brief study, attention was focussed on the case of silver bromide, though any of the other salts mentioned might have been chosen.

---

[1] **Present address: Virginia Chemical Corporation, Piney River, Virginia.**

EXPERIMENTAL

The general method of approach was that of illuminating a membrane-type silver bromide electrode and noting the resultant changes in potential. The pBr (negative logarithm of bromide-ion activity) of the solution was determined by immersing the usual type of silver–silver bromide electrode and measuring its potential against a saturated calomel electrode. This silver–silver bromide electrode (henceforth written Ag–AgBr) was made by anodizing a silver-plated platinum wire in 0.1 *N* potassium bromide for several minutes at 2 milliamperes; then it was thoroughly washed. These Ag–AgBr electrodes did not show such good inter-electrode agreement in the dark as do the corresponding Ag–AgCl or Ag–AgI types. Vanselow and Sheppard (7) describe similar difficulties. However, several electrodes were obtained agreeing to 0.001 volt, which is satisfactory for our purposes.[2] From the E.M.F. of the calomel|Ag–AgBr chain, the pBr of the solution was calculated, using −0.0711 volt as the normal electrode potential of silver bromide. Needless to say, both the calomel and the Ag–AgBr electrodes were at all times shielded from direct illumination.

The membrane-type silver bromide electrodes (henceforth written AgBr) were made as previously described (4) by fusing pure silver bromide into disk form, then cementing this salt disk with sealing wax to the end of a 10-mm. wide glass tube. A solution of 0.01 *N* potassium bromide was poured into the tube, and an inner reference Ag–AgBr electrode dipped into this. This unit consisting of disk, tube, and inner electrode is the so-called "AgBr" electrode. Two such membrane electrodes will not necessarily show the same potential in a given solution, owing to strain or asymmetry potentials in the salt disk, but they will show very nearly the same changes as the pBr of the solution varies.

The glass tube carrying the salt membrane was made L-shaped to allow direct illumination of the disk. It was also coated with sealing wax to shield the inner Ag–AgBr electrode from light, although preliminary tests showed this type gave only very feeble photopotentials with the intensity used.

The light source was simply a 32-C.P. carbon filament bulb at 20 cm. This low intensity was chosen so as to avoid too drastic photodecomposition of the silver bromide disk. A water-filled jar in front of the light source acted as a heat filter.

Potentials were measured with a vacuum-tube voltmeter employing an FP 54 Pliotron tube.

---

[2] After this work had been completed excellent papers by E. R. Smith and J. K. Taylor (J. Research Natl. Bur. Standards **20**, 837 (1938)) and by J. K. Taylor and E. R. Smith (J. Research Natl. Bur. Standards **22**, 307 (1939)) on the preparation of reproducible silver–silver halide electrodes appeared.

The pBr of the solutions was varied by starting with pure water and gradually adding potassium bromide to give low pBr values, or silver nitrate to give high ones. In this way no turbidity due to precipitated silver bromide existed at any time.

A run, then, consisted of placing the calomel, Ag–AgBr, and AgBr electrodes in the solution contained in a Pyrex beaker, working in dim light throughout. The E.M.F. of the calomel|Ag–AgBr pair was first measured, and the pBr computed from this. The calomel|AgBr couple was measured next, and this "dark value" noted. The bulb was then switched on, when the calomel|AgBr E.M.F. slowly changed during about 2 min. to a new and constant value. The bulb was then switched off, and the new "dark value" noted. This became constant after about 1 min. Then the pBr was altered by adding either potassium bromide or silver nitrate, and the cycle repeated.

RESULTS

It was found that on illuminating the silver bromide membrane electrodes, even with this comparatively feeble source, photovoltaic effects of several millivolts were easily detected.

Writing the electrode chain as

$$\mathrm{Ag} \mid \mathrm{AgBr(s)},\ \mathrm{Br^-}\ (0.01\ N) \mid \mathrm{AgBr(membrane)} \mid \mathrm{Br^-}\ (a) \mid \mid \mathrm{calomel\ (satd.)}$$

we adopt the convention that the sign of the E.M.F. is positive when positive current can flow from left to right as written, i.e., when the calomel electrode is positive to the silver bromide membrane unit. Hence an increase in the positive value of the cell E.M.F. on illumination signifies a change to more negative values in the silver bromide unit. Since the inside is shielded, such a change in the unit must be due to a change in the potential of the silver bromide surface itself.

Table 1 presents the data for two runs, using different membrane electrodes. Curves I and II in figure 1 depict these results graphically for runs 1 and 2, respectively, in table 1.

The interesting fact emerges from these data that the photovoltaic effect at pure silver bromide is *always* negative in sign, i.e., the potential becomes less positive on illumination. This is in contradiction to the results of the prior work cited above.

Furthermore, it is important to note that as the pBr of the solution is varied there is a sharp maximum found for the photopotentials. The magnitude of the effect falls off at higher concentrations of both silver and bromide ions. The maximum effect is seen to occur very close to pBr 6. The solubility product of silver bromide is about 4×10^{-13}, so this corresponds to the pBr of pure water saturated with the salt. In other words, the maximum photopotential is found near the silver bromide equivalence point.

So far as the reproducibility of the E values is concerned, it was found that practically the same potential shift was obtained on several successive illuminations, showing that the result is not fortuitous.

As will be seen from table 1, the potential of the silver bromide electrode does not return completely to its original value after being illuminated. The discrepancy does not seem to depend on the pBr value of the solution.

The effect of agitation is also worthy of mention. The experiments described were run using constant agitation throughout. It was observed, however, that in the absence of stirring the photopotentials obtained were much larger, and that the recovery time after cutting off illumination was much longer. Such behavior would point strongly to the presence of a soluble reaction product as a result of illumination.

TABLE 1

Photovoltaic changes in silver bromide electrodes

(All E.M.F.'s against saturated calomel)

INITIAL AgBr NO. 2 E.M.F.	ILLUMINATED AgBr NO. 2 E.M.F.	ΔE	FINAL AgBr NO. 2 E.M.F.	E.M.F. OF Ag-AgBr	pBr
Run No. 1					
volts	*volts*	*millivolts*	*volts*	*volts*	
+0.0457	+0.0479	−2.2	+0.0463	+0.0686	1.80
−0.0412	−0.0375	−3.7	−0.0400	−0.0257	3.40
−0.1230	−0.1162	−6.8	−0.1226	−0.1100	4.81
−0.1357	−0.1283	−7.4	−0.1350	−0.1233	5.03
−0.1552	−0.1492	−6.0	−0.1540	−0.1440	5.39
−0.2136	−0.2095	−4.1	−0.2129	−0.2038	6.41
−0.3140	−0.3128	−1.2	−0.3134	−0.3053	8.13
Run No. 2: As above but using AgBr No. 4					
+0.0776	+0.0783	−0.7	+0.0789	+0.1033	1.20
+0.0396	+0.0431	−3.5	+0.0404	+0.0540	2.05
+0.0080	+0.0121	−4.1	+0.0080	+0.0050	2.88
−0.0342	−0.0289	−5.3	−0.0340	−0.0610	4.00
−0.0980	−0.0902	−7.8	−0.0980	−0.1558	5.59
−0.1974	−0.1929	−4.5	−0.1956	−0.1952	6.26
−0.2253	−0.2228	−2.5	−0.2240	−0.2282	6.82
−0.2750	−0.2742	−0.8	−0.2748	−0.2750	7.62

To show that the effects were not due to adsorption of light by the potassium bromide being added to the solution, a silver bromide electrode was allowed to come to equilibrium with pure water. Its photopotential was −9.9 millivolts. Now the water in the heat filter was replaced by a saturated potassium bromide solution. This time the photopotential was −10.1 millivolts. Hence the effect of the dissolved salt on the light passed through is negligible.

It has been said, above, that any change in potential of the silver bromide electrode unit must be due to a change at the fused salt disk. The question of whether only the outer face, or also the inner one, of the transparent membrane is effective has not yet been discussed. If illumination affected the potential of the inner side of the disk, this effect would be constant, since the inner side is always in contact with a solution of constant pBr. Further, the result would be to lower the observed photopotential, owing to the direction of current in the galvanic chain. However, it would seem likely that much of the effective light is adsorbed in its passage through the 2-mm. disk, and hence effects at the inner face would be very small. Examination of the transmitted light with a hand spectroscope showed that practically all the blue and violet were cut off.

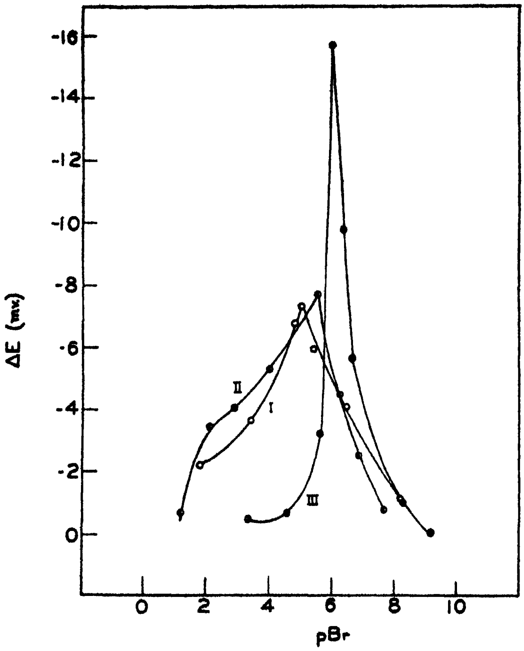

FIG. 1. Photopotentials of pure silver bromide membranes

Again, since the photopotential is less in concentrated solutions than in dilute ones, changing the 0.01 N internal solution to a concentrated one should eliminate any effect of the inner face and hence result in larger observed photopotentials. Actually, only very slight increases were found on trying this, indicating that the inner face does not contribute much.

Hence it would seem fairly safe to say that all observed photovoltaic effects of the composite silver bromide electrode are due mainly to potential changes at the outer face of the fused silver bromide disk.

In another experiment, instead of a fused disk of silver bromide as the membrane, a compressed tablet was used. The plasticity of the salt enables hard, non-porous tablets to be pressed with ease. The surfaces of this tablet were scraped clean, and it was soaked first in nitric acid and then bromine water to ensure the absence of all free silver. The electric conductivity of the opaque pressed tablet is very much greater than of the fused disks.

When the tablet was mounted as silver bromide electrodes in the usual way, it was found that only minute photopotentials could be obtained. This does not seem altogether in accordance with the previous statement that only the face of the disk is effective. Perhaps a penetration of some little distance into the salt is necessary before the light can become effective. In any event, replacement of the 32-c.p. bulb by a 100-watt tungsten type produced very much larger potentials. These results are given in curve III of figure 1.

TABLE 2

Variations of photopotential with pH

(E.M.F.'s against saturated calomel)

pH	INITIAL AgBr NO. 5 E.M.F.	ILLUMINATED AgBr NO. 5 E.M.F.	ΔE	FINAL AgBr NO. 5 E.M.F.	E.M.F. OF Ag–AgBr
	volts	*volts*	*millivolts*	*volts*	*volts*
1.95	−0.2015	−0.1955	−6.0	−0.2010	−0.1800
3.22	−0.2020	−0.1945	−7.5	−0.2017	−0.1811
5.69	−0.2003	−0.1903	−10.0	−0.2003	−0.1775
6.86	−0.1961	−0.1852	−10.9	−0.1950	−0.1738
8.10	−0.1920	−0.1816	−10.4	−0.1912	−0.1692
10.55	−0.1765	−0.1655	−11.0	−0.1755	−0.1650

After exposure to this high-intensity source, the yellow tablet was found to have taken on a violet tone.

Finally, a brief study was made of the effect of pH on the photopotentials at a definite pBr. The pH was varied by using a composite type of buffer and adding sodium hydroxide to it. A run was carried out by allowing the silver bromide and silver–silver bromide electrodes to come to equilibrium with the buffer, thus saturating it with silver bromide. Then the photopotential was measured at each pH. Table 2 indicates a tendency for lower photopotentials in acid solutions.

DISCUSSION

Previous theories of silver–silver halide photopotentials have variously ascribed them to change in solubility of the halide in light (3), to oxidation–reduction action of the solution on the halide under the influence of illumination (6), and to photoelectric emission of electrons by the electrodes into the solution (2). Vanselow and Sheppard (7) believe the primary effect is the splitting of a halogen ion in the solid silver halide, resulting in a free halogen atom and a free electron. The metallic silver may then be charged negatively by the electron, or positively by the halogen. Athanasiu (1) agrees that the free halogen is liberated, but apparently does not consider the resulting electron to reach the free metal of the electrode. Instead, the halogen is supposed to unite with hydroxyl ions in the solution to form the hypohalite

$$\mathrm{Br} + \mathrm{OH}^- = \mathrm{BrOH} + \text{electron}$$

and the electron thus released is what gives the metal its negative potential.

The results of the experiments recorded here would make it unnecessary to postulate free electrons as potential-determining factors. The most probable mechanism for the photovoltaic effect at metal-free silver bromide would seem to be mainly a photodecomposition, resulting in the liberation of a free bromine atom and an electron. The electron may then react to produce silver atoms, or simply take its place in the lattice according to the "perforated lattice" theory. In either case, this electron plays no rôle in the potential change, since we are dealing with a non-metallic system. The free bromine, however, can diffuse into the solution (a fact long recognized in photographic work) and there hydrolyze, giving hypobromite and bromide ions. It is these bromide ions that give the salt its negative potential, our earlier experiments having demonstrated that bromides make silver bromide negative.

The various effects described in this paper can be accounted for qualitatively by the above interpretation. The largest photovoltaic effect is observed at a pAg in the neighborhood of the equivalence point, where relatively small amounts of bromide formed cause a large change of pAg (see especially curve III, figure 1). The effects of stirring and of the pH are also in agreement with the above postulate. However, it should be emphasized that the small photovoltaic effects observed in solutions containing relatively large amounts of bromide or silver ions can hardly be attributed to the bromide formed by photodecomposition of the silver bromide. This secondary effect has not been further investigated. Possibly, it may be partly explained by a decrease in light sensitivity of the silver bromide in excess of silver or bromide ions.

The fact that positive photopotentials are never observed is due to the absence of free metal which may be oxidized by the bromine or hypobromite.

SUMMARY

Pure silver bromide has been shown to exhibit a photovoltaic effect even in the absence of all free metal. This has been explained as due mainly to the potential-determining action of bromide ions liberated by light at the salt-solution interface.

All previously reported photopotentials of silver–silver halide electrodes are complex functions of the above effect, plus the oxidizing action of free halogen or hypohalite on the metal, and hence almost impossible of exact interpretation or control.

REFERENCES

(1) ATHANASIU, M. G.: Ann. Physik **4**, 377 (1935).
(2) AUDUBERT, R.: Compt. rend. **179**, 682 (1924).
(3) GARRISON, A.: J. Phys. Chem. **28**, 333 (1924).
(4) KOLTHOFF, I. M., AND SANDERS, H. L.: J. Am. Chem. Soc. **59**, 416 (1937).
(5) SANDERS, H. L.: Thesis, McGill University, Montreal, 1937.
(6) TUCKER, C. W.: J. Phys. Chem. **31**, 1357 (1927).
(7) VANSELOW, W., AND SHEPPARD, S. E.: J. Phys. Chem. **33**, 331 (1929).

APPLICATION OF THE HYDROGEN-BRIDGE THEORY TO SORPTION FROM SOLUTION BY SILICA GEL[1]

ALBERT L. ELDER AND ROBERT A. SPRINGER

Department of Chemistry, Syracuse University, Syracuse, New York

Received August 7, 1939

In this paper some data are presented on sorption from solution, involving various solvents and solutes with silica gel as a sorbent. From the experimental facts an attempt has been made to draw some conclusions regarding the theoretical aspects of sorption phenomena. The principle of hydrogen bridging will be introduced as an explanation for the abnormalities observed in sorption work with silica gel.

EXPERIMENTAL

The manipulations necessary to obtain the data were very similar to those used by other investigators in the same field. In general, a series of acid solutions of varying concentration were made up in one of the organic solvents. Fifty cubic centimeters of each solution were introduced into a glass-stoppered flask and 5 g. of Patrick's silica gel (10 to 20 mesh) were added. The gel was previously washed five hundred times with distilled water in a Soxhlet apparatus and activated at 400°C. The flasks were then transferred to a shaking machine kept at 20°C. After 48 hr. of shaking, the flasks were allowed to stand in the bath until the gel had settled out. Twenty cubic centimeters of the supernatant liquid were removed and titrated to phenolphthalein end point with base to determine the equilibrium concentration.

---

[1] This article is based upon a thesis submitted by Robert A. Springer to the Faculty of the Graduate School of Syracuse University in partial fulfillment of the requirements for the degree of Master of Arts, June, 1939.

DISCUSSION OF RESULTS

In the accompanying figures the letter *C* expresses the equilibrium concentration of each solution in moles per liter. The letter *A* represents the milliequivalents of solute sorbed per gram of gel.

Figures 1, 2, and 3 express a comparison of various acids in a certain solvent. Figures 4, 5, and 6 represent results obtained by using a single acid and various solvents. It is apparent that sorption of the acids diminishes as the number of carbon atoms in the acid increases, i.e., acetic > propionic > crotonic > benzoic > palmitic. Also, sorption of the solute decreases with change in solvent: carbon tetrachloride > toluene > nitrobenzene > dioxane > water. In most cases the amount sorbed from water is so small that a good comparison cannot be shown by graphical methods. Neither has all the work with dioxane been shown, for sorption was very poor. An abnormality is observed in the case of crotonic acid in carbon tetrachloride and toluene solutions. In greater concentrations it is less sorbed than propionic acid, but this is reversed at low concentrations.

It is very apparent that two questions must be answered to account for the sorption of organic acids from solvents. First, using the same solute, why is a greater amount sorbed from one solvent than from another? Second, why is one organic acid sorbed in a greater amount than another from the same solvent?

On the basis of the gaseous sorption theory, Patrick and Jones (5) explained sorption from solution. However, many of the results in this paper could not be accounted for by their deductions. Mention has also been made in the literature by Holmes and McKelvey (1) that sorption is a function of polarity. Nevertheless a good correlation between sorption and dipole moments cannot be made. Thus there must be something more fundamental which has not as yet been mentioned in the literature in connection with sorption.

In 1936 Huggins (2) published an excellent review on hydrogen bridging, in which he discussed the work of others and greatly extended the theoretical aspects of bonding. According to this theory, a proton can form a bond between two electronegative atoms. It is, therefore, an application of this association phenomenon that we wish to suggest as an explanation of sorption from solution by silica gel.

Silica gel, activated so that it contains about 9.0 per cent water, has been found to have a maximum sorptivity (4). If almost all of the water

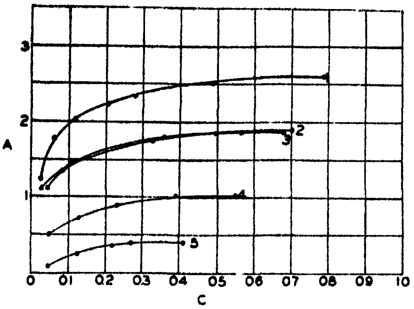

Fig. 1. Adsorption of organic acids from carbon tetrachloride. 1, acetic acid; 2, propionic acid; 3, crotonic acid; 4, benzoic acid; 5, palmitic acid.

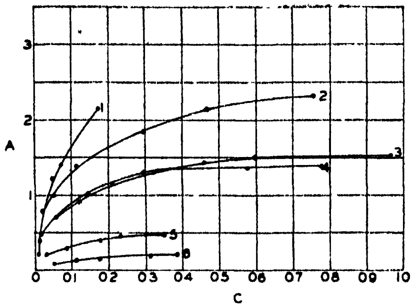

Fig. 2. Adsorption of organic acids from toluene. 1, formic acid; 2, acetic acid; 3, propionic acid; 4, crotonic acid; 5, benzoic acid; 6, palmitic acid.

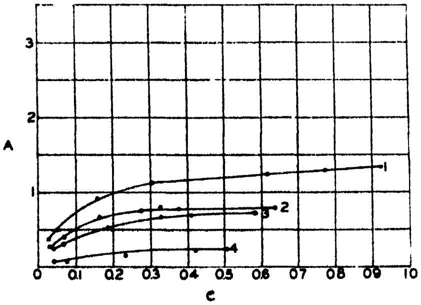

Fig. 3. Adsorption of organic acids from nitrobenzene. 1, acetic acid; 2, propionic acid; 3, crotonic acid; 4, benzoic acid.

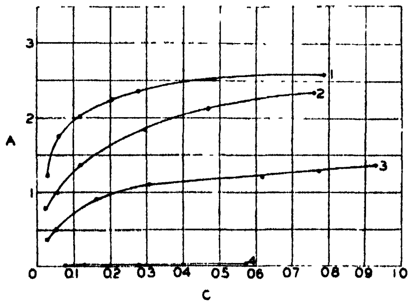

Fig. 4. Adsorption of acetic acid from various solvents. 1, carbon tetrachloride; 2, toluene; 3, nitrobenzene; 4, dioxane.

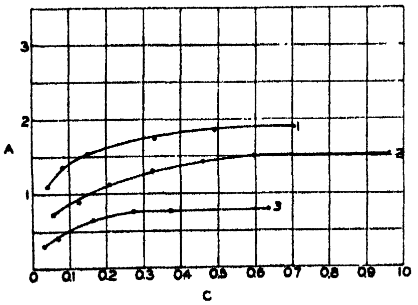

Fig. 5. Adsorption of propionic acid from various solvents. 1, carbon tetrachloride; 2, toluene; 3, nitrobenzene.

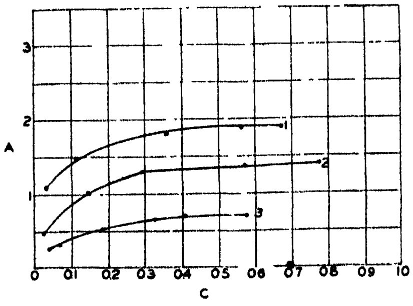

Fig. 6. Adsorption of crotonic acid from various solvents. 1, carbon tetrachloride; 2, toluene; 3, nitrobenzene.

has been driven out, the structure is changed and the gel is of no use as a sorbent. For this reason, it has been assumed by investigators (3) that one is not dealing with silicic anhydride containing small amounts of water, but with silicic acid itself. Substantially, this means that hydroxyl groups are present. In a gel containing 9 per cent of water by weight, there is approximately one molecule of water for every three molecules of silicon dioxide. Assuming that the water adds to the silicon dioxide with formation of hydroxyl groups, this would permit two hydroxyl groups for every three silicon dioxides. Since it is practically certain that the structure of the gel contains capillary openings which held the water before activation, it follows that many of these hydroxyl groups are necessarily on the surface of the capillaries. Yet it cannot be inferred that all the hydroxyl groups are on the surface, since there are so many of them; rather, they must be distributed throughout the network structure (otherwise, complete dehydration would not alter the structure).

Thomas (6), in his theory of colloidal systems, suggests that the particles are aggregates of molecules held together by covalent linkages in a regular pattern. The coagulation of silicic acid, followed by dehydration, would allow the hydroxyl groups to occupy definite positions in the silica-gel structure.

The fact that hydroxyl groups are present makes hydrogen bridging possible. The following points indicate that these bridges should be fairly stable. Silicon is a fairly metallic element and does not attract electrons of other elements very strongly. In silicic acid the electrons joining the silicon and oxygen will lie close to the oxygen. This would necessarily make the oxygen highly electronegative: thus it would have a strong attraction for protons and should therefore lend itself readily to hydrogen-bridge formation.

From the above discussion, it can be seen that hydrogen bridging is possible with silica gel. The following mechanism is suggested: A pair of electrons from an oxygen in the gel structure is bound to the labile hydrogen of the organic acid. In turn a pair of electrons from the oxygen of the carboxyl group is associated with the hydrogen in the hydroxyl group of the gel. This latter bridge is not as strong as the first one, because the hydrogen of the hydroxyl group in the silica gel is so tightly bound to its oxygen. Consequently, the bridge from the oxygen of the carboxyl group to the hydrogen of the silica gel is very unsymmetrical, whereas the bridge from the hydrogen of the carboxyl group to the oxygen of the silica gel should be fairly symmetrical. A planar representation of this is:

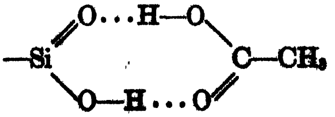

An attempt must be made to interpret the experimental results on the basis of the proposed theory. However, as will be shown in detail later, hydrogen bridging alone will not suffice to account quantitatively for all of the experimental results. It is necessary to attribute part of the effect to molecular size, and also to take into account the relative extent of formation of hydrogen bridges by solvent and solute.

The association of carboxyl groups with the hydroxyl groups of the gel will account qualitatively for the sorption. The quantitative results can also be accounted for to a certain extent. The tendency to form hydrogen bridges is in the following order: formic > acetic > propionic > palmitic. This is also the order of extent of sorption (figure 2). In degree of formation of hydrogen bridges, benzoic acid fits into this series between formic and acetic acids, but in extent of sorption it lies between propionic and palmitic acids. This discrepancy may be explained by assuming that molecular size and shape are factors in the sorption. Benzoic acid, being a bulky molecule in contrast to the linear aliphatic acids, is more difficultly sorbed. It may also be pointed out that the entire series, benzoic acid included, is in the order of molecular size. This factor may be even more important in determining the *extent* of sorption than the *relative tendency* to form hydrogen bridges. This idea receives some support from the behavior of crotonic acid. At the higher concentrations in all solvents, crotonic acid is less sorbed than propionic acid, which fits in with the order of molecular size but not with the order of tendency to form hydrogen bridges. In respect to formation of bridges, crotonic acid is very nearly equal to acetic acid. However, at low concentrations in solvents which themselves are only slightly sorbed by silica gel, such as toluene and carbon tetrachloride, crotonic acid is more highly sorbed than propionic acid (figure 6). It seems reasonable to assume that the relative tendency to form hydrogen bridges would be more important at low concentrations, where only the more available surfaces of the gel are involved and molecular size is not such an important consideration. This reversal of extent of sorption does not occur in nitrobenzene solution (figure 3), where crotonic acid is less sorbed than propionic acid at all concentrations. This anomalous behavior will be explained in the following paragraph.

Hydrogen bridging has been offered to account for differences in sorption of various organic acids by silica gel from any one solvent. Differences in behavior of the same acid in various solvents must now be explained. This is obviously an effect of the solvent, and can be accounted for on the same basis as the differences in sorption of different acids. For if one solvent is more sorbed by silica gel than another, then obviously an acid dissolved in the first solvent will be less sorbed than one dissolved in the second, owing to greater saturation of the gel by the first solvent. This hypothesis is fully borne out by the experimental results. Sorption for any acid from the following solvents *decreases* in the order carbon tetrachloride, toluene, nitrobenzene, dioxane, and water (figure 4). This is also the order of *increasing* sorption of the solvent by silica gel, according to the hydrogen-bridge theory. Furthermore, the sorption of crotonic acid from nitrobenzene bears out the hypothesis of hydrogen bridging. It has been mentioned that in nitrobenzene solution crotonic acid is less sorbed than propionic acid at all concentrations, while in carbon tetrachloride and toluene the crotonic acid is more sorbed at low concentrations and less at high concentrations. The low sorption at low concentrations in nitrobenzene may be explained by the assumption (which appears quite reasonable) that sorption of the nitrobenzene itself by the silica gel produces exactly the same effect as would a higher concentration of the acid. If this be so, it is possible that the crotonic acid might be more highly sorbed at very low concentrations. This range has not been investigated.

In a discussion of this paper with Dr. Maurice L. Huggins of the Eastman Kodak Company, it was suggested that there be indicated more specifically the competition effects produced in the system, i.e., bridging between solute molecules, between solvent molecules, and a competition of solute molecules for solvent molecules. The structure of the gel presents the possibility of a partial bridging between its hydroxyl groups. When a solution is put in contact with the gel, in addition to the bridging effects produced in the solution and within the gel itself, there is a gel–solvent and gel–solute competition set up. It is evident then that the amount sorbed by the gel is dependent on the equilibrium set up between these different bridging effects. This in turn depends on the strength of the different bridge formations. It is evident also that the breaking of the bridges in the gel, permitting other bridge formations, is of some consequence.

SUMMARY

1. Data have been presented on the sorption of formic, acetic, propionic, crotonic, benzoic, and palmitic acids from solutions in carbon tetrachloride, toluene, nitrobenzene, dioxane, and water by use of silica gel.

2. An hypothesis has been advanced to account for the results obtained, based on the formation of hydrogen bridges.

3. A semi-quantitative explanation of the results depends on at least three factors: (*a*) the relative extent of hydrogen bridging by the different acids; (*b*) the size and shape of the acid molecules; and (*c*) the relative extent of formation of hydrogen bridges by solute, solvent, and gel.

4. The presence of an unsaturated linkage in an aliphatic acid gives rise to certain abnormalities in the sorption, which afford further proof of the correctness of the hydrogen-bridge hypothesis.

REFERENCES

(1) HOLMES, H. N., AND MCKELVEY, J. B.: J. Phys. Chem. **32**, 1522 (1928).
(2) HUGGINS, M. L.: J. Org. Chem. **1**, 407 (1936).
(3) MAGNUS, A., AND KIEFFER, R.: Z. anorg. Chem. **179**, 215 (1929).
(4) MCGAVACK, J., AND PATRICK, W. A.: J. Am. Chem. Soc. **42**, 946 (1920).
(5) PATRICK, W. A., AND JONES, D. C.: J. Phys. Chem. **29**, 1 (1925).
(6) THOMAS, A.: Lecture given before the Syracuse Chapter of Sigma Xi, in 1939.

COMMUNICATION TO THE EDITOR

PHOTOCHEMICAL REDUCTION OF FERRIC IRON BY OXALIC ACID

The paper on "The Photochemical Oxidation of Oxalic Acid Sensitized by Ferric Ion," published by R. Livingston (J. Phys Chem. **44**, 601 (1940)), contains a statement which I should like to support by additional evidence. The results on the photochemical reduction of ferric ion by oxalic acid, as published in 1928 by E. Mencke and myself (Z. Elektrochem. **34**, 598 (1928)) must be discarded. In December, 1936, I repeated this investigation with Dr. H. Hoch in Vienna. We found the permanganate titration not reliable enough and adopted the titration with titanium trichloride, used by Allmand and Young (J. Chem. Soc. **1931**, 3079). Our experiments showed (*1*) that the velocity of the reaction was approximately proportional to the first power of the light intensity, which result was in agreement with the findings of Allmand and Young but contrary to those of Kornfeld and Mencke, who stated a dependence on the square root of the light intensity, and (*2*) that the reaction proceeded until the end, regardless of the presence of ferrous ions. This result also agreed with the findings of Allmand and Young and disagreed with those of Kornfeld and Mencke. For external reasons the investigation was not completed, and publication of the results was postponed. Since I have not been able to resume the investigation I should like to clarify the issue now, in connection with Dr. Livingston's paper.

GERTRUD KORNFELD.

Research Laboratories,
Eastman Kodak Company,
Rochester, New York.

NEW BOOKS

A Dictionary of Metals and their Alloys. First edition. By F. J. Camm. 245 pp. New York: The Chemical Publishing Company, Inc., 1939. Price: $3.00.

The author, apparently not a metallurgist, has had considerable experience in writing books in engineering, mechanics, wireless, etc., from the practical side. His *Dictionary of Metals* is written for the layman, in alphabetical fashion, but it should not be classed as an unabridged edition, because the book is very brief and of service only to the practical man for whom it is written. Many of the definitions are short, elementary, and wrong from the metallurgical standpoint. The list of alloys for different classes of metals is not too extensive, but should serve a useful purpose for shop men.

The author also has short treatises on plating, polishing, hardening and tempering, coloring, metal spraying, and rust-proofing, and includes tables on physical properties of materials which can be found elsewhere. If one is interested in a more complete list of alloys, your abstractor refers you to *Engineering Alloys* by Woldman and Dornblatt (American Society for Metals, Cleveland, Ohio, 1936, 622 pp.; price, $10.00). If Mr. Camm's book is a dictionary, *Engineering Alloys* is an encyclopedia.

Ralph L. Dowdell.

Theoretical and Applied Electrochemistry. Third edition. By Maurice de Kay Thompson. xxi + 535 pp.; 235 fig. New York: The Macmillan Company. Price: $5.00.

The format of the third edition of this text follows that adopted in the second edition, devoting one hundred and eighty some pages to "Theoretical Electrochemistry," one hundred and ninety-two pages to "Applied Electrochemistry of Aqueous Solutions," and ninety-nine pages to "Electric Furnaces and their Products." Twenty-one pages are devoted to the solution of problems. From the foregoing statement it is obvious that an adequate treatment of the principal topics necessitates masterly condensation to keep within the space allotted. Hasty perusal of the volume invites the opinion that it is characterized by overcondensation. Such judgment is quite unjustified when one becomes aware of the comprehensive number of original references included and the bibliography and problems at the end of each of the twenty-one separate chapters. One should also realize that the use of the book as a text presumes that the student has completed a thorough course in physical chemistry, and that the theoretical section aims to serve as a review, placing emphasis upon the theory underlying the applications discussed in the succeeding sections.

The author has obviously received abundant coöperation from industry. This is evidenced in the large number of facts included which have been privately communicated and in the generous number of hitherto unpublished illustrations and original line drawings which could not have been provided otherwise. The volume is intended for use as a text and not a reference work, and on that basis the omission of topics such as electronics, electrostatic and magnetic separation, photoelectric phenomena, and polarographic analysis may be justified. In the preface to the original edition the statement is made:—"It is believed that, by collecting in a single volume the material that would be comprised in a course aiming to give an account of the most important electrochemical industries, as well as the principal applications of electrochemistry in the laboratory, it will be possible to teach the subject much more satisfactorily." Dr. Thompson deserves distinct commendation for his success in attaining an objective which the writer recognizes as a most difficult task.

Hiram S. Lukens.

Chemical Computations and Errors. By THOMAS B. CRUMPLER AND JOHN H. YOE. 247 pp. New York: John Wiley and Sons, Inc., 1940. Price: $3.00.

At the present time many students of chemistry are graduated without adequate training in or appreciation of the thoroughly practical nature of the theory of measurements and errors. It is to be hoped that the present volume will stimulate interest in these subjects as well as serve as a useful text and elementary reference book.

The first eighty pages of this book are devoted to a detailed discussion of certain selected computational and algebraical methods which are of particular interest to students of physics and chemistry. The theories of measurements and errors, and their practical applications, are discussed in the next one hundred twenty pages. This section includes an elementary introduction to the mathematics of probability, as well as a careful analysis of some of the sources of the persistent (i.e., corrigible) errors which occur in the more common physicochemical measurements. The last chapter, twenty-four pages long, contains an account of some of the simpler methods of "curve fitting." The several chapters are followed by a number of interesting and practical problems, the numerical solutions of which are given in the appendix.

This book appears to be intended for the undergraduate student and is written so simply and in such detail that few students should experience any difficulty in using it for independent study. Although the treatment is straightforward and simple throughout, the authors have employed a rather scholarly style, somewhat uncommon in present-day texts. While it is primarily designed for undergraduates, this book contains some sections which should prove of value to many graduates as well as to a few more mature students of chemistry.

The book is attractively printed and appears to be unusually free from errors. Although it is of no importance in the context, it may be worth while to point out that 6.06×10^{23} (as given on page 2) is not at present "the accepted value" of Avogadro's number.

ROBERT LIVINGSTON.

Chemistry and Medicine. MAURICE B. VISSCHER, Editor. v + 296 pp.; 77 illustrations and graphs; 20 tables. Minneapolis: The University of Minnesota Press, 1940. Price: $4.50.

In this book are collected the revised and edited papers presented (October 12, 13, and 14, 1939) as the scientific program of the celebration of the Fiftieth Anniversary of the founding of the Medical School of the University of Minnesota. The scope of the topics discussed and the authority with which they are presented is demonstrated by the list of subjects and authors, *viz*: "Some Aspects of the Colloid Chemistry of Membranes," by Herbert Freundlich; "The Performance of Osmotic Work in Living Systems," by Maurice B. Visscher; "Some Reactions by Which Solutes May Be Differentially Concentrated by the Kidney," by John P. Peters; "Organic Chemistry in the Pursuit of Vitamin Research," by Lee Irvin Smith; "On the Necessity of Fats in the Diet," by George O. Burr; "Heparin and Thrombosis," by Charles H. Best; "Recent Chemical Trends in the Study of Immunity," by Michael Heidelberger; "The Biology of Animal Viruses," by Robert G. Green; "The Mode of Action of Sulfanilamide and its Derivatives," by Perrin H. Long; "Chemistry in Urinary Antisepsis," by Henry F. Helmholz; "The Physicochemical Approach to the Mechanisms of Convulsive Reactivity," by Irvine McQuarrie; "Methods of Analysis of Nervous Action," by Herbert S. Gasser; "The Nervous Regulation of Visceral Process," by Detlev W. Bronk; "The Argument for Chemical Mediation of Nerve Impulses," by Walter B. Cannon.

In all instances a sufficiently comprehensive review is presented to develop adequately the background for the description of the investigations reported by each author. In some cases, particularly with regard to the papers having reference to bacteriology, chemotherapy, and nerve physiology the papers are actually concise, complete, and well-organized reviews whose scope and content are well described by their titles. Each paper is supplemented by a list of references. The emphasis as to the work described naturally lies on that done in the laboratory of each author and upon the investigations contributory to that work. The result is that in no other book is it possible to find such a synthesis of the work and of the interpretations thereof of so many authorities.

The book is easily readable, even though there has been no sacrifice of exactness of description in an attempt at a popular style. This book should be read by all who have any interest in the modern applications of chemistry to biological processes.

W. D. ARMSTRONG.

Introduction to Bessel Functions. By F. BOWMAN. 22 × 14 cm.; 134 pp. London: Longmans, Green and Company, 1938. Price: 10s. 6d. net.

Mr. Bowman's small book has a value out of all proportion to its size, and will be welcomed by all students of physical science who desire to obtain rapidly an understanding of the more elementary properties of these functions. The author starts from the definition of a Bessel function of zero order in terms of a power series, and proceeds to a consideration of modified Bessel functions, definite integrals, asymptotic expansions, and Bessel functions of any real order.

There are a number of well-selected applications of physical interest, and each chapter is accompanied by a set of exercises of various grades of difficulty.

ALLAN FERGUSON.

The Nature of the Chemical Bond. Second edition, revised. By LINUS PAULING. 4.5 x 7 in.; xvi + 450 pp. Ithaca, New York: Cornell University Press, 1940. Price: $4.50.

In this second, revised, edition only relatively minor changes have been made from the text of the first edition, which was reviewed in this Journal recently (J. Phys. Chem. **44**, 827 (1940)). New material has been inserted in several places, increasing the total length by twenty pages. Particularly interesting are the increased discussion (pp. 217–21) of conjugated systems, and the new section on free and restricted rotation about single bonds (pp. 90–2).

ROBERT S. MULLIKEN.

The Ultracentrifuge. By THE SVEDBERG AND KAI O. PEDERSEN. In coöperation with J. H. Bauer and E. G. Pickels; G. Boestad; E. O. Kraemer and J. B. Nichols; O. Lamm; A. S. McFarlane; R. Signer. 478 pp. Oxford: The Clarendon Press, 1940. Price: $12.50.

All who are interested in biochemistry or, quite generally, in biology will welcome this extensive monograph on the ultracentrifuge and will find it most useful. The book is not confined to ultracentrifuges of the Svedberg type, but also contains a chapter (by J. H. Bauer and E. G. Pickels) giving a detailed description of the construction and operation of air-driven ultracentrifuges as developed by J. W. Beams, J. H. Bauer, and others.

The four major parts of the monograph are: I. Theory of Sedimentation. II. Construction and Operation of Ultracentrifuges. III. Methods of Measurement. IV. Results Obtained with Svedberg Ultracentrifuges. The last part contains two chapters,—one on proteins, the other on organic colloids (with the exception of proteins). A complete bibliography should be mentioned here too.

The most remarkable results so far obtained by Svedberg with the ultracentrifuge are that protein solutions are in many cases monodisperse and that the macromolecules of proteins are distributed among a limited number of classes according to their molecular weights, correlated with one another by fairly simple numerical proportions. There is an imposing amount of experimental work in favor of these assertions. There is also a series of experiments proving that particles of the same size as found in isolated proteins are present in the sera from which they were prepared. The results gained so far do not seem to allow any conclusions as to the state of proteins in living protoplasm.

The strong tendency of proteins to form macromolecules of well-defined molecular weight, in which they appear to differ from other large elementary particles of biologically important substances such as cellulose, chitin, rubber, etc., is drawing general attention, owing to its importance, in attempts to explain the chemical structure of proteins. This problem is discussed but briefly in this book, and the author of the chapter in question (K. O. Pedersen) is apparently rather sceptical concerning all hypotheses brought forward so far, both as to the conception of long chains (M. Bergmann, Astbury, and others) and as to the cyclic pattern (D. Wrinch).

H. Freundlich.

Electrocapillarity. By J. A. V. Butler. 5 x 8 in.; viii + 208 pp.; 56 diagrams; 1 plate. New York: The Chemical Publishing Company, Inc., 1940. Price: $5.00.

This book is remarkable, owing particularly to the subject matter which it covers. The author uses the word "electrocapillarity" in a wider sense than is generally done. The term is mostly reserved for our knowledge of the electrocapillary curves of liquid metals; one also finds it extended to include electrokinetic phenomena. Besides these subjects the author treats those parts of electrochemistry which deal with electrode processes as such, not with their usefulness in explaining the properties of electrolytes in solution.

Hence the first three chapters are concerned with the seat of electromotive force and with the thermodynamics and the mechanism of electrode potentials. Chapters IV and V treat the electrical double layer, electrocapillary curves, and electrokinetic phenomena. The last three chapters have to do with electrode reactions and overvoltage, concentration polarization and the deposition of metals, and some special electrode processes, passivity, etc.

The author is interested mainly in the recent development of his subject. He therefore takes full account of the investigations of Frumkin and his collaborators, of the conception of hydrated ions, as developed especially by Gurney, and of the experimental results of Tiselius, Abramson, Moyer, and others in cataphoresis, as well as his own work in this field. The advantage of closely connecting phenomena such as the Nernst potential with electrokinetics becomes very conspicuous when reading this book; an even more impressive success will be achieved as soon as we possess more quantitative results concerning that factor which is the link in the whole range of these phenomena,—namely, the electrical double layer.

H. Freundlich.

Physicochemical Methods. By Joseph Reilly and William Norman Rae. Volume I, 686 pp.; Volume II, 580 pp. New York: D. Van Nostrand Company, 1940. Price: $17.50.

The third edition of this well-known handbook is published in two volumes, totaling 1266 pages, at a price of $17.50, in contrast to the 822-page volume of the second edition which sold for $8.00. While this book undoubtedly remains the most useful work on the subject, the new edition scarcely satisfies the expectations raised by its increase in length and price.

The treatment of the several subjects varies greatly, not only in emphasis and detail, but in manner of presentation. For example, some subjects, such as "Thermionic Vacuum Tubes," are represented by clear and adequate outlines of their general principles and applications. In other cases, as the section on "Molecular Weights," there is a good detailed description of the more important experimental methods. A few chapters, the one on "Reaction Rates" being a particularly bad example, consist of very elementary theoretical discussions followed by the directions for a few experiments of the type commonly found in the older laboratory manuals of physical chemistry. Some topics which are of theoretical and practical interest have been omitted entirely. Amongst these we might mention propagation of flames, gaseous explosions, diffusion, and the rates of dissolution, evaporation, and crystallization. Photochemistry, fluorescence, phosphorescence, and chemiluminescence receive scant mention in the section on the "Photoelectric Effect."

Perhaps the greatest single improvement is the introduction in the edition of an extensive classified bibliography of specialized works on physicochemical methods. On the other hand, it is to be regretted that the excellent index of the second edition has been replaced by one so brief that it is practically useless.

The new edition shows a decided trend toward subjects of practical interest. It includes sections on such chemical engineering topics as "Plant Design and Press Filtration," but devotes relatively less space than formerly to the refined methods of specialized research. Several of the new chapters have been written by specialists in the subjects concerned.

In contrast to these practical subjects, the authors have introduced a rather abstract discussion under the general title "Measurement and Units." This chapter, 53 pages long, was written by Professor O'Rahilly. Without questioning the correctness or utility of Professor O'Rahilly's concepts and terminology (the reviewer lacks courage to cross cudgels with one who boasts (p. 92) that he has exploded the dimensions of the electrical text books with one swoop), it appears that this chapter is entirely out of place in a book which is devoted to the practical methods of physical chemistry.

The book is clearly printed and well bound. It appears to have been carefully edited. While the illustrations are adequate, the draughtsmanship of some of them could be improved.

ROBERT LIVINGSTON.

A New Dictionary of Chemistry. Edited by STEPHEN MIALL. 22 x 15 cm.; xv + 575 pp. London, New York, and Toronto: Longmans, Green and Company, 1940. Price: 42 shillings net.

This dictionary covers all branches of chemistry, including inorganic, organic, physical, pharmaceutical, and industrial, and also contains biographies of leading chemists. A table at the end gives the physical properties of about eighteen hundred organic compounds. The information in the inorganic and organic sections is surprisingly complete and up to date, and although the sections on physical chemistry are very brief they give much useful information to non-specialists. The book is one which is likely to prove very useful in libraries and to those wishing to obtain information rapidly, and it may be recommended with confidence.

J. R. PARTINGTON.

Molecular Spectra and Molecule Structure. I. Diatomic Molecules. By GERHARD HERZBERG. In the recent review of this book (This Journal **44**, 682 (1940)), it was not stated that the translation into English was made by Dr. J. W. T. Spinks of the University of Saskatchewan.

IMP. AGRI. ... NEW DELHI
3. JAN. 1941
LIBRARY

ABSOLUTE RATES OF SOLID REACTIONS: DIFFUSION

ALLEN E. STEARN
Department of Chemistry, University of Missouri, Columbia, Missouri
AND
HENRY EYRING
Frick Chemical Laboratory, Princeton University, Princeton, New Jersey

Received January 28, 1940

INTRODUCTION

It is ordinarily assumed (44) that diffusion through solids may take place by three different mechanisms, which may be termed solid solution, rift, and grain boundary diffusion, respectively. From another point of view all solid diffusion may be spoken of as (*a*) interface or (*b*) volume diffusion. Interface diffusion may occur (*1*) along the rifts ordinarily arising from mechanical working, (*2*) at the interface between the grain and the surrounding cementing material, and (*3*) at the surface of the crystal. Volume diffusion may be either through the grains or through the cementing material at the grain boundary. Since ordinarily only one molecule in 10^8 is located on a surface, the corresponding diffusion coefficients will appear anomalous by such a factor if one makes the mistake of calculating them as for volume diffusion, i.e., there will be a large negative apparent entropy of activation. On the other hand, if one calculates this interface diffusion on the basis of surface atoms only, then the only term which will in general differ from the D for volume diffusion will be the heat of activation, which will be smaller. Thus an inspection of an observed diffusion coefficient will sometimes suffice to distinguish between volume and surface diffusion.

Whatever the specific mechanism of solid diffusion, the rate can be expressed by the formulation

$$D = Ae^{-\frac{Q}{RT}} \tag{1}$$

where D is the diffusion coefficient, A is a term which varies only slightly with temperature, and Q is the heat of activation of the diffusion process.

A general equation has been developed on statistical grounds (17), which applies to any rate process in which the slow step involves surmounting a potential barrier. It has the form

$$k' = \frac{kT}{h}\frac{\mathcal{F}^{\ddagger}}{\mathcal{F}_n}e^{-\frac{E_0}{RT}} \tag{2}$$

where k' is the specific rate constant, T is the temperature, k and h are the Boltzmann and the Planck constants, respectively, and E_0 is the activation energy at absolute zero. $\mathcal{F}^{\ddagger}$ and $\mathcal{F}_n$ are the partition functions for the activated state and the initial state, respectively. In equation 2 as written we have taken the transmission coefficient as unity.

The activated complex may always be considered essentially as a molecular species, and thus the rate constant can be pictured as an equilibrium constant between activated complex and reactants at unit activity multiplied by the universal frequency kT/h. This permits formulation of the reaction rate in thermodynamic terms (71) in the form

$$k' = \frac{kT}{h}e^{-\frac{\Delta F^{\ddagger}}{RT}} = \frac{kT}{h}e^{\frac{\Delta S^{\ddagger}}{R}}e^{-\frac{\Delta H^{\ddagger}}{RT}} \tag{3}$$

where $\Delta F^{\ddagger}$, $\Delta S^{\ddagger}$, and $\Delta H^{\ddagger}$ are, respectively, the standard free energy' entropy, and heat increases when the activated complex is formed from the reactants. $\Delta H^{\ddagger}$ can be obtained from the temperature coefficient of k' by the relation

$$\Delta H^{\ddagger} = RT^2\frac{\mathrm{d}\ln k'}{\mathrm{d}T} - RT \tag{4}$$

Applied specifically to the rate process diffusion, it has been shown (18) that the diffusion constant is related to an activated rate process by the equation

$$D = \lambda^2 k' \tag{5}$$

where λ is the distance travelled in a single jump. Substituting equations 2 and 3 into 5 we obtain

$$D = \lambda^2\frac{kT}{h}\frac{\mathcal{F}^{\ddagger}}{\mathcal{F}_n}e^{-\frac{E_0}{RT}} \tag{6}$$

$$= \lambda^2\frac{kT}{h}e^{-\frac{\Delta F^{\ddagger}}{RT}} = \lambda^2\frac{kT}{h}e^{\frac{\Delta S^{\ddagger}}{R}}e^{-\frac{\Delta H^{\ddagger}}{RT}} \tag{7}$$

In the derivation (17) of equation 2 the partition function for that degree of freedom along the reaction coördinate was included in the frequency term, kT/h. Thus the partition function, $\mathcal{F}_n$, for the normal state contains a term for the reaction coördinate not appearing in $\mathcal{F}^{\ddagger}$.

If we neglect the changes in all the terms of the partition function on activation except those in the reaction coördinate, we may write

$$D = \lambda^2 \frac{kT}{h} \left(1 - e^{-\frac{h\nu}{kT}}\right) e^{-\frac{E_0}{RT}} \tag{8}$$

where $\left(1 - e^{-\frac{h\nu}{kT}}\right)^{-1}$ is the partition function, and ν the frequency of the normal state for that degree of freedom along the reaction coördinate. In the limit, when ν is extremely large, equation 8 reduces to

$$D = \lambda^2 \frac{kT}{h} e^{-\frac{E_0}{RT}} \tag{9}$$

In the range where ν is small enough so that $h\nu \ll kT$ and we can expand the exponential term retaining only the first power of the exponent, we obtain

$$D = \lambda^2 \nu e^{-\frac{E_0}{RT}} \tag{10}$$

If we treat the motion along the reaction coördinate as a translation and use classical mechanics in a manner previously adopted for liquids (16), we would have

$$D = \lambda^2 \frac{kT}{h} \left(\frac{h^2}{2\pi\mu kT}\right)^{1/2} \frac{1}{V_f^{1/3}} e^{-\frac{E_0}{RT}} \tag{11}$$

where

$$\left(\frac{2\pi\mu kT}{h^2}\right)^{1/2} V_f^{1/3}$$

is the corresponding partition function for the normal state. Here μ is the reduced mass of the two passing molecules and V_f is the free volume (20). This leads to the equation

$$D = \frac{\lambda^2}{V_f^{1/3}} \left(\frac{kT}{2\pi\mu}\right)^{1/2} e^{-\frac{E_0}{RT}} \tag{12}$$

which is of the form

$$D = aT^{1/2} e^{-\frac{E_0}{RT}} \tag{13}$$

It is seen that the various forms of the diffusion equation obtainable from absolute reaction rate theory cover the important equations which have from time to time been proposed. Thus Richardson's well-known equation (49)

$$D = (K/d)P^{1/2}T^{1/2}e^{-\frac{E}{2RT}}$$

is of the form of equation 13; the Dushman–Langmuir (13) equation

$$D = \frac{Q}{Nh}\delta^2 e^{-\frac{Q}{RT}}$$

is of the form of equation 10, as is also that of van Liempt (35). In most work the attention has been largely confined to the factors entering the term A in equation 1, but Braune (6), on the basis of Lindemann's theory of melting, related the activation energy with the absolute melting point of the solvent metal, and derived the expression

$$D = Ae^{-\frac{3b^2T_m}{T}}$$

where T_m is the melting point and b is a constant said to lie between 1 and 2 for different metals. For low-melting metals the data show b to be almost invariably greater than 2, and may approach 3 so that, since b enters as a squared multiplying factor in the exponent, a variation of 2 to 3 would mean a difference of over 100 times in the diffusion coefficient at the melting point of the metal, or a difference of 2×10^4 times at half that temperature.

II. DIFFUSION OF METALS THROUGH METALS

We investigate the applicability of equation 8 to the behavior of metals as given by diffusion data. For λ we take $(\bar{V}/N)^{1/3}$, where $\bar{V}$ is the gram-atomic volume and N is Avogadro's number. We estimate ν by taking the average frequency, which is three-fourths of the Debye limiting frequency. We then obtain

$$D = \left(\frac{\bar{V}}{N}\right)^{2/3}\frac{kT}{h}\left(1 - e^{-\frac{3\theta}{4T}}\right)e^{-\frac{E_0}{RT}} = Ae^{-\frac{E_0}{RT}} \qquad (14)$$

where θ is the Debye characteristic temperature. Using the properties of the solvent metal for systems for which data are available, we find that the value of the A term in equation 14 ranges from 0.0013 to 0.0042. From the diffusion data themselves, however, we find that the A term in equation 1 ranges from 10^{-5} to unity for bimetallic diffusion in most cases, and may reach higher values, up to 11, in the case of self-diffusion. In fact, in a particular unique case to be noted later, A is of the order of 10^{47}. Any method of choosing some average value for $\bar{V}$ or θ for bimetallic systems, in place of using the values characteristic of the solvent metal, will not affect the calculated range of the A term by more than a factor of 2 to 3, so that the explanation of the large discrepancies between A values calculated from equation 14 and those obtained from diffusion data must be sought elsewhere. No account is taken in the A term as just estimated of the effect of the process on the entropy of the crystal atoms other than those two which are passing each other. However, a satisfactory representation of the mechanism of diffusion can be obtained from equation 7.

We shall first consider the quantity $\Delta F^{\ddagger}$. The diffusion process may be pictured as (*1*) the passing by each other of two atoms, with the neighboring atoms suitably accommodating themselves to this event, or (*2*) the diffusion of an individual atom into empty lattice positions. The latter process may equally well be visualized as the diffusion of the hole.

To form a hole the size of a molecule (50, 18) requires an energy equal to the energy of sublimation aside from polarization forces. Thus we would expect activation energies approximately equal to this energy if mechanism 2 were responsible for diffusion. As will be seen later, the observed activation energies are in general enough smaller to render mechanism 2 highly improbable. Mechanism 1 proceeds by some combination of the deformations of types I and III proposed in the interesting paper of Wagner and Schottky (69), whereas our mechanism 2 must proceed by deformations of their type II.

To permit the passing by each other of two atoms by mechanism 1, the lattice must be slightly deformed, and a hole, or extra space, made available. Clearly the amount of this work of activation is the product of a volume factor largely determined by the dimensions of the passing atoms, and a second factor dependent on the resistance to compression of these atoms and their neighbors. The thermodynamic equation for calculating the free energy is

$$\Delta F = \int^{V} \frac{1}{\beta} \mathrm{d}V \tag{15}$$

The choice of β, the compressibility, and of the limit of integration will be determined by the model. In table 1, where most of the available data are collected, and upon which much of the discussion in this section of the paper is based, we have introduced the quantity α, defined as follows,

$$\alpha = \frac{\Delta F}{\Delta F^{\ddagger}} \tag{16}$$

where, in calculating ΔF in equation 15 we take the limit V equal to the arithmetic mean of the volumes of the two molecules passing each other, and β is taken as one-half the arithmetic mean of the β's of the two molecules passing each other plus one-half the compressibility of the neighboring molecules. This choice of β assumes that the compression is largely limited to the lattice immediately surrounding the passing pair of atoms and to the pair itself. Strictly speaking, we should know the values of β at the temperatures of the diffusion experiments, but in the present state of knowledge it was not considered advisable to attempt extrapolation to temperatures so far from those where direct experimental values

TABLE 1

METAL	T	$A_{\text{calcd.}}$ EQUATION 14	$A_{\text{measd.}}$	$\Delta S^{\ddagger}$	$E_{\text{act.}}$	n	$\Delta F^{\ddagger}$	α	REFERENCES
Solvent metal, Ag; $\Delta E_{\text{sub.}}$, 68 kg-cal.; $\Delta S^{\ddagger}_{\text{ideal}}$ (equations 14, 7), − 5.8									
	°A.		sec.$^{-1}$		kg-cal.		kg-cal.		
Pd	1000	0.002	6.4×10^{-6}	−15.5	20.2	3.36	35.5	7.5	(29)
Sn	1000	0.002	7.9×10^{-5}	−10.5	21.4	3.18	31.8	8.5	(58)
Sb	1000	0.002	5.3×10^{-5}	−11.3	21.7	3.13	32.8	7.5	(58)
Cd	1000	0.002	4.9×10^{-5}	−11.4	22.4	3.04	33.7	6.7	(58)
In	1000	0.002	7.3×10^{-5}	−10.6	24.4	2.79	34.9	6.5	(58)
Cu	1000	0.002	5.9×10^{-5}	−11.1	24.8	2.74	35.7	6.5	(58)
Au	1000	0.002	$4. \times 10^{-4}$	−10.7	26.6	2.56	33.7	8.5	(29, 28, 6)
Solvent metal, Pb; $\Delta E_{\text{sub.}}$, 46 kg-cal.; $\Delta S^{\ddagger}_{\text{ideal}}$, − 6.3									
Au	558	0.0013	0.97	6.8	14.	3.29	9.14	20.4	(56, 54)
Ag	558	0.0013	0.083	1.9	15.2	3.03	13.04	13.5	(56)
Cd	558	0.0013	0.0046	−3.8	15.4	3.00	16.44	10.2	(56, 55)
Bi	558	0.0013	0.0085	−2.6	18.6	2.47	18.96	10.3	(56)
Hg	460	0.0013	0.41	5.5	19.0	2.42	15.57	9.7	(55)
β-Tl	558	0.0013	0.054	1.1	21.0	2.19	19.31	9.8	(56)
Sn	558	0.0013	0.42	5.1	24.0	1.92	20.04	9.5	(56)
Pb	558	0.0013	6.6	10.6	28.0	1.64	20.99	9.3	(56)
Solvent metal, Cd; ΔE_{sub}, 26.5 kg-cal.; $\Delta S^{\ddagger}_{\text{ideal}}$, −4.8									
Hg	450	0.0018	2.6	9.6	19.6	1.35	14.38	8.9	(55)
Solvent metal, Ni; $\Delta E_{\text{sub.}}$, 96.7 kg-cal.; $\Delta S^{\ddagger}_{\text{ideal}}$, −4.8									
Cu	1000	0.0026	0.0010	−6.7	35.5	2.72	40.2	7.1	(40)
Solvent metal, Au; $\Delta E_{\text{sub.}}$, 89.4 kg-cal.; $\Delta S^{\ddagger}_{\text{ideal}}$, −6.2									
Cu	1000	0.0017	0.0011	−7.1	27.4	3.23	33.77	10.7	(29)
Pd	1000	0.0017	0.0011	−7.1	37.4	2.39	42.48	10.2	(29)
Pt	1000	0.0017	0.0012	−6.9	39.	2.29	43.86	10.7	(29)
Au	1100	0.0017	7.1	10.2	51.	1.75	46.43	10.0	(29)
Solvent metal, Cu; $\Delta E_{\text{sub.}}$, 80.5 kg-cal.; $\Delta S^{\ddagger}_{\text{ideal}}$, −5.1									
Zn	1000	0.0023	$3. \times 10^{-6}$	−18.3	19.7	4.09	36.04	5.8	(41)
Pd	1000	0.0023	1.6×10^{-6}	−19.5	21.9	3.68	39.49	7.1	(41)
Pd*	1000	0.0023	1.8×10^{-5}	−14.7	27.4	2.94	40.19	7.0	(41)
Au	1000	0.0023	6.8×10^{-6}	−16.7	22.5	3.58	37.22	8.2	(41)
Pt	1000	0.0023	1.0×10^{-6}	−20.5	21.9	3.67	40.42	7.5	(41)
Mn	1000	0.0023	7.1×10^{-6}	−16.6	23.2	3.47	37.83	6.3	(41)
Ni	1000	0.0023	6.5×10^{-5}	−12.2	29.8	2.70	40.04	6.1	(41)
Sn	1000	0.0023	4.1×10^{-3}	−4.0	31.2	2.58	33.21	8.4	(41)
Sn*	1000	0.0023	2.5×10^{-1}	4.2	39.9	2.02	33.76	8.3	(41)
Al	1000	0.0023	7.1×10^{-2}	1.7	39.1	2.06	35.45	7.3	(41)
Cu	1000	0.0023	11.	16.9	57.2	1.40	43.54	5.4	(67)

TABLE 1—*Concluded*

METAL	T	$A_{\text{calcd.}}$ EQUATION 14	$A_{\text{measd.}}$	$\Delta S^{\ddagger}$	$E_{\text{act.}}$	n	$\Delta F^{\ddagger}$	α	REFERENCES
Solvent metal, W; $\Delta E_{\text{sub.}}$, 199.8 kg-cal.; $\Delta S^{\ddagger}_{\text{ideal}}$, −6.4									
	°A.		sec.$^{-1}$		kg-cal.		kg-cal.		
Y	2000	0.0030	0.11	0.2	62.	3.22	56.5		(12)
Zr	2000	0.0030	1.1	4.8	78.	2.56	63.4	9.2	(12)
Ce	2000	0.0030	1.15	4.8	83.	2.41	68.2	4.8	(12)
Th	2000	0.0030	1.13	4.8	94.	2.13	79.3	6.7	(12)
U	2000	0.0030	1.14	4.8	100.	2.00	85.4	6.9	(12)
Mo†	2000	0.0030	$8. \times 10^{-4}$	−9.1	80.5	2.48	94.6	6.4	(35a)
Mo‡	2000	0.0030	$5. \times 10^{-3}$	−5.5	80.5	2.48	87.3	5.9	(35a)
Self-diffusion of various metals									
Au	1000	0.0017	7.1	10.2	51.	1.75	46.43	10.0	(39)
Pb	558	0.0013	6.6	10.6	28.	1.64	20.99	9.3	(26)
Cu	1000	0.0023	11.	16.9	57.2	1.41	43.54	5.4	(67)
Bi§	500	0.0016	0.0012	−6.4	31.	1.54	33.3	5.2	(51)
Bi¶	500	0.0016	$7. \times 10^{46}$	221.	140.	0.34	28.5	6.1	(51)
Effect of concentration in alloys; concentration of solute in atomic per cent Solvent metal, Cu; ΔE_{sub}, 80.4 kg-cal.; $\Delta S^{\ddagger}_{\text{ideal}}$, −5.1									
0% Zn	1073	0.0024	0.0166	−1.9	37.7	2.13	37.06	5.7	(48)
4% Zn	1073	0.0024	0.0525	0.4	40.	2.01	36.89	5.7	(48)
8% Zn	1073	0.0024	0.0776	1.2	40.	2.01	36.08	5.8	(48)
12% Zn	1073	0.0024	0.0275	−0.9	36.5	2.20	34.77	6.0	(48)
16% Zn	1073	0.0024	0.0046	−4.5	31.	2.59	33.09	6.3	(48)
18% Zn	1073	0.0024	0.0068	−3.7	31.	2.59	32.29	6.5	(48)
0% Sn	1073	0.0024	1.13	6.4	45.	1.79	35.37	8.0	(48)
4% Sn	1073	0.0024	0.0032	−5.2	30.5	2.64	33.40	8.4	(48)
0% Cd	1073	0.0024	$2. \times 10^{-9}$	−33.6	8.	10.05	41.32	5.6	(48)
½% Cd	1073	0.0024	$2. \times 10^{-8}$	−29.0	10.	8.04	38.42	6.0	(48)
0% Si	1073	0.0024	0.037	−0.4	40.	2.01	37.68	9.5	(48)
4% Si	1073	0.0024	0.405	9.0	48.2	1.67	35.86	10.0	(48)
8% Si	1073	0.0024	18.7	12.0	53.8	1.49	33.29	10.8	(48)
0% Be	1073	0.0024	2.3×10^{-4}	−10.4	28.	2.87	36.52	5.4	(48)
4% Be	1073	0.0024	7.1×10^{-4}	−8.2	30.	2.68	36.08	5.4	(48)
8% Be	1073	0.0024	3.3×10^{-2}	−0.5	37.	2.17	34.90	5.6	(48)
0% Al	1073	0.0024	0.0175	−1.8	37.7	2.13	36.94	6.5	(48)
4% Al	1073	0.0024	0.0454	0.1	39.5	2.04	36.72	6.5	(48)
8% Al	1073	0.0024	0.375	4.3	43.	1.87	35.72	6.7	(48)
12% Al	1073	0.0024	6.75	10.0	48.	1.68	34.57	6.9	(48)
16% Al	1073	0.0024	252.	17.1	54.	1.49	32.86	7.3	(48)

* Samples annealed before diffusion measurements were made.

† Monocrystal.

‡ Polycrystalline sample.

§ Diffusion parallel to the c-axis.

¶ Diffusion perpendicular to the c-axis.

of compressibility are available. Such extrapolation would lower the values of α somewhat. These values of α in table 1 average 7.6. That means, crudely speaking, that on the average, a space some 14 per cent of the mean atomic volume must be made available for the diffusion interchange to take place.

While it is true that α varies between, roughly, 5 and 10, the following rational regularities will be easily seen:

1. In every case α for the diffusion of a solute metal in some solvent metal is greater than α for the self-diffusion of the solvent metal. This is because the more nearly perfect the lattice the greater the free energy, $\Delta F^{\ddagger}$, required to pass to the comparatively disordered activated state, and a pure substance most closely approaches a perfect lattice. It will be noted that the highest values of α in the entire table 1 are associated with gold and silver diffusing in lead. This apparent anomaly is just what would be expected when the phase diagrams of the various binary systems are consulted. They show gold and silver nearly insoluble in lead (gold is soluble to a few hundredths of an atomic per cent in lead, and silver is about twice as soluble in lead as is gold). In no other case in the table does mutual solubility approach these small values. This means that the entrance of gold, especially, and to a somewhat lesser extent of silver, into the lead lattice causes a strain at that point which almost amounts to activation itself.

That the average values of α for the diffusion of the solute metals do not range haphazardly through the entire limits shown in the entire table, but are invariably higher than α for the self-diffusion of the particular solvent metal is shown by table 1. Thus for gold, α for self-diffusion is 10.0, whereas for the solute metals diffusing in gold the average value of α is 10.5, and it is in no case less than 10. In the case of copper, α for self-diffusion is 5.4, as compared with an average value of 6.9 for the solute metals diffusing in copper. With lead we find the value for α for self-diffusion is 9.3, which is to be compared with an average value of 11.5 for the solute metals diffusing in lead, or, if we exclude the very insoluble gold and silver, an average for the other solute metals of 9.8.

2. It will be seen that, in all cases considered in table 1, as the concentration of the solute metal increases and the lattice therefore becomes more strained, α increases. That is, there is required less additional strain to reach the activated state. This is reflected in the fact that $\Delta F^{\ddagger}$ invariably decreases with increase in concentration of solute metal. Also, in a two-phase, two-component system, it is clear that a concentration gradient does not insure a net passage of one component from the dilute to the more concentrated phase, i.e., in such a case the diffusion coefficient is zero. We therefore digress a moment to derive the appropriate relationship.

In figure 1 we have drawn the typical barrier over which the system passes in diffusing. If the activity coefficient, γ, of a diffusing molecule

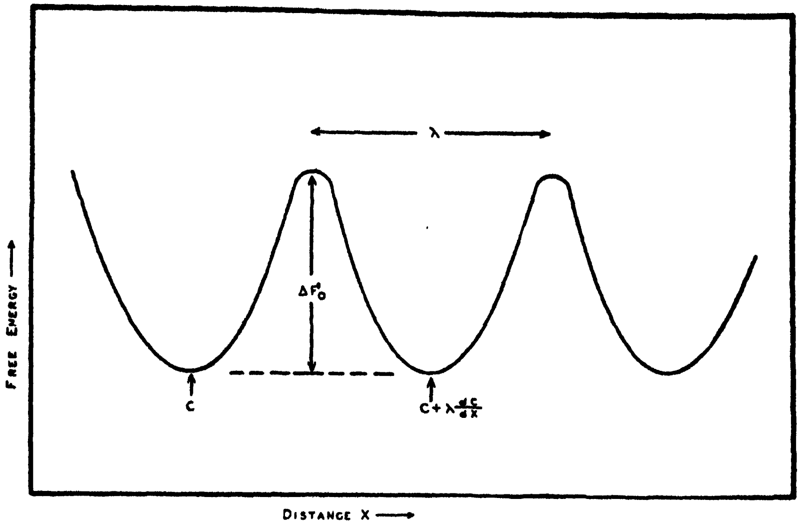

FIG. 1

is a function of concentration, then the number of molecules moving in the positive x-direction per square centimeter per second is

$$n_{\text{forward}} = \lambda c \frac{kT}{h} e^{-\frac{\Delta F_0^{\ddagger}}{RT}} e^{-\frac{d(RT \ln \gamma)}{RT\, dc} \frac{dc}{dx} \frac{\lambda}{2}} \tag{17}$$

and in the backward direction

$$n_{\text{reverse}} = \lambda \left(c + \lambda \frac{dc}{dx}\right) \frac{kT}{h} e^{-\frac{\Delta F_0^{\ddagger}}{RT}} e^{-\frac{d(RT\, d \ln \gamma)}{RT\, dc} \cdot \frac{dc}{dx} \cdot \frac{\lambda}{2}} \tag{18}$$

Setting

$$n_{\text{forward}} - n_{\text{reverse}} = -D \frac{dc}{dx}$$

and writing

$$e^{-\frac{d \ln \gamma}{dc} \frac{dc}{dx} \frac{\lambda}{2}} = 1 - \frac{d \ln \gamma}{dc} \frac{dc}{dx} \frac{\lambda}{2}$$

we obtain

$$D = \lambda^2 \frac{kT}{h} e^{-\frac{\Delta F_0^{\ddagger}}{RT}} \left(1 + \frac{d \ln \gamma}{d \ln c}\right) \tag{19}$$

$$= \lambda^2 \frac{kT}{h} e^{-\frac{\Delta F_0^{\ddagger}}{RT}} \frac{d \ln a}{d \ln c} \tag{20}$$

where a is the activity. Thus if the activity, a, in two successive layers is the same, we have $c_1\gamma_1 = c_2\gamma_2 = a$, or $c_1\gamma_1 =$ constant. Substituting this in the equation for D, we find $D = 0$ as it should. Thus we introduce a correction to the rate

$$\lambda^2 \frac{kT}{h} e^{-\frac{\Delta F_0^\ddagger}{RT}}$$

found by measuring the viscosity in a medium without a concentration gradient. As a consequence, instead of the relationship

$$D\eta = \frac{kT\lambda_1}{\lambda_2\lambda_3}$$

which has a considerable application in liquids, the proper relationship is

$$D\eta = \frac{kT\lambda_1}{\lambda_2\lambda_3}\left(1 + \frac{\mathrm{d} \ln \gamma}{\mathrm{d} \ln c}\right) = \frac{kT\lambda_1}{\lambda_2\lambda_3} \frac{\mathrm{d} \ln a}{\mathrm{d} \ln c} \tag{21}$$

This correction term, depending on $(\mathrm{d} \ln a)/(\mathrm{d} \ln c)$, can be added when vapor pressure or electromotive force data are available. For example, in cases where the activity plotted against the concentration shows a maximum or a minimum, the diffusion rate will drop to zero under the maximum or minimum conditions.

The equations 17, 18, etc. which lead to equation 21 presuppose that in passing from the normal to the activated state only one molecule moves. If, instead, the activated state is achieved by two unlike molecules each moving simultaneously toward the other along the gradient, we obtain equation 20 of a previous paper (66). Additional experimental data on vapor pressure and diffusion as functions of concentration will readily serve to decide in each case as to the applicability of one of these mechanisms or of some still more complicated way of building up the activated complex from the normal state of the atoms or molecules.

3. It is recognized that lattice imperfections may arise mechanically and that these may affect diffusion mechanisms. In the cases covered in table 1, however, the effect on $\Delta F^\ddagger$ is not great. In the data on diffusion in copper, two cases, lead and tin, are marked with asterisks. In these cases the samples were annealed before the diffusion measurements were made. As would be expected, some of the lattice strains tend to be "healed," and α tends to decrease ($\Delta F^\ddagger$ to increase), but this change is comparatively small. A somewhat greater effect is noted in the difference in α for diffusion of molybdenum through a single crystal and through polycrystals of tungsten. Whether the strains removed by heating are rifts or simply strained zones, their disappearance should have the observed effect of increasing $\Delta F^\ddagger$.

In column 7 of table 1 we have entered the ratio of the heat of sublimation of the solvent metal to the activation energy for diffusion of the various solute metals. The average value of this ratio, $n = 2.3$, is to be compared with values of n found for viscous flow in liquid metals (16) running from 9 to 20. This great difference in activation energies for the flow processes in liquid and solid metals is of course simply another aspect of the difference in rigidity.

The comparative fluidity of liquid metals has been explained (16) as being due to the atoms passing each other minus their conducting electrons, or at least with their outer shells highly deformed. Similarly, diffusion in the solid state should proceed more readily for metals than for nonmetals because of this deformability of the outer shell of the metals.

The great difference in the rate of diffusion of molecules in a solid and in a liquid in equilibrium with it (i.e., at the melting point) is a striking example of the fact that the diffusion rate is not determined alone by the activity of the diffusing molecules in their normal state. This rate process, like every other, is governed by the free-energy change in passing from the normal state to the activated state. The loosening of structure required to form the activated complex means the pushing back of the neighbors of the diffusing molecules. The process thus requires the coöperation of neighbors, and this coöperation is much more expensive in free energy for the interlocking atoms of a solid. Any rate process which has an activated complex more expanded than the normal state encounters this large negative catalytic effect on the rate in the solid state.

TABLE 2

Diffusion of thorium on or in tungsten

MECHANISM	$\Delta F^{\ddagger}$	$\Delta H^{\ddagger}$	$\Delta S^{\ddagger}$
	kg-cal.	*kg-cal.*	
Solid solution	105.7	116.0	5.18
Grain boundary	76.9	86.0	4.58
Surface	55.1	62.4	3.68

The case of diffusion of thorium on or in tungsten is of interest, since the diffusion rates have been measured for solid solution, grain boundary, and surface diffusion (33). In table 2 are collected the values of those quantities occurring in equation 7 which are characteristic of these different mechanisms.

The striking point here is that for surface diffusion one expects about half as many bonds to be broken on activation as for solid solution diffusion, and it will be noted that the heat of activation in the former case is about half (53.7 per cent) that in the latter. Since the entropies are small in both cases, it follows that the free energy of activation for surface diffusion is also about half (52.1 per cent) that for solid solution diffusion.

Investigations on the effect of external pressure on diffusion rate would enable one to differentiate two models as to how the extra volume for the passing of two molecules is made available in the activated state. In the first model a hole of suitable volume, V_h, appears at the required point without changing the average density of the adjacent molecules. This means that the whole system expands and does the work PV_h against the external pressure P. Thus the free energy of activation becomes

$$\Delta F_p^{\ddagger} = PV_h + \Delta F_i^{\ddagger} \tag{22}$$

where $\Delta F_i^{\ddagger}$ is that part of the free energy arising from the work against the internal forces, and will of course vary somewhat with the pressure. Such a model seems to represent very well the situation in normal liquids (16b).

In this second model the necessary cavity, V_h, is made by compressing adjacent molecules, and as this stress, because of crystalline structure, gradually disappears with distance from the cavity, the activation process would involve in the extreme case no expansion of the system as a whole. In this case $\Delta F_p^{\ddagger} = \Delta F_i^{\ddagger}$, and since $\Delta F_i^{\ddagger}$ may either increase or decrease with pressure depending on the resultant modification of the structure, we would have correspondingly a decrease or increase in the diffusion rate. Thus water, a system which possesses structure at low temperatures, actually becomes more fluid with increase in pressure for low pressures. This contrasts with the opposite behavior for normal liquids. Fluidity and diffusivity, according to our theory, are linearly proportional. This fact that this liquid, i.e., water, which has structure, approaches model 2 suggests that solids are likely to approach model 2 more nearly than 1.

As a very rough estimate, the diffusion in solids is not apt to decrease with pressure by factors much smaller than $e^{-\frac{PV_h}{RT}}$, and in certain cases may very well increase by factors comparable with the reciprocal of this, on the basis of model 1. For model 2 we would have

$$D_0 = Ae^{-\frac{V_h}{\beta_0 RT}} \tag{23}$$

and

$$D_p = A \exp\left(-\frac{V_h}{RT\left(\beta_0 - P\dfrac{\partial\beta}{\partial P}\right)}\right) \tag{24}$$

so that the corresponding factor for decrease of diffusion with pressure would be

$$\exp\left(-\frac{V_h P \dfrac{\partial\beta}{\partial P}}{RT\beta_0\left(\beta_0 - P\dfrac{\partial\beta}{\partial P}\right)}\right)$$

The very limited available experimental data on the effect of pressure indicate that it is very small (8). Using the relationship

$$D_0/D_p \cong e^{\frac{PV_h}{RT}}$$

we find the pressure necessary to make $D_0/D_p = 2$, for the case of diffusion in lead (for which, in table 1, $T = 560$, and the volume increase, V_h, necessary for activation is about 2 cc.) to be 11,000 atm. (The estimated value of 2 cc. for V_h is simply the molal volume divided by α.) Using the second model and the relationship

$$D_0/D_p = \exp\left(\frac{V_h P \dfrac{\partial\beta}{\partial P}}{RT\beta_0\left(\beta_0 - P\dfrac{\partial\beta}{\partial P}\right)}\right)$$

we find, on the other hand, for diffusion in lead at 560°C. that about 2600 atm. would be necessary to make $D_0/D_p = 2$. At higher temperatures the pressures necessary for the same change in diffusion would be greater. The pressures, 1000 to 1500 atm., so far employed in diffusion studies, would, on the basis of models 1 and 2, change the diffusion rate (in the specific case noted) by 10 per cent and 30 per cent, respectively, but this would not in general be differentiated from experimental error.

While the rate-determining magnitude for any process is the free energy of activation, further insight into specific behavior may sometimes be gained by breaking up the free energy into the corresponding heat and entropy changes. In table 1 are given the entropies of activation calculated by means of equation 7. (Corresponding values of $\Delta H^{\ddagger}$ can be obtained by subtracting RT from the values in the column containing $E_{\text{act.}}$) The idealized equation 14 yields values of $\Delta S^{\ddagger}$ lying between -4.8 and -6.4.

Three classes of effects on the lattice by the process of activation are suggested by the measured values of $\Delta S^{\ddagger}$.

1. In the simplest (though by no means the most frequent) case, the deformation of, or strain on, the lattice is not accompanied by marked alteration of its rigidity or general structure. Examples of this case are the diffusion of copper, palladium, and platinum in gold, where $\Delta S^{\ddagger}$ values of nearly $-7.$ in all cases are to be compared with the ideal -6.2.

2. In the second case $\Delta S^{\ddagger}$ is negative, and runs from $-11.$ to $-18.$ units. This can be interpreted as a great increase in the rigidity of the

activated as compared with the normal state. An alternative explanation is that only a fraction of the molecules—those located at interfaces, for example—diffuse at an appreciable rate. Evidence of this may be noted in the diffusion of the various metals in silver, where the average value of $\Delta S^{\ddagger}$ is -11.6 in place of the ideal -5.8. In certain cases of diffusion in copper the same thing is true.

3. Finally, we have cases which can be interpreted as a partial melting of the solvent around the activated pair, shown by an abnormally large value of $\Delta S^{\ddagger}$. Self-diffusion, in general, shows this behavior, as well as diffusion of many metals in lead. This "melting" varies from what may be interpreted as the loosening of one or two atoms to the apparent collapse of a unit cell of from seven to ten atoms, as estimated by the number

$$\frac{\Delta S^{\ddagger} - \Delta S^{\ddagger}_{\text{ideal}}}{\Delta S_{\text{melting}}}$$

If the data on the self-diffusion of bismuth can be taken at face value, there seems to be a slight stiffening of the lattice upon activation for diffusion parallel to the *c*-axis, but an enormous collapse of structure, amounting to the melting of nearly sixty atoms, for diffusion normal to this axis.

With respect to the effect of annealing on $\Delta S^{\ddagger}$, it will be seen that the partial healing of strains in the lattice by this process is accompanied by the expected increase in $\Delta S^{\ddagger}$, as shown by the behavior of palladium and tin diffusing in copper.

Effect of concentration

In the case of zinc diffusing in copper it is possible to test qualitatively the effect of change of activity with concentration on the diffusion rate (equation 20). In figure 2A we have plotted the logarithm of p/p_0 for zinc against its mole fraction in zinc–copper alloys. Here p is the partial pressure of zinc over the alloy, and p_0 is the vapor pressure of pure zinc (27). It will be seen that up to about 15 mole per cent of zinc the value of $(\mathrm{d} \log p/p_0)/(\mathrm{d} \log N_{\mathrm{Zn}})$ is about unity, but for concentrations of zinc above 15 mole per cent log p/p_0 increases more rapidly than log N_{Zn}. In figure 2B we have plotted D for the diffusion of zinc in copper at 800°C. (48) against mole fraction of zinc. The diffusion coefficient is seen to increase sharply somewhere between 12 and 16 mole per cent zinc. Dunn (11) also finds an increase in D for zinc in copper of five to seven times between alloys containing 9.6 and 29 per cent zinc, respectively.

III. DIFFUSION OF GASES IN METALS

In the case of diffusion of gases in metals, several qualitative facts must be borne in mind in approaching a treatment of any postulated mechanism.

1. "Only those gases which undergo activated adsorption by a metal can diffuse through it" (63).

2. At very low pressures the rate is proportional to the pressure.

3. At higher pressures the rate is proportional to the square root of the pressure unless, or until, some specific compound, as for example an oxide layer, holds the free energy of the gas constant at the point where diffusion starts, in which case the rate becomes independent of pressure. For the diffusion of oxygen through nickel at 900°C. this is the case when the oxygen pressure reaches about 0.25 mm. (65).

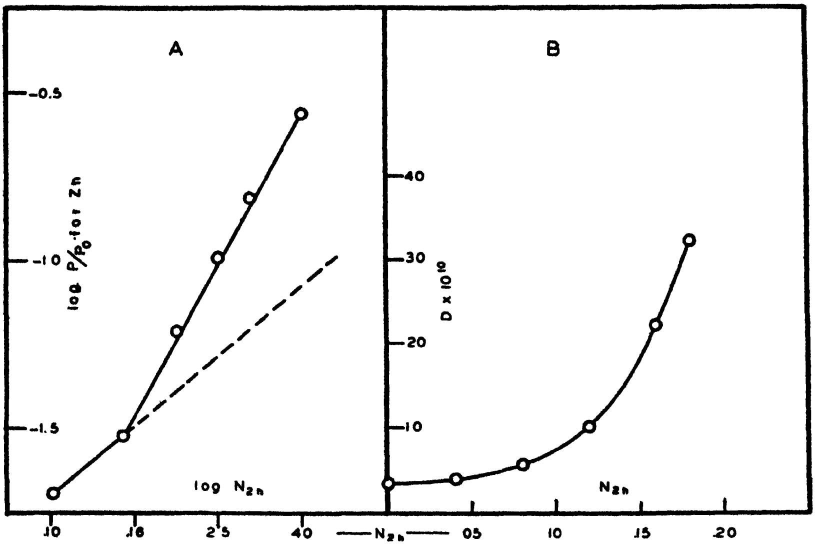

FIG. 2

4. If two sheets of metal, each 1 mm. thick, are clamped together, the rate at which hydrogen diffuses through the two sheets is the same as its rate of diffusion through a single sheet 2 mm. thick (36).

In general, the behavior of gases diffusing through metals can be described by an equation of the form of equation 7.

It is recognized that at sufficiently high pressures mechanical processes, such as a kind of effusion through crystal imperfections, are important. Such mechanisms doubtless contribute under any conditions, but it is thought that the general diffusion behavior in regions of temperature and pressure where kinetic experiments have been made indicates that lattice diffusion is the predominant mechanism, and that the slow process does not take place at either surface except as noted below. In table 3 are given values for the quantities occurring in equation 7 which have been calculated from certain typical diffusion data. It is sufficient for our purpose to obtain the data from the collection made by Smithells (63).

The reason for taking lattice diffusion as the important mechanism is based on the following points:

1. It is improbable that grain boundary diffusion through impurities or other semi-mechanical diffusion would be as *specific* as the data in table 3 indicate $\Delta F^{\ddagger}$ to be. For hydrogen diffusion this quantity varies by over twelve times, from only 2.17 kg-cal. in palladium to 24. kg-cal. in aluminum.

2. The close approximation of the square-root law for sufficiently high pressures is hard to reconcile with purely mechanical mechanisms.

3. There is no confirmation of the idea that grain size affects rate of diffusion. In particular, Baukloh and Kayser (1) could not detect any difference in the rate of diffusion of hydrogen through samples of nickel varying in grain size. Edwards (14), as well as Smithells and Ransley (64), found the rate of diffusion of hydrogen through a single crystal of iron to be identical with its rate through a sample having 100 grains per mm^2. These rates of diffusion remained equal through the entire temperature range studied, from 245° to 779°C.

TABLE 3

Diffusion of gases through metals

SYSTEM	T	$E_{act.}$	A	$\Delta H^{\ddagger}$	$\Delta S^{\ddagger}$	$\Delta F^{\ddagger}$
	°A.	kg-cal.		kg-cal.		kg-cal.
H_2-Ni	800	13.95	0.0386	12.35	0.9	13.2
H_2-Pt	750	18.80	0.0358	17.3	0.6	18.3
H_2-Mo	1200	20.20	0.0256	17.8	−1.0	21.4
H_2-Pd	800	4.33	0.113	2.73	2.7	2.17
H_2-Cu	600	18.15	0.0047	16.95	−2.67	19.8
H_2-Fe	800	10.00	0.0052	8.4	−3.0	12.4
H_2-Al	600	30.8	*ca.* 5.	29.6	10.7	24.4
O_2-Ag	850	22.6	0.08	20.9	1.8	21.1
N_2-Mo	1500	45.0	0.229	42.0	2.9	40.6
N_2-Fe	1000	23.8	0.0124	21.8	−1.7	25.5
CO-Fe	1000	18.6	0.0036	16.6	−4.2	22.8

D. P. Smith and coworkers (62) have suggested that rifts, i.e., slight openings in the lattice structure along slip planes formed during mechanical working or plastic deformation, furnish a "preferred path of diffusion." Whether such slip planes in actual practice contribute appreciably to diffusion rate or not, it is notable that we still have the high specificity of $\Delta F^{\ddagger}$ for the diffusion of hydrogen through various metals as noted above, which would necessitate, if rift diffusion dominates, either a high specificity of rifting among the various metals, or else the conclusion that diffusion through rifts is an activated atomic event just as it is through a more nearly perfect lattice. This last conclusion is borne out by the fact that, at least in the cases of nickel, palladium, and iron, the hydrogen in the rifts is dissociated or ionized. In this latter sense rifts might well afford a preferred path if they are available, since a certain lattice distortion is necessary in any case for activation.

That under most conditions neither surface process is the slow step is indicated by the qualitative fact noted above that the rate of diffusion through two metallic strips clamped together was found to be equal to the rate through a single strip of the same total thickness. . . . In specific instances one can be more definite. For example, Leypinsky (34) has shown that the activation energy for the adsorption of hydrogen on nickel is 3. kg-cal. or less per mole of hydrogen. For the adsorption of hydrogen and of deuterium on platinum Maxted and Moon (43) find 2.5 and 2.4 kg-cal. per mole, respectively. Since the value of $\Delta F^{\ddagger}$ for diffusion of hydrogen in palladium is only 2.17 kg-cal., it seems hardly probable that the hydrogen can lose an appreciable fraction of its entropy when the activation process of adsorption takes place. This means that the values of $\Delta H^{\ddagger}$ and $\Delta F^{\ddagger}$ for adsorption will probably be nearly the same and quite small. Thus, *in general,* adsorption cannot be the slow process. The energy of activation of the desorption process will be the sum of the heat of adsorption and the activation energy for the adsorption process. The activation energy for adsorption is 2.5 and 3. kg-cal. per mole of hydrogen in the two cases known and is probably not very different in other cases. To obtain the activation energy of desorption we must add 10 to 15 kg-cal. (for values and references see our reference 63) for the metals copper, nickel, platinum, and iron, giving an energy of activation for desorption of 14 to 18 kg.-cal. per mole of hydrogen, or 7 to 9 kg-cal. per gram-atom. Any small entropy increase will lower the corresponding free energy, but, as pointed out above, this will probably be negligible, so we may take 7 to 9 kg-cal. for $\Delta F^{\ddagger}$ for desorption for the metals mentioned and compare these values with 16.1 kg-cal. for the free energy of activation of diffusion in the case of iron, and up to 22.5 kg-cal. for copper. In the case of palladium, the data of Melville and Rideal (45) give a heat of solution for hydrogen of 2.24 kg-cal. per mole, or about 1.12 kg-cal. per gram-atom. If this value is good at 800°A., and if we assume that the energy of activation of hydrogen adsorption on palladium is at least no greater than on platinum, we would have for an upper limit of $\Delta F^{\ddagger}$ for desorption $2.5 - RT + 1.12 = 2.0$ kg-cal., which would be lowered by any $T\Delta S^{\ddagger}$ for desorption. This value, while not appreciably smaller than the value 2.17 kg-cal. for $\Delta F^{\ddagger}$ for diffusion activation, cannot make desorption the limiting process. Farkas (21) suggests sorption as the slow process for hydrogen through palladium, but this is on the basis of heat rather than free-energy considerations.

There are two general conditions under which the reaction at the entering surface becomes the limiting factor. In the first place, when the pressure of the gas is sufficiently lowered, the rate at which it enters the lattice is so slow that the activated positions are always nearly empty. This means that instead of the independent activation of the adsorbed hydrogen atoms in the diffusion process, two atoms almost simultaneously diffuse. This would result in a rate which is proportional to the gas pressure rather than to its square root. It may be remarked in passing that absolute rate theory does not involve equilibria intermediate between the initial and the activated state. Thus the concentration of hydrogen at the top of the activation energy barrier for diffusion remains proportional to the square root of the pressure of hydrogen gas up to pressures at which the surface may be covered, and even beyond, providing diffusion remains the slow process. The fundamental equilibrium is between the gaseous state and the activated positions.

The equivalent of higher pressures in the case of hydrogen seems to have been obtained by Borelius and Lindblom (4) and by Bodenstein (3) through furnishing nascent hydrogen to the surface of metal by electrolysis. The activation energy found by Borelius and Lindblom for the diffusion of electrolytic hydrogen through iron at ordinary temperatures was only slightly lower than that found for diffusion of gaseous hydrogen at higher temperatures. In fact, they have been considered essentially identical, though, as will be pointed out later, this is not the case even though the actual diffusion process through the metal be the same for gaseous hydrogen as for the electrolytically produced material. From their data Borelius and Lindblom found an approximate relationship between the current density and the gas pressure necessary for the same diffusion rate of the form

$$P = 17{,}000I \tag{25}$$

where I is the current density in amperes per cm.^{2}, and P is in atmospheres. A relationship of this general nature is exactly what the theory of absolute reaction rates would predict. In the study of diffusion of electrolytically produced hydrogen through metals three processes are of interest:

1. $\frac{dm}{dt} = -D\frac{dc}{dx}$ for the diffusion process (26)

2. $\frac{dm}{dt} = \frac{I}{F}$ for the liberation of hydrogen (27)

3. $\frac{dm}{dt} = c^2\frac{kT}{h}e^{-\frac{\Delta F^\ddagger}{RT}}$ for the combination of two hydrogen atoms into molecules (28)

Here we take m in gram-atoms of hydrogen, I in amperes per cm.^{2}, F is the Faraday, and c is the concentration of hydrogen in gram-atoms per cubic centimeter. To eliminate questionable activity coefficients at the metal surface we will take the concentration gradient as effective from just inside the entering surface of the metal to just inside the departing surface, taking the effective concentration at the departing surface as zero. We assume that the hydrogen just inside the entering surface is in essential equilibrium with that at the surface.

In the steady state the rate of process 2 above will be the sum of the rates of processes 1 and 3, but will be essentially equal to process 3, i.e., a very small fraction of the liberated hydrogen diffuses.

TABLE 4

The diffusion of hydrogen through iron

T	$-\log \frac{dm}{dt}$	I	$-\log D$	B
°A.				
293	12.50	0.0075		9130
	12.36	0.0150		8710
	12.19	0.030		9550
	12.09	0.045		10000
			13.42	9350 (ave.)
333	11.59	0.0075		12420
	11.45	0.0150		11860
	11.31	0.030		11320
	11.22	0.045		11320
			12.577	11730 (ave.)
370	10.98	0.0075		12030
	10.81	0.0150		13180
	10.67	0.030		12590
	10.58	0.045		12590
			11.96	12600 (ave.)

In obtaining the values given in table 4 we use the data of Borelius and Lindblom to calculate the constant B in the relationship (equation 25) $P = BI$. For the rate of the ordinary gaseous diffusion we employ their equation

$$D = 4 \times 10^{-7} e^{-\frac{9400}{RT}}$$

These values are given in column 4. Column 2 contains values for the electrolytic diffusion rates at different current densities measured in gram-atoms of hydrogen per second per square centimeter area per centimeter thickness. It will be seen that the value of the constant B changes with temperature. From this change the heat of activation of adsorption may be obtained as follows. Equation 28 may be written

$$\frac{dm}{dt} = c_{\mathrm{H}}^{2}\frac{kT}{h}e^{\frac{\Delta S^{\ddagger}}{R}}e^{-\frac{\Delta H^{\ddagger}}{RT}} = K_{eq}c_{\mathrm{H}_2}\frac{kT}{h}e^{\frac{\Delta S^{\ddagger}}{R}}e^{-\frac{\Delta H^{\ddagger}}{RT}} = -K_{eq}I = -\frac{P_{\mathrm{H}_2}}{B}$$

where K_{eq} is $c_{\mathrm{H}}^{2}/c_{\mathrm{H}_2}$, and I may be written as

$$c_{\mathrm{H}_2}\frac{kT}{h}e^{\frac{\Delta S^{\ddagger}}{R}}e^{-\frac{\Delta H^{\ddagger}}{RT}}$$

Thus if we plot $1/BT$ against $1/T$ we can obtain $\Delta H^{\ddagger}$ from the slope. The data give a satisfactorily straight line which yields a value of 1.5 kg-cal. for $\Delta H^{\ddagger}$. The sign will be negative for the reaction represented in equation 28, but positive if we are interested in the heat of activation of adsorption.

In figure 3 we have indicated in more detail the course of the diffusion phenomenon of a gas, particularly hydrogen, through a metal. The quantities noted in the figure are defined in the headings of table 5, where we have attempted to collect approximate values in the case of several metals, from the available data.

Since only those gaseous molecules which are able to combine with the solid can diffuse through it, a necessary condition for easy diffusibility of hydrogen is that the solid atoms have a low-lying orbital which can accommodate the hydrogen electron. All paramagnetic materials have such unpaired electrons as the paramagnetism itself shows, and the transition elements are in general conspicuous for their permeability to hydrogen as well as for their magnetic properties. Further, palladium, although it lies between nickel and platinum in the Periodic Table, is both more permeable to hydrogen and more inclined to keep its *d* shell filled if the electrons are available. This is shown, for example, by the fact that the 3*d* shell in normal nickel lacks two electrons of being full, the two extra electrons being in the 4*s* shell. In platinum the 5*d* shell lacks one electron of being full, the extra electron being in the 6*s* state, whereas in palladium the 4*d* shell is filled, with no electron able to overflow into the 5*s* state. This explains why solid palladium is more anxious to acquire an electron from hydrogen to fill the *d* shell, which has been partly emptied into higher states to form the metallic bonds. Other evidence than the permeability of the transition elements to hydrogen and a tendency to combine with the latter can be found in the nature of the coördination compounds which are formed (47).

When a metal is immersed in an electrolyte there is in general a preferential adsorption of the positive or negative ions on the surface. The ions of opposite charge then congregate on the opposite side of the double

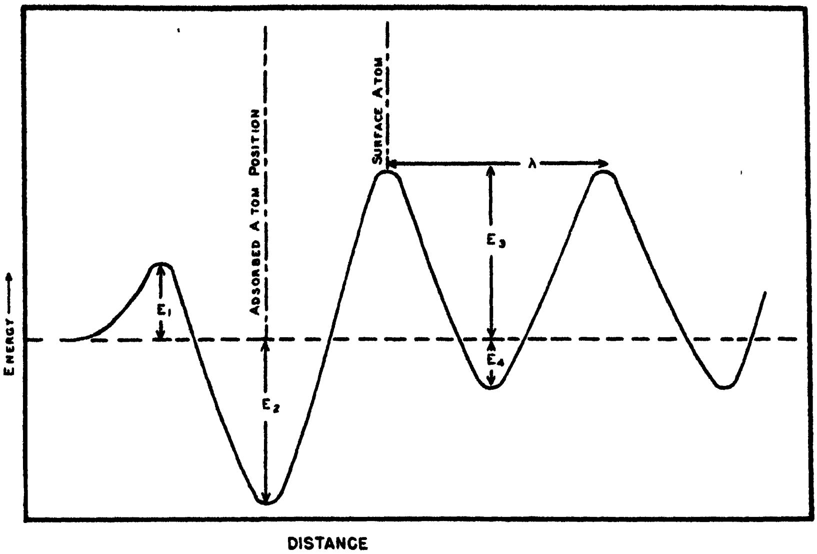

FIG. 3

TABLE 5

Various heat values per gram-atom of hydrogen

METAL	E_1 HEAT OF ACTIVATION OF ADSORPTION (TAKEN AS ENDOTHERMIC)		E_2 HEAT OF ADSORPTION (TAKEN AS EXOTHERMIC)		E_3 OVER-ALL ACTIVATION ENERGY OF DIFFUSION (TAKEN AS ENDOTHERMIC)		E_4 HEAT OF SOLUTION (TAKEN AS EXOTHERMIC)		$E_3 + E_4$ HEAT OF ACTIVATION OF THE LATTICE DIFFUSION PROCESS	
	Value	Reference	Value	Reference	Value	Reference	Value	Reference	Value	Reference
	kg-cal.		*kg-cal.*		*kg-cal.*		*kg-cal.*		*kg-cal.*	
Fe....	1.5	(4)	5.2	(15)	9.5	(64)	−3.5 ($T < 1100$) −4.1 ($T > 1100$)	(59)	6.0 5.4	
Pd...	2.9	(21)	Probably less than 1	(45)	4.33	(45, 38)	0.8 to 1.2	(45, 60)	5.1 to 5.5*	
Pt....	1.2	(43)	6.8	(42, 68)	18.8	(49, 23)	−7.8	(61)	11.0	
Ni....	1.5	(34)	5.0	(22)	13.9	(64, 4, 23, 37, 9)	−1.7	(59)	12.2	
Cu ..			6.2	(31, 2)	18.2	(64, 5)	−4.5	(59)	13.7	

* Direct experimental measurement of this quantity gives values lying between 4.1 and 6.7 (references 21, 7).

layer. The result is a definite change in the overvoltage which is a measure of the activation energy for the ion being transferred between electrode and electrolyte (19). This change in activation energy will arise whether the particle traversing the double layer carries a charge or not and whether or not the adsorbed molecules are charged. However, when both the diffusing and adsorbed particles carry charges we can anticipate an interesting difference arising from the polar nature of the double layer. In this case, if an electrolyte increases the rate of sorption, it should decrease the rate of desorption, since the ion traverses the double layer in opposite directions in the two cases. Since this effect has been observed by Kobozev and Monblanova (32) for the electrodiffusion of hydrogen through a palladium membrane between solutions containing potassium salts, we can conclude that the hydrogen passes over the barrier at the interface as an ion. Further, the fact that sorption is facilitated indicates that the negative ions are in this case preferentially adsorbed.

IV. ELECTROLYTIC CONDUCTION

The determination of the conductance and transference number of any constituent in a mixture gives information as to the average charge on the transported constituent. This can be calculated from the relationship between mobility and diffusion coefficient as follows: Given a solute with concentration gradient dc/dx, a potential barrier, and an applied field such that αw is the work done by the applied field in going to the top of the barrier, and $(1 - \alpha)w$ is the work done by the applied field in going from the top of the barrier to the trough. Then, if λ is the distance between two potential minima, we have for the number of particles crossing the barrier in the forward direction

$$\text{rate (forward)} = \lambda c k' e^{\frac{\alpha w}{kT}} \tag{29}$$

and

$$\text{rate (reverse)} = \lambda(c + \lambda\, dc/dx) k' e^{-\frac{(1-\alpha)w}{kT}} \tag{30}$$

where the forward direction is taken as that with the applied field, and k' is the specific rate constant. The net rate is thus

$$\text{rate (net)} = \lambda c k' e^{\frac{\alpha w}{kT}} - \lambda(c + \lambda\, dc/dx) k' e^{-\frac{(1-\alpha)w}{kT}} \tag{31}$$

Since w/kT will in general be small compared to unity, we may expand the exponentials, dropping terms beyond the first power of w/kT, and write in place of equation 31

$$\text{rate (net)} = \lambda c k'(1 + \alpha w/kT) - \lambda(c + \lambda\, dc/dx) k' \left(1 - \frac{(1-\alpha)w}{kT}\right) \tag{32}$$

$$= \frac{\lambda c k' w}{kT} - \lambda^2 k' \frac{dc}{dx}\left(1 - \frac{(1-\alpha)w}{kT}\right) \tag{33}$$

or, since $(1 - \alpha)w/kT \ll 1$, we may write

$$\text{rate (net)} = \frac{\lambda c k' w}{kT} - \lambda^2 k' \frac{\mathrm{d}c}{\mathrm{d}x} \tag{34}$$

If the applied field is electrical, we may put

$$w = \lambda \varphi z \epsilon \tag{35}$$

where φ is the potential gradient (in units to give work in ergs), and $z\epsilon$ is the effective charge, or z is the absolute value of the effective charge in electron units. Substituting in equation 34 we get

$$\text{rate (net)} = \frac{\lambda^2 c k' z \epsilon \varphi}{kT} - \lambda^2 k' \, \mathrm{d}c/\mathrm{d}x \tag{36}$$

But for the electrical flow we have

$$\text{rate (elec.)} = cB\varphi = \frac{\lambda^2 c k' z \epsilon \varphi}{kT} \tag{37}$$

where B is the mobility. However, since the diffusion coefficient, D, is $\lambda^2 k'$, we obtain

$$B = \frac{Dz\epsilon}{kT} \tag{38}$$

or

$$z = \frac{BkT}{D\epsilon} \tag{39}$$

Table 6 contains values of z calculated for four types of solid conduction systems, together with the value calculated for K^+ or Cl^- in potassium chloride solution (aqueous), for comparison.

The observed value of $z = 0.007$ for hydrogen diffusing in palladium can be understood if the migrating hydrogen has a charged activated state lying about 3 kg-cal. higher than the activated state. In this case about seven protons would migrate for each 993 uncharged hydrogen atoms which pass over the barrier. The alternate hypothesis that each diffusing hydrogen atom carries 0.7 per cent of a unit of charge seems unlikely.

The effect of hydrogen on the conductance of palladium gives some evidence as to the condition of the dissolved hydrogen. The effective charge on the hydrogen is seen from table 6 to be small. The decrease in conductivity caused by dissolving hydrogen in palladium is in part due to the diluting of the conducting metallic electrons, since the metal expands with increasing hydrogen concentration; but the conductivity decrease is greater than can be accounted for on this basis alone. In table 7, calcu-

TABLE 6

Values of z calculated for four types of solid conduction systems

SYSTEM	*B*	*D*	*T*	*z*	SIGN OF CHARGE	REFERENCE
	cm. per second per volt per cm.	*cm.^{2} * per second*	°*A.*			
H-Pd	2.5×10^{-5}	9.5×10^{-6}	308	0.007	H positive	(10)
Au-Pb (0.02 atom per cent Au)	4.73×10^{-8}	3.25×10^{-7}	473	0.006	Au negative	(53)
Pb-PbI$_2$	6.63×10^{-12}	2.97×10^{-13}	500	0.96	Pb positive	(52, 24)
Pd-Au	3.45×10^{-11}	1.17×10^{-10}	1173	0.03	Pd positive	(30, 29)
C-Fe	1.6×10^{-5} to 2.2×10^{-5}	$5. \times 10^{-7}$	1343	0.005	C positive	(57, 46)
K (or Cl)-H$_2$O	6.79×10^{-4}	1.69×10^{-5}	291	1.01		(72)

* *B* in units given in the table, may be calculated from the relationship

$$B_i = \frac{1000 n_i \kappa}{\mathfrak{F} c_i}$$

where κ is the specific conductance, n_i is the transference number of the i^{th} constituent, $\mathfrak{F}$ is the Faraday, and c is the concentration in gram-atoms per liter. Substituting for z, we get

$$z = \frac{8.9 \times 10^{-7} n_i \kappa T}{D c_i}$$

where D is the diffusion coefficient.

TABLE 7

Effect of dissolving hydrogen in palladium on the conducting electrons

HYDROGEN CONCENTRATION RATIO H/Pd	PER CENT CHANGE IN κ	PER CENT CHANGE IN VOLUME	PER CENT CHANGE IN κ CORRECTED FOR VOLUME CHANGE	CONDUCTING ELECTRONS BOUND PER H ATOM (Ratio column 4/column 5)	$\kappa \times 10^4$
0.000					9.321
0.060	11.47	5.27	6.2	1.03	8.252
0.12	17.52	6.63	10.89	0.91	7.6876
0.307	33.80	9.75	24.05	0.78	6.1712
0.459	41.70	11.98	29.72	0.65	5.4344
0.549	46.10	13.27	32.83	0.60	5.0233
0.645	50.73	14.80	35.93	0.56	4.5924

lated from the data of G. Wolf (70), we have estimated the number of conducting electrons effectively bound, per atom of hydrogen in the palladium.

We wish to thank Dr. John Turkevich for helpful discussions.

REFERENCES

(1) Baukloh, W., and Kayser, H.: Z. Metallkunde **26**, 156 (1934).
(2) Beebe, R. A.: Trans. Faraday Soc. **28**, 761 (1932).
(3) Bodenstein, M.: Z. Elektrochem. **28**, 517 (1922).
(4) Borelius, G., and Lindblom, S.: Ann. Physik **82**, 201 (1927).
(5) Braaten, E. O., and Clark, G. F.: Proc. Roy. Soc. (London) **153**, 504 (1936).
(6) Braune, H.: Z. physik. Chem. **110**, 147 (1924).
(7) Coehn, A., *et al.*: Z. Physik **62**, 1 (1930); **71**, 179 (1931); **83**, 291 (1933).
(8) Cohen, E., and Bruins, H. R.: Proc. Acad. Sci. Amsterdam **27**, 555 (1924).
van Ostrand, C. E., and Dewey, F. P.: U. S. Geol. Survey, Professional Paper No. 95 (1915).
Seith, W., and Etzold, H.: Z. Elektrochem. **40**, 829 (1934).
(9) Deming, H. G., and Hendricks, B. C.: J. Am. Chem. Soc. **45**, 2863 (1923).
(10) Duhm, B.: Z. Physik **94**, 434 (1935).
Coehn, A., and Jürgens, H.: Z. Physik **71**, 179 (1931).
(11) Dunn, J. S.: J. Chem. Soc. **129**, 2973 (1926).
(12) Dushman, S., Denison, D., and Reynolds, N. B.: Phys. Rev. **29**, 903 (1927).
(13) Dushman, S., and Langmuir, I.: Phys. Rev. **20**, 113 (1922).
(14) Edwards, C. A.: J. Iron Steel Inst. (London) **110**, 9 (1924).
(15) Emmett, P. H., and Harkness, R. W.: J. Am. Chem. Soc. **57**, 1631 (1935).
(16a) Ewell, R. H., and Eyring, H.: J. Chem. Phys. **5**, 726 (1937).
(16b) Frisch, D., Kincaid, J. F., and Eyring, H.: J. Chem. Phys., in press.
(17) Eyring, H.: J. Chem. Phys. **3**, 107 (1935).
(18) Eyring, H.: J. Chem. Phys. **4**, 283 (1936).
(19) Eyring, H., Glasstone, S., and Laidler, K.: J. Chem. Phys. **7**, 1053 (1939).
(20) Eyring, H., and Hirschfelder, J.: J. Phys. Chem. **41**, 249 (1937).
Kincaid, J. F., and Eyring, H.: J. Chem. Phys. **6**, 620 (1938).
(21) Farkas, A.: Trans. Faraday Soc. **32**, 1667 (1936).
(22) Fryling, C. F.: J. Phys. Chem. **30**, 818 (1926).
(23) Ham, W. R.: J. Chem. Phys. **1**, 476 (1933).
(24) Hevesy, G. v., and Seith, W.: Z. Physik **56**, 790 (1929).
(25) Hevesy, G. v., and Seith, W.: Z. Elektrochem. **37**, 528 (1931).
(26) Hevesy, G. v., Seith, W., and Kiel, A.: Z. Physik **79**, 197 (1932).
(27) *International Critical Tables*, Vol. III, p. 284. McGraw-Hill Book Company, Inc., New York (1928).
(28) Jost, W.: Z. physik. Chem. **B9**, 73 (1930).
(29) Jost, W.: Z. physik. Chem. **B21**, 158 (1933).
(30) Jost, W., and Linke. R.: Z. physik. Chem. **B29**, 127 (1935); we have taken 10^4 for the specific conductance of this alloy at 900°C.
(31) Kistiakowsky, G. B., Flosdorf, E. W., and Taylor, H. S.: J. Am. Chem. Soc. **49**, 2200 (1927).
(32) Kobozev, N. I., and Monblanova, V.: Acta Physicochim. U. S. S. R. **1**, 611 (1934); J. Phys. Chem. (U. S. S. R.) **6**, 308 (1935); *cf.* also reference 21.
(33) Langmuir, I.: Chem. Rev. **13**, 147 (1933); J. Franklin Inst. **217**, 543 (1934).
(34) Leypinsky, O. I.: Acta Physicochim. U. S. S. R. **2**, 737 (1935); J. Phys. Chem. U. S. S. R. **9**, 143 (1937).
(35) van Liempt, J. A. M. (a) Rec. trav. chim. **51**, 114 (1932); (b) Z. anorg. Chem. **195**, 366 (1931).
(36) Lombard, V.: Thesis, Paris, 1928.
(37) Lombard, V.: Rev. mét. **26**, 519 (1929).
(38) Lombard, V., and Eichner, C.: Bull. soc. chim. [4] **53**, 1176 (1933).

(39) McKay, H. A. C.: Trans. Faraday Soc. **34**, 845 (1938).
(40) Matano, C.: Mem. Coll. Sci., Kyoto Imp. Univ. **15**, 351 (1932).
(41) Matano, C.: Japan. J. Phys. **9**, 41 (1934); *cf.* also reference 11.
(42) Maxted, E. B., and Hassid, N.: J. Chem. Soc **1931**, 3313.
(43) Maxted, E. B., and Moon, C. H.: J. Chem. Soc. **1936**, 1542.
(44) *Cf.* Mehl, R. F.: Metals Tech. **3**, 1 (1936).
(45) Melville, H. W., and Rideal, E. K.: Proc. Roy. Soc. (London) **153**, 89 (1935).
(46) Paschke, M., and Hauttmann, A.: Arch. Eisenhüttenw. **9**, 305 (1935).
(47) *Cf.* Pauling, L.: *Nature of the Chemical Bond*, p. 231. Cornell University Press, Ithaca, New York (1939).
(48) Rhines, F. N., and Mehl, R. F.: Am. Inst. Mining Met. Engrs., Inst. Metals Div., Tech. Pub. 883 (1938).
(49) Richardson, O. W., Nicol, J., and Parnell, T.: Phil. Mag. [6] **8**, 1 (1904).
(50) Schottky, W.: Z. physik. Chem. **B29**, 335 (1935).
(51) Seith, W.: Z. Elektrochem. **39**, 538 (1933).
(52) Seith, W.: Z. Physik **56**, 802 (1929).
(53) Seith, W., and Etzold, H.: Z. Elektrochem. **40**, 829 (1934).
(54) Seith, W., and Etzold, H.: Z. Elektrochem. **41**, 122 (1935).
(55) Seith, W., Hofer, E., and Etzold, H.: Z. Elektrochem. **40**, 322 (1934).
(56) Seith, W., and Kiel, A.: Z. physik. Chem. **B22**, 350 (1933).
(57) Seith, W., and Kubaschewski, O.: Z. Elektrochem. **41**, 551 (1935).
(58) Seith, W., and Peretti, E. A.: Z. Elektrochem. **42**, 570 (1936).
(59) Sieverts, A.: Z. physik. Chem. **77**, 591 (1911).
(60) Sieverts, A.: Z. physik. Chem. **88**, 103 (1914).
(61) Sieverts, A., and Jurisch, E.: Ber. **45**, 221 (1912).
(62) Smith, D. P., and Derge, G. J.: Trans. Electrochem. Soc. **66**, 253 (1934); J. Am. Chem. Soc. **56**, 2513 (1934).
Moore, G. A., and Smith, D. P.: Trans. Electrochem. Soc. **71**, 545 (1937); Am. Inst. Mining Met. Engrs., Tech. Pub. 1065 (1939).
Moore, G. A.: Trans. Electrochem. Soc. **75**, 257 (1939).
(63) Smithells, C. J.: *Gases and Metals*, p. 107. John Wiley and Sons, Inc., New York (1937).
(64) Smithells, C. J., and Ransley, C. E.: Proc. Roy. Soc. (London) **150**, 172 (1935).
(65) Smithells, C. J., and Ransley, C. E.: Proc. Roy. Soc. (London) **157**, 292 (1936).
(66) Stearn, A. E., Irish, E. M., and Eyring, H.: J. Phys. Chem. **44**, 981 (1940).
(67) Steigman, J., Shockley, W., and Nix, F. C.: Phys. Rev. **56**, 13 (1939).
(68) Taylor, H. S., and Kistiakowsky, G. B.: Z. physik. Chem. **125**, 341 (1927).
(69) Wagner, C., and Schottky, W.: Z. physik. Chem. **B11**, 163 (1930). See also Jost, W.: *Diffusion und Chemische Reaktion in festen Stoffen.* Steinkopff, Dresden and Leipzig (1937). Hedvall, J. A.: *Reaktionsfähigkeit fester Stoffe.* Barth, Leipzig (1938).
(70) Wolf, G.: Z. physik. Chem. **87**, 575 (1914).
(71) Wynne-Jones, W. F. K., and Eyring, H.: J. Chem. Phys. **3**, 492 (1935).
(72) Zuber, R., and Sitte, K.: Z. Physik **79**, 306 (1932).

A THEORY OF DIFFUSION IN LIQUIDS

ALLEN E. STEARN
Department of Chemistry, University of Missouri, Columbia, Missouri
AND
EDWIN M. IRISH AND HENRY EYRING
Frick Chemical Laboratory, Princeton University, Princeton, New Jersey

Received January 28, 1940

INTRODUCTION

Although for the diffusion of large molecules through a solvent composed of smaller molecules the Stokes-Einstein law of diffusion has been found to describe satisfactorily the experimental results, it is unsatisfactory in principle in cases where solute and solvent molecules are nearly the same size. Eyring (3) has pointed out that the process of diffusion is the same as that for viscous flow, except that in diffusion the two molecules passing each other may have different properties, whereas for viscous flow, in a pure liquid at least, the two molecules passing each other are alike. The relation between the diffusion coefficient and the specific velocity constant given for an activated rate process was

$$D = \lambda^2 k' \tag{1}$$

where λ is the distance between two equilibrium positions of the diffusing molecule, and k' is the number of times per second that a particular molecule is engaged in passing a neighbor in any particular direction,—say the direction of diffusion.

The expression developed for viscosity was (3)

$$\eta = \lambda_1 kT/\lambda^2\lambda_2\lambda_3 k' \tag{2}$$

where λ has the same significance as in equation 1, namely, the distance between equilibrium positions in the direction of flow, λ_1 is the perpendicular distance between adjacent layers of molecules, λ_2 is the distance between adjacent molecules in the direction of flow, λ_3 is the distance between molecules in the plane of flow and normal to the direction of flow, and k' is the specific rate constant.

Taylor (18), using the combination

$$D = kT\lambda_1/\lambda_2\lambda_3\eta$$

of equations 1 and 2, found that it gave much more reasonable results than the Stokes-Einstein relation,

$$D = kT/6\pi r\eta$$

when the molecules diffusing into each other were similar.

Since viscosity was shown to exhibit an exponential variation with temperature (2), it follows that diffusion should exhibit a like temperature variation. For solid diffusion such a variation with temperature has long been recognized, but up until this time diffusion in liquids has frequently been considered as a linear function of temperature. The difficulty of measuring diffusion rates has restricted the advancement of investigation into this problem, and even Cohen and Bruins (1), whose data on the diffusion of tetrabromoethane in tetrachloroethane seem as yet the best available for determining the variation of diffusion rate with temperature, plot their rate values against both the first and the second powers of the temperature.

From absolute reaction rate theory (4) we may write for k' in equation 1

$$k' = \frac{kT}{h}\frac{\mathcal{F}^{\ddagger}}{\mathcal{F}_n}e^{-\frac{E_0}{RT}} \tag{3}$$

$$= \frac{kT}{h}e^{-\frac{\Delta F^{\ddagger}}{RT}} = \frac{kT}{h}e^{-\frac{\Delta S^{\ddagger}}{R}}e^{-\frac{\Delta H^{\ddagger}}{RT}} \tag{4}$$

where $\mathcal{F}^{\ddagger}$ and $\mathcal{F}_n$ are the partition functions of the reacting system in the activated and the normal state, respectively, $\Delta F^{\ddagger}$ $\Delta S^{\ddagger}$, and $\Delta H^{\ddagger}$ are, respectively, the standard free energy, entropy, and heat increases when the activated complex is formed from the reactants, E_0 is the difference in energy between the lowest level in the normal and in the activated state, k is the Boltzmann constant, and h is the Planck constant. We have taken the transmission coefficient as unity. The heat of activation is calculated from the relation

$$\Delta H^{\ddagger} = RT^2\frac{\mathrm{d}\ln k'}{\mathrm{d}T} - RT$$

From equations 1, 3, and 4 we obtain

$$D = \lambda^2\frac{kT}{h}\frac{\mathcal{F}^{\ddagger}}{\mathcal{F}_n}e^{-\frac{E_0}{RT}} \tag{5}$$

$$= \lambda^2\frac{kT}{h}e^{-\frac{\Delta F^{\ddagger}}{RT}} = \lambda^2\frac{kT}{h}e^{\frac{\Delta S^{\ddagger}}{R}}e^{-\frac{\Delta H^{\ddagger}}{RT}} \tag{6}$$

If we assume that the degree of freedom corresponding to flow is a translational one, and that the partition functions for other degrees of freedom are the same for the initial and activated states, then

$$\frac{\mathcal{F}^{\ddagger}}{\mathcal{F}_n} = \frac{h}{(2\pi mkT)^{1/2}v_f^{1/3}} \tag{7}$$

where v_f is the free volume for one molecule. Capital letters are used for the volume, V, and the free volume, V_f, when a mole is indicated.

If the unit process in diffusion (or in viscous flow) is the passing of two molecules in the sense of a partial rotation of a double molecule (10), extra space must be provided, though this may not necessarily have to be a hole the full size of a molecule. Therefore the energy of activation for diffusion will be some fraction of the energy of vaporization; $\Delta E_{\text{act.}} = \Delta E_{\text{vap.}}/n$. Considering the data of Cohen and Bruins (1), Taylor (18) concluded that in diffusion the size of the hole required is approximately the arithmetic mean of that required by the two pure substances in their respective viscous flows.

Substituting equation 7 into equation 5 and writing $\Delta E_{\text{vap.}}/n$ for E_0, we obtain

$$D = \lambda^2 \frac{kT}{h} \frac{h}{(2\pi mkT)^{1/2} v_f^{1/3}} e^{-\frac{\Delta E_{\text{vap.}}}{nRT}} \tag{8}$$

$$= \frac{\lambda^2}{v_f^{1/3}} \left(\frac{kT}{2\pi m}\right)^{1/2} e^{-\frac{\Delta E_{\text{vap.}}}{nRT}} \tag{9}$$

For λ, in the case of a pure liquid, we take $(V/N)^{1/3}$, where N is Avogadro's number. The free volume characteristic of a pure liquid has been estimated in various ways. Eyring and Hirschfelder (5) developed the relation

$$v_f^{1/3} = \frac{2RT}{V^{2/3}N^{1/3}(p + a/V^2)} \tag{10}$$

$$= \frac{2RTV^{1/3}}{N^{1/3}\Delta E_{\text{vap.}}} \qquad \text{if } a/V^2 = \Delta E_{\text{vap.}}/V \gg p \tag{11}$$

where $\Delta E_{\text{vap.}} = \Delta H_{\text{vap.}} - \Delta(pV)$. Kincaid and Eyring (13) find

$$v_f^{1/3} = v^{1/3} \frac{U_{\text{gas}}}{U_{\text{liq.}}} \tag{12}$$

where U is the velocity of sound.[1]

For more concentrated solutions the change in activity coefficients of the components with concentration will affect the free energy of activation. This effect can be calculated for the simple case of molecules of approximately equal size as follows: Let $\Delta F_0^\ddagger$ be the height of the energy barrier in figure 1. Then if γ_1 and γ_2 are, respectively, the activity coefficients of constituents 1 and 2, the rate at which constituent 1 will sur-mount the barrier in the forward direction (left to right) will depend not only on $\Delta F_0^\ddagger$ but also on the differences in γ_1 and γ_2 on the opposite sides of the barrier. For a symmetrical barrier the additional free energy, due to non-ideality of the solution, needed by constituent 1 to reach the top of the barrier in the forward direction will be

---

[1] There seems to be no significant difference in the values of the free volumes whether calculated from equation 11 or equation 12 except in the case of water. For five organic liquids the ratio of $v_f^{1/3}$ from equation 12 to that from equation 11 averages 0.95 and varies from about 0.85 to 1.07, whereas for water this ratio is about 2.5 (*cf.* reference 8). In the case of the values of free volume used later in this paper, we specify in all cases whether they were obtained from equation 11 or equation 12.

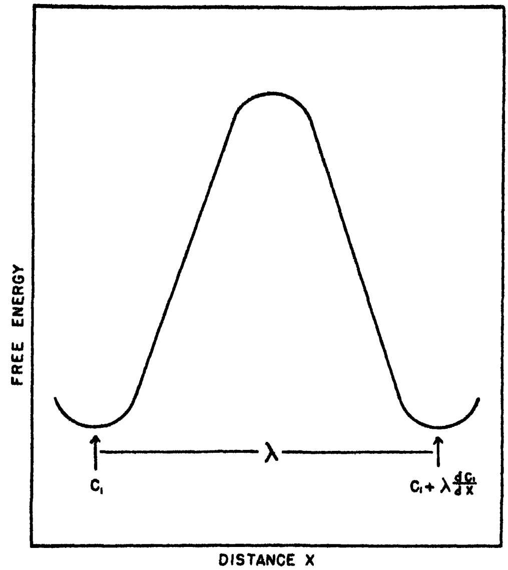

FIG. 1. Potential energy curve for diffusion

$$\frac{RT\,\mathrm{d}\ln\gamma_1}{\mathrm{d}N_1}\,\frac{\mathrm{d}N_1}{\mathrm{d}x}\,\frac{\lambda}{2}-\frac{RT\,\mathrm{d}\ln\gamma_2}{\mathrm{d}N_2}\,\frac{\mathrm{d}N_2}{\mathrm{d}x}\,\frac{\lambda}{2}$$

$$=\frac{RT\,\mathrm{d}\ln\gamma_1}{\mathrm{d}N_1}\,\frac{\mathrm{d}N_1}{\mathrm{d}x}\,\frac{\lambda}{2}+\frac{RT\,\mathrm{d}\ln\gamma_2}{\mathrm{d}N_2}\,\frac{\mathrm{d}N_1}{\mathrm{d}x}\,\frac{\lambda}{2}$$

where N_1 and N_2 are the mole fractions of constituents 1 and 2, and $\mathrm{d}N_1 = -\mathrm{d}N_2$.

We set

$$\frac{RT\,\mathrm{d}\ln\gamma_1}{\mathrm{d}N_1}=G_1,\qquad \frac{RT\,\mathrm{d}\ln\gamma_2}{\mathrm{d}N_2}=G_2$$

and

$$\frac{kT}{h}e^{-\frac{\Delta F_0^\ddagger}{RT}}=B$$

We may then write for the net rate[2] of constituent 1 in the forward direction

---

[2] When the effect of G_1 only is considered, we obtain the form of activity coefficient effect given by L. Onsager and R. M. Fuoss (J. Phys. Chem. **36**, 2687 (1932)).

$$\text{rate} = -D_1\,\mathrm{d}n_1/\mathrm{d}x = \lambda n_1 k'_{\text{forward}} - \lambda(n_1 + \lambda\,\mathrm{d}n_1/\mathrm{d}x)k'_{\text{reverse}} \tag{13}$$

$$= \lambda B n_1 \exp\left(-\frac{(G_1 + G_2)(\mathrm{d}N_1/\mathrm{d}x)(\lambda/2)}{RT}\right) - \lambda B(n_1 + \lambda\,\mathrm{d}n_1/\mathrm{d}x)\exp\left(\frac{(G_1 + G_2)(\mathrm{d}N_1/\mathrm{d}x)(\lambda/2)}{RT}\right) \tag{14}$$

Since

$$(G_1 - G_2)\frac{\mathrm{d}N_1\lambda}{\mathrm{d}x\ 2} \ll RT$$

we may expand the exponential in equation 14 and, neglecting higher powers of the exponent, write

$$-D_1\,\mathrm{d}n_1/\mathrm{d}x = -\lambda^2 B n_1 \frac{(G_1 + G_2)}{RT}\frac{\mathrm{d}N_1}{\mathrm{d}x} - \lambda^2 B\frac{\mathrm{d}n_1}{\mathrm{d}x}\left(1 + \frac{(G_1 + G_2)}{RT}\frac{\mathrm{d}N_1}{\mathrm{d}x}\frac{\lambda}{2}\right) \tag{15}$$

Noting that $n_1\,\mathrm{d}N_1/\mathrm{d}x = N_1\,\mathrm{d}n_1/\mathrm{d}x$, provided the molecules are about the same size so that $n_1 + n_2$ can be assumed constant, and that

$$\frac{(G_1 + G_2)}{RT}\frac{\mathrm{d}N_1}{\mathrm{d}x}\frac{\lambda}{2}$$

can be neglected compared to unity, we obtain

$$D_1 = \lambda^2 B(1 + N_1(G_1 + G_2)/RT) \tag{16}$$

Replacing G_1, G_2, and B by their respective values and noting that

$$\lambda^2 B = D_1^0 \text{ (equations 1 and 4)}$$

we have

$$D_1 = D_1^0\left(1 + N_1\left(\frac{\mathrm{d}\ln\gamma_1}{\mathrm{d}N_1} + \frac{\mathrm{d}\ln\gamma_2}{\mathrm{d}N_2}\right)\right) \tag{17}$$

$$= D_1^0\left(1 + \frac{\mathrm{d}\ln\gamma_1}{\mathrm{d}\ln N_1} - \frac{\mathrm{d}\ln\gamma_2}{\mathrm{d}\ln N_2} + \frac{\mathrm{d}\ln\gamma_2}{\mathrm{d}N_2}\right) \tag{18}$$

From the Duhem–Margules relation

$$\frac{\mathrm{d}\ln\gamma_1}{\mathrm{d}\ln N_1} = \frac{\mathrm{d}\ln\gamma_2}{\mathrm{d}\ln N_2}$$

equation 18 becomes

$$D_1 = D_1^0(1 + \mathrm{d}\ln\gamma_2/\mathrm{d}N_2) \tag{19}$$

$$= D_1^0\left(1 + \frac{\mathrm{d}\ln\gamma_1}{N_2\,\mathrm{d}\ln N_1}\right) \tag{20}$$

If we introduce the relation (9)

$$\ln \gamma_2 = \frac{1}{2}\beta_1 N_1^2$$

we may also write

$$D_1 = D_1^0(1 - \beta_1 N_1) \tag{21}$$

true when N_1 is small. Similarly, when N_2 is small we have

$$\ln \gamma_1 = \frac{1}{2}\beta_2 N_2^2$$

which when substituted in equation 20 gives

$$D_1 = D_1^0(1 - \beta_2 N_1) \tag{21a}$$

For large spherical molecules moving with a velocity u in a solution Stokes has shown that the force acting on such a molecule is

$$f = 6\pi r u \eta \tag{22}$$

where r is the radius of the molecule and η is the viscosity of the solution. For a solution containing n_1 of these large molecules per cubic centimeter, the total force acting on all these molecules in a column of solution of unit cross section and length δx is

$$\mathrm{d}f = 6\pi r \eta u n_1 \delta x \tag{23}$$

Now for a perfect solution $p = n_1 kT$, so that the osmotic force acting on the same column of solution is

$$-\mathrm{d}f = \frac{\mathrm{d}n_1}{\mathrm{d}x}\delta x kT \tag{24}$$

For an actual solution we have

$$-\,\mathrm{d}f = \frac{\mathrm{d}n_1}{\mathrm{d}x}\,\delta x\, kT + n_1\left(\frac{kT\,\partial \ln \gamma_1}{\partial N_1}\frac{\mathrm{d}N_1}{\mathrm{d}x}\,\delta x - \frac{\bar{V}_1}{\bar{V}_2}\frac{kT\,\partial\, ln\ \gamma_2}{\partial N_2}\frac{\mathrm{d}N_2}{\mathrm{d}x}\,\delta x\right) \tag{25}$$

where the second term is due to the change of activity coefficients with concentration. The factor $\bar{V}_1/\bar{V}_2$, the ratio of partial molal volumes, arises from the fact that when one large molecule flows from its initial position, enough small molecules must then flow in to fill the resulting hole. Noting that $\mathrm{d}N_1 = -\mathrm{d}N_2$, where N_i is the mole fraction and, since

$$\frac{n_1\bar{V}_1 + n_2\bar{V}_2}{N} = 1$$

(N being Avogadro's number here), that

$$n_1\,\mathrm{d}N_1/\mathrm{d}x = N_1\,\mathrm{d}n_1/\mathrm{d}x\left(\frac{N_2\bar{V}_2 + N_1\bar{V}_1}{\bar{V}_2}\right)$$

using the Duhem–Margules relation and simplifying,

$$-\mathrm{d}f = \frac{\mathrm{d}n_1}{\mathrm{d}x}\delta x\, kT\left[1 + \left(\frac{N_1\,\mathrm{d}\ln\gamma_1}{\mathrm{d}N_1} + \frac{\bar{V}_1}{\bar{V}_2}\,\frac{N_1\,\mathrm{d}\ln\gamma_2}{\mathrm{d}N_2}\right)\left(\frac{N_2\bar{V}_2 + N_1\bar{V}_1}{\bar{V}_2}\right)\right]$$

$$= \frac{\mathrm{d}n_1}{\mathrm{d}x}\delta x\, kT\left(1 + \frac{\mathrm{d}\ln\gamma_1}{\mathrm{d}\ln N_1}\,\frac{(N_2\bar{V}_2 + N_1\bar{V}_1)^2}{N_2\bar{V}_2^2}\right) \tag{26}$$

Equating expressions 23 and 26 and noting that $un_1 = \mathrm{d}n_1/\mathrm{d}t$, we obtain

$$\frac{\mathrm{d}n_1}{\mathrm{d}t} = -D\frac{\mathrm{d}n_1}{\mathrm{d}x} = -\frac{\mathrm{d}n_1}{\mathrm{d}x}\,\frac{kT}{6\pi r\eta}\left(1 + \frac{\mathrm{d}\ln\gamma_1}{\mathrm{d}\ln N_1}\,\frac{(N_2\bar{V}_2 + N_1\bar{V}_1)^2}{N_2\bar{V}_2^2}\right) \tag{27}$$

so that

$$D = \frac{kT}{6\pi r\eta}\left(1 + \frac{\mathrm{d}\ln\gamma_1}{\mathrm{d}\ln N_1}\,\frac{(N_2\bar{V}_2 + N_1\bar{V}_1)^2}{N_2\bar{V}_2^2}\right) \tag{28}$$

For large molecules which are not spherical, the right-hand side of equation 28 would have to be multiplied by another factor which would depend on the shape. For example, in the case of a prolate ellipsoid with the ratio of the short to the long axis a/b, this factor has been found to have the form (16)

$$\frac{(a/b)^{2/3}}{\sqrt{1-(a/b)^2}}\ln\frac{1+\sqrt{1-(a/b)^2}}{a/b}$$

Diffusion, like every other rate process, has a specific rate constant which depends on the mechanism, i.e., the nature of the activated complex. Whether the mechanisms that lead to equations 20 and 28 are correct can be ascertained only by comparison with experiment. They should be compared with equation 19 for a unimolecular mechanism in the accompanying article by Stearn and Eyring. With sufficient data, using these equations, it should be possible to choose definitely between a bimolecular and a unimolecular or some still more complicated mechanism.

COMPARISON WITH EXPERIMENTAL DATA

As a test of equation 9 we use the data of Cohen and Bruins (1) on the diffusion of tetrabromoethane in tetrachloroethane. They employed liquid mixtures up to a mole fraction of tetrabromoethane of 0.0783, and we have used this concentration for calculating the average values of the quantities occurring in equation 9. For these different quantities the following average values are chosen: For λ and $v_f^{1/3}$ we take the weighted arithmetical mean of the values characteristic of the pure constituents, e.g.,

$$\lambda_{\text{ave.}} = N_1\lambda_1 + N_2\lambda_2$$

For m we use the reduced mass of the two passing molecules, and for $\Delta E_{\text{vap.}}$ we use the geometric mean of the energies of vaporization of the two pure constituents, i.e.,

$$\Delta E_{\text{vap.ave.}} = (N_1\sqrt{\Delta E_{\text{vap.}_1}} + N_2\sqrt{\Delta E_{\text{vap.}_2}})^2$$

The heat of vaporization of tetrachloroethane is known, and, by assuming the same Trouton constant for tetrabromoethane, its theoretical heat of vaporization can be calculated at its boiling point, and from this can be obtained the corresponding energy of vaporization. For the temperature coefficient of the energy of vaporization we use the relation developed by Kincaid and Eyring (12)

$$\Delta E_T/\Delta E_B = V_B/V_T$$

where the subscripts B and T refer respectively to boiling point and the temperature of interest, and V is the molal volume. The results are given in table 1. Values of $v_f^{1/3}$ for the constituents were obtained with the use of equation 11, and from the results of Ewell and Eyring (2) and in agreement with Taylor (18), we take $n = 3$.

TABLE 1

Diffusion of tetrabromoethane in tetrachloroethane

T	$\lambda^2 \times 10^{15}$ (AVERAGE)	$V_f^{1/3} \times 10^9$ (AVERAGE)	$\Delta E_{\text{vap.}}$ (AVERAGE)	$D_{\text{obsd.}} \times 10^5$	$D_{\text{calcd.}} \times 10^5$	RATIO $D_{\text{obsd.}}/D_{\text{calcd.}}$
°*A.*			*kg.-cal.*	*cm.*^{2} *sec.*$^{-1}$	*cm.*^{2} *sec.*$^{-1}$	
273.44	3.124	6.45	9.852	0.351	0.64	0.55
280.7	3.140	6.69	9.784	0.419	0.77	0.54
288.0	3.155	6.92	9.719	0.497	0 92	0.54
298.0	3.174	7.25	9.624	0.611	1.14	0.54
308.61	3.195	7.59	9.525	0.741	1.42	0.52
324.1	3.230	8.13	9.383	0.954	1.89	0.51

The constancy of the ratio $D_{\text{obsd.}}/D_{\text{calcd.}}$ (column 7) shows that the calculated values of D reproduce the experimental temperature coefficient very closely. This ratio is less than unity, a fact which has been found generally true for diffusion in organic liquids, and which is commented on below.

Aqueous diffusion

Few data are available which suffice for obtaining satisfactory temperature coefficients in the case of aqueous diffusion. There are numerous cases where the value of the diffusion coefficient is reported for two temperatures, usually differing by not much more than 10 degrees. For such cases it was not thought advisable to attempt to calculate values for n. However, the value of n for the viscous flow of water varies (2) from 2.0

at 0°C. to 2.8 at 50°C. For room temperatures, where most aqueous diffusion data have been obtained, n for water is about 2.4. The data of Scheffer and Scheffer (17) on the diffusion of mannite in water between 0° and 70°C. were found to give a good straight line when log D was plotted against $1/T$. Its slope gave $\Delta E_{\text{act.}} = 4047$ cal., and this, with the average $\Delta E_{\text{vap.}}$ for water between 0 and 70°C., gives a value for n of 2.41. We therefore use the value 2.4 for n for water. In table 2 we compare values of D calculated by means of equation 9 with the experimental values of Scheffer and Scheffer. Besides the average value of $n = 2.4$, which we use through the temperature range, we use the average $\Delta E_{\text{vap.}}$ for water of 9700 cal.

We have calculated D using both equation 11 and equation 12 to obtain the free volumes. As was pointed out above, these two equations seem to give about the same values for most liquids, but not for water. In either case the constancy of the ratio $D_{\text{obsd.}}/D_{\text{calcd.}}$ indicates how well the calculated values of D reproduce the temperature coefficient. In the case of this aqueous solution it will be seen that the ratio $D_{\text{obsd.}}/D_{\text{calcd.}}$ is greater than 1. This is found to be generally true for diffusion in water, in contrast to values less than 1 for diffusion in organic liquids. That this ratio differs consistently from unity is at least partly due to a factor in equation 9 which has not been considered. For the case of a liquid with a structure such as water, rotation in the normal state will be hindered more strongly than in the activated state. Thus in cancelling out all but one term in the partition functions corresponding to the two states this factor is overlooked (13). This would lead to a calculated value too low. For liquids without such pronounced structure rotation may, on the other hand, be less hindered in the normal state, and the neglect of this factor would then lead to calculated results which are too high.

TABLE 2

Diffusion of mannite in water

T	$D_{\text{obsd.}} \times 10^5$	$D_{\text{calcd.}} \times 10^5$	RATIO $D_{\text{obsd}}/D_{\text{calcd.}}$	$D_{\text{calcd.}} \times 10^5$	RATIO $D_{\text{obsd.}}/D_{\text{calcd.}}$
		($V_f^{1/3}$ FROM EQUATION 12)		($V_f^{1/3}$ FROM EQUATION 11)	
°A.	$cm.^2\ sec.^{-1}$	$cm.^2\ sec.^{-1}$		$cm.^2\ sec.^{-1}$	
273.0	0.26	0.096	2.7	0.26	1.0
296.2	0.61	0.179	3.4	0.43	1.4
305.9	0.75	0.226	3.3	0.52	1.4
316.4	0.97	0.288	3.4	0.63	1.5
325.3	1.14	0.349	3.3	0.74	1.5
335.0	1.35	0.424	3.2	0.89	1.5
343.2	1.56	0.498	3.1	1.05	1.5

In table 3 we have collected data for a variety of solutes diffusing in water. These have been obtained from the Landolt-Börnstein *Tabellen*, and suffice for our purpose. For calculating the value of D we use the properties of water itself (except for the reduced mass of the passing molecules) to substitute into equation 9, and we have compared our calcu-

TABLE 3

Data for a variety of solutes diffusing in water

SUBSTANCE	CONCENTRATION	T	$D_{\text{obsd.}} \times 10^5$	$D_{\text{calcd.}} \times 10^5$	RATIO $D_{\text{obsd.}}/D_{\text{calcd.}}$
			($V_f^{1/3}$ FROM EQUATION 11)		
	per cent	°*A.*	*cm.*^{2} *sec.*$^{-1}$	*cm.*^{2} *sec.*$^{-1}$	
Methyl alcohol	0.25	291	1.37	0.386	3.5
Ethyl alcohol	0.25	291	1.10	0.382	3.0
Propyl alcohol	0.25	291	0.98	0.346	2.8
Butyl alcohol	0.25	291	0.88	0.343	2.6
Amyl alcohol	0.25	291	0.88	0.338	2.6
Allyl alcohol	0.25	291	0.99	0.353	2.8
Phenol	0.25	291	0.80	0.338	2.4
Glycerol	0.125*	293	0.83	0.36	2.3
Pyrogallol	0.25	291	0.66	0.329	2.0
Resorcinol	0.125	293	0.76	0.358	2 1
Hydroquinone	0.25	293	0 77	0.358	2.2
Saligenin	0.25*	293	0.72	0.353	2.0
Urea	0.25*	293	1.18	0.377	3.1
Acetamide	0.25*	293	1.0	0.377	2.7
Alloxan	0.125*	293	0.66	0.350	1.9
Urethan	0.25	291	0.87	0.338	2.6
Dicyandiamide	0.2*	293	1.04	0.365	2.8
Antipyrine	0.25	291	0.56	0.324	1.7
Caffeine	0.05*	293	0.57	0.343	1.7
Glucose	0.25	291	0.57	0.324	1.7
Salicin	0.06*	293	0.49	0.341	1.5
Maltose	0.25	291	0.41	0.317	1.3
Lactose	0.25	291	0.41	0.317	1.3
Sucrose	2.0	293	0.57	0.338	1.7
Raffinose	0.25	291	0.64	0.312	2.0
Acetylene		291	1.76	0.391	4.5
Carbon dioxide		291	1.46	0.367	4.0
Nitrogen		291	1.62	0.396	4.1
Hydrogen		291	3.59	1.04	3.5
Dyes (various)	0.008*	291	0.17 to 0.58	*ca.* 0.31	0.5 to 1.9
Proteins (various)		280 to 290	0.04 to 0.13	*ca.* 0.3	0.1 to 0.4

* These concentrations are in moles per liter.

lated values with experimental ones for the most dilute solutions for which data were available.

Non-aqueous diffusion

In tables 4 and 5 are collected representative data for non-aqueous diffusion. Table 4 shows diffusion behavior for several solutes diffusing in the same solvent, while table 5 has data for the same solute diffusing in several solvents. For table 4 the common solvent was benzene, and since the solutions were dilute we use the properties of benzene to obtain the values for substituting in equation 9 (except reduced mass). For viscous flow of benzene Ewell and Eyring (2) find $n = 3$, which value we use in equation 9. $v_f^{1/3}$ is the value given by equation 12.

TABLE 4
Diffusion in benzene
$T = 280.5°A.$

SOLUTE	$D_{obsd.} \times 10^5$	$D_{calcd.} \times 10^5$ (EQUATION 9)	RATIO $D_{obsd.}/D_{calcd.}$
	cm.² sec.⁻¹	*cm.² sec.⁻¹*	
Phenyl bromide	1.45	3.39	0.43
Phenyl iodide	1.35	3.27	0.42
o-Dichlorobenzene	1.62	3.44	0.48
m-Dichlorobenzene	1.57	3.44	0.45
p-Dichlorobenzene	1.42	3.44	0.42
1,2,4-Trichlorobenzene	1.34	3.33	0.40
1,2,4,5-Tetrachlorobenzene	1.24	3.27	0.38
Hexachlorobenzene	1.02	3.13	0.33
Bromocyclohexane	1.38	3.38	0.42
Naphthalene	1.19	3.52	0.34
Phenanthrene	0.95	3.34	0.29
α-Bromonaphthalene	1.07	3.26	0.33
α-Bromophenanthrene	0.95	3.17	0.30
Methyl iodide	2.06	3.46	0.59
Ethyl iodide	1.77	3.39	0.53
n-Propyl bromide	1.71	3.55	0.48
n-Propyl iodide	1.67	3.36	0.50
n-Butyl bromide	1.68	3.48	0.48
n-Butyl iodide	1.53	3.31	0.46
n-Amyl bromide	1.42	3.42	0.42
n-Amyl iodide	1.41	3.28	0.43
Octyl bromide	1.17	3.29	0.36
Ethylene chloride	1.77	3.71	0.48
Iodoform	1.12	3.04	0.37
Carbon tetrachloride	1.51	3.40	0.43
Carbon tetrabromide	1.12	3.08	0.37

In table 5 we also use the properties of the pure solvents to obtain the values for substituting in equation 9, using equation 11 to obtain the values of $v_f^{1/3}$. In treating the data included in table 5, the choice of n presents a problem. We have where possible used the value of n found by Ewell and Eyring to hold for the viscous flow of the solvent in question.

TABLE 5

SOLVENT	$E_{vap.}$	n	$D_{obsd.} \times 10^5$	$D_{calcd.} \times 10^5$	RATIO $D_{obsd.}/D_{calcd.}$
Diffusion of bromobenzene in various solvents. T = 280.5°A.					
	kg-cal.		$cm.^2\ sec.^{-1}$	$cm.^2\ sec.^{-1}$	
Ether	6.16	4*	3.50	16.5	0.21
Benzene	7.69	3*	1.41	3.1	0.45
Toluene	8.5	4*	1.59	7.4	0.22
Cyclohexane	7.59	3*	1.16	3.34	0.34
Hexane	7.0	4*	2.59	13.26	0.20
m-Xylene	9.77	4	1.52	4.90	0.31
m-Cymene	10.3	4	1.18	4.09	0.29
Diffusion of bromoform in various solvents. T = 293°A.					
Acetone	7.27	4*	2.69	11.97	0.23
Ether	6.1	4*	3.39	17.3	0.20
Benzene	7.45	3*	1.69	3.71	0.45
Methyl alcohol	8.44	3	1.93	2.64	0.71
Ethyl alcohol	9.97	3	0.97	1.25	0.77
Propyl alcohol	9.99	3	0.77	1.22	0.63
Amyl alcohol	10.6	3	0.52	0.94	0.56
Diffusion of iodine in various solvents. T = 293°A.					
Dibromoethane	8.25	3.5*	0.83	3.82	0.22
Benzene	7.45	3*	1.93	3.79	0.50
Carbon tetrachloride	8.0	3*	1.37	2.39	0.59
Toluene	7.99	4*	1.96	9.26	0.21
Chloroform	7.08	4*	2.12	10.08	0.21
Ethyl acetate	7.78	4*	2.15	9.79	0.22
Heptane	7.59	4*	2.77	11.39	0.24
Carbon disulfide	6.60	4*	3.12	12.41	0.25
m-Xylene	8.80	4	1.68	7.23	0.23
Isoamyl acetate	9.00	4	1.24	6.75	0.19
Bromobenzene	8.80	3	1.20	1.71	0.71

* Values found by Ewell and Eyring.

Such values are marked in the table with an asterisk. Values used for other solvents may be somewhat arbitrary, though they have been assigned values which are considered probable from analogy to chemically related liquids for which these values of n are known.

Effect of concentration

We compare available data with results calculated from a modification of equation 20. Besides the "gradient" effect on diffusion covered by the factor

$$\left(1+\frac{\mathrm{d}\ln\gamma_i}{N_2\,\mathrm{d}\ln N_i}\right)$$

there is a concentration effect on $\Delta F_0^{\ddagger}$ due to the change in $\Delta E_{\text{vap.}}$ with concentration. If we arbitrarily take a solution dilute with respect to constituent 2 as a standard or reference state, for which we can use $\Delta E_{1_{\text{vap.}}}$, λ_1^2, and $V_{f_1}^{1/3}$, for the reference value of the diffusion coefficient, we would then have

TABLE 6

Ratio of the two limiting diffusion rates of the dilute constituents in a binary solution

CONSTITUENT 1	CONSTITUENT 2	$D_{1\to 2}/D_{2\to 1}$ (EQUATION 30)	$D_{1\to 2}/D_{2\to 1}$ (OBSERVED)
Ethyl acetate	Ethyl benzoate	0.46	0.48
Acetone	Ethyl benzoate	0.41	0.42
Ethyl benzoate	Nitrobenzene	0.66	0.79
Acetone	Nitrobenzene	0.26	0.30
Ethyl acetate	Nitrobenzene	0.30	0.34
Benzene	Bromobenzene	0.68	0.72
Benzene	Nitrobenzene	0.26	0.44
Benzene	Carbon tetrachloride	1.1	1.0

$$D_1 = D_{\text{ref.}}\left(1+\frac{1}{N_2}\frac{\mathrm{d}\ln\gamma_i}{\mathrm{d}\ln N_i}\right)\left(e^{\frac{-[\Delta E_{\text{vap.ave.}}-\Delta E_{\text{vap.}_1}]}{nRT}}\right)\frac{\lambda^2_{\text{ave.}}}{\lambda^2_1}\,\frac{V_{f_1}^{1/3}}{V_{f_{\text{ave.}}}^{1/3}} \qquad (29)$$

In the limiting case we may compare D for the diffusion of constituent 1 in practically pure constituent 2 with that for the diffusion of constituent 2 in practically pure constituent 1. Equation 29 then becomes

$$D_{1\to 2} = D_{2\to 1}\exp\left(-\,\frac{\Delta E_{\text{vap.}_2}-\Delta E_{\text{vap.}_1}}{nRT}\right)\frac{\lambda_2^2}{\lambda_1^2}\,\frac{V_{f_1}^{1/3}}{V_{f_2}^{1/3}} \qquad (30)$$

In table 6 values of the ratio $D_{1\to 2}/D_{2\to 1}$ from diffusion data, obtained for several non-aqueous liquid pairs from the Landolt-Bornstein *Tabellen*, are compared with values of this ratio calculated from equation 30. We take $n = 3$ in all cases.

In order to test equation 29 it is necessary to have partial-pressure data or their equivalent for obtaining activity coefficients. Available data permit only rough average values of $D_1/D_{\text{ref.}}$ through finite, and sometimes fairly wide, composition ranges. In figure 2 we plot $D_1/D_{\text{ref.}}$ calculated from equation 29 against N_2 for several liquid pairs. The plot is never extended beyond $N_2 = 0.5$, in order to avoid multiplying the errors in γ_i too much for small values of N_2 (and large values of $1/N_2$). These calcu-

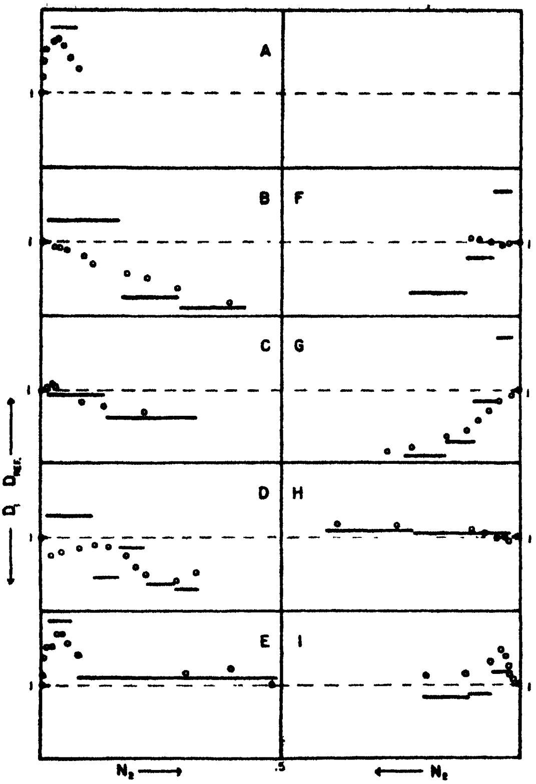

FIG. 2. Comparison of experimental values of $D_l/D_{ref.}$ (circles) with those calculated from equation 29, through composition ranges of $N_2 = 0$ to $N_2 = 0.5$ (heavy horizontal straight lines) for the following liquid pairs:

CURVE	CONSTITUENT 1	CONSTITUENT 2
A..........	Propyl alcohol	Water
B..........	Water	Propyl alcohol
C..........	Water	Methyl alcohol
D..........	Methyl alcohol	Water
E..........	Carbon tetrachloride	Nitrobenzene
F..........	Water	Ethyl alcohol
G..........	Ethyl alcohol	Water
H..........	Benzene	Carbon tetrachloride
I..........	Carbon tetrachloride	Benzene

lated values are compared with experimental values of $D_l/D_{ref.}$ obtained from measurements of Gerlach (7), of Münter (15), and of Franke (6). Partial-pressure data for the system carbon tetrachloride–nitrobenzene were obtained from the measurements of Linebarger (14), and for the other systems from the *International Critical Tables.* The average calculated values of $D_1/D_{\text{ref.}}$ are shown in the figure by straight lines covering the particular composition range for which they were calculated. The experimental values are denoted by circles. We have arbitrarily assumed perfect solutions for all compositions within 1 mole per cent of a pure constituent, an assumption which is apparently not true in some of the cases. The average values of λ^2, $V_f^{1/3}$, and $\Delta E_{\text{vap.}}$ were calculated as described earlier in this paper, and for d ln γ/d ln N we used the mean of the value of this coefficient for each constituent in the range covered. In spite, however, of the incompleteness of the data and the necessary crudeness of handling, the obvious correlations in figure 2 between the trends of the experimental points and the calculated averages of $D_1/D_{\text{ref.}}$ indicate the general soundness of equation 29.

James, Hollingshead, and Gordon (11) have recently published results for the diffusion of hydrochloric acid in water which agree very well with a formula due to Gordon (8). His formula has the same dependence on the gradient in activity as our own in the range of low mole fractions of hydrochloric acid for which agreement is found. Further precise experimental diffusion measurements covering the temperature variations will make it possible to assign diffusion mechanisms from a comparison of the observed rates with those calculated from the absolute rate theory using only thermodynamic data.

REFERENCES

(1) Cohen, E., and Bruins, H. R.: Z. physik. Chem. **103**, 404 (1923).

(2) Ewell, R. H., and Eyring, H.: J. Chem. Phys. **5**, 726 (1937).

(3) Eyring, H.: J. Chem. Phys. **4**, 283 (1936).

(4) Eyring, H.: J. Chem. Phys. **3**, 107 (1935); Wynne-Jones, W. F. K., and Eyring, H.: J. Chem. Phys. **3**, 492 (1935).

(5) Eyring, H., and Hirschfelder, J.: J. Phys. Chem. **41**, 249 (1937).

(6) Franke, G.: Ann. Physik **14**, 675 (1932).

(7) Gerlach, B.: Ann. Physik **10**, 437 (1931).

(8) Gordon, A. R.: J. Chem. Phys. **5**, 522 (1937).

(9) *Cf.* Hildebrand, J. H.: *Solubility of Non-Electrolytes*, 2nd edition, p. 44. Reinhold Publishing Corporation, New York (1936).

(10) *Cf.* Hirschfelder, J., Stevenson, D., and Eyring, H.: J. Chem. Phys. **5**, 896 (1937).

(11) James, W. A., Hollingshead, E. A., and Gordon, A. R.: J. Chem. Phys. **7**, 89 (1939).

(12) Kincaid, J. F., and Eyring, H.: J. Chem. Phys. **5**, 587 (1937).

(13) Kincaid, J. F., and Eyring, H.: J. Chem. Phys. **6**, 620 (1938).

(14) Linebarger, C. E.: J. Am. Chem. Soc. **17**, 690 (1895).

(15) Münter, E.: Ann. Physik **11**, 558 (1931).

(16) *Cf.* Neurath, H.: J. Am. Chem. Soc. **61**, 1841 (1939).

(17) Scheffer, J. D. R., and Scheffer, F. E. C.: Verslag Akad. Wetenschappen Amsterdam **25**, 67 (1916).

(18) Taylor, H. S.: J. Chem. Phys. **6**, 331 (1938).

WATER BOUND TO GELATIN AS SHOWN BY MOLECULAR STRUCTURE STUDIES[1]

O. L. SPONSLER, JEAN D. BATH, AND J. W. ELLIS

Physical-Biological Laboratories, University of California, Los Angeles, California

Received August 31, 1939

While attempting to obtain a dimensional, molecular picture of the living material of organisms, we found ourselves involved in the interrelationships which occur in protein–water mixtures. The water content of protoplasm in an actively growing period of the organism is about 85 per cent, and the protein content about 10 per cent; in a dormant period the water is greatly reduced, often to one-third or even less. This percentage of about 30 to 35 per cent water is also a critical region, experimentally, in the water content of many protein–water mixtures. Investigations of protein hydration have been carried out, to a great extent, with gelatin–water mixtures which have furnished a wealth of experiment and suggestions concerning these relations (38, 39, 40). Confirmation of these is beginning to come out of recent correlative investigations, among which infrared absorption and x-ray studies are playing an important part. When evidence from these physical methods is combined with that from chemical studies, a fairly complete story of gelatin–water relations is obtained.

The gelatin molecule is a long polypeptide chain and, as such, may be considered as fairly typical of the primary structure of the simple proteins (41). A small portion of a typical protein chain model built to scale, using known interatomic distances and bond angles (46), is reproduced in figure 1.

It has been suggested (38, 39, 40) that water will be held only by the constituent groups which contain oxygen and nitrogen atoms. Water relation studies by various methods, such as heat of imbibition (23, 44), imbibition pressure (21), freezing point determinations and expansion on freezing (4, 31, 43, 45), osmotic pressure and diffusion measurements (35, 36), and pressure-concentration curves (39), indicate a restriction in the freedom of motion of the water molecules when less than about 35 per cent water is present in the mixture. It seemed reasonable to suppose that the number of water molecules present in this 35 per cent mixture should be approximately equal to the number predicted when the present knowledge of the water molecule (9), of the nature of the oxygen and nitrogen atoms, and of the hydrogen bridge (46) are correlated with recent amino acid analyses of gelatin.

---

[1] Presented at the Sixteenth Colloid Symposium, held at Stanford University, California, July 6–8, 1939.

Computations of this nature, but more general in character, have been attempted (39) without sufficient experimental support concerning the details of water-protein coördination. It is now possible to take into consideration reports on investigations which show not only the numerical relationship between the water molecules and the hydrophilic groups, but also the spatial relations and the manner of bonding.

In order to estimate the number of water molecules which may be coördinated with a gelatin molecule, it is necessary to consider the recent model of the water molecule proposed by Bernal and Fowler (9) as well as the recent studies on the chemical and physical structure of gelatin. The water molecule may be thought of as a spherical particle in which the oxygen and hydrogen nuclei lie in a plane passing through the center of the molecule, as indicated in the diagrams of figure 2, A and B. The oxygen atom has two negative residual charges (46) indicated by *E* and *E'* in figure 2, A. These two negative charges and the two hydrogen protons are distributed at the four corners of a tetrahedron; each charge may be active in coördinating another water molecule, as shown in figure 4.

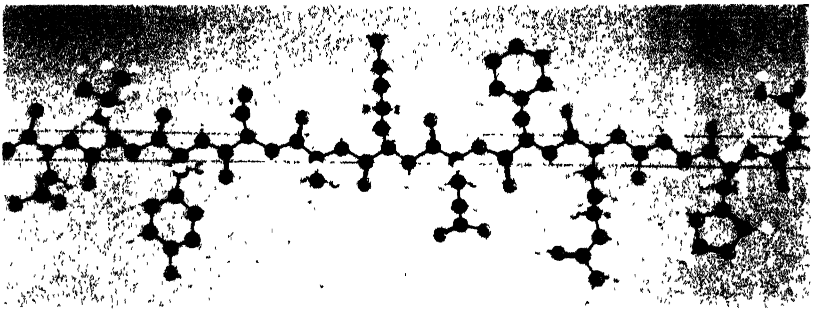

FIG. 1. A portion of a protein chain model showing twelve residues of various sorts attached to the zig-zag backbone indicated by the horizontal lines. The oxygen atoms have a dot in the center, the hydrogen atoms are small white balls, the carbon atoms are black, and the nitrogen atoms are slightly lighter and have three bonds.

X-ray structure analyses of various organic crystals have shown that this tetrahedral distribution of residual charges is characteristic of the oxygen and also of the nitrogen atom, especially where accompanying hydrogens occur (1, 5, 7, 11, 24, 25, 46, 52). These charges may be associated with the formation of a hydrogen bridge (9, 30, 46), as indicated in the diagram in figure 3, where the hydrogen proton of one water molecule is shown displaced towards the negative residual charge of a second water molecule (9), thus forming the hydrogen bridge. The molecular centers approach to about 2.7 Å. A water polymer consisting of four water molecules bridged in this manner to a fifth is shown in figure 4.

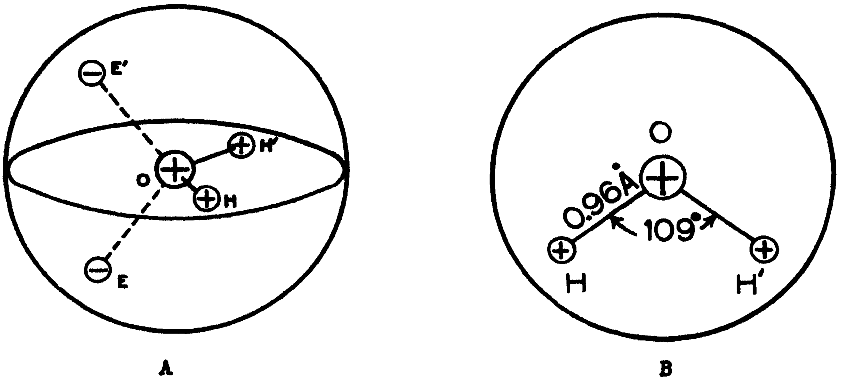

FIG. 2. (A) Diagram of a water molecule showing the plane made by the oxygen and hydrogen nuclei in relation to the two residual negative charges indicated by E and E′ (9); (B) diagram showing the dimensional relationship of the oxygen and hydrogen nuclei.

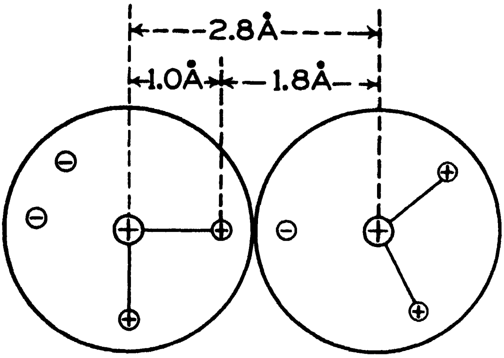

FIG. 3. Diagram illustrating the formation of a hydrogen bridge between two water molecules (9).

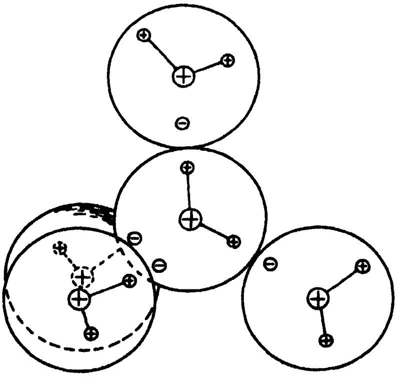

FIG. 4. Illustrating the coördination of four water molecules to a central molecule through hydrogen bridges, as in ice crystals. This also illustrates the tetrahedral nature of the oxygen atom (9).

Hydration centers on the protein chain are associated with the various atomic groups in which these two atoms, oxygen and nitrogen, occur (39). Many types of experimental evidence, such as x-ray analyses of crystalline hydrates (25, 47, 51) and studies of solubility curves (29) and of the heat and entropy of hydration of various compounds (10), have indicated the coördination of water with these groups (30, 37). The number of water molecules that may be coördinated in this manner with the various hydrophilic groups of the protein is given in table 1, where both experimental and theoretical amounts are presented.

It has been convenient to consider these hydration centers on the protein chain as separated into two groups,—those on the backbone and those on the ends of the amino acid residues. The total number per molecule obviously depends upon the length of the protein chain; and since the length for gelatin is known to be variable, an arbitrary choice of 288 residues is used here. In accordance with this, the backbone contains 288 double-bonded oxygens and the same number of nitrogen atoms, in contrast to 94 residues which have polar end groups. The number of potentially available coördination points supplied by the polar groups of the side chains is given in table 2 as 348.

TABLE 1

Water molecules coördinated with hydrophilic groups

HYDROPHILIC GROUPS	NUMBER OF WATER MOLECULES (THEORETICAL)	NUMBER OF WATER MOLECULES (EXPERIMENTAL)	REFERENCES (EXPERIMENTAL)
H_2O	4	4	(9)
$-OH$	3	3	(10)
$-COOH$	5-4	4	(30, 25)
$=O$	2	2	(10)
$-NH_2$	3	3	(10)
>NH	2		
>N—	1		

Both types of hydration centers on the backbone, =O and >NH, are potentially capable of forming hydrogen bridges to two water molecules, but when space restrictions, resulting from the close approach of atoms in the construction of the chain, are taken into consideration, only one for each group would be a reasonable estimate. Furthermore, in this firm, almost solid gel having about 65 per cent protein and 35 per cent water even this degree of hydration would probably be too great, since a certain amount of protein-to-protein cohesion through bridges between $>C{=}O$ and $>NH$ groups (18) is to be expected. An estimate of about 450 to 500 water molecules coördinated to the backbone has been made. This number is a rather crude estimate which standing alone would have relatively little value but, when supplemented by x-ray and infrared interpretations, becomes more significant. The total number of coördinated water molecules, when reasonable restrictions are taken into account, is then approximately 800 to 850 (39). This is in fairly good numerical agreement with the amount present in a 33 per cent water mixture in which the behavior, as indicated by the physical-chemical methods referred to previously, shows that the water is bound to the protein. This amount, computed on the basis of a chain molecule of 288 residues with a molecular weight of 27,000, is about 750 water molecules.

TABLE 2

Composition of gelatin

AMINO ACID	GRAMS PER 100 G. DRY GELATIN	REFERENCE	NUMBER OF AMINO ACID RESIDUES*	NUMBER OF HYDRATION CENTERS ON SIDE CHAINS	NUMBER OF COÖRDINATE WATER MOLECULES ON SIDE CHAINS
Glycine	25.5	(8, 13)	90		
Alanine	8.7	(13)	26		
Leucine	7.1	(13)	14		
Aspartic acid	3.4	(13)	7	7	28
Glutamic acid	5.8	(13)	11	11	44
Serine	0.4	(13)	1	1	3
Proline	19.7	(8)	45		
Hydroxyproline	14.4	(8, 13)	29	29	87
Phenylalanine	1.4	(13)	2		
Tyrosine	0.01	(13)	<1		
Hydroxylysine	0.3	(48)	<1		
Cystine	0.17	(42)	<1		
Arginine	8.2	(13)	12	12	84
Histidine	2.94	(50)	5	5	15
Lysine	5.92	(3, 50)	12	12	36
Not accounted for†	16.14		34	17	51
Total	120.08		288	94	348

* The number of residues is based on a chain molecule consisting of 288 residues. Average residue weight is equal to 93, thus making the average molecular weight 27,000.

† The undetermined portion was thought to consist of amino acids with higher molecular weights, and about half of them to contain hydrophilic groups (3, 13).

The assumption that both the backbone and the polar residues become hydrated is strengthened by x-ray diffraction patterns which were made from gelatin containing various percentages of water. The long chain-like nature of the gelatin molecule has been established by studies of diffraction patterns from various forms of air-dried gelatin, including powdered material and stretched films (27, 28, 32, 49). The number of diffraction spots is too small for a clean-cut decision concerning the lattice constants, but, when studied in connection with other similar materials, a reasonable interpretation may be made. The molecule appears to be a long chain with a repetition distance of about 2.8 Å. (040), a width of about 11 Å. (200), and a thickness of about 4.3 Å. (001). The repetition distance is the portion of the backbone allotted to each residue (see figure 1). In the fully extended protein chain it is about 3.5 Å., but in gelatin the distortions caused by the large number of proline residues probably account for the low value of 2.8 Å. The width is an average of various side-chain lengths, as illustrated in figure 1. The thickness is shown in figure 5, where an end view of the model is reproduced.

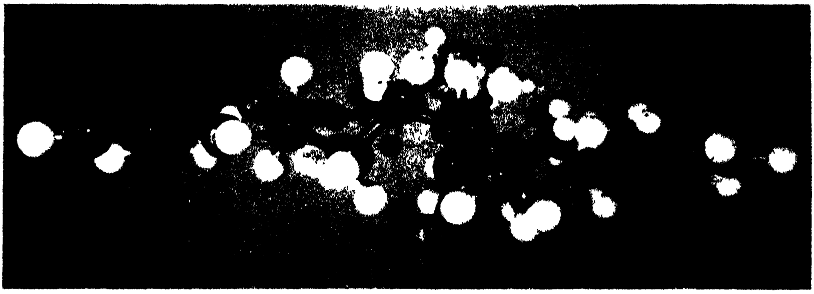

FIG. 5. End view of a model of a protein chain, reproduced to show the thickness of the chain, vertically 4.5 Å.

When water is allowed to penetrate a gelatin mass, the x-ray pattern changes considerably, and it is important to notice that the changes depend upon the amount of water present. Two reports have been made showing these changes (27, 32). Their values are in reasonable agreement with each other. One table of values, somewhat simplified, is quoted here (table 3). The repetition distance along the chain, 2.8 Å., remains the same regardless of water content, indicating that the chain remains unbroken. The side-chain spacing undergoes a rapid increase with the rise in the amount of water present, and the backbone spacing, 4.3 Å., apparently is altered when the amount of water is greater than about 15 per cent moisture, as in the air-dry condition.

The explanation of these changes becomes comprehensible when the spacings are considered in connection with the number of water molecules present. At 0.2 per cent moisture there would be only 4 or 5 water molecules present for each protein chain. The spacings given in this column in table 3 may be considered those for desiccated gelatin.

When 15 per cent water is present, the side-chain distance is increased by about 1 Å., and a diagonal, 7.5 Å., which is associated with the 11.3 Å. lattice spacing, appears, but no other change takes place. The number of water molecules, at 15 per cent, is about 260 for each protein molecule. The hydrophilic centers at the ends of the side chains have a coördination capacity of about 350 water molecules. It seems reasonable to think that the 260 water molecules present have to a very large extent become attached to these hydration centers and have caused the chains to spread from 10.4 to 11.3 Å., since there is no change in backbone spacing.

When 33 per cent water is present, the number of water molecules is increased to 750, enough to supply nearly all available hydration centers, those of the backbone as well as those of the side chains. This amount should spread the backbones 2.5 Å. to 3.0 Å. farther apart, about the thickness of a water molecule; that is, the backbone spacing should increase from 4.3 Å. to about 7 Å. It is probable that not all of the possible coördination points are satisfied, that some of the 4.3 Å. spacings are not disturbed. Three sets of backbone spacings then must occur: one from the undisturbed protein chains, 4.3 Å., and two from the protein chains interleaved with water layers. The latter give two spacings, one about 7.0 Å., and the other the half distance of 3.5 Å. The 3.5 Å. and 4.3 Å. spacings may be expected to fuse into a single ring at about 3.7 Å., and the 7.0 Å. to fuse with the 7.5 diagonal which still remains, as shown in table 3. The x-ray patterns are not sharply outlined, and exactness of spacing measurement is not very great. In addition to these changes lateral tensions have been diminished (2), and the side-chain spacing is increased to 13 Å.

TABLE 3

*Molecular spacings in hydrated powdered gelatin from x-ray diffraction patterns**

SPACINGS	PERCENTAGE OF WATER						
	0.2%	15%	33%	71%	78%	81%	93%
	SPACINGS IN Å.						
Side chain (width)	10.4	11.3	13.0	17.1			
Diagonal		7.5	7.5		7.5	7.5	7.2
Repetition (along backbone)	2.8	2.8	2.8		2.8	2.8	
Backbone (thickness)	4.4	4.3					
Backbone and water (alternate layers)			3.7		3.6	3.3	3.3

* Modified slightly from reference 27.

Increasing amounts of water greater than 35 per cent make the side-chain spacings larger, until the layers become too distorted to form diffraction patterns. Despite the disturbance of the side-chain distances, protein–water–protein backbone spacings of 3.5 and 7.0 Å. remain along with the repetition distance of 2.8 Å. in the chain, even up to a water content of 90 per cent. Space does not permit elaboration of further minor points which also fit into this interpretation.

HYDRATION OF GELATIN

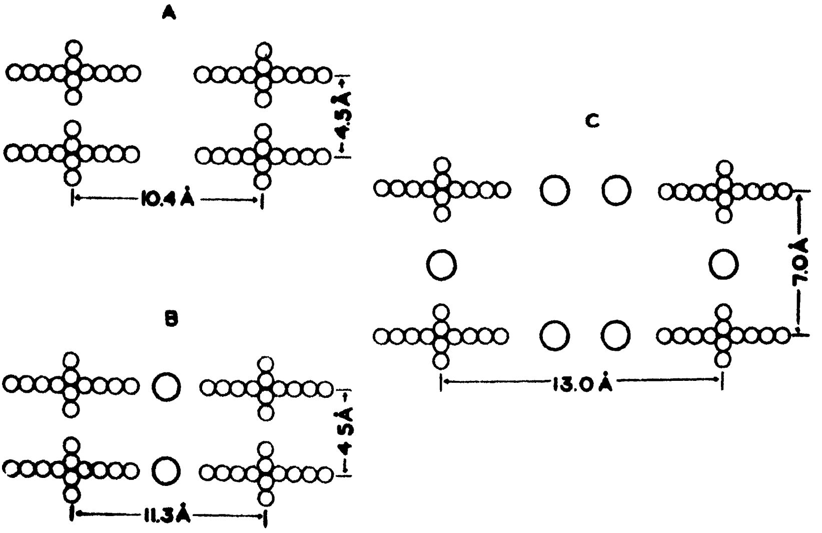

FIG. 6. Diagrams to show the increase in intermolecular spacings for A, desiccated gelatin; B, air dry, 15 per cent water; C, 35 per cent water. The large circles represent water molecules; the groups of small circles represent end views of protein chains.

The increase in intermolecular distances with increase in water is shown schematically in figure 6, where diagram A represents an end view of four protein chains with no water present; B represents the air-dry gelatin, containing 15 per cent water, with the water molecules between the side chains only; and C represents the gelatin, containing 35 per cent water, with the water between the backbones as well as between the side chains.[2]

The third part of this discussion concerns the more direct evidence for the manner of attachment of the water molecules to the protein chain.

[2] A similar spreading of molecular layers by insertion of water molecules has been reported by Sir William Bragg in connection with plasticity of clays, in a lecture at the Royal Institution of Great Britain, November, 1937.

It has been shown by reports from numerous investigations that infrared radiation may be absorbed by OH, NH, CH, and C=O groups (34). The absorption spectra from a high-dispersion quartz spectrograph, such as used in the work discussed here (14), consist of definite and specific bands which have been interpreted as caused primarily by vibrations within these oscillators. These vibrations may be affected by adjacent atomic groups to such an extent that the type of disturbance or perturbation thus produced may be interpreted from the characteristics of the absorption bands (20, 22). From these and other studies in which crystal structure and Raman spectra (12) play a part, the concept of the hydrogen bridge has been fairly well established. Among the substances which have been investigated are water (6, 12), alcohols (19, 33), acids (26), and, more specifically, sucrose (16), pentaerythritol (17), cellulose (18), and the proteins; silk (18), gelatin (15), and zinc insulinate (18).

Concerning gelatin, it was thought that if the water molecules were bridged to the oxygen and nitrogen atoms of the protein, a comparison of the spectrum from oven-dried gelatin with that from gelatin containing 35 per cent water would reveal something concerning the nature of the water bonding which is suggested by the physical-chemical methods mentioned earlier. For details of this infrared work the original publication must be consulted (15); here we present merely the conclusions.

These studies included a comparison of the absorption bands of water in the gelatin mixture with those of an equal amount of liquid water. When water molecules are present as individuals in a non-polar solvent, absorption bands may be observed at 1.4 μ ($\nu_\pi + \nu_\sigma$) and at 1.9 μ ($\nu_\sigma + \nu_\delta$). Corresponding bands from liquid water alone, however, are very much broader and are shifted considerably in the direction of the longer wave lengths. This is due to the perturbing effects of the closely attached, coördinated molecules of the water polymers in which the molecules are presumed to be attached to one another through their hydrogens (12). The amount of perturbation due to the number of ways by which the vibrations may be affected as well as the nature of the restriction of vibration is shown by the character of the band.

Turning now to the gelatin-water mixture in which 35 per cent water is present, the 1.4 μ band, a combination of the fundamental symmetric and asymmetric valence vibrations for water, is seen to be shifted slightly towards the longer wave lengths and is not as broad as when obtained from water alone. The removal of the short-wave-length portion which is associated with the single, vapor-like molecules is interpreted as showing that practically all of the water molecules present are bound; that is, that few, if any, are free as individuals in the mixture among the protein molecules. The diminished intensity on the long-wave-length side of the band indicates fewer ways of perturbation being effective than in liquid water, inasmuch as this long-wave-length portion of the band is identified with the coördination of water molecules to three or four coördination points (12). The 1.9 μ band ($\nu_\sigma + \nu_\delta$) obtained from this gelatin–water mixture has both the high and low frequency sides diminished in a similar manner. This again is considered as indicating a binding of the water molecules. Two smaller, less conspicuous bands at 1.79 μ ($\nu_\sigma + \nu_\delta + \nu_R$) and 1.35 μ ($\nu_\sigma + \nu_\pi + \nu_R$), involve restricted, oscillatory rotation about the symmetry axis of the water molecule and are interpreted as indicating that the water molecules are not vapor-like and are therefore bound.

Further confirmation is found in a comparison of the spectrum of the desiccated gelatin with that of the wet gelatin. Despite the structural complexity of the gelatin molecule it becomes relatively simple, from the point of view of infrared absorption, when considered as consisting of NH, CH, and C═O oscillators. One of the principal changes to be noted upon addition of water to the gelatin is the diminished intensity of the NH absorption bands. The intensity of the first overtone valence N—H band at 1.50 μ is greatly diminished by the addition of water molecules; the combination deformation-valence N—H bands at 2.05 μ and 2.18 μ are also reduced, but somewhat less than in the first case. A probable explanation is that some of the water molecules are bound to the NH and NH_2 groups through hydrogen bridges and that the hydrogen atoms of the bridges are being furnished by the nitrogen groups of the protein. Since by far the greater number of NH groups are those of the backbone, it seems probable that the diminished intensity of the NH bands is produced to a great extent by the binding of the water molecules through the hydrogen furnished by the NH groups of the backbone. This gives additional confirmation to the x-ray interpretation of the presence of a layer of water molecules between the backbones of the protein chains.

SUMMARY

Three lines of investigation are brought to bear on gelatin hydration. (*a*) Agreement is shown between the number of coördinate water molecules potentially possible in a 35 per cent water–65 per cent protein system and the number computed to be present. (*b*) The location and distribution of the water molecules on the gelatin chain molecule is shown by x-ray analyses. (*c*) The manner in which the water molecules are bound to the protein chain is shown by infrared absorption studies to be in all probability through hydrogen bridges.

REFERENCES

(1) ALBRECHT, G., AND COREY, R. B.: J. Am. Chem. Soc. **61**, 1087 (1939).
(2) ASTBURY, W. T., AND WOOD, H. J.: Nature **127**, 663 (1931).
(3) ATKINS, W. R.: J. Intern. Soc. Leather Trades' Chem. **17**, 575 (1933).
(4) BARNES, W. H., AND HAMPTON, W. F.: Can. J. Research **13B**, 218 (1935).
(5) BARNES, W. H.: Proc. Roy. Soc. (London) **125A**, 670 (1929).
(6) BAUER, E., AND MAGAT, M.: J. phys. radium **9**, 319 (1938).

(7) Beevers, C. A., and Schwartz, C. M.: Z. Krist. **91**, 157 (1935).

(8) Bergmann, M.: J. Biol. Chem. **110**, 471 (1935).

(9) Bernal, J. D., and Fowler, R. H.: J. Chem. Phys. **1**, 515 (1933).

(10) Butler, J. A. V.: Trans. Faraday Soc. **32**, 229 (1936).

(11) Corey, R. B., and Wyckoff, R. W. G.: Z. Krist. **86**, 8 (1933).

(12) Cross, P. C., Burnham, J., and Leighton, P. A.: J. Am. Chem. Soc. **59**, 1134 (1937).

(13) Dakin, H. D.: J. Biol. Chem. **44**, 499 (1920).

(14) Ellis, J. W.: Rev. Sci. Instruments **4**, 123 (1933).

(15) Ellis, J. W., and Bath, Jean D.: J. Chem. Phys. **6**, 723 (1938).

(16) Ellis, J. W., and Bath, Jean D.: J. Chem. Phys. **6**, 221 (1938).

(17) Ellis, J. W., and Bath, Jean D.: J. Chem. Phys. **7**, 862 (1939).

(18) Ellis, J. W., and Bath, Jean D.: Unpublished data.

(19) Errera, J., and Mollet, P.: J. phys. radium **6**, 281 (1935).

(20) Errera, J., and Sack, H.: Trans. Faraday Soc. **34**, 728 (1938).

(21) Freundlich, H.: *Lehrbuch der Kapillar-Chemie.* Leipzig (1930–32).

(22) Gordy, W.: J. Am. Chem. Soc. **60**, 605 (1938).

(23) Hedges, J. J.: Trans. Faraday Soc. **22**, 176 (1926).

(24) Hendricks, S. B.: Z. Krist. **91**, 48 (1935).

(25) Hendricks, S. B., and Jefferson, M. E.: J. Chem. Phys. **4**, 102 (1936).

(26) Herman, R. C., and Hofstadter, R.: Phys. Rev. **53**, 940 (1938).

(27) Herrmann, K., Gerngross, O., and Abitz, W.: Z. physik. Chem. **10**, 371 (1930).

(28) Hess, K., and Trogus, C.: Biochem Z. **262**, 131 (1933).

(29) Hildebrand, J. H.: Science **83**, 21 (1933).

(30) Huggins, M. L.: J. Org. Chem. **1**, 407 (1936).

(31) Jones, J. D., and Gortner, R. A.: J. Phys. Chem. **36**, 387 (1932).

(32) Katz, J. R., and Derksen, J. C.: Rec. trav. chim. **51**, 513 (1932).

(33) Kinsey, E. L., and Ellis, J. W.: J. Chem. Phys. **5**, 399 (1937).

(34) Krönig, R.: *Optical Basis of the Theory of Valency.* The Macmillan Company, New York (1935).

(35) Kunitz, M., and Northrop, J. H.: J. Gen. Physiol. **18**, 433 (1935).

(36) Kunitz, M., Anson, M. L., and Northrop, J. H.: J. Gen. Physiol. **17**, 365 (1934).

(37) Lassettre, E. N.: Chem. Rev. **20**, 259 (1937).

(38) Lloyd, D. J.: Biol. Rev. Cambridge Phil. Soc. **8**, 463 (1933).

(39) Lloyd, D. J., and Moran, F.: Proc. Roy. Soc. (London) **147A**, 382 (1934).

(40) Lloyd, D. J., and Phillips, H.: Trans. Faraday Soc. **29**, 132 (1933).

(41) Lloyd, D. J., and Shore, A.: *The Chemistry of the Proteins.* P. Blakiston's Son and Company, Philadelphia (1938).

(42) Looney, J. M.: J. Biol. Chem. **69**, 519 (1926).

(43) Mennie, J. H.: Can. J. Research **7**, 178 (1932).

(44) Moran, T.: Proc. Roy. Soc. (London) **135A**, 411 (1932).

(45) Moran, T.: Proc. Roy. Soc. (London) **118B**, 548 (1935).

(46) Pauling, L.: *The Nature of the Chemical Bond.* Cornell University Press, Ithaca, New York (1939).

(47) Robertson, J. M., and Woodward, I.: J. Chem. Soc. **1936**, 1817.

(48) Schryver, S. B., and Buston, H. W.: Proc. Roy. Soc. (London) **98B**, 58 (1925).

(49) Sponsler, O. L., and Bath, Jean D.: Unpublished data.

(50) Van Slyke, D. D.: *Handbuch der biologischen Arbeitsmethoden von Abderhalden,* Abt. I, Chemische Methoden, Teil 7, S. 51. Urban and Schwarzenberg, Berlin and Vienna (1923).

(51) Zachariasen, W. H.: Z. Krist. **89**, 442 (1934).

(52) Zachariasen, W. H., and Mooney, R. C. L.: J. Chem. Phys. **2**, 34 (1934).

THE MACLEOD CONSTANT AND ITS DEPENDENCE ON PHYSICOCHEMICAL FACTORS

DAVID T. LEWIS

Tatem Chemistry Laboratories, University College, Cardiff, Wales

Received August 29, 1939

The empirical equation advanced by Macleod (6) expressing the connection between the surface tension γ, and the densities D and d of the liquid and saturated vapor, respectively, takes the form

$$\gamma = C(D - d)^4 \tag{1}$$

where C is a characteristic constant for the substance concerned. The elaborate mathematical investigation of Fowler (3) suggests that this constant C is a function of the critical temperature, and this view has also been advanced by Lewis (5) for the case of chemically related series. Ferguson and Kennedy (2) have also demonstrated that the parachor P is given by the equation

$$P = MC^{1/4} = AT_c^{1/4}V_c^{7/8} \tag{2}$$

where the terms have their usual significance.

It is a well-known fact that for many liquids, e.g., glycerol, supercooling is possible over an extensive temperature range, and if this process be carried down to the absolute zero, we may write $\gamma_0 = C(D_0)^4$, where γ_0 and D_0 represent the surface tension and density at the absolute zero.

Cailletet and Mathias (1) have shown that the mean values of the density of any substance in the state of liquid and saturated vapor are linear functions of the temperature, and they suggest the equation

$$(D + d)/2 = D_c[1 + a(1 - T/T_c)] \tag{3}$$

which has been discussed by Young (12) and Timmermans (10) and is widely employed for the accurate determination of the critical volume.

If extrapolation with this equation is also possible to the absolute zero, the critical density D_c is given by

$$D_0 = 2D_c(1 + a) \tag{4}$$

since the vapor density, d_0, is negligible at this temperature. Eliminating the term D_c from equations 3 and 4 gives the following expression for D_0:

$$D_0 = \frac{(1 + a)(D + d)}{(1 + a) - aT/T_c} \tag{5}$$

Substitution of this expression in the Macleod equation and elimination of C gives the final result

$$\gamma^{1/4} = \gamma_0^{1/4} \frac{[(1 + a) - aT/T_c](D - d)}{(1 + a)(D + d)} \tag{6}$$

Comparison of equations 1 and 6 indicates that the Macleod constant is a function of the reduced temperature, T_r, the sum of the liquid and vapor densities, the surface tension γ_0, and the constant "a" of Cailletet and Mathias. It has been shown by Mathias (7) that a is practically unity and he states that "On aura la densité critique, à un ou deux centièmes près en général, en appliquant la formule"

$$D_c = (D + d)/2(2 - T/T_c) \tag{7}$$

which is equation 3 for the rectilinear diameter with the condition $a = 1$ incorporated. Young and Thomas (13) have suggested that the slight variation of the factor a is due to variations in the molecular weight and structure of the molecule, and their results for ten normal esters give strong evidence in support of this possibility. If $a = 1$, we derive the formula

$$\gamma^{1/4} = \gamma_0^{1/4} \frac{(2T_c - T)(D - d)}{2T_c(D + d)} \tag{8}$$

which expresses the variation of surface tension from absolute zero to the critical temperature.

This latter equation undergoes further simplification when d is small, i.e.,

$$\gamma^{1/4} = \gamma_0^{1/4}\ (2T_c - T)/2T_c \tag{9}$$

where γ_0 is invariant. Table 1 gives the calculated values for chloroform ($T_c = 536.1$°K) in the temperature range where the vapor density is negligible. Where d is not small, e.g., at 77.5°C., the more correct equations (8 or 6) should be used, and divergence from the simplified equation is observable.

Mathias (7) has given a comprehensive table of a values which can be used for the more exact calculations of surface tensions.

The values of γ_0 computed in this way should afford an excellent means of determining relative internal pressures, for at the absolute zero the intrinsic pressure due to molecular agitation will have vanished for all liquids, the remaining forces being wholly cohesional. Considering the thermodynamical equation

$$E = \gamma - T\,\mathrm{d}\gamma/\mathrm{d}T \tag{10}$$

it is apparent that the total surface energy, E, will be equal to γ_0 at the absolute zero, and the internal pressure is then calculable from the general formula

$$\text{Internal pressure} = \text{Const.} \times E/V^{1/3}$$

where V is the molar volume. The essential point is to derive an equation whose extrapolation to low temperatures is justifiable, and for that reason equation 6 derived in this paper is now compared with other equations which are known to hold up to the critical temperature.

TABLE 1

Calculated and observed values of γ for chloroform

γ_0 = 97.45 dynes per centimeter; $\gamma = 3.142(2T_c - T)/2T_c$

TEMPERATURE	$\gamma_{\text{obsd.}}$	$\gamma_{\text{calcd.}}$
°C.		
10	28.60	28.63
20	27.24	27.20
77.5	19.40	20.01

The Katayama (4) extension of the Eötvös equation

$$\gamma[M/(D - d)]^{2/3} = k(T_c - T) \tag{11}$$

is known to represent accurately results over this range, and if γ is eliminated by combination with the Macleod equation we have

$$(D - d)^{10/3} = k(T_c - T)/CM^{2/3}$$

which is the van der Waals type of equation proposed by Verschaffelt (11). From this equation it is simple to deduce that

$$\gamma = C(D - d)^4 = k^{6/5}(T_c - T)^{6/5}/C^{1/5}M^{4/5} \tag{12}$$

which was employed by Sugden (8) in the form

$$\gamma = \gamma_*(1 - T_r)^{6/5} \tag{13}$$

where γ_* is the surface tension at absolute zero.

This relation has been shown to represent with accuracy the variation of surface tension with temperature. Table 2 compares the experimental figures with γ_S calculated by Sugden and with γ_L calculated by means of of equation 6. The data refer to benzene, T_c = 561.5°, a = 0.9359, and a mean value of γ_0 equal to 92.72 dynes per centimeter. The liquid and vapor densities are those recorded in the *International Critical Tables.* It is apparent that both equations 6 and 13 represent the observed values over the entire range to the critical temperature. The literature affords insufficient data to test which of these equations would more accurately represent results for the surface tension at very low temperatures and which could thus be used to determine γ_0 by extrapolation. At low temperatures, equation 6 may be employed in the form

$$\gamma^{1/4} = \gamma_0^{1/4}\left[\frac{(1 + a) - aT/T_c}{(1 + a)}\right] \tag{14}$$

which gives the surface tension as a linear function of $f(T)$ raised to the fourth power. It is probable that the extrapolation of equations 14 and 13 will yield very different values for the surface tension of the supercooled liquid. That this is the case is indicated in table 3, where γ_0 values for a number of normal liquids have been calculated and are compared with the values γ_* obtained by Sugden (9).

TABLE 2

Comparison of experimental values of γ for benzene with γ_S calculated by Sugden and γ_L calculated by means of equation 6

TEMPERATURE	D	d	$\gamma_{\mathrm{obsd.}}$	$\gamma_{\mathrm{L\ calcd.}}$	$\gamma_{\mathrm{S\ obsd.}}$
°C.					
20	0.8770	Very	28.88	28.91	28.88
30	0.8676	small	27.58	27.65	
90	0.8041	0.0036	20.13	20.01	20.05
180	0.6906	0.0249	9.56	9.62	9.64
270	0.4984	0.1287	1.05	0.90	1.06
280	0.4514	0.1660	0.36	0.33	0.37
288.5	0.3045	0.3045	0.00	0.00	0.00

TABLE 3

Comparison of γ_0 values with the γ_* values

SUBSTANCE	T_c	a	D	γ_0	γ_*
Benzene	561.6	0.9359	1.171	70.26	92.72
Ether	466.9	0.9600	1.029	55.96	74.47
Carbon tetrachloride	556.2	0.9181	1.875	66.27	85.31
Fluorobenzene	559.6	0.9165	1.357		85.20
Chlorobenzene	632.3	0.9557	1.429	70.33	94.01
Iodobenzene	721.1	0.9572	2.274		97.81
Methyl formate	487.1	0.9970	1.393	75.85	104.8
Methyl acetate	506.8	1.049	1.332		99.84
Ethyl acetate	523.2	1.061	1.269	65.24	94.28

Since both equations are equally effective in the temperature range which has so far been studied, no criticism can be made of either until both have been tested with surface tension data obtained from a study of a normal liquid whose freezing point lies well below room temperature. At this low temperature, one of the equations should show considerable divergence from the anticipated figures. The relationship derived in this paper depends essentially on the applicability of the law of Cailletet and Mathias, and Timmermans has shown that for pentane the curvature of the rectilinear diameter is exceedingly slight even at −130°C. Other investigators have commented on a slight but measurable curvature as the critical temperature is approached, but at lower temperatures the diameter closely follows the linear law, and equation 6 should therefore represent surface tension determinations at low temperatures with great exactitude.

REFERENCES

(1) Cailletet and Mathias: Compt. rend. **104**, 1563 (1887).
(2) Ferguson and Kennedy: Trans. Faraday Soc. **32**, 1474 (1936).
(3) Fowler: Proc. Roy. Soc. (London) **A153**, 229 (1937).
(4) Katayama: Science Repts. Tohôku Imp. Univ. **4**, 373 (1916)
(5) Lewis: J. Chem. Soc. **1938**, 262.
(6) Macleod: Trans. Faraday Soc. **19**, 38 (1923).
(7) Mathias: *Le point critique des corps pur*, p. 164 (1904).
(8) Sugden: J. Chem. Soc. **125**, 32 (1924).
(9) Sugden: *The Parachor and Valency*, p. 24. Geo. Routledge and Sons, Ltd., London (1930).
(10) Timmermans: Sci. Proc. Roy. Dublin Soc. **13**, 310 (1912).
(11) Verschaffelt: Commun. Univ. Leiden 1896, No. 28.
(12) Young: Phil. Mag. **50**, 291 (1900).
(13) Young and Thomas: J. Chem. Soc. **63**, 1255 (1893).

NEW BOOKS

Electrochemistry and Electrochemical Analysis. Volume II. Gravimetric Electrolytic Analysis and Electrolytic Marsh Tests. By H. J. S. Sand. 18 x 12 cm.; ix + 149 pp. London: Blackie and Sons, 1940.

The second volume of Sand's *Electrochemistry* deals with gravimetric electrolytic analysis. The author commences with a full and detailed account of the apparatus required for electrolytic analysis; among other things descriptions are given of ammeters, voltmeters, capillary electrometers, the cathode-ray detector and potentiometers, together with an account of the principles on which the instruments depend. Many types of electrical stirring apparatus and auxiliary electrodes are also described and illustrated. The technique of electrochemical deposition is discussed at some length. The third chapter deals with the electrolytic deposition and estimation of some twenty-four individual metals and the quantitative deposition of the higher oxides of lead and thallium. The anodic deposition and estimation of chlorides, bromides, iodides, carbonates, ferro- and ferri-cyanides, phosphates, and sulfides is also considered. In many cases alternative methods are given, along with essential practical details. Very full descriptions are given of the electrolytic separation and quantitative estimation of silver, copper, bismuth, antimony, cadmium, nickel, cobalt, and zinc from solutions also containing other metals likely to be associated with them. The methods described in the earlier chapters are applied to the electrolytic analysis of several industrial alloys, including yellow metal alloys, white metal alloys, nickel bronzes, light aluminum alloys, and fusible metals. Internal analysis is dealt with in a very thorough manner, both from the theoretical and from the practical point of view. The methods of Pregl and of Sand and Lindsay for microchemical analysis are fully explained and illustrated by a description of a quantitative separation of lead and bismuth. Electrolytic Marsh tests of arsenic, antimony, and germanium are described in detail.

This book is a very useful and valuable one. It is well arranged and written and the descriptions are both clear and ample, so that a student following them could carry out any of the estimations described. The text is well illustrated, and a number of relevant references are included in it. The book may be unreservedly recommended to analysts and to chemists generally.

James F. Spencer.

Principles of Inorganic and Analytical Chemistry. By E. J. Baldwin. 506 pp. New York: D. Van Nostrand Company, 1940. Price: $3.25.

The book is divided in two parts, part I (204 pages) dealing with properties of atoms and molecules, and part II with the theory of reactions. The book is well written in a lucid style. "The author has intended to include in it the main features of the various theories of inorganic chemistry, together with their application to the reactions commonly used in analysis."

The book is intended for class-room study during the entire second year of chemistry. The reviewer doubts whether it will be a success in this respect. The book is not balanced, in so far as it gives a too detailed discussion of parts of physical chemistry and lacks a presentation of the application of many of the essentials to analysis. For example, an extensive discussion of covalence is given in part I, but the use of organic compounds in qualitative and quantitative analysis is not mentioned. Reaction velocity is discussed in the first chapter of part II, but the analytical significance of catalysis and induced reactions is not given in the book. On page 313 the author should have mentioned the significance of the velocity of precipitation, since the phenomena observed in the precipitation of metal sulfides cannot be understood on the basis of the principle of solubility product alone. One also misses a discussion of oxidation-reduction, adsorption and radioactive indicators, and of colorimetry and spectrophotometry.

The reviewer noticed some serious errors in the book. On page 292 the hydrolysis of silver phosphate and on page 308 that of cupric sulfide is neglected, making the results of the calculations greatly in error. The calculation of the pH of an acid salt, such as Na_2HPO_4 (page 376) and $NaHCO_3$ (page 413) is entirely wrong; so is Fig. 97, giving the neutralization curve of sodium carbonate with hydrochloric acid. In the discussion of "causes" of ionic reactions (chapter V, part II), the effect of complex formation is not mentioned; this omission is more serious in the rule for dissolving precipitates (page 309).

I. M. Kolthoff.

10. FEB. 1941
LIBRARY

A PHASE RULE STUDY OF THE SYSTEM SODIUM STEARATE-WATER[1]

JAMES W. McBAIN, ROBERT D. VOLD, AND MARY FRICK

Department of Chemistry, Stanford University, California

Received February 21, 1940

Sodium stearate, although one of the most important constituents of commercial soap, has not previously been studied from a phase rule point of view. This paper presents the results of an exploratory survey. Although this soap has not yet been investigated as extensively as sodium oleate (8), it has nevertheless been possible to construct a considerable portion of the phase rule diagram.

Recent work (6, 7, 8, 11) has shown that all the saturated sodium soaps and likewise sodium oleate pass through a sequence of mesomorphic states between room temperature and the melting point, instead of having only the single liquid crystalline form formerly recognized. Since the number of phases in this sequence is not always the same for different soaps, the generalization (1) that phase rule diagrams for different soaps do not differ from each other qualitatively must break down to some extent in the regions of concentration involving these new phases. One purpose of this work was to investigate the extent of the differences thus caused in the soap-water diagram.

A new maximum had been found in the solubility curve for sodium oleate (8), resulting in a curve for this soap qualitatively different from those previously reported for sodium palmitate (3) and sodium laurate (2, 5). When this same maximum was found for sodium stearate,—showing that it was not a special characteristic of the unsaturated soap sodium oleate,—sodium palmitate and sodium laurate were reinvestigated. The new maximum was found to be present in both these cases also.

All four sodium soaps,—laurate, palmitate, stearate, and oleate,—have curves defining the limits of existence of ordinary isotropic solution which are qualitatively comparable in shape, despite the newly discovered feature of the curve. It may therefore be possible to relate quantitative differences from soap to soap, at corresponding points in the phase rule diagram, to specific differences between the soap molecules.

---

[1] Parts of this work were presented at the meetings of the Pacific Division of the American Association for the Advancement of Science at San Diego in June, 1938, and at Stanford University in June, 1939.

MATERIALS AND EXPERIMENTAL METHODS

Sodium stearate was prepared[2] from stearic acid "Kahlbaum" by neutralization (phenolphthalein as indicator) of a hot alcoholic (95 per cent) solution of the acid with an alcoholic solution of sodium ethylate. Alcohol and water were driven off by heating in an air oven at 105°C. with frequent stirring to prevent burning. The acid from which the soap was made melted at 69.0°C. and had a molecular weight (by titration) of 284.3. Analysis of the soap (as used) by standard methods (2) gave the following results: real soap, 99.53 per cent; water, 0.41 per cent; free sodium hydroxide, 0.06 per cent. Allowance was made for the water in making up samples.

The sodium laurate and sodium palmitate were the same stock whose preparation has been described in previous publications (10, 11).

Details of the methods of study used in this work have been described previously (8). Values of T_i, the temperature at which isotropic soap solution separates an anisotropic liquid crystalline phase on slow cooling, were determined by visual observation of systems of known composition, sealed in thick-walled Pyrex tubes, and hung in an electric oven (4). Values of T_c, the temperature at which the last trace of curd fiber phase disappears on slow heating,--about one degree per five minutes in the vicinity of transitions,--were also determined visually. This change was a great deal more definitive and easily observed with sodium stearate than had been the case with sodium oleate (8). These results are given in table 1.

A few investigations were carried out with the polarizing microscope on samples sealed in small glass capillaries and examined in an electric furnace on the microscope stage (8, 11). These data are summarized in table 2. The temperatures T_0, at which a liquid crystalline phase first begins to melt to isotropic liquid on slow heating, are easily determined and very useful, since a few such points suffice to determine the phase boundaries of the fields of homogeneous liquid crystal. Other changes in microscopic appearance can also be detected, as indicated in the table, but these cannot be regarded as proof of phase changes without other substantiating evidence. Table 2 also shows the transition temperatures of anhydrous sodium stearate taken from the work of Vold, Macomber, and Vold (7).

A very useful check on the interpretation of the results was obtained by hanging a series of tubes in a viewing thermostat and examining their appearance by ordinary light and between crossed polaroids. Flow properties were also observed after the systems had remained a day or two at

---

[2] The authors are indebted to Dr. M. E. L. McBain for the preparation of this soap.

TABLE 1

Visual observations

SODIUM STEARATE	T_i	PROBABLE SEPARATING PHASE AT T_i	T_c
weight per cent	°C.		°C.
0.37			62.7
0.81			66.8
1.49			68.8
2.51			69.8
5.10			71.8
7.51			72.8
16.8			75.3
15.3			75.6
19.9	87	Middle soap	76.8
24.8	124		78.1
29.6	152		78.8
34.9	166		80.3
38.0	169		81.3
39.8	171		81.9
41.9	164		82.4
43.8	147		82.4
45.0	170	Either soap-boiler's neat soap or superneat soap	82.4
47.8	212		83
49.5	226		83
55.0	256		86
60.3	277		86
64.9	280		87
71.9	284		90
74.5	293		93
79.8	286		104
84.7	281		112
88.6	274		119
89.8	273		
91.2	272		
92.6	276		
92.8	276		
93.2	267		
94.6	274	Neat soap	
97.1	277		
99.6	284		
100.0	288		
SODIUM PALMITATE			
weight per cent			
97.2	286	Neat soap	
94.6	276	Neat soap	
92.2	274	Superneat soap	
85.4	280	Superneat soap	
SODIUM LAURATE			
weight per cent			
95.3	313	Neat soap	
89.5	296	Neat soap	
85.4	294	Superneat soap (?)	
81.3	290	Superneat soap	

each of several temperatures (8). The results of observation of nineteen systems, ranging in composition from 15 per cent to 100 per cent sodium stearate at temperatures from 96° to 161°C., are given in table 3.

EXPERIMENTAL RESULTS

The phase rule diagram constructed from these data is shown in figure 1. The T_i curve, which gives the limiting concentrations and temperatures of existence of isotropic soap solution, is fairly well defined. The two maxima in the curve are presumptive evidence for the existence of two aqueous soap phases, middle and superneat soap, which have no counterpart in the anhydrous soap. This conclusion receives further support from the qualitative observation that the change in viscosity at T_i is less between *ca.* 45 per cent and 95 per cent sodium stearate than at higher or lower soap concentrations.

TABLE 2

Possible transition temperatures obtained by microscopic observations

T_i	SODIUM STEARATE	T_0	INCIPIENT BRIGHTENING	BRIGHT STIPPLED APPEARANCE	COARSER BRIGHTER APPEARANCE	SLIGHTLY COARSER STRUCTURE
°C.	*weight per cent*	*°C.*	*°C.*	*°C.*	*°C.*	*°C.*
161	32.5	158	76	79		
165	41.5	143				
171	40.0	158		78		
228	49.5	142				
231	51.0	209		86		
256	55.0	245	82		138–143 ↑ 160 ↓	199(?)
270	90.5	267	90–98	128	168 or 183	
265	91.5	263				

The arrows in the table indicate whether the temperature was rising (↑) or falling (↓) when the change in appearance was observed at different temperatures in the two cases.

Anhydrous sodium stearate underwent the following changes in appearance: at 123°C. the original dull material was replaced by a bright, fine-grained, pebbled structure; at 166°C. the visible structure became coarser and brighter, and the color was still predominantly golden; at 203°C. there was some softening, the structure became markedly coarser and brighter, and some red, green, and blue color appeared; at 256°C. there was marked softening, bubbles became practically circular, there was marked orientation at the edges of the tube and a great increase in brightness, the variety and depth of color and the size of the structural units increased, and some small focal conics developed; at 285°C. the field became completely dark as the soap melted cleanly to isotropic liquid. In addition, there was a gradual brightening of the field around 90°C. and a gradual appearance of brighter golden material from 108° to 118°C.

The established transition temperatures (7), plotted in figure 1, are 69°, 90°, 117°, 132°, 169°, 203°, 256°, and 288°C.

The minimum temperature at which isotropic liquid can be present between middle soap and soap-boiler's neat soap, shown in figure 1 as

TABLE 3

Appearance of systems at various temperatures

SODIUM STEARATE	APPEARANCE OF SODIUM STEARATE SYSTEMS AT				
	96°C.	109°C.	126°C.	144°C.	161°C.
weight per cent					
15.3	I	I	I	I	I
19.9	IM	I	I	I	I
24.8	M	M	IM	I	I
29.6	M	M	M	M	I
34.9	M	M	M	M	M
39.8	MN(?)	M	MN(?)	MN	M
45.0	MN	MN	MN	MN	NI
49.5	N	N	N	MN	NI
55.0	N	N	N′	N	N
60.3	N	N′	N′	N	N′
64.9	N	N′	N′	N	N′
74.5	NC	N′	N′	N	N′
79.8	NC	NC	N′	N	N′
84.7	NC	NC	N′	N	N
89.8	NC	NC	N′	N	N
92.6	C	NC	NC	N	N
94.6	C	NC(?)	NC	NW	N
97.1	C	C	C	W	NW
99.6	C	C	C	W	W

In this table I represents a mobile isotropic liquid; M represents a nearly transparent, nearly rigid, anisotropic liquid crystal which is middle soap; N is a rather clear, translucent, anisotropic liquid crystal soft enough to slide in an inverted tube and is probably soap-boiler's neat soap; N′ represents systems very similar in appearance to those designated by N, except that they are considerably cloudier and less translucent; C is a rather lustrous, white, frequently fibrous, immobile crystalline material, which is probably curd fiber phase (very possibly not in the case of observations at 126°C.); and W is a rather opaque, whitish, waxy material somewhat deformable on pounding the tube, and is probably waxy soap. Two letters in the same space indicate that both phases were present, although in general phase segregation did not occur under the influence of gravity (49.5 per cent and 45.0 per cent systems did separate into layers at 161°C.). The apparent viscosities, judged by the ease with which systems flowed when the tubes were inverted and tapped, were in general greater toward the middle of the concentration range of a given homogeneous phase than towards its edges or in two-phase regions. Thus, at 161°C. a 79.8 per cent system flows less easily than either 84.7 per cent or 74.5 per cent systems.

145°C., is not entirely certain, since there was an indication of the possible presence of isotropic liquid at lower temperatures in a few of the samples studied microscopically. Likewise, the value of the minimum temperature of existence of isotropic liquid between neat soap and superneat soap, shown as 262°C., may require slight revision.

In the region of this latter minimum in the T_i curve visual values of T_i were occasionally found to be as much as 10°C. higher than the reproducible curve shown in figure 1. Although isotropic between crossed polaroids, the solutions were quite turbid. The turbidity can scarcely be due to hydrolysis products, since the soap actually contained a slight excess of alkali. In one instance it was noted that suspended dust particles were no longer free to move at temperatures several degrees above

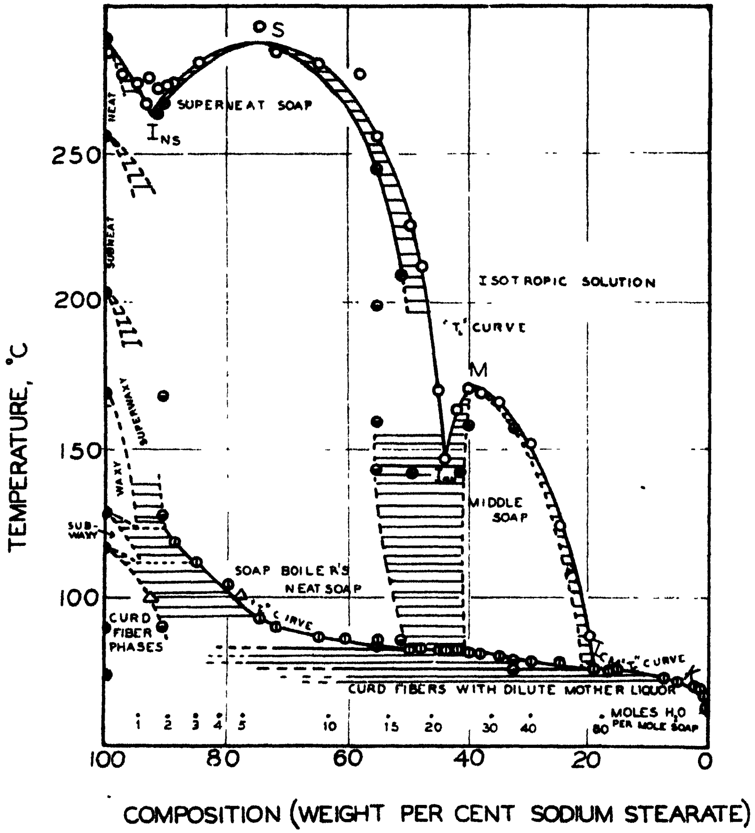

FIG. 1. Phase rule diagram of the system sodium stearate-water. ○, T_i; ⦶, T_c; ●, dilatometric results; ⊕, T_0; ◒, other microscopic observations; △, vapor pressure results, taken from preliminary unpublished work of W. W. Lee. This portion dealing with curd and subwaxy boundaries will be revised when those measurements are completed.

T_i, despite the absence of any apparent change in the fluidity of the solution as a whole. The phenomena may be related to the apparent existence of dull anisotropic patches in isotropic sodium oleate solutions of corresponding concentration (8).

Parts of the T_c curve, giving the maximum temperatures at which solid, white curd fiber phase can exist at any concentration, are also rather sharply defined. However, in concentrated systems where curd fiber phase may melt to a mixture of subwaxy soap and soap-boiler's neat soap, the change in appearance is not sufficiently striking to permit of precise visual determination. It is significant that the results of viewing experiments, with 2 days at each temperature, are in general accord with the T_c curve, obtained with a continuous rise in temperature of about 0.25°C. per minute. Thus, systems in the field of soap-boiler's neat soap were semi-fluid and translucent, while those of higher soap concentration (at temperatures below 128°C.) always had some lustrous white fibrous material, frequently with beautiful projecting individual fibers similar to those photographed in the case of sodium palmitate (9). This seems rather strange in view of the fact that anhydrous sodium stearate undergoes a transition to the subwaxy phase at 117°C. In a few instances the position of the T_c curve was confirmed microscopically by the change which occurred at this temperature from a dull, nearly opaque, featureless appearance to a much brighter appearance with a prominent structural pattern.

It is theoretically possible to determine the compositions of the intersections of the bounding curves of the middle-soap field with the T_c curve from the phase rule requirement that the T_c curve must be flat over the concentration range where two condensed phases are present on melting (3). In the case of sodium stearate this criterion was not particularly helpful, since the increase in T_c with increasing soap concentration is so gradual over most of the concentration range that it is difficult to say where the ends of the flats are because of the experimental uncertainty. The boundaries of the middle-soap field are nevertheless fairly well fixed by direct microscopic determination, in a few instances, of the temperature where melting commenced to isotropic liquid (T_0) and by the viewing experiments showing whether at a given temperature systems were homogeneous middle soap or a mixture of phases.

The lower boundary of the region of soap-boiler's neat soap is defined by the T_c curve. The right-hand boundary of this field is dotted in, partly from the results of viewing experiments and partly from a very rough estimate of the phase composition made from the relative volumes of neat soap and middle soap in the few cases where phase separation occurred.

The upper boundary of the field of superneat soap is rather well determined by the microscopic observations of T_0. The central portion of the diagram is left blank, since no boundaries have been determined nor

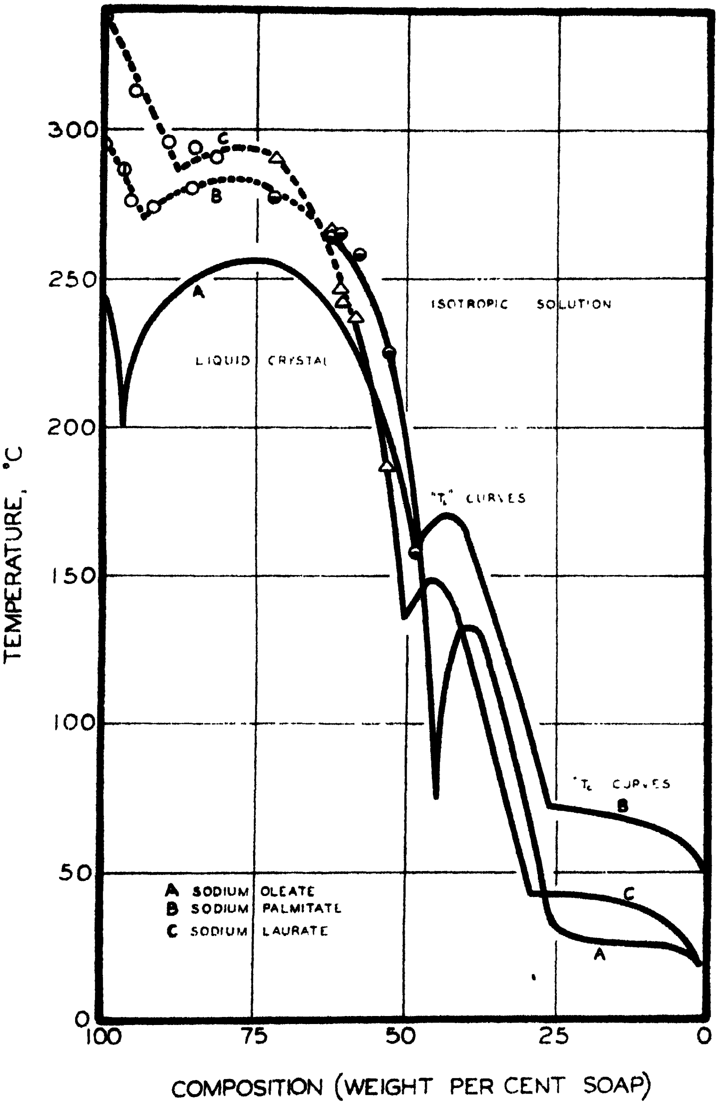

FIG. 2. Boundaries of the field of isotropic solution in various systems of soap and water. O, this work; ⦶, M. J. Vold; ◑, McBain, Lazarus, and Pitter; △, McBain, Brock, Vold, and Vold. Data are shown only for sodium palmitate and sodium laurate and then only in the region of the new maximum in the curve.

has the independent existence of superneat soap and soap-boiler's neat soap yet been demonstrated in this system.

No adequate investigation has yet been made of the phase behavior at very high soap concentrations. Transitions known to occur in the anhydrous soap (7) have been tentatively represented as giving rise to corresponding aqueous phases as in the sodium oleate system (8), but there is as yet no evidence as to their fields of existence or concerning the question of their difference from or identity with the aqueous phases existing at lower soap concentrations. The name "neat soap" has been retained for the phase which first separates on cooling anhydrous isotropic liquid sodium stearate and for very concentrated aqueous systems, but it seems likely, though still unproved, that this phase is not continuous with the aqueous phase known as soap-boiler's neat soap.

Anhydrous sodium stearate has an additional transition (at 90°C.) so far not detected in the case of sodium palmitate. Whether this is merely a change of crystal form or a transition to still another mesomorphic phase is not yet known. No attempt is made in figure 1 to indicate the phase boundaries in the binary system arising from either this transition or the genotypic transition (69°C.) of the anhydrous soap.

Nineteen systems were separated into groups on the basis solely of their visual appearance, without prior knowledge of their compositions, after they had been homogenized and cooled to room temperature. Those which had been isotropic liquid at 100°C. at room temperature were a dull white, coarse, granular material resembling plaster. Those which had been middle soap at 100°C. had an appearance at room temperature intermediate between the preceding and following groups. Those which had been soap-boiler's neat soap at 100°C. had a high sheen, were macroscopically homogeneous, of a fibrous nature, and had many fine fibers visible to the naked eye. Those which had been a mixture of curd fiber phase and neat soap at 100°C. were not quite so white (slight yellowish tinge), had a very high sheen, were very fibrous, and had many well-developed fibers. Those which had been curd fiber phase at 100°C. had less sheen, were less fibrous in appearance, and had a slight yellowish tinge. Hence it seems that the appearance at room temperature is somewhat dependent on the phase from which the curd was formed, despite the presumption that most of these systems ultimately consist of the same mixture of phases at room temperature.

The new results on the T_i curves of sodium laurate and sodium palmitate are shown in figure 2, together with previous results on these systems.

DISCUSSION

Since the series of phases of the anhydrous soap is not the same for all, it follows that qualitative differences must likewise exist in their phase rule behavior with water. However, comparison of figure 1 with figure 2 and with the diagram for sodium oleate (8) shows that sodium stearate, sodium palmitate, sodium laurate, and sodium oleate all have the same kind of T_i curve, and hence significant comparisons can be made, since presumably the phases involved are the same with the different soaps (except above *ca.* 95 per cent).

In order to compare the phase behavior it is desirable to select points at which the different soap systems will be in a corresponding condition, rather than to compare temperatures at some arbitrary composition or compositions at some arbitrary temperature. For this purpose the following six "corresponding points" on the T_i curve have been chosen: K, which is the temperature of maximum inflection in the solubility curve (closely related to the so-called Krafft point); I_{CM}, where isotropic solution is in equilibrium with both middle soap and curd fiber phase; M, where middle soap melts to isotropic liquid of the same composition; I_{MN}, where isotropic liquid is in equilibrium with both middle soap and soap-boiler's neat soap; S, where superneat soap melts to isotropic liquid of the same composition; and I_{NS}, where isotropic solution, superneat soap, and neat soap (subneat soap in the case of sodium oleate) are simultaneously in equilibrium.

TABLE 4

Compositions and temperatures at corresponding points on the phase rule diagrams of sodium laurate, sodium palmitate, sodium stearate, and sodium oleate*

SOAP	POINT K TEMPERATURE	POINT I_{CM}		POINT M		POINT I_{MN}		POINT S		POINT I_{NS}	
		Composition	Temperature	Composition	Temperature	Composition	Temperature	Composition	Temperature	Composition	Temperature
Sodium laurate (C_{12})	30	29.5	42	14.4	149	12.0	136	3.6	294	1.7	285
Sodium palmitate (C_{16})	62	44.0	71	20.5	171	16.2	159	4.5	284	1.1	269
Sodium stearate (C_{18})	67	72.5	76	26.6	171	21.6	145	6.0	287	1.5	262
Sodium oleate ($C_{18}^{=}$).	22	47.0	32	26.4	133	20.2	70	6.1	260	0.5	199

* Temperatures are in °C. and compositions in terms of moles of water per mole of soap.

Comparative results for sodium stearate and sodium oleate, which differ from each other by only a double bond, are shown in table 4. In all cases corresponding changes occur at lower temperatures with sodium oleate than with sodium stearate. The unsaturated soap is also much more soluble, as shown by the higher concentration of soap in the saturated solution (point I_{CM}) and by the very much lower temperature of the Krafft point (point K), the temperature below which the soap is nearly insoluble (<2 per cent). Although the maximum temperature at which middle soap and superneat soap can exist is lower for oleate than for stearate, the compositions at these points (M and S) are nearly the same in the two systems. There is a considerable difference in composition at point I_{NS}, which is to be expected, since in this instance the phases involved are no longer the same in the two systems, being neat soap, superneat soap, and isotropic liquid with sodium stearate and subneat soap, superneat soap, and isotropic liquid in the case of sodium oleate. A further difference is the much larger range of composition over which sodium oleate systems exist as a mixture of phases as opposed to sodium stearate systems, particularly with respect to the equilibria between soap-boiler's neat soap and middle soap or isotropic liquid.

Table 4 also shows the effect on the phase rule diagram of increasing the length of the hydrocarbon chain of the soap molecule. The values given for points S and I_{NS} must be regarded as provisional until a more exhaustive investigation has been made of this portion of the diagram. The solubility in hot water (point I_{CM}) decreases rapidly as the chain length increases. The composition of that middle soap which melts unchanged to isotropic liquid varies nearly linearly with the length of the hydrocarbon chain. This fact would seem to require that any satisfactory structural model of middle soap must dispose the water in such a way that its amount is related to the length of the chain and not only to the extent of hydration of the carboxylate groups.

A similar situation seems to prevail with respect to the composition of that superneat soap which melts to isotropic liquid without change of composition. Here, too, the concentration depends on the chain length, the water content at the maxima in the curves being in the ratio 11:13.7:18.3 for laurate, palmitate, and stearate, respectively, while the lengths of the hydrocarbon chains are in the ratio 11:15:17. Sodium oleate, despite its double bond, has almost exactly the same water concentration as sodium stearate at this corresponding point.

SUMMARY

A part of the phase rule diagram of the system sodium stearate–water has been constructed on the basis of visual observations of the temperatures at which phase changes occurred, supplemented by microscopic determinations and by viewing experiments at selected temperatures.

A much larger number of mesomorphic phases exist than had previously been recognized with saturated soaps. Except at very high soap concentrations the phase behavior in this system is qualitatively similar to that found with other soap systems.

Comparison has been made of the temperatures and compositions of corresponding points in the phase rule diagrams of water and the following soaps: sodium laurate, sodium palmitate, sodium stearate, and sodium oleate.

REFERENCES

(1) McBain, J. W.: Chapter V in Alexander's *Colloid Chemistry*, Vol. I. The Chemical Catalog Company, Inc., New York (1926).
(2) McBain, J. W., Brock, G. C., Vold, R. D., and Vold, M. J.: J. Am. Chem. Soc. **60**, 1870 (1938).
(3) McBain, J. W., Lazarus, L. H., and Pitter, A. V.: Z. physik. Chem. **A147**, 87 (1930).
(4) MacBain, J. W., Vold, R. D., and Jameson, W. T.: J. Am. Chem. Soc. **61**, 30 (1939).
(5) McBain, J. W., Vold, R. D., and Vold, M. J.: J. Am. Chem. Soc. **60**, 1866 (1938)
(6) Vold, M. J.: J. Am. Chem. Soc. **62**, December (1940).
(7) Vold, M. J., Macomber, M., and Vold, R. D.: J. Am. Chem. Soc. **62**, December (1940).
(8) Vold, R. D.: J. Phys. Chem. **43**, 1213 (1939).
(9) Vold, R. D., and Ferguson, R. H.: J. Am. Chem. Soc. **60**, 2066 (1938).
(10) Vold, R. D., and Vold, M. J.: J. Am. Chem. Soc. **61**, 37 (1939).
(11) Vold, R. D., and Vold, M. J.: J. Am. Chem. Soc. **61**, 808 (1939).

THE TIME OF SET OF SILICA GELS. V

THE EFFECT OF ALCOHOLS AND pH ON THE "HEAT OF ACTIVATION"

L. A. MUNRO AND J. A. PEARCE[1]

Department of Chemistry, Queen's University, Kingston, Canada

Received August 1, 1939

Hurd and Letteron (7) have discussed the application of the equations of chemical kinetics and the Arrhenius equation to the setting of silicic acid gels. A value of 16,940 cal. was obtained for the "heat of activation." This was independent of the soda–silica ratio (8) and the weak acid used (5) but varied when strong acids were used (6).

Prasad and Desai (13) have recently estimated the "heat of activation" of various inorganic gels of unrecorded pH.

Previous investigation (12) has shown that the effect of addition agents on the time of set of silica gels is specific at all pH values except 7.0 and changes in a regular manner as the acidity decreases. The heterogeneity of the gelating system and the difference in properties of acid and alkaline gels made it seem of interest to determine whether this change in behavior and the specific effect of addition agents would be reflected in the "heat of activation."

---

[1] Present address: Department of Chemistry, McGill University, Montreal, Canada.

EXPERIMENTAL

A stock silicate solution of sp. gr. 1.1569 containing 6.70 per cent SiO_2 was prepared from "Crystalline sodium silicate, $Na_2SiO_3 \cdot 9H_2O$" (Na_2O : SiO_2 = 1.00:1.02). The standard acetic acid was 1.636 *N* (100 cc. of glacial acetic acid + 1 liter of water). The experimental technique was the same as previously described (10, 11, 12).

RESULTS

The results for one concentration of addition agent (0.5 *M* per liter) are shown in tables 1, 2, and 3. The relation between concentration of addition agent and time of set was found to be similar to earlier work (11).

TABLE 1

Effect of alcohols upon the time of set of silica gels

ADDITION OF 25 CC. OF 3.35 PER CENT SiO_2 SOLUTION TO:	TEMPERATURE	TIME OF SET IN MINUTES					pH OF CONTROL GEL
		Control (t_c)	1-Propanol	Glycol	Glycerol	Mannitol†	
	°C.						
(a) 22 cc. of standard acid + water + addition agent (= 25 cc.)	0	863.	1000	930	906.	900.	5.74
	20	122.	155.	132	130	126.	5.61
	30	45.0	57.0	49.0	48.0	47.0	5.76
	50	8.87	10.5	9.75	9.20	9.10	5.93
(b) 15 cc. of acid* + water + addition agent (= 25 cc.)	0	60.0	Coagulated	Coagulated	75.0	256.	10.59
	20	185.	Coagulated	124.	215.	400.	10.50
	40	105.	Coagulated	70.0	90.0	137.	10.60
	50	53.0	Coagulated	37.5	45.7	66.6	10.63

* 100 cc. of glacial acetic acid + 1250 cc. of water.

† Mannitol values at 0.5 mole per liter of addition agent are obtained at the lower temperatures by extrapolation from smaller additions

The pH changes recorded are the corrected (3) initial pH and the pH on setting for the control gel. In the region of pH 9.5 to 11.0 the corrected glass-electrode readings were between 0.2 and 0.4 pH unit lower than that obtained by indicators (11).

Figure 1 (data in table 3(a)) shows the log time of set plotted against the reciprocal of the absolute temperature and is representative of the acid gels. Only limiting curves are shown, the remainder lying between and parallel to these. The "heats of activation" calculated for these acid gels are, respectively: 16,900; 16,500; 16,780; and 16,300 cal.,—essentially the same as reported by Hurd.

Data from table 3(c), for slightly alkaline gels, have been used to construct figure 2. In this figure the curve for methanol crosses, and that for 1-propanol approaches, the curve for the control gel (12). This appears

TABLE 2

Effect of alcohols upon the time of set of silica gels

ADDITION OF 25 CC. OF 3.63 PER CENT SiO_2 SOLUTION TO:	TEMPERATURE	TIME OF SET IN MINUTES						pH OF CONTROL GEL
		Control (t_c)	Methanol	1-Propanol	Glycol	Glycerol	Mannitol†	
	°C.							
(a) 22 cc. of standard acid + water + addition agent (= 25 cc.)	0	717.	765.	925.	765.	763.	732.	5.52
	20	91.5	98.8	118.	97.0	95.8	93.3	5.57
	30	35.8	38.7	41.0	37.8	37.3	37.0	5.55
	50	6.00	6.37	6.83	6.33	6.33	6.15	5.82
(b) 16 cc. of standard acid + water + addition agent (= 25 cc.)	0	2.92	1 00	Too fast	2.25	4.25	10.7	10.09-10.11
	20	5.00	1.90	Too fast	3.58	6.00	16.0	10.18-10.49
	30	4.75	1.75	Too fast	3.33	5.25	12.4	10.26-10.42
	50	2.66	1.00	Too fast	1.75	2.15	5.45	10.39-10.56

† Mannitol values at 0.5 mole per liter of addition agent are obtained at the lower temperatures by extrapolation from smaller additions.

TABLE 3

Effect of alcohols upon the time of set of silica gels

ADDITION OF 25 CC. OF 2.59 PER CENT SiO_2 SOLUTION (SP. GR. = 1.0569) TO:	TEMPERATURE	TIME OF SET IN MINUTES						pH CHANGES IN CONTROL GEL
		Control (t_c)	Methanol	1-Propanol	Glycol	Glycerol	Mannitol†	
	°C.							
(a) 15 cc. of standard acid + water + addition agent (= 25 cc.)	0	1852.	1955.	2307.	1958.	1910.	1910.	5.36
	20	276.	298.	320.	296.	292.	289.	5.49
	30	105.	117.	124.	113.	111.	108.	5 41
	50	16.6	18.0	20 4	18 0	17.5	17.1	5.60
(b) 14 cc. of standard acid + water + addition agent (= 25 cc.)	0	532.	559.	581.	552.	553.	550	5.70-5 81
	20	78.	85.5	94.0	83.0	82.0	80.0	6.02-6.35
	30	31.1	32.8	36.0	33.0	32.5	31.8	6.02-5.98
	50	5.25	5.50	6.17	5.62	5.50	5.50	6.24-6.29
(c) 13 cc. of standard acid + water + addition agent (= 25 cc.)	0	21.0	22.3	21.0	22.6	24.8	31.0	7.70-7.70
	20	7.50	7.25	6.33	8.00	8.25	9.83	7.92-8.12
	30	3.75	3.50	3.17	4.00	4.20	4.83	7.99-8.11
	50	1.33	1.23	0.97	1.42	1.40	1.58	8.20-8.38
(d) 12 cc. of standard acid + water + addition agent (= 25 cc.)	0	26.0	19.0	6.00	26.5	32.8	69.0	8.85-9.08
	20	19.3	12.8	5.00	19.0	23.0	37.8	9.20-9.68
	30	13.4	9.50	3.62	11.5	15.0	24.3	9.18-9.55
	50	6.66	4.62	1.94	5.57	7.00	10.9	9.57-9.90

† Mannitol values at 0.5 mole per liter of addition agent are obtained at the lower temperatures by extrapolation from smaller additions.

to be due to the change in pH with temperature. Such a shift in pH has been noted by Batchelor (1). The "heat of activation" calculated from the data for the control gel is 9820 cal. This differs greatly from Hurd's values.

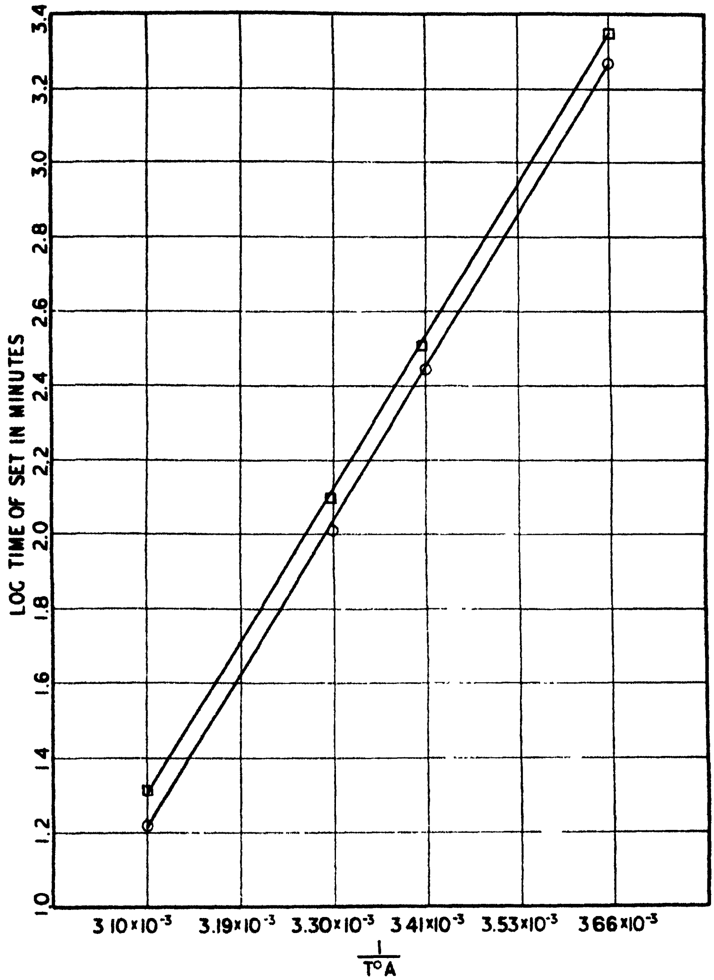

Fig. 1. Relation between time of set and absolute temperature for acid gels of different silica concentrations at different pH with or without addition agents. ○, control gel; □, 1-propanol.

Figure 3, from table 3(d), illustrates the same kind of a change in the case of glycol. It is no longer possible to calculate a "heat of activation." The values for gels containing glycerol approach the values for the control gel very closely at the higher temperatures.

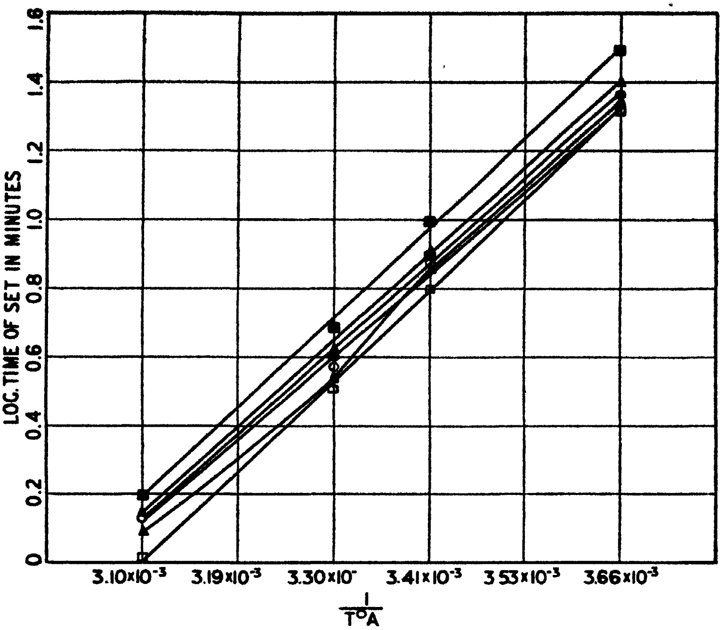

FIG. 2. Change in temperature-time of set relation at pH ~ 7.9 (SiO_2, 1.3 per cent). ○, control gel; △, methanol; □, 1-propanol; ●, glycol; ▲, glycerol; ■, mannitol.

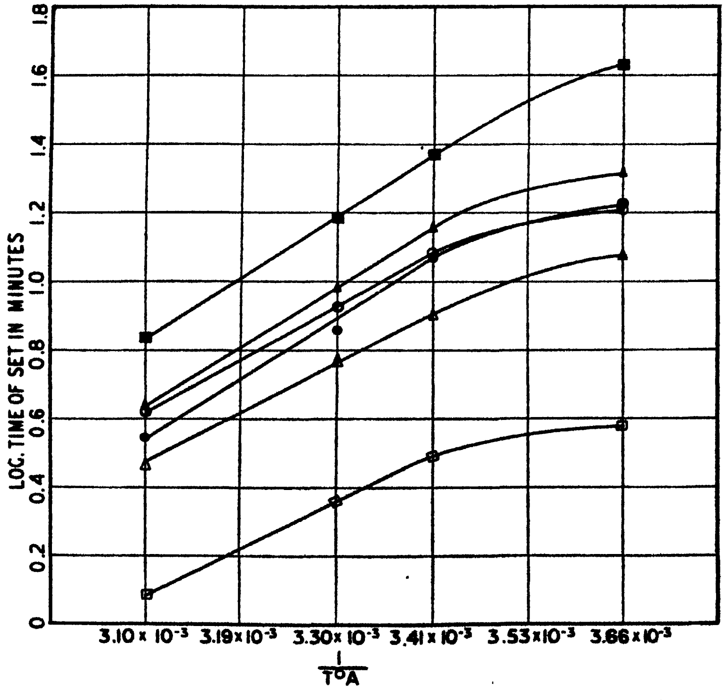

FIG. 3. Change in temperature-time of set relation at pH ∽ 9.2 (SiO_2, 1.3 per cent). ○, control gel; △, methanol; □, 1-propanol; ●, glycol; ▲, glycerol; ■, mannitol.

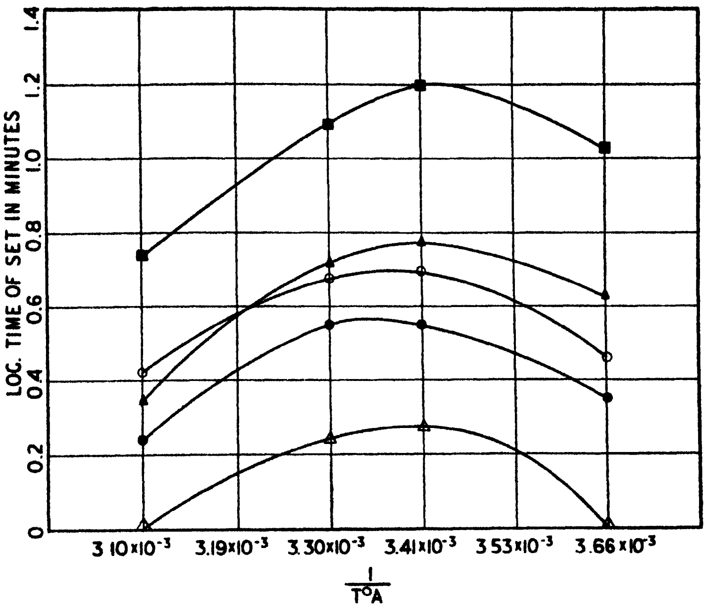

FIG. 4. Change in temperature-time of set relation at pH ~ 10.2 (SiO_2, 1.8 per cent). ○, control gel; △, methanol; ●, glycol; ▲, glycerol; ■, mannitol.

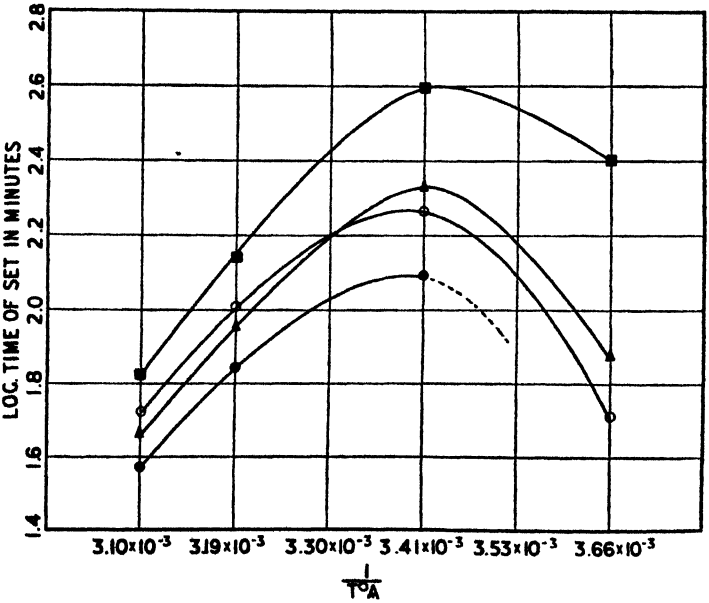

FIG. 5. Change in temperature-time of set relation at pH ~ 10.5 (SiO_2, 1.7 per cent). ○, control gel; ●, glycol; ▲, glycerol; ■, mannitol.

Table 2(b) and figure 4 show the effect at increased silica content and increased pH. It will be seen that the curving is more pronounced. At 50°C. glycerol has actually become an accelerator of gelation.

Table 1(b) gives the data for figure 5, at pH 10.59. As this is just inside the limit of alkalinity in which gels are formed (12, 15), these gels are very fragile. The readings, therefore, can only be approximations. The important points are that the curving of the lines is still more pronounced and that glycerol joins the accelerators between 30° and 40°C.

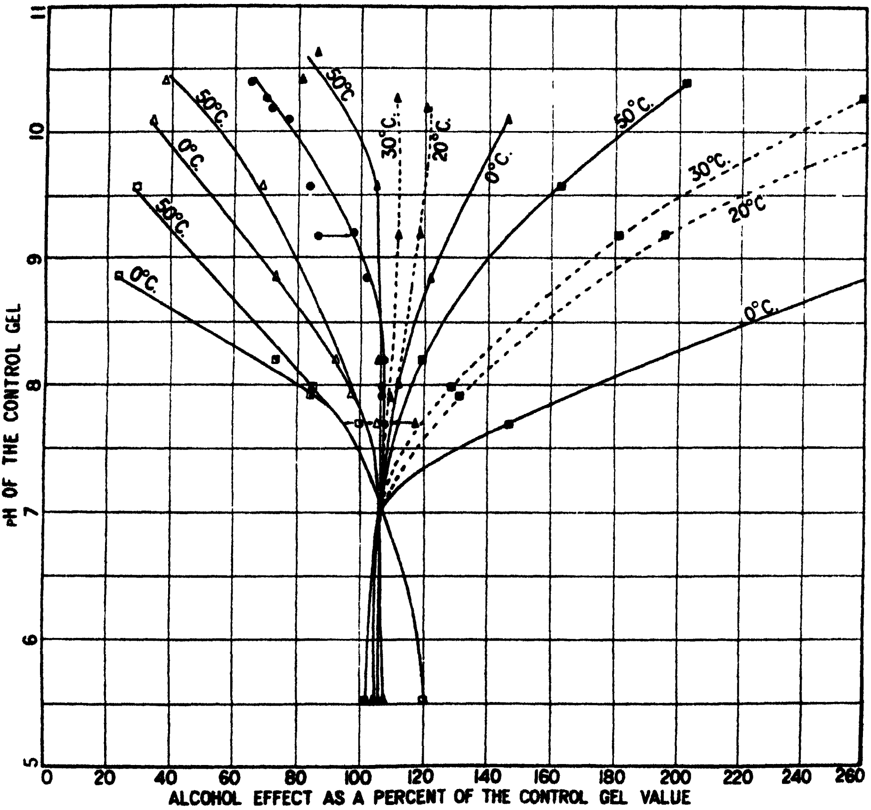

FIG. 6. Variation in specific effect of the alcohols ($100t_a/t_c$) with pH. △, methanol; □, 1-propanol; ●, glycol; ▲, glycerol; ■, mannitol.

Calculations on Batchelor's (1) data[2] gave a few straight lines for the "heat of activation" curves, but the slopes obtained were not the same as Hurd's. This might be explained by Batchelor's use of a mixture of strong acids and by his method of determining the time of set, which does not give exact readings in those gels which are definitely thixotropic. His data, in spite of these limitations, support our findings that the "heat of activation" is not constant over a pH range.

---

[2] Kindly supplied by the author.

THE GENERALIZATION FOR SILICA GELS WITH ALCOHOLS AS ADDITION AGENTS

When the time of set of a gel containing addition agent (t_a) expressed as a percentage of the time of set of the original or control gel (t_c) is plotted against the pH of the control gel, a system of smooth curves is obtained (12). In the present work this generalization is extended to other temperatures. A series of similar curves is obtained (figure 6). To avoid congestion experimental points have been omitted on the acid side. The deviations of the present 20°C. curves from those reported elsewhere are doubtless due to the pH discrepancy mentioned above and the difficulty of preparing silicate solutions of exactly the same colloidal properties.

Those addition agents that have the greatest specific action on the time of set are affected most by change in temperature. On the alkaline side, as the temperature is increased all reagents become less specific in their effect. For those alcohols which change from accelerators to retarders the pH of reversal is practically constant and is the same as previously noted (12). The effect of temperature on the glycol curve is astonishingly small.

The lack of specificity at pH 7.0 seems to indicate that the dielectric constant of the addition agent plays a minor rôle in the setting phenomenon. This is in opposition to the suggestion of Davis and Hay (2) that the most important variable of colloidal silica is the sign and magnitude of the electrokinetic potential.

DISCUSSION

Hurd, Raymond, and Miller (9) report that there is a straight-line relationship between the log time of set and the pH of acid gels. The former quantity plotted against the reciprocal of the absolute temperature also gives a straight-line relationship. Any changes in pH therefore that occur with temperature would not cause any curvature of the activation line for acid gels. Hurd (4) considers that there is a similar relationship for alkaline gels. It has been shown (12) that this is only true for a limited range, and that the curve goes through a pronounced minimum. Hence the change in pH with temperature may here be an important factor in causing a change in slope for alkaline gels.

Davis and Hay (2) appear to have confused "the heat evolved during the formation of the gel," which they refer to as the "heat of formation," with the "heat of activation." They suggest six possible sources of the heat evolved. Two of these, e.g., heat of neutralization and heat of dilution, are not determinative of the relatively slow gelation process. The term "heat of activation" is descriptive of the rate of the determining reactions which immobilize the sol and produce a standard rigidity, defining the time of set. Sorption of the dispersion medium, displacement of water from the silicic acid complex, surface energies, and loss of kinetic energy of the molecules are all factors that determine the so-called "heat of activation." If the importance of one or the other of these changes with temperature, a straight line will not be obtained.

In the presence of addition agents the importance of these factors might be expected to be altered and other factors introduced. The specific nature of the effect of alcohols on the alkaline side would point to the increasing importance of adsorption. This factor alone would tend to cause greater deviation from a theoretical "heat of activation." On the acid side the addition agents apparently affect but little the mechanism of gelation, although the time of set is altered.

Differences between acid and alkaline silica gels are shown in other respects than in their behavior towards addition agents. For acid silica gels syneresis is slow; for alkaline silica gels of similar concentration syneresis is rapid. Acid silica gels are more transparent, more rigid, and more elastic. Alkaline gels appear to be less stable and tend to be granular. It would seem that the setting of acid and of alkaline gels is governed by different factors. It is even doubtful if a theory of gelation for acid gels can be applied to alkaline systems. The difference in the curves for the Arrhenius equation, described above, supports this view.

SUMMARY

1. Calculations of the so-called "heat of activation" have been made for silica gels over a pH range.
2. The presence of addition agents does not essentially change the slope of the curve for acid gels.
3. For acid gels the values for the "heat of activation" were the same as those obtained by Hurd.
4. For alkaline gels the slope changes and finally a straight line is no longer obtained.
5. The generalized curve relating pH and per cent effect on the set for a series of alcohols is given for the temperatures studied.
6. It is concluded that the gelations of acid and alkaline gels are fundamentally different.

REFERENCES

(1) Batchelor, H. W.: J. Phys. Chem. **42**, 575 (1938).
(2) Davis, H. L., and Hay, K. D.: J. Am. Chem. Soc. **61**, 1020 (1939).
(3) Dole, M.: *Measuring pH with the Glass Electrode*, p. 12. Coleman Electric Co., Maywood, Illinois (1937).
(4) Hurd, C. B.: Chem. Rev. **22**, 403 (1938).
(5) Hurd, C. B.: J. Phys. Chem. **40**, 21 (1936).

(6) HURD, C. B., FREDERICK, K. J., AND HAYNES, C. R.: J. Phys. Chem. **42**, 85 (1938).
(7) HURD, C. B., AND LETTERON, H. A.: J. Phys. Chem. **36**, 604 (1932).
(8) HURD, C. B., AND MILLER, P. S.: J. Phys. Chem. **36**, 2194 (1932).
(9) HURD, C. B., RAYMOND, C. L., AND MILLER, P. S.: J. Phys. Chem. **38**, 663 (1934).
(10) MUNRO, L. A., AND ALVES, C. A.: Can. J. Research **B15**, 353 (1937).
(11) MUNRO, L. A., AND PEARCE, J. A.: Can. J. Research **B16**, 390 (1938).
(12) MUNRO, L. A., AND PEARCE, J. A.: Can. J. Research **B17**, 266 (1939).
(13) PRASAD, M., AND DESAI, D. N.: J. Indian Chem. Soc. **16**, 117 (1939).
(14) PRASAD, M., AND HATTIANGADI, R. R.: J. Indian Chem. Soc. **6**, 991 (1929).
(15) TOURKY, A. R.: Z. anorg. allgem. Chem. **240**, 198 (1939).

AN ANOMALOUS CONCENTRATION CELL. THE CONSTITUTION OF SOLUTIONS OF STANNOUS CHLORIDE IN WATER AND IN HYDROCHLORIC ACID

L. R. ALLISON, E. J. HARTUNG, AND E. HEYMANN
Department of Chemistry, University of Melbourne, Melbourne, Australia

Received June 20, 1939

Some time ago, a concentration cell of stannous chloride with the more dilute solution superimposed on the more concentrated was prepared for a lecture demonstration. The more concentrated solution (25 per cent) was prepared in 2.33 *N* hydrochloric acid, and the other by dilution in the ratio 1:10 with water. On superimposing one solution on the other, and introducing a small tin rod, it was found that the tin crystals, instead of being deposited in the more concentrated region, were formed in the dilute solution, contrary to what would be expected. It was later found that, when the two solutions were prepared in acid of the same normality, the cell behaved in a normal manner and the tin crystals were deposited in the concentrated region.

Subsequent investigation has shown that the behavior of the anomalous cell may be readily explained on the assumption that the activity of the stannous ions is smaller in the strongly acid solution of stannous chloride in high concentration than in the weakly acid solution of stannous chloride in low concentration. This is most probably due to the complexity of these solutions.

I. THE LIQUID-JUNCTION POTENTIAL

The anomalous cell

$$^{-}\mathrm{Sn}\left|\begin{matrix}25\%\ \mathrm{SnCl_2}\\ 2.33\ N\ \mathrm{HCl}\end{matrix}\right|\begin{matrix}2.5\%\ \mathrm{SnCl_2}\\ 0.233\ N\ \mathrm{HCl}\end{matrix}\left|\mathrm{Sn}^{+}\right.$$

shows an E.M.F. of −70 millivolts (the negative sign being used to indicate anomalous behavior). After introduction of a saturated potassium chloride bridge the E.M.F. is reduced to −35 to −40 millivolts, showing that the liquid-junction potential in the original cell is appreciable, but not great enough to account for the anomalous effect. Assuming that the liquid-junction potential is to a great extent destroyed by the salt bridge, its value would be approximately equal to the difference, namely $\sim$ 30 to 35 millivolts. Applying Cumming's (4) equation,[1] a value of 33 millivolts would be expected.

If the hydrochloric acid concentration is the same in both cells (2.33 N), the cell shows normal behavior, the E.M.F. being 30.9 millivolts. Introduction of a salt bridge reduces this value by less than 1 millivolt, showing that the liquid-junction potential is negligible in this case. Hence, in the anomalous cell, it is mainly due to the difference in concentration of hydrochloric acid.

II. SOLUTIONS OF STANNOUS CHLORIDE WITHOUT ADDITION OF ACID

To obtain an indication of the possible nature of the ions concerned in the phenomena mentioned above, the potential $Sn \mid Sn^{++}$ was first measured in solutions without addition of acid. The potentials were measured against a *saturated* calomel electrode, using a Tinsley potentiometer. From these values the potentials against the standard hydrogen electrode were calculated (E_H). Since neither the nature of the ions present nor the transport numbers in stannous chloride solutions are known with certainty, the value of the liquid-junction potential cannot be estimated. It will, however, be only small, since saturated potassium chloride solution has been used as intermediate liquid. In all experiments oxygen was excluded by keeping the system under nitrogen or carbon dioxide.

In figure 1 E_H is plotted against log c (c = molar concentration). It is seen that E_H does not vary linearly with log c, $dE/d \log c$ varying between 8 and 14 millivolts. This is considerably below the Nernst value of

$$\frac{2.303 \times RT}{2F} = 29 \text{ millivolts } (18°\text{C.})$$

which would be expected, if the activity coefficient were either unity or independent of c. Hence, on dilution, the activity (α_{Sn}) is reduced in a much smaller ratio than the concentration, as a consequence of a process in which new stannous ions are formed. Such a process consists presumably in the breaking up of complexes, such as $SnCl_4^{--}$ or $SnCl_3^-$. The suggestion of the presence of a large amount of the salt in an autocomplex form was first made by Foerster (6). From the experimental figures and from the standard potential of tin ($E_0 = -0.136$ volt (7,8)) the

---

[1] Cumming's equation is more suitable for concentrated systems than Henderson's equation, since it contains actual transport numbers instead of mobilities at infinite dilution and the conductance ratio instead of the concentration ratio.

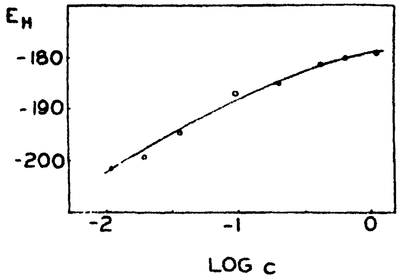

FIG. 1

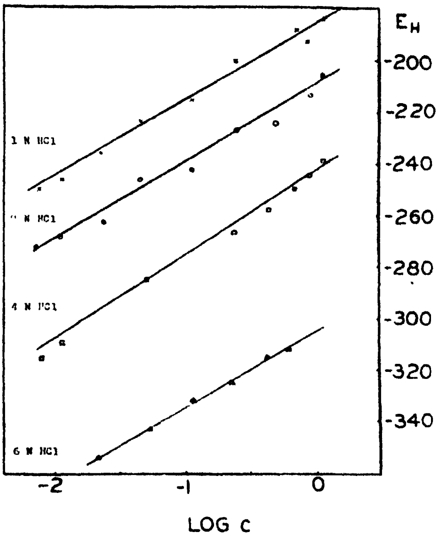

FIG. 2

FIG. 1. Plot of E_H against log c for stannous chloride solutions containing no hydrochloric acid

FIG. 2. Plot of E_H against log c for stannous chloride solutions containing various amounts of hydrochloric acid

TABLE 1

Stoichiometric activity coefficient γ_{Sn}

$E_0 = -136$ millivolts

c	E_H	a_{Sn}	γ_{Sn}
M	*millivolts*		
1.058	179.8	0.0309	0.029
0.634	180.5	0.0295	0.047
0.417	181.7	0.0270	0.065
0.202	185.6	0.0187	0.091
0.099	187.4	0.0170	0.17
0.037	194.8	0.0100	0.29
0.018	199.9	0.0063	0.35
0.011	201.4	0.0056	0.50

stoichiometric activity coefficient (γ_{Sn}) may be estimated. It varies from 0.03 to 0.5, when the concentration is reduced from 1.058 *M* to 0.011 *M* (table 1).

III. SOLUTIONS CONTAINING ACID

All potentials measured in acid solutions are corrected to eliminate the liquid-junction potential due to hydrochloric acid, using Cumming's equation. In figure 2 E_H is plotted against log c for solutions containing various amounts of hydrochloric acid. Addition of hydrochloric acid makes the potentials much more negative; hence the activity of Sn^{++} decreases strongly. Addition of 6.0 N hydrochloric acid to a 1.108 M stannous chloride solution decreases the activity from 3.6×10^{-2} to the order of 10^{-6}. Addition of potassium chloride and ammonium chloride has a similar effect (6). The reason for these effects is obviously an increase in the amount of complex ions, e.g., $SnCl_4^{--}$ and $SnCl_3^-$, on addition of acid.

Figure 2 shows further that, in acid solution, there is a linear relation between E_H and log c, dE/d log c being very near to the Nernst value of 29 millivolts. Table 2 shows the values for various acid concentrations, calculated from the slope of the curves.[2]

TABLE 2

Values of dE/d log c for various acid concentrations

HYDROCHLORIC ACID	$\frac{dE}{d \log c}$
N	*millivolts*
1	30.0
2	30.0
4	33.5
6	28.0

The striking discrepancy between the behavior of stannous chloride solutions containing acid (dE/d log $c \cong 29$ millivolts) and those containing no acid, except that originating from hydrolysis, (dE/d log $c \ll 29$ millivolts) is easily explained. Increasing addition of hydrochloric acid favors the formation of the complex, the stability of which is obviously so great in acid solution that its degree of dissociation is but little influenced by the total concentration of stannous chloride. The activity of stannous ions, which determines the potential, is then roughly proportional to the analytical concentration of the salt. Hence, conditions exist in which the variation of the potential with concentration is described by the Nernst equation.

From the slope of the E_H–log c curves in strongly acid solutions, information about the nature of the complex may be obtained by a method first employed by Bodländer (1). It can be shown that

---

[2] It may be mentioned that the slope of the curves is not affected by the uncertainty about the magnitude of the liquid-junction potential since, each set of experiments being carried out at constant hydrochloric acid concentration, the liquid-junction potential is practically independent of the stannous chloride concentration and therefore does not affect the slope of the E_H–log c curves.

$$\frac{dE}{d \log c} = \frac{2.303 \times RT}{2F \times n} = \frac{29}{n} \text{ millivolts (18°C.)}$$

where n is the number of tin atoms in the complex. Hence our results show conclusively that acid stannous chloride solutions contain in appreciable concentration only complexes with one atom of tin. Of these, $SnCl_4^{--}$ and $SnCl_3^-$ are the most probable ones, for a complex acid, $HSnCl_3 \cdot 3H_2O$, and salts of H_2SnCl_4 have been separated in crystalline form and some of them have been investigated by x-ray analysis (2, 3, 5, 6, 9). The existence of the higher negative chloro-complexes and that of a positive complex, such as $SnCl^+$, can, however, not be ruled out (8), although there is practically no direct experimental evidence for their occurrence.

IV. SUMMARY

1. An anomalous concentration cell is described and its mechanism discussed.

2. The potential Sn | Sn^{++} in stannous chloride solutions of various concentrations has been investigated. dE/d log c is much smaller than the "Nernst" value (29 millivolts). This is due to the breaking up of complex ions into simple ions on dilution.

3. Addition of hydrochloric acid makes the potential much more negative. Obviously the amount of complex ions, e.g., $SnCl_4^{--}$ or $SnCl_3^-$, is greatly increased at the expense of stannous ions.

4. The potential Sn | Sn^{++} in strongly acid solutions of stannous chloride varies linearly with the logarithm of the analytical concentration of stannous chloride, dE/d log c being very near to the "Nernst" value. This is due to the stabilizing effect of hydrochloric acid on the complex, which makes it insensitive to dilution. The activity of the remaining stannous ions, which determines the potential, is then roughly proportional to the analytical concentration of the salt.

5. The nature of the complex ions present in acid stannous chloride solutions is discussed.

REFERENCES

(1) BODLÄNDER, G., AND FITTIG, R.: Z. physik. Chem. **39**, 597 (1902); Z. anorg. Chem. **31**, 458 (1902); **39**, 197 (1904). *Cf.* also GLASSTONE, S.: *The Electrochemistry of Solutions*, Chap. 16. Methuen & Co., Ltd., London (1930).

(2) BRASSEUR, H., AND DE RASSENFOSSE, A.: Nature **143**, 333 (1939).

(3) COX, E. G., SHORTER, A. J., AND WARDLAW, W.: Nature **139**, 71 (1937).

(4) CUMMING, A. C.: Trans. Faraday Soc. **8**, 86 (1912).

(5) ENGEL, M.: Bull. soc. chim. [2] **50**, 96 (1888).

(6) FOERSTER, F., AND YAMASAKI, J.: Z. Elektrochem. **17**, 361 (1911).

(7) NOYES, A., AND TOABE, K.: J. Am. Chem. Soc. **39**, 1537 (1917).

(8) PRYTZ, MILDA: Z. anorg. Chem. **172**, 147 (1928).

(9) YOUNG, S. W.: J. Am. Chem. Soc. **23**, 21 (1901).

VISCOSITIES OF SEVERAL COMMON GASES BETWEEN 90°K. AND ROOM TEMPERATURE

HERRICK L. JOHNSTON AND KENNETH E. McCLOSKEY

Department of Chemistry, The Ohio State University, Columbus, Ohio

Received October 3, 1939

Although considerable work has been done on the viscosities of gases below the ice-point, the data have usually been taken at widely separated points on the temperature scale and would seem, with a few notable exceptions, to be none too reliable. In connection with a program of accurate low-temperature heat-capacity measurements on gases by the velocity of sound method, the authors have considered it advisable to carry out a series of viscosity measurements in the low-temperature range. In addition, it was felt that accurate viscosity data would furnish a worthwhile contribution to the study of interrelationships among heat capacities, thermal conductivities, data of state, viscosities, and intermolecular forces. This paper deals with a description of the method and apparatus used, together with results obtained on hydrogen, air, oxygen, nitrogen, nitric oxide, nitrous oxide, carbon dioxide, and methane.

METHOD AND APPARATUS

A careful consideration of the problem of measuring gas viscosities over the low-temperature range leads ultimately to the oscillating-disk method of Maxwell (21, 10, 8, 25). The apparatus (figure 1) was patterned after that of Sutherland and Maass (25), but included certain refinements which it was felt would increase the reliability of the results, especially in the measurement and control of temperature.

Temperature measurement and temperature control

Temperatures were determined by means of a copper-constantan thermocouple soldered directly to the bottom of the lower fixed disk. This had the advantage of measuring the temperature of thermally conducting metal adjacent to the portion of gas whose viscosity was determined. Subsequent measurements showed that the temperature of this region differed significantly from that of the bath, owing in part to conduction of heat by the gas which fills the central column of the apparatus. The thermocouple employed was one of several standardized in this laboratory against the Berkeley temperature scale (5) through the intermediate standard couple, designated as couple 101, calibrated by Milner and Greensfelder (17). Our scale is believed accurate to ± about 0.05°, which is better than our requirement. The couple was wound loosely around the supporting screws for several turns, to eliminate temperature gradients near the junction, and was taken out of the apparatus through a de Khotinsky seal at the top of the side tube F.

A large Dewar flask contained the bath for regulating the temperature of the gas. An air-driven stirrer, supported independently of the mount that held the apparatus, was run slowly enough to prevent noticeable vibrations.

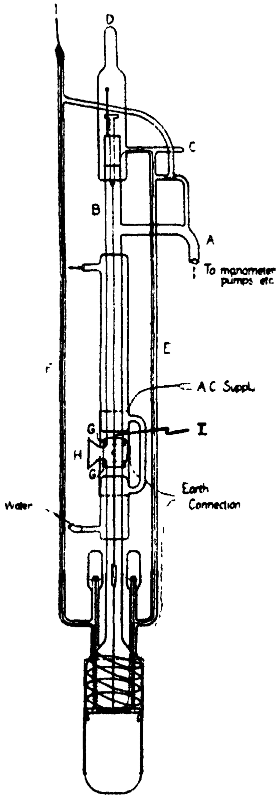

FIG. 1. Apparatus

Liquid oxygen was used for the bath at 90°K. At 118°K. a freezing mixture of dichlorodifluoromethane was maintained by inserting into the bath a copper flask containing liquid air to a suitable level. Between 130° and 150°K. a thin-necked copper Dewar flask was used with a bath of dichlorodifluoromethane. Regulation of the liquid air level in the Dewar flask and of the hydrogen pressure between its walls proved a sufficient means to offset heat leak into the bath or to reduce the warming rate to a few tenths of a degree per hour. Above 150°K. the bath was thermostatted with the use of accessory apparatus patterned after the precision cryostat of Scott and Brickwedde (24). Thermostatting was usually better than ± 0.05°. Dichlorodifluoromethane was employed as bath liquid to a temperature of 170°. Above this temperature a bath with the following composition was used: 19.4 per cent chloroform, 44.7 per cent ethyl bromide, 22.5 per cent trichloroethylene, and 13.9 per cent s-dichloroethylene.

For all runs two temperatures were read and recorded, both before and after the viscosity measurements: namely, that of the silver disk by means of the standard couple previously referred to, and that of the bath by means of a second copper–constantan couple submerged in the liquid. The two readings were usually not identical. In thermostatted runs the temperature of the disks usually exceeded that of the bath by a few hundredths of a degree owing, presumably, to heat conduction by the gas in the vertical column of the apparatus. In some trial runs in which the bath was permitted to warm at the rate of 2° or 3° an hour the conditions were reversed, the silver disks lagging behind approximately 1°. Rapid heating of the bath (1° per minute) produced temperature differences of 6° to 7° between the bath and the disks. These results indicate the necessity of measuring temperatures directly at the disks, in reporting viscosities.

Other variations from the design employed by Sutherland and Maass

(*a*) In order to maintain constant spacing between the oscillating disk and the fixed disks, in spite of temperature changes in the lower part of the apparatus, the section of brass rod below the ivory segment was made the same length as the three long screws which support the fixed disks. The desirability of maintaining constant spacings is shown by an equation given by Keesom and van Itterbeek (15)

$$C = \pi r^4 (d_1 + d_2)/4Id_1d_2 \qquad (1)$$

in which C is the apparatus constant (*cf.* equation 2), r the radius of the oscillating disk, d_1 and d_2 the distances which separate the oscillating disk and the upper and lower fixed disks, respectively, and I the moment of inertia of the oscillating system.

(*b*) Spiral springs of brass slip over the long brass supporting screws and bear against special washers placed just under the glass risers. These prevent permanent displacement of the fixed-disk assembly as the result of successive contractions and elongations of the supporting screws consequent on temperature changes in the bath.

(*c*) The hook and grooved eyelet, placed by Sutherland and Maass at the upper end of the suspension wire, were placed by us at the bottom, where they could be reached through the open window with a curved pair of tweezers. The window was cemented in place with a non-volatile cement, which could be easily softened with a flame. This variation in design was a considerable advantage for purposes of assembling or repairing the apparatus, since the whole suspension could be changed without removing the apparatus from its supports or necessitating adjustments below the window.

(*d*) Amplitudes of successive oscillations were observed by means of a telescope with cross hair, with the aid of an illuminated scale. The scale was set at approximately 10 feet from the apparatus, to obtain high sensitivity. To prevent any distortion of the mirror which might result if it were cemented directly to the brass rod, it was tied firmly with silk thread to a thin piece of cork which, in turn, was cemented to the rod by means of shellac. A small galvanometer mirror, which was ground to dimensions of about 2 mm. by 3 mm., was employed.

The apparatus was firmly clamped in a wooden support attached to a 3 ft. by 3 ft. concrete pillar which formed a portion of the foundation of the building.

PREPARATION AND PURIFICATION OF GASES

Hydrogen, investigated largely to test the reliability of the apparatus, was taken from a commercial tank of electrolytic hydrogen and was purified by slow passage through charcoal cooled with liquid air. Preliminary treatment of the charcoal involved evacuation at a dull red heat and subsequent washing with hydrogen at the same temperature.

Air, taken from outside the laboratory, was freed from carbon dioxide and water vapor by slow bubbling through concentrated potassium hydroxide solution and concentrated sulfuric acid, followed by passage first over stick potassium hydroxide and then over phosphorus pentoxide.

Oxygen was prepared and purified by the method outlined by Giauque and Johnston (7). The electrolytic cell used operated on a current of 5 amperes.

Nitrogen was prepared according to the procedure outlined by Giauque and Clayton (6).

Nitric oxide was prepared by the method of Johnston and Giauque (13), using the preparation and purification system set up by Johnston and Weimer (14).

Nitrous oxide was prepared by the procedure followed by Johnston and Weimer (14).

Carbon dioxide was prepared by the modification of the method of Maass and Cooper (19) and by the modification of the method of Meyers and Van Dusen (22) employed by Long (18).

Methane was prepared by the Grignard reaction, special precautions being taken to free the gas from ether vapor. The methane was fractionated several times in a closed glass system, the end fractions being discarded each time. This is essentially the procedure set forth by Duncan and Howe (3).

CALIBRATION

Maxwell (21) derived the following fundamental equation for the oscillating-disk viscosity apparatus:

$$\eta = (\lambda - x)/Ct \tag{2}$$

where η = viscosity, λ = logarithmic decrement, x = wire constant, t = period, in seconds, of one oscillation, and C = the apparatus constant.

We can put for the logarithmic decrement:

$$\eta = (\log L_n - \log L_{(n+i)})/i \tag{3}$$

where L_n is the full amplitude of the n^{th} oscillation (corrected for noncurvature of our scale) and n takes on the values $1, 2, \cdots i$. Our custom has been to take series of ten oscillations ($i = 5$) for gas runs. The five values for λ thus obtained in a single series ordinarily agreed to within 0.1 of 1 per cent.

Wire constant

To obtain the wire constant, which is a measure of energy losses in the wire alone, the logarithmic decrement was measured with the apparatus thoroughly evacuated.

Preliminary to each determination the apparatus was evacuated to a pressure of 10^{-6} mm. of mercury, or under, for from 12 to 24 hr., with the apparatus at room temperature. The bulb of the apparatus was immersed in liquid air for the determinations. For determinations of the wire constant, each run consisted of a series of 60 oscillations (that is, $i = 30$ (equation 3)). Table 1 indicates the degree of reproducibility obtained in the measurement of wire constants. These refer to measurements made within a single day.

Although Sutherland and Maass (25) assumed x to remain constant after several hours annealing at 100°C., our own preliminary measurements indicated small but significant irregularities that could be accounted for only by variations in x. Further investigations revealed (*1*) that x decreases normally with use, owing apparently to work hardening of the wire as the result of twisting, and (*2*) that x is increased markedly if glass blowing is done on or near the apparatus, even though there be little apparent opportunity for the wire to become heated. These observations are brought out clearly in figure 2, for a wire on which numerous determinations of the constant were made over a period of more than two months. Accordingly it was found necessary to repeat determinations of the wire constant at convenient intervals, and to interpolate to intermediate dates. Table 2 is a record of determinations of the wire constant within the period

TABLE 1

Determinations of the wire constant for suspension I

DATE	x
August 12, 1937	0.000866 0.000854 0.000861
Average	0.000860

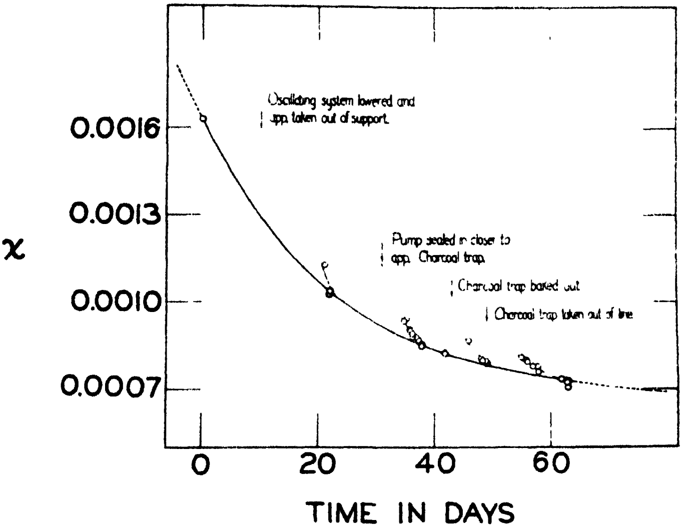

FIG. 2. Variations in the wire constant with time and with experimental adjustments

TABLE 2

Determinations of the wire constant for suspension II

DATE	x*
(a) Determinations prior to readjustment of zero setting	
September 10, 1937	0.000734
September 27, 1937	0.000676
(b) Determinations subsequent to readjustment of zero setting	
October 1, 1937	0.000747
October 10, 1937	0.000663

* There can be no doubt that these systematic variations in x are real and that a proper method of interpolation has been pursued in choosing x's to use with the viscosity data: namely, by using curves rough-drawn to the shape of that in figure 2. However, the entire effect is small. If the evidence of figure 2 and the reproducibility exhibited in successive determinations, as in table 1, were neglected, and the four values of table 2 were averaged as though they represented an experimental spread of error, the viscosity value most affected—that of methane at 90°—would be changed by only 0.25 of 1 per cent.

during which the majority of the viscosity data were collected. Each value is an average of several determinations, as in table 1. The wire (suspension II) had been previously annealed *in situ* at 100°C. *after* the rest point was adjusted and all glass seals completed. During the annealing process hydrogen was held in the apparatus to increase heat transfer between the wire and the condenser walls. The wire constant decreased slowly with time. Between September 27th and October 1st the rest point was readjusted, which necessitated opening and resealing the glass tubes C and D (figure 1). The wire was reannealed before the new calibration on October 1st.

Apparatus constant

The apparatus constant was determined by measurements of logarithmic decrements in air at temperatures close to 296.1°K. The viscosity of air was taken as $\eta = 1833.0 \times 10^{-7}$ poises at 296.1°K. This is the average of the following published results: 1829.2×10^{-7}, Houston (11); 1834.9×10^{-7}, Kellstrom (16); 1834.7×10^{-7}, Bond (2); 1834.4×10^{-7}, Majumdar and Vajifdar (20); 1833.3×10^{-7}, Banerjea and Plattanaik (1); 1830.3×10^{-7}, Rigden (23); 1834.1×10^{-7}, Fortier (4). This value, which is 0.57 per cent higher than the value of Harrington (9), 1822.6×10^{-7}, which has served as the standard for most of the recent work in the United States and Canada, agrees well with the standard generally accepted in Europe: namely, Vogel's (29) $\eta = 1724 \times 10^{-7}$ for air at 273.1°K., corresponding to $\eta = 1832 \times 10^{-7}$ for air at 296.1°K.

TABLE 3

Corrections to the viscosities made necessary by thermal contraction of the metal disks

T	CORRECTION
°K.	*per cent*
300	−0.005
200	+0.155
100	+0.316

Determinations of the apparatus constant, with air, were repeated at 4- to 5-day intervals during the period that active measurements of the several gases were in progress. Measurements on six different days prior to the readjustment of the zero setting averaged $C = 5.368$ with deviations from the mean equal to about 0.1 of 1 per cent. Three determinations subsequent to the readjustment of the zero setting averaged 5.380 with deviations of only 0.05 of 1 per cent from this mean. Within limits of experimental error, the wire constant appeared to be independent of time, but was somewhat affected by the readjustment of the zero. The value

5.368 was therefore employed as the apparatus constant for all data taken prior to October 1, 1937 and 5.380 for all data taken subsequent to that time.

THE DATA

The experimental data are given in tables 4 to 12 and are shown graphically in figure 3. These include a small correction made necessary at temperatures other than 296°K. by virtue of thermal changes in the dimensions of the oscillating-disk assembly. The need for this is made apparent from equation 1, which shows that the apparatus constant will vary directly with r^4/I and inversely with $d_1d_2/(d_1 + d_2)$. Neglecting the slight difference in the thermal expansion coefficients of brass and of silver and the contributions from both brass and silver to the $d_1d_2/(d_1 + d_2)$ portion of the correction, the net effect is that C varies directly with the first power of the linear expansion of silver. Taking the average coefficient

TABLE 4

Viscosity of hydrogen

DATE	T	$\eta \times 10^7$	AVERAGE $\eta \times 10^7$	DATE	T	$\eta \times 10^7$	AVERAGE $\eta \times 10^7$
	°K.				°K.		
October 2, 1937	90.28	390.6		October 3, 1937	216.06	717.2	
		391.2				718.2	717.7
		390.6	390.9		231.07	750.7	
October 5, 1937	117.48	474.2				751.5	751.1
		474.0	474.1		244.99	780.6	
	131.63	513.0	513.0			781.7	781.1
	132.69	515.4	515.4		259.87	812.4	
	145.30	548.2				813.5	813.0
		549.0	548.6		273.23	841.1	
	155.94	576.2				842.2	841.7
		575.3	575.7		286.78	869.2	
	169.07	603.9				868.5	868.8
		608.3	606.1	October 1, 1937	299.95	895.6	895.6
October 3, 1937	184.01	643.4		October 3, 1937	300.05	896.7	
		639.4	641.4			895.3	896.0
	200.67	683.1					
		682.1	682.6				

for silver to be 16.1×10^{-6} (12) over the temperature interval 90° to 300°K., the magnitudes of the corrections to viscosity are indicated in table 3. Wire constants were interpolated to the dates at which runs were made, in the manner previously indicated.

Pressures during the runs varied from 500 mm. at 90°K. to 760 mm. at 300°K., except as noted in table 11. An unrecorded run with methane

TABLE 5

Viscosity of air

DATE	T	$\eta \times 10^7$	AVERAGE $\eta \times 10^7$	DATE	T	$\eta \times 10^7$	AVERAGE $\eta \times 10^7$
	°K.				°K.		
September 11, 1937	90.22	645.4		October 11, 1937	215.23	1424.4	
		644.3				1423.5	
		646.7	645.5			1420.9	1422.9
October 10, 1937	90.28	646.1			230.52	1503.7	
		645.6	645.9			1502.7	1503.2
September 16, 1937	118.40	835.7		October 11, 1937	245.61	1584.4	
		834.4	835.0			1584.6	1584.5
	132.78	928.7			260.35	1655.4	
		929.8	929.3			1665.9	
						1662.0	1661.1
	146.19	1011.4					
		1010.3	1010.9	October 12, 1937	273.29	1725.9	
						1724.0	
	160.89	1110.2				1722.8	1724.2
		1099.4					
		1113.0	1107.5		284.60	1776.6	
						1778.4	1777.5
October 11, 1937	183.27	1235.3					
		1244.1			300.12	1851.3	
		1239.9				1851.0	
		1235.2	1238.6			1854.0	
						1849.2	1851.4
	201.59	1346.0					
		1347.8					
		1343.9	1345.9				

at 90°K. (suspension I) and a pressure of 78 mm. likewise showed no sensible dependence on the pressure. Sutherland and Maass (25) and van Itterbeek (27) have found viscosities to be independent of pressure over much wider limits.

Measurements on carbon dioxide were taken with suspension I. At the time of these measurements variations of the wire constant with time were unsuspected. However, several runs on air were taken just prior to the runs with carbon dioxide and several runs with methane were made just after the carbon dioxide runs. Comparison with the later data obtained on air and on methane, with suspension II, permitted evaluation of the wire constant values in the earlier runs and, by interpolation, the value of the wire constant during the carbon dioxide runs. The results obtained were consistent with the direct measurements recorded in table 1 and the character of variations with time and treatment revealed in figure 2. An apparatus constant was determined at the time of the carbon dioxide runs through calibration with air at 296°K. On account of this indirect manner of evaluating the wire constant for the carbon dioxide runs, the data are slightly less accurate than were obtained with the other gases. However, the added uncertainty from this source of error should not exceed 0.1 of 1 per cent.

TABLE 6

Viscosity of oxygen

DATE	T	$\eta \times 10^7$	AVERAGE $\eta \times 10^7$	DATE	T	$\eta \times 10^7$	AVERAGE $\eta \times 10^7$
	°K.				°K.		
September 13, 1937	90.28	692.7		September 14, 1937	215.17	1573.9	
		692.7	692.7			1573.5	1573.7
September 15, 1937	118.81	908.3			229.94	1666.4	
		909.6				1663.4	1664.9
		907.8	908.6				
					245.13	1756.7	
	131.29	998.0				1762.3	1759.5
		1000.5	999.4				
					260.11	1847.1	
September 15, 1937	144.94	1099.9				1846.6	1846.9
September 16, 1937		1098.3					
		1097.7	1098.6		273.16	1916.5	
						1918.9	
September 13, 1937	158.46	1185.6				1919.6	1918.4
		1184.3	1185.0				
					285.16	1988.5	
September 14, 1937	172.56	1286.4				1987.5	1888.0
		1290.1	1288.2				
				September 12, 1937	300.02	2071.9	
	184.61	1373.2				2070.7	2071.2
		1374.9	1374.0				
				September 14, 1937	300.05	2070.4	
	201.49	1483.4				2070.5	2070.5
		1483.5	1483.5				

Table 13 gives smoothed values of the viscosities read at 10° intervals from large-scale graphs.

ACCURACY OF RESULTS

The average deviation of two hundred and fifty-seven experimental points from the smooth curves of figure 3 is ± 0.13 per cent. The precision is somewhat less at low than at high temperatures. One hundred and three points below 200°K. deviate from the smooth curves by ± 0.17 per cent, whereas one hundred and fifty-four points above that temperature possess an average deviation of ± 0.10 per cent.

TABLE 7

Viscosity of nitrogen

DATE	T	$\eta \times 10^7$	AVERAGE $\eta \times 10^7$
	°K.		
September 18, 1937	90.17	631.9	
		630.9	
		631.5	631.4
September 17, 1937	118.26	817.5	
		815.4	816.4
	130.82	890.8	
		894.0	892.4
	140.98	954.1	
		955.6	954.7
	155.56	1039.7	
		1046.0	
		1039.9	1041.8
	169.4	1121.7	
		1120.2	
		1124.7	1122.5
September 19, 1937	184.72	1209.1	
		1210.9	1210.0
	200.16	1295.2	
		1301.2	1298.2

DATE	T	$\eta \times 10^7$	AVERAGE $\eta \times 10^7$
	°K.		
September 19, 1937	215.75	1381.0	
		1380.6	1380.8
	229.88	1451.9	
		1455.0	1453.5
	245.19	1532.1	
		1530.6	1531.3
	260.13	1603.4	
		1602.5	1603.0
	273.21	1664.6	
		1664.2	
		1666.3	1665.0
September 20, 1937	285.08	1718.3	
		1720.6	1719.5
	300.05	1785.1	
		1783.8	
		1785.8	1784.9
September 18, 1937	300.07	1788.4	
		1785.5	1787.0

The following systematic errors are considered:

1. *Temperature scale.* Our temperature scale is believed to be accurate to ± 0.05° over the range covered. An error of 0.05° at 296°K. would introduce an error of 0.013 per cent into determinations of the apparatus

TABLE 8

Viscosity of nitric oxide

DATE	T	$\eta \times 10^7$	AVERAGE $\eta \times 10^7$	DATE	T	$\eta \times 10^7$	AVERAGE $\eta \times 10^7$
	°K.				°K.		
October 6, 1937	118.95	836.2		September 21, 1937	230.03	1552.7	
		836.3				1552.6	1552.6
		835.8	836.1				
					245.18	1636.9	
	133.71	936.9	936.9			1636.5	1636.7
	134.55	945.4	945.4		260.03	1723.4	
						1726.7	1725.1
	143.05	1002.3					
		1004.0	1003.2		273.16	1793.2	
						1789.2	
	157.08	1097.3				1787.6	1790.0
		1097.9	1097.6				
				September 22, 1937	285.33	1856.9	
	170.21	1183.3				1853.2	1855.0
		1182.1	1182.7				
				September 21, 1937	300.12	1936.8	
September 21, 1937	184.04	1270.8				1933.5	
		1271.8	1271.3			1933.8	1934.7
	200.86	1375.1		September 22, 1937	300.17	1935.1	
		1375.8	1375.5			1935.4	1935.2
	215.72	1466.7					
		1468.2	1467.4				

TABLE 9

Viscosity of nitrous oxide

DATE	T	$\eta \times 10^7$	AVERAGE $\eta \times 10^7$	DATE	T	$\eta \times 10^7$	AVERAGE $\eta \times 10^7$
	°K.				°K.		
September 24, 1937	185.20	923.0		September 25, 1937	259.97	1293.9	
		926.3				1295.8	1294.8
		923.5	924.3				
					273.28	1362.6	
September 25, 1937	201.17	1013.1				1361.5	
		993.4				1361.0	1361.6
		1012.2	1006.2				
					285.77	1422.2	
	215.54	1075.7				1420.6	1421.4
		1077.4	1076.6				
					300.10	1488.0	
	229.94	1150.1				1490.2	1489.1
		1147.3	1148.7				
				September 24, 1937	300.15	1490.2	
	245.00	1217.4				1489.1	1489.7
		1219.8	1218.6				

TABLE 10

Viscosity of methane

DATE	T	$\eta \times 10^7$	AVERAGE $\eta \times 10^7$	DATE	T	$\eta \times 10^7$	AVERAGE $\eta \times 10^7$
	°K.				°K.		
October 8, 1937	90.39	366.8		October 8, 1937	200.06	775.5	
		367.1	367.0			775.9	775.7
October 7, 1937	118.63	471.6			215.48	835.9	
		472.8				836.0	836.0
		473.8	472.7				
					231.24	888.5	
	132.40	524.5				889.9	889.2
		525.6	525.0				
					246.10	939.2	
	146.19	578.2				939.4	939.3
		576.9	577.5				
					260.05	985.8	
	157.45	619.9				987.6	986.7
		619.9	619.9				
					273.18	1029.4	
	170.53	667.7				1030.6	1030.0
		667.4	667.6				
					284.85	1068.5	
	183.13	722.3				1069.0	1068.7
		714.1					
		714.9	717.1		300.00	1116.2	
						1116.4	
						1116.1	1116.2

TABLE 11

GAS	P	T	$\eta \times 10^7$
	mm.	°K.	
Hydrogen.	154	299.93	893.4
			894.0
	363	299.95	895.8
			893.8
	561	299.93	895.3
			895.6
	757	299.95	895.7
Methane	79	300.05	1114.7
			1114.2
	448		1116.1
	758		1116.2
			1116.4

constant and affect all subsequent measurements of viscosity by this same amount. An equal error at a temperature other than 296°K. would introduce errors into the viscosities in proportion to their magnitudes and their temperature coefficients. On a percentage basis the error would be largest for methane at 90°K., where it would amount to 0.052 per cent. For temperatures above 200°K. the error from this source could not exceed 0.025 per cent in the most unfavorable case. In view of the fact that the standard thermocouple is soldered directly to the disk assembly, it does not appear probable that there can be systematic temperature errors in excess of those inherent in the scale.

TABLE 12

Viscosity of carbon dioxide

DATE	T	$\eta \times 10^7$	AVERAGE $\eta \times 10^7$	DATE	T	$\eta \times 10^7$	AVERAGE $\eta \times 10^7$
	°K.				°K.		
August 16, 1937	197.86	1004.3		August 17, 1937	259.76	1302.8	
		1005.4	1004.8			1302.1	1302.5
	198.00	1004.0			273.13	1365.5	
		1006.2				1366.3	
		1007.9	1005.9			1365.3	1365.7
	214.75	1087.8			286.59	1430.5	
		1082.7				1431.9	1431.2
		1087.8	1086.1				
				August 16, 1937	298.44	1486.8	
August 17, 1937	230.17	1161.8				1487.7	1487.4
		1160.6	1161.2				
				August 17, 1937	300.32	1496.0	
	245.08	1231.6				1495.3	
		1233.6	1232.6			1497.8	1496.4

2. *Thermostatic control.* Owing to temperature fluctuation in the course of each run, the temperature assigned to the run on the basis of the thermocouple reading may deviate by a few hundredths of a degree from the true average temperature. Above 150°K. this effect can be 0.05° at most, owing to the excellent behavior of the thermostatic control. Below 150°K. this error may attain 0.1° or 0.2° for certain runs. However, this error would not be systematic in the viscosity runs, but makes its contribution to the average deviations of ± 0.13 per cent referred to above. To the extent to which it may have been present in runs to determine the apparatus constant it would contribute to the systematic errors introduced through this constant. Since the apparatus constant is itself determined as the average of several runs, the systematic error

from this source cannot attain the full 0.013 per cent characteristic of a temperature error of 0.05°.

3. Timing. Absolute errors, as in the accuracy of the stop watch, cancel out between the calibration against air (the apparatus constant) and the viscosity runs. Chance errors from this source are small (± 0.2 sec. in 500 to 600 sec.), but may contribute 0.04 per cent to the apparatus constant through the calibration runs.

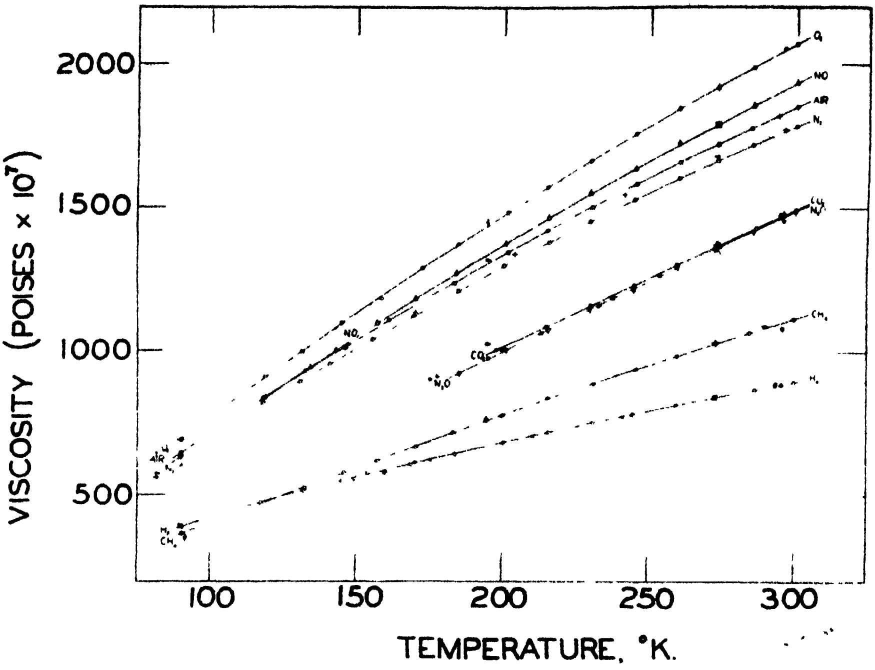

Fig. 3. Viscosity-temperature curves

ϙόο		This research			
+	Air	Sutherland and Maass	×	N_2O	Vogel
*	CO_2	Sutherland and Maass	♦	H_2	Yen
x	H_2	Sutherland and Maass	□	O_2	Yen
●	H_2	Kamerlingh Onnes, Dorsam,	-♦-	N_2	Yen
		and Weber	-o-	CH_4	Rankine and Smith
●-	Air	Vogel	♥	CH_4	Ishida
+	O_2	Vogel	▽	N_2O	Ishida
-●	N_2	Vogel	♦	CO_2	van Dyke; Ishida
ϙ	CH_4	Vogel	-+-	O_2	van Itterbeek and Keesom
o-	CO_2	Vogel	△	N_2	van Itterbeek and Keesom
⋈	NO	Vogel			

4. Scale readings. The amplitude of the scale readings averaged from 500 to 600 mm., and the scale was clearly readable with an accuracy of

0.1 or 0.2 mm. Ten such readings comprised a run. If it is assumed that the chance of making the readings in such a way that the errors cancel is equal to the chance that they are cumulative, there will be an error contribution of only 0.04 per cent in a determination of the apparatus constant.

TABLE 13

Smoothed values for the viscosities

T	HYDROGEN	AIR	OXYGEN	NITROGEN	METHANE	NITRIC OXIDE	NITROUS OXIDE	CARBON DIOXIDE
°*K*.								
90.0	390.2	644.1	691.2	629.8	364.9			
100.0	421.2	712.6	767.5	697.5	402.8			
110.0	451.5	780.2	842.8	763.1	440.7			
120.0	480.5	846.0	916.5	826.4	478.3	843.6		
130.0	508.1	910.6	999.2	887.6	516.0	912.7		
140.0	534.5	975.1	1060.9	948.4	559.7	981.4		
150.0	560.3	1037.1	1131.6	1008.3	591.4	1048.8		
160.0	585.4	1100.5	1201.9	1067.6	628.9	1115.0		
170.0	609.8	1161.3	1271.7	1125.3	666.1	1180.8		
180.0	634.0	1220.8	1340.6	1182.9	703.1	1244.9	898.2	
190.0	657.5	1279.2	1408.6	1239.4	740.6	1308.6	948.6	966.0
200.0	680.9	1336.4	1475.8	1295.4	777.8	1371.2	998.7	1015.0
210.0	703.9	1392.8	1541.1	1349.9	814.3	1432.9	1048.6	1063.5
220.0	726.7	1448.1	1604.4	1402.9	850.1	1493.0	1098.7	1111.7
230.0	749.1	1503.1	1666.2	1454.7	885.0	1552.0	1148.6	1160.1
240.0	770.7	1555.8	1727.6	1505.2	919.1	1609.7	1197.7	1208.5
250.0	792.5	1607.8	1786.3	1554.7	953.0	1665.9	1247.0	1256.0
260.0	813.8	1658.9	1845.3	1603.1	986.3	1710.7	1296.2	1303.2
270.0	835.0	1708.3	1902.3	1650.2	1019.8	1774.2	1345.1	1351.5
280.0	855.5	1756.4	1958.4	1696.0	1052.5	1837.6	1393.3	1399.6
290.0	875.8	1804.0	2015.3	1741.1	1084.4	1881.4	1441.3	1447.7
296.1	888.1	1833.0	2049.1	1768.4	1103.6	1913.6	1470.2	1476.8
300.0	895.9	1850.9	2070.6	1785.7	1115.9	1934.4	1488.9	1495.1

5. Wire constant. Errors in the wire constant will appear as systematic errors in the data and will enter various measured viscosities in rough inverse proportion to the magnitudes of the viscosities. Further, any error in the measured value will enter both the apparatus constant *C* and the viscosity term ($\lambda - x$) with compensating effect. Thus, for viscosities of close to 1832 × 10^{-7} poises the effect of an equal error in the values of x applied in the evaluation of C and of η will cancel substantially completely. A 1 per cent error in the x applied both to η and to C will produce an error of 0.05 per cent in the viscosity of methane at 90°K. We believe (*cf.* table 1) that our determinations of the wire constant are accurate to within 1 per cent. However, the error in certain of our interpolations of changing wire constant may be double this. A 2 per cent error in the value of x employed in evaluating ($\lambda - x$) in viscosity runs will influence viscosities in the neighborhood of room temperature by about 0.02 per cent and produce the maximum effect on hydrogen or methane at 90°K., where the error could be 0.13 per cent.

6. Apparatus. Systematic errors could be introduced from non-horizontality of the fixed disks, non-perpendicularity of the suspension rod to the movable disk, temperature variations in the relative positions of the movable and fixed disks, and stray magnetic fields. We believe that errors from these sources have been reduced to negligible proportions by the care exercised in constructing and assembling the apparatus. Likewise viscous drag on the mirror and permalloy armatures can be excluded as a source of significant error, because of the small dimensions of these parts.

Accumulation of the systematic errors referred to above can barely exceed 0.3 of 1 per cent in the more unfavorable cases at 90°K. or half this amount at 300°K. There may be in addition to these some residual electrostatic effects, for we are not certain that these were completely eliminated by the shielding. Certain of our runs gave some indication of a trend in the logarithmic decrements which we were able to attribute to no other source. Ordinarily no trouble of this sort was encountered.

With account taken of the chance deviations we believe that, with the exception of carbon dioxide, the inaccuracies in our smoothed values entered in table 13 are no greater than 0.7 of 1 per cent in the most unfavorable case,—that of methane at 90°K.,—and do not exceed 0.3 of 1 per cent in the more favorable values at 300°K. For carbon dioxide the inaccuracy may be somewhat larger, owing to the indirect manner in which the wire constant was evaluated. We estimate that the inaccuracy in this gas may range from 0.4 of 1 per cent at room temperature to 0.8 of 1 per cent at 190°K.

This discussion of error relates to the relative values, with air at 23°C. taken as standard.

COMPARISON WITH VALUES OF OTHER AUTHORS

Figure 3 shows to some extent the agreement between our results and those in the literature. The viscosities of other workers were corrected to $\eta^{\text{air}}_{296.1°} = 1833.0 \times 10^{-7}$ when such correction was indicated. For example, the published values of Sutherland and Maass, which were related to $\eta^{\text{air}}_{296.1°} = 1822.6 \times 10^{-7}$, must be corrected to our standard for any comparison. Likewise, we feel that we are justified in altering the absolute viscosities of Yen (30) for hydrogen, oxygen, and nitrogen and that of Van Dyke (26) for carbon dioxide, since both worked with the apparatus of Harrington (9).

Table 14 shows the excellent agreement thus obtained between our results and those of Yen and of Van Dyke at 296.1°K. and includes also a comparison with results obtained at Leiden (15, 27, 28) on hydrogen and on oxygen at 90°K. and on hydrogen at 293°K. Comparison with the Leiden value for nitrogen at 90°K. shows a considerable discrepancy, as is apparent on the graph. Our own value for nitrogen at 90°K. is more consistent with an interpolation between the values for oxygen and for air.

TABLE 14

Comparison of the results of this research with previously published results

GAS	T	$\eta \times 10^7$ (THIS RESEARCH)	$\eta \times 10^7$ (PUBLISHED)	REFERENCE
	°K.			
Hydrogen	296.1	888.1	887.2	Yen (30)
	293.0	881.8	882.7	van Itterbeek and Claes (28)
	90.2	390.8	389.5	van Itterbeek (27)
	89.4	388.3	387.1	van Itterbeek and Claes (28)
Oxygen.	296.1	2049.1	2054.0	Yen (30)
	90.2	692.7	688	Keesom and van Itterbeek (15)
Nitrogen	296.1	1768.4	1774.8	Yen (30)
Carbon dioxide.	296.1	1476.8	1479.9	Van Dyke (26)

Comparison with the data of Sutherland and Maass is of especial interest, since our apparatus is patterned after theirs. In general our data run higher than theirs. Differences run as much as 2 per cent on some of the low-temperature values. It is unlikely that possible changes in their wire constant could be of sufficient magnitude to account for this. Furthermore, the period of oscillation t for the Sutherland and Maass apparatus exhibited a remarkable consistency, indicating little change in x, whatever its value may have been. It also appears unlikely that so large a discrepancy can be attributed to the temperature scale. It appears probable to us, however, that the temperatures which Sutherland

and Maass measured were not the true gas temperatures but lay above the temperatures of the disk assembly. They measured bath temperatures on an unthermostatted bath. Their observation that "the variation in temperature due to warming up during a run did not exceed 1°C. and at the higher temperatures was much less than this" and our experience that a run requires about 10 min. imply that their bath may have warmed at the rate of about 6° per hour at the lower temperatures. As previously mentioned, we found in our own experience that the temperature of the disk assembly lagged considerably behind that of the bath under these conditions. In one experiment with nitric oxide in our apparatus the bath surrounding the bulb was cooled with dry ice and then allowed to warm for 45 min. At this time readings on the two thermocouples showed the temperature of the bath to be 206.4°K. and that of the disks 205.1°K. In another experiment with air in the apparatus the bath, which had been thermostatted for runs at 230.52°K., was allowed to warm for 1 hr. and 15 min. The bath had then reached a temperature of 232.6°K., and the disks a temperature of 231.4°K. Other experiences with very rapid warming (1° per minute) showed a lag of 7° to 8° in the disk temperatures.

TABLE 15

Differences between the data of Sutherland and Maass and those of this research on a temperature basis

T	GAS	TEMPERATURES OF SUTHERLAND AND MAASS HIGH BY
°K.		*°K.*
240	Air	3
	Hydrogen	1.5
	Carbon dioxide	1.5
200	Air	3
	Hydrogen	1
	Carbon dioxide	2
170	Air	4
	Hydrogen	2
145	Hydrogen	3.5
90	Air	2
	Hydrogen	0

Some confirmation of this explanation is found when the discrepancy between our results and those of Sutherland and Maass are put on a temperature basis. This is shown in table 15 for air, hydrogen, and carbon dioxide. The temperature differences are all of the correct sign to fit this explanation and those for air and carbon dioxide are of the correct order of magnitude to compare with our own observations with nitric oxide and with air. Also, as would be expected because of its higher thermal conductivity, the discrepancies with hydrogen (except for the 145°K. value) are distinctly lower than those with air.

SUMMARY

An apparatus patterned after that of Sutherland and Maass, for accurate measurement of gaseous viscosities, is described. The chief improvements, from the point of improved accuracy, are the introduction of a thermocouple soldered directly to the disk assembly and the use of a thermostatted bath. The introduction of brass springs to hold the fixed disks in place and the removal of the hook and slotted eyelet to the bottom of the suspension wire increase the ease of assembling and operating the apparatus and of making replacement of the suspension wire.

Variations were observed in the wire constant and are attributed to (*1*) work hardening of the metal and (*2*) the influence of glass working adjacent to the apparatus.

Viscosities relative to air at 296.1°K. (1833.0×10^{-7} poises) have been measured for hydrogen, air, oxygen, nitrogen, nitric oxide, nitrous oxide, carbon dioxide, and methane. Viscosities were measured at approximate 10° or 15° intervals from 90°K., or the boiling points of the respective gases, to 300°K. A table of smoothed values, read from large-scale graphs at even 10° intervals, is included. These values are believed accurate to from 0.3 per cent at 300°K. to 0.7 per cent or 0.8 per cent in the most unfavorable cases at low temperatures.

The data are graphed, and comparisons are given with the results by other investigators.

The authors are grateful to Mr. L. H. Booher, who assembled and calibrated the preliminary form of the apparatus; to Professor O. Maass, who kindly communicated details of construction omitted from his publication; to the Bell Telephone Laboratories, which contributed the permalloy needed for shielding; and to Mr. R. B. Leonard, the University glass blower, and Mr. John Betz, the shop technician, for skillful fabrication of the apparatus.

REFERENCES

(1) Banerjea, G. B., and Plattanaik, B.: Z. Physik **110**, 676 (1938).
(2) Bond, W. N.: Nature **137**, 1031 (1936).
(3) Duncan, A. B. F., and Howe, J. P.: J. Chem. Phys. **2**, 851 (1934).
(4) Fortier, A.: Compt. rend. **208**, 506 (1939).

(5) Giauque, W. F., Buffington, R. M., and Schulze, W. A.: J. Am. Chem. Soc. **49**, 2343 (1927).
(6) Giauque, W. F., and Clayton, J. O.: J. Am. Chem. Soc. **55**, 4875 (1933).
(7) Giauque, W. F., and Johnston, H. L.: J. Am. Chem. Soc. **51**, 2300 (1929).
(8) Gunther, P.: Z. physik. Chem. **110**, 626 (1924).
(9) Harrington, E. L.: Nature **8**, 738 (1916); *cf.* also Phys. Rev. **55**, 230 (1939).
(10) Hogg, J. L.: Proc. Am. Acad. Arts Sci. **42**, 115 (1906).
(11) Houston, W. V.: Phys. Rev. **52**, 751 (1937).
(12) *International Critical Tables*, Vol. II, p. 459. McGraw-Hill Book Company, Inc., New York (1926).
(13) Johnston, H. L., and Giauque, W. F.: J. Am. Chem. Soc. **51**, 3194 (1929).
(14) Johnston, H. L., and Weimer, H. R.: J. Am. Chem. Soc. **56**, 625 (1934).
(15) Keesom, W. H., and van Itterbeek, A.: Physica **2**, 97 (1935).
(16) Kellström, G.: Phil. Mag. **23**, 313 (1937).
(17) Latimer, W. M., and Greensfelder, B. S.: J. Am. Chem. Soc. **50**, 2205 (1928).
(18) Long, E. A.: Ph. D. Dissertation, The Ohio State University, 1934.
(19) Maass, O., and Cooper, D. LeB.: Can. J. Research **2**, 388 (1930).
(20) Majumdar, V. D., and Vajifdar, M. B.: Proc. Indian Acad. Sci. **8A**, 171 (1938).
(21) Maxwell, G. C.: Phil. Mag. **19**, 31 (1866); *Collected Works*, Vol. 2, p. 1, Cambridge University Press, London (1890).
(22) Meyers, C. H., and Van Dusen, M. S.: Bur. Standards J. Research **10**, 381 (1933).
(23) Rigden, P. J.: Phil. Mag. **25**, 961 (1938).
(24) Scott, R. B., and Brickwedde, F. G.: Bur. Standards J. Research **6**, 401 (1931).
(25) Sutherland, B. P., and Maass, O.: Can. J. Research **6**, 428 (1932).
(26) Van Dyke: Phys. Rev. **21**, 250 (1923).
(27) van Itterbeek, A.: 7th Intern. Congr. Refrig. (Cong. intern. du froid), 1st Comm. intern. Rapports et Commun., June, 1936, p. 81.
(28) van Itterbeek, A., and Claes, A.: Nature **142**, 793 (1938).
(29) Vogel, H.: Ann. Physik **43**, 1235 (1914).
(30) Yen, K.-L.: Phil. Mag. **38**, 582 (1919).

SYSTEMS OF SODIUM PALMITATE IN ORGANIC LIQUIDS[1]

ROBERT D. VOLD, CHARLES W. LEGGETT, and JAMES W. McBAIN

Department of Chemistry, Stanford University, California

Received July 3, 1940

The present work was undertaken as the first step in a systematic survey of the phase rule behavior of soaps in organic solvents.[2] This report includes the determination of solubility curves of anhydrous sodium palmitate in glycerol, diethylene glycol, Nujol, *n*-heptane, isopropyl alcohol, and palmitic acid, and a few observations with carbon tetrachloride. The different systems are characterized with respect to their appearance and nature at different temperatures, and an effort is made to correlate the type of solubility curve obtained, and the presence or absence of certain phases, with the physicochemical characteristics of the different solvents. The observed phenomena are interpreted for the most part in terms of the occurrence of a number of phase changes rather than by means of the less precise concepts of swelling and gel formation.

---

[1] Presented at the Seventeenth Colloid Symposium, held at Ann Arbor, Michigan, June 6–8, 1940.

[2] For previous work on sodium soaps and organic liquids see references 3, 11, 13, 6, 10, 1, 4, 18, and 22.

In the aqueous soap systems which have been extensively studied, both as to phase rule behavior (8, 15, 19, 20) and colloidal nature of the solutions (7), simple ions and other charged particles are always present, and their properties are important in explanations of the stability and behavior of the systems. Since soap in organic liquids forms colloidal systems in many instances in the absence of ions, as shown by the occurrence in these systems of jellies, gels, liquid crystalline phases, and syneresis, the nonionic factors must be emphasized in explaining the observed phenomena. Technically, systems containing soaps and organic liquids are important in such products as greases, shaving creams, and dry cleaning fluids.

TECHNIQUE

The technique employed in this work was very similar to that previously used in the study of aqueous systems (19, 9). Systems of any desired composition were prepared by weighing out the requisite amount of soap and solvent into thick-walled Pyrex tubes, taking care to prevent ingress of water by using containers protected by calcium chloride tubes. These tubes were then sealed and heated in a small electric oven until the contents were completely melted to a homogeneous isotropic liquid. They were then cooled slowly, being watched between crossed polaroids, until anisotropic material first began to form, this temperature being noted and designated as T_i. With more dilute systems, where some kind of waxy material was the separating phase rather than translucent liquid crystal, it was necessary to determine the temperature of the phase boundary by slow heating, or by allowing the system to stand successively at each of several increasing temperatures, since results obtained on cooling are frequently erroneously low, owing to undercooling. These values are referred to as T_w. Many of the systems contained a small amount of an insoluble flocculent white precipitate (possibly an impurity of sodium carbonate in the soap), which sometimes tended to obscure the end point.

A few additional phase boundaries were determined in the glycerol system. Close inspection as the temperature was slowly raised located the temperature at which concentrated systems changed from opaque waxy material to translucent liquid crystal, designated as the T_w curve in figure 3. Some systems involving "superneat soap," located under the hump in the T_i curve, separated into two layers on standing, liquid crystal on top and isotropic liquid on the bottom, thereby permitting approximate calculation of the compositions of the equilibrium phases from the relative volumes of the layers and the known total composition of the system. With four different tubes, the calculated composition of the liquid crystalline phase agreed within 3 per cent, well within the uncertainty of the relatively crude method employed, showing that the phase rule applies to the system in its conventional form, there being no effect on the equilibrium of changes in the concentration or in the absolute amount of systems whose compositions fall on the same tie line.

All systems were examined as they cooled from isotropic solution to room temperature, and an effort was made to detect any changes in appearance. Although these observations were not made sufficiently carefully to determine transition temperatures, even assuming the changes in appearance would be marked enough to make this possible, they do suffice to give a qualitative picture of the phenomena which occur on cooling.

The appearance of all systems was also noted after various lengths of time at room temperatures and was found to remain essentially unchanged. Since these observations were made on 5-g. systems, in 12-mm. diameter glass tubes, cooled from isotropic solution to room temperature in about half an hour, it is possible that undercooling or suspended transformation may have occurred in some instances. Larger samples, cooled more slowly, consequently might not always have the same appearance. The slight color of the systems may be due to their exposure to high temperatures.

MATERIALS

The sodium palmitate was the same preparation used in previous work (21). It was dried for 1 hr. at 105°C., before use.

The glycerol was a Baker and Adamson product of reagent quality; it was twice distilled under vacuum from barium oxide, only the central portion being kept; $n_D^{20°}$ for the glycerol = 1.4735.

The diethylene glycol was of the Eastman Kodak Company's best quality; it was twice distilled under vacuum, and only the central portion, $n_D^{20°} = 1.4472$, was retained.

Nujol, a medicinal paraffin oil produced under carefully controlled specifications, was the usual commercial product obtained at drug stores. It was used without purification.

The palmitic acid was Kahlbaum's best product and melted at 62.6°C. It was dried for 5 days over phosphorus pentoxide.

The isopropyl alcohol was an especially pure preparation obtained from the Shell Development Company of Emeryville, California. It was dried for 4 days with calcium oxide before use.

The *n*-heptane was of the Eastman Kodak Company's better quality, and was used without further purification.

The carbon tetrachloride was a Merck c.p. product. It was distilled before use, the central portion being retained; $n_D^{20°} = 1.4607$.

RESULTS

Appearance

Above 85 to 90 per cent soap all systems, regardless of the nature of the solvent, act rather like pure sodium palmitate. The isotropic solutions are slightly yellow and flow like a medium engine oil. The phase which forms first on cooling is a translucent liquid crystalline material, very bright between crossed polaroids, with a "wavy" elongated cellular structure resembling anhydrous neat soap. On further cooling, the systems become somewhat more opaque, having a rather waxy appearance. At lower temperatures they become entirely opaque and form a hard, nearly white mass which shrinks away from the glass walls of the tube. Although the phase changes known to occur in anhydrous sodium palmitate must persist to a certain extent into the binary systems, the present observations are inadequate to indicate their presence or absence.

The changes observed on cooling more dilute systems differ considerably from solvent to solvent. In general, the viscosity of the *isotropic* solutions (containing up to about 60 per cent soap) is not markedly greater than that of the solvents. The foaming power of the different solutions decreases in the order water, glycerol, diethylene glycol, isopropyl alcohol, Nujol, and heptane, being marked for water, slight for glycerol, and nearly absent for the others.

Usually the phase first formed on cooling systems containing less than 30 per cent soap is semi-translucent, anisotropic, soft, waxy material, somewhat resembling softened paraffin. On further cooling this changes first to a more opaque, less gray, harder wax-like aggregate, and finally to a very much whiter, more compact, completely opaque solid.

At room temperature the general appearance was rather similar in all the systems, although there were certain characteristic differences from solvent to solvent. Those containing less than about 30 per cent soap are usually anisotropic semi-transparent gels. With glycerol and diethylene glycol they somewhat resemble gelatin jellies, except for a slight yellow color and the absence of visible elasticity. After several months these become less translucent, possibly indicating incipient crystallization. The diethylene glycol gels are considerably less transparent than the glycerol gels. With the other solvents the gels look more like an aging silica gel. There was very extensive syneresis in the case of the Nujol, heptane, and isopropyl alcohol systems, but little or none with other solvents. With increasing concentration the cloudiness increased and the systems became less translucent.

Between 20 to 80 per cent soap the appearance was usually that of a moist wax-like material of uniform consistency (like a solid ointment) in contact with the glass, frequently having imbedded in it patches of harder, drier, whiter material at the higher soap concentrations. Concentrated systems all consist of relatively hard dry lumps which, on jarring, often break apart.

Phenomena near the critical temperature

As the temperature of a heptane system containing up to 36 per cent sodium palmitate approaches the critical temperature of heptane, the system first becomes homogeneous isotropic liquid at the temperature of the T_w curve, and then the solution separates into two immiscible isotropic liquid layers, both containing soap. At a still higher temperature, apparently slightly higher than the critical temperature of pure heptane (267°C.), the upper layer vaporizes but the lower layer apparently remains unchanged.

Solubilities

The quantitative results of this investigation are embodied in figures 1 and 2, which show the solubility curves for each system, giving the temperatures to which any mixture must be heated to obtain a homogeneous isotropic solution. Results on sodium palmitate and water are from McBain, Lazarus, and Pitter (12) and from McBain, Vold, and Frick (14); those with sodium palmitate and palmitic acid at less than 70 per cent soap are from McBain and Field (10). Figure 1 is plotted using weight per cent, since this is more nearly representative of the proportions in these systems than is the more customary mole fraction. A system which is 50 weight per cent soap would have a volume about double that of the solvent therein, even though the mole fraction of the soap is only about 0.05. The data are plotted on a mole fraction basis in figure 2, in order to show the great distortion due to the widely different molecular weights of soap and solvents, and to illustrate the apparent differences in relative solubility relations. The following discussion is in terms of figure 1.

In order to permit a more convenient comparison of the solubilities in the different solvents, values at representative temperatures and compositions are assembled in table 1.

These figures show clearly that at room temperature and even at moderately high temperatures (up to 50°C.) sodium palmitate is only very slightly soluble in any of the solvents here studied. At higher temperatures (100°C.) the differences in solubility are striking. In water and in

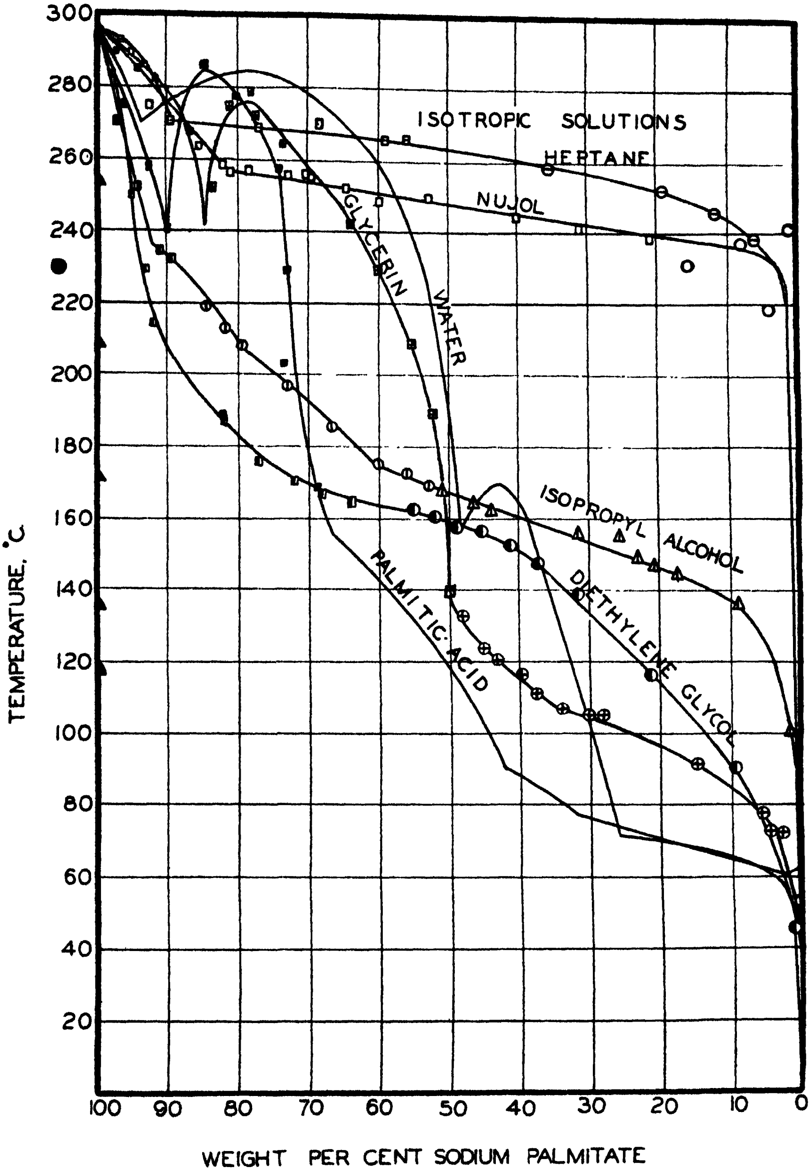

FIG. 1. Solubility curves of sodium palmitate in various solvents. Squares are T_i points; circles are T_w points. ⊟⊖, heptane; □○, Nujol; ◫⦶, isopropyl alcohol; ◧◐, diethylene glycol; ⊞⊕, glycerol; ■●, palmitic acid; ▲, transition temperatures of anhydrous sodium palmitate.

glycerol the solubility is relatively high. The same is true of palmitic acid, as would be expected from the fact that palmitic acid and sodium palmitate tend to react to form various acid soaps (10). The solubility in diethylene glycol and isopropyl alcohol is considerably smaller, while the

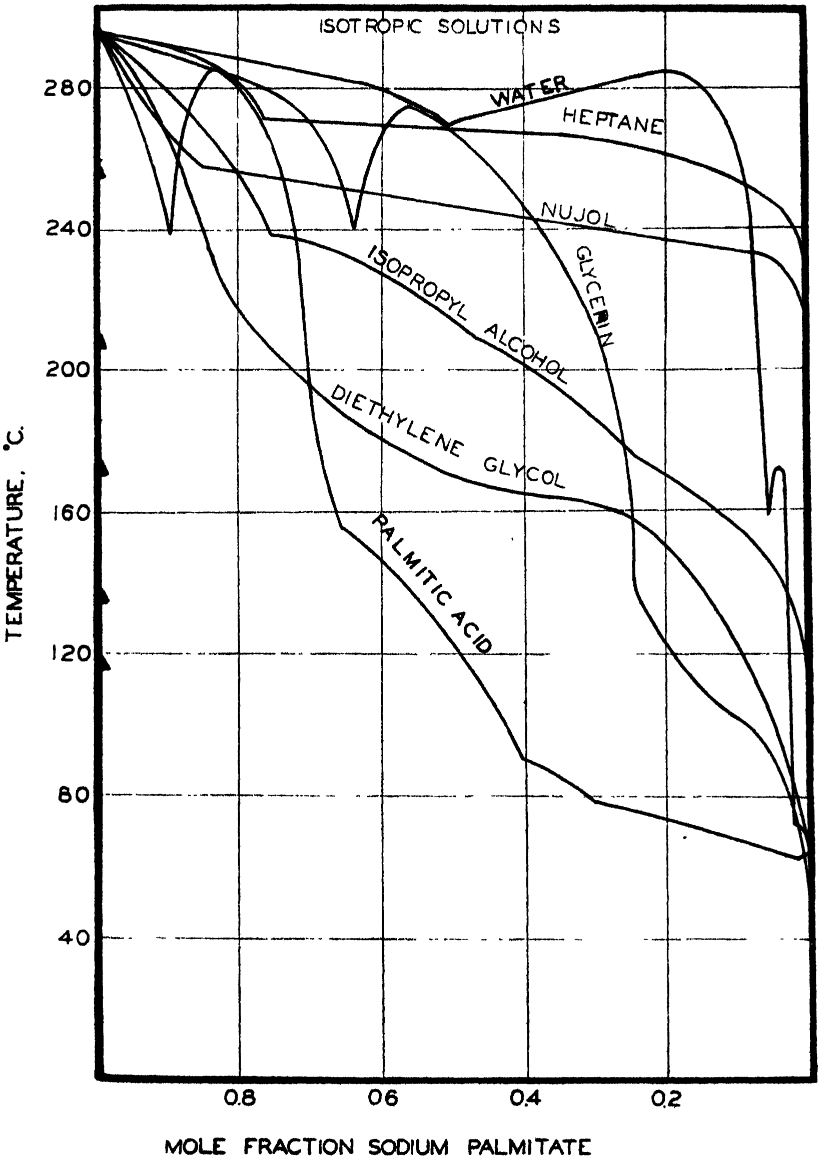

FIG. 2. Solubility curves of sodium palmitate in various solvents. ▲, transition temperatures of anhydrous sodium palmitate.

hydrocarbons Nujol and heptane dissolve so little soap, even at 100°C., that it cannot be accurately determined from the present curves.

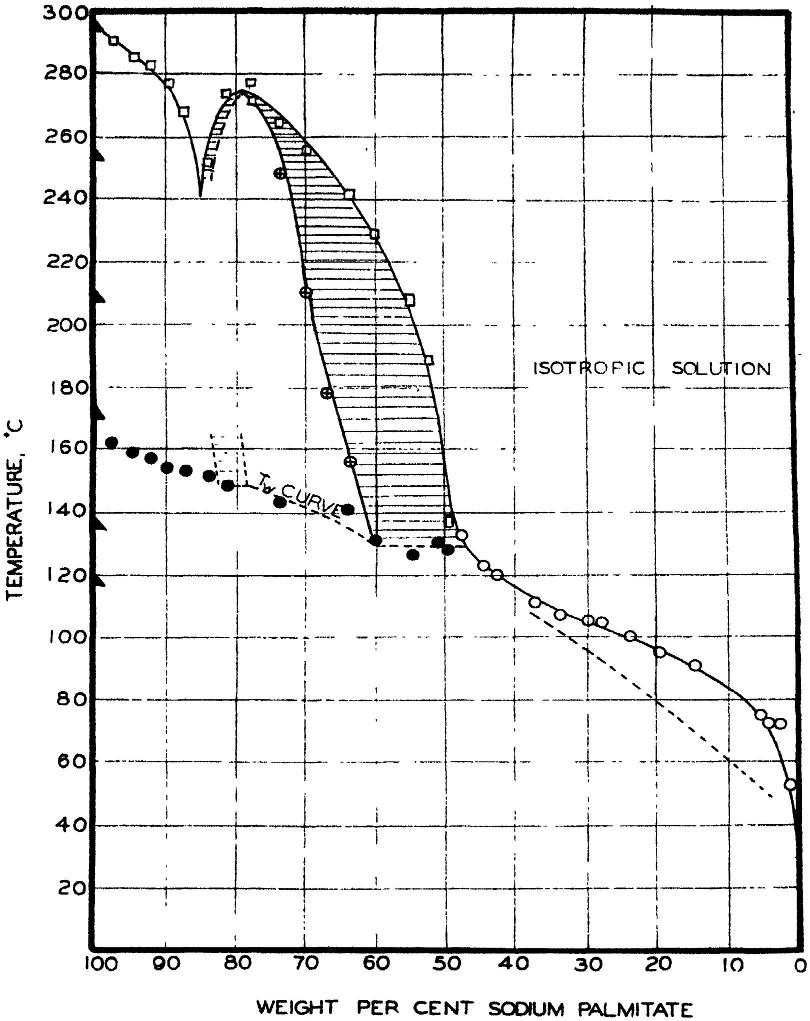

FIG. 3. Phase behavior of sodium palmitate and glycerol.[3] □, T_i; ○, T_w. ●, T_u points on transition to a liquid crystalline phase; ⊕, compositions calculated from the amounts of the separated phases; ▲, transition temperatures of anhydrous sodium palmitate.

---

[3] An additional dotted boundary is shown below the T_w curve with glycerol systems containing from 10 to 40 per cent of sodium palmitate. With sufficiently slow cooling a nearly invisible "honeycomb" structure develops at the upper curve and the material sets to a stiff gel, very faintly anisotropic under the polarizing microscope. On more rapid cooling no change is noted until the lower boundary is reached, at which temperature the formation of translucent, macroscopically anisotropic material occurs. On heating, the systems change only slightly until they become isotropic at the temperature of the upper curve. Three systems were studied dilatometrically and showed changes in slope agreeing within one degree with the full curve. There were also changes in slope at lower temperatures in the vicinity of, but not on, the dotted curve. Samples which stand a few minutes at temperatures between the two curves develop nearly transparent small spherulites, 1 to 4 mm. in diameter, which show dark interference crosses between crossed polaroids.

The same general picture emerges if the values of T_i at a given composition are taken as a measure of the mutual miscibility of the soap with the various solvents. At lower concentrations, mixtures of sodium palmitate with the polar hydroxylic solvents water, glycerol, and diethylene glycol all dissolve to form isotropic solutions below 100°C. Isopropyl alcohol occupies an intermediate position, while very high temperatures are required to bring about solution in the hydrocarbons. At higher soap concentrations the temperatures of formation of isotropic solution are all high and roughly comparable, independent of the solvent, suggesting that in these regions the structure of the liquid crystalline or waxy phase, determined by the soap, is the dominant factor which controls melting’ rather than the constants of the various solvents.

TABLE 1

Solubility of sodium palmitate in various solvents

SYSTEM	SOLUBILITY AT 50°C.	SOLUBILITY AT 100°C.	TEMPERATURE OF FORMATION OF ISOTROPIC SOLUTION WHEN NaP CONCENTRATION IS		
			10 per cent	40 per cent	80 per cent
	weight per cent	*weight per cent*	*°C.*	*°C.*	*°C.*
Sodium palmitate–water	*ca.* 1.0	29.9	66	164	283
Sodium palmitate–palmitic acid	Insoluble	44.5	66	88	278
Sodium palmitate–glycerol	*ca.* 1.0	24.0	84	115	275
Sodium palmitate–diethylene glycol	*ca.* 1.5	13.5	91	151	182
Sodium palmitate–isopropyl alcohol	*ca.* 0.6	*ca.* 1.8	137	160	208
Sodium palmitate–Nujol	Nearly insoluble	Very slightly soluble	236	245	257
Sodium palmitate–heptane	Nearly insoluble	Very slightly soluble	244	260	269
Sodium palmitate–carbon tetrachloride	When the concentration is 8.9 per cent sodium palmitate, T_i = *ca.* 115°C.				

In five out of the seven solvents the solubilities bear no relation to the melting point of palmitic acid, 62.6° C., the so-called Krafft point. Instead, for 10 per cent solution, the temperatures of complete solution range upwards from 66° to 244° C. This and the fact that any correspondence in aqueous solutions is confined only to sodium soaps would seem to rob the Krafft point of any significance except as to a progressive influence of the length of the hydrocarbon chain in an homologous series.

Carbon tetrachloride is in a separate category from the others, since at high temperatures it reacts with sodium palmitate with decomposition and formation of tar.

DISCUSSION

Relation between solubility and the characteristics of the solvents

There is a general correlation between the polarity of the solvents and the solubility of sodium palmitate in them. If the dielectric constant itself is taken as the yardstick, it is evident from examination of the curves of figure 1 and the constants in table 2 that the more polar the liquid the greater its solvent power for sodium palmitate. Thus the solubility curves for heptane and Nujol are at very high temperatures and that of isopropyl alcohol in an intermediate position, while those of water and glycerol are at low temperatures. This dependence of solubility on polarity may be related to the possibility of secondary-valence, non-stoichiometric complex formation between the polar solvent molecules and the dipole of the soap (5), although there is as yet no unambiguous evidence on this point.

TABLE 2

Physicochemical constants of the solvents

SOLVENT	$\Delta E/V$	AT t°C.	μ	ϵ	AT t°C.	μ^2/ϵ	σ IN DYNES PER CM.	AT t°C.
Water	552[e]	20	1.85[a]	80.0[a]	20	0.0428	72.75[f]	20
Oleic acid			1.7[c]	2.45[h]	20	1.18	33.3[e]	
Glycerol	279[f,g]	20		45.8[h]	20		63.14[g]	17
Diethylene glycol	140(?)[g]	245[e]						
Isopropyl alcohol	128[b]	20	1.58[b]	18.6[b]	20	0.134	21.7[b]	20
Nujol				*ca.* 2[j]			33.5[d]	27
Heptane	54.0[a]	25	0[a]	1.97[h]	20	0	*ca.* 20[f]	25
Carbon tetrachloride..	72.9[a]	25	0[a]	2 24[a]	20	0	26.8[f]	20

Approximate values were obtained or calculated from the following sources:

[a] HILDEBRAND, J. H.: *Solubility of Non-electrolytes.* Reinhold Publishing Co., New York (1936).

[b] *Petrohol.* Standard Alcohol Co., New York (1939).

[c] MOLL, W. L. H.: Kolloid-Beihefte **49**, 1 (1939).

[d] McBAIN, M. E. L., AND PERRY, L. H.: J. Am. Chem. Soc. **62**, 989 (1940).

[e] *Handbook of Chemistry and Physics.* Chemical Rubber Publishing Company, Cleveland, Ohio (1936).

[f] LANGE: *Handbook of Chemistry.* Handbook Publishers, Inc., Sandusky, Ohio (1937).

[g] LAWRIE, J. W.: *Glycerol and the Glycols.* Chemical Catalog Company, Inc , New York (1928).

[h] *International Critical Tables,* Vol. VI. McGraw-Hill Book Company, Inc , New York (1929).

[j] *International Critical Tables,* Vol. II. McGraw-Hill Book Company, Inc., New York (1927).

It is interesting that the polarity of the solvents should alone suffice to arrange them in the proper qualitative order with no explicit consideration of the forces acting between solvent and solute molecules or of the forces responsible for the formation of colloidal particles. Perhaps disregard of these factors is one of the reasons for the lack of quantitative correlation.

Palmitic acid and carbon tetrachloride are exceptions, both having low dielectric constants, although they have relatively high solvent power for sodium palmitate. In the case of palmitic acid this must be due to the tendency toward formation of acid soaps at lower temperatures. Carbon tetrachloride also tends to react chemically with sodium palmitate.

The order of solubilities is in accord also with the internal pressures (E/V, where E is the energy of vaporization at constant volume and V the molar volume) of the different solvents, even though some are nonpolar and some have permanent dipoles. Since the solubility is greatest in water and least in heptane, molten sodium palmitate itself must have a relatively high internal pressure.

Moll (16), utilizing concepts of solubility which have been extensively developed for molecular solutions (2), found that, when values of σ (surface tension) and μ^2/ϵ (the square of the dipole moment divided by the dielectric constant) were used as coördinates, all solvents having an appreciable action for each of such solutes as cellulose derivatives, polyvinyl acetate, rubber, etc., had constants placing them in the same region of the graph. This scheme does not appear to apply in the present instance, there being no apparent regularity between the positions of the various liquids in a μ^2/ϵ *versus* σ plot and the solvent action for sodium palmitate. Also, the solubilities are obviously not governed here by the value of the permanent dipole.

Conclusions from the shape of the solubility curves

It is possible to make some deductions concerning the phases present under the solubility curves from the appearance of the systems together with the shape of the curves themselves. For sodium palmitate and water, for example, the nearly perpendicular change in direction of the solubility curve at 26 per cent soap is caused by the change in the saturation phase from curd fiber to middle soap. The lower of the two maxima in the solubility curve is caused by the existence of the liquid crystalline solution phase, i.e., middle soap, and the higher by another liquid crystalline solution phase, i.e., superneat soap.

Examination of the curves from this point of view shows that water, palmitic acid, and glycerol all have a maximum which indicates the presence, in these three systems, of a phase which may be termed superneat soap. The maximum temperature of existence of the phase in the three cases is 284°, 286°, and 275°C., respectively, indicating an approximately equal thermal stability independent of the solvent, and suggesting that here the structure of the liquid crystalline soap phase is of greater importance than the nature of the solvent.

The ratios of the molal compositions under the superneat maxima in the solubility curves are in rough correspondence with the ratio of the lengths of the solvent molecules, the relative compositions being 1:4.0:22.6 for palmitic acid, glycerol, and water, respectively (the actual values being 0.199, 0.803, and 4.50 moles of solvent per mole of sodium palmitate), while the ratio of the lengths of water, glycerol, and palmitic acid molecules is 1:3.3:10.4 (calculated from atomic radii (17)). This shows that in superneat soap the association between sodium palmitate and solvent cannot be a one-to-one molecular interaction between the dipole of the solvent and the carboxylate group of the soap. Possibly the structure is micellar, the solvent essentially merely filling the interstices between soap aggregates, more of the small molecules being required for this purpose than of the longer molecules.

Only the curve for water exhibits a second maximum attributable to middle soap. It may be significant in this connection that of all the solvents used water is the most polar, has the smallest molecule, and constitutes the most highly ionizing medium.

Ferguson (1) has published a phase rule diagram showing middle soap in anhydrous glycerol, continuous in mixtures with aqueous middle soap. This seemed surprising in view of its apparent absence in the system sodium palmitate-glycerol, even though a sample containing 34.4 per cent sodium palmitate, 32.9 per cent glycerol, and 32.7 per cent water did have a phase having the typical stiffness and relative transparency of aqueous middle soap. Consequently a sample was made up containing 36.1 per cent sodium tallow soap (obtained from the National Oil Products Company) and 63.9 per cent anhydrous glycerol, melted to isotropic liquid, and then placed in a thermostat at 90°C. It was a great deal more turbid than aqueous middle soap and seemed to contain dispersed, yellow-white, soft wax-like material, although according to Ferguson's diagram only middle soap and isotropic liquid should have been present. Likewise a system which should have been homogeneous middle soap (46.6 per cent tallow soap, 53.4 per cent glycerol) had a similar turbid appearance. The discrepancy may be one of degree rather than kind, but it requires further investigation.

The solubility curve of sodium palmitate in isopropyl alcohol has a number of sharp inflections. The changes in the saturation phase responsible for these inflections may be related to phase transitions of the nonsolvated soap, since their temperatures are close to those of the transitions of anhydrous sodium palmitate.

Jellies, gels, and syneresis

For about 10°C. above the solubility curve, Nujol and heptane solutions containing less than about 25 per cent sodium palmitate, although themselves isotropic and flowing freely, flash bright between crossed polaroids when the tube is tapped, thereby demonstrating the existence of a strain anisotropy. Consequently, even though aggregation has not gone far enough to form a firm jelly or to constitute a second phase in the sense of the phase rule, the sodium palmitate molecules or micelles cannot be independent in the solution, but must be associated into some type of loose, ramifying structure.

The solubility curve appears to mark a classical phase change since, on heating, systems change reproducibly at this temperature from anisotropic gel to isotropic liquid. With more dilute systems, values obtained on cooling were generally 5 to 10°C. lower than the curve, but these values were not reproducible, suggesting that the difference is due to simple undercooling. In the case of the more dilute systems the formation of the anisotropic gel immobilizing all the solvent would seem therefore to be due to formation of a second phase in a finely divided form, possibly in more orderly structure, with a large adsorptive surface.

At lower temperatures syneresis occurs, some of the previously immobilized solvent being released. This indicates that there must have been an increase in the average particle size or in the compactness of the structure. Whether this is due to a gradual "ripening" of the aggregate or to further phase changes undergone on cooling, as Lawrence suggests for very dilute Nujol systems (4), cannot be determined without further investigation.

SUMMARY

Solubility curves have been determined over the whole range of temperature and composition for anhydrous sodium palmitate in each of the following solvents: palmitic acid, glycerol, diethylene glycol, isopropyl alcohol, Nujol, and heptane. At sufficiently high temperatures the soap is completely miscible in all proportions with these solvents, but at lower temperatures anisotropic gels, liquid crystalline phases, and wax-like or crystalline phases are formed.

The solubility depends on the internal pressure and polarity of the solvents, higher temperatures being required in general to bring about complete solution in the non-polar than in the polar liquids.

No phase completely analogous to aqueous middle soap was found in any of the organic liquids studied. A phase resembling aqueous superneat soap was found with palmitic acid and glycerol, but not with the less polar solvents.

REFERENCES

(1) FERGUSON, R. H.: Oil & Soap **14**, 115 (1937).
(2) HILDEBRAND, J. H.: *Solubility of Non-Electrolytes*. Reinhold Publishing Corporation, New York (1936).
(3) LAING, M. E.: J. Chem. Soc. **113**, 435 (1918).

(4) LAWRENCE, A. S. C.: Trans. Faraday Soc. **34**, 660 (1938).

(5) LAWRENCE, A. S. C.: Trans. Faraday Soc. **33**, 325 (1937).

(6) LEDERER, E. L.: *Kolloidchemie der Seifen.* Th. Steinkopff, Leipzig (1932).

(7) For references see McBAIN, J. W.: Nature **145**, 702 (1940).

(8) McBAIN, J. W.: In Alexander's *Colloid Chemistry*, Vol. I, Chap. 5. Chemical Catalog Company, Inc., New York (1926).

(9) McBAIN, J. W., BROCK, G. C., VOLD, R. D., AND VOLD, M. J.: J. Am. Chem. Soc. **60**, 1870 (1938).

(10) McBAIN, J. W., AND FIELD, M. C.: J. Chem. Soc. **1933**, 920.

(11) McBAIN, J. W., AND LAING, M. E.: Kolloid-Z. **35**, 18 (1924).

(12) McBAIN, J. W., LAZARUS, L. H., AND PITTER, A. V.: Z. physik. Chem. **A147**, 87 (1930).

(13) McBAIN, J. W., AND McCLATCHIE, W. L.: J. Phys. Chem. **36**, 2567 (1932).

(14) McBAIN, J. W., VOLD, R. D., AND FRICK, M.: J. Phys. Chem. **44**, 1013 (1940).

(15) McBAIN, J. W., VOLD, R. D., AND VOLD, M. J.: J. Am. Chem. Soc. **60**, 1866 (1938).

(16) MOLL, W. L. H.: Kolloid-Beihefte **49**, 1 (1939). This paper also gives numerous references to earlier work of Wo. Ostwald and collaborators.

(17) PAULING, L.: *The Nature of the Chemical Bond.* Cornell University Press, Ithaca, New York (1939).

(18) SMITH, E. L.: J. Phys. Chem. **36**, 2455 (1932).

(19) VOLD, R. D.: J. Phys. Chem. **43**, 1213 (1939).

(20) VOLD, R. D.: Soap and Sanitary Chemicals **16**, 31 (1940).

(21) VOLD, R. D., AND VOLD, M. J.: J. Am. Chem. Soc. **61**, 808 (1939).

(22) WHITBY, G. S.: Colloid Symposium Monograph **4**, 213 (1926).

QUANTITATIVE CAPILLARY LUMINESCENCE ANALYSIS[1]

FRANK E. E. GERMANN AND JAMES W. HENSLEY

Department of Chemistry, University of Colorado, Boulder, Colorado

Received July 3, 1940

Although attempts to determine concentrations by capillary adsorption methods have been made by Holmgren (10) and by Schmidt (21), little has been done along this line in the case of capillary luminescence analysis. Guyot (8) used the term "Quantitative Research" as applied to the determination of color and intensity of fluorescence, and Neugebauer (13) stated that he would publish methods for the determination of concentrations using the methods of capillary fluorescence analysis. This question has also been considered by Eisenbrand (1, 3).

Since the methods of capillary luminescence analysis are known to be valuable in identifying traces of material (4), it seemed worth while to study the quantitative aspects more closely by means of a direct vision fluorometer developed in this laboratory (5). The preparation of reproducible capillarized strips has been the subject of very extensive investigation in the pioneer work of Schoenbein (23) and of Goppelsroeder (6, 7) and in the more recent work of Platz (15), Neugebauer (12), Heinrici (9), and Rojahn (19). The factors involved include the nature of the solvent, the type of paper, the direction of cutting, the depth of immersion, the shape of the container, the concentration of the solution, the quantity of the solution, air currents, temperature, pressure, humidity (or degree of saturation of solvent vapors around the paper and above the solution), and illumination (in the case of photoactive substances).

---

[1] Presented at the Seventeenth Colloid Symposium, held at Ann Arbor, Michigan, June 6–8, 1940.

After studying the characteristics of various papers, including their own fluorescence, it was found that for our work the Carl Schleicher and Schüll paper No. 598 was most suitable. The height to which a given liquid will rise in a given paper depends upon the rate at which the liquid evaporates from the paper. If the container is sealed, the liquid will rise to the top of the paper. By changing the rate of evaporation by suitable means, one may obtain anything from very sharply defined to very broad "washed out" bands, as pointed out by various investigators (15, 18, 22, 14, 17, 18, 20). In one set of experiments the strip of paper was attached to the cork which closed the top of the cylinder, and the bottom was allowed to dip into 0.5 per cent solutions of phenanthrene, pyrene, and colchicine in acetone. When capillarization was allowed to continue in this way at constant temperature for 8 to 10 hr., the liquid rose to the top of the paper and most of the fluorescent material was deposited on the stopper. When capillarization was stopped before the liquid had reached the top, very little liquid had risen in the paper, and the fluorescent bands were faint. With more dilute solutions, the concentration of material in the bands was too low for definite tests.

The aim of the present work was to prepare a series of strips capillarized in a series of concentrations of the same compound or group of compounds in the same solvent in order to determine if there was any relation between concentration and the width, intensity, or position of the band. It was therefore decided to prepare each set of strips simultaneously and thus eliminate differences arising from variable external conditions such as temperature and pressure. Thus the strips in a given series should be comparable, even though they might not necessarily be comparable between sets. The work was carried out in a dark room in which the maximum temperature variation during a 12-hr. period at night was found to be 2°C., provided no one entered the room and the ventilation fan was off. Seven 10 x 40 cm. glass cylinders were used. Uniform 50-cc. glass beakers were placed in the bottom of the cylinders. Ten cubic centimeters of a solution containing 0.00025 g. of phenanthrene in 100 cc. of carbon tetrachloride was placed in each of the seven beakers, and strips were suspended, by means of a support at the top of each cylinder, so as just to touch the bottom of the beakers, the cylinders being left open to the air. Over a period of 8 hr. the solutions were completely absorbed and the solvent had evaporated, leaving the strips dry. Under these conditions all the strips showed the blue fluorescent band of phenanthrene about 17 cm. from the bottom of the paper. The bands were uniform in color and intensity as shown by the fluorometer, the only variation being that the position of the peak of the band showed a maximum shift of about 3 mm. as measured from the bottom of the paper. Strips from different series showed a slightly greater variation. Although every precaution was taken to clean pipets and beakers thoroughly, an occasional strip was found to be entirely different from the rest. However, such occurrences were infrequent, could be easily detected under the ultraviolet lamp, and serve to show the extreme sensitivity of the method.

In making fluorometer measurements, a horizontally placed slit with variable width was used. The length of the slit was thus placed across the 2 cm. width of the paper, which was susceptible to vertical motion. In this work the slit width was adjusted to 5 mm., so that the entire length of the strip was viewed by the photocell in successive sections 2 cm. wide and 0.5 cm. high. Thus the centers of successive areas measured were 0.5 cm. apart. Under these conditions, the sum of the individual galvanometer deflections is proportional to the total fluorescence energy of the entire strip. If the deflection given by the blank paper is subtracted from each reading, then the sum of the residual deflections is proportional to the total fluorescence energy of the adsorbed material on the strip. Rather than calculate the sum of the net ordinates, we may merely obtain the area under the curve, which will also be proportional to the total energy. The advantage of this is that it will not be necessary to take readings on every 0.5 cm., nor will the strips viewed have to be adjacent. They may overlap or, in case the intensity is varying gradually and uniformly along the length, they may be separated by finite intervals. All that is necessary is to know the exact position of the center of the slit from the lower end and to keep the slit width constant. When curves of this nature were plotted for the series of strips produced by the same concentrations, the areas were sensibly constant, although the peak of the band was not always at the same place, as shown in figure 1.

In order to see what possible relation existed between curves of this nature when the concentration was a variable, series of different concentrations of different materials were made up by dilution such that the concentrations varied in the order of 1, 1/2, 1/4, 1/8, 1/16, etc. Thus, starting with a solution containing 0.1 g. of phenyl-alpha-naphthylamine in 100 cc. of acetone, dilutions were made so as to give a series of concentrations of 0.1, 0.05, 0.025, 0.0125, 0.00625, and 0.00312 g. per liter. When filter paper strips were treated as described above with equal volumes of solutions of these concentrations, and fluorometer readings were taken, the series of curves shown in figure 2 was obtained. The areas under these curves increase progressively as the concentration increases, yet it is obvious that, although the area under curve 5 is approximately double the area under curve 6, the area under curve 1 is far from being double that under curve 2. The readings of intensities were made as rapidly as possible after the strips had been permitted to dry in the air and in the dark. Phenyl-alpha-naphthylamine was found to be quite photoactive, and the galvanometer readings fell off rapidly as a given section was being exposed to ultraviolet light. In a short time a distinct darkening of the fluorescence on the exposed area could be detected. When this series was run, no reference standard was used, but readings were made at approximately the same line voltage on the lamp, in order to keep its light intensity constant. As shown by later work, this was not as satisfactory as adjusting the voltage so as to give the same galvanometer reading when a standard barium platinocyanide powder was placed over the slit in front of the fluorometer.

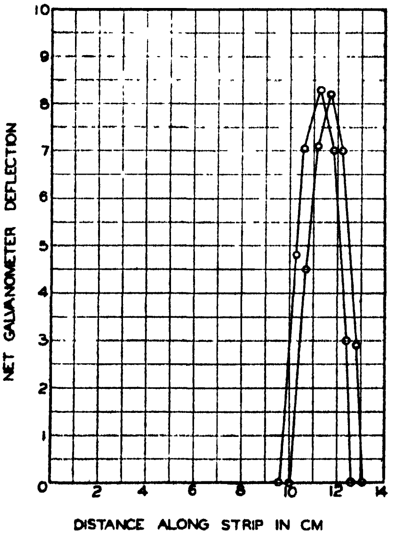

FIG. 1

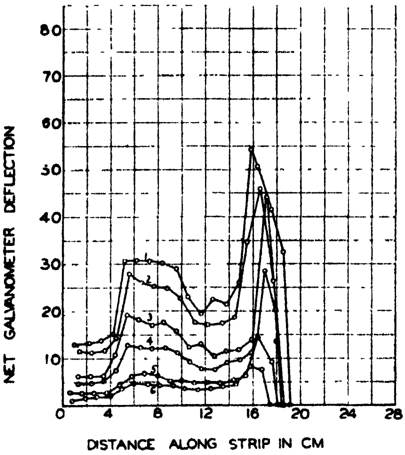

FIG. 2

FIG. 1. Fluorescence intensities along capillary strips prepared from carbon tetrachloride solutions containing 0.00025 g. of phenanthrene per cubic centimeter.

FIG. 2. Fluorescence intensities along capillary strips of phenyl-alpha-naphthylamine series. Acetone solutions. Curve 1, 0.001 g. per cubic centimeter; curve 2, 0.0005 g. per cubic centimeter; curve 3, 0.00025 g. per cubic centimeter; curve 4, 0.000125 g. per cubic centimeter; curve 5, 0.0000625 g. per cubic centimeter; curve 6, 0.0000312 g. per cubic centimeter.

The supposition that the energy of fluorescence will be proportional to the concentration rests on the assumption that all or a definite fraction of the material is exposed to the ultraviolet light. This holds true only on condition that the adsorbed fluorescent material is deposited in a very thin layer of microcrystals. If the crystals tend to become large, then the surface exposed to ultraviolet light is no longer proportional to the concentration. This offers one possible explanation of the area under curve 1 of figure 2 not being double that under curve 2. The nature of the filter paper might easily have an important action in the determination of the grain size, so that a paper might be found which would yield the area ratio desired even for these concentrations. It is, however, obvious that such a relation can be anticipated only for low concentrations or for small amounts of solution in the case of higher concentrations.

Another interesting point in figure 2 is the fact that there are two bands of the same fluorescence color from a solution presumably containing a single compound. Three possible causes for this may be advanced. The first is that the phenyl-alpha-naphthylamine used contained a highly fluorescent impurity. However, a more probable explanation is that the compound oxidized in part on exposure to the air in the presence of the solvent and as a result deposited in two places. Both of these possibilities are being checked at the present time, the latter by performing the experiment in an atmosphere of hydrogen. Other solvents are also being tried to determine what effect they have on the number and position of these bands. A third possibility which presents itself is that the phenyl-alpha-naphthylamine is adsorbed in the lower band, and that the unadsorbed material is carried on by the solvent to the higher point, where precipitation results from more rapid evaporation of solvent or from causes similar to those producing rhythmic precipitation in Liesegang rings.

Pyrene dissolved in acetone acts somewhat like phenyl-alpha-naphthylamine, as is shown in figure 3. In this case most of the fluorescent material is carried to a position near the end of the paper, where it is deposited in a very narrow, bright blue band.

The violet fluorescence band produced by fluorene dissolved in chloroform is shown graphically in figure 4. Although the character of the band is similar to that of pyrene, being deposited far up on the strip, it is nevertheless located somewhat below the capillary limit of the solvent. The small hump to the right of the high peak is the result of the extraction of fluorescent material from the paper and is present in all strips just as it is when pure solvent rises in the paper. It is always located at the upper limit to which the solvent rises. In a number of cases where this band is sharply defined and widely separated from that of the solute, it is not shown in the curves. It has been included, however, in several cases to show its general nature.

Phenanthrene dissolved in acetone yields a single blue fluorescence band. As shown in figure 5, these bands all start at practically the same distance from the base and increase both in width and intensity as the concentration increases. Areas under these curves, as determined with a planimeter, are in the same ratio as the concentrations, showing that in this case, at least in the range of concentrations considered, there is a quantitative relation between the total intensity of fluorescence radiation and the concentration of the original solution.

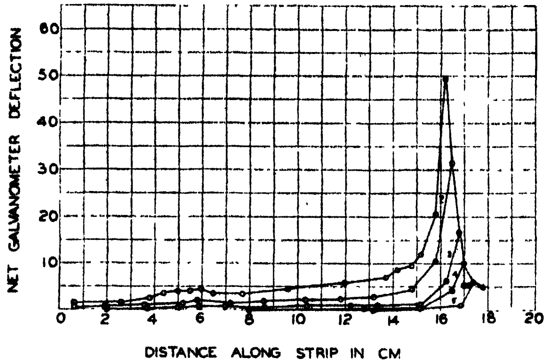

FIG. 3. Fluorescence intensities along capillary strips of pyrene series. Acetone solutions. Curve 1, 0.0008 g. per cubic centimeter; curve 2, 0.0004 g. per cubic centimeter; curve 3, 0.0002 g. per cubic centimeter; curve 4, 0.0001 g. per cubic centimeter; curve 5, 0.00005 g. per cubic centimeter.

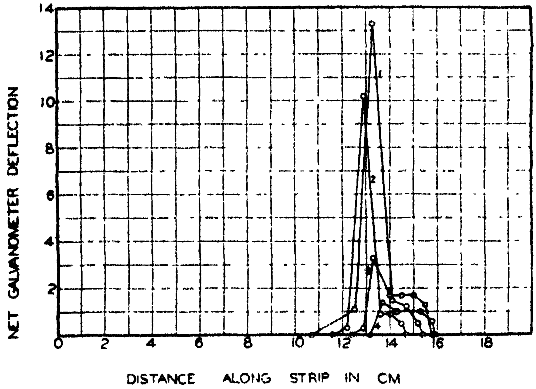

FIG. 4. Fluorescence intensities along capillary strips of fluorene series. Chloroform solutions. Curve 1, 0.008 g. per cubic centimeter; curve 2, 0.004 g. per cubic centimeter; curve 3, 0.002 g. per cubic centimeter; curve 4, 0.001 g. per cubic centimeter.

Salol dissolved in acetone possesses a weaker fluorescence than the materials previously described. Accordingly 20-cc. samples were used in order to obtain higher intensities. The principal band shows a tendency to have two peaks. The peak of rather constant height at the right in figure 6 is again the result of extraction from the paper, and was also obtained when pure acetone was allowed to rise in the paper.

Berberine sulfate shows an intense yellow fluorescence, so that only very low concentrations were necessary to produce brilliant bands. The fact that these bands start with the maximum intensity at the base of the strip, as seen in figure 7, probably can be explained by its very low solubility in chloroform. The narrow band at the right is again the result of the extraction of fluorescent material from the paper by the solvent. Capillary strips made with berberine sulfate are very stable, so that measurements made over a period of weeks showed little decrease in fluorescence intensity.

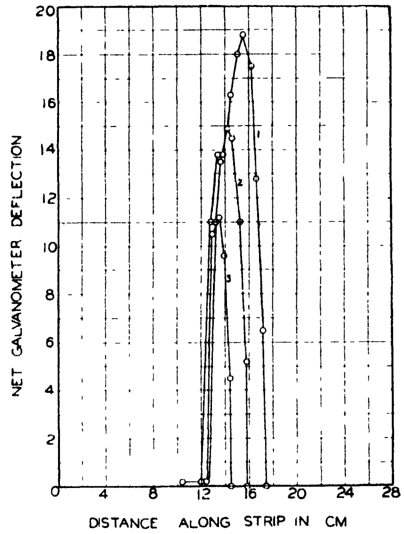

Fig. 5

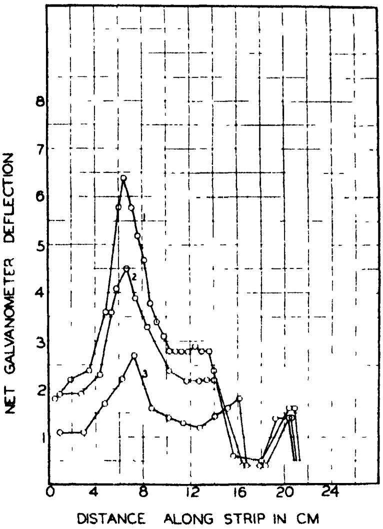

Fig. 6

Fig. 5. Fluorescence intensities along capillary strips of phenanthrene series. Acetone solutions. Curve 1, 0.001 g. per cubic centimeter; curve 2, 0.0005 g per cubic centimeter; curve 3, 0.00025 g. per cubic centimeter.

Fig. 6. Fluorescence intensities along capillary strips of salol series. Acetone solutions. Curve 1, 0.002 g. per cubic centimeter; curve 2, 0.001 g per cubic centimeter; curve 3, 0.0005 g. per cubic centimeter.

Any attempt at a determination of concentrations by capillary luminescence analysis will have to deal with solutions containing, in general, more than one substance in solution. One or more than one of these may fluoresce in filtered ultraviolet light. If the fluorescence bands of several

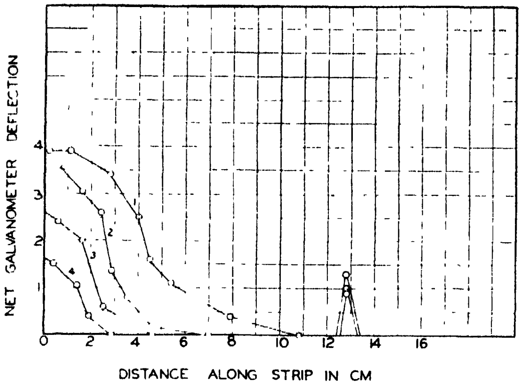

FIG. 7. Fluorescence intensities along capillary strips of berberine sulfate series. Chloroform solutions. Curve 1, 0.0003 g. per cubic centimeter; curve 2, 0.00015 g. per cubic centimeter; curve 3, 0.000075 g. per cubic centimeter; curve 4, 0.000037 g per cubic centimeter.

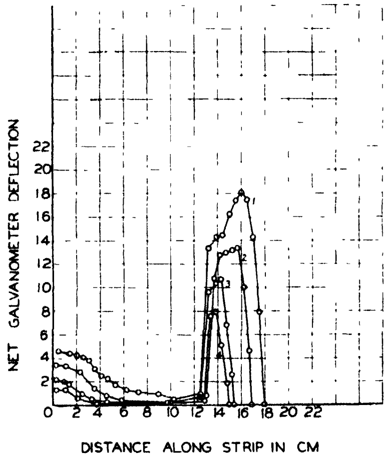

FIG. 8. Fluorescence intensities along capillary strips of phenanthrene-berberine sulfate series. Chloroform solutions.

	PHENANTHRENE	BERBERINE SULFATE
	g. per cc.	*g. per cc.*
Curve 1	0.001	0.00015
Curve 2	0.0005	0.000075
Curve 3	0.00025	0.000037
Curve 4	0.00012	0.000018

constituents overlap, then a spectroscopic resolution of the superimposed bands is probably the simplest method of identifying the individual constituents (13, 16, 2). If, on the other hand, the individual constituents give their characteristic bands in distinct positions on the paper, then the resolution has been accomplished by the very nature of the method.

The latter case frequently presents itself and is shown by figures 8 and 9. When the solution contains two compounds showing widely differing adsorption characteristics, such as phenanthrene and berberine sulfate, then the bands are widely separated and appear practically the same as they do from solutions of the pure constituents. This case is shown for these two substances dissolved in chloroform in figure 8, the concentrations of each being varied in the same proportion. Salol, which gives a band near the center of the capillary area, can be separated from all the other compounds tried which give bands at the top or bottom of the strip. On the other hand, compounds which form bands in approximately the same position can not in general be separated when present in the same solution. Thus pyrene alone gives an intense narrow band at the top of the capillary zone, while phenanthrene gives a wider, less bright band in about the same position. When these two substances were capillarized from the same solution, keeping the concentration of phenanthrene constant and varying the concentration of pyrene, a series of single maximum curves was obtained which might just as well have represented a series of a single component.

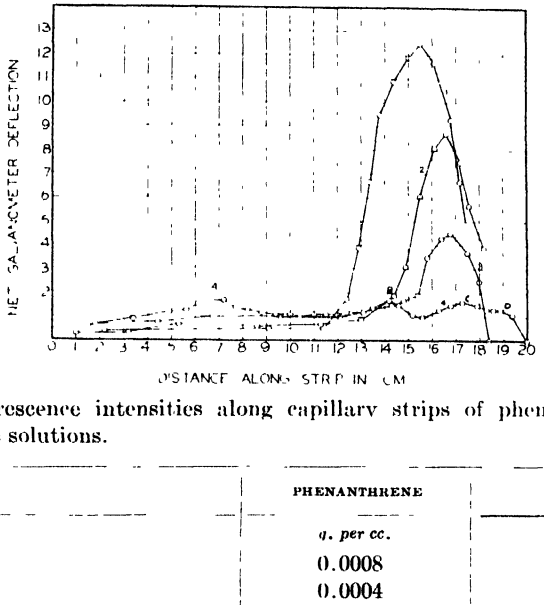

FIG. 9. Fluorescence intensities along capillary strips of phenanthrene-salol series. Acetone solutions.

	PHENANTHRENE	SALOL
	g. per cc.	*g. per cc.*
Curve 1	0.0008	0 0002
Curve 2	0.0004	0 0004
Curve 3	0.0002	0.0008
Curve 4	0.0001	0 0016

Figure 9 represents the results obtained from acetone solutions of salol and phenanthrene. In this series the concentration of phenanthrene was decreased, while that of salol was increased. Here the maxima representing the phenanthrene bands differ from those of the single component by virtue of the addition of intensities of fluorescence of the two components. In curve 4 of figure 9, representing the highest concentration of salol and the lowest of phenanthrene, the two separate maxima of the former are observed at *A* and *B* as in figure 6 for pure salol, where the concentrations were higher than in figure 9. The maximum at point *C* represents the phenanthrene band, and *D* is the band resulting from extraction of the filter paper by the acetone. In curves 1, 2, and 3 this hump was obscured by the intense phenanthrene band.

SUMMARY

The above series of experiments shows the feasibility of the application of the methods of capillary luminescence analysis to the quantitative determination of concentrations, within certain limits, of very dilute solutions of fluorescent substances. The solutions may contain one or more solutes. Although both the width and height of the band increase with increasing concentration, the most reliable measure of concentration is total fluorescence energy, which is proportional to the area under the curves. At higher concentrations the crystals may become so large that the light energy is no longer proportional to the concentration. In this case, the material to be tested may be diluted until concentration is proportional to fluorescence energy. The data obtained by means of our new fluorometer, using a quartz-capillary mercury-vapor lamp and photronic cell, has been shown to be very reliable in making energy measurements in the study of capillary luminescence analysis.

REFERENCES

(1) Danckwortt, P. W., and Eisenbrand, J.: *Lumineszenz-Analyse im filtrierten ultravioletten Licht*, 3rd edition. Akademische Verlagsgesellschaft, Leipzig (1934).
(2) Dhéré, C.: *La Fluorescence in Biochimie.* Les Presses Universitaires de France, Paris (1937).
(3) Eisenbrand, J., and Siewert, G.: Arch. Pharm. **272**, 428 (1934).
(4) Germann, F. E. E.: Univ. Colorado Studies, Series D, **1**, 7 (1940).
(5) Germann, F. E. E., and Hensley, J. W.: Univ. Colorado Studies, Series D, **1**, 37 (1940).
(6) Goppelsroeder, F.: Verhandl. Nat. Forscher-Ges. Basel **19**, 1 (1907); Chem. Zentr. **I**, 760 (1908).
(7) Goppelsroeder, F.: Kolloid-Z. **4**, 23 (1909).
(8) Guyot, M.: Ann. fals. **24**, 196 (1931).
(9) Heinrici, G.: Dissertation, Halle (S), 1932.
(10) Holmgren, J.: Biochem. Z. **14**, 181 (1908); Kolloid-Z. **4**, 219 (1909).

(11) Kreidl, A., and Lenk, E.: Chem. Zentr. **II,** 1272 (1911), Arch. ges. Physiol. (Pflügers) **141,** 541 (1911).
(12) Neugebauer, H.: Pharm. Ztg. **74,** 1511 (1929).
(13) Neugebauer, H.: *Die Kapillar-Lumineszenz Analyse im pharmazeutischen Laboratorium.* Verlag Dr. Willmar Schwabe, Leipzig (1933).
(14) Pfau, E.: Apoth. Ztg. **41,** 133 (1926).
(15) Platz, H.: *Über Kapillaranalyse*, 2nd edition. Verlag Dr. Willmar Schwabe, Leipzig (1922).
(16) Radley, J. A., and Grant, J.: *Fluorescence Analysis in Ultraviolet Light.* Chapman and Hall, Ltd., London (1935).
(17) Rapp: Pharm. Ztg. **73,** 1585 (1928).
(18) Rojahn, C. A.: Pharm. Ztg. **74,** 14 (1929).
(19) Rojahn, C. A., and Hellrung, A.: *Über die Identifizierung der Homoopathie gebrauchten Trockendrogen mit Hilfe chemischer Reaktionen und der Lumineszenz-Kapillaranalyse.* Akademische Verlagsgesellschaft, Halle(S) (1937).
(20) Rojahn, C. A., and Herzog, H.: Pharm. Zentralhalle **73,** 104 (1932).
(21) Schmidt, H.: Kolloid-Z. **13,** 146 (1914); **24,** 49 (1919).
(22) Schmidt, H.: In Liesegang's *Kolloid-chem. Technologie*, p 211. Th. Steinkopff, Dresden-Leipzig (1927).
(23) Schoenbein, C. F.: Trans Soc. Natural Philosophy Basel **3,** (2) 249 55 (1861), **4,** (1) (1864).

AN ELECTRON DIFFRACTION STUDY OF HYDROUS OXIDES AMORPHOUS TO X-RAYS[1]

HARRY B. WEISER and W. O. MILLIGAN

Department of Chemistry, The Rice Institute, Houston, Texas

Received July 3, 1940

In recent years, extended investigations have been carried out at The Rice Institute and elsewhere on the constitution of hydrous oxide gels by means of the simultaneous application of the techniques of x-ray diffraction and of isothermal and isobaric dehydration. The results of these investigations disclose that a large percentage of the precipitated oxides give x-ray diffraction patterns corresponding to a simple oxide or a simple oxide hydrate or hydroxide. It is concluded therefore that, in general, gelatinous precipitates of the oxides are not polymerized bodies or condensation products resulting from the splitting off of water from hypothetical metallic hydroxides. Instead, the gels are believed to consist of agglomerates of extremely minute crystals of oxide or simple hydrate (or hydroxide) which hold large amounts of water by adsorption and capillary forces (9, 14).

---

[1] Presented at the Seventeenth Colloid Symposium, held at Ann Arbor, Michigan, June 6-8, 1940.

A few of the hydrous oxide gels precipitated at room temperature are amorphous to x-rays, that is, they give x-ray diffraction patterns consisting of only one or two broad bands so diffuse that it is impossible to determine their constitution by x-ray analysis. Oxide gels of the following metals fall in this category: iron (Fe^{III}), aluminum (from aluminum sulfate), chromium, beryllium, gallium, yttrium, samarium, titanium, thorium, zirconium, columbium (Cb^{V}), tantalum (Ta^{V}).

Materials which give diffuse x-ray diffraction patterns frequently give electron diffraction patterns consisting of relatively sharp rings, because of the smaller wave length and the greater efficiency of diffraction of electrons. Accordingly, an electron diffraction study has been made of a number of the hydrous oxides which are amorphous to x-rays.

EXPERIMENTAL

General procedure

The procedure consists essentially in passing a beam of electrons through a very thin film of the sample of oxide and recording the position of the diffracted electrons on a photographic plate. A Seemann electron diffraction apparatus was employed, to which was attached a device for adjusting the filament accurately with respect to the focusing cup. The constant-potential high-voltage supply consisted of a 70,000-volt, 10-milliampere, oil-immersed Kenetron rectifying unit operated from an alternator driven by a synchronous motor. High-voltage measurements were made with a 2000-megohm resistance in series with a 0–50 microammeter. The apparatus was calibrated with gold foil in the usual manner.

With satisfactory equipment available, the problem of examining the precipitated oxides with electron waves resolves itself into obtaining films that possess the necessary properties. In the first place, the films must be sufficiently thin so that they will allow electrons accelerated by a potential of 30,000 to 70,000 volts to pass through. In the second place, the films must be sufficiently coherent so that they do not scrunch up on drying to give an open network of agglomerates so thick that they stop the electrons and of cracks through which the electrons pass without diffraction. The sample holder consists of a 300- or 400-mesh stainless-steel gauze. On this is first placed a very thin film of collodion (amyl acetate solution) or resoglas (benzene solution), on which the sample to be examined is subsequently deposited. This is accomplished by making a dilute colloidal suspension in water, placing a drop of the suspension on the supporting film, and allowing it to evaporate. By this procedure films suitable for examination by electrons are readily obtained for such substances as copper ferrocyanide, which is known to give a uniform coherent membrane, and for clays which, because of the plate-like shape of the crystals, give a thin uniform layer. Unfortunately, the property of readily forming a thin coherent film is not possessed by most of the hydrous oxide gels under investigation. In many instances a suitable film has been obtained only after many trials, and in some instances repeated attempts have failed to give a film with the necessary properties.

The brown gel of ferric oxide

The brown gel of hydrous ferric oxide, frequently misnamed ferric hydroxide, is commonly prepared by the addition of a base to a ferric salt. The gel, when freshly formed in the cold and dried in a vacuum, is amorphous to x-rays, but after standing at room temperature in contact with water for several weeks, it gives a band x-ray diffraction pattern corresponding to α-Fe_2O_3 or hematite (11); after several months the crystals have grown until the sample gives a sharp hematite pattern. The growth of the crystals takes place more rapidly at high temperatures. The gel thrown down at 100°C. gives at once a band pattern of α-Fe_2O_3; if maintained a few hours at this temperature, it gives a sharp pattern.

The above observations suggest that the brown gel thrown down in the cold consists of hematite crystals so small or poorly formed that it gives an amorphous x-ray pattern. Examination of this brown gel in the cold by means of electrons disclosed that this was the case. In figure 1 is given the electron diffraction pattern of the fresh gel thrown down at 25°C. from ferric nitrate solution. The rather broad diffraction rings are in the same position as the rings from a hematite sample crystalline to x-rays (*cf.* figures 2 and 6). Baccaredda and Beati (1) were unable to obtain a crystalline-type electron diffraction pattern from precipitated ferric oxide. Fordham and Tyson (3) reported that precipitated ferric oxide prepared by the interaction of ferric chloride and sodium hydroxide solutions gave an electron diffraction pattern corresponding to a cubic lattice with a_0 = 5.70 Å. In figure 3 is shown in diagram form (*a*) the x-ray diffraction pattern of sodium chloride, (*b*) Fordham and Tyson's electron diffraction pattern, and (*c*) an electron diffraction pattern of sodium chloride (sample prepared by evaporating a drop of very dilute sodium chloride solution on a collodion film). It is apparent that the pattern of Fordham and Tyson is from sodium chloride which was not washed out of the ferric oxide gel (*cf.* 1).

The newly formed brown gel thrown down from a cold solution of ferric chloride gives a pure hematite pattern, provided the solution is made up fresh. An old ferric chloride solution contains colloidal β-$Fe_2O_3 \cdot H_2O$ (12), which gives a distinctive electron diffraction pattern (figures 4 and 6). The gel thrown down from an old solution of ferric chloride or from an old sol of ferric oxide peptized by ferric chloride gives an electron diffraction pattern consisting of rings of both α-Fe_2O_3 and β-$Fe_2O_3 \cdot H_2O$ (figures 5

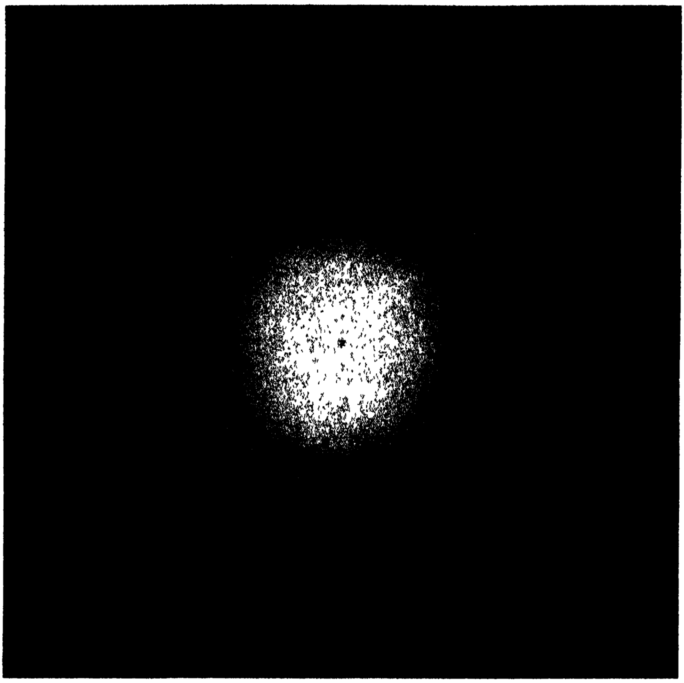

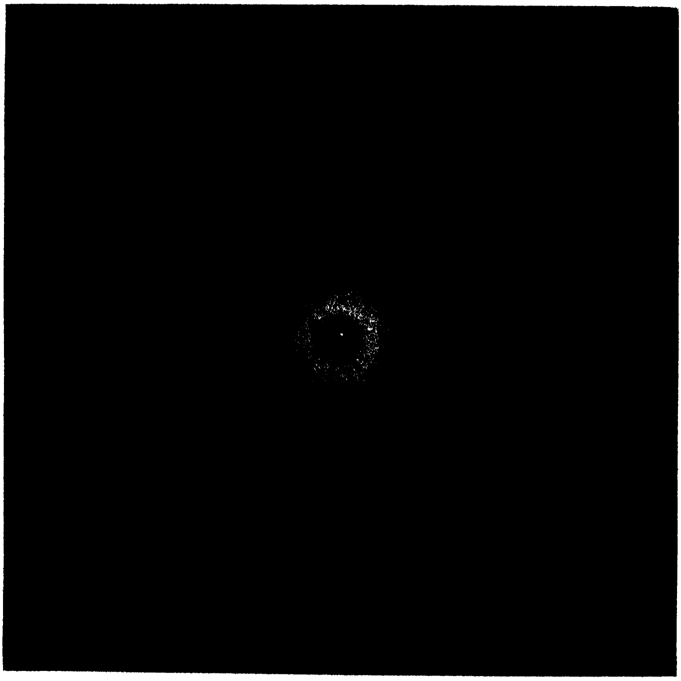

Fig. 1. (left) Electron diffraction pattern of ferric oxide (Fe_2O_3) gel precipitated from the nitrate at 25°C.

Fig. 2. (right) Electron diffraction pattern of ferric oxide (hematite pattern) precipitated from the nitrate at 100°C.

and 6). The electron diffraction patterns of α-FeOOH and γ-FeOOH have been studied by Smith (7).

The oxide gels of aluminum, gallium, and chromium

Alumina. The highly gelatinous precipitates thrown down at room temperature on adding slightly more than the equivalent amount of ammonia to *N*/10 solutions of aluminum salts are crystalline to x-rays, giving the x-ray diffraction pattern of γ-$Al_2O_3 \cdot H_2O$. The crystals are sufficiently large so that the diffraction rings are relatively sharp when the precipitate is thrown down from solutions of aluminum chloride and aluminum nitrate (figure 7, a and b). But samples precipitated from aluminum sulfate solution consist of such minute crystals that they give broad band patterns (figure 7, c). Indeed, the bands are so broad that such samples were identified tentatively as γ-$Al_2O_3 \cdot H_2O$ only because the position of the bands corresponded roughly to that of the sharpest lines in the pattern from the chloride and the nitrate. To establish definitely the constitution of the precipitate from the sulfate, its electron diffraction pattern was obtained (figure 8). It is obvious that the diffraction rings are in the same position as those from an aged sample of γ-$Al_2O_3 \cdot H_2O$ from the chloride (figure 9). The freshly formed precipitate from the sulfate is γ-$Al_2O_3 \cdot H_2O$; the crystals are too small to give a sharp x-ray diffraction pattern, but are large enough to give a sharp electron diffraction pattern.

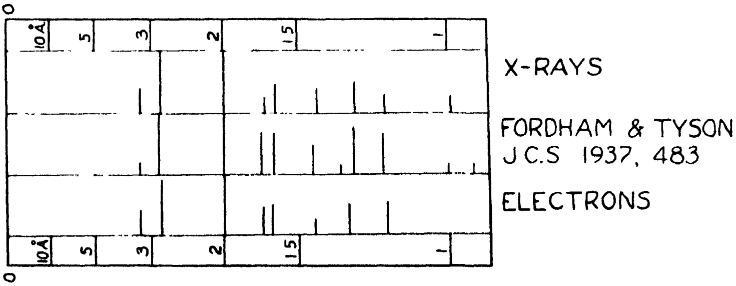

Fig. 3 Electron and x-ray diffraction patterns of sodium chloride

In an earlier paper it was shown that the alumina thrown down at pH 6 to 8 from the highly dilute aluminum sulfate solutions, such as are used in water purification, gives band x-ray diffraction patterns but sharp electron diffraction patterns corresponding to γ-$Al_2O_3 \cdot H_2O$ (15). In accord with earlier x-ray observations (*cf.* 9) γ-$Al_2O_3 \cdot H_2O$, aged in the cold in contact with water, gives an electron diffraction pattern corresponding to α-$Al_2O_3 \cdot 3H_2O$. Baccaredda and Beati (1) have also obtained an α-$Al_2O_3 \cdot 3H_2O$ electron diffraction pattern from an alumina gel.

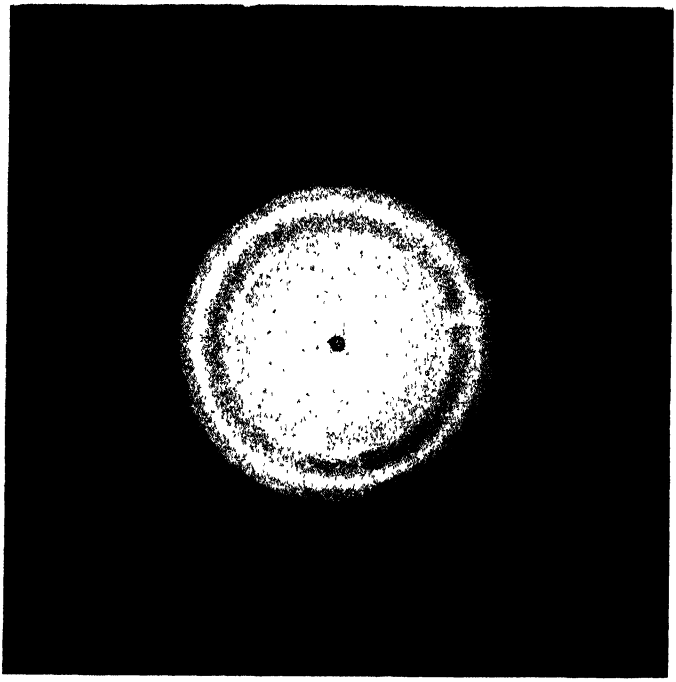

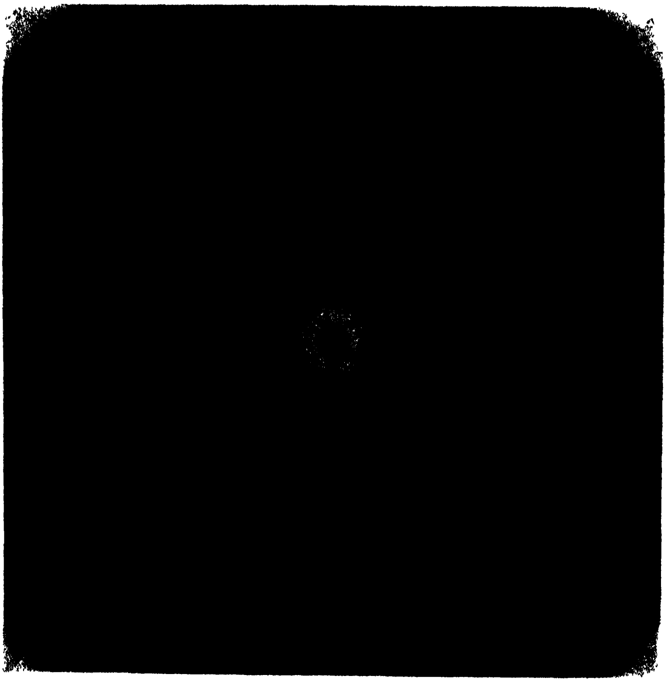

Fig. 4. (left) Electron diffraction pattern of β-FeOOH

Fig. 5. (right) Electron diffraction pattern of the gel thrown down from an aged ferric oxide sol

Gallia. Gallium oxide gel precipitated at 25° or 100°C. from a gallium chloride solution with a slight excess of ammonia gives an x-ray diffraction pattern consisting of two broad but distinct bands. Although in general it is not possible to identify a substance from an x-ray pattern consisting of but two bands, in this instance the position of maximum intensity of the bands corresponded to the position of the two sharp lines in the pattern obtained from relatively large crystals of α-Ga_2O_3 (13). Moreover, heat-treatment of the gel at various temperatures gave additional and sharper

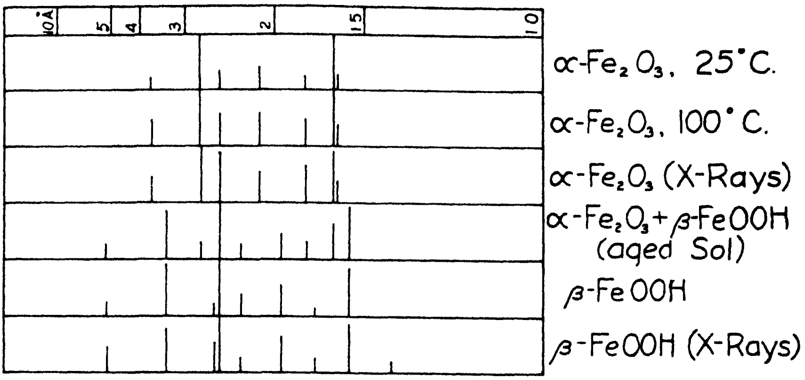

FIG. 6. Electron and x-ray diffraction patterns of ferric oxides

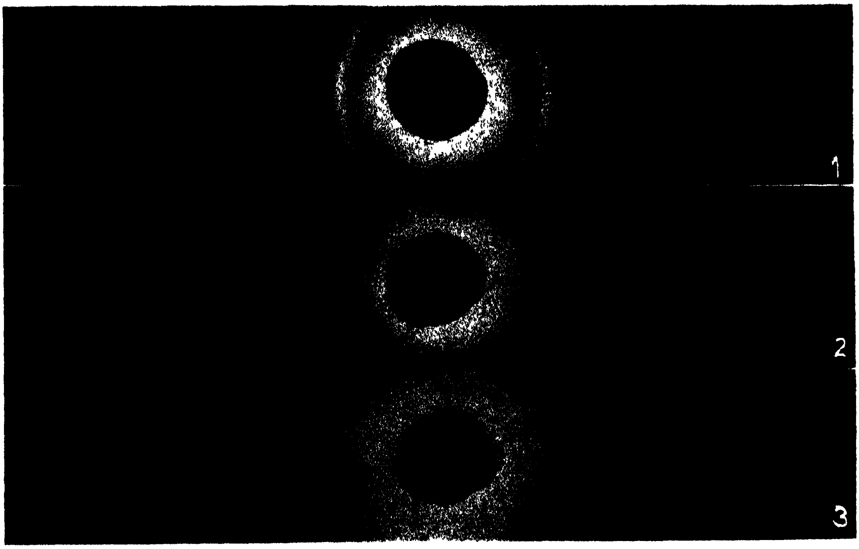

FIG. 7. X-ray diffraction patterns of γ-$Al_2O_3 \cdot H_2O$ from solutions of (1) the nitrate, (2) the chloride, and (3) the sulfate

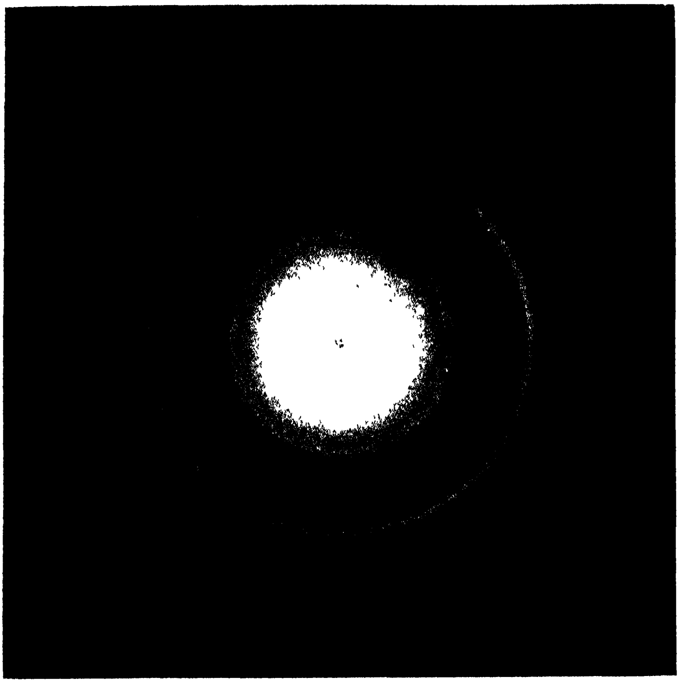

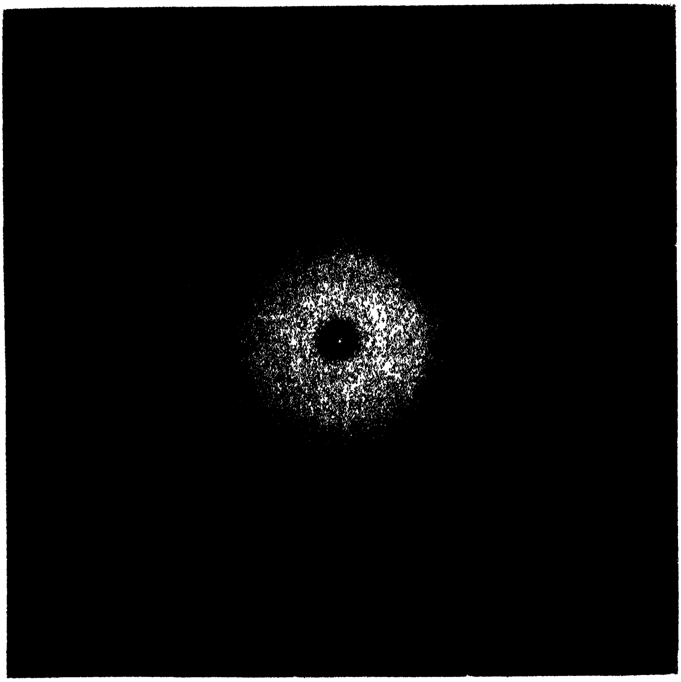

FIG. 8. (left) Electron diffraction pattern of γ-$Al_2O_3 \cdot H_2O$ from aluminum sulfate solution at 25°C.

FIG. 9. (right) Electron diffraction pattern of γ-$Al_2O_3 \cdot H_2O$ (standard sample) diffraction lines corresponding to α-Ga_2O_3. It was inferred (13) from these observations that the fresh gel consisted of minute particles of α-Ga_2O_3, but Laubengayer and Engle (5) question the accuracy of this deduction. Early attempts to get an electron diffraction pattern of the precipitated oxide were without success, since the evaporation of a drop of a dilute suspension of the gel failed to give a film with the necessary properties. The oxide agglomerates into clumps that are either too thick or too porous for examination by electrons. Addition of alcohol to the suspension of hydrous gallia made it possible to obtain a thin uniform film. In figure 10 is given an electron diffraction pattern of hydrous gallia precipitated at 25°C. The rings correspond to the pattern of α-Ga_2O_3 (figure 11), thus confirming our deductions from x-ray diffraction data.

Chromic oxide. The gel formed by the addition of alkali or ammonia to a chromic salt is amorphous to x-rays whether precipitated cold or hot. Moreover, the gel, after being heated for days or weeks in contact with water at the boiling point, gives an amorphous x-ray diffraction pattern. A crystalline type of diffraction pattern results after heating the gel in an autoclave for several hours at 180-250°C. The pattern from the sample heated in an autoclave is that of chromic oxide monohydrate.

The freshly formed gel of chromic oxide is readily peptized, and evaporation of the highly dilute sol gives a film suitable for examination by electrons. The preparation gives an amorphous electron diffraction pattern. We have been unable to confirm Baccaredda and Beati's (1) observation that a chromic oxide gel gives an electron diffraction pattern similar to that of α-$Al_2O_3 \cdot 3H_2O$.

Silica gel

The x-ray diffraction pattern of silica gel thrown down either at room temperature or at 100°C. consists of very broad bands. The precipitated oxide readily forms thin coherent films, which have been examined by electrons. The resulting electron diffraction pattern is definitely of the amorphous type. In accord with this observation Germer and Storks (4) found that a silica film formed by condensation of the vapors gives an electron diffraction pattern characteristic of an amorphous material.

Gels of the pentoxides of columbium and tantalum

The gels of columbium pentoxide and tantalum pentoxide resemble silica gel in appearance and properties (9) and are amorphous to x-rays. To investigate their behavior toward electrons the gels were thrown down from solutions of K_2CbOF_5 and K_2TaF_7, respectively, and were washed thoroughly by the aid of the centrifuge until they peptized. Evaporation of the highly diluted sols gave thin coherent films, which were examined in an electron beam. Like silica, both columbium and tantalum pentoxides give electron diffraction patterns of the broad-band, amorphous type.

The gels of titania, zirconia, and thoria

Titania. The gels of titania, zirconia, and thoria formed from solutions of the respective salts by precipitation with ammonia or alkali at room temperature are alike in being amorphous to x-rays. The dehydration isobars for the respective gels are smooth curves, indicating that the water in the gels is held by adsorption or capillary forces and not in chemical combination.

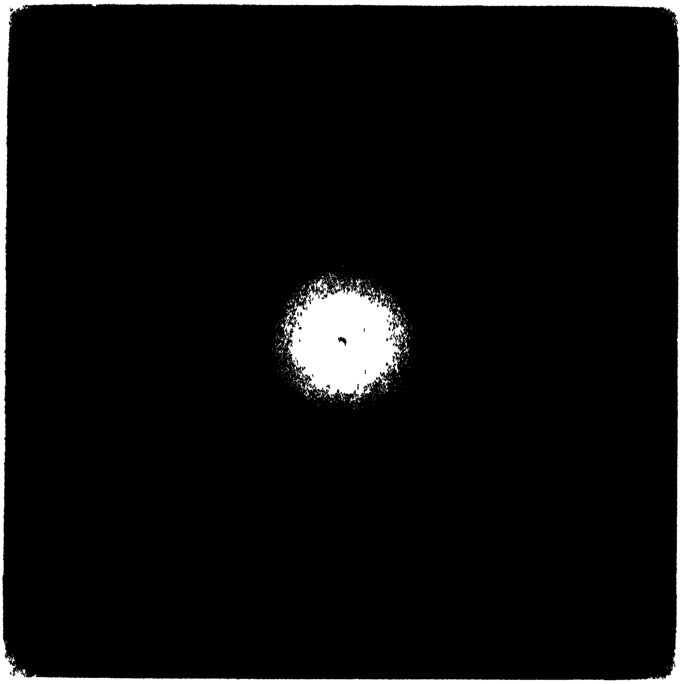

Fig. 10. Electron diffraction pattern of α-Ga_2O_3 gel

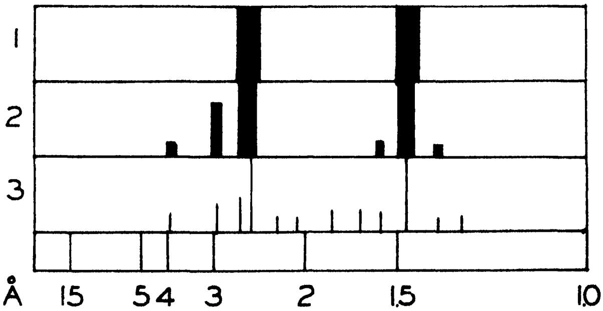

Fig. 11. X-ray and electron diffraction patterns of α-Ga_2O_3: (1) gel precipitated at 100°C (x-rays); (2) gel precipitated at 25°C. (electrons); (3) gel heated to 625°C.

Aging of precipitated titania for 8 months at room temperature or for 8 hr. at 100°C. produces materials that give narrow-band x-ray diffraction

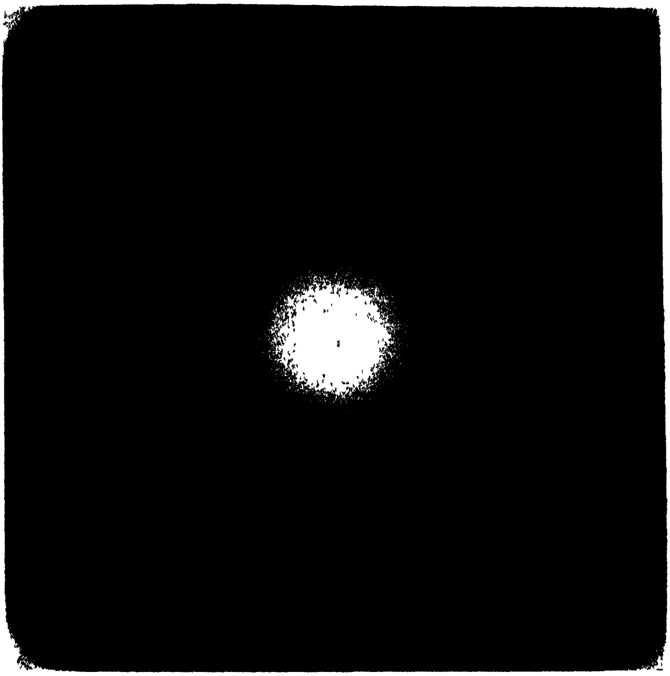

FIG. 12. Electron diffraction pattern of titania gel

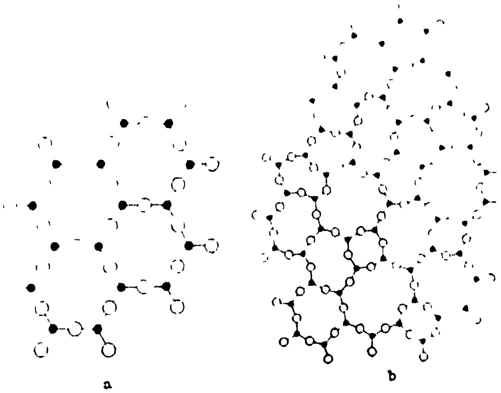

FIG. 13. Structure of two-dimensional crystals (a) and glasses (b) of M_2O_3 (after Zachariasen)

patterns corresponding to the mineral anatase, TiO_2 (10). The electron diffraction pattern of the freshly formed gel (figure 12) shows that it is made up of minute crystals. The pattern corresponds neither to the rutile nor to the anatase modification of titania. The composition of this crystalline material is being investigated further.

The oxide formed by the hydrolysis of titanium chloride or nitrate at 100°C. gives an x-ray pattern corresponding to the rutile modification of titania, whereas the product thrown down by hydrolysis of titanium sulfate gives a pattern corresponding to the anatase modification (10).

Zirconia and thoria. The minute crystals of precipitated zirconia and thoria both grow more slowly than titania crystals. Heating zirconia and thoria gels for several hours at 100°C. in contact with the mother liquor from which they separated produces materials that give broad-band x-ray diffraction patterns corresponding to zirconia and thoria, respectively (2). Because of difficulties in obtaining suitable films of cold precipitated zirconia and thoria, it is uncertain whether they give an amorphous electron diffraction pattern or whether the materials have not been examined.

DISCUSSION

Freshly formed gels of the hydrous oxides which are amorphous to x-rays fall into two classes: those which give electron diffraction patterns characteristic of crystals, and those which give electron diffraction patterns of the amorphous type. In the first class are the oxides of ferric iron, aluminum (from the sulfate), gallium, tetravalent titanium, and probably beryllium, which give relatively sharp ring electron diffraction patterns; in the second class are the oxides of chromium, silicon, pentavalent columbium, and pentavalent tantalum, which give broad-band, amorphous electron diffraction patterns. It is uncertain at present whether the oxides of zirconium and thorium belong in the first or the second class.

The oxide gels of the first class are crystalline, but the primary crystals thrown down at room temperature are so minute that they give only diffuse x-ray diffraction patterns. The oxide gels of the second class are amorphous in the sense that glasses are amorphous, the network of oxygen and metal atoms lacking the periodicity and symmetry which exist in definite crystals.

In order to account for the similarities in the mechanical properties of an oxide in the form of a glass which is amorphous and the same oxide in definite crystalline form, Zachariasen (16; *cf.* 8) assumes that the atoms in the glass are linked together by forces essentially the same as in crystals, and that over large ranges of temperatures the atoms in the glass, like those in crystals, are oscillating about definite equilibrium positions. It is further assumed that the atoms in the glass must form an extended three-dimensional network as they do in crystals. The essential difference between a crystal and a glass is that a crystal network possesses both symmetry and periodicity in the arrangement of the atoms, whereas a glass network possesses neither symmetry nor periodicity in the arrangement of the atoms.

It is difficult to represent in drawings the difference between a crystal and a glass network, because of the three-dimensional arrangement, but Zachariasen illustrates the difference by means of two-dimensional analogs as shown in figure 13. Part *a* represents diagrammatically the lattice of a two-dimensional crystal, M_2O_3, and part *b* the glass network of the same compound. The general arrangements of the atoms and the forces are similar in the crystal and the glass, but the symmetry and periodicity which characterize the crystal lattice are absent in the glass.

It is suggested that the precipitated oxides which give broad-band electron diffraction patterns are amorphous in the sense that Zachariasen assumes a glass to be amorphous, that is, the atoms are arranged in the form of a network which lacks both periodicity and symmetry.

SUMMARY

1. An electron diffraction study has been made of gels of the hydrous oxides which give x-ray diffraction patterns of the amorphous type.

2. Hydrous oxides which are amorphous to x-rays may be grouped in two classes: (*a*) oxides which give relatively sharp ring electron diffraction patterns and (*b*) oxides which give electron diffraction patterns of the amorphous type.

3. The oxide gels of the first class are crystalline, but the size of the primary crystals is so small that their x-ray diffraction pattern consists of broad bands. The precipitated oxides of the following metals belong in this class: ferric iron, aluminum (from the sulfate), gallium, titanium (Ti^{IV}), and probably beryllium.

4. The oxide gels of the second class are amorphous in the sense that glasses are amorphous, the atoms arranging themselves in the form of a network lacking the periodicity and symmetry which characterize a crystal lattice. The precipitated oxides of the following metals belong in the second class: chromium, silicon, columbium (Cb^V), and tantalum (Ta^V).

5. The gel of ferric oxide thrown down at room temperature consists of minute crystals of α-Fe_2O_3. The oxide gel thrown down from aluminum sulfate solution, like that from aluminum chloride or nitrate solution, is γ-$Al_2O_3 \cdot H_2O$. Gallia gel precipitated at room temperature is composed of minute crystals of α-Ga_2O_3.

REFERENCES

(1) Baccaredda and Beati: Atti X° congr. intern. chim. **2,** 99 (1938).
(2) Böhm and Niclassen: Z. anorg. allgem. Chem. **132,** 6 (1924).
(3) Fordham and Tyson: J. Chem. Soc. **1937,** 483.
(4) Germer and Storks: Ind. Eng. Chem., Anal. Ed. **11,** 583 (1939).
(5) Laubengayer and Engle: J. Am. Chem. Soc. **61,** 1210 (1939).

(6) MILLIGAN AND WEISER: J. Am. Chem. Soc. **59**, 1670 (1937).
(7) SMITH: J. Am. Chem. Soc. **58**, 173 (1936).
(8) WARREN: Chem. Rev. **26**, 237 (1940).
(9) WEISER: *Inorganic Colloid Chemistry, Vol. II. The Hydrous Oxides and Hydroxides.* John Wiley and Sons, Inc., New York (1935).
(10) WEISER AND MILLIGAN: J. Phys. Chem. **38**, 513 (1934).
(11) WEISER AND MILLIGAN: J. Phys. Chem. **39**, 25 (1935).
(12) WEISER AND MILLIGAN: J. Am. Chem. Soc. **57**, 238 (1935).
(13) WEISER AND MILLIGAN: J. Am. Chem. Soc. **59**, 1670 (1937).
(14) WEISER AND MILLIGAN: Chem. Rev. **25**, 1 (1939).
(15) WEISER, MILLIGAN, AND PURCELL: Ind. Eng. Chem. **32**, 1487 (1940).
(16) ZACHARIASEN: J. Am. Chem. Soc. **54**, 3841 (1932).

SKIN REACTIONS. IX

THE ELECTROPHORETIC DEMONSTRATION OF THE PATENT PORES OF THE LIVING HUMAN SKIN; ITS RELATION TO THE CHARGE OF THE SKIN[1]

HAROLD A. ABRAMSON AND MANUEL H. GORIN

Biological Laboratory, Cold Spring Harbor, Long Island, New York, and the Medical Service of Dr. George Baehr and the Laboratories of the Mount Sinai Hospital, New York, New York

Received July 3, 1940

INTRODUCTION

The active agent in dialyzed extracts of giant ragweed, of short ragweed, and of timothy pollen may be transported by electrophoresis into the human skin (1). Marked whealing is readily produced in the skin of individuals hypersensitive to these comparatively large molecules. It becomes of interest to ascertain by what means these substances of comparatively high molecular weight pass through the skin. There are three main channels of transport to be considered: (*1*) the pores or coils of the sweat glands; (*2*) the hair follicles and sebaceous glands; (*3*) the skin itself, that is, the keratin matrix linking the structures mentioned in (1) and (2).

The authors have investigated this problem by the electrophoresis of both basic and acid dyes as well as of copper ions. By means of "development" of the patterns produced by the electrophoretic technic, it is possible not only to trace more accurately the channels traversed during the electrical transport but also to describe more explicitly than hitherto the relationship between the electrical charge of the dye ion and that of the pores of the skin.

---

[1] Presented at the Seventeenth Colloid Symposium, held at Ann Arbor, Michigan, June 6-8, 1940.

HISTORICAL

Among those who in the latter part of the nineteenth century were especially interested in the electrical transport of drugs through the skin, was Morton. Morton (15) stated, "The skin and other membranes and tissues of the human body may be regarded as septa, and, this allowed, it follows that electric osmosis may be made to take place through such septa . . . .I prefer the term Electric Diffusion, which may be defined as the capacity possessed by an electric current for diffusing or transporting liquids and whatever they may contain in solution from one polarity toward the other, preferably through porous septa- thus being applicable to the tissues of the living body."

Morton (15), however, rejected the notion that the cataphoresis of ions into the tissues is dependent upon the charge of the particles. He wrote, "The theory of Arrhenius as to the free and electrically charged ion advances our views as to the nature of electrolysis and electrolytic conduction, but I cannot see that we are yet entitled to assume that the electrolytic double progression of the ions which occurs in only a small percent of the molecules which constitute the solution is, in reality, that movement known as cataphoresis or electric diffusion. . . .This view would involve the relation and behavior of electrostatically charged tubules of small calibre, namely, the porous septa."

Before Morton wrote his book, Vergnés (17), an electroplater who worked in Cuba, found that he had developed on his hand an incurable ulcer that had been produced by contact with solutions of metallic salts. He accidentally placed his hand in a bath already prepared for plating and found that the negative pole received a metallic coating. In other words, he observed reversed electrophoresis of the metal out of the skin and plating of the metal onto the electrode employed. He followed this with a similar number of electrophoretic treatments, using the negative pole. This resulted in a rapid cure of his ulcer. On the basis of this incident the Vergnés electrochemical bath was developed. Morton (15), to support his contention that the pores of the skin were important, did another interesting experiment. "I, also, there mentioned an experiment which I had tried upon myself and which showed the ease with which even solid particles might be driven into tissue by the action of an electric current. Some finely powdered lampblack or graphite was incorporated with some salicylate of soda and placed on my arm under the positive electrode. The current was turned on and the particles of graphite were carried into the sweat follicles, making small black spots, like bird shot, which were so deeply embedded that they did not disappear for several weeks." This was apparently the first demonstration that particles may go into the living human skin by electrophoresis.

Three decades later Rein (16) also noted that dyestuff seemed to be deposited in the pores of the skin. He maintained, however, that positively charged dyes were more readily introduced than negatively charged dyes. He explained this selectivity by assuming that negatively charged dyes were restricted in their passage by the negative charge of the keratin. Our findings are contrary to those of Rein.

Although not directly connected with the subject matter of this communication, the recent papers of Hopkins, Kesten, and Hazel (9), Harpuder (8), Kovacs (10), Kovacs, Saylor, and Wright (11), and Lowenfish (12) may be consulted for related phenomena.

METHODS

Commercially available dyes were employed without purification. These were methylene blue (U.S.P. and "vital"), eosin Y, prontosil sodium, sodium indigotetrasulfonate, pontamine blue, patent blue V, sodium phenolsulfonephthalein, neutral red, and basic and acid fuchsin. Concentrations from 0.1 per cent to 2 per cent were used, but, in general, a solution containing 0.5 per cent of the dye gave excellent results. The dye was applied to the skin through a piece of absorbent cotton or canton flannel.

The electrophoresis apparatus consisted of the usual galvanic circuit. Current densities from 0.3 to 1.0 milliampere per square centimeter were suitable, the higher currents being comfortably borne with the positive pole.

Observations were made (*1*) without magnification, (*2*) with a hand lens, or (*3*) with a Bausch and Lomb wide-angle dissecting microscope.

The patterns obtained were photographed by means of a specially designed attachment to an Argus camera. It allowed the camera to be held against the area to be photographed and at a fixed distance from it. The distance was chosen to make the ratio of image to object 1:1. Pictures obtained in this way were enlarged for detailed study.

EXPERIMENTAL

If a pledget of cotton wet with a 1 per cent solution of methylene blue is held against the skin of the forearm or of the palm of the hand, the skin stains fairly uniformly. With vigorous rubbing and washing the stained cornified layer of the skin may usually be removed, with no evidence of marked selective adsorption of the dyestuff by any particular skin structure. If, however, the pledget of cotton is made the positive pole of an electrophoretic circuit for 1 to 5 min., selective adsorption by the skin can be demonstrated. On superficial examination of the blue-stained area, differential staining of the skin surface may not be observed. If, however, the stained area of the skin is vigorously rubbed and washed free of the blue dye, a remarkable pattern of the channels traversed by the dye is "developed." An example of this pattern is illustrated in figure 1 (magnified 3 ×). Close examination of the skin in experiments of this type disclosed that the blue dots were the sites of the pores of the skin,—the orifices of the coils of the sweat glands. Little or no methylene blue was usually observed at the bases of the hair follicles, although exceptions occurred. The electrical transport of dye through the skin of the palm of the hand showed that the hair follicles need not be involved at all. Development of the pattern in the palm is more difficult. In certain adult cases the final pattern developed several days after electrophoresis of the dye, as the superficial epithelium was lost. With the uncalloused hand of a three-year-old child, however, pore patterns can be developed in the usual way. Figure 2 is a photograph of a pore pattern obtained in an adult on the hypothenar eminence.

Pore patterns produced with methylene blue by the technic described in the foregoing may remain clearly visible for several weeks. The pattern nearly always remains visible for a week. In the course of time an interesting transformation may occur in the appearance of the individual spots of blue which comprise the pattern. This is observed in figures 3a and 3b, which are photographs of pore patterns obtained after 24 hr. and 1 week, respectively. Note that the blue spots which have within them paler white areas have taken on the appearance of doughnut forms. Examination of the size and structure of these doughnut forms indicates that the methylene blue which persists is due to a selective staining of the walls of the sweat glands. The pale areas observed in the centers of the doughnut forms are the orifices of the sweat glands, which gradually clear themselves of the methylene blue contained within the ducts.

It is surprising that the methylene blue is not reduced to the leuco form. Evidently the diffusion of oxygen into the cells of the duct is sufficiently great to keep the dyestuff in the oxidized state. One of us with Taylor (6) has shown that adsorbed dyes may be reduced, but more slowly in all cases studied. In certain instances it has been observed that the cells of the ducts containing methylene blue grow outward from the skin. Tiny papillae may then be seen under the microscope at the sites of the blue-stained pores. Not all of the pores may be stained by methylene blue. This can be readily demonstrated by following the electrophoresis of methylene blue with a second electrophoresis of eosin Y. By this means, red staining pores not previously stained by the first application of methylene blue may in certain instances be observed to appear.

According to Rein (16), a negative charge on the skin surface facilitates the passage of positively charged basic dyes, whereas it retards the passage of negatively charged acid dyes. This is in decided contrast with our experience. Not only have we obtained definite patterns with positive dyes like patent blue V and basic fuchsin, but we have obtained similar patterns using the negative pole with neutral red, eosin Y, sodium prontosil, sodium indigotetrasulfonate, sodium phenolsulfonephthalein, and acid

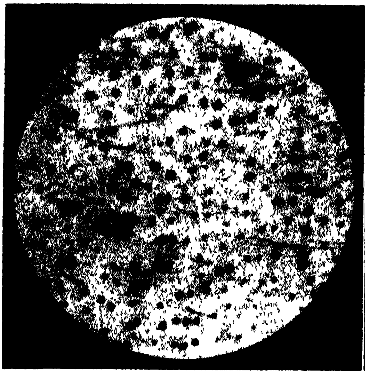

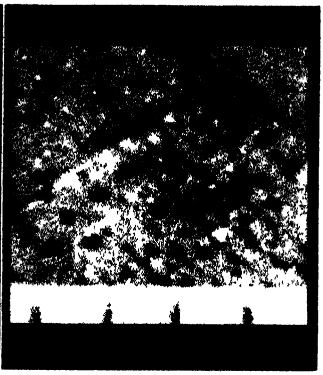

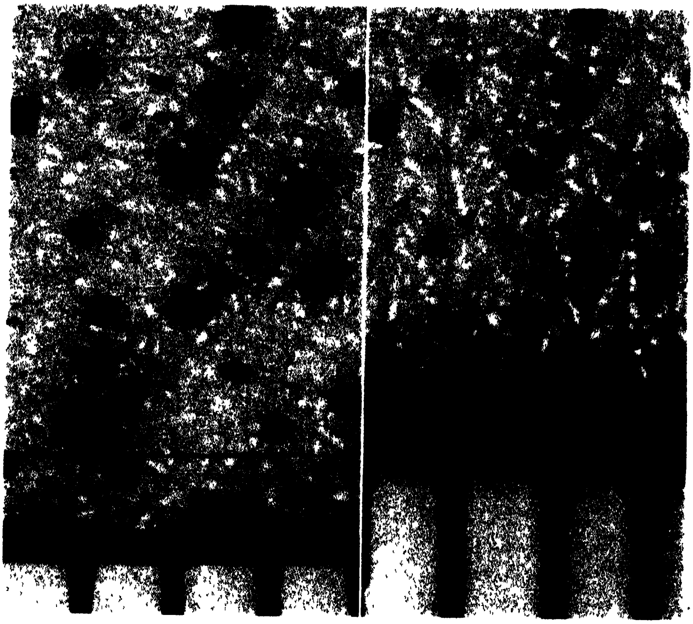

Fig. 1. (upper left) Magnification 3.2 ×. Pore pattern developed following electrophoresis of methylene blue into the skin of the anterior aspect of forearm of male adult. Note the arrangement of the dots in rows.

Fig. 2. (upper right) Electrophoresis of methylene blue into the pores of the palm of the hand. Note the more orderly arrangement of the pores in this region (hypothenar eminence). Millimeter scale.

Fig. 3. a (lower left): doughnut forms appearing 24 hr. after electrophoresis of methylene blue into the pores of the anterior aspect of the forearm. b (lower right): note the persistence of the pattern 1 week after the electrophoresis of the methylene blue. Millimeter scale.

fuchsin. Figures 4 and 5 are illustrations of patterns obtained by sodium phenolsulfonephthalein and by sodium indigotetrasulfonate.

There are differences in the skin reactions of certain individuals. Thus, in subject H. A. A. introduction of sodium phenolsulfonephthalein resulted in a red pattern which changed to yellow in time, the yellow pattern remaining for about a week. In an experiment on J. C., who had a different type of pore pattern, the red stage was not observed. Evidently in the cells of the pores the dye is in a different state than in the ducts of the pores. This is not unexpected.

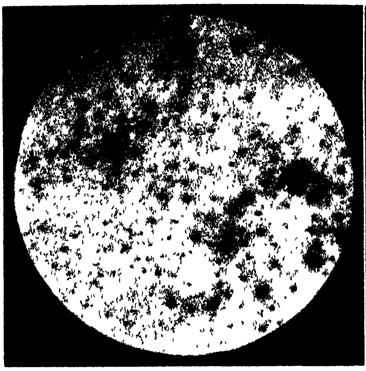

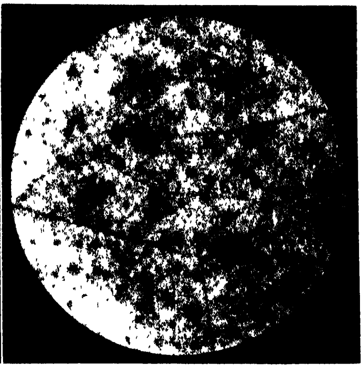

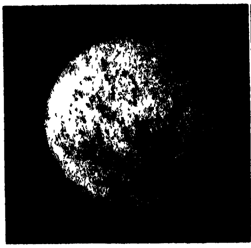

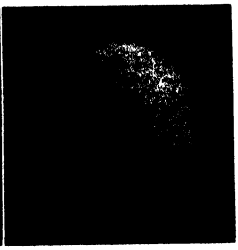

Fig. 4. (upper left) Negatively charged dyes like phenol indigotetrasulfonate form definite pore patterns in the skin. Note the more diffuse nature of the pattern when compared with positively charged methylene blue employed to obtain the pattern in figure 1. Magnification 3.2 ×.

Fig. 5. (upper right) Another illustration of a pore pattern obtained with phenol red, a negatively charged dye. The pattern appears to be more diffuse in this case also. Magnification 3.2 ×.

Fig. 6. (lower left) Pore pattern in a scar over 30 years old; natural size

Fig. 7. (lower right) Pore pattern in psoriasis; natural size

In experiments with sodium indigotetrasulfonate-doughnut forms appeared much more readily and rapidly than in the case of methylene blue. The rapid appearance of the doughnut forms is probably caused by reduction of some of the dye in special regions, following its introduction into the skin. In spite of this rapid initial reduction the pore pattern may remain visible for a week with large doughnut forms. Apparently the dye which has been absorbed by the cells lining the coils of the pores is not readily reduced.

In view of the development of recent technics (7) designed to introduce copper by electrical transport in the treatment of fungus diseases of the skin, the path taken by the copper ion was also studied. When copper is introduced into the skin by electrophoresis with the technic described in the foregoing, tiny red dots due to irritation appear and form a pattern of their own without the introduction of any dyestuff. It is not difficult to demonstrate that copper has been introduced through the pores, apparently in the same manner. Chemical tests in the pores for copper were positive.

APPLICATION TO DISEASES OF THE SKIN

Up to this point the experiments which have been described deal with the reaction of the normal skin. There is, however, a wide field of application to dermatological problems. Thus, scars and skin diseases like psoriasis, etc., may be investigated in this way. In figures 6 and 7 are illustrations of the type of application possible. Figure 6 is a pore pattern of a scar 30 years old, and figure 7 is a pore pattern in a lesion of psoriasis. It is hoped that the application of these technics to the study of skin diseases will lead to a more explicit structural and functional comprehension of the rôle that the pores of the skin play in these diseases.

DISCUSSION

The adherents of the pore or sieve theory of skin permeability (e.g., Rein (12)) maintain that the charge on the pores determines the restrictive forces which operate on the permeability of the membrane. Thus, negatively charged collodion membranes are well known to restrict the passage of negative ions but to permit positive ions to pass freely (13). In support of the point of view that the charge on the membrane determines the restrictive forces, Mond and Hoffmann (14) have shown that reversal of the sign of charge of the membrane by a dyestuff, rhodamine B, changes the nature of the permeability. This dye, by reversing the sign of the charge on collodion membranes, presumably permitted the passage of negative ions but restricted the passage of positive ions. It is evident that the pores of the skin readily permit the passage of both positively charged dye ions and negative ions like the phenolsulfonephthalein ion, in spite of the skin's negative charge. Indeed, one may easily imagine, according to Rein's scheme, that as positive ions are introduced into the skin they would reverse the sign of the surface charge, making the walls of the pores of the skin positive and in that way would progressively tend to restrict their own passage by reversal both of the charge and of the electroösmotic flow. It can be readily observed that if a dye is introduced electrophoretically for 0.5, 2, and 5 min., respectively, on separate sites, much more of the dye goes in as the experimental time increases. This illustrates that the adsorbed positive methylene blue ion apparently does not restrict its own passage as it accumulates on the cell surfaces. Similar observations have been made with other dyes. We are unable, therefore, to correlate the charge of the skin with the passage of the dyes under these circumstances. However, it would be of interest to make skin potential measurements of the type performed by Rein to determine whether these dyes do change the sign of the charge of the membrane which is assumed to give rise to the potentials observed.

It is useful to have the physical picture of the doughnut form in figures 3a and 3b. This enables us to visualize the pores of the skin discussed in detail (3) in a recent communication. It had been previously found that, contrary to the behavior of ordinary ions, the biologically active substance of giant and dwarf ragweed pollens migrated into the skin, not only from one pole but from both poles (1). In the case of giant ragweed, with the solutions employed, the positive pole was more efficacious than the negative pole; in the case of dwarf ragweed, the negative pole was more efficient. This type of electrophoretic behavior was unprecedented, for, as stated previously, usually only one pole is able to introduce an ion of the proper sign. The data were also not in keeping with preliminary measurements made on the electrical charge of the biologically active constituent of the ragweed pollen (5). More recently a single constituent which is negatively charged at pH 7.0 has been isolated (4) in the Tiselius apparatus. This negatively charged constituent can be introduced into the skin with the positive pole.

The fact that the skin acts as a reservoir for histamine and epinephrine, following electrophoresis of these substances (3, 2), may be correlated to a certain point with the persistence of dyes in the cells of the pores over long periods. Since histamine may be demonstrated in the skin for as long a period as a week, there must be some mechanism which prevents diffusion into the dermis. Although this mechanism is probably in some respects unlike that operating in the case of dyestuffs, the persistent pore patterns found for the dyes are presumptive evidence that a mechanism restricting diffusion does exist and that a similar general process may retain the histamine depots.

Obstruction of the pores need not prevent the formation of electrophoretic patterns. To investigate the effect of plugging the pores, an area was treated with albolene before electrophoresis of methylene blue. Although the initial resistance of the skin so treated was very much higher than that of a normal area, with sufficient voltage the resistance soon dropped to normal. With a current density of 0.5 milliampere for 5 min., a typical pore pattern was obtained. It is possible that electroösmotic forces drive the albolene out of the pores.

SUMMARY

When an electric current is applied across the living human skin, the skin may be considered to act like a system of pores through which transfer of substances like ragweed pollen extract may be achieved both by electrophoretic and by diffusion phenomena. The sites of these pores have been localized by forcing dyestuffs electrically into the skin, thus localizing the channels traversed. Both basic and acid dyes, as well as copper ions, localize primarily in the sweat glands, and pore patterns of the skin may be "developed" following electrophoretic transfer of basic dyes, acid dyes, and metallic ions. The pore patterns may persist for several weeks. During this time some of the small colored spots may decolorize in the center, leaving colored doughnut forms which correspond to selective staining of the cells comprising the orifices of the glands. Electrically patent pores may be plotted over the entire body. The pore patterns in scar tissue and in skin diseases like scleroderma and psoriasis may also be mapped, and in this way characteristics of these diseases be defined.

REFERENCES

(1) Abramson, H. A.: Science **87**, 299 (1938); N. Y. State J. Med. **39**, 611 (1939).
(2) Abramson, H. A.: Arch. Phys. Therapy, X-ray, Radium **21**, 261 (1940).
(3) Abramson, H. A., and Gorin, M. H.: J. Phys. Chem. **43**, 335 (1939); Chem. Products (London), February, 1940.
(4) Abramson, H. A., Moore, D. H., Gettner, H., Gagarin, J., and Jennings, L.: J. Am. Chem. Soc. **62**, 1627 (1940); Proc. Soc. Exptl. Biol. Med. **44**, 311 (1940).
(5) Abramson, H. A., Sookne, A. M., and Moyer, L. S.: J. Allergy **10**, 317 (1939).
(6) Abramson, H. A., and Taylor, I.: J. Phys. Chem. **40**, 519 (1936).
(7) Haggard, H. W., Strauss, M. J., and Greenberg: J. Am. Med. Assoc. **112**, 1229 (1939).
(8) Harpuder, K.: N. Y. State J. Med. **38**, 176 (1938).
(9) Hopkins, J. G., Kesten, B. M., and Hazel, O. G.: Arch. Dermatol. Syphilol. **38**, 679 (1939).
(10) Kovacs, J.: Am. J. Med. Sci. **188**, 32 (1934).
(11) Kovacs, J., Saylor, L. L., and Wright, I. S.: Am. Heart J. **11**, 53 (1936).
(12) Lowenfish, F. P.: Arch. Dermatol. Syphilol. **37**, 797 (1938).
(13) Michaelis, L.: Bull. Natl. Research Council, No. **69** (1929).
(14) Mond, R., and Hoffman, F.: Arch. ges. Physiol. **220**, 194 (1928).
(15) Morton, W. J.: *Cataphoresis or Electric Medicamental Surgery.* American Technical Book Company, New York (1898).
(16) Rein, H.: Z. Biol. **85**, 195 (1926).
(17) Vergnés: In Morton's *Cataphoresis or Electric Medicamental Surgery*, p. 21. American Technical Book Company, New York (1898).

ELECTRIC MOMENTS AND RELAXATION TIMES OF PROTEIN MOLECULES[1]

J. L. ONCLEY

Department of Physical Chemistry, Harvard Medical School, Boston, Massachusetts

Received July 3, 1940

The importance of the electric moments of molecules in the interpretation of their interactions with other molecules and with ions has long been recognized. Electric moments of a great many organic and inorganic substances have been measured in the past fifteen years, and have aided not only in the interpretation of molecular and ionic interactions but also in the study of molecular structure (5).

The electric moments of certain substances have been found to be of a much higher order of magnitude than is usually observed, and these substances have been shown, by both these and other measurements (2), to possess a very different type of structure, now commonly known as the "zwitter-ionic" or "dipolar-ionic" configuration. Substances with these configurations are found to possess many characteristic properties. Amino acids and peptides afford examples of substances of this type and have been widely studied.

This same "dipolar-ionic" configuration is one of the most important characteristics of the structure of protein molecules. The evaluation of electric moments of these materials was not attempted, however, until the past few years. Results of Wyman, Marinesco, Errera, and Shutt gave us the first indication of the order of magnitude of the dielectric increments of these materials, and the evaluation of electric moments from these data has been summarized by Cohn (2) and by Wyman (18). A considerable volume of work in this field has since been carried out by Andrews, Arrhenius, Elliott, Ferry, Oncley, Shack, and Williams, and has been summarized by Oncley, Ferry, and Shack (13).

Perhaps the most convenient way to compare the data obtained for these proteins is by means of their "low-frequency dielectric increment per gram per liter," defined as

$$(\Delta\epsilon_0/g) = (\epsilon_0 - \epsilon^0)/g \qquad (1)$$

where ϵ_0 is the dielectric constant at very low frequencies of a solution containing g grams of protein per liter, and ϵ^0 is the dielectric constant of the pure solvent. Values for this quantity for most of the proteins which have been studied and for a few typical amino acids and peptides are given in table 1. It is evident that the dielectric increments of proteins vary over an even wider range than do those of the amino acids and peptides.

---

[1] Presented at the Seventeenth Colloid Symposium, held at Ann Arbor, Michigan, June 6–8, 1940.

During the past year we have studied new fractions of serum albumin and serum pseudoglobulin-γ from the horse and of edestin from hemp seed. The serum albumin was prepared by McMeekin by crystallization of carbohydrate-free material as the sulfate from water at pH 4.0 (8), the serum pseudoglobulin by Green and by McMeekin, and the edestin by Bailey. The fractionations of these materials are being continued, and the results which have been obtained must be taken as preliminary in nature, since fractions of somewhat higher purity are now being prepared. Since these proteins afford good examples of both extremes of dielectric behavior, however, they have been chosen for discussion in this paper. Most of these fractions have also been studied by diffusion and by sedimentation velocity methods, and these determinations are of considerable importance in the evaluation of the results.

TABLE 1

Dielectric increments of certain proteins, amino acids, and peptides

SUBSTANCE	INCREMENT ($\Delta\epsilon_0/g$)	SUBSTANCE	INCREMENT ($\Delta\epsilon_0/g$)
α-Alanine	0.26	Egg albumin	0.1
Glycine	0.30	Gliadin	0.1
β-Alanine	0.39	Serum albumin (low)	0.1
γ-Aminobutyric acid	0.50	Carboxyhemoglobin	0.3
Diglycine	0.54	Insulin	0.3
ε-Aminocaproic acid	0.59	Zein	0.4
ζ-Aminoheptoic acid	0.59	Serum albumin (high)	0.4
Triglycine	0 60	Secalin	0.9
Heptaglycine	0.70	Serum pseudoglobulin	1.1
Lysylglutamic acid	1.26	Lactoglobulin	1.4

METHOD OF MEASUREMENT

The method used for the measurement of dielectric constant has been recently described (7, 10, 12). A substitution method is used, employing a somewhat modified General Radio Company Type 516 radio frequency bridge, a Leeds and Northrup Type 1188 standard condenser, an especially designed cell with concentric platinum thimble-shaped electrodes and a

Lucite top, and suitable oscillator, amplifier, and detector equipment for the frequency range from about 1,000 to 5,000,000 cycles.[2]

A brief description of the standard resistor used in this apparatus is necessary. Almost any type of resistor has a certain amount of residual capacitance or inductance. The resistors that we have employed have an almost constant residual inductance, and can be represented by a resistance R_a, variable from 0 to 111 ohms, and a series inductance, L_a, of about 1.1 ± 0.05 microheneries. A fixed resistance R_b with a capacitance C_b in parallel can as a first approximation (i.e., at low frequencies) be considered as a fixed resistance R_b and a fixed series inductance $-C_bR_b^2$. When we add this new combination in series with the constant inductance resistors, we have a total series resistance of $R_a + R_b$ and a series inductance of $L_a - C_bR_b^2$. By a proper choice of C_b we can reduce this series inductance to zero at low frequencies. Experimentally, we find this to be a perfectly feasible method for obtaining a variable resistor with very low residuals between 1,000 and 5,000,000 cycles. We have set R_b equal to 150 ohms, and C_b to about 50 micromicrofarads.

A complication due to the polarization capacitance at the electrodes has been found to exist at the lower frequencies. As a result of considerable study with various cells and electrolytes (7), we have adopted sand-blasted platinum as the electrode material and make a series of measurements on a reference solution consisting of the same solvent as was used for the protein solution with added potassium chloride so that the conductance is approximately equal to that of the protein solution. Capacitance increments are obtained by subtracting the capacitance of this reference solution, C'_x, from that of the protein solution, C_x, and these increments are plotted against $\nu^{3/2}$, ν being the frequency of the measurement (in megacycles). The slope, ΔB, of the best straight line resulting from this plot is then

---

[2] The equipment used in this laboratory consists of the following:

FREQUENCY RANGE	OSCILLATOR	AMPLIFIER	DETECTOR
50 to 8,000	Clough-Brengle Type 79-U audio frequency oscillator	General Radio Type 814A	Noise analyser, General Radio Company, Type 760
10,000 to 100,000	General Radio Type 648A modulated oscillator	General Radio Type 814A	Sargent all-wave receiver, model 11-UA
100,000 to 5,000,000	General Radio Type 648A modulated oscillator	None	Sargent all-wave receiver, model 11-UA

evaluated, and the dielectric increments, $\Delta\epsilon$, are calculated from the equation

$$\Delta\epsilon = (C_x - C_x' - \Delta B\nu^{-3/2})/Q \qquad (2)$$

where Q is the change in cell capacitance caused by a change of unity in the dielectric constant (i.e., the cell constant). This procedure has been shown to be quite adequate at frequencies above 10,000 cycles. Below this frequency slight errors may be introduced, increasing as the frequency is decreased (7).[3]

TABLE 2

Dielectric increments of serum albumin, serum pseudoglobulin-γ, and edestin preparations

SUBSTANCE	CONCENTRATION g	INCREMENT $\Delta\epsilon_0$	INCREMENT PER GRAM $\Delta\epsilon_0/g$	TOTAL INCREMENT PER GRAM $\Delta\epsilon_t/g$
Serum albumin	15.7	2.90	0.18	0.25
	26.2	4.51	0.17	0.24
	43.6	6.90	0.16	0.23
Serum pseudoglobulin-γ	9.9	8.6	0.87	(0.94)
	10.4	9.0	0.87	(0.94)
	16.3	13.2	0.81	(0.88)
	17.3	13.3	0.77	(0.84)
	27.4	20.3	0.74	(0.81)
	29.7	20.2	0.68	(0.75)
Edestin (in 2*M* glycine)	3.76	2.90	0.77	(0.84)
	6.38	4.50	0.71	(0.78)

DIELECTRIC INCREMENTS

The low-frequency dielectric increments for this albumin and γ-pseudoglobulin of normal horse serum and for edestin are recorded in table 2. Values for the total increment per gram, $\Delta\epsilon_t/g$, were estimated by adding 0.07 to the value for the low-frequency increment per gram - a value which has been found to closely approximate the usual value for $-\Delta\epsilon_\infty/g$. In the case of the albumin the value 0.07 was obtained by direct measurement,[4] since the contribution of the high-frequency increment is of much more importance in this case.

---

[3] Work toward the development of a new bridge and the use of cells with smaller cell constant, under progress in this laboratory, will probably increase the precision of the measurements at lower frequencies and allow measurements to be made on solutions of higher conductance at higher frequencies.

[4] The author is indebted to Professor Wyman for these measurements.

We have taken an average of the increment per gram values as representing the increment at infinite dilution in the cases of albumin and edestin,

TABLE 3

Data regarding the size, shape, and electric moments of serum albumin, serum pseudoglobulin-γ, and edestin preparations

MEASUREMENTS	SERUM ALBUMIN	SERUM PSEUDOGLOBULIN	EDESTIN[g]
Dielectric measurements:			
Low-frequency dielectric increment per gram, $\Delta\epsilon_0/g$ ..	0.17	1.1	0.7
Total increment per gram, $\Delta\epsilon_t/g$	0.24	(1.2)	(0.8)
Electric moment, μ, in Debye units	380	1200	1400
Relaxation time for equivalent sphere, $\tau_0 \times 10^8$ (in water at 25°C.)	6.0	22.	21.
Axial ratio, a/b	6	9	9
Dipole angle, θ	45°	45°	45°
Ultracentrifuge and diffusion measurements:			
Assumed molecular weight, M..	70,000	142,000	310,000
Partial specific volume, $\bar{v}$	0.748[a]	0.730[c]	0.744[a]
Sedimentation constant, $s_{20,w} \times 10^{13}$	4.5[a]	6.5[e]	12.8[a, f]
Diffusion constant, $D_{20,w} \times 10^7$	6.2[a]	4.1[d]	3.9[a]
Frictional ratio, f/f_0	1.25[a]	1.5	1.21[a]
Relaxation time for equivalent sphere (no hydration), $\tau_0 \times 10^8$ (H_2O, 25°C.)	5.7	11.3	25.
Axial ratio, a/b (assuming no hydration and elongated ellipsoidal shape).	5	9	4
Viscosity measurements:			
Viscosity coefficient, $1000(\eta - \eta_0)/(\eta_0\bar{v}g)$	6.5[b]	10[c]	
Axial ratio, a/b (assuming no hydration and elongated ellipsoidal shape).	6	8	.

[a] From Svedberg and Pedersen: *The Ultracentrifuge*, p. 406. Oxford University Press, London (1940).

[b] From Polson: Kolloid-Z. **88**, 51 (1939).

[c] Unpublished work of Armstrong (Harvard Medical School).

[d] Unpublished work of Mehl (Harvard Medical School).

[e] Measured in air-driven ultracentrifuge of the Bauer-Pickels type.

[f] A value of 14.6 for $s_{20,w} \times 10^{13}$ was obtained in some preliminary experiments on this material in our laboratory. A small amount (*ca.* 15 per cent) of this material had a somewhat higher sedimentation constant of about 18.

[g] Dissolved in 2*M* glycine solution with relative viscosity of 1.33.

while the values for γ-pseudoglobulin were extrapolated to zero concentration by plotting the increment per gram against the concentration. The values thus obtained are recorded in table 3, and may be compared with the results of Ferry and Oncley (6) upon a total pseudoglobulin (containing γ-pseudoglobulin together with other pseudoglobulins) and various albumin fractions. The low-frequency increment for the γ-pseudoglobulin is identical with the earlier result for the total pseudoglobulin, while that for the albumin lies between values previously obtained for fractions of low and high solubility. These increments, together with the "assumed molecular weights" recorded in table 3, are used to calculate the electric moment, μ, expressed in Debye units, as calculated (10) from the equation

$$\mu = 2.9\sqrt{M(\Delta\epsilon_t/g)} \tag{3}$$

The electric moments of these proteins which we obtained in this manner seem very large when compared with those of substances of low molecular weight, but this is due largely to the high molecular weights of the proteins. A comparison of the electrical symmetry of molecules of widely differing size can be made by calculating the diameter, R, which the molecule would have if it were spherical and then computing the number of unit charges, z, which must be located at each end of a dipole of this length in order to give the observed dipole moment, μ.[5] The values obtained in this way,—1.4 for the albumin, 3.4 for the γ-pseudoglobulin, and 3.4 for the edestin,—are all much smaller than half the total anionic and cationic charges found in these proteins, which range from perhaps 60 for the albumin to about 320 for the edestin. These molecules would accordingly have moments many times those reported here if they were very unsymmetrical electrically, and these measurements can be taken as proof of a fairly high degree of electrical symmetry.

RELAXATION TIMES

If we conduct dielectric constant measurements over a wide frequency range, we find a much more complex behavior than that described for the low-frequency measurements. In a certain frequency region we find that the dielectric increment drops from the low-frequency value we have been discussing to a value near zero, usually slightly negative. This behavior has been designated as "anomalous dispersion" (4, 10, 13); the frequency region in which the effect occurs depends upon the viscosity of the solvent and upon the size and shape of the protein molecules. The quantitative treatment of the problem has been carried out by Debye for spherical

---

[5] $$z = \mu/(eR) = 0.41\,[(\Delta\epsilon_t/g)^{1/2}M/\bar{v}^{1/3}] = 0.41\,[\delta_t^{1/2}/V^{1/3}] \tag{3a}$$

where M is the molecular weight, $(\Delta\epsilon_t/g)$ the total dielectric increment per gram per liter, and $\bar{v}$ the partial specific volume of the protein, and δ_t and V are the corresponding molal total increment and volume.

particles (4) and by Perrin (14) and by Budo, Fischer, and Miyamoto (1) for ellipsoidal particles.

The results of these treatments can perhaps best be described in the following manner: A hypothetical relaxation time, τ_0, for a spherical molecule with identical molecular weight, M, and partial specific volume, $\bar{v}$, can be calculated from the equation

$$\tau_0 = 3M\bar{v}\eta/(RT) \tag{4}$$

where η is the viscosity of the solvent medium, R the gas constant per mole (8.31×10^7 ergs per degree per mole), and T the absolute temperature. The dielectric dispersion of a spherical molecule could be completely characterized by this relaxation time, but molecules of other shapes would show a more complex behavior. If we assume that the molecule can be represented by an ellipsoid of revolution, the form of the dispersion curve will depend upon the axial ratio of the ellipsoid, a/b, and the angle between the geometric axis a of the ellipsoid and the electric moment vector, called the dipole angle,[6] θ. Here a is taken as the half-length of the ellipsoid along the geometric axis of rotation, and b as the equatorial

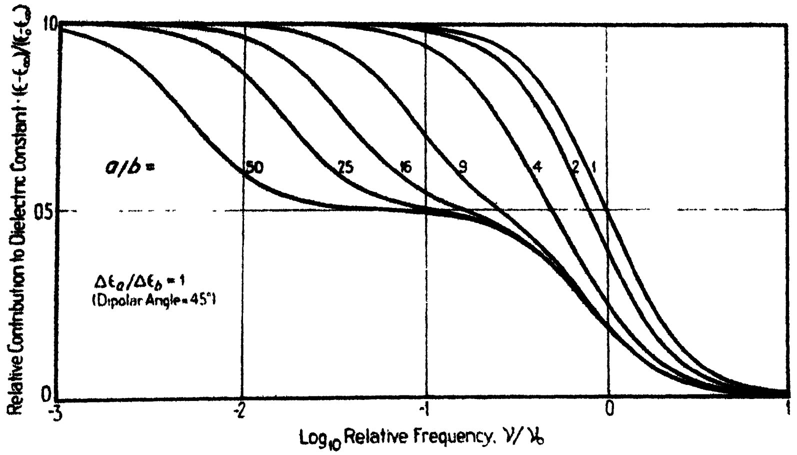

FIG. 1. Dielectric dispersion curves for elongated ellipsoids of revolution (according to Perrin). Constant dipole angle ($\theta = 45°$) and varying axial ratio (a/b from 1 to 50).

---

[6] The angle θ can be defined by the equation

$$\tan \theta = \mu_b/\mu_a = \sqrt{\Delta\epsilon_{t_b}/\Delta\epsilon_{t_a}} \tag{3b}$$

where μ_a and μ_b represent the components of the dielectric moment along the a- and b-axes, respectively, and $\Delta\epsilon_{t_a}$ and $\Delta\epsilon_{t_b}$ the increment contributions along these axes.

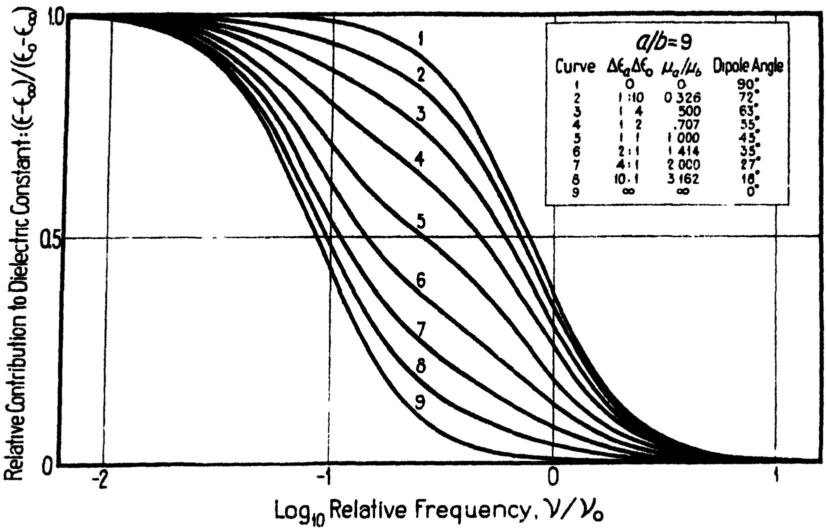

FIG. 2. Dielectric dispersion curves for elongated ellipsoids of revolution (according to Perrin). Constant axial ratio ($a/b = 9$) and varying dipole angle (θ from 0° to 90°).

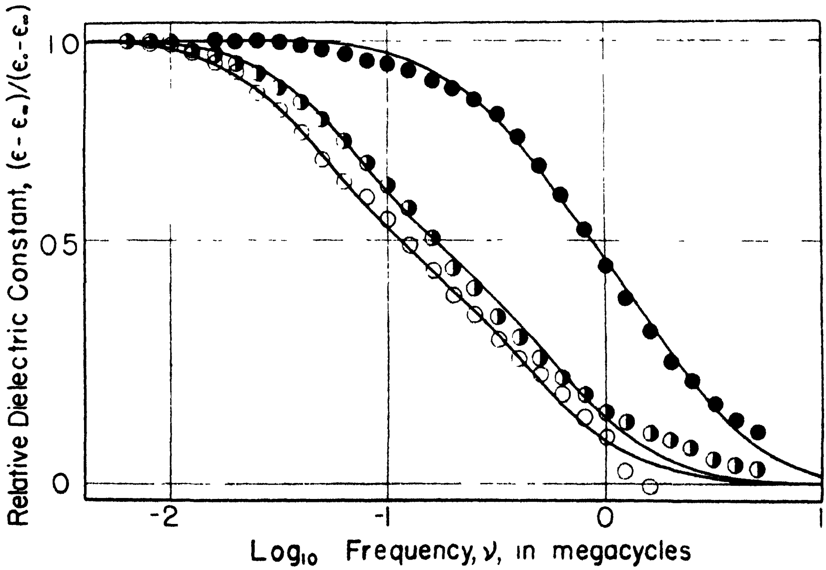

FIG. 3. Observed dielectric dispersion curves for certain proteins. ●, Serum albumin; ◑, serum pseudoglobulin-γ; ○, edestin. The curves are those calculated for the parameters recorded in table 3, lines 4, 5, and 6.

radius. Theoretical dispersion curves for various values of a/b and θ can then be computed, examples of such curves being shown in figures 1 and 2. Figure 1 is for the case of constant dipole angle ($\theta = 45°$) and varying axial ratio (with a/b varying from 1 to 50), while figure 2 is for the case of constant axial ratio ($a/b = 9$) and varying dipole angle (with θ from 0° to 90°). By comparing theoretical curves of this type with the observed dispersion curves shown in figure 3 we may pick values of θ, a/b, and τ_0 which best represent the experimental data, and such values are recorded in table 3. These observed dispersion curves are similar to those obtained by Ferry and Oncley (6), but additional measurements at both high and low frequencies have increased their reliability. The curves for the γ-pseudoglobulin are found to show the presence of dispersion over an even wider range of frequency than was previously observed for the total pseudoglobulin, giving rise to a somewhat larger amount of asym-

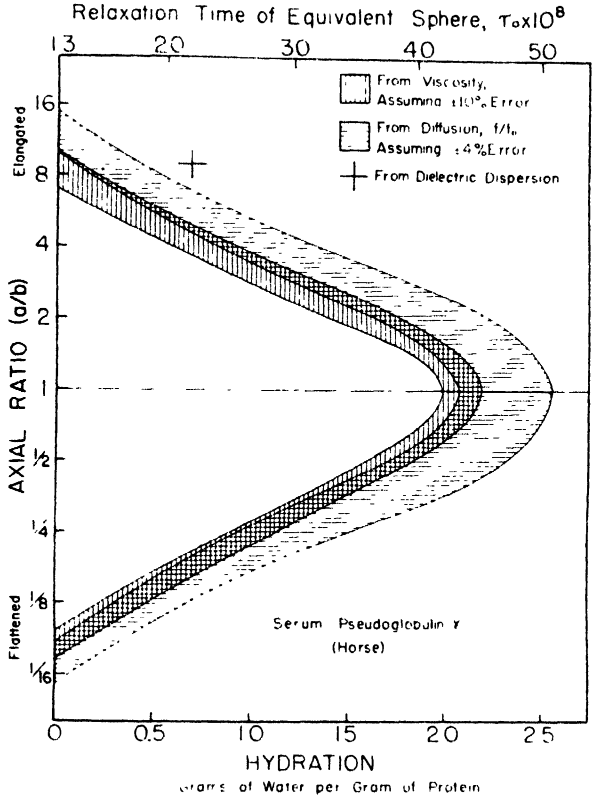

FIG. 4. Values of axial ratio and relaxation time (or hydration) consistent with viscosity and diffusion data for serum pseudoglobulin-γ.

metry for the γ-pseudoglobulin. Values of a/b less than unity (flattened ellipsoids) do not give curves of the type observed for the molecules under discussion here, and have therefore been omitted from figure 1.

The values selected in this manner for a/b and τ_0 must be consistent with values obtained from other reliable sources (3). Perhaps the most reliable data of this kind are obtained from measurements of sedimentation constant, diffusion constant, and viscosity coefficient of dilute protein solutions. A considerable amount of data of this type is available for the molecules under discussion here and is recorded in table 3. By the use of the equations of Perrin and of Simha we may use these data to evaluate the asymmetry (9, 15, 16, 17). Values for both a/b and τ_0 cannot be directly and unambiguously obtained from these data, however, since values for both the fractional ratio, f/f_0, and the viscosity coefficient, F, depend upon the amount of hydration (and hence the size) and the asymmetry. The values of these quantities as recorded in table 3 are calculated assuming no hydration and an elongated ellipsoidal shape.

The agreement between the values of a/b and τ_0 obtained in this way is good in the case of the albumin and fair for the edestin. The pseudoglobulin shows very poor agreement, however, since the values of τ_0 differ by a factor of 2. We have accordingly recorded in figure 4 all of the values of a/b and of τ_0 (or of the hydration) which are consistent with the viscosity and diffusion data for this molecule. The width of the bands was chosen to represent the probable range of values, but is somewhat arbitrary. The cross represents the result obtained from the dielectric dispersion studies, and the values $a/b = 8$ and $\tau_0 = 18 \times 10^{-8}$ (corresponding to a hydration of about 0.4 g. of water per gram of protein) might represent the best average of these data.

SUMMARY

The electric moments of serum albumin, serum pseudoglobulin-γ, and edestin were found to be about 380, 1200, and 1400 Debye units, respectively. These large electric moments are of considerable importance in the interpretation of the interaction of these molecules.

A study of the dielectric dispersion of these molecules gave relaxation times and shapes which are compared with those from diffusion, ultracentrifuge, and viscosity measurements. The agreement was good in the case of serum albumin and edestin without the assumption of any very large degree of hydration, but in the case of the serum pseudoglobulin-γ it appeared necessary to assume a moderate amount of hydration or some other complicating phenomenon.

I should like to express my thanks to Drs. T. L. McMeekin, A. A. Green, and K. Bailey for the preparation of proteins used in this investigation;

to Professor J. Wyman, Jr., Drs. S. H. Armstrong, Jr., J. D. Ferry and J. W. Mehl, and Mr. M. Melin for making certain of the measurements recorded here; and to Professor E. J. Cohn for his help throughout these investigations.

REFERENCES

(1) BUDO, FISCHER, AND MIYAMOTO: Physik. Z. **40,** 337 (1939).

(2) COHN: Ann. Rev. Biochem. **4,** 93 (1935).

(3) COHN: Chem. Rev. **24,** 203 (1939).

(4) DEBYE: *Polar Molecules* The Chemical Catalog Company, Inc., New York (1929).

(5) Dielectric Symposia: Trans. Faraday Soc., Volume **30** (1934).

(6) FERRY AND ONCLEY: J. Am. Chem. Soc. **60,** 1123 (1938).

(7) FERRY AND ONCLEY: J. Am. Chem. Soc., in press.

(8) MCMEEKIN: J. Am. Chem. Soc. **61,** 2884 (1939).

(9) MEHL, ONCLEY, AND SIMHA: Science **92,** 132 (1940)

(10) ONCLEY: J. Am. Chem. Soc. **60,** 1115 (1938).

(11) ONCLEY: Ann. N. Y. Acad. Sci., in press.

(12) ONCLEY, FERRY, AND SHACK: Cold Spring Harbor Symposia Quant. Biol. **6,** 21 (1938).

(13) ONCLEY, FERRY, AND SHACK: Ann. N. Y. Acad. Sci., in press

(14) PERRIN: J. phys. radium **5,** 497 (1934)

(15) PERRIN: J. phys. radium **7,** 1 (1936).

(16) SIMHA: J. Phys. Chem. **44,** 25 (1940)

(17) SVEDBERG AND PEDERSEN: *The Ultracentrifuge*. Oxford University Press, London (1940).

(18) WYMAN: Chem Rev **19,** 213 (1938)

A STUDY OF SOME PROPERTIES OF THIXOTROPIC GELS CONTAINING EGG ALBUMIN AS THE DISPERSE PHASE[1]

WILLIAM G. MYERS AND WESLEY G. FRANCE

Department of Chemistry, The Ohio State University, Columbus, Ohio

Received July 3, 1940

Jirgensons (19) investigated thixotropic gels containing 2 to 5 per cent of egg albumin in which the percentage by volume of normal propyl alcohol was varied between 40 and 60 and the concentrations of various salts were found to be optimal between 0.2 and 0.5 mole per liter. In attempting to check his results it was found that acetic acid, when added to diluted egg white, produced thixotropic gels. This result is in marked contrast to that reported by Loughlin and Lewis (25), Loeb (24), and others, who found that the viscosity of such protein solutions is independent of the hydrogen-ion concentration when strong mineral acids are used. Preliminary experiments showed that the thixotropic properties of the gels were greatly altered by the addition of small quantities of various salts. In view of the little work that had been done on thixotropic protein gels and in order to clear up, if possible, the discrepancy between our findings and those of Loughlin and Lewis, it was deemed desirable to investigate carefully the factors which were responsible in producing the thixotropic gels.

---

[1] Presented at the Seventeenth Colloid Symposium, held at Ann Arbor, Michigan, June 6–8, 1940.

Only a few other thixotropic systems containing proteins have been studied. Freundlich and Abramson (11) found that solutions containing between 1 and 8 per cent of gelatin were thixotropic. Muralt and Edsall (27) were able to extract the globulin, muscle myosin, which constitutes the main portion of the interior of muscle fibers, and found solutions of it to be thixotropic. Both Chambers (4) and Fauré-Frémiet (8) have described the thixotropic properties of protoplasm. Anson and Mirsky (1) studied the effects of acids, salts, and heat on the viscosity of denatured egg albumin and hemoglobin solutions. It is probable from their description that they were dealing with thixotropic gels in some of their work. Kopaczewski (22) studied thixotropic gels composed of impure serum proteins, casein, and mucoid in the presence of lactic acid and salts, and merely mentioned the fact that gels were produced when hydrochloric acid, pyridine, and sodium hydroxide were substituted for the lactic acid.

Many theories of protein structure have been formulated in attempts to depict the complex interrelationships among the thousands of atoms constituting each huge protein molecule and to correlate these with the changes in properties and thermodynamic quantities which result when these massive entities are acted upon by external agencies. The modern picture is far from a complete one, as the controversy around several points in the current literature will attest (31, 41, 42), but the main framework has been established to the satisfaction of most of the investigators in the field.

In 1906 Emil Fischer (9) introduced the concept of the peptide bond, and his subsequent brilliant researches established that this bond is the essential one in protein structure. From this arose the idea that a native protein molecule is composed of amino acid residues linked together by peptide bonds into a single continuous polypeptide chain. As the result of many experiments of great diversity, it is now generally agreed that this chain is not an extended one, but that it is twisted and folded upon itself to form a compact globule having either a spherical or a more or less elongated shape (29). Svedberg (38, 39) and his collaborators have shown that the particle weights of these globules vary for different protein species from about fifteen thousand to several millions. In 1931 Wu (43) first expressed the idea that the pattern of folding of the polypeptide chain im-parts to the molecule of each protein species the unique configuration which gives the molecule its specific characteristic properties.

Since the extended chain is a more random condition than the globular form and therefore is the more probable one, it follows that some kind or kinds of bonds must exist among different points on the chain to hold it in a rolled-up state. The nature of these non-peptide bonds is the principal cause of argument among workers in the field of proteins (2, 31, 37, 41, 42) at the present time. It is not our purpose to enter the controversy here; rather, we shall adopt the concepts which seem best fitted to explain the phenomena under study. Those most useful to us have appeared in the works of many authors, but they are summarized principally in the recent theoretical discussions of protein structure and protein behavior by Mirsky and Pauling (26), Anson (36, Chapter IX), and Eyring and Stearn (7).

According to these workers there are essentially two different types of cross-linkages, one of which, the cystine link (included here, also, are any possible inner ester links), plays a minor part in holding the chain wound up because of its paucity in most proteins.

The other type of cross-link is an internal salt-bridge, arising from the interaction of excess basic and acidic groups along the chain as well as from a basic and a carboxyl group not involved in a peptide bond at each end of the chain. The excess acidic groups along the chain are due to the monoaminodicarboxylic acids, aspartic, glutamic, and hydroxyglutamic, whereas the excess basic groups are due to the diaminomonocarboxylic acids, arginine, histidine, and lysine. The nature of the interaction of these basic and acidic groups is unsettled. We shall adopt the concept of Mirsky and Pauling (26): "Side-chain bonds in proteins we consider to involve usually an amino and a carboxyl group, the nitrogen atom forming a hydrogen bond with each of two oxygen atoms and holding also one unshared hydrogen atom. In acid solutions hydrogen bonds may be formed between two carboxyl groups, as in the double molecules of formic acid (30). . . .The bond is essentially electrostatic in nature." A scheme of such a bond between a lysine and a glutamic acid residue located at points along the polypeptide chain separated by . . .*n*. . . interposed amino acid residues appears in figure 1a. Figure 1b shows how the electrons are arranged in the salt-bridge according to the above description by Mirsky and Pauling. The small light-inked symbols between the heavy ones represent electrons the source of which is self-indicated. The dotted lines

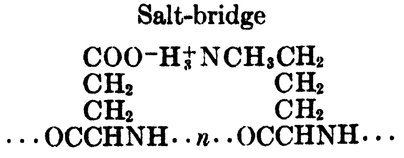
Salt-bridge

$$\begin{array}{lll} & \mathrm{COO^{-}H_3^{+}NCH_3CH_2} & \\ & \mathrm{CH_2} \qquad\qquad\quad \mathrm{CH_2} & \\ & \mathrm{CH_2} \qquad\qquad\quad \mathrm{CH_2} & \\ \cdots & \mathrm{OCCHNH} \cdot\cdot n \cdot\cdot \mathrm{OCCHNH} & \cdots \end{array}$$

FIG. 1a

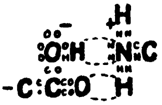

FIG. 1b

show where the hydrogen bonds are located. Rodebush (33) "regards the hydrogen bond as a case of coordination of the simplest cation, the proton." A fuller description of the nature of the hydrogen bond and of its applications appears in the reviews by Huggins (18) and Lassettre (23).

Now there is an excess of twenty-eight each of basic and acidic groups in egg albumin (5), among which there are presumably salt-bridges in the native protein molecule to hold it rolled up in its globular form. Evidence for this is that the native protein molecule loses many of its characteristic properties in a process known as denaturation, when it is acted upon by various agents which break the links holding the parts of the molecule in their specific relationships. "The denatured protein molecule is characterized by the absence of a uniquely defined configuration" (26).

Many different explanations have been offered by various authors in attempting to account for thixotropy. The most widely accepted theory is that thixotropy is due to the formation of solvated hulls around each of the particles of the dispersed phase (12, 13, 14, 15, 16, 17, 20, 32). These thick envelopes or lyospheres of oriented solvent molecules are supposed to be disrupted by shaking and to re-form again when the system is left undisturbed; the rigidity of the gel state arises from the fact that these lyospheres become so large as to interlock throughout the system.

Several lines of evidence may be adduced in favor of this hypothesis. Chief among these are the observations of the sol-gel transformation made under the ultramicroscope (10, 13, 16, 34, 35).

Evidence which may make the solvated hull theory seem untenable is the excessive thickness of these hulls that would be necessary in order for them to touch. Werner (40) calculated that the thickness would have to be up 3 μ for a gel containing kaolin, and Freundlich (10) found that it would have to be about 100 mμ for a bentonite gel.

A popular alternative hypothesis, which has been expressed variously (12, 13, 14, 34), attributes thixotropy to the formation of a network composed of chains, filaments, or sheets of the dispersed phase that pervades the entire gel and entraps the dispersion medium. These structures are readily broken down by shaking and form anew when the system is undisturbed. Factors affecting thixotropic gel formation are discussed fully in the reviews of Freundlich (13), Pryce-Jones (32), and Myers (28).

EXPERIMENTAL

Solutions of thrice-crystallized egg albumin were prepared by the method of Kekwick and Cannan (21). They were electrodialyzed free of salt and analyzed for protein content by evaporating a weighed amount of the solution to dryness at 110–140°C.

The pH of the solutions was measured with a Coleman glass-electrode assemblage and found to be around 4.85. This is in agreement with the results of Errera and Hirshberg (6), who found that prolonged electrodialysis always brought the pH to the isoelectric point of the protein.

An Ostwald-type viscosimeter immersed in a bath constant to ±0.02°C. was used. Time intervals were measured in fifths of seconds with a stop watch.

Whenever protein was a reagent being used in conjunction with a weak organic acid or base, the emptying periods of the viscosimeter were used only as bases for comparisons of the actions of reagents or of different durations of time upon the protein. This qualification is necessary, since chemical interactions within the systems caused their viscosities to increase continuously even while the emptying periods were being determined. Also it is doubtful that the emptying periods of the very viscous systems could be used validly for the determination of their viscosities, even though they had remained constant during the times of measurement, because such highly viscous systems probably do not obey Poiseuille's law relating viscosity with pressure for flow through a capillary. Greenberg (36, page 452) designates the viscosities of highly viscous systems, which vary with the rate of shear, as structural viscosities or plastic flow.

The method of mixing the reagents when 1 per cent egg albumin solution was used along with acetic acid was as follows: 2 cc. of a 5 per cent protein solution was allowed to flow into a test tube from a buret. Then an appropriate concentration of a salt solution in a volume calculated to give the desired final concentration when diluted to 10 cc. was added. Next, water was added to bring the total volume up to 7 cc. Finally 3 cc. of glacial acetic acid was added as quickly as possible. A cork was inserted in the test tube, and the contents were mixed by inverting the tube five times. Then the contents were quickly poured into the viscosimeter in the water bath and forced by air pressure to a point above the second file mark of the capillary of the viscosimeter. In order to obtain as comparable results as possible, 1 min. was allowed to elapse from the time that the addition of acetic acid was begun until the beginning of the emptying period of the viscosimeter was clocked.

After the emptying periods had been determined over the desired intervals of time, the contents of the viscosimeter were poured back into the test tube. The systems were then stored in test-tube racks for further observations of the effect of lapse of time upon them. Thixotropic gelation, flocculation, or syneresis were noted in particular.

In figure 2 the emptying periods of a viscosimeter containing a 1 per cent protein solution in the presence of 30 per cent of glacial acetic acid by volume at 25°C. are plotted against the time intervals after the mixing of the components. The curve is very smooth up to a point where the emptying period exceeds 260 sec., when it is thought that plastic flow or "structural" viscosity becomes dominant.

The emptying periods of a viscosimeter containing a 1 per cent solution of egg albumin in the presence of 30 per cent of glacial acetic acid by volume at 27°C., when increasing concentrations of sodium chloride are added, are given in table 1. Emptying periods are given in seconds and time intervals after mixing the components are given in minutes. The data are plotted in figure 3.

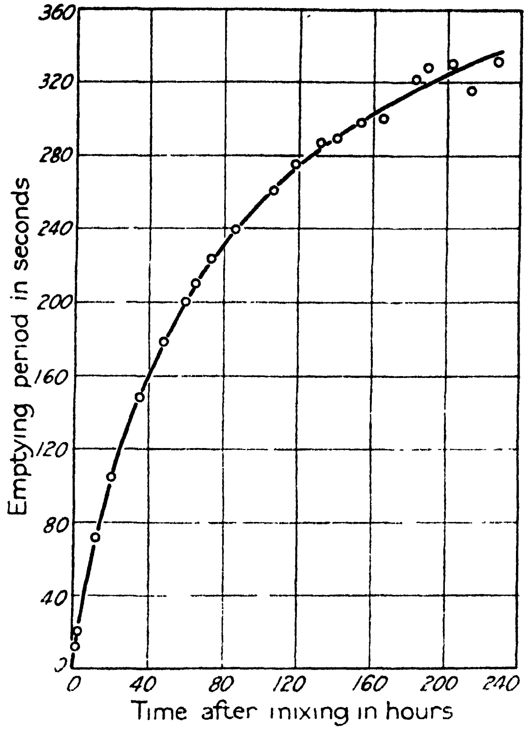

FIG. 2. Plot of the emptying periods of a viscosimeter against time intervals after mixing components. The viscosimeter contains 1 per cent protein solution in the presence of 30 per cent of glacial acetic acid by volume; no salt is present. Temperature, 25°C. The curve indicates gradual unwinding of the egg albumin molecule with time, owing to thermal agitation with simultaneous solvation by acetic acid *via* hydrogen bonds.

The systems which were 0.006–0.020 *N* with respect to sodium chloride showed increasing gel structure. They were thixotropic.

Similar data were obtained when sodium sulfate and sodium ferrocyanide were used. Here the emptying periods increased much more rapidly for a given concentration of salt than was the case with sodium chloride, as figure 4 illustrates.

Some qualitative observations concerning the effects produced by

TABLE 1

Emptying periods of viscosimeter containing egg albumin, acetic acid, and sodium chloride

CONCENTRATION OF NaCl	EMPTYING PERIODS IN SECONDS										
Time intervals	1 min.	3 min.	5 min.	7 min.	9 min.	11 min.	16 min.	21 min.	31 min.	46 min.	61 min.
0.002 *N*	11.2	11.2	11.2	11.4	11.6	11.8	12.0	12.2	13.0	14.2	15.6
0.004 *N*	11.2	11.4	11.6	11.8	12.2	12.6	13.4	14.4	16.6	20.6	23.8
0.006 *N*	11.0	11.4	12.0	12.6	13.4	14.2	16.2	18.2	22.0	27.8	33.4
0.008 *N*	10.8	11.6	13.0	13.8	15.4	16.6	19.4	22.4	28.2	37.2	46.4
0.010 *N*	10.8	12.4	14.2		17.4	19.2	23.4	27.2	35.8	49.0	61.6
0.020 *N*	12.4	19.2	25.4	30.8	37.0	43.0	64.4	105	416		
0.040 *N**											
0.060 *N*†											

* Set to gel immediately.

† Formed suspended flocs immediately and was white and opaque. Syneresis soon occurred.

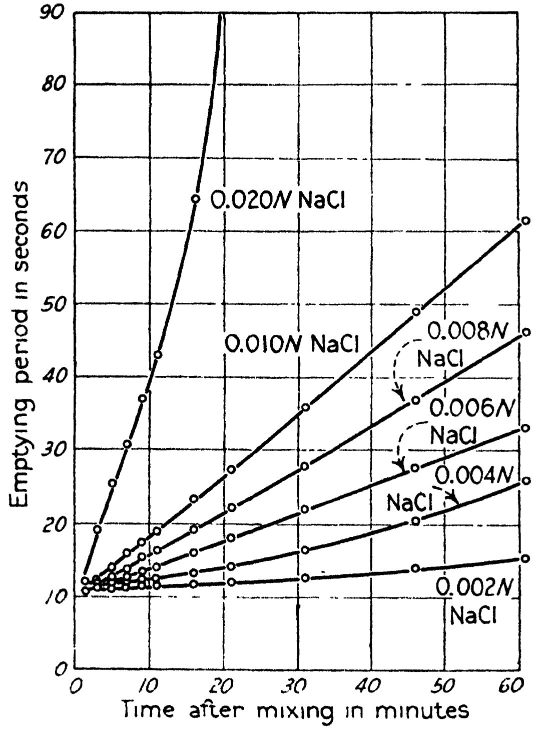

FIG. 3. Plot of the emptying periods of a viscosimeter against time intervals after mixing components. The viscosimeter contains a 1 per cent solution of egg albumin in the presence of 30 per cent of glacial acetic acid by volume and added sodium chloride. Temperature, 27°C.

weak organic acids and bases, including pyridine, were made. Propionic acid and lactic acid appeared to have the same effect as pyridine. Nicotine also produced thixotropic gels, but they were very viscous and showed very prolonged setting times. Piperidine produced very basic solutions when added to egg albumin, but these showed no tendency to develop a gel structure.

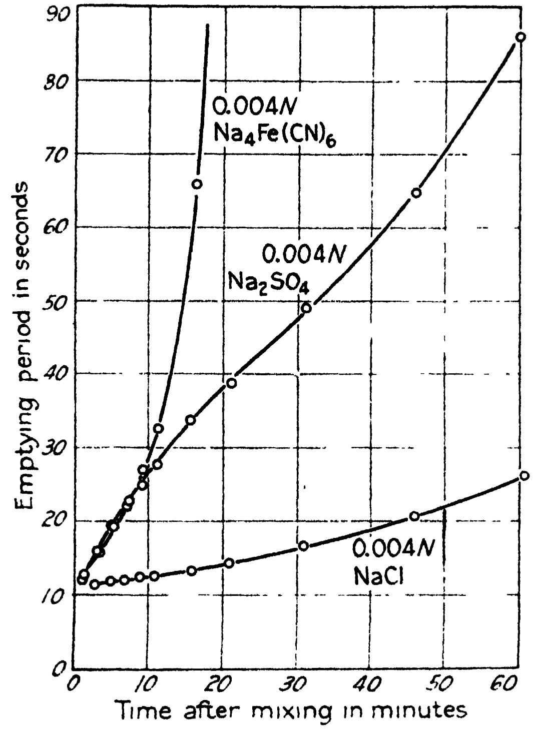

FIG. 4. Plot of the emptying periods of a viscosimeter against time intervals after mixing components. The viscosimeter contains a 1 per cent solution of protein in the presence of 30 per cent of glacial acetic acid by volume and added sodium ferrocyanide, sodium sulfate, or sodium chloride. Temperature, 27°C.

Figure 2 shows how the emptying period of a viscosimeter containing 1 per cent of egg albumin mixed with 30 per cent by volume of glacial acetic acid increases with the interval of time after the mixing of the components. This result is entirely different from that reported by Loughlin and Lewis (25) and by Loeb (24), who found that the viscosity of solutions of egg albumin was independent of the hydrogen-ion concentration when strong mineral acids were added. We also found that the viscosity of a 3 per cent solution of egg albumin was constant when sulfuric acid was used to produce the same hydrogen-ion concentration as that obtained by the addition of 30 per cent of glacial acetic acid.

Now this difference between the effect of a weak organic acid and that of a strong mineral acid cannot be accounted for on the basis of a difference in the number of salt-bridges neutralized, because the hydrogen-ion concentration in each case was great enough to insure the complete neutralization of all salt-bridges. We believe that, in addition to the formation of albumin acetate in a process identical with the formation of a protein salt by strong mineral acids, acetic acid present in sufficient concentration to give a pH of about 2 also solvates (through hydrogen bonds) the loose ends of the salt-bridges after neutralization has permitted them to separate. This is in harmony with the view of Mirsky and Pauling (26). Huggins also believes that such solvation can occur readily.

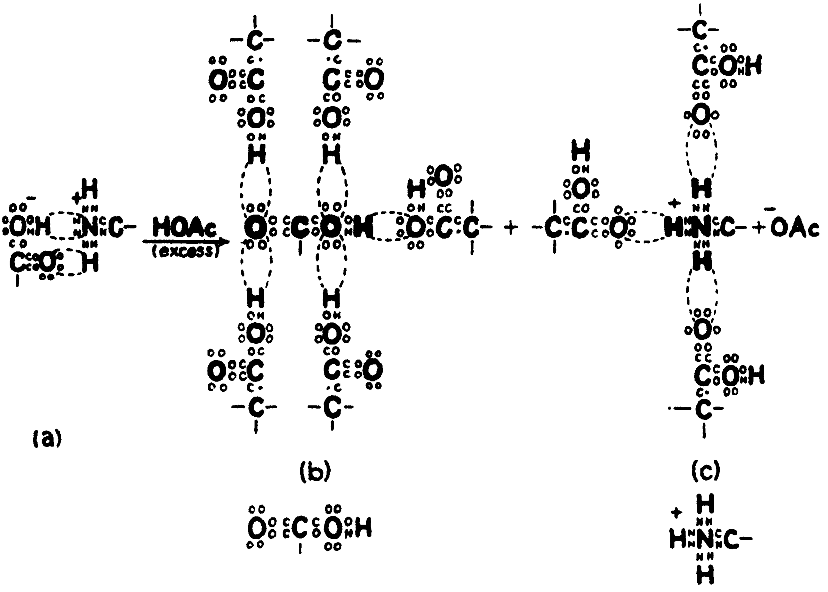

(Solvated by five acetic acid molecules through five hydrogen bonds)

(Solvated by three acetic acid molecules through three hydrogen bonds)

FIG. 5. A possible solvation mechanism

Carboxyl groups seem to be especially well adapted to bridge formation. The carboxyl hydrogen is held loosely enough so that it can be shared readily with a suitable electronegative atom elsewhere. The carboxyl oxygen atoms likewise act as receivers for hydrogen atoms held loosely enough elsewhere (18).

A depiction of a possible solvation mechanism appears in figure 5, where the source of the electrons is indicated by the small symbols and the hydrogen bonds are indicated by the broken lines. The two hydrogen bonds between the nitrogen atom and the two oxygen atoms in figure 5 a, —postulated by Mirsky and Pauling,—are broken at the pH (about pH = 2.0) under consideration, with a subsequent solvation of the free carboxyl to the maximum extent of five molecules of acetic acid (figure 5 b) and of the free H_3^+N— to the extent of three molecules of acetic acid (figure 5 c) through hydrogen bonds. It is unlikely that the carboxyl group could form the maximum of five hydrogen bonds with acetic acid if correct bond angles and bond distances were observed.

An even greater solvation is probable if one considers the possibilities of hydrogen-bond formation at each peptide link, as shown in figure 6. There are three lone pairs of electrons and a hydrogen attached to the nitrogen which are available for solvation by four acetic acid molecules through hydrogen bonds. Since there are 288 amino acid residues in the egg albumin molecule (3), the total maximum solvation by acetic acid through hydrogen bonds is (287 × 4) + (28 × 8) = 1372 molecules. Multiplying by the molecular weight of acetic acid adds 82,320 to the particle weight, owing to solvation. As pointed out before, the maximum solvation is probably prevented when the bond angles and distances are considered. However, the above calculation is concerned only with the maximum solvation directly through hydrogen bonds. If one examines figure 5 it is apparent that each directly solvated molecule presents a great many opportunities for further indirect solvation by acetic acid. It is known that acetic acid readily forms hydrogen bonds with itself and with water as well, so that one immediately realizes that he is here dealing with a logical mechanism for lyosphere formation without having to resort to the postulation of any vague and unknown forces (10, 13, 15, 20, 40) acting over comparatively enormous distances.

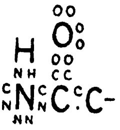

FIG. 6. Possibilities of hydrogen-bond formation at each peptide link

The picture thus far then is that weak organic acids and bases, which form hydrogen bonds readily, neutralize the salt-bridges in the protein molecule and then solvate onto the loosened ends as well as onto the atoms attached to and involved in the peptide bonds. These solvate molecules are in turn solvated by others like themselves as well as by water, so that a huge lyosphere is built up with a more or less extended polypeptide chain as its central strut. The interlocking of such lyospheres in moving past each other is thought to impart an increase in viscosity to the system which is a function of the size and shape of the lyospheres as well as of the fraction of the space occupied by them and the amount of interlocking.

We believe that figure 2 indicates that when the salt-bridges are neutralized the polypeptide chain does not unwind at once to form its extended and most random configuration but that unwinding occurs slowly from rotation on bonds produced by thermal agitation. The unwinding successively makes more of the polypeptide chain available for solvation. The gradual increase in the duration of the emptying periods with the lapse of time is interpreted to mean that the increase in the elongation and solvation processes is responsible. The maximum in the duration of the emptying periods, which was reached 284 hr. after the acetic acid and the solution of egg albumin had been mixed, is interpreted to mean that the configuration of the polypeptide chain has reached its highest state of randomness and that the solvation has become a maximum.

It is quite probable that the polypeptide chain also unwinds after the salt-bridges have been neutralized by sulfuric acid, but, since there is very little of the sulfuric acid present, solvation of the chain does not have an appreciable effect.

We believe that the lyospheres, which are formed according to the mechanism described above, may penetrate each other somewhat, but that in general they repel each other, owing to like charges on the polypeptide chains. In the case of denaturation by acetic acid each lyosphere should carry twenty-eight positive charges, which are balanced by a like number of acetate contraions. On this basis it is believed that, by selective adsorption, the anions of added salts neutralize the positive charges on the protein cation. After electrical neutralization there are no repelling forces between the elongated lyospheres, so that collisions between them can result in cohesion and flocculation. However, the addition of variable quantities of salts, which are sufficient to effect only a partial electrical neutralization, results in variable degrees of cohesion of the lyospheres when they collide, owing to the interpenetration of the overlapping portions of the lyospheres with hydrogen-bond formation among the solvating molecules. In this manner chains of lyospheres are built up which cross each other in entirely random directions. At the points of crossing of these chains there will be cohesion by the same mechanism that is operative when lyospheres link together to form chains. That a multivalent anion can also act at a point of crossing of these chains to hold them in association by electrically neutralizing a positive charge on each one of as many lyospheres as the valency of the anion is indicated by figures 3 and 4. Such a mechanism accounts for the greater effectiveness of salts having multivalent anions over those having univalent anions in increasing the viscosity.

Any of the liquid medium which is not immobilized in the formation of the lyospheres has a high viscosity, owing to hydrogen-bond formation among acetic acid and water molecules. It is then thought to become entrapped in the three-dimensional meshes of the cohering lyosphere chains. The rigidity of the resulting gel depends upon: (*1*) The protein concentration. (*2*) The completeness of unwinding of the denatured egg albumin molecules, and hence the time interval which has elapsed since the mixing of the components. Figures 2, 3, and 4 all illustrate this point. (*3*) The amount of solvation of the polypeptide chain, and hence the concentration of the solvating molecules as well as their relative ability to form many and strong hydrogen bonds. (*4*) The concentration of salt and the valency of the effective ion. This is well illustrated by figures 3 and 4. Figure 4 shows the greater effectiveness of higher concentrations of a tetravalent anion over corresponding concentrations of a divalent anion and, in turn, of the divalent anion over a univalent anion.

Varying these factors in all possible ways gives systems which have any degree of viscosity or which have gel structures of any rigidity. There result sols of variable viscosity, labile gels, thixotropic gels, rigid gels, gels in which the disperse phase shows variable flocculation, and coagulated systems having low viscosities.

We believe that the solation of the thixotropic gels by mechanical shear is due to the breaking of the relatively weak hydrogen bonds which hold the lyospheres together. After the shearing stress is removed, there occurs a re-formation of these hydrogen bonds either at the same or (much more likely) at different points than was the case previous to solation. The amount of time required for the gel to re-form depends upon the degree of disruption of the three-dimensional meshwork of lyospheres and hence upon the vigor with which and the duration of time for which the system is shaken.

RESUMÉ

The explanation given above to account for the gel structures and the thixotropic breakdown and re-formation of the systems studied is a combination of the common theories of gel structure. We have given a logical explanation of the elongation and solvation of the disperse phase to form anisometric lyospheres without postulating any unknown forces acting over large distances in order to account for the formation of solvated hulls. In this way the greatest weakness of the solvated hull theory has been avoided. Also, we do not follow this theory to the extent that the interlocking of the lyospheres is alone thought to be responsible for the establishment of a gel structure. Instead we describe a mechanism according to which the elongated lyospheres are able to link together to form chains and three-dimensional meshworks which entrap any of the dispersion medium not involved in the formation of the solvated hulls. In this way we have modified the network theory of gel structure by postulating that the filaments making up the network are highly solvated previous to their linking together, instead of simply being the disperse phase alone. Also, we have modified the repulsion–attraction equilibrium theory by postulating that added salts decrease the repulsion between the like-charged particles of the disperse phase which have already become highly solvated before the salt is added. The salt is then thought to decrease the repulsion between the elongated lyospheres to the extent that they can cohere enough so as to permit them to link together by the formation of hydrogen bonds among the molecules of the interpenetrating solvated hulls.

REFERENCES

(1) Anson, M. L., and Mirsky, A. E.: J. Gen. Physiol. **15**, 341 (1931).
(2) Astbury, W. T.: Trans. Faraday Soc. **29**, 193 (1933).
(3) Bergmann, M., and Niemann, C.: Science **86**, 187 (1937).
(4) Chambers, R.: Proc. Soc. Exptl. Biol. Med. **19**, 87 (1921).
(5) Cohn, E. J.: Cold Spring Harbor Symposia Quant. Biol. **6**, 8 (1938).
(6) Errera, J., and Hirshberg, Y.: Biochem. J. **27**, 764 (1933).
(7) Eyring, H., and Stearn, A. E.: Chem. Rev. **24**, 253 (1939).
(8) Fauré-Frémiet, E.: Trans. Faraday Soc. **26**, 779 (1930).
(9) Fischer, E.: *Untersuchungen über Aminosäuren, Polypeptide und Protein.* J. Springer, Berlin (1906).
(10) Freundlich, H.: Kolloid-Z. **46**, 289 (1928).
(11) Freundlich, H., and Abramson, H. A.: Z. physik. Chem. **131**, 278 (1928).
(12) Freundlich, H.: *Kapillarchemie,* 4th edition, Vol. II. Akademische Verlagsgesellschaft m.b.H., Leipzig (1932).
(13) Freundlich, H.: *Thixotropy.* Hermann et Cie., Paris (1935).
(14) Freundlich, H.: Proc. Roy. Inst. Gt. Brit., March 20, 1936.
(15) Hamaker, H. C.: Rec. trav. chim. **56**, 727 (1937).
(16) Hauser, E. A.: Kolloid-Z. **48**, 57 (1929).
(17) Hauser, E. A.: J. Rheol. **2**, 5 (1931).
(18) Huggins, M. L.: J. Org. Chem. **1**, 407 (1936).
(19) Jirgensons, B.: Kolloid-Z. **74**, 300 (1936).
(20) Kallmann, H., and Willstätter, M.: Naturwissenschaften **20**, 952 (1932).
(21) Kekwick, R. A., and Cannan, R. K.: Biochem. J. **30**, 227 (1936).
(22) Kopaczewski, W.: Protoplasma **29**, 180 (1937).
(23) Lassettre, E. N.: Chem. Rev. **20**, 259 (1937).
(24) Loeb, J.: *Proteins and the Theory of Colloidal Behavior.* McGraw-Hill Book Company, Inc., New York (1924).
(25) Loughlin, W. J., and Lewis, W. C. M.: Biochem. J. **26**, 476 (1932).
(26) Mirsky, A. E., and Pauling, L.: Proc. Natl. Acad. Sci. U. S. **22**, 439 (1936).
(27) Muralt, A. L., and Edsall, J. T.: J. Biol. Chem. **89**, 315 (1930).
(28) Myers, W. G.: Master's Thesis, The Ohio State University, 1937.
(29) Neurath, H.: J. Am. Chem. Soc. **61**, 1841 (1939).
(30) Pauling, L., and Brockway, L. O.: Proc. Natl. Acad. Sci. U. S. **20**, 336 (1934).
(31) Pauling, L., and Niemann, C.: J. Am. Chem. Soc. **61**, 1860 (1939).
(32) Pryce-Jones, J.: J. Oil Colour Chem. Assoc. **17**, 305 (1934).

(33) Rodebush, W. H.: Chem. Rev. **19**, 59 (1936).
(34) Russell, J. L., and Rideal, E. K.: Proc. Roy. Soc. (London) **A154**, 540 (1936).
(35) Schalek, E., and Szegvari, A.: Kolloid-Z. **32**, 318 (1923); **33**, 326 (1923).
(36) Schmidt, C. L. A. (Editor): *The Chemistry of the Amino Acids and Proteins.* Charles C. Thomas, Springfield, Illinois (1938).
(37) Sponsler, O. L., and Dore, W. H.: Ann. Rev. Biochem. **5**, 63 (1936).
(38) Svedberg, T.: Chem. Rev. **20**, 81 (1937).
(39) Svedberg, T.: Ind. Eng. Chem., Anal. Ed. **10**, 113 (1938).
(40) Werner, H.: Ber. **62B**, 1525 (1929).
(41) Wrinch, D. M.: Nature **137**, 411 (1936); **138**, 241 (1936); **139**, 972 (1937).
(42) Wrinch, D. M.: Phil. Mag. **26**, 313 (1938).
(43) Wu, H.: Chinese J. Physiol. **5**, 321 (1931).

THE INFRARED ABSORPTION OF PROTEINS IN THE 3 μ REGION. XII[1]

A. M. BUSWELL, KARL F. KREBS, and W. H. RODEBUSH

Department of Chemistry, University of Illinois, Urbana, Illinois

Received July 3, 1940

INTRODUCTION

The study of bound water in biological tissues has been handicapped from its inception by the weaknesses inherent in the methods used for the determination of bound water. None of the various methods gives any clue as to the mechanism of bonding, and all are subject to criticism on the basis of the fundamental assumptions involved (12).

A possible mechanism for the bonding of water was suggested by Buswell in 1928 (3). His suggestion that water was bonded to gelatin by means of the hydrogen bond followed from a correlation of the paper by Latimer and Rodebush (17), who suggested the hydrogen-bond hypothesis, and the classic work in spectroscopy of Coblentz (9), who had noticed peculiarities in the infrared absorption of water at 1.5 μ when present as "water of constitution" in certain minerals and in a gelatin film.

The work of Wulf and Liddel (21, 13), who showed that the first harmonic of the hydroxyl group disappeared when opportunities for hydrogen bonding were present, indicated that the infrared absorption technique offered a method of testing this proposed mechanism, and also gave promise of being adaptable to quantitative determination of bound water in biological hydrogels.

---

[1] **Presented at the Seventeenth Colloid Symposium, held at Ann Arbor, Michigan, June 6–8, 1940.**

In a previous publication (6) a curve was given for the absorption spectrum for gelatin in various stages of hydration. Absorption bands were found at 3.37, 3.2, and 3 μ. At that time the 3.4 was assigned to the HC vibration, and the 3 μ band, since it varied widely with water content, was assumed to be a measure of bound water. Although the 3.2 band appeared to vary somewhat with the water content, it was tentatively assigned to O—H—N or N—H—N bonding. Recent work now rules out the possibility of NH—N (10).

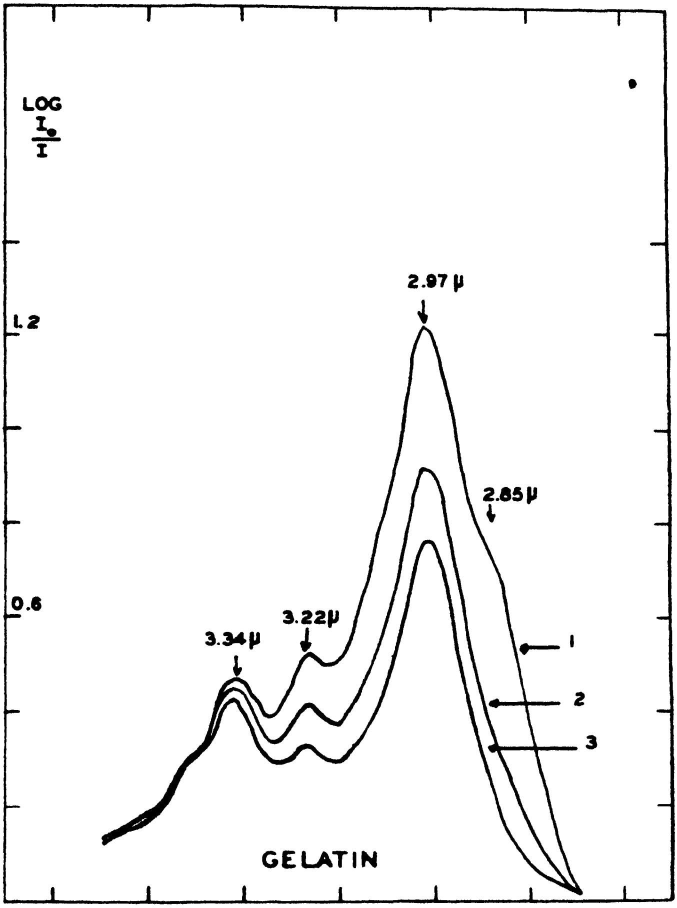

FIG. 1. Absorption curves for gelatin. Curve 1, air-dried; curve 2, dried at 102°C. for 2 hr.; curve 3, dried at 152°C. for 4 hr.

On the replotting of our data (see figure 1), placing the height of the 3.37 bands at the same elevation in all cases (a procedure which we now find to be justified), there appears to be practically no variation in the

3.2 band with water content and no change in the height of the 3 μ band between specimens dried at 102° and 152°C. Curves of specimens of appreciable moisture content show a distinct broadening or shoulder at the shorter wave length, at about 2.90 μ.

It also appears that the suggestion of Ellis and Bath (11) that "the absorption at 3 μ . . . in a gelatin specimen dried for 14 hours at 122°C. is caused by protein NH groups rather than by residual water" is a valuable one and at least partially correct. It must be pointed out, however, that the NH frequency itself is relatively weak, while the 3 μ band in dry gelatin is very strong. It is further known that the HN frequency is much shorter than 3 μ, namely, 2.83 to 2.93 (7). However, as in the case of water, the shift to longer frequency with bonding results in greatly increased intensity of absorption. This 3 μ band now appears to be due to a linear NHO bonding plus the effect of absorbed water. The hydration of proteins, as shown in this earlier work as well as in that on zinc insulinate as presented in this paper (figure 2), is evidenced by greatly increased absorption in the 3 μ region, with distinct broadening and in some cases a shoulder at approximately 2.90 μ.

Owing to the complexity of the NH and OH absorption spectra in the bonded state, it has been necessary to determine the various bonding frequencies of these groups in simple organic molecules and also to work out their absorption spectra when present in such complicated structures as the proteins. This work is reported elsewhere (10). The present work is then a report of the infrared absorption of a series which includes members of several of the classes of proteins based upon solubilities.

EXPERIMENTAL

The spectrometer used was one of the prism type, built in this laboratory in 1936. The source of radiation was a street-lamp bulb, which was supplied with a current of 7 amperes from the 110 D.C. line balanced against six 2-volt storage batteries to avoid line fluctuations. A more detailed discussion of the instrument is available in a previous publication (8).

The materials studied were all too insoluble in suitable solvents to permit study in the solution form, and so a method for obtaining them in the form of a thin film was devised. The solution of the protein was evaporated on a 24 x 50 mm. microscope cover slide floating on mercury. The use of 0.5 cc. of a 1 per cent solution of the protein in water, 0.6 per cent ammonium hydroxide, or 70 per cent alcohol, depending upon the properties of the protein, gave a film of the desired thickness.

Films built up by the Langmuir technique (2, 16) were also tried, but were abandoned in favor of the simpler deposition method when no appreciable qualitative differences in the two types of film were found. The method would have a distinct advantage in quantitative determinations, in that the molecular absorption coefficient could be calculated from the known number of layers. The preparation of such films would be laborious, since they would have to be about five thousand layers in thickness.

In the hydration studies on two of the proteins, gelatin and insulin, a cell provided with air ducts to permit the passage of air across the film was used. This arrangement made it possible to regulate the degree of hydration of the film without removing it from the absorption cell. Different degrees of hydration were effected by passing the air through saturated salt solutions of known vapor pressure.

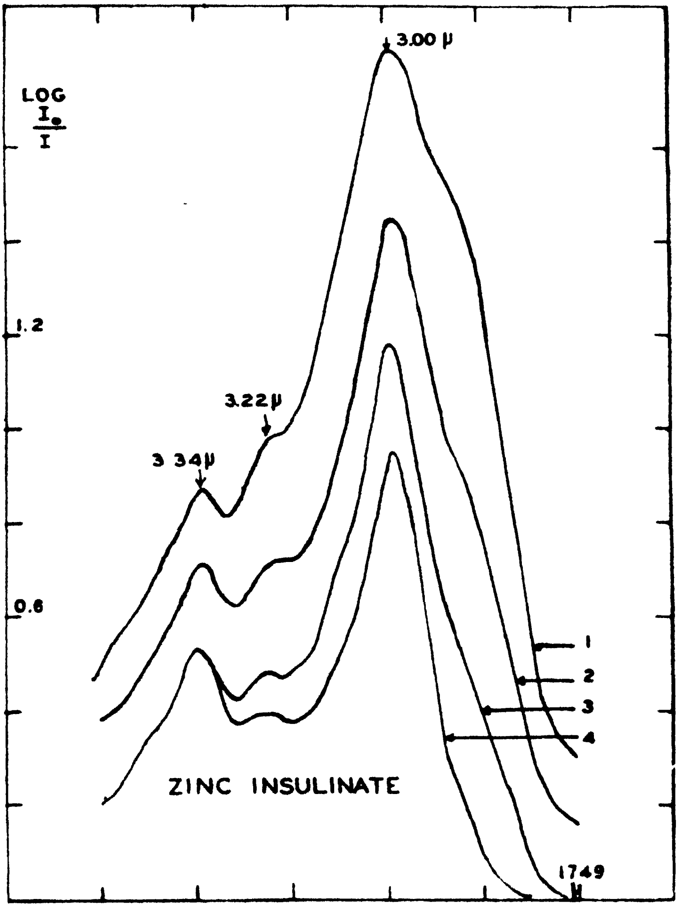

Fig. 2. Absorption curves for zinc insulinate. Curve 1, over barium chloride solution; curve 2, over magnesium nitrate solution; curve 3, air-dried; curve 4, over phosphorus pentoxide.

Data on the molecular extinction coefficient of absorbed water are necessary to complete the solution of the problem. It has been impossible to obtain such data with the experimental technique outlined above, for the following reasons: the material is very opaque and the absorption due to water is very intense. It is therefore necessary to use very thin films in order to permit the passage of sufficient energy to obtain satisfactory galvanometer readings. The actual change in weight of a 24 x 50 mm. film between different degrees of hydration is very close to the limit of error of even a microbalance. A large number of attempts to determine molecular extinction coefficients of absorbed water, at both 1.44 and 3 μ, have been unsuccessful.

TABLE 1

Absorption bands in sixteen proteins

COMPOUND	ABSORPTION PEAKS (WAVE LENGTH IN μ)					
Peptone	2.91	3.00		3.22	3.33	
Gelatin		2.97		3.22	3.34	
Rennet		2.97		3.20	3.38	
Zein		2.99		3.21	3.35	
Gliadin		2.99		3.21	3.34	
Hemoglobin		2.99		3.22	3.35	
Insulin		3.00		3.22	3.35	
Hordein		3.00		3.21	3.35	
Pepsin		3.01		3.22	3.35	
Salmine		3.01	3.09	3.20	3.35	
Glutenin		3.01		3.22	3.36	
Edestin		3.01		3.20	3.34	
Soybean protein		3.02		3.20	3.35	
Ficin		3.02		3.22	3.34	
Casein		3.02		3.22	3.34	
Egg albumin		3.03		3.22	3.34	
Glucose		2.96			3.40	
Agar		2.92			3.35	
β-Amylose		2.96			3.39	
Glycyl-*dl*-alanine	2.85		3.09	3.22	3.36	
α-Bromoisocaproylleucine	2.79	3.03		3.23	3.35	
Alanine				3.23	3.40	3.48
Proline		2.97	3.14		3.34	
Urea	2.91	2.99 and 3.04				
N-Butylurea		2.97 and 3.04			3.36	3.42
Thiourea	2.96	3.03	3.12			
N-Phenyl-N′,N′-dibutylthiourea		3.05		3.24	3.36	3.43

RESULTS

The absorption bands found in the sixteen proteins studied are given in table 1, together with the data obtained in the study of certain other related compounds.

DISCUSSION

A. Proteins

The interpretation of the absorption peaks found in the proteins is based upon considerable experimental data obtained from the study of simple organic nitrogen compounds, as mentioned above (10).

The most logical interpretation of the results obtained from the study of compounds having a linkage of the amide type

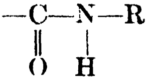

$$\begin{array}{ccccc} -\mathrm{C} & - & \mathrm{N} & - & \mathrm{R} \\ \| & & | & & \\ \mathrm{O} & & \mathrm{H} & & \end{array}$$

is that the absorption found at 3.00 μ is due to a single NH—O bond and that the band at 3.22 μ arises as a result of double NH—O bonds in a ring-dimer structure

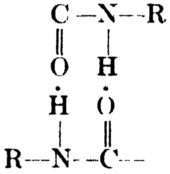

$$\begin{array}{ccccccc} & & \mathrm{C} & - & \mathrm{N} & - & \mathrm{R} \\ & & \| & & | & & \\ & & \mathrm{O} & & \mathrm{H} & & \\ & & \cdot & & \cdot & & \\ & & \mathrm{H} & & \mathrm{O} & & \\ & & | & & \| & & \\ \mathrm{R} & - & \mathrm{N} & - & \mathrm{C} & - & \end{array}$$

Gelatin and peptone (figure 3, curves 1 and 2) show relatively strong absorption at 3.22 μ, the band being distinct from the broad 3 μ band. This band resembles the absorption at 3.22 of *N*-ethylacetamide (7).

The natural proteins show much less pronounced absorption at 3.22. This is shown by a low peak in glutenin, ficin, zein, and gliadin (figure 4, curves 3 to 6) or by a mere shoulder on the 3 μ peak in the case of egg albumin, rennet, edestin, and soybean protein (figure 5, curves 7 to 10).

In the case of acid casein and rennet casein (figure 6, curve 11) there is more pronounced absorption at 3.22 in the former than in the latter. Also, among the natural proteins there is a distinct indication that the less drastic the method of isolation the less pronounced is the absorption at 3.22 μ. This cumulative evidence suggests a relation between the structure related to this band and the phenomenon of denaturation. As mentioned above, this 3.22 band is associated with the ring-dimer structure. In nature one might expect that in the presence of excess water it would bond to half the hydrophilic groups, thus

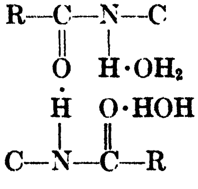

$$\begin{array}{ccccccc} \mathrm{R} & - & \mathrm{C} & - & \mathrm{N} & - & \mathrm{C} \\ & & \| & & | & & \\ & & \mathrm{O} & & \mathrm{H}\cdot\mathrm{OH_2} & & \\ & & \cdot & & & & \\ & & \mathrm{H} & & \mathrm{O}\cdot\mathrm{HOH} & & \\ & & | & & \| & & \\ \mathrm{C} & - & \mathrm{N} & - & \mathrm{C} & - & \mathrm{R} \end{array}$$

preventing ring formation. This water may be considered as "water of constitution." At the same time the natural products contain a large and variable amount of water which may be removed by mild desiccation and may be reabsorbed or reimbibed repeatedly. But on severe dehydration the water of constitution would be irreversibly removed and the ring structure, which is very stable, would be formed. The resulting material would be less soluble and less active in many ways. The above is not put forward as a complete theory of denaturation but only as a suggestion of a mechanism of part of the process.

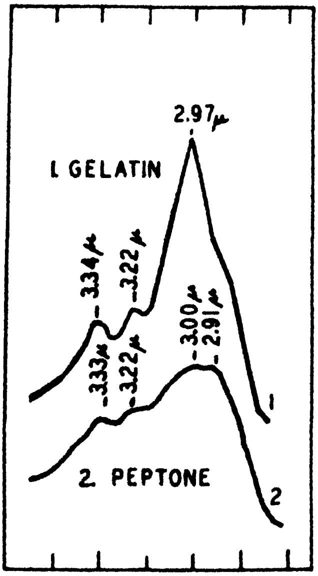

FIG. 3

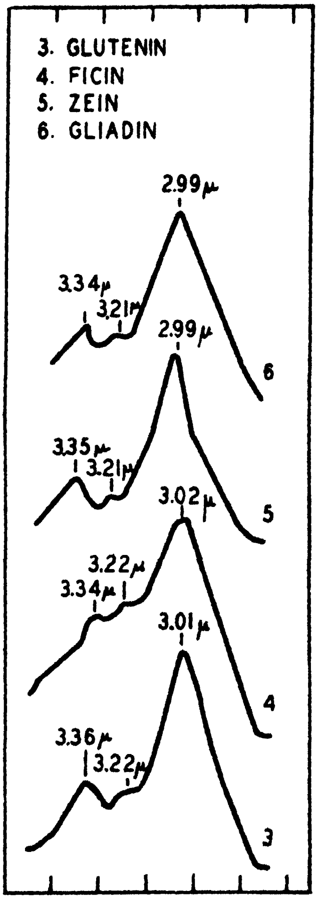

FIG. 4

FIG. 3. Absorption curves for gelatin and peptone
FIG. 4. Absorption curves for glutenin, ficin, zein, and gliadin

The appearance of the 3.22 and 3.00 μ bands in all of the proteins studied suggests the important rôle that the hydrogen bond plays in the structure of the proteins. These data afford experimental justification to the postulates of protein structures involving hydrogen bonds which have been made by several authors (18, 14, 15).

The spiralled beta-keratin structure suggested by Neurath (19) appeals to the authors as being highly probable, in that it would appear to permit a closer approach of adjacent polypeptide chains and thus allow hydrogen bonding of the ring-dimer type between the peptide links. This type of linkage would explain the appearance of both the 3.22 and 3.00 μ bands. The spiralled structure might be compared to two twisted threads with the peptide links as the points of contact. Of course, for fully extended polypeptide chains the situation is different.

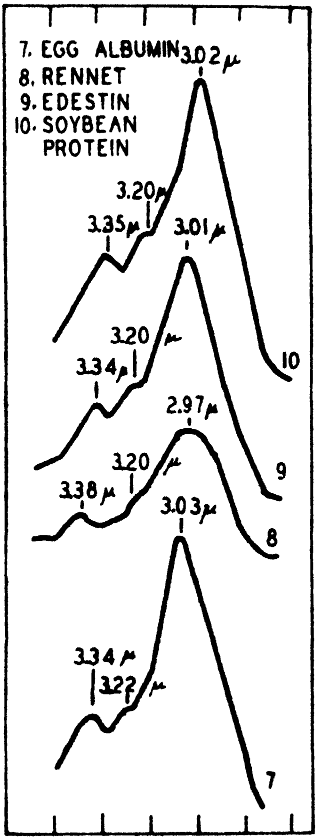

Fig. 5

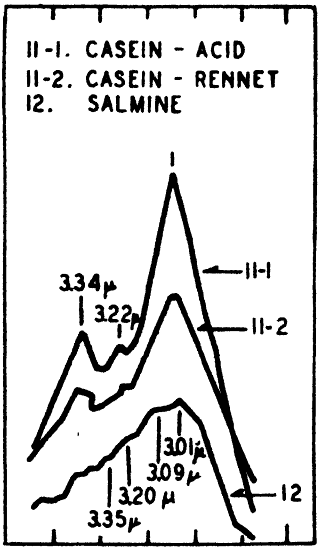

Fig. 6

Fig. 5. Absorption curves for egg albumin, rennet, edestin, and soybean protein
Fig. 6. Absorption curves for acid casein, rennet casein, and salmine

Salmine is a member of the protamine class of proteins; these yield on hydrolysis comparatively few amino acids, among which the basic ones predominate. Salmine, obtained from salmon sperm, contains 87 per cent of arginine, $NH_2C(=NH)NHCH_2CH_2CH_2CHNH_2COOH$, which has, in addition to the usual amino group, three extra nitrogen-hydrogen groups, one of which is an imino group. The typical protein, on the other hand, is made up of many different amino acids. Only a very small per cent of these amino acids contain NH groups other than the amino group.

One would expect, therefore, that salmine would show an absorption spectrum different from that obtained from most proteins. The band at 3.09 μ appearing in the absorption spectrum for salmine (figure 4, curve 12) is unique in the protein spectra so far obtained. It undoubtedly arises as a result of the large excess of nitrogen-hydrogen groups in the protein. One might predict that NH—O bonds involving the imino groups would appear at a wave length differing from the ordinary NH—O absorption. These NH—O bonds could be formed either through the $—NH_2$ or the $=NH$ groups of the amino acid side chains. Since this wave length is not far from the absorption at 3.16 μ in glycine and at 3.14 μ in unsubstituted acetamide, it seems probable that it is to be assigned to association through $—NH_2$ rather than $=NH$.

The need for further study of this protein and of simpler compounds containing the imino linkage is indicated. It is quite probable that very interesting structures could be postulated for salmine, if more exact data as to the type of bonding were available.

One is naturally concerned with the possibility of nonpeptide-nitrogen bonds in other proteins. In going through the structures of the amino acids which have been found in the proteins, one finds five amino acids containing non-peptide nitrogens:

Tryptophan,

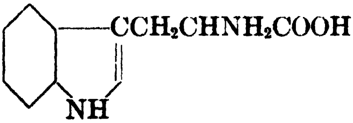

Histidine,

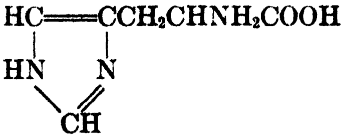

Lysine, $NH_2CH_2CH_2CH_2CH_2CHNH_2COOH$

Arginine, $NH_2C{=}NHNHCH_2CH_2CH_2CHNH_2COOH$

Citrulline, $NH_2CONHCH_2CH_2CH_2CHNH_2COOH$

Of these amino acids tryptophan is rarely present in amounts greater than 3 per cent, histidine is also low in most proteins, lysine varies from 0 to 8 per cent in the proteins considered here, the presence of citrulline in most proteins has not been verified, and arginine varies from 1 to 15 per cent in the usual protein.

The characteristics of the spectrum of salmine should be apparent in the spectrum of thymus histone, which contains 27 per cent of arginine, 9.7 per cent of lysine, and 5.8 per cent of histidine (20).

It can be seen that the hydrogen bondings due to the presence of these amino acids in the ordinary protein would be only a very small contribution to the total bonding due to the peptide linkage. Since the amino acids are probably arranged in some sort of periodic arrangement in the proteins (1), it would not be logical to assume that very many of these extra NH groups would be close enough together in the peptide chain to permit bonding. The absorption of the free N—H groups in the protein would probably resemble that of the primary and secondary aliphatic amines. This type of N—H absorption has been shown to be very weak in intensity (4), and therefore the presence of these few free amino groups, e.g., lysine, might very well be missed in the spectra of the proteins. The effect of the small amounts of histidine and tryptophan occurring in certain proteins cannot be detected in the absorption spectra with the present methods. One would expect, therefore, that there would be a great similarity in the absorption spectra in this region.

Peptone (figure 3) also shows a peculiarity in the infrared absorption, in that it has a distinct shoulder on the short-wave side of the 3.00 μ band. This peak, if separated from the 3.00 μ band, would occur a little below 2.9 μ. It appears likely that the band represents unbonded NH groups (10) in the protein fragments that make up the peptone. This might be expected in such a mixture of components, since there would be lack of orientation and complete randomness of arrangement.

So far in this discussion no mention has been made of differences appearing in the CH absorption of the proteins due to differences in the side-chain residues. The reason for this is that the CH band is not very prominent, and no significant observations can be made either as to prominence or exact location of the absorption maxima. The only differences detectable would be in the relative amounts of aliphatic and aromatic carbon-hydrogen, but the relative percentages of those amino acids having aromatic rings is fairly constant in the proteins and the percentage is also relatively low.

Bonding between hydroxyl or carboxyl groups in proteins is possible, but resolving power available does not permit their observation. Their number would be small in comparison to bonds involving nitrogen.

Structural linkages other than the hydrogen bond between chains are not detectable in the 3 μ region. Of these proposed linkages the disulfide might be expected to appear at a wave length greater than 10 μ, and the ester or salt linkages between acidic and basic amino acids might be detected in the carbonyl region at 5.8 μ.

B. Hydration studies

The bonded frequency for water-like hydroxyl groups has been shown to appear at a wave length slightly lower than 3 μ (5). The results from the study of the carbohydrates support these data, in that the bonded frequency occurs at 2.96 μ. The superposition of the absorption due to structural hydrogen bonding and of the absorption of bonded water hydroxyls make hydration studies on the carbohydrates impracticable in the 3 μ region. In the proteins these two types of bonding are separated to some extent, since the predominant type of structural hydrogen bonding involves the NH groups which show absorption in the bonded state at slightly longer wave length than the hydroxyl groups do. The shoulder that appears on the short-wave side of the 3 μ band (figures 1 and 2) gives a qualitative picture of water bonding, but the separation is not great enough for any quantitative measurements with the present technique and instrument. It is hoped that improvements in the weighing technique and the use of an instrument of greater resolving power will enable a quantitative determination to be made in the future.

SUMMARY

It has been shown that:

1. The proteins are characterized by absorption at about 3.4 μ (HC), at 3.22 μ (believed to be due to a ring formed by two peptide links bonded NH to O), and at 3 μ (a broad band due to linear NH to O).

2. Salmine shows additional absorption at 3.09μ (attributed to excess NH_2).

3. The band at 3.22 μ is much weaker in "unaltered" natural proteins than in gelatin, etc. It is suggested that this explains in part the mechanism of denaturation.

4. Hydration causes a broadening of the 3 μ band with a shoulder at about 2.9 μ.

REFERENCES

(1) Bergmann, M.: Harvey Lectures **31**, 37 (1936).

(2) Blodgett, K. B.: J. Am. Chem. Soc. **57**, 1007 (1935).

(3) Buswell, A. M.: *The Chemistry of Water and Sewage Treatment*, American Chemical Society Monograph No. 38, pp. 53, 60. Reinhold Publishing Corporation, New York (1928).

(4) Buswell, A. M.: Unpublished data from this laboratory.

(5) Buswell, A. M., Deitz, V., and Rodebush, W. H.: J. Chem. Phys. **5**, 501 (1937).

(6) Buswell, A. M., Krebs, K. F., and Rodebush, W. H.: J. Am. Chem. Soc. **59**, 2603 (1937).

(7) Buswell, A. M., Rodebush, W, H., and Roy, M. F.: J. Am. Chem. Soc. **60**, 2444 (1938).
(8) Claussen, W. F.: Thesis, University of Illinois, 1939.
(9) Coblentz, K. K.: J. Franklin Inst. **172**, 309 (1911).
(10) Downing, J. R.: Thesis, University of Illinois, 1940.
(11) Ellis, J. W., and Bath, J. D.: J. Chem. Phys. **6**, 108 (1938).
(12) Fisher, H.: Thesis, University of Illinois, 1936.
(13) Hilbert, G. E., Wulf, O. R., Hendricks, S. B., and Liddel, U.: J. Am. Chem. Soc. **58**, 548 (1936).
(14) Huggins, M. L.: J. Am. Chem. Soc. **61**, 755 (1939).
(15) Huggins, M. L.: Paper presented at Ninety-ninth Meeting of the American Chemical Society, held at Cincinnati, Ohio, April, 1940.
(16) Langmuir, I.: Science **85**, 76 (1937).
(17) Latimer, W. M., and Rodebush, W. H.: J. Am. Chem. Soc. **42**, 1419 (1920).
(18) Mirsky, A. E., and Pauling, L.: Proc. Natl. Acad. Sci. U. S. **22**, 439 (1936).
(19) Neurath, H.: J. Phys. Chem. **44**, 296 (1940).
(20) Schmidt, C. L. A. (Editor): *Chemistry of the Amino Acids and Proteins.* Charles C. Thomas, Springfield, Illinois (1938).
(21) Wulf, O. R., and Liddel, U.: J. Am. Chem. Soc. **57**, 1464 (1935).

ULTRACENTRIFUGATION STUDIES ON TOBACCO MOSAIC AND BUSHY STUNT VIRUSES[1]

MAX A. LAUFFER

Department of Animal and Plant Pathology, The Rockefeller Institute for Medical Research, Princeton, New Jersey

Received July 3, 1940

The plant viruses which have thus far been obtained in a highly purified state may be divided into two groups,--those which are rod-shaped and those which are essentially spherical. Of the first group, tobacco mosaic virus (20) is the easiest to study, for it is highly stable and may be isolated as a crystalline protein in comparatively large quantities. Of the second group, only tomato bushy stunt virus (2) is available in crystalline form. Much information is available concerning the physical properties of both of these materials. Tobacco mosaic virus solutions exhibit strong double refraction of flow (11), electrical double refraction (10), and anomalous viscosity (7, 19). Concentrated solutions give rise to micro-tactoids which separate out into liquid crystalline phases (3). The material crystallizes in the form of rod-like para-crystals of microscopic size (20), and the virus particle itself is a rod-like body from 12 to 15 mμ thick and from 300 to 500 mμ in length (12, 13). The bushy stunt virus, on the other hand, does not exhibit stream double refraction, and it crystallizes in the form of beautiful dodecahedra (2, 21). From a consideration of the diffusion and the sedimentation rates of this virus, it has been suggested that the particle is either hydrated to an appreciable extent or has an asymmetry of about 5:1 (15); x-ray diffraction studies, on the other hand, indicate that the particles are essentially spherical (4). It seems probable that the degree of asymmetry is small. Although both of these viruses have been the subject of ultracentrifugation studies in the past (5, 15, 22), it was thought that a direct comparison of the behavior of the two in the ultracentrifuge under comparable conditions would be of interest from a colloid-chemical point of view.

---

[1] Presented at the Seventeenth Colloid Symposium, held at Ann Arbor, Michigan, June 6-8, 1940.

METHOD AND MATERIALS

An air-driven ultracentrifuge of the type described by Bauer and Pickels (1), equipped with a "turret" drive (18) and a Lamm scale (8) optical system, was used in this study. It was operated at room temperature at a speed of 18,000 R.P.M. for the bushy stunt virus and at a speed of 14,400 R.P.M. for the tobacco mosaic virus. The speed was measured stroboscopically, utilizing a flashing neon lamp actuated by the vibrations of standard 60-cycle alternating current. A thermocouple was employed to measure the temperature of the rotor before and after each run, and the mean temperature was used in correcting the sedimentation rate to its value in water at 20°C. This computation, involving a correction for the viscosity of the solvent and the density of the solution, was carried out in the manner described in a previous publication (14). In the cases of the more dilute solutions, the density of the solution was assumed to be equal to that of the solvent, but for the more concentrated solutions the effect of the solute was taken into consideration in calculating the density. The partial specific volume of tobacco mosaic virus was taken to be 0.730 and that of the bushy stunt virus 0.739.

Four different preparations of bushy stunt virus were used. Preparations 1 to 3, inclusive, were isolated by means of differential centrifugation from tomato and *Datura stramonium* plants. Sample 4 was isolated from the same supply of plants as was sample 3, but chemical means were used. These four samples are described in detail by Stanley (21). They correspond to samples 2, 5, 6, and 6a, respectively, as described in his paper. Three preparations of tobacco mosaic virus were used. All were isolated from freshly harvested diseased Turkish tobacco plants by subjecting the expressed juice to three or four differential centrifugation cycles. Although dipotassium phosphate is often added to the ground plant material before extracting the juice, no phosphate was used in the isolation of the three samples of tobacco mosaic virus under consideration. Water was used to dissolve the pellets of virus obtained upon centrifugation, and the samples were stored dissolved in water. Just before making a run with either tobacco mosaic or bushy stunt virus, sufficient molar phosphate buffer at about pH 7 was added to a virus solution of the desired concentration to bring the phosphate content to 0.1 *M*. The molar phosphate buffer consisted of a mixture of molar solutions of monopotassium and dipotassium phosphate in the ratio of 1:2.2.

DISCUSSION OF RESULTS

The character of the sedimenting boundaries

In the Lamm method, a picture of a finely ruled scale is taken through the sedimenting column. At the virus-buffer boundary there is a refraction gradient which causes the photographic image of the scale to be distorted. By plotting the displacements of the scale against the distances through the boundary, one is able to get a graphic picture of the degree of diffuseness of the boundary. In figure 1 are represented more or less typical sedimenting boundaries of bushy stunt virus and tobacco mosaic virus. It may be observed that, as the sedimentation progresses away from the center of rotation, both the tobacco mosaic virus and the bushy stunt virus boundaries tend to become more diffuse. In the case of materials like the ones under consideration, in which diffusion proceeds very slowly, this broadening of the boundary could be due either to mechanical mixing of some sort or to heterodispersity of the virus. It is not possible at present to eliminate either of these possibilities. It is important to observe that, at least qualitatively, the tobacco mosaic virus boundary is similar to that of the bushy stunt virus. Both boundaries resemble those obtained by Eriksson-Quensel and Svedberg (5) for tobacco mosaic virus, which were interpreted as being evidence of particle heterodispersity, rather than those obtained by McFarlane and Kekwick (15) for bushy stunt, which were interpreted as being evidence of unusual homogeneity. Boundaries for both tobacco mosaic and bushy stunt viruses which show much less tendency to become diffuse than those here shown have been obtained, but only with more concentrated solutions. No attempt is made to interpret the curves here shown quantitatively in terms of a distribution of particle sizes, because the natures of their bases are not known with sufficient certainty.

Variation in the estimate of the sedimentation constant

The results of the sedimentation experiments on bushy stunt virus at various concentrations in *M*/10 phosphate buffer at pH 7 are summarized in table 1, and those on tobacco mosaic virus under similar conditions in table 2. The identities of the samples, the concentrations of virus, and the sedimentation constants corrected to water at 20°C. are listed in the tables. In figure 2 the sedimentation constants are plotted as functions of virus concentrations. The straight lines representing both sets of data were fitted by the method of least squares, and the probable error of estimate for each curve was calculated. The formal interpretation of this

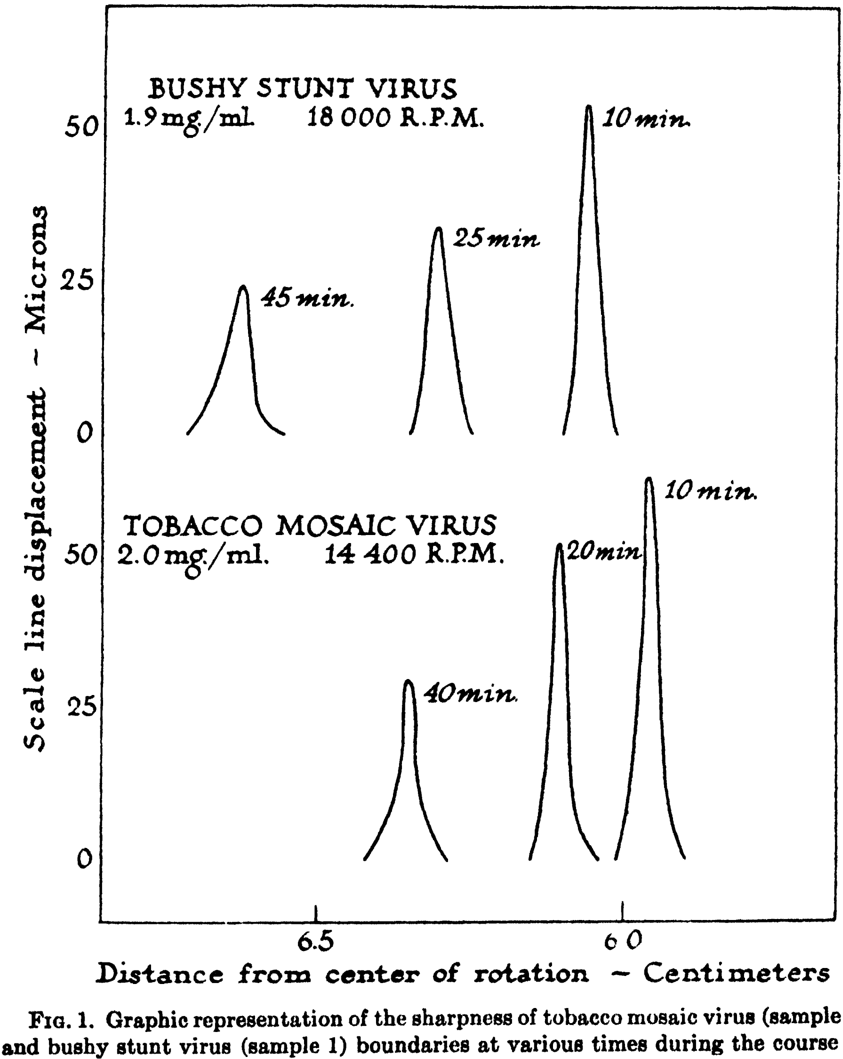

FIG. 1. Graphic representation of the sharpness of tobacco mosaic virus (sample 1) and bushy stunt virus (sample 1) boundaries at various times during the course of sedimentation. As ordinates are plotted the displacements of scale lines in microns, which are proportional to the refraction gradients, and as abscissas are plotted the positions of the distorted lines measured in centimeters from the axis of rotation. Distance from scale to cell = 1.8 cm.; scale to objective = 300 cm. Enlargement factor = 1.0.

statistic as here calculated is that, for a given virus concentration, there is a 50-50 chance that a single determination of the sedimentation constant will not differ from the value represented by the regression line by more than the probable error. For both viruses the probable error is fairly high, ±1.9 × 10^{-13} for bushy stunt and ±4.9 × 10^{-13} for tobacco mosaic. As yet, the reason for this variability has not been determined. However, in most of the sedimentation studies that have been published on viruses, variability of this order of magnitude was encountered.

TABLE 1

Sedimentation constants of tomato bushy stunt virus at various concentrations in M/10 phosphate buffer at pH 7

SAMPLE	CONCENTRATION OF VIRUS	$S_{w20} \times 10^{13}$	SAMPLE	CONCENTRATION OF VIRUS	$S_{w20} \times 10^{13}$
	mg. per ml.			*mg. per ml.*	
1	0.76	130.3	1	3.8	135.2
1	0.95	131.3	1	3.8	134.2
1	0.95	133.3	2	2.1	127.8
1	1.5	134.2	2	10.7	132.2
1	1.7	129.2	3	2.2	134.7
1	1.7	129.2	3	8.5	128.0
1	1.9	136.2	3	10.0	127.5
1	1.9	128.2	4	7.5	128.5
1	3.1	127.2			

TABLE 2

Sedimentation contants of tobacco mosaic virus at various concentrations in M/10 phosphate buffer at pH 7

SAMPLE	CONCENTRATION OF VIRUS	$S_{w20} \times 10^{13}$	SAMPLE	CONCENTRATION OF VIRUS	$S_{w20} \times 10^{13}$
	mg. per ml.			*mg. per ml.*	
1	1.6	188.8	2	2.1	182.5
1	1.8	179.9	2	3.3	177.3
1	1.8	196.2	2	4.1	182.2
1	1.9	184.3	2	4.9	187.8
1	2.0	189.8	2	4.9	185.3
1	2.1	185.8	2	6.6	184.8
1	2.2	177.3	2	8.2	163.8
1	2.2	179.9	2	11.5	159.1
1	2.3	190.8	2	14.8	142.3
1	3.6	189.2	2	14.8	159.0
1	7.1	177.9	3	2.0	177.5
1	14.3	159.5	3	12.7	139.6
1	25.7	124.5	3	27.7	109.0
2	1.0	193.3	3	27.7	106.7

The sedimentation constant as a function of virus concentration

It becomes evident upon inspection of figure 2 that there is a strong dependence of the sedimentation constant of tobacco mosaic virus on the concentration of virus. The slope of the best fitting straight line is -2.93×10^{-13}, which means that the sedimentation constant is decreased 2.93×10^{-13} units when the concentration of the virus solution is increased 1 mg. per milliliter. This effect is probably associated with relatively strong forces between virus particles. The slope of the line would indicate that these forces diminish fairly rapidly as the solution is diluted. This conclusion is entirely consistent with many other facts that are known concerning the properties of tobacco mosaic virus solutions, for, although there can be no doubt that strong interaction exists in concentrated solutions of tobacco mosaic virus, viscosity, stream double refraction, electrical double refraction, and diffusion data all indicate that these forces largely disappear in solutions as dilute as a few milligrams per milliliter (13).

The great effect of the tobacco mosaic virus concentration on the sedimentation rate made it seem desirable to investigate the possibility that these virus solutions behave like gels rather than like sols in the ultracentrifuge. The sedimentation constant, S, is defined by the expression

$$S = \frac{1}{\omega^2 x} \frac{dx}{dt}$$

where ω is the angular velocity of the centrifuge, t is the time, and x is the distance of the sedimenting boundary from the center of rotation. Since, in an ideal solution at a definite temperature, the sedimentation constant is a characteristic of the solute, it is obvious from the above equation that if, in an experiment on an ideal solution in which the angular velocity is held constant, the logarithm of x is plotted against t, a straight line should be obtained, the slope of which may be used to evaluate S. According to Pedersen (17), when a gel sediments in the ultracentrifuge, the sedimentation velocity is not a constant but decreases asymptotically as the gel approaches an equilibrium condition, after which no further sedimentation takes place. This equilibrium is attained when the swelling pressure of the gel, which is thought to be approximately proportional to its concentration, just equals the hydrostatic pressure caused by the centrifugal field. In figure 3 the logarithm of the distance of the boundary from the center of rotation (x) is plotted against time of centrifugation (t) of tobacco mosaic virus solutions at concentrations of 25.7, 14.3, and 7.1 mg. per milliliter. No one of the curves shows any indication of the boundary approaching an equilibrium position. This means that, with respect to this criterion, even these very concentrated tobacco mosaic virus solutions behave more nearly like ideal solutions than like gels. Or, stated in other words, if the virus solutions are gels, their swelling pressures are very low compared to the hydrostatic pressure due to the centrifugal field.

As may be seen in figure 2, the dependence of the sedimentation constant of the bushy stunt virus upon the concentration is negligible compared to that of tobacco mosaic virus. Even the apparent relationship that is obtained may not be real, for it can be shown by a statistical procedure that there are about three chances in ten that the slope here shown could be due entirely to random errors in sampling a supply in which there is no correlation. This behavior tends to emphasize the fundamental difference between the properties of essentially symmetrical and extremely anisometric colloidal materials.

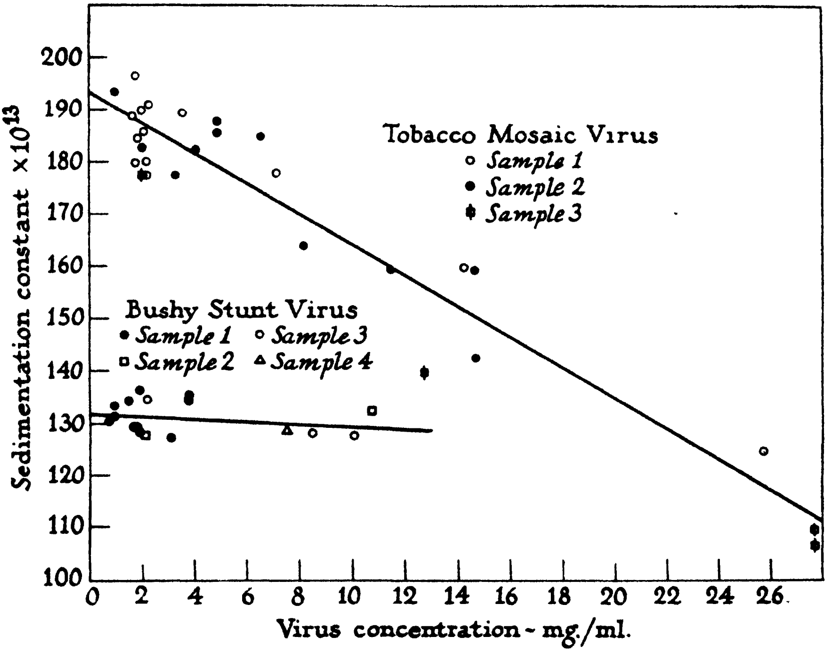

FIG. 2. Graphs showing the relationships between the sedimentation constants and the concentrations of bushy stunt and tobacco mosaic viruses.

The sedimentation constant at zero concentration

The variation of the sedimentation constant with the concentration is direct experimental evidence that tobacco mosaic virus solutions do not fulfill the requirements essential to the validity of Stokes' law; that is, the particles do not behave like isolated objects in a continuous medium of infinite extent. This conclusion was anticipated by Frampton (6), although direct experimental evidence has heretofore been lacking. This limitation may be circumvented readily by extrapolating the sedimentation

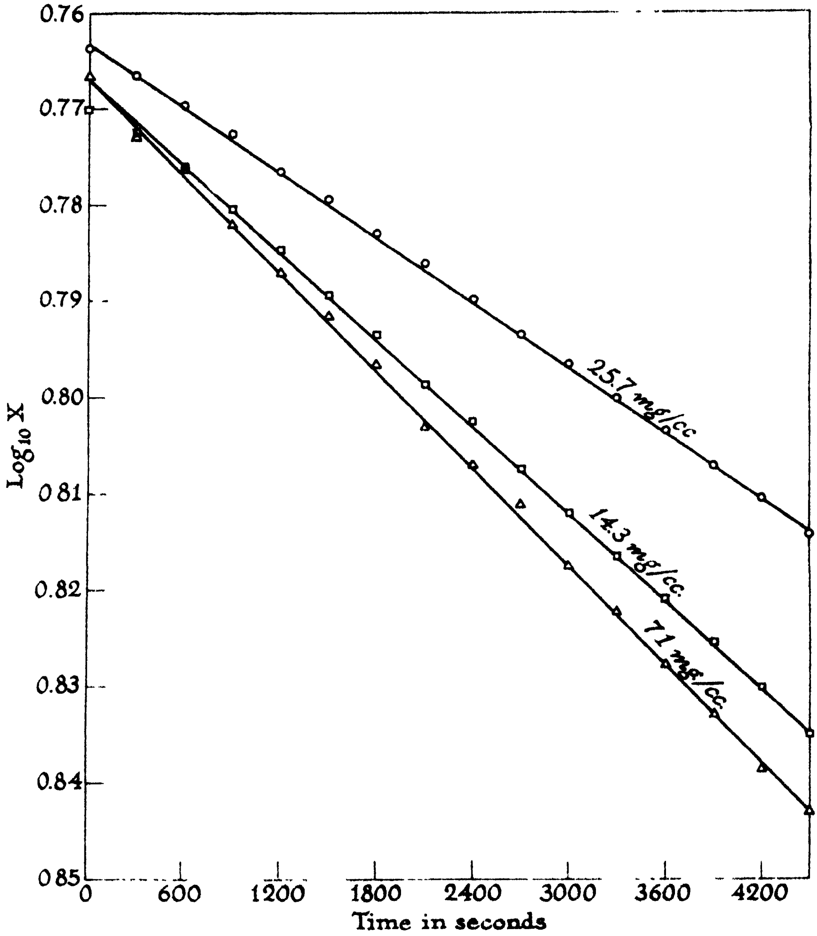

FIG. 3. Graphs showing the relationships between $\log_{10}$ of the positions of sedimenting boundaries measured in centimeters from the axis of rotation and the time of centrifugation in seconds for concentrated tobacco mosaic virus solutions (sample 1).

constant-concentration curve to zero concentration, thus obtaining the value that the sedimentation constant would have if the particles were absolutely independent of each other. The nature of the data in figure 2 makes it seem reasonable to extrapolate by simply extending the straight line. This procedure is at least partially justified by the fact that the stream double refraction and the viscosity of tobacco mosaic virus solutions more dilute than a few milligrams per milliliter are directly proportional to concentration (13), for these observations may be interpreted to mean that the interaction at concentrations of 2 mg. per milliliter should not be much greater than at infinite dilution, indicating that in the extrapolation the slope of the line should not be increased. The sedimentation constant of tobacco mosaic virus at infinite dilution obtained by extrapolating as suggested is 193 × 10^{-13} cm. per second unit field. This value is only about 3 per cent higher than the value for a virus concentration of 2 mg. per milliliter, indicating that the failure of such dilute solutions to obey Stokes' law rigidly introduces no really serious complication. Hence this factor, contrary to the impression left by a discussion by Frampton (6), probably has very little bearing on the validity of the attempts that have been made to interpret the sedimentation constant of tobacco mosaic virus in terms of particle size (9). This estimate of the sedimentation constant may be compared with the 174 × 10^{-13} reported as an average value by Wyckoff (22). It should not be confused with the sedimentation constant of the second component, about 200 × 10^{-13}, reported by Wyckoff, for we have on occasion obtained two boundaries in our studies, the slower of which corresponded to the 193 × 10^{-13} reported above, and the faster of which had a sedimentation constant about 33 units higher. When the sedimentation constant concentration curve for bushy stunt virus is extrapolated to zero concentration, a value for the sedimentation constant of 132.0 × 10^{-13} is obtained. This value does not differ appreciably from the average value of 131.6 × 10^{-13} which was reported previously for some of the same data here recorded (14). It may be compared with the average value of 146 × 10^{-13} obtained by McFarlane and Kekwick (15) for chemically purified virus. As we have reported previously, in a coöperative study on a single sample of bushy stunt virus isolated in our laboratory in which five centrifugation laboratories, including those of McFarlane and the writer, participated, the agreement from laboratory to laboratory was very good (14). In view of this, the sedimentation constants here recorded for bushy stunt and tobacco mosaic viruses are regarded as reasonably accurate values for the samples of the viruses actually studied. The disagreement between the values reported in the present paper and those of other workers may, in some instances, represent actual differences in the properties of the virus preparations studied.

SUMMARY

Several samples of bushy stunt and tobacco mosaic viruses, prepared by means of differential centrifugation, were studied at various concen-

trations in the ultracentrifuge. The sedimenting boundaries of the two viruses are qualitatively similar. Both become diffuse more rapidly than they should owing to diffusion alone. There is considerable variability in the estimates of the sedimentation constants of these viruses. It has been established that there is a strong dependence of the sedimentation constant of tobacco mosaic virus upon the concentration of the virus. However, the virus does not behave like a gel in the ultracentrifuge. The sedimentation constant of bushy stunt virus is almost independent of the virus concentration. The sedimentation constant at infinite dilution of tobacco mosaic virus is 193×10^{-13}, and that of bushy stunt virus is 132.0×10^{-13} cm. per second per unit field.

REFERENCES

(1) Bauer, J. H., and Pickels, E. G.: J. Exptl. Med. **65**, 565 (1937); In T. Svedberg and K. O. Pedersen's *The Ultracentrifuge*, p. 191, Oxford University Press, London (1940).
(2) Bawden, F. C., and Pirie, N. W.: Nature **141**, 513 (1938); Brit. J. Exptl. Path. **19**, 251 (1938).
(3) Bawden, F. C., Pirie, N. W., Bernal, J. D., and Fankuchen, I.: Nature **138**, 1051 (1936).
(4) Bernal, J. D., Fankuchen, I., and Riley, D. P.: Nature **142**, 1075 (1938).
(5) Eriksson-Quensel, I.-B., and Svedberg, T.: J. Am. Chem. Soc. **58**, 1863 (1936).
(6) Frampton, V. L.: Phytopathology **29**, 495 (1939).
(7) Frampton, V. L.: J. Biol. Chem. **129**, 233 (1939).
(8) Lamm, O.: Z. physik. Chem. **A138**, 313 (1928).
(9) Lauffer, M. A.: Science **87**, 469 (1938).
(10) Lauffer, M. A.: J. Am. Chem. Soc. **61**, 2412 (1939).
(11) Lauffer, M. A., and Stanley, W. M.: J. Biol. Chem. **123**, 507 (1938).
(12) Lauffer, M. A., and Stanley, W. M.: Chem. Rev. **24**, 303 (1939).
(13) Lauffer, M. A., and Stanley, W. M.: Kolloid-Z. **91**, 62 (1940).
(14) Lauffer, M. A., and Stanley, W. M.: J. Biol. Chem. **135**, 463 (1940).
(15) McFarlane, A. S., and Kekwick, R. A.: Biochem. J. **32**, 1607 (1938).
(16) Neurath, H., and Cooper, G. R.: J. Biol. Chem. **135**, 455 (1940).
(17) Pedersen, K. O.: In T. Svedberg and K. O. Pedersen's *The Ultracentrifuge*, p. 28. Oxford University Press, London (1940).
(18) Pickels, E. G.: Rev. Sci. Instruments **9**, 358 (1938).
(19) Robinson, J. R.: Proc. Roy. Soc. (London) **A170**, 519 (1939).
(20) Stanley, W. M.: Science **81**, 644 (1935).
(21) Stanley, W. M.: J. Biol. Chem. **135**, 437 (1940).
(22) Wyckoff, R. W. G.: J. Biol. Chem. **121**, 219; **122**, 239 (1937).

NEW BOOKS

Kinetics of Chemical Change. By C. N. HINSHELWOOD. 269 pp. London: Oxford University Press, 1940. Price: $4.50.

The present volume may be regarded as a fourth edition of the author's well-known work entitled *The Kinetics of Chemical Change in Gaseous Systems.* Instead of allowing it to expand to encyclopedic dimensions, which would be necessary to encompass all of the experimental material in this active field, the author has "cut the Gordian knot" by confining it to the general principles of chemical kinetics.

The illustrative examples of reaction types are suitably drawn from a wide field which is no longer limited to gaseous systems. The author aptly states that "successive editions of a book should get smaller and smaller." That this condensation has been effected in a very skillful and acceptable manner may be generally agreed.

S. C. LIND

Electrochemistry and Electrochemical Analysis. Vol. I. Electrochemical Theory. By HENRY J. S. SAND. 12 x 18.5 cm.; viii + 133 pp.; 9 fig.; 1 plate. New York; Chemical Publishing Co., Inc., 1939. Price: $2.00.

The primary object of this little book, written by one of the pioneers in the field of quantitative electroanalysis, is to explain the fundamental principles of electrochemical analysis, and incidentally to provide a review of electrochemical theory. The subject matter of the book covers all the main aspects of electrochemistry, as is evident from the following chapter headings: "Electrolysis and the Ionic Theory"; "Conduction of Current in the Interior of the Electrolyte"; "Application of the Law of Mass Action"; "Electromotive Force"; Activity and Theories of Interionic Attraction"; "Electrode Potentials and Liquid Junction Potentials"; and "Irreversible Electrode Processes."

The treatment, on the whole, is clear and accurate, although there appears to be room for improvement in some of the portions dealing with thermodynamics. A commendable feature is the consideration of all reversible electrodes as oxidation-reduction systems; the same standard equation for the electrode potential which covers all cases is then derived from the reaction isotherm, as suggested by Bancroft many years ago. The convention as to the sign of the electrode potential is the one generally employed by European physical chemists, which is not the same as that widely adopted in America; the author's arguments for the adoption of this convention (page 73) are, however, not convincing. The discussion of solubility product, of acids and bases, and of indicators follows classical lines; nevertheless, the book provides an excellent introduction to the principles of electrochemistry, and undoubtedly fulfills the author's purpose. The companion volume, dealing with the practical aspects of electrolytic methods of analysis, will be awaited with interest.

S. GLASSTONE.

Intermediate Chemical Calculations. By PARTINGTON AND STRATTON. 239 pp. London: Macmillan and Co., 1940. Price: $1.65.

This book consists of a collection of problems illustrating several of the laws and principles of general chemistry and of elementary physical chemistry. Each set of exercises is preceded by a brief statement of the quantitative laws to be illustrated and by one or two computations carried through in numerical detail. Answers to the problems are given at the end of the book. Most of the problems can be solved by direct substitution in formulae; however, a few, particularly in the chapter on "Organic Analysis," do require some thought on the part of the student. These more difficult exercises are carefully distinguished by asterisks, thereby preventing the discouragement of duller or less interested students who might otherwise have blundered onto them.

The authors have placed special emphasis on the gas laws, stoichiometric computations, and those calculations which are involved in quantitative analysis. By contrast, the field of physical chemistry is dealt with rather sketchily. Several subjects (including electromotive force, the properties of liquids and solids, reaction velocity, and surface phenomena) which are commonly included even in introductory or "short course" discussions of physical chemistry are completely omitted from this survey.

While this book is not adapted to the educational system of most American universities, it may prove useful to students who are attempting an independent review of their elementary chemistry or to teachers who wish to add a few straightforward practical problems to their list of exercises.

ROBERT LIVINGSTON.

Electronic Structure and Chemical Binding (with special reference to inorganic chemistry). By O. K. RICE. 6 x 9 in.; 511 pp. New York and London: McGraw-Hill Book Company, Inc., 1940. Price: $5.00.

The author discusses the modern theory of the chemical bond, drawing his references to experimental facts mainly from the field of inorganic chemistry. Since the book is written primarily for students of chemistry at the level of first-year graduate work, the content and mode of presentation have been determined with this aim in mind. Here the author meets a serious difficulty. On the one hand the problems of chemical binding must certainly be discussed on a broad background of atomic structure. This latter topic can only be rendered satisfactorily nowadays on the basis of our modern ideas of wave mechanics. This science therefore also forms the foundation of the modern notions of the structure of molecules and hence of the chemical bond. Therefore any book or treatise on theoretical chemistry must be written with these latest ideas as a cornerstone. Thus the problem arises as to how much knowledge of wave mechanics do the potential reader and students have? It is clear that a complete discussion of all of the problems involved in a book concerned with the fundamentals of theoretical chemistry on the basis of wave mechanics is out of the question, merely from the point of view of space. Hence the author cuts the Gordian knot of this difficulty by simply stating the results of wave mechanics on the supposition that the reader either has the knowledge or will be interested enough to acquire an acquaintance with modern concepts. Of course this method of procedure requires the use of such phrases as "it can be shown" or "on the basis of wave mechanics it can be demonstrated" etc. throughout the book, but it also forces the student to the realization that he must acquaint himself with modern concepts if he would understand the present theory of chemical binding. The demonstration of this need is really one of the definite accomplishments by the author. To any one familiar with modern ideas of wave mechanics the book is to be recommended, because the author has a very happy and clear mode of stating theoretical problems in a way that makes them living counterparts to the related facts.

The first eight chapters contain a very brief summary of the atomic theory of chemistry, the constitution of matter in its wave and corpuscular aspects, an elementary consideration of quantum theory of the hydrogen atom, the idea of electron spin, the Pauli principle, and a discussion of the many-electron atoms. Molecular potential-energy curves are used to discuss molecular spectra and the energy of dissociation. The hydrogen molecule is rendered on the basis of the Heitler–London treatment and the Hund–Mulliken method. These theories and Lewis' theory of valency are compared in chapter XI. Naturally the polar and covalent bonds are discussed fully, as are also the concepts of bond energy, electronegativity, and polarizability. The idea of resonance between different structures of a molecule is mentioned but is not stressed as much as might be expected. Chapters XIII and XIV contain a discussion of the solid state based on ionic radii, lattice energy, and the Born-Haber cycle. The problem of the covalent bond, directional valency, and magnetic considerations as to bond type find a brief discussion in chapter XV. What might be termed old-style advanced inorganic chemistry, i.e., the chemistry of complex compounds based on the concepts of coördination number, etc., is contained in chapter XVI, along with the one- and three-electron bond and the important problem of the hydrides of boron. van der Waals forces and molecular crystals are treated in chapter XVII, the metallic state in chapter XVIII, and the structure of water and solutions in chapter XIX. Every chapter ends with a short list of pertinent problems.

It is seen that this volume covers a tremendous field, and it is no wonder that many topics are mentioned only in barest outline. If students just entering the science of chemistry on the graduate level, for whom the book is intended, will study the modern science of wave mechanics, they will derive great benefit from a perusal of this edition.

Geo. Glockler.

International Union of Chemistry. Tables and Committee Reports.

International Table of Atomic Weights. Tenth Report, 1940. Committee: G. P. Baxter, *Chairman*; M. Guichard, O. Hönigschmid, R. Whytlaw-Gray.

International Table of Stable Isotopes. Fifth Report, 1940. Committee: F. W. Aston, *Chairman*; N. Bohr, O. Hahn, W. D. Harkins, F. Joliot, R. S. Mulliken, M. L. Oliphant.

Rules for Naming Inorganic Compounds. Report of the Committee, 1940. W. P. Jorissen, *Chairman*; H. Bassett, A. Damiens, F. Fichter, H. Remy.

S. C. Lind.

INDEX

Absolute rates of solid reactions, 955
Absorption, infrared, of proteins, 1126
Acetic acid-chloroform-acetone-water system, 683
Acetone-acetic acid-chloroform-water system, 683
  colloidal suspensions in, 21
Activated carbon as a catalyst in certain oxidation-reduction reactions, 70
Activities, solute, calculation of, from activities of the solvent, 306
  solute, in dilute solutions of non-electrolytes, approximate rules for, 313
Activity of the constituents in mixtures of *n*-butyl alcohol and water, 917
Addition compounds of iodine with alkali bromides and thiocyanates, 640
Adsorption of ions by pectin, 409
  of water vapor by gelatin sols and gels, 185
Agent, emulsifying, hydrous lanthanum hydroxide as, 259
Aging and coprecipitation, 921
  thermal, of imperfect barium sulfate, 921
Alanine, effects of certain salts on the dissociation of, 880
Alcohol, methyl, colloidal suspensions in, 12
  -water-benzene system, 404
Alcohols, effect of, on the heat of activation of silica gels, 1024
  sugar, 862
Aliphatic hydrocarbons, boiling point relationships among, 730
Alkyl fluorides, 275
Aluminum oxide-sodium oxide-water system, 909
  oxide, translucent films of, 401
  sulfate-silver sulfate-water, 256
Amino acids, reaction of formaldehyde with, 874
Ammonium polyiodides, 322, 325
Apparatus, vapor pressure, 574
Arginine, effects of certain salts on the dissociation of, 893
Aspartic acid, effects of certain salts on the dissociation of, 893
Asphaltic bitumen as colloid system, 139
  bitumens, rheological properties of, 149
Azeotropic system alcohol-water-benzene, 404

Barbituric acids, substituted, apparent dissociation constants of, 449
Barium sulfate, electrokinetic potentials of, 265
  sulfate, imperfect, thermal aging of, 921
Bentonites, metallized, catalysis by, 180
Benzene-alcohol-water system, 404
  colloidal suspensions in, 12
Bitumen, asphaltic, as colloid system, 139
Bitumens, asphaltic, rheological properties of, 149
Boiling point relationships among aliphatic hydrocarbons, 730
Boric acid, dissociation constant of, effect of anhydrides of sorbitol on, 862
Brønsted's criticism of classical thermodynamics, 713
Brownian movement, influence of, on the viscosity of solutions, 25
Bury's rule, generalized form of, 313
Bushy stunt viruses, 1137
Butyl alcohol-ethyl acetate-toluene system, 377
  alcohol-water mixtures, activity of the constituents in, 917

Calcite, fluorescent, 435
Calcium carbonate, precipitation from ammoniacal solutions, inhibiting action of minute amounts of sodium hexametaphosphate on, 535, 552

Calcium oxalate, solubility of, in various salt solutions, 166
Capillary luminescence analysis, 1071
Carbon, activated, as a catalyst in certain oxidation-reduction reactions, 70
  black, suspensions of, in mineral oil, 652
Catalysis by metallized bentonites, 180
Catalyst in certain oxidation-reduction reactions, activated carbon as, 70
Catalysts for hydrogenation, 670
Catalytic hydrolysis of chlorobenzene in the vapor phase, 727
  oxidation of hydrogen on platinum, 235
Cell, anomalous concentration, 1033
Cells, galvanic, subject to fields of force, theory of, 463
  galvanic, with liquid-liquid junctions, 101
  photovoltaic, with silver-silver bromide electrodes, 411
Cellulose, coagulated, fiber structures from, 513
  fibers, x-ray studies of crystallite orientation in, 513
Chlorobenzene, catalytic hydrolysis of, in the vapor phase, 727
Chloroform-acetic acid-acetone-water system, 683
Clays, colloidal behavior of, as related to their crystal structure, 1
Coefficient of thixotropy of suspensions of carbon black in mineral oil, 652
Colloid, protective, for manganese dioxide sols, 422
Colloidal behavior of clays as related to their crystal structure, 1
  behavior of Hevea latex, effect of proteins and electrolytes on, 788
  suspensions in non-aqueous solvents, preparation of, 12, 21
  systems, particle size determination in, 584
Concentration cell, anomalous, 1033
Conductance of salts in monoethanolamine, 388
Conduction, quasi-reversible, 101
Conductivity, electrical, of gelatin sols and gels, 185
Constant, Macleod, 1007
Constants, apparent dissociation, of substituted barbituric acids, 449
Convergence of tie lines in ternary liquid systems, 446
Copper-chromium oxide hydrogenation catalysts, 670
  single crystals of, 35
  sulfate, reaction with sodium silicate, 439
Coprecipitation, 921
Crystal structure and colloidal behavior of clays, 1
Crystallite orientation in cellulose fibers, x-ray studies of, 513
Crystals, single, of copper, 35
Cybotaxis at interfaces, 592

Dentine, normal human, light scattering in, 745
Derivation of the equilibrium conditions in physical chemistry on the basis of the work principle, 699
Deuterium water, solubilities in, 207
Development, photographic, by hydroquinone, 42
  photographic, mechanism of, 42
Dielectric properties of the system gelatin-water, 716
Diffusion, 955
  in liquids, theory of, 981
Dioxane, colloidal suspensions in, 21
  -potassium carbonate-water system, 629
Dissociation constant of boric acid, effect of anhydrides of sorbitol on, 862
  constants, apparent, of substituted barbituric acids, 449
  of alanine, effects of certain salts on, 880
  of aspartic acid, arginine, and ornithine, effects of certain salts on, 893
Dyes, optical sensitizing by, 411

Electric moments and relaxation times of protein molecules, 1103
Electrokinetics, 265
Electrolytes, strong, freezing points in mixtures of, 427
Elements, liquid state of, 808
Emulsifying agent, hydrous lanthanum hydroxide as, 259

Equilibrium conditions in physical chemistry on the basis of the work principle, derivation of, 699
Errata, 834
Erythrocytes, effect of Roentgen irradiation upon, 172
Ethanolamine, conductance of salts in, 388
Ether, colloidal suspensions in, 21
Ethyl acetate–butyl alcohol–toluene system, 377
Ethylene glycol-potassium carbonate–water system, 629

Ferric ion, photochemical reduction of, by oxalic acid, 949
Fiber structure, intermicellar hole and tube system in, 764
Fibers, cellulose, x-ray studies of crystallite orientation in, 513
Figures in thin layers of grease and viscous liquids, 612
Films, adsorbed, wetting characteristics of solid surfaces covered with, 86
  translucent, of aluminum oxide, 401
Flocculation values, influence of sol concentration on, 62
Fluorescent calcite, 435
Fluorides, alkyl, 275
Formaldehyde, reaction with amino acids, 874
Freezing points in mixtures of strong electrolytes, 427

Galvanic cells subject to fields of force, theory of, 463
  cells with liquid–liquid junctions, 101
Gas imperfection, 835
Gases, viscosities of, 1038
Gel, silica, sorption from solution by, 943
Gelatin gels, structure of, 185
  sols, structure of, 185
  water bound to, 996
  -water system, dielectric properties of, 716
Gels, gelatin, structure of, 185
  silica, time of set of, 1024
  silicic acid, 57, 847
  thixotropic, 1113
Gold sol formation, pH change in, 247
Grease, figures in thin layers of, 612

Hevea latex, effect of proteins and electrolytes on colloidal behavior of, 788
Hydrocarbons, aliphatic, boiling point relationships among, 730
  determination of second virial coefficients for, 835
Hydrogen on platinum, catalytic oxidation of, 235
  -bridge theory, application to sorption from solution by silica gel, 943
Hydrogenation catalysts, 670
Hydrolysis, catalytic, of chlorobenzene in the vapor phase, 727
Hydroquinone, photographic development by, 42
Hydrous oxides, electron diffraction study of, 1081

Interfaces, cybotaxis at, 592
Intermicellar hole and tube system in fiber structure, 764
Iodides of some polyvalent metals, 647
Iodine, addition compounds of, with alkali bromides and thiocyanates, 640
Irradiation, Roentgen, effect of, upon erythrocytes, 172

Lanthanum hydroxide as an emulsifying agent, 259
Latex, Hevea, effect of proteins and electrolytes on colloidal behavior of, 788
Light scattering in normal human dentine, 745
Liquid state of the elements, 808
  systems, ternary, convergence of tie lines in, 446
Liquids, theory of diffusion in, 981
  viscous, figures in thin layers of, 612
Luminescence analysis, capillary, 1071

Macleod constant, dependence on physicochemical factors, 1007
Manganese dioxide sols, silicic acid as a protective colloid for, 422
Mechanism of photographic development, 42
Metallized bentonites, catalysis by, 180
Metals, polyvalent, iodides of, 647

Methyl alcohol, colloidal suspensions in, 12
Mineral oil, coefficient of thixotropy of suspensions of carbon black in, 652
Molal volumes of solutes, 619
Moments, electric, and relaxation times of proteins, 1103

Non-electrolytes, solutions of, approximate rules for solute activities in, 313

Optical sensitizing by dyes, 411
Ornithine, effects of certain salts on the dissociation of, 893
Oxalic acid, photochemical oxidation of, 601
  acid, photochemical reduction of ferric ion by, 949
Oxidation, catalytic, of hydrogen on platinum, 235
  photochemical, of oxalic acid, 601
Oxides, hydrous, electron diffraction study of, 1081

Particle size determination of colloidal systems by the supercentrifuge, 584
Pectin, ion adsorption by, 409
pH change in gold sol formation, 247
  effect of, upon the time of set of silicic acid gels, 57
Phosphors, zinc silicate, 851
Photochemical oxidation of oxalic acid sensitized by ferric ion, 601
  reduction of ferric ion by oxalic acid, 949
Photographic development, mechanism of, 42
Photoöxidations, dye-sensitized, quantum yields of, 865
Photovoltaic behavior of pure silver bromide, 936
  cells with silver-silver bromide electrodes, 411
Platinum, catalytic oxidation of hydrogen on, 235
Polyiodides of ammonium, 322, 325
  of potassium, 350
  of rubidium, 633
Polypeptide chains, intramolecular folding of, in relation to protein structure, 296
Potassium carbonate-dioxane-water system, 629
  carbonate-ethylene glycol-water system, 629
  chloride solutions, specific heats of, 483, 494
  polyiodides, 350
Potentials, electrokinetic, of barium sulfate, 265
Precipitation of calcium carbonate from ammoniacal solution, inhibiting action of minute amounts of sodium hexametaphosphate on, 535, 552
  of silver chromate, 751
Protein molecules, electric moments and relaxation times of, 1103
  structure, intramolecular folding of polypeptide chains in relation to, 296
Proteins, infrared absorption of, 1126

Quantum yields of some dye-sensitized photoöxidations, 865

Radioactive standards, 824
Rates, absolute, of solid reactions, 955
Reaction of copper sulfate with sodium silicate, 439
  of formaldehyde with amino acids, 874
Reactions, solid, absolute rates of, 955
Reduction, photochemical, of ferric ion by oxalic acid, 949
Rheological properties of asphaltic bitumens, 149
Roentgen irradiation, effect of, upon erythrocytes, 172
Rubidium, polyiodides of, 633

Sensitizing by dyes, optical, 411
Silica gel, sorption from solution by, 943
  gels, time of set of, 1024
Silicic acid as a protective colloid for manganese dioxide sols, 422
Silicic acid gels, 57, 847
Silicon dioxide-sodium oxide-water system, 909
Silver bromide, pure, photovoltaic behavior of, 936
  chromate, precipitation of, 751
  sulfate-aluminum sulfate-water, 256
Skin reactions, 1094
Sodium chloride solutions, specific heats of, 483, 494

hexametaphosphate, inhibiting action on the precipitation of calcium carbonate from ammoniacal solutions, 535, 552
  iodide-water system, 373
  oxide-aluminum oxide-water system, 909
  oxide-silicon dioxide-water system, 909
  silicate, reaction with copper sulfate, 439
  stearate-water system, 1013
Sol concentration, influence of, on flocculation values, 62
  gold, 247
Solid reactions, absolute rates of, 955
Sols, gelatin, structure of, 185
  of manganese dioxide, silicic acid as a protective colloid for, 422
Solubilities of certain inorganic compounds in ordinary water and in deuterium water, 207
Solubility of calcium oxalate in various salt solutions, 166
Solute activities, calculation of, from activities of the solvent, 306
  activities in dilute solutions of non-electrolytes, approximate rules for, 313
Solutes, molal volumes of, 619
Solutions of non-electrolytes, approximate rules for solute activities in, 313
  viscosity of, influence of Brownian movement on, 25
Solvents, non-aqueous, chemical preparation of colloidal suspensions in, 12, 21
Sorbitol, anhydrides of, effect on the dissociation constant of boric acid, 862
Sorption from solution by silica gel, 943
Specific heats of some aqueous sodium and potassium chloride solutions, 483, 494
Stannous chloride, constitution of solutions in water and in hydrochloric acid, 1033
State, liquid, of the elements, 808
Sugar alcohols, 862
Supercentrifuge, particle size determination of colloidal systems by, 584
Suspensions, colloidal, in non-aqueous solvents, 12, 21
  of carbon black in mineral oil, coefficient of thixotropy of, 652
System acetic acid-chloroform-acetone-water, 683
  alcohol-water-benzene, 404
  ammonium iodide-iodine-water, 325
  butyl alcohol-ethyl acetate-toluene, 377
  dioxane-potassium carbonate-water, 629
  ethylene glycol-potassium carbonate-water, 629
  gelatin-water, dielectric properties of, 716
  intermicellar hole and tube, in fiber structure, 764
  potassium iodide-iodine-water, 350
  silver sulfate-aluminum sulfate-water, 256
  sodium iodide-water, 373
  sodium oxide-aluminum oxide-water, 909
  sodium oxide silicon dioxide-water, 909
  sodium stearate-water, 1013
Systems, colloidal, particle size determination in, 584
  ternary liquid, convergence of tie lines in, 446

Theory of diffusion in liquids, 981
  of galvanic cells subject to fields of force, 463
Thermodynamics, classical, Brønsted's criticism of, 713
Thixotropy, coefficient of, 652
Tie lines, convergence of, in ternary liquid systems, 446
Time of set of silicic acid gels, 57
Tobacco mosaic viruses, 1137
Toluene-butyl alcohol-ethyl acetate system, 377

Ultracentrifugation studies on tobacco mosaic and bushy stunt viruses, 1137

Vapor pressure apparatus, 574
Viruses, tobacco mosaic and bushy stunt, 1137

Viscosities of several common gases, 1038
Viscosity of solutions, influence of Brownian movement on, 25
Volumes, molal, of solutes, 619

Water-alcohol-benzene system, 404
  bound to gelatin, 996
  vapor, adsorption of, by gelatin sols and gels, 185
Wetting characteristics of solid surfaces covered with adsorbed films, 86
Work principle, derivation of the equilibrium conditions in physical chemistry on the basis of, 699

Zinc silicate phosphors, 851

AUTHOR INDEX

Abramson, Harold A., and Gorin, Manuel H. Skin reactions. IX. The electrophoretic demonstration of the patent pores of the living human skin; its relation to the charge of the skin, 1094

Addlestone, J. A., Marsh, L. R., and Hall, G. C. The system silver sulfate-aluminum sulfate-water, 256

Allison, L. R., Hartung, E. J., and Heymann, E. An anomalous concentration cell. The constitution of solutions of stannous chloride in water and in hydrochloric acid, 1033

Alrich, Miss F. R. *See* Briggs, T. R.

Anderson, Harold V., and Hochgesang, Frank P. The copper sulfate-sodium silicate reaction, 439

Arnold, J. E., and Goodeve, C. F. The coefficient of thixotropy of suspensions of carbon black in mineral oil, 652

Bachman, Irvin. Convergence of tie lines in ternary liquid systems, 446

Ballard, K. H. *See* Briggs, T. R.

Barclay, Raymond W. *See* Hurd, Charles B.

Bartell, F. E., and Bristol, Kenneth E. Wetting characteristics of solid surfaces covered with adsorbed films, 86

Batchelder, A. C., and Schmidt, Carl L. A. The effects of certain salts on the dissociation of alanine. II. Experiments on cells without liquid-junction potentials, 880

  and Schmidt, Carl L. A. The effects of certain salts on the dissociation of aspartic acid, arginine, and ornithine, 893

Bath, Jean D. *See* Sponsler, O. L.

Bell, Frederick K., Carr, C. Jelleff, and Krantz, John C., Jr. Sugar alcohols. XXI. A study of the effect of the anhydrides of sorbitol on the dissociation constant of boric acid, 862

Benton, Arthur F. *See* Gwathmey, Allan T.

Bonner, John F. *See* Manly, Richard S.

Bonner, Walter D., and Williams, Max B. The azeotropic system alcohol-water-benzene, 404

Brancker, A. V., Hunter, T. G., and Nash, A. W. The quaternary system acetic acid-chloroform-acetone-water at 25°C., 683

Briggs, T. R., and Ballard, K. H. Polyiodides of ammonium. I. Ammonium iodide and iodine, 322

  Ballard, K. H., Alrich, Miss F. R., and Wikswo, J. P. Polyiodides of ammonium. II. The ternary system ammonium iodide, iodine, and water, 325

  Clack, K. D. G., Ballard, K. H., and Sassaman, W. A. Polyiodides of potassium. II. The ternary system potassium iodide-iodine-water, 325

  and Geigle, W. F. Note on the system sodium iodide-water, 373

Briscoe, H. T., and Dirkse, Thedford P. The conductance of salts in monoethanolamine, 388

Bristol, Kenneth E. *See* Bartell, F. E.

Brønsted, J. N. The derivation of the equilibrium conditions in physical chemistry on the basis of the work principle, 699

Broughton, Geoffrey. Catalysis by metallized bentonites, 180

Buehrer, T. F. *See* Reitemeier, R. F.

Buswell, A. M., Krebs, Karl F., and Rodebush, W. H. The infrared absorption of proteins in the $3\,\mu$ region. XII, 1126

CARR, C. JELLEFF. *See* Bell, Frederick K.
CHANDLER, RAY CALVIN. A sensitive static vapor pressure apparatus, 574
CLACK, K. D. G. *See* Briggs, T. R.
CORSON, B. B. *See* Ipatieff, V. N.

DIRKSE, THEDFORD P. *See* Briscoe, H. T.
DITTMAR, C. *See* Sheppard, S. E.
DRUMMOND, D. H., TOLLMAN, J. P., AND RICHARDS, F. L. The effect of Roentgen irradiation upon erythrocytes, 172
DULL, R. B. *See* Egloff, Gustav

EDDY, ROBERT D., AND MENZIES, ALAN W. C. The solubilities of certain inorganic compounds in ordinary water and in deuterium water, 207
EGLOFF, GUSTAV, SHERMAN, J., AND DULL, R. B. Boiling point relationships among aliphatic hydrocarbons, 730
ELDER, ALBERT L., AND SPRINGER, ROBERT A. Application of the hydrogen-bridge theory to sorption from solution by silica gel, 943
ELLIS, J. W. *See* Sponsler, O. L.
EYRING, HENRY. *See* Stearn, Allen E.

FIDIAM, J. F. *See* Ford, T. F.
FISHER, E. D., AND SORUM, C. H. The influence of sol concentration on flocculation values, 62
FLEISCHER, MICHAEL. *See* Foote, H. W.
FONDA, GORTON R. The preparation of fluorescent calcite, 435
The yellow and red zinc silicate phosphors, 851
FOOTE, H. W., AND FLEISCHER, MICHAEL. Addition compounds of iodine with alkali bromides and thiocyanates, 640
AND FLEISCHER, MICHAEL. Solid polyiodides of rubidium, 633
AND FLEISCHER, MICHAEL. The iodides of some polyvalent metals, 647
FORD, T. F., LOOMIS, A. G., AND FIDIAM, J. F. The colloidal behavior of clays as related to their crystal structure, 1
FRANCE, WESLEY G. *See* Myers, William G.
FRICK, MARY. *See* McBain, James W.
FRICKE, HUGO, AND PARKER, EDWARD. The dielectric properties of the system gelatin-water. II, 716

GEIGLE, W. F. *See* Briggs, T. R.
GERMANN, FRANK E. E., AND HENSLEY, JAMES W. Quantitative capillary luminescence analysis, 1071
GOODEVE, C. F. *See* Arnold, J. E.
GORIN, MANUEL H. *See* Abramson, Harold A.
GRAMKEE, BRUCE E. *See* Hess, C. B.
GRINNELL, S. W. *See* Koenig, F. O.
GROSSE, ARISTID V., WACKHER, RICHARD C., AND LINN, CARL B. Physical properties of the alkyl fluorides and a comparison of the alkyl fluorides with the other alkyl halides and with the alkyls of the elements of period II, 275
GWATHMEY, ALLAN T., AND BENTON, ARTHUR F. The growth, orientation, and preparation of the surface of single crystals of copper, 35

HALL, G. C. *See* Addlestone, J. A.
HANDLER, PHILIP. *See* Smith, Allan K.
HAPP, G. P. *See* Sheppard, S. E.
HARTUNG, E. J. *See* Allison, L. R.
HAUSER, E. A., AND SCHACHMAN, H. K. Particle size determination of colloidal systems by the supercentrifuge, 584
HAZEL, FRED. Silicic acid as a protective colloid for manganese dioxide sols, 422
HAZLEHURST, T. H., AND NEVILLE, HARVEY A. Cybotaxis at interfaces, 592
HENSLEY, JAMES W. *See* Germann, Frank E. E.
HESS, C. B., AND GRAMKEE, BRUCE E. The specific heats of some aqueous sodium and potassium chloride solutions at several temperatures. I, 483
HEYMANN, E. *See* Allison, L. R.
HOCHGESANG, FRANK P. *See* Anderson, Harold V.

HODGE, HAROLD C. *See* Manly, Richard S.

HOUCK, R. C. *See* Sheppard, S. E.

HUME-ROTHERY, WILLIAM. The liquid state of the elements, 808

HUNTER, T. G. *See* Brancker, A. V.

HURD, CHARLES B., AND BARCLAY, RAYMOND W. Studies on silicic acid gels. X. The time of set of gel mixtures containing high concentrations of mineral acids, 847

AND PATON, HARRIS W. Studies of silicic acid gels. IX. The effect of a change of pH upon the time of set of some acid gels, 57

HURD, FRANK, AND LIVINGSTON, ROBERT. The quantum yields of some dye-sensitized photoöxidations, 865

HUTCHINSON, I. W., JR. *See* Litkenhous, E. E.

IPATIEFF, V. N., CORSON, B. B., AND KURBATOV, J. D. Mixed copper-chromium oxide hydrogenation catalysts, 670

IRISH, EDWIN M. *See* Stearn, Allen E.

JAMES, T. H. Mechanism of photographic development. II. Development by hydroquinone, 42

JOHNSTON, HERRICK L., AND MCCLOSKEY, KENNETH E. Viscosities of several common gases between 90°K. and room temperature, 1038

JOSEPH, GLENN H. A note concerning ion absorption by pectin, 409

KEMP, A. R., AND STRAITIFF, W. G. Hevea latex: effect of proteins and electrolytes on colloidal behavior, 788

KOBE, KENNETH A., AND STONG, JOSEPH P., JR. The ternary systems ethylene glycol-potassium carbonate-water and dioxane-potassium carbonate-water, 629

KOENIG, F. O. On quasi-reversible conduction and galvanic cells with liquid-liquid junctions, 101

AND GRINNELL, S. W. On the theory of galvanic cells subject to fields of force. I. The gravitational field, 463

KOLTHOFF, I. M., AND MACNEVIN, W. M. Studies on aging and coprecipitation. XXXIII. The thermal aging of imperfect barium sulfate, 921

See Sanders, Herbert L.

KORNFELD, GERTRUD. Photochemical reduction of ferric ion by oxalic acid, 949

KRAHL, M. E. The effect of variation in ionic strength and temperature on the apparent dissociation constants of thirty substituted barbituric acids, 449

KRANTZ, JOHN C. *See* Bell, Frederick K.

KREBS, KARL F. *See* Buswell, A. M.

KUMLER, W. D. Figures in thin layers of grease and viscous liquids, 612

KURBATOV, J. D. *See* Ipatieff, V. N.

LABOUT, J. W. A. *See* Saal, R. N. J.

LARSEN, ELMER C., AND WALTON, JAMES H. Activated carbon as a catalyst in certain oxidation-reduction reactions, 70

LAUFFER, MAX A. Ultracentrifugation studies on tobacco mosaic and bushy stunt viruses, 1137

LEWIS, DAVID T. The Macleod constant and its dependence on physico-chemical factors, 1007

LIBBY, W. F. *See* Randall, Merle

LINN, CARL B. *See* Grosse, Aristid V.

LITKENHOUS, E. E., VAN ARSDALE, J. D., AND HUTCHINSON, I. W., JR. The physical properties of the ternary system butyl alcohol-ethyl acetate-toluene, 377

LIVINGSTON, ROBERT. The photochemical oxidation of oxalic acid sensitized by ferric ion, 601

See Hurd, Frank

LONGTIN, BRUCE. *See* Randall, Merle

LOOMIS, A. G. *See* Ford, T. F.

MACDOUGALL, F. H. Brønsted's criticism of classical thermodynamics, 713

MACNEVIN, W. M. *See* Kolthoff, I. M.

MANLY, RICHARD S., BONNER, JOHN F., AND HODGE, HAROLD C. Light scattering in normal human dentine. The calculation of absorption and scattering constants, 745

Mark, H. Intermicellar hole and tube system in fiber structure, 764
Marsh, L. R. *See* Addlestone, J. A.
McBain, James W., Vold, Robert D., and Frick, Mary. A phase rule study of the system sodium stearate–water, 1013
McCloskey, Kenneth E. *See* Johnston, Herrick L.
Menzies, Alan W. C. *See* Eddy, Robert D.
Milligan, W. O. *See* Weiser, Harry B.
Moeller, Therald. Hydrous lanthanum hydroxide as an emulsifying agent, 259
Mrgudich, J. N. *See* Smith, Allan K.
Munro, L. A., and Pearce, J. A. The time of set of silica gels. V. The effect of alcohols and pH on the "heat of activation," 1024
Myers, William G., and France, Wesley G. A study of some properties of thixotropic gels containing egg albumin as the disperse phase, 1113

Nash, A. W. *See* Brancker, A. V.
Nelson, Harrison A. *See* Vernon, Arthur A.
Neurath, Hans. Intramolecular folding of polypeptide chains in relation to protein structure, 296
Neville, Harvey A. *See* Hazlehurst, T. H.

Oncley, J. L. Electric moments and relaxation times of proteins, 1103
Ouellet, C. *See* Potvin, R.

Pall, D. B. *See* Shehyn, H.
Parker, Edward. *See* Fricke, Hugo
Paton, Harris W. *See* Hurd, Charles B
Pearce, D. W. *See* Sprauer, J. W.
Pearce, J. A. *See* Munro, L. A.
Pfeiffer, J. Ph., and Saal, R. N. J. Asphaltic bitumen as colloid system, 139
Potvin, R., and Ouellet, C. The catalytic oxidation of hydrogen on platinum. A search for chemiluminescence and ionization, 235

Randall, Merle, Libby, W. F., and Longtin, Bruce. Approximate rules for solute activities in dilute solutions of non-electrolytes. Generalized form of Bury's rule, 313
  and Longtin, Bruce. Calculation of solute activities from activities of the solvent. Limiting behavior of the *h* and *j* functions in dilute solutions, 306
  and Longtin, Bruce. Freezing points in mixtures of strong electrolytes, 427
  and Weber, Heinz P. The activity of the constituents in mixtures of *n*-butyl alcohol and water at 30°C., 917
Redlich, Otto. Molal volumes of solutes. IV, 619
Reitemeier, R. F., and Buehrer, T. F. The inhibiting action of minute amounts of sodium hexametaphosphate on the precipitation of calcium carbonate from ammoniacal solutions. I. Quantitative studies of the inhibition process, 535
  and Buehrer, T. F. The inhibiting action of minute amounts of sodium hexametaphosphate on the precipitation of calcium carbonate from ammoniacal solutions. II. Mechanism of the process, with special reference to the formation of calcium carbonate crystals, 552
Richards, F. L *See* Drummond, D. H.
Rodebush, W. H. *See* Buswell, A. M.
Roper, Edwin E. Gas imperfection. I. Experimental determination of second virial coefficients for seven unsaturated aliphatic hydrocarbons, 835
Ruyssen, R. G. Electrokinetics. XXII. Electrokinetic potentials of barium sulfate in solutions of electrolytes and in fifty per cent ethanol, 265

Saal, R. N. J., and Labout, J. W. A. Rheological properties of asphaltic bitumen, 149
  See Pfeiffer, J. Ph.

Sanders, Herbert L., and Kolthoff, I. M. Photovoltaic behavior of pure silver bromide, 936
Sassaman, W. A. *See* Briggs, T. R.
Schachman, H. K. *See* Hauser, E. A.
Schmidt, Carl L. A. *See* Batchelder, A. C.
Shehyn, H., and Pall, D. B. The solubility of calcium oxalate in various salt solutions, 166
Sheppard, S. E., Houck, R. C., and Dittmar, C. The structure of gelatin sols and gels. VI. The adsorption of water vapor and the electrical conductivity, 185
    Vanselow, W., and Happ, G. P Photovoltaic cells with silver-silver bromide electrodes. III. Optical sensitizing by dyes, 411
Sherman, J. *See* Egloff, Gustav
Simha, R. The influence of Brownian movement on the viscosity of solutions, 25
Sisson, Wayne A. X-ray studies of crystallite orientation in cellulose fibers. III Fiber structures from coagulated cellulose, 513
Smith, Allan K., Handler, Philip, and Mrgudich, J N. The reaction of formaldehyde with amino acids: X-ray diffraction patterns, 874
Sorum, C. H. *See* Fisher, E. D.
    See Throckmartin, C L.
Sponsler, O. L., Bath, Jean D, and Ellis, J. W. Water bound to gelatin as shown by molecular structure studies, 996
Sprauer, J. W., and Pearce, D. W. Equilibria in the systems Na_2O–SiO_2–H_2O and Na_2O-Al_2O_3–H_2O at 25°C., 909
Springer, Robert A. *See* Elder, Albert L.
Stearn, Allen E., and Eyring, Henry. Absolute rates of solid reactions: diffusion, 955
    Irish, Edwin M., and Eyring, Henry. A theory of diffusion in liquids, 981
Stong, Joseph P., Jr. *See* Kobe, Kenneth A.
Straitiff, W. G. *See* Kemp, A. R

Thompson, Francis X. *See* Vernon, Arthur A.
Throckmartin, C. L., and Sorum, C. H. pH change in gold sol formation, 247
Tollman, J. P. *See* Drummond, D. H.

Van Arsdale, J. D *See* Litkenhous, E. E.
Van Hook, Andrew. The precipitation of silver chromate, 751
Vanselow, W. *See* Sheppard, S. E.
Vernon, Arthur A., and Nelson, Harrison A. Chemical preparation of colloidal suspensions in non-aqueous solvents I. Methyl alcohol and benzene, 12
    and Nelson, Harrison A. Chemical preparation of colloidal suspensions in non-aqueous solvents. II. Ether, dioxane, and acetone, 21
    and Thompson, Francis X. Catalytic hydrolysis of chlorobenzene in the vapor phase, 727
Vold, Robert D *See* McBain, James W.
Vollrath, Richard E. Translucent films of aluminum oxide, 401

Wackher, Richard C. *See* Grosse, Aristid V.
Walton, James H. *See* Larsen, Elmer C.
Weber, Heinz P. *See* Randall, Merle
Weiser, Harry B., and Milligan, W. O. An electron diffraction study of hydrous oxides amorphous to x-rays, 1081
White, Chester M. The specific heats of some aqueous sodium and potassium chloride solutions at several temperatures. II, 494
Wikswo, J. P. *See* Briggs, T. R.
Williams, Max B. *See* Bonner, Walter D.

INDEX TO NEW BOOKS

Abridged Scientific Publications from the Kodak Research Laboratories, Vol. XX, 829
Adam, N. K. The Physics and Chemistry of Surfaces, 829
Anderson, Arthur K. Essentials of Physiological Chemistry, 137

Balarew, D. Der disperse Bau der festen Systeme, 136
Baldwin, E. J. Principles of Inorganic and Analytical Chemistry, 1012
Barton, A. W. A Text-Book of Light, 138
Becker, R., and Döring, W. Ferromagnetismus, 531
Berthoud, A. Précis de Chimie Physique, 137
Bowman, F. Introduction to Bessel Functions, 952
Butler, J. A. V. Electrocapillarity, 953

Camm, F. J. A Dictionary of Metals and their Alloys, 950
Chalmers, Bruce. The Physical Examination of Metals. Vol. I. Optical Methods, 831
Chemistry and Medicine (edited by Maurice B. Visscher), 951
Crumpler, Thomas B., and Yoe, John H. Chemical Computations and Errors, 951

Dictionary of Chemistry (edited by Stephen Miall), 954

Eve, A. S. Rutherford, 832

Fowler, R. H., and Guggenheim, E. Statistical Thermodynamics, 831

Gaudin, A. M. Principles of Mineral Dressing, 532

Herzberg, Gerhard. Molecular Spectra and Molecule Structure. I. Diatomic Molecules, 682, 954
Hibben, James H. The Raman Effect, 681
Hinshelwood, C. N. Kinetics of Chemical Change, 1147

International Union of Chemistry. Tables and Committee Reports, 1149

Jauncey, G. E. M., and Langsdorf, A. S. M. K. S. Units and Dimensions and a Proposed M. K. O. S. System, 825
Jellinek, K. Kurzes Lehrbuch der physikalischen Chemie. Heft 2, 829
Jost, Wilhelm. Explosions- und Verbrennungs-vorgänge in Gasen, 529

Krczil, Franz. Technische Adsorptionstoffe in der Kontaktkatalyse, 530

Maass, O., and Steacie, E. W. R. An Introduction to the Principles of Physical Chemistry, 397
MacDougall, F. H. Thermodynamics and Chemistry, 825
Mann, W. B. The Cyclotron, 828
McKenna, N. C. Theoretical Electrochemistry, 679
Mellor's Modern Inorganic Chemistry, 136
Miller, Elmer S. Quantitative Biological Spectroscopy, 680

O'Rahilly, Alfred. Electromagnetics: A Discussion of Fundamentals, 397

Partington and Stratton. Intermediate Chemical Calculations, 1147
Pauling, Linus. The Nature of the Chemical Bond, 827, 952

Reilly, Joseph, and Rae, William Norman. Physicochemical Methods, 953

Rheological Memoirs (edited by Eugene C. Bingham), 829

Rice, O. K. Electronic Structure and Chemical Binding, 1148

Roberts, J. K. Some Problems in Adsorption, 833

Sage, Bruce H., and Lacey, William N. Volumetric and Phase Behavior of Hydrocarbons, 680

Sand, Henry J. S. Electrochemistry and Electrochemical Analysis. Vol. I, 1147 Vol. II, 1011

Schreinemakers, F. A. H. Lectures on Osmosis, 533

Scott, Blair G. W. Einführung in die technische Fliesskunde, 826

Semat, Henry. Introduction to Atomic Physics, 830

Sherwood, T. K., and Reed, C. F. Applied Mathematics in Chemical Engineering, 530

Sutermeister, Edwin, and Browne, Frederick L. Casein and its Industrial Applications, 834

S[illegible] Pedersen, Kai O. The Ultracentrifuge, 952

Thompson, Maurice de Kay. Theoretical and Applied Electrochemistry, 950

Thorpe, Jocelyn Field, and Whiteley, M. A. Thorpe's Dictionary of Applied Chemistry, 399

van Arkel, A. E. (Editor). Reine Metalle, 531

Visscher, Maurice B. (Editor). Chemistry and Medicine, 951

Weiser, Harry Boyer. Colloid Chemistry, 534

Indian Agricultural Research Institute (Pusa)
LIBRARY, NEW DELHI-110012

This book can be issued on or before.....................

Return Date	Return Date